Methods in Ecosystem Science

Osvaldo E. Sala
Robert B. Jackson
Harold A. Mooney
Robert W. Howarth

Editors

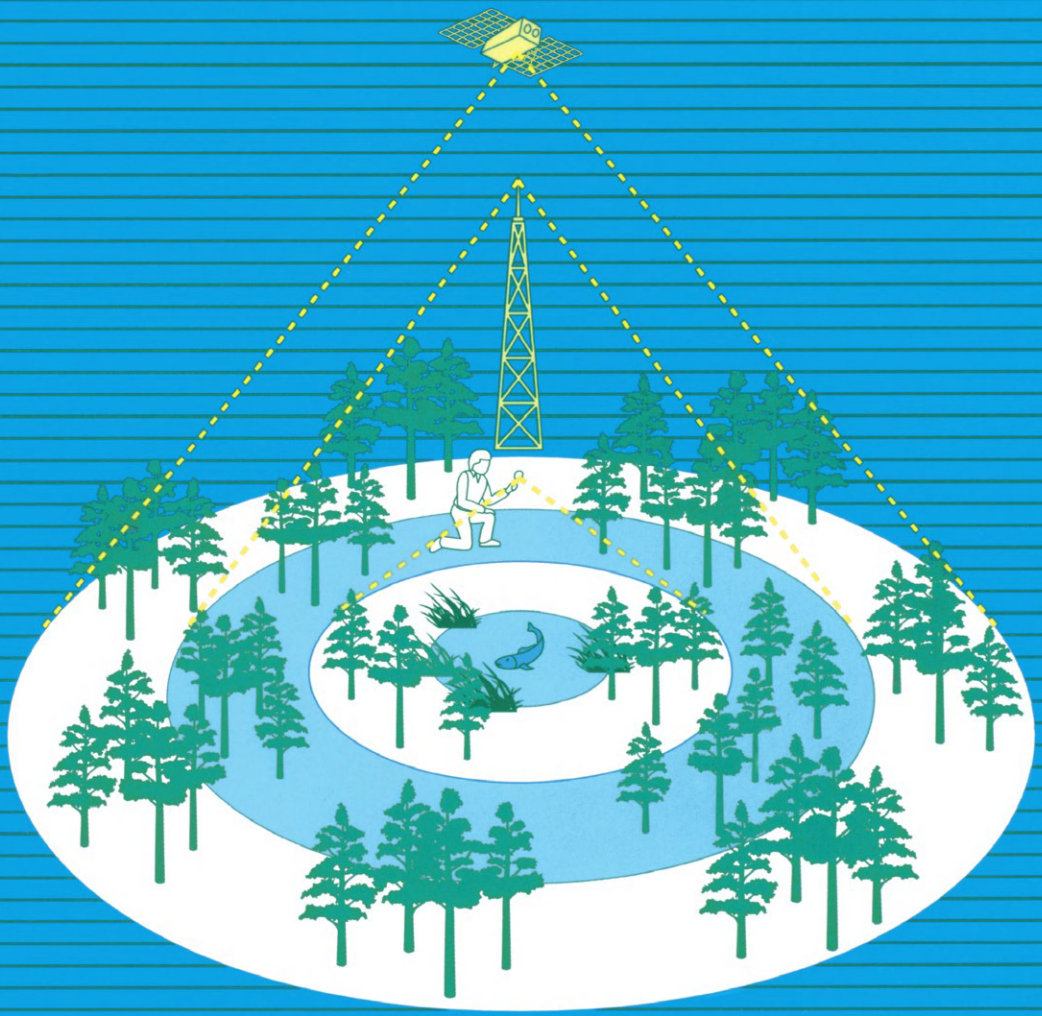

Methods in Ecosystem Science

Springer Science+Business Media, LLC

Osvaldo E. Sala Robert B. Jackson
Harold A. Mooney Robert W. Howarth
Editors

Methods in Ecosystem Science

Foreword by Eugene P. Odum

With 90 Illustrations

Springer

Osvaldo E. Sala
IFEVA
Cátedra de Ecología
Facultad de Agronomía
Universidad de Buenos Aires
Av. San Martin 4453
Buenos Aires 1417
Argentina

Robert B. Jackson
Department of Biology and Nicholas
School of the Environment
Phytotron Building
Duke University
Durham, NC 27708
USA

Harold A. Mooney
Department of Biological
Sciences
Stanford University
Stanford, CA 94305
USA

Robert W. Howarth
Program in Biogeochemistry and
Environmental Change
Section of Ecology and Systematics
Corson Hall
Cornell University
Ithaca, NY 14853
USA

Cover illustration: Diagram developed by A. T. Austin and O. E. Sala representing the different scales of study in ecosystem science. The questions asked by the ecosystem scientist will determine the scale of study and the variables to be evaluated, which range from interpretation of satellite imagery at the global scale to microbial populations in a milliliter of water or a gram of soil. A multidisciplinary approach and a broad range of methodology are necessary to address the newest challenges in ecosystem science.

Library of Congress Cataloging-in-Publication Data
Methods in ecosystem science / editors, Osvaldo E. Sala ... [et al.].
p. cm
Includes bibliographical references and index (p.).
ISBN 978-0-387-98743-9 ISBN 978-1-4612-1224-9 (eBook)
DOI 10.1007/978-1-4612-1224-9
1. Ecology. I. Sala, Osvaldo E.
QH541.M43 2000
577—dc21 99-087691

Printed on acid-free paper.

© 2000 Springer Science+Business Media New York
Originally published by Springer-Verlag New York, Inc. in 2000
Softcover reprint of the hardcover 1st edition 2000
All rights reserved. This work may not be translated or copied in whole or in part without the written permission of the publisher (Springer Science+Business Media New York),
except for brief excerpts in connection with reviews or scholarly analysis. Use in connection with any form of information storage and retrieval, electronic adaptation, computer software, or by similar or dissimilar methodology now known or hereafter developed is forbidden.
The use of general descriptive names, trade names, trademarks, etc., in this publication, even if the former are not especially identified, is not to be taken as a sign that such names, as understood by the Trade Marks and Merchandise Marks Act, may accordingly be used freely by anyone.

Production coordinated by Impressions Book and Journal Services, Inc., and managed by Steven Pisano; manufacturing supervised by Joe Quatela.
Typeset by Impressions Book and Journal Services, Inc., Madison, WI.

9 8 7 6 5 4 3 2 1

SPIN 10556922 (softcover)
SPIN 10708731 (hardcover)

Foreword

The ecosystem is the first (or lowest) unit in the molecule-to-ecosphere levels-of-organization hierarchy that is complete, that is, has all of the components, biological and physical, necessary for survival. Accordingly, it is the basic unit around which to organize both theory and practice in ecology. As the shortcomings of the "piecemeal" short-term technological and economic approaches to dealing with complex environmental problems become ever more evident with each passing year, ecosystem management emerges as the challenge for the present and future.

As ecologists and resource managers move up from the species and population levels to the ecosystem level, the biological ecologist needs the help of the physical scientist when it comes to methods, as is evident in the layout of this book on ecosystem methods. About half of the 51 authors of the 26 chapters are chemists, hydrologists, limnologists, soil scientists, and others associated with ecology and environmental and resource sciences departments and schools rather than biology departments. Many of these are not current members of the Ecological Society of America.

Chapters are about evenly divided between aquatic and terrestrial environments in the four sections: 1, energetics (ten chapters); 2, nutrient and water cycling (eight chapters); 3, experimental approaches (six chapters); and 4, modeling (two chapters). Measurement of organic production is a special focus. Primary production is easier to measure by gaseous exchange in water than on land. Gross production is very difficult to measure on land, especially in large biomass ecosystems such as forests, so attention is focused on net primary production (four chapters). Estimating productivity at the biome and global levels by satellite remote sensing is very promising, but such estimates have to be ultimately calibrated by "ground truth" measurement.

In this era of multiauthored books, we can say that this one has a very high author diversity! The message is that measurements at the ecosystem and landscape levels require a lot of team effort.

Eugene P. Odum
Institute of Ecology
University of Georgia
Athens, GA 30602
USA

Acknowledgments

This book had its intellectual origin during a productive sabbatical leave at Stanford University where most of the editors met and freely discussed ideas about science in general and ecology in particular. At that time, we realized that there was a gap in ecology and that a book synthesizing methods in ecosystem science was badly needed. From the origin of the idea until completion of the book, we benefited from the help and encouragement of many people and institutions. We are deeply indebted to Amy Austin for her constant support, encouragement, and insightful discussions. We are very grateful to the authors for producing such high-quality chapters and for tolerating our multiple demands. We want to thank our responsible reviewers who, with their anonymous work, assured the excellent quality of all the chapters. Janet Slobodien provided excellent guidance and support throughout this project. We specially want to thank Anne Schram, Jazmín Vrsalovic, and Christian Micieli who contributed in many ways to the completion of this project. Finally, the Guggenheim and Mellon Foundations, the University of Buenos Aires, CONICET, and the Inter-American Institute for Global Change Research supported OES while the U.S. Department of Energy supported RBJ during the period when the ideas for this book fermented.

Osvaldo Sala
Rob Jackson
Hal Mooney
Bob Howarth

Contents

Foreword v
Acknowledgments vii
Contributors xix

Introduction. Methods in Ecosystem Science: Progress, Tradeoffs, and Limitations 1
Osvaldo E. Sala, Robert B. Jackson, Harold A. Mooney, and Robert W. Howarth

References 3

Part 1. Carbon and Energy Dynamics 5

1 Stand Structure in Terrestrial Ecosystems 7
Frank W. Davis and Dar Roberts

Introduction 7
Methodological Approaches 7
Models of Canopy Architecture 8
Remote Sensing Instrumentation for Indirect Methods 11
Portable Ground Instruments 11
Aerial Remote Sensing 12
Approaches for Estimating Stand Structure 18
Canopy Height 19
Vertical Foliar Distribution 19
Stand Density 21
Cover and Leaf Area 22
Biomass 23
Three-Dimensional Structure 24
References 25

2 Methods of Estimating Aboveground Net Primary Productivity 31
Osvaldo E. Sala and Amy T. Austin

Introduction 31
Methods to Estimate ANPP in Fast Turnover Ecosystems 33
Estimates of Aboveground Biomass 35

Methods to Estimate ANPP in Slow Turnover Ecosystems 36
Errors Associated with Estimates of ANPP 37
Optimal Methodology to Estimate ANPP 41
Summary 41
References 42

3 Global Terrestrial Gross and Net Primary Productivity from the Earth Observing System 44
Steven W. Running, Peter E. Thornton, Ramakrishna Nemani, and Joseph M. Glassy

Introduction 44
Theoretical Basis for the Algorithm for Global NPP 44
Relating NPP and APAR 45
Relating APAR and NDVI 45
Biophysical Variability of ε 45
Parameterization of ε with Global BIOME-BGC Simulations 46
Algorithm Implementation Logic in EOS 50
Satellite-Derived Input Variables 50
Final NPP Algorithm 51
Validation of Global NPP 53
Summary 55
References 55

4 Methods of Estimating Belowground Net Primary Production 58
William K. Lauenroth

Introduction 58
Concepts 58
Methods 59
Biomass 59
Ingrowth Cores 60
Isotopes 61
Carbon Balance 62
Nitrogen Balance 63
Minirhizotrons 63
Uncertainty in Estimates of BNPP 65
Summary 69
References 69

5 The Measurement of Primary Production in Aquatic Ecosystems 72
Robert W. Howarth and Anthony F. Michaels

Introduction 72
Light and Dark Bottle Oxygen Technique 74
Carbon-14 Technique 75
Problems and Challenges with Light and Dark Bottle and Carbon-14 Techniques 77
In Situ Diel Approaches 79
Remote Sensing Techniques 82
References 82

6 Benthic Respiration in Aquatic Sediments 86
Bo Thamdrup and Donald E. Canfield

Introduction 86
Total Benthic Mineralization, Flux Measurements 88
Other Total Mineralization Assays 89
Respiratory Pathways, Oxygen Respiration 90
Nitrate Reduction 91
Manganese and Iron Reduction 92
Sulfate Reduction 95
Methanogenesis 96
Conclusions 97
References 97

7 Decomposition and Soil Organic Matter Dynamics 104
G. Philip Robertson and Eldor A. Paul

Introduction 104
Plant Litter Decomposition 106
Fine Litter Decomposition Rates 106
Woody Detritus 109
Reciprocal Transplants and Standard Substrates 109
Soil Organic Matter Dynamics 110
Soil Organic Matter Stores 110
Physical Fractionation of Soil Organic Matter 110
Biological Soil Organic Matter Fractions 111
Use of Tracers 113
References 113

8 Stable Isotope Tracers and Mathematical Models in Soil Organic Matter Studies 117
Ronald Amundson and W. Troy Baisden

Introduction 117
Soil Organic Matter Pools and Dynamics 117
SOM Pools 117
SOM Additions 118
SOM Losses 118
Internal SOM Transfers 119
SOM Transformations 119
Stable Carbon Isotopes in Organic Matter 119
Well-Mixed One Box Model of C Isotopes in SOM 119
Uses of Well-Mixed Box Models in SOM C Studies 122
Models for Vertical Variations in the $\delta^{13}C$ Value of SOM 123
Stable Nitrogen Isotopes in Organic Matter 128
Well-Mixed One Box Soil Ecosystem Model of N Isotopes 129
Use of N Isotopes in SOM as a Tracer 132
Model of Vertical Variations in $\delta^{15}N$ Value of SOM 132
Conclusions 134
References 134

9 Microbial Carbon Cycling in Pelagic Ecosystems: Microbial Methods for Ecosystem Scientists 138
Jonathan J. Cole

Introduction 138
Abundance and Biomass 139
Epifluorescent Direct Count 140
Sample Preservation 141
Count by Flow Cytometry 141
Active and Inactive Cells 141
Cell Size and Biomass 142
Growth and Respiration of Planktonic Bacteria 143
Bacterial Secondary Production 143
Bacterial Respiration 144
Uptake and Turnover of Specific Substrates 144
Substrates Supporting Bacterial Growth 144
Conclusions 146
References 147

10 Herbivory in Terrestrial Ecosystems 151
Martín Oesterheld and Samuel J. McNaughton

Introduction 151
Consumption 151
Animal-Based Methods 151
Plant-Based Methods 152
Differential Use of the Two Approaches 154
Effect of Herbivores on Primary Production 154
Compensatory Growth 154
Approaches 155
References 156

Part 2. Nutrient and Water Dynamics 159

11 Canopy Fluxes 161
John B. Moncrieff, Paul G. Jarvis, and Ricardo Valentini

Introduction 161
The Canopy Scale 161
The Surface Boundary Layer 161
Net Ecosystem Exchange 163
Flux Footprint 164
Methodologies 166
Aerodynamic Method 167
Energy Balance/Bowen Ratio 167
Eddy Covariance 168
Conditional Sampling 174
Errors in Long-Term Measurements of Fluxes of Carbon and Water 174
Related Techniques 175
Conclusions 177
References 177

12 Assessing Ecosystem-Level Water Relations Through Stable Isotope Ratio Analyses 181
James R. Ehleringer, John Roden, and Todd E. Dawson

Introduction 181
Stable Isotopes: Natural Abundances and δ Notation 181
Isotope Ratio Mass Spectrometry 181
Meteoric Water Line 183
Evaporative Enrichment 183
Methods for Water Sampling, Extraction, and Analysis 184
Water Sample Collection and Storage 184
Soil, Leaf, and Stem Water Extraction 185
δD Analysis of Water 185
$\delta^{18}O$ Analysis of Water 186
Methods for Leaf and Stem Organic Matter Sampling, Extraction, and Analysis 186
Total Tissue Versus Cellulose Analysis 186
Leaf Sampling Considerations 187
Tree Ring Separation and Cellulose Purification 187
$\delta^{13}C$ Analysis of Organic Matter 188
δD Analysis of Organic Matter 189
$\delta^{18}O$ Analysis of Organic Matter 189
Short-Term, Ecosystem Process–Level Applications 189
Partitioning of Water Resources Among Plants Within Ecosystems 189
Using δD and $\delta^{18}O$ Water Pulses and Interpretation of Mixing Models 191
Water-Use Efficiency 192
Short-Term, Regional Process–Level Applications Across Ecosystems 193
Recycling of Water Among and Between Ecosystems 193
$\delta^{18}O$ of Atmospheric Carbon Dioxide 193
Long-Term, Temporal Scaling of Ecosystem Processes 193
Decadal-to-Century: Tree Rings 193
Millennial: Caliche 194
Animals 194
Short-Term Indicators of Water Source 194
Long-Term Indicators of Water Source 194
References 195

13 Measuring Water Availability and Uptake in Ecosystem Studies 199
Robert B. Jackson, Laurel J. Anderson, and William T. Pockman

Introduction 199
Theory and Currencies for Measuring Water in the Environment 199
Methods for Estimating Plant and Soil Moisture 201
Gravimetric Measurements of θ_m and θ_v 201
Techniques for Direct Measurement of ψ 202
Time Domain Reflectometry 204
Remotely Sensed Data Using Microwave Radiometers 206

Estimating the Vegetative Component of Ecosystem Water Fluxes 207
Sap Flow Measurements 208
Whole Root/Shoot Hydraulic Conductance 209
Summary 210
References 211

14 Nutrient Transformations 215
John M. Stark

Introduction 215
Non-Isotope Methods 217
Net Rate Measurements with Inhibitors 217
Rate Measurements Obtained from Nutrient Budgets 221
Net Rate Measurements with "Super Sinks" 221
Rate Measurements Using Substrate Analogs 222
Isotope Methods 223
Tracer Measurements 223
Isotope Dilution Measurements 224
Estimation of Rates by Modeling Methods 229
Natural Abundance Isotope Methods 230
Application of Methods to Other Nutrient Transformations 231
References 231

15 Biogenic Trace Gas Exchanges 235
Pamela Matson and Allen Goldstein

Approaches for Estimation of Fluxes 235
Enclosure Methods 236
Micrometeorological Approaches 242
Analytical Methods for Trace Gases 242
Multiple Approaches for Understanding and Estimating Fluxes 244
References 244

16 Ecosystem Nutrient Balance and Dynamics 249
Kate Lajtha

Introduction 249
Input–Output Ecosystem Budgets at the Watershed Scale 250
Atmospheric Inputs 251
Stream Outputs 252
Other Budget Approaches 253
Stand-Level Budgets Using Lysimetry 253
Monolith Lysimetry and Sandbox Experiments 256
Nitrogen-15 Studies at the Ecosystem Scale 258
References 259

17 Deposition of Nutrients and Pollutants to Ecosystems 265
Lars O. Hedin

Role of Atmospheric Deposition 265
Vectors of Delivery 266
Scales of Inquiry 266

Wet Deposition 267
Dry Deposition 268
Cloud Deposition 270
Mass-Balance Techniques 271
Stable Isotope and Other Tracer Techniques 272
Summary and Prospects 273
References 274

18 Landscape and Regional Biogeochemistry: Approaches 277
Ingrid C. Burke

Introduction 277
Pattern Analysis: Design for Field Studies 278
Stratified Sampling and Discrete Units 278
Sampling Continuous Variation 279
Spatially Explicit Analyses 280
Field Analyses 280
Modeling Movement 281
Extrapolating to the Regional or Landscape Scale 282
Field Analysis 282
Modeling 283
Summary 283
References 284

Part 3. Manipulative Ecosystem Experiments 289

19 Nutrient Manipulations in Terrestrial Ecosystems 291
Valerie T. Eviner, F. Stuart Chapin III, and Charles E. Vaughn

Introduction 291
Ecological Questions Addressed by Nutrient Addition 291
Nature of Nutrient Limitation 292
Commonly Limiting Nutrients 293
Single Versus Multiple Nutrient Limitation 293
Experimental Design 293
General Approach 293
Experimental Setup 294
Experimental Design 294
Time Scale of Response 295
Addition Rates 295
How to Add? 295
Form of Nutrients Added 296
Nitrogen 296
Phosphorus 298
Potassium 299
Sulfur 299
Isotopes 300
Alternatives to Nutrient Addition Experiments 302
Summary and Conclusions 303
References 303

20 Biotic Manipulation of Aquatic Ecosystems 308
Daniel E. Schindler, Brian R. Herwig, and Stephen R. Carpenter

Introduction 308
Manipulation of Species 308
Species Removals 308
Species Introductions 309
Habitat Manipulations 310
Macrophyte Restoration and Removal in Lakes 310
Restoration of Other Structural Features 311
Wetland Restoration 311
Simulation Modeling, Manipulation Strength, and Statistical Power 311
Future Prospects 313
Field Guide to Keystones 313
Humans and Ecosystems 313
Adaptive Management 314
References 315

21 Biotic Manipulations Involving Belowground Animals 318
Diana H. Wall and O. James Reichman

Introduction 318
Soil Biota 318
Exclusions as Biotic Manipulations 320
Physical Exclusion Methods 320
Chemical Exclusions 321
Natural Gradients as Treatments 322
Habitat Manipulations 323
Physical Alteration 323
Introductions and Transplants 323
Resource Manipulations 324
Laboratory Studies 324
Summary 325
References 325

22 Assessing the Effects of Acidification on Aquatic Ecosystems: Insights from Lake Experiments 330
Thomas M. Frost and Janet M. Fischer

Introduction 330
The Chemistry of Acidification 331
What Controls the Anthropogenic Acidification of Aquatic Ecosystems? 331
Ecological Consequences of Acidification 332
Smaller-Scale Experiments to Evaluate the Effects of Acidification 332
Large-Scale Experiments to Evaluate the Effects of Acidification 334
References 338

23 Large-Scale Water Manipulations 341
Paul J. Hanson

Introduction 341
Active Versus Passive Manipulations 342
Artificial Rainfall 343
Throughfall Interception 344
Verification of Water Treatments 345
Measurement Approaches 345
Dealing with Spatial Variation 346
Collection of Adequate Weather Data 348
Confounding Issues 348
Plot Size and Edge Effects 348
Statistical Replication 349
Conclusions 349
References 350

24 Ecosystem Climate Manipulations 353
Karin P. Shen and John Harte

Introduction 353
Global Climate Change and Ecosystems 353
Methods of Ecosystem Climate Manipulation 355
Laboratory Methods: Growth Chambers 355
Field Manipulations: General Considerations 356
Field Manipulations: Warming Experiments 357
Field Methods: Other Climate Variables 362
Field Methods: Enhancing UV-B Radiation 363
General Recommendations 364
References 365

Part 4. Synthesis and Conclusions 371

25 Ecosystem Modeling 373
Herman H. Shugart

Introduction 373
Lexical Phase 373
Parsing Phase 374
Modeling Phase 375
A Simple Population Model 376
Compartment Models and Material Flow 376
Formulation of Compartment Models for Ecosystem Studies 378
Analysis Phase 381
Model Validation 381
Sensitivity Analysis 381
Stability Analysis 383
Future Directions: Multiple Commodity Models and Individual-Based Models 383
Multiple Commodity Models 383
Individual-Based Models 385
Conclusions 386
References 386

26 Stoichiometric Analysis of Pelagic Ecosystems: The Biogeochemistry of Planktonic Food Webs 389
James J. Elser

Introduction 389
Biogeochemical Structure of Planktonic Food Webs 390
Dynamics Under Stoichiometric Constraints: The Andersen Model 397
What About the Microbes? 400
Methodological Issues 401
Applications 402
Implications 403
References 404

Index 407

Contributors

Ronald Amundson, Division of Ecosystem Sciences, University of California, Berkeley, CA, USA

Laurel J. Anderson, Department of Horticulture, Pennsylvania State University, University Park, PA, USA

Amy T. Austin, IFEVA and Cátedra de Ecología, Facultad de Agronomía, Universidad de Buenos Aires, Buenos Aires, Argentina

W. Troy Baisden, Division of Ecosystem Sciences, University of California, Berkeley, CA, USA

Ingrid C. Burke, Department of Forest Sciences, Colorado State University, Fort Collins, CO, USA

Donald E. Canfield, Institute of Biology, Odense University, Denmark

Stephen R. Carpenter, Center for Limnology, University of Wisconsin, Madison, WI, USA

F. Stuart Chapin III, Institute of Arctic Biology, University of Alaska, Fairbanks, AK, USA

Jonathan J. Cole, Institute of Ecosystem Studies, Cary Arboretum, AB, Millbrook, NY, USA

Frank W. Davis, Department of Geography, University of California, Santa Barbara, CA, USA

Todd E. Dawson, Center for Stable Isotope Biogeochemistry, Department of Integrative Biology, University of California, Berkeley, CA, USA

James R. Ehleringer, Stable Isotope Ratio Facility for Environmental Research, Department of Biology, University of Utah, Salt Lake City, UT, USA

James J. Elser, Department of Biology, Arizona State University, Tempe, AZ, USA

Valerie T. Eviner, Department of Integrative Biology, University of California, Berkeley, CA, USA

Janet M. Fischer, Department of Biology, Franklin and Marshall College, Lancaster, PA, USA

Thomas M. Frost, Trout Lake Station, Center for Limnology, University of Wisconsin, Madison, WI, USA

Joseph M. Glassy, Numerical Terradynamic Simulation Group, School of Forestry, University of Montana, Missoula, MT, USA

Allen Goldstein, Environmental Science, Policy and Management, Division of Ecosystem Sciences, University of California, Berkeley, CA, USA

Paul J. Hanson, Environmental Sciences Division, Oak Ridge National Laboratory, Oak Ridge, TN, USA

John Harte, Energy and Resources Group, University of California, Berkeley, CA, USA

Lars O. Hedin, Section of Ecology and Systematics, Cornell University, Ithaca, NY, USA

Brian R. Herwig, Illinois Natural History Survey, Center for Aquatic Ecology, Champaign, IL, USA

Robert W. Howarth, Program in Biogeochemistry and Environmental Change, Section of Ecology and Systematics, Cornell University, Ithaca, NY, USA

Robert B. Jackson, Department of Biology and Nicholas School of the Environment, Duke University, Durham, NC, USA

Paul G. Jarvis, Institute of Ecology and Resource Management, University of Edinburgh, Edinburgh, UK

Kate Lajtha, Department of Botany and Plant Pathology, Oregon State University, Corvallis, OR, USA

William K. Lauenroth, Department of Rangeland Ecosystem Science and Natural Resource Ecology Laboratory, Colorado State University, Fort Collins, CO, USA

Pamela Matson, Department of Geological and Environmental Sciences, Stanford University, Stanford, CA, USA

Samuel J. McNaughton, Biological Research Laboratories, Syracuse University, Syracuse, NY, USA

Anthony F. Michaels, Wrigley Institute for Environmental Studies, University of Southern California, Los Angeles, CA, USA

John B. Moncrieff, Institute of Ecology and Resource Management, University of Edinburgh, Edinburgh, UK

Harold A. Mooney, Department of Biological Sciences, Stanford University, Stanford, CA, USA

Ramakrishna Nemani, Numerical Terradynamic Simulation Group, School of Forestry, University of Montana, Missoula, MT, USA

Martín Oesterheld, IFEVA and Cátedra de Ecología, Facultad de Agronomía, Universidad de Buenos Aires, Buenos Aires, Argentina

Eldor A. Paul, Department of Crop and Soil Sciences, Michigan State University, East Lansing, MI, USA

William T. Pockman, Department of Botany, University of New Mexico, Albuquerque, NM, USA

O. James Reichman, Department of Ecology, Evolution, and Marine Biology and National Center for Ecological Analysis and Synthesis, University of California, Santa Barbara, CA, USA

Dar Roberts, Department of Geography, University of California, Santa Barbara, CA, USA

G. Philip Robertson, W.K. Kellogg Biological Station, Michigan State University, Hickory Corners, MI, USA

John Roden, Department of Biology, Southern Oregon University, Ashland, OR, USA

Steven W. Running, Numerical Terradynamic Simulation Group, School of Forestry, University of Montana, Missoula, MT, USA

Osvaldo E. Sala, IFEVA and Cátedra de Ecología, Facultad de Agronomía, Universidad de Buenos Aires, Buenos Aires, Argentina

Daniel E. Schindler, Department of Zoology, University of Washington, Seattle, WA, USA

Karin P. Shen, Energy and Resources Group, University of California, Berkeley, CA, USA

Herman H. Shugart, Department of Environmental Sciences, University of Virginia, Charlottesville, VA, USA

John M. Stark, Department of Biology and the Ecology Center, Utah State University, Logan, UT, USA

Bo Thamdrup, Max Planck Institute for Marine Microbiology, Bremen, Germany, and Institute of Biology, Odense University, Odense, Denmark

Peter E. Thornton, Numerical Terradynamic Simulation Group, School of Forestry, University of Montana, Missoula, MT, USA

Ricardo Valentini, Department of Forest Science and Environment, University of Tuscia, Viterbo, Italy

Charles E. Vaughn, Hopland Research and Extension Center, University of California, Hopland, CA, USA

Diana H. Wall, Natural Resource Ecology Laboratory and Department of Rangeland Ecosystem Science, Colorado State University, Fort Collins, CO, USA

Introduction. Methods in Ecosystem Science: Progress, Tradeoffs, and Limitations

Osvaldo E. Sala, Robert B. Jackson, Harold A. Mooney, and Robert W. Howarth

Ecosystem science is a relatively young field of ecology dealing with all of the organisms in an area and their relationships with the physical environment (Odum 1959). It includes plants, animals, and microorganisms, and studies the interactions among them and with the soil, water, and the atmosphere. In pursuing general patterns at the ecosystem level, and when trying to understand the mechanisms controlling these patterns, ecosystem scientists study the flow of energy and the cycling of material, including water and elements, such as carbon, nitrogen, and phosphorus. The rapid growth in ecosystem science during the last 20 years partially resulted from its unique relationship to other disciplines. Ecosystem science has articulated the role of organisms with the physical environment and emphasized the feedback of human activities with the atmosphere, rivers, and open oceans. The demands of global change research and earth-system studies are only likely to increase the importance of ecosystem studies in the future.

As ecosystem science grew and gained its identity, scientists began to develop their own methods for studying ecosystem processes. Some of these methods were developed ex novo, while some others were adapted from such disciplines as chemistry, physics, and physiology. The development of new tools fostered new concepts in ecosystem science, while new theories led to the development of new techniques in a synergistic interaction between theory and methods. For example, continuous flow mass spectrometers opened the possibility of using stable isotopes as a tool for studying water and nutrient dynamics in ecosystems. These new capabilities, in turn, stimulated a wealth of model and theoretical developments on isotopic discrimination by different ecosystem processes (see Chapters 8 and 12). The progress of ecosystem science is limited simultaneously by both theory and methods, as has been demonstrated by the benefits of introducing simulation models and remote sensing tools into ecological research (see Chapters 3 and 25). This book suggests that there are methods limitations, such as real-time root observation techniques, automated tissue grinders, or chamberless methods for flux measurements. These represent just some examples of methodological constraints, but they are not necessarily the only or the most important limitations.

The objectives of this book are to review the methods most commonly used in ecosystem science and to assess their advantages and disadvantages. Each chapter reviews the basic ecological concepts behind each method, describes the methods most commonly used and those increasing in importance, and examines tradeoffs among alternatives. The aim of the book is to help scholars explore new areas and make decisions about the best methods to answer particular ecosystem questions. Because of the breadth of ecosystem science, the book cannot possibly describe all methods in detail, but instead provides information for choosing among methods and guidance for locating detailed information about particular techniques. When good reviews of particular techniques exist, some authors have chosen to direct the reader to those reviews, and concentrate on other methods less well described.

The range of methods in ecosystem science is one of our discipline's strengths, but it also poses

a challenge. Methods change quickly and are adapted to the needs of researchers locally. This local need sometimes conflicts with the need of our discipline to synthesize results across systems. If every researcher uses a different technique to measure an ecosystem process, we may be unable to compare results quantitatively across studies. This inability hinders some aspects of ecosystem science today and limits our ability to synthesize data for use by other disciplines. Another goal of this book, then, is to clarify differences and similarities among methods and suggest the extent to which results collected using different tools could be compared.

The book discusses tools to address similar questions in aquatic and terrestrial ecosystems. Differences between methods used in these two ecosystem types stem from differences in their natures and differences in the histories of the disciplines. Aquatic and terrestrial scientists have often worked in isolation as a result of the barriers imposed by the structure of institutions, such as funding agencies, universities, or scientific societies. Although structure is necessary and fosters efficiency, it sometimes leads to duplication and intellectual isolation. This book therefore attempts to present, in one volume, methods for aquatic and terrestrial ecosystems because we think that this intellectual interaction will be fruitful. Developments in one area may stimulate ideas in the other. The book attempts to cover the breadth of aquatic and terrestrial ecosystem science in a structure that is roughly parallel, but the reader will undoubtedly find gaps. For example, description of the manipulations of nutrients in terrestrial ecosystems does not have an aquatic counterpart in the book, and the analysis of animal manipulations belowground lacks a counterpart of the aboveground manipulations. Similarly, the book describes most types of manipulations of the abiotic environment but it misses some important manipulations, such as carbon dioxide.

Ecosystem science is a complex discipline spanning different spatial and temporal scales, from the square meter to the region and from minutes to centuries. As temporal and spatial scales change, not only the researcher's perspective changes but also the nature of the process and its controls change. Important controlling variables at one scale become white noise at a coarser scale, and what may have been considered constant now becomes a driving variable (Allen and Starr 1982; O'Neill et al. 1986). For example, in the case of carbon fixation, the same process can be studied at the scale of patches with a diameter of a few meters, at the landscape level, or at the regional level. Whereas differences in soil texture, through changes in water and nutrient availability, account for most of the variability in terrestrial carbon fixation at the finer levels of the hierarchy, they are overshadowed by climate variability at coarser scales (Sala et al. 1988). In contrast, while climate could be easily considered as a constant at the finer scale, it is certainly one of the major determinants of primary production patterns at the regional scale.

Important basic and applied questions in ecosystem science need to be addressed at each of these levels. The rate of primary production at the scale of a paddock or lake and its variability in space and time are critical tools when managing commercial fish stocks, herds of grazers, or forests stands. Carbon balance at the regional level is currently an important item in global negotiations for carbon trade among countries. Different tools and methods are necessary to address the same kind of questions at different scales. This book attempts to describe methods to address this nested hierarchy of ecosystem questions.

Chapters in this book do not prescribe a method or technique but emphasize tradeoffs among tools. A clear description of advantages and disadvantages will aid scientists in how to test hypotheses and answer questions. When discussing tradeoffs, the authors point out not only issues of scale but cost–accuracy or accuracy–understanding tradeoffs. Methods that yield the best results at a fine scale may not be the most appropriate at the regional scale. Similarly, the errors associated with methods sometimes are negatively associated with its costs. Consequently, the question and the accuracy needed for the estimate of the variable help to determine the best methodological option. Some chapters make a thorough analysis of the errors associated with each technique. In some cases, methods that provide estimates closest to the real value are not necessarily those that are most detailed (for example, see Chapters 2 and 4). A very detailed estimate of a large number of process components certainly yields a better understanding of the role of the different pieces. This bottom-up approach and the error inevitably associated with aggregation yield, in many cases, results that are farther away

from the real value. For example, when estimating primary production from a time series of total biomass versus from time series of individual species biomass, the latter yields valuable information about the behavior of individual species but an estimate of total production that is farther from the real value than if just total values were used (see Chapters 2, 4, and 18 for examples of errors associated with aggregation). Similarly, nutrient estimates at the mouth of a river yield better estimates of the biogeochemical behavior of the watershed than could have been obtained by laboriously measuring individual units in the watershed (Howarth et al. 1996). When the purpose of the study is the accurate estimate, then integrating measurements at the questions' scale are usually preferred. In contrast, when the main purpose is mechanistic understanding of ecosystem processes, detail estimates at finer scales than the level of interest are preferred.

Ecosystem science is complex and interacts with many other disciplines, such as atmospheric science, soil science, plant and animal physiology, as well as microbiology, zoology, and botany. The nature of ecosystem questions calls for such interdisciplinary work. Consequently, ecosystem studies incorporate pieces of methods from other disciplines and adapt them to satisfy ecosystem questions, which have their own scales and their own emphasis on interactions. The multiscale nature of ecosystem science, the wealth of interactions with other disciplines, the breadth of ecosystem studies, and the relatively recent development of its major concepts may explain the lack of a book to date that summarizes the methods used in ecosystem science.

One of the strengths of ecosystem science is the focus on the interactions among levels and between biotic and abiotic factors. This same strength results in a challenge to organize a methods book because most techniques examine the patterns and dynamics of more than one factor. Similarly, experimental manipulation of ecosystems that alter one part of the ecosystem frequently affect many other compartments and processes. This book is organized in four parts: the first encompasses methods related to carbon and energy dynamics, the second discusses those related to water and nutrient dynamics, the third describes experimental manipulations of abiotic and biotic factors, and the fourth discusses tools to synthesize our understanding about ecosystems.

References

Allen, T.; Starr, T. *Hierarchy: Perspectives for Ecological Complexity.* Chicago: Univ. Chicago Pr.; 1982.

Howarth, R.; Billen, G.; Swaney, D.; Townsend, A.; Jaworski, N.; Lajtha, K.; Downing, J.; Elmgren, R.; Caraco, N.; Jordan, T. et al. Regional nitrogen budgets and riverine N & P fluxes for the drainages to the North Atlantic Ocean: Natural and human influences. Biogeochemistry: 35:75–139; 1996.

Odum, E. *Fundamentals of Ecology.* Philadelphia: Saunders; 1959.

O'Neill, R.; DeAngelis, D.; Waide, J.; Allen, T. *A Hierarchical Concept of Ecosystems.* Princeton, NJ: Princeton Univ. Pr.; 1986.

Sala, O.E.; Parton, W.J.; Lauenroth, W.K.; Joyce, L.A. Primary production of the central grassland region of the United States. Ecology 69:40–45; 1988.

Part 1

Carbon and Energy Dynamics

1

Stand Structure in Terrestrial Ecosystems

Frank W. Davis and Dar Roberts

Introduction

This chapter provides a brief overview of instrumentation and methods for characterizing vegetation structure at the stand level, where a stand is defined as an area of relatively uniform physical environmental conditions, vegetation structure, and plant community composition (Barbour et al. 1987). By vegetation structure we mean the three-dimensional distribution of aboveground phytomass integrated over some period of time. We will not consider the temporal components of stand structure, such as diurnal variation in leaf orientation or seasonal phenology, focusing instead on methods for estimating structural variables at a particular point in time.

Knowledge of vegetation structure is essential for describing the exchange of energy and mass between vegetation and its environment. At leaf, branch, and canopy scales, vegetation structure influences the interception of precipitation, absorption of photosynthetically active radiation, and the turbulent exchange of momentum, heat, and mass. At the stand or regional scale, the density, height, and crown dimensions of canopies modify the availability of light and moisture and thus influence rates of plant establishment, growth, and succession. At all of these scales, vegetation structure influences the rates at which carbon is assimilated, stored, and transported through ecosystems and thus has a major impact on the cycling of carbon, water, and other nutrients.

Stand structure is also of fundamental importance to many other disciplines, for example, wildlife biology, phytosociology, forestry, range science, and fire ecology. Not surprisingly, an enormous array of qualitative and quantitative procedures has been developed to estimate different stand structural properties, and those procedures have tended to be tailored to the specific needs and perspectives of the different disciplines. The focus of this chapter is on recently developed procedures of special interest to ecosystem ecologists. We do not go into any detail on traditional, direct measurement methods, which are well described in reference works such as Ross (1981), Bonham (1989), Husch et al. (1982), and Norman and Campbell (1989). Instead, we emphasize indirect approaches that make use of recent advances in remote sensing and image analysis.

The chapter is organized as follows: First, we summarize and contrast direct versus indirect approaches for measuring vegetation structure, followed by an overview of models of canopy architecture that guide the analysis of vegetation structure and can form the basis for indirect approaches. Next, we describe some remote sensing instruments of special importance for indirect measurement of vegetation structure. The final section reviews some widely used direct and indirect methods for estimating common descriptors of vegetation structure at the stand level.

Methodological Approaches

Elements of stand structure include stems, branches, twigs, leaves, and other specialized organs, whole plants, and groups of plants (e.g., cohorts, members of a stratum, etc.), which can be

further described by position and condition (e.g., dead vs. living, standing vs. fallen, photosynthetic vs. nonphotosynthetic, etc.). The distribution of these elements can be summarized at many levels from individual plants to whole canopies, stands, landscapes, and regions.

An exact reconstruction of three-dimensional stand structure is currently not practical. Instead, summary descriptors must be estimated in one, two, or three dimensions. Common vertical descriptors include canopy height, canopy depth, stratification, and foliar profile. Common horizontal descriptors include cover, canopy closure, canopy or stem density, leaf area, stem basal area, and phytomass per unit area. Three-dimensional descriptions incorporate additional information on element size distribution within the stand volume, element position, and orientation. For some applications, the void between biomass elements (e.g., canopy gaps) is the variable of interest, although the methods will tend to be the same for estimating either phytomass distribution or its complement.

Structural descriptors can be estimated visually or from point, line, image, or volumetric samples. These samples consist of one or more measurements taken using a particular set of instruments and procedures (Bonham 1989). Vegetation structure generally has high fractal dimensionality, meaning that structural estimates depend strongly on the measurement scale (e.g., probe diameter, line interval, pixel area, etc.). Some methods, in fact, exploit the scaling features of vegetation to estimate structural properties such as canopy gap fraction (Chen et al. 1994) or three-dimensional distribution of biomass (Kruijt 1989).

Norman and Campbell (1989) distinguish ground-based direct methods that involve manual (contact) measurement of individual plants or plant organs from indirect methods involving remote sensing of stand properties. We adopt this terminology and further subdivide indirect methods into ground-based versus aerial (i.e., by aircraft or orbiting satellite) remote sensing.

Any investigation of stand structure must ultimately employ direct methods, at least for calibration and/or validation of indirect techniques. Most direct methods are labor-intensive and rely on relatively simple estimation procedures, such as statistical summarization (e.g., mean height) or application of allometric equations, to indirectly estimate one structural variable from another that can be measured directly (e.g., leaf area from directly measured sapwood area). Direct methods have severe practical limits over large areas or heterogeneous vegetation and have the added disadvantage that they usually require disturbing the vegetation. Direct investigation of the structure of tall forest canopies poses a special challenge, and may require felling trees or use of elaborate rope systems, cranes, or suspended walkways (Koike and Syahbuddin 1993; Parker et al. 1992; Lowman and Nadkarni 1995).

Indirect methods are based on canopy–light interactions and range from very simple optical tools, such as gridded concave mirrors, to sophisticated hardware and software, such as radar scatterometers or satellite-borne radiometers. Data acquisition is generally much faster than with direct methods and can be conducted over larger areas. However, estimation procedures can be considerably more complex, involving calibration of indirect measures (e.g., regression modeling to retrieve biomass from radar backscatter power) or the inversion of empirical or physically based models (e.g., inversion of gap fraction data obtained from hemispherical photography to estimate total leaf area). Rapid advances in remote sensing theory over the past 20 years have led to general and robust indirect methods that, for many structural parameters, can provide more reliable estimates than the traditional direct methods. Lack of familiarity, equipment cost, and the complexity of data reduction methods are probably the main factors preventing even wider use of indirect approaches by ecosystem ecologists.

Models of Canopy Architecture

Many modern methods for characterizing plant structure at the plant or stand level are based on underlying models of plant geometry and canopy–light interactions. These canopy models have been developed for various purposes, for example, to explore the adaptive significance of canopy geometries (Horn 1971; Oker-Blom et al. 1989) or the effects of canopy shape on crown shadowing and light penetration in gaps (Kuuluvainen and Pukkala, 1989; Van Pelt and North 1996). Early efforts focused primarily on modeling the distribution of

leaves (e.g., Monsi and Saeiki 1953; Horn 1971) and branching patterns (Halle et al. 1978; Honda et al. 1981).

Radiative transfer models based on foliage amount and leaf angle distributions (LADs) are commonly used to estimate properties such as canopy cover and leaf area index (LAI) from integrated light measurements from quantum light sensors or upward-looking, hemispherical photographs. An example of such measurements is provided in Figure 1.1, which contrasts light profiles for late seral Douglas fir–hemlock forest and a plantation forest of broad-leaved *Populus*. Of special significance is the use of simple radiative transfer models to derive LAI from measured canopy "gap fraction," that is, the fraction of a field of view through a canopy that is not blocked by the canopy. One approach to derive LAI from gap fraction data uses the Beer–Lambert law of exponential extinction of light though a canopy as a function of that canopy's extinction coefficient (e.g., Marshall and Waring 1986). A second related approach inverts a one-dimensional model that is based on exponential extinction of light as a function of zenith angle, foliar density, and LAD (Norman and Campbell 1989; Welles 1990). Instruments and methods for gap fraction analysis are discussed in more detail later in this chapter.

Branch models by Honda et al. (1981) have been used to simulate growth patterns in tropical trees. More recent efforts have focused on fractal descriptions of branching patterns as a means of describing canopy architecture and modeling three-dimensional radiative transfer (Myneni et al. 1990; Chen et al. 1994). Fractal models of trees are attractive because complex branching patterns can be described by a few simple equations and still generate remarkably realistic architectures (Zeide 1991, 1993).

Canopy-to-stand scale models have primarily focused on the use of geometrical optical models and crown shadows (Li and Strahler 1985). Geometrical optical models generally assume canopies can be described as simple geometrical shapes, such as cones, spheroids, and ellipsoids, and focus on modeling the reflected light as consisting of illuminated and shadowed ground and sunlit and shadowed canopy. Early models disallowed mutual shadowing and were thus most applicable to open forests and shrublands (e.g., Pech et al. 1986; Franklin and Strahler 1988). More recent models account for mutual shadowing (Li and Strahler 1992).

Understanding of the interaction between microwaves and vegetated surfaces has been advanced by theoretical canopy backscatter models. One class of models treats vegetation as a continuous random medium above a reflecting soil surface (e.g., Bush and Ulaby 1976; Attema and Ulaby 1978). A second class represents vegetation as an aggregation of individual scatterers, such as leaves and stems, over a continuous soil surface and uses estimated probabilities of microwaves passing though canopy gaps or intersecting crowns and stems to calculate backscatter and attenuation (e.g., Lang and Sidhu 1983). Most current forest backscatter models are based on realistic forest geometry, specified by size, shape, orientation, density, and dielectric constant of cylindrical or disk-shaped scattering elements. These models compute microwave scattering from multiple sources (trunk, ground, crown, trunk–ground double-bounce, etc.) and evaluate net forest backscatter using a radiative transfer approach. Such physically based models have been formulated for use with both continuous and discontinuous canopies. Continuous models treat the canopy as a randomly organized layer of scatterers (Richards et al. 1987; Ulaby et al. 1990), whereas discontinuous models treat it as separate crowns, in which the scatterers are aggregated into crown-shaped volumes (Sun et al. 1991; McDonald and Ulaby 1993). The discontinuous models use estimated probabilities of microwaves intersecting crowns and stems or passing through canopy gaps to calculate backscatter and attenuation. More recently, Sun and Ranson (1995) have introduced a three-dimensional forest backscatter model that also accounts for the size distribution and spatial arrangement of trees within a modeled pixel. Canopy backscatter models have helped elucidate the mechanisms of microwave scattering in forests (e.g., McDonald et al. 1990; Wang et al. 1993; Imhoff 1995). However, the complexity of surface–microwave interaction is such that current physically based models can only be inverted under very restrictive assumptions about vegetation structure and ground conditions (e.g., Polatin et al. 1994).

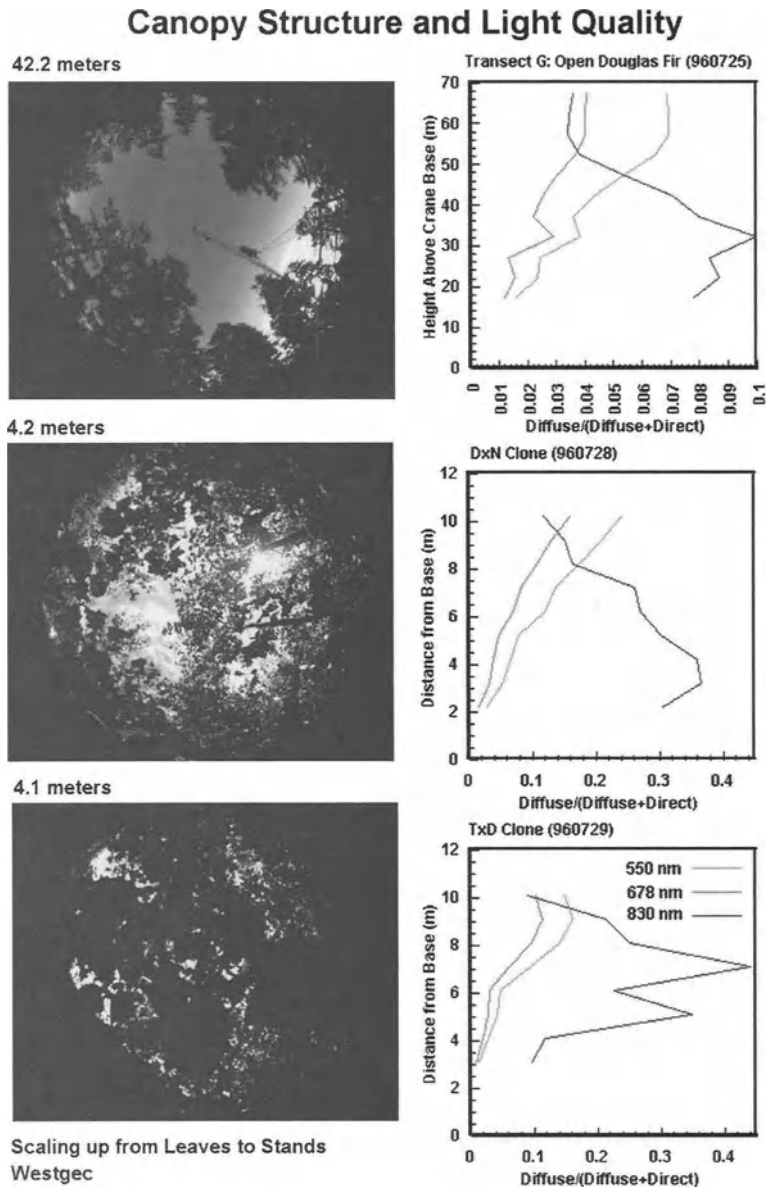

FIGURE 1.1. Color hemispherical photographs late seral Douglas fir forest and two clonal *Populus,* one with more vertically oriented leaves (*P. deltoides* × *P. nigra* = D×N) and one with more horizontally distributed leaves (*P. trichocarpa* × *P. deltoides* = T×D). Hemispherical photographs were measured at at least 10 heights within each crown. Vertical light profiles measured at the same location as the hemispherical photographs are shown to the right. At 42.2 m above the ground, the Douglas fir canopy is relatively open, consisting primarily of clustered foliage and branches (top). In comparison, the clonal *Populus* canopies consist of more uniformly distributed leaves. Major differences at 4.2 m height between the D×N (middle) and T×D (bottom) clones are due to leaf angles. Light penetration is highest in the D×N clone due to its more vertically oriented leaves. All three canopies show a decrease in diffuse red and green light and an increase in NIR. The largest difference among the profiles occurs in the T×D clone, which shows a rapid decrease in visible light and an initial rapid increase in diffuse NIR followed by a decrease. In contrast, both the D×N and Douglas fir profiles show more gradual changes in light and only a minor decrease in NIR closest to the forest floor. The difference between the T×D clone and the other canopies can attributed primarily to the more horizontal leaf orientation in the T×D clone. Higher diffuse light in the D×N and T×D clone profiles can be attributed to partially cloudy conditions, which did not block direct light but produced side-scattered diffuse radiation. *(See color plate.)*

Remote Sensing Instrumentation for Indirect Methods

Colwell (1983) defines remote sensing as "the measurement or acquisition of information of some property of an object or phenomenon, by a recording device that is not in physical or intimate contact with the object or phenomenon under study." Active remote sensing systems, such as laser (light amplification by stimulated emission of radiation) and active microwave systems, measure an electromagnetic signal sent by the sensor and returned by the illuminated surface. Passive sensor systems, such as film cameras or optical multispectral scanners, measure the brightness of sun-illuminated surfaces or the longwave thermal or microwave emission of surfaces.

Portable Ground Instruments

Rangefinders

Distance measurements are required to lay out plot boundaries as well as for many methods of estimating stand structure. Distance can be measured by direct comparison (measuring tape or wheel), optical instruments, or by electromagnetic devices (Curtis 1995). Because tapes are cumbersome and impractical over large distances or heights, optical or electromagnetic instruments are often the preferred alternative. Optical instruments can be based on angular observation of a reference length at the targeted distance (e.g., survey stadia) or on focusing of split images created by mirrors and lenses (coincidence rangefinders). Optical systems are relatively inexpensive, are usually practical over distances up to 300 m, and provide precision of roughly $\pm 1\%$.

Electromagnetic instruments, such as ultrasonic, infrared, and laser rangefinders, measure distance by comparing transmitted and received wave patterns or by measuring the round-trip travel time of short pulses of radiation. The simplest hand-held systems allow rapid measurements up to 100 m with an accuracy of $\pm 1\%$. More-sophisticated infrared or laser surveying systems can measure distances up to several kilometers with accuracies of ± 5 mm $\pm$ 0.0001%. Professional surveying systems also measure inclination and compass bearing to derive heights, volumes, and three-dimensional position (Curtis 1995). These more-expensive systems can be coupled to global positioning systems (GPSs) to map absolute locations in three dimensions within a few meters or to submeter accuracy depending on system configuration. All systems depend on a clear line of sight and are sensitive to atmospheric effects. Some systems require a special target, which limits their use for measuring forest canopies and in rugged terrain, although leaves and stems serve as suitable reflecting targets for most laser rangefinders.

Instruments for Gap Fraction Analysis

Several classes of instruments can be used beneath plant canopies to indirectly measure canopy gap fraction. Line quantum sensors integrate diffuse photosynthetically active radiation (PAR) measured by a linear array of photodiodes, whereas fisheye light sensors measure diffuse PAR using azimuthally arranged photodiodes. Upward-looking photographs taken through a hemispherical lens can also be processed to estimate canopy fraction (Rich 1990). Pulse laser systems have also been developed that scan the canopy and estimate the fraction of pulses intercepted by leaves (e.g., the Decagon Devices Leaf Laser, Decagon Devices, Inc., Pullman, Washington). As discussed in detail by Welles (1990), these systems vary considerably in sky condition requirements, calibration, sample size, time per site, and in the kinds of vegetation that can be measured. Welles and Cohen (1996) provide a current overview of the design of commercially available systems. Understory light sensors must be calibrated in the open and perform best under relatively continuous canopies and in diffuse light conditions when the sun is obscured.

Photography

Ground photography has been used for over 150 years to record features of vegetation, such as canopy height, closure, and composition. The major variables to consider are film format (35-mm cameras are defined as small format and low resolution), film type (panchromatic, normal color, color-infrared), lens focal length and field of view, speed of film advance, and scale of reproduction (Philipson 1997). Simple equipment, such as mounted, downward- or side-looking 35-mm cameras can be used to acquire mono or stereo color photographs

to monitor stand structural features, such as height and cover (e.g., Wimbush et al 1967). As mentioned above, upward-looking hemispherical photography is a long-standing method of obtaining information on canopy gap fraction and derived variables, such as LAI or foliar distribution (reviewed by Rich 1990). Furthermore, photographs can be readily scanned to generate digital images for quantitative analysis.

Video and digital cameras lack the spatial resolution of film photography but are a convenient means of producing panchromatic or color imagery for digital image analysis of vegetation. Most systems are based on solid-state, charge coupled device (CCD) array sensors. Video images generally must be converted from analog (videotape) to digital form using a frame grabber. Digital cameras, on the other hand, acquire and store digital images directly. The maximum spatial resolution (measured as resolution elements per square millimeter of surface) of current video and low-cost digital cameras is roughly 5 to 10 times coarser than that of standard film products (King 1995), although cost-performance is improving rapidly. More-expensive professional systems offer 1600 × 1200 or greater resolution and are beginning to approach the resolution of film while offering the advantage of real-time image editing, enhancement, and production.

Aerial Remote Sensing

Laser Altimetry

Aircraft- and satellite-borne laser systems transmit and analyze monochromatic light that interacts with and is partially reflected by the illuminated surface. LIDAR (light detection and ranging) laser systems measure the travel time of short pulses of light to estimate the sensor-surface distance, while more sophisticated systems measure changes in light quality to measure absorptive properties of the atmosphere (differential absorption LIDAR) or the velocity of a moving target (Doppler LIDAR). Beam divergence from airborne LIDAR systems can be widened to increase the illuminated ground area or "footprint," which typically ranges from 0.5 to 10 m. Time-varying return signals from targets at different distances from the sensor are sampled at high frequency to construct a "waveform" of distances to targets along the flightline. The waveform of heights can be analyzed to estimate the vertical distribution of vegetation and ground surface within the footprint.

Although low penetration of lasers through dense vegetation can lead to underestimation of vegetation height, LIDAR profiles obtained from aircraft show real promise for estimating vegetation height, stratification, and canopy closure over large regions (Nelson et al. 1988; Weltz et al. 1994; Nilsson 1996). In the United States, the National Aeronautics and Space Administration (NASA) has deployed several aircraft-borne laser altimeters, the most recent known as the laser vegetation imaging sensor (LVIS) (Blair et al. 1994; Blair and Coyle 1996). Nilsson (1996) describes an airborne Scandinavian system that uses a near-infrared (NIR) beam to measure distance to the surface or canopy, and a green beam to measure vegetation height profiles based on analysis of the waveform. In 2000, NASA is scheduled to launch the vegetation canopy LIDAR (VCL), a five-laser system designed to obtain global measurements of surface and vegetation height at 25-m horizontal resolution and 1-m vertical accuracy along sampling tracks separated by 2 km (http://essp.gsfc.nasa.gov/vcl).

Aerial Photography and Videography

Aerial photography has been in widespread use since the first quarter of the century and it continues to be the primary means for mapping and inventorying vegetation structural features, such as timber volume, shrub or tree crown diameter, crown closure, and vegetation height (reviewed in Philipson 1997). Large-scale (<1:100) photography can be obtained from balloons, cherrypickers, towers, and other low platforms. Medium- to small-scale photography is obtained from aircraft or satellite. Standard large-format film (23 × 23 cm) still provides the highest resolution, readily available, remotely sensed imagery.

Stand-level analyses generally employ true color and color-infrared film and acquire photos at 1:12,000 to 1:24,000 scale. Scale or "representative fraction" is used to measure distance in rectified photography. Shadow length in a single image or image parallax in stereo photo pairs can be used to measure object heights. Dot grids and other photogrammetric tools are typically used to estimate crown closure and composition.

Airborne video systems provide a relatively inexpensive source of high-resolution color or multispectral imagery (reviewed in King 1995). Multispectral imagery can be obtained by using multiple cameras with selective light filters (e.g., Everitt et al. 1995) or a single camera with either a rotating filter wheel or a beam splitter. Spectral bandwidths as narrow as 10 to 25 nm can be measured at visible and NIR wavelengths. Commercial airborne systems typically acquire multispectral imagery with a frame size of 2 × 1.4 km and an effective spatial resolution of 1 to 3 m. In addition to relatively high spatial resolution, airborne video systems have the advantage over satellite systems that the user can select the spectral bands, bandwidths, target location, date, and time. On the other hand, band-to-band registration and geometrical rectification of the imagery can be difficult. In this decade, videography has been made even more useful by the integration of GPSs, development of radiometric calibration capabilities, and evolution of digital camera sensors, which provide full-frame images instead of interlaced paired frames produced by video systems (King 1995).

Satellite-Borne Multispectral Scanners

Passive optical systems exploit the distinctive spectral properties of leaves and nonphotosynthetic structural components, such as branches and stems, to derive information related to light absorption and vegetation structure. The types of materials present, their relative abundance, and orientation influence the spectral quality of visible and NIR radiation scattered absorbed and reflected by vegetation. Most notably, canopy reflectance is a product of leaf optical properties, which include strong absorptance at less than 0.7 μm and high NIR scattering between 0.7 and 1.3 μm (Fig. 1.2). Changes in the relative proportion of reflected NIR and red radiation can be used to infer absorbed PAR, canopy cover, and LAI among other structural parameters (see Chapter 3). Leaf orientation and leaf area distribution modify these relationships by changing the light-scattering regime and changing the relative proportion of shadowed and unshadowed leaves. The relative proportion of nonphotosynthetic components and exposed soil modify the reflected signal, in general causing an increase in red reflectance, decrease in NIR (0.7 to 1.3 μm), and increase beyond 1.5 μm (see Fig. 1.2). At the scale of individual plants, crown geometry interacts with solar energy to modify the types of shadows cast by plants and the relative proportion of sunlit and shadowed crown. At the stand level, the density, types, and variation in crown height interact as a source of variance in canopy reflectance and shadowing across the landscape. For example, old-growth coniferous forest is distinguished from other forest and landcover types by high within-stand heterogeneity relative to second growth, and lower reflectance due to extensive shadowing (Fig. 1.3). In general, little floristic (taxonomic) information can be obtained from most systems, but broad functional vegetation types can be mapped (Graetz 1990). In contrast to broadband systems, recent advances using imaging spectrometers have shown promise for mapping select plant species in some ecosystems (Roberts et al. 1998a).

Since the advent of the LANDSAT program of orbiting multispectral scanners in 1972, much research has been devoted to retrieval of canopy cover, LAI, and canopy condition using digital multispectral imagery acquired from satellite platforms. Spaceborne remotely sensed data have an advantage over standard aerial photography in that they sample wavelengths that cannot be measured using photographic film and provide a standardized digital product, long-term and rapid-repeat coverage, and regional to global data sets. The primary limiting factor for spaceborne data is spatial resolution, which ranges from 10 m for SPOT panchromatic to as large as 8 km (AVHRR GAC data). A secondary limitation is the wavelengths that are sampled. For example, AVHRR samples only two wavelengths in the visible/NIR, SPOT samples three, whereas LANDSAT Thematic Mapper (TM) samples seven channels, three in the visible, one in the NIR, two in the shortwave infrared, and one in the thermal. Limitations in spatial and spectral sampling, combined with the spectral and spatial attributes of vegetation, interact to influence the types of information that can be derived remotely. Common airborne sensors include NS001, Daedalus, AVIRIS, CASI, ADAR, ASAR, and MAS, representing a range in spatial resolution to as low as 1 m (ADAR) and spectral resolution up to 224 bands (AVIRIS). Most recent research has focused on the use of LANDSAT TM data at a spatial resolution of 30 m.

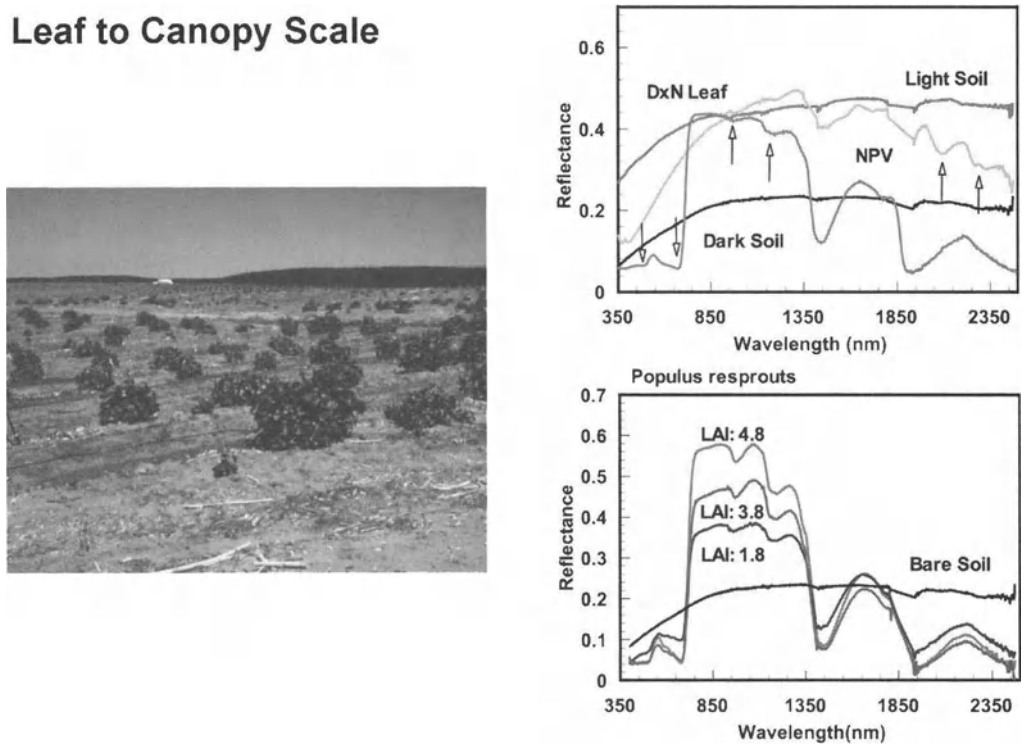

FIGURE 1.2. Leaf and canopy scale spectra of natural materials. The photograph on the left shows *Populus* resprouts (*P. deltoides* × *P. nigra* = D×N) located in the vicinity of Wallula, WA. Plants were flagged and placed in five height classes covering a range of heights and LAIs. Multiple spectra were collected from each resprout. A subset of 25 plants was destructively harvested to determine LAI for each plant and compared with canopy spectra and several spectral indices. Example spectra of a leaf, bare soil, and a *Populus* stump are shown in the upper right frame. Diagnostic absorptions for chlorophyll in the visible, liquid water in the NIR, and lignocellulose in the shortwave infrared are marked by arrows. Four spectra, sampled from bare soil and three canopies with LAIs ranging from 1.8 to 4.8, are shown in the lower right frame. Note the general decrease in red reflectance and increase in NIR reflectance with increasing LAI. Details on LAI sampling and spectral analysis are provided in Roberts et al., (1998b). *(See color plate.)*

In December 1999 NASA launched the first earth observing system (EOS) platform, which will include the much-anticipated moderate resolution imaging spectroradiometer (MODIS). MODIS can observe most of the earth every two days via 36 spectral bands at nadir instantaneous-fields-of-view of 250, 500, and 1000 m (Barnes et al. 1998). The MODIS imagery will be acquired in concert with LANDSAT 7 and ASTER (advanced spaceborne thermal emission and reflection radiometer) to allow multiscale sampling and land surface monitoring. The MODIS science team will derive and distribute several "standard data products" for monitoring regional and global vegetation dynamics, including surface reflectance, land surface temperature, albedo, vegetation indices, fraction of absorbed photosynthetically active radiation (FPAR), LAI, fires, landcover, and net primary productivity (NPP) (see Justice et al. [1998] for details).

Radar Remote Sensing

Active microwave sensors yield a wide range of information about earth surfaces, notably surface topography, surface roughness, soil moisture, and vegetation structure and composition (Henderson and Lewis 1998). All active microwave sensors share the advantages of being independent of solar

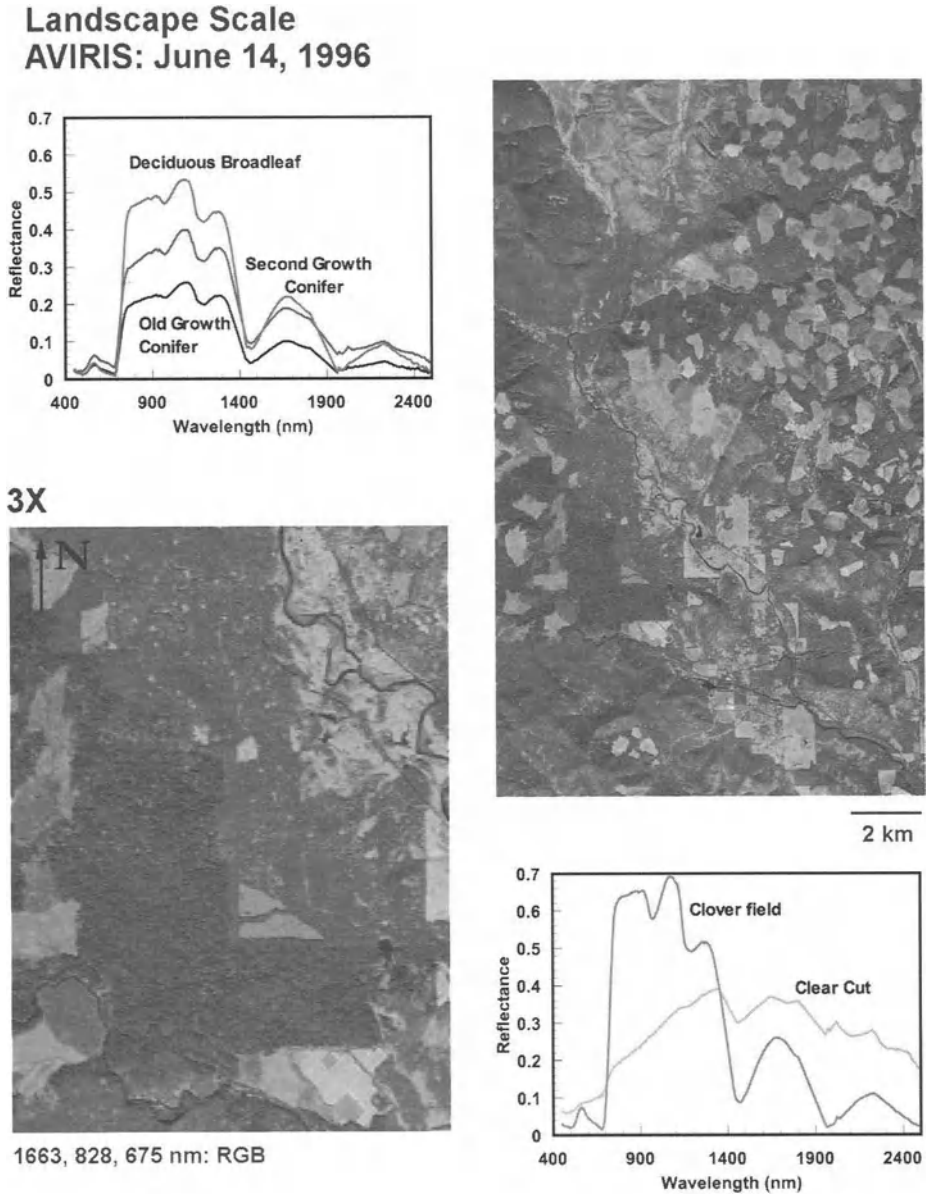

FIGURE 1.3. AVIRIS image acquired on June 14, 1996, over the Wind River Canopy Crane Research Facility (Carson, Washington). The frame on the upper right shows a false color composite with 1663, 828, and 657 nm displayed as red, green, and blue, respectively. In this rendition, vegetation is green and bare soil and slash are magenta. Old-growth forest is distinguished from second-growth forest and broadleaf plants by low reflectance due to shadowing. The frame on the lower left is 3× blowup centered over the T.T. Munger Research Natural Area. Old growth is distinguished from all other landcover types by its heterogeneity. In forest types, the highest reflectance occurs in the deciduous broadleaf trees, with second growth mixed hemlock and Douglas fir having intermediate reflectance between old-growth and broadleaf trees. Reflectance differences among these forest types are a combination of architecturally derived shadows and the different optical properties of leaves and needles. Nonforested landcover includes a clover field and clearcuts. Note, while visible reflectance tends to be lower in canopies than at leaf scales, NIR reflectance can be higher, as is shown by the clover field. Associated spectra for all five landcover types are shown. *(See color plate.)*

illumination and atmospheric turbidity. In this section, we focus on three specific radar systems that can provide valuable structural data. These include profiling radars, imaging synthetic aperture radar (SAR), and interferometric SAR.

Radar sensors operate by transmitting microwave radiation of a specific wavelength and polarization and then measuring the power of backscatter from the illuminated surface. Radars may transmit horizontally (H) or vertically (V) polarized microwave energy and may receive either polarization, resulting in four linear polarizations: HH, HV, VH, and VV. Backscatter is measured as radar "cross-section" in square meters. This scattering "area" is equivalent to actual area only for a perfectly reflecting isotropic target. As a result of forward scattering and absorption, most natural targets have cross-sections smaller than their physical areas, but, in some cases, the scattering geometry focuses energy back toward the antenna, causing very bright returns. The "normalized backscatter coefficient" (σ_0) equals the backscatter cross-section, σ, normalized by actual horizontal pixel area. This coefficient is unity for a perfectly reflecting isotropic surface and ranges over many orders of magnitude depending on radar wavelength, polarization, and local incidence angle, as well as on the size, orientation, and dielectric properties of the target. For this reason, backscatter is usually reported as σ_0 in decibels (that is, $\sigma_0 = 10 * \log_{10}(\sigma/\text{Area})$).

Structure and water content are the major controls of vegetation on radar backscatter. Soil surface roughness and moisture may also have a large effect on backscatter from low-biomass or discontinuous vegetation and at steep radar incidence angles where microwaves penetrate the canopy. Because of their high moisture content, plant structural components (leaves, branches, trunks, fruits) have high dielectric constants and thus behave as microwave scatterers and attenuators. Both microwave scattering and attenuation depend on the size and orientation of the scattering elements in relation to the wavelength, polarization, and incidence angle of the radar. Longer wavelengths (P-band [30 to 100 cm] and L-band [15 to 30 cm]) penetrate deeply into a forest canopy, attenuated to some degree by leaves and small branches. Thus, backscatter originates mainly from large branches and (in some forests) trunk–ground "double-bounce" reflections, in which microwaves are reflected from the ground surface, then off of standing stems, and finally back to the radar. Shorter wavelengths (C-band [3.75 to 7.5 cm] and X-band [2.4 to 3.75 cm]) are backscattered by small branches and leaves; penetration is shallow, except as it may occur through canopy gaps. Dry soils are more absorptive than wet soils, and flooded, vegetated surfaces can generate very high backscatter because the smooth reflective water surface enhances double-bounce reflection (Hess et al. 1990). P- and L-bands may find their best applications in forests (e.g., detection of flooding, estimation of biomass, monitoring forest regrowth) while C- and X-bands may be best applied to low-biomass vegetation (e.g., rangelands, wetlands, agriculture). Because the various bands and polarizations have been found highly complementary, multiband, multipolarization radars are desirable for vegetation study.

The round-trip travel time of the microwave signal from the radar antenna to the target provides a precise measure of distance to the target. Different systems utilize the positional information in different ways. Applied to vegetation canopies, a ranging scatterometer records backscatter as a function of distance into the canopy. A scatterometer or radar profiler traveling above the canopy and pointed downward samples the canopy depth profile. Radars such as SAR that are aimed obliquely down to the side of the flight track construct two-dimensional images of the canopy, in which each pixel represents backscatter integrated through the canopy depth. Interferometric imaging SARs can provide information on the depth dimension as well.

Scatterometers and Radar Profilers

Any calibrated radar can be a scatterometer, but scatterometers used for study of vegetation are most commonly nonimaging, ranging scatterometers, which record backscatter as a function of range distance (based on signal travel time). Typical resolutions are on the order of 10 cm to several meters. Laboratory scatterometers and truck-mounted field scatterometers have been used extensively to examine scattering and attenuation properties of plant structural components and canopies, forest included (e.g., Zoughi et al. 1986).

Scatterometry has also been used to study changes in backscatter associated with changes in vegetation moisture status and soil moisture content (e.g., Way et al., 1991). The main purpose of such studies has been to develop and validate models for microwave scattering and attenuation by vegetation, and to develop a sound basis for interpreting SAR images.

Profiling radars are nonimaging, airborne scatterometers that illuminate the surface with a near-vertical beam. These systems have direct application for forest inventory (e.g., Hyyppä and Hallikainen 1996). Over the past decade several systems have been deployed and tested in Europe. For example, the Helsinki University of Technology scatterometer (HUTSCAT) is a multipolarization C- and X-band helicopter-borne scatterometer with vertical resolution of 0.65 m (Hallikainen et al. 1993). Profiling radars return strong signals from the canopy top and from the ground, permitting direct calculation of tree height. Profiling radars also have demonstrated potential to discriminate structurally different vegetation types in diverse forests.

Synthetic Aperture Radar

Of available radar data, SAR data from aircraft and orbiting satellites provide the most useful information on stand structure over large areas (reviewed by Waring et al. [1995] and Kasischke et al. [1997]). SAR systems acquire multiple observations of a targeted area made from different locations in order to obtain backscatter properties at relatively high spatial resolution. Most spaceborne SAR systems have a fixed look angle between 20 and 50° with images covering a few degrees from near edge to far edge. An exception is RADARSAT, whose angle can be varied from from 20 to 59°. Today's spaceborne SAR systems also have relatively fine spatial resolution of 20 to 40 m and sampling frequencies of 20 to 40 days.

SAR imagery has been used to map landcover classes, inundation patterns, phytomass, canopy cover, and the freeze/thaw status of trees (Hess et al. 1990; Ranson and Sun 1997; Way et al. 1997). Despite their utility in cloudy regions and for deriving vegetation structural properties, SAR data have had little application in ecosystem ecology. Impediments to wider use include the complex nature of polarized backscatter data (especially in areas with significant vertical relief), poor data coverage, image speckle, and the need for specialized image processing software for calibration, rectification, and feature extraction (Kasischke et al. 1997). However, in recent years several operational systems have been placed in orbit, calibrated data are more widely available, and software has become available for the nonspecialist.

Differences in the types of information that can be obtained from radar and optical systems, such as LANDSAT TM, can be illustrated by comparing images collected over the same region (Fig. 1.4). Spaceborne imaging radar systems that are now in operation include: ERS-1, JERS-1, SIR-C/X-SAR, RADARSAT, and ERS-2. The ERS-2 follow-on, known as advanced SAR or ASAR, will be deployed on the planned European ENVISAT and consists of a dual-polarized C-band SAR. It will have both copolarized channels (HH and VV), but not crosspolarized (HV). The planned "wide swath" mode has a 400-km swath width and 100-m resolution.

Radar Interferometry

Interferometric measures of vegetation structure have the potential of providing canopy height, crown depth, canopy attenuation (extinction coefficient), and the density of canopy elements (Hagberg et al., 1995; Treuhaft et al., 1996), as well as more standard measures of ground surface elevation (Zebker and Goldstein, 1986). For interferometric radar, the phase of each returning microwave pulse is measured along with backscatter power and polarization. If two pulses travel slightly different distances, they can interfere constructively, increasing the amplitude of the return pulse, or destructively, creating a decrease. Different path lengths can be generated by shifting the origin of the pulse, either by using two microwave antennae separated by a known distance, known as the baseline, or by synthesizing a baseline by analysis of two SAR data sets recorded on different orbits or flights. Single-pass systems that use two antennae separated by a known baseline may be best for vegetation study, because vegetation movement between orbits causes image decorrelation. However, the decorrelation itself may yield information about vegetation structure and permit

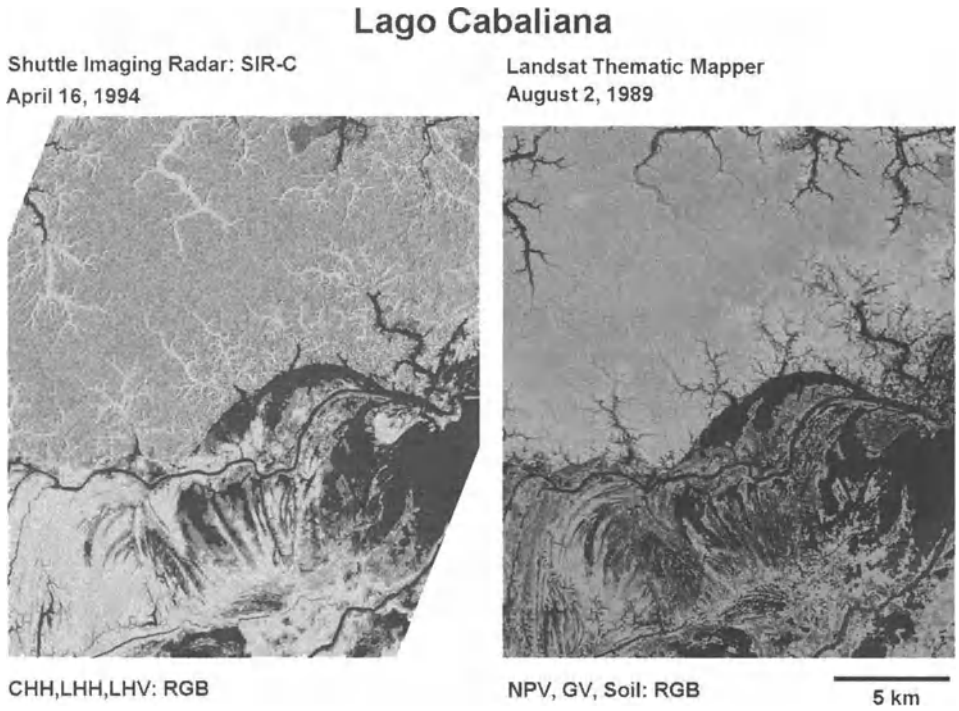

FIGURE 1.4. Comparison of SIR-C data and LANDSAT TM data for Lago Cabaliana, approximately 60 km southwest of the city of Manaus in central Amazonia. SIR-C CHH, LHH and LHV data from April, 1994, are displayed on the left as red, green, and blue, respectively. Flooded forests are evident as regions that are yellowish white due to a strong LHH double-bounce return, high C and low LHV. Recent clearcuts in the northeastern portion of the image have low returns in all three channels due to low standing biomass. The image to the right shows a LANDSAT TM scene acquired in same area on August 2, 1989. This image has been analyzed using spectral mixture analysis, generating fraction images for nonphotosynthetic vegetation, green vegetation, and soil, displayed as red, green, and blue (Roberts et al., 1993). Unlike the SAR image, the optical data are relatively insensitive to the presence of standing water and do not differentiate macrophytes from flooded forests. Spectral fractions vary primarily in response to the materials within the field of view and subpixel shadowing due to variation in leaf angles, crown shading, and the presence of canopy gaps. In this image, second-growth forest is readily separated from primary forest by a low shade content, which produces light green vegetation along the margins of rivers. Flooded forest, which commonly has a more uniform crown height than upland forest, is more homogeneous and is differentiated in many places by a lower shade content. Recent clearcuts are modeled primarily as nonphotosynthetic vegetation due to the presence of fallen logs and senesced grasses. *(See color plate.)*

accurate forest mapping. The phase shift induced by two returning pulses from a canopy is a product of the ground surface height, density of scatterers, crown depth, and degree of attenuation of the microwave pulse within the crown, which is frequency- and polarization-dependent (Treuhaft et al., 1996). Because the return signal from the canopy layer is a weighted return dependent on the degree of penetration within the crown, sophisticated models are required to retrieve canopy height.

Approaches for Estimating Stand Structure

This section briefly reviews direct and indirect methods and approaches for estimating stand height, vertical foliar profile, density, cover, LAI, biomass, and three-dimensional architecture. The reader is referred to the cited works for more detail on the actual procedures and analytical techniques required to apply these methods.

Canopy Height

Direct Methods

In herbaceous and shrubland vegetation, canopy height and stratification can be measured using pin probes at sample points, which are often arrayed along line transects or belts (Bonham 1989). Range scientists have also developed the "swardstick," which consists of a plate centered on a graduated vertical pole that, when properly calibrated, provides rapid estimates of sward height and density (e.g., Earle and McGowan 1979). In tall forest vegetation, one can access the canopy by ropes or cranes, trees can be felled to measure height and foliar profile directly (e.g., Maguire et al. 1996), or tree height can estimated allometrically from sapwood area measurements (Husch et al. 1982).

Indirect Methods

In low vegetation, ground cameras have been used to estimate canopy height both from horizontal profiles and from vertical stereo photographic pairs (e.g., Ivanov et al. 1994). Active ground sensors have not seen much use in herbaceous or shrubland types, although Hutchings et al. (1990) tested the use of ultrasonic rangefinders to estimate canopy height in grasslands and found the estimates of height and mass to be closely related to those obtained by direct swardstick measurements.

Many ground-based methods of tree height estimation have been developed. The time-honored approach uses hypsometers that measure the angle to a reference height in the canopy for a known distance from the base of the tree, and then applies trigonometric principles to derive tree height (Husch et al. 1982). Vertical optical rangefinders can also be used at sample points or along transects to measure canopy stratification (e.g., Clark et al. 1996). Unfortunately, all of the distance-based approaches depend on obtaining unobstructed views of canopy elements and are difficult to apply in rugged terrain and dense or multilayered forests.

For over 60 years, aerial photographs have been used to estimate shrub and forest canopy height based on either shadow lengths or parallax measurements (Philipson 1997). The use of stereo pairs depends on obtaining clear views of nearby ground surface as well as the canopy. Submeter accuracy of tree heights can be obtained from stereo aerial photographs depending on choice of camera, flying height, and equation.

Weltz et al. (1994) tested the use of an airborne laser profiling system against ground-estimated height of semiarid vegetation types and found that the two were in general agreement, although the waveform analysis method used did not perform as well in very clumped vegetation or very sparse shrublands. Nilsson (1996) tested the use of a helicopter-borne LIDAR system for estimating tree heights and stand volume in a 12- to 13-m tall pine plantation and found that mean tree height was sensitive to footprint size and was systematically underestimated by 2.1 to 3.7 m. Means et al. (1997) have obtained very promising results using aircraft laser altimetry to estimate tree height, foliar biomass, and total biomass in conifer forests of the western Cascades of Oregon (Fig. 1.5).

Profiling radar scatterometers have been used successfully to estimate canopy height. For instance, Hyyppä and Hallikainen (1996) reported rms errors of 1 m for estimates in 17- to 19-m pine and spruce stands. Forest height has also been correlated with backscatter data from airborne synthetic aperture radar systems. Working in temperate forests, Dobson et al. (1995) stratified vegetation into general structural types based on form, branching pattern, and leaf type, and used calibrated regression equations to estimate height from like-polarized or crosspolarized C-band, L-band, and/or X-band data, attaining moderate to high accuracy, depending on the forest type.

In a recent test of the applications of interferometric SAR (INSAR), Treuhaft et al. (1996) estimated ground surface height and canopy depth to an average accuracy of 5 m over a range of 25 m using a C-band system. They found that INSAR systematically overestimated canopy depth and that the magnitude of error in canopy depth and ground surface heights increased with increasing tree height. Multiple baselines and multifrequency SAR would be expected to increase accuracy (Hagberg et al. 1995; Treuhaft et al. 1996).

Vertical Foliar Distribution

Direct Methods

Foliar profiles of herbaceous and shrubland vegetation can be obtained directly by stratified probing or clipping of the canopy. Ross (1981) and Bonham

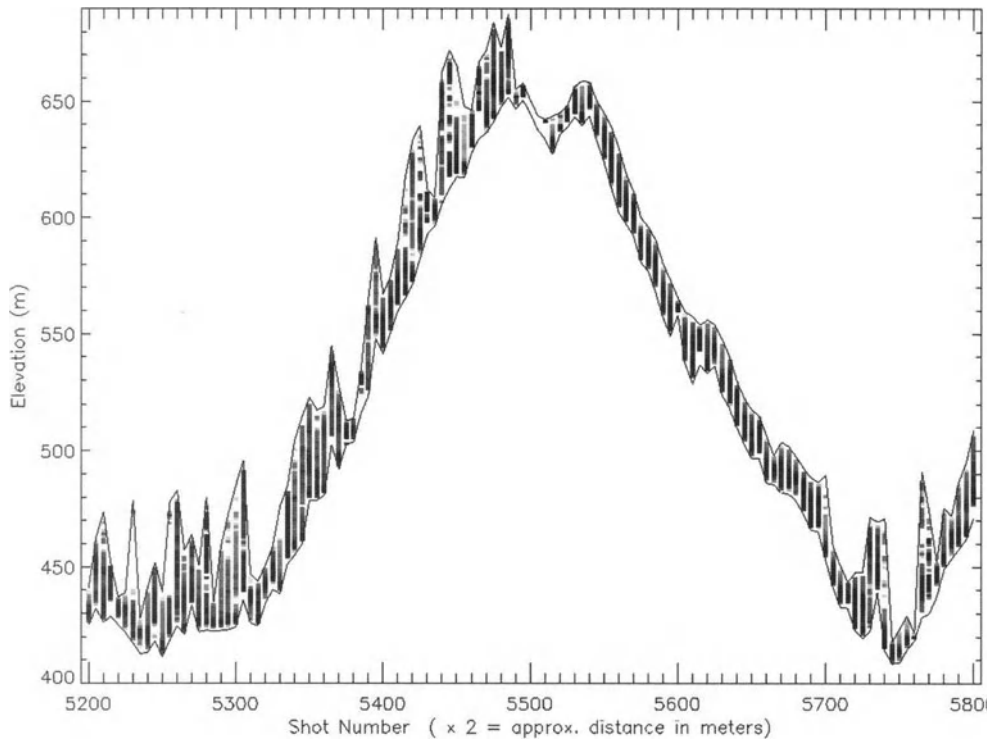

FIGURE 1.5. Profile of SLICER laser altimetry data from conifer forests in the Cascades Range in western Oregon. The gray scale is proportional to the density of reflective surfaces in the vertical profile. Each pixel is approximately 10 m in diameter. This 600-m transect over Blue Ridge (viewer faces SW) starts in the Lookout Creek valley on the left (the creek is in the lowest spot), continues up the south side of the ridge in mixed old-growth and mature forest, down the north side of the ridge through a uniform plantation of 50-year-old Douglas fir, and crosses Blue River on the right. At the top of the ridge, the dip in the ground topography is the top of Watershed 10. On both sides of Blue River one can see 20 to 30-m-wide riparian buffers, and the road is visible on the north (right) side of the river.

(1989) describe the use of point intercept methods for estimating foliar cover and orientation and emphasize that the approach may require very large sample sizes to obtain reliable estimates. Stratified clipping allows for detailed and precise measurements but is destructive and laborious. In forest, the distortion of the canopy makes it difficult to develop accurate profiles from felled trees. Kruijt (1989) developed a nondestructive, multiscale technique for developing vertical leaf and branch profiles based on direct measurements of sampled trees that appears practical for relatively low-statured forests (<15 m). Cameras or probes suspended from rope systems or cranes have also been used to nondestructively sample the forest canopy for vertical profiles (Koike and Syahbuddin 1993; Parker et al. 1992).

Daughtry (1990) summarizes direct methods for measuring leaf area and LAI. These include leaf tracing, matching sampled leaves to standard leaf shapes and sizes, estimation based on linear measurements, mass-based estimates, and areal measurement of harvested material using optical scanning or video planimeters. Linear measurements are especially well suited to estimating surface area of conifer needles, stems, and spines. For simple, planar leaves, portable optical planimeters provide rapid, accurate estimates of LAI and are the method of choice when a large number of samples is involved.

Indirect Methods

As noted in the previous section, rangefinders can be used to obtain vertical profiles of foliar density. The main concern is the length of time needed to obtain a sufficient number of distances to accurately characterize foliar height frequency distribution. To facilitate reconstruction of foliar profiles of low vegetation, such as crops, Sinoquet et al. (1993) mounted a mobile laser rangefinder in a 5 × 5 m frame above the canopy, acquiring a large number of sensor-plant distances to profile light interception in the canopy.

Koike (1985) describes a tomographic approach for obtaining two-dimensional vertical profiles of foliar distribution in forests using horizontal photographs taken from several locations in a section plane of the canopy. One-dimensional profiles are now routinely obtained by acquiring gap fraction data at a series of heights below the canopy. As mentioned previously, there are several methods for analyzing gap fraction data to retrieve LAI, but all depend on the assumption of random foliar distribution. This assumption appears reasonable for many canopy types (Nilson 1971), an important exception being that of conifer canopies (e.g., Norman and Jarvis 1974). Bidlake and Black (1989), working in *Larix occidentalis* forests, compared allometric estimates of LAI to indirect estimates using gap fraction analysis of hemispherical photographs and found that gap fraction procedures underestimated LAI by nearly 50% due to clumping of leaves and branches. However, the estimates were highly correlated and a calibration factor could be used to bring the approaches into close agreement. Martens et al. (1993) compared the one-dimensional inversion model of Norman and Campbell (1989) to the Beer-Lambert estimation procedure (Marshall and Waring 1986) for estimating the LAI of needle-leaved and broad-leaved trees, and found that results depended strongly on both the instrument used to measure gap fraction and the analytical technique. One-sided LAI estimates ranged from 2.93 to 8.98 for conifer forest and 2.1 to 6.56 for walnut orchard, and there were no consistent patterns that allowed for simple cross-calibration of methods.

The ability of lasers and microwaves to penetrate plant canopies raises the possibility of obtaining information on vertical leaf distribution in forests from profiling systems. Efforts to date have focused on height retrieval, although Hyyppä and Hallikainen (1996) also estimated the average height of the crown base with a precision of 1.5 m. Others (e.g., Hallikainen et al. 1993) show histograms of backscatter as a function of depth in the canopy, from which estimates of vertical foliar distribution can potentially be derived.

Stand Density

Direct Methods

Density, or the number of individuals per unit area, is a common descriptor of stand structure, although limited in its applicability to ecosystem studies, where other measures of abundance, such as cover, volume, and biomass, are usually desired. Bonham (1989) provides a detailed treatment of distance-based, angle-order, transect, and plot methods for direct measurement of density. Distance-based or "plotless" methods are frequently used to estimate tree and shrub density (e.g., Cottam and Curtis 1956), and can also be used to map individual plant locations (Rohlf and Archie 1978). Such methods are greatly expedited by optical and electromagnetic rangefinders, as are those methods that require laying out large sample plots.

Aerial Indirect Methods

Strahler et al. (1986) distinguish two different scene models for remote sensing, the high-resolution (H-resolution) model in which the elements of the scene are larger than individual pixels, and low-resolution (L-resolution) models in which the opposite is true. For density estimation, the elements of interest are individual plants or plant canopies. Most applications of remote sensing to density estimation have involved H-resolution approaches in which individual plants are resolvable in the imagery, for example, the use of film photography or aerial videography to estimate shrub or tree density in open shrublands and woodlands. Accurate density measurement requires rectified imagery or some other method to minimize effects of image distortion on area estimation.

Image processing methods have been developed to exploit spatial variance or texture in H-resolution imagery. For example, Cohen et al. (1990) applied variogram analysis to 1-m digital aerial photogra-

phy and found that variation in crown size was primarily related to the range of the variogram, whereas crown closure affected the sill. Cohen and Spies (1992) showed high correlation between canopy tree density and texture in SPOT HRV 10-m panchromatic imagery.

Low-resolution optical geometrical models have been used with some success to estimate tree and shrub density over large areas. For example, Wu and Strahler (1994) inverted an optical geometrical forest canopy reflectance model to estimate crown size and density in various conifer stand types in the northwestern United States. The inversion procedure systematically underestimated both crown size and density, but the estimates were highly correlated with field measurements ($r^2 > 0.9$ for density).

Cover and Leaf Area

Direct Methods

In general, cover refers to the vertical projection of vegetation onto the ground when viewed from above. (Unfortunately, crown density is often used synonymously with cover in the forest mensuration literature [Philipson 1997]). Point and line intercepts are the most common means for directly measuring cover, and there are many variations on the general approach (reviewed by Bonham 1989). Because cover is so tedious to measure directly, visual cover estimation has been widely used for survey and phytosociological studies (Mueller-Dombios and Ellenberg 1974), although not without bias (Gotfryd and Hansell 1985). McAuliffe (1990) devised a method for rapid and less-biased estimation of cover in sparse shrublands based on using logarithmic series of canopy density and diameter classes.

Indirect Methods

On the ground, cover can be measured indirectly based on the point intercept method using optical or electromagnetic devices, such as an upward-or downward-pointed "moosehorn" with bubble levels (Mueller-Dombios and Ellenberg 1974) or an upward-looking gridded concave mirror (spherical densiometer, Lemmon 1956). Alternatively, gap fraction methods can be used to estimate cover in both low and tall vegetation.

Many techniques have been developed to estimate canopy cover from aerial photographs. Most are based on either subjective visual estimation, a sampling approach (e.g., dot grids, line intercept), or area estimation (e.g., planimetering of tree crowns) (Husch et al. 1982). Aerial photographs may also be used as one stage in a multistage estimation procedure based on the measured relationship between cover measured in ground samples and estimates of the same areas made from large-scale aerial photographs (e.g., Pitt et al. 1996). Image processing methods have been used with mixed success to automatically delineate tree or shrub crowns in H-resolution digital imagery in order to measure crown size, cover, or density (Gougeon 1995).

Multispectral aircraft and satellite imagery has been extensively applied to estimate canopy cover. At scales ranging from 5 to 60 m, vegetation structure is expressed as subpixel mixtures of canopy components, including shadows, green leaves, branches, trunks, and exposed soil/litter, as well as interpixel variation in crown illumination due to stand scale heterogeneity in crown shape, density, and tree height. Analysis techniques at subpixel scales can be placed into two broad categories, ratio-based indices and linear techniques. Ratio-based indices primarily include the standard ratio (near infrared/red) and the normalized difference vegetation index (NDVI) (Tucker, 1979; Sellers 1985). They have been used to quantify LAI, FPAR, and percentage cover and have been highly successful in agricultural applications and in some analyses of forest structure (see Chapter 3). Although most applications have used data from operational orbiting LANDSAT or NOAA sensors, forest LAI has also been measured with high accuracy from aircraft-borne imaging spectrometers using simple regression models and spectral indices (Gong et al. 1995). Time series of NDVI images generated from global AVHRR data sets have been applied to monitor seasonal and interannual changes in canopy greenness and ecosystem primary production (Reed et al. 1994, reviewed by Defries et al. 1995). Recently, Myneni et al. (1997) demonstrated a relatively simple and robust algorithm for retrieving LAI and FPAR at continental to global scale.

Linear techniques include indices, such as the perpendicular vegetation index (PVI); (Richardson

and Wiegand 1977), KT transform (Kauth and Thomas 1976; Crist and Cicone 1984), and a diversity of spectral mixture models (Adams et al. 1993; Roberts et al. 1993). All of these techniques are based on the assumption that reflected radiance can be modeled as the sum of reflected radiance weighted by the aerial proportions of components within the field of view. In the case of the PVI, vegetation is modeled as the orthogonal distance in the NIR to red plane from a soil brightness line. The KT transform extends this analysis to include up to the six bands of LANDSAT TM, yet develops the orthogonal indices from a library of soil spectra. Spectral mixture models derive the mixing lines (analogous to soil brightness lines and axes from greenness and brightness) either by deriving pure spectra from the image (image endmembers) or from a library of measured field or laboratory spectra (reference endmembers). Vegetation structure is expressed as variation in either spectral fractions or one of the other linear measures. For example, a forested ecosystem might be best modeled as a mixture of green leaves, shadows, and exposed branches or litter (nonphotosynthetic vegetation, NPV). Early regeneration of conifers might be distinguished from old-growth forest by a decrease in green leaves, an increase in canopy shadows (gaps), and an increase in wood as exposed branches and snags (Heilman et al., 1996).

Radar profilers and SAR (notably L-band) have established capability to discriminate forest from nonforest, but topographic effects pose a real problem. In addition, SAR has demonstrated capacity to classify landcover types (Pierce et al. 1994). Thus far, the combined use of radar and optical systems for classification and cover estimation has not received much attention.

Biomass

Direct Methods

For herbs and small shrubs, biomass may be estimated by harvesting and weighing (Bonham 1989; Chiariello et al. 1989), although large sample sizes are needed to account for usually high local spatial variance. Point intercept methods have also been applied, although the quality of the estimates varies depending on plant growth form (Frank and Mcnaughton 1990). For some herbs and shrubs, the notion of reference units has proven useful. In this approach, small units of the plant are sampled and weighed, and then the number of reference units in the larger sample is counted (Andrew et al. 1981; Carpenter and West 1987).

Nondestructive methods for herbs, shrubs, and trees depend on allometric relationships between biomass and more readily obtained direct measures of cover, LAI, height, basal area, canopy diameter, or volume (reviews in Causton 1985; Bonham 1989; Husch et al. 1982; Etienne 1989). Thousands of allometric models have been developed for individual species, structural components, and environments. For example, Means et al. (1994) compiled over 1150 allometric equations for estimating biomass and other components of structure for common plant species growing in the western United States. They also produced public domain software (BIOPAK, http://www.fsl.orst.edu/rogues.tsuga/meansj/biopak.htm) to facilitate modeling based on these equations.

Indirect Methods

In herbaceous vegetation, biomass can be highly correlated with LAI, and thus gap fraction methods may be used to retrieve biomass based on fitted allometric equations. In shrublands, crown height, diameter, or volume may be estimated by ocular methods or from large-scale aerial photographs, and then dimensional equations applied to predict biomass (reviewed by Etienne 1989). Total aboveground forest biomass has been estimated through a variety of techniques based on ocular estimates of stand basal area, height, and/or density, and commercial inventory stand and stock tables (Husch et al. 1982). Stereo aerial photographs have been used extensively to estimate timber volume based on forest type, stand height, and crown diameter and/or closure (reviewed by Howard 1991).

Some traditional methods of biomass estimation exploit a multistage sampling approach to reduce the variance in biomass estimates obtained over large areas. These approaches incorporate ocular methods, aerial photographs, or satellite imagery at one or more scales to estimate biomass, and then measure biomass directly by harvesting or other techniques from a smaller number of subsamples of the same area (Bonham 1989; Heller and Ulliman 1983). These approaches can be extremely ef-

fective as long as there is moderate to high correlation between the indirect estimates and direct biomass measures (The theory of multistage sampling is presented in detail by Brewer and Hanif [1983].)

Ratio-based indices, linear models, and geometrical optical models have been used to estimate a variety of canopy biophysical properties directly linked to primary productivity including LAI, intercepted PAR, and phytomass (e.g., Tucker 1979; Asrar et al. 1989; see also Chapter 3). Indices, such as the NDVI and spectral ratio (SR), and linear techniques, such as the KT transform and PVI, have been used to estimate green biomass primarily through empirical relationships developed for crop plants and grassland ecosystems. Alternative approaches include the use of process-based models that link vegetation indices to meteorological variables, canopy aerodynamic resistance, net radiation, and physiological variables to compute seasonal changes in aboveground biomass (e.g., Running and Coughlan 1988, Asrar et al., 1989). These approaches have been highly successful for agriculture and grassland ecosystems and somewhat less successful in forested ecosystems (Hall et al., 1995). Myneni et al. (1995) provide a current review of models and algorithms used to derive vegetation structural information from optical imagery.

Geometrical optical models offer an alternative approach toward estimating green biomass and timber volume in woodland and forested ecosystems. For example, Wu and Strahler (1994) inverted an optical geometrical model to estimate tree crown radius and stand density and then used allometric equations to predict foliar, woody, and total biomass for nine conifer forest stands. Estimates of foliar biomass were highly correlated with direct estimates based on measured basal area (r^2 = 0.75). Indirect and direct methods were not as strongly correlated for total biomass (r^2 = 0.63). Hall et al. (1995) linked linear spectral mixture analysis with a cylindrical canopy geometrical model to model reflectance of boreal forests as a product of sunlit and shadowed canopy fractions. Using this approach, they were able to estimate biomass, density, average diameter at breast height (DBH), LAI, and aboveground NPP. In comparison, they found the NDVI was a poor predictor of canopy biophysical properties in these forests.

Because optical indices saturate at low levels of biomass, much attention has focused on the use of radar imagery for mapping and monitoring biomass in shrubland and forest ecosystems. Radar profilers look especially promising because they can accurately retrieve forest height. Kasischke et al. (1997) cite numerous studies that have demonstrated the sensitivity of imaging radar backscatter to woody plant biomass. Radar backscatter saturates at low to moderate levels of biomass (10 to 20 kg m^{-2}) and is highly dependent on radar wavelength and polarization, with the saturation level being higher for longer wavelengths. Among single band systems, P-HV and L-HV have proven the most useful wavelengths and polarizations.

Using multiband imagery and multistep estimation procedures, it may be possible to overcome saturation effects and obtain quite good estimates of forest biomass over large regions. For example, Dobson et al. (1995) first segmented the region into more uniform forest structural types and then used different wavelengths and polarizations to obtain separate estimates of canopy biomass, canopy height, and basal area, and then combined these to estimate total forest biomass in mixed coniferous–deciduous stands of northern Michigan. They achieved a correlation (r^2) of 0.95 between SAR-estimated and allometrically estimated biomass without any obvious saturation effect. Other studies have not attained such high accuracies and have not overcome saturation effects beyond 15 to 20 kg m^{-2} (Ranson and Sun 1997, Harrell et al. 1997). This could be due in part to the effects of other scene-dependent factors, such as soil moisture and surface roughness. All such studies are also subject to significant uncertainties in ground-based estimates of total biomass for the test stands.

Three-Dimensional Structure

Direct Methods

Nearly all work to reconstruct three-dimensional structure directly has been conducted in crops and other herbaceous vegetation and has emphasized the architecture of foliar elements. At a minimum, measures of leaf height, area, and orientation (normal to the leaf surface) are needed to reconstruct three-dimensional foliar structure. Stem structure requires measures of stem length, circumference,

and orientation (zenith and azimuth). Foliar orientation can be measured using a protractor, compass, and ruler (Ross 1981, Daughtry 1990). Lang (1990) describes a mechanical probe for measuring canopy structure that consists of four linked arms whose geometry is precisely measured to calculate the three-dimensional location of the probe tip within a sample volume of 1 m^3. Individual leaves are characterized by several to many point locations, and leaf area and orientation are derived analytically.

Martens et al. (1991) describe a method for reconstructing three-dimensional structure of tree canopies and demonstrate its applicability in a walnut orchard. The process involves stratified sampling of stem size and orientation in different size classes at the scale of the orchard (stand), tree, and branch levels to yield data that can be synthesized at the orchard level. Based on comparisons with plumb-line measures of three-dimensional position, the approach provides highly accurate estimates of canopy architecture and LAD. Fournier et al. (1996) characterized the canopy architecture of several conifer plantations using a "tree vectorization" method that involves sampling of structural components (trunk, branching structure, foliage distribution, and leaf size and orientation) and application of similarity principles to simulate individual trees. These trees were then used to simulate hemispherical photographs that closely resembled actual photographs from the field sites and allowed systematic investigation of effects of scale dependence, nonrandom foliar and branch distributions, and solar zenith angle on light extinction in forest canopies. Most recently, Sinoquet and Rivet (1997) describe a method that utilizes a three-dimensional digitizing device to reconstruct tree canopy architecture based on branching pattern, plant geometry, and shoot morphology. The method worked well when applied to a 7-m walnut tree. Needless to say, all of the aforementioned direct measurement methods for tree canopies work best for simple stand structures, such as plantations, and for relatively short, open-grown (symmetrical) trees.

Indirect Methods

Ross (1981) provides a theoretical basis for characterizing vertical leaf area distribution and leaf angle distribution (LAD) based on projected leaf area measured from multiple points of reference. Using these concepts, Vanderbilt et al. (1990) employed a laser much like a pin probe to estimate the probability of the beam being intercepted by various canopy elements as a function of height in the canopy and view direction. Vertical foliar profile and LAD were estimated using these probabilities.

Machine vision techniques have been successful at reconstructing simple three-dimensional objects and topographic surfaces from digital stereo imagery. However, these same methods have met with only limited success when applied to complex plant canopies, the main problem being the number of hidden leaf surfaces. Ivanov et al. (1994) were able to partly overcome this problem to reconstruct a maize canopy by taking sequential photos of the same canopy after removing successive leaf layers. It remains to be seen whether approaches based on machine vision will eventually evolve to handle the very heterogeneous structures encountered in natural plant stands.

Acknowledgments. We gratefully acknowledge John Day's contribution to the sections on radar remote sensing, Kim Brown for LAI measurements at Wallula and Keir Keightley for help with figures. Helpful advice and references were provided by Bryan Blair, Peng Gong, Joe Means, Nalini Nadkarni, and Steve Running. Data for Figures 1.1 to 1.3 were acquired with funding supplied by WESTGEC/NIGEC award WEGEC 95-062A. Partial support for F. Davis was provided through a NASA SIR-C/X-SAR project (Jet Propulsion Lab Contract # 958468).

References

Adams, J.B.; Smith, M.O.; Gillespie, A.R. Imaging spectrometry: Interpretation based on spectral mixture analysis. In: Pieters C.M.; Englert P., eds. *Remote Geochemical Analysis: Elemental and Mineralogical Composition.* Vol. 7. New York: Cambridge Univ. Pr.; 1993: 145–166.

Andrew, M.H.; Noble, I.R.; Lange, R.T.; Johnson, A.W. The measurement of shrub forage weight: Three methods compared. Aust. Range J. 3:74–82; 1981.

Asrar, G.; Myneni, R.B.; Kanemasu, E.T. Estimation of plant-canopy attributes from spectral reflectance measurements. In: Asrar, G., ed. *Theory and Applications*

of Optical Remote Sensing. New York: Wiley; 1989:252–296.

Attema, E.P.W.; Ulaby, F.T. Vegetation modeled as a water cloud. Radio Sci. 13:357–364; 1978.

Barbour, M.G.; Burk, J.H.; Pitt, W.D. *Terrestrial Plant Ecology.* 2nd ed. Menlo Park, CA: Benjamin Cummings; 1987.

Barnes, W.L., Pagano, T.S.; Salomonson, V.V. Prelaunch characteristics of the Moderate Resolution Imaging Spectroradiometer (MODIS) on EOS-AM1. IEEE Trans. Geosci. Remote Sens. 36:1088–1100; 1998.

Bidlake, W.R.; Black, R.A. Vertical distribution of leaf area in *Larix occidentalis:* A comparison of two estimation methods. Can. J. For. Res. 19:1131–1136; 1989.

Blair, J.B.; Coyle, D.B. Vegetation and topography mapping with an airborne laser altimeter using a high-efficiency laser and a scannable field-of-view telescope. In: *Proceedings of the Second International Airborne Remote Sensing Conference and Exhibition.* Vol. 2; Ann Arbor, MI: Environmental Research Institute of Michigan (ERIM); 1996:403–407.

Blair, J.B.; Coyle, D.B.; Bufton, J.L.; Harding, D.J. Optimization of an airborne laser altimeter for remote sensing of vegetation and tree canopies. Proc. IGARSS'94:939–941; 1994.

Bonham, C.D. *Methods of Vegetation Analysis.* New York: Wiley; 1989.

Brewer, K.R.W.; Hanif, H. *Sampling with Unequal Probabilities. Lecture Notes in Statistics 15.* New York: Springer-Verlag; 1983.

Bush, T.F.; Ulaby, F.T. Radar return from a continuous vegetation canopy. IEEE Anten. Propag. AP-24:269–276; 1976.

Carpenter, A.; West, N. Validating the reference-unit method of aboveground phyromass estimation on shrubs and herbs. Vegetatio 72:75–79; 1987.

Causton, D.R. Biometrical, structural and physiological relationships among tree parts. In: Cannell, M.G.R.; Jackson, J.E., eds. *Attributes of Trees as Crop Plants.* Huntingdon, UK: National Environmental Research Council; 1985:137–159.

Chen, S.G.; Ceulemans, R.; Impens, I. A Fractal-based *Populus* canopy structure model for the calculation of light interception. For. Ecol. Manage. 69:97–110; 1994.

Chiariello, N.R.; Mooney, H.A.; Williams, K. Growth, carbon allocation, and cost of plant tissues. In: Pearcy, R.W.; Ehleringer, J.; Mooney, H.A.; Rundel, P.W., eds. *Plant Physiological Ecology: Field Methods and Instrumentation.* London: Chapman and Hall; 1989:327–365.

Clark, D.B.; Clark, D.A.; Rich, P.M.; Weiss, S.; Oberbauer, S.F. Landscape-scale evaluation of understory light and canopy structure: Methods and application in a neotropical lowland rain forest. Can. J. For. Res. 26:747–757; 1996.

Cohen, W.G.; Spies, T.A. Estimating structural attributes of Douglas-fir/western hemlock forest stands from Landsat and SPOT imagery. Remote Sens. Environ. 41:1–17; 1992.

Cohen, W.B.; Spies, T.A.; Bradshaw, G.A. Semivariograms of digital imagery for analysis of conifer canopy structure. Remote Sens. Environ. 34:167–178; 1990.

Colwell, R.N., ed. *Manual of Remote Sensing.* Falls Church, VA: American Society of Photogrammetry and Remote Sensing; 1983.

Cottam, G; Curtis, J.T. The use of distance measures in phytosociological sampling. Ecology 37:451–460; 1956.

Crist, E.P.; Cicone, R.C. A physically-based transformation of Thematic Mapper data: The TM tasseled cap. IEEE Trans. Geosci. Remote Sens. GE-22:256–263. 1984.

Curtis, K.S. Linear measurements. In: Brinker, R.C.; Minnick, R. *The Surveying Handbook.* 2nd ed. New York: Chapman and Hall; 1995:42–50.

Daughtry, C.S.T. Direct measurements of canopy structure. Remote Sens. Rev. 5:45–60; 1990.

Defries, R.S.; Field, C.B.; Fung, I.; Justice, C.O.; et al. Mapping the land surface for global atmosphere-biosphere models: Toward continuous distributions of vegetations functional properties. J. Geophys. Res. Atmos. 100:20867–20882; 1995.

Dobson, M.C.; Ulaby F.T.; Pierce L.E.; Sharik T.L.; Bergen, K.M.; Kellndorfer, J.; Kendra, J.R.; Li, E.; Lin, Y.C.; Nashashibi, A.; Sarabandi, K.; Siquiera, P. Estimation of forest biophysical characteristics in northern Michigan with SIR-C/X-SAR. IEEE Trans. Geosci. Remote Sens. 33:877–895; 1995.

Earle, D.F. McGowan, A.A. Evaluation and calibration of an automated rising plate meter for estimating dry matter yield of pasture. Aust. J. Exp. Agric. Anim. Husb. 19:337–350; 1979.

Etienne, M. Nondestructive methods for evaluating shrub biomass: A review. Acta Oecol. Oecol. Appl. 10:115–128; 1989.

Everitt, J.H.; Escobar, D.E.; Cavazos, I.; Noriega, J.R.; Davis, M.R. A three-camera multispectral digital video imaging system. Remote Sens. Environ. 54:333–337; 1995.

Fournier, R.A.; Landry, R.; August, N.M.; Fedosejevs, G.; Gauthier, R.P. Modelling light obstruction in three conifer forests using hemispherical photography and fine tree architecture. Agric. For. Meteorol. 82:47–72; 1996.

Frank, D.A.; Mcnaughton, S.J. Aboveground biomass estimation with the canopy intercept method: A plant growth form caveat. Oikos 57:57–60; 1990.

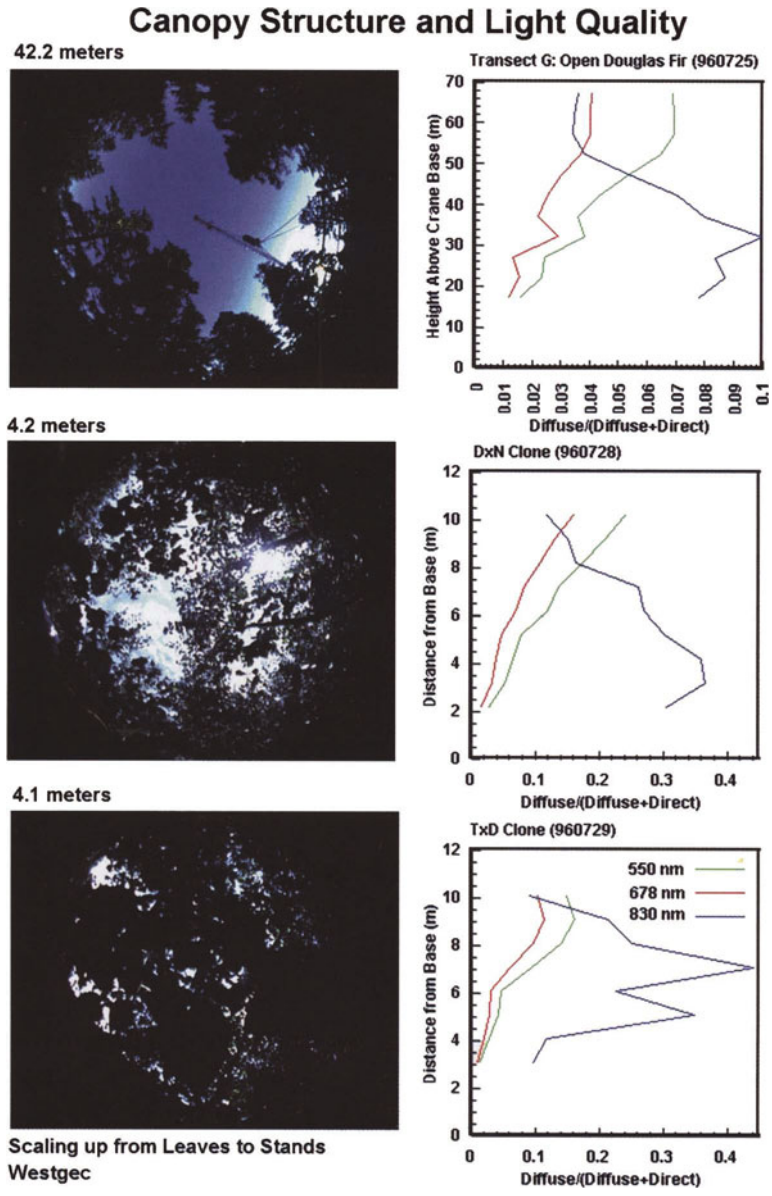

FIGURE 1.1. Color hemispherical photographs late seral Douglas fir forest and two clonal *Populus,* one with more vertically oriented leaves (*P. deltoides* × *P nigra* = D × N) and one with more horizontally distributed leaves (*P. trichocarpa* × *P deltoides* = T × D). Hemispherical photographs were measured at at least 10 heights within each crown. Vertical light profiles measured at the same location as the hemispherical photographs are shown to the right. At 42.2 m above the ground, the Douglas fir canopy is relatively open, consisting primarily of clustered foliage and branches (top). In comparison, the clonal *Populus* canopies consist of more uniformly distributed leaves. Major differences at 4.2 m height between the D × N (middle) and T × D (bottom) clones are due to leaf angles. Light penetration is highest in the D × N clone due to its more vertically oriented leaves. All three canopies show a decrease in diffuse red and green light and an increase in NIR. The largest difference among the profiles occurs in the T × D clone, which shows a rapid decrease in visible light and an initial rapid increase in diffuse NIR followed by a decrease. In contrast, both the D × N and Douglas fir profiles show more gradual changes in light and only a minor decrease in NIR closest to the forest floor. The difference between the T × D clone and the other canopies can attributed primarily to the more horizontal leaf orientation in the T × D clone. Higher diffuse light in the D × N and T × D clone profiles can be attributed to partially cloudy conditions, which did not block direct light but produced side-scattered diffuse radiation.

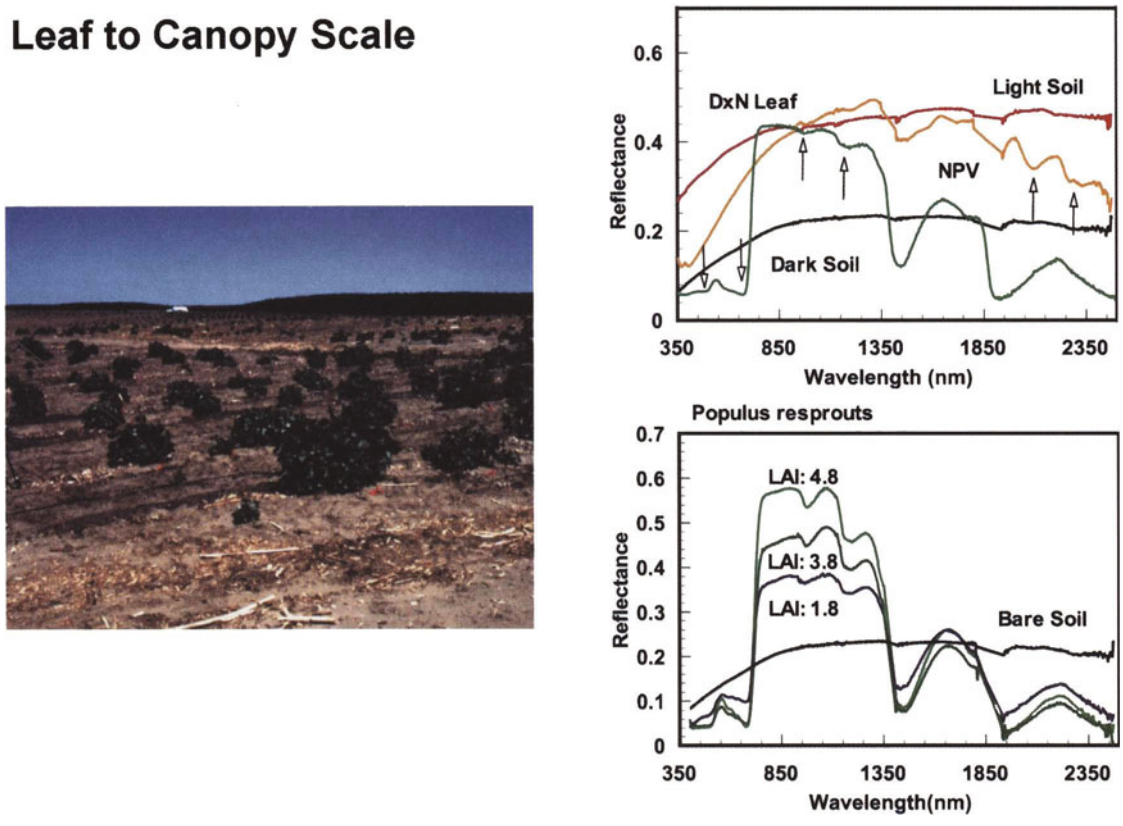

FIGURE 1.2. Leaf and canopy scale spectra of natural materials. The photograph on the left shows *Populus* resprouts (*P. deltoides* × *P. nigra* = D × N) located in the vicinity of Wallula, WA. Plants were flagged and placed in five height classes covering a range of heights and LAIs. Multiple spectra were collected from each resprout. A subset of 25 plants was destructively harvested to determine LAI for each plant and compared with canopy spectra and several spectral indices. Example spectra of a leaf, bare soil, and a *Populus* stump are shown in the upper right frame. Diagnostic absorptions for chlorophyll in the visible, liquid water in the NIR, and lignocellulose in the shortwave infrared are marked by arrows. Four spectra, sampled from bare soil and three canopies with LAIs ranging from 1.8 to 4.8, are shown in the lower right frame. Note the general decrease in red reflectance and increase in NIR reflectance with increasing LAI. Details on LAI sampling and spectral analysis are provided in Roberts et al., (1998b).

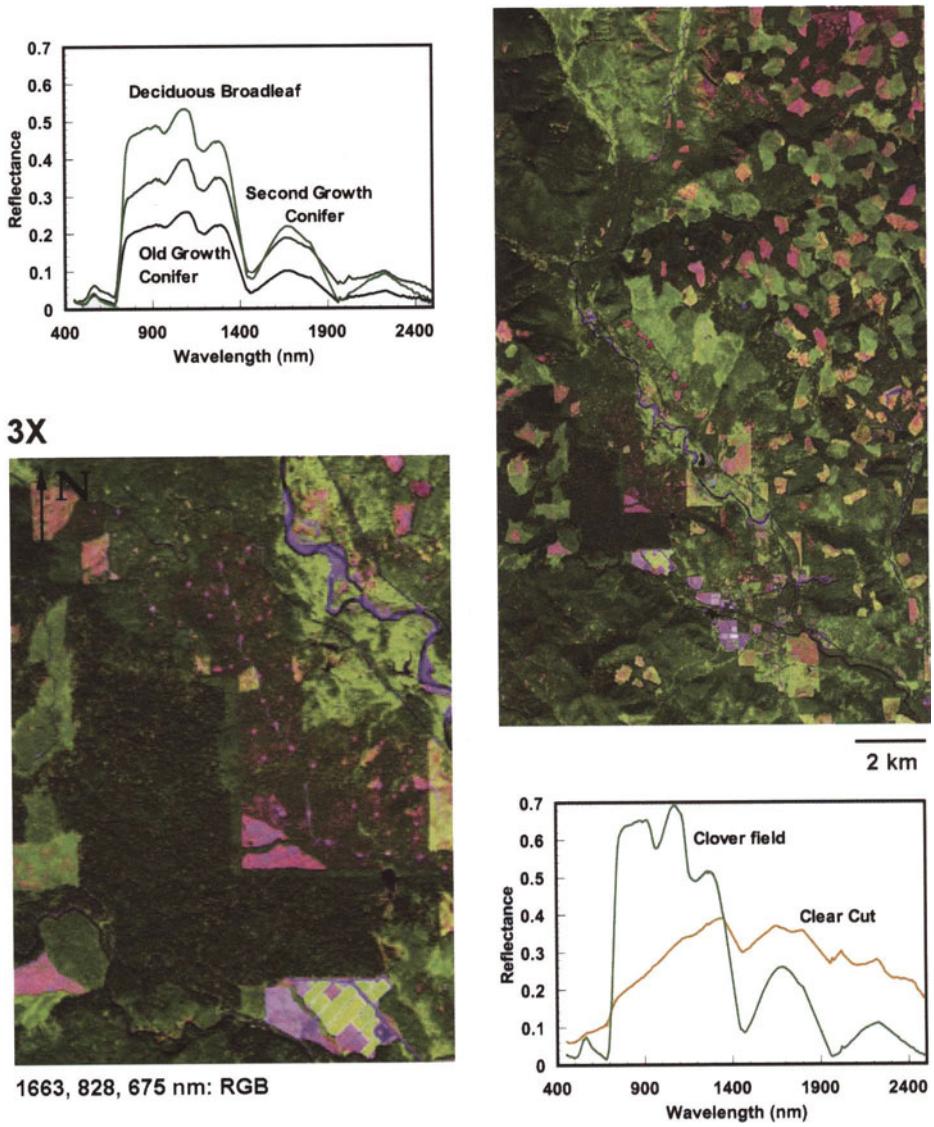

FIGURE 1.3. AVIRIS image acquired on June 14, 1996, over the Wind River Canopy Crane Research Facility (Carson, Washington). The frame on the upper right shows a false color composite with 1663, 828, and 657 nm displayed as red, green, and blue, respectively. In this rendition, vegetation is green and bare soil and slash are magenta. Old-growth forest is distinguished from second-growth forest and broadleaf plants by low reflectance due to shadowing. The frame on the lower left is 3 × blowup centered over the T.T. Munger Research Natural Area. Old growth is distinguished from allover landcover types by its heterogeneity. In forest types, the highest reflectance occurs in the deciduous broadleaf trees, with second growth mixed hemlock and Douglas fir having intermediate reflectance between old-growth and broadleaf trees. Reflectance differences among these forest types are a combination of architecturally derived shadows and the different optical properties of leaves and needles. Nonforested landcover includes a clover field and clearcuts. Note, while visible reflectance tends to be lower in canopies than at leaf scales, NIR reflectance can be higher, as is shown by the clover field. Associated spectra for all five landcover types are shown.

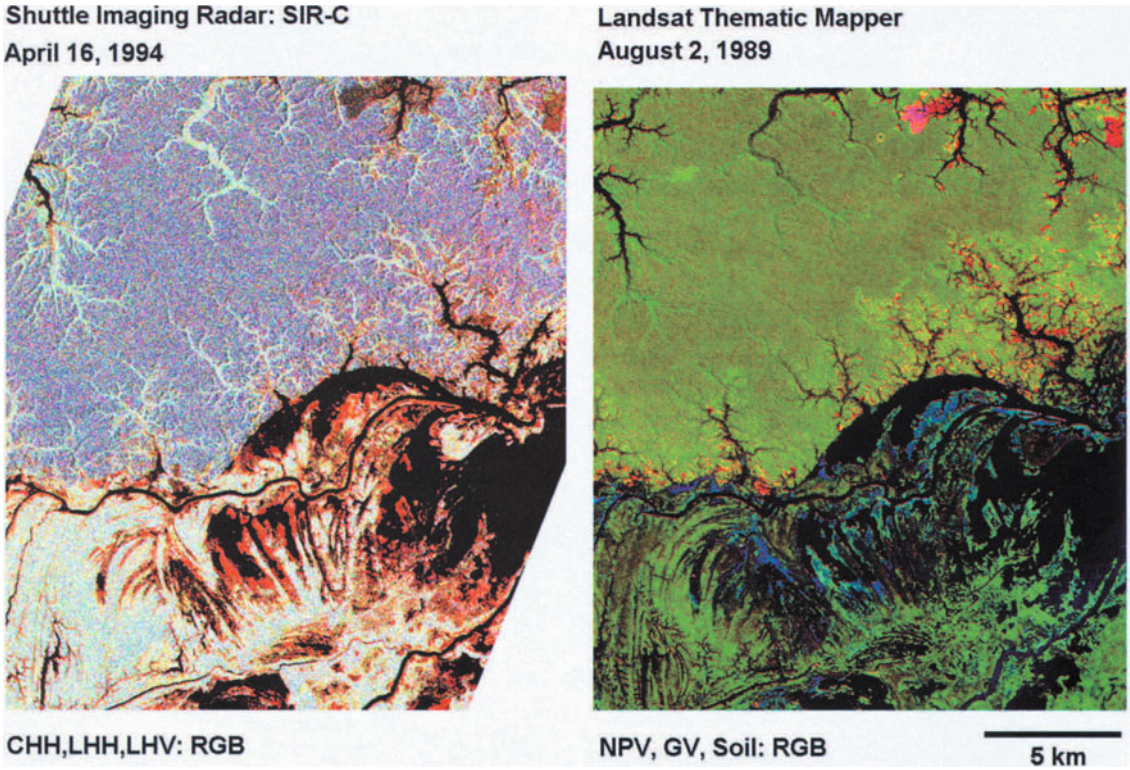

FIGURE 1.4. Comparison of SIR-C data and LANDSAT TM data for Lago Cabaliana, approximately 60 km southwest of the city of Manaus in central Amazonia. SIR-C CHH, LHH and LHV data from April, 1994, are displayed on the left as red, green, and blue, respectively. Flooded forests are evident as regions that are yellowish white due to a strong LHH double-bounce return, high C and low LHV. Recent clearcuts in the northeastern portion of the image have low returns in all three channels due to low standing biomass. The image to the right shows a LANDSAT TM scene acquired in same area on August 2, 1989. This image has been analyzed using spectral mixture analysis, generating fraction images for nonphotosynthetic vegetation, green vegetation, and soil, displayed as red, green, and blue (Roberts et al., 1993). Unlike the SAR image, the optical data are relatively insensitive to the presence of standing water and do not differentiate macrophytes from flooded forests. Spectral fractions vary primarily in response to the materials within the field of view and subpixel shadowing due to variation in leaf angles, crown shading, and the presence of canopy gaps. In this image, second-growth forest is readily separated from primary forest by a low shade content, which produces light green vegetation along the margins of rivers. Flooded forest, which commonly has a more uniform crown height than upland forest, is more homogeneous and is differentiated in many places by a lower shade content. Recent clearcuts are modeled primarily as nonphotosynthetic vegetation due to the presence of fallen logs and senesced grasses.

Franklin, J.F.; Strahler, A.H. Invertible canopy reflectance modeling of vegetation structure in semiarid woodland. IEEE Trans. Geosci. Remote Sens. 26:809–825; 1988.

Gong, P.; Pu, R.; Miller, J.R. Coniferous forest leaf area index estimation along the Oregon transect using Compact Airborne Spectrographic Imager Data. Photogram. Eng. Remote Sens. 61:1107–1117; 1995.

Gougeon, F.A. A crown following approach to the automatic delineation of individual tree crowns in high spatial resolution aerial images. Can. J. Remote Sens. 21(3):274–284; 1995.

Gotfryd, A; Hansell, R.I. The impact of observer bias on multivariate analysis of vegetation structure. Oikos 45:223–234; 1985.

Graetz, A.R.D. Remote sensing of ecosystem structure: An ecologist's pragmatic view. In: Hobbs, E.R.J.; Mooney, H.A., eds. *Remote Sensing and Biosphere Functioning.* New York: Springer-Verlag; 1990:5–30.

Hagberg, J.O.; Ulander, L.M.H.; Askne, J. Repeat-pass SAR interferometry over forested terrain. IEEE Trans. Geosci. Remote Sens. 33:331–340; 1995.

Hall, F.G.; Shimabukuro, Y.; Huemmrich, K.F. Remote sensing of forest biophysical structure using mixture decomposition and geometric reflectance models. Ecol. Applic. 5:993–1013; 1995.

Halle, F.R.; Oldeman, A.A.; Tomlinson, P.B. *Tropical trees and forests.* Berlin: Springer-Verlag; 1978.

Hallikainen, M., Hyyppä, J.; Haapanen, J.; Taresl, J. A helicopter-borne 8 channel ranging scatterometer for remote sensing. IEEE Trans. Geosci. Remote Sens. 31:161–169; 1993.

Harrell, P.A.; Kasischke, E.S.; Bourgeau-Chavez, L.L.; Haney, E.M.; et al. Evaluation of approaches to estimating aboveground biomass in southern pine forests using SIR-C data. Remote Sens. Environ. 59(2):223–233; 1997.

Heilman, P.E.; Hinckley, T.M.; Roberts, D.A.; Ceulemans, R. Production physiology. In: Stettler R.F.; Bradshaw, H.W.; Heilman, P.E.; Hinckley, T.M., eds. *Biology of Populus and Its Implications for Management and Conservation.* Washington, D.C.: NRC Research Press; 1996:459–490.

Heller, R.C.; Ulliman, J.J. Forest resources assessments. In: Colwell, R.N., ed. *Manual of Remote Sensing.* Falls Church, VA: American Society of Photogrammetry and Remote Sensing; 1983; Ch. 34.

Henderson, F.M.; Lewis, A.J., eds. *Principles and Applications of Imaging Radar. Manual of Remote Sensing,* 3rd ed. Vol. 2 New York: Wiley; 1998.

Hess, L.L.; Melack, J.M.; Simonett, D.S. Radar detection of flooding beneath the forest canopy: A review. Int. J. Remote Sens. 11:1313–1325; 1990.

Honda, H.; Tomlinson, P.B.; Fisher, J.B. Computer simulation of branch interaction and regulation by unequal flow rates in botanical trees. Am. J. Bot. 68:569–585; 1981.

Horn, H.S. *The Adaptive Geometry of Trees.* Princeton, NJ: Princeton Univ. Pr.; 1971.

Howard, J.A. *Remote Sensing of Forest Resources: Theory and Application.* London: Chapman and Hall; 1991.

Husch, B.; Miller, C.I.; Beers, T.W. *Forest Mensuration.* 3rd ed. New York: Wiley; 1982.

Hutchings, N.J.; Phillips, A.H.; Dobson, R.C. An ultrasonic rangefinder for measuring the undisturbed surface height of continuously grazed grass swards. Grass Forage Sci. 45:119–128; 1990.

Hyyppä, J.; Hallikainen, M. Applicability of airborne profiling radar to forest inventory. Remote Sens. Environ. 57:39–57; 1996.

Imhoff, M.L. A theoretical analysis of the effect of forest structure on synthetic aperture radar backscatter and the remote sensing of biomass, IEEE Trans. Geosci. Remote Sens. 33:341–352; 1995.

Ivanov, N.; Boissard, P.; Chapron, M.; Valery, P. Estimation of the height and angles of orientation of the upper leaves in the maize canopy using stereovision. Agronomie 14:183–1194; 1994.

Justice, C.O.; Vermote, E.; Townshend, J.R.G.; Defries, R.; et al. The Moderate Resolution Imaging Spectroradiometer (MODIS): Land remote sensing for global change research. IEEE Trans. Geosci. Remote Sens. 36:1228–1249; 1998.

Kasischke, E.S.; Melack, J.M.; Dobson, M.C. The use of imaging radars for ecological applications: A review. Remote Sens. Environ. 59:141–156; 1997.

Kauth, R.J.; Thomas, G.S. The tasselled cap: A graphic description of the spectral-temporal development of agricultural crops as seen by LANDSAT. In: *Proceedings of the Third Symposium on Machine Processing of Remotely Sensed Data.* West Lafayette, IN: LARS, Purdue Univ.; 1976:4B-41–4B-51.

King, D. Airborne multispectral digital camera and video sensors: A critical review of system design and applications, Can. J. Remote Sens. 21:245–256; 1995.

Koike F. Reconstruction of two-dimensional tree and forest canopy profiles using photographs. J. Appl. Ecol. 22:921–929; 1985.

Koike, F.; Syahbuddin. Canopy structure of a tropical rain forest and the nature of an unstratified layer. Funct. Ecol. 7:230–235; 1993.

Kruijt, B. Estimating canopy structure of an oak forest at several scales. Forestry 62:269–284; 1989.

Kuuluvainen, T.; Pukkala, T. Simulation of within-tree and between-tree shading of direct radiation in a forest canopy: Effect of crown shape and sun elevation. Ecol. Model. 49:89–100; 1989.

Lang, A.R.G. An instrument for measuring canopy. Remote Sens. Rev. 5:61–71; 1990.

Lang, R.H.; Sidhu, J.S. Electromagnetic backscattering from a layer of vegetation: A discrete approach. IEEE Trans. Geosci. Remote Sens. GE-21:62–71; 1983.

Lemmon, P.E. A spherical densiometer for estimating forest overstory density. For. Sci. 2:314–320; 1956.

Li, X.W.; Strahler, A.H. Geometric-optical bidirectional reflectance modeling of a conifer forest canopy. IEEE Trans. Geosci. Remote Sens. Ge-24:906–919; 1985.

Li, X.; Strahler, A.H. Geometric-optical bidirectional reflectance modeling of the discrete crown vegetation canopy: Effect of crown shape and mutual shadowing. IEEE Trans. Geosci. Remote Sens. 30:276–292; 1992.

Lowman, M.D.; Nadkarni, N.M., eds. *Forest Canopies.* London: Academic Press; 1995.

Maguire, D.A.; Bennett, W.S. Patterns in vertical distribution of foliage in young coastal Douglas-fir. Can. J. For. Res. 26:1991–2005; 1996.

Marshall, J.D.; Waring, R.H. Comparison of methods for estimating leaf-area index in old-growth Douglas-fir. Ecology 67:975–979; 1986.

Martens, S.N.; Ustin, S.L.; Norman, J.M. Measurement of tree canopy architecture, Int. J. Remote Sens. 12(7):1525–1545; 1991.

Martens, S.N.; Ustin, S.L.; Rousseau, R.A. Estimation of tree canopy leaf area index by gap fraction analysis. For. Ecol. Manage. 61:91–108; 1993.

McAuliffe, J.R. A rapid survey method for the estimation of density and cover in desert plant communities. J. Vegetat. Sci. 1:653–656; 1990.

McDonald, K.C.; Dobson, M.C.; Ulaby, F.T. Using MIMICS to model L-band multiangle and multitemporal backscatter for a walnut orchard. IEEE Trans. Geosci. Remote Sens. 28:477–491; 1990.

McDonald, K.C.; Ulaby, F.T. Radiative transfer modelling of discontinuous tree canopies at microwave frequencies. Int. J. Remote Sens. 14:2097–2128; 1993.

Means, J.E.; Acker, S.A.; Harding, D.A.; Lefsky, M.A.; Cohen, W.B.; Harmon, M.; Mckee, W.A. Use of laser altimetry to estimate forest stand characteristics in the western Cascades of Oregon. Unpublished manuscript; 1997.

Means, J.E.; Hansen, H.A.; Koerper, G.J.; Alaback, P.B.; M.W.; Klopsch, M.W. *Software for Computing Plant Biomass: BIOPAK User's Guide.* Gen. Tech. Rep. PNW-GTR-340. Portland, Oregon: U.S. Department of Agriculture, Forest Service, Pacific Northwest Research Station; 1994.

Monsi, M.; Saeki, S. Uber den Lichtfaktor in den Pflanzengesellschaften und seine Bedeutung fur den Stoffproduktion. Jpn. J. Bot. 14:22–52; 1953.

Mueller-Dombois, D.; Ellenberg, H. Aims and methods of vegetation ecology. New York: Wiley; 1974.

Myneni, R.B.; Asrar, G.; Gerstl, S.A.W. Radiative transfer in three dimensional leaf canopies, Trans. Theory Stat. Phys. 19:205–250; 1990.

Myneni, R.B.; Maggion, S.; Iaquinto, J.; Privette, J.L.; et al. Optical remote sensing of vegetation: Modeling, caveats and algorithms. 51(1):169–188; 1995.

Myneni, R.B.; Nemani, R.R.; Running, S.W. Estimation of global Leaf Area Index and absorbed PAR using radiative transer models. IEEE Trans. Geosci. Remote Sens. Environ. 35:1380–1393; 1997.

Nelson, R.; Swift, R.; Krabill, W. Using airborne laser to estimate forest canopy and stand characteristics. J. For. 86:31–38; 1988.

Nilson, T. A theoretical analysis of the frequency of gaps in plant stands. Agric. Meteorol. 8:25–38; 1971.

Nilsson, M. Estimation of tree heights and stand volume using an airborne lidar system. Remote Sens. Environ. 56:1–7; 1996.

Norman, J.M.; Campbell, G.S. Canopy structure. In: Pearcy, R.W.; Ehleringer, J.; Mooney, H.A.; Rundel, P.W., eds. *Plant Physiological Ecology: Field Methods and Instrumentation.* London: Chapman and Hall; 1989:301–325.

Norman, J.M.; Jarvis, P.G. Photosynthesis in Sitka spruce (*Picea sitchensis* (Bong.) Carr.). III. Measurements of canopy structure and interception of radiation. J. Appl. Ecol. 11:375–398; 1974.

Oker-Blom, P.; Pukkala, T.; Kuuluvainen, T. Relationship between radiation interception and photosynthesis in forest canopies: Effect of stand structure and latitude. Ecol. Model. 49:73–87; 1989.

Parker, G.G.; Smith, A.P.; Hogan, K.P. Access to the upper forest canopy with a large tower crane sampling the treetops in three dimensions. Bioscience 42:664–670; 1992.

Pech, R.P.; Graetz, R.D.; Davis, A.W. Reflectance modelling and the derivation of vegetation indices for an Australian semi-arid shrubland. Int. J. Remote Sens. 7:389–403; 1986.

Philipson, W.R., ed. *Manual of Photographic Interpretation.* 2nd ed. Falls Church, VA: American Society for Photogrammetry and Remote Sensing; 1997.

Pierce, L.E.; Ulaby, F.T.; Sarabandi, K.; Dobson, M.C. Knowledge-based classification of polarimetric SAR images. IEEE Trans. Geosci. Remote Sens. 32:1081–1086; 1994.

Pitt, D.G.; Glover, G.R.; Jones, R.H. 1996. Two-phase sampling of woody and herbaceous plant communities using large scale aerial photographs. Can. J. For. Res. 26:509–524; 1996.

Polatin, P.K.; Sarabandi, K.; Ulaby, F.T. An iterative inversion algorithm with application to the polarimetric radar response of vegetation canopies. IEEE Trans. Geosci. Remote Sens. 30:412–415; 1994.

Ranson, K.J.; Sun, G. An evaluation of AIRSAR and SIR-C/X-SAR images for mapping northern forest attributes in Maine, U.S.A. Remote Sens. Environ. 59:203–222; 1997.

Reed, B.C.; Brown, J.F.; Vanderzee D.; Loveland T.R.; et al. Measuring phenological variability from satellite imagery. J. Vegetat. Sci. 5:703–714; 1994.

Rich, P.M. Characterizing plant canopies with hemisherical photographs. Remote Sens. Rev. 5:13–29; 1990.

Richards, J.A.; Sun, G.O.; Simonett, D.S. L-band radar backscatter modeling of forest stands. IEEE Trans. Geosci. Remote Sens. GE-25:487–498; 1987.

Richardson, A.J.; Wiegand, C.L. Distinguishing vegetation from soil background information. Photogram. Eng. Remote Sens. 43:1541–1552; 1977.

Roberts, D.A.; Adams, J.B.; Smith, M.O. Discriminating green vegetation, non-photosynthetic vegetation and soils in AVIRIS data. Remote Sens. Environ. 44:1–25; 1993.

Roberts, D.A.; Gardner, M.; Church, R.; Ustin, S.; Scheer, G.; Green, R.O. Mapping chaparral in the Santa Monica Mountains using multiple endmember spectral mixture models. Remote Sens. Environ. 65:267–279; 1998a.

Roberts, D.A.; Brown, K.J.; Green, R.; Ustin, S.; Hinckley, T. Investigating the relationship between liquid water and leaf area in clonal Populus, Proc. 7th AVIRIS Earth Science Workshop JPL 97-21, Pasadena, CA 91109, 10 p; 1998b.

Rohlf, F.J.; Archie, J.W. Least-squares mapping using interpoint distances. Ecology 59:126–132; 1978.

Ross, J.P. The radiation regime and architecture of plant stands. The Hague, Netherlands: Dr. W. Junk; 1981.

Running, S.W.; Coughlan, J.C. A general model of forest ecosystem processes for regional applications. Ecol. Model. 42:125–154; 1988.

Sellers, P.J. Canopy reflectance, photosynthesis and transpiration. Int. J. Remote Sens. 6:1335–1372; 1985.

Sinoquet, H; Rivet, P. Measurement and visualization of the architecture of an adult tree based on a three-dimensional digitising device. Tree 11(5):265–270; 1997.

Sinoquet, H.; Valmorin, M.; Cabo, X.; Bonhomme, R. DAOLI: An automated laser distance system for measuring profiles of vegetation. Agric. For. Meteorol. 67:43–64; 1993.

Strahler, A.H.; Woodcock, C.E.; Smith, J.A. On the nature of models in remote sensing. Remote Sens. Environ. 20:131–139; 1986.

Sun, G.; Ranson, K.J. A three-dimensional radar backscatter model of forest canopies. IEEE Trans. Geosci. Remote Sens. 33:372–382; 1995.

Sun, G.; Simonett, D.S.; Strahler, A.H.; A radar backscattering model for discontinuous coniferous forests. IEEE Trans. Geosci. Remote Sens. 29:639–650; 1991.

Treuhaft, R.N.; Madsen, S.N.; Moghaddam, M.; van Zyl, J.J. Vegetation characteristics and underlying topography from interferometric radar. Radio Sci. 31:1449–1485; 1996.

Tucker, C.J. Red and photographic infrared linear combinations for monitoring vegetation. Remote Sens. Environ. 8:127–150; 1979.

Ulaby, F.T.; Sarabandi, K.; McDonald, K.C.; Whitt, M.; Dobson, M.C. Michigan microwave canopy scattering model (MIMICS). Int. J. Remote Sens. 11:1223–1253; 1990.

Vanderbilt, V.C.; Silva, L.F.; Bauer, M.E. Canopy architecture measured with a laser. Appl. Opt. 29:99–106; 1990.

Van Pelt, R; North, MP. Analyzing canopy structure in Pacific Northwest old-growth forests with a stand-scale crown model. Northwest Sci. 70:15–30; 1996.

Wang, Y.; Davis, F.W.; Melack, J.M. Simulated and observed backscatter at P-, L-, and C-bands from ponderosa pine stands, IEEE Trans. Geosci. Remote Sens. 31:871–879; 1993.

Waring, R.H.; Way, J.; Hunt, E.R. Jr.; Morrissey, L.; Ranson, K.J.; Weishampel, J.F.; Oren, R.; Franklin, S.E. Imaging radar for ecosystem studies. Bioscience 45:715–723; 1995.

Way, J.; Paris, J.; Dobson, M.C.; McDonald, K.; Ulaby, F.T.; Weber, J.A.; Ustin, S.L.; Vanderbilt, V.C.; Kasischke, E.S. Diurnal change in trees as observed by optical and microwave sensors: The EOS synergism study. IEEE Trans. Geosci. Remote Sens. 29:807–821; 1991.

Way, J.; Zimmermann, R.; Rignot, E.; McDonald, K.; Oren, R. Winter and spring thaw as observed with imaging radar at BOREAS. J. Geophys. Res. Atmos. 102(ND24):29673–29684; 1997.

Welles, J.M. Some indirect methods of estimating canopy structure. Remote Sens. Rev. 5:31–43; 1990.

Welles, J.M.; Cohen, S. Canopy structure measurement by gap fraction analysis using commercial instrumentation. J. Exp. Bot. 47:1335–1342; 1996.

Weltz, M.A.; Ritchie, J.C.; Fox, H.D. Comparison of laser and field measurements of vegetation height and canopy cover. Water Resources Res. 30:1311–1319; 1994.

Wimbush, D.J.; Barrow, M.D.; Costin, A.B. Color stereo-photography for the measurement of vegetation. Ecology 48:150–152; 1967.

Wu, Y.; Strahler, A.H. Remote estimation of crown size, stand density, and biomass on the Oregon transect. Ecol. Applic. 4:299–312; 1994.

Zebker, H.; Goldstein, R. Topographic mapping from interferometric synthetic radar observations, J. Geophys. Res. 91:4993–5001; 1986.

Zeide, B. Fractal geometry in forestry applications, For. Ecol. Manage. 46(3–4):179–188; 1991.

Zeide, B. Analysis of growth equations, For. Sci. 39(3):594–616; 1993.

Zoughi, R.; Wu, L.K.; Moore, R.K. Identification of the major backscattering sources in trees and shrubs at 10 GHz. Remote Sens. Environ. 19:269–290; 1986.

2

Methods of Estimating Aboveground Net Primary Productivity

Osvaldo E. Sala and Amy T. Austin

Introduction

Estimating net primary productivity (NPP) has been a central goal of basic and applied ecologists. Very important questions rely on good estimates of NPP: the global carbon balance, the location of the missing carbon sink, and predictions of global climate change (see Chapter 3). Primary productivity represents the major input of carbon and energy into ecosystems and McNaughton (1989) proposed NPP as an integrative variable of the functioning of the whole ecosystem because of its relationships with animal biomass, secondary productivity, and nutrient cycling. From an applied perspective, primary production of grasslands determines forage availability and constrains animal carrying capacity whereas primary production of forests is directly related to wood yield.

The concept of primary productivity is related to the ideas of energy flow in ecosystems (Odum 1971). A portion of the photosynthetically active radiation (PAR, radiation in the 400- to 700-nm wave band) received by an ecosystem is absorbed by green plants (Fig. 2.1). The absorbed energy is either re-radiated, lost as latent heat, or stored by the activity of photosynthesis in organic substances. The last flow is known as *gross primary productivity.* Plants use the stored energy in these organic compounds fixed in photosynthesis for their own respiration (autotrophic respiration). The balance between carbon fixation in photosynthesis and carbon loss in plant respiration is *net primary productivity,* or as Odum (1971) defined it: "net primary productivity is the rate of storage of organic matter in plant tissues in excess of the respiratory utilization by plants." Along the trophic web, herbivores eat part of the organic matter stored in plants (herbivore consumption) but a portion is not consumed and goes directly to decomposers. This flow of matter and energy that represents the fraction of NPP not consumed by heterotrophs is named *net community productivity.* Only a portion of the consumed substances is assimilated since part is lost in animal feces and urine. The assimilated products are then used in supporting heterotrophic respiration or accumulation of herbivore biomass. The rate of accumulation of organic substances in herbivores is named *secondary productivity.* This pattern of partitioning of energy into the categories of assimilated, nonassimilated, and nonutilized is repeated along the food web. Finally, *net ecosystem productivity* is the rate of storage or loss of organic matter in the ecosystem in excess of the respiration by all its organisms in all the different trophic levels from autotrophs to decomposers.

All types of productivity are flow rates of matter and energy through different portions of the ecosystem; they are represented by arrows in the scheme of figure 2.1, and they have units of mass or energy per unit area per unit time (e.g., $g\ m^{-2}\ yr^{-1}$ or $kJ\ m^{-2}\ yr^{-1}$). The terms production and productivity are used as synonyms here. In contrast, biomasses of plants and animals are quantities or state variables where mass and energy accumulate; they are represented by boxes in Figure 2.1, and they have units of mass or energy per unit area (e.g., $g\ m^{-2}$ or $kJ\ m^{-2}$). These two concepts, biomass and productivity, although very different, are often confounded. In part, this confusion arises because biomass is used to estimate productivity in

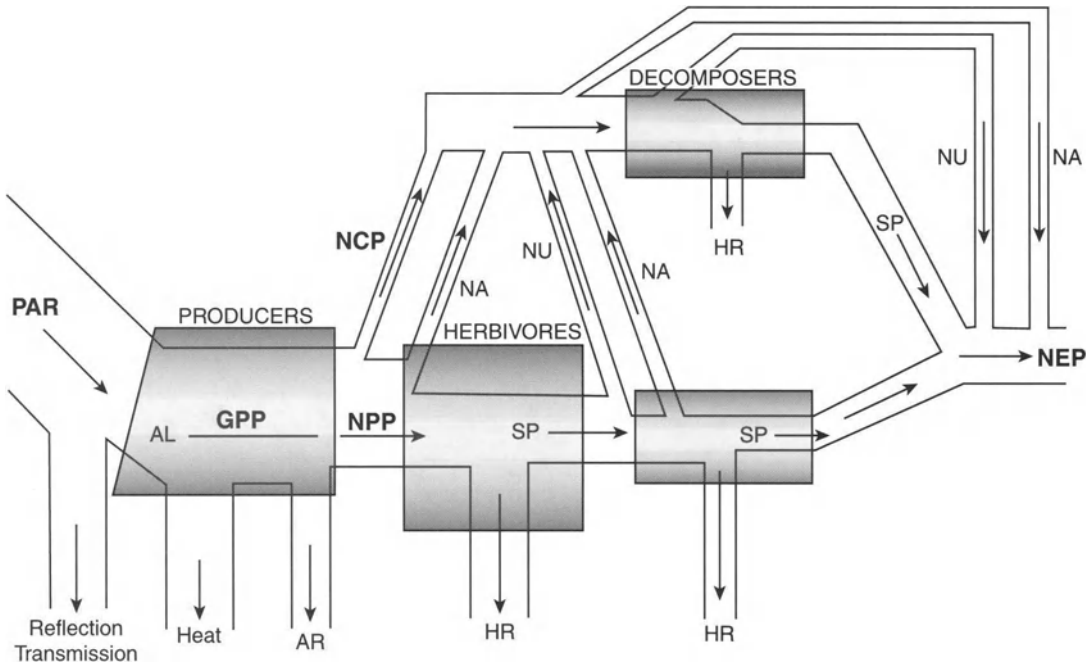

FIGURE 2.1. Schematic energy flow throughout an ecosystem showing the different kinds of productivity. GPP, gross primary production; NPP, net primary productivity; NCP, net community productivity; and NEP, net ecosystem productivity. The associated flows are PAR, photosynthetically active radiation; AL, absorbed light; AR, autotrophic respiration; NU, not utilized; NA, not assimilated; HR, heterotrophic respiration; and SP, secondary productivity.

some cases, as we will discuss later. The concepts associated with both words are identical although production is usually reserved for those cases with an annual time scale. Productivity is usually the preferred term when the scale of interest is less than a year.

The objectives of this chapter are to review the most commonly used methods to estimate aboveground NPP (ANPP) of terrestrial ecosystems using ground measurements and to analyze the tradeoffs among them. This chapter is closely related to several other chapters in this book: Chapter 3 describes remote sensing tools to measure ANPP, Chapter 4 assesses methods for estimating belowground NPP, Chapter 5 reviews the different approaches to measure NPP in aquatic ecosystems, and, finally, Chapter 11 describes micrometeorological techniques to assess primary production. The issue of estimating primary productivity is discussed throughout the book from different perspectives, indicating the importance of the topic and the attention that it has received in ecosystem science.

Different flows and state variables associated with the transfer of energy and matter in ecosystems are measured in assessing primary productivity (Fig. 2.2). *Production* is the flow of carbon from the atmosphere into the *green biomass* of plants. Green leaves and twigs *senesce* and form part of the *standing dead* compartment made up of dead material still attached to the original plant. *Detachment* of dead leaves from original plant incorporates them into the *litter* pool, which is made up of dead plant material lying on the ground. Finally, litter is *decomposed* by the action of microorganisms and part of its carbon returns to the atmosphere as carbon dioxide while another portion is incorporated into microbial biomass or remains in the ecosystem as soil organic matter.

We grouped methods to estimate ANPP in two categories depending on the rate of biomass turnover of the ecosystem. Grasslands and steppes are among the fast turnover ecosystems with high ANPP/biomass ratios, and characterized by small individuals of relatively short life span. In contrast,

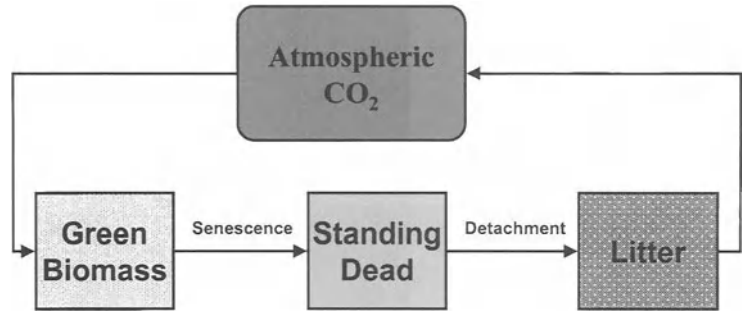

FIGURE 2.2. Schematic of carbon flow through an ecosystem, primary productivity, and the associated flows and state variables used in different methods to assess primary production.

forests belong to the slow turnover rate group with low ANPP/biomass ratio, and large individuals of relatively long life span. Shrubland ecosystems are intermediate between grasslands and forests and usually require the use of a hybrid method combining those of fast and slow turnover ecosystems.

Many methods have been developed to assess primary productivity and many papers have been written on this topic. This chapter describes methods to estimate ANPP in fast and slow turnover ecosystems, and reviews errors and costs associated with the major methods in an attempt to identify costs, benefits, and tradeoffs among the different methodologies.

Methods to Estimate ANPP in Fast Turnover Ecosystems

Singh et al. (1975) thoroughly reviewed the methods for estimating ANPP used during the International Biological Program (IBP) and described the effects of the different methods on the ANPP estimate along the different IBP sites. In ecosystems such as grasslands and steppes, it is difficult to estimate ANPP directly, and most methods take advantage of the characteristics of these ecosystems that live biomass varies broadly among seasons. In some extreme cases, such as the California annual grasslands, green biomass approaches zero during part of the year. In most cases, there are clear minima and maxima for green biomass.

The simplest method to estimate ANPP in grasslands (method 1) is to assess peak biomass and to equate this value with annual productivity. This method assumes that minimum biomass is zero or close to zero and that it increases up to a point (peak biomass) after which senescence starts. It also assumes that there is no carryover from one growing season to the next. Simplicity and low cost are among the most important advantages of this method. A more thorough analysis of the errors associated with this method and the costs and benefits of each method are discussed later in this chapter.

The next method (method 2) relaxes the assumption of no carryover and estimates both minimum and maximum biomass. ANPP is then calculated as the difference between maximum and minimum biomass. This method still assumes a monotonic increase of biomass from a minimum to a maximum value and a separation in time of the processes of production and senescence.

Grassland productivity is usually constrained during the growing season by water availability, which results in a seasonal pattern of biomass with several peaks and troughs (Fig. 2.3). Taking into account just one biomass peak may underestimate total productivity during the studied period. Methods 1 and 2 have the problem of the missing intermediate peaks in biomass since they assume a single maximum. In order to take into account this potential source of error, method 3 relaxes the assumption of the monotonic biomass increase and sums all the differences between consecutive troughs and peaks. This method requires multiple biomass estimates along the growing season instead of one or two as in methods 1 and 2, and therefore significantly increases the costs.

An important assumption of these three methods is that productivity and senescence occur in different periods during the growing season. This assumption may hold only in an annual crop, such as wheat. In most multispecies ecosystems subjected to a variety of stresses, productivity and

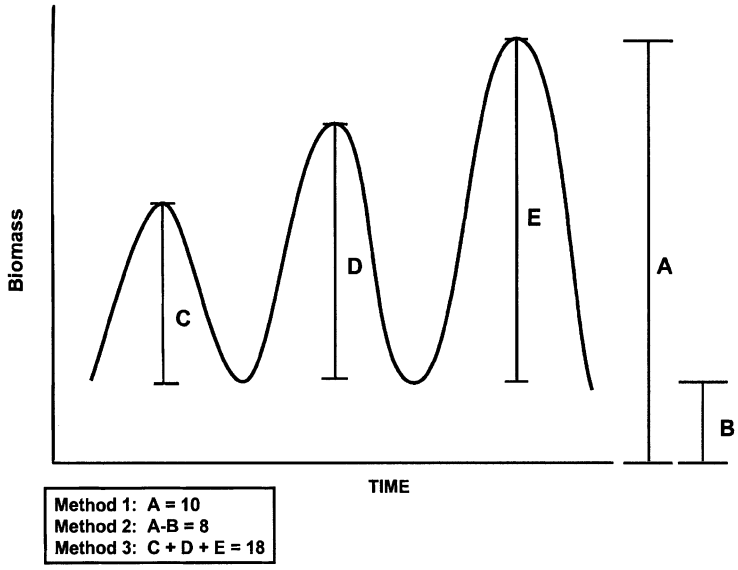

FIGURE 2.3. Idealized seasonal pattern of green biomass. Estimates of primary production using method 1, peak biomass; method 2, maximum minus minimum; and method 3, summation of peaks minus troughs.

senescence occur simultaneously. New leaves emerge at the same time that others senesce or fall to the ground; short periods dominated by production may be followed by others dominated by senescence. The green biomass compartment then reflects the net balance between input and output, productivity and senescence (see Fig. 2.2). Increases in the green biomass compartment underestimate primary production since part of the productivity that occurred during that period replaces tissue that senesced during the same period. It is possible for green biomass to remain constant when production is indeed occurring if senescence is equal to production.

The problem of the simultaneity of production and senescence has been recognized by several authors who suggested different solutions. Wiegert and Evans (1964) proposed to use paired plots, in one of which they harvested dead biomass at time 0 (W0), and in the other they clipped green vegetation at time 0 and harvested dead material at time 1 (W1). Then W1 − W0 yielded the disappearance rate of dead material and this value was added to the estimates of production.

Sala et al. (1981) proposed a method based on a time series of green biomass, standing dead, and litter. The method used data sets in which green biomass was separated among the component species but standing dead and litter were considered in pools undifferentiated by species.

$$ANPP_t = \sum Pi + Sc + Fc \qquad (2.1)$$

where Pi was the productivity of individual species "I" in the time interval t. Sc and Fc were correction factors that accounted for the simultaneous nature of productivity, senescence, and decomposition.

$$Sc = (\Delta^{+}SD/\Delta t) - \sum Si \qquad (2.2)$$

where Sc represented the increments (Δ^{+}) in standing dead (SD) not accounted for by the sum of decrements in the green biomass of individual plant species (Si). Sc took a value greater than 0 when the sum of all the specific green biomass compartments that decreased during the period was smaller than the increase in the standing dead compartment. Sc assessed part of the productivity that occurred during the period but that it was not detected as an increase in green biomass. Similarly,

$$Fc = (\Delta^{+}L - \Delta^{-}SD)/\Delta t \qquad (2.3)$$

where Fc represented the portion of the productivity that was not detected in the green biomass or standing dead compartments. Fc acquired a positive value when the increases in litter ($\Delta^{+}L$) were larger than the decreases in standing dead ($\Delta^{-}SD$).

The errors associated with the simultaneous nature of productivity, senescence, and decomposition probably increase as the diversity of plant species and functional groups of species increases. A single species shows a partial separation in time of pro-

ductivity and senescence. In contrast, ecosystems made up of species with different phenologies and life cycles, such as early-and late-season species, C_3 and C_4, or annuals and perennials, have a high overlap of productivity, senescence, and decomposition. For example, the senescence of the early-season C_3 species in the Pampas masked the productivity of the late-season C_4-dominated species (Sala et al. 1981). The overlap error becomes less important in ecosystems with lower diversity of species or functional groups. One approach to reduce the overlap error has been to measure productivity by species and then sum them to calculate total productivity.

Estimates of Aboveground Biomass

The discussion about estimates of primary productivity in fast turnover ecosystems assumed that a time series of biomass estimates was available. This section discusses the different ways of obtaining biomass estimates and focuses on how to take into account spatial variability; the temporal variability issue and sampling frequency are discussed in the following section. This section focuses on the issues related exclusively to biomass estimates and does not deal with statistical sampling issues. Sampling is a large section of statistics devoted to the theory and solution of applied problems and its scope goes beyond that of this chapter (Scheaffer et al. 1979).

In grasslands and shrublands, harvests of aboveground biomass have been the most frequently used technique. The number of samples is mostly determined by the variability of the ecosystem and the budget available or the accepted error. The size and shape of the sampling quadrats try to minimize the variance of the estimate (Greig-Smith 1983). The optimal size of the sampling quadrats is related to the pattern of vegetation. The variance of the estimates is maximum when the size of vegetation patches coincides with the quadrat size and decreases as they become larger or smaller. Another consideration is that as the quadrat size becomes smaller, the length of the quadrat boundary per unit area increases. Consequently, the edge effect increases because the person clipping biomass includes individuals or parts of individuals that should not be included and vice versa. Different shapes also affect the magnitude of the edge effect. Circular plots have the lower boundary/area ratio, while rectangular strips located perpendicular to boundaries between patches show lower variance than rectangles and circles. Rectangular strips encompass efficiently the natural variability of vegetation, which otherwise would require huge circles or rectangles. The sampling scheme chosen, which could be random, stratified random, or systematic, depends on the patterns of variability of biomass and on the available budget (see Scheaffer et al. [1979] for a description of sampling techniques' costs and benefits).

After the harvest in the field, biomass is transferred to a freezer as soon as possible to avoid mass losses as a result of plant respiration. Later, material is separated into the different compartments, which can be specific compartments or functional compartments, such as green biomass, standing dead, and litter, depending on the objectives of the study. Finally, the different samples are oven-dried at 70°C for two days to obtain dry weights.

Harvest techniques are expensive and, consequently, many double sampling techniques have been developed to reduce costs. Double sampling techniques consist of establishing the correlation between an expensive variable, such as biomass, and a less-expensive variable, and then using the inexpensive variable in the correlation for future estimates of the expensive variable. Double sampling techniques work as long as the treatment or factor under study does not affect the relationship between the expensive and inexpensive variables. For example, if the purpose of the experiment is to assess the effect of fertilization on productivity and the fertilization alters the relationship between greenness and productivity, then double sampling using greenness is not a good technique.

Capacitance is another variable used for double sampling (Currie et al. 1973; Neal et al. 1976; Neal and Neal 1973; Vickery et al. 1980). Changes in canopy capacitance correlate well with aboveground biomass and small easy-to-use devices have been developed that provide instant readings. Capacitance is mostly correlated with leaf area, and meters need to be calibrated often when water content of the canopy changes. The correlation with dry weight changes with species composition. This is a simple technique mostly used in extension when rapid estimates are needed.

Another group of double sampling techniques uses characteristics of the structure of the community or its individuals. Good results have been obtained using a pin that passes through the vegetation and assesses canopy interception (Frank and McNaughton 1990). The r^2 for the relationship between canopy interception and biomass ranged between 0.831 and 0.956 but the relationship changed with leaf size and thickness, indicating the need to use new calibration curves when there are changes in plant growth forms in space, time, or treatment (e.g., grazed vs. ungrazed plots). At the level of individuals, there are good correlations ($r^2 = 0.997$) between stem diameter and aboveground biomass for a large number of species spanning orders of magnitude of biomass (Freedman 1983).

Methods to Estimate ANPP in Slow Turnover Ecosystems

Ecosystems with marked differences in the turnover time of their aboveground components represent a challenge for effectively assessing primary production. For example, forests, woodlands, and shrublands have two separate components of aboveground primary production: leaves that are produced in a given time interval, and growth increment of woody material. Each has a different turnover time and the methodology used to estimate its primary production is different. As a result of these characteristics of ecosystems with woody vegetation, proximate measurements of biomass are used more frequently than in the case of systems dominated by herbaceous vegetation.

Production estimates for leaves and small twigs in forests usually involve the use of baskets or litter traps distributed in the forest understory (Whittaker and Marks 1975). The objective is to collect leaves and small twigs over a time course of at least a year, with the litterfall representing the aboveground production in the given time interval. Seasonality of litterfall, rate of litter decomposition, and climatic factors all must be taken into account when designing a sample scheme for litterfall collections. Litter traps should be located at random within a defined plot area, with care taken to avoid edge effects of the plot. The number of litter traps necessary will be determined largely by the heterogeneity of the system, with a minimum of 10 traps per plot area. The traps can be constructed of mesh-screen or nylon fabric, attached to a plastic or wooden frame, and elevated off the ground to avoid contamination with soil and waterlogging. Depending on the dynamics of the forest under study, pickups of litter may need to be completed weekly in the case of some tropical forests (e.g., Wright and Cornejo 1990), at a fixed time interval (e.g., Ogden and Schmidt 1998), or at the end of the season in temperate deciduous forests. Once taken from the field, litter is sorted by type or species and dried in an oven at 70°C for 48 hours for determinations of dry mass.

Additionally, a double sampling technique has been developed to estimate leaf production. Leaf area index (LAI), which is the leaf area in square meters of leaf area per square meter of ground area, is estimated by measuring light intensity at the bottom and top of the canopy using a commercial device called a plant canopy analyzer (e.g., Li-Cor 1992). Leaf area index is then modeled using the following equation: $IL/IO = e^{-kLAI(L)}$, where IL is incident light at the bottom of the canopy, IO is incident light at the top of the canopy, and k is the light extinction coefficient, which varies according to the type of vegetation and angle of inclination of the leaves (Aber and Melillo 1991). Changes in LAI over time can be converted to leaf biomass and used to represent leaf production in forests.

The development of methods for measurements of the woody component of ANPP in forest ecosystems came primarily from yield assessment of lumber for silviculture and forestry. As a result, there is allometric information on many economically important tree species with regression equations that relate tree height and diameter at breast height (DBH) to biomass (e.g., Curtin 1970; Curtis and Reukema 1970). For species that do not have published yield tables, however, which is the case for most nonmanaged forest ecosystems, it is necessary to measure species-specific allometric relationships (i.e., the shape of the trunks and how trunk diameters change with height) in order to estimate biomass and tree production. Because of the logistic difficulty of multiple measurements of all components of woody biomass, dimensional analysis is often used (e.g., Whittaker and Marks 1975; Whittaker and Woodwell 1968). This approach in-

volves taking measurements of several "easy-to-measure" parameters, which, when used with regression equations on a small sample of intensively measured individuals, give information about many of the "hard-to-measure" parameters, including woody biomass and net growth increments. These accessible measurements include DBH, tree height, and basal circumference, which are translated with the use of regression equations to measurements of woody biomass and tree production. In cases in which even the intensive sampling and harvest of even a few individuals cannot be done, some generalizations can be made and they are useful when working in native forests or protected areas where little background information is available. For example, Whittaker and Marks (1975) suggested as an estimate of tree biomass:

$$TB = 0.5 * BABH * TH \qquad (2.4)$$

where TB is tree biomass, BABH is basal area at breast height, and TH is tree height. Similarly, tree production is estimated as:

$$TNPP = 0.5 * AWI * TH \qquad (2.5)$$

where TNPP is tree net primary production and AWI is annual wood increment (at breast height). Additionally, some general relationships of DBH and biomass have been developed for specific regions, such as tropical forests (Brown and Iverson 1992), and in site-specific studies in particular forest ecosystems (e.g., Bormann and Gordon 1984; Raich et al. 1997; Singh et al. 1994).

Wood production per unit area can be estimated in two ways (Binkley et al. 1997). One is to sum the increments of individual trees in a unit area and extrapolate to a hectare basis. Individual increments can be estimated from repeated estimates as described above or using tree cores. The second way of estimating wood production is to make repeated estimates of total stand biomass through time. As will be discussed later, these two different ways of estimating wood production have interesting implications for the estimates of ANPP error.

Branch production is another component of forest ANPP. In some cases, branch plus trunk production can be estimated using regression equations with tree height and diameter (Newbould 1970). When branch production varies among treatments, an independent assessment has been preferred. Researchers have measured the diameter of branches at the base and correlated it with direct measurements of branch dry weight.

Once the woody and branch increments and the litterfall have been accurately assessed, a further complication that can occur in deciduous forests (where some part of the year has substantial light intercepted at the soil surface) is the productivity of understory biomass. In some cases, this vegetation can represent a substantial component of NPP and cannot be ignored or assumed to be a constant fraction of woody production. Peak biomass harvests or sequential harvests over time (such as those described in the previous section) may be used and combined with overstory measurements for the total production estimate.

Shrublands and steppes share characteristics of grasslands and forests and usually require methods that are a hybrid of those used in fast and slow turnover ecosystems. Generally, the two components are assessed separately and combined for a total measure of NPP. Shrubs present some of the same challenges as trees, and various methods have been developed to assess shrub productivity. For example, Fernández et al. (1991) developed a method to measure shrub production in which they harvested annual growth of shrubs (leaves and small twigs) in a small quadrat (10 × 25 cm) located on top of several shrub individuals. They also measured height and two diameters of several individuals. Based on allometric studies of these shrub species and on data about their densities, they extrapolated the quadrat results to a shrub individual and finally expressed their results on an areal basis.

Errors Associated with Estimates of ANPP

The section on estimating ANPP in fast turnover ecosystems highlighted a series of methods to estimate ANPP. The more complicated methods tried to take into account different sources of errors ranging from the missing peaks in biomass to the simultaneous nature of productivity, senescence, and decomposition. All these errors tend to underestimate ANPP. Sala et al. (1988) named this kind of error *errors leading to underestimation (ELUs).*

Singh et al. (1984) and Lauenroth et al. (1986) demonstrated that there are other kinds of errors when estimating NPP that always lead to overestimation of NPP. These are the *errors leading to overestimation (ELOs),* which stem from the fact that random errors in estimates of biomass do not compensate but accumulate, leading to a positive bias when estimating NPP (Sala et al. 1988). ELOs result directly from the estimation of NPP. In all cases, NPP is estimated as the increase in biomass during a period of time. An increase in biomass during a time period is considered an estimate of production. However, a decrease in biomass in the same interval yields a production equal to zero. Consider the case in which the real value of biomass at time 0 (B0) is equal to biomass at time 1 (B1) (Fig. 2.4). Both B0 and B1 are random variables and therefore, when sampling them, sometimes B1 will be larger than B0, sometimes B0 will be larger than B1, and occasionally they will be equal. Because of the definition of productivity (increments in biomass), when $B1 > B0$ it is considered an estimate of production, but when $B1 < B0$ the estimate of production will be zero. In synthesis, when random errors result in a positive difference, it is accepted as productivity, but when they result in a negative difference, it is ignored.

Singh et al. (1984) and Lauenroth et al. (1986) developed simulation models that yielded "true" values of below- and aboveground biomass and production. They sampled biomass from both models, calculated productivity using several of the standard methods, and compared them against the true values of production from the models. They found that the ELOs were very large; belowground NPP estimates were up to 5 times higher than the true value (Singh et al. 1984) and aboveground estimates were up to 33% higher than the true value (Lauenroth et al. 1986).

The works of Singh et al. (1984) and Lauenroth et al. (1986) were empirical demonstrations of ELOs and their magnitude. Sala et al. (1988) later calculated the distribution function of the estimator of productivity NPP which is nonnormal and demonstrated analytically that NPP derived from changes in biomass is a biased estimator of the true value of productivity. Based on the distribution function of NPP, it was possible to calculate the distribution function of the *overestimation error (OE)* and to assess the determinants of its magnitude.

$$OE = (\sigma/\sqrt{2\pi})e^{-1/2(\mu/\sigma)^2} - q\mu \qquad (2.6)$$

where μ is the true difference in biomass between time 1 and time 0, σ is the standard deviation of the difference, and q is the probability of $B1 - B0 \leq 0$. Independently of the mathematical reasoning that led to the distribution function of OE, it can be

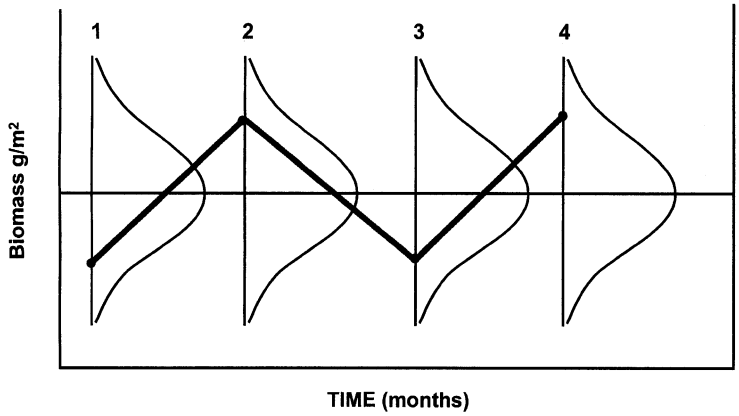

FIGURE 2.4. Example demonstrating how random errors in estimates of biomass do not compensate but rather accumulate and result in a positive bias in estimates in productivity. The horizontal line represents the true value of biomass which, in the example, does not change. Biomass estimates are random variables that have a normal distribution and a mean that coincides with the real mean. Sampling from this normal distribution yields, by chance, values that are slightly higher or lower than the true value. Increases in biomass through time are accepted as productivity but decreases are considered as zero.

seen that the size of the overestimation error depends on the variance and the true value of productivity. The larger the variance and the lower the true value of productivity, the larger is the overestimation error.

The larger the variance of the estimates of biomass used in calculating NPP, the greater will be the possibility of having only by chance a negative difference between biomass at time 0 and time 1 when in fact the true difference was positive. Similarly, the smaller the true value of productivity and of the true difference in biomass (B1 − B0), the higher will be the probability of obtaining by chance only a negative value of B1 − B0. Equation 2.6 indicates that the magnitude of the overestimation error depends on the probability of obtaining by chance a negative value for B1 − B0.

Biondini et al. (1991) developed an example for a grassland with a biomass at time 0 B0 = 110 g m^{-2}, SD = 10, and a biomass at time 1 B1 = 120, SD = 20 g m^{-2} (Fig. 2.5). The distribution of B1 − B0 had a mean of 10 g m^{-2} and a SD of 22.4, and the probability of B1 − B0 being less than 0 was 0.33. The mean and standard deviation of NPP can be calculated using the distribution calculated by Sala et al. (1988). In this example, NPP had a mean of 14.6 g m^{-2}, SD 16.3, the probability of NPP being equal to 0 was 0.33, and the probability of NPP being greater than 0 was 0.67. The overestimation error was 4.6 g m^{-2} and it was cal-

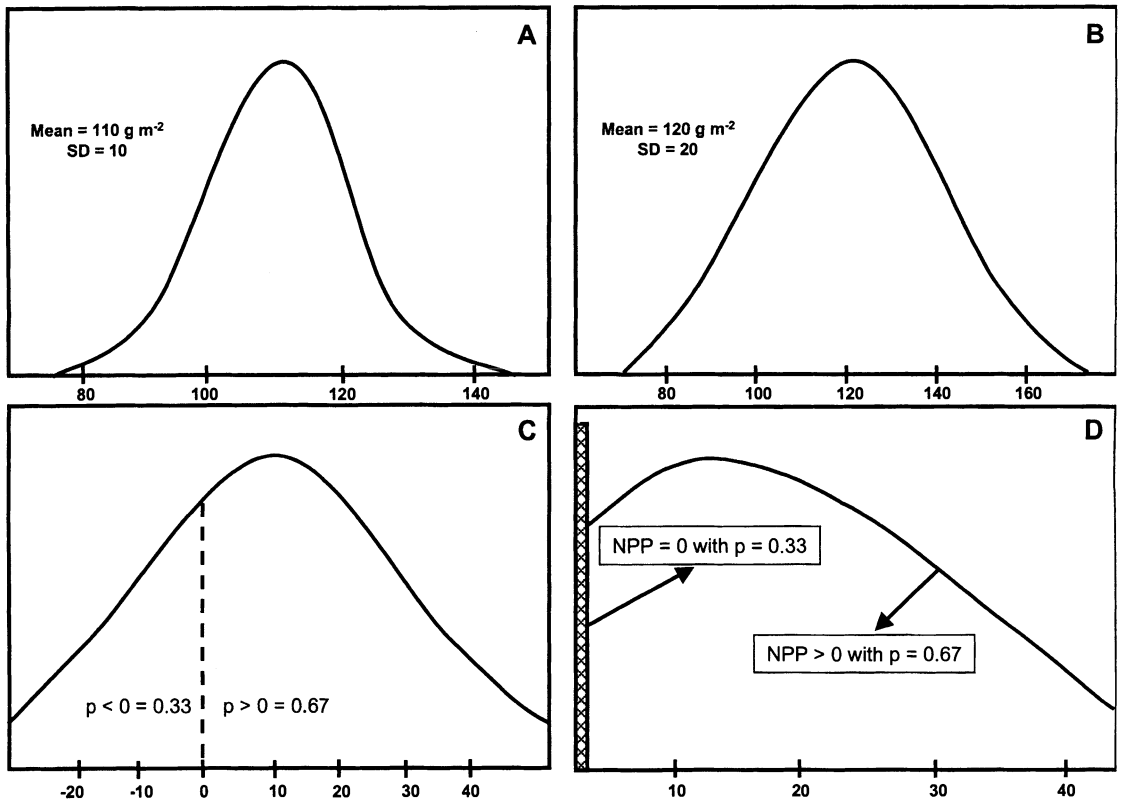

FIGURE 2.5. Example of the occurrence of overestimation error in estimates of productivity. A, Frequency distribution of biomass estimates at time 0. B, Frequency distribution of biomass estimates at time 1. C, Frequency distribution of the B1 − B0. D, Frequency distribution of net primary productivity (NPP) estimates. Note that although the real difference between B1 − B0 is 10 g m^{-2}, in 33% of the cases, the difference B1 − B0 is negative. Because negative values are discarded, NPP estimates are biased and an overestimation error occurs. The mean of B1 − B0 is 10 g m^{-2}, the mean of NPP is 14.6 g m^{-2}, and the overestimation error is 4.6 g m^{-2}. For calculation details see text and Biondini et al. (1991).

culated as the difference between the mean of the distribution of B1 − B0 and the estimated NPP. Biondini et al. (1991) developed software that, given the biomass values at times 0 and 1 and the corresponding standard deviation, calculates OE and corrected NPP value. The software is free and available from M. Biondini, North Dakota State University (biondini@plains.nodak.edu).

Using a similar example, we now show the effect of decreasing the variance of the biomass estimates on the overestimation error (Table 2.1). A 50% reduction in the standard deviation of the biomass estimates with respect to the example depicted in Figure 2.5 (case 1) while maintaining the other variables unchanged, reduces the probability of B1 − B0 < 0 from 0.32 to 0.18 and the overestimation error from 4.6 g m^{-2} (case 1) to 1.1 g m^{-2} (case 2). Similarly, a reduction in the true difference between biomass at time 1 and time 0 increases the overestimation error. In case 3, the variability is the same as in case 1 but the true difference (B1 − B0) is reduced (see Table 2.1). This 50% reduction in the true value of productivity resulted in an increase of the probability of obtaining negative differences in B1 − B0 from 0.32 to 0.41 and a large increase in the overestimation error from 4.6 to 6.5 g m^{-2}.

An important deduction from the analysis of the determinants of the overestimation error is that an increase in the sampling frequency necessarily results in an increase in the error. An increase in the sampling frequency results in a reduction of the true value of productivity that is being estimated. For example, the true value of productivity to be measured when samples are taken monthly will be smaller than if they are taken bimonthly. The reduction in the true value as shown above necessarily results in an increase in the overestimation. The idea just described, that higher frequency results in larger overestimation errors, has been mathematically proven (Sala et al. 1988). Similarly, it has been demonstrated that an increase in error occurs as a result of increasing the number of components used in estimating productivity. For example, estimates of productivity based on the sum of the increases of individual species biomass have a larger overestimation error than estimates based on changes in total biomass.

TABLE 2.1. Examples demonstrating the effect of variance and the true value of productivity on the overestimation error of productivity estimates.

	Case	Case 2	Case 3
Biomass at time 0, g m^{-2}	110	110	110
Biomass at time 1, g m^{-2}	120	120	115
B1 − B0	10	10	5
Standard deviation B0	10	5	10
Standard deviation B1	20	10	20
Standard deviation B1 − B0	22	11	22
Probability of B1 − B0 < 0	0.32	0.18	.41
Overestimation error, g m^{-2}	4.6	1.1	6.5

The errors associated with ANPP in ecosystems dominated by woody plants with slow turnover ecosystems are different from those characteristic of fast turnover ecosystems. Errors associated with litterfall are quite straightforward since the baskets integrate the litterfall flow during a period of time. Consequently, litter accumulated in the traps is an unbiased estimator of true litterfall and there are no errors of under- or overestimation. Sampling errors in estimates of litterfall depend on the forest heterogeneity and the sampling effort, which is mostly constrained by resource availability. Estimates of wood increments have two sources of error, errors estimating average tree growth per tree and errors in extrapolating to a hectare basis. Estimates of tree growth per tree, in turn, have two main sources of error, the estimates of DBH and the error in the allometric equations used to convert DBH data into trunk volume or weight. Tree mortality between two consecutive estimates of stand biomass introduces another source of error when extrapolating from trees to stands (Binkley et al. 1997). The magnitude of this error depends largely on the way stemwood ANPP is calculated. If wood production is calculated by summing the growth per tree in an area, the death of trees during that period represents an underestimation of ANPP. The production of trees that grew during that period and died is missed. Binkley et al. (1997) estimated that tree mortality is usually low and this error would not be larger than 1 to 2% per year. On the contrary, if wood ANPP is calculated as the difference in total stand wood biomass between two sampling dates, the error resulting from tree mortality could be very large. The fall of a big tree will result in a major underestimate of production during the period. All the wood biomass accumulated in the fallen tree during many years is now subtracted

from the estimate of wood production for the study period. Consequently, tree mortality results in a large underestimation error when the method of differences in stand biomass is used to calculate wood production.

Optimal Methodology to Estimate ANPP

The optimal methodology to assess ANPP depends on the objective of the study. Analysis of the errors associated with estimates of productivity provides the tools to choose the best method given certain objectives and budget. Methods that try to minimize ELUs necessarily increase ELOs. The sources of ELUs are the missing peaks and the simultaneous nature of productivity and decomposition. The way to reduce these errors is to increase the sampling frequency to reduce the number of missing peaks and troughs. The increase in the frequency also decreases the possibility of overlap between productivity and decomposition. Estimating productivity by species and then adding them up to assess total NPP also reduces ELUs, as discussed above. However, the increase in sampling frequency and the estimates by species all increase ELOs since they reduce the true value of NPP and increase the variance of the estimates of B1 − B0. Similarly, reductions in the sampling frequency and in the number of components analyzed reduce ELOs but increase ELUs.

If the purpose of the study is to obtain an estimate of annual production, and the ecosystem has a clear seasonality, the best method will be a single harvest at peak biomass. If the ecosystem has even productivity distributed throughout the year or frequent peaks and troughs, a more frequent sampling scheme will be desirable. One possibility of resolving the tradeoff between reducing ELUs and ELOs is to use a detailed method and estimate the overestimation error using the algorithm developed by Sala et al. (1988).

It is important to distinguish between methods that are conceptually more correct and methods that provide an answer that is closer to the true value. Methods that study the independent pattern of individual species or those that take into account numerous functional compartments are closer to the concept of primary production. However, the results that they yield may be further from the real value than those resulting from simpler methods. Here it is crucial to take into account the uncertainty associated with each one of the terms used in the calculation. O'Neill (1973) pointed out that uncertainty of the results increases as the uncertainty of the individual components increases. In the production case, higher variability in the biomass estimates means larger overestimation error. An extreme example is to try to estimate annual production from gas exchange estimates from individual leaves or small patches that then are extrapolated to longer time frames and larger areas. Photosynthesis is a fast variable that varies in a matter of minutes and consequently the errors associated with extrapolating from the leaf to the hectare and from minutes or hours to months and years are so large that they make the results irrelevant. Although the annual estimate of production through the gas exchange method may contain large errors, it may still be very close to the concept of productivity.

Summary

There is not a best method to measure aboveground primary productivity. Decisions about methods are even more complicated, because methods that reduce one kind of error increase other kinds of errors. It is somehow counterintuitive that the more complicated and expensive methods, which take into account most of the flows involved in primary productivity, may yield results with the largest errors. Although these methods are closest to the concept of primary productivity, they may yield results that are the farthest from the real value of productivity. Uncertainty in the variables used to estimate primary productivity results in greater uncertainty in the final estimates of productivity. Because of the way productivity is calculated, uncertainty in the input variables always results in overestimation of productivity. This chapter described of the kinds of errors associated with each method and how they relate to the ecosystem characteristics, as well as the costs and benefits of the different methodological alternatives. The best method will depend on the characteristics of the ecosystem, such as turn-

over time, seasonality, etc., and on the objectives of the study.

Acknowledgments We gratefully acknowledge W.K. Lauenroth for helpful discussions about many of the ideas described in this chapter and J.M. Paruelo and D. Binkley for insightful comments on an earlier version of this manuscript.

References

Aber, J.D.; Melillo, J.M. *Terrestrial Ecosystems.* Philadelphia: Saunders; 1991.

Binkley, D.; O'Connell, A.; Sankaran, K. Stand development and productivity. In: Sadanandan N.; Brown A., eds. *Management of Soil, Nutrients and Water in Tropical Plantation Forests.* Canberra: Australian Centre for International Agriculture Research; 1997: 419–441.

Biondini, M.E.; Lauenroth, W.K.; Sala, O.E. Correcting estimates of net primary production: Are we overestimating plant production in rangelands? J. Range Manage. 44:194–197; 1991.

Bormann, B.T.; Gordon, J.C. Stand density effects in young red alder plantations: Productivity, photosynthate partitioning, and nitrogen fixation. Ecology 65:394–402; 1984.

Brown, S.; Iverson, L.R. Biomass estimates for tropical forests. World Resourc. Rev. 4:366–384; 1992.

Currie, P.O.; Morris, M.J.; Neal, D.L. Uses and capabilities of electronic capacitance instruments for estimating standing herbage. Part 2. Sown Ranges. J. Br. Grassland Soc. 28:155–160; 1973.

Curtin, R.A. Dynamics of tree and crown structure in *Eucalyptus obliqua.* For. Sci. 16:321–328; 1970.

Curtis, R.O.; Reukema, D.L. Crown development and site estimates in a Douglas fir plantation spacing test. For. Sci. 16:287–301; 1970.

Fernández, R.J.; Sala, O.E.; Golluscio, R.A. Woody and herbaceous aboveground production of a Patagonian steppe. J. Range Manage. 44:434–437; 1991.

Frank, D.A.; McNaughton, S.J. Aboveground biomass estimation with the canopy intercept method: A plant growth form caveat. Oikos 57:57–60; 1990.

Freedman, B. The relationship between the aboveground dry weight and diameter for a wide size range of erect land plants. Can. J. Bot. 62:2370–2374; 1983.

Greig-Smith, P. *Quantitative Plant Ecology.* Oxford: Blackwell; 1983.

Lauenroth, W.K.; Hunt, H.W.; Swift, D.M.; Singh, J.S. Estimating aboveground net primary production in grasslands: A simulation approach. Ecol. Model. 33:297–314; 1986.

Li-Cor. *LAI 2000 Plant Canopy Analyzer Operating Manual.* Lincoln, NE: Li-Cor Inc.; 1992.

McNaughton, S.J.; Oesterheld, M.; Frank, D.A.; Williams, K.J. Ecosystem-level patterns of primary productivity and herbivory in terrestrial habitats. Nature 341:142–144; 1989.

Neal, D.L.; Currie, P.O.; Morris, M.J. Sampling herbaceous native vegetation with an electronic capacitance instrument. J. Range Manage. 29:74–77; 1976.

Neal, D.L.; Neal, J.L. Uses and capabilities of electronic capacitance instruments for estimating herbage. Part 1. History and development. J. Br. Grassland Soc. 28:81–89; 1973.

Newbould, P. *Methods for Estimating the Primary Production of Forests.* Oxford: Blackwell; 1970.

Odum, E. *Fundamentals of Ecology.* Philadelphia: Saunders; 1971.

Ogden, A.E.; Schmidt, M.G. Litterfall and soil characteristics in canopy gaps occupied by vine maple in a coastal western hemlock forest. C. J. Soil Sci. 77:703–711; 1998.

O'Neill, R. Error analysis of ecological models. In: Nelson O., ed. *Radionuclides in Ecosystems.* Washington, DC: USAEC-CONF Technical Information Division; 1973: 898–908.

Raich, J.W.; Russell, A.E.; Vitousek, P.M. Primary productivity and ecosystem development on Mauna Loa, Hawaii. Ecology 78:707–721; 1997.

Sala, O.; Deregibus, V.; Schlichter, T.; Alippe, H. Productivity dynamics of a native temperate grassland in Argentina. J. Range Manage. 34:48–51; 1981.

Sala, O.E.; Biondini, M.E.; Lauenroth, W.K. Bias in estimates of primary production: An analytical solution. Ecol. Model. 44:43–55; 1988.

Scheaffer, R.; Mendenhall, W.; Ott L. *Elementary Survey Sampling.* North Scituate, Ma: Duxbury; 1979.

Singh, J.S.; Lauenroth, W.K.; Hunt, H.W.; Swift, D.M. Bias and random errors in estimators of net root production: A simulation approach. Ecology 65:1760–1764; 1984.

Singh, J.S.; Lauenroth, W.K.; Steinhorst, R.K. Review and assessment of various techniques for estimating net aerial primary production in grasslands from harvest data. Bot. Rev. 41:181–232; 1975.

Singh, S.P.; Adhikari, B.S.; Zobel, D.B. Biomass, productivity, leaf longevity and forest structure in the central Himalaya. Ecol. Monogr. 64:401–421; 1994.

Vickery, P.J.; Bennett, I.L.; Nicol, G.R. An improved electronic capacitance meter for estimating herbage mass. Grass Forage Sci. 35:247–252; 1980.

Whittaker, R.; Marks, P. Methods of assessing terrestrial productivity. In: Lieth H.; Whittaker R., eds. *Primary*

Productivity of the Biosphere. New York: Springer-Verlag; 1975:55–118.

Whittaker, R.H.; Woodwell, G.M. Dimension and production relations of trees and shrubs in the Brookhaven Forest, New York. J. Ecol. 56:1–25; 1968.

Wiegert, R.; Evans, F.C. Primary production and the disappearance of dead vegetation on an old field. Ecology 45:49–63; 1964.

Wright, S.J.; Cornejo, F.H. Seasonal drought and leaf fall in a tropical forest. Ecology 71:1165–1175; 1990.

3

Global Terrestrial Gross and Net Primary Productivity from the Earth Observing System

Steven W. Running, Peter E. Thornton, Ramakrishna Nemani, and Joseph M. Glassy

Introduction

Probably the single most fundamental measure of "global change" of highest practical interest to humankind is the change in terrestrial biological productivity. Biological productivity is the source of all the food, fiber, and fuel by which humans survive, and so defines most fundamentally the habitability of Earth. The spatial variability of net primary productivity (NPP) over the globe is enormous, from about 1000 $g\,C\,m^{-2}$ for evergreen tropical rain forests to less than 30 $g\,C\,m^{-2}$ for deserts (Scurlock et al. 1999). With increased atmospheric carbon dioxide (CO_2) and global climate change, NPP over large areas may be changing (Myneni et al. 1997a, VEMAP 1995, Melillo et al. 1993). Understanding regional variability in carbon cycle processes requires a more spatially detailed analysis of global land surface processes. Since December 1999, the U.S. National Aeronautics and Space Administration (NASA) Earth Observing System (EOS) produces a regular global estimate of (gross primary productivity, GPP) and annual NPP of the entire terrestrial earth surface at 1-km spatial resolution, 150 million cells, each having GPP and NPP computed individually.

The GPP and NPP products are designed to provide an accurate, regular measure of the production activity or growth of terrestrial vegetation. These products will have both theoretical and practical utility. The theoretical use is primarily for defining the seasonally dynamic terrestrial surface CO_2 balance for global carbon cycle studies, such as solving the "missing sink question" of carbon (Tans et al. 1990; Ciais et al. 1995; Randerson et al. 1997; Field et al. 1998). The spatial and seasonal dynamics of CO_2 flux are also of high interest in global climate modeling, because CO_2 is an important greenhouse gas (Keeling et al. 1996; Hunt et al 1996). Currently, global carbon cycle models are being integrated with climate models, toward the goal of integrated Earth Systems Models that will represent the dynamic interaction between the atmosphere, biosphere, and oceans. The weekly GPP is most useful for theoretical questions, and more correctly defines terrestrial CO_2 fluxes than simple normalized difference vegetation index (NDVI) correlations currently done. These analyses will increase understanding of how the seasonal fluxes of net photosynthesis and respiration are related to seasonal variations of atmospheric CO_2.

The practical utility of these GPP/NPP products is as a measure of crop yield, range forage and forest production, and other economically and socially significant products of vegetation growth. The value of an unbiased, regular source of crop, range, and forest production estimates for global policy and economic decision making is immense. These products will be available for all users worldwide. This chapter summarizes the conceptual background and implementation details of these new EOS satellite products.

Theoretical Basis for the Algorithm for Global NPP

The history of the theoretical basis for this satellite estimate of terrestrial NPP has three components: the idea that plant NPP is directly related to ab-

sorbed solar energy, the theoretical connection between absorbed solar energy and satellite vegetation indices, and the analysis of the causes of variation in the final conversion efficiency. We will consider each step in sequence.

Relating NPP and APAR

The original logic of Monteith (1972, 1977) suggested that the NPP of well-watered and fertilized annual crop plants was linearly related to the amount of solar energy they absorbed. This logic combined the meteorological constraint of available sunlight reaching a site with the ecological constraint of the amount of leaf area absorbing that solar energy, yet avoided many complexities of carbon balance theory. *Absorbed photosynthetically active radiation (APAR)* integrates the geographic and seasonal variability of day length and potential incident radiation with daily cloud cover and aerosol attenuation of sunlight. Additionally, APAR quantifies implicitly the amount of leaf area the vegetation is displaying to absorb radiation, that is, the leaf area index (LAI). A conversion efficiency, ε, then translates the APAR in energy units to final tissue growth, NPP, in biomass. There can be some conceptual ambiguity in relating APAR directly to growth, as often photosynthate is stored by the plant temporarily before growth occurs. Daily net photosynthesis (GPP) is the daily total of photosynthesis minus all autotrophic respiration over a 24-hour day. Net primary production (NPP) is the annual sum of daily GPP. So, for generalized global-scale purposes, we assume that, summed over a given time interval:

$$\text{GPP} = \varepsilon * \text{APAR} \tag{3.1}$$

where ε is the PAR conversion efficiency (g MJ^{-1}), see Landsberg et al. (1996). Plant respiration costs are included in the ε term, as described below.

$$\text{NPP} = \varepsilon * \sum \text{APAR} = \sum \text{GPP} \tag{3.2}$$

Relating APAR and NDVI

Sellers (1987), Asrar et al. (1992) and Myneni et al. (1997b) have shown that APAR could be estimated from remote sensing. Spectral vegetation indices (SVIs) derived from remote sensing data have several forms, the most widely used currently is the normalized difference vegetation index (NDVI), which uses reflectances from red and near-infrared (NIR) wavelengths as:

$$\text{NDVI} = (\text{NIR} - \text{Red})/(\text{NIR} + \text{Red}) \tag{3.3a}$$

and

$$\text{APAR/PAR} \approx \text{NDVI} \tag{3.3b}$$

where PAR is the incident radiation in photosynthetic wavelengths. Consequently, SVIs such as NDVI most directly quantify the *fraction of photosynthetically active radiation that is absorbed, (FPAR):*

$$\text{FPAR} = \text{APAR/PAR} \approx \text{NDVI} \tag{3.4}$$

When FPAR derived by a spectral vegetation index is driven by daily incident radiation (PAR) and converted with ε as in Equation 3.2:

$$\begin{aligned} \text{GPP} &= \varepsilon * \text{FPAR} * \text{PAR} \\ &= \varepsilon * \text{NDVI} * \text{PAR} \end{aligned} \tag{3.5}$$

and when summed annually:

$$\begin{aligned} \text{NPP} &= \varepsilon * \sum (\text{FPAR} * \text{PAR}) \\ &= \varepsilon * \sum (\text{NDVI} * \text{PAR}) \end{aligned} \tag{3.6}$$

It should be noted that the EOS MODIS (moderate resolution imaging spectroradiometer) instrument computes more advanced SVIs using three or four wavelengths, then the simple two-wavelength NDVI used for these general derivations (Running et al. 1994; Justice et al. 1998). These relationships derived between a satellite radiometric index and vegetation canopy radiative properties are the critical logical connections that now allow scientists to use remote sensing to spatially extrapolate ecosystem carbon cycle processes.

Biophysical Variability of ε

The PAR conversion efficiency, ε, varies widely with different vegetation types (Field et al. 1995; Ruimy et al. 1994; Prince and Goward 1995). There are two principal sources of this variability. First, with any vegetation, some photosynthesis is immediately used for maintenance respiration costs. For the annual crop plants from the original theory of Monteith (1972), these respiration costs were minimal. However, this respiration cost increases with perennial plants that must sustain permanent

tissue. Prince (1991) summarized values of ε for herbaceous vegetation to be from 1.0 to 1.8 g C MJ^{-1} for plants with the C_3 photosynthetic pathway, and higher ε for plants with the C_4 photosynthetic pathway. Running and Hunt (1993) and Hunt (1994) found published ε values for woody vegetation were lower, from about 0.2 to 1.5 g C MJ^{-1}. and hypothesized that this was the result of respiration from the living cells in the sapwood of woody stems.

The second source of variability in ε is due to suboptimal climatic conditions. To extrapolate Monteith's original theory, designed for well-watered crops only during the growing season, to perennial plants living year around, certain severe climatic constraints must be treated. Evergreen vegetation, such as conifer trees or schlerophyllous shrubs, absorb PAR all during the nongrowing season, yet during subfreezing temperatures execute minimal photosynthetic activity, because stomata are closed by frozen water in the leaves (Waring et al. 1995; Waring and Running 1998). So, as a global generalization, we truncate GPP on days when the minimum temperature is below 0°C. Additionally, high vapor pressure deficits, >20 hPa, have been shown to induce stomatal closure in unirrigated native plants. This level of daily atmospheric water deficit is commonly reached in semiarid regions of the world for much of the growing season. So, our algorithm mimics this physiological control by progressively limiting daily GPP when high vapor pressure deficits are computed from the surface meteorology.

Other biophysical factors regularly constrain the conversion of APAR into biomass growth. All plants have an optimum temperature for photosynthesis, but acclimation is so rapid that a global general temperature limit cannot be easily defined. Progressive seasonal soil water stress also limits plant growth, but cannot be quantified without a water balance calculation. For our global logic here, we assume that continuous soil water stress ultimately results in reduction in vegetation leaf area, which is then reflected in the NDVI or FPAR terms of Equations 3.5 and 3.6 (Nemani and Running 1989). Finally, we also assume nutrient constraints on vegetation growth to be quantified by limiting leaf area, rather than attempting to compute a constraint through ε. This is not entirely accurate, as ranges of leaf nitrogen and photosynthetic capacity occur in all vegetation types (Schulze et al. 1994).

Parameterization of ε with Global BIOME-BGC Simulations

In order to quantify this biome- and climate-induced range of ε, we have simulated global NPP in advance with a complex ecosystem model, BIOME-BGC, and computed the ε, or conversion efficiency, from APAR to final NPP (Fig. 3.1). This complete global range of ε is incorporated into a biome parameter look-up table (BPLUT) (Table 3.1). Operating this simple PAR conversion efficiency model rather than the complex ecosystem model to compute NPP is roughly 100 times faster in computer execution, an important consideration when 150 million cells must be computed each day.

To capture as much of the global range of variation in climate and landcover as possible for determining ε, we performed daily simulations over a global 1° × 1° grid. Meteorological input was from the 14-year daily data set developed at Scripps Oceanographic Institute (Piper and Stewart 1996). Gridded soil physical parameters were estimated from the Zobler soil texture database (Zobler, 1986). The standard at-launch EOS global 1-km landcover data set was obtained (Hansen et al. 1999). This consisted of two separate data sets: a discrete classification of biome types that is also the at-launch MODIS landcover product, and a continuous fields product that describes the fractional cover of woody species in each grid cell and also discriminates woody cover fraction by leaf longevity and leaf morphology (DeFries et al. 1999). For each grid cell, a separate (independent) BIOME-BGC simulation was performed for each functional vegetation type having greater than 1% of the total vegetated land area within the cell. The Scripps meteorological data set contains 14 years of daily gridded surfaces for maximum and minimum temperature and precipitation. We used these variables to estimate daily humidity (Kimball et al. 1997a) and radiation (Thornton and Running 1999) over the grid. Day length was calculated for each grid cell from standard geometrical relationships.

The interactions between the carbon and water budgets of the BIOME-BGC model have been described in considerable detail elsewhere (Running

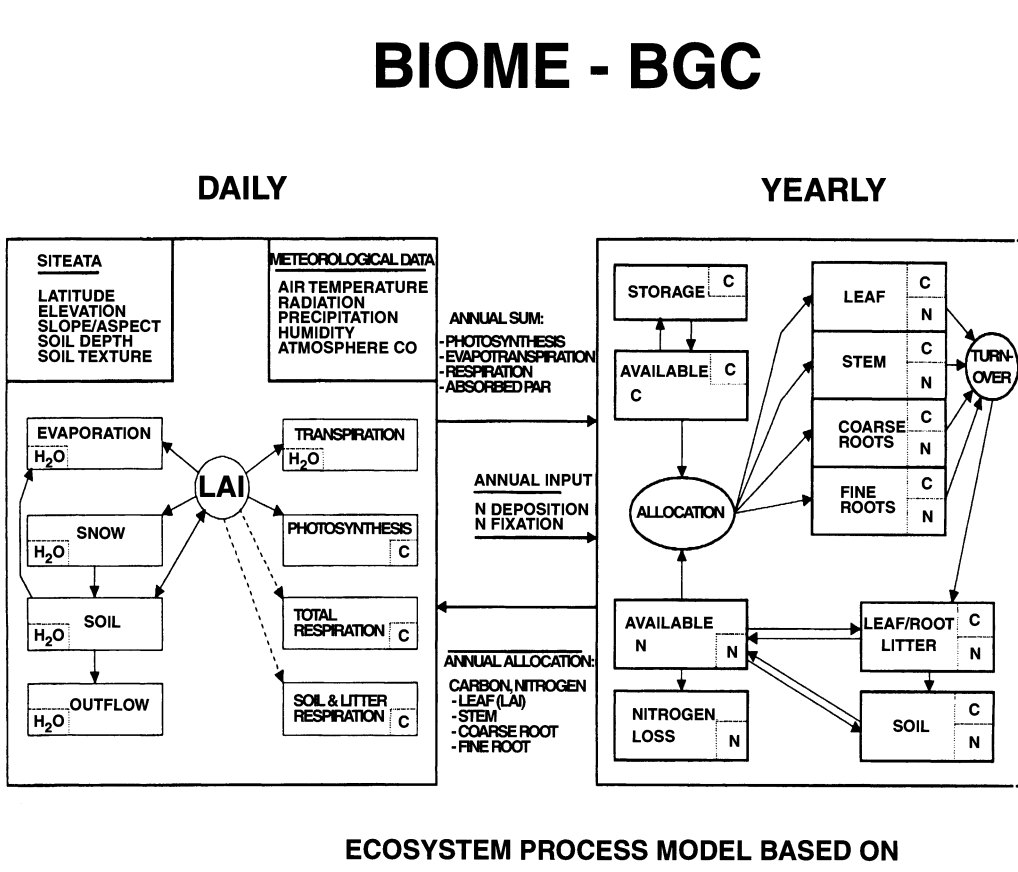

FIGURE 3.1. Compartment flow diagram for the ecosystem process model BIOME-BGC used to compute the global biome specific parameters for ε. (Running and Hunt 1993).

and Gower 1991; Running and Hunt 1993; Kimball et al. 1997b, c). Carbon (C) and nitrogen (N) allocation is controlled by fixed C/N ratios, so new growth is dependent on there being an adequate supply of both C, from the gross photosynthesis process, and N, taken up by the plants from the soil mineral N pool. In the case of excess C coming from the photosynthesis predictions, with respect to the N available from the soil mineral N pool, gross photosynthesis is reduced, effectively attenuating the N use efficiency under N-limiting conditions. The implication of this interaction is that in addition to the direct environmental controls on photosynthesis that influence the radiation conversion efficiency relationship, there are indirect controls that operate through the influence of environmental conditions on the mineralization of N from decomposing litter and soil organic matter. These influences appear in the daily GPP outputs, and can be at least partly captured in the estimates of ε_{max} derived from those outputs.

There is a strong dependence of plant C and N allocation on soil mineral nutrition status, and this dependency translates to variation in optimized parameters for the radiation conversion efficiency logic. Model spinup runs were performed that allowed the soil organic matter and mineral nutrient pools to stabilize. Our approach was to start all soils with no organic matter, and plants with a very low initial biomass, and let the soil organic matter and plant biomass agrade over many cycles (≈2000 yr) through the 14-year daily driver record. These spinup runs describe a hypothetical global steady state for primary production (as well as net ecosystem exchange) characteristic of the preindustrial atmosphere and N cycles. Because the optimized GPP parameters are sensitive to the soil nutrient status, anthropogenic influences on

TABLE 3.1 Biome Property Lookup table (BPLUT)[a]

Parameter name	EOS biome class[b]										
	ENF	EBF	DNF	DBF	MF	WL	WGrass	CShrub	OShrub	Grass	Crop
epsilon_max	0.001008	0.001259	0.001103	0.001044	0.001116	0.000864	0.000768	0.000888	0.000774	0.000604	0.000604
Daily											
tmin_max	8.31	9.09	10.44	7.94	8.50	10.24	11.39	8.61	8.80	12.02	12.02
tmin_min	−8.00	−8.00	−8.00	−8.00	−8.00	−8.00	−8.00	−8.00	−8.00	−8.00	−8.00
vpd_max	4100	4100	4100	4100	4100	4100	4100	4100	4100	4100	4100
vpd_min	930	930	930	930	930	930	930	930	930	930	930
sla	22.1	17.3	30.0	26.2	21.5	33.8	39.8	12.0	28.5	45.0	45.0
q10_mr	2.0	2.0	2.0	2.0	2.0	2.0	2.0	2.0	2.0	2.0	2.0
Annual											
froot_leaf_ratio	1.3	1.1	1.3	1.1	1.1	1.5	1.8	1.0	1.5	2.0	2.0
livewood_leaf_rat	0.081	0.162	0.152	0.203	0.132	0.107	0.051	0.079	0.040	0.000	0.000
leaf_mr_base	0.00653	0.00604	0.00805	0.00778	0.00677	0.00824	0.00869	0.00519	0.00714	0.00908	0.00908
froot_mr_base	0.00519	0.00519	0.00519	0.00519	0.00519	0.00519	0.00519	0.00519	0.00519	0.00519	0.00519
livewood_mr_base	0.00322	0.00397	0.00297	0.00371	0.00372	0.00212	0.00100	0.00436	0.00218	0.00000	0.00000
leaf_gr_base	0.3	0.3	0.3	0.3	0.3	0.3	0.3	0.3	0.3	0.3	0.3
froot_leaf_gr_rati	1.3	1.1	1.3	1.1	1.1	1.5	1.8	1.0	1.5	2.0	2.0
livewood_leaf_gr_r	0.16	0.20	0.15	0.19	0.19	0.11	0.05	0.22	0.11	0.0	0.0
deadwood_leaf_gr_r	1.6	1.1	1.5	1.6	1.8	1.0	0.5	0.0	0.0	0.0	0.0

[a]**Long names and units for BPLUT parameters:**

epsilon_max	maximum radiation conversion efficiency (kgC/MJ)
tmin_max	daily minimum temperature at start of temperature reduction to epsilon_max (C)
tmin_min	daily minimum temperature at full temperature reduction to epsilon_max (C)
vpd_max	daylight average vapor pressure deficit at full humidity reduction to epsilon_max (Pa)
vpd_min	daylight average vapor pressure deficit at start of humidity reduction to epsilon_max (Pa)
sla	specific leaf area (projected m^2/kg leaf C)
q10_mr	Q10 for maintenance respiration (unitless)
froot_leaf_ratio	new fine root:new leaf (kgC/kgC)
livewood_leaf_rat	annavg livewood:annmax leaf (kgC/kgC)
leaf_mr_base	leaf maintenance respiration base (kgC/kgC/day, 20C)
froot_mr_base	fine root maintenance respiration base (kgC/kgC/day, 20C)
livewood_mr_base	livewood maintenance respiration base (kgC/kgC/day, 20C)
leaf_gr_base	leaf growth respiration base (kgC respired/kgC grown)
froot_leaf_gr_rati	fine root:leaf, growth respiration (kgC/kgC)
livewood_leaf_gr_r	livewood:leaf, growth respiration (kgC/kgC)
deadwood_leaf_gr_r	deadwood:leaf, growth respiration (kgC/kgC)

[b]**EOS biome class key:**

ENF = evergreen needleleaf forest
EBF = evergreen broadleaf forest
DNF = deciduous needleleaf forest
DBF = deciduous broadleaf forest
MF = mixed forest
WL = woodland
WGrass = wooded grassland
CShrub = closed shrubland
OShrub = open shrubland
Grass = grassland
Crop = cropland

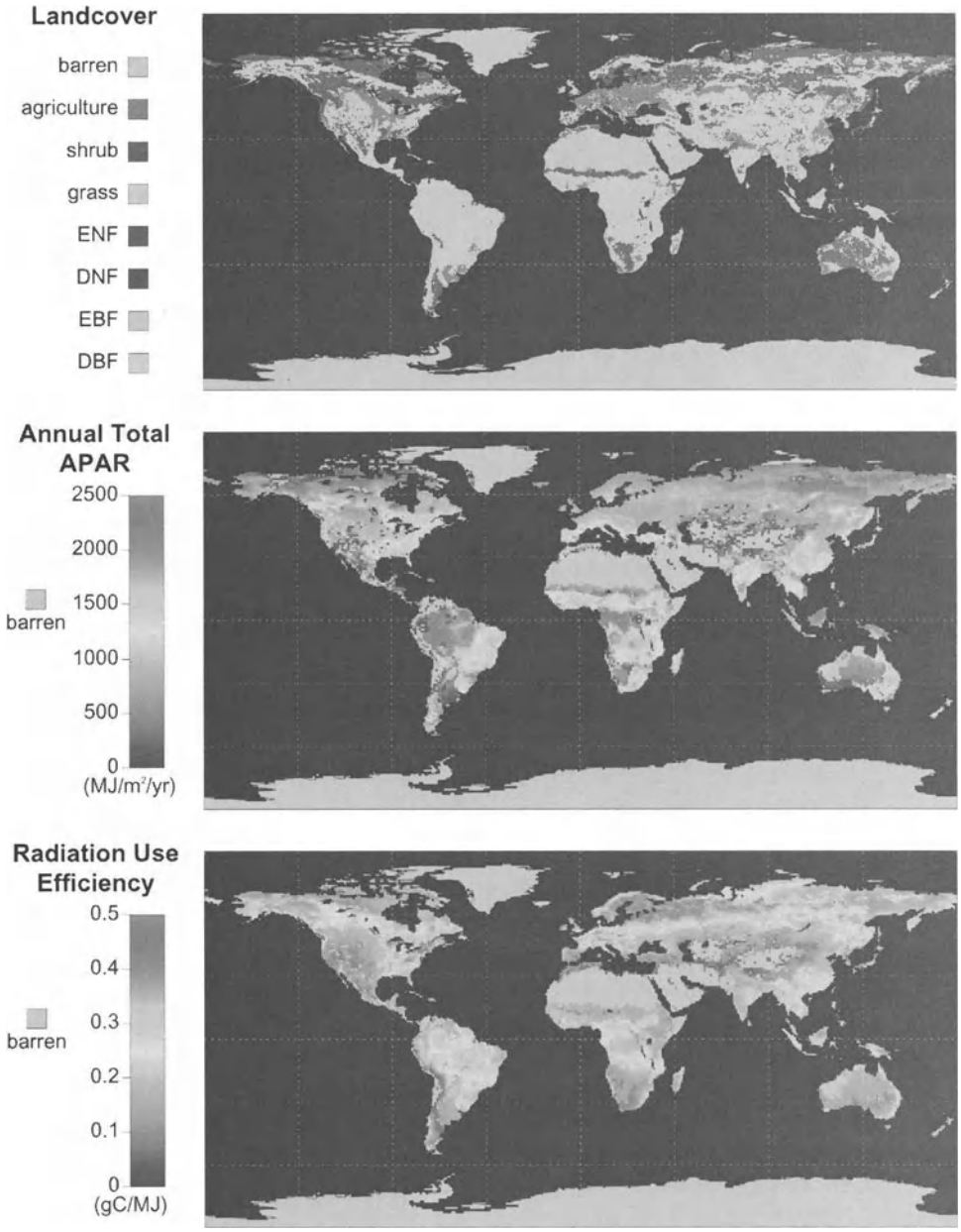

FIGURE 3.2. Example of the landcover (top), annual APAR (middle), and ε (bottom) global data inputs needed to compute the NPP algorithm. *(See color plate.)*

such variables as atmospheric concentrations of CO_2 and the rate of N deposition have important consequences influencing soil organic matter and plant biomass states (Hudson et al. 1994; Keeling et al. 1996). For this reason, we extended the preindustrial spinup runs into the historical record of increasing atmospheric CO_2 and atmospheric N deposition, assuming 1895 as a starting point, and following the record of CO_2 established for use in VEMAP (vegetation/ecosystem modeling and analysis project) (VEMAP 1995).

To reiterate, these intensive global simulations with BIOME-BGC have been done in advance of EOS launch to define the BPLUT with as much ecological accuracy as possible (see Table 3.1). Next, we will cover the simple implementation algorithm that will be executed within the EOS computing system to compute global NPP.

Algorithm Implementation Logic in EOS

Each day the EOS data system will ingest calibrated and atmospherically corrected reflectances from each spectral channel of the MODIS sensor for each cloud-free pixel. In order to make the daily GPP computation for each global terrestrial pixel, three other variables must first be retrieved: the biome type, which changes no more than annually; the FPAR, which can change weekly during rapid vegetation growth and senescence; and the daily surface climate conditions, which change diurnally.

Satellite-Derived Input Variables

Biome Classes

From earlier analyses, we define the major differences in vegetation biogeochemistry by defining key biome classes with markedly different nutritional constraints and carbon cycling dynamics, often called functional types (Running et al. 1995). The difference in our analysis, though, was to define these biome attributes from characteristics that would be amenable to remote sensing (Nemani and Running 1997). For example, deciduous foliage and evergreen foliage have different lignin/nitrogen ratios that control the rate of litter decomposition and N mineralization. Grasslands and annual crops have very aerodynamically smooth surfaces, whereas forests have very aerodynamically rough surfaces, affecting the energy, momentum, water and CO_2 fluxes. Forests have large respiring masses of living wood (sapwood), whereas grasslands and annual crops do not. Broadleaf forests have different radiative transfer properties compared with needleleaf forests. These differences in vegetation biophysics and biogeochemistry are defined implicitly by the biome classification.

From sensitivity analyses with BIOME-BGC and remote sensing data, we determined that seven fundamental biome classes were needed to represent essential differences in biogeochemical cycling of different global vegetation types (Running et al. 1995; Nemani and Running 1996). The standard global 1-km biome classification for EOS defines 11 classes, incorporating some additional fractional cover combinations (see Table 3.1) (Fig. 3.2, top) (Hansen et al. 1999). Grasslands may have either the C_3 or C_4 photosynthetic pathways, controlling ε_{gross}. We assume that C_4 photosynthesis occurs in tropical and arid climates and C_3 photosynthesis occurs in moist, temperate climates, and use long-term climatic conditions to make this distinction globally (Piper and Stewart 1996).

The biome class for each pixel is planned to be updated once each year to reflect changes in global landcover (John Townshend, personal communication). Consequently, each pixel will be reevaluated for biome changes resulting from deforestation and reforestation, new agriculture or urbanization, large-scale disturbances, and successional development.

FPAR and LAI

For each pixel, an algorithm using the MODIS sensor measures the FPAR (the radiometric equivalent of LAI) each day, and this is averaged over an 8-day period (see Fig. 3.2, middle) (Myneni et al. 1997b). As the spring growing season begins around the world, emerging leaves will be quantified by increasing FPAR at each 1-km pixel. Conversely, at fall senescence or crop harvest, the FPAR will decline. Consequently, this FPAR will also provide a measure of continental phenology in addition to quantifying the vegetation canopy every 8 days for the NPP algorithm (White et al. 1997).

Climatology Inputs from the DAO

The NASA Data Assimilation Office (DAO), ingests all available surface weather observations globally every 3 hours. The DAO then interpolates and grids these point data, runs a short-time sequence global climate model, and produces surface climatic conditions at $1° \times 1°$ for the world. From this data output, the NPP algorithm retrieves

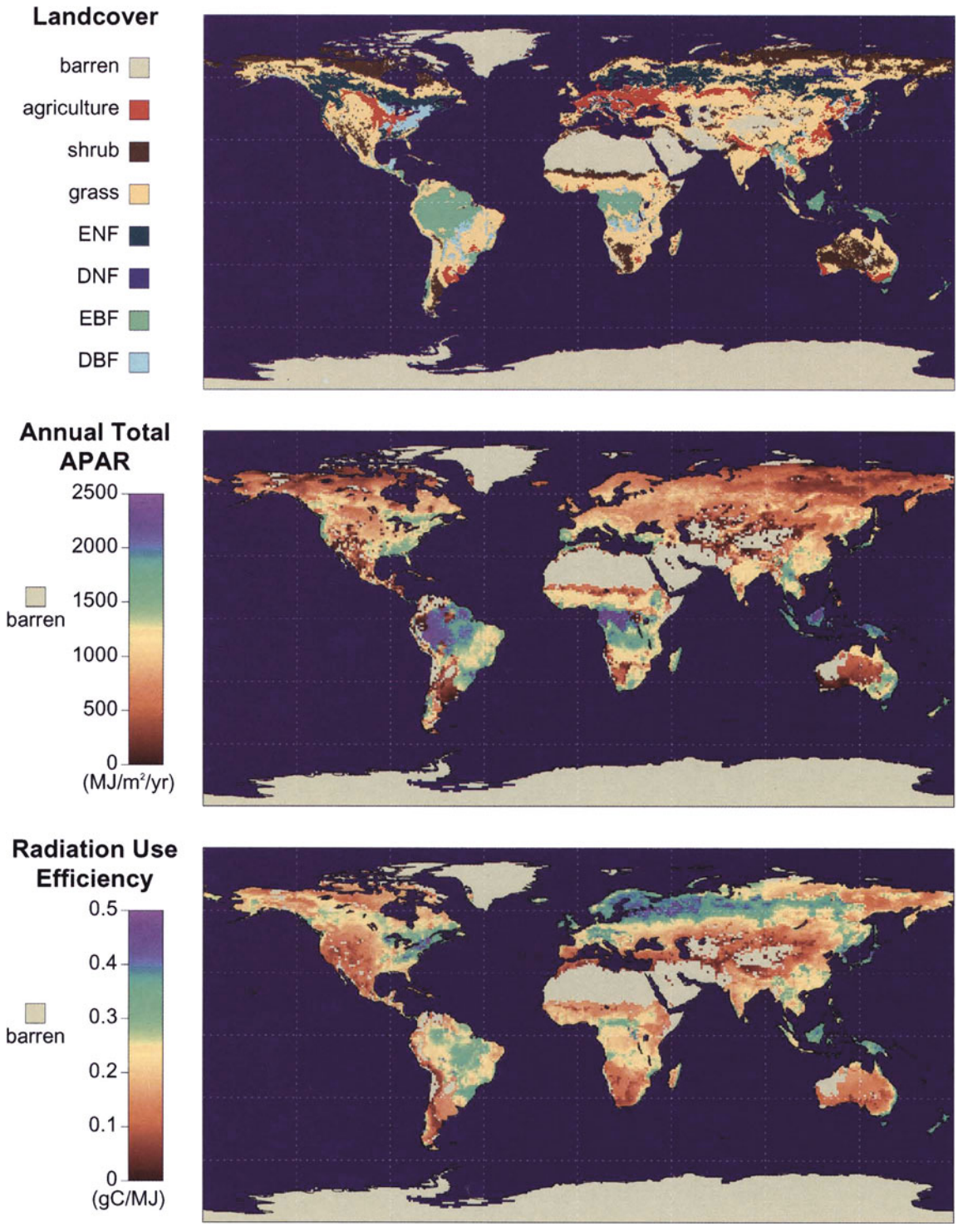

FIGURE 3.2. Example of the landcover (top), annual APAR (middle), and ϵ (bottom) global data inputs needed to compute the NPP algorithm.

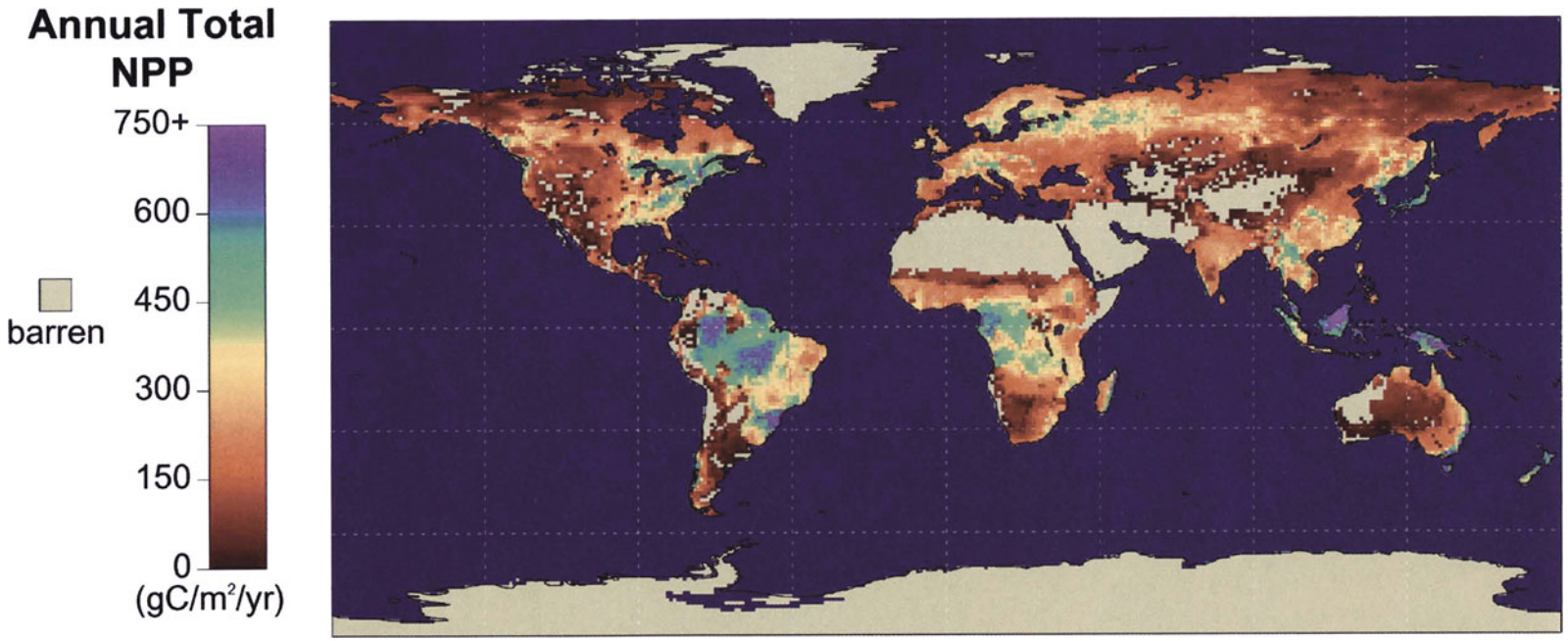

FIGURE 3.5. An example of the final global NPP that will be produced every 8 days at 1-km resolution by the Earth Observing System.

1. average 24-hour daily temperature (°C),
2. daily 24-hour minimum temperature (°C),
3. actual vapor pressure (derived from DAO specific humidity, in Pa units), and
4. incident shortwave solar radiation (MJ m^{-2} per 3-hr timestep).

These surface weather "observations" are then used in the final computation of the NPP algorithm by the EOS data system.

Final NPP Algorithm

Daily Estimation of GPP

The following steps are performed to calculate each day's intermediate GPP, subtract maintenance respiration (GPP − R_m), and accumulate NPP variables (Fig. 3.3).

1. A PAR conversion efficiency (ε) is first extracted from the global BPLUT in Table 3.1 for the appropriate pixel. This retrieved ε_{max} applied to a maximum value established for each vegetation (biome) type is attenuated by two controls. These controls are
   a. stomatal closure due to cold night temperature (TMIN) and
   b. stomatal control due to daytime vapor pressure deficit (VPD).
2. The simple daily GPP for the model day is then calculated as a function of net incident shortwave radiation, FPAR, and ε.
3. The daily maintenance respiration "costs" are then estimated, using a Q_{10} function from a 20°C base temperature. Next we calculate a cumulative daily term for estimating annual NPP:
4. To incrementally build the annual NPP term, we maintain a series of daily terms for each pixel, calculating the annual growth (for live wood, leaf, and roots), to appropriately take plant and root respiration into account.

The two parameters for TMIN and the two parameters for VPD are used to calculate two scalars that attenuate ε_{max} to produce the final ε used to predict GPP (see Fig. 3.2, bottom). These attenu-

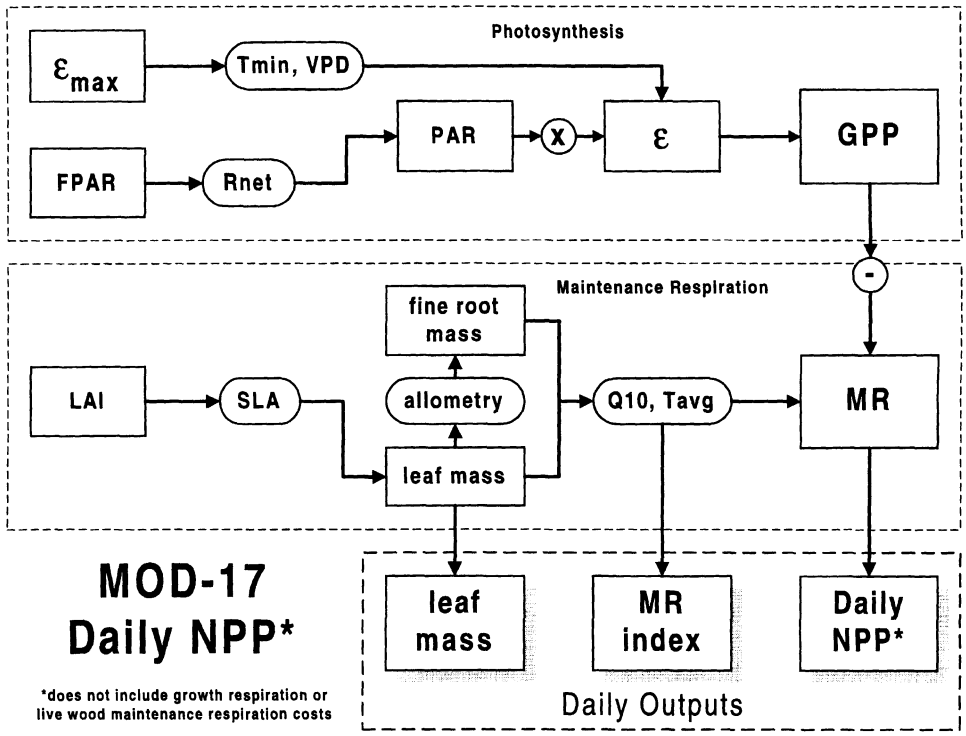

FIGURE 3.3. Logical and data flow diagram for the daily NPP algorithm.

ation scalars are simple linear ramp functions of daily TMIN and VPD. The estimate of maintenance respiration costs for leaves and fine roots is based on a standard exponential function of daily average air temperature (Sprugel et al. 1995; Ryan et al. 1997; Maier et al. 1998), scaled by the biomass of leaves and fine roots. We use the daily LAI from MODIS to estimate leaf mass, based on a specific leaf area (SLA) from Table 3.1. Fine root mass is assumed to be present in a constant ratio to leaf mass. The following parameters from Table 3.1 are required for these calculations: SLA, froot_leaf_ratio, leaf_mr_base, froot_mr_base, q10_mr.

Annual Estimation of NPP

Given outputs from the daily algorithm as specified in the previous section, the annual algorithm finishes the estimation of annual NPP by first estimating live woody tissue maintenance respiration, then estimating the growth respiration costs for leaves, fine roots, and woody tissue. Finally, these components are subtracted from the accumulated daily NPP* to produce the estimate of annual NPP (Fig. 3.4). The annual maximum leaf mass, as estimated from the output of daily leaf mass, is the primary input for estimates of both live wood maintenance respiration and whole-plant growth respiration. This approach relies on empirical studies relating annual growth of leaves to annual growth of other plant tissues (Cannell 1982). In addition to the annual maximum leaf mass, an estimate of leaf longevity (the inverse of leaf turnover rate) is required to predict the annual leaf growth for evergreen types. For deciduous types, leaf longevity is assumed to be less than one year, so the total leaf mass must be grown each year.

Growth respiration costs depend only on the amount of tissue grown and the type of tissue. Although our implementation of the annual algorithm leaves open the possibility of having different growth costs for different tissues, our current implementation uses the same growth cost per unit of new carbon in leaves, fine roots, live wood, and deadwood (Larcher, 1995). The annual algorithm

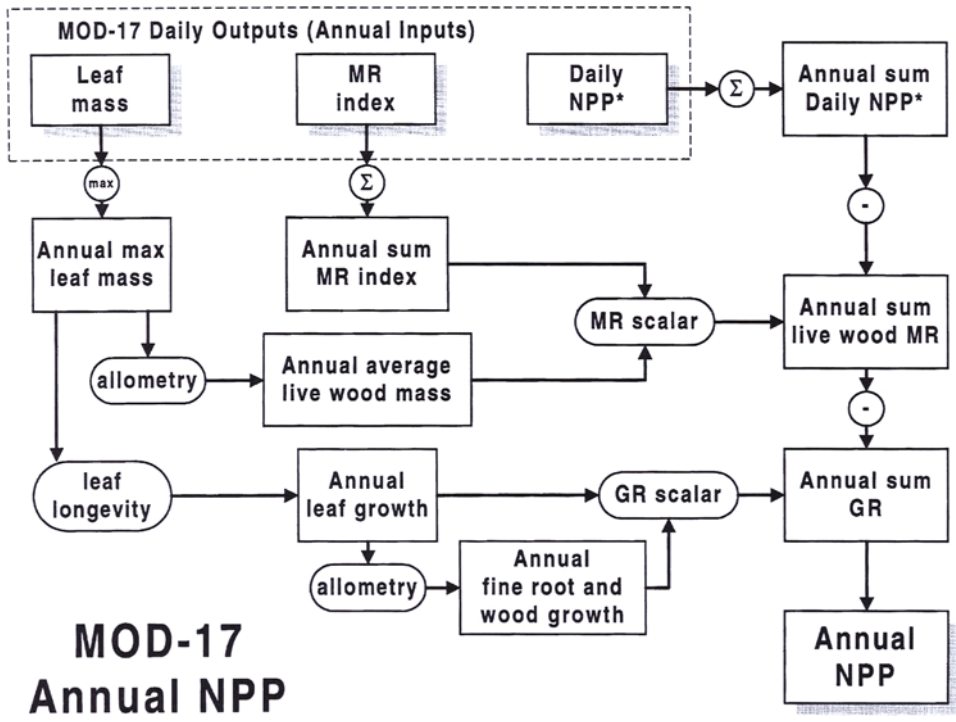

FIGURE 3.4. Logical and data flow diagram for the annual NPP algorithm.

uses maximum leaf mass and the leaf longevity to assess leaf growth respiration, and then uses empirical coefficients to relate annual leaf growth respiration costs to fine root, live wood, and deadwood growth respiration. These parameters are calculated directly from similar parameters used in the BIOME-BGC model.

Availability and Retrieval of Global NPP Data

The final global NPP computed every 8 days will generate a map similar to Figure 3.5, but at 1-km spatial resolution. The file to produce this global data set will be 1.4 GB in the standard EOS data format, but can be reduced substantially by translation to different resolution and projection. The official policy of EOS is that global data sets such as NPP will be available at no more than the cost of reproduction to the international scientific community. The NPP data set will be archived and distributed from a NASA-authorized data center (Justice et al. 1998). Within 2 days of the end of each 8-day computational period, current plans are that the new 8-day NPP will be available for ordering from an internet web site. The first EOS satellite was launched in December 1999, but these plans are yet to be activated.

Validation of Global NPP

No biophysical variable is directly measurable globally; consequently, none can be comprehensively validated. A number of techniques are being used to attempt a credible global validation of NPP but each has severe limitations. Collectively, the strategy is that a validation protocol can be assembled from these various components that provides confidence in global NPP.

In situ field measurements of NPP would seem to provide the most dependable validation, and a collection of published field NPP data is now being assembled for validation purposes (Scurlock et al. 1999). However, these field samples are usually measured on <1-ha areas, and for only one growing season. They do not quantify 150 million km^2 of land productivity adequately, or quantify year-to-year variations in productivity. The Global Terrestrial Observing System (GTOS) is initiating a plan to coordinate future international field sampling of NPP.

Another attempt at global validation has been to compare measured and simulated atmospheric CO_2 concentrations from the global flask network (Hunt et al. 1996; Randerson et al. 1997). In these analyses, a terrestrial carbon cycle model first computes

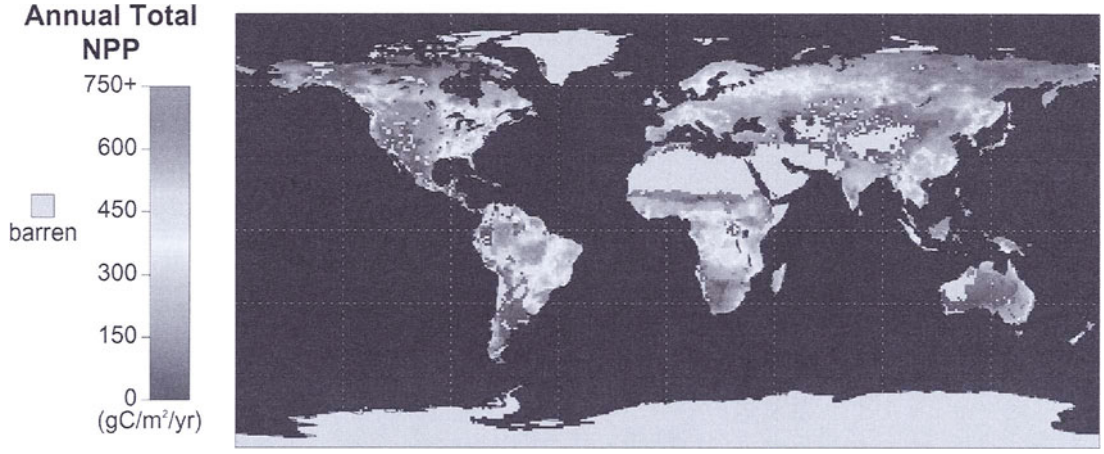

FIGURE 3.5. An example of the final global NPP that will be produced every 8 days at 1-km resolution by the Earth Observing System. *(See color plate.)*

daily CO_2 flux, which is then coupled to an atmospheric mixing model to transport the land surface fluxes into the atmosphere to match the flask sampling. This computation can be done for the few dozen sampling sites that exist around the world, providing some regional analysis of carbon source and sink dynamics that can be very revealing of biospheric dynamics (e.g., Keeling et al. 1996). Nemery et al. (1999) found that terrestrial biospheric models quantify northern hemisphere CO_2 seasonality adequately, but all models miss the southern hemisphere cycle, possibly because of poor representation of tropical rain-green phenology. Of course, atmospheric CO_2 is not vegetation production, so again this technique cannot directly validate NPP.

A new technique for large-scale carbon cycle validation incorporates eddy covariance flux towers that detect terrestrial CO_2 fluxes continuously (Baldocchi et al. 1996; Goulden et al. 1996). A coordinated network of 80 towers currently operates globally called FLUXNET, and CO_2 fluxes are measured year around. Again, these fluxes must be transformed into vegetation NPP to be a direct validation. The carbon allocation theory needed to transform a tower net ecosystem exchange (NEE) into aboveground NPP equivalent to the MODIS variable requires partitioning GPP into respiration and growth components, and separating soil heterotrophic respiration (Waring and Running 1998). Additionally, the towers only sample roughly 1 to 5 km^2 of land area, so spatial scaling procedures must be established to even approach a global analysis of NPP (Running et al. 1999). Nevertheless, these NEE data provide the highest precision and most temporally continuous carbon cycle measurements available (Kimball et al. 1997b).

The only way to generate complete coverage of NPP in both space and time is by model computations that incorporate some of these measurements. These global NPP models are initialized and operated with a variety of real measurements of the terrestrial biophysical system, but certainly cannot be called a direct validation. Some use regular satellite mapping of global LAI, most use global weather station data, and some use flux and/or isotopic data to define the ecosystem. These modeled NPP allow analyses that usually are not possible with individual field data. For example, the environmental space occupied by global NPP gives an opportunity to evaluate the general climatic controls on productivity (Fig. 3.6) (Churkina and Run-

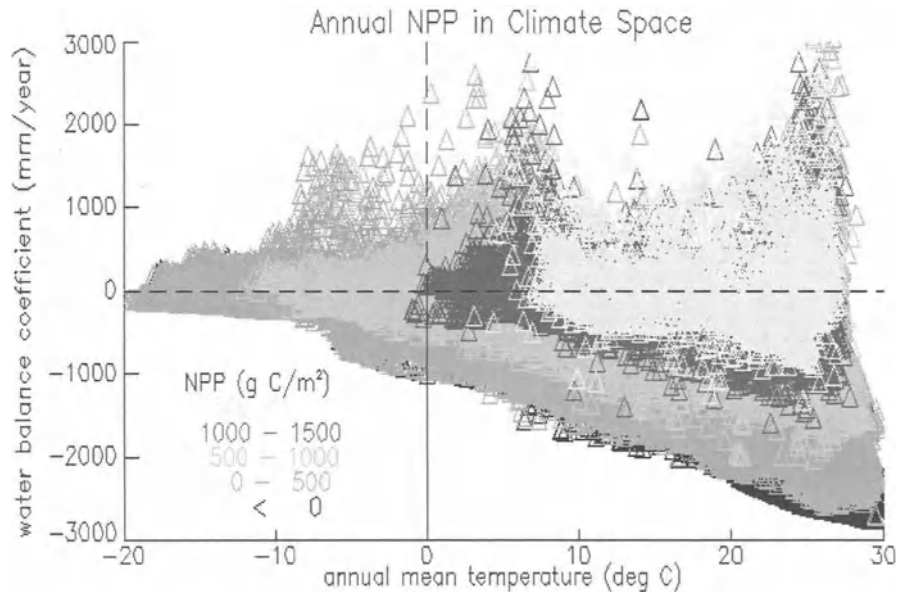

FIGURE 3.6. An analysis of global annual NPP in climate space, defined by annual temperature and water balance, to understand the range and limitation of NPP by climatic constraints. (From Churkina and Running [1998].)

ning 1998; Churkina et al. 1999). A formal intercomparison of 17 global NPP models was presented in a complete issue of *Global Change Biology* (Cramer and Field 1999). These intercomparisons help highlight our areas of greatest uncertainty in global NPP. For example, midsummer boreal forest and dry-season tropical evergreen forest NPP had the highest disagreement among models (Kicklighter et al. 1999). Schloss et al. (1999) found the greatest variability among models in areas that were simultaneously limited by both temperature and precipitation, and Churkina and Running (1998) estimated that 52% of global terrestrial area has NPP fundamentally limited by water availability. Bondeau et al. (1999) found greatest errors in tracking the rain-green phenology of subtropical savannas. Despite not being actual data, the models do give some critical insight into global-scale NPP variability and dynamics.

In the future, a combination of these techniques of measurements at various scales interpolated and extrapolated with ecosystem models will be required to determine the validity of the regular global NPP produced by EOS. More local validation activities will immediately be possible by extracting the local area from the global EOS NPP data set and comparing with any local measurements available (Running et al. 1999).

Summary

A near-weekly calculation of global terrestrial NPP driven by EOS satellite data began in 2000. This NPP will be computed for 150 million km^2 of the vegetated terrestrial surface of Earth. These data will be available for nominal cost to scientists worldwide, and should initiate a new era of more easily attainable spatially georeferenced biophysical information for landscape ecological study and management.

Acknowledgments This research was funded by the Earth Science Enterprise at NASA. As much of this work is in progress, updates on this global data availability will be available at http://www.forestry.umt.edu/ntsg.

References

Asrar, G.; Myneni, R.; Choudhury, B.J. Spatial heterogeneity in vegetation canopies and remote sensing of absorbed photosynthetically active radiation: A modeling study. Remote Sens. Environ. 41:85–103; 1992.

Baldocchi, D.; Valentini, R.; Running, S.W.; Oechel, W.; Dahlman, R. Strategies for measuring and modelling carbon dioxide and water vapor fluxes over terrestrial ecosystems. Global Change Biol. 2:159–168; 1996.

Bondeau, A.; Kicklighter, J.; Kaduk, J.; and participants of the Potsdam NPP Model Intercomparison. Comparing global models of terrestrial net primary productivity (NPP): Importance of vegetation structure on seasonal NPP estimates. Global Change Biology 5:35–45; 1999.

Cannell, M.G.R. *World Forest Biomass and Primary Production Data.* London: Academic; 1982.

Churkina, G.; Running, S.W. Contrasting climatic controls on the estimated productivity of different biomes. Ecosystems 1:206–215; 1998.

Churkina, G.; Running, S.W.; Schloss, A.L.; PIK-NPP Participants. Comparing global models of terrestrial net primary productivity (NPP): The importance of water availability. Global Change Biol. 5:46–55; 1999.

Ciais, P., Tans, P.P., Trolier, M., White, J.W.C., and Francey, R.J. A large northern hemisphere terrestrial CO_2 sink indicated by $^{13}C/^{12}C$ of atmospheric CO_2. Science 269:1098–1102; 1995.

Cramer, W.; Field, C.B. Comparing global models of terrestrial net primary productivity (NPP): Introduction. Global Change Biol. 5:iii–iv; 1999.

DeFries, R.S.; Townshend, J.R.G.; Hansen, M.C. Continuous fields of vegetation characteristics at the global scale at 1 km resolution. J. Geophys. Res. Atmos. 104(D14):16911–16924; 1999.

Field, C.B.; Behrenfeld, M.J.; Randerson, J.T.; Falkowski, P. Primary production of the biosphere: Integrating terrestrial and oceanic components. Science 281:237–240; 1998.

Field, C.B.; Randerson, J.T.; Malmstrom, C.M. Global net primary production: Combining ecology and remote sensing. Remote Sens. Environ. 51:74–88; 1995.

Goulden, M.L., Munger, J.W., Fan, S-M., Daube, B.C., and Wofsy, S.C. Exchange of carbon dioxide by a deciduous forest: Response to interannual climate variability. Science 271:1576–1578; 1996.

DeFries, R.S.; Hansen, M.C.; Townshend, J.R.G.; Sohlberg, R. Global land cover classification at 8 km spatial resolution: the use of training data derived from Landsat imagery in decision tree classifiers. Internat. J. Remote Sens. 19(16):3141–3168.

Hudson, R.J.M.; Gherini, S.A.; Goldstein, R.A. Modeling the global carbon cycle: Nitrogen fertilization of the terrestrial biosphere and the "missing" CO_2 sink. Global Biogeochem. Cycl. 8(3):307–333; 1994.

Hunt, E.R., Jr. Relationship between woody biomass and PAR conversion efficiency for estimating net primary production from NDVI. Internat. J. Remote Sens. 15:1725–1730; 1994.

Hunt, E.R., Jr., Piper, S.C.; Nemani, R.R.; Keeling, C.D.; Otto, R.D.; Running, S.W. Global net carbon exchange and intra-annual atmospheric CO_2 concentrations predicted by an ecosystem process model and three-dimensional atmospheric transport model. Global Biogeochem. Cycl. 10:431–456; 1996.

Justice, C.O.; Running, S.W.; et al. The Moderate Resolution Imaging Spectroradiometer (MODIS): Land remote sensing for global change research. IEEE Trans. Geosci. Remote Sens. 36(4):1228–1249; 1998.

Keeling, C.D.; Chin, J.F.S.; Whorf, T.P. Increased activity of northern vegetation inferred from atmospheric CO_2 measurements. Nature 382:146–149; 1996.

Kicklighter, D.W.; Bondeau, A.; Schloss, A.L.; Kaduk, J.; McGuire, A.D.; and participants of the Potsdam NPP Model Intercomparison. Comparing global models of terrestrial net primary productivity (NPP): Global pattern and differentiation by major biomes. Global Change Biol. 5:16–24; 1999.

Kimball, J.; Running, S.W.; Nemani, R.R. An improved method for estimating surface humidity from daily minimum temperature. Agric. For. Meteorol. 85:87–98; 1997a.

Kimball, J.S.; Thornton, P.E.; White, M.A.; Running, S.W. Simulating forest productivity and surface-atmosphere carbon exchange in the BOREAS study region. Tree Physiol. 17:589–599; 1997b.

Kimball, J.S.; White, M.A.; Running, S.W. BIOME-BGC simulations of stand hydrologic processes for BOREAS. J. Geophys. Res. 102(D24):29043–29051: 1997c.

Landsberg, J.J.; Prince, S.D.; Jarvis, P.G.; McMurtrie, R.E.; Luxmoore, R.; Medlyn, B.E. Energy conversion and use in forests: The analysis of forest production in terms of radiation utilization efficiency. In: Gholz, H.L.; Nakane, K., eds. *The Use of Remote Sensing in the Modeling of Forest Productivity at Scales from the Stand to the Globe.* London: Kluwer; 1996.

Larcher, W. *Physiological Plant Ecology.* Springer-Verlag, Berlin; 1995.

Maier, C.A.; Zarnoch, S.J.; Dougherty, P.M. Effects of temperature and tissue nitrogen on dormant season stem and branch maintenance respiration in a young loblolly pine (*Pinus taeda*) plantation. Tree Physiol. 18:11–20; 1998.

Melillo, J.M.; McGuire, A.D.; Kicklighter, D.W.; Moore, B., III; Vorosmarty, C.J.; Schloss, A.L. Global climate change and terrestrial net primary production. Nature 363:234–240; 1993.

Monteith, J.L. Solar radiation and productivity in tropical ecosystems. J. Appl. Ecol. 9:747–766; 1972.

Monteith, J.L. Climate and the efficiency of crop production in Britain. Philosoph. Trans. R Soc. Lond. 281:277–294; 1977.

Myneni, R.B.; Keeling, C.D.; Tucker, C.J.; Asrar, G.; Nemani, R.R. Increased plant growth in the northern high latitudes between 1981–1991. Nature 386:698–702; 1997a.

Myneni, R.B.; Nemani, R.R.; Running, S.W. Estimation of global LAI and FPAR from radiative transfer models. IEEE Trans. Geosci. Remote Sens. 35:1380–1393; 1997b.

Nemani, R.R.; Running, S.W. Testing a theoretical climate-soil-leaf area hydrologic equilibrium of forests using satellite data and ecosystem simulation. Agric. For. Meteorol. 44:245–260; 1989.

Nemani, R.R.; Running, S.W. Implementation of a hierarchical global vegetation classification in ecosystem function models. J. Vegetat. Sci. 7:337–346; 1996.

Nemani, R.R.; Running, S.W. Land cover characterization using multi-temporal red, NIR and thermal-IR AVHRR data. Ecol. Applic. 7:79–90; 1997.

Nemery, B.; Francois, L.; Gerard, J.C.; Bondeau, A.; Heimann, H.; and participants of the Potsdam NPP Model Intercomparison. Comparing global models of terrestrial net primary productivity (NPP): Analysis of the seasonal atmospheric CO_2 signal. Global Change Biol. 5:65–76; 1999.

Piper, S.C.; Stewart, E.F. A gridded global data set of daily temperature and precipitation for terrestrial biospheric modeling. Global Biogeochem. Cycl. 10:757–782; 1996.

Prince, S.D. A model of regional primary production for use with coarse resolution satellite data. Internat. J. Remote Sens. 12:1313–1330; 1991.

Prince, S.D.; Goward, S.N. Global primary production: A remote sensing approach. J. Biogeogr. 22:815–835; 1995.

Randerson, J.T.; Thompson, M.V.; Conway, T.J.; Fung, I.Y.; Field, C.B. The contribution of terrestrial sources and sinks to trends in the seasonal cycle of atmospheric carbon dioxide. Global Biogeochem. Cycl. 11:535–560; 1997.

Ruimy, A.; Saugier, B. Methodology for the estimation of terrestrial net primary production from remotely sensed data. J. Geophys. Res. 99:5263–5283; 1994.

Running, S.W.; Baldocchi, D.D.; Turner, D.P.; Gower, S.T.; Bakwin, P.S.; Hibbard, K.A. A global terrestrial monitoring network integrating tower fluxes, flask sampling, ecosystem modeling and EOS satellite data. Remote Sens. Environ. 70(1):108–127; 1999.

Running, S.W.; Gower, S.T. FOREST-BGC, A general model of forest ecosystem processes for regional applications. II. Dynamic carbon allocation and nitrogen budgets. Tree Physiol. 9:147–160; 1991.

Running, S.W.; Hunt, Jr., E.R. Generalization of a forest ecosystem process model for other biomes, BIOME-BGC, and an application for global-scale models. In: Ehleringer, J.R.; Field, C., eds. *Scaling Physiological Processes: Leaf to Globe.* Orlando, FL: Academic; 1993.

Running, S.W.; Justice, C.; Salomonson, V.; Hall, D.; Barker, J.; Kaufmann, Y.; Strahler, A.; Huete, A.; Muller, J.P.; Vanderbilt, V.; Wan, Z.M.; Teillet, P.; Carneggie, D. Terrestrial remote sensing science and algorithms planned from EOS/MODIS. Internat. J. Remote Sens. 15:358–3620; 1994.

Running, S.W.; Loveland, T.R.; Pierce, L.L.; Nemani, R.R.; Hunt Jr., E.R. A remote sensing based vegetation classification logic for global land cover analysis. Remote Sens. Environ. 51:39–48; 1995.

Ryan, M.G.; Binkley, D.; Fownes, J.H. Age-related decline in forest productivity: Pattern and Process. Adv. Ecol. Res. 27:213–261; 1997.

Schloss, A.L.; Kicklighter, D.W.; Kaduk, J.; Wittenberg, U.; and the participants of the Potsdam NPP Model Intercomparison. Comparing global models of terrestrial net primary productivity (NPP): Comparison of NPP to climate and the Normalized Difference Vegetation Index (NDVI). Global Change Biol. 5:25–34; 1999.

Schulze, E.D.; Kelliher, F.M.; Korner, C.; Loyd, J.; Leuing, R. Relationships among maximum stomatal conductance, ecosystem surface conductance, carbon assimilation rate and plant nitrogen nutrition. Annu. Rev. Ecol. Syst. 25:629–660; 1994.

Scurlock, J.M.O.; Cramer, W.; Olson, R.J.; Parton, W.J.; Prince, S.D. Terrestrial NPP: Towards a consistent data set for global model evaluation. Ecol. Applic. 9(3):913–919; 1999.

Sellers, P.J. Canopy reflectance, photosynthesis and transpiration. II. The role of biophysics in the linearity of their interdependence. Remote Sens. Environ. 21:143–183; 1987.

Sprugel, D.G.; Ryan, M.G.; Brooks, J.R.; Vogt, K.A.; Martin, T.A. Respiration from the organ level to stand level. In Smith, W.K.; Hinkley, T.M., eds. *Resource Physiology of Conifers.* San Diego, CA: Academic; 1995:255–299.

Tans, P.P.; Fung, I.Y.; Takahashi, T. Observational constraints on the global atmospheric CO_2 budget. Science 247:1431–1438; 1990.

Thornton, P.E.; Running, S.W. An improved algorithm for estimating incident daily solar radiation from measurements of temperature, humidity, and precipitation. Agric. For. Meteorol. 93:211–228; 1999.

VEMAP [Vegetation/Ecosystem Modeling and Analysis Project] Members. Comparing biogeography and biogeochemistry models in a continental scale study of terrestrial ecosystem responses to climate change and CO_2 doubling. Global Biogeochem. Cycl. 9:407–437; 1995.

Waring, R.H.; Law, B.; et al. Scaling gross ecosystem production at Harvard Forest with remote sensing: A comparison of estimates from a constrained quantum-use efficiency model and eddy correlation. Plant Cell Environ. 18:1201–1213; 1995.

Waring, R.; Running, S.W. *Forest Ecosystems: Analysis at Multiple Scales.* San Diego, CA: Academic; 1998.

White, M.E.; Thornton, P.E.; Running, S.W. A continental phenology model for monitoring vegetation responses to inter-annual climatic variability. Global Biogeochem. Cycl. 11(2):217–234; 1997.

Zobler, L.A. *A World Soil File for Global Climate Modeling.* Tech. Memo. 87802. U.S. National Aeronautics and Space Administration (NASA), Greenbelt, MD; 1986.

4

Methods of Estimating Belowground Net Primary Production

William K. Lauenroth

Introduction

Despite much recent attention over the past 30 years, belowground net primary production (BNPP) remains one of the poorest understood attributes of terrestrial ecosystems (Milchunas and Lauenroth 1992; Nadelhoffer and Raich 1992). Estimates of the ratio of BNPP to net primary production (NPP) across ecosystem types range from less than 0.20 to more than 0.80 (Bray 1963, Coleman 1976). Part of this range can be explained by differences among ecosystems, but a portion of it is the result of differences among methods. For instance, Aber et al. (1985) reported ratios of fine root production by two different methods for the same sites ranging from close to 1 to more than 10. In addition to a wide range of estimates of the importance of BNPP across ecosystem types, estimates within ecosystems also vary widely. For instance, Sims and Singh (1978) found that BNPP accounted for 24 to 87% of NPP over a range of grassland ecosystems and Vogt (1991) reported that fine root production accounted for 7 to 76% of NPP over a range of forest ecosystems. How much of this variability is the result of differences among ecosystems and how much is the result of differences among methods? While there is no agreement on the answer to this question, there is abundant evidence that all of the current methods have important strengths and limitations. The objective of this chapter is to describe the most frequently used methods to estimate BNPP and their strengths and weaknesses. The first section provides definitions of terms and descriptions of concepts. The next section describes the methods, comments on their strengths and weaknesses, and provides references in which they have been applied. The last section evaluates the degree to which uncertainty (variability) in input data influences the uncertainty of the resulting estimate of BNPP.

Concepts

Belowground net primary production is not a directly observable characteristic of an ecosystem. One cannot go to the field and in a strict sense measure BNPP. Consequently, approaches to assessing BNPP consist of a collection of methods to approximate the amount of biomass or carbon that gets assimilated belowground over a particular interval. Each method consists of a technique to collect the relevant information in the field and an assumed mathematical relationship between the variable(s) sampled in the field and BNPP.

Conceptually, BNPP during the interval from $t = 1$ to $t = 2$ is:

$$BNPP = \Delta B + \Delta H + \Delta E + \Delta D \quad (4.1)$$

where ΔB is the change in belowground biomass between $t = 1$ and $t = 2$, ΔH is the amount of biomass consumed by herbivores, ΔE is the amount of biomass lost to exudation and sloughing, and ΔD is the amount of biomass lost to death and detachment—all during the interval between $t = 1$ and $t = 2$. The most common time interval encountered in the literature for estimates of BNPP is a year. The most frequently encountered quantities are annual BNPP (grasslands) or annual net

fine root production (NFRP) (forests and shrublands). In ecosystems dominated by herbaceous plants, it is possible to assess BNPP (all belowground plant organs) because of the lack of large woody roots. In ecosystems dominated by woody plants, effectively all of the data are for NFRP because of the difficulties associated with estimating the increment to large woody roots. Fine roots (<3 mm in diameter) represent the most dynamic component of the root systems of woody plants (Hendrick and Pregitzer 1992) and a large fraction of the annual carbon balance of ecosystems dominated by woody plants (Nadelhoffer and Raich 1992). The relationship between NFRP and BNPP is unknown. Unless stated otherwise, all further references in this chapter to either BNPP or NFRP will assume an annual time scale. Furthermore, I will use BNPP as a generic term to refer to both belowground net primary production and net fine root production. I will use NFRP when I specifically mean net fine root production.

Estimating BNPP requires, at the minimum, an estimate of ΔB from Equation 4.1. Many of the differences among methods are related to how ΔB is determined. None of the methods deals explicitly with herbivory (H) and therefore it represents a source of underestimation except for the carbon isotope turnover method in which it is lumped with decomposition as a portion of total loss. Although there is evidence that belowground herbivory is large and on the same order as aboveground herbivory, very few data exist (Lauenroth and Milchunas 1992). Exudation and sloughing (E) are likewise ignored by all methods except carbon isotope turnover (Milchunas and Lauenroth 1992). Estimates from field and laboratory experiments suggest that, at least in grasslands, E can account for a measurable loss from BNPP (Milchunas et al. 1985; Milchunas and Lauenroth 1992). Death and detachment (D) have received considerable attention in methods for aboveground NPP (ANPP) (Wiegert and Evans 1964; Long et al. 1989), but they are ignored in methods for BNPP, except those using minirhizotrons, and represent a loss of unknown magnitude. Death and detachment losses are thought to be large for estimates of ANPP from ecosystems dominated by herbaceous plants, especially those in tropical climates (Long et al. 1989, 1992).

Methods

Biomass

The majority of the estimates of BNPP in the literature have been calculated from data that were collected by directly sampling belowground biomass (Milchunas and Lauenroth 1992; Nadelhoffer and Raich 1992; Publicover and Vogt 1993). This process involves two steps at which the decisions that are made have a large influence on the resulting estimate of BNPP. The first step involves a decision about when to sample and how to collect and process the samples. The decision about when and how often to sample will be influenced by the specific characteristics of the ecosystem and project objectives. Some of the complications involved with sampling frequency are discussed in Chapter 2 with respect to ANPP. The issues are directly applicable to BNPP as well and therefore do not need to be repeated here. The most common sampling procedures involve collecting volumetric soil samples using either a coring device or an auger (Böhm 1979[1]). The samples are then processes by sieving and flotation after which the resulting organic material is dried and weighed (Lauenroth and Whitman 1971; Böhm 1979; Smucker et al. 1982). In some cases, the organic material is sorted into categories such as live roots and dead roots (e.g., Aerts et al. 1989; McClaugherty et al. 1982; Hook et al. 1994), although there is considerable uncertainty associated with such separations (Böhm 1979). Another controversial topic has been whether there is a need to correct the organic matter values for ash content. High ash contents (≥50%) and high sample-to-sample variability argue for the need for such corrections (Böhm 1979).

The second step involves a decision about how the biomass data will be used to calculate BNPP (Singh et al. 1984). While there are a large number of possibilities (Singh et al. 1984), there are two common methods of calculation. The first is to subtract the annual minimum in root biomass from the annual maximum (max-min method); the second is to calculate differences in biomass between each pair of sample dates and sum the positive changes (Dahlman and Kucera 1965; Lauenroth and Whit-

[1]This small book is the authoritative reference on collection and processing root biomass samples.

man 1977; Persson 1978; Singh et al. 1984). Calculations using belowground biomass data are illustrated in Table 4.1.

Biomass methods are appealing because they directly assess the variable of interest, belowground plant biomass. The limitations of the methods can be categorized by whether they are related to the collection and preparation of the biomass samples or whether they are related to how the data are used in the calculations of BNPP. However, in most cases, the two categories of limitations interact. Our inability to distinguish roots of different species and the lack of reliable methods to separate live and dead roots influence all methods of estimating BNPP, including those using biomass. The inability to separate root biomass by species means that it is not possible to account for differences in phenology among species. If species reach their peaks in root biomass at different times during the growing season, the influence of these differences on BNPP will be missed. The lack of reliable methods to separate live and dead roots either introduces an additional source of variability (inexact separation) or means that the temporal dynamics of belowground biomass will be heavily influenced by the large amount of dead roots in most ecosystems. This can lead to large sensitivity of estimates to random errors (Singh et al. 1984; Kurtz and Kimmins 1987; Milchunas and Lauenroth 1992; Publicover and Vogt 1993). If only positive changes in biomass are included in the calculation of BNPP, the result will have a positive bias (Persson 1978; Sala et al. 1988).

Because biomass methods are so widely used, the issue of their limitations has received considerable attention (Singh et al. 1984; Aber et al. 1985; Kurtz and Kimmins 1987; Santantonio and Grace 1987; Milchunas and Lauenroth 1992; Nadelhoffer and Raich 1992; Neill 1992; Publicover and Vogt 1993; Burke and Raynal 1994). Most of this work has focused on comparison of estimates by different methods or analysis of deviations of the estimates of BNPP from a known or theoretical value for BNPP. The major message from all of this work is that estimates of BNPP based upon biomass methods have substantial limitations with well-identified conceptual inaccuracies. Many of the alternative methods were developed as a result of dissatisfaction with biomass methods.

TABLE 4.1 Example calculations of BNPP using belowground biomass data. Biomass data were estimated from Figure 2, page 512, in Persson (1978). Both live-root strata from the original data were combined and only data from 1974 were used.

Approximate date		Biomass ($g\ m^{-2}$)	$Biomass_{t+1} - Biomass_t$
May	1	149	
	15	104	−45
June	5	130	26
	15	171	41
July	3	100	−71
	15	108	8
August	5	141	33
	10	153	12
September	1	194	41
	15	82	−112
October	10	189	107
November	1	156	−33

The maximum-minimum method involves finding the maximum and minimum values of root biomass in the data set and subtracting them to obtain an estimate of BNPP:

$$BNPP\ (g\ m^{-2}) = 194 - 82 = 112$$

The summation of positive changes method involves comparing each pair and summing only the differences that are positive. This method introduces a positive bias in the calculated values of BNPP (Persson 1978, Sala et al. 1988).

$$BNPP\ (g\ m^{-2}) = 26 + 41 + 8 + 33 + 12 + 41 + 107 = 268$$

Ingrowth Cores

This method consists of removing the roots from a volume of soil and monitoring the regrowth of roots (Jordan and Escalante 1980; Persson 1983, Neill 1992). Operationally, cores are removed from the soil and all of the roots are either sieved or hand picked from the sample. The root-free soil is then placed in a mesh bag and returned to the hole from which it came. After a period of time, the mesh bag is removed from the soil and the roots are again separated from the soil. This second sample of root biomass is an estimate of the amount of root biomass produced during the interval (see Jordan and Escalante [1980] for a variant on this method). The choices that the researcher has to make that influence the estimate of BNPP are the size, depth, number, and frequency of collection of the ingrowth cores.

Jordan and Escalante (1980) compared six different ingrowth methods in a tropical rainforest and found that estimates of biomass accumulation were similar among methods. Persson (1979, 1983) and Neill (1992) found that estimates of BNPP by ingrowth cores were similar to those produced by a biomass method. Limitations of ingrowth methods include the stimulation or depression of root growth caused by collecting the initial root core, inability to deal with simultaneous growth and death or herbivory, and the different conditions associated with roots growing into root-free soil (Neill 1992).

Isotopes

Although radioactive isotopes have been used in several ways in root studies, the only isotope that has been used to estimate BNPP is carbon = 14 (^{14}C) (Dahlman and Kucera 1967; Caldwell and Camp 1974; Milchunas et al. 1985; Milchunas and Lauenroth 1992). The assumption implicit in this method is that by exposing the photosynthetically active tissue of a plant or group of plants to an atmosphere containing $^{14}CO_2$, a portion of the ^{14}C that is translocated to the roots will be incorporated into structural root tissue (Fig. 4.1).

Caldwell and Camp (1974) used ^{14}C dilution to estimate BNPP. This consisted of a pulse labeling of the vegetation to establish a $^{14}C/^{12}C$ ratio followed by sampling to detect changes in the ratio. A key assumption of this method is that following the pulse labeling, only ^{12}C is added to the root system. A turnover coefficient (TC) was calculated as:

$$TC = \frac{^{14}C_{t1}/^{12}C_{t1}}{^{14}C_{t2}/^{12}C_{t2}} - 1 \qquad (4.2)$$

The ^{14}C dilution method requires that sampling not begin until the labile pool of ^{14}C has all been incorporated into structural tissue (see Fig. 4.1). Milchunas et al. (1985) tested the method using seedlings grown in pots and found that the amount of time necessary for all of the labile ^{14}C to be incorporated into structural tissue was considerably longer than the 5 days recommended by Caldwell and Camp (1974). Once the values were corrected for labile ^{14}C, Milchunas et al. (1985) found very good agreement between actual production and the estimate by ^{14}C dilution.

Milchunas and Lauenroth (1992) were unable to obtain estimates of BNPP using the ^{14}C dilution method in a field experiment, which they attributed

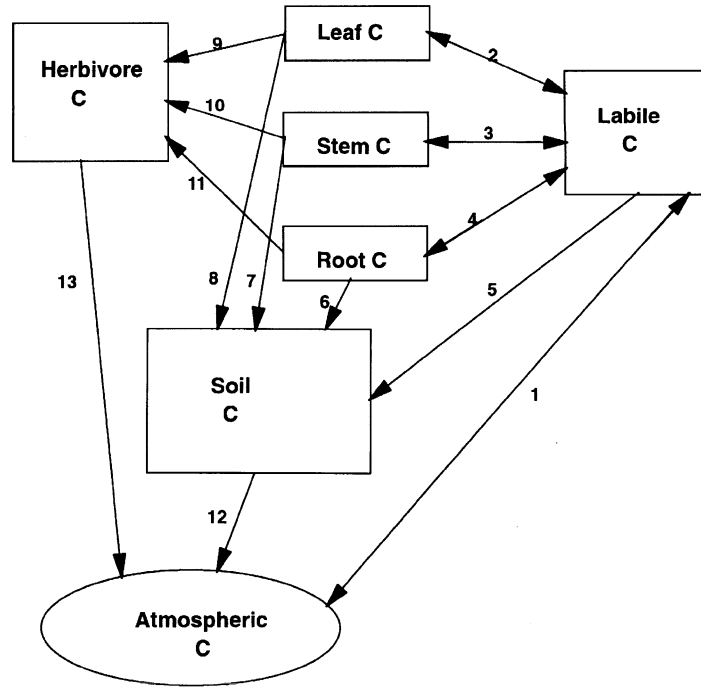

FIGURE 4.1. Diagram of the carbon (C) budget of a plant or a collection of plants in an ecosystem. 1, Photosynthesis and respiration; 2, translocation of labile carbon compounds to and from leaves; 3, translocation of labile carbon compounds to and from stems; 4, translocation of labile carbon compounds to and from roots; 5, loss of labile carbon directly to the soil via leaching or exudation; 6, transfer of root litter to the soil; 7, transfer of stem litter to the soil; 8, transfer of leaf litter to the soil; 9, consumption of leaves by herbivores; 10, consumption of stems by herbivores; 11, consumption of roots by herbivores; 12, decomposition; and 13, herbivore respiration.

to differential herbivory and decomposition of ^{14}C compared with ^{12}C. They subsequently adopted a ^{14}C turnover method first described by Dahlman and Kucera (1967). This method is similar to the ^{14}C dilution method in that it requires an initial pulse labeling. The decrease in ^{14}C in the root system is then followed for a period sufficient to describe the rate of loss. After 2 years, Dahlman and Kucera (1967) fit a linear regression to their loss data and concluded that the root system would turn over every 4 years. Milchunas and Lauenroth (1992) fit a linear regression to their loss data after 3 years and estimated that the root system would turn over every 5 to 7 years. In addition to information about the dynamics of ^{14}C in the root system, the carbon isotope methods require an estimate of belowground biomass. The turnover coefficient calculated from the tracer data is multiplied by the biomass data to obtain an estimate of BNPP.

Dahlman and Kucera (1965, 1967) estimated root turnover using biomass methods and ^{14}C turnover and found good agreement between the two methods. Milchunas and Lauenroth (1992) calculated both ANPP and BNPP using the ^{14}C turnover method and found excellent agreement between the estimate for ANPP using ^{14}C turnover and an estimate based upon biomass. Milchunas and Lauenroth (1992) interpreted this agreement as support for the use of ^{14}C turnover to estimate BNPP. The limitations of the ^{14}C turnover method are largely related to the difficulty of introducing the label and working with radioactive materials. The requirement to be able to label the vegetation limits the applicability to ecosystems dominated by short-statured plants, such as grasslands and shrublands. Use of ^{13}C would solve the radioactive materials problem, but it is substantially more expensive than ^{14}C. This is an excellent method for grasslands and shrublands if the problems with the labeled material can be resolved.

Carbon Balance

This and the following method using nitrogen balance exploit knowledge about element budgets to estimate BNPP. The carbon balance method uses the law of conservation of mass to derive the following conceptual model (Nadlehoffer et al. 1998):

$$TRCA \approx R_s - P_a + E + \Delta C_r - \Delta C_s \quad (4.3)$$

where *TRCA* is total root carbon allocation, R_s is soil respiration, P_a is aboveground litterfall, E is export as a result of leaching or erosion, ΔC_r is the change in root carbon (coarse + fine), and ΔC_s is the change in soil carbon. Site-specific application of the method relies on estimates of R_s and P_a and either measurements of E, ΔC_r and ΔC_s, or an assumption of steady state (Binkley and Ryan 1998).

Raich and Nadlehoffer (1989) developed a statistical model for ecosystems at or near steady state by assuming that:

$$R_h \approx P_a + P_b \quad (4.4)$$

where R_h is heterotrophic respiration and P_b is belowground litter production. Recognizing that soil respiration comprises both root (R_r) and heterotrophic respiration, estimates of *TRCA* ($P_b + R_r$) can be calculated by the relationship:

$$P_b + R_r \approx R_s - P_a \quad (4.5)$$

This relationship effectively shifts the problem of estimating BNPP from estimating the change in belowground plant biomass to estimating aboveground litter production (see Chapter 2) and soil respiration (Chapter 7). Both P_a and R_s have been measured for many ecosystems, and Raich and Nadelhoffer (1989) reported significant regressions between P_a and R_s ($r^2 = 0.71$) and between TRCA and P_a ($r^2 = 0.52$). Their final statistical model is

$$TRCA = 1.92\ P_a - 130 \quad (4.6)$$

Accepting these relationships further reduces the problem of estimating BNPP to one of only estimating aboveground litter production (P_a).

Raich and Nadelhoffer (1989) suggested that their relationships were useful to place an upper constraint on the amount of carbon allocated to roots (for tissue production and respiration), and therefore NFRP, and Nadelhoffer and Raich (1992) recommended that estimates of NFRP always be compared with TRCA. They also warned that the large scale of their analysis may have overlooked important smaller-scale variability (Raich and Nadelhoffer 1989) and seasonal and yearly variability within sites (Nadelhoffer and Raich 1992). Gower et al. (1996) tested the utility of the Raich and Nadelhoffer (1989) statistical model to estimate TRCA and NFRP at a range of temperate forest sites and concluded that it should not be used at the individual site scale. In a rejoinder to the Gower et

al. (1996) analysis, Nadlehoffer et al. (1998) argued that the Gower et al. (1996) analysis was largely inappropriate and added no new information to the question of the applicability the TRCA method. Smith and Resh (1999) successfully applied the conceptual (not the statistical) TRCA approach to a group of stands to evaluate whether increasing allocation to BNPP as forests age would provide an explanation for the widely observed decline in ANPP with increasing age. They were able to reject the increasing belowground allocation hypothesis as a single explanation for the decline in ANPP, suggesting that a detailed carbon budget evaluation can provided useful information in an analysis of BNPP and NFRP.

Nitrogen Balance

This method assumes that all available nitrogen is taken up by plants and allocated to either aboveground litter, woody tissue, or fine roots (Aber et al. 1985; Nadelhoffer et al. 1985; see also Chapter 16). The amount of nitrogen allocated to fine roots is:

$$N_{fr} = N_a - N_w - N_{al} \tag{4.7}$$

where N_{fr} is the amount of nitrogen allocated to fine roots, N_a is available nitrogen, N_w is nitrogen allocated to woody tissue, and N_{al} is nitrogen allocated to aboveground litter. NFRP is then calculated by:

$$NFRP = \frac{N_{fr}}{N_{conc}} \tag{4.8}$$

where N_{conc} is the concentration of nitrogen in fine roots. This method transforms the problem of estimating BNPP from a focus on changes in root biomass to a focus on annual nitrogen availability (see Chapter 14) and the amounts of nitrogen allocated to aboveground litter and to wood (see Chapters 2 and 16). Available nitrogen is calculated using the following assumption:

$$N_a = N_m + N_p - N_l \tag{4.9}$$

where N_m is measured nitrogen mineralization (see Chapter 14), N_p is the amount of nitrogen received in precipitation (see Chapter 17) and N_l is the amount of nitrogen lost to leaching (see Chapter 16). A sample calculation is illustrated in Table 4.2.

This method has not been widely used. Aber et al. (1985) compared the nitrogen balance method to a biomass method and concluded that for stands with low nitrification the two methods compared very well. For stands with high nitrification, Aber et al. (1985) suggested that the larger estimates of NFRP from the nitrogen balance method were better estimates than those from the biomass method. The limitations of this method are related to the assumptions that it makes about nitrogen allocation and the accuracy of estimates of annual nitrogen availability and nitrogen concentration in fine roots (Aber et al. 1985; Nadelhoffer and Raich 1992).

Minirhizotrons

Root observation methods are among the oldest methods to be used to evaluate root and rhizome dynamics (Böhm 1979). However, it has only been since the recent availability of small video cameras that the method has been considered for estimating BNPP (Upchurch and Ritchie 1983; Ferguson and Smucker 1989; Cheng et al. 1990; Hendrick and Pregitzer 1992).

The method involves placing transparent tubes in the soil to a depth determined by the objective of the study (Brown and Upchurch 1987). Observations of roots intersecting the tubes are made at intervals and the images are recorded on videotape (Brown and Upchurch 1987). The video images must be converted to digital images for analysis, which requires digitizing the root outline (Hendrick and Pregitzer 1992) or counting the number of intersections of roots with the tube (Merrill and Upchurch 1994). While the potential for automating the digitizing step exists, to date the problem of extracting the root images from the background of organic debris has proven to be very difficult (Smucker 1993). Manually digitizing the root images is very time consuming.

Root length is measured at each sample date and the change in root length is expressed as a proportion of the root length on the first sample date (Hendrick and Pregitzer 1992, 1993). The amount of root length added as a proportion of the initial amount is a turnover coefficient. Production can be expressed either in terms of root length (Hendrick and Pregitzer 1992) or in terms of biomass (Hendrick and Pregitzer 1993). NFRP or BNPP is calculated by assuming that the turnover in root length

TABLE 4.2 Means of input variables for Monte Carlo uncertainty analysis of the nitrogen (N) balance method[a] for calculating net fine root production.[b]

Variable	Definition[c]	Mean	Distribution
N_{m1}	January net N mineralization	0.2	Normal
N_{m2}	February net N mineralization	0.2	Normal
N_{m3}	March net N mineralization	0.2	Normal
N_{m4}	April net N mineralization	0.2	Normal
N_{m5}	May net N mineralization	12	Normal
N_{m6}	June net N mineralization	7	Normal
N_{m7}	July net N mineralization	20	Normal
N_{m8}	August net N mineralization	15	Normal
N_{m9}	September net N mineralization	12	Normal
N_{m10}	October net N mineralization	2	Normal
N_{m11}	November net N mineralization	2	Normal
N_{m12}	December net N mineralization	0.2	Normal
N_p	Amount of N in precipitation	8	Normal
N_l	Amount of N lost to leaching	0.1	Normal
N_w	N allocated to wood	9.9	Normal
N_{al}	N allocated to aboveground litter	40	Normal
N_c	N concentration in fine roots	0.0105	Normal

[a]

$$NFRP = \frac{\sum_{i=1}^{12} N_{mi} + N_p - N_l - N_w - N_{al}}{N_c}$$

[b]Net fine root production (NFRP) for this example is:

$$NFRP = (71 + 8 - 0.1 - 9.9 - 40)/0.0105$$
$$= 2762 \text{ g m}^{-2} \text{ yr}^{-1}$$

[c]All units in kg N ha^{-1} yr^{-1} except N concentration, which is in (kg kg^{-1}).

density (cm cm^{-2}) is the same as the turnover in biomass (Hendrick and Pregitzer 1993). Hendrick and Pregitzer (1993) used the equation

$$NFRP = B_i \frac{Alp}{Ild} \tag{4.10}$$

to estimate NFRP where B_i is initial root biomass (kg ha^{-1}), *Alp* is annual root length production (mm cm^{-2} yr^{-1}) and *Ild* is initial root length density (mm cm^{-2}). A sample calculation is illustrated in Table 4.3.

The use of minirhizotrons to estimate NFRP is relatively new and few estimates are available. Aerts et al. (1989) compared minirhizotrons with a biomass method of estimating root turnover and concluded that the minirhizotron estimates were more reliable. They calculated root length turnover rate (yr^{-1}) (RLT) for each tube using the following equation

$$RLT = \frac{Rlp}{Arl} \tag{4.11}$$

where *Rlp* is annual root length production (cm) and *Arl* is average living root length (cm). Hendrick and Pregitzer (1992) found that a substantial amount of the growth and death of fine roots in a northern hardwood forest occurred simultaneously and that methods that were not able to separate growth and mortality would produce underestimates of root length production. Hendrick and Pregitzer (1993) compared their estimates of NFRP using minirhizotrons to the estimates of other researchers using different methods and, in general, found that the minirhizotron estimates were greater. The limitations of the minirhizotron method are related to assumptions about the effect of the observation tubes on the demography of roots, the equivalence of turnover of biomass and length, the

TABLE 4.3. Means of input variables for Monte Carlo uncertainty analysis of the minirhizotron method,[a] of calculating net fine root production.[b]

Variable	Definition	Mean	Distribution
B_i	Initial biomass ($g\ m^{-2}$)	6110	Normal
Alp	Annual root length production ($mm\ cm^{-2}\ yr^{-1}$)	3.38	Normal
Ild	Initial root length density ($mm\ cm^{-2}$)	3.34	Normal

[a]

$$NFRP = B_i \frac{Alp}{Ild}$$

[b]Net fine root production for this example is:

$$NFRP = 6110 * (3.38/3.34)$$
$$= 6183\ g\ m^{-2}\ yr^{-1}$$

amount of time required to collect and process the data, and the high cost of the camera and digitizing and analysis equipment.

Uncertainty in Estimates of BNPP

The reason that BNPP represents one of the major weaknesses in our understanding of terrestrial ecosystems is that all of the methods for estimating it have important limitations. Many of the specific limitations of each method have been mentioned. This section addresses a problem that affects all methods to a varying degree, namely, the uncertainty associated with the estimate of BNPP. Previous authors have dealt with one aspect of uncertainty, how variability in the input data for various methods influences the degree to which they over- or underestimate BNPP (Singh et al. 1984; Kurtz and Kimmins 1987; Publicover and Vogt 1993). Here, I want to tackle a related but different aspect of uncertainty associated with estimates of BNPP, that of how variability in the input data affects variability in the estimate of BNPP. The objective of this analysis is not to exhaustively analyze the methods of estimating BNPP, but to use a few examples to illustrate the importance of assessing the uncertainty associated with estimates of BNPP.

Uncertainties in estimates of BNPP arise as a result of uncertainties in the components used to calculate the estimate. If the variables that go into a particular calculation of BNPP can be measured with great precision, then the resulting estimate will have low uncertainty associated with it. The most common situation, however, is that some of the components are sampled with high precision (low variance) while others are sampled with low precision (high variance). How the precision of a variable or its variance is propagated through a calculation depends upon the characteristics of the calculation. If the calculation is a linear combination (sums or differences), the problem of propagating the variance of each component through to the final result can be solved analytically (Box et al. 1978). Propagating uncertainty through sums and differences is the easiest part of the problem of calculating uncertainty associated with estimates of BNPP. The most difficult part is dealing with nonlinear calculations (multiplication, division, and logarithms). Nonlinear functions are difficult because there are no general equations that one can use to calculate the variance of the result from the variances of the components. An effective method for nonlinear equations is Monte Carlo analysis (O'Neill 1973; Gardner and O'Neill 1981; O'Neill et al. 1982). An example of the calculations for the Monte Carlo method is presented in Table 4.4.

While all of the methods can be subjected to Monte Carlo uncertainty analysis, I have chosen several of them to illustrate the importance of understanding the influence of variability in input data on the uncertainty in the estimate of BNPP or NFRP. The methods I chose for analysis are the biomass method described by Publicover and Vogt (1993) (see Table 4.4 for equations and means), the nitrogen balance method as described by Aber et al. (1985) (see Table 4.2), and the minirhizotron method as described by Hendrick and Pregitzer (1993) (see Table 4.3). The analysis involved 100,000 estimates of BNPP or NFRP, which were based upon 100,000 random samples of the input variables. The means for the input variables were taken from the papers that describe the method or from a reference they cited. All of the input variables were assumed to be normally distributed and independent. The assumption of independence can, in the case of correlated input variables, lead to an overestimate of uncertainty (O'Neill et al. 1982). Each analysis was repeated for a range of coeffi-

TABLE 4.4. Example of using Monte Carlo uncertainty analysis to propagate variance through calculations of belowground net primary production. The example uses data from Publicover and Vogt (1993).

The information necessary for Monte Carlo uncertainty analysis is the mean, the variance, and a reasonable range for all of the input variables and an assumption about the distribution for each variable. If the distribution type is not known, a uniform distribution can be used (O'Neill et al. 1982). The uncertainty of the final result is determined by making a large number of calculations (≥10,000) each with a sample of the input variables drawn from their respective distributions. A mean and variance of the result is then calculated from the results of the Monte Carlo simulations. This example uses data from months 3 and 4 from Table 1 on page 1180 of Publicover and Vogt (1993) and calculates net fine root production for that single interval.

Month	LFR	DFR	P	MR	DR	M	D
0	.	.	.	.	.	.	.
1	.	.	.	.	.	.	.
2	.	.	.	.	.	.	.
3	554.3	369.8	.	0.1	0.15	45	61
4	671.1	391.2	200	0.15	0.15	83	62
.	.	.	.	.	.	.	.
.	.	.	.	.	.	.	.
.	.	.	.	.	.	.	.

I assumed that live fine roots (LFR, g m^{-2}) and dead fine roots (DFR; g m^{-2}) had coefficients of variation of 10% (Publicover and Vogt 1993), and that mortality rate (MR, g g^{-1}) and disappearance rate (DR, g g^{-1}) also had coefficients of variation of 10%. All, but especially those for MR and DR, are conservative estimates (Publicover and Vogt 1993, Burke and Raynal 1994). I also assumed normal distributions for all of the variables and made 100,000 calculations of net fine root production (P_t, g m^{-2}) using the following formulas from Publicover and Vogt (1993):

$$P_t = (LFR_t - LFR_{t-1}) + (DRF_t - DFR_{t-1}) + D_t \quad (1)$$

Equation 1 was suggested by McClaugherty et al. (1982) as appropriate for estimating net fine root production during periods when live and dead fine root biomass both increase. D_t was calculated as proposed by Publicover and Vogt (1993):

$$D_t = \left(DFR_{t-1} + \frac{LFR_{t-1}MR}{2}\right)DR_t \quad (2)$$

The following table contains a sample of 50 values for each of the variables and for P_t. These 50 were selected from the 100,000 values generated for the analysis. The mean and coefficient of variation of P_t for these 50 values are 221 g m^{-2} and 48%. The results for the entire analysis indicate that a coefficient of variation of 10% for all of the input data produces a mean P_t of 199.7 g m^{-2} and a coefficient of variation of 50%. See Figure 4.2 for the results of an analysis for a range of coefficients of variation of the input variables.

LFR(t)	LFR(t − 1)	DFR(t)	DFR(t − 1)	MR(t)	DR(t)	P(t)
.	.	.	.	.	.	.
.	.	.	.	.	.	.
.	.	.	.	.	.	.
739.8	567.2	426.9	418.5	0.16	0.15	251
659.7	575.0	388.6	406.5	0.16	0.15	135
591.9	486.0	457.0	285.3	0.15	0.15	327
686.1	512.3	413.4	387.2	0.14	0.17	271
626.1	576.8	333.7	355.8	0.14	0.16	92
657.8	482.1	376.5	403.9	0.13	0.15	214
745.5	586.1	319.8	385.6	0.18	0.18	170
726.2	450.5	396.5	376.7	0.12	0.15	357
687.0	480.5	296.0	344.5	0.14	0.15	213
606.4	529.6	391.1	337.4	0.16	0.16	192
786.8	528.5	331.8	375.0	0.16	0.14	275
569.4	550.3	449.1	373.3	0.13	0.17	164
697.2	562.7	392.1	355.3	0.16	0.16	234
694.6	619.4	349.4	351.1	0.14	0.12	123
739.2	485.7	400.9	453.9	0.15	0.15	272
741.4	508.7	399.2	389.3	0.15	0.16	311
637.5	596.0	395.7	349.6	0.15	0.18	157

(*continued*)

TABLE 4.4. (continued).

LFR(t)	LFR(t − 1)	DFR(t)	DFR(t − 1)	MR(t)	DR(t)	P(t)
785.5	642.1	420.8	385.2	0.17	0.15	243
769.0	609.8	398.3	371.5	0.14	0.14	242
700.0	706.7	341.5	432.2	0.15	0.18	−12
647.3	591.6	393.3	353.5	0.16	0.18	166
670.0	582.3	339.6	413.2	0.14	0.14	80
618.8	539.4	431.1	379.0	0.14	0.14	190
589.2	564.8	418.9	358.0	0.16	0.17	152
667.6	654.2	351.2	429.7	0.15	0.15	6
708.7	469.5	428.9	360.3	0.16	0.14	362
734.1	502.8	417.3	372.1	0.15	0.18	349
716.4	568.6	415.1	251.4	0.15	0.17	363
667.3	523.8	364.8	422.2	0.16	0.13	147
636.4	554.6	345.7	340.4	0.16	0.13	139
666.3	632.9	461.0	326.8	0.17	0.13	219
543.1	574.9	338.7	344.3	0.14	0.16	23
634.3	654.6	434.7	369.2	0.13	0.13	99
638.8	468.6	370.3	405.8	0.15	0.12	185
673.3	628.3	446.4	355.1	0.16	0.13	190
635.8	441.4	378.6	429.8	0.14	0.16	217
740.6	494.7	388.4	286.6	0.15	0.15	396
798.4	548.7	389.4	306.1	0.16	0.16	388
749.1	483.4	469.8	384.5	0.14	0.12	402
654.1	607.0	404.5	409.7	0.17	0.11	92
660.6	506.1	405.0	363.2	0.14	0.12	244
744.7	546.5	425.6	352.9	0.13	0.16	334
689.3	499.4	380.8	397.9	0.17	0.15	239
763.4	625.8	417.6	311.2	0.16	0.15	297
720.5	493.3	374.3	380.7	0.15	0.13	277
723.8	551.9	448.4	360.7	0.14	0.16	322
715.5	506.8	381.6	323.6	0.17	0.15	321
687.2	487.4	382.6	316.5	0.14	0.15	320
629.2	735.6	417.6	350.8	0.15	0.15	23
700.2	547.5	402.4	320.7	0.15	0.16	291
.	.	.	.	.	.	.
.	.	.	.	.	.	.
.	.	.	.	.	.	.

cients of variation (CVs) for the input variables from 5 to 30% in steps of 5%.

Variability in the input variables had a large effect on the amount of uncertainty associated with the estimate of BNPP for all three methods (Figs. 4.2 to 4.4). The CV_{NFRP} for the biomass method was linearly related to the CV_{Input} ($CV_{NFRP} = 5.03\ CV_{Input}$) (see Fig. 4.2). A CV_{Input} of 5% resulted in a CV_{NFRP} of 25%. By the time the CV_{Input} reached 25%, the CV_{NFRP} was greater than 100%. The CVs of NFRP for both the nitrogen balance and minirhizotron methods had threshold responses to CV_{Input} (see Figs. 4.3 and 4.4). Between CV_{Input} of 5 and 20%, the CV_{NFRP} increased linearly from 10 to 44% for the nitrogen balance method and from 9 to 38% for the minirhizotron method. Between CV_{Input} of 20 to 30%, CV_{NFRP} for the nitrogen balance method increased from 44 to 672% and CV_{NFRP} for the minirhizotron method increased from 38 to 181%. In both cases, a large part of the reason for the increase is that, as the CV_{Input} becomes large, the probability of selecting a value for the denominator in the equations very close to zero also becomes large, causing the result to become unstable. This emphasizes the sensitivity of these methods to errors in fine root nitrogen concentra-

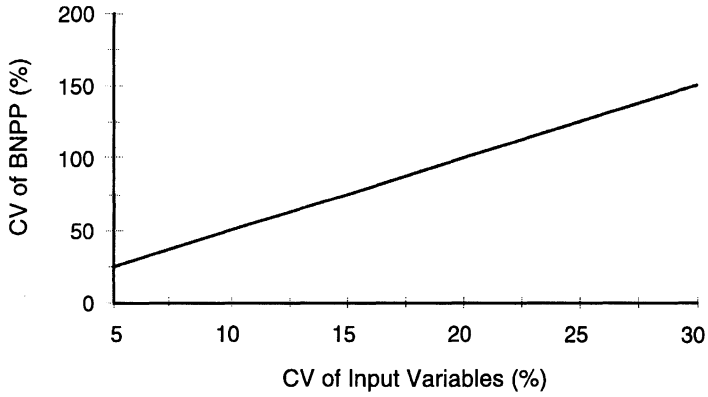

FIGURE 4.2. The relationship between the coefficient of variation (CV) of the input variables and the coefficient of variation of the estimate of BNPP by the biomass method described by Publicover and Vogt (1993).

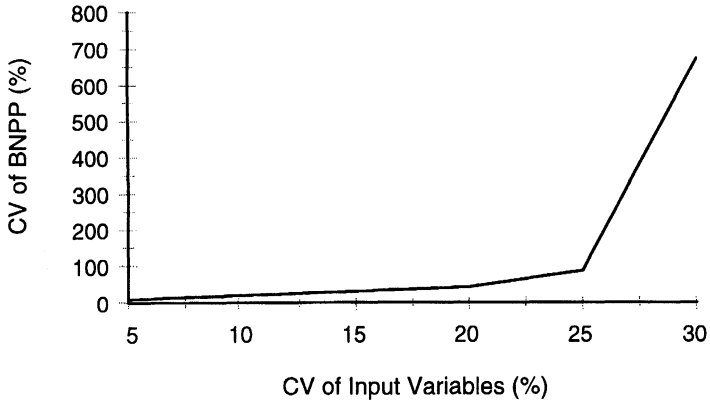

FIGURE 4.3. The relationship between the coefficient of variation (CV) of the input variables and the coefficient of variation of the estimate of BNPP by the nitrogen balance method described by Aber et al. (1985).

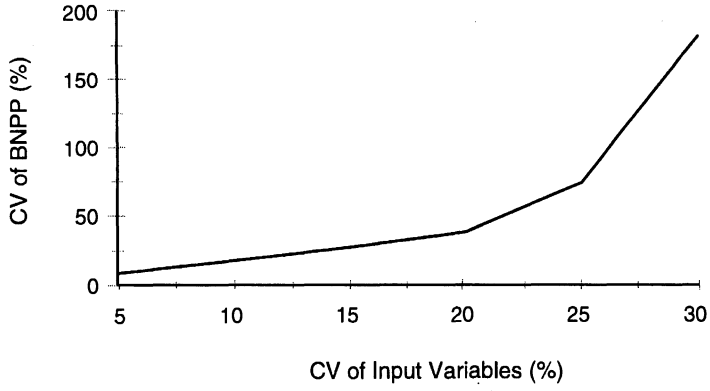

FIGURE 4.4. The relationship between the coefficient of variation (CV) of the input variables and the coefficient of variation of the estimate of BNPP by the minirhizotron method described by Hendrick and Pregitzer (1993).

tion in the case of the nitrogen balance method and initial root length density in the case of the minirhizotron method.

Two important points emerge from these analyses. First, the amount of uncertainty associated with published estimates of BNPP and NFRP can be, and in most cases probably is, large. This underscores the importance of attempting to assess the uncertainty associated with all published estimates of BNPP. This is analogous to always including a standard deviation or a standard error for every mean. This or more elaborate statistical analyses

have become the accepted norm for all ecological papers published in the refereed literature. A similar standard for estimates of BNPP would provide a useful way for readers to assess the importance of particular estimates in the range of numbers they encounter.

Currently, there is no standard by which small and large estimates can be judged. We have been told that more elaborate methods produce "better" estimates (e.g., Long et al. 1989, 1992). However, because these "better" estimates often entail making measurements of more variables, they often have higher uncertainty associated with them. There can be large differences among methods that are the result of an interaction between the kind of calculation made and the amount of variability in the input data. The calculations made for the Publicover and Vogt (1993) method involved addition, subtraction, and division by a constant. The relationship between the uncertainties of the input and output variables was linear. In the cases of the nitrogen balance and minirhizotron methods, both involved division by a variable. In the case of the nitrogen balance method, the denominator (nitrogen concentration) will always be very small compared with the numerator (amount of nitrogen allocated to fine roots), which means that the estimate of NFRP will be very sensitive to the estimate of the nitrogen concentration in fine roots. For the minirhizotron method, the data from Hendrick and Pregitzer (1993) suggest that the numerator and denominator will be of similar magnitudes, which should increase the stability of the calculation.

Decisions about which method to choose to estimate BNPP should be based upon the objective of the study, which will dictate the kind of estimate that is required. The final choice should include a consideration of the potential of the method to produce an estimate with an acceptable level of uncertainty.

Summary

There is no best way to estimate BNPP. All of the methods have conceptual strengths and weaknesses, numerous practical considerations, and differing relationships between variability of the input variables and uncertainty in the estimate of BNPP. Each of these factors should be evaluated relative to the objectives of the particular project in arriving at a decision about which method to use. In some cases, the decision will be quite simple. The practical considerations in using the carbon isotope turnover method in a mature forest will lead to its quick elimination as a possibility. Other decisions will be more difficult, such as deciding between the biomass or minirhizotron methods in a grassland. While there are substantial practical considerations associated with each method, there are few that completely overwhelm the decision-making process. The initial costs are different, the amounts and types of field work required are different, the amounts of analysis after the field sampling differ, and the relationships between the variability of the input variables and the uncertainty in the estimates of BNPP differ between the methods. Each of these factors will have to be considered in relation to the project objectives before a decision can be reached.

Acknowledgments I thank Daniel Milchunas and Osvaldo Sala for many stimulating discussions about belowground net primary production. I also thank Martyn Caldwell, Dennis Knight, F.W. Smith and Daniel Milchunas for helpful comments on an earlier draft. Funding for this work was provided by the Shortgrass Steppe Long Term Ecological Research project which is supported by the National Science Foundation (BSR 90-13888) and the Colorado State University Experiment Station (1-50661).

References

Aber, J.D.; Melillo, J.M.; Nadelhoffer, J.K.; McClaugherty, C.A.; Pastor, J. Fine root turnover in forest ecosystems in relation to quantity and form of nitrogen availability: A comparison of two methods. Oecologia 66:317–321; 1985.

Aerts, R.; Berendse, F.; Klerk, N.M.; Bakker, C. Root production and root turnover in two dominant species of wet heathlands. Oecologia 81:374–378; 1989.

Binkley, D.; Ryan, M.G. Net primary production and nutrient cycling in replicated stands of *Eucalyptus saligna* and *Albizia facaltaria.* For. Ecol. Manage. 112:79–85; 1998.

Böhm, W. *Methods of Studying Root Systems.* Berlin: Springer-Verlag; 1979.

Box, G.E.P.; Hunter, W.G.; Hunter, J.S. Statistics for experimenters: An introduction to design, data analysis, and model building. New York: Wiley Sons; 1978:87–89.

Bray, J.R. Root production and the estimation of net productivity. Can. J. Bot. 41:65–72; 1963.

Brown, D.A.; Upchurch, D.R. Minirhizotrons: A summary of methods and instruments in current use. In: Taylor, H.M., ed. *Minirhizotron Observation Tubes: Methods and Applications for Measuring Rhizosphere Dynamics.* Madison, WI: American Society of Agronomy; 1981:15–30.

Burke, M.K.; Raynal, D.J. Fine root growth phenology, production and turnover in a northern hardwood forest ecosystem. Plant Soil 162:135–146; 1994.

Caldwell, M.M.; Camp, L.B. Belowground productivity of two cool desert communities. Oecologia 17:123–130; 1974.

Cheng, W.; Coleman, D.C.; Box, J.E., Jr. Root dynamics, production and distribution in agroecosystems on the Georgia Piedmont using minirhizotrons. J. Appl. Ecol. 27:592–604; 1990.

Coleman, D.C. A review of root production processes and their influence on soil biota in terrestrial ecosystems. In: Anderson, J.M.; Macfadyen, A., eds. *The Role of Terrestrial and Aquatic Organisms in Decomposition Processes. Proceedings of the British Ecological Society Symposium, Coleraine, N. Ireland, April 15–18, 1975.* Oxford: Blackwell; 1976:417–434.

Dahlman, R.C.; C.L. Kucera. Carbon-14 cycling in the root and soil components of a prairie ecosystem. *Proceedings of the 2nd National Symposium on Radioecology, Ann Arbor, Michigan, May 15–17, 1967.* Wahsington DC: U.S. Government Printing Office; 1967:652–660.

Dahlman, R.C.; Kucera, C.L. Root productivity and turnover in native prairie. Ecology 46:84–89; 1965.

Ferguson, J.C.; Smucker, A.J.M. Modifications of the minirhizotron video camera system for measuring spatial and temporal root dynamics. Soil Sci. Soc. Am. J. 53:1601–1605; 1989.

Gardner, R.H.; O'Neill, R.V. A comparison of sensitivity analysis and error analysis based on a stream ecosystem model. Ecol. Model. 12:173–190; 1981.

Gower, S.T.; Pongracic, S.; Landsberg, J.J. A global trend in belowground carbon allocation: Can we use the relationship at smaller scales. Ecology 77:1750–1755; 1996.

Hendrick, R.L.; Pregitzer, K.S. The demography of fine roots in a northern hardwood forest. Ecology 73:1094–1104; 1992.

Hendrick, R.L.; Pregitzer, K.S. The dynamics of fine root length, biomass and nitrogen content in two northern hardwood ecosystems. Can. J. For. Res. 23:2507–2520; 1993.

Hook, P.B.; Lauenroth, W.K.; Burke, I.C. Spatial patterns of roots in a semiarid grassland: Abundance of canopy openings and regeneration gaps. J. Ecol. 82:485–494; 1994.

Jordan, C.F.; Escalante, G. Root productivity in an Amazonian rain forest. Ecology 61:14–18; 1980.

Kurtz, W.A.; Kimmins, J.P. Analysis of some sources of error in methods used to determine fine root production in forest ecosystems: A simulation approach. Can. J. For. Res. 17:909–912; 1987.

Lauenroth, W.K.; Milchunas, D.G. Shortgrass steppe. In: Coupland, R.T., ed. *Natural Grasslands: Introduction and Western Hemisphere.* Amsterdam: Elsevier, 1992:183–226.

Lauenroth, W.K.; Whitman, W.C. A rapid method for washing roots. J. Range Manage. 24:308–309; 1971.

Lauenroth, W.K.; Whitman, W.C. Dynamics of dry matter production in a mixed-grass prairie in western North Dakota. Oecologia 27:339–351; 1977.

Long, S.P.; Jones, M.B.; Roberts, M.J., eds. *Primary Productivity of Grass Ecosystems of the Tropics and Subtropics.* London: Chapman and Hall; 1992:267.

Long, S.P.; Garcia Moya, E.; Imbamba, S.K.; Kamnalrut, A.; Piedade, M.T.F.; Scurlock, J.M.O.; Shen, Y.K.; Hall, D.O. Primary productivity of natural grass ecosystems of the tropics: A reappraisal. Plant Soil 115:155–166; 1989.

McClaugherty, C.A.; Aber, J.D.; Melillo, J.M. The role of fine roots in the organic matter and nitrogen budgets of two forest ecosystems. Ecology 63:1481–1490; 1982.

Merrill, S.D.; Upchurch, D.R. Converting root numbers observed at minirhizotrons to equivalent root length density. Soil Sci. Soc. Am. J. 58:1061–1067; 1994.

Milchunas, D.G.; Lauenroth, W.K. Carbon dynamics and estimates of primary production by harvest, C-14 dilution and C-14 turnover. Ecology 73:1593–1607; 1992.

Milchunas, D.G.; Lauenroth, W.K.; Singh, J.S.; Cole, C.V.; Hunt, H.W. Root turnover and production by C-14 dilution: implications of carbon partitioning in plants. Plant Soil 88:353–65; 1985.

Nadelhoffer, K.J.; Aber, J.D.; Melilo, J.M. Fine roots, net primary production, and soil nitrogen availability: A new hypothesis. Ecology 66:1377–1390; 1985.

Nadelhoffer, K.J.; Raich, J.W. Fine root production estimates and belowground carbon allocation in forest ecosystems. Ecology 73:1139–1147; 1992.

Nadelhoffer, K.J.; Raich, J.W.; Aber, J.D. A global trend in belowground carbon allocation: Comment. Ecology 79:1822–1825; 1998.

Neill, C. Comparison of soil coring and ingrowth methods for measuring belowground production. Ecology 73:1918–1921; 1992.

O'Neill, R.V. Error analysis of ecological models. In: Nelson, D.J., ed. *Radionuclides in Ecosystems.* Washington, DC: U.S. Atomic Energy Commission; 1973:898–908.

O'Neill, R.V.; Gardner, R.H.; Carney, J.H. Parameter constraints in a stream ecosystem model: Incorporation of a priori information in Monte Carlo error analysis. Ecol. Model. 16:51–65; 1982.

Persson, H.A. Root dynamics in a young Scots pine stand in central Sweden. Oikos 30:508–519; 1978.

Persson, H.A. Fine root production, mortality and decomposition in forest ecosystems. Vegetatio 41:101–109; 1979.

Persson, H.A. The distribution and production of fine roots in boreal forests. Plant Soil 71:87–101; 1983.

Publicover, D.A.; Vogt, K.A. A comparison of methods for estimating forest fine root production with respect to sources of error. Can. J. For. Res. 23:1179–1186; 1993.

Raich, J.W.; Nadelhoffer, K.J. Belowground carbon allocation in forest ecosystems: Global trends. Ecology 70:1346–1354; 1989.

Sala, O.E.; Biondini, M.E.; Lauenroth, W.K. Bias in estimates of primary production: An analytical solution. Ecol. Model. 44:43–55; 1988.

Santantonio, D.; Grace, J.C. Estimating fine root production and turnover from biomass and decomposition data: A compartment flow model. Can. J. For. Res. 17:900–908; 1987.

Sims, P.L.; Singh, J.S. The structure and function of ten western North American grasslands. III. Net primary production, turnover and efficiencies of energy capture and water use. J. Ecol. 66:573–97; 1978.

Singh, J.S.; Lauenroth, W.K.; Hunt, H.W.; Swift, D.M. Bias and random errors in estimators of net root production: A simulation approach. Ecology 65:1760–1764; 1984.

Smith, F.W.; Resh, S.C. Age-related changes in production and below-ground carbon allocation in *Pinus contorta* forests. For. Sci. 45:1–9; 1999.

Smucker, A.J.M. Soil environmental modifications of root dynamics and root measurement. Annu. Rev. Phytopathol. 31:193–216; 1993.

Smucker, A.J.M.; McBurney, S.L.; Srivastava, A.K. Quantitative separation of roots from compacted soil profiles by the hydropneumatic elutriation system. Agron. J. 74:500–503; 1982.

Upchurch, D.R.; Richie, J.T. Root observations using a video recording system in minirhizotrons. Agron. J. 75:1009–15; 1983.

Vogt, K.A. Carbon budgets of temperate forests. Tree Physiol. 9:69–86; 1991.

Wiegert, R.G.; Evans, F.C. Primary production and the disappearance of dead vegetation on an old field in southeastern Michigan. Ecology 45:49–63; 1964.

5

The Measurement of Primary Production in Aquatic Ecosystems

Robert W. Howarth and Anthony F. Michaels

Introduction

All biological systems exist as a result of continual inputs of energy to maintain structure and order. At the scale of the ecosystem, most of this energy comes from sunlight, which is converted into the energy of organic matter in living biomass through the process of primary production, and from imports of organic matter from adjacent ecosystems. This import of energy in organic matter is, of course, dependent upon primary production in the "upstream" ecosystem. Thus, a critical aspect of understanding the functioning of an ecosystem is an accurate estimate of its rate of primary production.

Primary production in aquatic ecosystems is also of great interest for practical concerns. Eutrophication, or the excess primary production caused by accelerated nutrient inputs, is one of the greatest environmental problems facing both freshwater and coastal marine ecosystems (NRC 1993; Vitousek et al. 1997; Carpenter et al. 1998). On the positive side, primary production in oceans makes up 30 to 60% of global primary production (Sakshaug et al. 1997), and the balance between primary production and respiration is important in regulating carbon dioxide uptake by the oceans, and therefore climate change.

In aquatic ecosystems, both phytoplankton and benthic autotrophs, such as vascular plants, macroalgae, and mats of photosynthetic bacteria, can contribute to primary production. In this chapter, we concentrate on approaches to measuring primary production by phytoplankton (Table 5.1). Methods for measuring primary production by benthic macroalgae and vascular plants in aquatic ecosystems often have more in common with methods used to measure production in terrestrial ecosystems (see Sand-Jensen and Krause-Jensen 1997; see also Chapter 2 and 4). Among the phytoplankton community, primary production is performed by both microscopic algae and photosynthetic bacteria (particularly cyanobacteria).

Gross primary production (GPP) is defined as the total rate of production of new organic matter by phytoplankton through photosynthesis. Net primary production (NPP) is GPP minus the organic matter respired by the phytoplankton themselves, that is, the rate of accumulation of new phytoplankton biomass. Net ecosystem production (NEP; also referred to as net community production, or NCP) is the difference between NPP and the respiration of all of the heterotrophs in the ecosystem (equivalent to the difference between GPP and all respiration by both autotrophs and heterotrophs). All three of these rates are of ecological interest, and we will discuss all in this chapter.

Primary production can be simply illustrated as the following reaction:

$$CO_2 + H_2O \xrightarrow{\text{light}} CH_2O + O_2 \qquad (5.1)$$

where CH_2O represents generic organic matter. In theory, one could estimate primary production by measuring the rate of change in any of the products or reactants, or even other biomass constituents that are stoichiometrically related to the production rate (i.e., nutrient uptake). In practice, however, almost all measurements of primary production in planktonic systems are based on mea-

TABLE 5.1. Comparison of commonly used methods for estimating primary production in aquatic ecosystems.

Method	Items measured	Advantages	Problems
Light and dark bottles	GPP and water-column respiration	Relatively easy; measures well-defined processes	Historically, low sensitivity (now less of a problem); difficulty with scaling to light availability; "bottle effects" such as reduced turbulence; must assume that respiration is equal in light and dark
$^{14}CO_2$	Some rate of primary production between NPP and GPP; no estimate for respiration	Relatively easy; very sensitive	Process being measured not well defined (particularly with longer incubations or in systems with low light); difficulty with scaling to light availability; "bottle effects" such as reduced turbulence
In situ diel	GPP, whole-ecosystem respiration, and NEP	Measures well-defined processes; no "bottle effects"	Historically, low sensitivity (now less of a problem); must assume that respiration is equal during day and at night; can be some error estimating atmospheric exchange, particularly in shallow systems

suring the rate of uptake of carbon dioxide (CO_2) or the rate of production of dissolved oxygen (O_2), and this chapter is largely devoted to describing such methods. They can roughly be divided into two categories, analysis of the time-dependent behavior of the constituents in the reaction and the use of radioactive tracers to follow the conversion rate of carbon.

In terrestrial ecosystems, primary production is often estimated from changes in the standing stock of plant biomass (see Chapters 2 and 4), that is, the rate of change in organic carbon (C) in the above reaction representing primary production. However, in planktonic systems, the primary producers are often rapidly consumed by grazing animals (both zooplankton and benthic filter feeders); the turnover of the phytoplankton community can be as rapid as 1 day. Without an accurate measure of this mortality and turnover, primary production in planktonic systems cannot be estimated from the change in organic C in primary producers. Unfortunately, it is quite difficult to measure rates of grazing on phytoplankton. Net ecosystem production (NEP or NCP) can be measured through the changes in biomass with time and, during the expansion phase of a phytoplankton bloom, this can provide a lower bound on the rate of NPP.

The H_2O term in the primary production equation, the rate of change of H_2O from primary production, is much too small to measure among the huge pool of H_2O in an aquatic system. Primary production can be measured by spiking a water sample with $H_2^{18}O$ and measuring the production of $^{18}O_2$ by mass spectrometry (Bender et al. 1987), but this is basically a measure of O_2 production rather than H_2O consumption.

Some efforts have also been made to estimate rates of primary production by quantifying the rate of energy capture or energy flux through phytoplankton communities. This method has a rich history, beginning with attempts to relate the light absorption characteristics of populations of phytoplankton to the profiles of light availability in the ocean (Ryther, 1956). Recently, these techniques have become more sophisticated as they follow the flow of energy through phytoplankton and quantitatively begin to measure the relationships between absorption, fluorescence, and the formation of chemical energy in the cell. Many of these techniques allow for rapid sampling with electronic optical devices and very detailed profiles. All of them have to be calibrated against the standard measures of carbon uptake or oxygen evolution to be useful from an ecological perspective. See Li and Maestrini (1993) for a thorough discussion of new, developing approaches for measuring primary production.

Light and Dark Bottle Oxygen Technique

The light and dark bottle oxygen technique was the first method used to measure primary production in an aquatic ecosystem (Gaarder and Gran 1927) and is still commonly used (e.g., Arîstegui et al. 1996). This method compares the rate of change in oxygen in bottles held in the light (which includes the net effects of production and respiration) with those held in the dark (respiration only) to calculate the primary production rate by difference. Water samples containing ambient plankton populations are placed into sets of incubation bottles or other containers, with some bottles clear and others covered so as to be opaque. The bottles are then incubated at in situ temperatures either in situ in the water column (hung from a buoy or pier) or in an incubator (either outdoors using sunlight, or with artificial lights). The more sophisticated incubators are both temperature controlled and correct the color of the light to approximate the spectral composition at depth (Lohrenz et al. 1992). At the end of the incubation period, the oxygen concentration is measured in both the light (clear) bottles and the dark (opaque) bottles and compared with the oxygen concentration in the water column at the time the bottles were filled. The change in oxygen in the light bottle over time is the combined result of GPP and respiration by all of the organisms in the bottle (phytoplankton, but also heterotrophic bacteria and zooplankton). The decrease in oxygen in the dark bottle is a measure of this rate of respiration. Thus, GPP can be estimated by subtracting the rate of change of oxygen in the dark bottle from the rate of change of oxygen in the light bottle.

$$\text{GPP} = \Delta O_2 \text{ (light)} - \Delta O_2 \text{ (dark)} \quad (5.2)$$

where ΔO_2 (light) = $[O_2]$ final − $[O_2]$ initial in the light bottles, and ΔO_2 (dark) = $[O_2]$ final − $[O_2]$ initial in the dark bottles.

Usually the oxygen concentration increases in the light bottle and decreases in the dark bottle. In low-light or in organic-rich waters, the oxygen concentration in the light bottle can decrease if the rate of respiration exceeds GPP. Still, in this case, the rate of oxygen decrease in the light bottle will be less than the rate of decrease in the dark bottle, so that when the dark bottle result (decrease in O_2) is subtracted from the light bottle change (smaller decrease in O_2), GPP will be a positive value.

The comparisons with the initial oxygen concentration allow an estimate of the rate of planktonic community respiration and net planktonic community production on the time-scale of the incubation. Note, however, that these rates measured in the dark bottle are measures of planktonic respiration and production only. They are not measures of whole-ecosystem respiration and whole-system net ecosystem production, since benthic respiration (see Chapter 6) and respiration by large animals such as fish (which are not sampled and placed in the incubation bottles) are not included. Since the dark bottle measures total planktonic respiration, including respiration by heterotrophic organisms and not just respiration by phytoplankton, addition of this rate to the rate of change of oxygen in the light bottle yields an estimate of GPP, and not NPP. There is no way to estimate NPP from the light and dark bottle technique, unless there is some independent way to estimate the rate of respiration by phytoplankton alone. As discussed below, phytoplankton respiration is very difficult to estimate. As also discussed below, rates of respiration in the dark may not equal rates of respiration in the light, which introduces some error into the light and dark bottle method of assessing GPP.

The light and dark bottle method yields an estimate of GPP in units of rate of change of oxygen per volume of water. Generally, rates are converted to units of carbon by assuming some stoichiometric relationship between O_2 produced and organic C fixed: the photosynthetic quotient. The equation for production, above, suggests a stoichiometry of one mole O_2 produced per mole of organic C fixed. However, phytoplankton also incorporate nitrogen into their biomass during primary production and can produce organic carbon that is more reduced than represented by the generic representation of organic matter as CH_2O. Consequently, in general, more moles of O_2 are produced in GPP than the number of moles of organic C that are fixed. Generally, the assumed stoichiometric ratios of O_2/C for GPP range from 1.0 to 1.3 when phytoplankton are growing on ammonium and from 1.4 to 1.8 when algae grow on nitrate (Raine, 1983, Platt and Harrison, 1986). The higher ratio for nitrate assimilation represents the extra photosynthate required to reduce nitrate to amine before incorporation, some

of which comes directly from the products of the light reaction. There is a similar enhancement of the photosynthetic quotient when phytoplankton produce large amounts of lipid or other highly reduced compounds.

Rather than measuring changes in O_2 in light and dark bottles, changes in dissolved inorganic carbon (DIC, or the sum of dissolved CO_2 gas, HCO_3^- and CO_3^{2-}) can be measured instead. However, in seawater and in freshwaters with significant carbonate alkalinity, CO_2 is much more soluble than O_2 and DIC concentrations are very high. Thus, measuring changes in DIC requires a large relative accuracy and usually results in a much less sensitive method. In lakes with low carbonate alkalinity, DIC concentrations can sometimes be less than O_2 concentrations, making changes in DIC a more sensitive method.

Historically, the light and dark bottle method could only be used in ecosystems where the rate of GPP was reasonably high. The resolution of the traditional Winkler titration for oxygen is of the order 0.2 to 1% in the surface ocean (0.4 to 2 μmol O_2 kg^{-1}). In oligotrophic ecosystems, such as many lakes and the majority of oceanic waters, where the GPP rates over the range of the euphotic zone are often only 1 to 10 μg C $liter^{-1}$ day^{-1}, the oxygen change during the day is usually less than 1 μmol $liter^{-1}$. Traditional analytical techniques for measuring oxygen concentrations simply lacked the precision necessary to apply this technique in oligotrophic, "blue" oceanic waters. However, during the past two decades, analytical techniques for measuring oxygen have improved dramatically. Instruments for automated endpoint detection (e.g., Williams and Jenkinson 1982) have pushed the precision of the Winkler chemistry to 0.1 μmol $liter^{-1}$. With the large amount of replication made relatively simple by rapid automated titrators, statistically significant comparisons of light and dark treatments that vary by as little as 0.03 μmol O_2 $liter^{-1}$ are now possible. As a result, the light and dark bottle technique could now be applied in systems with extremely low productivity, and this measurement of GPP would be a powerful complement to the estimates from radiotracers and other techniques.

There are a variety of problems with the light and dark bottle technique that are associated with scaling from volume to surface area, with scaling in time, with sampling water, and with isolating a parcel of water in a bottle during incubations. These problems are all shared with the carbon-14 technique (presented next) and so are discussed in a later section. A more fundamental problem with applying this technique in open ocean ecosystems is that the incubation bottles must be gas-impermeable. Also, the most common gas bottles (BOD bottles) are extremely difficult to make "trace-metal clean." Quartz bottles, which can be appropriately cleaned, are extremely expensive. This issue of the standard of trace-element cleanliness appropriate for oceanic ecosystems is discussed in more detail below.

Carbon-14 Technique

With the advent of readily available radioisotopes following World War II, Steemen Nielsen (1952) introduced the use of the carbon-14 (^{14}C) method for measuring primary production in planktonic ecosystems. This approach increased the sensitivity for measuring production by at least 10-fold over the light and dark bottle oxygen technique as it was applied in the 1950s through the 1970s, and the ^{14}C method gained rapid favor. It remains today the most common method for measuring primary production in both lakes and marine ecosystems, despite the fact that the light and dark bottle technique has now been improved sufficiently so as to be sensitive enough in many oligotrophic ecosystems (see above). The ease of the method, the high sensitivity, and the ability to follow carbon through explicit subcomponents of the ecosystem are all advantages shared by no other method.

In the ^{14}C method, water samples with ambient plankton are placed in clear incubation bottles, and a tracer quantity of ^{14}C-labeled DIC is added (typically 1 to 20 μCi $liter^{-1}$). The samples are incubated, either in situ or in an incubator, as for the light and dark bottle technique. Generally, at the end of the incubation (typically 2 to 24 hours), the water is filtered, the sample acidified to remove inorganic ^{14}C and the ^{14}C on the filter counted in a scintillation counter. By measuring the ratio of ^{14}C to total inorganic carbon in the incubation, the rate of accumulation of ^{14}C in the particulate matter can be converted to a rate of uptake of carbon.

Many investigators use both light and dark bottles for a ^{14}C incubation. However, in this case, dark bottles are a combined measure of particulate contamination in the tracer (a blank control that should be subtracted) and dark carbon fixation, a real process for incorporating carbon into plankton that is temporally independent of light. The careful application of killed controls or deep-water samples can partially clarify this distinction. In careful incubations, much of the dark bottle uptake is dark carbon fixation. For an estimate of the total carbon incorporation into the ecosystem, this rate should be added to the light bottle rate. For an estimate of the light-dependent production rate, it should be subtracted. Fortunately, the dark carbon fixation rate is rarely more than 5% of the total integrated production, so, at the ecosystem level, it is a minor issue compared with some of the larger concerns with the accuracy and interpretation of the method.

As with the light and dark bottle oxygen method, there are many problems with this technique regarding the scaling from volume to surface area, the scaling from the time period of the incubation to a daily rate, the sampling of the water, and the isolating of the water sample in a bottle during incubations. These problems are discussed in the section on sampling issues below.

There are some problems or concerns specific to the $^{14}CO_2$ method. One of these is that ^{14}C-labeled organic matter formed during the incubation is sometimes released to solution, either excreted by the living phytoplankton or lysed from cells during the filtration. This results in an underestimation of primary production, if as is usually the case, the soluble ^{14}C material is not counted. An alternative to filtering the samples at the end of the incubation is to acidify the sample or filtrate, bubble off the remaining ^{14}C that has not been fixed in primary production, then sample some of the degassed water and count the ^{14}C (which represents both particulate and dissolved ^{14}C-labeled organic matter if it was not filtered) on a scintillation counter. Unfortunately, the rather small volume that can be counted in a scintillation results in a less sensitive assay than can be obtained by concentrating the particles from a larger volume onto a filter. Also, care must be taken to ensure that no ^{14}C-labeled DIC remains in solution (dark or killed controls can confirm this). The converse of this correction is that it allows the explicit separation of the productivity into particulate and soluble, a valuable distinction in ecosystems dominated by the microbial food web. Even here, the interpretation will have a few caveats as the glass-fiber filters commonly used for these experiments adsorb some of the dissolved organic matter, and some of the excreted dissolved organic matter will be respired to ^{14}C-labeled DIC by bacteria during the course of the incubation.

A conceptual problem with the ^{14}C technique is that it measures neither GPP nor NPP, but rather, in many ecosystems, some rate between these two (Peterson 1980; Bender et al. 1987; Collos et al. 1993). Simply stated, the method would measure GPP if incubations were instantaneously short. As an incubation starts, none of the organic matter within phytoplankton is labeled with ^{14}C, and so none of the organic matter respired by phytoplankton is labeled with ^{14}C. Therefore, in some types of ecosystems, a very short incubation measurement can sometimes approach an estimate of GPP (Collos et al. 1993), particularly in systems with high light irradiance (Sand-Jensen and Krause-Jensen 1997). However, as the incubation proceeds in time, more and more of the phytoplankton biomass is labeled with the radioisotope, and so an increasing percentage of the phytoplankton respiration includes respiration of the ^{14}C-labeled tissues. That is, as the incubation time increases, the net rate of ^{14}C uptake decreases from the rate of GPP and moves toward the rate of NPP. If phytoplankton were not grazed and the extracellular products of photosynthesis were not consumed by bacteria, then eventually a steady state would be approached where the phytoplankton biomass would be uniformly labeled and the amount of $^{14}CO_2$ respired would be a constant percentage of the total CO_2 respired. At this point, the ^{14}C method would be measuring NPP (assuming that the incubation included the nighttime dark cycle). However, it is unclear how long a time is required for an incubation to truly represent a measure of NPP, and the necessary length of time for this to occur probably varies among ecosystems, being faster in ecosystems with higher rates of turnover of the phytoplankton biomass. Zooplankton grazing on phytoplankton and bacterial consumption of dissolved organic carbon aggravate the interpretation of the ^{14}C method, for with longer incubations, these processes increasingly include the ingestion and respiration of labeled ^{14}C. Thus, long incubations may tend to-

ward measuring the net community production (NCP) of the plankton community. Note, however, that in many ecosystems at many points in time, NCP can be a negative number; although rarer, negative rates of NPP also occur. The ^{14}C method, however, always shows a positive rate of uptake. Note also that long incubations generally are not desirable since they aggravate what are called "bottle effects" (see below).

Some researchers have attempted to correct for the algal respiration that occurs during ^{14}C incubation (Wofsy 1983; Cole et al. 1992). However, the relationship between photosynthesis and respiration in phytoplankton is not easily predictable or measured. Respiration rates for phytoplankton vary from 5 to 50% of the rate of light-saturated photosynthesis (Raven and Beardall 1981). This makes it difficult to determine an empirical relationship between ^{14}C-labeled DIC assimilation and rates of GPP or NPP. Since the ^{14}C technique does not truly measure GPP (or NPP, NEP, or NCP), results are most commonly reported as just "primary production" or "^{14}C production." Despite problems with interpretation, using such data in a comparative manner across ecosystems has proven quite useful. For instance, Nixon et al. (1996) have demonstrated that ^{14}C production is well correlated with nitrogen inputs to estuarine and marine ecosystems across a wide range of inputs. However, one cannot use estimates of ^{14}C production to prepare carbon or nutrient budgets without making assumptions about how these rates relate to GPP and NPP (Howarth et al. 1996).

Problems and Challenges with Light and Dark Bottle and Carbon-14 Techniques

Photosynthesis is generally a nonlinear function of light intensity (irradiance). Production rates increase linearly with irradiance at low light levels. At some moderately high light level, photosynthetic rates saturate and then actually decrease at higher levels of irradiance due to photoinhibition processes. This relationship between light and photosynthesis is commonly called the "P versus I curve" (for photosynthesis vs. irradiance), and the relationship varies among different ecosystems, presumably because phytoplankton are well adapted or acclimated to the in situ light levels of the ecosystem where they occur (Gallegos and Platt 1981; Falkowski and LaRoche 1991). Therefore, when measuring production by either the light and dark bottle method or the ^{14}C technique, one ideally measures production rates over a range of light intensities that encompasses the spectrum seen by the plants. By using short-term in situ light measurements over depth in the ecosystem and the empirically determined P versus I curves, one can scale the rate measurements and estimate the in situ rate of production per square meter (Gallegos and Platt 1981). The use of an incubation chamber with a well-characterized gradient of light intensities simplifies this approach (Fee 1973, 1980), but P versus I curves can also be determined from incubating bottles in situ in the ecosystem if bottles are incubated at different depths (light intensity decreases with depth) and the irradiance is measured at each depth (Bower et al. 1987). Alternatively, one can incubate the samples for the entire diel period and trade off an increase in the accuracy of the light field for a longer incubation (with the concomitant increase in the potential for bottle artifacts).

In water masses where phytoplankton are continually buoyed in well-lit surface waters, the ^{14}C technique works fairly well when rates are extrapolated by use of a P versus I curve, as shown by good agreement with rates so derived and rates determined by whole-lake additions of ^{14}C-labeled DIC (Hesslein et al. 1980; Bower et al. 1987). However, simple integration of ^{14}C uptake rates measured in a series of bottles incubated in situ over depth can underestimate rates compared with whole-lake ^{14}C-labeled DIC additions (Bower et al. 1987). In some ecosystems, phytoplankton get mixed in the water column to depths below the compensation depth (the depth at which photosynthesis equals respiration by phytoplankton). This commonly occurs in deep, turbid rivers and, in the ocean, during deep winter mixing at high latitudes. To estimate ^{14}C production in such systems, one must be able to estimate what percentage of time phytoplankton spend at different light levels while being mixed through the water column (Lewis 1988; Cole et al. 1991, 1992). In such systems, ^{14}C production can be quite difficult to interpret, as phytoplankton respiration is such a great percentage of GPP due to the high percentage of time spent

in the dark. GPP can be many times greater than either ^{14}C production or NPP, and NPP can in fact be a negative value if phytoplankton spend too large a proportion of their day below the compensation depth and total daily respiration by phytoplankton exceeds GPP (Cole et al. 1991, 1992; Howarth et al. 1996). In ocean systems, the depth above which rates of GPP and phytoplankton respiration are equal when integrated over the water column is called the "critical depth." When the depth of the mixed layer is greater than this critical depth, so that phytoplankton are mixed in such a way that their total respiration rate integrated over the water column exceeds their total rate of GPP, NPP is negative. When the depth of mixing is shallow compared with the critical depth, GPP becomes proportionally greater than phytoplankton respiration, and NPP increases. This concept has shown great utility in explaining the seasonal limits to phytoplankton growth in the North Atlantic Ocean (Sverdrup 1953).

Perhaps the greatest challenge associated with the use of incubation techniques is the difference between the natural ecosystem and the portion of the system that is contained in the bottle. These so-called "bottle effects" have been the focus of large amounts of study, most of which has been more valuable for highlighting the problems than for providing an unambiguous set of solutions. A few of the key issues are discussed below.

One area of concern that now seems to have achieved consensus regards contamination with trace metals. From the earliest incubation experiments, it was recognized that contamination of the sample in the bottle would compromise the measurement. Rigorous cleaning regimes were defined with most methods. However, in the 1980s, a revolution in the analytical ability to measure trace metals in seawater completely changed the perspective of the word "clean" for the open ocean. Trace metals that had been thought to exist at micromolar concentrations were found to exist at nanomolar and even picomolar concentrations (Bruland 1980; Boyle et al. 1981). Careful incubations that compared natural concentrations with the previous levels of cleanliness showed large differences in production rates, with production usually higher at the natural levels of trace metals and production partially suppressed due to toxic effects from the higher levels of trace metals found usually traditional techniques (e.g., Fitzwater et al. 1982). Conversely, small additions of trace metals above background levels sometimes seem to enhance production after a few days, particularly in parts of the ocean where macronutrients persisted through the year (Martin et al. 1989). These experiments indicated that trace metal limitation for iron, zinc, and perhaps other metals could be an important control on these ecosystems.

In the past decade, a standard, trace-metal clean protocol has evolved for oceanic ecosystems. This protocol carefully redefines every step of the ^{14}C protocol to remove even trace levels of contamination in the sample. All of the sampling gear and the incubation bottles are rigorously cleaned with a multistage acid-cleaning procedure. Samples are collected with samplers that can pass through the air–sea interface closed and open and close at depth to gather the sample. General Oceanics Go-Flo bottles are most commonly used. These are deployed on nonmetal cables (usually Kevlar) or on trace-metal clean rosettes. Samples are drawn into the incubation bottles using the same precautions that the trace-metal chemists use to prevent contamination. The ^{14}C innoculum is prepared to either reduce the trace-element concentration or cleaned by passing it through a chelation column. Using these precautions, trace-metal concentrations in the incubation bottles are near background. Rates of production with "clean techniques" appear to be two- to fourfold higher than those from before these techniques were adopted (Michaels and Knap 1996). In coastal waters and most freshwater systems, trace-element concentrations are naturally higher and these extreme measures may not be required.

Another general problem with both the light and dark bottle method and the ^{14}C technique is the inherent isolation of the phytoplankton from the natural system by placement in a bottle (Collos et al. 1993). Within the incubation bottle, turbulence is reduced, which may reduce the rate of nutrient uptake due to increased boundary layers around cells, particularly in high-turbulence ecosystems such as rivers and estuaries (Nixon et al. 1979; Richey et al. 1990; Howarth et al. 1992). The total nutrient pools or pools of DIC and CO_2 in incubation bottles may also become depleted to the extent the water is isolated from pathways of remineralization and mixing. Within 6 to 24 hours, there can be signifi-

cant changes in the community structure within the bottle compared with the natural system, particularly in the bacteria. Some of these changes are due to the growth of organisms that live on surfaces (the wall of the bottle) and thus not representative of the purely aqueous system. The large aggregate particles called "marine snow" become destroyed by the collection process or settle to the bottom of the sampler and are underrepresented in the sample (Gardner 1977). Further, the incubation bottles rarely exceed a liter in volume. Large grazing animals will not be included in the incubation bottles and the change in grazing pressure may affect rates of production (Collos et al. 1993).

In Situ Diel Approaches

In situ diel methods use changes in dissolved O_2, CO_2 or particle matter over a 24-hour period to infer rates of GPP and respiration. Where this approach is feasible, it is often preferable to bottle-incubation methods since natural levels of turbulence, grazing, nutrient availability, and light fields are maintained and since accurate integration in space and time is possible. The basic approach is simple and relatively easy to apply to nonflowing systems with relatively high rates of production, such as ponds. In oceanic environments, similar methods have been used where spatial heterogeneity on scales of kilometers seems smaller than the diurnal variability.

For the dissolved gas methods, the in situ concentration of O_2 or CO_2 is measured over time both during daylight and at night. The rate of change during daylight hours is a function of GPP, respiration by all organisms, and exchange of gases with the atmosphere. The rate of change in oxygen overnight is the net result of respiration by all organisms and the exchange of gases with the atmosphere. Generally O_2 decreases at night and increases during the day, while CO_2 increases at night and decreases during the day, but this need not always be so. For instance, O_2 concentrations can decrease during daylight hours if rates of respiration are sufficiently greater than GPP or if the supersaturation of the surface waters by cooling or previous production causes a gas flux to the atmosphere that exceeds net ecosystem production during the day.

By correcting for the atmospheric exchange of O_2 (or CO_2) at night, the rate of whole-ecosystem respiration can be estimated by the nighttime changes in concentration. For instance, if O_2 is undersaturated in the water body, there is a flux of O_2 from atmosphere to the water, and this needs to be added to the rate of decrease in O_2 during the night to estimate respiration; if O_2 is supersaturated, there is a net flux of O_2 from the water to the atmosphere, and this must be subtracted from the rate of decrease in dissolved O_2 to estimate respiration. Approaches for estimating atmospheric exchanges are discussed below. If one assumes that the rate of respiration is the same during the day as at night, then the daily rate of respiration can be estimated by multiplying the hourly nighttime respiration by 24 hours. This assumption that respiration rates are constant between night and day is not necessarily true, as diel temperature changes, photorespiration by phytoplankton, or bacterial responses to organic carbon excretion from phytoplankton during active photosynthesis may all tend to make respiration rates greater during the daytime.

GPP can be estimated by determining the hourly rate of O_2 change during daylight hours, adding the rate of whole-ecosystem respiration determined at night to this (since the O_2 would have increased more rapidly during the day if some of it were not being respired away), and correcting for atmospheric exchange of O_2. To obtain a daily rate of GPP, this hourly rate is multiplied by the number of daylight hours. If changes in CO_2 are used rather than O_2, then the respiration rate is subtracted from the rate of change of CO_2 during daylight. Generally, changes in O_2 rather than CO_2 are used because the measurement is analytically easier, often changes are easier to detect (if concentrations of dissolved O_2 are less than dissolved CO_2, as is true in seawater), and nonbiological processes such as carbonate precipitation and dissolution need not be considered. However, a detailed comparison of using both gases to measure production in estuarine mesocosms yielded similar results (Oviatt et al. 1986).

Some of the first uses of in situ diel methods to estimate GPP were in small streams and rivers (Odum 1956; Edwards and Owens 1962). In such systems, rates of gas exchange with the atmosphere can be estimated from the partial-pressure gradient between the water and the atmosphere

and an estimate of turbulence caused by the flowing waters interacting with bottom topography (O'Connor and Dobbins 1958; Bennet and Rathbun 1972; O'Connor 1984; Roberts 1984). However, in deeper waters, currents and bottom topography have little or no influence on gas exchange with the atmosphere; rather, gas exchange is controlled by turbulence generated through wind shear on the surface (Jirka and Brutsaert 1984; Marino and Howarth 1993). Marino and Howarth (1993) found relatively good agreement among a variety of methods for estimating gas exchange with the atmosphere in a variety of lakes, estuaries, and open-ocean sites. Using that compilation, atmospheric exchange of oxygen can be estimated by the equation:

$$F = k[C_w - (P_a \times K_h)] \qquad (5.3)$$

where F is the gas flux per surface area of water, k is the "piston velocity," C_w is the molar concentration of gas in solution, P_a is the partial pressure of gas in the atmosphere, and K_h is the Henry's Law constant (Fig. 5.1). The term $[C_w - (P_a \times K_h)]$ describes the partial pressure gradient of the gas. The piston velocity, k, is a function of wind velocity, with ln K increasing linearly with increasing wind. Thus, for many lakes, open-ocean systems, estuaries, and relatively deep rivers, the atmospheric exchange of oxygen can be estimated from data on wind and the extent of oxygen undersaturation or supersaturation (Marino and Howarth 1993; Howarth et al. 1992). However, care should be taken to ensure that this estimation approach will work in any particular ecosystem of interest. Recently, Kremer et al. (1999) have demonstrated for one

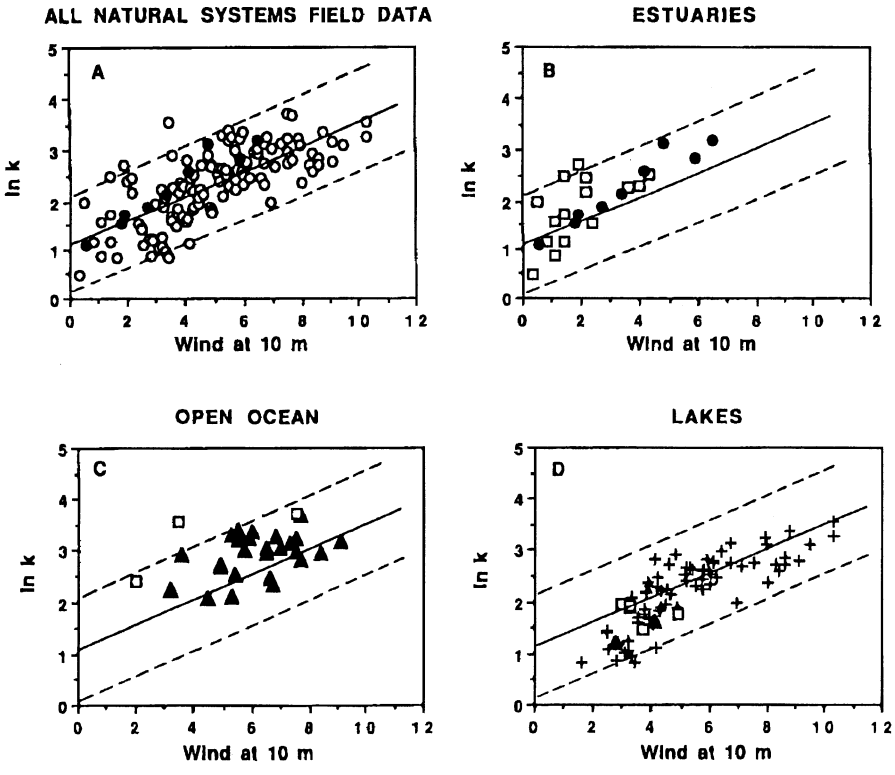

FIGURE 5.1. The relationship between wind and the "piston velocity" controlling oxygen exchange with the atmosphere for a variety of lakes, estuaries, and open-ocean sites. Upper left panel includes all data from the other three panels. The dashed lines indicate 95% confidence limits for the regressions. See text for further explanation. (From Marino and Howarth [1993].)

shallow estuary that rates of oxygen exchange at any given wind velocity were less than predicted from the regression in Marino and Howarth (1993), perhaps because the shallowness of the water column reduced the amount of surface turbulence created by the wind shear.

In situ diel techniques work best when the correction for atmospheric exchange is relatively small, since there can be a significant error associated with this correction (Howarth et al. 1992; Marino and Howarth 1993). The exchange of oxygen with the atmosphere is a function both of wind and of the gradient in partial pressures; thus, this correction is least when oxygen concentrations are near saturation levels. Consequently, the atmospheric exchange becomes greater as either GPP becomes much greater than respiration (leading to degassing of oxygen from the water to the atmosphere) or as respiration becomes much greater than GPP (leading to large fluxes from atmosphere to water). Further, for a given amount of production per area, changes in oxygen concentration are greater in more shallow water columns, leading to steeper gradients with the atmosphere. Consequently, in situ diel techniques have the greatest precision and accuracy in deeper water columns and in ecosystems where GPP and respiration are roughly equal and relatively high (Marino and Howarth 1993).

When applied to nonflowing waters, in situ diel techniques can simply measure changes in O_2 or CO_2 over 24 hours at one location (Nixon and Oviatt 1972; Oviatt et al. 1986). The situation is more complex in flowing waters. One approach has been to sample at only one location, and simply assume that the waters upstream are homogenous so that the one station represents the entire ecosystem (Odum 1956). Another approach in rivers is to compare dissolved gas concentrations at two stations, and infer rates of metabolism from the difference between the two stations and a knowledge of the time of travel for water between the two stations (Owens 1969). A third approach used in a tidal river with a high rate of mixing but with water advection changing direction over the tidal cycle is to measure diel changes at many stations spaced more broadly than the range of tidal flow over a day and simply average the station results (Howarth et al. 1992). In large, partially mixed estuaries with complex circulation patterns, the use of in situ diel techniques for estimating GPP and respiration has proven problematical (Kemp and Boynton 1980). However, recently Swaney et al. (1999) have demonstrated a multistation technique in which oxygen concentrations are regressed across stations as a function of depth, salinity, and time. The time-dependent rate of change of oxygen as a function of depth and salinity can be used to obtain reasonably high-precision estimates of GPP and respiration despite complex estuarine circulation.

An analogous approach has been developed for diel changes in particles in the oceanic water column (Siegel et al. 1989; Walsh et al. 1995). In this approach, an optical instrument called a beam transmissometer is used as a rapid profiler to collect data on the vertical patterns in the attenuation of light. The instrument emits a 25-cm-long beam of light at 665-nm wavelength. The attenuation of this beam of light is recorded and corrected for the attenuation of pure water to estimate the attenuation from the scattering by particles. Samples of the suspended particles are collected on filters and compared with the optical measurement to determine a regression between optical attenuation and particulate organic carbon.

The attenuation of light in oceanic waters sometimes shows a marked diel pattern with daytime maxima and nighttime minima. The variable fraction of the particulate matter is likely due to biological production and removal terms, although changes in cell size, particle aggregation, and other processes can cause diel patterns that are not related to biomass (Durand and Olson, 1996). After correction to suspended particulate variations with the calculated regression, this approach allows an estimate of the diurnal fluctuations in particulate organic matter. These correlate well with the production measured by ^{14}C incubations (Siegel et al. 1989). As with the gas methods, the nocturnal decrease is a measure of particle removal or respiration. The daylight increase is the total particle production (analogous to NPP). When corrected for the nocturnal respiration (with the same assumptions as above), the total production is probably analogous to GPP. This method has a variety of assumptions that are difficult to test. It has the advantage that it is very easy to make and it can be done automatically from moorings or electronic profiling packages.

Remote Sensing Techniques

The advent of ocean color satellites provides an opportunity to measure aquatic biology from space with global coverage and near-daily temporal resolution. The Coastal Zone Color Scanner provided limited data through the late 1970s and early 1980s and the SeaWiFS satellite now provides global resolution on a daily basis (e.g., Gordon and Morel 1983; McClain et al. 1998). This has resulted in a suite of bio-optical approaches for determining primary production from space-based platforms (e.g., Platt et al. 1991; Bidigare et al. 1992; Antoine and Morel, 1996; Behrenfeld and Falkowski, 1997).

Ocean color satellites work by measuring the amount of upwelled radiance from the earth's surface in a limited number of visible wavelengths. They provide a spatial resolution of about 1 km and thus can be usable for larger lakes and the oceans. However, the data from these satellites can be quite tricky to work with. First, there are nontrivial issues associated with determining the stability and accuracy of the satellite-determined radiance measurements and correcting them for atmospheric influences. This provides a determination of the water leaving radiance, or the ocean color spectrum.

The second complicating factor is the conversion of the ocean color spectrum into a measurement of interest, such as the chlorophyll concentration. An excellent comparison of methods to determine chlorophyll from ocean color determinations can be found in O'Reilly et al. (1998). Other recent techniques allow for the determination of the amount of chlorophyll, detritus, and colored organic material concentrations, as well as particulate backscattering intensity (e.g., Garver and Siegel, 1997).

The third major issue is the specification of photo-physiological parameters (P vs. I characteristics, quantum yields for carbon assimilation, etc.) for use in bio-optical primary production models. A variety of approaches have been used. Some investigators assume that these parameters are fixed for a given biogeochemical province (e.g., Platt et al. 1991). Obviously, this method subsumes much of the natural ecosystem variability into the algorithm. Other investigators parameterize them in terms of measurable quantities (e.g., Bidigare et al. 1992; Antoine and Morel, 1996). In all, the success of these approaches is rather poor, accounting for 30 to 40% of the variability in production within an ecosystem and not much more when evaluated globally (e.g., Balch et al. 1992; Campbell and O'Reilly, 1988; Siegel et al. 1995). However, all of these remote sensing techniques make up for their accuracy limitations by the enormous increase in information on spatial and temporal patterns that are seen from space. Carefully used in conjunction with field measurements, these tools can and will help to revolutionize our understanding of aquatic productivity.

Acknowledgments Dave Siegel provided valuable advice on remote sensing techniques. We thank Tom Butler, Jon Cole, and Roxanne Marino for helpful comments on an earlier draft of this chapter. Preparation of the manuscript was supported in part by a grant to RWH from the Hudson River Foundation, a not-for-profit foundation with headquarters in New York.

References

Antoine, D.; and Morel, A. Oceanic primary production. 1. Adaptation of a spectral light-photosynthesis model in view of application to satellite chlorophyll observations. Global Biogeochem. Cycl. 10:43–55; 1996.

Arîstegui, J.; Monero, M.F.; Ballesteros, S.; Basterretxea, G.; van Lenning, K. Planktonic primary production and microbial respiration measured by ^{14}C assimilation and dissolved oxygen changes in coastal waters of the Antarctic peninsula during austral summer: Implications for carbon flux studies. Mar. Ecol. Prog. Ser. 132:191–201; 1996.

Balch, W.M., Evans, R.; Brown, J.; Feldman, G.; McClain, C.; W. Esaias, W. The remote sensing of ocean primary productivity—the use of a new data compilation to test satellite algorithms. J. Geophys. Res. 97:2279–2293; 1992.

Behrenfeld, M.J.; and Falkowski, P.G. Photosynthetic rates derived from satellite-based chlorophyll concentration. Limnol. Oceanogr. 42:1–20; 1997.

Bender, M.; Grande, K.; Johnson, K.; Marra, J.; Williams, P.J.L.; Sieburth, J.; Milson, M.; Langdon, C.; Hitchock, G.; Orchardo, J.; Hunt, C.; Donaghay, P.; Heinemann, K. A comparison of four methods for determining planktonic community production. Limnol. Oceanogr. 32:1085–1098; 1987.

Bennet, J.P.; Rathbun, R.E. *Reaeration in Open-Channel Flow.* U.S. Geological Survey (USGS) Paper 737.

Washington, DC: U.S. Government Printing Office; 1972.

Bidigare, R.R.; Prézelin, B.B.; and Smith, R.C. Bio-optical models and the problems of scaling. In: Falkowski, P.B.; Woodhead, A.D., eds. *Primary Productivity and Biogeochemical Cycles in the Sea.* New York: Plenum; 1992:175–212.

Bower, P.M.; Kelly, C.A.; Fee, F.J.; Shearer, J.A.; DeClercq, D.R.; Schindler, D.W. Simultaneous measurement of primary production by whole-lake and bottle radiocarbon additions. Limnol. Oceanogr. 32:299–312; 1987.

Boyle, E.A.; Huested, S.S.; Jones, S.P. On the distribution of Cu, Ni, and Cd in the surface waters of the North Atlantic and North Pacific Oceans. J. Geophys. Res. 86:8048–8066; 1981.

Bruland, K.W. Oceanographic distributions of cadmium, zinc, nickel and copper in the North Pacific. Earth Planet. Sci. Lett. 47:176–198; 1980.

Carpenter, S.R.; Caraco, N.F.; Correll, D.L.; Howarth, R.W.; Sharpley, A.N.; Smith, V.H. Nonpoint pollution of surface waters with phosphorus and nitrogen. Ecol. Applic. 8:559–568; 1998.

Cole, J.J.; Caraco, N.F.; Peierls, B. Phytoplankton primary production in the tidal, freshwater Hudson River, New York (USA). Verh. Int. Verein. Limnol. 24:1715–1719; 1991.

Cole, J.J.; Caraco, N.F., Peierls, B. Can phytoplankton maintain a positive carbon balance in a turbid, freshwater, tidal estuary? Limnol. Oceanogr. 37:1608–1617; 1992.

Collos, Y.; Descolas-Gros, C.; Fontugne, M.; Mortain-Bertrand, A.; Chretiennot-Dinet, M.J.; Frikha, M.G. Chemical, isotopic and enzymatic monitoring of free and enclosed seawater: implications for primary production estimates in incubation bottles. Mar. Ecol. Prog. Ser. 93:49–54; 1993.

Durand, M.D.; Olson, R.J. Contributions of phytoplankton light-scattering and cell concentration changes to diel variations in beam attenuation in the equatorial Pacific from flow cytometric measurements of picoplankton, ultraplankton and nanoplankton. Deep-Sea Res. 43:891–906; 1996.

Edwards, R.W.; Owens, M. The effects of plants on river conditions. IV. The oxygen balance of a chalk stream. J. Ecol. 50:207–220; 1962.

Falkowski, P.G.; LaRoche, J. Acclimation to spectral irradiance in algae. J. Phycol. 27:8–14; 1991.

Fee, E.J. Modeling primary production in water bodies: A numerical approach that allows vertical inhomogeneities. J. Fish. Res. Bd. Can. 30:513–522; 1973.

Fee, E.J. Important factors for estimating annual phytoplankton production in the Experimental Lakes Area. Can. J. Fish. Aquat. Sci. 37:513–522; 1980.

Fitzwater, S.E.; Knauer, G.A.; Martin, J.H. Metal contamination and its effect on primary production measurement. Limnol. Oceanogr. 27:544–551; 1982.

Gaarder, T.; Gran, H.H. Investigation of the production of plankton in the Oslo Fjord. Rapp. P.-v. Cons. Int. Explor. Mer. 42:1–48; 1927.

Gallegos, C.L.; Platt, T. Photosynthesis measurements on natural populations of phytoplankton: Numerical analysis. Can. Bull. Fish. Aquat. Sci. 210:103–112; 1981.

Gardner, W.D. Incomplete extraction of rapidly settling particles from water samplers. Limnol. Oceanogr. 22:764–768; 1977.

Garver, S.A.; Siegel, D.A. Inherent optical property inversion of ocean color spectra and its biogeochemical interpretation. 1. Time series from the Sargasso Sea. J. Geophys. Res. Oceans 102:18607–18625; 1997.

Gordon, H.R.; Morel, A.Y. *Remote assessment of ocean colour for interpretation of satellite visible imagery: A review.* Lecture Notes on Coastal and Estuarine Studies, 4. New York: Springer-Verlag; 1983.

Hesslein, R.H.; Broecker, W.S.; Quay, P.D. Whole-lake radiocarbon experiment in an oligotrophic lake at the Experimental Lakes Area, northwestern Ontario. Can. J. Fish. Aquat. Sci. 37:454–463; 1980.

Howarth, R.W.; Marino, R.; Garritt, R.; Sherman, D. Ecosystem respiration and organic carbon processing in a large, tidally influenced river: The Hudson River. Biogeochem. 16:83–102; 1992.

Howarth, R.W.; Schneider, R.; Swaney, D. Metabolism and organic carbon fluxes in the tidal freshwater Hudson River. Estuaries 19:848–865; 1996.

Jirka, G.A.; Brutsaert, W. Measurements of wind effects on water-side controlled gas exchange in riverine systems. In: Brutsaert, W.; Jirka, G.H., eds. *Gas Transfer at Water Surfaces.* Dordrecht: Reidel; 1984: 437–446.

Kemp, W.M.; Boynton, W.R. Influence of biological and physical process on dissolved oxygen dynamics in an estuarine system: Implication for measurement of community metabolism. Est. Coast. Mar. Sci. 11:407–431; 1980.

Kremer, J.N.; Reischauer, A.; D'Avanzo, C. Estuary-specific variation in the air-water gas exchange coefficient for oxygen. Estuaries, submitted; 1999.

Lewis, W.M. Primary production in the Orinoco River. Ecology 69:679–692; 1988.

Li, W.K.W; Maestrini, S.Y., eds. *Measurement of Primary Production from the Molecular to the Global Scale.* ICES Symposium Vol. 197. Copenhagen: ICES Secretariat; 1993.

Lohrenz, S.E.; Wiesenburg, D.A.; Rein, C.R.; Arnone, R.A.; Taylor, C.D.; Knauer, G.A.; Knap, A.H. A comparison of in situ and simulated in situ methods for estimating oceanic primary production. J. Plank. Res. 14:201–221; 1992.

Marino, R.; Howarth, R.W. Atmospheric oxygen exchange in the Hudson River: Dome measurements and comparison with other natural waters. Estuaries 16:433–445; 1993.

Martin, J.H.; Gordon, R.M.; Fitzwater, S.; Broenkow, W.W. VERTEX: Phytoplankton/iron studies in the Gulf of Alaska. Deep-Sea Res. 36:649–680; 1989.

Michaels, A.F.; Knap, A.H. Overview of the U.S. JGOFS Bermuda Atlantic Time-series Study and the Hydrostation S Program. Deep-Sea Res. II 43:157–198; 1996.

McClain, C.R.; Cleave, M.L.; Feldman, G.C.; Gregg, W.W.; Hooker, S.B.; Kuring, N. Science Quality SeaWiFS Data for Global Biosphere Research. Sea Technol. September:10–16; 1998.

[NRC] National Research Council. *Managing Wastewater in Coastal Urban Areas.* Washington, DC: National Academy; 1993.

Nixon, S.W.; Ammerman, J.W.; Atkinson, P.; Berounsky, V.M.; Billen, G.; Boicourt, W.C.; Boynton, W.R.; Church, T.M.; DiToro, D.M.; Elmgren, R.; Garber, J.H.; Giblin, A.E.; Jahnke, R.A.; Owens, N.J.P.; Pilson, M.E.Q.; Seitzinger, S.P. The fate of nitrogen and phosphorus at the land-sea margin of the North Atlantic Ocean. Biogeochem. 35:141–180; 1996.

Nixon, S.W.; Oviatt, C.A. Preliminary measurements of midsummer metabolism in beds of eelgrass, *Zostera marina.* Ecology 53:150–153; 1972.

Nixon, S.W.; Oviatt, C.A.; Buckley, B.A. Turbulent mixing in mesocosms—some relative measures and ecological consequences. In: Jacoff, F.S. ed. *Advances in Marine Environmental Research.* U.S. Environmental Protection Agency (EPA) Report EPA-600/9-79-035. Narragansett, RI: US EPA; 1979:382–409.

O'Connor, D.J. Turbulent transfer across smooth and rough surfaces. In: Brutsaert, W.; Jirka, G.H., eds. *Gas Transfer at Water Surfaces;* Dordrecht: Reidel; 1984:321–331.

O'Connor, D.J.; Dobbins, W.E. Mechanism of reaeration in natural streams. Am. Soc. Civ. Eng. Trans. 123:641–684; 1958.

Odum, H.T. Primary production in flowing waters. Limnol. Oceanogr. 1:102–117; 1956.

OReilly, J.E.; Maritorena, S.; Mitchell, B.G.; Siegel, D.A.; Carder, K.L.; Garver, S.A.; Kahru, M.; McClain, C. Ocean color chlorophyll algorithms for SeaWiFS. J. Geophys. Res. Oceans 103:24937–24953; 1998.

Oviatt, C.A.; Rudnick, D.T.; Keller, A.A.; Sampou, P.A.; Almquist, G.T. A comparison of system (O_2 and CO_2) and C-14 measurements of metabolism in estuarine mesocosms. Mar. Ecol. Prog. Ser. 28:57–67; 1986.

Owens, M. Some factors involved in the use of dissolved-oxygen distributions in streams to determine productivity. In: Goldman, C.R., ed. *Primary Productivity in Aquatic Environments.* Berkeley, CA: Univ. of California Pr.; 1969.

Peterson, B.J. Aquatic primary productivity and the ^{14}C-CO_2 method: A history of the productivity problem. Annu. Rev. Ecol. Syst. 11:359–385; 1980.

Platt, T.; Caverhill, C.M.; Sathyendranath, S. Basin-scale estimates of oceanic primary production by remote sensing: The North Atlantic. J. Geophys. Res. 96:15147–15159; 1991.

Platt, T. Harrison, W.G. Reconciliation of carbon and oxygen fluxes in the upper ocean. Deep-Sea Res. 33:273–276; 1986.

Raine, R.C.T. The effects of nitrogen supply on the photosynthetic quotient of natural phytoplankton assemplages Botanica Marina 26:417–423; 1983.

Raven, J.A.; Beardall, J. Respiration and photorespiration. Can. Bull. Fish. Aquat. Sci. 210:55–82; 1981.

Richey, J.E.; Devol, A.H., Hedges, J.I., Forsber, B.R.; Victoria, R.L.; Martinellis, L.A.; Ribeiro, N. Distributions and flux of carbon in the Amazon River. Limnol. Oceanogr. 35:352–371; 1990.

Roberts, P.V. Dependence of oxygen transfer rate on energy dissipation during surface aeration and in stream flow. In: Brutsaert, W.; Jirka, G.H., eds. *Gas Transfer at Water Surfaces.* Dordrecht: Reidel; 1984.

Ryther, J.H. Photosynthesis in the ocean as a function of light intensity. Limnol. Oceanogr. 1:61–70; 1956.

Sakshaug, E.; Bricaud, A.; Dandonneau, Y.; Falkowski, P.G.; Kiefer, D.A.; Legendre, L.; Morel, A.; Parslow, J.; Takahaski, M. Parameters of photosynthesis: Definitions, theory, and interpretation of results. J. Plank. Res. 19:1637–1670; 1997.

Sand-Jensen, K.; Krause-Jensen, D. Broad-scale comparison of photosynthesis in terrestrial and aquatic plant communities. Oikos 80:203–208; 1997.

Siegel, D.A.; Dickey, T.D.; Washburn, L.; Hamilton, M.K. Mitchell, B.G. Optical determination of particulate abundance and production variations in the oligotrophic ocean. Deep-Sea Res. 36:211–222; 1989.

Siegel, D.; Michaels, A.F.; Sorensen, J.C.; O'Brien, M.C.; Hammer, M. Seasonal variability of light availability and its utilization in the Sargasso Sea. J. Geophys. Res. 100:8695–8713; 1995.

Steeman Nielsen, E. The use of radioactive carbon (^{14}C) for measuring organic production in the sea. J. Cons. Int. Explor. Mer. 18:117–140; 1952.

Sverdrup, H.U. On conditions for the vernal blooming of phytoplankton. J. Cons. Int. Explor. Mer. 18:287–296; 1953.

Swaney, D.P.; Howarth, R.W.; Butler, T.J. A novel approach for estimating ecosystem production and respiration in estuaries: Application to the oligohaline

and mesohaline Hudson River estuary. Limnol. Oceanogr. 44:1509–1521; 1999.

Vitousek, P.M.; Aber, J.D.; Howarth, R.W.; Likens, G.E.; Matson, P.A.; Schindler, D.W.; Schlesinger, W.H.; Tilman, D. Human alteration of the global nitrogen cycle: Sources and consequences. Ecol. Applic. 7:737–750; 1997.

Walsh, I.D.; Chung, S.P., Richardson, M.J.; Gardner, W.D. The diel cycle in the integrated particle load in the Equatorial Pacific: A comparison with primary production. Deep-Sea Res. 42:465–477; 1995.

Williams, P.J.L.; Jenkinson, N.W. A transportable microprocessor-controlled precise Winkler titration suitable for field station and shipboard use. Limnol. Oceanogr. 27:576–584; 1982.

Wofsy, S.C. A simple model to predict extinction coefficients and phytoplankton biomass in eutrophic waters. Limnol. Oceanogr. 28:1144–1155; 1983.

6

Benthic Respiration in Aquatic Sediments

Bo Thamdrup and Donald E. Canfield

Introduction

Sediments make up an important compartment in the energy flow of aquatic ecosystems. On the continental shelves, 10 to 50% of the primary production reaches the sea-floor, most of which is mineralized there (Suess 1980; Wollast 1991; Canfield 1993). Through the balance between retention and release of nutrients, benthic mineralization influences the nutrient dynamics of the ecosystem (e.g., Howarth 1988), and through their regulatory effect on the burial of residual carbon and associated nutrients, mineralization processes may also affect the global cycles of these elements (Canfield 1994; Hedges and Keil 1995).

The mineralization of organic matter, that is, its biologically catalyzed degradation to inorganic carbon and nutrients, proceeds in sediments through several different pathways involving different organisms. The generalized scheme involves extracellular hydrolysis, fermentative transformations, and respiratory oxidation. In addition to the respiration with oxygen by bacteria and zoobenthos, nitrate, manganese oxides, iron oxides, and sulfate may serve as terminal electron acceptors in bacterial respiration (Table 6.1). Only organisms that respire with oxygen or nitrate are able to carry out the complete oxidation of hydrolysates to carbon dioxide (CO_2), while the anaerobic bacteria depend on coexisting fermentative organisms that transform the hydrolysates to secondary substrates such as acetate and hydrogen. Some CO_2 may be released during fermentations (Schink 1988) but as the reduced fermentation products are rapidly consumed, an overall balance of CO_2 production and respiration is expected (Sørensen et al. 1981; Parkes et al. 1989). In the absence of inorganic electron acceptors, organic matter is mineralized through methanogenesis without any net oxidation of carbon (see Table 6.1).

The relative importance of the different mineralization pathways in a given sediment depends on factors such as bottom water chemistry, sedimentation rate, and bulk sediment composition. Locations have been found where any of the pathways in Table 6.1 dominates carbon degradation (reviewed by Jørgensen 1983; Henrichs and Reeburgh 1987; Canfield 1993; see also Aller 1990; Canfield et al. 1993a). Sediments typically exhibit a vertical redox zonation where the oxidants are depleted in the order oxygen > nitrate > manganese oxide > iron oxide > sulfate (e.g., Froelich et al. 1979; Canfield et al. 1993a). However, the exclusion of less favorable pathways of respiration is often not complete, and a considerable spatial overlap between respiratory types is observed (Canfield and Des Marais 1991; Jørgensen and Bak 1991; Canfield et al. 1993a; Brandes and Devol 1995).

Parallel to carbon oxidation, the electron acceptors are also consumed in the reoxidation of the reduced inorganic metabolites produced during mineralization. These include reduced manganese and iron, sulfide, and methane (see Table 6.1), as well as ammonia. Each reduced species can potentially be oxidized with an electron acceptor higher in the redox sequence listed above, and many of these pathways appear to function in sediments through either abiotic reaction, lithotrophic bacterial catalysis, or both. This adds considerable complexity to the benthic processes (Fig. 6.1). Reoxi-

TABLE 6.1. Generalized stoichiometries of carbon mineralization pathways in sediments.

Oxygen respiration:

$$CH_2O + O_2 \rightarrow CO_2 + H_2O$$

Denitrification:

$$5CH_2O + 4NO_3^- \rightarrow 5HCO_3^- + 2N_2 + H^+ + 2H_2O$$

Manganese reduction:

$$CH_2O + 2MnO_2 + H_2O \rightarrow HCO_3^- + 2Mn^{2+} + 3OH^-$$

Iron reduction:

$$CH_2O + 4Fe(OH)_3 \rightarrow HCO_3^- + 4Fe^{2+} + 7OH^- + 3H_2O$$

Sulfate reduction:

$$2CH_2O + SO_4^{2-} \rightarrow 2HCO_3^- + 2HS^-$$

Methanogenesis:

$$2CH_2O \rightarrow CO_2 + CH_4$$

dation is an essential part of manganese, iron, and sulfur cycles in sediments where typically 90% or more of the reduced species produced during mineralization are recycled (Jørgensen 1982; Canfield et al. 1993b; Thamdrup et al. 1994a). Also, a large part of the ammonia formed is nitrified to nitrate. Thus, a substantial amount of electron acceptor utilization may be coupled to reoxidation. No methods are available for the direct, separate quantification of organotrophic, lithotrophic, and abiotic consumption of electron acceptors, and it is a major challenge in the measurement of benthic respiration to distinguish among these different types of processes.

In this paper, we review methods for the quantification of total rates of benthic mineralization as well as of the individual respiratory pathways. Our emphasis is on the conditions met on the continental margins from coast to slope, but the application of the methods to freshwater and deep-sea sediments is also discussed. We further focus on direct experimental techniques rather than quantifications

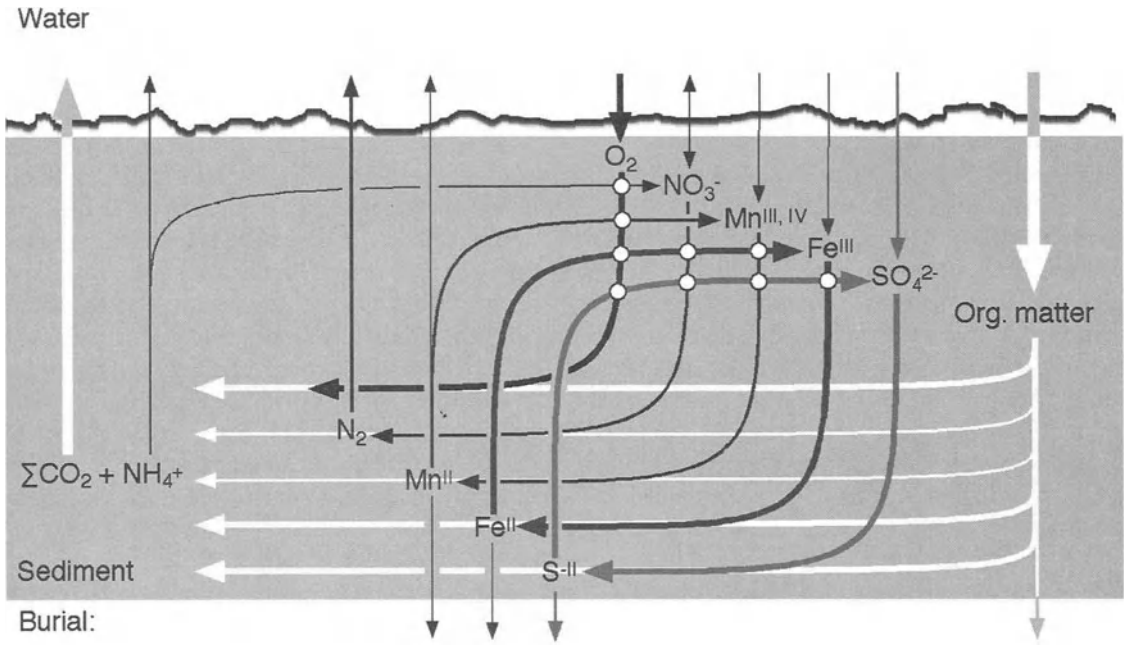

FIGURE 6.1. Interactions of C, O, N, Mn, Fe, and S cycles in the sediment. A rough indication of the importance of the individual fluxes and reactions in continental margin sediments is given by the width of the arrows. Circles at intersections indicate reoxidation reactions that have been identified in sediments (see text for details).

based on diagenetic models. Such models are generally not an alternative to direct rate measurements, mainly due to limitations in the mathematical description of transport through bioturbation. In combination with direct measurements, however, models are an extremely useful tool for, for example, verifying experimental results, extracting information on processes that cannot be measured directly, and testing hypothetical scenarios (Berner 1980; Wang and Van Cappellen 1996; Boudreau 1997).

Total Benthic Mineralization, Flux Measurements

The earliest and still most widely used measure of total benthic mineralization is the oxygen (O_2) uptake of the sediment (Pamatmat 1977; Smith and Hinga 1983). Its use, even in sediments where anaerobic respiration predominates, is based on the general observation that in sediments underlying well-oxygenated waters, reduced inorganic metabolites are largely reoxidized within the sediment, and that O_2 is therefore the ultimate acceptor of nearly all electron equivalents from organic carbon (C) (see Fig. 6.1). The nitrogen gas (N_2) formed during denitrification is an obvious exception, which, however, only accounts for a major fraction of mineralization in sediments that contact bottom water with a low oxygen/nitrate (O_2/NO_3^-) ratio (see later section on nitrate reduction). In sediments with methanogenesis at shallow depth, electron equivalents may also escape the sediment by methane (CH_4) ebullition (Martens and Klump 1980). Benthic fluxes of reduced manganese (Mn^{2+}), iron (Fe^{2+}), and hydrogen sulfide (H_2S) are insignificant as long as O_2 is not depleted (Balzer 1982; Hall et al. 1989; Thamdrup et al. 1994b). Sulfide burial, mainly in the form of pyrite, is the largest sink for electron equivalents from C oxidation next to O_2 consumption in most sediments, but typically represents 10% or less of C mineralization (Jørgensen 1982). The minor sinks listed here can all be individually quantified and added to the O_2 consumption for a more accurate determination of benthic C mineralization. The O_2 uptake should further be corrected for the contribution from nitrification, which can be estimated as the sum of denitrification and NO_3^- efflux from the sediment (e.g., Canfield et al. 1993a). During the aerobic mineralization of typical, "Redfieldian" organic matter, the oxygen demand from nitrification makes up about 20% of the total (Anderson and Sarmiento 1994).

An important uncertainty in using O_2 uptake as a measure of mineralization lies in the assumption that anaerobic respiration and reoxidation of inorganic species are at steady state. Most reduced Mn, Fe, and sulfur (S) is in particulate form, and sediment reworking, for example, by bioturbation, is crucial for its reoxidation. The nature of particle transport in sediments is poorly understood, and it is not clear whether reoxidation occurs in pulses or continuously relative to the time scale of O_2 uptake measurements. On monthly or seasonal time scales the inventory of reduced inorganic compounds in a sediment may vary in response to changes in supply of organic substrate or oxidants (e.g., Luther et al. 1991; Thamdrup et al. 1994a), which implies a temporal uncoupling of anaerobic mineralization and reoxidation. In special cases, reoxidation may be dominated by discrete events such as wind or current-induced resuspension, so that the benthic O_2 uptake during calm periods may underestimate total mineralization (Aller et al. 1996; Jørgensen 1996).

The uncertainties related to reoxidation are avoided if the benthic flux of dissolved inorganic C, ΣCO_2, rather than O_2 is used as a measure of C mineralization (Teal and Kanwisher 1961; Hargrave and Phillips 1981). Dissolved inorganic C is the immediate product of all mineralization pathways, and ΣCO_2 distributions respond rapidly to changes in production rates. However, roughly a 10-fold higher precision is required for ΣCO_2 compared with O_2 analysis due to a higher background concentration. Also, ΣCO_2 fluxes may be affected by carbonate dissolution or precipitation (Hammond et al. 1985; Anderson et al. 1986), though this contribution has rarely been quantified in shelf sediments. In active coastal sediments, calcium carbonate ($CaCO_3$) dissolution has been estimated to account for approximately 15% of the ΣCO_2 flux as an annual average (Hammond et al. 1985; Jørgensen 1996). The dissolution of foraminiferal tests was estimated to be >30% of ΣCO_2 fluxes from Long Island Sound sediments during some seasons, while at other times net precipitation occurred (Green et al. 1993). On the continental slope,

$CaCO_3$ dissolution may account for most of the ΣCO_2 flux (Berelson et al. 1987; Reimers et al. 1992). Significant carbonate precipitation has been described for iron-rich Amazon shelf sediments, where a large part of the ΣCO_2 production precipitates as ferrous carbonate ($FeCO_3$) and ΣCO_2 is released during vigorous reworking events (Aller et al. 1996).

For the comparison of measurements of C mineralization based on oxidant consumption or ΣCO_2 production, the oxidation state of the metabolized organic C must be known. Estimates based on a variety of approaches including both aerobic and anaerobic mineralization range from -0.7 to 0 corresponding to $O_2/\Sigma CO_2$ ratios of 1.0 to 1.2 (Hammond et al. 1996; Roden and Wetzel 1996; Thamdrup and Canfield 1996; and references therein). The $O_2/\Sigma CO_2$ flux ratio will be somewhat higher than this due to the additional oxygen consumption by nitrification (see above).

Flux measurements are made either with benthic flux chambers in situ (e.g., Pamatmat 1977; Smith 1978; Tengberg et al. 1995) or with retrieved cores in closed or continuous flow incubations (Pamatmat 1977; Rasmussen and Jørgensen 1992; Miller-Way and Twilley 1996). Sediment retrieved from depths greater than approximately 1 km and incubated on shipboard has strongly enhanced O_2 uptake compared with in situ rates, which has been ascribed to physical and biological decompression and temperature effects (Smith 1978; Reimers et al. 1986; Glud et al. 1994). Conversely, higher in situ than laboratory O_2 uptake rates have been reported from shallower depths (Devol and Christensen 1993; Glud et al. 1994, 1998; Jørgensen 1996). In this case, the difference between in situ and laboratory results correlated with faunal biomass, and was interpreted to result from decreased bioirrigation due to both disturbance of the fauna by coring and to selection against larger fauna through the relatively smaller area of individual cores (20 to 80 cm^2) relative to benthic chambers (400 to 900 cm^2). Thus, in lab incubations, the effects of core area and possible selectivity during coring should be carefully considered.

It is important that in situ hydrodynamic conditions are simulated during flux determinations. The thickness of the diffusive boundary layer (DBL) influences diffusive exchange rates, particularly of O_2 (Boudreau and Guinasso 1982), and the water phase should therefore be stirred to create a DBL of a thickness comparable to the natural conditions (Sweerts et al. 1989; Gundersen and Jørgensen 1990; Rasmussen and Jørgensen 1992). Optimally, flow rates or DBL thicknesses in the experimental set-up can be mapped, so that the effect of deviations between the natural and experimental conditions can be evaluated (Buchholtz-ten Brink et al. 1989; Glud et al. 1995). Most set-ups involve rotational stirring, which induces radial hydrostatic pressure gradients. In sandy sediments with high permeability, this induces substantial advective pore water flow, and it can cause flushing of U-shaped burrows in less permeable sediments (Huettel and Gust 1992; Glud et al. 1996). To avoid this problem, benthic fluxes from permeable sediments may alternatively be determined in flume-type set-ups under a unidirectional flow (Forster et al. 1996; Huettel et al. 1996).

In closed incubations, the incubation time should be chosen to yield the minimum necessary changes in the overlying water. The diffusional O_2 flux in active sediments decreases with decreasing bottom water concentration (Hall et al. 1989; Rasmussen and Jørgensen 1992), and changes in O_2 concentration may also affect the irrigating activity of infauna (Forster et al. 1995). Furthermore, pumping activity by suspension-feeding organisms may stop when the overlying water has been cleared for phytoplankton, and clearing of the shallow water column typically enclosed in flux determinations can be extremely rapid (e.g., Vedel et al. 1994).

Other Total Mineralization Assays

As an alternative to benthic fluxes, total mineralization rates can be determined from the accumulation rate of ΣCO_2 in pore water in closed, anoxic "jar" incubations. Sediment sectioned in discrete depth intervals and homogenized under anoxic conditions can be incubated in centrifuge tubes that are sacrificed for sampling serially (Mackin and Swider 1989; Aller et al. 1996) or as a single batch in gas-tight plastic bags each of which is sampled several times (Canfield et al. 1993b; Kruse 1993; Thamdrup and Canfield 1996). By reducing the variability between subsamples, the bag incubations give a higher accuracy and thereby require shorter incubation times (1 to 5 days vs. 2 to 30+ days). In a

slightly different approach, the change in pore water distribution of ΣCO_2 in intact cores, which have been incubated with both ends sealed, is determined relative to the initial profile, and the depth distribution of C mineralization rates is estimated using a non–steady state transport-reaction model (Aller and Mackin 1989; Aller et al. 1996). Ammonia accumulation rates in closed incubations also have been used to estimate mineralization rates based on experimentally obtained $\Sigma CO_2/NH_4^+$ accumulation ratios (Mackin and Swider 1989; Canfield et al. 1993b).

As with ΣCO_2 fluxes, the significance of carbonate dissolution and precipitation must be considered. Under anoxic conditions, little $CaCO_3$ dissolution is expected since little or no acidity is generated during metal oxide or sulfate (SO_4^{2-}) reduction (Canfield and Raiswell 1991). Also, $CaCO_3$ dissolution has not been observed (Mackin and Swider 1989; Thamdrup and Canfield 1996). Precipitation of other carbonate phases, for example, ferrous carbonate, has been indicated during long incubations of iron-rich sediments (Aller et al. 1996). Generally, though, little is known about the magnitude of authigenic carbonate formation in coastal marine sediments.

The main benefit of the closed sediment incubations is that the depth distribution of rates can be used to quantify pathways and dynamics of C mineralization (see later section on manganese and iron reduction). In non–steady state systems, the incubations may provide better estimates of mineralization rates than do benthic fluxes (Aller et al. 1996), though this is likely not the case in general, since less manipulation of the sediment is necessary for flux measurements. In a direct comparison in Long Island Sound sediment, very similar rates were determined with homogenized sediment and in whole-core incubations, and the depth-integrated rates were also in close agreement with benthic ΣCO_2 fluxes. This indicated that neither homogenization nor the imposed anoxia affected total mineralization rates (Aller and Mackin 1989; Mackin and Swider 1989). Also, in sediments underlying anoxic bottom water, good agreement has been found with ΣCO_2 fluxes measured in situ (Thamdrup and Canfield 1996).

The heat production of sediments has been used as a direct measure of total benthic metabolism in terms of energy flow (Pamatmat et al. 1981; Pamatmat 1982). The technique has mainly been applied to the study of temporal dynamics (Graf 1992). The principle of the method is that heat is produced during all metabolic processes and can be measured in a calorimeter, and it is assumed that heat production from other kinds of reactions in sediments are negligible. The measured heat can be converted to carbon or oxidant equivalents if the overall reaction stoichiometry is known, but the metabolic pathways producing the heat have not been separately quantified, and only a conversion factor for oxic respiration has been applied. The difficulties in interpreting the results in chemical equivalents, together with its technical requirements have kept the technique from gaining wider use.

Electron transport system activity (ETSA) is used as a proxy for benthic respiration (Christensen and Packard 1977; Relexans 1996a,b). The ETSA assay involves the extraction of electron transport chains from the sediment and an in vitro measurement of their potential activity using synthetic electron donors and acceptors. The potential rate is correlated to bacterial biomass, and is converted to in situ rates by a calibration factor, which depends on in situ substrate levels and varies more than an order of magnitude between sites (Relexans 1996b). The technique is rapid and very sensitive, and therefore often applied to deep-sea sediments. Due to the uncertainties in the calibration factor, however, direct determinations of respiration are preferable. The respiration/ETSA ratio can possibly give information on the nutritional state of the microbenthic community (Relexans 1996b).

Respiratory Pathways, Oxygen Respiration

Oxygen is globally the most important electron acceptor in benthic respiration. In open ocean sediments with deep oxic zones, the process dominates C oxidation completely, and it has been estimated to account for 50% of C oxidation in coastal sediments (Jørgensen 1983; Henrichs and Reeburgh 1987; Canfield 1993), though this figure has recently has been questioned (see below).

In sediments, O_2 is consumed by organotrophic respiration, lithotrophic respiration, and by abiotic

reactions (see Fig. 6.1). There are no assays for the separate determination of any of these pathways. In early studies of benthic O_2 consumption, it was attempted to distinguish oxic organotrophic respiration and reoxidation of inorganic compounds by poisoning sediment cores with, for example, formaldehyde since all reoxidation was assumed to be chemical and therefore not affected by poisoning (Pamatmat 1977). In the following years the role of lithotrophic microorganisms in reoxidation has become apparent (e.g., Jørgensen 1989) and such approaches are not recommended.

In active sediments, where all three O_2 sinks may be important, oxic organotrophic respiration rates are estimated as the difference between the total benthic O_2 uptake (see previous discussion) and the O_2 demand from inorganic reoxidation. The largest uncertainties are associated with the reoxidation term. Until recently, SO_4^{2-} reduction has been considered the only significant anaerobic respiration in sediments, and the reoxidation term has therefore been calculated from the balance of SO_4^{2-} reduction rates and sulfide burial (Jørgensen 1982; see also later section on sulfate reduction). Recent studies have shown that the reoxidation of Mn(II) and Fe(II) from organotrophic Mn and Fe reduction contributes significantly to O_2 consumption in many continental margin sediments, so that less O_2 is left for aerobic respiration than previously thought (Aller 1990; Canfield et al. 1993a; Thamdrup and Canfield 1996; see also later section on manganese and iron reduction). The best estimate of the O_2 consumption coupled to inorganic reoxidation is therefore obtained from the sum of Mn, Fe, and SO_4^{2-} reduction rates *plus* O_2 consumption by nitrification *less* the burial flux of reduced Mn, Fe, and reduced S (Canfield et al. 1993a). As discussed for the use of total O_2 uptake as a measure of total C mineralization, a major uncertainty lies in the poorly validated assumption of a tight temporal coupling between anaerobic mineralization and reoxidation.

The depth distribution of O_2 consumption can be determined from the O_2 profiles obtained with microsensors (Revsbech 1989). This may aid in distinguishing pathways of consumption, since the oxidation of dissolved inorganic species is often focused near the oxic–anoxic interface (e.g., Jørgensen and Revsbech 1983, Rasmussen and Jørgensen 1992). The analysis can be strengthened by microsensor measurements of dissolved Mn^{2+}, Fe^{2+}, and H_2S distributions (Revsbech et al. 1983; Brendel and Luther 1995). The reoxidation of solid reduced inorganic phases is not included in such measurements, however, and since these phases dominate in bioturbated sediments (see later section on manganese and iron reduction), this approach may not allow a separate determination of organotrophic O_2 consumption there.

Nitrate Reduction

Bacterial NO_3^- reduction follows two main pathways: denitrification with N_2 as the final product, and reduction to ammonium (NH_4^+). In recent studies, the latter pathway has been found to be of little importance in sediments (Binnerup et al. 1992; Rysgaard et al. 1993). In addition to organic C, reduced inorganic compounds (Fe^{2+}, H_2S) may serve as electron donors for both pathways (Kuenen et al. 1985; Dannenberg et al. 1992; Straub et al. 1996). A separate quantification of organotrophic and lithotrophic NO_3^- reduction is mostly not attempted due to the relatively minor role of NO_3^- as electron acceptor in sediments (but see Fossing et al. 1995; Thamdrup and Canfield 1996).

The main interest in NO_3^- reduction measurements arises from the role of benthic denitrification as an important sink in the marine nitrogen cycle which influences primary productivity on both local and global scales (Christensen et al. 1987; Middelburg et al. 1996b). Global estimates of the contribution of benthic denitrification to C oxidation fall in the range 3 to 11% (Jørgensen 1983; Middelburg et al. 1996b). The process may be of greater importance in sediments underlying O_2-depleted water with associated elevated NO_3^- levels or in areas with high NO_3^- levels due to eutrophication (Jørgensen and Sørensen 1985; Canfield 1993).

As a tight coupling between nitrification and denitrification is often observed (Nishio et al. 1983), with a rapid turnover of the pore water NO_3^- pool and NO_3^- depletion very close to the oxic–anoxic interface (Christensen et al. 1989; Brandes and Devol 1995), accurate determinations of denitrification rates require that the natural O_2 and NO_3^- gradients and associated microenvironments are not disturbed. A multitude of techniques have been used to determine denitrification and NO_3^- reduc-

tion rates in sediments (Koike and Sørensen 1988; Seitzinger 1988). We will limit our discussion to the most widespread and accurate assays, including the most recent developments.

The acetylene inhibition technique has been one of the most widely used and relies on the inhibition by acetylene of nitrous oxide reduction, the final step in the denitrification pathway (Sørensen 1978). The accumulation of nitrous oxide is monitored at a high sensitivity, which allows incubation times of few hours. Unfortunately, acetylene also inhibits nitrification, which leads to an underestimation of rates in sediments where this process is the dominating source of NO_3^-. Additionally, inhibition can be incomplete at low NO_3^- concentrations or in the presence of H_2S (Koike and Sørensen 1988; Binnerup et al. 1992).

Denitrification rates may be determined directly from benthic N_2 fluxes (Kaplan et al. 1979). This requires minimal manipulation of the sediment, and is possible both in situ with benthic flux chambers (Devol 1991; Devol and Christensen 1993) and in core incubations (Lamontagne and Valiela 1995). The main disadvantage is that the high background concentration of N_2 in water calls for high analytical precision and relatively long incubations, which may lead to O_2 depletion and thereby change the nitrification activity and the diffusion distance for bottom water NO_3^- (Rysgaard et al. 1993; Lamontagne and Valiela 1995; Blackburn 1996). N_2 fluxes are also sensitive to temperature-dependent solubility changes (Lamontagne and Valiela 1995). Alternatively, cores can be depleted for background N_2 before the flux determination (Seitzinger et al. 1980). This, however, requires either an equilibration time of approximately 10 days to deplete pore water N_2, or separate determination of the nonbiogenic N_2 flux in anoxic cores, with possible artifacts due to ceasure of bioirrigation (Nowicki 1994).

A third approach involves the use of the stable isotope nitrogen-15 (^{15}N) (pioneered by Goering and Pamatmat 1970). Rates of both denitrification, NO_3^- reduction to ammonia, and nitrification can be obtained by parallel incubation of cores in a continuous flow system with $^{15}NO_3^-$ or $^{15}NH_4^+$ added to the inflowing water when the isotopic composition of effluent nitrogen compounds is monitored (Nishio et al. 1982, 1983). In such assays, natural NO_3^- (>99% $^{14}NO_3^-$) and O_2 concentrations and the associated chemical gradients can be maintained. A significant improvement was achieved with the isotope pairing technique, which is based on $^{15}NO_3^-$ addition, separate determination of $^{15}N^{14}N$ and $^{15}N^{15}N$ fluxes, and calculation of the $^{14}N^{14}N$ flux assuming random isotope pairing (Nielsen 1992). The assay includes the nitrification-coupled denitrification. It can be applied in both closed and continuous flow modes (Rysgaard et al. 1993; Risgaard-Petersen and Rysgaard 1995) as well as in situ in benthic flux chambers (Nielsen and Glud 1996). It is robust and, in the no-flow mode, rapid and easy to apply. The use of the method is restricted to sediments with a relatively thin NO_3^- zone, where a homogeneous mixing of the $^{15}NO_3^-$ with the indigenous NO_3^- pool can be rapidly achieved. Mathematical simulations have shown that the basic assumptions hold to a good approximation (Middelburg et al. 1996a), and it has been confirmed experimentally that the addition of labeled NO_3^- to the system does not significantly affect the turnover of the indigenous NO_3^- pool (Nielsen and Glud 1996). The rate from the assay can be operationally separated into denitrification based on nitrified and water-column NO_3^-, but the reality behind this separation has recently been debated (Middelburg et al. 1996a; Nielsen et al. 1996). This separation was introduced to illustrate the regulatory controls on denitrification rates, but for mass balances of the N cycle, only total denitrification rates are needed, and the separation itself may be somewhat confusing.

Manganese and Iron Reduction

Oxidized manganese and iron, Mn(III, IV) and Fe(III), are found in sediments in a wide variety of solid phases from free hydr(oxides) to silicate minerals with an associated large variation in reactivity (Lovley and Phillips 1986; Burdige et al. 1992; Canfield et al. 1992). Also, most Mn(II) and Fe(II) formed in sediments is either adsorbed or precipitated and only a small fraction is found in the pore water (Sørensen 1982; Canfield et al. 1993b). The deposition flux of reactive Mn and Fe in sediments is low compared with the organic C flux and recycling is therefore necessary for these elements to be of importance in C oxidation. Due to the predominant association with solids, such recycling depends strongly on sediment reworking by infauna

or through physical processes (Aller 1990; Canfield et al. 1993b; Aller et al. 1996).

Oxidized Mn and Fe in sediments can be reduced through bacterial respiration coupled to the oxidation of organic matter or hydrogen (Lovley 1991). Fermentative organisms may also utilize the metals as electron sinks, though this process is a minor part of their metabolism (Lovley 1991) and, therefore, likely of little significance in C oxidation. Bacterial Mn and Fe reduction competes with rapid abiotic reactions with H_2S and, for manganese, Fe^{2+} (Pyzik and Sommer 1981; Postma 1985; Yao and Millero 1993). Manganese reduction by sulfide may also be bacterially catalyzed (Aller and Rude 1988; Lovley and Phillips 1994). Humic substances have been shown to shuttle electrons from bacteria to Fe oxides during the oxidation of organic matter in some pure cultures (Lovley et al. 1996). Whether such interactions play a role in sedimentary iron reduction is not yet known.

Dissimilatory Mn and Fe reductions are the most rarely quantified pathways of benthic respiration. They may contribute significantly to C oxidation in some continental margin and freshwater wetland sediments (Aller 1990; Canfield et al. 1993a; Roden and Wetzel 1996; Thamdrup and Canfield 1996), whereas in some cases Fe and, in particular, Mn reductions are mainly coupled to inorganic reoxidation (Canfield et al. 1993a; Aller 1994; Thamdrup et al. 1994a). For a recent review see Thamdrup (2000).

Due to the co-occurrence of respiratory reduction and reactions with reduced inorganic species, similar problems are met in the quantification of Mn and Fe respiration as for aerobic respiration, with additional complications associated with the analysis of oxidized and reduced Mn and Fe pools. The use of radiolabeled Fe(III) oxide as a tracer of Fe reduction is precluded by rapid electron exchange that causes the formation of labeled Fe(II) without net Fe reduction (Roden and Lovley 1993). Iron reduction rates have been estimated by monitoring Fe(III) consumption or Fe(II) production by means of wet chemical Fe extractions in anoxic incubations of homogenized sediment from discrete depth intervals (Sørensen 1982; Lovley and Phillips 1986; Roden and Wetzel 1996). This approach has some potential with freshwater sediments with low rates of SO_4^{2-} reduction and, hence, of H_2S production. There are, however, several complications associated with the use of changes in Fe pools for measuring Fe reduction. Long incubation times (approximately 10 days) are mostly necessary to obtain sufficient changes in the Fe(II) or Fe(III) pools due to high background levels. Also, it is not clear that iron extractions retrieve all reacting Fe(III) or produced Fe(II). Particularly, lattice-bound Fe in clay minerals, which is not targeted by conventional extractions, may be redox active (Wallmann et al. 1993; Kostka et al. 1996). The extraction efficiency toward Fe reduced during incubation may be tested by measuring the Fe reduction/ΣCO_2 production ratios in sediment known to be dominated by Fe reduction (Roden and Wetzel 1996). As a further problem, oxidation or reduction artifacts may be associated with the extractions (Phillips and Lovley 1987; Jensen and Thamdrup 1993; Petersen 1993). Mössbauer spectroscopy has been used as an alternative to, and a calibration of, wet extractions, but this technology is not generally accessible (Wallmann et al. 1993). If SO_4^{2-} reduction is of significance, interpretation of Fe(III) consumption is difficult as it is not clear to what extend the H_2S formed reacts with Fe(III). Independence of Fe reduction on H_2S oxidation has been demonstrated by addition of molybdate to inhibit SO_4^{2-} reduction, or by direct determination of SO_4^{2-} reduction rates with radiotracer (Sørensen 1982; Canfield 1989; Roden and Wetzel 1996). However, inhibition of SO_4^{2-} reduction with molybdate does not exclude the reaction of Fe(III) with reduced S already present in the sediment. Finally, Fe reduction may also be obscured by a rapid reoxidation of Fe(II) by Mn oxides. To exclude this reaction, Ferrozine, a strong Fe^{2+} chelator has been added to the incubated sediment (Canfield et al. 1993b).

Manganese reduction rates have been estimated from the accumulation of dissolved Mn^{2+}, either by assuming an adsorption coefficient or by incubating sediment in large volumes of anoxic water in order to minimize adsorption or precipitation (Aller and Mackin 1989; Aller 1990, 1994). Reduction of Mn by reduced Fe or S was, however, not excluded in these experiments. Furthermore, adsorption and precipitation of Mn^{2+} is poorly understood, and rates based on Mn^{2+} may seriously underestimate actual rates of reduction (Aller and Rude 1988; Canfield et al. 1993b; Aller 1994). Changes in oxidation state of solid-phase Mn have

been determined in sediment incubations to calculate manganese reduction rates (Canfield 1993b). The available techniques are, however, only applicable to very Mn-rich sediments.

The only experimental approach to determine in situ rates of organotrophic Mn and Fe reduction in sediments presented so far is based on a comparison of rates of total C oxidation and of SO_4^{2-} reduction in anoxic incubations of homogenized sediment sectioned into discrete depth intervals (Fig. 6.2; Canfield et al. 1993a,b; Aller 1994; Thamdrup and Canfield 1996). Total C oxidation rates are determined from the accumulation of ΣCO_2 (see previous section on other total mineralization assays), and SO_4^{2-} reduction rates are measured in subsamples by the $^{35}SO_4^{2-}$-technique (see following section). The C oxidation rate corresponding to the measured SO_4^{2-} reduction is calculated and subtracted from the total C oxidation rate. Based on the measured depth distributions of O_2 and NO_3^-, a zone where only Mn and Fe reduction can account for the excess C oxidation may be distinguished. With further support from the depth distributions of reactive Mn and Fe oxides and from the accumulation of Mn^{2+} and Fe^{2+} during the incubation, the contributions of Mn and Fe reduction to C oxidation can be partitioned. The sediment is incubated with no head-space in "Würgler" bags of laminated gas-tight plastic (Kruse 1993). In this way, all samples are taken from the same batch of sediment, which can be mixed intermittently. This minimizes the variability among samples considerably and thereby increases the total precision, which allows for brief incubation times of one to a few days with coastal sediments. Short incubation times preclude the depletion of the reactive Mn and Fe pools during the incubation and minimize other effects of the inhibition of vertical transport caused by discrete interval sediment sampling.

One limitation of this method is that Mn and Fe reduction in, and often a little below, the O_2/NO_3^- zone cannot be quantified due to a limited spatial resolution of 0.5 to 1 cm. The potential underestimation is probably larger for Mn since Mn cycling is often focused very close to the oxic–anoxic interface (e.g., Canfield et al. 1993b; Thamdrup et al. 1994a). A further concern is associated with the stoichiometry of C oxidation by SO_4^{2-} reduction, but considering the crudeness of the method in general this potential error is relatively small.

The greatest consideration about the accuracy of the method concerns the effect of sediment homogenization on C oxidation rates. In our study off Chile (Thamdrup and Canfield 1996), there was a general agreement between C oxidation rates and in situ ΣCO_2 fluxes where both parameters were measured, and also between SO_4^{2-} reduction rates in incubations of homogenized sediment and intact sediment cores (Ferdelman et al. 1997). Close matches have previously been reported between intact cores and homogenized (but not slurried) sediment for rates of both SO_4^{2-} reduction and total

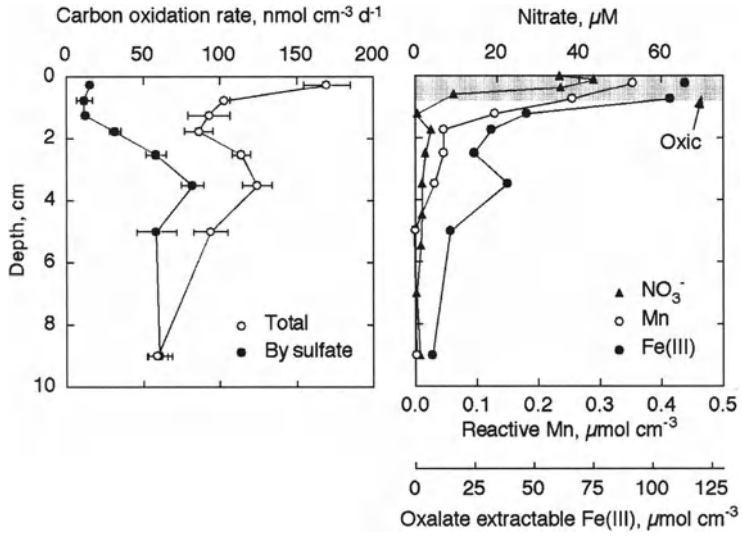

FIGURE 6.2. Results from anoxic bag incubation experiments with sediment from a station at 2000-m depth off Chile (data from Thamdrup and Canfield 1996). Left: Total C oxidation rates (measured as CO_2 production), and C oxidation rates due to SO_4^{2-} reduction (measured with $^{35}SO_4^{2-}$). Right: Depth distribution of oxidants. Near the surface, SO_4^{2-} reduction contributes little to carbon oxidation but at 9-cm depth, all carbon oxidation is explained by SO_4^{2-} reduction. Below 1.5 cm, Fe(III) is the only significant oxidant other than SO_4^{2-}, and the excess C oxidation below this depth is attributed to Fe reduction.

mineralization (Jørgensen 1978; Mackin and Swider 1989). In recent experiments with coastal Costa Rican, Danish, and Northeast Greenland sediments, we have noticed a tendency for higher SO_4^{2-} reduction rates in the homogenized sediment compared with whole-core incubations (Thamdrup et al. 1996; Rysgaard et al. 1998; B. Thamdrup unpublished results). The source of these differences is not yet clear. Homogenization could stimulate mineralization by relieving metabolite inhibition of bacterial metabolism around organic-rich microenvironments, but the observed differences could also be due to an undersampling of active hot-spots in the small cores (3 to 4 cm i.d.) used for whole-core SO_4^{2-} reduction measurements.

The internal consistency of the results from the incubation technique has been confirmed by multicomponent diagenetic modeling (Wang and Van Cappellen 1996). The incubation technique is very work intensive, but it has provided quantitative evidence for the importance of Mn and, in particular, Fe reduction for benthic C oxidation in a wide variety of continental margin sediments, and at the moment it appears to be the only way to obtain good estimates of the rates of these processes in sediments where SO_4^{2-} reduction is of importance.

Sulfate Reduction

Benthic SO_4^{2-} reduction has been extensively studied (Jørgensen 1982; Howarth 1984; Skyring 1987). The process is exclusively catalyzed by SO_4^{2-}-reducing bacteria that couple it to the oxidation of organic matter or H_2, and produce H_2S as the only immediate extracellular sulfur product (Widdel and Hansen 1991). Intense SO_4^{2-} reduction can, however, occur without detectable accumulation of H_2S due to rapid precipitation of iron sulfides and S^0 (e.g., Canfield 1989; Thamdrup et al. 1994a). Sulfate reduction typically contributes about 50% of the C oxidation in shallow coastal sediments with oxic bottom water (Jørgensen 1982), and the contribution may be even higher in salt marsh and sheltered subtidal sediments (Howarth 1984; Mackin and Swider 1989), whereas in the deep sea it is of little importance (Jørgensen 1982; Canfield 1991; Canfield 1993). In freshwater sediments, the process is limited by the shallow penetration depth of SO_4^{2-} which results from low SO_4^{2-} concentrations in freshwater, though volume-specific rates can be as high as in marine sediments (e.g., Capone and Kiene 1988; Bak and Pfennig 1991).

The most widespread assay for SO_4^{2-} reduction is the radiotracer technique (Sorokin 1962; Jørgensen 1978). Microliter volumes of carrier-free $^{35}SO_4^{2-}$ tracer are injected into intact sediment cores, and incubation times are typically from 1 hour to 1 day. Injections have been performed at the seafloor using a benthic lander (Greeff et al. 1998). Since the discovery that significant amounts of tracer may be incorporated into pyrite and S^0 (Howarth 1979; Howarth and Jørgensen 1984), reduced radiolabeled S has been recovered by distillation with a hot acidic chromous solution that reduces these species to H_2S (Zhabina and Volkov 1978; Fossing and Jørgensen 1989). A small amount of radiolabel may be distilled from unreacted $^{35}SO_4^{2-}$ tracer, possibly due to slight contamination from other S species, and it is therefore advisable to include a zero-time blank (Howarth and Jørgensen 1984; Spratt et al. 1987; Roden and Tuttle 1993b). In freshwater sediments, 10 to 40% of total reduced tracer in SO_4^{2-} reduction rate incubations has been recovered as organic C–bonded S, quantified as the residue after sequential distillation with chromium (Cr^{2+}) and hydroiodic acid (Wieder and Lang 1988; Spratt and Morgan 1990; Roden and Wetzel 1996).

The radiotracer technique has been validated by comparison to SO_4^{2-} depletion in long-term incubations (Jørgensen 1978; Westrich 1983; Crill and Martens 1987; Canfield and Thamdrup 1996), to sulfide accumulation or benthic H_2S fluxes (Jørgensen 1978; Chanton et al. 1987; Roden and Tuttle 1993a), and to total C mineralization rates (Thamdrup and Canfield 1996). With the radiotracer technique, SO_4^{2-} reduction rates can be measured in oxidized and even oxic sediment where sulfide reoxidation is possible (Canfield and Des Marais 1991; Jørgensen and Bak 1991). Determination of SO_4^{2-} reduction rates is possible with concomitant reoxidation when the reduced tracer is diluted into an unlabeled pool of reduced S compounds, and the incubation time is kept short relative to the turnover time of this pool (Fossing et al. 1995). The dependence of the rate on incubation time can be used to evaluate the effects of reoxidation on the measurements (Jørgensen 1978; Canfield and Des Marais 1993). Detailed time courses in oxidized surface

sediments have shown decreasing SO_4^{2-} reduction rates over the initial 0.25 to 1 hour of incubation after which rates became constant (Moeslund et al. 1994; Fossing 1995; Isaksen and Finster 1996). This was interpreted as a result of reoxidation of tracer from a small (undetectable) H_2S pool that rapidly became saturated with tracer, after which the measured rate represented the rate of net incorporation of S into the solid reduced pools. The results were not conclusive, however, and further investigations are needed to constrain to what extent, and under which conditions, the radiotracer technique may underestimate rates of SO_4^{2-} reduction in oxidized sediments.

When the technique is used with freshwater sediments, special attention must be paid to an accurate determination of SO_4^{2-} concentrations due to low levels and steep gradients, and incubation times must be kept short due to the brief turnover time of the SO_4^{2-} pool (e.g., Bak and Pfennig 1991; Roden and Tuttle 1993b; Urban et al. 1994). High SO_4^{2-} reduction rates are in some cases measured at what appears to be threshold level SO_4^{2-} concentrations based on the concentration profile. Rapid recycling of SO_4^{2-} has been suggested as an explanation, but recently, such high rates have been found to significantly exceed total C mineralization rates corrected for the contribution of methanogenesis, which indicated that the reduction rates were overestimated (Roden and Wetzel 1996). It has been suggested that the threshold concentrations represent a nonreducible SO_4^{2-} pool of unknown nature (Bak and Pfennig 1991; Roden and Tuttle 1993b). A more extensive comparison of total mineralization rates measured as ΣCO_2 accumulation to the sum of individual degradative pathways, similar to the approach of Roden and Wetzel (Roden and Wetzel 1996), could serve as control on SO_4^{2-} reduction rate measurements in freshwater sediments.

Sulfate reduction rates can also be determined from SO_4^{2-} depletion in the incubation of sediment in discrete depth intervals (e.g., Goldhaber et al. 1977; Swider and Mackin 1989; Bak and Pfennig 1991). This approach yields only net reduction rates, however, it has far lower sensitivity than the tracer technique, and it requires longer incubation times. In the deep sea where SO_4^{2-} reduction is restricted to below the zone of bioturbation and irrigation, rates are more easily quantified from SO_4^{2-} concentration profiles (Bender and Heggie 1984; Canfield 1991; but see also Parkes et al. 1995).

Methanogenesis

In the absence of inorganic electron acceptors, the mineralization of organic matter will proceed by fermentative processes with methanogenesis as the terminal step. Due to competitive inhibition, methanogenesis is insignificant when inorganic electron acceptors are present (Lovley and Klug 1986; Capone and Kiene 1988). In marine sediments, therefore, the onset of methanogenesis generally lies far below the sediment surface where little reactive organic matter is left, and decomposition through this pathway is estimated to be only 10% of the C oxidation through SO_4^{2-} reduction (Canfield 1993). Higher contributions are found in coastal sediments with extreme deposition rates and SO_4^{2-} depletion only a few decimeters below the surface (Martens and Klump 1984). In freshwater sediments, methanogenesis accounts for 20 to 90% of organic decomposition (Capone and Kiene 1988).

In marine sediments where the onset of methanogenesis is below the zone of bioturbation, CH_4 production rates can be obtained by modeling concentration profiles provided that loss through bubble ebullition, either in situ or as a result of decompression after sediment collection, can be excluded (Reeburgh 1976, 1983). Under these conditions and the assumption of steady state, areal rates can also be estimated from rates of CH_4 oxidation determined directly using radiolabeled $^{14}CH_4$ (Reeburgh 1980). Acetate and $H_2 + CO_2$ are generally found to be the most important substrates for methanogenesis (Capone and Kiene 1988), and rates can therefore be determined directly by monitoring the incorporation of ^{14}C into CH_4 from ^{14}C-labeled acetate or CO_2 (Crill and Martens 1987; Kuivila et al. 1989). Methanogenesis co-occurring with SO_4^{2-} reduction is to a large extend attributed to "noncompetitive" substrates, mainly C_1 compounds such as methyl amines, and can be quantified in incubations with radiolabeled versions of these compounds (King et al. 1983; Ferdelman et al. 1997).

Conclusions

Although aquatic sediments may appear rather dull to the eye, they are highly structured communities harboring a metabolic diversity that is matched by few other environments. Steep chemical gradients at the surface and around animal burrows and plant roots provide a range of different microenvironments, and much remains to be learned about the interactions between micro- and macroorganisms. It must therefore be a prime concern in measurements of sediment processes to minimize the disturbance of the sediment community. The techniques described in this chapter achieve this to a quite variable extent. Clearly, in situ flux measurements involve the least manipulation and should be applied as widely as possible, and in situ techniques should be extended to other processes as well. Their cost in both time and funds is large, however, and they are not a priori free of experimental artifacts. In the deep sea, in situ flux measurements are indispensable due to decompression artifacts. The indications that laboratory incubations with shallow-water sediments underestimate mineralization rates compared with benthic flux chambers deserve more attention. Paradoxically, efforts to obtain "undisturbed" sediment cores may cause an undersampling of sediment with larger infauna and therefore, in essence, a serious disturbance of the sediment community. The behavioral response of the infauna to coring and incubation is another main concern. Information on the lifestyle of dominating fauna may help to constrain such effects as well as patterns of bioturbation in the sediment in general (e.g., Blair et al. 1996; Wheatcroft and Martin 1996), and thereby provide insights to the regulation of carbon oxidation pathways.

The partitioning of carbon oxidation according to individual respiratory pathways has been improved through recent developments in assays for denitrification and Mn and Fe reduction. For denitrification, the N_2-flux and isotope pairing techniques complement each other and should be used as mutual controls. The bag incubation technique for Mn and Fe reduction has closed a methodological gap and shown that these processes must be considered in benthic C oxidation. The technique is rather crude compared with the other assays, and it is important that results are verified by comparison with other rate determinations and through modeling in combination with quantifications of sediment reworking. The measurement of Mn and Fe reduction is particularly dependent on an accurate determination of SO_4^{2-} reduction rates. The radiotracer technique for measuring such rates is well tested and widely used. Still, a possible underestimation of sulfate reduction rates in oxidized sediment due to reoxidation needs further investigation.

The contribution of oxic respiration to C oxidation can only be estimated from the difference between total and anaerobic mineralization rates, and therefore this pathway probably has the largest associated uncertainty. The suggestion, raised by the inclusion of Mn and Fe reduction in anaerobic mineralization rates, that oxic mineralization plays a lesser role than previously thought needs further investigation. The role of oxic mineralization is an important question in benthic ecology, and furthermore, the balance between oxic and anoxic mineralization has been suggested to play a key role in the regulation of carbon preservation in sediments with implications for the global C cycle (cf. Canfield 1994). Hence, a better quantification of oxic mineralization rates is an important task for future research.

Acknowledgments During the writing of this chapter, we were supported by the Max Planck Society and the Danish National Science and Research Foundations.

References

Aller, R.C. Bioturbation and manganese cycling in hemipelagic sediments. Philos. Trans. R. Soc. Lond. A331:51–58; 1990.

Aller, R.C. The sedimentary Mn cycle in Long Island Sound: Its role as intermediate oxidant and the influence of bioturbation, O_2, and C_{org} flux on diagenetic reaction balances. J. Mar. Res. 52:259–295; 1994.

Aller, R.C.; Blair, N.E.; Xia, Q.; Rude, P.D. Remineralization rates, recycling, and storage of carbon in Amazon shelf sediments. Continental Shelf Res. 16:753–786; 1996.

Aller, R.C.; Mackin, J.E. Open-incubation, diffusion methods for measuring solute reaction rates in sediments. J. Mar. Res. 47:411–440; 1989.

Aller, R.C.; Rude, P.D. Complete oxidation of solid phase sulfides by manganese and bacteria in anoxic marine

sediments. Geochim. Cosmochim. Acta 52:751–765; 1988.

Anderson, L.A.; Sarmiento, J.L. Redfield ratios of remineralization determined by nutrient data analysis. Global Biogeochem. Cycl. 8:25–35; 1994.

Anderson, L.G.; Hall, P.O.J.; Iverfeldt, Å.; Rutgers van der Loeff, M.M.; Sundby, B.; Westerlund, S.F.G. Benthic respiration measured by total carbonate production. Limnol. Oceanogr. 31:319–329; 1986.

Bak, F.; Pfennig, N. Microbial sulfate reduction in littoral sediment of Lake Constance. FEMS Microbiol. Ecol. 85:31–42; 1991.

Balzer, W. On the distribution of iron and manganese at the sediment/water interface: Thermodynamic versus kinetic control. Geochim. Cosmochim. Acta 46:1153–1161; 1982.

Bender, M.L.; Heggie, D.T. Fate of organic carbon reaching the deep-sea floor: A status report. Geochim. Cosmochim. Acta 48:977–986; 1984.

Berelson, W.M.; Hammond, D.E.; Johnson, K.S. Benthic fluxes and the cycling of biogenic silica and carbon in two southern California borderland basins. Geochim. Cosmochim. Acta 51:1345–1363; 1987.

Berner, R.A. *Early Diagenesis.* Princeton, NJ: Princeton Univ. Pr.; 1980.

Binnerup, S.J.; Jensen, K.; Revsbech, N.P.; Jensen, M.H.; Sørensen, J. Denitrification, dissimilatory reduction of nitrate to ammonium and nitrification in a bioturbated estuarine sediment as measured with ^{15}N and microsensor techniques. Appl. Environ. Microbiol. 58:303–313; 1992.

Blackburn, T.H. Nitrogen gas flux from sediments: Insights from simulation modelling. Aquat. Microb. Ecol. 10:209–211; 1996.

Blair, N.E.; Levin, L.A.; DeMaster, D.J.; Plaia, G. The short-term fate of fresh algal carbon in continental slope sediments. Limnol. Oceanogr. 41:1208–1219; 1996.

Boudreau, B.P. *Diagenetic Models and Their Implementation.* Berlin: Springer-Verlag; 1997.

Boudreau, B.P.; Guinasso, N.L., Jr. The influence of a diffusive sublayer on accretion, dissolution, and diagenesis at the sea floor. In: Fanning, K.A.; Manheim, F.T., eds. *The dynamic environment at the ocean floor.* Lanham, MD: Lexington; 1982:115–145.

Brandes, J.A.; Devol, A.H. Simultaneous nitrate and oxygen respiration in coastal sediments: Evidence for discrete diagenesis. J. Mar. Res. 53:771–797; 1995.

Brendel, P.J.; Luther, G.W., III. Development of a gold amalgam voltammetric microelectrode for the determination of dissolved Fe, Mn, O_2, and S(− II) in porewaters of marine and freshwater sediments. Environ. Sci. Technol. 29:751–761; 1995.

Buchholtz-ten Brink, M.R.; Gust, G.; Chavis, D. Calibration and performance of a stirred benthic chamber. Deep-Sea Res. 36:1083–1101; 1989.

Burdige, D.J.; Dhakar, S.P.; Nealson, K.H. Effects of manganese oxide mineralogy on microbial and chemical manganese reduction. Geomicrobiol. J. 10:27–48; 1992.

Canfield, D.E. Reactive iron in marine sediments. Geochim. Cosmochim. Acta 53:619–632; 1989.

Canfield, D.E. Sulfate reduction in deep-sea sediments. Am. J. Sci. 291:177–188; 1991.

Canfield, D.E. Organic matter oxidation in marine sediments. In: Wollast, R.; Mackenzie, F.T.; Chou, L., eds. *Interactions of C, N, P, and S Biogeochemical Cycles and Global Change.* Berlin: Springer-Verlag; 1993:333–363.

Canfield, D.E. Factors influencing organic carbon preservation in marine sediments. Chem. Geol. 115:315–329; 1994.

Canfield, D.E.; Des Marais, D.J. Aerobic sulfate reduction in microbial mats. Science 251:1471–1473; 1991.

Canfield, D.E.; Des Marais, D.J. Biogeochemical cycles of carbon, sulfur, and free oxygen in a microbial mat. Geochim. Cosmochim. Acta 57:3971–3984; 1993.

Canfield, D.E.; Jørgensen, B.B.; Fossing, H.; Glud, R.; Gundersen, J.; Ramsing, N.B.; Thamdrup, B.; Hansen, J.W.; Nielsen, L.P.; Hall, P.O.J. Pathways of organic carbon oxidation in three continental margin sediments. Mar. Geol. 113:27–40; 1993a.

Canfield, D.E.; Raiswell, R. Carbonate precipitation and dissolution, its relevance to fossil preservation. In: Allison, P.A.; Briggs, D.E.G., eds. *Taphonomy: Releasing the Data Locked in the Fossil Record.* New York: Plenum; 1991:411–453.

Canfield, D.E.; Raiswell, R.; Bottrell, S. The reactivity of sedimentary iron minerals toward sulfide. Am. J. Sci. 292:659–683; 1992.

Canfield, D.E.; Thamdrup, B. Fate of elemental sulfur in an intertidal sediment. FEMS Microbiol. Ecol. 19(2):95–103; 1996.

Canfield, D.E.; Thamdrup, B.; Hansen, J.W. The anaerobic degradation of organic matter in Danish coastal sediments: Fe reduction, Mn reduction and sulfate reduction. Geochim. Cosmochim. Acta 57:2563–2570; 1993b.

Capone, D.G.; Kiene, R.P. Comparison of microbial dynamics in marine and freshwater sediments: contrasts in anaerobic catabolism. Limnol. Oceanogr. 33:725–749; 1988.

Chanton, J.P.; Martens, C.S.; Goldhaber, M.B. Biogeochemical cycling in an organic-rich coastal marine basin. 7. Sulfur mass balance, oxygen uptake and sulfide retention. Geochim. Cosmochim. Acta 51:1187–1199; 1987.

Christensen, J.P.; Packard, T.T. Sediment metabolism in the northwest African upwelling system. Deep-Sea Res. 24:331–343; 1977.

Christensen, J.P.; Murray, J.W.; Devol, A.H.; Codispoti, L.A. Denitrification in continental shelf sediments has major impact on the oceanic nitrogen budget. Global Biogeochem. Cycl. 1:97–116; 1987.

Christensen, P.B.; Nielsen, L.P.; Revsbech, N.P.; Sørensen, J. Microzonation of denitrification activity in stream sediments as studied by a combined oxygen and nitrous oxide microsensor. Appl. Environ. Microbiol. 55:1234–1241; 1989.

Crill, P.M.; Martens, C.S. Biogeochemical cycling in an organic-rich coastal marine basin. 6. Temporal and spatial variations in sulfate reduction rates. Geochim. Cosmochim. Acta 51:1175–1186; 1987.

Dannenberg, S.; Kroder, M.; Dilling, W.; Cypionka, H. Oxidation of H_2, organic compounds and inorganic sulfur compounds coupled to reduction of O_2 or nitrate by sulfate-reducing bacteria. Arch. Microbiol. 158:93–99; 1992.

Devol, A.H. Direct measurements of nitrogen gas fluxes from continental shelf sediments. Nature 349:319–321; 1991.

Devol, A.H.; Christensen, J.P. Benthic fluxes and nitrogen cycling in sediments of the continental margin of the eastern North Pacific. J. Mar. Res. 51:345–372; 1993.

Ferdelman, T.G.; Lee, C.; Pantoja, S.; Harder, J.; Bebout, B.M.; Fossing, H. Sulfate reduction and methanogenesis in a *Thioploca*-dominated sediment off the coast of Chile. Geochim. Cosmochim. Acta 61:3065–3079; 1997.

Forster, S.; Graf, G.; Kitlar, J.; Powilleit, M. Effects of bioturbation in oxic and hypoxic conditions: A microcosm experiment with a North Sea sediment community. Mar. Ecol. Prog. Ser. 116:153–161; 1995.

Forster, S.; Huettel, M.; Ziebis, W. Impact of boundary layer flow on oxygen utilization in coastal sediments. Mar. Ecol. Prog. Ser. 143:173–185; 1996.

Fossing, H. ^{35}S-radiolabelling to probe biogeochemical cycling of sulfur. In: Vairavamurthy, M.A.; Schoonen, M.A.A., eds. *Geochemical Transformations of Sedimentary Sulfur.* Washington, DC: American Chemical Society; 1995:348–364.

Fossing, H.; Gallardo, V.A.; Jørgensen, B.B.; Hüttel, M.; Nielsen, L.P.; Schulz, H.; Canfield, D.E.; Forster, S.; Glud, R.N.; Gundersen, J.K.; Küver, J.; Ramsing, N.B.; Teske, A.; Thamdrup, B.; Ulloa, O. Concentration and transport of nitrate by the mat-forming sulphur bacterium *Thioploca.* Nature 374:713–715; 1995.

Fossing, H.; Jørgensen, B.B. Measurement of bacterial sulfate reduction in sediments: Evaluation of a single-step chromium reduction method. Biogeochemistry 8:223–245; 1989.

Froelich, P.N.; Klinkhammer, G.P.; Bender, M.L., Luedtke, N.A.; Heath, G.R.; Cullen, D.; Dauphin, P.; Hammond, D.; Hartman, B.; Maynard, V. Early oxidation of organic matter in pelagic sediments of the eastern equatorial Atlantic: Suboxic diagenesis. Geochim. Cosmochim. 43:1075–1090; 1979.

Glud, R.N.; Forster, S.; Huettel, M. Influence of radial pressure gradients on solute exchange in stirred benthic chambers. Mar. Ecol. Prog. Ser. 141:303–311; 1996.

Glud, R.N.; Gundersen, J.K.; Jørgensen, B.B.; Revsbech, N.P.; Schultz, H.D. Diffusive and total oxygen uptake of deep-sea sediments in the eastern South Atlantic Ocean: In situ and laboratory measurements. Deep-Sea Res. I41:1767–1788; 1994.

Glud, R.N.; Gundersen, J.K.; Revsbech, N.P.; Jørgensen, B.B.; Hüttel, M. Calibration and performance of the stirred flux chamber from the benthic lander *Elinor.* Deep-Sea Res. I42:1029–1042; 1995.

Glud, R.N.; Holby, O.; Hoffmann, F.; Canfield, D.E. Benthic mineralization and exchange in Arctic sediments (Svalbard). Mar. Ecol. Progr. Ser. 173:237–251; 1998.

Goering, G.G.; Pamatmat, M.M. Denitrification in sediments of the sea off Peru. Invest. Pesq. 35:233–242; 1970.

Goldhaber, M.B.; Aller, R.C.; Cochran, J.K.; Rosenfeld, J.K.; Martens, C.S.; Berner, R.A. Sulfate reduction, diffusion, and bioturbation in Long Island Sound sediments: Report from the FOAM group. Am. J. Sci. 277:193–237; 1977.

Graf, G. Benthic-pelagic coupling: A benthic view. Oceanogr. Mar. Biol. Annu. Rev. 30:149–190; 1992.

Greeff, O.; Glud, R.N.; Gundersen, J.; Holby, O.; Jørgensen, B.B. A benthic lander for tracer studies in the seabed: In situ measurements of sulfate reduction. Cont. Shelf Res. 18:1581–1590; 1998.

Green, M.A.; Aller, R.C.; Aller, J.Y. Carbonate dissolution and temporal abundances of Foraminifera in Long Island Sound sediments. Limnol. Oceanogr. 38:331–345; 1993.

Gundersen, J.K.; Jørgensen, B.B. Microstructure of diffusive boundary layers and the oxygen uptake of the sea floor. Nature 345:604–607; 1990.

Hall, P.O.J.; Anderson, L.G.; Rutgers van der Loeff, M.M.; Sundby, B.; Westerlund, S.F.G. Oxygen uptake kinetics in the benthic boundary layer. Limnol. Oceanogr. 34:734–746; 1989.

Hammond, D.E.; Fuller, C.; Harmon, D.; Hartman, B.; Korosec, M.; Miller, L.G.; Rea, R.; Warren, S.; Berelson, W.; Hager, S.W. Benthic fluxes in San Francisco Bay. Hydrobiologia 129:69–90; 1985.

Hammond, D.E.; McManus, J.; Berelson, W.M.; Kilgore, T.E.; Pope, R.H. Early diagenesis of organic material in equatorial Pacific sediments: stoichiometry and kinetics. Deep-Sea Res. II43:1365–1412; 1996.

Hargrave, B.T.; Phillips, G.A. Annual in situ carbon dioxide and oxygen flux acros a subtidal marine sediment. Estuarine Coastal Shelf Sci. 12:725–737; 1981.

Hedges, J.I.; Keil, R.G. Sediment organic matter preservation: an assessment and speculative synthesis. Mar. Chem. 49:81–115; 1995.

Henrichs, S.M.; Reeburgh, W.S. Anaerobic mineralization of marine sediment organic matter: Rates and the role of anaerobic processes in the oceanic carbon economy. Geomicrobiol. J. 5:191–237; 1987.

Howarth, R.W. Pyrite: Its rapid formation in a salt marsh and its importance in ecosystem metabolism. Science 203:49–51; 1979.

Howarth, R.W. The ecological significance of sulfur in the energy dynamics of salt marsh and coastal marine sediments. Biogeochemistry 1:5–27; 1984.

Howarth, R.W. Nutrient limitation of net primary production in marine ecosystems. Annu. Rev. Ecol. Syst. 19:89–110; 1988.

Howarth, R.W.; Jørgensen, B.B. Formation of ^{35}S-labelled elemental sulfur and pyrite in coastal marine sediments (Limfjorden and Kysing Fjord, Denmark) during short-term $^{35}SO_4^{2-}$ reduction measurements. Geochim. Cosmochim. Acta 48:1807–1818; 1984.

Huettel, M.; Forster, S.; Klöser, S.; Fossing, H. Vertical migration in the sediment-dwelling sulfur bacteria *Thioploca* spp. in overcoming diffusion limitations. Appl. Environ. Microbiol. 62:1863–1872; 1996.

Huettel, M.; Gust, G. Solute release mechanisms from confined sediment cores in stirred benthic chambers and flume flows. Mar. Ecol. Prog. Ser. 82:187–197; 1992.

Isaksen, M.F.; Finster, K. Sulphate reduction in the root zone of the seagrass *Zostera noltii* on the intertidal flats of a coastal lagoon (Arcachon, France). Mar. Ecol. Prog. Ser. 137:187–194; 1996.

Jensen, H.S.; Thamdrup, B. Iron-bound phosphorus in marine sediments as measured by bicarbonate-dithionite extraction. Hydrobiologia 253:47–59; 1993.

Jørgensen, B.B. A comparison of methods for the quantification of bacterial sulfate reduction in coastal marine sediments. I. Measurement with radiotracer techniques. Geomicrobiol. J. 1:11–27; 1978.

Jørgensen, B.B. Mineralization of organic matter in the sea bed: Role of sulphate reduction. Nature 296:643–645; 1982.

Jørgensen, B.B. Processes at the sediment-water interface. In: Bolin, B.; Cook, R.B., eds. *The Major Biogeochemical Cycles and Their Interactions.* New York: Wiley; 1983:477–509.

Jørgensen, B.B. Biogeochemistry of chemoautotrophic bacteria. In: Schlegel, H.G.; Bowien, B., eds. *Autotrophic Bacteria.* Madison, WI: Science Tech; 1989:117–146.

Jørgensen, B.B. Case study: Aarhus Bay. In: Jørgensen, B.B.; Richardson, K., eds. *Eutrophication in Coastal Marine Ecosystems.* Washington, DC: American Geophysical Union; 1996:137–154.

Jørgensen, B.B.; Bak, F. Pathways and microbiology of thiosulfate transformations and sulfate reduction in a marine sediment (Kattegat, Denmark). Appl. Environ. Microbiol. 57:847–856; 1991.

Jørgensen, B.B.; Revsbech, N.P. Colorless sulfur bacteria, *Beggiatoa* spp. and *Thiovolum* spp. in O_2 and H_2S microgradients. Appl. Environ. Microbiol. 45:1261–1270; 1983.

Jørgensen, B.B.; Sørensen, J. Seasonal cycles of O_2, NO_3^- and SO_4^{2-} reduction in estuarine sediments: the significance of an NO_3^- reduction maximum in the spring. Mar. Ecol. Prog. Ser. 24:65–74; 1985.

Kaplan, W.A.; Valiela, I.; Teal, J.M. Denitrification in a marsh ecosystem. Limnol. Oceanogr. 24:726–734; 1979.

King, G.M.; Klug, M.J.; Lovley, D.R. Metabolism of acetate, methanol, and methylated amines in intertidal sediments of Lowes Cove, Maine. Appl. Environ. Microbiol. 45:1848–1853; 1983.

Koike, I.; Sørensen, J. Nitrate reduction and denitrification in marine sediments. In: Blackburn, T.H.; Sørensen, J., eds. *Nitrogen Cycling in Coastal Marine Environments.* New York: Wiley; 1988:251–273.

Kostka, J.E.; Stucki, J.W.; Nealson, K.H.; Wu, J. Reduction of structural Fe(III) in smectite by a pure culture of *Shewanella putrfaciens* strain MR-1. Clays Clay Miner. 44:522–529; 1996.

Kruse, B. Measurement of plankton O_2 respiration in gastight plastic bags. Mar. Ecol. Prog. Ser. 94:155–163; 1993.

Kuenen, J.G.; Robertson, L.A.; Van Gemerden, H. Microbial interactions among aerobic and anaerobic sulfur-oxidizing bacteria. In: Marshall, K.C., ed. *Advances in Microbial Ecology.* New York: Plenum; 1985:1–59.

Kuivila, K.M.; Murray, J.W.; Devol, A.H. Methane production, sulfate reduction and competition for substrates in the sediments of Lake Washington. Geochim. Cosmochim. Acta 53:409–416; 1989.

Lamontagne, M.G.; Valiela, I. Denitrification measured by a direct N_2 flux method in sediments of Waquoit Bay, MA. Biogeochemistry 31:63–83; 1995.

Lovley, D.R. Dissimilatory Fe(III) and Mn(IV) reduction. Microbiol. Rev. 55:259–287; 1991.

Lovley, D.R.; Coates, J.D.; Blunt-Harris, E.L.; Phillips, E.J.P.; Woodward, J.C. Humic substances as electron acceptors for microbial respiration. Nature 382:445–448; 1996.

Lovley, D.R.; Klug, M.J. Model for the distribution of sulfate reduction and methanogenesis in fresh water sediments. Geochim. Cosmochim. Acta 50:11–18; 1986.

Lovley, D.R.; Phillips, E.J.P. Availability of ferric iron for microbial reduction in bottom sediments of the

freshwater tidal Potomac River. Appl. Environ. Microbiol. 52:751–757; 1986.

Lovley, D.R.; Phillips, E.J.P. Novel processes for anaerobic sulfate production from elemental sulfur by sulfate-reducing bacteria. Appl. Environ. Microbiol. 60:2394–2399; 1994.

Luther, G.W., III; Ferdelman, T.G.; Kostka, J.E.; Tsamakis, E.J.; Church, T.M. Temporal and spatial variability of reduced sulfur species (FeS_2, $S_2O_3^{2-}$) and porewater in salt marsh sediments. Biogeochemistry 14:57–88; 1991.

Mackin, J.E.; Swider, K.T. Organic matter decomposition pathways and oxygen consumption in coastal marine sediments. J. Mar. Res. 47:681–716; 1989.

Martens, C.S.; Klump, J.V. Biogeochemical cycling in an organic-rich coastal marine basin. I. Methane sediment-water exchange processes. Geochim. Cosmochim. Acta 44:471–490; 1980.

Martens, C.S.; Klump, J.V. Biogeochemical cycling in an organic-rich coastal marine basin. 4. Carbon budget for sediments dominated by sulfate reduction and methanogenesis. Geochim. Cosmochim. Acta 48:1987–2004; 1984.

Middelburg, J.J.; Soetaert, K.; Herman, P.M.J. Evaluation of the nitrogen isotope pairing method for measuring denitrification: a simulation analysis. Limnol. Oceanogr. 41:1839–1844; 1996a.

Middelburg, J.J.; Soetaert, K.; Herman, P.M.J.; Heip, C.H.R. Denitrification in marine sediments: A model study. Global Biogeochem. Cycles 10:661–673; 1996b.

Miller-Way, T.; Twilley, R.R. Theory and operation of continuous flow systems for the study of benthic-pelagic coupling. Mar. Ecol. Prog. Ser. 140:257–269; 1996.

Moeslund, L.; Thamdrup, B.; Jørgensen, B.B. Sulfur and iron cycling in a coastal sediment: Radiotracer studies and seasonal dynamics. Biogeochemistry 27:129–152; 1994.

Nielsen, L.P. Denitrification in sediment determined from nitrogen isotope pairing. FEMS Microbiol. Ecol. 86:357–362; 1992.

Nielsen, L.P.; Glud, R.N. Denitrification in a coastal sediment measured in situ by the nitrogen isotope pairing technique applied to a benthic flux chamber. Mar. Ecol. Prog. Ser. 137:181–186; 1996.

Nielsen, L.P.; Risgaard-Petersen, N.; Rysgaard, S.; Blackburn, T.H. Reply to the note by Middelburg et al. Limnol. Oceanogr. 41:1845–1846; 1996.

Nishio, T.; Koike, I.; Hattori, A. Denitrification, nitrate reduction, and oxygen consumption in coastal and estuarine sediments. Appl. Environ. Microbiol. 43:648–653; 1982.

Nishio, T.; Koike, I.; Hattori, A. Estimates of denitrification and nitrification in coastal and estuarine sediments. Appl. Environ. Microbiol. 45:1983; 1983.

Nowicki, B.L. The effect of temperature, oxygen, salinity, and nutrient enrichment on estuarine denitrification rates measured with a modified nitrogen gas flux technique. Estuarine Coastal Shelf Sci. 38:137–156; 1994.

Pamatmat, M.M. Benthic community metabolism: a review and assessment of present status and outlook. In: Coull, B.C., ed. *Ecology of Marine Benthos.* Columbia, SC: Univ. South Carolina Pr.; 1977: p. 89–111.

Pamatmat, M.M. Heat production by sediment: Ecological significance. Science 215:395–397; 1982.

Pamatmat, M.M.; Graf, G.; Bengtsson, W.; Noval, C.S. Heat production, ATP concentration and electron transport activity of marine sediments. Mar. Ecol. Prog. Ser. 4:135–143; 1981.

Parkes, R.J.; Cragg, B.A.; Bale, S.J.; Goodman, K.; Fry, C. A combined ecological and physiological approach to studying sulphate reduction within deep marine sediment layers. J. Microbiol. Methods 23:235–249; 1995.

Parkes, R.J.; Gibson, G.R.; Mueller-Harvey, I.; Buckingham, W.J.; Herbert, R.A. Determination of the substrates for sulphate-reducing bacteria within marine and estuarine sediments with different rates of sulphate reduction. J. Gen. Microbiol. 135:175–187; 1989.

Petersen, S.O. Influence of liquid cattle manure on reduction processes in soil. Biol. Fertility Soils 15:137–143; 1993.

Phillips, E.J.P.; Lovley, D.R. Determination of Fe(III) and Fe(II) in oxalate extracts of sediments. Soil Sci. Soc. Am. J. 51:938–941; 1987.

Postma, D. Concentrations of Mn and separation from Fe in sediments. 1. Kinetics and stoichiometry of the reaction between birnessite and dissolved Fe(II) at 10°C. Geochim. Cosmochim. Acta 49:1023–1033; 1985.

Pyzik, A.J.; Sommer, S.E. Sedimentary iron monosulfides: Kinetics and mechanism of formation. Geochim. Cosmochim. Acta 45:687–698; 1981.

Rasmussen, H.; Jørgensen, B.B. Microelectrode studies of seasonal oxygen uptake in a coastal sediment: role of molecular diffusion. Mar. Ecol. Prog. Ser. 81:289–303; 1992.

Reeburgh, W.S. Methane consumption in Cariaco trench waters and sediments. Earth Planet. Sci. Lett. 28:337–344; 1976.

Reeburgh, W.S. Anaerobic methane oxidation: Rate depth distributions in Skan Bay sediments. Earth Planet. Sci. Lett. 47:345–352; 1980.

Reeburgh, W.S. Rates of biogeochemical processes in anoxic sediments. Annu. Rev. Earth Planet. Sci. 11:269–298; 1983.

Reimers, C.E.; Fischer, K.M.; Merewether, R.; Smith, K.L., Jr.; Jahnke, R.A. Oxygen microprofiles mea-

sured in situ in deep ocean sediments. Nature 320:741–744; 1986.

Reimers, C.E.; Jahnke, R.A.; McCorkle, D.C. Carbon fluxes and burial rates over the continental slope and rise off central California with implications for the global carbon cycle. Global Biogeochem. Cycles 6:199–224; 1992.

Relexans, J.C. Measurements of the respiratory electron transport activity in marine sediments: State-of-the-art and interpretation. I. Methodology and review of literature data. Mar. Ecol. Prog. Ser. 136:277–287; 1996a.

Relexans, J.C. Measurements of the respiratory electron transport activity in marine sediments: State-of-the-art and interpretation. II. Significance of ETS activity data. Mar. Ecol. Prog. Ser. 136:289–301; 1996b.

Revsbech, N.P. An oxygen electrode with a guard cathode. Limnol. Oceanogr. 34:474–478; 1989.

Revsbech, N.P.; Jørgensen, B.B.; Blackburn, T.H.; Cohen, Y. Microelectrode studies of photosynthesis and O_2, H_2S, and pH profiles of a microbial mat. Limnol. Oceanogr. 28:1062–1074; 1983.

Risgaard-Petersen, N.; Rysgaard, S. Nitrate reduction in sediments and waterlogged soil measured by ^{15}N techniques. In: Alef, K.; Nannipieri, P., eds. *Anaerobic Microbial Activities in Soil.* London: Academic; 1995:287–310.

Roden, E.E.; Lovley, D.R. Evaluation of ^{55}Fe as a tracer of Fe(III) reduction in aquatic sediments. Geomicrobiol. J. 11:49–56; 1993.

Roden, E.E.; Tuttle, J.H. Inorganic sulfur cycling in mid and lower Chesapeake Bay sediments. Mar. Ecol. Prog. Ser. 93:101–18; 1993a.

Roden, E.E.; Tuttle, J.H. Inorganic sulfur turnover in oligohaline estuarine sediments. Biogeochemistry 22:81–105; 1993b.

Roden, E.E.; Wetzel, R.G. Organic carbon oxidation and suppression of methane production by microbial Fe(III) oxide reduction in vegetated and unvegetated freshwater wetland sediments. Limnol. Oceanogr. 41:1733–1748; 1996.

Rysgaard, S.; Risgaard-Petersen, N.; Nielsen, L.P.; Revsbech, N.P. Nitrification and denitrification in lake and estuarine sediments measured by the ^{15}N dilution technique and isotope pairing. Appl. Environ. Microbiol. 59:2093–2098; 1993.

Rysgaard, S.; Thamdrup, B.; Risgaard-Petersen, N.; Fossing, H.; Christensen; P.B., and Dalsgaard, T. Seasonal carbon and nutrient mineralization in a high-Arctic coastal marine sediment, Young Sound, Northeast Greenland. Mar. Ecol. Progr. Ser. 175:261–276; 1998.

Schink, B. Principles and limita of anaerobic degradation: Environmental and technological aspects. In: Zehnder, A.J.B., ed. *Biology of Anaerobic Microorganisms.* New York: Wiley; 1988:771–846.

Seitzinger, S.P. Denitrification in freshwater and coastal marine ecosystems: ecological and geochemical significance. Limnol. Oceanogr. 33:702–724; 1988.

Seitzinger, S.P.; Nixon, S.W.; Pilson, M.E.; Burke, S. Denitrification and N_2O production in nearshore marine sediments. Geochim. Cosmochim. Acta 44:1853–1860; 1980.

Skyring, G.W. Sulfate reduction in coastal ecosystems. Geomicrobiol. J. 5:295–374; 1987.

Smith, K.L., Jr. benthic community respiration in the N.W. Atlantic Ocean: In situ measurements from 40 to 5200 m. Mar. Biol. 47:337–347; 1978.

Smith, K.L., Jr.; Hinga, K.R. Sediment community respiration in the deep sea. In: Rowe, G.T., ed. *The Sea.* New York: Wiley; 1983:331–379.

Sørensen, J. Denitrification rates in a marine sediment as measured by the acetylene inhibition technique. Appl. Environ. Microbiol. 36:139–143; 1978.

Sørensen, J. Reduction of ferric iron in anaerobic, marine sediment and interaction with reduction of nitrate and sulfate. Appl. Environ. Microbiol. 43:319–324; 1982.

Sørensen, J.; Christensen, D.; Jørgensen, B.B. Volatile fatty acids and hydrogen as substrates for sulfate-reducing bacteria in anaerobic marine sediment. Appl. Environ. Microbiol. 42:5–11; 1981.

Sorokin, Y.I. Experimental investigation of bacterial sulfate reduction in the Black Sea using ^{35}S. Mikrobiologiya 31:402–410; 1962.

Spratt, H.G.; Morgan, M.D. Sulfur cycling in a cedar-dominated, freshwater wetland. Limnol. Oceanogr. 35:1586–1593; 1990.

Spratt, H.G., Jr.; Morgan, M.D.; Good, R.E. Sulfate reduction in peat from a New Jersey Pinelands cedar swamp. Appl. Environ. Microbiol. 53:1406–1411; 1987.

Straub, K.L.; Benz, M.; Schink, B.; Widdel, F. Anaerobic, nitrate-dependent microbial oxidation of ferrous iron. Appl. Environ. Microbiol. 62:1458–1460; 1996.

Suess, E. Particulate organic carbon flux in the ocean-surface productivity and oxygen utilization. Nature 288:260–263; 1980.

Sweerts, J.P.R.A.; St Louis, V; Cappenberg, T.E. Oxygen concentration profiles and exchange in sediment cores with circulated overlying water. Freshwater Biol. 21:552–556; 1989.

Swider, K.T.; Mackin, J.E. Transformations of sulfur compounds in marsh-flat sediments. Geochim. Cosmochim. Acta 53:2311–2323; 1989.

Teal, J.M.; Kanwisher, J. Gas exchange in a Georgia salt marsh. Limnol. Oceanogr. 6:388–399; 1961.

Tengberg, A.; De Bovee, F.; Hall, P.; Berelson, W.; Chadwick, D.; Ciceri, G.; Crassous, P.; Devol, A.; Emerson, S.; Gage, J.; Glud, R.; Grazziottini, F.; Gundersen, J.;

Hammond, D.; Helder, W.; Hinga, K.; Holby, O.; Jahnke, R.; Khripounoff, A.; Lieberman, S.; Nuppenau, V.; Pfannkuche, O.; Reimers, C.; Rowe, G.; Sahami, A.; Sayles, F.; Schurter, M.; Smallman, D.; Wehrli, B.; De Wilde, P. Benthic chamber and profiling landers in oceanography: A review of design, technical solutions and functioning. Prog. Oceanogr. 35:253–294; 1995.

Thamdrup, B. Bacterial manganese and iron reduction in aquatic sediments. Adv. Microb. Ecol. 16:41–84; 2000.

Thamdrup, B.; Canfield, D.E. Pathways of carbon oxidation in continental margin sediments off central Chile. Limnol. Oceanogr. 41:1629–1650; 1996.

Thamdrup, B.; Canfield, D.E.; Ferdelman, T.G.; Glud, R.N.; Gundersen, J.K. A biogeochemical survey of the anoxic basin Golfo Dulce, Costa Rica. Rev. Biol. Tropical 44(suppl. 3):19–33; 1996.

Thamdrup, B.; Fossing, H.; Jørgensen, B.B. Manganese, iron, and sulfur cycling in a coastal marine sediment, Aarhus Bay, Denmark. Geochim. Cosmochim. Acta 58:5115–5129; 1994a.

Thamdrup, B.; Glud, R.N.; Hansen, J.W. Manganese oxidation and in situ fluxes from a coastal sediment. Geochim. Cosmochim. Acta 58:2563–2570; 1994b.

Urban, N.R.; Brezonik, P.L.; Baker, L.A.; Sherman, L.A. Sulfate reduction and diffusion in sediments of Little Rock Lake, Wisconsin. Limnol. Oceanogr. 39:797–815; 1994.

Vedel, A.; Andersen, B.B.; Riisgård, H.U. Field investigations of pumping activity of the facultatively filter-feeding polychaete *Nereis diversicolor* using an improved infrared phototransducer system. Mar. Ecol. Prog. Ser. 103:91–101; 1994.

Wallmann, K.; Hennies, K.; König, I.; Petersen, W.; Knauth, H.D. A new procedure for the determination of "reactive" ferric iron and ferrous iron minerals in sediments. Limnol. Oceanogr. 38:1803–1812; 1993.

Wang, Y.; Van Cappellen, P. A multicomponent reactive transport model for early diagenesis: Application to redox cycling in coastal marine sediments. Geochim. Cosmochim. Acta 60:2993–3014; 1996.

Westrich, J.T. The consequences and controls of bacterial sulfate reduction in marine sediments. Ph.D. thesis, Yale University; 1983.

Wheatcroft, R.A.; Martin, W.R. Spatial variation in short-term (^{234}Th) sediment bioturbation intensity along an organic-carbon gradient. J. Mar. Res. 54:763–792; 1996.

Widdel, F.; Hansen, T.A. The dissimilatory sulfate- and sulfur-reducing bacteria. In: Balows, H. et al., eds. *The Procaryotes.* Berlin: Springer-Verlag; 1991:583–624.

Wieder, R.K.; Lang, G.E. Cycling of inorganic and organic sulfur in peat from Big Run Bog, West Virginia. Biogeochemistry 5:221–242; 1988.

Wollast, R. The coastal organic carbon cycle: Fluxes, sources, and sinks. In: Mantoura, R.F.C.; Martin, J.-M.; Wollast, R., eds. *Ocean Marine Processes in Global Change.* New York: Wiley; 1991:365–381.

Yao, W.; Millero, F.J. The rate of sulfide oxidation by δMnO_2 in seawater. Geochim. Cosmochim. Acta 57:3359–3365.

Zhabina, N.N.; Volkov, I.I. A method of determination of various sulfur compounds in sea sediments and rocks. In: Krumbein, W.E., ed. *Environmental Biogeochemistry and Geomicrobiology.* Ann Arbor, MI: Ann Arbor Science; 1978:735–746.

7

Decomposition and Soil Organic Matter Dynamics

G. Philip Robertson and Eldor A. Paul

Introduction

Decomposition is the process whereby dead organic material is broken down to its constituent parts, ultimately to carbon dioxide (CO_2) and inorganic ions such as ammonium (NH_4^+), calcium (Ca^{2+}), potassium (K^+), and other elements originally assimilated by the organisms now decomposing. At various points along this path the decomposing organic matter is consumed and metabolized by other organisms, which themselves will die and decompose. Decomposition is thus a dynamic recursive process that involves a complex array of physical, chemical, and biological interactions that complete the biogeochemical nutrient cycles.

Rates of decomposition vary tremendously as a function of the structure and chemical composition of the organic matter being decomposed (substrate quality), the abiotic environment in which decomposition is occurring (temperature, moisture, and aeration status in particular), and the degree to which the decomposing substrate is exposed to heterotrophs, both microbial and faunal (Kurcheva 1960; Bunnell et al. 1977; Jenny et al. 1949; Swift et al. 1979; Paustian et al. 1997). One might thus expect differences in rates of decomposition both within and between ecosystems. Within-ecosystem variability will occur as different materials are deposited and decompose in microhabitats that range from plant canopies to different positions along topographic gradients, different positions within soil profiles, and even different positions within soil aggregates. Differences among ecosystems arise from expressions of environmental and biotic gradients at larger scales, especially with respect to climate, ecosystem fertility, and successional status (Olson 1963; Meentemeyer 1978; Melillo et al. 1982; Wallace and Freedman 1986; Aber et al. 1990).

Operationally, in terrestrial ecosystems, decomposition typically defines the breakdown of organic matter into either inorganic ions or into an organic matter size class that permits its entry into the soil organic matter (SOM) pool. The SOM pool receives the breakdown products of decomposition, and the further decomposition and humification of these products falls under the general rubric of SOM dynamics—which also includes the turnover of microbes and soil invertebrates that further oxidize and assimilate SOM.

Typically, decomposition is measured as mass and nutrient loss from dead organic material placed in that part of the ecosystem in which it normally occurs—usually the soil surface for senescent plant leaves, branches, stems, and other aboveground litter, and various soil horizons for roots, fungi, and other belowground organisms or parts thereof. More often than not, the usual strategy for assessing mass loss is to entrain a known quantity of material at a specific location and to then periodically evaluate it or a subsample for mass and nutrient loss.

Methods for assessing organic matter dynamics (as opposed to decomposition per se) are varied and often more difficult to interpret than decomposition assays owing to the heterogeneous nature of SOM. The most comprehensive and least controversial measure is that of the total SOM pool itself. Combustion techniques provide an adequate representation of total organic carbon (C) stores in soil and can be used to document changes in these stores

over decadal to century intervals. These measures are particularly important for assessing changes in soil C pools as a function of land use change (e.g., Haas 1957) and as a function of changes in potential feedbacks in the global C budgets in response to climate change (e.g., Schlesinger 1990; IPCC 1996). Combustion techniques are less useful for understanding the role of SOM in ecosystem C dynamics because combustion techniques do not adequately measure C availability.

The availability of C to heterotrophs differs markedly from one ecosystem to another and can be independent of total C stores. For example, ecosystems with identical soil C stores may have very different soil C cycles because of marked differences in the availability of C stores to the heterotrophic community. Soil C takes a wide variety of organic forms, ranging from simple sugars to humified substances with large molecular weights and complex aromatic structures. These latter compounds are highly resistant to microbial attack, especially when protected by association with stable soil aggregates and clay minerals, and may thus have turnover times on the order of millennia.

Efforts to characterize SOM in ecologically meaningful ways have provided a variety of fractionation methods designed to separate SOM into functional pools. Classical fractionation procedures separate SOM into humic acid, fulvic acid, and humin components as a function of relative solubility in strong acid and base solutions (Sollins et al. 1999). The humic acid component is soluble in base but not acid, the fulvic acid component is soluble in both base and acid, and the humin component is insoluble in base. However, few of these fractions have been shown to be ecologically relevant across widely different ecosystems, soil types, and management or disturbance regimes (Duxbury et al. 1990; Collins et al. 1999; Sollins et al. 1999). More useful are two simple chemical fractionations: water-soluble C extracts, which appear related to carbon readily available to microbes, and C released by acid hydrolysis. Acid hydrolysis appears to provide a reasonable measure of the resistant C pool in many soils; Leavitt et al. (1997) found for a variety of soils that nonhydrolyzable C is on average 1400 years older than the total C.

Physical fractionation methods use wet sieving, density flotation gradients, or chemical dispersal to separate SOM into pools of different size and stability classes. Recent work in the U.S. Great Plains (Cambardella and Elliott 1993) underscores the potential importance of soil aggregate formation for protecting SOM. Earlier work in a wide variety of soils (e.g., Ladd and Amato 1980; Spycher et al. 1983; Baldock et al. 1990; Christensen 1992) has shown that SOM particles of different densities decompose at different rates. Light fractions are typically comprised of partially decomposed plant residues with high decomposition rates (Gregorich and Janzen 1996). That aggregate formation and the distribution of SOM density classes are under largely biological control and subject to disturbances imposed by management practices (Oades 1993; Gregorich and Janzen 1996) suggests ecological relevance for these measures.

The proportional composition for any particular soil appears to be best quantified via microbial bioassays in which CO_2 release is followed over long-term incubations of a year or more. This biological fractionation relies on the in situ microbial and microarthropod community to define ecologically relevant SOM fractions. Biological fractionation schemes have arisen concurrent with the development of quantitative soil C models over the past two decades. These models have resulted from efforts to predict the loss rate and the eventual level of soil C following disturbance, and most now incorporate the concept of multiple soil C pools with different turnover times (Jenkinson et al. 1987; Parton et al. 1987; Paustian et al. 1992). Usually these models recognize at least three SOM pools (Fig. 7.1): an active fraction that turns over on the order of months to years, comprised of recent residues and microbial biomass and metabolites; a slow fraction that turns over on the order of decades, comprised of stabilized decomposition products; and a resistant fraction of highly stabilized, recalcitrant organic matter that turns over on the order of centuries to millennia.

The curves describing CO_2 release during long-term incubations can be parameterized into two or more components related to their proportional composition, as described later. These components have intrinsic ecological relevance, and a further value for their application in soil C models (e.g., see Fig. 7.1). The application of these models is becoming increasingly important for evaluating historical and future global change scenarios (e.g.,

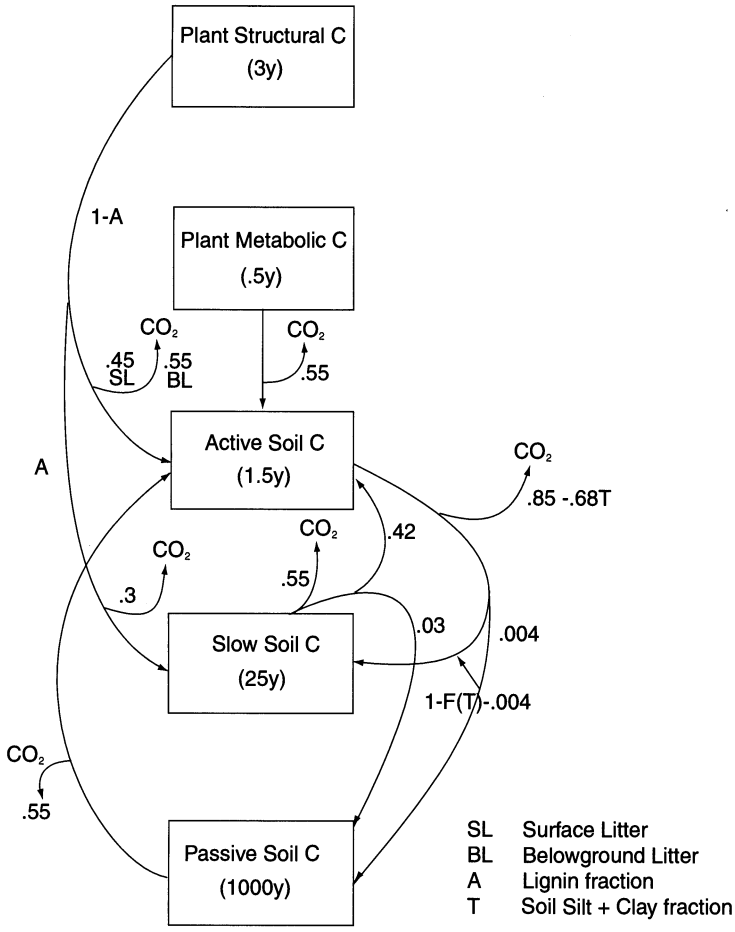

FIGURE 7.1. Structural components of the CENTURY soil organic matter model. Values adjacent to arrows are transfer coefficients for the noted carbon pools; parenthetical values are approximate turnover times. (From Paustian et al. [1992].)

Schlesinger 1984; Jenkinson et al. 1991; IPCC 1996).

In the remainder of this chapter we present and discuss appropriate methods for assessing plant litter decomposition and organic matter dynamics in terrestrial ecosystems. Dozens of contributions in the past decade have presented methods for assessing one or the other of these processes. We concentrate on those methods that have ecological relevance and that appear to be sufficiently well standardized to be usable for cross-ecosystem comparisons. This latter criterion is becoming increasingly important as the diversity of available methods limits opportunities for a posteriori syntheses of independently collected data from multiple sites and studies. Our contribution is intended to complement rather than complicate emerging efforts to standardize current soil methods for ecological research (e.g., Robertson et al. 1999b).

Plant Litter Decomposition

Fine Litter Decomposition Rates

The decomposition of plant leaves and other relatively fine material is typically assayed by following mass and nutrient changes in litter placed in mesh bags on the soil surface. As the organic material decomposes, changes in mass document the decomposition rate, and changes in nutrient composition document rates of nutrient release, retention, and immobilization (e.g., Falconer et al. 1933; Bocock et al. 1960; Gosz et al. 1973; Melillo et al. 1982; Heal et al. 1997).

Decomposition is carried out by a complex array of heterotrophic organisms that vary widely in size and function. Commonly these organisms are grouped into size (body-width) classes that correspond to the groups microflora and -fauna, and

macro-, meso-, and megafauna. The microheterotrophs are <100 μm and include mainly bacteria, fungi, nematodes, protozoans, and rotifers; the mesofauna are generally <2 mm in width and include mites, springtails, diplurans, and enchytraeids; and the macro-fauna include earthworms, isopods, spiders, molluscs and other organisms >2 mm width. Many of these organisms are detritovores, some are carnivores, and all appear to be important parts of the soil food web (Swift 1979; Beare et al. 1995; Coleman and Crossley 1996).

Investigations of decomposition with litter bags have employed different mesh sizes, sometimes to experimentally exclude different groups in order to determine their functional significance for decomposition (e.g., Heath et al. 1964). Generally, however, mesh size has been chosen to optimize the access of all organisms to entrained litter while minimizing excessive particle loss in situ. Particle loss to mineral soil is an important part of decomposition, and too small a mesh size will not only exclude certain organisms but will also inhibit particle loss. Mesh size may also affect litter microclimate (Witkamp and Olson 1963) if it inhibits air flow and water flux, and can also alter root ingrowth.

Although litter bag studies are compromised somewhat by mesh size limitations, alternatives to litter bags suffer from equal or greater problems. For example, litter baskets with mesh bottoms and mostly-open tops (Stevenson and Dindal 1981; Blair et al. 1991) allow greater access for macroinvertebrates and better represent the soil surface microclimate, but also allow additional litterfall inputs. Tethered material (Witkamp and Olson 1963; Lang 1974) is completely exposed to the biotic and abiotic soil surface environment but even large pieces that fragment from the original material can be difficult to recover for later weighing and chemical analysis. Thus, litter bags with an appropriate mesh size remain the preferred means for directly estimating fine litter mass loss (Harmon et al. 1999).

Indirect measures of estimating decomposition include estimates of the decomposition rate constant k using litter input: forest floor ratios (Olson 1963), and annual differences in the lowest and highest stores of litter (e.g., Loomis 1975). These methods are usually less preferable than direct means because of their underlying assumption of steady state conditions and the requirement for precise measurements of litter stores, especially where decomposition rates are low. In some environments, most notably annual cropping systems, these indirect techniques to estimate mass loss can be quite accurate.

To allow access to macrofauna, litter bag mesh size must be >2 mm although 1-mm nylon mesh has been used in most recent litter bag studies. Harmon et al. (1999) recommend a 1.5-mm fiberglass mesh for high-light environments in which nylon and other organic materials will be subject to ultraviolet (UV) attack. This is probably a reasonable compromise that allows access for most mesofauna, that preserves a near-normal litter layer microclimate, and that avoids excessive loss of large litter fragments. No mesh size will be free of compromising assumptions, however, and results from any litter bag study must be interpreted accordingly. Coleman et al. (1999) recommend specific procedures for assessing macroinvertebrate contributions to decomposition rates, and these should be consulted for ecosystems in which macroinvertebrates will substantially affect decay rates.

The size of the litter bag must also be appropriate to the litter under investigation; 20 × 20 cm is conventional, but bags may need to be larger for larger litter or for litter from more diverse plant communities. Depending on the purpose of the study, the contents of each litter bag should be proportionately representative of the target ecosystem: single versus mixed-species litter bags are known to exhibit different decomposition dynamics (Blair et al. 1990), and in many plant communities it will be appropriate to include fine woody debris (e.g., twigs). Litter should be freshly senesced.

The number of litter bags to deploy at a site will vary as a function of expected decomposition rate and the microclimatic heterogeneity of the site. The minimum number of bags must be sufficient to describe the decay curve with enough confidence that the decomposition rate constant k can be adequately estimated. Usually a geometric sampling interval is appropriate, that is, more bags are retrieved from the field earlier than later in the study. Often 3 to 6 collections arranged by season are adequate for the first year of the study and 2 to 4 collections in subsequent years. Most studies have examined decomposition dynamics over 1- to 3-year periods; consequently we know less about late-term decom-

position in most environments, so there is, in fact, considerable value for extending studies to >5 years (Harmon et al. 1999).

At least 4 to 5 litter bags should be retrieved at each sampling interval for each experimental or landscape replicate, which should be chosen to avoid pseudoreplication. Thus, it is not uncommon to deploy 100 or more litter bags to appropriately characterize decomposition within an ecosystem. For postcollection chemical analyses it may be appropriate to composite samples after drying and weighing. Samples to be chemically analyzed should be dried at 55°C to avoid heat-induced chemical changes in C content. Both litter mass and sometimes chemical content must be corrected for contaminating soil that is commonly collected with the litter bags, especially at later stages of decomposition. Mass can be corrected by combusting each sample and calculating an ash-free dry mass proportion to estimate the litter versus soil portion of the sample. Where contaminating soil has a high organic matter content or can affect nutrient analyses, a more involved correction is necessary (Blair 1988; Harmon et al. 1999).

The decomposition rate constant k can usually be calculated by fitting mass loss to the single negative exponential model (Jenny et al. 1949; Olson 1963):

$$x_t/x_o = e^{-kt} \quad (7.1)$$

where x_t/x_o is the proportion of original mass remaining at time t, t is elapsed time in years, and k is the decomposition rate constant.

Least-squares regression (e.g., Fig. 7.2) will provide values for k, for the y-intercept, and confidence intervals. The y-intercept can be used to indicate the presence of initial decomposition stages that are more accelerated or slower than that predicted by the model (Harmon et al. 1999). In these cases, alternative models may be more appropriate.

A wide variety of chemical analyses have been applied to decomposing litter in attempts to identify functional predictors of decay and nutrient mineralization rates (see Heal et al. 1996 for a recent review). Recent efforts have identified total polyphenol content and protein-binding capacities of litter as useful predictors of rates (Palm and Sanchez 1991; Handayanto et al. 1997) in addition to the more conventional nitrogen and lignin contents

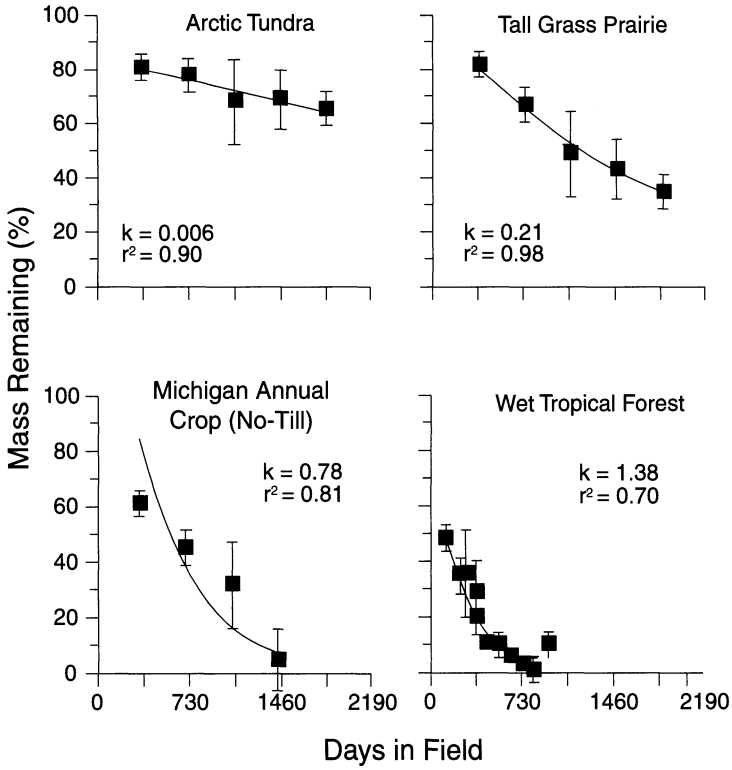

FIGURE 7.2. Mass loss from litter bags containing wheat litter from a southern Michigan agricultural site placed in four different ecosystems. The decomposition rate constant k is calculated by fitting the exponential decay equation noted in text and diagrammed in each graph. (From Halstead et al. [1996].)

(e.g., Melillo et al. 1982; Aber et al. 1990). Palm and Rowland (1997) suggest a standard set of analyses for characterizing plant litter quality, as do Harmon and Lajtha (1999).

Woody Detritus

Woody detritus includes both fine and coarse woody debris. Fine fractions are defined operationally as dead trees and branches <10 cm in diameter and <1 m long, as well as twigs and roots too large for litter bags. Coarse fractions include boles, branches, and roots larger than fine fractions. The principal reason for dividing woody detritus into these fractions is mode of study: fine fractions can be weighed intact while coarse fractions must be subsampled in the field.

Methods for studying woody detritus are analogous to litter bag methods but usually without the need for litter confinement. Woody material can be cut to standard lengths (a typical length is 10 times longer than the mean diameter of the material), tethered and marked for later collection, and placed in the field in microclimates that would be normally encountered—on the litter layer, suspended above the soil surface (for standing dead material such as dead branches still attached to stems), or buried (for coarse roots).

At intervals appropriate to the climatic environment and composition of the wood, tethered pieces are collected and taken to the laboratory for drying, weighing, and chemical analysis. A minimum of 10 sample collections will likely be needed, spaced at 1- to 3-year intervals. Any given study may take decades to complete.

Decomposition of woody material is a function of size and species as well as placement, so the number of samples initially deployed will need to be chosen carefully to provide a geometric range of diameter classes and an appropriate range of genera. It is usually not necessary to sample below the genus level except for genera with diverse heartwood contents. Because bark, sapwood, and heartwood decay at different rates, it is important to record the proportions of these materials in the pieces initially deployed. As for fine litter, replication should be organized to avoid pseudoreplication. Sample preparation, chemical analyses, and calculations are similar to those for fine plant litter, though analyses should be performed separately for bark, sapwood, and heartwood.

Because it is impractical to weigh large woody debris, one can remove trimmed end pieces from the field for weighing and chemical analyses. Prior to initial sampling, it is necessary to estimate the mass of each piece that will eventually be removed; this should be done at the outset of the study by measuring in situ the volume of each segment that will be removed and assuming an initial density ($g\ cm^{-3}$) equal to the density of the first sample. Formulas for determining the volume of complex shapes are provided in Harmon et al. (1999).

Reciprocal Transplants and Standard Substrates

The relative influence of climate versus litter quality for controlling decomposition rates can be evaluated using reciprocal litter transplants and standard substrates. Reciprocal litter transplants usually involve exchanging litter bags or tethered wood among two or more sites: litter from ecosystem A is allowed to decompose in both ecosystem A and ecosystem B, as is litter from ecosystem B. This scheme effectively removes litter quality as an explanation for differences in the decomposition rates of litter from the two ecosystems. For example, ecosystem A litter should decompose at the same rate in each ecosystem if the decomposition environment of ecosystem A is similar to that of ecosystem B; a faster rate of litter disappearance in ecosystem B means a more favorable environment in ecosystem B (see Fig. 7.2).

Different rates of decay are usually interpreted to mean different abiotic conditions among sites, that is, between-site differences in moisture, temperature, and (for buried litter) aeration regimes. However, differences in the biotic environment can also lead to different decomposition rates among ecosystems, and these differences need also to be kept in mind when interpreting transplant results. For example, differences in the soil invertebrate community and, perhaps to a lesser extent, differences in the microbial community may accelerate decomposition in one ecosystem relative to another; separating abiotic from biotic factors requires a more elaborate experimental design. Notwithstanding the difficulty of separating the effects of the abiotic from the biotic environment, recip-

rocal transplants can provide a valuable approach for evaluating differences in substrate quality as an explanation for decomposition rate differences among divergent ecosystems.

Substituting a standard substrate for native litter provides a similar and logistically simple means for evaluating substrate quality versus environment differences. In this technique (e.g., Binkley 1984; Sinsabaugh et al. 1993; O'Lear et al. 1996) a single organic substrate, usually one that is manufactured and thus commercially available, is placed in litter bags or buried across a range of two or more ecosystems. Studies have employed cellulose filter paper and hardwood dowels as substrate standards. Both filter paper and dowels vary somewhat in their substrate composition, however—filter paper can contain small but varying amounts of nitrogen, and dowels can contain different amounts of decay-resistant heartwood—so it is necessary to select materials carefully. Because of substrate differences, results may still be interpretable only within the scope of a particular study. Harmon et al. (1999) recommend dowels be made of basswood (*Tilia* spp.), birch (*Betula* spp.), or ramin (*Gonystylus bancannus*), 6 mm in diameter by 60 cm in length. Placement, recovery, and analysis of standardized substrates follow the same procedures as for fine and coarse woody litter, above.

Soil Organic Matter Dynamics

Soil Organic Matter Stores

Soil organic matter is defined operationally as C and associated nutrients entrained in soil mineral horizons, in forms no longer easily identifiable as plant residues. The O horizon or litter layer is by convention excluded from SOM stores, because it can be identified as specific plant residues that in modeling are handled by separate equations. In most soils, the mass of C in mineral horizons far outweighs the mass of C in the litter horizon. Soil, however, includes the entire solum, and especially in ecosystem studies it is important to include C in horizons both above and below the more commonly analyzed A horizon when calculating total ecosystem SOM stores. This may mean sampling to a meter or more in many soils. Sites in which significant decomposition occurs in the tree or grass canopy present a special challenge, as this material also is part of ecosystem decomposition.

Litter stores are easily evaluated by collecting litter from known-area quadrants (e.g., 1 m^2) and analyzing for C and nutrients as for leaf and woody material, above. In most ecosystems, stores will vary by season and collections should be staggered accordingly. Stores of organic C in mineral soil are usually evaluated by whole-soil combustion. Any inorganic C that may be present is either removed beforehand or analyzed separately and subtracted from combustion results. Inorganic C can be a major fraction of total C in calcareous soils low in SOM; this is often the case for soils in arid and semiarid environments, for young soils developed on carbonate parent materials, and for agricultural soils limed for pH control.

Modern C and N (CN) analyzers oxidize small samples at high temperatures (>1000°C) in an O_2-enriched atmosphere, then measure the resulting gases by gas chromatography (CO_2 and N gases) or infrared gas analysis (CO_2 only) (Nelson and Sommers 1996). Small sample size (usually <20 mg) means that great care must be taken to adequately subsample and powder the soil to be analyzed; inadequate grinding is the leading source of analytical variability for most soils (Sollins et al. 1999). Conversion of gravimetric results (e.g., g C/g $soil^{-1}$) to an areal extent (e.g., g C m^{-2}) is crucial for including SOM C in total ecosystem carbon budgets and for making comparisons of SOM across ecosystems with different soil types and depths. It is thus critically important to have accurate values for both soil bulk density (g soil cm^{-3}), stone content, and soil horizon depths. Bulk density values are needed to convert from gravimetric values to areal values, stone volume must be excluded from the conversion, and estimates must be weighted by horizon depths, including the depth of the O or litter layer horizon (Sollins et al. 1999). Alternately, single soil cores taken to a depth of minimal soil C content can be homogenized and analyzed for total C content, and this total-core value then divided by the sampled stone-free surface area to yield an areal estimate for SOM C.

Physical Fractionation of Soil Organic Matter

The two most promising strategies for physically separating SOM into differentially reactive fractions are fractionations based on density and size

of both the plant residues and soil aggregates. Soils are typically comprised of a wide variety of particles that differ in size, shape, mineral composition, and density. Typically, these particles exhibit associated differences in C content and the availability of this C to microbial oxidation. Ecosystem-level differences in these properties can provide insight into differences among ecosystems and disturbance regimes with respect to SOM dynamics.

Density fractionation is useful where lighter particles exhibit different C dynamics than heavier particles; most obvious are density differences between organic materials, most of which are light, and mineral-associated materials, most of which are heavy (Gregorich and Janzen, 1996). At intermediate densities are a wide range of materials, including amorphous, mineral material adsorbed onto organic fractions, secondary minerals such as clays coated with different thicknesses of organic compounds, and soil aggregates of differential stabilities (Turchenek and Oades 1978; Spycher et al. 1983; Tisdall 1996; Sollins et al. 1999). The type of mineral present can greatly affect decomposition rates, especially when clays with mixed exchange characteristics are involved (Sollins et al. 1999).

Soils are most easily separated into density fractions using flotation. The simplest method is to mix the soil with an inert heavy liquid such as sodium iodide (NaI) or sodium polytungstate (NaPT) and remove the floating fraction (Strickland and Sollins 1987). By sequentially adjusting the density of the NaI or NaPT, soil fractions of differing densities can be collected sequentially, usually across an initial range of 1.0 to 2.0 g cm^{-3}. Initial suspensions can be mixed or sonicated to disperse aggregates of different stabilities. Each fraction can then be analyzed for C and N content. Sollins et al. (1999) provide a specific procedure.

Size fractionation (as opposed to density fractionation) is based on the fact that different particle sizes are differentially reactive because of differences in specific surface areas. For example, clay-size particles (<2 μm in diameter) have a surface area that is 10^4 larger than the surface area of sand-size particles (<2 mm in diameter): approximately 10^2 versus 10^6 $cm^2/g\ soil^{-1}$, respectively. One might thus expect the smaller particles to have adsorbed a greater fraction of organic material that will also be more accessible (because of its larger surface area) to microbial oxidation.

A number of techniques are available for sorting soil into size classes for subsequent chemical analysis (Gee and Bauder 1986; Elliott et al. 1999). Efforts to correlate SOM size class fractions with ecosystem attributes have successfully used within-aggregate particulate organic matter (Cambardella and Elliott, 1992, 1993) and light fraction (Gregorich and Janzen 1996) components. These coarse particulate organic matter fractions appear to correlate well with land use management and vegetation changes and with differences in CO_2 evolution in extended laboratory incubations. Carter and Stewart (1996) review the relationship between soil structure, various soil C fractions, and SOM storage and turnover.

Biological Soil Organic Matter Fractions

Biological fractions are defined by the relative rates of SOM turnover in short- versus long-term soil incubations. Rates of CO_2 release during incubations typically follow an exponential decay curve, that is, CO_2 release is much faster earlier in the incubation than later. As the more labile C is oxidized in the incubation, the slow-turnover material is unmasked and both fractions can then be compared with the total C pool to derive fast- and slow-turnover SOM fractions (Fig. 7.3). The turnover of the old resistant pool can be determined by acid hydrolysis (and if necessary confirmed by C dating) and is expressed as mean residence time. The amount of C coming from the old pool is small in laboratory incubations. The mean residence time therefore has little effect on the determination of the dynamics of the active and slow pools, although the size of the old pool enters into the calculations and should be estimated independently by acid hydrolysis.

Laboratory-derived decomposition rate constants can be converted to mean residence times by the knowledge that in first order reactions at steady state, mean residence time is $1/k$. The laboratory mean residence times can be converted to field mean residence times through the use of Q_{10} relationships and knowledge of the field mean annual temperatures. As noted above, the resistant pool is measured with acid hydrolysis (Martel and Paul 1974, Leavitt et al. 1997). These three pools analytically define the conceptual pools of the same names that are incorporated in leading SOM mod-

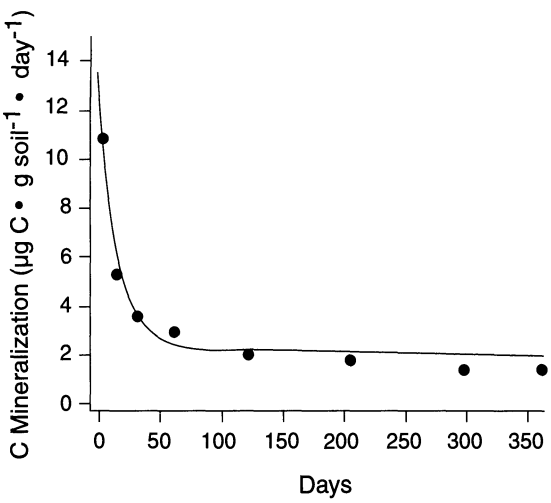

FIGURE 7.3. Long-term carbon mineralization in a cultivated soil from an agricultural site in southwest Michigan. The solid line is fit with the 2-pool nonlinear model noted in text. The model provides estimates of the fast and slow turnover pools; the passive or resistant pool can be estimated by acid hydrolysis. (From Paul et al. [1999].)

els (see Fig. 7.1) (Paul et al. 1999, in press). Models make it possible to correct for the effects of microbial growth and the knowledge that materials in soil move from one pool to the other. Analytically determined SOM decomposition kinetics greatly assist model improvement and in turn benefits our empirical understanding and application of SOM knowledge (Paustian et al. 1992; Paul et al. 1997)

A variety of short-term incubation techniques have been developed that involve measuring CO_2 release from incubated soil over 1- to 24-hour incubation periods. This release provides a quick snapshot of the quantity of readily mineralizable C in one soil versus another. Methods range from simple incubations of intact soil cores brought to some optimal proportion of water-holding capacity in the laboratory (e.g., Robertson et al. 1988; Collins et al. 1999) to more elaborate shaken-slurry incubations that—when accompanied by a glucose-amended companion slurry—can provide a relative measure of microbial biomass (e.g., Anderson and Domsch 1989; Beare et al. 1990).

In many soils, an initial CO_2 flush associated with soil sampling, mixing, and sieving can distort estimates of the size of the fast turnover pool, so some methods—especially long-term incubations—employ a preincubation interval of several days. Preincubation is not important for within-site comparisons of immediately available SOM C or for intact-core samplings, but for cross-study comparisons in which samples may be dried, differentially mixed, sieved, or brought to a new moisture content, preincubation can be important to normalize for differential sampling effects and for differences in rainfall and temperature patterns in the days immediately prior to sampling.

Robertson et al. (1999a) recommend a technique in which unamended soil is brought to the laboratory and, after sieving, is incubated at optimal water content (approximately 60% water-holding capacity) in an aerobic atmosphere for 7 days. At the end of 7 days, the soil's respiration potential is assessed by measuring the rate of CO_2 release over a 2 to 3-hour period during which soil head-space is sealed from the atmosphere. Carbon dioxide is readily measured by introducing 1-ml samples into a stream of N_2 carrier gas connected to an infrared gas analyzer. This technique can be amended to follow long-term CO_2 release by repeating CO_2 analyses at geometrically increasing intervals (e.g., 14, 28, 42, 63, 84, 105, 140, 196, and 252 days). Long-term N release can be followed concomitantly by sacrificing subsamples at each interval for inorganic N analysis.

Long-term incubations can be used to estimate multiple SOM pools by fitting the following model to a graph of CO_2 production (e.g., CO_2-C g^{-1} day^{-1} or CO_2-C cm^{-2} day^{-1}) versus incubation time:

$$\text{C Mineralization}_t = k_1(C_1e^{-k_1t}) + k_2(C_2e^{-k_2t}) \quad (7.2)$$

where C_1 is carbon content of the active or fast turnover pool, k_1 is the rate constant for the C_1 pool, C_2 is carbon content of the intermediate or slow turnover pool, k_2 is the rate constant for the intermediate pool, and t is incubation time in days.

The third, resistant pool can be very roughly estimated as total C (SOM stores, above) less C_1 and C_2. A more accurate estimate of the resistant pool can be made by using acid hydrolysis to define its size and by using the ^{14}C age of the hydrolysis residue to estimate the rate constant for this pool (Paul et al. 1998). Because of the great age of this pool, an average age of 500 y can be assumed or one can

use a two-pool constrained model once the size of the resistant pool is known (Paul et al. 2000).

Statistical analysis of the curves is most easily accomplished when the CO_2 evolution data are expressed on a rate per unit time basis rather than as cumulative curves (Hess and Schmidt 1995). Use of all the data in a single regression equation with separate parameter estimates for each treatment provides much greater statistical power than analyzing each treatment in a separate regression (Willson et al. in press). The effect of possible autocorrelation from repeated measurements of the same sample also can be statistically corrected (Paul et al. in press).

Use of Tracers

The isotopes of C include the radioactive ^{14}C occurring in minute quantities in the atmosphere and ^{13}C, which has a stable natural abundance of 1.1%. The $^{14}CO_2$ produced in the atmosphere by the interaction of cosmic radiation with N_2 is incorporated into plants during photosynthesis at a fairly constant rate, and can be measured with carbon dating techniques (Goh 1991). This is expensive and not readily accessible, but together with acid hydrolysis gives the best estimates of the size and turnover of the old resistant SOM fraction (Paul et al. 1998; Leavitt et al. 1997). Added ^{14}C, in the form of uniformly labeled plant residues exposed to a high ^{14}C atmosphere, give exceptionally useful information on organic matter breakdown and the incorporation of C into microbial biomass (Wolf et al. 1994). It is difficult to produce uniformly labeled substrates, but field experiments can be undertaken with commercially available, specifically labeled substrates if adequate health and safety precautions for working with a radioactive isotope are followed (Schimel 1993).

The stable isotope ^{13}C has been utilized in experiments in which plants have been ^{13}C-labeled in the laboratory in a fashion similar to that used for radioactive elements. Reliable automated mass spectrometers to measure the stable isotopes are available in many laboratories. The naturally occurring discrimination against $^{13}CO_2$ by plants with a C_3 photosynthetic pathway relative to those with a C_4 pathway provides a powerful, naturally occurring label in many parts of the world. This requires a C_3–C_4 plant growth switch, such as the growth of C_4 corn or sorghum on sites previously forested with C_3 trees, or the growth of C_3 wheat, rice, cold season grasses, or most trees on prairie or savanna soils that previously had C_4 native vegetation. Sites that have a mixed signal make it possible to grow either a C_3 or C_4 test species. The ^{13}C either enriched or depleted in the test species can be used to measure the fate of test species plant residues—both their incorporation into various soil biological, chemical, and physical fractions as well as changes in their pool sizes and flux rates.

^{13}C studies are particularly useful when combined with CO_2 evolution studies (Paul et al. 1999). The measurement of the $^{13}CO_2$ evolved during extended laboratory incubation yields estimates of the active and slow pool sizes and decomposition kinetics for the labeled material. Details of these techniques are available in Schimel (1993), Boutton (1996), Coleman and Fry (1991), and Paul et al. (1998, 1999). The element N is closely associated with soil C, and the stable isotope ^{15}N has been utilized in many residue decomposition and SOM turnover studies. It, too, can provide much important information on decomposition as well as on the microbial growth and N immobilization that occurs during decomposition (Hauck et al. 1994).

Acknowledgments We thank a number of individuals for providing helpful discussion and insights during the preparation of this chapter. We thank in particular discussants at the 1996 LTER Soil Methods Standardization Workshop held in Sevilleta, New Mexico, and especially M.E. Harmon, J.M. Blair, P. Sollins, E.T. Elliott, and D. Harris. This work was supported by the National Science Foundation LTER program and the Michigan Agricultural Experiment Station.

References

Aber, J.D.; Melillo, J.M.; McClaugherty, C.A. Predicting long-term patterns of mass loss, nitrogen dynamics, and soil organic matter formation from initial fine litter chemistry in temperate forest ecosystems. Can. J. Botany 68:2201–2208; 1990.

Anderson, T.; Domsch, K.H. Ratios of biomass carbon to total organic carbon in arable soils. Soil Biol. Biochem. 21:471–479; 1989.

Baldock, J.A.; Oades, J.M.; Vasallo, A.M.; Wilson, M.A. Solid-state CP/MAS ^{13}C NMR analysis of particle size

and density fractions of a soil incubated with uniformly labeled ^{13}C-glucose. Aust. J. Soil Res. 28:193–212; 1990.

Beare, M.H.; Coleman, D.C.; Crossley, D.A.J.; Hendrix, P.F.; Odum, E.P. A hierarchical approach to evaluating the significance of soil biodiversity to biogeochemical cycling. Plant Soil 170:5–22; 1995.

Beare, M.H.; Neely, C.L.; Coleman, D.C.; Hargrove, W.L. A substrate-induced respiration (SIR) method for measurement of fungal bacterial and total microbial biomass on plant residues. Soil Biol. Biochem. 22:585–594; 1990.

Binkley, D. Ion exchange resin bags: Factors affecting estimates of nitrogen availability (adsorption of ammonium and nitrate, *Pinus taeda*). Soil Sci. Soc. Am. J. 48:1181–1184; 1984.

Blair, J.M. Nutrient release from decomposing foliar litter of three tree species with special reference to calcium, magnesium, and potassium dynamics. Plant Soil 110:49–55; 1988.

Blair, J.M.; Crossley, D.A., Jr.; Callaham, L.C. A litter basket technique for measurement of nutrient dynamics in forest floor. Agric. Ecosyst. Environ. 34:465–471; 1991.

Blair, J.M.; Parmelee, R.W.; Beare, M.H. Decay rates, nitrogen fluxes and decomposer communities of single- and mixed-species foliar litter. Ecology 71:1976–1985; 1990.

Bocock, K.L.; Gilbert, O.J.; Capstick, C.K.; Twinn, D.W.; Waid, J.S.; Woodmann, M.J. Changes in leaf litter when placed on the surface of soils with contrasting humus types. I. Losses in dry weight of oak and ash leaf litter. J. Soil Sci. 11:1–9; 1960.

Boutton, T.W. Stable carbon isotope ratios of soil organic matter and their use as indicators of vegetation and climate change. In: Boutton, T.W.; Yamasaki, S., eds. *Mass Spectrometry.* New York: Marcel Dekker; 1996:47–82.

Bunnell, F.L.; Tait, D.E.N.; Flanagan, P.W.; VanCleve, K. Microbial respiration and substrate loss. I. A general model of the influences of abiotic factors. Soil Biol. Biochem. 9:33–40; 1977.

Cambardella, C.A.; Elliott, E.T. Particulate soil organic matter changes across a grassland cultivation sequence. Soil Sci. Soc. Am. J. 56:777–783; 1992.

Cambardella, C.A.; Elliott, E.T. Carbon and nitrogen distribution in aggregates from cultivated and native grassland soils. Soil Sci. Soc. Am. J. 57:1071–1076; 1993.

Carter, M.R.; Stewart, B.A., eds. *Structure and Organic Matter Storage in Agricultural Soils.* Boca Raton, FL: CRC; 1996.

Christensen, B.T. Physical fractionation of soil and organic matter in primary particle size and density separates. Adv. Soil Sci. 20:1–90; 1992.

Coleman, D.C.; Blair, J.M.; Elliott, E.T.; Freckman, D.W. Soil invertebrates. In: Robertson, G.P.; Bledsoe, C.S.; Coleman, D.C.; Sollins, P., eds. *Standard Soil Methods for Long-Term Ecological Research.* New York: Oxford Univ. Pr.; 1999:349–377.

Coleman, D.C.; Crossley, D.A., Jr. *Fundamentals of Soil Ecology.* San Diego, CA: Academic; 1996.

Coleman, D.C.; Fry, B. *Carbon Isotope Techniques.* San Diego, CA: Academic; 1991.

Collins, H.P.; Paul, E.A.; Blevins, R.L.; Bundy, L.G.; Christenson, D.R.; Dick, W.A.; Huggins, D.R.; Lyon, D.J.; Peters, S.E.; Turco, R.F. Carbon pools and dynamics in Corn Belt agroecosystems. Soil Sci. Soc. Am. J. 63:584–589; 1999.

Duxbury, J.M.; Smith, M.S.; Doran, J.W. Soil organic matter as a source and a sink of plant nutrients. In: Coleman, D.C.; Oades, J.M.; Uehara, G., eds. *Dynamics of Soil Organic Matter in Tropical Soils.* Honolulu, HI: Univ. Hawaii Pr.; 1990:33–67.

Elliott, E.T.; Heil, J.W.; Kelly, E.F.; Monger, H.C. Soil structural and other physical properties. In: Robertson, G.P.; Bledsoe, C.S.; Coleman, D.C.; Sollins, P, eds. *Methods of Soil Analysis.* New York: Oxford Univ. Pr.; 1999:74–88.

Falconer, G.J.; Wright, J.W.; Beall, H.W. The decomposition of certain types of fresh litter under field conditions. Am. J. Bot. 55:1632–1640; 1933.

Gee, G.W.; Bauder, J.W. Particle size analysis. Agronomy 9:383–411; 1986.

Goh, K.M. Bomb carbon. In: Coleman, D.C.; Fry, B., eds. *Carbon Isotope Techniques.* San Diego, CA: Academic; 1991:147–154.

Gosz, J.R.; Likens, G.E.; Bormann, F.H. Nutrient release from decomposing leaf and branch litter in the Hubbard Brook Forest, New Hampshire. Ecol. Monogr. 43:173–191; 1973.

Gregorich, E.G.; Janzen, H.H. Storage of soil carbon in the light fraction and macroorganic matter. In: Carter, M.R.; Stewart, B.A., eds. *Structure and Organic Matter Storage in Agricultural Soils.* Boca Raton, FL: CRC; 1996: 167–190.

Haas, H.J.; Evans, C.E.; Miles, E.F. *Nitrogen and Carbon Changes in Great Plains Soils as Influenced by Cropping and Soil Treatments.* Washington, DC: United States Department of Agriculture (USDA) Technical Bulletin 1164; 1957.

Halstead, S.J.; Paul, E.A., Paustian, K.; Harmon, M. Decomposition rates of wheat straw across a network of ecosystems. Agron. Abstr. 232; 1996.

Handayanto, E.; Giller, K.E.; Cadisch, G. Regulating N release from legume tree prunings by mixing residues of different quality. Soil Biol. Biochem. 29:1417–1426; 1997.

Hauck, R.D.; Meisinger, J.J.; Mulvaney, R.L. *Practical Considerations in the Use of Nitrogen Tracers in Ag-*

ricultural and Environmental Research. SSSA book series 5. Madison, WI: Soil Science Society of America; 1994:907–950.

Harmon, M.E.; Lajtha, K. Analysis of detritus and organic horizons for mineral and organic constituents. In: Robertson, G.P.; Bledsoe, C.S.; Coleman, D.C.; Sollins, P., eds. *Standard Soil Methods for Long-Term Ecological Research.* New York: Oxford Univ. Pr.; 1999:143–165.

Harmon, M.E., Nadelhoffer, K.J.; Blair, J.M. Measuring decomposition, nutrient turnover, and stores in plant litter. In: Robertson, G.P.; Bledsoe, C.S.; Coleman, D.C.; Sollins, P., eds. *Standard Soil Methods for Long-Term Ecological Research.* New York: Oxford Univ. Pr.; 1999:202–240.

Heal, O.W.; Anderson, J.M.; Swift, M.J. Plant litter quality and decomposition: An historical overview. In: Cadisch, G.; Giller, K.E., eds. *Driven by Nature: Plant Litter Quality and Decomposition.* Wallingford, UK: CAB International; 1997:3–30.

Heath, G.W.; Edwards, C.A.; Arnold, M.K. Some methods for assessing the activity of soil animals in the breakdown of leaves. Pedobiologica 4:80–87; 1964.

Hess, T.F.; Schmidt, S.K. Improved procedure for obtaining statistically valid parameter estimates from soil respiration data. Soil Biol. Biochem. 27:1–7; 1995.

[IPCC] Intergovernmental Panel on Climate Change. *Climate Change 1995. The Science of Climate Change.* Cambridge: Cambridge Univ. Pr.; 1996.

Jenkinson, D.S.; Adams, D.E.; Wild, A. Model estimates of CO_2 emissions from soil in response to global warming. Nature 351:304–306; 1991.

Jenkinson, D.S.; Hart, PBS; Rayner, J.H.; Parry, L.C. Modeling the turnover of organic matter in long-term experiments at Rothamsted. INTECOL Bull. 15:1–8; 1987.

Jenny, H.; Gessel, S.P.; Bingham, F.T. Comparative study of decomposition rates of organic matter in temperate and tropical regions. Soil Sci. 68:419–432; 1949.

Kurcheva, G.F. The role of invertebrates in the decomposition of oak leaf litter. Pocroredenie 4:16–23; 1960.

Ladd, J.N.; Amato, M. Studies of nitrogen immobilization and mineralization in calcareous soils. IV. Changes in the organic nitrogen of light and heavy subfractions of silt and fine clay-size particles during nitrogen turnover. Soil Biol. Biochem. 12:185–189; 1980.

Lang, G.E. Dynamics in a mixed oak forest on the New Jersey Piedmont. J. Torrey Bot. Club 101:277–286; 1974.

Leavitt, S.W.; Follett, R.F.; Paul, E.A. Estimation of slow- and fast-cycling soil organic carbon pools from 6N HCl hydrolysis. Radiocarbon 38:231–239; 1997.

Loomis, R.M. *Annual Changes in Forest Floor Weights under a Southeastern Missouri Oak Stand.* Washington, DC: United States Department of Agriculture (USDA) Forest Service Research Note NC-184; 1975.

Martel, Y.A.; Paul, E.A. The use of radiocarbon dating of organic matter in the study of soil genesis. Soil Sci. Soc. Am. Proc. 38:501–506; 1974.

Meentemeyer, V. Microclimate and lignin control of decomposition rates. Ecology 59:465–472; 1978.

Melillo, J.M.; Aber, J.D.; Muratore, J.M. Nitrogen and lignin control of hardwood leaf litter decomposition dynamics. Ecology 63:621–626; 1982.

Nelson, D.; L. Sommers. Total carbon, organic carbon, and organic matter. In: Sparks, D.L.; Page, A.; Helmke, P.; Loeppert, R.; Soltanpour, P.; Tabatabai, M.; Johnston, C.; Sumner, M. eds. *Methods of Soil Analysis: Chemical Methods.* 2nd edition. Madison, WI: American Society of Agronomy; 1996: 961–1010.

Oades, J.M. The role of biology in the formation, stabilization and degradation of soil structure. Geoderma 56:377–400; 1993.

O'Lear, H.A.; Seastedt, T.R.; Briggs, J.M.; Blair, J.M.; Ramundo, R.A. Fire and topographic effects on decomposition rates and nitrogen dynamics of buried wood in tall grass prairie. Soil Biol. Biochem. 28:322–329; 1996.

Olson, J.S. Energy storage and the balance of producers and decomposers in ecological systems. Ecology 44:322–331; 1963.

Palm, C.A.; Rowland, A.P. A minimum dataset for characterization of plant quality for decomposition. In: Cadisch, G.; Giller, K.E., eds. *Driven by Nature: Plant Litter Quality and Decomposition.* Wallingford, UK: CAB International; 1997:379–392.

Palm, C.A.; Sanchez, P.A. Nitrogen release from the leaves of some tropical legumes as affected by their lignin and polyphenolic contents. Soil Biol. Biochem. 23:83–88; 1991.

Parton, W.J.; Schimel, D.S.; Cole, C.V.; Ojima, D.S. Analysis of factors controlling soil organic matter levels in Great Plains grasslands. Soil Sci. Soc. Am. J. 51:1173–1179; 1987.

Paul, E.A.; Collins, H.P.; Harris, D.; Schulthess, U.; Robertson, G.P. Evolution of CO_2 and soil carbon dynamics in biologically managed, row-crop agroecosystems. Appl. Soil Ecol. 11:53–65; 1999.

Paul, E.A.; Morris, S.J.; Bohm, S. The determination of soil C pool sizes and turnover rates: Biophysical fractionation and tracers. In Lal, R.; Kimble, J.; Follett, R., eds. *Assessment Methods for Soil C Pools.* Boca Raton, FL: CRC; in press.

Paul, E.A.; Paustian, K.A.; Elliott, E.T.; Cole, C.V. *Soil Organic Matter in Temperate Ecosystems: Long-Term Experiments in North America.* Boca Raton, FL: CRC; 1997.

Paul, E.A.; Smucker, A.J.M.; Collins, H.P.; Haile-Mariam, S. Analytical determination of soil C dynamics. 16th International Congress on Soil Science, Montpellier, France, 16–20 August; 1998.

Paustian, K.; Agren, G.I.; Bosatta, E. Modeling litter quality effects on decomposition and soil organic matter dynamics. In: Cadisch, G.; Giller, K., editors. *Driven by Nature: Plant Litter Quality and Decomposition.* Wallingford, UK: CAB International; 1997:313–335.

Paustian, K.; Parton, W.J.; Persson, J. Modeling soil organic matter in organic-amended and nitrogen-fertilized long-term plots. Soil Science Society of America Journal 56:476–488; 1992.

Robertson, G.P.; Blair, J.M.; Groffman, P.M.; Harris, D.; Holland, E.; Nadelhoffer, K.; Wedin, D. Soil carbon and nitrogen availability: Nitrogen mineralization, nitrification, and soil respiration potentials. In Robertson, G.P.; Bledsoe, C.S.; Coleman, D.C.; Sollins, P., eds. *Standard Soil Methods for Long-Term Ecological Research.* New York: Oxford Univ. Pr.; 1999a:258–271.

Robertson, G.P.; Bledsoe, C.S.; Coleman, D.C.; Sollins, P., eds. *Standard Soil Methods for Long-Term Ecological Research.* New York: Oxford Univ. Pr.; 1999b.

Robertson, G.P.; Huston, M.A.; Evans, F.C.; Tiedje, J.M. Spatial variability in a successional plant community: Patterns of nitrogen availability. Ecology 69:1517–1524; 1988.

Schimel, D.S. *Theory and Application of Tracers.* San Diego, CA: Academic; 1993.

Schlesinger, W.H. Soil organic matter: A source of atmospheric CO_2. In: Woodwell, G.M., ed. *The Role of Terrestrial Vegetation in the Global Carbon Cycle.* New York: Wiley; 1984:111–127.

Schlesinger, W.H. Evidence from chronosequence studied for a low carbon-storage potential of soils. Nature 348:232–234; 1990.

Sinsabaugh, R.L.; Antibus, R.K.; Linkins, A.E.; McClaugherty, C.A.; Rayburn, L.; Repert, D.; Weiland, T. Wood decomposition: Nitrogen and phosphorus dynamics in relation to extracellular enzyme activity. Ecology 74:1586–1593; 1993.

Sollins, P.; Glassman, C.; Paul, E.A.; Swanston, C.; Lajtha, K.; Heil, J.; Elliott, T.E. Soil carbon and nitrogen pools and fractions. In: Robertson, G.P.; Bledsoe, C.S.; Coleman, D.C.; Sollins, P., eds. *Standard Soil Methods for Long-Term Ecological Research.* New York: Oxford Univ. Pr.; 1999:89–105.

Spycher, G.; Sollins, P.; Rose, S. Carbon and nitrogen in the light fraction of a forest soil: Vertical distribution and seasonal patterns. Soil Sci. 135:79–87; 1983.

Stevenson, B.G.; Dindal, D.L. A litter box method for the study of litter arthropods. J. Georgia Entomol. Soc. 16:151–156; 1981.

Stevenson, F.J.; Elliott, E.T.; Cole, C.V.; Ingram, J.; Oades, J.M.; Preston, C.; Sollins, P.J. Methodologies for assessing the quantity and quality of soil organic matter. In: Coleman, D.C.; Oades, J.M.; Uehara, G., eds. *Dynamics of Soil Organic Matter in Tropical Ecosystems.* Honolulu, HI: Univ. Hawaii Pr.; 1989: 173–199.

Strickland, T.C.; Sollins, P. An improved method for separating light and heavy-fraction organic material from soils. Soil Sci. Soc. Am. J. 51:1390–1393; 1987.

Swift, M.J.; Heal, O.W.; Anderson, J.M. *Decomposition in Terrestrial Ecosystems.* Berkeley, CA: Univ. California Pr.; 1979.

Tisdall, J.M. Formation of soil aggregates and accumulation of soil organic matter. In: Carter, M.R.; Stewart, B.A., eds. *Structure and Organic Matter Storage in Agricultural Soils.* Boca Raton, FL: CRC; 1996:57–96.

Turchenek, L.W.; Oades, J.M.. Organo-mineral particles in soils. In: Emerson, W.W.; Bond, R.D.; Dexter, A.R., eds. *Modification of Soil Structure.* Chichester, UK: Wiley; 1978:137–144.

Wallace, E.S.; Freedman, B. Forest floor dynamics in a chronosequence of hardwood stands in central Nova Scotia. Can. J. For. Res. 16:293–302; 1986.

Willson, T.C.; Schabenberger, O.; Paul, E.A.; Harwood, R.R. Seasonal changes in nitrogen mineralization potential in soils under agricultural management. Soil Sci. Soc. Am. J., in press.

Witkamp, M.; Olson, J.S. Breakdown of confined and non-confined oak litter. Oikos 14:138–147; 1963.

Wolf, D.C.; Legg, J.O.; Boutton, T.W. *Isotopic Methods for the Study of Soil Organic Matter Dynamics.* SSSA Book Series 5. Madison, WI: Soil Science Society of America; 1994:865–907.

8

Stable Isotope Tracers and Mathematical Models in Soil Organic Matter Studies

Ronald Amundson and W. Troy Baisden

Introduction

Light stable isotopes have become widely used biogeochemical tracers in earth science and ecology research during the last half of this century. With some exceptions, these applications have originated as a result of pioneering geochemical research at the University of Chicago and the California Institute of Technology in the 1950s and 1960s (Taylor et al. 1991). The breadth of isotopic tracer studies in present-day ecosystem sciences is now so great that it eludes even the most ambitious review article or book.

In this chapter, we limit our focus to the use of natural abundance levels of stable carbon (C) and nitrogen (N) isotopes as tracers of soil organic matter (SOM) cycling. The use of natural abundance levels of carbon-14 (^{14}C) as a SOM tracer has been discussed elsewhere (Trumbore 1993). Stable isotopes offer alternatives to ^{14}C as a tracer in certain settings: lower cost per analysis and (particularly with N) the ability to trace different SOM processes. We define SOM as a continuum of substances ranging from fresh litter to humic substances in the mineral soil, all of which is ultimately derived from both above- and belowground plant material. As we discuss below, the isotopic composition of SOM reflects the balance between organic inputs and losses—losses (in the case of C) being dominated by heterotrophic respiration of carbon dioxide (CO_2). From this perspective, this chapter is a companion piece to our recent article on the carbon and oxygen (O) isotope composition of soil and soil-respired CO_2 (Amundson et al., 1998). In both, our approach is the same: the isotopic composition of both organic matter and CO_2 can each be described by their own mass balance expressions, the expressions differing slightly for the individual isotope being considered. In both, we review the pioneering work and modeling of other researchers, supplementing and expanding it with recent modeling and empirical measurements in our laboratory. We hope to provide a clear conceptualization of the mathematics required to construct realistic models of the behavior of C and N isotopes in SOM.

The key to modeling is identifying relevant pools and fluxes that must be represented mathematically. In the next section, we discuss SOM pools and identify the fluxes of C and N that are relevant to understanding stable isotope dynamics in SOM.

Soil Organic Matter Pools and Dynamics

SOM Pools

Conceptually, SOM can be considered in terms of "boxes" or "pools." One common division in terms of modeling has been to consider O horizons (if present) and mineral horizons separately. In this chapter, we focus on the stable isotope composition of SOM in mineral horizons although our discussion is applicable, with modification, to O horizons. We will take two approaches in our view of the mineral soil SOM pool: (1) We will review simple models that consider SOM as a homogenous, well-mixed pool and (2) we will review and develop models that recognize that the characteristics of the

SOM pool vary as a function of depth—at any depth the SOM pool may undergo additions, losses, and transformations, as well as the exchange of material with the soil above and below. Insights into SOM cycling can be gained from either simple or complex models of the SOM pool, and we will review, at the end of each section, applications of these approaches to problems of ecological significance.

SOM Additions

Carbon (and related elements in organic matter) is added to soil via a variety of processes: (1) surficial litter (i.e., leaves, branches, crop residue, etc.), (2) root inputs (i.e., root death, root exudation), and (3) downward (i.e., leaching via dissolved or suspended modes in water, bioturbation) or upward (bioturbation) transport (Fig. 8.1). A quantitative understanding of these processes in most soil systems is often poor due to the difficulty of monitoring them in the field.

It is likely easiest to quantify surficial litter inputs (via litter traps, standing biomass measurements, etc.) (see Chapter 2). However, these inputs only contribute to the SOM pool if they are incorporated via transport processes. These are discussed below. It is far more difficult to measure rates of root inputs into the soil (see Chapter 4), and a good understanding of these additions is not available for all ecosystems.

With respect to N, there are several important processes in addition to those discussed above for C. First, biological N fixation is an important N addition in many ecosystems. An additional input is atmospheric deposition of nitrate (NO_3^-) and ammonia (NH_3) via wet and dry pathways (Schlesinger 1991). The deposition rates appear to vary greatly from one location to another (Galloway et al. 1994; see also Chapter 17), and in some regions have been greatly modified by industrial and agricultural activity (Kinzig and Soclow 1994). Finally, fertilizer additions have, in some areas, exceeded natural N additions (Kinzig and Soclow 1994).

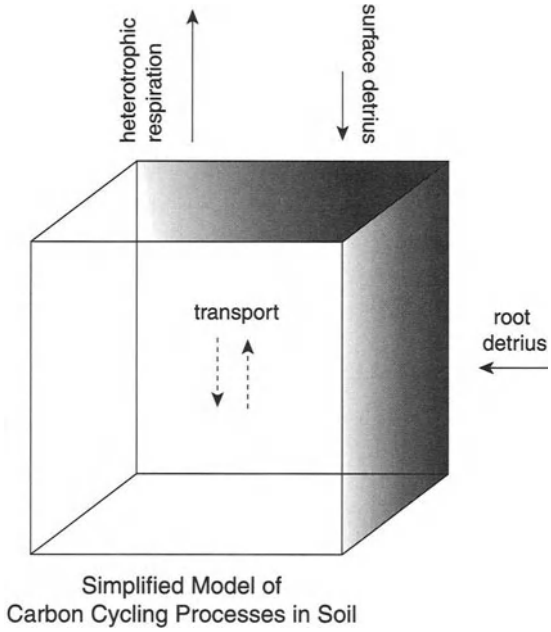

FIGURE 8.1. Carbon processes in the soil environment.

SOM Losses

With respect to C, most losses from soils are via (1) CO_2 produced through heterotrophic decomposition of SOM, (2) dissolved organic C (DOC) removal with downward percolating water, and (3) erosion. In most soils, respiration dominates the losses. Soil respiration (CO_2 flux across the soil–atmosphere interface) can be relatively easy to quantify (e.g., via sodium hydroxide [NaOH] traps, infrared [IR] gas analyzers, etc.). However, total soil respiration consists of CO_2 released via decomposition of SOM as well as CO_2 produced from the respiration of living plant roots. The proportion of total respiration due to decomposition of humic substances versus living root respiration is poorly known, although estimates of the humus contribution to respiration have been made based on comparisons of the net primary productivity (NPP) of a site to the total soil respiration (Schlesinger 1977) and natural abundance carbon-14 (^{14}C) (Dörr and Münnich 1986) and carbon-13 (^{13}C) (Robinson and Scrimgeour 1995; Rochette and Flanagan 1997) mass balance approaches.

In established ecosystems, soil N loss pathways include (1) plant uptake, with lesser losses via (2) gaseous losses (nitrous oxide [N_2O], nitric oxide [NO], N_2, NH_3) (see Chapter 15), (3) dissolved losses (NO_3^-, ammonium [NH_4^+], dissolved or-

ganic N [DON]), and (4) erosion. While plant uptake rates can be measured (see Chapter 11), the remaining fluxes remain poorly quantified in most, but not all (Riley and Vitousek, 1995), soil systems.

Internal SOM Transfers

The magnitude of the direct downward transport of surficial litter into the underlying soil remains largely unknown in many environments. In some ecosystems with large earthworm populations, direct incorporation of surface litter into the mineral soil pool represents a very important and quantifiable process (Darwin 1881). The influence of other mesofauna on litter incorporation is possibly less well quantified.

It is well accepted that in certain soils, such a Spodosols, downward transport of organic molecules with water constitutes the main, or in some cases the only, source of organic matter for certain horizons (e.g., Bhs or Bh horizons). However, the importance in other soils is far less constrained. Recent modeling of ^{14}C, cesium-137 (^{137}Cs), and lead-210 (^{210}Pb) in some forest soils of Germany have placed some constraints on rates of downward transport in certain environments (Dörr and Münnich 1989); however, this approach needs to be expanded to other ecosystems and soil environments to provide a general framework for modeling purposes.

SOM Transformations

The fate of plant detritus in soils continues to be an area of active research involving many unresolved issues concerning the pathways of organic matter decay (Oades 1995). A common simplification of modeling these complex C cycling processes is to assume that decomposition of organic compounds, and the resulting production of CO_2 and various humic substances, is a first order decay reaction (e.g., Cerling et al. 1991; Trumbore 1993; Wang et al. 1994). The CO_2 produced in this process diffuses to the atmosphere (Cerling et al. 1991; Amundson et al. 1998) while the remaining humic substances can undergo further modification or be stabilized in relatively nonreactive states or sites. The decay constant, k, while assumed to be constant with depth and time in relatively simple models, is likely a function of both variables.

Similar modeling approaches may be taken for soil N, although the reactions and products are considerably more numerous than for C (Schlesinger 1991). Soil organic N is mineralized to NH_4^+ which can either undergo plant uptake, microbial immobilization, volatilization, or nitrification. During nitrification, NH_4^+ is oxidized to NO_3^-, although N_2O may also be produced during this process (Goreau et al. 1980). Finally, oxidized forms of N can be reduced ultimately to N_2 during the process of denitrification. As we discuss later in this chapter, the modeling of these diverse processes in SOM N isotope studies has not been attempted, but various simplifying approaches can be made.

Stable Carbon Isotopes in Organic Matter

The central problem in understanding the temporal and spatial isotopic variations in soil organic matter (regardless of the isotope being considered) is the reality that organic compounds are not homogeneous isotopically or chemically. Plant compounds (the ultimate source of most soil organic matter) vary greatly structurally (e.g., lipids, cellulose, lignin, etc.), and each structural component can have widely varying stable isotope ratios. Additionally, SOM is likely even more heterogeneous, with widely varying susceptibilities to decomposition and (in particular for ^{14}C) widely differing isotopic ratios.

Below we examine two contrasting approaches to modeling C isotopes in SOM, differing in the number of processes captured and in the resulting mathematical complexity. Each of these contrasting approaches can provide important insights into C cycling—allowing comparisons between ecosystems or determining depth-dependent processes within a given soil. This discussion also serves as the introduction for the modeling of N isotopes in SOM.

Well-Mixed One Box Model of C Isotopes in SOM

As a simplifying assumption for any SOM horizon, or for the soil profile as a whole, the mass of organic matter can be thought of as a well-mixed pool that

can be described as a function of time by a mathematical approach first introduced to SOM research by Jenny et al. (1949):

$$\frac{dX}{dt} = I - L \tag{8.1}$$

where X is element X in soil organic matter, I is inputs, and L is losses. Equation 8.1 states that the rate of change of the mass of SOM is the difference between the rates of additions and losses from the soil system. The manner in which I and L are expressed (and the number of processes included in them) may vary greatly from one soil to another, or (as quite common) from one SOM compartment to another.

In order to utilize isotope ratios as natural tracers, separate mass balance equations must be established for the rare and common isotopes of interest, and these equations must be combined in order to evaluate the observed isotopic composition of the SOM being studied:

$$\frac{d}{dt}\left(\frac{X^*}{X}\right) = \frac{dR_{SOM}}{dt} = \frac{I^* - L^*}{(I - L)} = \frac{R_I I - R_L L}{I - L} \tag{8.2}$$

where X* is the mass of rare isotope, X is the mass of abundant isotope[1], and R_I and R_L are X*/X in the inputs and losses, respectively. The ratio of rare to abundant isotopes in element X in SOM (R_{SOM}) is related to the standard "delta" notation by:

$$\delta^r X_{SOM} = \left(\frac{R_{SOM}}{R_{std}} - 1\right)1000 \tag{8.3}$$

where r is the rare isotope of element X (e.g.,$\delta^{13}C$) and the SOM and std refer to the rare to abundant isotope ratios in the SOM and the internationally accepted standard, respectively. The resulting delta value is the per mil (‰) deviation of the isotopic ratio of the sample from that of the standard. The standards are the PDB carbonate for stable C isotopes ($^{13}C/^{12}C$) (Craig 1957) and N_2 in air for N isotopes ($^{15}N/^{14}N$) (Mariotti 1983).

[1]The assumption that the mass of an element in bulk organic matter = mass of the abundant isotope of that same element introduces a minor error into isotopic ratio calculations that is not significant in most, but not all, applications. Other authors take the more rigorous, but algebraically cumbersome, approach and calculate the abundant isotope mass directly.

Developing a mass balance model of soils can be as simple or complex as that required by the experimental conditions (or the patience of the experimentalist). The simplest (and most common) approach assumes that inputs into soil are homogenous, that the SOM pool is homogeneous and well-mixed, and that the loss of organic matter can be described by a first order decay model. In this case, for C isotopes, Equation 8.1 for the abundant isotope ^{12}C becomes:

$$\frac{dC}{dt} = I - kC \tag{8.4a}$$

and for the rare isotope ^{13}C:

$$\frac{dC^*}{dt} = R_I I - kC^* \tag{8.4b}$$

where C* is ^{13}C, R_I is $^{13}C/^{12}C$ in inputs, and k is the first order decay constant for the organic matter pool. The rate of decomposition (loss) is proportional to the size of the SOM pool. In this type of model, 1/k represents the residence time of C in organic matter. The solutions to this model for ^{12}C and ^{13}C are, respectively:

$$C(t) = \frac{1}{k}(I - Ie^{-kt}) \tag{8.5a}$$

$$C^*(t) = \frac{1}{k}(R_I I - R_I Ie^{-kt}) \tag{8.5b}$$

The ratio of Equations 8.5b and a describes the isotopic ratio of the soil organic matter pool at any time t:

$$R(t) = \frac{C^*}{C}(t) = \frac{\frac{1}{k}(R_I I - R_I Ie^{-kt})}{\frac{1}{k}(I - Ie^{-kt})} \tag{8.6}$$

For stable C isotope ratios, it is commonly assumed that the $\delta^{13}C$ value of the standing biomass represents the isotopic composition of the inputs (R_I) (see Equation 8.3 for relationship between $\delta^{13}C$ values and R). Additionally, it has been shown that, to a large degree, the $\delta^{13}C$ value of soil respiration (and hence SOM losses) is about the same as that of the standing biomass (Cerling et al. 1991). Thus, under these conditions, Equation 8.6 reduces to:

$$R_{SOM} = R_I \tag{8.7}$$

In other words, the $\delta^{13}C$ value of soil matter is time invariant and is the same as the $\delta^{13}C$ value of the plant inputs.

While this simplification describes much about the $\delta^{13}C$ value of SOM (i.e., it is commonly similar isotopically to that of the standing biomass), it is not entirely accurate. For example, the isotopic composition of plants is usually a few per mil less than that of the pooled SOM (e.g., Balesdent et al. 1993). Secondly, there are commonly 1 to 3‰ increases in the $\delta^{13}C$ value of soil organic matter with depth (Nadelhoffer and Fry 1988; Stout and Rafter 1978) (Fig. 8.2A) which indicates one or more modes of isotopic fractionation in soil organic matter formation: (1) preferential decomposition of organic compounds with more negative $\delta^{13}C$ values, (2) preferential retention of ^{13}C in the cells of soil microorganisms, (3) downward loss of ^{13}C-depleted compounds, and/or (4) accumulation of ^{13}C-enriched compounds from overlying horizons.

The preferential removal of $^{12}CO_2$ (or $^{13}CO_2$) during the decomposition process is called a *kinetic isotope effect* and leads to an observable isotopic enrichment or depletion (*fractionation*) in the re-

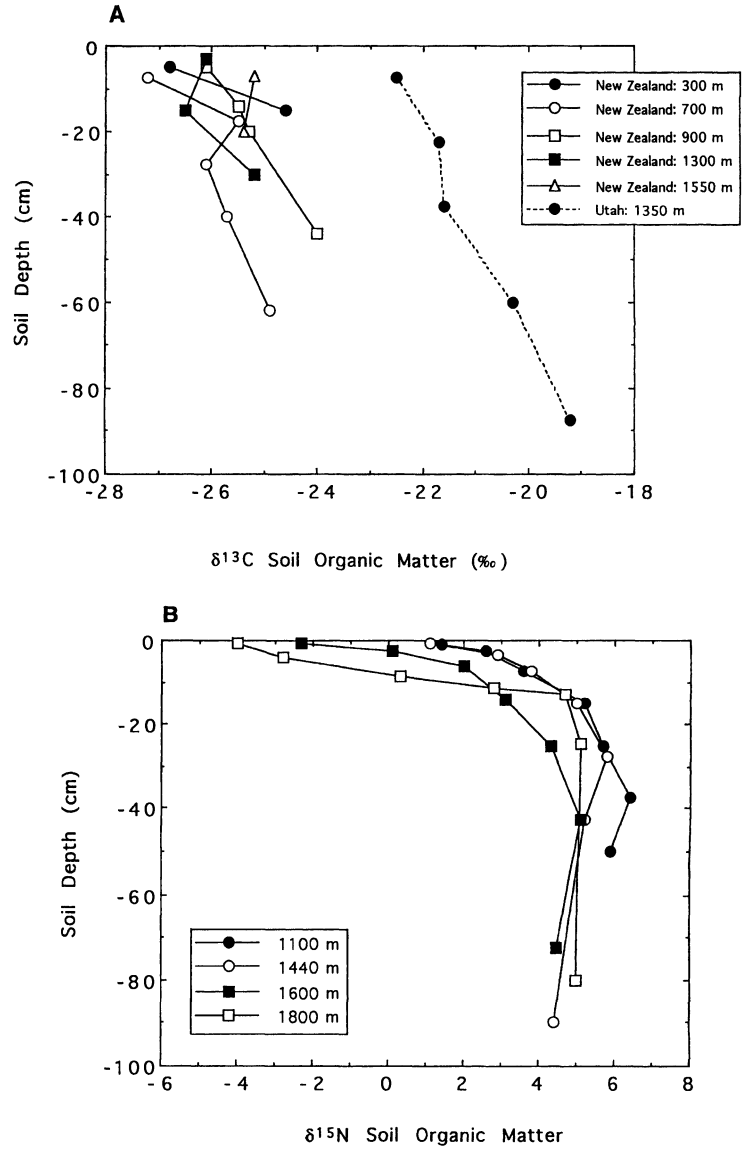

FIGURE 8.2. Variations in the (A) $\delta^{13}C$ and (B) $\delta^{15}N$ value of SOM with soil depth. Data in (A) from Stout and Rafter (1978) (New Zealand) and Dzurec et al. (1985) (Utah). Data in (B) from Mariotti et al. (1980).

maining SOM (Hayes 1982). The isotope effect is proportional to the ratio of the decay constants of the rare (k*) and common (k) isotopes, and can be incorporated into Equation 8.4b above by adding a fractionation term, α, to the decomposition of organic matter. For a given process, the fractionation factor α is defined as the instantaneous ratio of the isotopic composition of products and reactants:

$$\frac{k^*}{k} = \alpha = \frac{R_{prod}}{R_{react}} \qquad (8.8)$$

Values of α in processes relevant to SOM are typically close to 1; if $\alpha < 1$, there is a preferential loss of ^{12}C during a reaction, and if $\alpha > 1$, there is a preferential loss of ^{13}C. A related relationship, useful if the δ values of either a reactant or product are known, is (Friedman and O'Neil 1977):

$$10^3 \ln \alpha \cong \delta^{13}C_{prod} - \delta^{13}C_{react} \qquad (8.9)$$

With respect to Equation 8.4b, the kinetic isotope effect for the rare isotope ^{13}C is incorporated in the following manner:

$$\frac{dC^*}{dt} = R_I I - k\alpha C^* \qquad (8.10)$$

If a soil has had time to reach steady state, the mass balance equations can be greatly simplified. At steady state, dC/dt and $dC^*/dt = 0$, and Equations 8.4a and 8.10 become easy to solve algebraically. The ratio of the solution is:

$$R_{SOM} = \frac{C^*}{C} = \frac{\frac{R_I I}{k\alpha}}{\frac{I}{k}} = \frac{R_I}{\alpha} \qquad (8.11a)$$

where R_{SOM} is the isotopic ratio in SOM. In delta notation (Faure 1986), Equation 8.11a is expressed as:

$$\delta^{13}C_{SOM} = \left[\frac{\delta^{13}C_I + 1000}{\alpha}\right] - 1000 \qquad (8.11b)$$

where the SOM is the same as in Equation 8.11a. Thus, for this simple model, the isotopic ratio of soil organic matter is related to the isotopic values of the inputs (which in the absence of downward transport is nearly constant with depth) (Wedin et al. 1995) and the isotopic fractionation factors associated with decomposition (α).

Uses of Well-Mixed Box Models in SOM C Studies

One potential use of the well-mixed box model of SOM is the establishment of geographic or climatic variations in soil-ecosystem scale C isotope fractionations (i.e., the climatic dependence of the value of α in Equation 8.11). If the steady state $\delta^{13}C$ values of SOM and plant inputs can be quantified along climatic gradients, α can then be calculated. Unfortunately, this proves to be difficult in practice for several reasons. First, the $\delta^{13}C$ value of the atmosphere (and plant inputs) has decreased by about 1.3‰ in the past 150 years due to global SOM decomposition, biomass burning, and fossil fuel consumption (a corollary of the Suess effect) (Freidli et al., 1986). This shift in plant inputs is large relative to the approximate range of isotopic enrichment during decomposition (up to approximately 2‰ based on litter decomposition studies [e.g., Nadelhoffer and Fry 1988; Mary et al. 1992]). Therefore, these ecosystem-scale comparisons may not prove to be very rewarding for comparative purposes.

In contrast, there has been enormous success using C isotopes to evaluate SOM turnover in agricultural settings where crop photosynthetic pathways differ from precultivation plants (Balesdent and Mariotti 1996). In these approaches, the whole soil can be viewed as a well-mixed pool or, more commonly, each soil horizon can be viewed as a separate pool and modeled individually. The model used to calculate the fraction of new C added since a crop change is (Balesdent et al. 1988):

$$F = \frac{\delta^{13}C_t - \delta^{13}C_i}{\delta^{13}C_p - \delta^{13}C_i} \qquad (8.12)$$

where F is the fraction of SOM gained following vegetation change, $\delta^{13}C_t$ is the isotopic composition of SOM at time t, $\delta^{13}C_i$ is the isotopic composition of SOM prior to vegetation change, and $\delta^{13}C_p$ is the isotopic composition of the cultivar. Isotopic fractionations associated with decomposition are commonly ignored in these comparisons due to the large difference in $\delta^{13}C$ values between C_3 (-27 ± 4‰) and C_4 (-12 ± 3‰) plants (Bender 1968; Smith and Epstein 1971). When combined with total C measurements, the total quantity of cultivar-derived C in the soil can be determined. Additionally, the dynamics of the loss

of C accumulated prior to vegetation change can be determined if the precultivation mass of C is known:

$$C_t = C_o e^{-kt} \quad (8.13)$$

where C_t is the amount of C at time t, C_o is the original C content, and t is the elapsed time since vegetation change. This application is a good means of understanding SOM turnover times in particular agricultural management schemes, and has been one of the main applications of stable C isotopes as a "tracer" in SOM cycling (Balesdent and Mariotti 1996).

The use of SOM $\delta^{13}C$ values following C_3 or C_4 vegetation shifts is a potentially useful, and relatively inexpensive, means of quantifying organic C dynamics. We do not cover it in great detail here because it has been reviewed in several recent articles (Balesdent and Mariotti 1996; Boutton, 1996). It is important here to identify several factors that may add complexity to the use of Equation 8.12: (1) the $\delta^{13}C$ value of atmospheric CO_2 has decreased from -6.5 to $-8.0‰$ in the past century, changing the value of $\delta^{13}C_p$ continuously over time, (2) isotopic discrimination, or preferential preservation of certain compounds, during decomposition may shift the true C isotope composition of the inputs from that of $\delta^{13}C_p$, and (3) there is usually a fairly wide range in the $\delta^{13}C$ values of plants (particularly C_3 plants [Farquhar et al. 1989]) due to a variety of environmental stresses, all of which will add uncertainty to the value assigned to $\delta^{13}C_p$. While all these issues add uncertainty to the use of this approach to quantifying C dynamics, they do not undermine the potential of the approach in many applications.

A related use of C isotopes is to identify vegetation shifts along forest/grassland ecotones (Wang et al. 1993; Ambrose and Sikes, 1991) or C_3 to C_4 desert shrub ecotones (e.g., Dzurec et al. 1985; Boutton 1996; Connin et al. 1997). In these cases, C isotopes serve in a qualitative capacity, identifying whether a vegetation shift has or has not occurred. If the timing of the shift is known, then Equations 8.12 and 8.13 can be used to understand the SOM turnover rates.

A recent application, more appropriate to nonagricultural settings, is the use of the known decrease in the $\delta^{13}C_p$ value of atmospheric CO_2 during the past 150 years (as a result of land conversion and fossil fuel burning) as a means of estimating SOM turnover rates at regional or global scales. The principle is that in the past 150 years there has been approximately a $1.3‰$ decrease in the $\delta^{13}C$ value of the atmosphere due to fossil fuel burning. If this decrease is fully or partially registered in the SOM, it implies turnover times of a century or less (Bird et al. 1996). While this approach has been used, in conjunction with ^{14}C in SOM, to estimate residence times of surficial SOM as a function of latitude (Bird et al. 1996), some uncertainties in turnover estimates exist due to: (1) uncertainties in the $\delta^{13}C$ value of preindustrial SOM, (2) uncertainties in the value of the isotopic composition of the atmosphere (and therefore plant inputs) at various times over the past century, and (3) the extremely small isotopic differences that are being examined ($1.3‰$ or less) versus the large natural variability in the isotopic composition of SOM. Nonetheless, this is an innovative approach that may receive more attention in large-scale ecological studies.

In summary, several useful methods using C isotopes to monitor SOM dynamics have been developed. Each relies on a shift in the $\delta^{13}C$ value of plant inputs in order to derive information about the turnover of SOM. Next we discuss more complicated models that address the intrasoil isotopic heterogeneity.

Models for Vertical Variations in the $\delta^{13}C$ Value of SOM

The simple models we discuss above do not attempt to explain the commonly observed increase in the $\delta^{13}C$ value of SOM with depth shown in Figure 8.2a (Nadelhoffer and Fry 1988; Balesdent et al. 1993). While it is possible that the fractionation factor for SOM decomposition changes as a function of depth, the trend in $\delta^{13}C$ values versus depth may also relate to two other phenomena: (1) depth dependence of plant inputs combined with vertical transport of C within the soil profile and (2) multiple pools of SOM with different C turnover rates. For simplicity, we will discuss these two phenomena separately, in this and the next section, respectively. A model attempting a full mechanistic representation of SOC dynamics should include both approaches (Elzein and Balesdent 1995).

It is worthwhile to note that the trend in the $\delta^{13}C$ values of SOM with depth is rarely a simple, mono-

tonic increase. More often, it is a rapid increase of approximately 1‰ over litter values in the first 20 cm of the mineral soil, followed by a slower increase. This trend is particularly typical of temperate deciduous forests (Balesdent et al. 1993), but may be interrupted by a sharp decrease in $\delta^{13}C$ values in the E horizons of podzols (Bertram and Schleser 1982). Because the ^{13}C enrichment of SOM as a function of depth does not always begin to appear during the initial phases of litter decomposition (Melillo et al, 1989; Balesdent et al., 1993), this observation is difficult to study mechanistically. Thus, models that explain the observed trends in C isotopes represent a useful method for identifying the processes responsible for this soil property.

Generalized C Isotope Model

Introducing depth into the model as a continuous variable has two important implications. First, in the mass balance expression, C concentration is now a function of both time and depth, which makes the overall expression a partial differential equation. Second, boundary conditions at the upper and lower limit of the soil profile must be considered. Introducing z as depth in cm, and following the work of Elzein and Balesdent (1995), we begin with the following generalized mass balance expression for SOC concentration, C:

$$\frac{\partial C}{\partial t} = D\frac{\partial^2 C}{\partial z^2} - \nu\frac{\partial C}{\partial z} - kC + f_d \quad (8.14)$$

The terms on the right represent diffusive transport, advective transport, decomposition, and plant inputs, respectively. Each term (and the process it represents) is discussed completely in sequence below. In order to completely describe the system, we must first define upper and lower boundary conditions. These boundary conditions may be in any one of three forms:

$$C = \kappa \quad (8.15a)$$

$$D\partial C/\partial z - \nu C = f_s \quad (8.15b)$$

$$C + D\partial C/\partial t - \nu C = \kappa + f_s \quad (8.15c)$$

In each case, κ and f_s are constants (which for the lower boundary are often set equal to zero). Equation 8.15a represents a constant concentration boundary condition. Equation 8.15b represents a constant flux boundary condition, as one might expect given a constant flux of litter, f_s, to the soil surface. Equation 8.15c represents a combination of the first two.

Returning to the mass balance expression Equation 8.14, the first two terms on the right-hand side of the equation represent modes of physical transport. The first of these terms represents diffusive transport along a SOC concentration gradient given a diffusion coefficient, D. In soils, the diffusive movement of SOM is not truly governed by the Brownian motion of molecules, but results from larger-scale processes which result in mixing: mesofaunal transport, shrinking/swelling, freezing/thawing and perhaps DOC transport in the absence of leaching. This diffusion term was introduced and evaluated for both $\delta^{13}C$ and $\delta^{14}C$ values by O'Brien and Stout (1978). They obtained a value for D of 13 $cm^2\ yr^{-1}$; Elzein and Balesdent (1995) obtained values ranging from 1.0 to 17 $cm^2\ yr^{-1}$.

The diffusion term is appropriate if transport is multidirectional. If, on the other hand, transport is entirely downward (e.g., leaching of DOC and colloids), then the process is advective and represented by the second term in Equation 8.14. This term describes the downward movement of the SOC stock at a given depth with a "velocity" given by the coefficient of advection, ν. Dörr and Münnich (1989) calculated values for the advection coefficient, ν in several forested soils of 0.8 to 1.6 $mm\ yr^{-1}$. Elzein and Balesdent (1995) obtained lower values (0.1 to 0.6 $mm\ yr^{-1}$) while considering diffusional processes as well. Qualitatively, downward movement of SOM is recognized as being critical to the formation of Spodosols and other forested soils (McKeague et al. 1983). In non-forested soils, the importance of either diffusional or advective transport is less well recognized, although recent work with cosmogenic isotopes indicates it does occur (Monaghan et al. 1983; Tsai 1989). Assuming that both D and ν are constant with soil depth (a simplifying assumption that may not describe the situation in most natural settings), Elzein and Balesdent (1995) suggest that for both temperate and tropical forest soils, diffusive transport dominates over advective transport. Thus, it may be appropriate to consider only diffusive transport for many soils, ignoring the advective term. Soils where advective transport may domi-

nate include very sandy soils, and particularly Spodosols.

The third term on the right hand side of Equation 8.14 represents loss of SOC from the profile due to heterotrophic respiration or leaching of DOC. It is analogous to the decomposition term presented in Equation 8.4. Here, we assume that k is constant with depth. The notion that a single decomposition rate, k, is inadequate to fully represent SOC dynamics has led to the development of models that consider multiple pools of SOM: either simply as we present in the next section (Trumbore 1993) or by introducing multiple simultaneous versions of Equations 8.14 and 8.15, each for different SOM pools (O'Brien and Stout 1978; Elzein and Balesdent, 1995).

The final term on the right side of Equation 8.14 (f_d) represents inputs of SOC from plant roots. The flux of aboveground litter at the soil surface must also be considered in the upper boundary condition. O'Brien and Stout (1978) successfully account for the distribution of ^{13}C and ^{14}C in a forest soil, converted to pasture, while considering only inputs of litter at the soil surface. Fitting a multi-pool version of Equation 8.14 to SOC concentration and ^{14}C content, Elzein and Balesdent (1995) obtain relatively similar results with and without including root inputs. Thus, it may be appropriate to ignore the last term in Equation 8.14 in systems such as forests, or shallowly rooted pastures, where most root activity is near the mineral soil surface or in the litter layers. Alternatively, a model that considers only surface inputs may suffer by not recognizing the large inputs of SOM directly from living and recently deceased plant roots. In many environments, such as grassland and steppes, where much of the photosynthetic productivity of the plants is directed below ground (e.g., Lauenroth and Whitman 1977), the distribution of SOM with depth is well correlated with root densities (Gile et al. 1979; Amundson et al. 1989). For these environments, root inputs clearly must be considered: it is common for grasslands to have belowground/aboveground inputs ratios of 2:1 or more (Bray 1963; Volobuev 1964; Kononova 1966; Lauenroth and Whitman, 1977), while in forests, the ratio can commonly be <1 (Bray 1963; Volobuev 1964; Vogt 1991).

Finally, a version of Equation 8.14 is needed for the rare isotope, ^{13}C:

$$\partial C^*/\partial t = D\frac{\partial^2 C^*}{\partial z^2} - \nu\frac{\partial C^*}{\partial z} - \alpha k C^* + f_d R_I \qquad (8.16)$$

Here, the diffusive and advective processes are assumed to be nonfractionating. The decomposition of organic matter is assumed to have a fractionation factor, α, and the inputs are multiplied by the isotope ratio in the root inputs, R_I. Similarly, the boundary conditions described for ^{13}C must be multiplied by the appropriate ratio, normally R_I for the constant flux of surface litter, although the actual ratio $^{13}C/^{12}C$ measured in SOM may be used for a non-zero constant upper concentration boundary condition.

A Solution for the C Isotope Model

To solve the differential Equations 8.14 and 8.16 analytically, one must make several simplifications. This process is a tradeoff, since neglecting terms reduces the mechanistic reality of the result, but decreases the number of adjustable parameters that must be fitted to available data. As an example, we simplify the general model to resemble the model that O'Brien and Stout (1978) presented for their forest/pasture soil in New Zealand, neglecting advective transport and root input terms, leaving only the diffusion and decomposition terms on the right-hand side of Equation 8.14. If it assumed that the system is at steady state, then:

$$\partial C/\partial t = 0 = D\frac{\partial^2 C}{\partial z^2} - kC \qquad (8.17)$$

where C is the C concentration (g cm^{-3}), D is diffusivity (assumed to be constant with depth) ($cm^2\ yr^{-1}$), and k is the rate constant for decomposition of C (yr^{-1}). We impose the following boundary conditions:

$$\frac{\partial C}{\partial z} = 0 \ @\ z = -\infty, \qquad (8.18a)$$

and

$$\frac{\partial C}{\partial z} = \frac{f_s}{D} \ @\ z = 0 \qquad (8.18b)$$

where Equation 8.18b is a constant flux boundary condition in which f_s is the flux of litter (g $cm^{-2}\ yr^{-1}$). This flux is assumed to be entirely litter from aboveground plant parts, but could also

include the root inputs in many ecosystems if they occur in a depth increment that is small compared with the value of D. For Equation 8.17, with the given boundary conditions, we obtain the solution (from the mathematical software program MATLAB®):

$$C(z) = \frac{f_s}{\sqrt{kD}} e^{z\sqrt{k/D}} \quad (8.19)$$

For ^{13}C, the solution is:

$$C^*(z) = \frac{f_s R_p}{\sqrt{\alpha kD}} e^{z\sqrt{\alpha k/D}} \quad (8.20)$$

where R_p is the $^{13}C/^{12}C$ of plant inputs and α is a fractionation factor, which if <1 explains the ^{13}C enrichment of SOM with depth. Dividing Equation 8.20 by Equation 8.19 gives the steady state equation for the isotopic ratio of SOM as a function of depth:

$$R(z) = \frac{R_p}{\sqrt{\alpha}} e^{[\sqrt{k/D}][z\sqrt{\alpha}-1]} \quad (8.21)$$

In Figure 8.3A total SOC is plotted versus depth (Equation 8.19) and in Figure 8.3B the $\delta^{13}C$ value of the SOM versus depth is illustrated (Equation 8.21). The equations have been fitted to the soil data of O'Brien and Stout (1978), which are shown as open circles. Figure 8.3A shows that the relatively simple model solution (Equation 8.19) provides a good representation of the SOC concentration in the upper portion of the profile. Below 60 cm in depth, the model fit deviates from the profile data. This may be due to the need to consider a second pool of more inert organic matter with a residence time of centuries or millennia. O'Brien and Stout's (1978) analysis of their radiocarbon data supports this interpretation, suggesting that "old" SOC accounts for a small proportion of the total above 50 cm, but half of the total SOC at the lowest measured depth.

The linear trend in $\delta^{13}C$ values with depth suggested by Equation 8.21 and plotted in Figure 8.3B also appears to describe the data of O'Brien and Stout (1978). The values of the plant material ($-29‰$) and fractionation associated with decomposition ($10^3 \ln \alpha = -2.5$) that fit the data are well within reasonable values observed in nature or in experiments. However, it is not clear that this is the only appropriate means of explaining the data. First, the effect of the decrease in the atmospheric $\delta^{13}C$ value during the twentieth century (approximately 1.3‰) is not considered. Second, the data may also be explained by a shift in vegetation from forest to pasture at the site, with a concomitant decrease in the $\delta^{13}C$ value of plant inputs of approximately 4‰. Moreover, it may be appropriate to consider the isotope effects associated with the transfer of SOC to a more inert pool that accounts for the bulk of the SOC at lower soil depths. Finally, we note that we have neglected root inputs without proving that this assumption is justified.

Although this model is relatively simple, it appears to capture the dynamics of the natural system. It is likely that simple models of this type, balanced with numerical solutions to more general models such as Equation 8.14 that include belowground inputs, may prove useful in improving our understanding of SOC dynamics. In particular, these models provide an important counterpart to ecosystem biogeochemistry simulations which do not recognize soil depth as a continuous variable.

Multi-Box SOM Isotope Models

All the modeling approaches taken thus far assume that plant inputs and SOM each act as homogeneous pools. It has long been recognized, from ^{14}C measurements, that the only way to reconcile observed isotopic changes of SOM with time is to partition SOM into pools with different residence times (Trumbore 1993). In using this approach, the isotopic composition of inputs into all pools is considered to be the same, while the isotopic composition of losses varies with the SOM pool being considered. For ^{12}C:

$$dC/dt = \sum_{i=1}^{n} (I_i - k_i C_i) \quad (8.22a)$$

and for ^{13}C:

$$dC^*/dt = \sum_{i=1}^{n} (R_I I_i - k_i \alpha_i C^* i) \quad (8.22b)$$

where I_i = inputs of soil organic matter to each pool, and decay constants (k) and fractionation factors (α) refer to pool-specific values. More complicated models, involving transfers between pools, require either matrix models (Baisden and Amund-

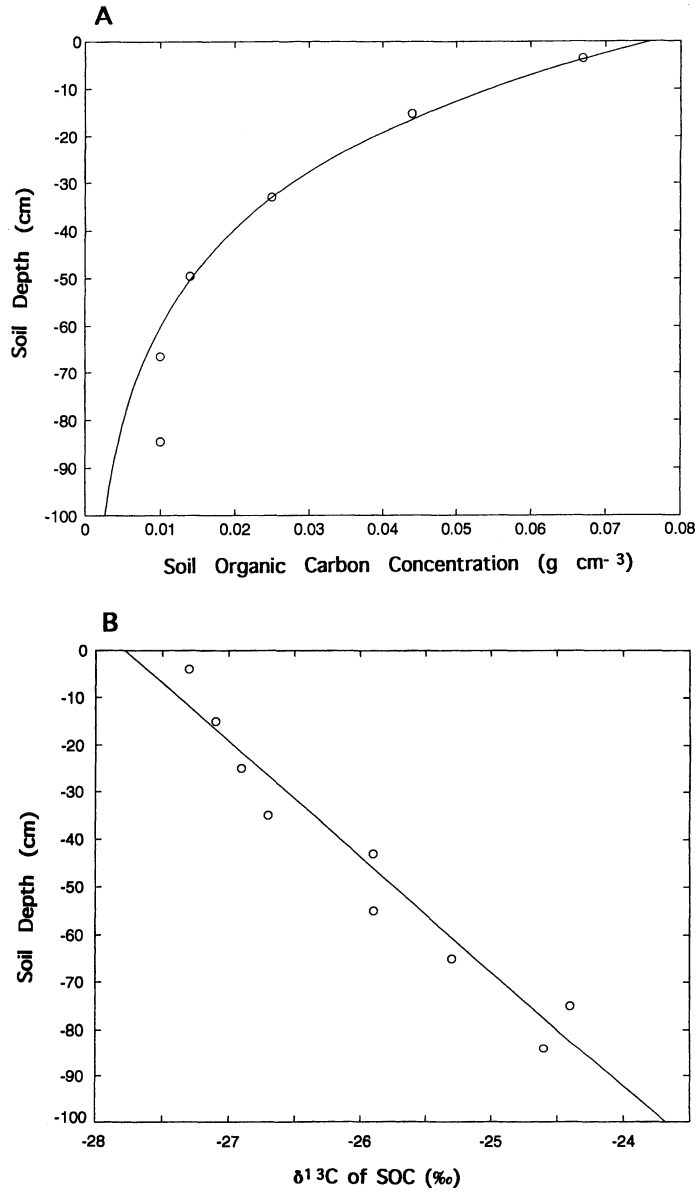

FIGURE 8.3. The solutions for: (A) The C concentration as a function of depth (Eq. 8.19) fitted to the data of O'Brien and Stout (1978). Values for constants are $k = 0.0163\ yr^{-1}$, $D = 14\ cm^2\ yr^{-1}$, and $f_s = 0.036\ g\ cm^{-2}\ yr^{-1}$. (B) The $\delta^{13}C$ value as a function of depth (Equation 8.21) fitted to the data of O'Brien and Stout (1978). The value of α was chosen such that $10^3 \ln \alpha = -2.5$ and the value of R_p was chosen such that $\delta^{13}C$ value of plant inputs $= -29‰$.

son 1997) or numerous coefficients to express the transfers between pools.

While plant components, such as lipids, proteins, cellulose, etc., have differing $\delta^{13}C$ values (Benner et al., 1987; Parker, 1964), there is not much evidence that differential preservation of these primary compounds in well-drained soils leads to the observed isotopic gradients with depth (Nadelhoffer and Fry 1988; Mellilo et al. 1989; Balesdent et al. 1993). However, in less-oxidized environments, such as bogs and marshes, there may indeed be differential decomposition of plant compounds that leads to preferential enrichment of lignin and other complex polymers (Benner et al. 1987; Hedges and Mann 1979). In these environments, a comprehensive SOM isotopic mass balance model would therefore include mass expressions for each individual organic component in plant inputs. The expression for ^{12}C in this scenario would be the same as Equation 8.22a, while the expression for ^{13}C is:

$$\frac{dC^*}{dt} = \sum_{i=1}^{n} (RI - k\alpha C^*)_i \qquad (8.23)$$

The only difference between Equations 8.22 and 8.23 is that the isotopic ratio of each input in Equation 8.23 is different (whereas they are the same in Equation 8.22). In Equation 8.23, I may also represent transfers from other pools, which is likely to be a very important part of SOM cycling that is included in some of the most complex SOM models (e.g., Elzein and Balesdent 1995).

The multiple pool approach for modeling stable C isotopes in SOM is difficult (Townsend et al. 1995), but various forms of this approach serve as the basis for the understanding of the ^{14}C content of SOM (Trumbore 1993; Elzein and Balesdent 1995) and the $\delta^{13}C$ value of SOM (Arrouays et al. 1995).

Stable Nitrogen Isotopes in Organic Matter

In terms of SOM dynamics and processes, observed patterns of stable N isotopic ratios in SOM have thus far proven frustrating because they have eluded quantitative interpretive models. In general, the relevant soil processes controlling N isotopes are well understood. Nitrogen enters the SOM pool via several pathways (Fig. 8.4): (1) wet and dry deposition, (2) biological fixation of atmospheric N_2, (3) nitrogenous fertilizers, and (4) plant inputs—each of which may have different $\delta^{15}N$ values. Once in the SOM pool, this N is subject to a variety of biological and inorganic transformations, each of which may cause small to very large isotopic fractionations (Table 8.1). Therefore, an understanding of the N isotope chemistry of soils is arguably more complex than the situation for stable carbon isotopes.

A "one pool, no fractionation" model (Equation 8.6) does not adequately describe SOM N isotope mass balances for three reasons. (1) There are two or more major sources of N in most soil ecosystems, each with differing $\delta^{15}N$ values, and (2) in many soils, the $\delta^{15}N$ value of SOM is up to 8 to 10‰ enriched relative to one or more of the N inputs (Shearer and Kohl 1986, 1988), indicating that discriminatory processes can be very important. These processes can vary greatly both spatially and temporally. Finally (3), with respect to in-soil processes, the $\delta^{15}N$ value of SOM commonly increases several or more ‰ with increasing soil depth (see Fig. 8.2b).

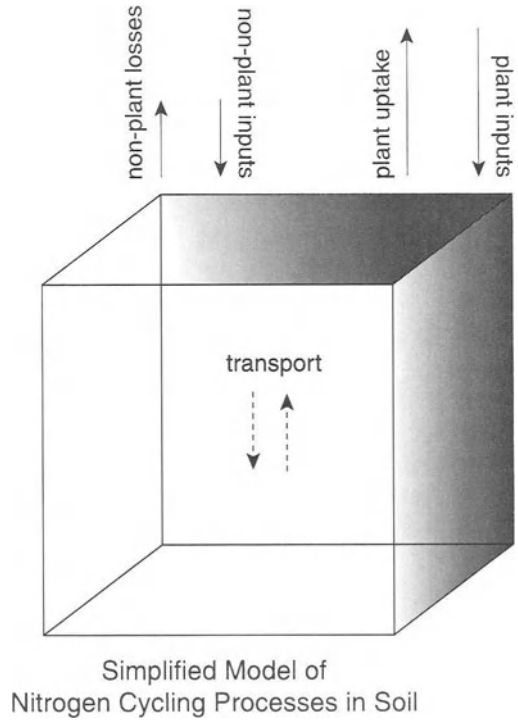

FIGURE 8.4. Nitrogen processes in the soil environment.

There have been several innovative efforts to mechanistically model the $\delta^{15}N$ value of SOM (Focht 1973; Shearer et al. 1974). These early models appear to have received little attention in the subsequent use of N isotopes in ecological research. Two of the difficulties of these models (in addition to their mathematical complexity) is the uncertainty in the absolute values of fractionation factors for all relevant N reactions in soils and uncertainty in the relative rates of various N transformations for a given soil. We believe that these models, or variations of them, will prove useful in future research. However, here we begin with a far more elementary approach to modeling soil $\delta^{15}N$ values in order to understand N cycling processes at a more generalized level.

TABLE 8.1. Isotopic fractionation for some important biological N transformations in the soil environment.

Process	β[a]	$10^3 \ln \beta$ (‰)	Source
N_2 fixation	0.998–1.020	−2 to 2	Shearer and Kohl (1986)[b]
Nitrification	1.012–1.029	11.9 to 28.6	Mariotti et al. (1982) soils
	1.000–1.040	0.0 to 39.2	Delwiche and Steyn (1970) cultures
			Miyake and Wada (1971)
			Domenach and Chalamet (1977)
			Mariotti et al. (1981)
Denitrification	1.000–1.030	0.0 to 29.6	Mariotti et al. (1981)
			Blackmer and Bremner (1977)
			Chien et al. (1977)
			Wellman et al. (1968)
			Delwiche and Steyn (1970)
			Cook et al. (1973)
			Bryan et al. (1983)
NH_3 volatilization	1.027–1.025	26.6 to 24.7	Mariotti (1982) steady state
	1.008–1.032	8.0 to 31.5	Mariotti (1982) non-steady state

[a] $\beta = R_{reactant}/R_{product} = 1/\alpha$
[b] Range of values compiled from 34 published measurements.

Well-Mixed One Box Soil Ecosystem Model of N Isotopes

The purpose of this section is to develop simple mass balance models of N isotopes in SOM somewhat analogously to what was done previously for C isotopes. However, since the models we develop are novel with respect to their application to N isotopes, we will also simultaneously illustrate their relevance via comparison to published data.

In order to gain some insight into processing of N at a soil-ecosystem scale, a simplified approach may be made. First, all SOM may be considered a well-mixed pool (which avoids the vertical variations present in the real world). Second, it may be assumed that N inputs into soil are from two main sources: (1) plant inputs (the major source in most established ecosystems) and (2) atmospheric or "external" inputs (which are likely to be small relative to plants in most environments). If these two sources have differing isotopic values, the expression for the common isotope, ^{14}N, is:

$$\frac{dN}{dt} = I_e - k_e N + I_p - k_p N \quad (8.24a)$$

and the expression for ^{15}N is:

$$\frac{dN^*}{dt} = R_e I_e - k_e \alpha_e N^* + R_p I_p - k_p \alpha_p N^* \quad (8.24b)$$

where e is external inputs and returns and p is plant inputs and returns. If Equations 8.24a and b are solved (including the simplifying assumption that plant inputs are not a function of time) and Equation 8.24b is divided by Equation 8.24a, the resulting expression is:

$$R_{SOM-N}(t) = \left(\frac{1}{k_e\alpha + k_p\alpha_p}((R_e I_e + R_p I_p) - (R_e I_e + R_p I_p)e^{-(k_e\alpha_e + k_p\alpha_p)t})\right) \div \left(\frac{1}{k_e + k_p}(I_e + I_p) - (I_e + I_p)e^{-(ke+kp)t}\right) \quad (8.25)$$

where $R_{SOM-N} = {}^{15}N/{}^{14}N$ in SOM N, R_e and R_p = N isotopic ratios of external and plant inputs, respectively; and α_e and α_p = fractionation factors associated with external losses and plant uptake, respectively. To quantitatively evaluate Equation 8.25 as a function of time requires knowledge or reasonable estimates for various inputs and losses (and their isotopic composition). However, qualitatively, the model suggests that for early stages of SOM accumulation, the $\delta^{15}N$ value of SOM will be dominated by inputs (with the deficiency in Equation 8.25 that plant inputs are overestimated relative to nonplant inputs at t = 0 because inputs are not modeled as being time-dependent). As time pro-

gresses, the net effect of the fractionating losses will become magnified and reflected in the remaining SOM pool.

There is some support for many of the simplifications and assumptions of Equation 8.25. Vitousek et al. (1989) measured the $\delta^{15}N$ values of plant and soil organic matter along a chronological sequence of soils in Hawaii (Fig. 8.5). These data suggest that for young ecosystems, whose only source of N is atmospheric deposition, the $\delta^{15}N$ values of the plants and SOM are close to the expected range for inorganic atmospheric additions (approximately $-5‰$). As the systems age, the $\delta^{15}N$ value of the plants and SOM increase, reflecting the combination of a variety of highly fractionating N losses (denitrification, nitrate loss, etc.) (Vitousek et al. 1989; Riley and Vitousek 1995).

If steady state is achieved, Equation 8.25 simplifies to:

$$R_{SS} = \frac{I_e[R_e F_e + R_p(1 - F_e)]}{(N)(Fe)(k_e\alpha_e + k_p\alpha_p)} \quad (8.26)$$

where R_{SS} = steady state $^{15}N/^{14}N$ ratio of SOM and $F_e = I_e/(I_e + I_p)$. Equation 8.26 states that if rates and isotopic composition of inputs are known (and the values of the fractionations associated with losses), the average $\delta^{15}N$ value of the soil ecosystem can be calculated.

To use either Equation 8.26 or 8.25, one must know the isotopic composition of the SOM, plants, and nonplant inputs at steady state (which potentially can be measured). Additionally, the fractionations associated with plant uptake and nonplant loss must be determined. These may be estimated as follows.

If it is assumed that the $\delta^{15}N$ value of plant N uptake = $\delta^{15}N$ value of plant N inputs at steady state (true for ecosystems with negligible N fixation), then the fractionation associated with plant uptake from the bulk SOM pool is (Equation 8.11):

$$\alpha_p = R_p/R_{SOM-N}$$

Table 8.2 shows the apparent α_p (for convenience, $10^3 \ln \alpha_p$) as a function of mean annual precipitation for a variety of locations (assuming that N fixation is not important in the systems). Regardless of temperature and moisture conditions, the fractionation between total SOM N and plant N is remarkably constant ($10^3 \ln \alpha_p = -6.7 \pm 1.5‰$) (see Table 8.2). This fractionation is far less than the fractionation associated with nitrification, and implies that the rate limiting step in the production of plant-available N is likely somewhere in the mineralization processes (see Shearer and Kohl, 1986 for discussion of rate limiting steps) or elsewhere in the N cycling pathway.

Plant–soil systems are not closed, and at steady state the losses via erosion, denitrification, volatilization, and nitrate loss are balanced by inputs from the atmosphere. Both the number of atmospheric inputs and soil loss pathways are large, but as a first order approximation of the fractionation involved

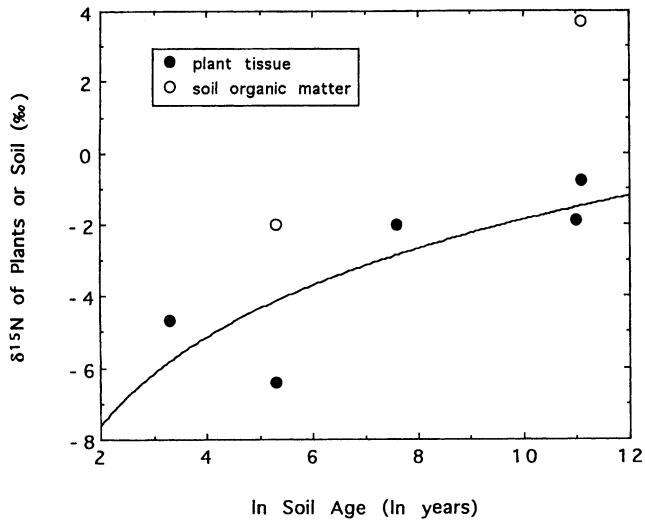

FIGURE 8.5. $\delta^{15}N$ values of plants and SOM as a function of soil age in Hawaii (Vitousek et al. 1989).

TABLE 8.2. $\delta^{15}N$ value of soil organic matter ($\delta^{15}N_s$) and vegetation ($\delta^{15}N_p$), and the value of the apparent soil to plant N isotopic fractionation factor (α_p), for a variety of non-agricultural ecosystems.

Location	$\delta^{15}N_s$ (‰)	$\delta^{15}N_p$ (‰)	α_p[a]	$10^3 \ln \alpha$[b] (‰)	MAT (°C)	MAP (cm)	elevation (m)
France[c]	5.1	−1.9	.9930	−7.0	—	—	1100
	4.8	−1.8	.9934	−6.6	—	—	1440
	3.8	−5.0	.9912	−8.8	—	—	1600
	3.0	−3.1	.9939	−6.1	—	—	1800
Tanzania[d]	4.5	−1.1	.9944	−5.6	15	167	2454
	4.9	−1.5	.9936	−6.4	14	157	2545
	5.4	−2.1	.9925	−7.5	12	132	2990
	6.0	−3.1	.9910	−9.1	9	104	3505
Wisconsin[e]	4.0	−3.8	.9922	−7.8	8	95	—
Mass.[f]	6.5	0	.9937	−6.3	—	—	—
Hawaii[g]	3.7	−0.8	.9955	−4.5	21	36	450
	−2.0	−6.4	.9956	−4.4	17	206	1160

[a] $\alpha_p = (\delta^{15}N_p + 1000)/(\delta^{15}N_s + 1000) = R_p/R_s$
[b] ‰ discrimination (Freidman and O'Neil, 1977).
[c] Mariotti et al. (1980). Weighted mean $\delta^{15}N$ of SOM to 50 cm.
[d] Uebersax (1996). Weighted mean $\delta^{15}N$ of SOM to 50 cm except at 3505 m, where it is calculated to 25 cm.
[e] Nadelhoffer and Fry (1988). Mean $\delta^{15}N$ of SOM to 20 cm.
[f] Melillo et al. (1989). Weighted mean $\delta^{15}N$ of SOM to 45 cm.
[g] Vitousek et al. (1989). $\delta^{15}N$ of SOM to 15 cm.

in these combined processes (i.e., α_e), an overall fractionation for loss can be calculated:

$$\alpha_e = \frac{R_e}{R_{SOM-N}}$$

The $\delta^{15}N$ value of atmospheric N inputs is variable. N fixed via biological processes is approximately 0‰ while N deposition is variable isotopically and must be determined locally.

Many measurements of the $\delta^{15}N$ value of SOM have been made, particularly in agricultural settings. These measurements initially revealed no discernible geographic pattern in SOM $\delta^{15}N$ values, suggesting that N isotopes may not be sensitive indicators of environmentally induced effects on soil N transformations. However, more recent measurements, conducted over strong climatic gradients (Mariotti et al. 1980; Uebersax 1996; Austin and Vitousek 1998), have demonstrated large variations in SOM $\delta^{15}N$ values with changes in climate. In general, total soil N increases and the $\delta^{15}N$ value of SOM decreases with increasing mean annual precipitation, an observation first noted by Shearer et al. (1978). Such a climatic variation is interpretable with the "two input/loss" model discussed above, where α_e is an apparent function of climate. Next we estimate α_e for two tropical climate gradients.

Uebersax (1996) measured the $\delta^{15}N$ value of SOM along elevation transects in the tropics. For an elevation transect in Hawaii, the $\delta^{15}N$ value of atmospheric inputs was estimated by the $\delta^{15}N$ value of lichens growing on bare rock surfaces (−5.1‰) (Vitousek et al. 1989). Similarly, atmospheric N inputs for an elevation transect of Mt. Kilamanjaro may vary between 0 and −5‰ (Heaton, 1987a). Using these values as approximate extremes, α_e was calculated as a function of precipitation for these two tropical elevation transects (Fig. 8.6). The calculations indicate large apparent increases in fractionation of "external" or nonplant N losses with decreasing precipitation (from a maximum fractionation of −18‰ in the low-precipitation systems to a minimum fractionation of −3‰ in the highest precipitation sites). While these curves are based on very limited data (with some important assumptions), they correspond with published data by Austin and Vitousek (1998) for a rainfall gradient in Hawaii and with Heaton (1987b) for plants collected along a rainfall gradient in South Africa and Nambia. Austin and Vitousek (1998) show that the high-rainfall montane tropical soils they ex-

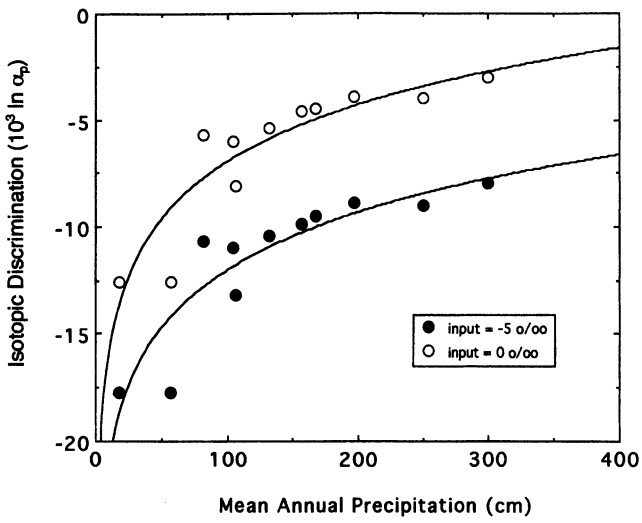

FIGURE 8.6. Estimates of apparent nonplant N loss isotope fractionation factor as a function of mean annual precipitation for two tropical ecosystems: Hawaii and Tanzania. The two curves represent apparent fractionation factors assuming nonplant inputs = 0‰ and −5‰, respectively. Soil data from Uebersax (1996).

amined are N-limiting to plants, and that products of mineralization are rapidly consumed. The isotopic data from all the transects also imply that the main external N losses in high-rainfall environments are relatively nonfractionating (e.g., erosion, DON leaching, etc.). In contrast, dry environments may be less N-limited (or have seasonal gaps in N demand when plant uptake is minimal [Jackson et al. 1988]), and plants are not consuming all the N that is mineralized, leading to fractionating N losses from these soils and ecosystems.

Use of N Isotopes in SOM as a Tracer

While the use of the $\delta^{15}N$ value of SOM as a tracer of natural N cycling is only in its formative stages, there is a long history of using N isotopes in soil/plant systems as a tracer of the magnitude of N fixation in agricultural or natural settings. Since the $\delta^{15}N$ value of biologically fixed N is well known (range of −2 to +2‰, Shearer and Kohl 1986), if the $\delta^{15}N$ value of soil-derived N sources can be characterized, a two component mixing model can be used to determine the proportion of total plant N obtained via biological fixation (Shearer and Kohl 1986, 1988):

$$\%N_F = \left(\frac{\delta N_s - \delta^{15}N_p}{\delta^{15}N_s - \delta^{15}N_f}\right)100 \qquad (8.27)$$

where $\%N_F$ = percentage of plant N derived from N_2 fixation, $\delta^{15}N_S$ = value of soil-derived N, $\delta^{15}N_F$ = value of fixed N, and $\delta^{15}N_P$ = value of the plant.

This application has an important ecological significance, and has been the impetus behind the interest in stable N isotopes in SOM since the 1960s (Bremner 1965). However, this section has revealed that there may be important new avenues for N isotope research: directions that focus on natural processes, such as comparisons between differing ecosystems or within-soil processes.

Model of Vertical Variations in $\delta^{15}N$ Value of SOM

The simple one box soil ecosystem model ignores the real variations in the $\delta^{15}N$ value of SOM with depth. For example, the variation in the $\delta^{15}N$ value of SOM with depth along an elevation transect in France is illustrated in Figure 8.2B. While in many areas, the $\delta^{15}N$ value of SOM increases with increasing depth, it has also been observed in a few locations (such as tropical volcanic soils in Hawaii) that there is no discernible isotopic trend with depth (Uebersax, 1996).

Following our approach for describing depth variation in the $\delta^{13}C$ values of SOM, we derive equations describing N isotope variation with depth for two separate cases: one assuming that transport of soil N is by diffusion and another assuming that transport is by advection. We develop these two models individually because this analysis will allow us to discuss these models in relation to previous approaches that have been used to evaluate

the observed depth variations in the $\delta^{15}N$ value of SOM. In both cases, we again make the simplifying (and unrealistic) assumption that N is added at the soil surface and moves downward, and that no N is added via root processes.

At steady state, the general model describing soil N, assuming that SOM moves downward via advection, is:

$$\frac{\partial N}{\partial t} = 0 = -\upsilon \frac{N}{z} - kN \qquad (8.28)$$

The model, assuming that transport is via diffusion, is (see also Equation 8.17):

$$\frac{\partial N}{\partial t} = 0 = D \frac{\partial^2 N}{\partial z^2} - kN \qquad (8.29)$$

If we assume that the abundant N isotope (N) concentration at $z = 0$ is the concentration in the added plant material (N_p), and that the rare N isotope ($*N$) = $*N_p$ at $z = 0$, we can solve Equations 8.28 and 8.29 for both the common and rare isotopes of N. By dividing the solution for the rare isotope by the solution for the common isotope, we can compare these two approaches to evaluating $\delta^{15}N$ values with depth z with that of the added plant material:

Advection/decomposition model:

$$\frac{R(z)}{R(p)} = e^{(-kz/\nu)(\alpha-1)} = f_A^{(\alpha-1)} \qquad (8.30)$$

Diffusion/decomposition model:

$$\frac{R(z)}{R(p)} = \frac{1}{\sqrt{\alpha}} e^{z\sqrt{k/D}(\sqrt{\alpha}-1)} \cong f_D^{(\sqrt{\alpha}-1)} \qquad (8.31)$$

where k is the decomposition constant for the release of N from SOM, D is the diffusion coefficient for N movement, and ν is the advection coefficient for N movement. Our final simplification is to denote f_A and f_D as the fraction of N remaining at depth z relative to that found at the surface in the form of plant inputs. The main point from a comparison of Equations 8.30 and 8.31 is that the N isotope ratio of SOM at depth z relative to that of plant inputs is dependent on the isotopic fractionation factor α if advective transport is operative, but it is dependent on the square root of α if diffusion operates.

In recent years, some researchers (e.g., Nadelhoffer and Fry 1988) have used a "Rayleigh distillation model" to interpret observed variations in the $\delta^{15}N$ value of SOM with depth:

$$R_{SOM-N} = R_o f_R^{(\alpha-1)} \qquad (8.32)$$

where $R_o = {}^{15}N/{}^{14}N$ ratio of the original SOM, f_R = fraction of inputs remaining, and α = isotopic fractionation associated with losses. A Rayleigh model describes any process in which a reactant is consumed by a process with a fixed fractionation factor. This is an appropriate model to use in laboratory incubation studies. For soil profiles, the model has no predictive value because space and time are not explicitly parameters in this model. On the other hand, if transport of SOM is assumed to be advective, and no root inputs are added, then it can be rearranged and used to calculate the fractionation factor for N isotopes in an identical way to advection (Equation 8.30).

We can convert Equations 8.30 and 8.31 to the familiar delta notation, and express the fractionation factor α as the commonly used discrimination term ε, if we use the following relationships:

$$1000 \ln \frac{R(z)}{R(p)} \cong \delta_z - \delta_p$$

and

$$(\alpha - 1)1000 \cong \varepsilon.$$

Following substitution and algebraic manipulation:

Rayleigh and advection models:

$$\varepsilon = \frac{\delta_z - \delta_p}{\ln f_x} \qquad (8.33)$$

Diffusion model:

$$\varepsilon = 2 \frac{\delta_z - \delta_p}{\ln f_D} \qquad (8.34)$$

Where f_x in Equation 8.33 refers to f_R for the Rayleigh model and f_A for the advection model. Equations 8.33 and 8.34 show that a Rayleigh model and an advection model result in identical interpretations of isotopic discrimination during decomposition. In contrast, if SOM is diffusively transported downward, then the apparent discrimination is twice that evaluated using Equation 8.33. Given our uncertainty in SOM transport processes, it is difficult to determine for any soil which model is most appropriate, however, it is likely that "diffusion" (both upward and downward movement of N by

biological processes) occurs in or dominates many biologically active soils. Exceptions to this may be coarse-textured Spodosols, where SOM is believed to be transported downward through advection. Previous estimates of ε have been based on rearranging Equation 33 so the data (δ_z vs. ln f) fit on a line with slope ε and intercept δ_p. Therefore, we suggest that previous estimates of ε (Nadelhoffer and Fry 1988; Evans and Ehleringer 1993; Piccolo et al. 1996) may underestimate isotopic discrimination because they were based on Equation 8.33 alone. Finally, it is likely that future advection and diffusion models that incorporate direct root inputs will add additional complexity, but also reality, to the analysis of depth variations in the SOM $\delta^{15}N$ values.

Ultimately, we believe that the isotopic trend with depth for N isotopes in SOM must be described using a variation of a production-decomposition-dispersion model (i.e., Equation 8.14) with multiple N sources and pathways, an approach first made in early papers (Focht 1973; Shearer et al. 1974). In the meantime, much remains to be learned of natural patterns of the rates and isotopic composition of N inputs, the natural patterns in SOM $\delta^{15}N$ values, and the rates of various soil N transformations—information needed to constrain any model that may be constructed to explain these interesting N transformation processes.

Conclusions

With some exceptions, stable isotopes in organic matter have been used as a tracer in SOM processes primarily in "mixing model" approaches. In the case of C isotopes, changes in $\delta^{13}C$ values, usually resulting from C_3/C_4 shifts, allow for the quantification of rates of SOM cycling. In the case of N, the isotopic differences between biologically fixed N and that derived from SOM mineralization provide a means of detecting N fixation in unknown plants or as a means of quantifying total rates of N fixation in agricultural settings.

In contrast, the differences in the isotopic composition of SOM relative to inputs, or the common increases in heavy isotopes with soil depth, have not been examined with nearly the same intensity. We believe that these observations can be analyzed with models of varying complexity with rewarding results. First, in the case of N, if soils are considered to be well-mixed pools of SOM, comparisons of inputs to the SOM pool at steady state can lead to important insights into the similarities or differences in the processes of N additions and losses in contrasting environments. For both C and N, the widely ranging increases in δ values with increasing depth hint at interesting combinations of processes, which may be ultimately captured by analytical or numerical mathematical models.

As the interest in ecosystem functioning grows, isotopes combined with mathematical modeling will play an important role in understanding the type and magnitude of SOM cycling processes. Despite nearly 30 years of research on SOM isotope chemistry, this is still a largely unexplored field of research—one which will provide many challenging opportunities for years to come.

Acknowledgments This research was supported by a NASA Earth System Science Fellowship to W.T. Baisden and by University of California Agricultural Experiment Station, University of California Committee on Research, and Kearney Foundation of Soil Science funding to R. Amundson. We thank Professor Sue Trumbore for her review of the chapter and Professor Peter Vitousek, Kitty Lohse, and Dana Brenner for helpful comments on an earlier version of the manuscript.

References

Ambrose, S.H.; Sikes, N.E. Soil carbon isotope evidence for Holocene habitat change in the Kenya Rift Valley. Science 252:1402–1405; 1991.

Amundson, R.; Chadwick, O.A.; Sowers, J.M.; Doner, H.E. Soil evolution along an altitudinal transect in the eastern Mojave Desert of Nevada, U.S.A. Geoderma 43:349–371; 1989.

Amundson, R.; Stern, L.; Baisden, T.; Wang, Y. The isotopic composition of soil and soil-respired CO_2. Geoderma 82:83–114, 1998.

Arrouays, D.; Balesdent, J.; Mariotti, A.; Girardin, C. Modeling organic carbon turnover in cleared temperate forest soils coverted to maize cropping by using ^{13}C natural abundance measurements. Plant Soil 173:191–196; 1995.

Austin, A.T.; Vitousek. P.M. Nutrient dynamics on a precipitation gradient in Hawaii. Oecologia 113:519–529; 1998.

Baisden, W.T.; Amundson. R.G. Matrix methods to model terrestrial ecosystem C and N dynamics. Suppl. Bull. Ecol. Soc. Am. 1997 Annu. Meet. 78(4):218; 1997.

Balesdent, J.; Girardin, C.; Mariotti, A. Site-related $\delta^{13}C$ of tree leaves and soil organic matter in a temperate forest. Ecology 74:1713–1721; 1993.

Balesdent, J.; Mariotti, A. Measurement of soil organic matter turnover using ^{13}C natural abundance. In: Boutton, T.; Yamasaki, S., eds. *Mass Spectrometry of Soils.* Marcel Dekker, New York; 1996:83–111.

Balesdent, J.; Wagner, G.H.; Mariotti, A. Soil organic matter turnover in long-term field experiments as revealed by carbon-13 natural abundance. Soil Sci. Soc. Am. J. 52:118–124; 1988.

Bender, M.M. Mass spectrometric studies of carbon 13 variations in corn and other grasses. Radiocarbon 10:468–472; 1968.

Benner, R.; Fogel, M.L.; Sprague, E.K.; Hodson, R.E. Depletion of ^{13}C in lignin and its implications for stable carbon isotope studies. Nature 329:708–710; 1987.

Bertram, H.-G.; Schleser, G.H. The $^{13}C/^{12}C$ isotope ratios in a north-German podzol. In: Schmidt, H.-L.; Förstel, H.; K. Heinzinger, K., eds. *Stable Isotopes.* Amsterdam: Elsevier; 1982:115–120.

Bird, M.I.; Chivas, A.R.; Head, J. A latitudinal gradient in carbon turnover times in forest soils. Nature 381:143–146; 1996.

Blackmer, A.M.; Bremner, J.M. Nitrogen isotope discrimination in denitrification of nitrate in soils. Soil Biol. Biochem. 9:73–77; 1977.

Boutton, T.W. Stable carbon isotope ratios of soil organic matter and their use as indicators of vegetation and climate change. In: Boutton, T.; Yamasaki, S, eds. *Mass Spectrometry of Soils.* New York: Marcel Decker; 1996:47–82.

Bray, J.R. Root production and the estimation of net productivity. Can. J. Bot. 41:65–72; 1963.

Bremner, J.M. Isotope-ratio analysis of nitrogen in nitrogen-15 tracer investigations. In: Black, C.A.; Evans, D.D.; Ensminger, L.E.; White, J.L.; Clark, F.E.; Dinauer, R.C., eds. *Methods of Soil Analysis. Part 2. Chemical and Microbiological Properties.* Madison, WI: American Society of Agronomy; 1965:1256–1286.

Bryan, B.A.; Shearer, G.; Skeeters, J.; Kohl, D.H. Variable expression of the nitrogen isotope effect associated with denitrification of nitrate. J. Biol. Chem. 258:8613–8617; 1983.

Cerling, T.E.; Solomon, D.K.; Quade, J.; Bowman, J.R. On the isotopic composition of carbon in soil carbon dioxide. Geochim Cosmochim Acta 55:3404–3405; 1991.

Chien, S.H.; Shearer, G.; Kohl, D.H. The nitrogen isotope effect associated with nitrate and nitrite loss from waterlogged soils. Soil Sci. Soc. Am. J. 41:63–69; 1977.

Cook, F.D.; Wellman, R.P.; Krouse, H.R. Nitrogen isotope fractionation in the nitrogen cycle. In: E. Ingersen, E., ed. *Proceedings of Symposium on Hydrogeochemistry and Biogeochemistry.* Vol. 2. Washington, DC: Clark; 1973:49–64.

Connin, S.L.; Virginia, R.A.; Chamberlain, C.P. Carbon isotopes reveal soil organic matter dynamics following arid shrub expansion. Oecologia 110:374–386; 1997.

Craig, H. Isotopic standards for carbon and oxygen and correction factors for mass spectrometric analyses of carbon dioxide. Geochim Cosmochim Acta 12:133–149; 1957.

Darwin, C. *The Formation of Vegetable Mould Through the Action of Worms, with Observations on Their Habits.* London: John Murray; 1881.

Delwiche, C.C.; Steyn, P.L. Nitrogen isotope fractionation in soils and microbial reactions. Environ. Sci. Tech. 4:929–935; 1970.

Domenach, A.M.; Chalamet, A. Rapports isotopiques naturels de l'axote. I. Premiers resultats. Sols des Dombes. Rev. Ecol. Biol. Sol. 14:279–287; 1977.

Dörr, H.; Münnich, K.O. Annual variations of the ^{14}C content of soil CO_2. Radiocarbon 28:338–345; 1986.

Dörr, H.; Münnich, K.O. Downward movement of soil organic matter and its influence on trace-element transport (^{210}Pb, ^{137}Cs) in the soil. Radiocarbon 31:655–663; 1989.

Dzurec, R.S.; Boutton, T.W.; Caldwell, M.M.; Smith, B.N. Carbon isotope ratios of soil organic matter and their use in assessing community composition changes in Curlew Valley, Utah. Oecologia 66:17–24; 1985.

Elzein, A.; Balesdent, J. Mechanistic simulation of vertical distribution of carbon concentrations and residence times in soils. Soil Sci. Soc. Am. J. 59:1328–1335; 1995.

Evans, R.D.; Ehleringer, J.R. A break in the nitrogen cycle in aridlands? Evidence from $\delta^{15}N$ of soils. Oecologia 94:314–317; 1993.

Farquhar, G.D.; Ehleringer, J.R.; Hubick, K.T. Carbon isotope discrimination and photosynthesis. Annu. Rev. Plant Physiol. Plant Mol. Biol. 40:503–537; 1989.

Faure, G. *Principles of Isotope Geology.* 2nd Ed. New York: Wiley; 1986.

Focht, D.D. Isotope fractionation of ^{15}N and ^{14}N in microbial transformations: a theoretical model. J. Environ. Qual. 2:247–252; 1973.

Freidli, H.; Lötscher, H.; Oeschger, H.; Seigenthaler, U.; Stauffer, B. Ice core record of the $^{13}C/^{12}C$ ratio of atmospheric CO_2 in the past two centuries. Nature 324:237–238; 1986.

Freidman, I.; O'Neil, J.R. Chapter, KK. Compilation of stable isotope fractionation factors of geochemical in-

terest. In: Fleischer, M., ed. *Data of Geochemistry.* 6th Ed. United States Geological Survey (USGS) Professional Paper 440-KK. Washington, DC: U.S. Government Printing Office; 1977.

Galloway, J.N.; Levy, H.; Kashibhatla, P.S. Year 2020—Consequences of population growth and development on deposition of oxidized nitrogen. Ambio 23:120–123; 1994.

Gile, L.; Grossman, R.B. *The Desert Soil Project Monograph.* Washington, DC: U.S. Department of Agriculture (USDA), Soil Conservation Service; 1979.

Goreau, T.J.; Kaplan, W.A.; Wofsy, S.C.; McElroy, M.B.; Valios, F.W.; Watson, S.W. Production of NO_3^- and N_2O by nitrifying bacteria at reduced concentrations of oxygen. Appl. Environ. Microbiol. 40:526–532; 1980.

Hayes, J.M. Fractionation, et al. An introduction to isotopic measurements and terminology. Spectra 8:3–8; 1982.

Heaton, T.H.E. $^{15}N/^{14}N$ ratios of nitrate and ammonium in rain at Pretoria, South Africa. Atm. Environ., 21:843–852; 1987a.

Heaton, T.H.E. The $^{15}N/^{14}N$ ratios of plants in South Africa and Namibia: Relationship to climate and coastal/saline environments. Eocologia 74:236–246; 1987b.

Hedges, J.I.; Mann, D.C. The lignin geochemistry of marine sediments from the southern Washington coast. Geochim Cosmochim Acta 43:1809–1818; 1979.

Jackson, L.; Strauss, R.; Firestone, M.; Bartolomne, J. Plant and soil nitrogen dynamics in California annual grassland. Plant Soil 110:9–17; 1988.

Jenny, H.; Gessel., S.P.; Bingham, F.T. Comparative study of decomposition rates of organic matter in temperate and tropical regions. Soil Sci 68:419–432; 1949.

Kinzig, A.P.; Socolow, R.H. Human impacts on the nitrogen cycle. Physics Today. November 1994:24–31; 1994.

Kononova, M.M. *Soil Organic Matter.* 2nd Ed. Oxford: Pergamon; 1966.

Lauenroth, W.K.; Whitman, W.C. Dynamics of dry matter production in a mixed-grass prairie in western North Dakota. Oecologia 27:339–351; 1977.

Mariotti, A. *Apports de al Geóchimie isotopiue a la connaissance du cycle de l'azote. Memoires des Sciences de la Terré.* Universite P. et M. Cure Paris, No. 82-13; 1982.

Mariotti, A. Atmospheric nitrogen is a reliable standard for natural ^{15}N abundance measurements. Nature 303:685–687; 1983.

Mariotti, A.; Germon, J.C.; Hubert, P.; Kaiser, P.; Letolle, R.; Tardieux, A.; Tardieux, P. Experimental determinations of nitrogen kinetic isotope fractionation: Some principles. Illustration for the denitrification and nitrification processes. Plant Soil 62:413–430; 1981.

Mariotti, A.; Mariotti, F.; Champigny, M.L.; Amarger, N.; Moyse, A. Nitrogen isotope fractionation associated with nitrate reductase activity and uptake of NO_3^- by pearl millet. Plant Physiol 69:880–884; 1982.

Mariotti, A.; Pierre, D.; Vedy, J.C.; Brukert, S.; Guillemot, J. The abundance of natural nitrogen-15 in the organic matter of soils along an altitudinal gradient. Catena 7:292–300; 1980.

Mary, B.; Mariotti, A.; Morel, J.L. Use of ^{13}C variations at natural abundance for studying the biodegradation of root mucilage, roots, and glucose in soil. Soil Biol. Biochem. 24:1065–1072; 1992.

McKeague, J.A.; DeConinck, F.; Franzmeier, D.P. Spodosols. In: Wilding, L.P.; Smeck, N.E.; Hall, G.F., eds. *Pedogenesis and Soil Taxonomy. II. The Soil Orders.* Developments in Soil Science 11B. New York: Elsevier; 1983:217–252.

Melillo, J.M.; Aber, J.D.; Linkins, A.E.; Ricca, A.; Fry, B.; Nadelhoffer, K.J. Carbon and nitrogen dynamics along the decay continuum: Plant litter to soil organic matter. Plant Soil 115:189–198; 1989.

Miyake, Y.; Wada, E. The isotope effect on the nitrogen in biochemical oxidation-reduction reactions. Rec. Oceanogr. Works Jpn 11:1–6; 1971.

Monaghan, M.C.; Krishnaswami, S.; Thomas, J.H. ^{10}Be concentrations and the long-term fate of particle-reactive nuclides in five soil profiles from California. Earth Planet. Sci. Lett. 65:51–60; 1983.

Nadelhoffer, K.J.; Fry, B. Controls on the natural nitrogen-15 and carbon-13 abundances in forest soil organic matter. Soil. Sci. Soc. Am. J. 52:1633–1640; 1988.

Oades, J.M. An overview of processes affecting the cycling of organic carbon in soils. In; Zepp, R.; Sontagg, C., eds. *The Role of Nonliving Organic Matter in the Earth's Carbon Cycle.* New York: Wiley; 1995:293–304.

O'Brien, J.B.; Stout, J.D. Movement and turnover of soil organic matter as indicated by carbon isotope measurements. Soil Biol. Biochem. 10:309–317; 1978.

Parker, P.L. The biogeochemistry of the stable isotopes in a marine bay. Geochim Cosmochim Acta 28:1155–1164; 1964.

Piccolo, M.C.; Neill, C.; Melillo, J.M.; Cerri, C.C.; Steudler, P.A. ^{15}N natural abundance in forest and pasture soils of the Brazilian Amazon Basin. Plant Soil 182:249–258; 1996.

Riley, R.H.; Vitousek, P.M. Nutrient dynamics and nitrogen trace gas flux during ecosystem development in montaine rain forest. Ecology 76:292–304; 1995.

Robinson, D.; Scrimgeour, C.M. The contribution of plant C to soil CO_2 measured using delta C-13. Soil Biol. Biochem. 27:1653–1656; 1995.

Rochette, P.; Flanagan, L.B. Quantifying rhizosphere respiration in a corn crop under field conditions. Soil Sci. Soc. Am. J. 61:466–474; 1997.

Schlesinger, W.H. Carbon balance in terrestrial detritus. Annu. Rev. Ecol. Syst. 8:51–81; 1977.

Schlesinger, W.H. *Biogeochemistry. An Analysis of Global Change.* New York: Academic; 1991.

Shearer, G.; Duffy, J.; Kohl, D.H.; Commoner, B. A steady-state model of isotopic fractionation accompanying nitrogen fractionations in soil. Soil Sci. Soc. Am. Proc. 38:315–322; 1974.

Shearer, G.; Kohl, D.H. N_2-fixation in field settings: Estimations based on natural ^{15}N abundance. Aust. J. Plant Physiol. 13:699–756; 1986.

Shearer, G.; Kohl, D.H. Estimates of N_2 fixation in ecosystems: The need for and basis of the ^{15}N natural abundance method. In: Rundel, P.W.; Ehleringer, J.R.; Nagy, K.A., eds. *Stable Isotopes in Ecological Research.* New York: Springer-Verlag, 1988:342–374.

Shearer, G.; Kohl, D.H.; Chein, S.H. The nitrogen-15 abundance in a wide variety of soil. Soil Sci. Soc. Am. J. 42:899–902; 1978.

Smith, B.N.; Epstein, S. Two categories of $^{13}C/^{12}C$ for higher plants. Plant Physiol. 47:380–384; 1971.

Stout, J.D.; Rafter, T.A. The $^{13}C/^{12}C$ isotopic ratios of some New Zealand tussock grassland soils. In: Robinson, B.W., ed. *Stable Isotopes in the Earth Sciences.* Wellington, New Zealand: Department of Scientific and Industrial Research; 1978:75–83.

Taylor, H.P., Jr.; O'Neil, J.R.; Kaplan, I.R. Samuel Epstein: Scientist, teacher, and friend. In: Taylor, H.P., Jr.; O'Neil, J.R.; Kaplan, I.R., eds. *Stable Isotope Geochemistry: A Tribute to Samuel Epstein.* Special Publication No. 3. San Antonio, TX: The Geochemical Society, Trinity Univ.; 1991:xiii–xvi.

Townsend, A.R.; Vitousek, P.M.; Trumbore, S.E. Soil organic matter dynamics along gradients in temperature and land use on the island of Hawaii. Ecology 76:721–733; 1995.

Trumbore, S.E. Comparison of carbon dynamics in tropical and temperate soil using radiocarbon measurements. Global Biogeochem. Cycl. 9:515–528; 1993.

Tsai, P.-T. *Strontium 90 Translocation in Undisturbed Soil Profiles.* M.S. thesis, University of Utah, Salt Lake City, UT; 1989.

Uebersax, A. *The Content and Stable Isotope Systematics of Carbon and Nitrogen in Soil Organic Matter from Elevation Transects in Hawaii (USA) and Mt. Kilimanjaro (Tanzania).* M.S. thesis, University of California, Berkeley, CA; 1996.

Vitousek, P.M.; Shearer, G.; Kohl, D.H. Foliar ^{15}N natural abundance in Hawaiian rainforest: Patterns and possible mechanisms. Oecologia 78:383–388; 1989.

Volobuev, V.R. *Ecology of Soils.* Jerusalem: Israel Program for Scientific Translations; 1964.

Vogt, K. Carbon budgets of temperate forest ecosystems. Tree Physiol. 9:69–86; 1991.

Wang, Y.; Amundson, R.; Trumbore, S.A. model for soil $^{14}CO_2$ and its implications for using ^{14}C to date pedogenic carbonate. Geochim. Cosmochim. Acta 58:393–399; 1994.

Wang, Y.; Cerling, T.E.; Effland, W.R. Stable isotope ratios of soil carbonate and soil organic matter as indicators of forest invasion of prairie near Ames, Iowa. Oecologia 95:365–369; 1993.

Wedin, D.A.; Tieszen, L.L.; Dewey, B.; Pastor, J. Carbon isotope dynamics during grass decomposition and soil organic matter formation. Ecology 76:1383–1392; 1995.

Wellman, R.P.; Cook, F.D.; Krouse, H.R. Nitrogen-15: Microbial alteration of abundance. Science 161:269–270; 1968.

9

Microbial Carbon Cycling in Pelagic Ecosystems: Microbial Methods for Ecosystem Scientists

Jonathan J. Cole

Introduction

In almost any ecosystem, microorganisms are responsible for most of the respiration and a large portion of the nutrient cycling. It is understandable, then, that ecologists working at the ecosystem scale would be naturally drawn to the study of microorganisms. The factors that regulate the abundance, distribution, growth rate, and respiration of these microorganisms are in large measure the factors that regulate some of the functioning of the ecosystem.

For a microbiologist interested in ecosystem processes, planktonic systems have some distinct advantages over most other environments as a focus for study. Planktonic bacteria are reasonably well dispersed, at least at the scale of milliliters to liters (see Duarte and Vaque 1992; Vaque and Pace 1992). The dilute nature of planktonic systems implies that bacteria will usually be found surrounded by water rather than attached to particles. And, although water chemistry does vary substantially among different types of aquatic ecosystems, most are dilute enough that techniques developed in one type are generally transferable to another without a great deal of modification. For these reasons process-level microbiology has progressed more rapidly in planktonic systems than in some others.

In this chapter, I discuss some of the techniques in use by microbiologists interested in carbon cycling in planktonic systems. While this restriction reduces the topic to the tractable, it also leaves out a great deal of new and exciting work on microbial diversity and genetics, microbial processes in other types of aquatic habitats (sediments, wetlands, groundwater) and microbial cycling of other elements. I focus on several aspects of microbial communities and processes: abundance and biomass, secondary production, respiration, growth efficiency, and use of specific substrates. I try to highlight new methodological developments that would be of use to ecosystem scientists.

To guide the discussion, I show two examples of the importance of bacteria to carbon (C) cycling in pelagic ecosystems in Figure 9.1. Bacteria draw on organic substrates from the pool of dissolved organic C (DOC). This DOC can originate from primary production within the system (autochthonous source) and from the input of organic C from outside of the system (allochthonous sources). When bacteria process this organic matter, they produce new bacterial biomass (bacterial secondary production) and they respire organic C to dissolved inorganic C (DIC). Figure 9.1A represents the pelagic region of the open ocean; Figure 9.1B represents an oligotrophic clearwater lake. Broadly similar patterns are seen in humic lakes (Hessen et al. 1990; Vezina and Pace 1994) and coastal waters as well (Vezina and Platt 1988). Planktonic bacterial respiration accounts for more than 30% of the total respiration of all heterotrophs and is of similar magnitude to the respiration of all zooplankton. Bacterial secondary production is coequal with that of zooplankton, and averages, among systems, about 20 to 30% of planktonic primary production (Cole et al. 1988; Simon et al. 1992) (Figure 9.2). This bacterial secondary production is an important food source to grazers, and can support the demands of protozoans and a sub-

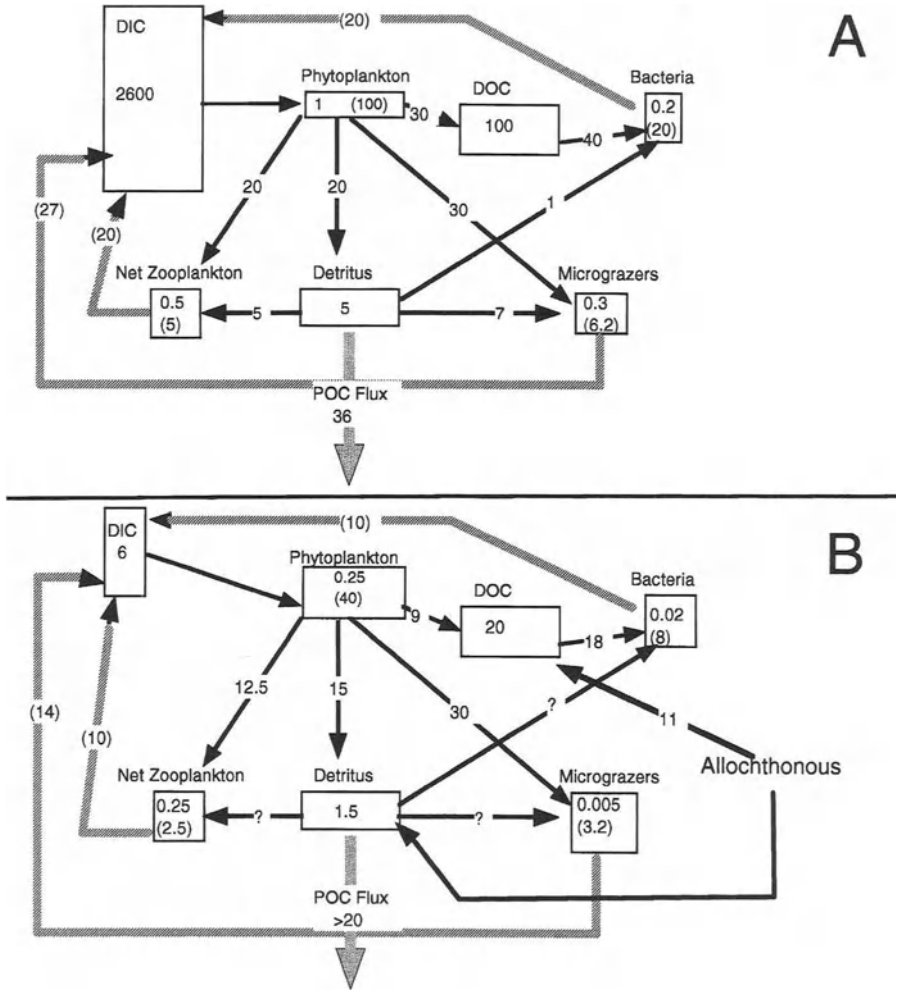

FIGURE 9.1. Carbon cycling in marine (A) and freshwater (B) pelagic environments showing the role of planktonic bacteria. Each box represents a pool; the magnitude (g C m^{-2}) is shown as the upper number in each box. For some boxes a rate of production (g C m^{-2} yr^{-1}) is also shown as a lower number and in parentheses. The arrows represent transfers between pools (g C m^{-2} yr^{-1}). Repriartion is shown as a transfer from an organic pool to the pool of dissolved inorganic C (DIC). Part A represents an open-water marine site with a mixed depth of about 100 m, and is modified from Peterson (1981) with data from Fasham et al. 1990 and Sarmiento et al. 1993. Part B represents and oligotrophic lake with an epilimnetic depth of 5 m, and is modified from Cole and Caraco (1993) and Cole et al. (1989). All numbers should be considered as approximate only.

stantial portion of the demands of zooplankton as well (see Fig. 9.1). Clearly, the abundance, biomass, production, and respiration of pelagic bacteria are key to understanding C cycling in pelagic environments.

Abundance and Biomass

Bacteria are the most abundant organisms in the plankton, and can be the most abundant particles in some systems. In oligotrophic systems, bacteria can

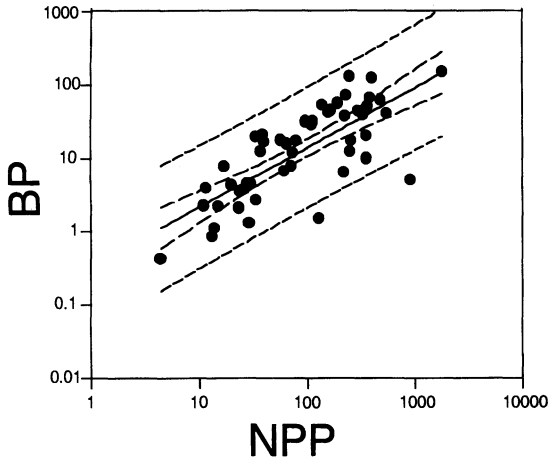

FIGURE 9.2. Bacterial secondary production versus phytoplankton primary production across a series of freshwater and marine systems. Each point represents the average of seasonal NPP and BP measurements in a different lake, estuary, or marine site. The equation for the regression is log (BP) = $-0.483 + 0.814 \times$ log (NPP); $r^2 = 0.6$; $n = 54$ systems; $p < 0.0001$. The Model II slope is 1.06. (Redrawn from the data of Cole et al. 1988.)

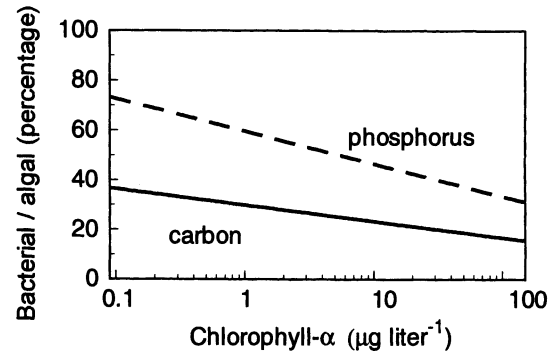

FIGURE 9.3. Modeled ratio of bacterial to algal carbon (solid line) and phosphorus (dashed line) along a gradient from ultraoligotrophic to hypereutrophic. The curves are derived from the relationships between bacterial abundance and chlorophyll-α (Bird and Kalff 1984); an assumed C/chlorophyll ratio (for phytoplankton) of 50:1; an assumed C/P for phytoplankton of 106:1. We further assumed a bacterial cell size of 0.12 μm; bacterial C content of 1.2×10^{-7} μg μm^{-3}; and a bacterial C/P ratio of 50:1. (Modified from Cole and Caraco 1993 and data therein.)

be the major reservoirs of some limiting elements, such as phosphorus (P) (Cho and Azam 1990; Cole and Caraco 1993) (Figure 9.3). Because bacterial abundance varies by several orders of magnitude across systems, it is often necessary to quantify it in a system of interest.

Epifluorescent Direct Count

Since the late 1970s, bacterial abundance has been measured by direct count using epifluorescent microscopy. Such procedures are designed to give the total direct count, that is the total number of intact bacterial cells in a sample. It was long ago realized that various culturing techniques greatly underestimated the total number of bacterial cells in natural waters (Hobbie et al. 1977). Thus, the total direct count, usually by epifluorescent microscopy, has been the standard way to enumerate bacteria for more than 20 years.

In these procedures, cells are stained with one of several types of fluorescent stains, filtered onto a 0.2-μm pore size filter and enumerated in known field sizes, typically at magnifications of 1000 to 1200 diameters using epifluorescent microscopy (Daley and Hobbie 1975). The type of filter used can greatly affect the outcome because some kinds of filters (those with a cellulose-acetate tortuous weave, such as Millipore-HA) have enough thickness that many cells are hidden from view (Hobbie et al. 1977). The use of polycarbonate filters (which have discrete, punctured holes and very little depth, e.g., Nuclepore or Poretics) yields significantly higher counts (Hobbie et al. 1977). Since the cells are viewed from above using the fluorescence of the stained bacteria, best results are achieved when the filters are stained black. A suitable black stain can be achieved using Irgalan Black (Hobbie et al. 1977) or by purchasing black filters from Poretics. An excellent, detailed protocol for sample preparation and staining is provided by Turley (1993).

The two stains in greatest use at present are acridine orange (AO; Hobbie et al. 1977) and 4′6-diamidino-2-phenylindole (DAPI) (Porter and Feig 1980). Both are nucleic acid fluorochromes but neither binds only to nucleic acids. In most samples, this nonspecific binding is a minor annoyance. In some samples, however, especially those from eutrophic waters, highly turbid waters or waters rich

in humic substances, nonspecific binding can cause a great deal of difficulty. Under the epifluorescent microscope, bacteria are recognized as stain-positive particles that resemble bacteria. Clearly, some experience and training are needed before a novice can count proficiently. Many researchers choose one or the other of the stains for different situations. Although agreement in counts is expected between DAPI and AO, the agreement is not always perfect. In a formal test, Suzuki et al. (1993) found that DAPI counts averaged about 70% of AO counts in the samples they tested. Where possible, we recommend checking representative samples with both stains and choosing the most effective. For a review of the use of fluorochromes for direct enumeration of planktonic bacteria, refer to Kepner and Pratt (1994).

While most counting is still done manually, the use of image-analysis systems to enhance or partially automate the procedure is gaining use but the equipment is costly (Sieracki et al. 1989; Psenner 1993).

The sources of variance and statistics of manual counting have been reviewed by Kirchman (1993) and Kirchman et al. (1982b). From a practical consideration of trying to optimize both effort and accuracy, Kirchman (1993) suggests taking two preserved samples, making one filtered preparation per sample, and counting about 10 microscopic fields per sample. The amount of sample (or field size) should be adjusted to yield about 30 cells per field. Less than this results in high variance among fields. With too many cells per field, the counter's eyes can become fatigued causing underestimation (Kirchman 1993).

Sample Preservation

Samples can be preserved at two stages. Investigators usually fix the initial, aqueous, samples upon collection with formalin (0.5 to 2% final concentration), glutaraldehyde (2.5% final concentration), or either of these fixatives with buffers. While these fixatives, with the samples stored cold (<5°C), are usually adequate to prevent further microbial growth, countable cells tend to decrease over time. Turley and Hughes (1992) observed a 39% decrease in AO counts over a 40-day period. Better preservation is achieved by making the complete slide preparation within 12 hours of sample collection and then storing the slide frozen (Turley 1993).

Count by Flow Cytometry

An exciting recent development has been the use of high-resolution flow cytometry to count bacterial samples. Cells are again stained with a nuclear fluorochrome but are counted directly in a flow cytometer. The cytometer can resolve event frequency, forward scatter, and fluorescence intensity of stained cells. Using these parameters it should be possible to obtain information on abundance, size distribution, and possibly activity (Button and Robertson 1993). Some of the initial difficulties with the cytometric approach were that different groups of bacteria stained differently with DAPI due to differences in adenine + thymine/guanine + cytosine (AT/GC) ratios. Further, because of the lack of suitable standards, it has proven difficult both to get size information and to know if the smaller cells were being counted with high efficiency (Button and Robertson 1993). Some of these problems have been overcome by using a different nuclear stain (SYTO 13) (del Giorgio et al. 1996b). In a calibration study using samples from 18 Canadian lakes, del Giorgio et al. (1996b) obtained excellent agreement between cytometer cell counts and those done by traditional epifluorescent microscopy. The obvious advantages of the cytometer are speed and precision. In the same data set, the mean coefficient of variation for epifluorescent counts was 14.5%, while for the flow cytometer it was 2.5%. Bacterial cell size may in theory be obtained from forward light scatter (Robertson and Button 1989), although planktonic bacteria are often close to the limits of resolution of most instruments (Davey and Kell 1996). In addition to total abundance and cell size, it is also possible to obtain data on the amount of DNA per cell and other cellular structural and physiological characteristics (Davey and Kell 1996; Wallner et al. 1997; see also below).

Active and Inactive Cells

Total direct counts of bacteria vary reasonably, predictably among environments, from $<5 \times 10^6$ to approximately 5×10^8 cells per liter. This variance tends to track trophic richness and is reasonably well correlated with the biomass of phytoplankton

(Bird and Kalff 1984; Cole et al. 1988; Simon et al. 1992) or nutrients (Currie 1990). Despite these relationships, total direct counts include populations of both active and inactive cells. Bacterial assemblages in natural aquatic systems are composed of cells in a wide range of physiological conditions, and the techniques used for total counts provide no information on the physiological condition of individual bacterial cells. There is now widespread consensus that traditional culture techniques greatly underestimate the number of metabolically active and viable cells (Roszak and Colwell 1997), so a number of alternative approaches, some relatively new, have been used to try to distinguish between populations of highly active and dormant or inactive bacteria (reviewed by McFeters et al. 1995). Briefly, these approaches include the use of:

1. microautoradiography, in which the uptake of radiolabeled compounds by single cells can be detected (Karner and Fuhrman 1997);
2. fluorogenic compounds that can diffuse through bacterial cell walls and membranes only when the integrity of the membranes has been compromised (Jepras et al. 1995);
3. universal 16s rRNA-targeted oligonucleotide probes to identify bacterial cells that contain sufficient ribosomal ribonucleic acid (rRNA) to be potentially metabolically active (Karner and Fuhrman 1997);
4. a destaining method developed by Zweifel and Hagstrom (1995) for specifically staining with DAPI only the nucleoid region of in situ bacterial cells. This eliminates nonspecific DAPI staining of other cellular components. Zweifel and Hagstrom suggested that only those cells with identifiably stained nucleoid regions should be considered to be alive. The nonnucleoid cells (called "ghosts") are presumably inactive since they contain either no or little deoxyribonucleic acid (DNA). Choi et al. (1996), working in coastal waters off Oregon, confirmed the finding that a large portion of the AO or DAPI countable cells did not have visible nucleoids. However, under conditions that stimulated cell growth, cells with visible nucleoids became nearly 100% of the population. The work of Choi et al. (1996) suggests that the ghost cells are capable of becoming active cells; and
5. stains that change upon reduction by intercepting energy along the biological electron transport system (ETS). Among the various stains used for this, tetrazolium salts have received the most attention. The tetrazolium salt, 5-cyano-2,3,-ditolyl tetrazolium chloride (CTC), becomes fluorescent upon reduction by the ETS system and can be visualized using epifluorescence microscopy (Rodriguez et al. 1992; Gasol et al. 1996; Smith 1998) and by flow cytometry (del Giorgio et al. 1997b). The newer work suggests that only a fraction of the total bacterial cells are active and that this fraction varies from $<5\%$ in ultraoligotrophic regions to $>50\%$ in very productive waters (del Giorgio and Scarborough 1995).

Most of these techniques can be coupled to flow cytometry (Davey and Kell 1996), and this effectively increases the sensitivity, speed, and precision of most determinations. In addition, subpopulations characterized by their level of activity or genetic composition can be physically sorted and used for further molecular or metabolic assays (Wallner et al. 1997).

Cell Size and Biomass

For ecosystem scientists, biomass, rather than numbers per se, is usually of more significant interest. The standard way to obtain the biomass of planktonic bacteria is to multiply the abundance by the cell volume. Cell volume is most often determined by direct measurement of size and shape either under the microscope itself or from photographic images of the microscopic preparation (Psenner 1993). One then has to adopt a model relating linear dimensions to volume. The most common of these is:

$$V = (\pi/4)W^2(L - W/3) \qquad (9.1)$$

where V is volume, L is length, and W is width. This model assumes all cells to be straight rods, but it works equally well for spherical cocci (Bratbak 1993). The various advantages of using epifluorescent microscopy or scanning or transmission electron microscopy have been reviewed by Bratbak (1993).

The estimation of cell biomass from cell volume is not straightforward. Cell volumes vary over three orders of magnitude, and biomass and volume appear to be related (Norland 1993). Many research-

ers routinely assume that there is a constant ratio between measured cell volume and biomass (Watson et al. 1977), or assume that all bacteria have the same C content per cell (20 fg cell^{-1}). There is some experimental support for both of these extremely opposite approaches. However, most researchers now assume that there is a power function relating biomass (m) to volume (V):

$$m = CV^a \quad (9.2)$$

where C is the conversion factor (pg C μg^{-3}) between biomass and volume, and a is the scaling factor. Simon and Azam (1989) suggest a scaling factor of 0.6, and that $C = 0.09V^{0.6}$.

Growth and Respiration of Planktonic Bacteria

Bacterial metabolism is important to two different aspects of the C cycle (see Fig. 9.1). Bacterial respiration converts organic C into inorganic C. The growth of bacterial cells (bacterial production) converts DOC into new bacterial biomass. Bacteria are the only organisms that use DOC to a significant degree, but many higher organisms can consume bacteria (Pace et al. 1990; Cole 1982; Azam et al. 1983; Sherr and Sherr 1996). Thus, the conversion of DOC into bacterial biomass represents a potential recovery of organic C that is lost to the rest of the food web (Paerl 1978).

Bacterial production (BP) is secondary production and is theoretically unconstrained by the inputs of organic C to the system from primary production or other sources (Strayer 1988; Scavia 1988; Jahnke and Craven 1995). Bacterial respiration, on the other hand, cannot exceed the inputs of organic C from primary production plus allochthonous sources (Cole and Pace 1995; Cole et al. 1989).

Bacterial Secondary Production

Bacterial production is most often measured with one of two techniques, both using radioactive tracers. By measuring the incorporation of ^{3}H-thymidine into bacterial DNA, or by measuring the incorporation of ^{3}H-leucine into bacterial protein, one can estimate BP. The details for both methods are available in user-friendly literature (Bell 1993; Kirchman 1993) and there has been considerable critical review of the thymidine method in particular (Robarts and Zohary 1993). Both methods depend on the fact that other organisms in the sample take up little or none of the label at the concentrations added, and that bacteria will take these up. Both methods use relatively short (<1 hour) incubations under ambient conditions to avoid container effects. There are a number of steps and potential pitfalls in getting actual estimates of BP from these measurements. The substrate needs to be added at a level that saturates the uptake kinetics. On the other hand, if the substrate is added at too high a level one can stimulate catabolic processes. Thus, the rate of uptake needs to be measured as a function of added substrate to determine the correct amount to be added. Unlabeled substrate present in the water or synthesized by the microbe during the incubation can dilute the specific activity of the added substrate. This isotope dilution can also be dealt with kinetically by adding a constant amount of labeled substrate while varying the amount of unlabeled substrate (Pollard and Moariaty 1984; Simon and Azam 1989). Finally, once the absolute rate of either thymidine or leucine uptake has been established, it needs to be related to cell growth with a series of conversion factors. For thymidine, we need to relate thymidine uptake to DNA synthesis, DNA synthesis to the number of cells produced, and C content per cell to express growth rate in units of C. For leucine, we need to relate leucine uptake to protein synthesis, and protein synthesis to C. (BP is expressed usually as μg C liter^{-1} hr^{-1} or cells liter^{-1} hr^{-1}). These conversion factors can be measured directly, based on theoretical values, or can be side-stepped by using empirical factors based on regrowth studies in dilution cultures (Kirchman et al. 1982a).

In their original forms, for both methods, the labeled bacteria were concentrated initially by filtration. In either method, there can be some nonspecific labeling. That is, some of the ^{3}H from the added thymidine can be incorporated into molecules other than DNA. Similarly, some of the ^{3}H from leucine can be incorporated into molecules other than protein. The nontarget molecules are therefore washed away by a series of extractions, and numerous protocols have been developed, especially for the thymidine method (Robarts and Zohary 1993 and references therein).

For leucine uptake, at least, it is possible to do the incubation in microcentrifuge tubes and to use centrifugation to concentrate the cells (Smith and Azam 1993). The extractions (done in this case with 5% trichloroacetic acid) occur in the centrifuge tube. Best of all, scintillation fluid can be added directly to the same centrifuge tube which is then dropped into a dry scintillation vial for the radioactive counting. This modification is faster, less expensive, and gives lower variance than earlier methods.

Bacterial Respiration

In soils, bacterial respiration (BR) is more commonly measured than BP is. In planktonic systems, it is actually difficult to measure BR and it is much less commonly measured than is BP. In order to get measurable changes in dissolved oxygen (DO) or in DIC, the incubation has to be much longer than that for BP. In oligotrophic waters, the incubation may have to be 24 hours or more to provide measurable oxygen changes. Further, the total community respiration in a water sample consists of the respiration of bacteria and other organisms, especially phytoplankton. Typically, differential filtration is used to separate bacteria from these larger organisms. This physical separation also removes bacteria from one possible substrate (new phytoplankton growth) and from most grazers. Many researchers estimate BR from literature values of bacterial growth efficiency (BGE), which have been measured by a variety of different approaches.

$$\text{BGE} = \text{BP}/(\text{BP} + \text{BR}) * 100\% \quad (9.3)$$

since the term BP + BR is the assimilation of substrate, BGE is analogous to assimilation efficiency for higher organisms.

The various approaches for measuring BGE include:

1. measuring the appearance of a representative ^{14}C-labeled substrate (glucose, acetate, labeled phytoplankton exudates) into bacterial biomass and into DIC or ^{3}H substrates into biomass and water;
2. measuring the disappearance of ambient DOC (which equals BP + BR) and the simultaneous increase in bacterial biomass (which equals BP); and
3. measuring BP (by thymidine or leucine uptake) and simultaneous consumption of DO or production of DIC.

Unfortunately, values of BGE show a large range in the literature (table from Jahnke and Craven 1995; Cole and Pace 1995; Roland and Cole in press). Thus the practice of estimating BR from an assumed value of BGE is subject to large uncertainty. Interest in directly measuring BR or BGE is growing and advances in the near future are likely (del Giorgio and Cole 1998).

Uptake and Turnover of Specific Substrates

The modern age of aquatic microbiology was ushered in during the mid-1960s when researchers began adding small amounts of radioactive organic compounds to water samples and examining the uptake (Wright and Hobbie 1966; Wetzel 1967) and respiration (Hobbie et al. 1969) of these. The original goal of this research was largely to see how active bacteria were in various environments (Hobbie et al. 1969; Hobbie and Rublee 1977) and how fast specific substrates were being turned over. These approaches demonstrated early on that many simple sugars and amino acids were being turned over by microbes on a time scale of minutes to hours. A major disappointment of these early measurements of heterotrophic potential was that they did not provide a measure of total BP. Thus, we could measure the turnover time and V_{max} for glucose (or any other labeled substrate) but we had no way of knowing the total array and quantity of substrates in use by the bacterial community. The glucose V_{max} was used as an index of bacterial heterotrophic potential (Hobbie and Rublee 1977; Wetzel 1967).

Substrates Supporting Bacterial Growth

The thymidine and leucine methods (above) provided a means by which total BP could be approached, albeit with some uncertainty. With an estimate of total BP, the use of specific substrates or suites of compounds takes on a new interest. We can now begin to ask what fraction of BP is supported by what kind of molecule. In this approach one adds a tracer amount of a labeled substrate. One

then measures the uptake and/or respiration of the labeled compound along with a chemical or kinetic measurement of the total pool size of that molecule. The fraction utilized per unit time (obtained from the tracer addition) is multiplied by the pool size for the total rate of utilization of that substrate.

This approach has revealed that relatively large fractions of total BP can often be supported by a few classes of molecules. For example, by measuring both BP and the kinetics of the uptake of dissolved free amino acids (DFAA) Kirchman et al. (1993) found that about 20% of total BP was supported by DFAA during the spring bloom in the Eastern North Atlantic (Kirchman et al. 1993). Using a similar approach, Rich et al. (1996) found that although dissolved neutral monosaccharides (DNMS) were in low concentration in the equatorial pacific, the uptake of glucose alone supported 15 to 47% of BP. In interpreting this work one has to keep in mind that what is measured is the proximate substrate and not its ultimate source. It is still interesting to learn where the DFAA or DNMS comes from. Further, it is intriguing to consider the type of molecule supporting the remaining, large fraction of BP not explained by the known simple substrates.

In both marine and freshwaters, much of the DOC is in large, high-molecular weight polymers. Further, particulate organic carbon (POC) can be the ultimate source of the small molecules in turbid systems and in sediments. Bacteria generally cleave very large molecules into simple compounds using extracellular enzymes. An approach to examining the array of complex substrates that support bacterial production has been to examine the suites of these exoenzymes present in different environments. The idea is to choose broad classes of enzymatic processes of interest and assay for these using model substrates that release either a colored or fluorescent endproduct or intermediate (see Sinsabaugh et al. 1997). This approach has also been used with some success in marine planktonic aggregates (marine snow, Karner and Herndl 1992), freshwater lakes (Chrost et al. 1989), and estuarine systems (Hoppe 1993). Recently, Karner and Rassoulzadegan (1995) examined α- and β-glucosidase and aminopeptidase activity in the Mediterranean Sea and found striking variations in the amounts and proportions of these enzymes at time scales from the diel to the seasonal. This study suggests the need to examine enzymatic responses on several time scales before strong conclusions about patterns can be drawn.

From an ecosystem perspective, one of the most intriguing applications of the exoenzyme approach has been done in river and streams using techniques that had been developed largely for working in sediments (Sinsabaugh et al. 1997; Findlay et al. 1998). Sinsabaugh et al. (1997) recently began looking at enzyme activity in the water column. In this approach, unfiltered water is challenged with a series of model substrates at a range of concentrations. The model substrates contain 4-methylumbelliferyl (MUF) attached to a substrate of interest. To measure fatty acid esterase, for example, the model substrate is MUF-acetate; to measure β-*N*-acetylglucosaminidase the model substrate is MUF-*N*-acetyl-β-glucosaminide. The enzyme cleaves the MUF, which becomes fluorescent. The fluorescence is proportional to MUF concentration. Relative new technology has made this type of assay rapid and many samples can be processed. The reactions are performed in multi-well microliter plates and fluorescence is read in a microfluor platereader. This degree of automation allows one to investigate enzyme kinetics over a range of concentrations and obtain both K_m and V_{max} values for each assay. This approach has recently been applied a range of coastal ecosystems in which the activities of eight different enzymes were assayed in five ecosystems (Hopkinson et al. in press). The multivariate data were then subjected to principal components analysis with interesting results (Fig. 9.4). Two of the eight principal components accounted for 62% of the total variability. Plotted on the space defined by these two, all of the ecosystems separated, indicating that substrate use was quite different among them. Samples near the upper right (e.g., Columbia River) would have higher standing stock of substrates that can be degraded by peptidases and esterases. Samples near the origin (e.g., Satilla River) are enriched in xylosidases and glucosaminidase. The implication is that the bacteria in the Satilla River are more dependent on complex plant polysaccharides and amino sugars while those in the Columbia are more dependent on proteins and fatty acids. Coupled with other descriptions about bacterial production, activity, and substrate composition, these enzyme tech-

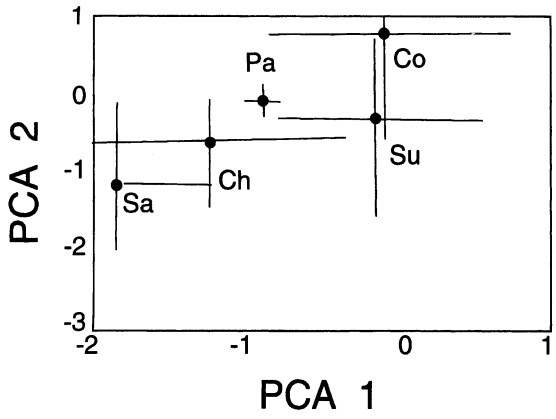

FIGURE 9.4. Results of a principle components analysis (CPA) of extracellular enzyme activity for the water column bacteria in a series of riverine and estuarine sites. Sites include the Child's River (Ch; Massachusetts); the Columbia River (Co); the Susquehanna River (Su); the Parker River (Pa, Massachusetts); and the Satilla River (Sa; Georgia). The principal component scores and their standard deviations in both dimensions are plotted. (Data are redrawn from Hopkinson et al. (1998) and data on the rivers and methods used can be found there.)

niques may offer a powerful way to examine how different ecosystems process complex molecules.

Conclusions

While it is clear that C cycling in pelagic ecosystems is often dominated by bacterial processes a number of intriguing unresolved questions remain. First, we have no widely accepted unifying theory of bacterial production or respiration, although there have been some noble attempts (Thingstad and Lignell 1997; Valino et al. 1997). That is, we can crudely predict these processes across environments but we do not have a simple, physiologically based model for either BP or BR (Valino et al. 1997). Phytoplankton primary production, in contrast, is much better understood from a theoretical and physiological perspective than is bacterial production (Pace and Cole 1994). Second, there is usually a very large pool of DOC relative to instantaneous bacterial demand (see Fig. 9.1). In soils, where there is also a large organic C pool, moisture clearly limits microbial activity in most environments. What, then, limits BP and BR in aquatic systems? While a number of studies show significant stimulation of BP by adding inorganic nutrients (Elser et al. 1995; Waiser and Robarts 1995; Pace and Funke 1991; Toolan et al. 1991) many others show stimulation of BP by the addition of labile C sources (Coveney et al. 1995; Wetzel et al. 1995). We know less about planktonic BR. Are bacteria nutrient-limited and competing with phytoplankton for inorganic nitrogen and phosphorus (see Currie 1990)? Does the addition of labile C sources (e.g., from new phytoplankton production) allow bacteria to co-metabolize the more refractory allochthonous sources? Further, in many environments, BR appears to exceed the input of C from autotrophic primary production (del Giorgio et al. 1997a). This heterotrophy in excess of primary production ("net heterotrophy") (Cole et al. 1994; Howarth et al. 1996) implies that allochthonous substrates are being used by bacteria. On the other hand, several broad comparative studies have shown that BP varies systematically with primary production among diverse environments (Cole et al. 1988; White et al. 1991). If allochthonous inputs are important to bacterial production and respiration, why do these processes co-vary with the primary production (Caraco et al. 1992)? Bacteria are capable of metabolizing a large amount of DOC. At a middling value of BP of 10 μg C liter^{-1} day^{-1} and a growth efficiency of 30%, bacteria utilize (BP + BR) about 12 mg C liter^{-1} yr^{-1}. Typical values for DOC in freshwaters are between 1 and 10 mg C liter^{-1}. With a water residence time on the order of 1 year (a good value for many lakes), bacteria should turn over the entire DOC pool once or more each year. In what ways, then, do aquatic bacteria modify the amount or composition of DOC, and what consequences might these modifications have for the ecosystem? We tended to look at bacterial processes in response to alterations in eutrophication (Hobbie and Cole 1984): primary production (White et al. 1991; Cole et al. 1988), grazing pressure from protozoa and zooplankton (Porter et al. 1985; Sanders et al. 1992), and top-down changes in food web structure (del Giorgio et al. 1996a; Vaque and Pace 1992). What are the important feedbacks by which the microbial food web regulates or influences other components of the ecosystem?

References

Azam, F.; Fenchel, T.; Field, J.G.; Gray, J.S.; Meyer-Reil, L.A.; Thingstad, F. The ecological role of water-column microbes in the sea. Mar. Ecol. Prog. Ser. 10:257–263; 1983.

Bell, R.T. Estimating production of heterotophic bacterioplankton via incorporation of tritiated thymidine. In: Kemp, P.F.; Sherr, B.F.; Sherr, E.B.; Cole, J.J., eds. *Handbook of Methods in Aquatic Microbial Ecology.* Ann Arbor, MI: Lewis; 1993:495–504.

Bird, D.F.; Kalff, J. Empirical relationships between bacterial abundance and chlorophyll concentration in fresh and marine waters. Can. J. Fish. Aquat. Sci. 41:1015–1023; 1984.

Bratbak, G. Microscope methods for measuring bacterial biovolume: Epiflourescence microscopy, scanning electron microscopy and transmission electron microscopy. In: Kemp, P.F.; Sherr, B.F.; Sherr, E.B.; Cole, J.J., eds. *Handbook of Methods in Aquatic Microbial Ecology.* Ann Arbor, MI: Lewis; 1993:309–318.

Button, D.K.; Robertson, B.R. Use of high resolution flow cytometry to determine the activity and distribution of aquatic bacteria. In: Kemp, P.F.; Sherr, B.F.; Sherr, E.B.; Cole, J.J., eds. *Handbook of Methods in Aquatic Microbial Ecology.* Ann Arbor, MI: Lewis; 1993:163–174.

Caraco, N.F.; Cole, J.J.; Likens, G.E. New and recycled primary production in an oligotrophic lake: Insights for summer phosphorus dynamics. Limnol. Oceanogr. 37:590–602; 1992.

Cho, B.C.; Azam, F. Biogeochemical significance of bacterial biomass in the ocean's euphotic zone. Mar. Ecol. Prog. Ser. 63:253–259; 1990.

Choi, J.W.; Sherr, E.B.; Sherr, B.F. Relation between presence-absence of a visible nucleoid and metabolic activity in bacterioplankton cells. Limnol. Oceanogr. 41:1161–1168; 1996.

Chrost, R.J.; Munster, U.; Rai, H.; Albrect, D.; Witzel, K. Overbeek, J. Photosynthetic production and exoenzymatic degradation of organic matter in the euphotic zone of a eutrophic lake. J. Plank. Res. 11:223–242; 1989.

Cole, J.J. Interactions between bacteria and algae in aquatic ecosystems. Annu. Rev. Ecol. Syst. 13:291–314; 1982.

Cole, J.J.; Caraco, N.F. The pelagic microbial food webs of oligotrophic lakes. In: Ford, T., ed. *Aquatic Microbiology.* New York: Blackwell; 1993:101–112.

Cole, J.J.; Caraco, N.F.; Kling, G.W.; Kratz, T.K. Carbon dioxide supersaturation in the surface waters of lakes. Science 265:1568–1570; 1994.

Cole, J.J.; Caraco, N.F.; Strayer, D.L.; Ochs, C.; Nolan, S. A detailed organic carbon budget as an ecosystem-level calibration of bacterial respiration in an oligotrophic lake during midsummer. Limnol. Oceanogr. 34:286–296; 1989.

Cole, J.J.; Findlay, S.; Pace, M.L. Bacterial production in fresh and saltwater ecosystems: A cross-system overview. Mar. Ecol. Prog. Ser. 43:1–10; 1988.

Cole, J.J.; Pace, M.L. Bacterial secondary production in oxic and anoxic freshwaters. Limnol. Oceanogr. 40:1019–1027; 1995.

Coveney, M.F.; Wetzel, R.G. Biomass, production and specific growth rate of bacterioplankton and coupling to phytoplankton in an oligotrophic lake. Limnol. Oceanogr. 40:1187–1200; 1995.

Currie, D.J. Large-scale variability and interactions among phtyoplankton, bacterioplankton and phosphorus. Limnol. Oceanogr. 35:1437–1455; 1990.

Daley, R.J.; Hobbie, J.E. Direct counts of aquatic bacteria by a modified epifluorescence technique. Limnol. Oceanogr. 20:875–886; 1975.

Davey, M.M.; Kell, D.B. Flow cytometry and cell sorting of heterogeneous microbial populations: The importance of single-cell analyses. Microbiol. Rev. 60:641–696; 1996.

del Giorgio, P.A.; Bird, D.; Prairie, Y.T.; Planas, D. Flow cytometric determinations of bacterial abundance in lake plankton with the green nucleic acid stain SYTO 13. Limnol. Oceanogr. 41:783–789; 1996a.

del Giorgio, P.A.; Cole, J.J. Bacterial growth efficiency in natural aquatic ecosystems. Annu. Rev. Ecol. Syst. 29:503–541; 1998.

del Giorgio, P.A.; Cole, J.J.; Cimbleris, A. Respiration rates in bacteria exceed phytoplankton production in unproductive aquatic systems. Nature 385:148–151; 1997a.

del Giorgio, P.A.; Gasol, J.M.; Vaque, D.; Mura, P.; Agusti, S.; Duarte, C.M. Bacterioplankton community structure: Protists control net production and the proportion of active bacteria in a coastal marine community. Limnol. Oceanogr. 41:1169–1179; 1996b.

del Giorgio, P.A.; Prairie, Y.T.; Bird, D.F. Coupling between rates of bacterial production and the abundance of metabolically active bacteria in lakes, enumerated using CTC reduction and flow cytometry. Microb. Ecol. 34:144–154; 1997b.

del Giorgio, P.A.; Scarborough, G. Increases in the proportion of metabolically active bacteria along gradients of enrichment in freshwater and marine plankton: Implications for estimates of bacterial growth and production rates. J. Plank. Res. 17:1905–1924; 1995.

Duarte, C.M.; Vaque, D. The scale dependence of bacterial patchiness. Mar. Ecol. Prog. Ser. 84:95–100; 1992.

Elser, J.J.; Stabler, L.B.; Hassett, R.P. Nutrient limitation of bacterial growth and rates of bacterivory in lakes

and oceans: A comparative study. Aquat. Microb. Ecol. 9:105–110; 1995.

Fasham, J.R.; Ducklow, H.W.; McKelvie, S.M. A nitrogen-based model of plankton dynamics in the oceanic mixed layer. J. Mar. Res. 48:591–639; 1990.

Findlay, S.F.; Hickey, C.W.; Quinn, J.M. Microbial enzymatic response to catchment-scale variations in supply of dissolved organic carbon. N.Z. J. Mar. Freshwat. Res. 32:701–706; 1998.

Gasol, J.M.; del Giorgio, P.A.; Massana, R.; Duarte, C.M. Active versus unactive bacteria: Size-dependence in a coastal marine plankton community. Mar. Ecol. Progr. Ser. 128:91–97; 1996.

Hessen, D.O.; Anderson, T.; Lyche, A. Carbon metabolism in a humic lake: Pool sizes and cycling through zooplankton. Limnol. Oceanogr. 35:84–99; 1990.

Hobbie, J.E.; Cole, J.J. Response of a detrital food web to eutrophication. Bull. Mar. Sci. 35:357–363; 1984.

Hobbie, J.E.; Crawford, C.C.; Webb, K.L. Amino acid flux in an estuary. Science 159:1463–1464; 1969.

Hobbie, J.E.; Daley, R.J.; Jasper, S. Use of nuclepore filters for counting bacteria by fluorescence microscopy. Appl. Environ. Microbiol. 22:1225–1228; 1977.

Hobbie, J.E.; Rublee, P. Radioisotope studies of heterotrophic bacteria in aquatic ecosystems. In: Cairns, J., ed. *Aquatic Microbial Communities.* New York: Garyland Publishing; 1977:441–476.

Hopkinson, C.; Buffam, I.; Hobbie, J.; Valino, J.; Perdue, M.; Eversmeyer, B.; Prahl, F.; Covert, J.; Hodson, R.; Moran, M.A.; Smith, E.; Baross, J.; Crump, B.; Findlay, S.; Foreman, K. Terrestrial inputs of organic matter to coastal ecosystems: An intercomparison of chemical characteristics and bioavailability. Biogeochemistry 43(3):211–234; 1998.

Hoppe, H. Use of flourogenic model substrates for extracellular enzyme activity (EEA) measurement of bacteria. In: Kemp, P.F.; Sherr, B.F.; Sherr, E.B.; Cole, J.J., eds. *Handbook of Methods in Aquatic Microbial Ecology.* Ann Arbor, MI: Lewis; 1993:423–432.

Howarth, R.W.; Schneider, R.; Swaney, D. Metabolism and organic carbon fluxes in the tidal freshwater Hudson River. Estuaries 19:848–865; 1996.

Jahnke, R.A.; Craven, D.B. Quantifying the role of heterotrophic bacteria in the carbon cycle: A need for respiration rate measurements. Limnol. Oceanogr. 40:436–441; 1995.

Jepras, R.I.; Pearson, S.C.; Paul, F.E.; Wilkinson, M.J. Development of a robust flow cytometric assay for determining numbers of viable bacteria. Appl. Environ. Microbiol. 61:2696–2701; 1995.

Karner, M.; Fuhrman, J.A. Determination of active marine bacterioplankton: A comparison of universal 16s rRNA probes, autoradiography, and nucleoid staining. Appl. Environ. Microbiol. 63:1208–1213; 1997.

Karner, M.; Herndl, G.J. Extracellular enzymatic activity and secondary production in free-living and marine-snow-associated bacteria. Mar. Biol. 113:341–347; 1992.

Karner, M.; Rassoulzadegan, F.R. Extracellular enzyme activity: Indications for high short term variability in a coastal marine ecosystem. Microb. Ecol. 30:143–156; 1995.

Kepner, R.L., Jr.; Pratt, J.R. Use of fluorochromes for direct enumeration of total bacteria in environmental samples: past and present. Microb. Rev. 58:615; 1994.

Kirchman, D.L. Leucine incorporation as a measure of biomass production by heterotrophic bacteria. In: Kemp, P.F.; Sherr, B.F.; Sherr, E.B.; Cole, J.J., eds. *Handbook of Methods in Aquatic Microbial Ecology.* Ann Arbor, MI: Lewis; 1993:509–512.

Kirchman, D.L.; Ducklow, H.; Mitchell, R. Estimates of bacterial growth from changes in uptake rates and biomass. Appl. Environ. Microbiol. 44:1296–1307; 1982a.

Kirchman, D.L.; Sigda, J.; Kapuscinski, R.; Mitchell, R. Statistical analysis of the direct count method for enumerating bacteria. Appl. Environ. Microbiol. 43:781; 1982b.

McFeters, G.A.; Yu, F.P.; Pyle, H.; Stewart, P.S. Physiological assessment of bacteria using fluorochromes. J. Microbiol. Methods 21:1–13; 1995.

Norland, S. The relationship between biomass and volume of bacteria. In: Kemp, P.F.; Sherr, B.F.; Sherr, E.B.; Cole, J.J., eds. *Handbook of Methods in Aquatic Microbial Ecology.* Ann Arbor, MI: Lewis; 1993:303–308.

Pace, M.L.; Cole, J.J. Comparative and experimental approaches to top-down and bottom-up regulation of bacteria. Microb. Ecol. 28:181–193; 1994.

Pace, M.L.; Funke, E. Regulation of planktonic microbial communities by nutrients and herbivores. Ecol. 72:904–914; 1991.

Pace, M.L.; McManus, G.B.; Findlay, S.E.G. Planktonic community structure determines the fate of bacterial production in a temperate lake. Limnol. Oceanogr. 35:795–808; 1990.

Paerl, H. Microbial organic carbon recovery in aquatic ecosystems. Limnol. Oceanogr. 23:927–935; 1978.

Peterson, B.J. Synthesis of carbon stocks and flows in the open ocean mixed layer. In: Hobbie, J.E.; Williams, P.J.; Ie, B., eds. *Heterotrophic activity in the Sea.* New York: Plenum; 1981:547–554.

Pollard, P.C.; Moriarty, D.J.W. Validity of the tritiated thymidine method for estimating bacterial growth rates: Measurement of isotope dilution during DNA synthesis. Appl. Environ. Microbiol. 48:1076–1083; 1984.

Porter, K.G.; Feig, Y.S. The use of DAPI for identifying and counting the microflora. Limnol. Oceanogr. 25:943–948; 1980.

Porter, K.G.; Sherr, E.B.; Sherr, B.F.; Pace, M.; Sanders, R.W. Protozoa in planktonic food webs. J. Protozool. 32:409–415; 1985.

Psenner, R. Determination of size and morphology of aquatic bacteria by automated image analysis. In: Kemp, P.F.; Sherr, B.F.; Sherr, E.B.; Cole, J.J., eds. *Handbook of Methods in Aquatic Microbial Ecology.* Ann Arbor, MI: Lewis; 1993:339–345.

Rich, J.H.; Ducklow, H.; Kirchman, D.L. Concentrations and uptake of neutral monosaccharides along 140° W in the equatorial Pacific: Contribution of glucose to heterotrophic bacterial activity and the DOM flux. Limnol. Oceanogr. 41:595–604; 1996.

Robarts, R.D.; Zohary, T. Fact or fiction—Bacterial growth rates and production as determined by [methyl ^{3}H]-thymidine? Adv. Microb. Ecol. 13:371–425; 1993.

Robertson, B.R.; Button, D.K. Characterizing aquatic bacteria according to population, cell size, and apparent DNA content by flow cytometry. Cytometry 10:70–76; 1989.

Rodriguez, G.G.; Phipps, D.; Ishiguro, K.; Ridgeway, H.F. Use of a fluorescent redox probe for direct visualization of actively respiring bacteria. Appl. Environ. Microbiol. 58:1801–1808; 1992.

Roland, F; Cole J.J. Regulation of bacterial growth efficiency in a large turbid estuary. Aquat. Microb. Ecol. 20:31–38; 1999.

Roszak, D.B.; Colwell, R. Survival strategies of bacteria in the natural environment. Microbiol. Rev. 51:365–379; 1997.

Sanders, R.W.; Caron, D.A.; Berninger, U.-G. Relationships between bacteria and heterotrophic nanoplankton in marine and freshwaters: An inter-ecosystem comparison. Mar. Ecol. Prog. Ser. 86:1–14; 1992.

Sarmiento, J.L.; Slater, R.D.; Fasham, J.R.; Ducklow, H.W.; Toggweiler, J.R.; Evans, G.T. A seasonal three-dimensional ecosystem model of nitrogen cycling in the north Atlantic euphotic zone. Global Biogeochem. Cycl. 7:417–450; 1993.

Scavia, D. On the role of bacteria in secondary production. Limnol. Oceanogr. 33:1220–1224; 1988.

Sherr, E.B.; Sherr, B.F. Temporal offset in oceanic production and respiration implied by seasonal changes in atmospheric oxygen: the role of heterotrophic microbes. Aquat. Microb. Ecol. 11:91–100; 1996.

Sieracki, M.E.; Johnson, P.W.; Webb, K.L. Detection, enumeration and sizing of planktonic bacteria by image-analyzed epiflourescence microscopy. Appl. Environ. Microbiol. 49:799–814; 1989.

Simon, M.; Azam, F. Protein content and protein synthesis rates of planktonic marine bacteria. Mar. Ecol. Prog. Ser. 51:201–213; 1989.

Simon, M.; Cho, B.C.; Azam, F. Significance of bacterial biomass in lakes and the ocean: Comparison to phytoplankton biomass and biogeochemical implications. Mar. Ecol. Prog. Ser. 86:103–110; 1992.

Sinsabaugh, R.L.; Findlay, S.; Franchini, P.; Fischer, D. Enzymatic analysis of riverine bacterioplankton production. Limnol. Oceanogr. 42:29–38; 1997.

Smith, D.C.; Azam, F. A simple economical method for measuring bacterial protein synthesis rates in seawater using tritiated leucine. Mar. Microb. Food Webs 6:107–114; 1993.

Smith, E.M. Coherence of microbial respiration rate and cell-specific bacterial activity in a coastal planktonic community. Aquat. Microb. Ecol. 16:27–35; 1998.

Strayer, D.L. On the limits to secondary production. Limnol. Oceanogr. 33:1217–1220; 1988.

Suzuki, M.; Sherr, E.B.; Sherr, B.F. DAPI direct counting underestimates bacterial abundance and average cell size compared to AO direct count. Limnol. Oceanogr. 38:1566–1569; 1993.

Thingstad, T.F.; Lignell, R. Theoretical models for the control of bacterial growth rate, abundance, diversity and carbon demand. Aquat. Microb. Ecol. 13:19–27; 1997.

Toolan, T.; Wehr, J.D.; Findlay, S. Inorganic phosphorus stimulation of bacterioplankton production in a mesoeutrophic lake. Appl. Environ. Microbiol. 57:2074–2078; 1991.

Turley, C.M. Direct estimates of bacterial numbers in seawater samples without incurring cell loss due to sample storage. In: Kemp, P.F.; Sherr, B.F.; Sherr, E.B.; Cole, J.J., eds. *Handbook of Methods in Aquatic Microbial Ecology.* Ann Arbor, MI: Lewis; 1993:143–148.

Turley, C.M.; Hughes, D.J. Effects of storage on direct estimates of bacterial numbers of preserved seawater samples. Deep Sea Res. 39:375–382; 1992.

Valino, J.J.; Hopkinson, C.S.; Hobbie, J.E. Modeling bacterial utilization of dissolved organic matter: Optimization replaces Monod growth kinetics. Limnol. Oceanogr. 41:1591–1609; 1997.

Vaque, D.; Pace, M.L. Grazing on bacteria by flagellates and cladocerans in lakes of contrasting food-web structure. J. Plank. Res. 14:307–321; 1992.

Vezina, A.; Pace, M.L. An inverse model analysis of planktonic food webs in experimental lakes. Can. J. Fish. Aquat. Sci. 51:2034–2044; 1994.

Vezina, A.F.; Platt, T. Food web dynamics in the ocean. I. Best estimates of flow networks using inverse models. Mar. Ecol. Prog. Ser. 42:269–284; 1988.

Waiser, M.J.; Robarts, R.D. Microbial nutrient limitation in prairie saline lakes with high sulfate concentrations. Limnol. Oceanogr. 40:566–574; 1995.

Wallner, G.; Spring, S.; Beisker, W.; Amman, R. Flow sorting of microorganisms for molecular

analysis. Appl. Environ. Microbiol. 63:4223–4231; 1997.

Watson, S.W.; Novitsky, T.J.; Quincy, H.L.; Valois, F.W. Determination of bacterial number and biomass in the marine environment. Appl. Environ. Microbiol. 33:940–946; 1977.

Wetzel, R.G. Dissolved organic compounds and their utilization in marl lakes of northern Indiana. Hidrologia Kozlony 47:298–303; 1967.

Wetzel, R.G.; Hatcher, P.G.; Bianchi, T.S. Natural photolysis by ultraviolet irradiance of recalcitrant dissolved organic matter to simple substrates for rapid bacterial metabolism. Limnol. Oceanogr. 40:1369–1380; 1995.

White, P.A.; Kalff, J.; Rasmussen, J.B.; Gasol, J.M. The effect of temperature and algal biomass on bacterial production and specific growth rate in freshwater and marine habitats. Microb. Ecol. 21:99–118; 1991.

Wright, R.T.; Hobbie, J.E. Use of glucose and acetate by bacteria in aquatic ecosystems. Ecology 47:464; 1966.

Zweifel, U.L.; Hagstrom, A. Total counts of marine bacteria include a large fraction of non-nucleoid-containing bacteria (ghosts). Appl. Environ. Microbiol. 61:2180–2185; 1995.

10

Herbivory in Terrestrial Ecosystems

Martín Oesterheld and Samuel J. McNaughton

Introduction

" . . . I marked all the seedlings of our native weeds as they came up, and out of 357 no less than 295 were destroyed, chiefly by slugs and insects. If turf which has long been mown (and the case would be the same with turf closely browsed by quadrupeds) be let to grow, the more vigorous plants gradually kill the less vigorous. . . . Within the last ten years, large spaces have been enclosed [so that cattle could not enter] and self-sown firs are springing up in multitudes . . . we see that cattle absolutely determine the existence of fir."

Darwin, *The Origin of Species*

The study of herbivory in relation to ecosystem science has been closely related to the methodological procedures outlined by Darwin in these lines. Ecologists have attempted to quantify herbivory in a variety of ways and systems, much like Darwin quantified consumption of weed seedlings. They have tried to simulate herbivory through defoliation, mowing, fertilization, and artificial trampling, much like Darwin used a mown turf as a substitute for a lawn grazed by quadrupeds. Finally, they have relied on herbivore exclusion by fencing or poisoning, much like Darwin did to assess the effect of cattle on fir populations.

In this chapter, we review the major approaches to quantifying and simulating herbivory and to assessing its effects at the ecosystem level. Considering a general model of energy flow through an ecosystem (see Chapter 2), we are concerned with two major fluxes and an interaction between them: the quantification of consumption, the quantification of primary productivity in systems under the effect of herbivores, and the effect of consumption on primary productivity.

Consumption

Consumption, or herbivory, is the rate at which energy or materials enter the herbivore compartment of an ecosystem. It is expressed as a velocity in absolute terms or as a proportion of primary productivity, plant biomass, leaf area, or other ecosystem attributes. Differences among plant–herbivore systems determine the existence of different methodologies. However, there are essentially two approaches: one is based on an estimate of what the animals have consumed given their density and mean individual performance, whereas the other is based on estimates of missing plant biomass. Both approaches have advantages and disadvantages and they only partially overlap in terms of the objectives they are prepared to fulfill.

Animal-Based Methods

This approach determines consumption as the product of two variables: herbivore density and individual consumption. The latter is estimated from mean individual performance (growth, respiration) and the amount of plant biomass or energy needed to meet the corresponding animal requirements. This latter variable is actually a composite of two other complex variables: the conversion factor between assimilated energy and animal performance, which is closely related to body size, and the conversion factor between consumed and assimilated energy

(i.e., digestibility), which, in turn, depends on attributes of the plants (i.e., lignin content) and the animals (i.e., digestive system).

Measuring each of these compartments for a given situation is hardly feasible, so researchers must either take most of them from the literature or make strong simplifications. For example, Milchunas and Lauenroth (1993) converted stocking rates into animal consumption based on a figure proposed by the Society for Range Management indicating that a 454-kg cow consumes 12 kg day^{-1} of plant dry-matter. That approach implies assumptions for the whole sequence described above, from animal performance through digestibility. This may be satisfactory for studies aimed at describing broad regional patterns in which consumption may vary by orders of magnitude, but is too coarse for studies aimed at evaluating environmental modifications within a system. Essentially identical approaches are used to estimate consumption in systems dominated by arthropod herbivores. For example, Schowalter et al. (1981) estimated sap-feeder consumption in forest ecosystems from determinations of abundance and the assumption, based on laboratory studies, that individual consumption was 2.5 mg dry sap mg^{-1} dry insect day^{-1}. Similarly, to estimate belowground herbivory by nematodes, Ingham and Detling (1986) measured density and estimated individual consumption from relationships between metabolic rate and temperature and a fixed assimilation efficiency taken from the literature.

What sort of potential error is associated with this approach? This may be better visualized in the series of equations that lead to final consumption (Scott 1979):

$$C = D \times F \tag{10.1}$$

where C is consumption, D is animal density, and F is individual food demand.

$$F = (G + R)/A \tag{10.2}$$

where G is growth, R is respiration, and A is assimilation efficiency. Thus, estimating C will require good estimates not only of animal density, but also of performance and assimilation efficiency. This, in turn, will depend on animal condition and physiology and on the digestibility and other nutritional properties of the forage.

The magnitude of these potential errors depends on the variation that researchers may leave unaccounted for at each step of the process. Regarding assimilation efficiency (A), plant digestibility may strongly vary because of seasonality and species composition. In vitro dry-matter digestibility of whole plants of *Lolium rigidum* decreased from 58% at anthesis to 36% 69 days later (Ballard et al. 1990). Even greater variations were observed among species fed to black-tailed deer, which ranged between 37 and 72% (Hanley et al. 1992). Plant digestibility may also vary among animal species grazing or browsing a common forage. Different digestive systems, gut capacities, body sizes, and glandular systems affect the digestibility of a forage (Demment and Van Soest 1985). For example, tannins strongly decrease cell wall digestion in domestic sheep, but do not affect mule deer, probably due to different salivary secretions (Robbins et al. 1987). Regarding animal performance (G and R), metabolic needs for maintenance, which depend on body weight raised to 0.75, increase as body size decreases (in relative terms). Thus, metabolic rates per unit mass may vary by 40% among differentially sized individuals of the same or different species (e.g., cattle from 300 to 700 kg of live weight) (Bondi 1989). Maintenance is not the only metabolic activity; similarly sized calves may need twice as much energy if they are growing at a rate of 1 kg day^{-1} than if they are just meeting maintenance requirements (Bondi 1989). Thus, animal density cannot be translated directly into consumption unless a series of variables related to the plants and the animals are determined or assumed.

Plant-Based Methods

The second approach to estimate herbivore consumption is based on estimates of missing plant biomass that was removed by herbivores. For most systems dominated by herbaceous vegetation and vertebrate herbivores, the difference between caged and uncaged plots is used (McNaughton et al. 1996). The cages may be set in place for an entire season and a single biomass determination made at the end or at peak biomass, or they may be moved with some frequency and biomass determinations made at each move. Although this method seems straightforward, it also implies many assumptions and involves a reduction of spatial scale compared

with the animal-based approach. There are two major assumptions and, as usual, controlling for the risk of violating one increases the risk of violating the other. The first assumption is that initial biomass inside and outside cages is the same. Thus, a reasonably high number of cages must be installed if relatively low values of consumption are to be detected. The second assumption is that growth rate inside and outside cages will be the same. The risk of violating this assumption increases with the length of time the cages are kept in one place (McNaughton et al. 1996). Usually, researchers have limited time or money to allocate to setting cages and clipping biomass. That total budget will be the product of the number of replicated cages, which controls for the first assumption, and the number of times the cages are moved, which controls for the second assumption. That tradeoff must be solved through individual judgment in each case. Low herbivore load and large spatial heterogeneity in plant biomass and animal distribution will need more replicates and less frequent movement, whereas high herbivore loads and high vegetation and animal homogeneity will call for fewer replicates and more frequent cage movement.

What is the magnitude of the bias associated to these two sources of error? The first error, initial biomass differences between caged and uncaged plots, is a simple sampling error (see Chapter 2). Coefficient of variation of biomass for reasonable sample sizes becomes higher as data on particular biomass compartments, such as species or functional groups, are required. Since consumption is a difference between two variables, its variance is actually the sum of the variances of the two variables. The second error, the differential growth rate between caged and uncaged plots will depend on the effect of grazing on production. Recent reviews for grasslands and savannas indicate that grazing may increase or decrease production by as much as 50% (Milchunas and Lauenroth 1993; Oesterheld et al. 1999).

For systems dominated by arthropod herbivores, there is a different method also based on the plants. Although it is practical to exclude arthropod herbivores by means of poisoning, this is generally done to study their effects on plant community dynamics or ecosystem function, but not to assess consumption (e.g., Brown and Gange 1992). This likely results from the low levels of consumption in systems where the herbivore trophic level is dominated by arthropods (McNaughton et al. 1989, 1991; Oesterheld et al. 1999). Detecting 0 to 10% levels of consumption by differences between poisoned and control plots may be unfeasible. Fortunately for researchers, herbivore arthropods, particularly chewing insects in forests, leave marks of their consumption on the leaves, and these marks are the core of the plant-based approach to determine consumption levels.

This approach is based on the quantification of the proportion of leaf area that is accounted for by various kinds of herbivore damage: holes, mines, galls, and scraped surfaces (Bray 1964). There are some problems associated with this determination of damaged leaf area, particularly for the case of chewing insects. If damage occurs while the leaf is growing and the quantification of the damage is done at the end of the growing season, several distortions caused by the continuous growth of the leaf and the holes arise (Reichle et al. 1973; Coleman and Leonard 1995). By measuring the relative increase of hole and leaf area after punching holes in expanding leaves, Reichle et al. (1973) showed that consumption is overestimated when damage is evaluated as percentage of total leaf area at the end of the growing season. This error may be slight for tree species with quick and simultaneous leaf growth, and severe for tree species with continuous growth throughout the season (Reichle et al. 1973). The error can be reduced by performing sequential estimations of leaf area and damaged area throughout the growing season, arriving at a daily percentage of removal (Reichle et al. 1973).

Another potential error is the integration process of individual leaf measurements into an average ecosystem level. First, the integration into an average proportion of leaf area for the whole stand must be done as the ratio of total defoliated area to total leaf area, instead of the average of the ratios for individual leaves (Williams and Abbott 1991). The results from either calculation method may be considerably different if individual leaves are very different in size (Williams and Abbott 1991). Second, a determination of percentage of leaf area damaged, even if it is error-free, will not return directly a value of biomass or energy consumption at the ecosystem level. In order to have consumption values in these terms, total leaf area must be deter-

mined and translated into biomass according to the leaf specific area, the area per unit of leaf weight.

Although this value can be obtained at the ecosystem level by standard methods, its pattern of variability among species and individuals, together with behavioral preferences by herbivores on leaves with different leaf specific area may be an important source of error. Specific leaf area of Amazonian trees ranges from 50 to 200 $cm^2\ g^{-1}$ (Reich and Walters 1994), it shows about a twofold variation between northern pin oak (*Quercus ellipsoidalis*) and sugar maple (*Acer saccharum*) (Reich et al. 1991), it may vary seasonally within a species by 50 or 70% (Reddy et al. 1989; Reich et al. 1991), and it may vary by almost 100% within single individuals because of leaf age or position within the canopy (Basset 1991). If this variation is superimposed on dietary preferences of herbivores toward leaves according to their leaf specific weights (Basset 1991; Choong et al. 1992), it becomes clear that gross average translation of leaf area consumed to biomass or energy consumed may be biased.

Consumption by browsers is also estimated by surveying marks left by the animals on plants. The number of twigs consumed may be counted because apical growth stops after consumption. The number and diameter of these marks is recorded and then transformed into biomass from previously determined regressions between twig biomass and diameter (e.g., Edenius 1993). The type of scar left by different browsers is sometimes so characteristic that consumption may be quantified by species (McInnes et al. 1992).

Differential Use of the Two Approaches

For practical reasons, animal-based and plant-based methods are tightly related to spatial scale. Because of the data they require and the sort of errors they handle relatively well, they are used with different purposes. The animal-based methods require data on animal density which usually have a spatial resolution that integrates different components of a landscape or even different landscapes of a region. Instead of being affected by structural patchiness and spatial heterogeneity, they integrate it. Methods based on establishing cages or sampling leaf or twig marks are usually applied to homogeneous environmental units, such as single plant communities, in which plant traits can be accurately estimated with a reasonable effort.

Effect of Herbivores on Primary Production

The effect of herbivores on primary production must be estimated by comparing the rates of production of grazed and ungrazed systems. However, since most methods of estimating primary production are based on determinations of plant biomass (see Chapter 2), the presence of herbivores, which consume plant biomass, may introduce an underestimation bias. For example, if herbivore consumption exactly matched daily primary production, sequential determinations of plant biomass would reveal no accumulation and would erroneously return a production value equal to zero. As a result, most approaches to assess the effect of herbivores on primary production involve the exclusion of herbivores. However, if production is not estimated from biomass determinations but from some measurements of canopy functioning, such as gas exchange rates or intercepted radiation (see Chapters 2 and 3), there would be no need to remove the herbivores from the grazed treatment.

In this section we discuss advantages and disadvantages of these approaches. However, we first review a few central concepts regarding the effect of herbivores on productivity. As in the previous section, our text is complemented by the reviews on methods to estimate aboveground and belowground production in Chapters 2, 3, and 4.

Compensatory Growth

There are a number of alternative responses of productivity to grazing, depending on how grazing affects the growth rate per unit of biomass or relative growth rate (McNaughton 1979; Hilbert et al. 1981; Belsky 1986; Oesterheld and McNaughton 1991). When relative growth rate decreases as a consequence of grazing, the response is called damage. When it increases, the response is called compensatory growth. Depending on the effect that this increase in relative growth has on the absolute growth rate or productivity, three different compensatory responses may be distinguished. When the

increase in relative growth rate is not high enough to result in equal productivity of grazed and ungrazed systems, the response is called partial compensation or undercompensation. When the increase is enough to equal the productivity of ungrazed systems, the response is called full compensation. Finally, when the increase is such that productivity under grazing is larger than in ungrazed situations, the response is called overcompensation (Belsky 1986; Oesterheld and McNaughton 1991). If there were neither compensatory growth nor damage, the effect of grazing on productivity would be equivalent to consumption, so measuring either one would return the value of the other.

Overcompensation and full compensation may be detected by simple comparisons of productivity of grazed and ungrazed treatments. In contrast, when productivity under grazing is lower than controls, simple determinations of productivity will not suffice to discriminate between partial compensation and damage. In that case, a determination of initial biomass of grazed and control plots is required to calculate relative growth rates. Lack of these data and loose usage of terms frequently results in two different errors: some researchers refer to "compensatory responses" only in cases in which overcompensation was observed, ignoring that there may be compensation even when grazing reduced productivity; whereas others refer to partial compensation or undercompensation in all cases in which productivity is reduced by grazing, ignoring that some of those cases may represent damage.

Approaches

One of the approaches to estimating the effect of herbivory on production is based on the comparison of productivity of ungrazed systems with that of grazed systems from which herbivores have been temporarily removed. This herbivore exclusion may be done in different ways: fencing (for large herbivores), poisoning (for insects), or individual removals (rodents). We here discuss in more detail the methods based on fencing because they are the most frequently used, but most of our considerations are valid for the other methods. As we described above, fencing is also used to estimate consumption. Thus, both consumption and production may be estimated in the same study by a combination of cage movements (McNaughton et al. 1996): as we showed before, the difference of biomass between caged and uncaged plots estimates consumption, and, as we will show now, the rate of accumulation of biomass inside cages estimates production.

Compensatory growth affects the choice among different approaches to study the effect of herbivory on primary productivity (McNaughton et al. 1996). The moveable-cage method uses moveable exclosures that are moved with a frequency timed to reflect the intensity of herbivory. Compared with the season-long–cage method, in which herbivores are excluded for the entire season, it has the advantage that what is sampled inside moveable cages better resembles the real grazed system. The season-long–cage method seems to be suitable to assess the long-term effect of grazing on productivity, rather than the current effect of the herbivores. For example, comparing 30-year-old exclosures with continuously grazed areas by placing season-long cages in the grazed area answers the question, "What is the effect of long-term grazing on primary productivity in a year without grazing?" Short-term compensatory regrowth will be missed by this approach and the grazed systems being evaluated will soon resemble the structure of ungrazed systems, particularly in regions with high productivity (McNaughton et al. 1996). For both methods, however, production must be simultaneously estimated in comparable, ungrazed controls (see Chapter 2).

The decision of how frequently to move exclosures and sample biomass in ungrazed controls is crucial for the moveable-cage method (McNaughton et al. 1996). Since productivity estimates are affected by the frequency of biomass sampling (Sala et al. 1988; Biondini et al. 1991; see Chapter 2), care should be taken in order to avoid introducing differences of frequency between grazed and ungrazed treatments. Once this is taken care of, increasing frequency will maximize both the resemblance between the cages and the grazed system and the likelihood of detecting regrowth. However, the statistical errors common to any determination of productivity will also increase (Sala et al. 1988; Biondini et al. 1991; McNaughton et al. 1996; see Chapter 2). There is not a simple rule to decide about this tradeoff, but certainly sampling effort at each biomass sampling and harvest frequency will have to be correlated. Maximizing the detection of

compensatory regrowth by increasing the frequency of movement will need a parallel increase in sampling effort to avoid statistical errors.

Clipping inside cages or exclosures to simulate grazing or browsing has the advantages and disadvantages of any simulation: simplicity is gained and realism is lost. Because the same plots are sampled throughout the season, movement is not necessary and bias associated with false peaks and troughs generated by spatial heterogeneity is not a source of error. However, several difficulties arise when trying to simulate grazing or browsing by clipping: the spatial and temporal pattern of consumption is difficult to replicate and other effects of grazing different from consumption, such as nutrient return and trampling, are not included (McNaughton et al. 1996).

Moving the animals to allow for regrowth determinations during times of vacancy may not be practical while working with large herbivores, but can be successful with small herbivores. The frequency of animal movements will have here the same effect on production estimates as the frequency of cage movement in the moveable-cage method (McNaughton et al. 1996). An additional application of this approach is in livestock production systems managed with rotational grazing. This management generates a pattern of utilization and vacancy that may be timed with growth determinations during times of vacancy.

These three approaches share the need for herbivore removal and biomass determinations. The "grazed" vegetation being sampled is then different from the real grazed vegetation. Assuming a full accuracy in biomass determinations, the effect of the difference between the real and the sampled situations on productivity will result in a bias. Controlling for this bias, which means controlling for the difference between real and sampled situations, goes against the assumption of full accuracy in biomass determination unless sampling effort is proportionally increased.

The observation that spectral data may be translated into productivity because they are an integration of absorbed photosynthetic active radiation (see Chapter 3) (Paruelo et al. 1997) suggests a way out of this tradeoff. Net primary productivity is the product between absorbed photosynthetic radiation and a coefficient that represents the conversion of radiation into biomass growth (see Chapter 3). Sequential determinations of canopy reflectance from remote sensing devices or hand-held radiometers may be integrated and provide estimates of production values of systems being grazed. The accuracy of these determinations will depend on the empirical calibration between production and reflectance (see Chapter 3). Also, differences in canopy structure, tissue composition, and water status between the grazed and ungrazed systems to be compared may require differential calibrations for each treatment.

Acknowledgments An anonymous reviewer made valuable comments on a previous version of this manuscript. Supported by University of Buenos Aires and Consejo Nacional de Investigaciones Cientificas y Técnicas (CONICET).

References

Ballard, R.A.; Simpson, R.J.; Pearce, G.R. Losses of the digestible components of annual ryegrass (*Lolium rigidum* Gaudin) during senescence. Aust. J. Agric. Res. 41:719–732; 1990.

Basset, Y. Influence of leaf traits on the spatial distribution of insect herbivores associated with an overstorey rainforest tree. Oecologia 87:388–393; 1991.

Belsky, A.J. Does herbivory benefit plants? A review of the evidence. Am. Natur. 127:870–892; 1986.

Biondini, M.E.; Lauenroth, W.K., Sala, O.E. Correcting estimates of net primary production. Are we overestimating plant production in rangelands? J. Range Manage. 44:194–198; 1991.

Bondi, A. *Nutrición Animal.* Zaragoza: Acribia; 1989.

Bray, J. Primary consumption in three forest canopies. Ecology 45:165–167; 1964.

Brown, V.K.; Gange, A.C. Secondary plant succession: How is it modified by insect herbivory? Vegetatio 101:3–13; 1992.

Choong, M.F.; Lucas, P.W.; Ong, J.S.Y.; Pereira, B.; Tan, H.T.W.; Turner, I.M. Leaf fracture toughness and sclerophylly: Their correlations and ecological implications. New Phytol. 121:597–610; 1992.

Coleman, J.S.; Leonard, A.S. Why it matters where on a leaf a folivore feeds. Oecologia 101:324–328; 1995.

Demment, M.W.; Van Soest, P.J. A nutritional explanation for body-size patterns of ruminant and nonruminant herbivores. Am. Natur. 125:641–672; 1985.

Edenius, L. Browsing by moose on Scots pine in relation to plant resource availability. Ecology 74:2261–2269; 1993.

Hanley, T.A.; Robbins, C.T.; Hagerman, A.E.; McArthur, C. Predicting digestible protein and digestible dry matter in tannin-containing forages consumed by ruminants. Ecology 73:537–541; 1992.

Hilbert, D.W.; Swift, D.M.; Detling, J.K.; Dyer, M.I. Relative growth rates and the grazing optimization hypothesis. Oecologia 51:14–18; 1981.

Ingham, R.; Detling, J. Effects of defoliation and nematode consumption on growth and leaf gas exchange in *Bouteloua curtipendula.* Oikos 46:23–28; 1986.

McInnes, P.F.; Naiman, R.J.; Pastor, J.; Cohen, Y. Effects of moose browsing on vegetation and litter of the Boreal Forest, Isle Royale, Michigan, USA. Ecology 73:2059–2075; 1992.

McNaughton, S.J. Grazing as an optimization process: Grass-ungulate relationships in the Serengeti. Am. Natur. 113:691–703; 1979.

McNaughton, S.J.; Milchunas, D.G.; Frank, D.A. How can net primary productivity be measured in grazing ecosystems? Ecology 77:974–977; 1996.

McNaughton, S.J.; Oesterheld, M.; Frank, D.A.; Williams, K.J. Ecosystem-level patterns of primary productivity and herbivory in terrestrial habitats. Nature 341:142–144; 1989.

McNaughton, S.J.; Oesterheld, M.; Frank, D.A.; Williams, K.J. Primary and secondary production in terrestrial ecosystems. In: Cole, J.; Lovett, G.; Findlay, S., eds. *Comparative Analyses of Ecosystems: Patterns, Mechanisms, and Theories.* New York: Springer-Verlag; 1991:120–139.

Milchunas, D.G.; Lauenroth, W.K. Quantitative effects of grazing on vegetation and soils over a global range of environments. Ecol. Monogr. 63:327–366; 1993.

Oesterheld, M.; Loreti, J.; Semmartin, M.; Paruelo, J.M. Grazing, fire, and climate effects on primary productivity of grasslands and savannas. In: Walker, L.R. Ed. *Ecosystems of Disturbed Ground.* Ecosystems of the World Series. Amsterdam: Elsevier; 1999. pp. 287–306.

Oesterheld, M.; McNaughton, S.J. Effect of stress and time for recovery on the amount of compensatory growth after grazing. Oecologia 85:305–313; 1991.

Paruelo, J.M.; Epstein, H.E.; Lauenroth, W.K.; Burke, I.C. ANPP estimates from NDVI for the Central Grassland Region of the United States. Ecology 78:953–958; 1997.

Reddy, V.R.; Acock, B.; Baker, D.N.; Acock, M. Seasonal leaf area-leaf weight relationships in the cotton canopy. Agron. J. 81:1–4; 1989.

Reich, P.B.; Walters, M.B. Photosynthesis-nitrogen relations in Amazonian tree species. 2. Variation in nitrogen vis-a-vis specific leaf area influences mass-based and area-based expressions. Oecologia 97:73–81; 1994.

Reich, P.; Walters, M.B.; Ellsworth, D.S. Leaf age and season influence the relationships between leaf nitrogen, leaf mass per area and photosynthesis in maple trees. Plant Cell Environ. 14:251–259; 1991.

Reichle, D.; Goldstein, R.; Van Hook, R.; Dodson, G. Analysis of insect consumption in a forest canopy. Ecology 54:1076–1084; 1973.

Robbins, C.T.; Mole, S.; Hagerman, A.E.; Hanley, T.A. Role of tannins in defending plants against ruminants: Reduction in dry matter digestion? Ecology 68:1606–1615; 1987.

Sala, O.E.; Biondini, M.E.; Lauenroth, W.K. Bias in estimates of primary production: An analytical solution. Ecol. Model. 44:43–57; 1988.

Schowalter, T.; Webb, J.; Crossley, D. Community structure and nutrient content of canopy arthropods in clearcut and uncut forest ecosystems. Ecology 62:1010–1019; 1981.

Scott, J. An ecosystem-level trophic-group arthropod and nematode bioenergetics model. In: French, N. eds. *Perspectives in Grassland Ecology.* New York: Springer Verlag; 1979:107–116.

Williams, M.R.; Abbott, I. Quantifying average defoliation using leaf-level measurements. Ecology 72:1510–1512; 1991.

Part 2

Nutrient and Water Dynamics

11

Canopy Fluxes

John B. Moncrieff, Paul G. Jarvis, and Ricardo Valentini

Introduction

One of the foremost challenges for ecologists is to integrate observations made at a range of scales so that they become useful to others working at a different scale. An example of this would be scaling observations of carbon and water exchange made at leaf or plot scale to be of direct use to global climate modelers. Micrometeorological techniques, which operate at intermediate scales to these two extremes, are being used increasingly to validate and parameterize such models (Baldocchi and Meyers 1998). In turn, micrometeorological techniques can be validated against suitably scaled observations at a smaller scale. Progress in closing the carbon budget for example, must rely on such an interdisciplinary approach. When made in combination with detailed biophysical field experiments, such observations can reveal the atmospheric and biophysical variables that control carbon and water exchange. In this review, we describe briefly the most common micrometeorological methods used to measure fluxes of carbon and water at the scale of the canopy, focusing in particular on the direct techniques of eddy covariance and eddy accumulation. We also describe flux measurements at related scales that are commonly used to give added value to canopy-scale fluxes.

This review comprises material available up until the end of 1998. Readers interested in the eddy covariance methodology may wish also to consult Aubinet et al. (2000).

The Canopy Scale

In general, micrometeorological methods are usually reported over a time period of about half an hour and integrate fluxes over a spatial scale of about 1 km^2. The space scale is influenced by the height of the measuring point above the top of the canopy and the length scales of atmospheric turbulence, which are a result of both mechanical (surface friction) and thermal effects that influence atmospheric stability. The reporting time for surface fluxes of about 30 minutes is related to the need to make observations over a suitably long period such that the majority of the spectrum of flux-carrying eddies are sampled, yet not too long so that natural diurnal variability in scalar concentrations or forcing functions such as solar radiation are included. Micrometeorological methods are nondestructive in that they only sample the air as it advects past the sensor.

The Surface Boundary Layer

All micrometeorological measurements are made within the atmospheric boundary layer (ABL) and the depth and structure of this layer present opportunities and challenges (Fig. 11.1). The ABL as defined by Lenschow (1995) is "the lower part of the atmosphere that interacts with the biosphere and is closely coupled to the surface by turbulent exchange processes." The depth of the ABL depends on the degree of mechanical (caused by surface friction) and buoyant mixing (thermals rising from the warmed surface) and its depth can also be dic-

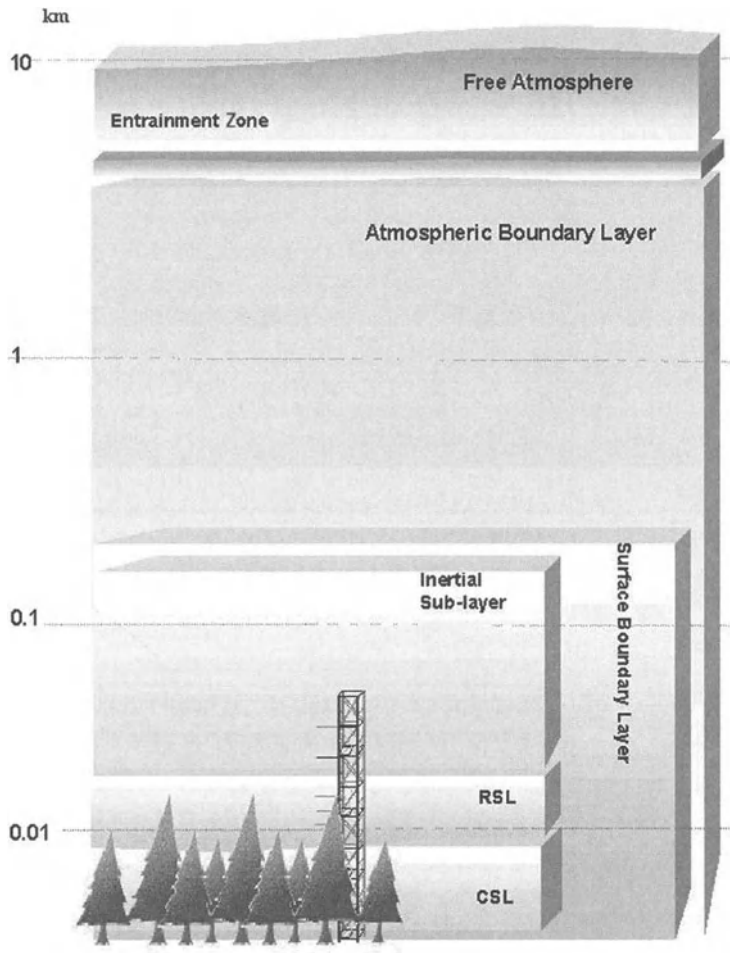

FIGURE 11.1. The atmospheric boundary layer and its sublayers. The lower 10% or so of the atmospheric boundary layer is the surface layer and this is where most conventional micrometeorological measurements are made from towers. More specifically, direct flux measurements by techniques, such as eddy covariance and eddy accumulation, can take place in any part of the surface boundary layer. Most indirect techniques based on measuring gradients of scalars should not be made within the roughness or canopy sublayers.

tated by synoptic scale motions such as anticyclonic subsidence. The ABL is sometimes also called a convective boundary layer (CBL) when several kilometers deep as a result of the development of thermals rising during the day. At night, the ABL may be perhaps only a few tens of meters deep.

The top of the ABL represents a fairly sharp boundary between the turbulent, chaotic motions of the ABL and the smoother, streamlined flow of the free atmosphere above. The rate of change in vertical profiles of temperature, water vapor, and carbon dioxide (CO_2) is highest near the active surface, in a region typically about one-tenth the depth of the ABL that is called the surface boundary layer (SBL). It is in this region that most conventional micrometeorological measurements are made. The SBL can further be divided into two sublayers: inertial and roughness (Raupach and Thom 1981). In the inertial sublayer, wind profiles in neutral stability conditions are logarithmic with height and well-established scaling schemes apply (Kaimal and Finnegan 1994). Fluxes are considered constant with height (or at least within 10% of their surface values). Close to surface vegetation lies an interfacial layer in which turbulence is enhanced over that in the inertial sublayer above by wake turbulence or thermal effects. The depth of this so-called "roughness sublayer" has been variously estimated to be three times the height of the vegetation (Kaimal and Finnegan 1994) or sometimes three times the spacing between the vegetation elements (Raupach and Legg 1984). The implication of the enhanced diffusivities in the

roughness layer is that micrometeorological methods that rely on establishing eddy diffusivities are difficult to apply in this layer. By going beyond the roughness sublayer however, concentration gradients can become small and difficult to measure over rough vegetation and this poses further problems.

The top of the surface layer is not physically as well defined as the top of ABL. Although most tower-based flux measurements are made within the SBL, the evolving structure of the ABL over a day does present opportunities for other measurements using aircraft, tethersondes, and ABL budget methods, which we shall mention in passing.

Net Ecosystem Exchange

Fluxes of carbon and water measured by micrometeorological methods above the canopy are the net fluxes from the whole system and are measures of the net ecosystem exchange of carbon (NEE) or total evaporation (ET) from the canopy, its elements and the ground surface (Fig. 11.2). Instrumentation placed above the upper system boundary (USB) measures the net exchange of material passing through that arbitrary level and of itself cannot distinguish the pathways by which that flux arrived at the sensor. Thus the NEE is the measured flux (F_c) above the USB plus that component that represents storage of carbon between the point of observation and the ground, i.e., $F_c + \Delta S$. (It is assumed that there are no advective fluxes in this representation but this assumption will be examined later.) Profiles of CO_2 concentration within the canopy and up to the height at which the flux measurements are made are used to measure changes in storage of carbon.

The NEE is the net sum of a number of component processes that take place within the stand. These include the gains of carbon in photosynthesis by the foliage of the trees, understory, and mosses, and the losses from respiration by the aboveground foliage and wood as well as the belowground roots, mycorrhizas, and heterotrophic microorganisms (the so called "soil respiration"). Of these, the major components are the gains by photosynthesis and the losses through soil respiration.

Techniques to measure the gains through foliage photosynthesis and the respiration losses of leaves and shoots using cuvettes have been described many times (Sestak et al. 1971) as have been techniques of measuring soil respiration (Hutchinson and Livingston 1993; Fang and Moncrieff 1998). The crux of the problem in the present context is to sample adequately the heterogeneity of the forest system so as to obtain adequate spatial integration on a continuous basis for comparison with the NEE.

Scaling up from leaf cuvettes to the stand requires a large number of cuvettes to estimate CO_2 gains and losses of foliage in different positions,

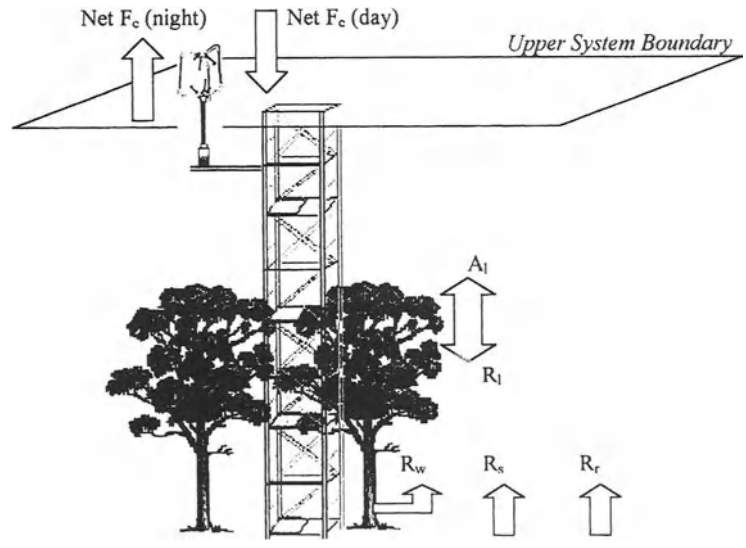

FIGURE 11.2. Fluxes above and within the canopy. The upper system boundary (USB) marks the level through which the vegetation exchanges carbon and water with the atmosphere. Direct micrometeorological methods, such as eddy covariance, operate at this level. Below the USB A_l and R_l are the net assimilatory and respiratory exchanges by the leaves; The subscripts w, s, and r refer to respiratory fluxes from wood, soil, and roots respectively. (Redrawn from Jarvis and Sandford, 1986.)

from leaves of different ages. Branches represent an intermediate scale that can be more readily scaled up to the stand if the sample is sufficient. Recently, branches in bags (branch bags) have been used as chambers within which photosynthesis can be measured continuously from spring to fall to scale up the gains and losses of the foliage on branches to stand scale in boreal forests (Rayment and Jarvis 1999). Similarly, open, air-sealed soil chambers have been used to measure the soil CO_2 efflux from spring to fall (Rayment and Jarvis 1997). In both cases, the main problem is not methodological but is a classical sampling problem—how many replicates are required to give an estimate within appropriate confidence limits (Livingston and Hutchinson 1995)?

The data obtained with such techniques can be used to compute detailed carbon budgets by summation of the component fluxes to yield estimates of NEE that can be compared with the measurements of NEE obtained by eddy covariance and, if the sample is adequate, used to validate the estimates of NEE by eddy covariance. Perhaps more importantly, the component fluxes measured in this way may explain how the NEE is made up and thus enable predictions of the likely effects of global change on NEE. A carbon budget for a boreal forest stand of black spruce built up using these techniques is shown in Figure 11.3, for comparison with the measured NEE. While the two approaches yield different estimates of the NEE, the sign and order of magnitude of the estimates are similar, providing support for both methodologies.

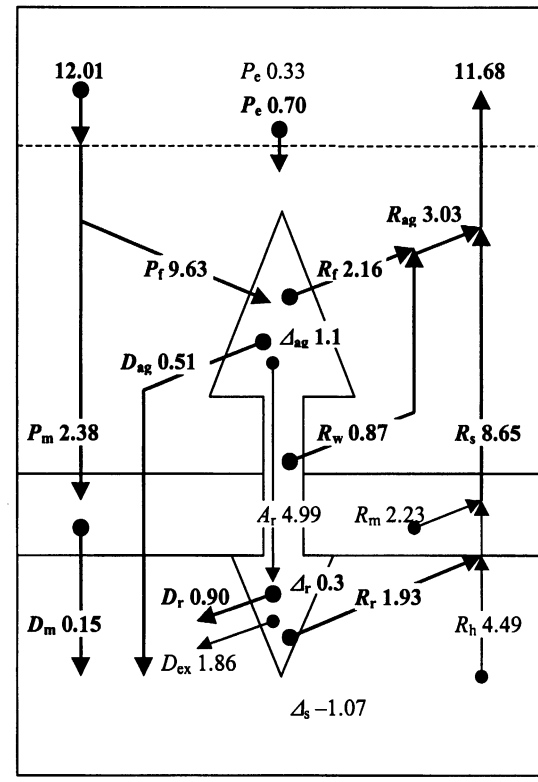

FIGURE 11.3. Estimated annual carbon balance for the BOREAS Southern Supersite Old Black Spruce site for a period of 366 days, ending day 332 of 1996. Fluxes are in Mg (C) $ha^{-1}\ yr^{-1}$. Arrows and values in **bold** were measured directly, other fluxes were derived by mass balance. Two estimates of the net ecosystem exchange, P_e, are given, the direct measurement by eddy covariance (**bold**) and the difference between the total gross uptake and the total efflux (plain). The other fluxes are: P_f, tree foliage gross photosynthesis; P_m, moss gross photosynthesis (data from Dr. L.B. Flanagan, University of Lethbridge, Alberta); R_f, tree foliage total respiration; R_w, aboveground woody biomass respiration (Ryan et al. 1997; Lavigne and Ryan 1997); R_{ag}, aboveground tree biomass respiration, R_m, moss respiration; R_r, root respiration (Ryan et al. 1997); R_h, heterotrophic respiration in soil; R_s, soil surface efflux; D_{ag}, aboveground detritus (Gower et al. 1997); D_m, moss turnover (Harden et al. 1997); D_r, root detritus and fine root turnover (Steele et al. 1997); D_{ex}, root exudate; A_r, carbon allocation to belowground parts; Δ_{ag} aboveground NPP (Gower et al. 1997); Δ_r, belowground NPP (Steele et al. 1997); Δ_s, change in soil organic matter pool. (From Rayment, [1998].)

Flux Footprint

Fluxes measured by micrometeorological sensors are effectively the integration of fluxes from a variety of sources and sinks in the landscape for a distance of several hundred meters upwind from the measuring point. The height at which the measurements are chosen to be made must be determined both by consideration of the frequency response of the instrumentation and also the "fetch" or extent of the upwind area from which the signal comes. Eddies become progressively larger with height up to the depth of the planetary boundary layer, typically 1 km by day, and this means that instrumentation with a slower response can be used successfully at heights well above the vegetation. As the

surface is approached, however, the spectrum of turbulence includes a larger proportion of smaller eddies that actively exchange mass and momentum between the surface and the atmosphere. The instrumentation must therefore be capable of sampling high-frequency eddies, typically up to 10 Hz. In principle, one could use an eddy covariance system well above the canopy in order to avoid the problem of frequency response of analyzers. However, as we move up in height, the area of flux integration becomes larger and the requirements of surface homogeneity become more and more stringent. In fact, if the instruments are placed too high above the surface it is possible that they could extend out of the boundary layer representative of the nearby vegetation and be measuring some component of fluxes from a different type of vegetation further upwind. A convenient rule-of-thumb suggests a fetch/height ratio of about 100:1; thus a fetch of 500 m would allow instruments to be placed up to a height of about 5 m above the surface. The fetch/height ratio depends on atmospheric stability and surface roughness insofar as they influence the degree of mixing of internal boundary layers as they are advected over different types of surface (Mulhearn 1977; Gash 1986; Grelle and Lindroth 1996).

One promising approach is to define a "footprint" or source region that is a measure of the relative importance of sources upwind that contribute to the measured flux. This area can be regarded as contributing most of the flux measured, and its areal extent and position can be calculated from a knowledge of surface roughness, atmospheric stability, wind speed and direction (e.g., Schuepp et al. 1990, Schmid and Oke 1990). The approach is based on the same theory as underlies dispersion modeling of pollutants using the familiar Gaussian plume approach. A number of models are available concerning footprint calculation based either on lagrangian or particle trajectory models (Schuepp et al. 1990; Finn et al. 1996; Flesch 1995) or analytical dispersion models (Horst and Weil 1994; Schmid 1994). At present, however, most are of limited application in the roughness sublayer.

Ideally, the measurement site should be extensive, flat, and horizontally uniform to ensure that fluxes are measured in the constant flux layer. To a first order approximation, the error $F_z - F_0$, following a change in surface with a flux of F_1 to one with flux F_0 may be estimated using

$$\frac{F_z - F_0}{F_1 - F_0} = 10z/x \frac{\ln(z/z_0)}{\ln(x/10z_0)} \qquad (11.1)$$

where x is the upwind distance from the change in surface and z_0 is the roughness length of the downwind surface (obtained from wind profiles) (Moncrieff et al. 1996). From this expression, it is clear that the error in the flux measurement, $F_z - F_0$, is proportional to the difference in fluxes of the upwind and downwind surfaces, $F_1 - F_0$. The error also diminishes as z/x decreases, and is $< 5\%$ of $F_1 - F_0$ for $z/x < 0.01$, in conformity with the micrometeorological rule-of-thumb that the measurement height should be $< x/100$ to ensure accurate measurements. This ratio needs to be increased for stable conditions and may be relaxed under unstable stratification (Kaimal and Finnigan 1994). According to (Schuepp et al. 1990) the relative contribution to the vertical flux $[(1/Q_0)(dQ/dx)]$ at height z, coming from an infinite crosswind source of unit width at an upwind distance x, in neutral conditions is given by:

$$\frac{1}{Q_0}\frac{dQ}{dx} = \frac{u(z-d)}{u^* k x^2} e^{-u(z-d)/(ku^* x)} \qquad (11.2)$$

and the upwind position (x_{max}) of the peak of the cumulative flux of the source area is:

$$x_{max} = \frac{u(z-d)}{u^* 2k} \qquad (11.3)$$

where u is the mean wind velocity at height z, d the zero-plane displacement (obtained from wind profiles), u^* the friction velocity, and k the von Karman constant (0.41). Figure 11.4 is an example of the distribution of the relative contribution to the vertical flux as a function of height of measurement. Increasing the height of measurements, the peak of the flux footprint becomes more and more distant from the point of measurement. Similarly, the peak contribution moves closer to the point of measurement as the atmosphere becomes more unstable. With increasing stability, the peak contribution moves further from the point of measurement.

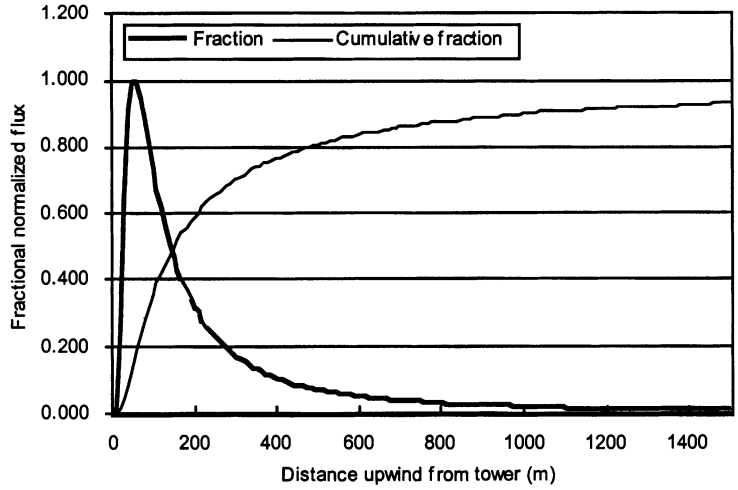

FIGURE 11.4. Flux footprints by measurement height. The solid line shows the relative contribution to the total measured flux contributed by sources at various distances upwind from the measuring point. The data are normalized such that the flux at the distance of maximum source contribution appears as a peak in this representation. In this simulation, the peak source distribution is within about 50 m of the measurement point. The contribution from sources upwind decreases exponentially with distance from the tower. The line showing the cumulative fraction shows that even at a distance of about 1500 m from the tower, only about 95% of the measured flux has been accounted for by sources within this distance or "footprint." Both the peak and cumulative fraction are dependent on measurement height and atmospheric stability.

Methodologies

The transport of gases, heat, and pollutants in the atmosphere is produced by the eddying motion of the atmosphere as air parcels are displaced from one level to another. Micrometeorological methods used to quantify this turbulent exchange can either sample the air as it flows past a sampling point for its vertical windspeed and direction and its gas concentration directly (the *eddy covariance* or *eddy accumulation* methods) or they can be based on quantifying the rate of diffusion down concentration gradients (the *aerodynamic* and *Bowen ratio* methods). The direct method of eddy covariance involves sampling at one height only but with relatively sophisticated sensors and logging equipment. The methods based on measuring gradients require measurements at two or more heights but use simpler sensors. The disadvantage of the gradient techniques is, however, that a number of empirical functions are required to account for thermal stratification of the atmosphere; additionally, the gradients in atmospheric properties become very small above vegetation canopies and the aerodynamic technique in particular cannot be used inside plant canopies. All three techniques, when used above vegetation, require that steady state conditions exist, that is, that atmospheric conditions are not changing rapidly over the sampling period; they also all require extensive upwind areas of the vegetation, that is, these methods cannot be used on isolated plots or small fields. If these conditions are met, it is assumed that the flux measured just above the vegetation is equal to that at the ground or plant surfaces and fluxes are constant with height up to a level dependent on the extent of upwind surface homogeneity and atmospheric mixing.

The question of which method to use depends not only on the available resources but also crucially on the surface type over which the measurements are to be made. For example, over very rough surfaces in an aerodynamic sense, such as forests, gradients of scalars are small and their measurement places extreme emphasis on the precision of sensors—under these conditions, gradient techniques are problematic. On the other hand, as turbulence is enhanced over forests, the eddy covariance technique is made easier as the size of the fluctuations in vertical windspeed and other at-

mospheric properties is increased. Measurements over smooth surfaces, such as water or ice, are difficult using any of the techniques mentioned. Increasingly, eddy covariance–based systems are being integrated into global observing networks both to monitor carbon and water exchange on the global scale and to validate remotely sensed products (Running et al. 1999).

Aerodynamic Method

The vertical exchange of atmospheric entities such as momentum, temperature, water vapor, and CO_2 by turbulent transport is driven by and is proportional to their vertical concentration gradients. We can describe the transport process in a flux-gradient form which defines the constant of proportionality K known as an eddy diffusivity. In generic form, the flux density (F_X, the amount of that entity transported vertically through unit area in unit time) of any scalar (X) is:

$$F_x = -K_x \frac{dX}{dz} \tag{11.4}$$

The eddy diffusivities for scalars such as temperature, water vapor, and CO_2 have been the subject of much experimentation over several decades as their relative magnitudes depend on both surface and atmospheric features. In practice, the diffusivities are related to the eddy diffusivity for momentum, which can be established from profiles of wind speed. Wind profiles are used to calculate the friction velocity, a measure of the degree of atmospheric mixing and from which $K_X = ku^*(z - d)$ is calculated (Thom 1975). The gradients of the scalar in question need to be precisely determined and obtaining accurate gradients over rough vegetation can be difficult because of the substantial degree of atmospheric mixing over such canopies (McNeil and Shuttleworth 1975). One of the concerns about the aerodynamic technique is that a number of empirical corrections are required to account for changes in atmospheric stability (which influences the shape of wind profiles). A number of semiempirical formulae have been extensively investigated and are well accepted (e.g., Webb 1970; Paulson 1970). The aerodynamic technique has been used extensively in the past to obtain fluxes of sensible and latent heat over forests (e.g., Thom 1975; Lindroth 1984) and extended to other trace gas species over different surface types (e.g., Fowler and Unsworth 1979; Sutton et al. 1993). It is not possible to use the aerodynamic technique in the roughness sublayer or within the canopy as the variation in sources and sinks for heat, water vapor, and CO_2 invalidate the underlying assumptions in the method (Raupach and Legg, 1984).

Energy Balance/Bowen Ratio

The energy balance at the surface is

$$R_n - G - S = H + LE \tag{11.5}$$

Where R_n is net radiation absorbed by the vegetation, G is soil heat flux, and S is heat stored in the vegetation. The ratio of sensible heat (H) to latent heat (LE) flux is known as the Bowen ratio (β) and by writing the fluxes in their flux-gradient form, an equation can be found that permits either flux to be found from measurements of the gradient of temperature (T) and humidity (e), irrespective of atmospheric stability:

$$\beta = 1/\gamma \frac{dT}{de} \tag{11.6}$$

where γ is the psychrometric constant (Monteith and Unsworth 1990). Once β has been obtained, substituting for LE and H in Equation 11.5 we get

$$H = \frac{R_n - G - S}{1 + \beta^{-1}} \tag{11.7}$$

and

$$LE = \frac{R_n - G - S}{1 + \beta} \tag{11.8}$$

This method can also be used to measure fluxes of other gases or pollutants by rewriting a more generalized form of the flux-gradient equation by combining H and LE as before to yield

$$R_n - G - S = K\rho c_p \frac{dT_e}{dz} \tag{11.9}$$

where K is an eddy diffusivity assumed equal for all entities (other than momentum), c_p is the specific heat at constant pressure, ρ is air density and T_e is the equivalent temperature, $(T + e/\gamma)$ (Monteith and Unsworth 1990). If all pollutants and gases share this value of K then the flux density for

any scalar, as determined by the energy balance method, can be written as:

$$F_x = (R_n - G - S)\frac{dx}{dT_e} \qquad (11.10)$$

The gradient for any scalar x, can be found by plotting x against T_e at the same height for a number of measurement levels. The available energy $(R_n - G - S)$ can be found using net radiometers, soil heat flux plates and from profiles of temperature within the canopy.

The technique is reliable in most conditions but when the available energy becomes small, for example, at night, or the gradients are small, as over rough vegetation, then large errors can occur. Also the method involves measuring G and S, and this poses problems. In low windspeed conditions, where the aerodynamic method fails because of stalling of anemometers, the Bowen ratio method works well. The Bowen ratio method can also be used in the roughness sublayer because it only requires the assumption of equality between the eddy diffusivities for sensible heat and water vapor; that is, there is no need for stability factors invoking similarity with K_M as are needed with the aerodynamic method (Lenschow 1995). Miranda et al. (1984) used the Bowen ratio method to measure evaporation over heather moorland and Barr et al. (1994) have demonstrated its use over forests.

Eddy Covariance

Theory

The eddy covariance technique measures the flux of a scalar (heat, mass) or momentum at a point centered on instruments placed at some height above the surface. For these measurements to be identical to the flux at the underlying surface, the instruments must be located in the internal boundary layer where the flux is constant with height. A clear understanding of the conditions required for a constant flux layer is obtained by examining the conservation equation for a scalar quantity in a control volume placed over the surface:

$$\frac{\partial \bar{s}}{\partial t} + \frac{\partial \overline{u_i s}}{\partial x_i} - D\frac{\partial^2 \bar{s}}{\partial x_i^2} = S \qquad (11.11)$$

In this equation, s is the density of the scalar, t is time, u_i is the wind velocity component in the orthogonal directions x_i $(i = 1, 2, 3)$, D is the molecular diffusivity for quantity s in air, S is the volumetric source/sink strength, and the overbar represents a time average. The first term on the left is the mean rate of change of mass per volume, while the second and third terms are the flux divergence arising from net advection and molecular diffusion through the sides of the control volume. A constant flux layer requires stationarity $(\partial \bar{s}/\partial t = 0)$ and the absence of sources or sinks between the surface and the instruments $(S = 0)$. Also, most micrometeorologists have assumed that over a horizontally homogeneous surface for a sufficiently long upwind area, the mean vertical velocity or the dry air flux will be zero so that $\partial(\overline{u_i s})/\partial x_i = 0$ and $D[(\partial^2 \bar{s})/(\partial x_i^2)] = 0$ $(i = 1, 2)$. When these assumptions are met (and we explain below that this is now thought to be unlikely), we obtain

$$\frac{\partial \overline{ws}}{\partial z} - D\frac{\partial^2 \bar{s}}{\partial z^2} = 0 \qquad (11.12)$$

where w is the vertical windspeed, and z is the vertical coordinate. Turbulence is suppressed near the surface, while turbulent transport is many orders of magnitude larger than molecular diffusion at height z above the surface (Businger, 1986). Thus, integrating this equation and using the Reynolds convention that $w = w' + \bar{w}$ and $s = s' + \bar{s}$, yields

$$F_0 = -D\left(\frac{\partial \bar{s}}{\partial z}\right)_0 = (\overline{w's'})_z = F_z \qquad (11.13)$$

where F_0 is the flux resulting from molecular diffusion at the underlying soil and leaf surfaces, and F_z is the turbulent eddy flux at height z. Note that the eddy flux can also be written as

$$F_z = r_{ws}\sigma_w\sigma_s \qquad (11.14)$$

where r_{ws} is the correlation coefficient and σ_w and σ_s are the standard deviations of w and s, respectively.

Under non–steady state but horizontally homogeneous conditions, Equation 11.13 may be integrated with respect to height to give

$$F_z - F_0 = -\int_0^z \frac{\partial \bar{s}}{\partial t}\,\partial z \qquad (11.15)$$

The term on the right represents the change in storage of s in the air mass between the surface and the height z. Baldocchi et al. (1988) showed that these errors are generally small during the day but can be significant at dusk, overnight, and at dawn when

turbulent mixing is low. This is particularly relevant to flux measurements over forests, as discussed later.

Equation 11.13 shows that we must have instrumentation that can sample vertical wind speeds and scalar concentrations and be able either to perform real-time analysis in which means are subtracted from raw data to yield the fluctuating components from which cross-products are formed or to store all the raw data for later processing in the laboratory.

In principle, then, Equation 11.13 defines the eddy covariance method but, in reality, there are a number of corrections that have to be applied to allow for instrumental and software effects on the final flux. Of more concern however, is the acceptance, based on recent field studies, that large-scale subsidence in the ABL and nocturnal (katabatic) drainage can induce a non-zero mean vertical velocity and thus a mass flux that has to be taken into account in any study using eddy covariance. If, in expansion of the conservation equation (Equation 11.11) we omit the molecular terms and concentrate on the x-z plane for clarity (x being aligned with the mean wind direction and z is perpendicular to the local ground surface) and we use c for scalar concentration then

$$\frac{\partial c}{\partial t} + \frac{\partial (uc)}{\partial x} + \frac{\partial (wc)}{\partial z} = S \qquad (11.16)$$

After Reynold's decomposition as before, we get:

$$\frac{\partial \bar{c}}{\partial t} + \frac{\partial \overline{u'c'}}{\partial x} + \bar{u}\frac{\partial c}{\partial x} + \bar{c}\frac{\partial \bar{u}}{\partial x} + \frac{\partial \overline{w'c'}}{\partial z} + \frac{\partial (\bar{w}\bar{c})}{\partial z} = S \qquad (11.17)$$

Given the not unreasonable assumption that air is incompressible over the small heights involved, Lee (1998) writes:

$$\frac{\partial \bar{u}}{\partial x} = -\frac{\partial \bar{w}}{\partial z} \approx -\frac{\bar{w}_r}{z_r} \qquad (11.18)$$

and a more complete equation for a flux by eddy covariance becomes (Equation 11.19)

$$F_0 = \int_0^{z_r} \frac{\partial \bar{c}}{\partial t}\, dz + (\overline{w'c'})_r + \bar{w}_r(\bar{c}_r - \langle \bar{c} \rangle) \qquad (11.19)$$

(overbars represent means over a specified averaging period, subscript r represents parameters at the reference level) where z_r is the reference or measurement height, $\langle c \rangle$ is the mean scalar concentration between the ground and the reference level, w_r is the vertical velocity at the reference height. Thus the simple Equation 11.13 has been modified to acknowledge that canopy storage below the level of measurement has to be measured (the first term on the right-hand side of Equation 11.19), together with the eddy flux itself (second term), *plus* a mass flow term (third term) to allow for horizontal flow convergence/divergence or a non-zero mean vertical velocity.

Mention has been made already of the relatively small size of the storage correction during the day, but at night it can be substantial. The correction term for non-zero mean velocity or convergence arises at even seemingly ideal field sites for micrometeorology. Atmospheric subsidence is common in highly convective conditions and in synoptic-scale subsidence; local circulations, such as lake breezes (Sun et al. 1998) and katabatic drainage even on slopes as little as 1:1000, can induce a non-zero mean vertical velocity, as drainage flow on a slope is compensated by a descending motion. According to Lee (1998) a mean vertical velocity of 3 cm sec^{-1} could be generated on a slope of only 1°. The implications for long-term flux measurement over a forest site of a trace gas such as CO_2 are important. Lee (1998) showed that the mass flow mechanism may contribute as much as 12 μmol m^{-2} sec^{-1} with a mean vertical velocity of only 0.5 cm sec^{-1}. He also gives the example of a typical flux site with a slope of 1°, which induced a mean vertical velocity at night of 1 cm sec^{-1}, sufficient to induce a mass flux that was twice the size of the measured eddy flux. As Lindroth et al. (1998) point out, for their long-term flux site in an old-growth spruce plantation in Sweden, a 1 μmol m^{-2} sec^{-1} bias averaged over 12 hours per day for 365 days would be equivalent to 200 g C m^{-2} yr^{-1} and large enough to change the sign of the net carbon flux over this period. Since the size of the correction term is proportional to height, the problem is not so large over short canopies, such as cereals.

Correction Terms in Eddy Covariance

Although the eddy covariance technique is widely considered to carry with it the least amount of empirical baggage of any micrometeorological tech-

nique, there are two other main sets of corrections that need to be applied:

1. The concentration of a trace gas may require correction if its partial pressure is measured rather than mixing ratio, as changes to air density arise from the simultaneous transfer of sensible and latent heat.
2. Corrections that apply to the whole system arise from the unavoidable fact that any measuring system has some influence on the measurement itself and no sampling system can be regarded as responding perfectly to all flux-carrying eddies. Although eddy covariance is the most direct micrometeorological method for measuring surface fluxes, the limitations of sensor response and data acquisition hardware introduce some uncertainty in the flux measurements.

We can summarize the required corrections as:

1. corrections to constituent density because of simultaneous transfer of sensible heat (to be discussed below);
2. the sensor may not be capable of responding quickly enough to all of the flux-carrying eddies moving past it;
3. the sensor for w may be too far from the scalar sensor and flux loss can occur (by reducing the covariance between the signals);
4. the entity in question must be averaged to some extent by the finite sampling volume of the sensor, for example, typically 20 cm between sonic transducers or between the source and detector of infrared radiation in an open-path analyzer;
5. the data acquisition hardware may not sample rapidly enough to capture high-frequency eddies; and
6. in the special case of using a closed-path analyzer, when the air is brought to the analyzer through a sampling tube, some meters long, some of the turbulent structure will be lost, particularly the higher frequencies and, unless accounted for, this will result in flux underestimation.

Corrections for Changes in Air Density

A paper by Webb, Pearman, and Leuning (1980), hereafter WPL, drew attention to the need to consider corrections to the measured flux because of changes to air density. The simultaneous transfer of sensible and latent heat causes fluctuations in air density that can be erroneously attributed to fluctuations in CO_2 and latent heat in sensors that measure the partial density of CO_2 or H_2O in air. A number of papers have explored the consequences of the WPL corrections; for example, Leuning et al. (1982) provided experimental proof of the WPL corrections, Leuning and Moncrieff (1990) developed the arguments for a closed-path system, and Leuning and King (1992) applied the equations to both open- and closed-path systems. For a closed-path system, the relationship between the CO_2 density in air (ρ_c) and that measured inside the optical bench of the infrared gas analyzer (IRGA) is

$$\rho_c = \left[\frac{pT_i}{p_i T}\right]\rho_{ci} \qquad (11.20)$$

where the subscript i refers to conditions inside the optical bench. The final working equation for CO_2 measured by a closed-path analyzer is

$$F_c = \left[\frac{\overline{pT_i}}{\bar{p}_i\bar{T}}\right][\overline{w'\rho'_{ci}} + \mu(\bar{\rho}_c/\bar{\rho}_a)\overline{w'\rho'_{vi}}] \qquad (11.21)$$

This equation assumes that both water vapor and CO_2 are brought to a common temperature and pressure within the optical bench. This is true for the Li-Cor 6262, an IRGA commonly used in closed-path systems; if the latent heat flux is measured by an open-path instrument, the latent heat flux has to be WPL corrected also before it can be used in Equation 11.8 (Leuning and Moncrieff, 1990). In a closed-path system, evaporation can be found from:

$$E = \left[\frac{\overline{pT_i}}{\bar{p}_i\bar{T}}\right](1 + \mu\sigma)\overline{w'\rho'_{vi}} \qquad (11.22)$$

where E is water vapour flux; $\mu = m_a/m_v$, the ratio of the molecular masses of dry air to water vapor; $\sigma = \rho_v/\rho_a$, the ratio of mean water vapor density to that of dry air; T is Kelvin temperature; the overbars indicate time averages; and the primes denote fluctuations.

Instrumentation and Site Requirements for Eddy Covariance

Sensors

The primary requirement for sensors that are to be used in eddy covariance is the ability to respond to the full range of flux-carrying eddies. If we refer to

our model of eddy transport, we can argue that the total flux of any scalar will be carried by the eddies with a range of sizes. Although eddies are continually undergoing change, it can help to describe eddies either by their cross-sectional diameter or wavelength, l, in the space domain, or by their frequency, n, in the time domain. Taylor's "frozen turbulence" model relates the two measures by the horizontal windspeed (u)

$$n = u/l \tag{11.23}$$

a relationship that is adequate for eddies with a wavelength under about 100 m, whereas larger eddies may not move at the local average wind speed. The intensity of an eddy is proportional to its kinetic energy and the total flux density of any scalar is carried by all the eddies in the spectrum, albeit not all contributing equally to the transport.

In order to compare spectra at different heights above the surface and in different wind speeds, we can use a normalized frequency (f) where

$$f = n(z - d)/u \tag{11.24}$$

It has been established by experiment that almost all of the flux is carried by eddies in the range $0.001 < f < 10$ (McBean 1972; Anderson et al. 1986). Such knowledge is important if fluxes are to be correctly calculated. For example, Garratt (1975) showed that CO_2 fluxes measured in a system using a Gill propeller anemometer (whose response time was about 0.5 sec) at a height of 1.5 m above the vegetation were 40% in error. If the anemometer had been placed at a height of about 5 m, the error would have been reduced to about 14%. Thus, the instrument frequency response time should be $10(z - d)/u$ or, on the other hand, it implies that the height of the instrument over the zero plane should be at least equal to $n_c u/10$ where n_c is the intrinsic cutoff frequency.

For closed-path analyzers, the intrinsic cutoff frequency (n_c) is in the order of 2.5 to 5 Hz, which typically decreases to about 0.5 Hz because of the damping effect induced by the sampling tube. Corrections for these effects are now well known and a system can be designed at the outset to have particular characteristics of frequency response (Leuning and Moncrieff 1990; Leuning and Judd 1996).

Since signals of two sensors become increasingly uncorrelated with increasing separation distance, the correct separation distance between instruments should be less than the length scale of the smallest eddy to be detected. Kristensen and Fitzjarrald (1984) indicated that the maximum separation distance (d_1) between two sensors measuring scalar quantities (e.g., sensible heat, water vapor, CO_2) should be:

$$d_1 \leq \frac{z - d}{5} \tag{11.25}$$

Sensors appropriately installed are important to minimize the effect of flow distortion. As recommended by Wyngaard (1988) the design of an eddy covariance array must be vertically symmetrical about its horizontal midplane to minimize the flow distortion effect. It is also recommended to place the inlet of the tube just below the sonic anemometer head, in order to minimize effects on w (Valentini et al 1996).

Instrument noise affects the uncertainty of a flux measurement for a given sampling period. The eddy covariance technique is inherently a noise rejection method since the flux contribution from random noise tends to be zero (i.e., the random noise of vertical wind speed and scalar measurements is not correlated). However, under certain circumstances, this general principle does not hold, especially when the statistics of turbulence are not enough to reduce the correlated random noise. Lumley and Panofsky (1964) derived the following expression to estimate the sampling time (T_s) required to obtain a given level of accuracy (α) of flux determination:

$$T_s = \frac{2\tau\sigma_\xi^2}{(\alpha\bar{\xi}^2)} \tag{11.26}$$

where $\bar{\xi}$ and σ_ξ^2 are the mean and variance of a turbulent quantity, and τ is an integral time scale usually approximated as $(z - d)/u$.

The ratio σ_ξ^2/ξ^2 is often assumed to be equal to 5 (Auble and Meyers 1992), and thus a simple expression for the required sampling time (seconds) in order to obtain an accuracy of 10% in the flux estimate is:

$$T_s = 1000 \frac{z - d}{u} \tag{11.27}$$

To satisfy these error requirements, sampling periods of about two hours are often found. However, such long sampling periods may invalidate the

steady state condition requirement under field conditions. To avoid undesirable effects, typically from the diurnal variation in important micrometeorological variables (e.g., solar radiation, air temperature, humidity), it is generally accepted that a 30-minute sampling interval is adequate to achieve an overall accuracy of about 10%, in near-neutral conditions (Lenschow et al. 1994; Baldocchi et al. 1988; Verma 1990). Longer averaging times to measure covariance are generally not suggested.

It is not possible to create an eddy covariance system that has no effect whatsoever on the fluxes it is designed to measure. Instruments do not have an infinitesimally small response time, nor can nearly co-located instruments sample exactly the same parcel of air simultaneously. As for actually digitizing and recording the signal, the sampling frequency and time constraints of analog or digital filters also influence the magnitude of the loss of signal. In this section, we describe the errors introduced into flux measurements by the components of a typical closed-path system as described by Moncrieff et al. (1997). The corrections that need to be applied are frequency-dependent, that is, they depend on the spectra and co-spectra shapes. Typically, a small fraction of the total flux may be carried by small, high-frequency eddies that cannot be detected by the measuring system. The approach used here is to ascribe this "flux loss" to its component origins by a series of transfer functions. A transfer function is simply a multiplier in the range 0 to 1 that varies with frequency. Moore (1986) proposed a scheme whereby a series of transfer functions could be defined for each of the correction terms required in an eddy covariance system. We can write the fractional error in measured flux ($\Delta F_c/F_c$) as

$$\frac{\Delta F_c}{F_c} = 1 - \frac{\int_0^\infty T_{w\rho_c}(n) C_{w\rho}(n) \mathrm{d}n}{\int_0^\infty C_{w\rho}(n) \mathrm{d}n} \qquad (11.28)$$

where $T_{w\rho_c}(n)$ is the convolution of all the transfer functions applicable to the measurement and $C_w\rho(n)$ is the cospectrum of the flux F_c. n is the natural frequency. The transfer functions have been verified for individual eddy covariance systems described elsewhere (Shuttleworth et al. 1988; Moncrieff et al. 1997).

Sonic Anemometer. A typical ultrasonic anemometer used in eddy covariance systems is a three-axis design, manufactured by Gill Instruments (Solent A1012R, Gill Instruments, Lymington, UK). The instrument is fully waterproof, consumes 700 mW of power and can operate at windspeeds up to 60 m sec^{-1}. The time-of-flight principle is employed to produce u, v, w and speed of sound (which is used to calculate virtual temperature). Sets of eight transmissions are made between each pair of transducers at a rate of 21 Hz, producing an accuracy of 2 cm sec^{-1} in horizontal and vertical components. The virtual temperature is obtained from the transit time of the ultrasonic pulses (Kaimal and Businger 1963; Kaimal and Gaynor 1991) using the relation

$$c_s = 403\, T_{air}\left(1 + 0.32\,\frac{e}{p}\right) \qquad (11.29)$$

where c_s is the speed of sound in air, T_{air} is Kelvin air temperature, e is the vapor pressure of water in air and p is the absolute atmospheric pressure. A sonic temperature (T) is defined as

$$T = \frac{c_s^2}{403} = T_{air}\left(1 + 0.32\,\frac{e}{p}\right) \qquad (11.30)$$

According to Stull (1988) the sonic temperature is close to the virtual or potential temperature

$$\theta = T_{air}\left(1 + 0.38\,\frac{e}{p}\right) \qquad (11.31)$$

Using the sonic virtual temperature for the calculation of sensible heat flux will be adequate under most conditions. At high wind speeds there are additional errors resulting from wind speed and momentum stress that need to be considered (Schotanus et al. 1983).

Infrared Gas Analyzer. A common closed-path infrared gas analyzer used in eddy covariance is the Li-Cor 6262 (Li-Cor, Lincoln, NE, USA), which measures CO_2 and H_2O in air with a quoted cutoff frequency of 5 Hz. Software on the IRGA can be used to correct CO_2 measurements for water vapor dilution and band-broadening effects. Changes in barometric pressure affect the analyzer span but this can be corrected for in software by continuous measurement of the pressure in the atmosphere and the

sample tube of the analyzer. Changes in instrument temperature affect zero drift. Power consumption of the IRGA is 8 to 12 watts, dependent on temperature.

Figure 11.5 depicts the air circuit part of a typical eddy covariance system with air being drawn through the analyzer by a pump at the end of the sampling line (Moncrieff et al. 1997). The material of the sample tube should not interact with CO_2 and water vapor, and we have successfully used Dekabon 1300 tubing (6-mm internal diameter, Samual Moore, OH, USA). Tube diameter affects flow rate, pressure drop, and the energy required to draw air through the system. More importantly, the internal diameter of the tubing can be chosen to ensure either turbulent or laminar flow (Leuning and Moncrieff 1990). The mass flow controller (Tylan FC2900B, Tylan General, Swindon, UK) maintains the flow rate in the tube within a small range and thus ensures that the time of travel for any air sample remains nearly constant.

Evaluation of Eddy Covariance Systems

The quality of eddy covariance data sets can be tested by a number of quality checks as suggested by Foken and Wichura (1996). Basic tests for water vapor flux would include closure of the surface energy balance (e.g., Verma et al. 1986; Valentini et al. 1991; Greco and Baldocchi 1996) but for CO_2

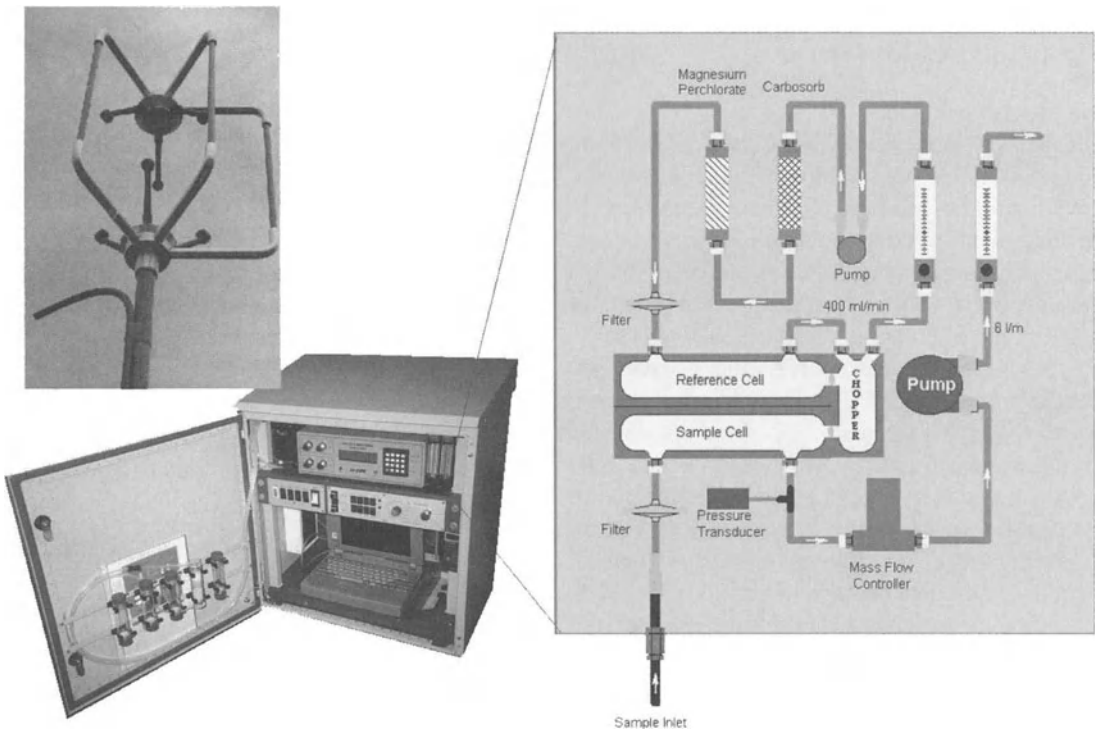

FIGURE 11.5. A schematic of a typical eddy covariance system. A sonic anemometer (top left) above the canopy measures the turbulent fluxes of horizontal and vertical wind speeds. Air is sucked down an inlet tube near the sonic head to a fast-responding infrared gas analyzer (bottom left) at the base of the tower. The expanded schematic (right) shows the gas path within the gas analyzer. A mass flow controller and pressure transducer can be used to maintain a constant rate of flow down the sample tube (and hence constant lag of gas sample between the sonic head and optical bench of the IRGA). Gas concentrations in the sample cell are measured relative to a reference cell in which air is dried and scrubbed of carbon dioxide.

flux, no such closure scheme is possible. Consequently, one tries to test either individual components of the system or the system as a whole by comparing its behavior against some parameter that is based on well-established and, hopefully, rigorous theory. For example, the adequacy of the frequency response of the eddy covariance system can be tested by spectral analysis of the scalar fluxes. In particular, because of the attenuation of fluctuations through the tube in a ducted system, the frequency response for CO_2 and H_2O fluxes is significantly reduced. One way to evaluate the magnitude of this problem is to compare the sensible heat flux density co-spectra, which is measured at the entrance to the tube, with the H_2O and CO_2 flux density co-spectra measured in the analyzer. The difference, usually found at the high-frequency end of the power spectra, can be used to account for the loss of fluxes, determined by frequency losses within the system (Leuning and Moncrieff 1990).

Conditional Sampling

Conditional sampling is a conceptually simple micrometeorological technique in which air is sampled into one of two sampling reservoirs (or sampling lines for on-line analysis), according to whether an up- or down-draught of air is measured by a sonic anemometer. After a suitable interval of time, say 30 to 60 minutes, the net vertical flux of the trace gas species of interest is proportional to the difference in gas concentration between the sampling reservoirs. The method is attractive as it can be used for trace gases or pollutants for which no suitable fast-response sensor is available and hence the alternative technique of eddy covariance is unsuitable (e.g., Majewski et al. 1993). The requirement for a fast sensor to measure vertical windspeed remains, but there is considerable relaxation in the speed requirement for the chemical analyzer. A further advantage is that by accumulating gas into reservoirs, the difference between the samples is enhanced and it is then possible to use high-precision gas analyses in the laboratory to determine the differences (Businger and Delaney 1990)

The method was first suggested by Desjardins (1977) for sensible heat flux and given the name eddy accumulation. Although attractive in principle, early studies using this method sampled air at a rate proportional to the magnitude of the vertical windspeed and this was technically difficult to achieve with the required accuracy. Hicks and McMillen (1984) suggested, almost as an aside, that a simplified method might work which would eliminate some of the practical difficulties. The simple method would be to sample air at a constant rate into either bag rather than at a rate proportional to vertical windspeed. One bag will then contain air collected in updraughts and the concentration of CO_2, say, would be c^+; the downdraught bag will have a CO_2 concentration of c^-. The idea was taken up by Businger and Oncley (1990) who wrote the flux (F_c) for a gas with concentration c, as

$$F_c = \beta\sigma_w(c^+ - c^-) \qquad (11.32)$$

where β is an empirical coefficient usually determined by experiment, σ_w is the standard deviation of the vertical windspeed, and $(c^+ - c^-)$ is the gas concentration difference between the two sampling bags at the end of the sampling period. As Businger and Oncley point out, the measurement of $(c^+ - c^-)$ is a direct difference of concentration not weighted by the magnitude of vertical wind speed in the original method. Thus in this method they *relax* the conditions for the original eddy accumulation and the method is based simply on sampling air into different reservoirs on the condition of either upward- or downward-moving air. The technique is known equally as conditional sampling or relaxed eddy accumulation (CS/REA). Figure 11.6 shows a schematic of a typical conditional sampling system in which fluxes of methane (CH_4) were routinely monitored on-line within a CS/REA system. In general, the CS/REA method has been well validated over the past few years although for fluxes of carbon and water, eddy covariance remains the more appropriate choice (Pattey et al. 1992; Oncley et al. 1993). Conditional sampling has a role in measuring fluxes of biogenic compounds and other trace gases for which no suitable eddy covariance sensors exist, for example, nitrous oxide (N_2O), non-methane hydrocarbons, and CH_4 (Moncrieff et al. 1998).

Errors in Long-Term Measurements of Fluxes of Carbon and Water

There are a number of sources of uncertainty associated with flux measurements made above the canopy by the micrometeorological methods de-

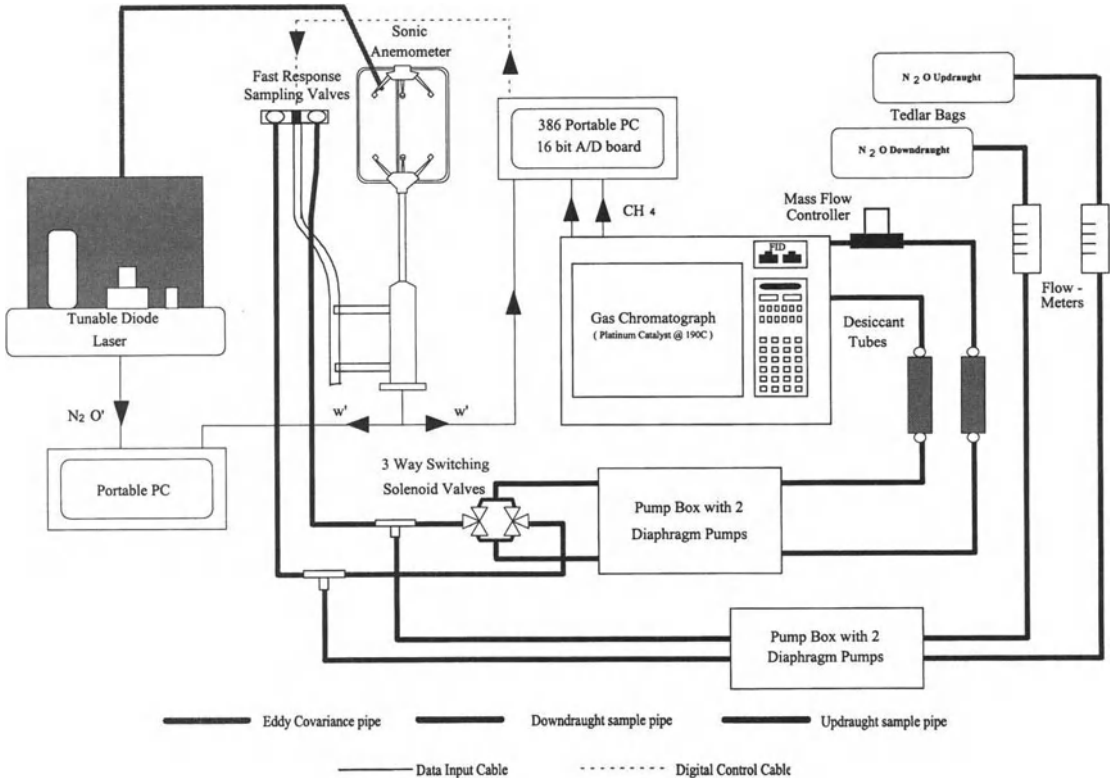

FIGURE 11.6. A schematic of a conditional sampling system. In this representation, the system is set up to measure simultaneous fluxes of methane and nitrous oxide. The vertical wind speed is measured by a sonic anemometer (center left of the diagram) and, dependent on whether an updraught or downdraught has been measured, the appropriate sample valve is opened and air is sucked into a reservoir or passed into a gas analyser. Further details of the systems shown here can be found in Beverland et al. 1996. (The tunable diode laser in this schematic is operating as part of a ducted eddy covariance system.)

scribed above. It is generally accepted that the variability in the natural environment (surface and atmosphere) coupled with the inevitability of an imperfect sensing system, gives rise to uncertainties in flux estimates on the order of 10 to 20% (Wesely and Hart 1985). The implication of this degree of uncertainty (and this assumes that all else being equal, the site of flux measurements is ideal and that the underlying assumptions are not invalidated) has been explored in a number of studies reporting long-term estimates of carbon and water exchange. It is possible to quantify errors into random and systematic types and to arrive at a final uncertainty estimate for the overall net flux. Moncrieff et al. (1996) show that for a site in the Amazon, it was possible to state unequivocally that it was a sink for carbon given the likely nature of the errors identified. Goulden et al. (1996) report that with careful checks on data quality, it is possible to reduce the overall uncertainty in annual flux estimates to $\pm 5\%$.

Related Techniques

Eddy covariance sensors can be adapted for flight on-board aircraft and flown through the ABL at heights of 100 m and more. When such measurements are made in conjunction with tower-based flux estimates, much of the difference in flux estimates comes down to differences in flux footprint as seen by the different systems (Desjardins et al.

1992). Aircraft-based techniques remain expensive to buy and maintain, and operate for only limited periods at a time. A more practical alternative is required that can be used by many research groups. One method currently being tested is a mass budget of the CBL, developed by Raupach et al. (1992). Under commonly encountered daytime conditions, a CBL is present over the surface of the earth. At the top of this layer is a temperature inversion, which effectively separates the air that has been influenced by the surface from the overlying air of the free atmosphere. Over the course of a day, the CBL grows from tens of meters in the early morning to a height of 1 to 3 km in the late afternoon, entraining air from the free atmosphere as it rises. As the photosynthetic rate increases with irradiance, the CO_2 concentration in the CBL is reduced below that in the free atmosphere above.

In principle, the CBL can be treated as a huge cuvette, in which the surface fluxes can be inferred from measured changes in CO_2 concentration and CBL height over time. The method is based on the conservation of mass equation for CO_2 in the *well-mixed* CBL, which can be written in integral form as:

$$F_c = [(\rho_2 h_2 + \rho W_t(t_2 - t_1))(C_t - C_{m2}) - \rho_2 h(C_t - C_{m1})]/(t_2 - t_1) \quad (11.33)$$

where F_c is the flux of CO_2 integrated between time t_1 and t_2, ρ is air density averaged over the CBL, h is the height of the CBL, W_t is the vertical velocity above the CBL, and C_m and C_t are the CO_2 concentrations in the mixed layer of the CBL and the free troposphere above, respectively. Equation 11.33 yields cumulative surface fluxes representing the area traversed by a column of air in the course of a day, and so may extend a few hundred kilo-

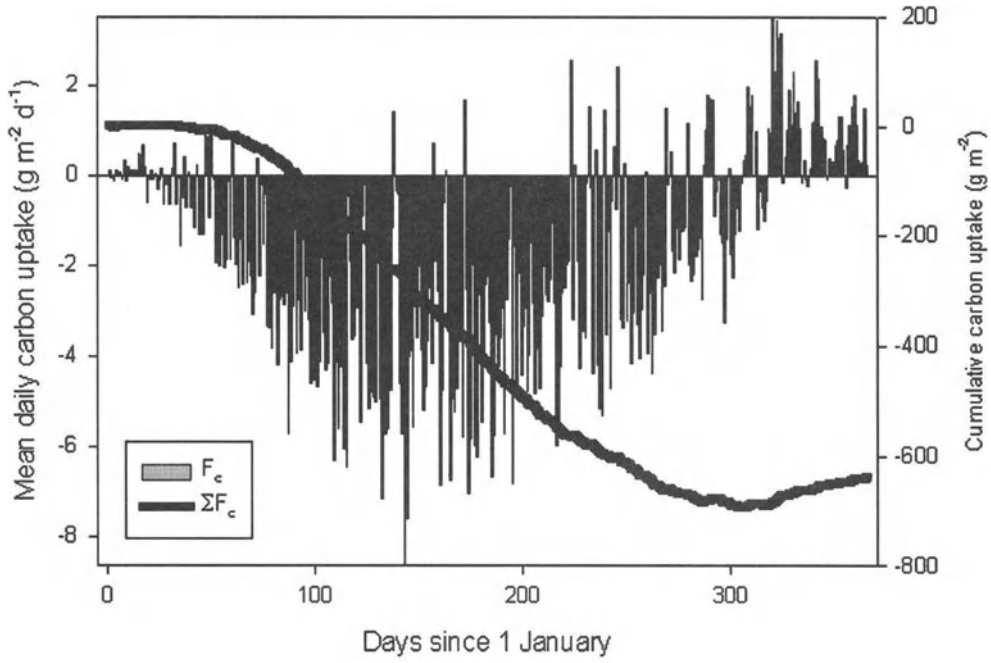

FIGURE 11.7. Typical long-term flux measurements at a EUROFLUX site, Griffin forest, UK. The narrow bars represent the daily carbon uptake (g m^{-2} day^{-1}) from the start of 1997. The heavy solid line shows the cumulative carbon uptake (g m^{-2}) over the course of the year. The growing season was 255 days long at this site in 1997 and the forest sequestered 638 g C m^{-2} over the whole year. For 1998 and 1999, the total C sequestered was 621 and 615 g C m^{-2}, respectively, at this site.

meters upwind and cover an area of 1000 to 10,000 km^2 (Raupach et al. 1992).

The budget method requires an estimate of the CO_2 concentrations of the air that is entrained as the CBL grows over the day. Tropospheric values (C_t) may be estimated from oceanic sites. Also, if there is a significant residual layer in the morning, the concentration in this layer can be measured with tethered balloon-borne instruments. The budget method has been tested in a number of field experiments so far (Munley and Hipps, 1991; Denmead et al. 1996; Levy et al. 1999), generally with encouraging results.

Again, as with aircraft platforms, the flux obtained by this boundary-layer budget approach is unlikely to be exactly the same as that obtained by tower-based systems because of the different source areas for the two fluxes. The height of the CBL (for inclusion in Equation 11.31) can be monitored by a radiosonde system or modeled according to best practice. Vertical velocity (W_t) can also be obtained from radiosonde data if it is assumed that horizontal divergence is constant with height (Gryning and Batchvarova 1998) or from operational analysis from major weather forecasting bureaux. Profiles of CO_2 concentration can be obtained either from balloon-borne systems or from tall towers. The method is sensitive to the value for C_t and this is best obtained with an aircraft-borne system.

Conclusions

Measuring canopy fluxes by micrometeorological methods bridges the gap between plot- and leaf-scale process studies on the one hand and aircraft- or space-borne platforms on the other. All such techniques are complementary and are best deployed in combination with process-based models of ecosystem functioning. Micrometeorological flux measurements above the canopy can be made routinely and can operate indefinitely given appropriate resources. They are a direct form of measurement, are nondestructive, and fluxes obtained from them are the spatial average of several km^2 upwind from the measuring point. Careful implementation of these techniques in appropriate parts of the landscape can mean that long-term canopy measurements of carbon and water can be reported to have an accuracy of more than 90 to 95%. The proposed networks of flux stations based on eddy covariance systems in particular, promise to deliver routine and long-term measurements of the cycling of energy, water, and carbon in a range of important ecosystems (Baldocchi et al. 1996, Figure 11.7). Such networks are essential to investigate and monitor ecosystems as they undergo change in the future.

References

Anderson, D.E.; Verma, S.B.; Clement, R.J.; Baldocchi, D.D.; Matt, D.R. Turbulence spectra of CO_2, water vapor, temperature and velocity over a deciduous forest. Bound. Lay. Meteorol. 38:81–99; 1986.

Auble, D.L.; Meyers, T.P. An open path, fast response infrared-absorption gas analyzer for H_2O and CO_2. Bound. Lay. Meteorol. 59:243–256; 1992.

Aubinet, M.; Grelle, A.; Ibrom, A.; Rannik, Ü.; Moncreiff, J.; Foken, T.; Kowalski, G.S.; Martin, P.H.; Berbigier, P.; Bernhofer, Ch.; Clement R.; Elbers, J.; Wranier, A.; Grünwald, T.; Morgenstern, K.; Pilegaard, K.; Rebmann, C.; Snijders, W.; Valentini, R.; Vesala, T. Estimates of the annual net carbon and water exchange of forests: the EUROFLUX methodology. Adv. Ecol. Res. 30:113–175; 2000.

Baldocchi, D.D.; Hicks, B.B.; Meyers, T.P. Measuring biosphere-atmosphere exchanges of biologically related gases with micrometeorological methods. Ecology 69:1331–1340; 1988.

Baldocchi, D.D.; Valentini, R.; Running, S.; Oechel, W.; Dahlman, R. Strategies for measuring and modelling carbon dioxide and water vapour fluxes over terrestrial ecosystems. Global Change Biol. 2:159–168; 1996.

Baldocchi, D.D.; Meyers, T. On using eco-physiological, micrometeorological and biogeochemical theory to evaluate carbon dioxide, water vapor and trace gas fluxes over vegetation: A perspective. Agric. For. Meteorol. 90:1–25; 1998.

Barr, A.G.; King, K.M.; Gillespie, T.J.; den Hartog, G.; Neumann, H.H. A comparison of bowen ratio and eddy correlation sensible and latent heat flux measurements above deciduous forest. Bound. Lay. Meteorol. 71:21–41; 1994.

Beverland, I.J.; Óhéill, D.; Scott, S.L.; Moncrieff, J.B. Design, construction and operation of flux measurement systems using the conditional sampling system. Atmos. Env. 30:3209–3220; 1996.

Businger, J.A. Evaluation of the accuracy with which dry deposition can be measured with current micrometeorological techniques. J. Clim. Appl. Meteorol. 25:1100–1124; 1986.

Businger, J.A.; Delaney, A.C.; Chemical sensor resolution required for measuring surface fluxes by three

common micrometeorological techniques. J. Atmos. Chem. 10:399–410; 1990.

Businger, J.A.; Oncley, S.P. Flux measurement with conditional sampling. J. Atmos. Ocean. Technol. 7:349–352; 1990.

Denmead, O.T.; Raupach, M.R.; Dunin, F.X.; Cleugh, H.A.; Leuning, R.L. Boundary layer budgets for regional estimates of scalar fluxes. Global Change Biol. 2:255–264; 1996.

Desjardins, R.L. Description and evaluation of a sensible heat flux detector. Bound. Lay. Meteorol. 11:147–154; 1977.

Desjardins, R.L.; Hart, R.L.; MacPherson, J.I.; Schuepp, P.H.; Verma, S.B. Aircraft- and tower-based fluxes of carbon dioxide, latent, and sensible heat. J. Geophys. Res. 97:18477–18485; 1992.

Fang, C.; Moncrieff, J.B. An open-top chamber for measuring soil respiration and the influence of pressure differences on CO_2 efflux measurement. Func. Ecol. 12:319–325; 1998.

Finn, D.; Lamb, B.; Leclerc, M.Y.; Horst, T.W. Experimental evaluation of analytical and lagrangian surface-layer flux footprint models. Bound. Lay. Meteorol. 80:283–308; 1996.

Flanagan, L.B.; Brooks, J.R.; Ehleringer, J.R. Photosynthesis and carbon respiration in boreal forest ecosystems in relation to species and climate. J. Geophys. Res. 102:28861–28869; 1997.

Flesch, T.K. Backward-time lagrangian stochastic dispersion models and their application to estimate gaseous emissions. J. Appl. Meteorol. 34:1320–1332; 1995.

Foken, Th.; Wichura, B. Tools for quality assessment of surface-based flux measurements. Agric. For. Meteorol. 78:83–105; 1996.

Fowler, D.; Unsworth, M.H. Turbulent transfer of sulphur dioxide to a wheat crop. Q. J. Roy. Meteorol. Soc. 105:767–783; 1979.

Garratt, J.R. Limitations of an eddy correlation technique for the determination of turbulent fluxes near the surface. Bound. Lay. Meteorol. 8:255–255; 1975.

Gash, J.H.C. A note on estimating the effect of limited fetch on micrometeorological evaporation measurements. Bound. Lay. Meteorol. 35:409–414; 1986.

Goulden, M.L.; Munger, J.W.; Fan, S-M.; Daube, B.C.; Wofsy, S.C. Measurements of carbon sequestration by long-term eddy covariance: Methods and a critical evaluation of accuracy. Global Change Biol. 2:169–182; 1996.

Gower, S.T.; Vogel, C.A.; Norman, J.M.; Kucharik, C.J.; Steele, S.J.; Stow, T.K. Carbon distribution and aboveground net primary production in aspen, jack pine and black spruce stands in Saskatchewan and Manitoba, Canada. J. Geophys. Res. 102:29029–29041; 1997.

Greco, S.; Baldocchi, D.D. Seasonal variations of CO_2 and water vapour exchange rates over a temperate deciduous forest. Global Change Biol. 2:183–197; 1996.

Grelle, A.; Lindroth, A. Eddy-correlation system for long-term monitoring of fluxes of heat, water vapour and CO_2. Global Change Biol. 2:297–307; 1996.

Gryning, S.E.; Batchvarova, E. Estimation of sensible heat fluxes from the growth of the daytime boundary layer. Agric. Forest Meteorol. 98–99:159–167; 1999.

Harden, J.W.; O'Neill, K.P.; Trumbore, S.E.; Veldhius, H.; Stocks, B.J. Moss and soil contributions to the annual carbon flux of a maturing boreal forest. J. Geophys. Res. 102:28805–28816; 1997.

Hicks, B.B.; McMillen, R.T. A simulation of the eddy accumulation method for measuring pollutant fluxes. J. Clim. Appl. Meteorol. 23:637–643; 1984.

Horst, T.W.; Weil, J.C. How far is far enough? The fetch requirements for micrometeorological measurements of surface fluxes. J. Atmos. Ocean. Technol. 11:1018–1025; 1994.

Hutchinson, G.L.; Livingston, G.P. Use of chamber systems to measure trace gas fluxes. In: Harper, L.A.; Moiser, A.R.; Duxburg, J.M.; Rolston, D.E., eds. *Agricultural Ecosystem Effects on Trace Gases and Global Climate Change.* American Society of Agronomy Special Publication No. 55. Madison, WI: American Society of Agronomy, Crop Science Society of America, and Soil Science Society of America; 1993:63–78.

Jarvis, P.G.; Sandford, A.P. Temperate forest. In: Baker, N.R.; Long, S.P., eds. *Topics in Photosynthesis. Vol. 7. Photosynthesis in contrasting environments.* Amsterdam: Elsevier 1986:199–236.

Kaimal, J.C.; Businger, J.A. A continuous wave sonic anemometer-thermometer. J. Appl. Meteorol. 2:156–164; 1963.

Kaimal, J.C.; Gaynor, J.E. Another look at sonic thermometry. Bound. Lay. Meteorol. 56:401–410; 1991.

Kaimal, J.C.; Finnegan, J.J. Atmospheric Boundary Layer Flows. Their Structure and Measurement. New York: Oxford Univ. Pr.; 1994.

Kristensen, L.; Fitzjarrald, D.R. 1984. The effect of line averaging on scalar flux measurements with a sonic anemometer near the surface. J. Atmos. Ocean. Technol. 1:138–146; 1984.

Lavigne, M.B.; Ryan, M.G. Growth and maintenance respiration rates of aspen, black spruce and jack pine stems at northern and southern BOREAS sites. Tree Physiol. 17:543–551; 1997.

Lee, X. On micrometeorological observations of surface-air exchange over tall vegetation. Agric. For. Meteorol. 91:39–49; 1998.

Lenschow, D.H. Micrometeorological techniques for measuring biosphere-atmosphere trace gas exchange.

In: Matson, P.A.; Harris, R.C., eds. *Biogenic Trace Gases: Measuring Emissions from Soil and Water.* Methods In Ecology Series. New York: Blackwell; 1995:126–163.

Lenschow, D.H.; Mann, J.; Christens, L. How long is long enough when measuring fluxes and other turbulence statistics? J. Atmos. Ocean. Technol. 11:661–673; 1994.

Leuning, R.; Denmead, O.T.; Lang, A.R.G.; Ohtaki, E. Effects of heat and water vapour transport on eddy covariance measurement of CO_2 fluxes. Bound. Lay. Meteorol. 23:209–222; 1982.

Leuning, R.L.; Judd, M. The relative merits of open- and closed-path analysers for measurement of eddy fluxes. Global Change Biol. 2:241–254; 1996.

Leuning, R.L.; King, K.M. Comparison of eddy covariance measurements of CO_2 fluxes by open- and closed-path CO_2 analysers. Bound. Lay. Meteorol. 59:297–311; 1992.

Leuning, R.L.; Moncrieff, J.B. Eddy covariance CO_2 flux measurements using open- and closed-path CO_2 analysers: Corrections for analyser water vapour sensitivity and damping of fluctuations in air sampling tubes. Bound. Lay. Meteorol. 53:63–76; 1990.

Levy, P.E.; Grelle, A.; Lindroth, A.; Molder, M.; Jarvis, P.G.; Kruijt, B.; Moncrieff, J.B. Regional-scale CO_2 fluxes over central Sweden by a boundary layer budget method. Agric. For. Meteorol. 98–99(1–4):169–180; 1999.

Lindroth, A. Gradient distribution and flux profile relations above a rough forest. Q. J. Roy. Meteorol. Soc. 110:553–563; 1984.

Lindroth, A.; Grelle, A.; Moran. A. Long term measurements of boreal forest carbon balance reveal large temperature sensitivity. Global Change Biol. 4:443–450; 1998.

Livingston, G.P.; Hutchinson, G.L. Enclosure-based measurement of trace gas exchange: Applications and sources of error. In: Matson, P.A. and Harriss, R.C., eds. *Biogenic Trace Gases: Measuring Emissions from Soil and Water.* Methods In Ecology Series. New York: Blackwell; 1995:14–51.

Lumley, J.L.; Panofsky, H.A. The structure of atmospheric turbulence. New York: Wiley; 1964.

Majewski, M.S.; Desjardins, R.L.; Rochette, P.; Pattey, E.; Seiber, J.N.; Glotfelty, D.E. A field comparison of an eddy accumulation and an aerodynamic-gradient system for measuring pesticide volatilization fluxes. J. Environ. Sci. Tech. 27:121–128; 1993.

McBean, G.A. Instrument requirements for eddy correlation measurements. J. Appl. Meteorol. 11:1078–1084; 1972.

McNeil, D.; Shuttleworth, W.J. Comparative measurements of the energy fluxes above a pine forest. Bound. Lay. Meteorol. 9:297–313; 1975.

Miranda, A.; Jarvis, P.G.; Grace, J. Transpiration and evaporation from heather moorland. Bound. Lay. Meteorol. 28:227–243; 1984.

Moncrieff, J.B.; Beverland, I.J.; O'Neill, D.H.; Cropley, F.D. Controls on trace gas exchange observed by a conditional sampling method. Atmos. Env. 32:3265–3274; 1998.

Moncrieff, J.B.; Malhi, Y.; Leuning, R.L. The propagation of errors in long-term measurements of land-atmosphere fluxes of carbon and water. Global Change Biol. 2:231–254; 1996.

Moncrieff, J.B.; Massheder, J.M.; DeBruin, H.; Elbers, J.; Friborg, T.; Huesunkveld, B.; Kabat, P.; Scott, S.L.; Soegaard, H.; Verhoef, A. A system to measure surface fluxes of momentum, sensible heat, water vapour and carbon dioxide. J. Hydrol. 188–189:589–611; 1997.

Monteith, J.L.; Unsworth, M.H. *Principles of Environmental Physics.* 2nd ed. London: Arnold; 1990.

Moore, C.J. Frequency response corrections for eddy correlation systems. Bound. Lay. Meteorol. 37:17–35; 1986.

Mulhearn, P.J. Relations between surface fluxes and mean profiles of velocity, temperature and concentration, downwind of a change in surface roughness. Q. J. Roy. Meteorol. Soc. 103:785–802; 1977.

Munley, W.G.; Hipps, L.E. Estimation of regional evaporation for a tallgrass prairie from measurements of properties of the atmospheric boundary layer. Water Resour. Res. 27:225–230; 1991.

Oncley, S.P.; Delaney, A.C.; Horst, T.W. Verification of flux measurements using relaxed eddy accumulation. Atmos. Environ. 27:2417–2426; 1993.

Pattey, E.; Desjardins, R.L.; Boudreau, F.; Rochette, P. Impact of density fluctuations on flux measurements of trace gases: implications for the relaxed eddy accumulation technique. Bound. Lay. Meteorol. 59:195–203; 1992.

Paulson, C.A. The mathematical representation of wind speed and temperature profiles in the unstable atmospheric surface layer. J. Appl. Meteorol. 9:857–861; 1970.

Raupach, M.R.; Denmead, O.T.; Dunin, F.X. Challenges in linking atmospheric CO_2 concentrations to fluxes at local and regional scales. Aus. J. Bot. 40:697–716; 1992.

Raupach, M.R.; Legg, B.J. The uses and limitations of flux-gradient relationships in micrometeorology. Agric. Water Manage. 8:119–131; 1984.

Raupach, M.R.; Thom, A.S. Turbulence in and above canopies. Annu. Rev. Fluid Mech. 13:97–129; 1981.

Rayment, M.R. Carbon and water fluxes in a boreal forest ecosystem. PhD Thesis University of Edinburgh, p. 145; 1998.

Rayment, M.B.; Jarvis, P.G. An improved open chamber system for measuring soil CO_2 effluxes in the field. J. Geophys. Res. 102:28779–28784; 1997.

Rayment, M.B.; Jarvis, P.G. Seasonal gas exchange of black spruce using an automatic branch bag system. Can. J. For. Res. 29:1528–1538; 1999.

Running, S.W.; Baldocchi, D.; Cohen, W.; Gower, S.T.; Turner, D.; Bakwin, P.; Hibbard, K. A global terrestrial monitoring network integrating tower fluxes, flask sampling, with ecosystem modelling and EOS satellite data. Remote Sens. Environ. 70(1):108–127; 1999.

Ryan, M.G.; Lavigne, M.B.; Gower, S.T. Annual carbon cost of autotrophic respiration in boreal forest ecosystems in relation to species and climate. J. Geophys. Res. 102:28877–28883; 1997.

Schmid, H.P. Source areas for scalars and scalar fluxes. Bound. Lay. Meteorol. 67:293–318; 1994.

Schmid, H.P.; Oke, T.R. A model to estimate the source area contributing to turbulent exchange in the surface layer over patchy terrain. Q. J. Roy. Meteorol. Soc. 116:965–988; 1990.

Schotanus, P.; Nieuwstadt, F.T.M.; de Bruin, H.A.R. Temperature measurements with a sonic anemometer and its application to heat and moisture fluxes. Bound. Lay. Meteorol. 26:81–93; 1983.

Schuepp, P.H.; Leclerc, M.Y.; Macpherson, J.I.; Desjardins, R.L. Footprint prediction of scalar fluxes from analytical solutions of the diffusion equation. Bound. Lay. Meteorol. 50:355–376; 1990.

Sestak, Z.; Catsky, J.; Jarvis, P.G. *Plant Photosynthetic Production. Manual of methods.* The Hague, Netherlands: Dr W. Junk; 1971.

Shuttleworth, W.J.; Gash, J.H.C.; Lloyd, C.R.; McNeil, D.D.; Moore, C.J.; Wallace, J.S. An integrated micrometeorological system for evaporation measurement. Agric. For. Meteorol. 43:295–317; 1988.

Steele, S.J.; Gower, S.T.; Vogel, C.A.; Norman, J.M. Root mass, primary production and turnover in aspen, jack pine and black spruce forests in Saskatchewan and Manitoba, Canada. Tree Physiol. 17:577–587; 1997.

Stull, R.B. *An Introduction to Boundary Layer Meteorol.* London: Kluwer; 1988.

Sun, J.; Desjardins, R.; Mahrt, L.; MacPherson, J.I. Transport of carbon dioxide, water vapor and ozone by turbulence and local circulations. J. Geophys. Res. 103:25873–25885; 1998.

Sutton, M.A.; Fowler, D.; Moncrieff, J.B. The exchange of atmospheric ammonia with vegetated surfaces. I. Unfertilized vegetation. Q. J. Roy. Meteorol. Soc. 119:1023–1045; 1993.

Thom, A.S. Momentum, mass and heat exchange. In: Monteith, J.L., ed. *Vegetation and the Atmosphere.* Chichester, UK: Academic; 1975:57–109.

Valentini, R.; De Angelis, P.; Matteucci, G.; Monaco, R.; Dore, S.; Scarascia Mugnozza, G.E. Seasonal net carbon dioxide exchange of a beech forest with the atmosphere. Global Change Biol. 2:199–207; 1996.

Valentini, R.; Scarascia Mugnozza, G.E.; De Angelis, P.; Bimbi, R. An experimental test of the eddy correlation technique over a Mediterranean macchia canopy. Plant Cell Environ. 14:987–994; 1991.

Verma, S.B. Micrometeorological methods for measuring surface fluxes. Remote Sens. Rev. 5:99–115; 1990.

Verma, S.B.; Baldocchi, D.D.; Anderson, D.E.; Matt, D.R.; Clement, R.I. Eddy fluxes of CO_2, water vapour and sensible heat over a deciduous forest. Bound. Lay. Meteorol. 36:71–91; 1986.

Webb, E.K. Profile relationships: the log-linear range and extension to strong stability. Q. J. Roy. Meteorol. Soc. 96:67–90; 1970.

Webb, E.K.; Pearman, G.I.; Leuning, R.L. Correction of flux measurements for density effects due to heat and water vapour transfer. Q. J. Roy. Meteorol. Soc. 106:85–100; 1980.

Wesely, M.L.; Hart, R.L. Variability of short term eddy correlation estimates of mass exchange. In: Hutchison, B.A.; Hicks, B.B., eds. *The Forest-Atmosphere Interaction.* Dordrecht, Netherlands: Reidel; 1985:591–612.

Wyngaard, J.C. Flow-distortion effects on scalar flux measurements in the surface layer: Implications for sensor design. Bound. Lay. Meteorol. 42:19–26; 1988.

12

Assessing Ecosystem-Level Water Relations Through Stable Isotope Ratio Analyses

James R. Ehleringer, John Roden, and Todd E. Dawson

Introduction

Virtually all elements of biological interest have multiple stable isotopic forms and the fractionation events associated with biological and physical processes help to create spatial and temporal variations in isotopic abundance that can be used to understand the dynamics of ecological systems. Stable isotope ratio analyses at natural abundance levels can provide integrated information on ecosystem functioning, such as variations in water-use activities by different elements within an ecosystem (Ehleringer et al. 1993; Dawson and Ehleringer 1998). Stable isotope ratio analyses do not provide information on water flux rates through the ecosystem, but instead they help constrain the analysis of flux data, such as through identifying those specific soil layers that are the source of current moisture use by the vegetation or the ratio of carbon dioxide–to–water (CO_2-to-H_2O) flux.

Stable Isotopes: Natural Abundances and δ Notation

Most elements are present in multiple stable forms, although one isotope is usually far more abundant than the others. Rather than consider the abundances of different stable isotopes in absolute terms, it is much more common and convenient to describe the abundance of stable isotopes as the molar ratios of the heavy-to-light forms (R) in a sample (R_{sample}) relative to that of an international standard ($R_{standard}$). This is the so called delta notation (δ) where

$$\delta = \left(\frac{R_{sample}}{R_{standard}} - 1\right) \cdot 1000‰ \quad (12.1)$$

and the δ value has units of parts per thousand, or per mil (‰).

With regard to water relations functions within ecosystems, carbon (C), hydrogen (H), and oxygen (O) isotopes are most relevant. Table 12.1 presents the typical background value for different isotopic forms as well as the range of δ values that one might encounter when investigating different ecosystem components on a global basis.

Isotope Ratio Mass Spectrometry

In isotope ratio mass spectrometry, light gases are introduced into a chamber maintained at a very low pressure ($<10^{-6}$ torr), in which there is an electron source. The gases (in our case H_2 or CO_2) are bombarded by this electron source, resulting in ion formation in approximately 1 out of every 1000–4000 molecules. The most likely molecular possibilities that are ionized include $^1H^1H$ and $^2H^1H$ for H_2 and $^{12}C^{16}O^{16}O$, $^{13}C^{16}O^{16}O$, and $^{12}C^{18}O^{16}O$ for CO_2, although other rarer combinations most certainly occur. These charged ions are then accelerated and pass along a flight tube with an even lower pressure (10^{-8} torr). During this flight, their trajectory is deflected by a magnet located at the center point. The extent of an ion's magnetic deflection depends on its m/e (i.e., mass to charge) ratio. Thus, $^1H^1H^+$ is deflected more than $^2H^1H^+$ and likewise $^{12}C^{16}O^{16}O^+$ more than $^{12}C^{18}O^{16}O^+$. At the end of the flight tube are a

TABLE 12.1. The stable isotopes that are of primary interest for addressing water relations issues within ecosystems. $R_{standard}$ is the molar abundance ratio of the heavy to light isotopic forms of the international standard. The range of expected variation is presented in delta notation with units of ‰. The reference standards are Standard Mean Ocean Water (SMOW) and Pee Dee Belemnite (PDB). Standards values are from Hayes (1983).

Element	Isotopic abundance (%)	$R_{standard}$	Typical range of δ values for different ecosystem components (‰)
Hydrogen	^{1}H 99.985	$^{2}H/^{1}H = 0.00015576$ (SMOW)	−200 to +50
	^{2}H 0.015		
Carbon	^{12}C 98.89	$^{13}C/^{12}C = 0.0112372$ (PDB)	−80 to +15
	^{13}C 1.11		
Oxygen	^{16}O 99.759	$^{18}O/^{16}O = 0.0020671$ (SMOW)	−30 to +40
	^{17}O 0.037		
	^{18}O 0.204		

series of ion current counters that measure the intensity of different mass signals that strike Faraday cups positioned to measure specific m/e ratios. From these current measurements, the relative ratio of the different masses can be determined and the isotope ratios of the sample calculated relative to that of the working and international standards.

Samples are introduced into the mass spectrometer by one of two conventional means. The first and more traditional approach is called the dual inlet mode, because its involves introducing the clean sample into one variable volume bellows and the standard into a second variable volume bellows. Both samples are then alternately introduced 6 to 12 times into the mass spectrometer from their bellows via a capillary connection to the source chamber. The isotope ratio calculation is based on the average of these 6 to 12 individual, short-term observations. This approach yields the highest precision measurement and typically the precision is ±0.006‰, ±0.25‰, and ±0.012‰ for carbon, hydrogen, and oxygen isotope ratios, respectively (Platzner et al. 1997). The second approach for introducing the sample into the chamber is called the continuous flow mode. In this approach, the sample and standard gases are carried into the mass spectrometer by a helium (He) (or argon [Ar]) carrier stream. The mass spectrometer gets a single, but longer time interval to measure the sample or standard signal. The stated precision of the continuous flow approach by different instrument manufacturers is ±0.3‰ and ±0.3‰ for carbon and oxygen isotope ratios, respectively (continuous flow hydrogen analysis is not routinely available). This lower precision arises because of the single versus multiple observation constraint and because of a reduction in ionization efficiency introduced by the presence of the He carrier. However, in practice, the precision can be much higher (<0.1‰) for carbon and oxygen isotope ratios of CO_2 gas samples (Ehleringer and Cook 1998) and ±0.1‰ and ±0.2‰ for carbon and oxygen isotope ratios of CO_2 from organic samples (Saurer et al., 1998).

Historically, the conversion of sample material from either water or organic matter into the gases that are introduced into the mass spectrometer was done off-line and the sample gases were introduced into the mass spectrometer using the dual inlet approach. Today, the continuous flow approach is becoming much more frequent because of its ease of use, which then allows peripheral instruments to be directly linked to the mass spectrometer for an on-line sample preparation and analysis (Brand 1996). It is now common to find that elemental analyzers or gas chromatographs are combined with isotope ratio mass spectrometers. For organic samples, the furnace of the elemental analyzer is used for a flash combustion reaction that ultimately allows for the sequential measurement of $\delta^{13}C$ and $\delta^{15}N$ ratios from the same sample (Platzner et al. 1997). If the combustion reaction is instead replaced by a pyrolysis reaction, measurements of $\delta^{13}C$ and $\delta^{18}O$ ratios are possible from the same sample (Saurer et al. 1998).

Meteoric Water Line

The isotopic composition of ocean water is approximately $\delta D = 0$ and $\delta^{18}O = 0$. Since the bonding is stronger when heavier isotopes are involved, the evaporating water vapor is depleted in the heavier isotopes relative to its water source. Under equilibrium conditions and at 25°C, the water vapor is depleted by approximately $-74‰$ and $-9.2‰$ for δD and $\delta^{18}O$, respectively, relative to the water source (Gat and Gonfiantini 1981). When this moisture condenses from clouds during precipitation events, the precipitation is slightly enriched in the heavier isotopes relative to the vapor remaining in the clouds. As a consequence, subsequent precipitation events from this cloud produce precipitation that is progressively more depleted in the heavier isotopes. The slope of the relationship of δD and $\delta^{18}O$ in these precipitation events should follow vapor pressure differences (i.e., $\Delta\delta D/\Delta\delta^{18}O \approx 74/9.2 \approx 8$).

The observed relationship between δD and $\delta^{18}O$ of precipitation collected from stations throughout the world generally follows a slope of 8 (Fig. 12.1). This regression is known as the meteoric water line (MWL). While local variations do exist in this relationship, the MWL serves as a foundation for predicting the isotopic composition of precipitation in different locations and allowing measurement of one isotope without always requiring the second isotopic measurement. Because the isotopic composition of subsequent precipitation events along a storm trajectory will follow Rayleigh distillation kinetics, the δD and $\delta^{18}O$ of precipitation will become progressively more negative as the storm moves inland (Mazor 1991). The isotopic depletion of water from inland regions serves as a valuable signal that can is recorded in both plants and animals. The δD and $\delta^{18}O$ of precipitation are related to temperature (Gat and Gonfiantini 1981). Summer precipitation events have higher δD and $\delta^{18}O$ values than winter precipitation events, which provides a basic mechanism for creating isotopic variation throughout the soil moisture profile (Mazor 1991; Gat 1996).

Evaporative Enrichment

While the isotopic composition of incoming precipitation follows the MWL, evaporating bodies (e.g., lakes, leaves, soils) within the ecosystem tend to exhibit a $\Delta\delta D/\Delta\delta^{18}O$ slope that is substantially less than 8 (see Fig. 12.1). Both the upper soil layers and leaves exhibit a strong evaporative enrichment relative to the input source water under nat-

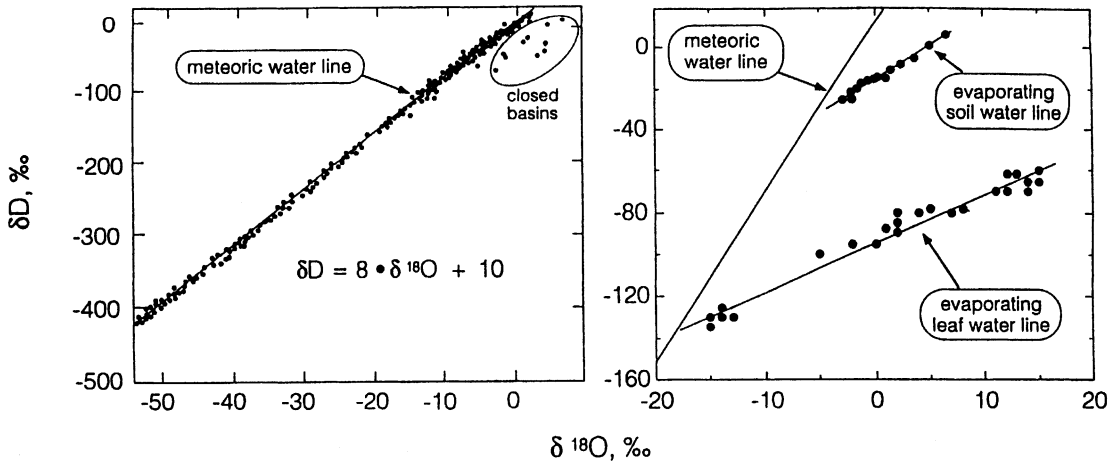

FIGURE 12.1. Left, A plot of the relationships between hydrogen isotope and oxygen isotope ratios for precipitation globally. Right, A plot of the relationships between hydrogen isotope and oxygen isotope ratios for an evaporating soil and leaf water values of different leaves in the same environment. (Data from Allison et al. [1983], Craig [1961], and Flanagan et al. [1991a].)

ural conditions. Craig and Gordon (1965), Allison et al. (1983), and Flanagan et al. (1991b) provide the quantitative models necessary to predict the isotopic composition of open waters, drying soils, and leaf water, respectively, from environmental parameters. Under strict conditions, it is possible to extrapolate evaporatively enriched water from either drying soils or leaves back to the isotopic composition of the original, unevaporated source waters (see Moreira et al. 1997).

Methods for Water Sampling, Extraction, and Analysis

Water Sample Collection and Storage

Representative sampling and prevention of evaporative enrichment are the primary concerns when collecting samples for determining the stable isotopes in water. When collecting water samples from an open water surface (e.g., lake), do not sample from a still surface, which may be enriched relative to deeper water. Stirring up the sample area can help to ensure a representative aliquot. Collect stream water from the site of interest, since evaporative enrichment will occur as water moves down the length of a river. Sampling from well water is often a good proxy for ground water, but do not keep the first water coming out of the pipe since it may be enriched relative to the source. Fill the vials and seal the lid with parafilm. It is desirable to store water samples at cold temperatures (5°C), but short-term storage at room temperature is adequate if the vials are well sealed.

Similar concerns apply to sampling leaves for extraction of water (i.e., sealed in a vial immediately). Remember when sampling for leaf water that the degree of evaporative enrichment in leaf water will be a function of local humidity and leaf temperature (Flanagan et al. 1991a). Thus, it is essential that there be consistency in sampling leaves that are experiencing the same microclimatological patterns (e.g., sun versus shade leaves). The portions of the leaf that are subject to evaporative enrichment are those regions away from the major veins (Yakir et al. 1989). Therefore, some investigators prefer to use a punch to cut out those interveinal regions for sampling. Samples should be stored in a freezer as soon as possible after sampling and kept there until the water is extracted.

Since there is no fractionation during water uptake, sampling xylem waters becomes a convenient and reliable approach for determining the current water source used by a plant (Ehleringer and Dawson 1992). Stems or other suberized tissues are a convenient means of sampling xylem water in order to determine plant water sources from the soil. Emphasis should be placed on sampling organs with a rapid water turnover. For example, sampling of small suberized stems is better than sampling a tree trunk, where external and internal portions may be turning over water at different rates. Use only suberized stem materials, as green stem tissues are subject to evaporative enrichment (Dawson and Ehleringer 1993).

Collection of precipitation from open areas should be done immediately after the storm to avoid evaporation. On the other hand, within a forest, some evaporative enrichment will occur as throughfall makes its way into the soil, in which case, it makes more sense to sample the throughfall since this is what actually enters the soil (Dawson 1998). Soil samples must be collected across the range of possible rooting depths since water in surface soils is exposed to evaporative enrichment. Soil samples are usually stored in the same type of glass vials used to store leaf or stem samples.

If precipitation input and transpiration activity occur at roughly the same time, then it is likely that the atmospheric water vapor will be in isotopic equilibrium with that of the input precipitation. However, these input and loss processes are often temporally offset and may be offset by as much as several months in regions where precipitation occurs primarily in the winter and growth occurs later in the spring and summer. In most cases, it is essential that atmospheric water vapor be collected, since its isotopic value has such a strong influence in determining the isotopic composition of leaf water. Atmospheric vapor is collected by using a pump to flow air through a condensing-loop trap. This requires a very cold trap (dry ice in an ethanol slush) to ensure complete vapor extraction, since any water vapor that escapes would be isotopically altered. For later data interpretation, it is best to also measure air temperature and humidity at the time of vapor collection.

Soil, Leaf, and Stem Water Extraction

Water is extracted from the bulk sample by cryogenic extraction. The entire frozen leaf, stem, or soil sample along with the vial is placed into the sample holder shown in Figure 12.2, which is then immersed in liquid nitrogen. Once the sample is frozen, the sample and holder are evacuated. Once the sample is under vacuum, it is warmed by substituting boiling water for the liquid nitrogen. The collection tube is then immersed into liquid nitrogen to draw the moisture from the sample into this collection tube. [Hint: The frozen tissue still retains some atmospheric gases. Once thawed, these gasses will also migrate to the collection tube. Prevent bubbles from forming within the ice, which will cause problems later when trying to seal the collection tube.] In order to eliminate fractionation, all of the water must be moved from the sample into the collection tube. Continue the cryogenic extraction procedure until no further condensation occurs on the vacuum line walls; this process normally requires 45 to 90 minutes. Thaw the ice and collect the water for isotopic analysis. [Hint: Precut stems into small sections prior to extraction in order to reduce the time required for complete water extraction.]

δD Analysis of Water

Perhaps the most common method for obtaining δD of water involves reducing the H in H_2O to H_2 using a zinc (Zn) catalyst (Coleman et al. 1982). A 2-μl subsample of water (using a capillary) is placed in a Pyrex tube preloaded with 100 mg of Zn contaminated with a small amount of alloy and backfilled with nitrogen (the most reliable Zn is obtained from the Geology Department at Indiana University). The tube is then frozen with liquid nitrogen, evacuated, and sealed. The samples can then be batch processed. The samples are heated to 500°C for 60 minutes. The resulting H_2 gas (sole gas within the sealed tube) can then be directly introduced into the mass spectrometer for analysis. The overall precision of this approach is ± 1‰.

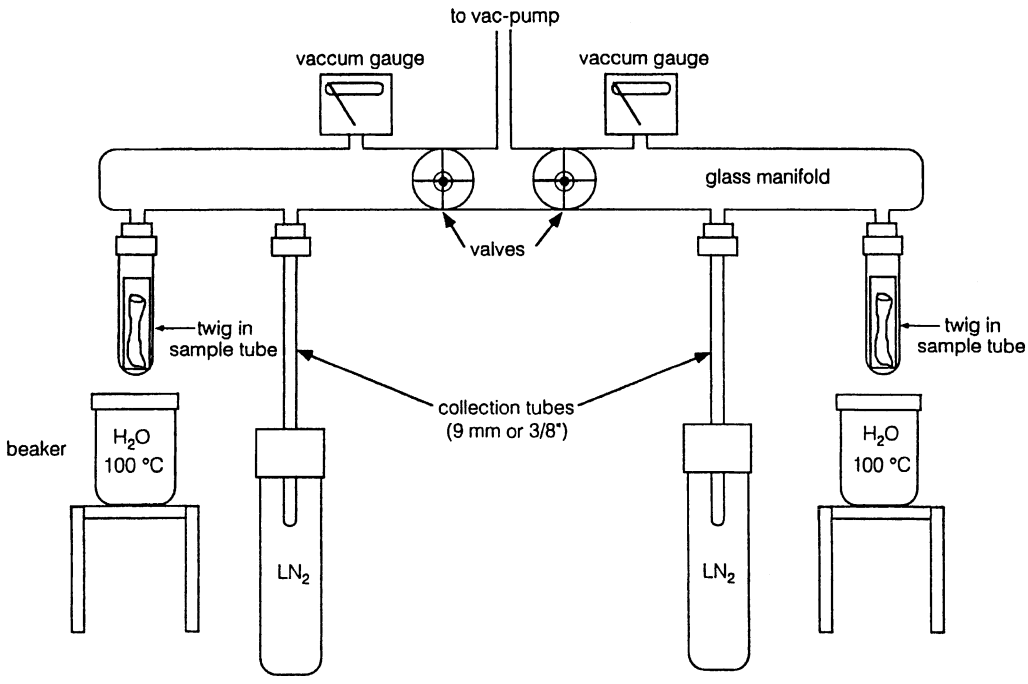

FIGURE 12.2. A cryogenic vacuum line for extracting water from leaves, stems, and soils. Samples are introduced into a chamber and placed under vacuum. The chamber is then heated with boiling water to drive all of the water to a collection tube, which is surrounded by liquid nitrogen (−196°C).

A promising new, on-line method for determination of δD in water uses a chromium reaction furnace (Gehre et al. 1996). The reaction unit, which is directly coupled to the mass spectrometer inlet, is filled with chromium powder (<0.3 mm) and set to 900°C. Very small sample sizes (1 μl) are injected through a layered septum into a preevacuated reaction furnace, and are subject to flash evaporation and reduction to H_2 upon contact with the hot chromium. The H_2 gas flows directly into the bellows of the sample side in the dual inlet mode, because of pressure gradients. One advantage of this approach is that no special sample preparation is needed since the hot chromium reduces water while simultaneously binding other elements in the sample (C, N, O, sulfur [S], and halogens) to thermally stable compounds (Gehre et al. 1996). The overall precision of this approach is ±1‰.

$\delta^{18}O$ Analysis of Water

For relatively large volumes of water (0.2 to 0.5 ml), the $^{18}O/^{16}O$ composition is determined by equilibration with CO_2 of known isotopic composition (Dugan et al. 1985; Compston and Epstein 1958). A volume of CO_2 adequate for analysis on the mass spectrometer is placed along with the water sample in a preevacuated tube. After equilibration in a constant temperature water bath for at least 24 hr, the CO_2 is extracted cryogenically using liquid nitrogen along with dry ice/ethanol traps to prevent water vapor and other gases from entering the collection tube. The CO_2 collected will have the $^{18}O/^{16}O$ signature of the water since the oxygen in the water should completely exchange with the much smaller mole fraction of oxygen in the CO_2. This method is easily batched, but requires large volumes of water and is time consuming. This method has a precision better than ±0.2‰.

Equilibration techniques have also been developed for much smaller sample sizes (40 to 50 μl) (Kishima and Sakai 1980; Socki et al. 1992). These methods add the sample using a micropipet into the bottom of 9-mm Pyrex tube that was previously evacuated and backfilled with dry nitrogen or argon. The sample is frozen with liquid nitrogen, evacuated, and then 250 μl of CO_2 is injected through a septa port. The tube is sealed under vacuum and equilibrated in a constant temperature water bath for at least 24 hr. After equilibration, the CO_2 is extracted as discussed above and ready for the mass spectrometer. An external liquid nitrogen trapping device (similar to a cold finger) has proven useful for enhancing the mass spectrometer precision for the small volumes of CO_2 utilized. A variation on this method can be found in Scrimgeour (1995).

Even smaller volumes (5 to 10 μl) of water can be analyzed by reacting with guanidine hydrochloride to produce CO_2 (Dugan et al. 1985; Wong et al. 1987). The water and guanadine hydrochloride are heated in an evacuated sealed tube at 260°C for 16 hr. The two gases formed in this reaction are ammonia (NH_3) and CO_2. Upon cooling, the CO_2 combines with NH_3 to form an ammonium carbamate. The CO_2 is released from the ammonium carbamate by reacting it with phosphoric acid and trapped at liquid nitrogen temperatures. The method is most useful when very small sample sizes are required, otherwise the method is more time consuming than the H_2O-CO_2 equilibration methods. The precisions of both techniques are similar, 0.2‰.

Methods for Leaf and Stem Organic Matter Sampling, Extraction, and Analysis

Total Tissue Versus Cellulose Analysis

Most isotopic studies on water relations utilize cellulose since it has very slow turnover rates (Lea and Leegood 1993) and represents the water signature at the time of fixation. The study of various components of organic matter can yield information regarding the dynamics of isotopic fractionation during metabolism. However, for considerations of water relations, the differences in δD between various components (e.g., lipids and carbohydrates, Sternberg et al. 1984) make whole tissue samples more difficult to interpret. Although the carbon-bound H is considered nonexchangeable, post-photosynthetic heterotrophic metabolism has been shown to modify the δD of plant carbohydrates as they are exposed to isotopically different water fractions (Yakir 1992). Even though the O of organic matter tends to be less exchangeable than H, the use of cellulose rather than total tissue is particularly important for $\delta^{18}O$ studies due to the com-

plications caused by nitric oxides formed upon combustion when nitrogenous compounds are present. Whole tissue samples are often used for measurements of time-averaged water use efficiency even though the $\delta^{13}C$ of various metabolites can vary considerably. The choice of what fraction to measure depends greatly on the purpose of the study, but in general α-cellulose is a good choice for information on water relations.

Leaf Sampling Considerations

The isotopic composition within a plant varies due to differences in source water, environmental effects, genetic differences, biochemical composition, phenology, etc., and a sampling plan must take all these factors into consideration. Sampling should be done at the same time of the day as diurnal changes in isotopic composition can occur. Samples should be collected from the same canopy position, since differences in microenvironment will affect the extent of evaporative enrichment in the leaves. Since incident light levels can be quite variable throughout a canopy, it is important to be consistent in sampling only sunlit or shaded leaves from all four cardinal directions. While leaves have been commonly used in the past, there is now increasing interest in other tissues and plant parts (Farquhar et al. 1989). The number of plants sampled is dependent on the research question being addressed, and will be affected by the amount of environmental and genetic heterogeneity expected. It is appealing to bulk samples to save time and money, but there is likely some information on population-level genetic variation in isotopic composition that then will be lost.

After harvesting, plant samples should be dried immediately to avoid changes in chemical composition associated with slow drying of living material. If that is not possible, then freezing the tissue at time of collection (dry ice works well) and drying later is adequate. Dried material can be stored at room temperature for extended periods. Dried tissues are ground to pass a 40-mesh screen or in a mortar and pestle for analysis of the isotopic composition of organic matter. Finely ground material burns more uniformly as well as enhances the efficiency of extraction procedures (e.g., cellulose purification). Since the amount of tissue required for analysis is so small (<3 mg or <0.1 mg with a cold finger) care must be taken to ensure sample homogeneity. Often there will be greater variation in the repeated analysis of the same "bulk sample" than in repeated analysis of an individual sample through the mass spectrometer.

Tree Ring Separation and Cellulose Purification

Most approaches to tree ring separation involve simply cutting along visibly delineated rings. With the aid of a dissecting microscope or a microtome, it is possible to subdivide annual rings into finer temporal resolution in order to quantify seasonal variation in δ values (Loader et al. 1995). Care must be taken to ensure that false rings and other anomalies are avoided (Stokes and Smiley 1996). Although destructive, the best way to get at tree rings is by cutting out an entire cross-section of the bole. Preliminary sampling should be done when using increment cores to determine how many cores will be required to obtain enough material for isotopic analysis from a typical annual ring. Due to potential variation along the stem, it is best to sample increment cores from all four cardinal directions (Leavitt and Long 1986).

There has been a tendency for long-term, multiple-year studies to focus sampling only on α-cellulose from organic matter. To obtain α-cellulose from a bulk plant sample (either leaf or tree ring), various modifications of the Wise (1944) method have been used. The approach used by Leavitt and Danzer (1993) allows one to batch process many samples at once. Basically, the preparation of plant material into α-cellulose involves a delipification step (using a Soxlet apparatus), followed by repeated boiling (to remove any water-soluble compounds, such as sugars), bleaching with sodium chlorite and acetic acid (to remove lignins and proteins), and washing of the sample to produce cellulose (α-cellulose and hemicellulose). Since hemicelluloses have exchangeable O atoms, it is important to remove them in a strong sodium hydroxide solution followed by an acetic acid wash. The resulting α-cellulose is then ready for $\delta^{18}O$ analysis. For δD analysis, the α-cellulose must first be nitrated in order to remove the exchangeable H atoms (see below).

$\delta^{13}C$ Analysis of Organic Matter

The off-line analysis of the $\delta^{13}C$ in organic matter involves an in-tube combustion with cupric oxide and a silver foil catalyst (Buchanan and Corocoran 1959). Quartz tubes are loaded with 2 to 3 mg dried organic matter, 1 g cupric oxide, and silver foil (if halogens or S is present), which are then sealed under vacuum. The materials are combusted at 850°C for 4 hr and then allowed to slowly cool. The resulting gases, CO_2, H_2O, and N_2, are separated using a utility vacuum line (Fig. 12.3). In such a line, the sample gases pass through a series of traps to freeze H_2O (ethanol/dry ice) (trap 1) and then CO_2 (liquid nitrogen) (trap 2). The N_2 is pumped away by the vacuum pump. The CO_2 is then isolated by closing valves in the vacuum line and is then cryogenically moved from trap 2 into a collection tube, which can then be sealed so that the sample can be later analyzed on the mass spectrometer operating in a dual inlet mode. Organic samples should be cleaned up soon after combustion, because H_2O and CO_2 will slowly interact with the copper present to form copper carbonate, potentially affecting the isotopic composition of the CO_2. The overall $\delta^{13}C$ precision of this off-line preparation and analysis is $<0.1‰$.

The development of the continuous flow mode and linking an elemental analyzer to the mass spectrometer have greatly simplified the measurement of $\delta^{13}C$ in organic matter, but does so by providing an analysis of somewhat lower precision (precision varies between ± 0.15 to $\pm 0.3‰$). For on-line analysis, dried organic matter (1 to 2 mg) is placed into a tin cup, which is then dropped into a hot (1060°C) quartz combustion furnace flooded with oxygen-enriched helium. As the tin cup ignites (flash combustion) the temperature rises to 1800°C. A helium carrier stream carries the sample products from the combustion furnace through to the mass spectrometer. The combustion products (primarily CO_2, H_2O, and N_2) first flow through an oxidation column (containing chromium oxide), which facilitates complete oxidation, and then through a reduction column (reduced copper to remove excess O and reduce nitrogen oxides to N_2). Water is then removed using magnesium perchlorate, and the remaining gases (CO_2 and N_2) are separated by gas chromatography before they are sent into the mass spectrometer for analysis. Both $\delta^{13}C$ and $\delta^{15}N$ can thus be obtained from a single analysis (Platzner et al. 1997). If the initial sample is weighed precisely, then %N and %C contents can be derived by measurement of the peak area. A typical cycle time for this analysis is approximately 12 minutes and by using an autosampler attached to the elemental analyzer, larger numbers of samples can be run with ease.

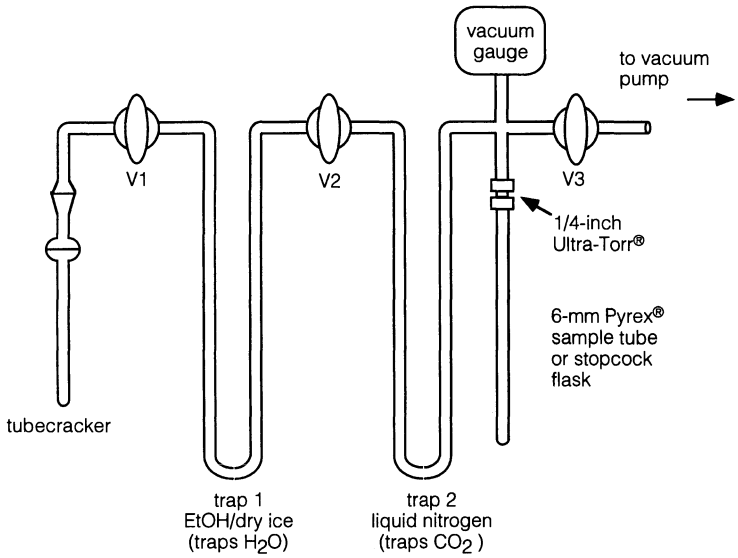

FIGURE 12.3. A general vacuum line for the separation of water (ethanol slush trap at -78°C) and CO_2 (liquid nitrogen trap at -196°C) from other gases.

δD Analysis of Organic Matter

All carbohydrates contain hydroxyl groups that can exchange their hydrogens with those in water, and thus in order to determine the δD of organic matter at the time of formation, only nonexchangeable hydrogens (C-H bonds) can be analyzed for isotopic composition. The most common process is nitration in which each hydroxyl group is exchanged for a nitrate (NO_3). The purified organic material (α-cellulose, see above) is placed in a flask with a solution of nitric acid and acetic anhydride on ice due to the exothermic nature of the reactions (Bennett and Timell 1955; DeNiro 1981; Yapp and Epstein 1982). The material is then washed, dissolved in acetone and then precipitated in water to obtain purified tri-nitrated cellulose (all three hydroxyls per glucose are nitrated). The material is then freeze-dried for storage.

The nitrated material (9 to 14 mg) is then placed into a tube with cupric oxide (1 g), evacuated, sealed, and combusted for 3 hr at 520°C. Following combustion, the gases are separated on the same type of vacuum line (see Figure 12.3) as used for organic $\delta^{13}C$, only instead of trapping CO_2, water vapor is trapped by using the ethanol/dry ice slush to control the water movement while evacuating the other gases. The water is then transferred to a tube containing a Zn catalyst (see section on δD analysis of water above) for reduction to diatomic hydrogen and input into the mass spectrometer. Although this procedure yields good precision (<2‰), it is also labor intensive and requires relatively large sample sizes for the nitration.

$\delta^{18}O$ Analysis of Organic Matter

Conversion of organic matter to CO_2 for $\delta^{18}O$ analysis involves a pyrolytic reaction. For off-line conversion, the α-cellulose (see above) is placed in a tube with mercuric chloride, evacuated, sealed, and then heated for 6 hr at 550°C to form carbon monoxide (CO), CO_2, and hydrochloric acid (HCl) gases. The CO is converted to CO_2 in an ionization chamber and the HCl is reacted with Zn. After a distillation step, the CO_2 is then ready for the mass spectrometer. This procedure, especially the conversion of CO to CO_2 in the spark chamber, is time consuming and along with the toxicity of mercuric chloride makes this technique much less appealing than newer on-line techniques.

Similar to on-line analysis of $\delta^{13}C$ (see above), the use of continuous flow and an elemental analyzer as an automated pyrolysis device has greatly simplified the estimation of $\delta^{18}O$ in organic matter (Saurer et al. 1998). Dried α-cellulose (1 to 2 mg) contained in a silver cup is dropped into a hot (1100°C) quartz combustion furnace containing glassy carbon catalyst in a stream of He. The excess C from the catalyst facilitates the conversion at high temperatures to the thermodynamically favorable products of CO and N_2. These two gases are then separated by a chromatographic column and sent into the mass spectrometer for analysis. A typical cycle time is around 20 minutes and many samples can be run by using an autosampler. If care is taken to reduce memory effects (repeated sampling is recommended) then this method has proven to be robust and precise (<0.4‰).

Short-Term, Ecosystem Process–Level Applications

Our understanding of ecosystem-level water use on a short-term basis has been significantly advanced with the application of stable isotope methods. This is particularly true if the isotopic methods and data collected are linked with other methods at the plant, catchment, and atmospheric levels (Dawson and Ehleringer 1998). If chemical and/or physical reactions result in differential representation of the heavy and light isotopes (Figure 12.4), the isotopic distributions of the reactants and products can inform us about "processes" (i.e., reaction conditions) (Peterson and Fry 1987). The different distributions of stable isotopes, in water for example, can also help to identify and then trace the origin of different water resources in the ecosystem as well (Ehleringer and Dawson 1992). The isotopic values (signatures) of source pools then provide a baseline with which to assess process-level information by looking for changes in the isotopic signature along a reaction pathway (termed isotope fractionation or discrimination) (Peterson and Fry 1987; Hoefs 1987; Lajtha and Michener 1994).

Partitioning of Water Resources Among Plants Within Ecosystems

There are now a number of very good examples of how different plant species may partition soil water resources that have used H or O stable isotope anal-

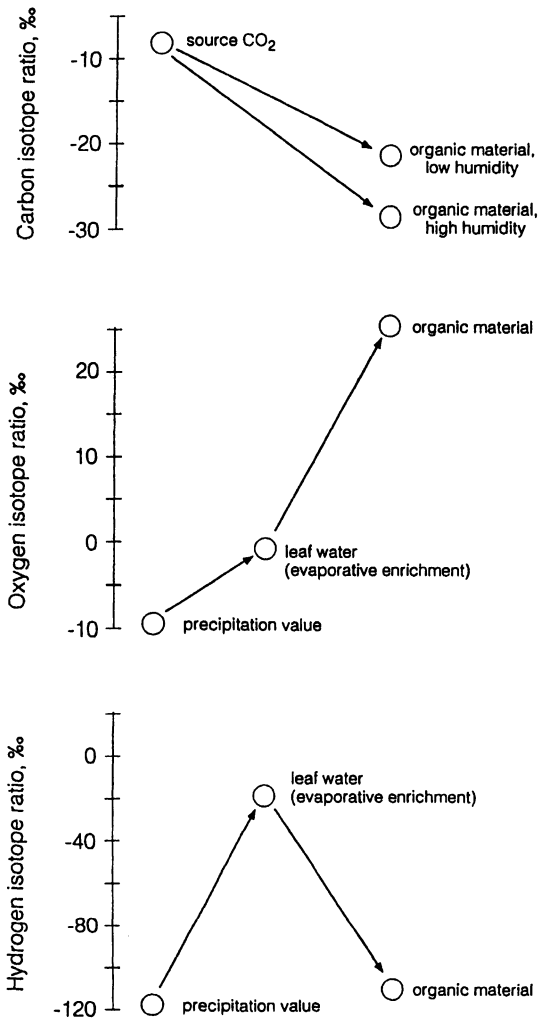

FIGURE 12.4. Stylized relationships between the carbon isotope ratios of organic matter relative to source CO_2 as a function of humidity growth conditions (top) and the oxygen and hydrogen isotope ratios of source water, leaf water, and cellulose (middle and bottom).

yses of both source and plant water (reviewed in Ehleringer and Dawson 1992; Dawson 1993a; Dawson and Ehleringer 1998). Because there is no isotopic fractionation during water uptake by terrestrial plants (Wershaw et al. 1966; but see Lin and Sternberg 1993), if one carefully samples the different potential sources of water used by the vegetation (e.g., soil water, ground water, recent precipitation, fog drip, etc.) as well as the water within the plants themselves (xylem sap), it is possible to qualitatively assess which water sources are being used by coexisting species within a particular community. In the case in which two different water sources can be clearly identified, a simple two-end-member mixing model can be used to estimate the proportional use of each water source (e.g., shallow vs. deep soil water) (see White 198; Brunel et al. 1995; Dawson 1993b) being utilized by different species (Flanagan et al. 1992; Jackson et al. 1995; Ehleringer et al. 1998), in relation to plant distribution along natural gradients of water availability (Dawson and Ehleringer 1991; Sternberg and Swart 1987; Thorburn et al. 1993; Mensforth et al. 1994), over time between, say, wet and dry seasons (Ehleringer et al. 1991; Dawson and Pate 1996; Dawson 1998), or in relation to life history stages or strategies (Ehleringer et al. 1991; Feild and Dawson 1998), overall plant size (Dawson 1996), or in proximity to neighbors (Dawson 1993b). Such information can inform us about the degree of water resource partitioning among plants within and among communities or ecosystems, providing important information which contributes to our understanding of patterns.

When more than two different water sources are present, assessing the proportional use of each becomes more problematic. Recent quantitative models have been developed, however, and are providing a means to assess where the water being used by particular plants comes from when roots at several different zones of the soil profile are active (see Cramer et al. 1999) or at different times of the growing season (Dawson et al., unpublished manuscript). While these sorts of models require more detailed information about the spatial and temporal variation of water resources within an ecosystem, they may be the only way to quantitatively access resource use and partitioning among vegetation elements within an ecosystem; in some instances, that may also be the only way to more powerfully interpret a host of different data sets in cases in which simple two-source models cannot or should not be applied (Thorburn and Dawson in prep.). In ecosystems in which only two water sources (shallow and deep) can be identified (e.g., arid and semiarid systems), water pulses can be used to better understand patterns of plant water use and the possible partitioning of water resources among species (Schwinning and Ehleringer 2000 and below).

Using δD and $\delta^{18}O$ Water Pulses and Interpretation of Mixing Models

Even though the soil forms a continuum of moisture availabilities, it is often appropriate to distinguish two distinct soil water sources for plants (see above and Dawson and Ehleringer 1998; Dawson et al. 1998). One, the rain-fed shallow soil layer is dominated by pulse dynamics, where generally low soil moisture availability is punctuated by short episodes of high soil moisture availability. These pulses may occur naturally or artificially by augmenting the irrigation water with either ^{2}H- or ^{18}O-enriched water (both readily available commercially). Second, the deeper soil layer is not or is very little affected by single rainfall events and is dominated instead by seasonal dynamics in which soil moisture is depleted during spring and summer and replenished during fall and winter. In many ecosystems, such as grasslands and deserts, the division of soil space and its resources among plants is central to explaining competitive relationships among plants and the community consequences of a changing climate. Stable isotope methods can help quantify the absolute and relative division of shallow and deep soil moisture sources among plant species.

Shallow and deep soil water pools often have distinct isotopic composition, particularly in temperate ecosystems and ecosystems receiving bimodal precipitation. If minimal isotopic differences exist within the soil profile, they can also be enhanced, creating artificial moisture pulses with ^{2}H- or ^{18}O-enriched irrigation water. As stated above, plants do not discriminate between isotopically different forms of water (Ehleringer and Dawson 1992). Thus, the isotopic composition of xylem water reveals the relative contribution from two distinct water sources. The question becomes how much ecologically relevant information can we obtain from the xylem signal?

There are several levels of sophistication in interpreting the xylem water signal. At the simplest level, the composition of xylem water merely informs whether one or two water sources are available to the plant at the time of measurement (Fig. 12.5). For example, if xylem water is indistinguishable from one of the two water sources this would suggest that the plant uses only one water source,

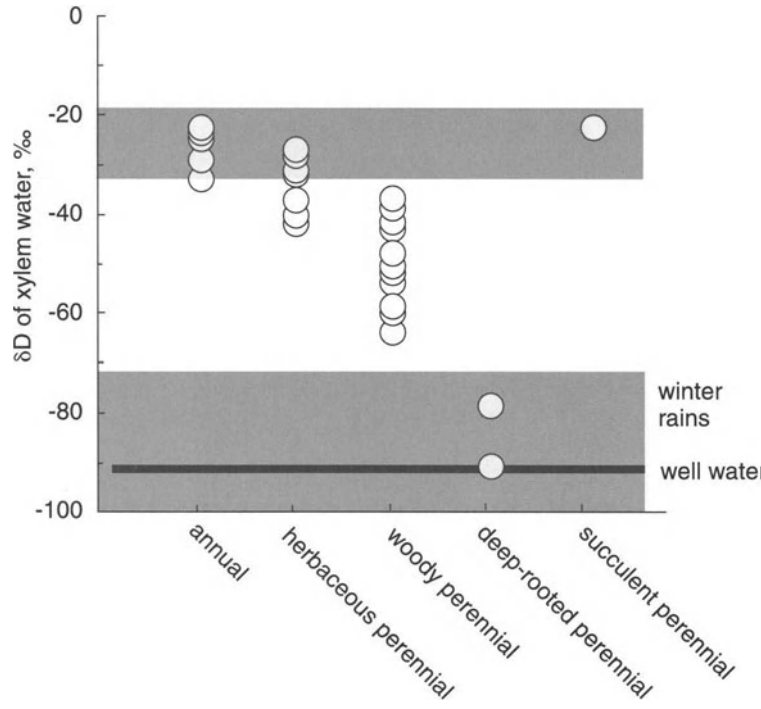

FIGURE 12.5. Hydrogen isotope ratios of xylem water during the summer monsoon period for different species, co-occurring within a desert ecosystem. (Data from Ehleringer et al. [1991].)

while an intermediate isotopic composition would suggests that both water sources are being used. A more precise quantification of the relative or absolute utilization of the two water sources is more difficult and requires additional measurements, such as of water flow rate through the plant and the exchangeable water volume. This is particularly important when one of the two water sources becomes available as a pulse.

This can be shown in a simple dynamic mixing model, where we consider a constant transpiration flow (E) through a well-mixed constant volume (V), fed in part (f) by a labeled source and in part (1 − f) by an unlabeled source. The concentration of label in the fixed volume depends not only on the relative contribution, f, of the labeled source to the uptake, but also on the flow-to-volume ratio, E/V. When this ratio is low, the concentration of label lags behind the true fraction, f, of labeled source in the total flow, E. Thus, the true utilization fraction of a pulsed source is likely to be underestimated, unless the dynamics of xylem water composition, as affected by E/V, are accounted for. Actual pulse label dynamics are often more complicated, because water uptake rates and ratios may not remain constant during or after a pulse. Thus, any one-time estimation of the fraction of water from a pulsed source in the transpiration stream would give incomplete information on overall pulse utilization. In this case, pulse utilization can be quantified precisely only when xylem composition and transpiration rates are monitored during and after the pulse. Then, total pulse utilization can be estimated by integrating, over time, the fraction of pulsed resource in the xylem and the whole plant transpiration rate. Since such intensive data collection is often not possible, methods have been developed to estimate integrated pulse utilization based on substantially less information.

In studies in which the utilization of single pulses is the focus, simplified models of pulse utilization dynamics have been used to fill the gaps left by limited data collection. Schwinning and Ehleringer (2000) suggested that relative pulse utilization by plants with contrasting life history strategies can be estimated within an accuracy of 10 to 20% based on only four data points: the time and magnitude of the maximal fraction of pulsed source water in the xylem, and two estimates of the whole-plant E/V ratios during and after the pulse. Schwinning and Ehleringer (2000) suggest that seasonally integrated pulse utilization can be estimated by randomly sampling xylem water composition and whole-plant transpiration rates throughout the season, regardless of time since last pulse. This method makes no assumption on pulse dynamics, but simply represents a statistical estimate of the seasonally integrated pulse-fed transpiration rate, based on randomly selected subsamples.

Water-Use Efficiency

If water sources are differentially available to plants with either different rooting depths or requirements for water, this could influence their water use behavior and thereby the efficiency with which they fix carbon. Differences in water use behavior have been assessed with the use of carbon isotope analyses of plant leaves (Farquhar et al., 1989) or tree ring cellulose (see Livingston and Spittlehouse, 1993). In plants with the C_3 photosynthetic pathway, variation in the leaf carbon isotope ratio ($\delta^{13}C$) can be correlated with the long-term efficiency with which the water resource is used (see Ehleringer 1991). This is because, during the photosynthetic process, C_3 leaves discriminate differentially against $^{13}CO_2$ more than $^{12}CO_2$, particularly when the leaf stomata are fully opened (Farquhar et al. 1989). Therefore, if plants within an ecosystem are using different water sources and experiencing different levels of water stress that lead to differences among species or over time in the water use behaviors, this could be "recorded" in the leaf or wood carbon being synthesized at that time. More conservative water use behavior should therefore, for example, in shallowly rooted species that experience more water stress, lead to a different leaf or wood $\delta^{13}C$ than more deeply rooted species that are using deeper, more stable water sources. This sort of pattern has been documented in arid land systems by Flanagan et al. (1992). Assessments of the variation in $\delta^{13}C$ have also been used to estimate evapotranspiration components over simple plant canopies (see Bariac et al. 1989; Ebdon et al. 1998). This sort of approach has the potential to help link water sources and water use behavior to the total system water flux in ecosystem-level investigations.

Short-Term, Regional Process–Level Applications Across Ecosystems

Recycling of Water Among and Between Ecosystems

The terrestrial biosphere influences global cycles of CO_2 and water. Stable isotopes can be used to probe these cycles since biological fractionation and subsequent exchange with the atmosphere alters ambient isotopic signatures of CO_2 and water vapor (Hsieh et al., 1998). For example, Gat and Matsui (1991) used the δD and $\delta^{18}O$ of precipitation across a longitudinal gradient to quantify the relative contribution of evaporation and transpiration to the recycling of water vapor in the Amazon basin. There is a predictable isotopic depletion of water in precipitation as storm fronts progress (the continental effect) due to Rayleigh distillation effects, and deviations imply that a source of isotopically enriched vapor must be coming from the biosphere. The source can be further delineated since vapor from evaporation processes (lakes, rainfall, stemflow, soil water, etc.) should be isotopically depleted relative to that from transpiration (Gat and Matsui 1991; Martinelli et al. 1996). Rather than sampling precipitation, Moreira et al. (1997) used flasks located on towers and balloons to sample atmospheric vapor directly and, using simple isotope mixing models, demonstrated that canopy transpiration can be a major source of water vapor recycling in Amazonia. These kinds of studies can also elucidate the effects of land use changes on ecosystem water cycles.

$\delta^{18}O$ of Atmospheric Carbon Dioxide

The biosphere can also have a significant influence on the oxygen isotope ratio of atmospheric CO_2 (Francey and Tans 1987; Farquhar et al. 1993; Flanagan et al. 1997). The equilibrium isotope effect that occurs between oxygen in CO_2 and oxygen in water may be the primary factor influencing the $\delta^{18}O$ of respired CO_2 (Farquhar and Lloyd 1993). However, discrimination against $C^{18}O^{16}O$ during photosynthesis acts to enrich atmospheric CO_2 in ^{18}O, while respiration has the opposite effect by releasing CO_2 depleted in ^{18}O. Thus, ecosystem respiration flux can be partitioned into soil and plant components due to the differences in the $\delta^{18}O$ of medium water (Flanagan et al. 1997; Ehleringer and Cook 1998; Flanagan et al. 1999). In addition, global-scale partitioning of CO_2 fluxes can be studied since the $\delta^{18}O$ of water differs widely between marine and terrestrial sources (even between different biomes and latitudes) helping to resolve conflicts over the relative role of the oceans in net CO_2 uptake (Farquhar et al. 1993).

Long-Term, Temporal Scaling of Ecosystem Processes

Decadal-to-Century: Tree Rings

Tree rings have been frequently used as a record of long-term climatic fluctuations. The hydrogen and oxygen isotopic composition of tree ring cellulose reflects, to a first approximation, precipitation inputs (Yapp and Epstein 1982; Lawrence and White 1984; White et al. 1994), and many studies have used the variations in δD and $\delta^{18}O$ in tree rings for temperature reconstruction (Gray and Thompson 1976; Epstein and Yapp 1977). However, White et al. (1985) observed that pine trees from wet and dry microsites, that presumably receive similar precipitation inputs, exhibited differences in their cellulose δD values, suggesting that water stress and/or humidity differences may alter leaf water δD and thus tree ring cellulose δD. There has been substantial controversy over exactly what environmental information is recorded in the δD and $\delta^{18}O$ of tree ring cellulose (e.g., DeNiro and Cooper 1989; Edwards 1990). However, Roden et al. (1999) have recently developed and tested a mechanistic model for the interpretation of hydrogen and oxygen isotope ratios in cellulose and have concluded that both water source and humidity information are recorded in tree rings.

The $\delta^{13}C$ of tree ring cellulose has also been used to study temperature and humidity signals (Loader et al. 1995; Lipp et al. 1996), climate change (Leavitt and Long 1991), water use efficiency (Duquesnay et al. 1998), soil moisture availability (Saurer et al. 1997), atmospheric $\delta^{13}C$, and the global CO_2 cycle (Switsur and Waterhouse 1998) over century-long time scales. These relationships are derived from the Farquhar et al. (1982) model for carbon

isotope discrimination and environmental influences on c_i/c_a. Some studies have found it useful to measure both $\delta^{13}C$ and $\delta^{18}O$ to separate out changes in precipitation input and local environmental conditions (Lipp et al. 1996; Saurer et al. 1997). Although tree rings are most often used to study long-term changes in the water relations of ecosystems, they can also be subdivided and provide fine-scale seasonal climatic information (Loader et al. [1995] subdivided an annual ring into 20 units).

Millennial: Caliche

Pedogenic carbonates are formed from soil-respired CO_2 and are therefore long-term indicators of the vegetation within an ecosystem. The variation in paleosol carbonate $\delta^{13}C$ signals at depth have been used to indicate shifts in C_3 and C_4 vegetation (Cole and Monger 1994; Quade and Cerling 1995; Liu et al. 1996). However, the $\delta^{18}O$ in the CO_2 evolved (using phosphoric acid) can also provide climatic information. For example, the lack of a change in $\delta^{18}O$ with changes in $\delta^{13}C$ implies that shifts in photosynthetic pathway may be due more to shifts in CO_2 concentration than climate (Cole and Monger 1994; Quade and Cerling 1995). Variation in the $\delta^{18}O$ of pedogenic carbonates may be caused by a number of climatic factors, including temperature change, shift in the amount of precipitation, shifts in precipitation patterns (summer vs. winter), and shifts in regional moisture sources (Quade and Cerling 1995), and are therefore a valuable long-term record of ecosystem water relations.

Animals

Short-Term Indicators of Water Source

Stable isotope ratio analyses can provide direct evidence of short-term animal movements across the landscape. Often, more than 60% of an animal's mass is water. The isotopic composition of water in animals reflects that of their drinking source modified by the isotopic effects of evaporative enrichment, in much the same way that leaf water reflects both a source water component and an evaporative enrichment component. Longinelli (1984) first showed that a strong linear relationship existed between the $\delta^{18}O$ values of blood and an animal's source water (Fig. 12.6). He further provided evidence for seasonality in the $\delta^{18}O$ values of blood, reflecting the seasonal changes in the $\delta^{18}O$ values of precipitation. Because different animals vary in overall water turnover rates and have different relative water rates of water loss through evaporation versus excretion, the slope of the $\delta^{18}O$ of source water and blood are different across species. Only microliter quantities are required for these analyses. Consequently, analyses of the $\delta^{18}O$ values of blood is a viable and less expensive alternative to radiotransmitters for tracing the recent movement patterns of animals between ecosystems and across the landscape.

Long-Term Indicators of Water Source

The $\delta^{18}O$ values of water in blood are recorded in bone phosphate (see Figure 12.6). Longinelli (1984) first showed that a linear 1:1 relationship

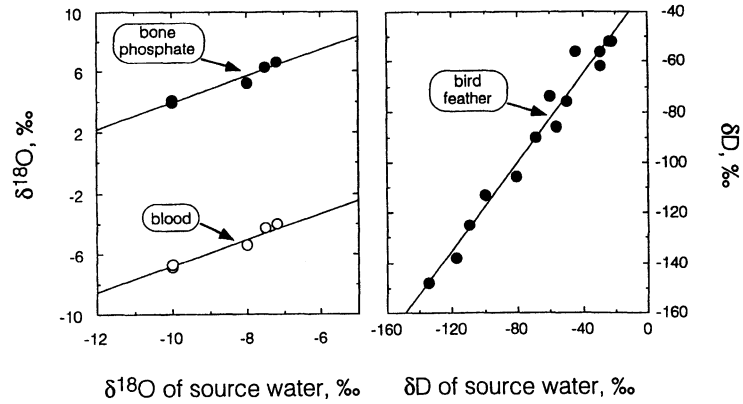

FIGURE 12.6. Relationships between source water and oxygen isotope ratios of blood and bone phosphate (left) (Longinelli 1984), and hydrogen isotope ratios of bird feathers (right) (Hobson and Wassenaar 1997).

existed between the $\delta^{18}O$ values of source water and bone phosphate. Ecological applications have included studies of the distribution of white-tailed deer across North America (Luz et al. 1990). Similar approaches have been used to show that the δD values of bone phosphate and bone gelatin also reflect source waters (Cormie et al. 1994). More recently, Hobson and Wassenaar (1997) have shown that the δD and $\delta^{18}O$ values of bird feathers also reflect that of their source water, which has far reaching implications for tracing long-distance bird migrations (see Figure 12.6). While many migratory animals, such as insects, lack bones, they too record long-term information about the source water of the ecosystem in which they were reared. Hobson et al. (1999) have shown that it is feasible to trace the migratory origins of monarch butterflies from the δD and $\delta^{18}O$ values of the organic matter in their wings. Further exploration of this approach is likely to have widespread ecosystem-level applications in cases in which animals move back and forth between adjacent ecosystems.

References

Allison, G.B.; Barnes, C.J.; Hughes, M.W. The distribution of deuterium and ^{18}O in dry soils. 2. Experimental. J. Hydrol. 64:377–397; 1983.

Bariac, T.; Rambal, S.; Jusserand, C.; Berger, A. Evaluating water fluxes of field-grown alfalfa from diurnal observations of natural isotope concentrations, energy budget and ecophysiological parameters. Ag. For. Meteorol. 48:263–283; 1989.

Bennett, C.F.; Timell, T.E. Preparation of cellulose trinitrate. Sven. Papperstidn. 58:281–286; 1955.

Brand, W. High precision isotope ratio monitoring techniques in mass spectrometry. J. Mass Spec. 31:226–235; 1996.

Brunel, J.-P.; Walker, G.R.; Kennett-Smith, A.K. Field validation of isotopic procedures for determining sources of water used by plants in a semi-arid environment. J. Hydrol. 167:351–368; 1995.

Buchanan, D.L.; Corocoran, B.J. Sealed tube combustions for the determination of carbon-14 and total carbon. Anal. Chem. 31:1635–1638; 1959.

Cole, D.R.; Monger, H.C. Influence of atmospheric CO_2 on the decline of C_4 plants during the last deglaciation. Nature 368:533–536; 1994.

Coleman, M.C.; Shepherd, T.J.; Durham, J.J.; Rouse, J.D.; Moore, G.R. Reduction of water with zinc for hydrogen isotope analysis. Anal. Chem. 54:993–995; 1982.

Compston, W.; Epstein, S. A method for the preparation of carbon dioxide from water vapor for oxygen isotope analysis. Trans. Am. Geophys. Union 39:511–512; 1958.

Cormie, A.B.; Schwarcz, H.P.; Gray, J. Determination of the hydrogen isotopic composition of bone collagen and correction for hydrogen exchange. Geochim. Cosmo. Acta 58:265–375; 1994.

Craig, H. Isotopic variations in meteoric waters. Science 133:1702–1703; 1961.

Craig, H.; Gordon, L. Deuterium and oxygen-18 variations in the ocean and the marine atmosphere. In: Tongiorgi, E., ed. *Stable Isotopes in Oceanographic Studies and Paleotemperatures, Spoleto 1965.* Pisa: Consiglio Nazionale delle Ricerche, Laboratorio di Geologia Nucleare; 1965:9–130.

Cramer, V.; Thorburn, P.; Fraser, G.; Stewart, G. Transpiration and groundwater uptake from farm forest plots of *Casuarina glauca* and *Eucalyptus camaldulensis* in saline areas of southeast Queensland, Australia. Ag. Water Manage. 39:(2–3):187–204; 1999.

Dawson, T.E. Water sources of plants as determined from xlyem-water isotopic composition: Perspectives on plant competition, distribution, and water relations. In: Ehleringer, J.R.; Hall, A.E.; Farquhar, G.D., eds. *Stable Isotopes and Plant Carbon-Water Relations.* San Diego, CA: Academic; 1993a:465–496.

Dawson, T.E. Hydraulic lift and water use in plants: Implications for performance, water balance and plant-plant interactions. Oecologia 95:565–574; 1993b.

Dawson, T.E. Determining water use by trees and forests from isotopic, energy balance and transpiration analyses: the roles of tree size and hydraulic lift. Tree Physiol. 16:263–272; 1996.

Dawson, T.E. Fog in the California redwood forest: Ecosystem inputs and use by plants. Oecologia 117:476–485; 1998.

Dawson, T.E.; Ehleringer, J.R. Stremside trees that do not use stream water. Nature 350:335–337; 1991.

Dawson, T.E.; Ehleringer, J.R. Isotopic enrichment of water in the "woody" tissues of plants: Implications for water source, water uptake, and other studies which use the stable isotopic composition of cellulose. Geochim. Cosmo. Acta 57:3487–3492; 1993.

Dawson, T.E.; Ehleringer, J.R. The role of plants in catchment-level hydraulic processes: Insights from stable isotope studies. In: Kendall, C.; McDonnell, J.J., eds. *Isotope Tracers in Catchment Hydrology.* Amsterdam: Elsevier; 1998:165–202.

Dawson, T.E.; Pate, J.S. Seasonal water uptake and movement in root systems of Australian phreatophytic plants of dimorphic root morphology: A stable isotope investigation. Oecologia 107:13–20; 1996.

Dawson, T.E.; Pausch, R.C.; Parker, H.M. The role of hydrogen and oxygen stable isotopes in understanding

water movement along the soil-plant-atmosphere continuum. In: Griffiths, H., ed. *Stable Isotopes: Integration of Biological, Ecological and Geochemical Processes.* Oxford: BIOS; 1998:169–183.

DeNiro, M.J. The effects of different methods of preparing cellulose nitrate on the determination of the D/H ratios of non-exchangeable hydrogen in cellulose. Earth Planet Let. 54:177–185; 1981.

DeNiro, M.J.; Cooper, L.W. Post photosynthetic modification of oxygen isotope ratios of carbohydrates in the potato: implications for paleoclimatic reconstruction based upon isotopic analysis of wood cellulose. Geochim. Cosmochim. Acta 53:2573–2580; 1989.

Dugan, J.P.; Borthwick, J.; Harmon, R.S.; Gagnier, M.A.; Glahn, J.E.; Kinsel, E.P.; MacLeod, S.; Viglino, J.A.; Hess, J.W. Guanidine hydrochloride method for determination of water oxygen isotope ratios and the oxygen-18 fractionation between carbon dioxide and water at 25°C. Anal. Chem. 57:1734–1736; 1985.

Duquesnay, A.; Bréda, N.; Stievenard, M.; Dupouey, J.L. Changes of tree-ring $\delta^{13}C$ and water-use efficiency of beech (*Fagus sylvatica* L.) in north-eastern France during the past century. Plant Cell Environ. 21:565–572; 1998.

Ebdon, J.S.; Petrovic, A.M.; Dawson, T.E. Relationship between carbon isotope discrimination, water use efficiency and evapotranspiration rate in Kentucky bluegrass turfgrass. Crop Science 38:157–162; 1998.

Edwards, T.W.D. New contributions to isotope dendroclimatology from studies of plants. Geochim. Cosmochim. Acta 54:1843–1844; 1990.

Ehleringer, J.R. $^{13}C/^{12}C$ fractionation and its utility in terrestrial plant studies. In: Coleman, D.C.; Fry, B., eds. *Carbon Isotope Techniques.* New York: Academic; 1991:187–200.

Ehleringer, J.R.; Cook, C.S. Carbon and oxygen isotope ratios of ecosystem respiration along an Oregon conifer transect: preliminary observations based upon small-flask sampling. Tree Physiol. 18:513–519; 1998.

Ehleringer, J.R.; Dawson, T.E. Water uptake by plants: Perspectives from stable isotope composition. Plant Cell Environ. 15:1073–1082; 1992.

Ehleringer, J.R.; Evans, R.D.; Williams, D. Assessing sensitivity to change in desert ecosystems: A stable isotope approach. In: Griffiths, H., ed. *Stable Isotopes: Integration of Biological, Ecological and Geochemical Processes.* Oxford: BIOS; 1998:223–237.

Ehleringer, J.R.; Hall, A.E.; Farquhar, G.D., eds. *Stable Isotopes and Plant Carbon/Water Relations.* San Diego, CA: Academic; 1993.

Ehleringer, J.R.; Phillips, S.L.; Schuster, W.F.S.; Sandquist, D.R. Differential utilization of summer rains by desert plants: Implications for competition and climate change. Oecologia 88:430–434; 1991.

Epstein, S.; Yapp, C. Isotope tree thermometers. Nature 266:477–478; 1977.

Farquhar, G.D.; Ehleringer, J.R.; Hubick, K.T. Carbon isotope discrimination and photosynthesis. Annu. Rev. Plant Physiol. 40:503–537; 1989.

Farquhar, G.D.; Lloyd, J. Carbon and oxygen isotope effects in the exchange of carbon dioxide between plants and the atmosphere. In: Ehleringer, J.R.; Hall, A.E.; Farquhar, G.D., eds. *Stable Isotopes and Plant Carbon/Water Relations.* San Diego, CA: Academic; 1993:47–70.

Farquhar, G.D.; Lloyd, J.; Taylor, J.A.; Flanagan, L.B.; Syversten, J.P.; Hubick, K.T.; Wong, S.C.; and Ehleringer, J.R. Vegetation effects on the isotopic composition of oxygen in atmospheric CO_2. Nature 363:439–443; 1993.

Farquhar, G.D.; O'Leary, M.H.; Berry, J.A. On the relationship between carbon isotope discrimination and the intercellular carbon dioxide concentration in leaves. Aust. J. Plant Physiol. 9:121–137; 1982.

Feild, T.S.; Dawson, T.E. Water sources used by *Didymopanax pittieri* at different life stages in a tropical cloud forest. Ecology 79:1448–1452; 1998.

Flanagan, L.B.; Bain, J.F.; Ehleringer, J.R. Stable oxygen and hydrogen isotope composition of leaf water in C_3 and C_4 plant species under field conditions. Oecologia 88:394–400; 1991a.

Flanagan, L.B.; Brooks, J.R.; Varney, G.T.; Ehleringer, J.R. Discrimination against $C^{18}O^{16}O$ during photosynthesis and the isotopic ratio of respired CO_2 in boreal forest ecosystems. Global Biogeochem. Cycl. 11:83–98; 1997.

Flanagan, L.B.; Comstock, J.P.; Ehleringer, J.R. Comparison of modeled and observed environmental influences on the stable oxygen and hydrogen isotope composition of leaf water in *Phaseolus vulgaris* L. Plant Physiol. 96:588–596; 1991b.

Flanagan, L.B.; Ehleringer, J.R.; Marshall, J.D. Differential uptake of summer precipitation among co-occurring trees and shrubs in a pinyon-juniper woodland. Plant Cell Environ. 15:831–836; 1992.

Flanagan, L.B.; Kubien, D.S.; Ehleringer, J.R. Spatial and temporal variation in the carbon and oxygen isotope ratio of respired CO_2 in a boreal forest ecosystem. Tellus; in press.

Francey, R.J.; Tans, P.P. Latitudinal variation in oxygen-18 of atmospheric CO_2. Nature 327:495–497; 1987.

Gat, J. Oxygen and hydrogen isotopes in the hydrologic cycle. Annu. Rev. Earth Planet. Sci. 24:225–262; 1996.

Gat, J.R.; Gonfiantini, R., eds. *Stable Isotope Hydrology. Deuterium and Oxygen-18 in the Water Cycle.* Vienna: IAEA; 1981.

Gat, J.R.; Matsui, E. Atmospheric water balance in the Amazon basin: An isotopic evapotranspiration model. J. Geophys. Res. 96:13179–13188; 1991.

Gehre, M.; Hoefling, R.; Kowaski, P.; Strauch, G. Sample preparation device for quantitative hydrogen isotope analysis using chromium metal. Anal. Chem. 68:4414–4417; 1996.

Gray, J.; Thompson, P. Climatic information from $^{18}O/^{16}O$ ratios of cellulose in tree rings. Nature 262:481–482; 1976.

Hayes, J.M. Practice and principles of isotopic measurements in organic geochemistry. In: Meinschein, W.G., ed. *Organic Geochemistry of Contemporaneous and Ancient Sediments.* Bloomington, In: Society of Economic Paleontologists and Mineralogists; 1983:5–31.

Hsieh, J.C.C.; Chadwick, O.A.; Kelly, E.F.; Savin, S.M. Oxygen isotopic composition of soil water: Quantifying evaporation and transpiration. Geoderma 82:269–293; 1998.

Hobson, K.A.; Wassenaar, L.I. Linking breeding and wintering grounds of neotropical migrant songbirds using stable hydrogen isotopic analysis of feathers. Oecologia 109:142–148; 1997.

Hobson, K.A.; Wassenaar, L.I.; Taylor, O.R. Stable isotopes (δD and $\delta^{13}C$) are geographic indicators of natal origins of monarch butterflies in eastern North America. Oecologia 120(3):397–404; 1999.

Hoefs, J. *Stable Isotope Geochemistry.* Heidelberg: Springer-Verlag; 1987.

Jackson, P.C.; Cavelier, J.; Goldstein, G.; Meinzer, F.C.; Holbrook, N.M. Partitioning of water resources among plants of a lowland tropical forest. Oecologia 101:197–203; 1995.

Kishima, N.; Sakai, H. Oxygen-18 and deterium on a single water sample of a few milligrams. Anal. Chem. 52:356–358; 1980.

Lajtha, K.; Michener, R.H., editors. *Stable Isotopes in Ecology and Environmental Science.* London: Blackwell; 1994.

Lawrence, J.R.; White, J.W.C. Growing season precipitation from D/H ratios of eastern white pine. Nature 311:558–560; 1984.

Lea, P.J.; Leegood, R.C. *Plant Biochemistry and Plant Molecular Biology.* New York: J Wiley; 1993.

Leavitt, S.W.; Danzer, S.R. Method for batch processing small wood samples to holocellulose for stable-carbon isotope analysis. Anal. Chem. 65:87–89; 1993.

Leavitt, S.W., Long, A. Seasonal stable-carbon isotope variability in tree rings: Possible paleoenvironmental signals. Chem. Geol. 87:59–70; 1991.

Leavitt, S.W., Long, A. Stable-carbon isotope variability in tree foliage and wood. Ecology 67:1002–1010; 1986.

Lin, G., Sternberg, L.d.S.L. Hydrogen isotopic fractionation by plant roots during water uptake in coastal wetland plants. In: Ehleringer, J.R.; Hall, A.E.; Farquhar, G.D., eds. *Stable Isotopes and Plant Carbon-Water Relations.* San Diego, CA: Academic; 1993:497–510.

Lipp, J.; Trimborn, P.; Edwards, T.; Waisel, Y.; Lin, D. Climatic effects on the $\delta^{18}O$ and $\delta^{13}C$ of cellulose in the desert tree *Tamarix jordanis.* Geochim. Cosmochim. Acta 60:3305–3309; 1996.

Liu, B.; Phillips, F.M.; Campbell, A.R. Stable carbon and oxygen isotopes of pedogenic carbonates, Ajo Mountains, southern Arizona: Implications for paleoenvironmental change. Palaeogeogr. Palaeoclimatol. Palaeoecol. 124:233–246; 1996.

Livingston, N.J., Spittlehouse, D.L. Carbon isotope fractionation in tree rings in relation to the growing season water balance. In: Ehleringer, J.R.; Hall, A.E.; Farquhar, G.D., eds. *Stable Isotopes and Plant Carbon-Water Relations.* San Diego, CA: Academic; 1993:141–153.

Loader, N.J.; Switsur, V.R.; Field, E.M. High resolution stable isotope analysis of tree rings: implications of "microdendroclimatology" for paleoenvironmental research. Holocene 5:457–460; 1995.

Longinelli, A. Oxygen isotopes in mammal bone phosphate: A new tool for paleohydrological and paleoclimatological research? Geochim. Cosmochim. Acta 48:385–390; 1984.

Luz, B.; Cormie, A.B.; Schwarcz, H.P. Oxygen isotope variations in phosphate of deer bones. Geochim. Cosmochim. Acta 54:1723–1728; 1990.

Mazor, E. Stable hydrogen and oxygen isotopes. In: Mazor, E., ed. *Applied Chemical and Isotopic Groundwater Hydrology.* Buckingham, UK: Open University Press; 1991:pp.122–146.

Martinelli, L.A.; Victoria, R.L.; Sternberg, L.S.L.; Ribeiro, A.; Moreira, M.Z. Using stable isotopes to determine sources of evaporated water to the atmosphere in the Amazon basin. J. Hydrol. 183:191–204; 1996.

Mensforth, L.J.; Thorburn, P.J.; Tyerman, S.D.; Walker, G.R. Sources of water used by riparian *Eucalptus camaldulensis* overlying highly saline groundwater. Oecologia 100:21–28; 1994.

Moreira, M.Z.; Sternberg, L.d.S.L.; Martinelli, L.A.; Victoria, R.L.; Barbosa, E.M.; Bonates, L.C.M.; Nepstad, D.C. Contribution of transpiration to forest ambient vapour based on isotopic measurements. Global Change Biol. 3:439–450; 1997.

Peterson, B.J.; Fry, B. Stable isotopes in ecosystem studies. Annu. Rev. Ecol. Systemat. 18:293–320; 1987.

Platzner, I.T.; Habfast, K.; Walder, A.J.; Goetz, A. *Modern Isotope Ratio Mass Spectrometry.* New York: Wiley; 1997.

Quade, J.; Cerling, T.E. Expansion of C_4 grasses in the Late Miocene of northern Pakistan: Evidence from stable isotopes in paleosols. Palaeogeogr. Palaeoclimatol. Palaeoecol. 115:91–116; 1995.

Roden, J.S.; Lin, G.; Ehleringer, J.R. A mechanistic model for the interpretation of hydrogen and oxygen isotope ratios in tree-ring cellulose. Geochim. Cosmochim. Acta 64:21–35; 2000.

Saurer, M.; Allen, K.; Siegwolf, R. Correlating $\delta^{13}C$ and $\delta^{18}O$ in cellulose of trees. Plant Cell Environ. 20:1543–1550; 1997.

Saurer, M.; Robertson, I.; Siegwolf, R.; Leuenberger, M. Oxygen isotope analysis of cellulose: An interlaboratory comparison. Anal. Chem. 70:2074–2080; 1998.

Schwinning, S.; Ehleringer, J.R. The interpretation of D_2O pulse experiments in ecological research on desert plants. (in preparation).

Scrimgeour, C.M. Measurement of plant and soil water isotope composition by direct equilibration methods. J. Hydrol. 172:261–274; 1995.

Socki, R.A.; Karlsson, H.R.; Gibson, E.K. Extraction technique for the determination of oxygen-18 in water using pre-evacuated glass vials. Anal. Chem. 64:829–831; 1992.

Sternberg, L.d.S.L.; Swart, P.K. Utilization of freshwater and ocean water by coastal plants of southern Florida. Ecology 68:1898–1905; 1987.

Sternberg, L.; DeNiro, M.J.; Ajie, H. Stable hydrogen isotope ratios of saponifiable lipids and cellulose nitrate from CAM, C_3 and C_4 plants. Phytochemistry 23:2475–2477; 1984.

Stokes, M.A.; Smiley, T.L. *An Introduction to Tree-Ring Dating.* Tucson, AZ: Univ Arizona Pr.; 1996.

Switsur, R.; Waterhouse, J. Stable isotopes in tree ring cellulose. In: Griffiths, H., ed. *Stable Isotopes: Integration of Biological, Ecological and Geochemical Processes.* Oxford: BIOS; 1998:303–321.

Thorburn, P.J.; Dawson, T.E. Partitioning water source use by plants using isotopic mixing models: a précis.; in preparation.

Thorburn, P.J.; Walker, G.R.; Brunel, J.-P. Extraction of water from Eucalyptus trees for analysis of deuterium and oxygen-18: Laboratory and field techniques. Plant Cell Environ. 16:269–277; 1993.

Wershaw, R.L.; Friedman, I.; Heller, S.J. Hydrogen isotope fractionation of water passing through trees. In: Hobson, F.; Speers, M., eds. *Advances in Organic Geochemistry.* New York: Pergamon; 1966:55–67.

White, J.W.C. Stable hydrogen isotope ratios in plants: a review of current theory and some potential applications. In: Rundel, P.W.; Ehleringer, J.R.; Nagy, K.A., eds. *Stable Isotopes in Ecological Research.* Ecological Studies, Vol. 68. Heidelberg: Springer-Verlag; 1988:142–162.

White, J.W.C.; Cook, E.R.; Lawrence, J.R.; Broecker, W.S. The D/H ratio of sap in trees: Implications for water sources and tree ring D/H ratios. Geochim. Cosmochim. Acta 49:237–246; 1985.

White, J.W.C.; Lawrence, J.R.; Broecker, W.S. Modeling and interpreting D/H ratios in tree rings: A test case of white pine in northeastern United States. Geochim. Cosmochim. Acta 58:851–862; 1994.

Wise, L.E. *Wood Chemistry.* New York: Reinhold; 1944.

Wong, W.W.; Lee, L.S.; Klein, P.D. Oxygen isotope ratio measurements on carbon dioxide generated by reaction of microliter quantities of biological fluids with Guanidine Hydrochloride. Anal. Chem. 59:690–693; 1987.

Yakir, D. Variations in the natural abundance of oxygen-18 and deuterium in plant carbohydrates. Plant Cell Environ. 15:1005–1020; 1992.

Yakir, D.; DeNiro, M.J.; Rundel, P.W. Isotopic inhomogeneity of leaf water: Evidence and implications for the use of isotopic signals transduced by plants. Geochim. Cosmochim. Acta 53:2769–2773; 1989.

Yapp, C.J.; Epstein, S. A reexamination of cellulose carbon-bound hydrogen δD measurements and some factors affecting plant-water D/H relationships. Geochim. Cosmochim. Acta 46:955–965; 1982.

13

Measuring Water Availability and Uptake in Ecosystem Studies

Robert B. Jackson, Laurel J. Anderson, and William T. Pockman

Introduction

Terrestrial productivity depends strongly on the availability of water in the environment (Lieth 1972). Measuring the availability and movement of water among soil, plants, and the atmosphere requires methods from ecosystem studies, plant physiology, soil science, and biogeochemistry (Casper and Jackson 1997). Techniques for estimating the water status of soils have been reviewed recently (Rundel and Jarrell 1989; Boyer 1995) and those for measuring plant water status at cellular and whole-plant levels are thoroughly described in physiological ecology and plant physiology texts (e.g., Koide et al. 1989; Kramer and Boyer 1995). Rather than reviewing all methods for estimating plant and soil water, we emphasize techniques that are increasing in importance or changing rapidly for ecosystem studies. We include methods for determining the water content of soil, the availability of that water for plant uptake, and the transport of water through the plant (Fig. 13.1). Since many of these methods are also used in physiological ecology, our chapter is designed to bridge the gap between the scales of physiological and ecosystem ecology, as a foundation for other contributions in this book.

We begin by defining terms that describe water in the environment, including a brief discussion of water potential, the currency that allows the water status of soil, plants, and the atmosphere to be compared and the direction of flow to be predicted (Slatyer and Taylor 1960). We describe various techniques for measuring soil water in the field, emphasizing such recent innovations as time domain reflectometry and remotely sensed data. We also discuss methods for estimating the vegetative component of ecosystem water fluxes, including sap flow measurement and whole root/shoot hydraulic conductivity. Such techniques for estimating whole-plant water use are important for interpreting canopy and ecosystem water fluxes in eddy covariance and other net ecosystem approaches (see Chapter 11). We summarize the advantages and disadvantages of various techniques and recommend some future directions for research.

Theory and Currencies for Measuring Water in the Environment

To understand differences among methods it is helpful first to describe common ways of estimating water availability. The three most common terms for expressing soil water attributes are mass water content, volumetric water content, and soil water potential. Soil water content calculated on a mass basis, θ_m, is defined as

$$\theta_m = \frac{\text{soil water mass}}{\text{soil dry mass}} = \frac{(\text{wet soil mass} - \text{oven-dry soil mass})}{\text{oven-dry soil mass}} \quad (13.1)$$

θ_m is a proportion; the mass water percentage (P_m) is calculated by multiplying θ_m by 100%. The volumetric water content, θ_v, is defined as

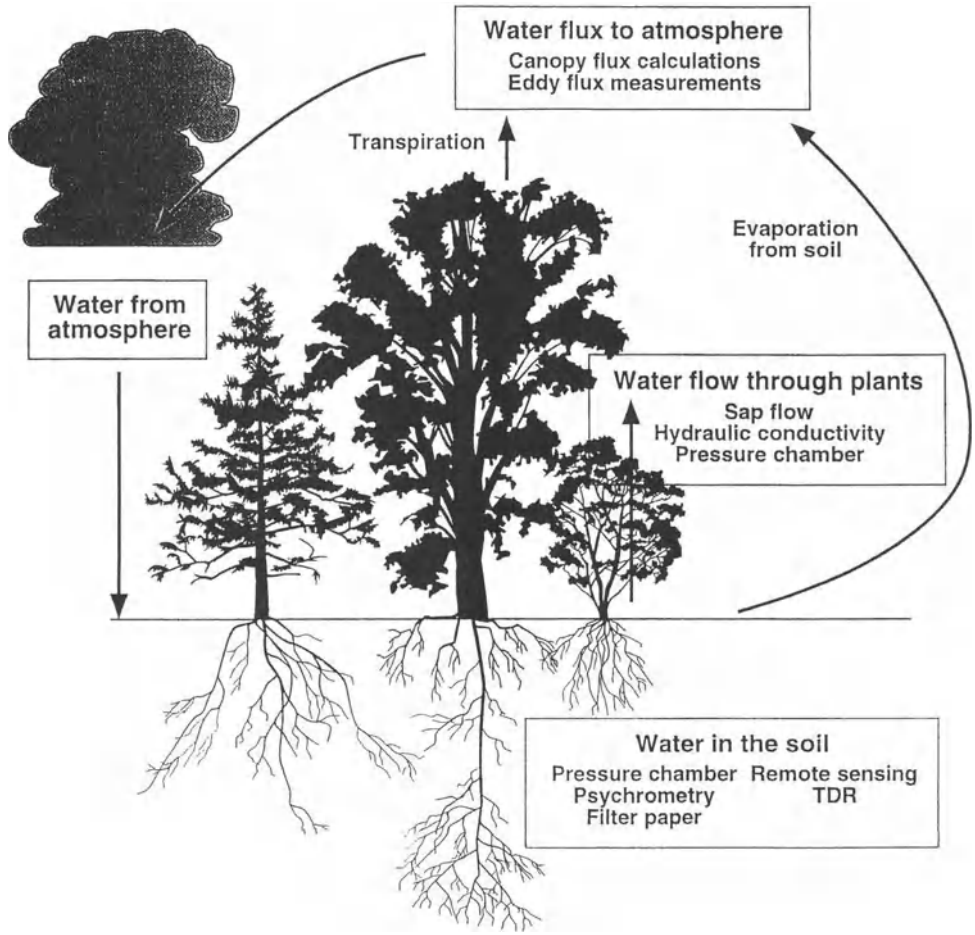

FIGURE 13.1. A simplified water cycle and some of the approaches used to measure water availability and movement in ecosystem studies.

$$\theta_v = \frac{\text{water volume}}{\text{bulk soil volume}} = \frac{\text{soil water mass}/\rho_w}{\text{bulk soil volume}} \qquad (13.2)$$

where ρ_w is the density of water. θ_v is also a proportion and can be converted to the volumetric water percentage (P_v) by multiplying by 100%. Further details can be found in Hanks and Ashcroft (1986) and Donahue et al. (1983).

Although θ_m and θ_v are important for understanding soil water properties, there is no consistent way to link either to the state of water in the atmosphere or in plants. To create a common currency for water in the environment, Slatyer and Taylor (1960) introduced water potential, ψ, based on the chemical potential of water:

$$\psi = \frac{(\mu_w - \mu_w^0)}{\bar{V}w} \qquad (13.3)$$

where μ_w is the chemical potential of water in the system under study, μ_w^0 is the chemical potential of pure, free water at a reference height and temperature and at atmospheric pressure (the reference state), and $\bar{V}_w$ is the partial molal volume of water (volume per mole of water) (Slatyer 1967). The upper term in the equation reflects the disequilibrium between the state of water in the experimental system and in its defined reference state, or, in thermodynamic terms, a measure of the work that may

be obtained from this disequilibrium. Water potential is most commonly expressed in units of pressure such as megapascals (MPa, and 1 Pa = 1 N m^{-2} = 1 (kg m s^{-2}) m^{-2}). The total water potential of most systems is usually negative (see below) because the reference state is defined as $\psi = 0$. When comparing two experimental states, such as the soil and an adjacent root, water flows from the system with a less negative ψ to that with a more negative ψ.

Total water potential, ψ_w, can be broken down into several components:

$$\psi_w = \psi_g + \psi_o + \psi_m + \psi_p \quad (13.4)$$

where g, o, m, and p refer to the gravitational, osmotic, matric, and pressure components of water potential. The gravitational component reflects the work required to lift water and is described by $\psi_g = \rho_w g h$, where g is the acceleration due to gravity and h is the vertical change in height. The value of ψ_g changes approximately 0.01 MPa per meter of difference in height, so relatively large values of h are required for ψ_g to become significant. The osmotic component, ψ_o, is described by the Van't Hoff relation for dilute ideal solutions: $\psi_o = cRT$, where T is absolute temperature, R is the universal gas constant (8.314 m^3 Pa mol^{-1} K^{-1}), and c is the osmolality of the solution. The matric component, ψ_m is a function of the surface tension of water among soil particles: $\psi_m = (-2\gamma\cos\vartheta)/r$, where γ is the surface tension of the liquid, ϑ is the contact angle between liquid and soil, and r is the radius of the soil pore (Hanks and Ashcroft 1986 but see Tyree and Karamanos, 1980; Sperry, 1997). The pressure, ψ_p, is generally taken as zero in the soil where the system is at atmospheric pressure. In the plant, ψ_p is typically negative in the apoplast and positive in the symplast due to turgor generated by osmosis. More detailed descriptions of water potential and the accompanying thermodynamics are presented in Slatyer (1967), Nobel (1991), and Kramer and Boyer (1995).

Conversions between ψ, θ_m, and θ_v are generally based on correlations with soil texture (the proportion of sand [0.05 to 2 mm], silt [0.002 to 0.05 mm] and clay [<0.002 mm] particles that make up the soil). The amount of available soil water (the difference between field capacity and the permanent wilting percentage) is smallest for a sandy soil, greatest for a loam, and intermediate for a clay soil (Fig. 13.2, bottom). Moisture tension release curves showing the relationship between ψ and θ_m or θ_v are generated by measuring ψ directly with thermocouple psychrometry (see below) and then destructively harvesting the soil to measure θ_m or θ_v (see Fig. 13.2, top).

Methods for Estimating Plant and Soil Moisture

We describe four approaches for measuring water status in the environment. The first is a brief discussion of gravimetric techniques, included because most other methods are calibrated against gravimetric θ_m and θ_v. The second approach is methods for measuring ψ directly in the environment, including the plant pressure chamber, thermocouple psychrometry, and the filter-paper method. The third is time domain reflectometry, an increasingly important technique described in some detail. The fourth and final approach is microwave radiometry for remotely sensing soil moisture, a technique with considerable promise for ecosystem and landscape studies.

Gravimetric Measurements of θ_m and θ_v

The mass water content of soils (θ_m) is determined simply and accurately using gravimetric techniques. Field samples are collected in soil cores sealed in plastic bags or in metal tins sealed with electrical tape. The wet samples are best weighed with a balance in the field, but transporting them to the laboratory in a cooler for weighing is also common. After drying the soil to constant weight at 105°C, the wet soil mass and oven-dry soil mass are used to calculate θ_m in Equation 13.1. The volumetric water content of soils (θ_v) is similarly obtained by collecting soil samples of known volume and assuming a density of 1 g cm^{-3} for water. Both θ_m and θ_v are easily converted if the soil's bulk density is known.

The advantages of the gravimetric method are its simplicity and low cost, requiring only a drying oven and a balance. This technique is used to calibrate other soil moisture instruments and can be applied under a range of soil depths and moisture conditions; it is one of the only techniques accurate

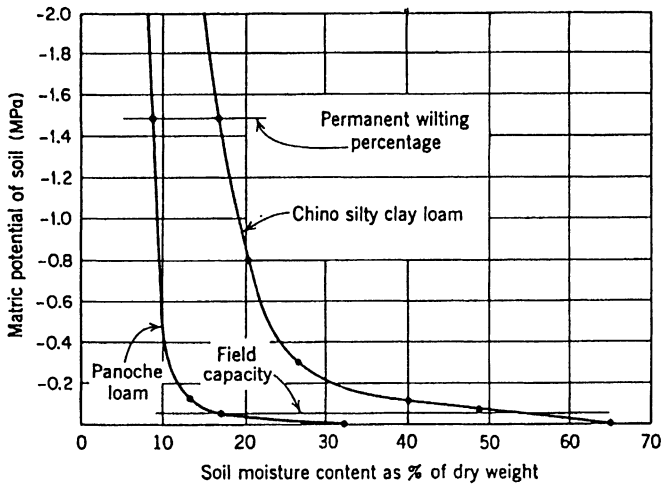

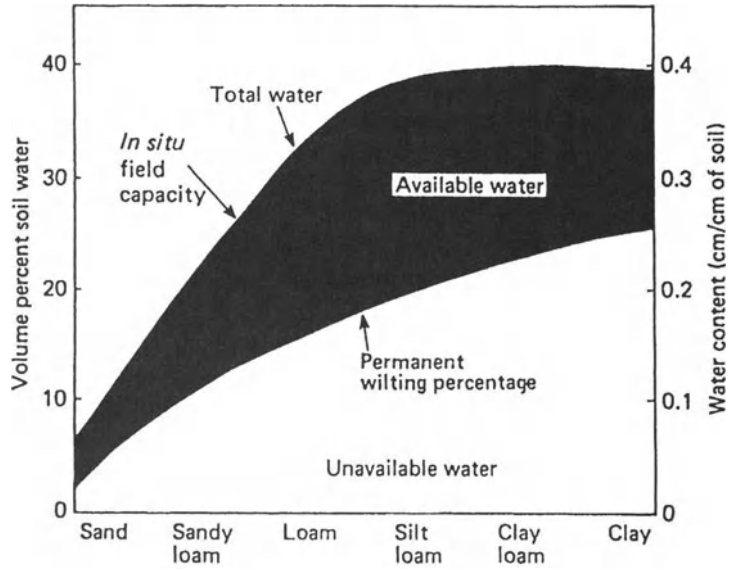

FIGURE 13.2. Top, Soil matric potential (MPa) for two sandy loam and clay loam soils as a function of soil water content. Bottom, Available and unavailable soil water across a range of soil textures (volume %, left axis; cm H_2O cm^{-1} soil, right axis). (From Kramer and Boyer [1995]. Used by permission of Academic Press.)

in very wet and very dry soils. Its major limitation is the requirement for destructive sampling. Other complications arise for stony soils, where θ_m and θ_v can be underestimated by including the mass and trivial water-holding capacity of stones. Stones >2 mm in diameter should be sieved from all samples and removed from calculations of θ_m and θ_v (Gardner 1986; Rowell 1994), though the volume of stones must be taken into account when ecosystem estimates of total water content are calculated. Sampling an accurate soil volume for θ_v can also be difficult in stony soils. Rowell (1994) discusses practical approaches for soil sampling and bulk density calculations in stony soils. Gardner (1986) gives a detailed treatment of the gravimetric method.

Techniques for Direct Measurement of ψ

There are at least two advantages to measuring water potential directly in the soil–plant–atmosphere continuum. First, water status anywhere along the continuum may be directly compared. Second, soil water can be expressed in terms of the energy needed by a plant to remove a unit of water from the soil. The two most commonly used techniques

to measure ψ in ecosystem studies are thermocouple psychrometry and the plant pressure chamber; both methods are widely used and have been reviewed elsewhere (e.g., Rundel and Jarrell 1989; Boyer 1995). We provide an overview of each approach and direct the reader to more detailed sources. We also outline a filter paper method that is a low-cost alternative for measuring soil ψ in some conditions.

Thermocouple Psychrometry

Water potential (expressed in units of pressure) may be described based on the relative vapor pressure of water in the experimental system compared with that of free, pure water at an equivalent temperature and pressure:

$$\psi = \frac{RT}{\bar{V}_w} \ln\left(\frac{e}{e_0}\right) \qquad (13.5)$$

where R is the universal gas constant, T is absolute temperature in °K, $\bar{V}_w$ is the partial molal volume of water, and e and e_0 are the vapor pressures of water in the experimental system and in the free, pure state, respectively. The ability to measure the vapor pressure of water in equilibrium with an in situ volume of soil or quantity of leaf tissue provides a convenient method to estimate ψ in thermocouple psychrometry.

Thermocouple psychrometry is based on the Seebeck effect: If a circuit consists of two metals and if the two metal junctions are at different temperatures, then a current flows around the circuit in a direction dependent on the metals chosen and the junction temperatures. A microvoltmeter may be used to measure the voltage in the circuit and, consequently, the temperature difference between the two junctions. The thermocouple junction used to measure relative humidity typically consists of fine chromel and constantan wires <25 μm in diameter (Brown 1970). The reference junction is typically a series of gold or copper posts to which the wires are connected. Ceramic or screen-cage covers allow the measurement junction to come into equilibrium with ψ in the surrounding soil solution.

The most common method for measuring in situ soil ψ is Peltier thermocouple psychrometry. By applying a current to the circuit, the measurement junction in equilibrium with the soil solution is cooled below the dew point of the surrounding air, causing droplets of water to form on the junction. When the Peltier current is turned off, the water on the junction begins to evaporate at a rate dependent on e in Equation 13.5. Isopiestic psychrometry ("iso" = equal, "piestic" = pressure) is a second type of psychrometry used to measure leaf ψ and ex situ soil ψ (Boyer and Knipling 1965). Drops of a series of solutions of known ψ, created using the Van't Hoff relationship discussed earlier, are placed on looped thermocouple wire and allowed to come to equilibrium with a leaf or soil sample. The solution that provides the same output as a dry thermocouple, neither warming nor cooling the junction, yields the sample ψ. Although no calibration is required and the technique is very accurate (± 0.01 MPa) (Boyer 1995), it is also time consuming and can not be automated or used for in situ soil analysis.

Thermocouple psychrometry is a powerful, accurate technique for estimating ψ in a small soil volume, but it has a number of difficulties. Except for the isopiestic technique, each psychrometer must be calibrated individually, making the method laborious and expensive. Contaminants, particularly salts, present on the measurement junction can alter the rate of evaporation and lead to inaccurate estimates of e (Rundel and Jarrell 1989). Because of problems with thermal gradients (Wiebe et al. 1977), in situ thermocouple psychrometers are usually positioned horizontally (making sure that the wire leading to them cannot act as a conduit for flowing water) and are generally only used below 30-cm soil depth. Thermocouple psychrometers are also not especially accurate in very wet soils. Boyer (1995) provides a much more detailed description of the theory of thermocouple psychrometry and its use in measuring ψ in plant tissue; Rundel and Jarrell (1989) provide an overview of thermocouple psychrometry for soil measurements. Commercial manufacturers include JRD Merrill Specialty Equipment (Logan, UT), Wescor, Inc. (Logan, UT), and Isopiestics Co. (Lewes, DE).

Plant Pressure Chamber

A second technique for measuring ψ in the environment is the plant pressure chamber. First used in the 1800s (Dixon 1914), the modern version dates to Scholander et al. (1965). A stem, branch, or leaf is cut from a plant and placed upside-down in an air-tight chamber with the point of excision

protruding outside the chamber through a rubber stopper. Pressurized gas (usually N_2) is gradually applied to the chamber until the pressure is sufficient to force water back to the cut surface. The pressure at which this occurs is an estimate of ψ for the tissue being measured. Assuming a rehydrating plant comes to equilibrium with the soil overnight, predawn measurements of ψ also provide an indication of the wettest soil ψ in which the plant's roots are actively taking up water. Midday measurements of ψ provide an indication of the water stress a plant experiences (Jackson et al. 1994).

The plant pressure chamber provides a simple, inexpensive method for estimating plant ψ and soil ψ within the active rooting zone of the plant. Measurements should be obtained within minutes after cutting the plant and the tissue should be placed in a sealed plastic bag to minimize evaporation until measurement. The point of excision should not be re-cut at any time during the procedure and it should protrude minimally outside the chamber. In some cases, it may be important to standardize the age/position of selected leaves where large phenological or physiological gradients occur. Some disadvantages of the pressure chamber are that it is labor intensive and difficult to automate. Because compressed gas is used, safety glasses should be worn and the plant sample should be viewed from the side rather than from above. For a more comprehensive treatment of the theory and assumptions behind the pressure chamber see Koide et al. (1989) and Boyer (1995).

Filter Paper Method

The filter paper method is a simple, low-cost alternative for determining soil ψ. The technique was developed by hydrologists and soil scientists, and its use has been largely restricted to these fields (Gardner 1937; Fawcett and Collis-George 1967; Hamblin 1981; Greacen et al. 1989). The method uses a known relationship between ψ_m and the gravimetric water content of a homogeneous porous material such as filter paper to estimate soil ψ (Gardner 1937). Filter paper disks are placed in contact with field soil, extracted core samples, or loose soil samples and left undisturbed until equilibrium is established between the paper and soil. The filter paper disk is either sandwiched between two intact core sections bound together or placed within loose soil samples lightly tamped down to establish soil–paper contact. While field equilibration must occur under prevailing conditions, laboratory samples are placed in a sealed container in an isothermal environment and left for periods between 1 hour (saturated soils) to 6 days (dry soils) to establish equilibrium between soil and paper.

After equilibration, the filter paper is removed, weighed immediately, and the gravimetric water content calculated using the oven-dry weight. Soil water potential is determined either from published calibrations for the selected filter paper or from local calibrations. While local calibration is required at high soil water potentials (soil $\psi > -0.1$ MPa), reliable measurements are possible using published data for the drier conditions often observed in the field (e.g., Whatman's No. 42 paper, Greacen et al. 1986; Greacen et al. 1989). The major sources of error are poor contact between paper and soil, temperature gradients/fluctuations during equilibration, and insufficient time for equilibration (e.g., Campbell and Gee 1986). When these errors are avoided, the approach may offer a low-cost alternative for estimating soil Ψ over a wide range of conditions.

Time Domain Reflectometry

Time domain reflectometry (TDR) measures soil θ_v and is based on the relationship between the apparent dielectric constant (K_a) of a soil and the soil's free water content (Davis and Chudobiak 1975). The unitless dielectric constant, also known as relative permittivity, is the ratio of electric field strength in a vacuum to that in a polarized substance (the dielectric)—the more polarized the dielectric, the greater the reduction in field strength (Parker 1983). As the dielectric constant for water (80) is much greater than that for air (1) or dry soil (3 to 7), the dielectric value for field soil is determined primarily by soil moisture (Cassel et al. 1994). Dalton and van Genuchten (1986) discuss the physical and mathematical principles of dielectric constants in detail.

Time domain reflectometry estimates K_a by measuring the time needed for an electromagnetic pulse emitted by a TDR instrument to travel along a probe in soil and reflect back to the soil surface from the probe end (Fig. 13.3). K_a is related to the propagation velocity (V) of an electromagnetic wave:

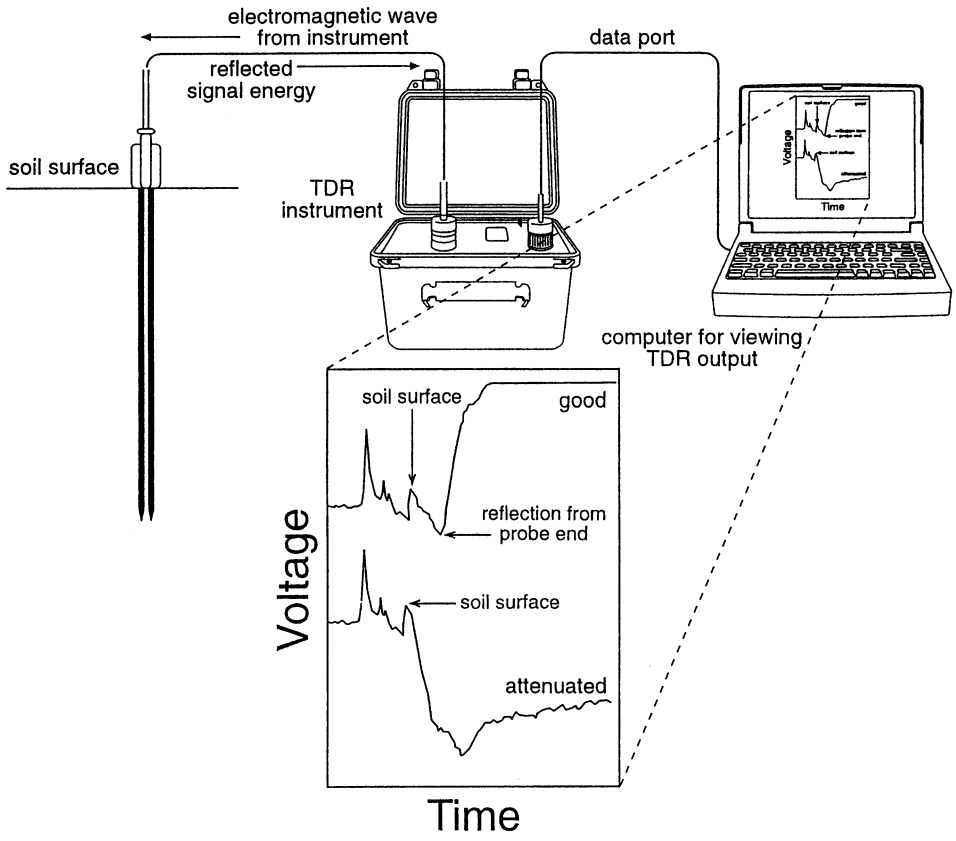

FIGURE 13.3. The basic components of a TDR system (not to scale) and two typical waveform outputs. The graph panel shows an example of a waveform associated with a good measurement of soil moisture and one with problems of attenuation. Waveforms can have different shapes than those shown here depending on the instrument and soil conditions.

$$V = c/(K_a)^{1/2} \tag{13.6}$$

where c is the speed of light. V can also be expressed as $V = 2l/t$ where t is the travel time for the pulse, and l is the probe length. K_a is therefore related to the length and travel time:

$$K_a = (ct/2l)^2 \tag{13.7}$$

Once K_a is estimated, θ_v averaged over the probe length is calculated from a calibration curve (Cassel et al. 1994). Early research suggested that soil characteristics other than water content, such as bulk density, mineral and organic content, and temperature, did not influence K_a significantly (Topp et al. 1980, 1982). Consequently, K_a for all soils could be converted to θ_v using a universal calibration (Topp et al. 1980):

$$\theta_v = -5.3 \times 10^{-2} + (2.92 \times 10^{-2} * K_a) - (5.5 \times 10^{-4} * K_a^2) + (4.3 \times 10^{-6} * K_a^3) \tag{13.8}$$

Further work revealed that this relationship, while robust for many soils, is not sufficiently accurate for all types, particularly finely textured or highly organic soils (Topp et al. 1980, Roth et al. 1992). Some workers have found that variation in bulk density, the fraction of bound water, and temperature affect TDR (Dasberg and Hopmans 1992; Dirksen and Dasberg 1993; Pepin et al. 1995). Other "universal" equations, including linear relationships between K_a and θ_v (e.g., Herkelrath et al. 1991, Whalley 1993), and dielectric mixing models that calculate θ_v using the volume fractions and dielectric constants of soil, air, and water (e.g., Roth

et al. 1990, Dirksen and Dasberg 1993) have been proposed. Relationships for specific soil types such as organics, minerals, and peats have also been suggested (e.g., Roth et al. 1992). Depending on the goals and soils in each study, these published curves may be appropriate (Zegelin et al. 1992). However, local calibration curves significantly improve estimates of soil moisture (e.g., Dasberg and Hopmans 1992; Gray and Spies 1995). Despite claims of TDR manufacturers whose instruments output θ_v using universal curves, a calibration for each soil should be generated by the user. Calibrations are done using packed soil columns or field soil cores.

Raw TDR output is a wave trace showing voltage changes in the electromagnetic wave as it reflects back to the instrument (see Fig. 13.3). These voltage changes correspond to variations in impedance, defined as the total opposition to current flow in an electrical circuit (Parker 1983). Mismatches in impedance between different materials along the TDR circuit path cause part of the signal energy to reflect back. Strong reflections occur at the soil surface and probe end, showing as peaks on the wave trace (Fellner-Feldegg 1969, Cassel et al. 1994). The distance from the soil surface peak to the final upward inflection represents the travel time of the electromagnetic wave t, used to calculate K_a. Early TDR required manual measurement of this distance on the wave trace (e.g., Topp et al. 1982), but many instruments now do this automatically using computer algorithms that search for characteristic changes in slope (e.g., Baker and Allmaras 1990).

Wave traces can vary substantially from the shape in Figure 13.3, making identification of the soil surface or probe end difficult. In highly conductive media, such as clays or saline soils, the electromagnetic pulse dissipates such that the final reflection is weak, called "signal attenuation" (see Fig. 13.3). While there are instrument and probe modifications that can address this problem, TDR is limited in very wet, conductive soils (Zegelin et al. 1992).

A wide variety of TDR probes (or wave guides) can be purchased or built. The most basic design includes a connection to conduct current from the coaxial cable into a set of stainless steel rods in the soil and a mechanism for holding the rods parallel. Probes generally range from 10 cm to 2 m in length and may be inserted into the soil at any angle (Topp and Davis 1985). They can be installed permanently or moved from site to site. Hook et al. (1992) created probes with diodes in the handles that switch from open to short circuits during a measurement. A shorted diode produces a strong reflection, but allows signal energy to pass into the soil when open. This identifies the soil surface without reducing signal strength. These workers also used diodes to divide long probes into segments, allowing measurements of moisture at different depths from one probe. For simple probe designs see Topp et al. (1984), Zegelin et al. (1989), and Heimovaara (1993).

Advantages of TDR include minimal soil disturbance and rapid, reliable measurements. Some probes can be built relatively cheaply. While TDR measures only the soil adjacent to the probe rods (Baker and Lascano 1989), θ_v is averaged over the probe length, providing an integrated measurement. Multidiode probes allow simultaneous sampling of moisture in different soil layers, which could give important insights into patterns of water flow and storage in ecosystems. Multiple probes can be connected to a data logger to allow simultaneous, regular readings at many sites (Baker and Allmaras 1990, Herkelrath et al. 1991).

Limitations of TDR include probe installation problems in stony or shallow soils. Signal attenuation in conductive soils may limit the probe lengths that can be used. Air pockets may form next to probes in soils that crack as they dry, causing measurement errors (Hokett et al. 1992). Sharply layered soils or large changes in the water profile with depth can create unexpected reflections in the wave trace, complicating interpretation (Nadler et al. 1991). Due to the variability of waveforms that can be generated in the field, TDR requires training and practice to use with confidence. Companies that sell TDR instrumentation include Environmental Sensors, Inc. (San Diego, CA), Soil Moisture Equipment Corporation (Goleta, CA), and Tektronix, Inc. (Redmond, OR). Detailed reviews of TDR are given in Zegelin et al. (1992) and Cassel et al. (1994).

Remotely Sensed Data Using Microwave Radiometers

Remotely sensed data for estimating soil moisture have been used for several decades (e.g., Schmugge et al. 1974). Existing methods can be separated into

two broad categories, passive and active techniques. Passive techniques measure the natural microwave radiation emitted by the ground surface (plants and the soil), while active techniques generate a pulse of microwave radiation and measure the backscatter to the sensor. The wavelengths most commonly used to minimize interference from the atmosphere are those greater than 5 cm (or a frequency of <6 GHz, where $v = c/\lambda$ and v is frequency, λ is wavelength, and c is the speed of light). Data are generally taken with truck-mounted equipment or from airplanes, but satellite measurements are becoming increasingly common (e.g., Owe et al. 1988).

Soil brightness temperature (T_B) as measured by a radiometer is related to soil temperature (T_{soil}) by the following relationship for a bare surface and isothermal soil (the Rayleigh-Jeans approximation to Planck's law):

$$T_B = (1 - r)T_{soil} = \varepsilon T_{soil} \qquad (13.9)$$

where r is reflectivity, ε is emmisivity, and $r = 1 - \varepsilon$. The emissivity is dependent on surface roughness and the dielectric constant of the soil (Engman and Chauhan 1995). The ability to assess soil moisture remotely is therefore based on the same dielectric effect used by time domain reflectometers—an increase in the soil dielectric constant K from <5 in dry soils to >25 in wet soils. Emissivity varies as a nonlinear function of K from approximately 0.95 in dry soils to 0.6 in wet soils, for a decrease in soil brightness temperature of more than 100°K (Schmugge 1990). Such large changes in T_B are easily measurable with microwave radiometers.

Several factors must be taken into account for interpreting remotely sensed soil moisture values. Surface roughness tends to increase emissivity and decrease reflectivity because of the increased surface area. The following equation was developed by Choudury et al. (1979) to incorporate roughness into the estimate of emissivity:

$$\varepsilon = R_0(1 - e^{-h}) \qquad (13.10)$$

where h is an empirical roughness parameter and R_0 is the smooth surface reflectivity (<0.1 for dry soils and up to 0.4 for wet). A rough surface (e.g., root mean square height variations of 5 cm) can result in a T_B that differs by 50°K compared with the same soil with a smooth surface (Choudury et al. 1979). A second complication arises from vegetation semitransparent to microwave radiation (Jackson and O'Neill 1987). With sufficient leaf area, the brightness temperature reflects the vegetation rather than the soil temperature. Corrections based on the water content of the vegetation are possible but complicated (Schmugge 1990). Additional factors for consideration are soil texture and the angle of measurement (if different from perpendicular).

The use of remotely sensed data is certain to increase. Overall, remote sensing of the moisture in the top 5 cm of the soil has great potential in deserts, crop systems, and some grasslands, and a number of field campaigns have shown good correlations between field and remotely sensed data across broad spatial scales (e.g., Lin et al. 1994). However, there are three primary disadvantages for microwave approaches in ecosystem research. The first is that current technologies are difficult to use in systems with high leaf area indices, such as forests, because the vegetation attenuates the microwave signal from the soil (Engman and Chauhan 1995). A dense thatch or dead vegetation layer causes similar problems (Schmugge et al. 1988). The second disadvantage is that microwave approaches are unlikely to provide information on soil layers deeper than 10 cm in the near future. The final disadvantage is that the approach is expensive, requiring airplane flights, truck-or tower-mounted equipment, or satellite imagery. Despite these problems, no existing technique has such potential for landscape and regional integration of soil moisture availability. Combining its use with ground-based methods and modeling provides a powerful approach for the coming century.

Estimating the Vegetative Component of Ecosystem Water Fluxes

The above methods are used to determine soil water potential, water content, and the availability of water to plants. Measuring the amount of water transferred to the atmosphere by plants is also important for many ecosystem studies (e.g., Jackson et al. 1998). Methods for determining total canopy or ecosystem water fluxes are described in Chapters

11 and 12. In all but the simplest systems, these methods can obscure the contributions of different vegetative constituents to total water fluxes. To understand the contributions of individual species and to predict changes in ecosystem water fluxes associated with vegetation change, ecosystem-level measurements must be combined with measurements of individuals from the dominant species or functional types.

Numerous studies have addressed leaf-level gas exchange and plant water use, but scaling such measurements to provide reliable estimates of stand or ecosystem fluxes is difficult (Jarvis 1993; Ansley et al. 1994; Verhoef 1997). In this section, we address two approaches with considerable promise for ecosystem studies: sap flow methods and measurements of whole plant hydraulic conductance. Sap flow methods are used for measuring water fluxes through stems of a variety of species. When combined with canopy or eddy correlation measurements, these methods help partition the contribution of species and plant functional groups to ecosystem water fluxes. They can also be coupled with stable isotope measurements (see Chapter 12) to estimate the volume of water transpired from different soil sources. The second useful approach is measuring the hydraulic conductance of entire root and shoot systems. As context for ecosystem studies, hydraulic measurements provide a mechanistic perspective on the contribution of different species and functional types.

Sap Flow Measurements

Sap flow techniques estimate the axial flow rate of water through root or stem xylem by applying heat and measuring the temperature of surrounding tissues. The methods used can be divided into three general groups: heat pulse, heat balance, and thermal dissipation techniques. Taken together, these methods permit measurement of sap flow through the roots and stems of herbs, grasses, crops, shrubs, and trees spanning a wide range of basal diameters (Lott et al. 1996; Baker and van Bavel 1987; Allen and Grime 1995; Kostner et al. 1992; Barrett et al. 1995). Several recent reviews cover various aspects of these methods (Pearcy et al. 1989; Swanson 1994; Edwards et al. 1996; Smith and Allen 1996).

Heat Pulse Method

The heat pulse method measures sap velocity through the xylem of woody stems. Two temperature probes are inserted in a stem above and below a heating element that is also inserted in the xylem of a woody stem. The lower temperature probe is positioned closer to the heater than the upper probe. Following the application of a 1- to 2-sec heat pulse, the temperature of both probes is measured continuously to determine the time (t_e) required for the two probes to reach the same temperature. The heat pulse velocity (v_h) is calculated as:

$$v_h = \frac{X_l - X_u}{2t_e} \tag{13.11}$$

where X_l and X_u are the distances between the heater and the lower and upper temperature sensors, respectively. Measured values of v_h are converted to sap velocity by accounting for sensor materials, wound effects, installation geometry, and the loss of heat to the stem during the measurement (e.g., Marshall 1958; Swanson and Whitfield 1981). Measuring the sap flow of entire stems often requires probes inserted to different depths and at different points around the stem to account for stem variation in sap flow. Integration of the resulting sap flow profile yields whole-plant water use (Green and Clothier 1988).

Heat Balance Methods

As the name suggests, heat balance methods apply heat (P) to the plant and measure the contribution of sap flow to the distribution of that heat. The amount applied is calculated from the heater resistance and the voltage. For the stem heat balance method, generally used with stems <120 mm in diameter, a heater is wrapped around the circumference of the stem and surrounded by insulation. Thermocouples are positioned to measure the radial and vertical temperature differences used to solve the heat balance (Sakuratani 1981; Baker and van Bavel 1987). For larger-diameter stems, a trunk sector heat balance method applies heat internally to a stem sector using embedded electrodes and thermocouples to measure vertical and lateral temperature differences (Cermak et al. 1984). The heat balance for both approaches is given by:

$$P = q_v + q_r + q_l + q_f \quad (13.12)$$

where q_v, q_r, q_l, and q_f are the vertical, radial, and lateral heat loss by conduction and the heat transferred by convection in the xylem sap, respectively. The lateral heat loss term q_l is only applicable in the trunk sector heat balance method since stem heat balance method applies heat evenly around the stem circumference. In both methods, q_f is calculated by subtracting q_v, q_r, and q_l from P. Sap flow is then calculated using q_f and the specific heat of water.

To determine q_r accurately, both heat balance approaches require measurements during periods of no flow for estimating the thermal conductance of insulation around the heater (Baker and van Bavel 1987).

Thermal Dissipation

The thermal dissipation method uses the installation of two probes in a woody stem, one probe directly above the other (Granier 1985, 1987). The upper probe contains a thermocouple junction and a heater powered by constant current, while the lower probe contains only a thermocouple. The temperature difference between probes (ΔT) is a function of the sap flow rate past the installation; the maximum difference occurs under conditions of no flow (ΔT_0) and the difference decreases as sap flow carries more heat away from the upper (heated) probe. Addition of a thermocouple array helps remove the confounding effects of naturally occurring vertical and lateral temperature gradients in the stem (Goulden and Field 1994). According to an empirical calibration for three tree species (Granier 1985), volumetric sap flux density (u_v) is given by:

$$u_v = 0.000119\left(\frac{\Delta T_0 - \Delta T}{\Delta T}\right)^{1.231} \quad (13.13)$$

Although this calibration may apply to other woody species (Granier et al. 1990), independent calibration may be required (Smith and Allen 1996).

Advantages and Disadvantages

The primary advantage of these methods is that they provide continuous measurements of sap flow in individuals over a wide range of plant sizes and functional types. It is thus possible to partition total plant water fluxes into the contributions of different species, at least in relatively simple systems. Simultaneous measurements at ecosystem and whole-plant scales can be combined in this way to address questions about the role of different species, life forms, or functional groups for ecosystem functioning (e.g., Ham et al. 1990; Kostner et al. 1992).

Sap flow methods are not without difficulties. Calibration is one important problem. The stem heat balance, trunk sector heat balance, and thermal dissipation methods depend on reliable measurements under no-flow conditions. If these conditions cannot be met, the accuracy of the methods is questionable (Smith and Allen 1996). A recently developed heat balance gauge may avoid this requirement through the incorporation of two heating elements (Peressotti and Ham 1996). In some installations, field values obtained using these methods can be checked by comparison with measurements of hydraulic conductance through the portion of the measured tissue containing the sap flow installation (e.g., Goulden and Field 1994).

Several other potential problems should also be considered. Heterogeneity in flow may confound whole-plant scaling when measuring flow in only a portion of the stem (Edwards et al. 1996). The accuracy of sap flow measurements may be compromised by tissue damage caused by prolonged heating effects (Smith and Allen 1996), toxic effects of silicone compounds used to improve thermal contact between heater and stem (Wiltshire et al. 1995), or wound responses and physical damage where portions of the apparatus are installed (Barrett et al. 1995). Finally, an error due to heat storage in the stem has been detected in some applications (Grime et al. 1995).

Whole Root/Shoot Hydraulic Conductance

Measurement of whole-plant hydraulic conductance is useful for mechanistic studies of ecosystem water fluxes and in determining the relative importance of individual plant species to total plant transpiration. Hydraulic conductance is defined as the mass flow rate for a given pressure difference (e.g., kg sec^{-1} MPa^{-1}) and may increase with the production of new xylem or decrease with cavitation caused by freezing or water stress. Seasonal and interspecific changes in hydraulic conductance can

have important consequences for plant gas exchange, which may be extended to understanding changes in ecosystem water fluxes.

Whole plant hydraulic conductance can be calculated using the pressure chamber and stem flow methods already described (Cohen et al. 1983; Tyree et al. 1994). The pressure difference across the plant can be taken as the difference between soil ψ estimated by predawn leaf water potential (ψ_l) and midday ψ_l. The pressure difference can be further divided into above- and belowground components by adding measurements of midday stem xylem pressure near the root crown. Pressure chamber measurements of a leaf or small branch attached to the main stem at ground level, and wrapped in advance with aluminum foil to eliminate flow, are used to measure stem xylem pressure. The hydraulic conductance of the whole plant, stem, or root system can be calculated by dividing the transpiration rate measured with sap flow methods by the appropriate pressure difference. These calculations assume the contribution of capacitance to the transpiration stream is negligible and that predawn ψ_l accurately reflects the ψ_s where water uptake occurs (Tyree et al. 1994).

Direct measurements of hydraulic conductance are also made by applying a pressure difference across the roots or shoots and measuring the flow through the system (Sperry and Pockman 1993; Kolb et al. 1996). Roots of potted plants can be measured by enclosing the soil and root system in a gas-tight container and measuring flow when the chamber pressure is increased (Saliendra and Meinzer 1992) or decreased by applying partial vacuum (Kolb et al. 1996). Until recently, field measurements have been more difficult because of the difficulty of generating a pressure difference without disturbing the root–soil interaction. The high pressure flowmeter (HPFM) (Tyree et al. 1993) permits the simultaneous application of pressure and measurement of flow into the cut stem or detopped root system. As originally developed, the HPFM method required the application of constant pressure over a period of hours until steady state flow was observed. During this extended measurement of roots, the accumulation of solutes caused by reverse flow through the roots changed the measured hydraulic conductance (Tyree et al. 1994). To minimize the effects of solute accumulation, a modified method measures flow as the applied pressure is increased at a constant rate (3 to 7 kPa sec^{-1}, Tyree et al. 1995). Using this approach, the hydraulic conductance of the measured tissue is calculated as the slope of the relationship between flow rate and applied pressure, and evidence suggests that this technique provides improved measurement of hydraulic conductance (Tsuda and Tyree 1997).

The development of the HPFM provides one method for measuring stem and root hydraulic conductances. Besides application to whole-plant physiology (Tyree et al. 1995), the availability of a technique for measurement of water transport through entire, intact root systems may prove useful in future ecosystem studies. In particular, measurements of whole-root systems and shallow and deep roots of the same plants may improve our understanding of how the characteristics of plant water transport influence ecosystem water fluxes.

Summary

Ecosystem studies are becoming increasingly important for monitoring and solving today's problems, such as those associated with global environmental change. This chapter is meant to be integrated with Chapters 11 and 12 for designing a well-conceived study of ecosystem water fluxes. Our chapter describes the necessary background and accompanying field measurements that may be taken for interpreting canopy fluxes and eddy covariance data. Promising methods include time domain reflectometry, remotely sensed data, and stem flow measurements. By combining such measurements with those discussed in the other chapters of this section, net ecosystem water fluxes across the landscape can be determined meaningfully and interpreted mechanistically.

Acknowledgments This research was supported by grants from the National Science Foundation (DEB 97-333333), NIGEC DOE, and the Andrew W. Mellon Foundation, and a USDA postdoctoral fellowship (#98-35100-6079) to W.T.P. M. Shawn Brumbaugh, J.R. Ehleringer. W.A. Hoffmann, and E.G. Jobbágy provided helpful suggestions on the manuscript.

References

Allen, S.J.; Grime, V.L. Measurements of transpiration from savannah shrubs using sap flow gauges. Agric. For. Meteorol. 75:23–41; 1995.

Ansley, R.J.; Dugas, W.A.; Heuer, M.L.; Trevino, B.A. Stem flow and porometer measurements of transpiration from honey mesquite (*Prosopis glandulosa*). J. Exp. Bot. 45:847–856; 1994.

Baker, J.M.; Allmaras, R.R. System for automating and multiplexing soil moisture measurement by time-domain reflectometry. Soil Sci. Soc. Am. J. 54:1–6; 1990.

Baker, J.M.; Lascano, R.J. The spatial sensitivity of time-domain reflectometry. Soil Sci. 147:378–384; 1989.

Baker, J.M.; van Bavel, C.H.M. Measurement of mass flow of water in the stems of herbaceous plants. Plant Cell Environ. 10:777–782; 1987.

Barrett, D.J.; Hatton, T.J.; Ash, J.E.; Ball, M.C. Evaluation of the heat pulse velocity technique for measurement of sap flow in rainforest and eucalypt forest species of south-eastern Australia. Plant Cell Environ. 18:463–469; 1995.

Boyer, J.S. *Measuring the Water Status of Plants and Soils.* San Diego, CA: Academic; 1995.

Boyer, J.S.; Knipling, E.B. Isopiestic technique for measuring leaf water potentials with a thermocouple psychrometer. Proc. Nat. Acad. Sci. USA 54:1044–1051; 1965.

Brown, R.W. *Measurement of Water Potential with Thermocouple Psychrometers: Construction and Applications.* United States Department of Agriculture (USDA), Forest Service Research Paper INT-80. Washington, D.C.: U.S. Government Printing Office; 1970.

Campbell, G.; Gee, G. Water potential: Miscellaneous methods. In: Klute, A., ed. *Methods of Soil Analysis. Part 1. Physical and Mineralogical Methods.* Agronomy Monograph 9. Madison, WI: American Society of Agronomy and Soil Science Society of America; 1986:619–633.

Casper, B.B.; Jackson, R.B. Plant competition underground. Annu. Rev. Ecol. Syst. 28:545–570; 1997.

Cassel, D.K.; Kachanoski, R.G.; Topp, G.C. Practical considerations for using a TDR cable tester. Soil Technol. 7:113–126; 1994.

Cermak, J.; Jenik, J.; Kucera, J.; Zidek, V. Xylem water flow in a crack willow tree *Salix fragilis* in relation to diurnal changes of environment. Oecologia 64:145–151; 1984.

Choudury, B.J.; Schmugge, T.J.; Chang, A.; Newton, R.W. Effect of surface roughness on the microwave emission from soils. J. Geophys. Res. 84:5699–5706; 1979.

Cohen, Y.; Fuchs, M.; Cohen, S. Resistance to water uptake in a mature citrus tree. J. Exp. Bot. 34:451–460; 1983.

Dalton, F.N.; van Genuchten, M.T. The time-domain reflectometry method for measuring soil water content and salinity. Geoderma 38:237–250; 1986.

Dasberg, S.; Hopmans, J.W. Time domain reflectometry calibration for uniformly and nonuniformly wetted sandy and clayey loam soils. Soil Sci. Soc. Am. J. 56:1341–1345; 1992.

Davis, J.L.; Chudobiak, W.J. In-situ meter for measuring relative permittivity of soils. Geol. Surv. Can. Ottawa. Paper 75-1A:75–79; 1975.

Dirksen, C.; Dasberg, S. Improved calibration of time domain reflectometry soil water content measurements. Soil Sci. Soc. Am. J. 57:660–667; 1993.

Dixon, H.H. *Transpiration and the Ascent of Sap in Plants.* London: Macmillan; 1914.

Donahue, R.L.; Miller, R.W.; Shickluna, J.C. *Soils: An Introduction to Soils and Plant Growth.* Englewood Cliffs, NJ: Prentice-Hall; 1983.

Edwards, W.R.N.; Becker, P.; Cermak, J. A unified nomenclature for sap flow measurements. Tree Physiol. 17:65–67; 1996.

Engman, E.T.; Chauhan, N. Status of microwave soil moisture measurements with remote sensing. Remote Sens. Environ. 51:189–198; 1995.

Fawcett, R.; Collis-George, N. A filter paper method for determining the moisture characteristic of soil. Aust. J. Exp. Agric. Anim. Husb. 7:162–167; 1967.

Fellner-Feldegg, J. The measurement of dielectrics in the time domain. J. Phys. Chem. 73:616–623; 1969.

Gardner, R. A method of measuring capillary tension of soil moisture over a wide moisture range. Soil Sci. 43:277–283; 1937.

Gardner, W.H. Water content. In: Klute, A., ed. *Methods of Soil Analysis. Part 1. Physical and Mineralogical Methods.* Madison, WI: American Society of Agronomy and Soil Science Society of America; 1986:493–544.

Granier, A. A new method of sap flow measurement in tree stems. Annales des Sciences Forestieres 42:193–200; 1985.

Granier, A. Evaluation of transpiration in a Douglas-fir stand by means of sap flow measurements. Tree Physiol. 3:309–320; 1987.

Granier, A.; Bobay, V.; Gash, J.; Gelpe, J.; Saugier, B.; Shuttleworth, W. Vapour flux density and transpiration rate comparisons in a stand of maritime pine (*Pinus pisaster* Ait.) in Les Landes forest. Agric. For. Meteorol. 51:309–319; 1990.

Goulden, M.L.; Field, C.B. Three methods for monitoring the gas exchange of individual tree canopies: Ventilated-chamber, sap-flow and Penman-Monteith

measurements on evergreen oaks. Func. Ecol. 8:125–135; 1994.

Gray, A.N.; Spies, T.A. Water content measurement in forest soils and decayed wood using time domain reflectometry. Can. J. For. Res. 25:376–385; 1995.

Greacen, E.; Walker, G.; Cook, P. Evaluation of the filter paper method for measuring soil water suction. *International Conference on the Measurement of Soil and Plant Water Status.* Logan, UT: Utah State Univ.; 1986:137–143.

Greacen, E.; Walker, G.; Cook, P. *Procedure for the Filter Paper Method of Measuring Soil Water Suction.* Divisional Report 108. Canberra, Australia: CSIRO Division of Soils; 1989.

Green, S.; Clothier, B. Water use of kiwifruit vines and apple trees by the heat-pulse technique. J. Exp. Bot. 39:115–123; 1988.

Grime, V.L.; Morison, J.I.L.; Simmonds, L.P. Including the heat storage term in sap flow measurements with the stem heat balance method. Agric. For. Meteorol. 74:1–25; 1995.

Ham, J.M.; Heilman, J.L.; Lascano, R.J. Determination of soil water evaporation and transpiration from energy balance and stem flow measurements. Agric. For. Meteorol. 52:287–302; 1990.

Hamblin, A. Filter paper method for routine measurement of field water potential. J. Hydrol. 53:355–360; 1981.

Hanks, R.J.; Ashcroft, G.L. *Applied Soil Physics.* Berlin: Springer-Verlag; 1986.

Heimovaara, T.J. Design of triple-wire time domain reflectometry probes in practice and theory. Soil Sci. Soc. Am. J. 57:1410–1417; 1993.

Herkelrath, W.N.; Hamburg, S.P.; Murphy, F. Automatic, real-time monitoring of soil moisture in a remote field area with time domain reflectometry. Water Resourc. Res. 27:857–864; 1991.

Hokett, S.L.; Chapman, J.B.; Cloud, S.D. Time domain reflectometry response to lateral soil water content heterogeneities. Soil Sci. Soc. Am. J. 56:313–316; 1992.

Hook, W.R.; Livingston, N.J.; Sun, Z.J.; Hook, P.B. Remote diode shorting improves measurement of soil water by time domain reflectometry. Soil Sci. Soc. Am. J. 56:1384–1391; 1992.

Jackson, R.B.; Paruelo, J.M.; Sala, O.E.; Mooney, H.A. Ecosystem water fluxes for two grasslands in elevated CO_2: A modeling analysis. Oecologia 113:537–546; 1998.

Jackson, R.B.; Sala, O.E.; Field, C.B.; Mooney, H.A. CO_2 alters water use, carbon gain, and yield for the dominant species in a natural grassland. Oecologia 98:257–262; 1994.

Jackson, T.J.; O'Neill, P. Temporal observations of surface soil moisture using a passive microwave sensor. Remote Sens. Environ. 21:281–296; 1987.

Jarvis, P. Prospects for bottom-up models. In: Ehleringer, J.; Field, C., eds. *Scaling Physiological Processes: Leaf to Globe.* San Diego: Academic; 1993:115–126.

Koide, R.T.; Robichaux, R.H.; Morse, S.R.; Smith, C.M. Plant water status, hydraulic resistance and capacitance. In: Pearcy, R.W.; Ehleringer, J.; Mooney H.A.; Rundel, P.W., eds. *Plant Physiological Ecology: Field Methods and Instrumentation.* London: Chapman and Hall; 1989:161–183.

Kolb, K.J.; Sperry, J.S.; Lamont, B.B. A method for measuring xylem hydraulic conductance and embolism in entire root and shoot systems. J. Exp. Bot. 47:1805–1810; 1996.

Kostner, B.; Schulze, E.-D.; Kelliher, F.; Hollinger, D.; Byers, J.; Hunt, J.; McSeveny, T.; Meserth, R.; Weir, P. Transpiration and canopy conductance in a pristine broad-leaved forest of Nothofagus: An analysis of xylem sap flow and eddy correlation measurements. Oecologia 91:350–359; 1992.

Kramer, P.J.; Boyer, J.S. Water relations of plants and soils. San Diego: Academic; 1995.

Lieth H. Modelling the primary productivity of the world. Nature Resourc. 8:5–10; 1972.

Lin, D.-S.; Wood, E.F.; Troch, P.A.; Mancini, M.; Jackson, T.J. Comparisons of remotely sensed and model-simulated soil moisture over a heterogeneous watershed. Remote Sens. Environ. 48:159–171; 1994.

Lott, J.E.; Khan, A.A.H.; Ong, C.K.; Black, C.R. Sap flow measurements of lateral tree roots in agroforestry systems. Tree Physiol. 16:995–1001; 1996.

Marshall, D. Measurement of sap flow in conifers by heat pulse transport. Plant Physiol. 33:385–396; 1958.

Nadler, A.; Dasberg, S.; Lapid, I. Time domain reflectometry measurements of water content and electrical conductivity in layered soil columns. Soil Sci. Soc. Am. J. 55:938–943; 1991.

Nobel, P.S. Physiochemical and environmental plant physiology. San Diego: Academic; 1991.

Owe, M.; Chang, A.; Golus, R.E. Estimating surface soil moisture from satellite microwave measurements and a satellite derived vegetation index. Remote Sens. Environ. 24:331–345; 1988.

Parker, S.P., ed. *McGraw-Hill Encyclopedia of Physics.* New York: McGraw-Hill; 1983.

Pearcy, R.; Schulze, E.-D.; Zimmermann, R. Measurement of transpiration and leaf conductance. In: Pearcy, R.; Ehleringer, J.; Mooney, H.; Rundel, P., eds. *Plant Physiological Ecology: Field Methods and Instrumentation.* New York: Chapman and Hall; 1989:137–160.

Pepin, S.; Livingston, N.J.; Hook, W.R. Temperature-dependent measurement errors in time domain reflectometry determinations of soil water. Soil Sci. Soc. Am. J. 59:38–43; 1995.

Peressotti, A.; Ham, J.M. A dual-heater gauge for measuring sap flow with an improved heat-balance method. Agron. J. 88:149–155; 1996.

Roth, C.H.; Malicki, M.A.; Plagge, R. Empirical evaluation of the relationship between soil dielectric constant and volumetric water content as the basis for calibrating soil moisture measurements by TDR. J. Soil Sci. 43:1–13; 1992.

Roth, K.; Schulin, R.; Fluhler, H.; Attinger, W. Calibration of time domain reflectometry for water content measurement using a composite dielectric approach. Water Resourc. Res. 26:2267–2273; 1990.

Rowell, D.L. *Soil Science: Methods and Applications.* New York: Longman; 1994.

Rundel, P.W.; Jarrell, W.M. Water in the environment. In Pearcy, R.W.; Ehleringer, J.; Mooney H.A.; Rundel, P.W., eds. *Plant Physiological Ecology: Field Methods and Instrumentation.* London: Chapman and Hall; 1989:29–56.

Sakuratani, T. A heat balance method for measuring sap flow in the stem of an intact plant. Agricultural Meteorology 37:9–17; 1981.

Saliendra, N.Z.; Meinzer, F.C. Genotypic developmental and drought-induced differences in root hydraulic conductance of contrasting sugarcane cultivars. J. Exp. Bot. 43:1209–1217; 1992.

Schmugge, T. Measurements of surface soil moisture and temperature. In Hobbs, R.J.; Mooney, H.A., eds. *Remote Sensing of Biosphere Functioning.* New York: Springer-Verlag; 1990:31–63.

Schmugge, T.; Gloersen, P.; Wilheit, T.; Geiger, F. Remote sensing of soil moisture with microwave radiometers. J. Geophys. Res. 79:317–323; 1974.

Schmugge, T.; Wang, J.R.; Asrar, A. Results from the push broom microwave radiometer flights over the Konza Prairie in 1985. IEEE Trans. Geosci. Remote Sens. 26:590–596; 1988.

Scholander P.F.; Hammel, H.T.; Bradstreet, E.D.; Hemmingsen, E.A. Sap pressure in vascular plants. Science 148:339–346; 1965.

Slatyer, R.O. *Plant-Water Relationships.* London: Academic; 1967.

Slatyer, R.O.; Taylor, S.A. Terminology in plant- and soil-water relations. Nature 187:922–924; 1960.

Smith, D.M.; Allen, S.J. Measurement of sap flow in plant stems. J. Exp. Bot. 47:1833–1844; 1996.

Sperry, J. Why you water the garden. BioScience 47:256–258; 1997.

Sperry, J.S.; Pockman, W.T. Limitation of transpiration by hydraulic conductance and xylem cavitation in *Betula occidentalis.* Plant Cell Environ. 16:279–287; 1993.

Swanson, R.H. Significant historical developments in thermal methods for measuring sap flow in trees. Agric. For. Meteorol. 72:113–132; 1994.

Swanson, R.; Whitfield, D. A numerical analysis of heat pulse velocity: Theory and practice. J. Exp. Bot. 32:221–239; 1981.

Topp, G.C.; Davis, J.L. Measurement of soil water content using time-domain reflectometry (TDR): A field evaluation. Soil Sci. Soc. Am. J. 49:19–24; 1985.

Topp, G.C.; Davis, J.L.; Annan, A.P. Electromagnetic determination of soil water content: Measurements in coaxial transmission lines. Water Resourc. Res. 16:574–582; 1980.

Topp, G.C.; Davis, J.L.; Annan, A.P. Electromagnetic determination of soil water content using TDR: I. Applications to wetting fronts and steep gradients. Soil Sci. Soc. Am. J. 46:672–678; 1982.

Topp, G.C.; Davis, J.L.; Bailey, W.G.; Zebchuk, W.D. The measurement of soil water content using a portable TDR hand probe. Can. J. Soil Sci. 64:313–321; 1984.

Tsuda, M.; Tyree, M. Whole-plant hydraulic resistance and vulnerability segmentation in *Acer saccharinum.* Tree Physiol. 17:351–357; 1997.

Tyree, M.T.; Karamanos, A.J. Water stress as an ecological factor. In: Grace, J.; Ford, E.; Jarvis, P., eds. *Plants and Their Atmospheric Environment.* Oxford: Blackwell; 1980:237–261.

Tyree, M.T.; Patino, S.; Bennink, J.; Alexander, J. Dynamic measurements of root hydraulic conductance using a high-pressure flowmeter in the laboratory and field. J. Exp. Bot. 46:83–94; 1995.

Tyree, M.T.; Sinclair, B.; Lu, P.; Granier, A. Whole shoot hydraulic resistance in *Quercus* species measured with a new high-pressure flowmeter. Ann. Sci. For. 50:417–423; 1993.

Tyree, M.T.; Yang, S.; Cruiziat, P.; Sinclair, B. Novel methods of measuring hydraulic conductivity of tree root systems and interpretation using AMAIZED. Plant Physiol. 104:189–199; 1994.

Verhoef, A. The effect of temperature differences between porometer head and leaf surface on stomatal conductance measurements. Plant Cell Environ. 20:641–646; 1997.

Whalley, W.R. Considerations on the use of time-domain reflectometry (TDR) for measuring soil water content. J. Soil Sci. 44:1–9; 1993.

Wiebe H.H.; Brown, R.W.; Barker, J. Temperature gradient effects on in situ hygrometer measurements of water potential. Agron. J. 69:933–939; 1977.

Wiltshire, J.J.J.; Wright, C.J.; Colls, J.J.; Unsworth, M.H. Effects of heat balance stem-flow gauges and associ-

ated silicone compound on ash trees. Agric. For. Meteorol. 73:135–142; 1995.

Zegelin, S.J.; White, I.; Jenkins, D.R. Improved field probes for soil water content and electrical conductivity measurement using time domain reflectometry. Water Resourc. Res. 25:2367–2376; 1989.

Zegelin, S.J.; White, I.; Russell, G.F. A critique of the time domain reflectometry technique for determining field soil-water content. In: Topp, G.C.; Reynolds, W.D.; Green, R.E., eds. *Advances in Measurement of Soil Physical Properties: Bringing Theory into Practice.* Madison, WI: Soil Science Society of America; 1992:187–208.

14

Nutrient Transformations

John M. Stark

Introduction

A question often asked in ecosystem studies is: What controls rates of release of plant-available nutrients? Nutrient elements are converted from unavailable to available forms through a wide variety of transformation processes (Stevenson 1986; Schlesinger 1991); however, there are some general cycling patterns that are common to all nutrients (Fig. 14.1). For example, most plant macronutrients exist in both organic and mineral forms. Therefore, the processes of mineralization (conversion of organic to mineral forms) and assimilation (conversion of mineral to organic forms) are common to these nutrients. Other nutrients also form insoluble compounds and, thus, dissolution and precipitation processes represent important pathways for release and immobilization of plant-available forms. While procedures used to measure concentrations of different nutrients vary considerably, the approaches used to measure these transformation rates are generally quite similar.

In this section, I discuss a variety of approaches that can be used to measure nutrient transformation rates. Rather than describing the details of specific procedures, I emphasize the theory, assumptions, advantages, and disadvantages of the various approaches. For descriptions of specific procedures, the reader should consult one of several excellent methodology texts (e.g., Weaver et al. 1994; Knowles and Blackburn 1993; Sparks et al. 1996). In the following discussion, the methods are divided into two groups: non-isotope methods and isotope methods. Methods for measuring nitrogen (N) cycling processes will often be used as examples for two reasons: N is the nutrient that most frequently limits net primary production in ecosystems, and many of the methods were originally developed to measure rates of N transformations. With appropriate modifications, however, these methods can be used to measure transformation rates of a variety of other nutrients.

Before discussing specific approaches, it is important to distinguish among some terms often used to describe rate estimates. The term "gross rate" refers to the unidirectional flow of a nutrient from one pool to another. It is the rate that is represented by individual arrows in Fig. 14.1. In contrast, a "net rate" is the difference between the flows into a pool (production processes) and the flows out of a pool (consumption processes). Net rates are determined simply by measuring the change in a pool size (nutrient concentration) over a period of time:

$$\begin{aligned}\text{net production rate} &= \frac{P_t - P_0}{t} \\ &= \sum \text{gross production rates} \\ &\quad - \sum \text{gross consumption rates} \end{aligned} \quad (14.1)$$

where P_0 is the nutrient concentration at the beginning of the incubation (time 0) and P_t is the concentration at the end of the incubation (time t). For consistency and ease of use in mass balance calculations, rates should be expressed in terms of the amount of element transferred, not the amount of compound. For example, rates of assimilation of phosphate (PO_4^{3-}) into plant biomass would be expressed in units of g P ha^{-1} day^{-1} rather than g PO_4^{3-} ha^{-1} day^{-1}.

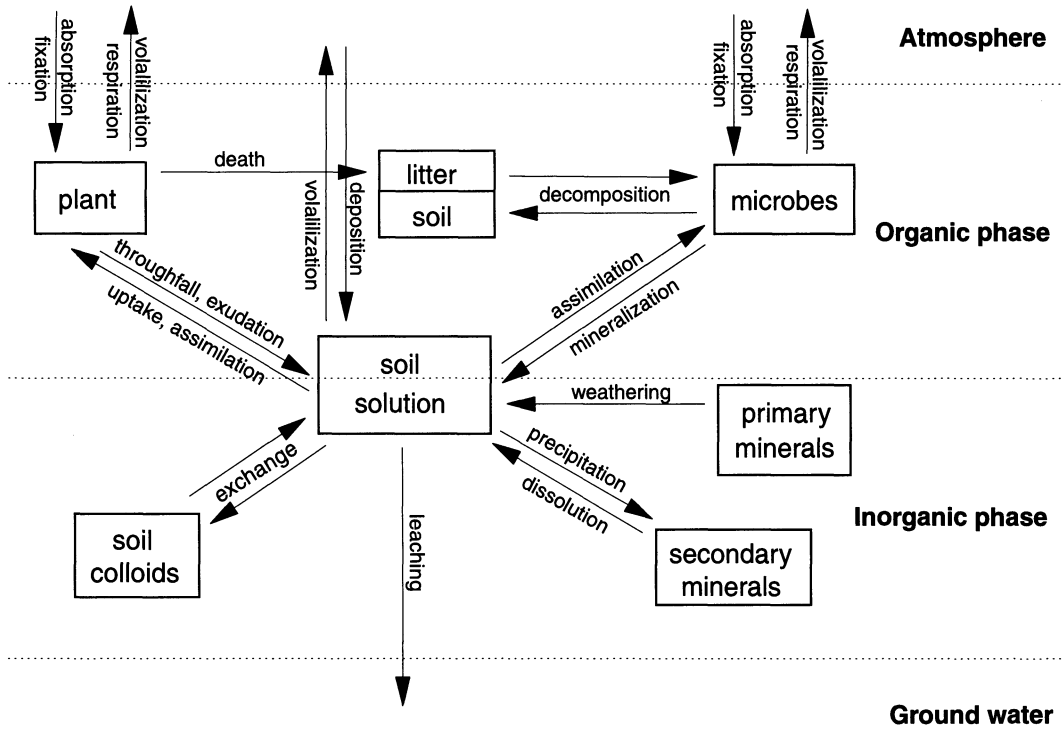

FIGURE 14.1. Generalized nutrient cycle for terrestrial ecosystems. (Modified from Aber and Melillo [1991].)

It can be seen from Equation 14.1 that the net production rate equals the gross production rate only when consumption processes are insignificant. When nutrient consumption occurs simultaneously with production, net rates underestimate gross rates. Measurement of the net change in nutrient concentration is the most common method for estimating transformation rates; however, when nutrient concentration is all that is measured, it is impossible to know for certain if production and consumption are co-occurring. For this reason, I will use the term "net rate" whenever a rate estimate is based solely on changes in concentration. I will use the term "gross rate" when isotopes are used to evaluate whether production and consumption are occurring simultaneously.

A third term often used to describe rates is the term "potential rate." This term is used to indicate that the incubation conditions were not representative of actual field conditions. In some, but not all cases, the term implies that the rates are maximal. For example, in the nitrification potential assay of Belser and Mays (1980), net rates of nitrate (NO_3^-) production are measured in shaken soil slurry samples incubated under nearly optimal conditions of moisture, temperature, and substrate availability. Under these conditions, gross nitrification rates approach maximum values (V_{max}), and NO_3^- consumption is inhibited so that net rates equal gross rates. In other assays measuring "potential rates," however, both consumption and production may be stimulated such that net rates are neither maximal nor indicative of gross rates. Examples are the nitrification potential and mineralization potential assays described by Stanford and Smith (1972) and Robertson and Vitousek (1981) in which moist sieved soil samples are incubated in the laboratory for various time periods (1 to 30 weeks), and net rates of inorganic N production are measured. In this assay, mixing and sieving tends to increase the availability of organic matter, which stimulates microbial activity. Because both production and consumption of inorganic N are stimulated, the potential net mineralization rate is not a good indicator of the gross mineralization rate. Instead, it is better used as an indicator of the quality

(e.g., C/N ratio) of the substrate available to the soil microbial community (Hart et al. 1994b).

Non-Isotope Methods

Non-isotope methods for estimating nutrient transformation rates can be divided into the following categories: (1) net rate measurements combined with inhibitors, (2) net rate estimates from nutrient budgets, (3) net rate measurements with "super sinks," and (4) net rate measurements using substrate analogs as non-isotope tracers. In the vast majority of experiments, estimates of transformation rates are obtained by combining net rate measurements with some type of inhibitor.

Net Rate Measurements with Inhibitors

As discussed previously, changes in nutrient concentration provide information on gross process rates only in extremely simple systems in which either only production or only consumption occurs. For example, the weathering rate of a primary mineral might be estimated from the changes in the quantity of mineral present at two points in time (see Fig. 14.1). The assumptions of this method are that (1) there are no confounding production or consumption processes and (2) rates are fast enough relative to measurement error that a significant change in concentration occurs during the course of the incubation period. Unfortunately, few systems are simple enough that changes in concentrations alone provide much information on gross process rates. Instead, net rate measurements are almost always combined with process inhibitors of some type to block confounding processes.

Inhibitors used to block confounding processes may be either physical or chemical. Physical barriers that prevent nutrient losses by mass flow and diffusion, or that exclude plant roots and prevent plant uptake are the most commonly used inhibitors. These include metal or plastic cylinders, solid or mesh partitions, or soil covers. A variety of chemical compounds are also frequently used to inhibit specific biogeochemical processes (Table 14.1) (Oremland and Capone 1988).

An experiment reported by Schimel et al. (1984) provides an elegant example of how gross process rates can be estimated in a complicated system by measuring net rates in the presence of inhibitors. Their objective was to measure rates of heterotrophic nitrification during laboratory incubations of forest soil samples. Heterotrophic nitrification involves the conversion of ammonium (NH_4^+) or organic N to nitrite (NO_2^-) and nitrate (NO_3^-), and in contrast to autotrophic nitrification (in which NH_4^+ is converted to NO_2^- and NO_3^-), heterotrophic nitrification is unaffected by acetylene. Schimel et al. (1984) used a modification of the nitrification potential assay described by Belser and Mays (1980) (Fig. 14.2). They incubated soil slurries in flasks, which obviously eliminated leaching and plant uptake as consumptive processes; they shook the samples to maintain high oxygen (O_2) concentrations, which blocked denitrification; they added NH_4^+, which inhibited microbial assimilation of NO_2^- and NO_3^-; and they added acetylene to block autotrophic nitrification. By blocking all production and consumption processes except the one process of interest (heterotrophic nitrification) they were able to use the net rate of NO_2^- and NO_3^- production to estimate the gross production rate.

Sometimes it is not possible to block all of the confounding processes. An alternative approach is to block the process of interest in one soil sample, and compare net rates in this sample with net rates in another sample in which the process has not been blocked. Assuming that all other process rates are the same in both soil samples, the difference between the two net rates provides an estimate of the gross rate. For example, Stark and Hart (1997) estimated field rates of gross nitrification in soils from a variety of forest ecosystems by comparing net rates of nitrate production in samples either exposed or not exposed to acetylene (C_2H_2). In samples not exposed to C_2H_2, net NO_3^- production equals the difference between gross nitrification and gross NO_3^- consumption:

$$\text{net } NO_3^- \text{ production} = \text{gross nitrification} - \text{gross } NO_3^- \text{ consumption} \quad (14.2)$$

In samples exposed to C_2H_2, gross nitrification is blocked:

$$\text{net } NO_3^- \text{ production}_{(w/C_2H_2)} = -\text{gross } NO_3^- \text{ consumption} \quad (14.3)$$

substituting Equation 14.3 into Equation 14.2 gives:

TABLE 14.1. Examples of chemical inhibitors that have been used during transformation rate measurements.

Process inhibited	Inhibitor	Reference
Autotrophic nitrification		
$NH_4^+ \rightarrow NO_2^-$	Acetylene, nitrapyrin, and others	Berg et al. (1982), Bedard and Knowles (1989)
$NO_2^- \rightarrow NO_3^-$	Chlorate	Belser and Mays (1980)
Nitrogen fixation	Carbon monoxide	Nohrstedt (1983), Tann and Skujins (1985)
Denitrification		
$N_2O \rightarrow N_2$	Acetylene	Balderston et al. (1976), Mosier and Klemedtsson (1994)
Ammonium assimilation (glutamine synthetase activity)	Methionine sulfoximine	Genetet et al. (1984), Schimel and Firestone (1989)
Nitrate assimilation	Ammonium	Betlach et al. (1981), Rice and Tiedje (1989)
Methanotrophy		
$CH_4 \rightarrow CO_2$	Acetylene and others	Bedard and Knowles (1989)
	Methyl fluoride	Oremland and Culbertson (1992)
Anaerobic respiration (denitrification; methanogenesis; Fe^{3+}, Mn^{4+}, and SO_4^{2-} reduction; etc.)	Oxygen and other terminal e-acceptors	Tiedje (1988)
Sulfur oxidation	N-ethylmaleimide	Pichtel and Dick (1991)
	2-Iodoacetamide	
Iron oxidation	Azide	Pichtel and Dick (1991)
Respiration		
Bacterial	Streptomycin	Anderson and Domsch (1975), Scheu & Parkinson (1994)
Fungal	Cycloheximide	
General microbial processes (decomposition, mineralization, respiration, etc.)	Azide	Wolf and Skipper (1994)
	Mercuric chloride	Wolf and Skipper (1994)
	Phenyl mercuric acetate	Bremner (1982)
	Thimerosal	Steffens and Sparks (1997)
	Complete sterilization	Wolf and Skipper (1994)

$$\text{net } NO_3^- \text{ prod}_{(w/oC2H2)} = \text{gross nitrification} + \text{net } NO_3^- \text{ prod}_{(w/C_2H_2)} \quad (14.4)$$

or:

$$\text{net } NO_3^- \text{ prod}_{(w/oC_2H_2)} - \text{net } NO_3^- \text{ prod}_{(w/C_2H_2)} = \text{gross nitrification} \quad (14.5)$$

Nitrification rates estimated using this acetylene inhibition technique had nearly a 1:1 correlation with gross nitrification rates measured by a $^{15}NO_3^-$ isotope dilution technique (described later).

The "buried bag" technique (Eno 1960; Gordon et al. 1987) is a similar approach that has been used extensively to estimate rates of net N mineralization and plant uptake of soil inorganic N. For example, Nadelhoffer et al. (1984) collected soil core samples from several deciduous forests. They measured initial concentrations of inorganic N by extracting subsamples with a salt solution (1 *M* KCl), and then they reburied other subsamples in polyethylene bags for 1-month field incubations. At the end of 1 month, soil from inside buried bags and from nearby undisturbed areas was extracted to determine inorganic N concentrations. By subtracting the net rate of N mineralization in the undisturbed soil (with plant uptake) from the net rate in the bag (without plant uptake), they estimated the amount of inorganic N taken up by plants during the 1-month period (Fig. 14.3).

Zou et al. (1992) describe a technique for estimating gross phosphorus (P) mineralization and immobilization that utilizes different sterilization treatments to inhibit specific P transformations (Fig. 14.4 and Table 14.2). Gamma irradiation kills living organisms but allows exoenzymes such as phosphatases to remain active. Therefore, this treatment inhibits P immobilization but not P mineralization. Gamma irradiation plus autoclaving kills living organisms and inactivates exoenzymes, which results in inhibition of both P immobilization and mineralization. Net rates of phosphate (PO_4^{3-}) accumulation on anion-exchange resins (see section

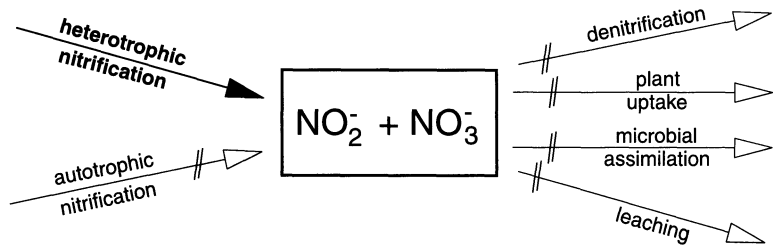

FIGURE 14.2. Processes involved in production and consumption of nitrite and nitrate in soil. When inhibitors are used to block all but one process (heterotrophic nitrification), the net change in pool size (concentration) can be used to estimate the gross rate (see Schimel et al. 1984).

on "super-sinks" below) are compared in control samples (no sterilization), irradiated samples, and irradiated plus autoclaved samples. Differences in net rates are then used to calculate gross rates of P mineralization and immobilization and net rates of P dissolution or precipitation from minerals (see Table 14.2).

When using any type of inhibitor, it is absolutely critical to evaluate how completely the inhibitor blocks the target processes and whether the inhibitor influences any nontarget processes. Antibiotics are frequently less than 100% effective due to the prevalence of antibiotic resistance in soil microbial populations. Many other compounds are competitive inhibitors, and thus their effectiveness varies with the nutrient concentration. Inhibitors that are less than 100% effective or that have unintended side effects on other processes can result in erroneous rate estimates unless corrections can be made. For example, Zou et al. (1992) found that in certain soils, irradiation reduced phosphatase activity by 20 to 30% and increased initial resin-extractable PO_4^{3-} concentrations relative to untreated soils, and that it was necessary to account for these effects during rate calculations.

In the technique described earlier in which gross rates of nitrification were estimated by acetylene inhibition (Stark and Hart 1997), blocking NO_3^- production causes a decline in the NO_3^- concentration. If NO_3^- consumption is limited by NO_3^- availability, then consumption rates in the presence of C_2H_2 will be lower than rates in the absence of C_2H_2. This would cause gross nitrification rates to be underestimated; however, incubation of samples for short time periods will minimize pool depletion, and thus minimize the error (Stark and Hart 1997).

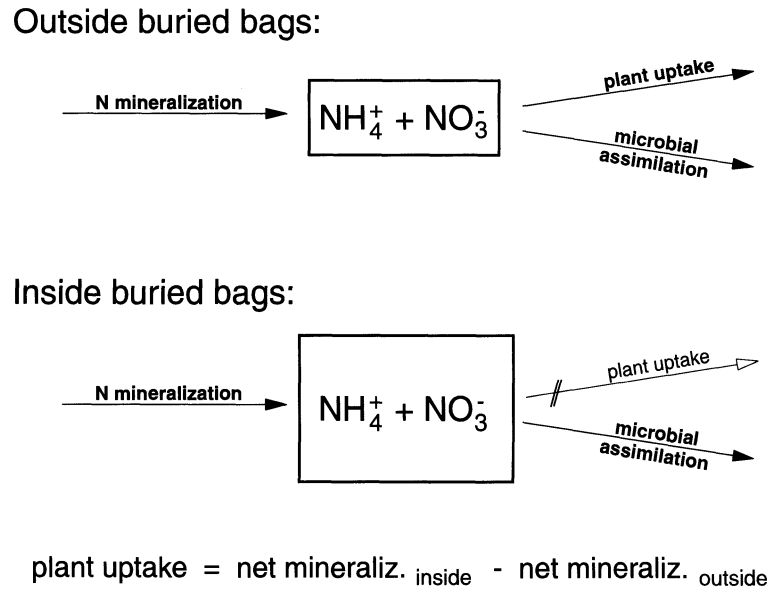

FIGURE 14.3. Use of the "buried bag" technique to estimate rates of plant uptake of inorganic N. Net N mineralization rates will be greater inside buried bags of soil than in undisturbed soil outside the bag because plant uptake has been eliminated. Assuming that all other process rates are unaffected by incubating soil in bags, the difference in net mineralization rates will equal the rate of plant uptake (e.g., Nadelhoffer et al. 1984).

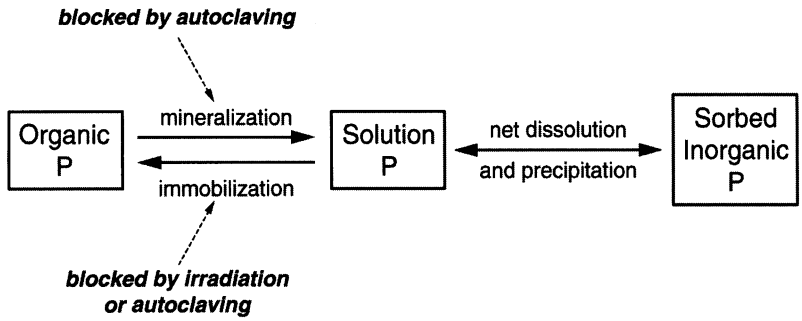

FIGURE 14.4. Use of inhibitors (irradiation or autoclaving) to estimate phosphorus transformation rates. See Table 14.2 for further explanation of the technique.

In the example in which plant uptake was estimated by incubation of buried bag samples (Nadelhoffer et al. 1984), elimination of plant uptake resulted in increased inorganic N pools. In N-limited systems, other consumption processes such as microbial assimilation may be stimulated, and plant uptake rates will be underestimated. For this reason, net mineralization rates in buried bags only provide accurate estimates of plant uptake when microbial assimilation is not N-limited (Hart et al. 1994b).

Another problem with the buried bag technique is that the soil is protected from precipitation, leaching, and soil moisture extraction by plant roots. Therefore, soil moisture in the buried bag may not follow the same temporal patterns as in undisturbed soil. Differences in moisture dynamics may produce unrepresentative rates inside the buried bags. This problem has been minimized in some studies by driving plastic or metal cylinders into the soil to collect intact soil cores, replacing the lower 1 cm of soil in the core with an ion exchange resin disk, and re-burying the cylinder + soil + resin disk in its original position (DiStefano and Gholz 1986). This open-topped resin core allows wetting and evaporation to occur, but the resin disk traps nutrients that would be lost by leaching. At the end of the incubation period, nutrient concentrations in both the soil and the ion exchange resins are determined. The quantity of nutrient trapped by the resin is added to the nutrient increase in the soil to calculate the net mineralization rate.

TABLE 14.2. Technique for estimating gross phosphorus mineralization and immobilization and net phosphorus dissolution or precipitation rates in soil. Based on procedure described by Zou et al. (1992).[a]

Treatment	Effect	P transformations occurring
Control (c)	—	Net dissolution/precipitation Gross mineralization Gross microbial immobilization
Radiation (r)	Sterilize soil	Net dissolution/precipitation Gross mineralization
Radiation + autoclaving (ra)	Sterilize soil Denature enzymes	Net dissolution/precipitation

[a]Rate calculations:

$$\text{net dissolution} = \Delta P_{ra}$$
$$\text{gross mineralization} = \Delta P_r - \Delta P_{ra}$$
$$\text{gross immobilization} = \Delta P_r - \Delta P_c$$

where ΔP is the resin-extractable PO_4^{3-} measured during 1-day incubations of samples from the different soil treatments. Note that ΔP_r and ΔP_{ra} must be corrected to account for any non-target effects of irradiating and autoclaving.

Rate Measurements Obtained from Nutrient Budgets

Nutrient budgets can be used to estimate nutrient transformation rates if information is available on a variety of nutrient pools and rates of associated production and consumption processes. First, the net change in all associated nutrient pools is calculated, or if the system is at steady state a net change of zero may be assumed. Then the sum of all known consumption rates is subtracted from the sum of all known production rates. Any discrepancy between the net change in nutrient pools and the balance of production and consumption (i.e., the left- and right-hand sides of Equation 14.1) is attributed to the unknown process rate. Nutrient budgets have been most frequently used to estimate ecosystem inputs or outputs of nutrients over relatively long time scales (Bormann et al. 1977; Peterjohn and Schlesinger 1990; Binkley et al. 1992b). For example, rates of N fixation for entire ecosystems have been estimated by directly measuring inputs, such as wet and dry deposition, and outputs, such as leaching and denitrification, and then either measuring the increase in N in the ecosystem or assuming that steady state exists (for examples see Chapter 16 and references in Boring et al. 1988). Budgets can also be used for smaller units than ecosystems. For example, net changes in plant N can be used to estimate N fixation rates if other plant N gains and losses can be quantified. A nutrient budget approach could also have been used to estimate the rate of heterotrophic nitrification (see Fig. 14.2) if the net change in NO_2^- and NO_3^- were known, and if instead of blocking the other rates (autotrophic nitrification, plant uptake, microbial assimilation, denitrification, and leaching), it were possible to measure them directly.

One of the most important problems with the use of budgets is that the rate of interest is estimated by difference, and thus the error for the rate estimate represents the sum of the errors for all other rate estimates. Therefore, rate estimates from budgets often have very large uncertainties (Binkley et al. 1992a).

Net Rate Measurements with "Super Sinks"

In some cases, it is possible to add a component that absorbs the nutrient of interest. If the sink strength of this component is great enough, it will compete with other consumptive processes for the nutrient, and it will not release the nutrient back into the system. Accumulation of nutrients in the added sink can then be used to estimate rates. Examples of such "super sinks" are acid traps, base traps, and ion exchange resins.

Traps containing a strong acid, such as hydrochloric acid (HCl) or sulfuric acid (H_2SO_4), have been used to trap ammonia (NH_3) gas that has volatilized from soil or plant surfaces (e.g., Schlesinger and Peterjohn 1991), and traps containing a strong base, such as potassium hydroxide (KOH) or lime, have been used to trap carbon dioxide (CO_2) (Van Cleve et al. 1979). Dishes or vials containing the acid or base can be placed inside soil covers, or a known volume of air can be circulated through traps (Van Cleve et al. 1979; Klubeck and Skujins 1981). When used correctly, these traps are highly efficient and do not release the nutrient back into the system. Precautions must be taken to ensure that the trapping capacity is sufficient so that the traps do not approach saturation during the incubation period. Also, the surface area of the absorbing portion of the trap must be high enough that diffusion into the trap is not restricted. Raich and Nadelhoffer (1989) observed that during measurement of CO_2 flux from soils, the area of the alkali trap should be at least 6% of the area occupied by the soil cover.

Ion exchange resins (IERs) are typically used to examine production of soluble nutrient ions, either as an index to how much plant-available nutrient is produced or to measure leaching losses of nutrients (Sibbeson 1977, Binkley and Hart 1989). Ion exchange resin beads are placed in nylon mesh bags (made from nylon stockings) and then buried in the soil for time periods ranging from a few weeks to several months, depending on nutrient flux rates and the exchange capacity of the IER (Binkley and Matson 1983). The resin bags are retrieved, extracted in a strong salt solution (e.g., 2 *M* KCl), and the extract is analyzed for nutrient concentrations. Either cation or anion exchange resins may be used, depending on whether the nutrient exists as a cation (e.g., Ca^{2+}, Mg^{2+}), anion (e.g., PO_4^{3-}, SO_4^{2-}), or both (e.g., NH_4^+, NO_3^-). Mixed-bed resins, which contain a mixture of both cation and anion exchange resins, are most commonly used because they act as a sink for a variety of nutrient ions. Various placement methods have been used. The

bag may be simply buried at a particular depth in the soil; however, this results in soil disturbance and precludes repeated measurements at the same location. Plastic access tubes have been placed at an angle in the soil, and then the resin bag is lowered down the tube with a string until it contacts the soil at the end of the tube. A wooden rod can be used to press the resin bag firmly against the soil. Attachment of a string to the bag allows it to be withdrawn and replaced at various time intervals. Other researchers have placed a ring of stiff rubber tubing inside each resin bag to force the bag into a disk shape. This ion exchange disk can be placed horizontally in the soil or attached to the base of a soil core to measure leaching rates of nutrients (DiStefano and Gholz 1986; Hart and Firestone 1989; Zou et al. 1992). Use of circular ion exchange disks with known areas allows the flux rates to be expressed per unit area of soil surface. In another approach, ion exchange membranes, rather than IER beads, are buried in soil (Gibson 1986, Subler et al. 1995). A known area of membrane is wrapped around a metal stake, which is driven into the soil to a predetermined depth. This "IER spike" can then be removed and replaced with a fresh one for repeated measurement at the same location with minimal soil disturbance.

One problem with interpretation of nutrient data collected using IERs is that fluxes are a function not only of nutrient production processes and competing consumption processes, but also of nutrient transport processes. Ions with higher diffusivities will appear in greater concentrations on IERs than ions with low diffusivities. Differences in soil water contents will cause different nutrient accumulation rates on IERs because of differences in rates of diffusion or leaching. In soils with greater moisture contents, transport processes will be faster, and a larger volume of soil will be "sampled" by the resin. This makes it difficult to express flux rates on a soil weight or area basis. The use of IER disks attached to plastic or metal cylinders containing soil cores, or the use of IER membranes may help solve this problem.

Another problem with the use of IERs for estimating process rates is that it is usually not known how efficiently the IERs compete with other processes. If the IERs are a perfect competitor with a particular consumption process, then the rate of accumulation of nutrient ions on the IERs will provide a good estimate of the gross rate of that consumption process. If they are only an incomplete competitor, then data from the IERs will underestimate the gross rate. For example, IER disks sealed to the base of plastic or metal soil cores are very efficient at stripping NH_4^+ and NO_3^- out of water that passes through the IER disk, and thus they are essentially perfect competitors with the leaching process. On the other hand, IER bags do not absorb all of the nutrient ions released by mineralization processes before microorganisms or plant roots take up the ions. Therefore, the rate of accumulation of nutrient ions on IER bags will underestimate gross mineralization rates. Because of this, IER methods are considered to provide an index to mineralization rates and plant uptake rather than an estimate of actual gross rates (Binkley and Hart 1989).

Rate Measurements Using Substrate Analogs

Enzymes responsible for nutrient transformations are often capable of transforming other compounds as well. If these alternate substrates are normally present in low concentrations, and if relatively simple methods are available for quantification of either the substrate or the product, then this substrate may be used as a non-isotope tracer for calculating rates. Examples of compounds that have been used are: acetylene for estimating rates of N fixation (Weaver and Danso 1994), sodium *p*-nitrophenyl phosphate for estimating rates of P mineralization, and 2,3,5-triphenyltetrazolium chloride for estimating rates of microbial respiration (dehydrogenase activity) (Tabatabai 1994). While techniques utilizing substrate analogs as non-isotope tracers have been used extensively in laboratory studies, they have been used relatively little for field measurements. One reason for this is that conversion factors are necessary to calculate nutrient transformation rates based on rates of transformation of the substrate analog. The conversion factors often vary with the incubation conditions (e.g., moisture content, temperature, soil disturbance, etc.), and control of these incubation conditions may not be possible under field conditions. A second problem is that addition of the substrate analog is likely to stimulate rates. Therefore, transformation rates estimated using substrate analogs are usually re-

ferred to as potential rates or enzyme activity measurements.

Isotope Methods

For discussion purposes, I divide isotope methods into four general categories: (1) tracer techniques, (2) isotope dilution techniques, (3) isotope models utilizing numerical solutions, and (4) natural abundance techniques. Of these approaches, isotope dilution techniques and isotope modeling have the greatest utility for estimating gross nutrient transformation rates in ecosystems; therefore, I emphasize these in my discussion. Additional discussions of specific isotope techniques can be found in Chapters 8 and 12 and Knowles and Blackburn (1993), Schimel (1993), Hart et al. (1994b), Wolf et al. (1994), and Lajtha and Michener (1994).

Tracer Measurements

In ecosystem studies, the most common use of isotopes is as tracers. A small amount of a radioactive or stable isotope is added in a particular molecular form (e.g., $^{15}NH_4^+$ or $^{15}NO_3^-$) in order to label a source pool. Flow of the isotope out of the source pool into various sink pools is then monitored over time. Based on the amount of isotope recovered in a sink pool, one can calculate the total amount of nutrient that flowed into that pool from the labeled source pool. For example, the total flow of a nutrient from pool A to pool B in Figure 14.5 is calculated as:

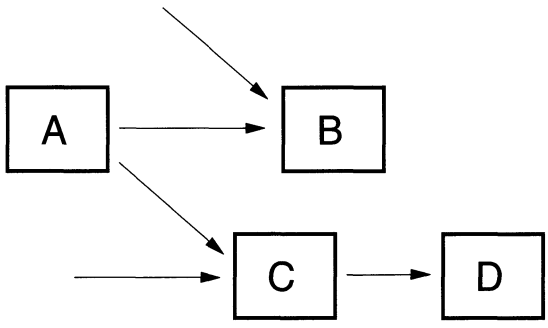

FIGURE 14.5. Hypothetical flow of nutrients during a tracer experiment.

$$M_{AB} = \frac{P_B \cdot I_B}{I_A} \tag{14.6}$$

where M_{AB} is total amount of nutrient (added plus natural isotopes) that flowed from pool A to pool B during the incubation period (e.g., mg N kg^{-1} soil); P_B is the size of the sink pool (B) at the end of the incubation (e.g., mg N kg^{-1} soil); I_B is the relative amount of isotope, in excess of background, that is found in pool *B* at end of the incubation (measured as atom % excess if a stable isotope is used or specific activity if a radioactive isotope is used); and I_A is the relative amount of isotope, in excess of background, that is present in the source pool, A (units are the same as for I_B). The total flow of nutrient from A to B calculated from Equation 14.6 is converted to a rate by dividing M_{AB} by the length of the incubation period.

The assumptions of the tracer method are: (1) The added isotope acts the same as the naturally occurring isotope (i.e., no significant discrimination or fractionation occurs), (2) the source pool is uniformly labeled by the isotope, (3) addition of the isotope does not stimulate rates, (4) no additional nutrient moves into the source pool (the source pool has a constant enrichment), and (5) nutrients are not lost from the sink pool.

The first assumption, that discrimination or fractionation does not occur, is frequently not valid. Different isotopes often have different reaction rates (Handley and Raven 1992). The differences are usually very small (<2%), however, and errors due to isotope discrimination or fractionation can usually be ignored when one is working with isotope enrichments that are well above natural abundance.

The second assumption, of uniform labeling of the source pool, is often more difficult to achieve than it seems. In studies of decomposition rates, ^{14}C-labeled plant material may be prepared by growing plants in an atmosphere containing $^{14}CO_2$. Frequently, plants are exposed to $^{14}CO_2$ for a single short period of time, as part of a "pulse labeling technique"; however, uniform distribution of ^{14}C among structural and soluble plant components may not occur even when the plant is grown in the presence of the isotope for several months (Lynch and Whipps 1990). In other studies measuring rates of soil nutrient transformations, a syringe maybe used to inject an isotope solution into soil (e.g.,

Davidson et al. 1991). This method promotes uniform distribution of the isotope throughout the soil volume; however, if ambient nutrient concentrations are heterogeneous, then the isotopic enrichment will also be heterogeneous because microsites with low ambient concentrations will become more highly enriched than microsites with high concentrations. In tracer and isotope dilution studies where soils have had low NH_4^+ or NO_3^- concentrations, researchers have sometimes combined NH_4^+ and NO_3^- pools for isotope analysis. This approach also violates the assumption of uniform distribution of isotope because the NH_4^+ and NO_3^- pools are likely to have different enrichments (Schimel 1996). For example, if the NH_4^+ pool is more highly enriched in ^{15}N, then consumption of NH_4^+ will result in greater ^{15}N uptake than the same rate of NO_3^- consumption. Modeling studies have shown that errors in rate estimates caused by non-uniform isotope distributions depend on how isotope is distributed relative to transformation rates (Davidson et al. 1991; Milchunas and Lauenroth 1992). If the non-uniformity in isotope distribution is random with respect to rates, then little error results; however, if the most active pools are more highly enriched in isotope, then rates will be overestimated. The importance of non-uniform isotope enrichments as a source of error in soil transformation rate measurements needs further evaluation.

Stimulation of rates by addition of isotope may be another important source of error in tracer studies. Many nutrient transformation rates are substrate limited, and thus, increased substrate availability will increase transformation rates. For this reason, the amount of isotope added should be just high enough to ensure that detectable quantities will appear in sink pools at the end of the incubation. To decide how much isotope to add, one must have initial estimates (guesses) of source and sink pool sizes and gross transformation rates. Preliminary experiments may be necessary to obtain this information.

Flow of nutrients either into the labeled source pool or out of the sink pool can cause large errors in rate estimates based on tracer calculations. If nutrients flow into the source pool, the isotopic enrichment (I_A in Equation 14.6) will decline during the incubation, and thus, a greater total number of nutrient atoms will be transferred to the sink pool for each atom of isotope that is transferred. When dilution of the isotopic enrichment of the source pool occurs, isotope dilution calculations must be used to accurately estimate rates (see next section, Equations 14.10 and 14.11).

If nutrients flow out of sink pools during the incubation period, then the amount of isotope that is recovered in the sink pool will underestimate the amount of isotope that really flowed into that pool. For example, the tracer equation (Equation 14.6) will underestimate the flow of nutrient from pool A into pool C because some of the isotope moved into pool D (see Fig. 14.5). The error can be eliminated, if the amount of isotope that flowed out of pool C and into pool D (or other pools) can be quantified. For example, the mass of isotope in pool D (i.e., $[P_D \cdot I_D]$) should be added to the mass recovered in pool C before dividing by the enrichment of the source pool:

$$M_{AC} = \frac{(P_C \cdot I_C) + (P_D \cdot I_D)}{I_A} \quad (14.7)$$

If it is not possible to quantify outflows from the sink, then keeping the incubation time as short as possible will minimize errors. This is because initially, while the enrichment of the sink pool is very close to background, the flow of isotope into the sink greatly exceeds the flow out of the sink, and thus the net rate of increase in isotope is similar to the gross rate (Fig. 14.6). As the length of the incubation increases, however, the enrichment will approach a steady state where the isotopic enrichment of nutrient flowing into the pool is equal to the enrichment of nutrient flowing out of the pool. In this case, the net change in isotope simply reflects the net change in pool size.

Because of the potential for dilution of isotope in the source pool and loss of isotope from sink pools, tracer approaches are of limited use in calculating gross rates. In many cases in which tracer techniques have been used, the same information could have been obtained more easily and with less expense by simply measuring net rates. If the objective is to measure gross rates, then the best approach is usually either an isotope dilution or isotope modeling approach.

Isotope Dilution Measurements

The term "isotope dilution" has been used to describe at least three different techniques. Originally, the term was used to describe a technique for esti-

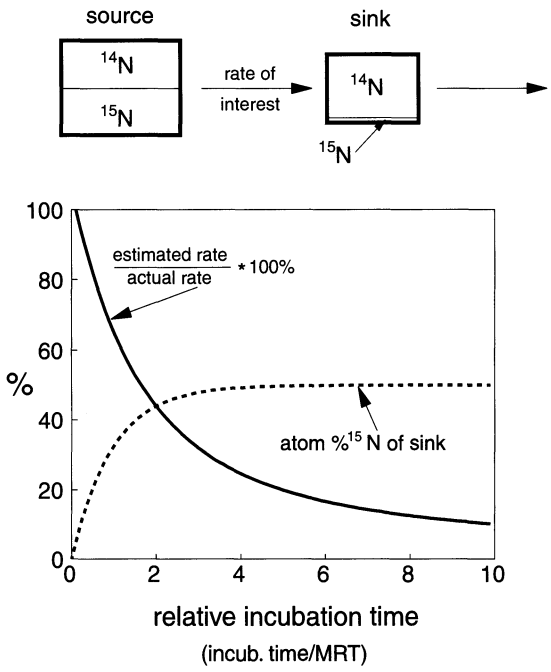

FIGURE 14.6. Model showing how movement of isotope out of a sink pool will influence the atom % enrichment of the sink pool and produce errors in rate estimates based on tracer calculations (Equation 14.6). The model assumes that the enrichment of the source pool is 50 atom % ^{15}N throughout the incubation, and that size of the sink pool does not change (i.e., inputs = outputs). The incubation time is expressed relative to the mean residence time (MRT) for the pool (pool size/flow rate). For example, if the sink pool has a MRT of 1 day and the experiment is carried out for 2 days, the rate estimated from tracer calculations will be only 43% of the actual rate.

mating pool size. A known quantity of labeled material was added to a particular pool, and following an equilibration period, the relative amounts of labeled and unlabeled material were determined. The original pool size was then calculated based on how much dilution of the labeled material occurred. The technique is analogous to the practice used by fish biologists of releasing tagged fish into a lake, and then estimating the fish population size from the proportion of tagged and untagged fish that are recaptured at a later date. This technique has been used frequently with soils to measure the amount of labile P (Kuo 1996), and to a lesser extent labile potassium (K), sulfur (S), zinc (Zn), and nickel (Ni) (Frossard and Sinaj 1997; Echevarria et al. 1998). To quantify labile inorganic P concentrations in soil, a small quantity of radioactive phosphate ($^{32}PO_4^{3-}$) is added to a shaken soil suspension along with chloroform or toluene to inhibit microbial uptake. The $^{32}PO_4^{3-}$ is allowed to equilibrate with naturally occurring sorbed and solution PO_4^{3-} during a 1-day incubation, and then the amount of labile sorbed P is determined from the following equation (Kuo 1996):

$$P_{sorb} = P_{soln} \cdot v \cdot \left(\frac{^{32}P_{init}}{^{32}P_{soln} \cdot v} - 1 \right) \quad (14.8)$$

where P_{sorb} is sorbed P capable of exchanging with PO_4^{3-} in solution within 1 day (mg P kg^{-1}); P_{soln} is the concentration of PO_4^{3-} in solution (mg P $liter^{-1}$); $^{32}P_{init}$ is the specific activity of ^{32}P initially added to the suspension (Bq kg^{-1}); $^{32}P_{soln}$ is the specific activity of ^{32}P in solution after 1-day equilibration (Bq $liter^{-1}$); and v is the solution to soil ratio (liter kg^{-1}).

When using this technique, labile P is defined in terms of the length of the equilibration period (1 day). True equilibrium is not reached after 1 day, and longer equilibration periods will result in greater disappearance of ^{32}P (although subsequent rates are slower than the initial rate). Measurement of ^{32}P several times during longer incubations provides more useful information on rates of exchange between solution PO_4^{3-} and a variety of less labile P fractions (Frossard and Sinaj 1997; Sinaj et al. 1997; He and Zhu 1998). This technique has been referred to more recently as an "isotope exchange kinetic technique."

Kirkham and Bartholomew (1954) recognized that after addition of label to a pool, dilution continues to occur over time as new material is produced and as material disappears from the pool due to consumption processes. They developed a set of "isotope dilution" equations to calculate gross rates of production and consumption based on the rates of dilution and disappearance of labeled material from the pool. More recently, the term "isotope dilution" has also been used to describe a technique for estimating rates of N fixation. Soil N is more highly enriched in ^{15}N than atmospheric N (see later section on natural abundance methods). Therefore, fixation of atmospheric N by plants will result in "dilution" of the ^{15}N obtained from the soil. This latter technique is really a "source iden-

tification" approach (Handley and Raven 1992) which I describe in the section on natural abundance methods. In this chapter, I use the term isotope dilution in the same sense as Kirkham and Bartholomew (1954).

The isotope dilution equations of Kirkham and Bartholomew (1954) calculate gross production and consumption rates based on how rapidly isotope enrichment declines and how rapidly isotope disappears from the labeled pool. In contrast to tracer techniques, the researcher adds isotope to the pool that is the *product* of the transformation of interest. The gross production rate is then estimated from the rate at which the added isotope (e.g., ^{15}N) is "diluted" by influx of the natural isotope (e.g., ^{14}N) (Fig. 14.7). The gross consumption rate can also be calculated based on the rate at which the isotope disappears from the pool. To calculate gross rates of production and consumption, data are required on the nutrient concentration and isotopic enrichment at the beginning and end of the incubation (Hart et al. 1994b):

Gross production rate (GPR)

$$= \frac{P_0 - P_t}{t} \cdot \frac{\log(I_0/I_t)}{\log(P_0/P_t)} \quad (14.9)$$

Gross consumption rate

$$= GPR - \frac{P_t - P_0}{t} \quad (14.10)$$

where P_0 is nutrient concentration at the beginning of the incubation (e.g., mg N kg^{-1} soil); P_t is nutrient concentration at the end of the incubation; I_0 is the relative amount of isotope, in excess of background, that is found in the nutrient pool at the beginning of the incubation (measured as atom % excess if a stable isotope is used or specific activity if a radioactive isotope is used); I_t is the relative amount of isotope, in excess of background, that is present in the nutrient pool at the end of the incubation; and t is the length of the incubation time.

Some of the same assumptions required for tracer techniques are required for isotope dilution techniques: The added isotope acts the same as the naturally occurring isotope, and the pool is uniformly labeled by the isotope. Additional assumptions are that rates are constant during the incubation period, and the isotopic enrichment of the source pool is constant (i.e., there is no recycling of isotope back into the source pool during the incubation) (Kirkham and Bartholomew 1954).

The isotope dilution method works best when used with short-term laboratory incubations of mixed water, sediment, or soil samples (e.g., Blackburn 1979; Glibert et al. 1982, Vitousek and Andariese 1986; Hart et al. 1994a, Stark and Firestone 1996; Low et al. 1997). Short incubation periods (24 to 48 hr for many N transformation rates) usually prevent significant recycling of isotope into the source pool. Incubation in the laboratory allows temperature control so that rates are less likely to fluctuate, and use of mixed samples promotes uniform distribution of isotope and reduces the subsample variance.

The isotope dilution method has also been used with field incubations of intact soil cores (e.g., Schimel et al. 1989; Davidson et al. 1990; Davidson et al. 1992; Stark and Hart 1997). Isotope di-

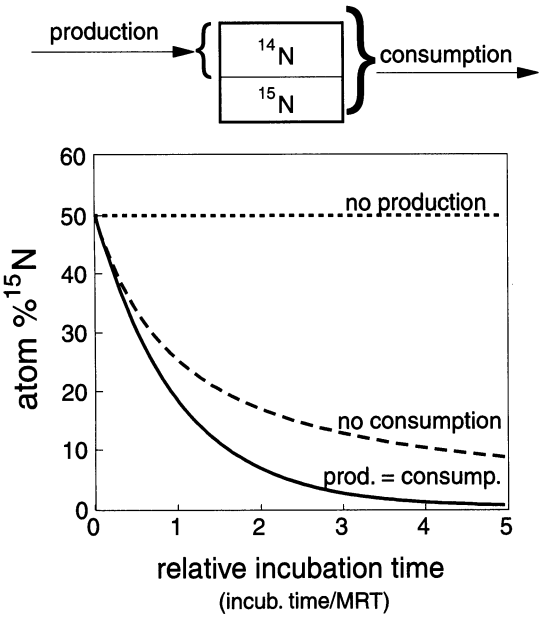

FIGURE 14.7. Changes in isotopic enrichment during an ^{15}N isotope dilution experiment when either production rates are zero, consumption rates are zero, or the production rate equals the consumption rate. The incubation time is expressed relative to the mean residence time (MRT) for the pool (initial pool size/flow rate). For example, in the case in which production = consumption, if the pool has a MRT of 1 day and the experiment is carried out for 2 days, the atom % ^{15}N excess will decline from 50 to 7%.

lution measurement of gross rates in intact soil cores presents some additional problems, however (Davidson et al. 1991; Hart et al. 1994b). The first problem is obtaining an accurate estimate of the nutrient concentration and enrichment in the intact soil core at time 0. Subsamples of soil collected adjacent to the intact core can be extracted to determine initial nutrient concentrations; however, the greater the fine-scale spatial heterogeneity, the greater the error associated with these estimates. This error can be minimized by pounding a large-diameter cylinder into the soil in a concentric circle around the cylinder used for the intact soil core (Fig. 14.8). The soil between the outer and inner cylinders is homogenized and extracted immediately. The soil in the inner cylinder is left intact, injected with isotope solution, incubated, and then harvested at the end of the incubation period. Theoretically, it should be possible to estimate the initial concentration in the intact inner core by summing the concentration measured in the soil between the inner and outer cylinders with amount of isotope added per unit mass of soil. A number of experiments using $^{15}NH_4^+$ and $^{15}NO_3^-$ have shown that considerably less than 100% of the ^{15}N is recovered in NH_4^+ or NO_3^- pools even when the soil is extracted within minutes of adding ^{15}N solution (Davidson et al. 1991; Hart et al. 1994b, Berntson and Aber 2000); thus, for ^{15}N dilution experiments, this method results in overestimation of the initial concentration in the intact core and overestimation of isotope enrichment. Because recovery of isotope is often <100% and varies from soil to soil, it is necessary to inject the same isotope solution into a replicate soil core, which is then extracted immediately to determine the extraction efficiency (amount of isotope recovered/amount of isotope injected) (Hart et al. 1994b). The extraction efficiency is then used to estimate how much isotope would have been measured in the intact core at time 0, if it had been extracted. Sample calculations showing how isotope dilution measurements can be made with intact cores are presented in Table 14.3.

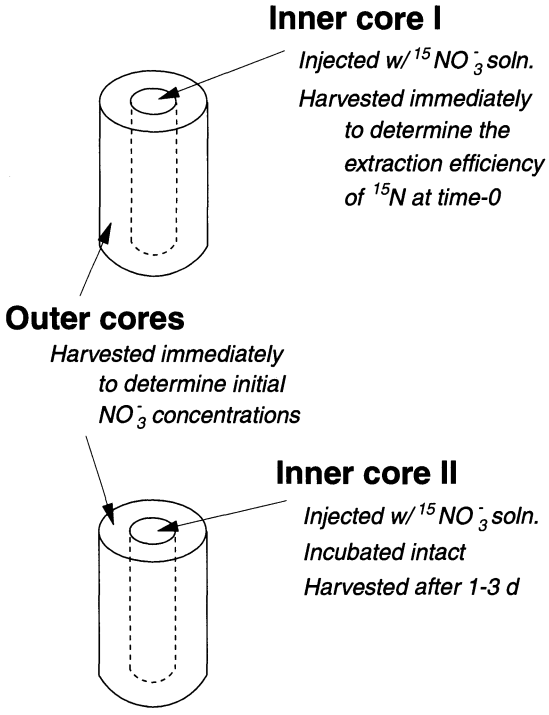
Inner core I
Injected w/ $^{15}NO_3^-$ soln.
Harvested immediately to determine the extraction efficiency of ^{15}N at time-0
Outer cores
Harvested immediately to determine initial NO_3^- concentrations
Inner core II
Injected w/ $^{15}NO_3^-$ soln.
Incubated intact
Harvested after 1-3 d

FIGURE 14.8. Concentric core design used during $^{15}NO_3^-$ isotope dilution measurements of gross nitrification and nitrate consumption rates in intact soil cores. See Table 14.3 for sample calculations.

As with tracer experiments, the amount of isotope required depends on detection limits for isotope measurement, the size of the pool to be labeled, and gross rates of production and consumption. For example when ^{15}N is used, >20 μg N are usually required for analysis by diffusion techniques and direct combustion–mass spectrometry (Barrie et al. 1989, Stark and Hart 1996). If ambient concentrations in soil are low, then it is generally wise to add enough N in the isotope solution to ensure that at least 20 μg of $^{14}N + {}^{15}N$ will be recovered in soil extracts. It is also necessary to add enough isotope that changes in enrichment during the incubation can be detected. In this case, detection is not limited by isotope analysis; it is limited by the ability to accurately estimate time-0 concentrations and enrichments. Because time-0 concentrations are estimated from soil adjacent to the intact core, errors in estimates may frequently be as high as ±20% (J. Stark, unpublished data). For this reason, sufficient isotope is usually added to create enrichments of 40 to 60 atom % ^{15}N. During 24- to 48-hr incubations of soils with active microbial populations, enrichments will often decline to 10 to 30 atom % ^{15}N, which is a change that can be easily detected.

TABLE 14.3. Sample calculations for a 1-day $^{15}NO_3^-$ isotope dilution experiment performed in intact soil cores (see Fig. 14.8 for sampling method). Based on procedure described in Hart et al. (1994b) and Davidson et al. (1991).

	Core pair I		Core pair II	
soil sample:	inner	outer	inner	outer
time harvested (days):	t0	t0	t1	t0
Data				
mass of $^{15}NO_3^-$ − N injected/core (@ 99.9 atom % ^{15}N) (μg N)[a]:	300	—	300	—
mass of <2 mm oven-dry soil in core (g o.d. soil):	320	—	290	—
2 *M* KCl-extractable NO_3^- − N (μg N g^{-1} o.d. soil):	2.3	1.6	2.0	2.5
mole fraction ^{15}N in KCl-extractable NO_3^-:	0.3820	0.0037[b]	0.1760	0.0037
Calculated Values				
mass of ^{15}N added (μg N g^{-1} o.d. soil):	300/320 = **0.938**		300/290 = **1.034**	
mass of excess ^{15}N recovered (μg N g^{-1}):	(2.3 * 0.382) − (1.6 * 0.0037) = **0.873**			
extraction efficiency:	0.873/0.938 = **0.931**			
mole fraction ^{15}N excess estimated to be in the intact core at time −0:	(1.034 * 0.931 + 2.5 * 0.0037)/(2.5 + 1.034 * 0.931) − 0.0037 = **0.277**			

	time-0	time-1
Calculation of Gross Rates		
pool size (μg N/g o.d. soil):	2.5 + 1.034 * 0.931 = **3.46**	**2.0**
mole fraction ^{15}N excess:	**0.277**	0.1760 − 0.0037 = **0.1723**
gross nitrification rate (μg N g^{-1} o.d. soil day^{-1}):	$\frac{(3.46 - 2.0)}{1} * \frac{\log(0.277/0.1723)}{\log(3.46/2.0)} = \mathbf{1.26}$	
gross nitrate consumption rate (μg N g^1 o.d. soil day^{-1}):	$1.26 - \frac{(2.0 - 3.46)}{1} = \mathbf{2.72}$	

[a]All N masses are expressed in terms of the equivalent weight of ^{14}N (i.e., 1 mole of ^{14}N or ^{15}N = 14 g N).
[b]Natural abundance of ^{15}N

For isotope dilution experiments, the isotope is added as a solution to promote uniform distribution throughout the soil. Generally, the greater the quantity of solution that is added, the more uniform the distribution will be. Unfortunately, water addition may stimulate nutrient transformation rates. Typically, the volume of solution has ranged from about 3 to 6 ml per 100 g of soil. Techniques for adding isotope through the gas phase have been tested, but these methods generally result in more than one soil pool being labeled. Exposure of soil to ^{15}NO gas results in appearance of a high proportion of the ^{15}N in soil NO_3^- and NO_2^- pools and smaller proportions in NH_4^+ and soil organic N pools (Stark and Firestone 1995; Rudolph et al. 1996). Exposure of soils to $^{15}NH_3$ results in labeling of soil organic N as well as soil NH_4^+ (Burge and Broadbent 1961; Nommik and Vahtras 1982). Labeling of nontarget pools complicates the analysis considerably, and in some cases violates the assumptions for use of the isotope dilution equations.

The type of extractant used to determine concentrations can effect the rate estimates obtained by isotope dilution. For example, dilute salt solutions such as 0.5 *M* KCl or 0.5 *M* potassium sulfate (K_2SO_4) may not extract as much exchangeable NH_4^+ as 2 *M* KCl does. Therefore, when dilute salt solutions are used as the extractant during $^{15}NH_4^+$ dilution measurements, adsorption of $^{15}NH_4^+$ onto exchange sites may be confused with NH_4^+ consumption, and desorption of $^{14}NH_4^+$ from exchange sites may be confused with mineralization. When one designs an isotope dilution experiment, it is critical that an extractant is selected that measures a well-defined pool, and that all flows affecting that pool are understood.

Isotope dilution measurements have a number of advantages relative to tracer measurements. First,

estimates of gross rates can be obtained even in complex systems where production and consumption occur simultaneously. Second, isotope is added to the product pool rather than the substrate pool, and thus, gross production rates will not be stimulated by addition of substrate. The isotope dilution equations also provide an estimate of gross consumption rates; however, these rates may be stimulated due to addition of isotope (Hart et al. 1994b).

The gross production rate estimated by isotope dilution is for all production processes combined. If production consists of more than one process and rate estimates of individual processes are desired, it may be possible to use isotope dilution in combination with inhibitors to estimate gross rates of individual processes.

The gross consumption rate estimated by isotope dilution is also for all consumption processes combined. In contrast to production rates, gross rates of individual consumption processes can be measured directly based on appearance of the isotope in other pools. For example, in an experiment in which $^{15}NO_3^-$ is added to soil as part of an isotope dilution experiment, measurement of ^{15}N in the plant and microbial biomass at the end of the incubation allows one to estimate how much of the consumption was due to either plant or microbial uptake. This approach is similar to the tracer approach described previously (Equation 14.6); however, it is necessary to use equations slightly more complicated than the simple tracer equation because the isotopic enrichment of the source pool (e.g., $^{15}NO_3^-$) changes throughout the incubation. Depending on how rapidly the source pool is diluted, one of two equations should be used. If rates are slow relative to the size of the pool or the length of the incubation, the enrichment of the source pool will decline in a nearly linear fashion. In this case, the mean enrichment of the source pool can be used in place of the initial enrichment of the source pool (I_A) in the tracer equation (Equation 14.6):

$$M_{AB} = \frac{P_{Bt} \cdot I_{Bt}}{(I_{A0} + I_{At})/2} \qquad (14.11)$$

where M_{AB} is the total amount of nutrient (added plus natural isotopes) that flowed from the source pool (A) to the sink pool (B) during the incubation (e.g., mg N kg^{-1} soil); P_{Bt} is the concentration of B (the sink pool) at the end of the incubation (e.g., mg N kg^{-1} soil); I_{Bt} is the relative amount of isotope, in excess of background, that is found in pool B at end of the incubation; I_{A0} is the relative amount of isotope, in excess of background, that is present in the source pool at the beginning of the incubation; and I_{At} is the relative amount of isotope, in excess of background, that is present in the source pool at the end of the incubation.

On the other hand, if rates are rapid relative to the concentration or incubation period, the enrichment of the source pool will decline exponentially, rather than linearly. In this case, the following equation provides a better estimate of the total amount of nutrient that flows into the sink (Davidson et al. 1991):

$$M_{AB} = \frac{P_{Bt} \cdot I_{Bt}}{I_{A0}(1 - e^{-k})/k} \qquad (14.12)$$

where $k = \ln(I_{A0}/I_{At})/t$, and t is the length of the incubation time. As with the tracer equation, M_{AB} must be divided by the length of the incubation period to calculate the gross rate. This method has some of the same limitations as the tracer method: Increased substrate concentration due to addition of isotope may stimulate rates, and movement of isotope out of sinks will result in underestimation of rates.

Estimation of Rates by Modeling Methods

In many experiments, it may not be possible to meet the assumptions required for the isotope dilution approach. Rates may not be constant throughout the incubation period, and isotope may recycle back into the source pool. Simulation modeling combined with a numerical approximation technique provides an extremely powerful tool for estimating gross rates in more complex experimental systems (Myrold and Tiedje 1986; Barraclough and Smith 1987, Bjarnson 1988; Tietema and Van Dam 1996; Mary et al. 1998). While the isotope dilution equations described previously (Equations 14.9 to 14.11) require the assumption of zero order kinetics, simulation modeling allows one to describe individual rates with first order, mixed order (e.g. Michaelis-Menten), or higher order kinetics. Modeling also allows one to include the influence of temperature, moisture, or other variables on rate constants. Depending on how much information is

available, rates (or rate constants) can be estimated using very simple or relatively complicated models.

When using a modeling approach with numerical approximation, separate, but identical submodels are used to describe flow of the two isotopes (natural and added isotopes) through the system. All of the rate constants used in the two submodels are linked mathematically so that as the rate constant for one process is adjusted, flow of both isotopes changes. Initial values for pool sizes (concentrations) and rate constants are provided for the model, either based on actual data or best guesses, and a simulation is performed. At the end of the simulation, the enrichment predicted by the model for one of the sink pools is compared with the actual enrichment measured for that pool during experimentation. Rate constants are adjusted, and a new simulation is performed. Enrichments are compared again, and rate constants are readjusted. This iterative process continues until the error between predicted and actual enrichments becomes lower than some value predetermined by the modeler. While this approach requires some proficiency in programming, modeling software, such as Time-Zero (Quaternary Software, Fort Collins, CO), is available that greatly simplifies the numerical approximation procedure. In addition, software is currently available that uses numerical methods to estimate gross rates of specific processes such as N mineralization, immobilization, and nitrification (e.g., Mary et al. 1998).

Natural Abundance Isotope Methods

Isotope fractionation and discrimination processes cause the relative abundance of naturally occurring isotopes to differ slightly from one pool to another. For example, N_2 in the atmosphere is 0.3663% ^{15}N and 99.6337% ^{14}N (on a mole basis), whereas N in soil typically ranges from about 0.3670 to 0.3718% ^{15}N (Shearer et al. 1978). Changes in the relative abundance of naturally occurring isotopes from one pool to another have been used to estimate gross rates of nutrient transformations. Natural abundance approaches fall into two categories: kinetic models and source-identification approaches. The approach using kinetic models is nearly identical to the modeling and numerical approximation method described in the previous section. The only difference is that slightly different rate constants are used for the two isotopes to model fractionation or discrimination processes. For example, during nitrification, the rate constant for $^{14}NH_4^+$ oxidation is about 3% higher than the rate constant for $^{15}NH_4^+$ (i.e., $\beta = 1.03$) (Handley and Raven 1992). In contrast, during N fixation, the rate constant for $^{14}N_2$ reduction is nearly equal to the rate constant for $^{15}N_2$ ($\beta = 1.002$). Relatively few kinetic models have been used to estimate transformation rates in ecosystems, however (e.g., Shearer et al. 1974; Herman and Rundel 1989).

The most frequent way that natural isotope abundances are used to estimate transformation rates is by combining a source identification approach with net rate measurements. Source identification approaches are used when an element flows into a sink pool from two sources, and the two sources differ significantly in isotope composition. For example, a source identification approach has been frequently used to estimate rates of N fixation by plants of natural and agro-ecosystems (Shearer and Kohl 1986; Handley and Raven 1992; Ladha et al. 1993). The two sources of N for N-fixing plants are the soil and the atmosphere. As discussed earlier, the N from these two sources may differ by as much as 0.006 atom % ^{15}N (or 15‰). Isotope discrimination during fixation of atmospheric N and during uptake of soil N is relatively small (Handley and Raven 1992). Therefore, if a plant obtains 100% of its N from N fixation, then the isotope abundance of the plant N will be approximately equal to that of the atmosphere. Conversely, if the plant obtains 100% of its N from the soil, then the isotope abundance of the plant N will be approximately equal to that of the soil plant-available N pool. If the plant N is derived from both sources, then the isotope abundance will be a weighted average of the abundances of the atmosphere and the soil, where the weights are the proportion of N obtained from each source. Typically the ^{15}N abundance of the soil plant available N pool cannot be measured directly, but instead the ^{15}N abundance in a non–N-fixing "control" plant, that obtains all of its N from the soil, is measured and assumed to represent the plant-available N pool (e.g., Ladha et al. 1993). These source identification calculations only provide information on the relative amount of N obtained from two different sources. To convert these relative flow rates to absolute rates, the total rate of increase of N in the plant must also be measured.

This is usually done by plant harvesting and measurement of plant N at two points in time. Thus, the natural abundance method is really dependent on how well net rate measurements approximate gross rates.

Application of Methods to Other Nutrient Transformations

All of the approaches described in this chapter require estimation of nutrient concentrations at the beginning and end of an incubation period. Approaches utilizing isotopes require additional measurements of isotope abundances (enrichment or specific activity). Therefore, to use these approaches, procedures must be available that allow precise measurement of the nutrient pool of interest. In many cases, the greatest limitation to using these methods is the lack of a procedure for measuring a specific nutrient pool. The researcher must be careful in choosing a procedure because use of different concentrations or types of extractant may result in measurement of slightly different pools, and thus produce different estimates of nutrient transformation rates. With careful consideration of the system being studied and the objectives of the research, the approaches discussed in this chapter can be adapted for use in measuring transformation rates of a wide variety of nutrients.

Acknowledgments This work was supported by grants from the National Science Foundation (DEB-9208212 and DEB-9807097) and USDA-NRICGP (92-37101-7976).

References

Aber, J.D.; Melillo, J.M. Terrestrial ecosystems. San Francisco: Saunders; 1991.

Anderson, J.P.E.; Domsch, K.H. Measurement of bacterial and fungal contributions to respiration of selected agricultural soils. Arch. Microbiol. 21:314–322; 1975.

Balderston, W.L.; Sherr, B.; Payne, W.J. Blockage by acetylene of nitrous oxide reduction in *Pseudomonas perfectomarinus*. Appl. Environ. Microbiol. 31:504–508; 1976.

Barraclough, D.; Smith M.J. The estimation of mineralization, immobilization and nitrification in nitrogen-15 field experiments using computer simulation. J. Soil Sci. 38:519–530; 1987.

Barrie, A.; Davies, J.E.; Park, A.J.; Workman, C.T. Continuous-flow stable isotope analysis for biologists. Spectroscopy 4:44–52; 1989.

Bedard, C.; Knowles, R. Physiology, biochemistry, and specific inhibitors of CH_4, NH_4^+, and CO oxidation by methanotrophs and nitrifiers. Microbiol. Rev. 53:68–84; 1989.

Belser, L.W.; Mays, E.L. Specific inhibition of nitrite oxidation by chlorate and its use in assessing nitrification in soils and sediments. Appl. Environ. Microbiol. 39:505–510; 1980.

Berg, P.; Klemedtsson, L.; Rosswall, T. Inhibitory effect of low partial pressures of acetylene on nitrification. Soil Biol. Biochem. 14:301–303; 1982.

Berntson, G.M.; Aber, J.D. Fast nitrate immobilization in N saturated temperate forest soils. Soil Biol. Biochem. 32:151–156; 2000.

Betlach, M.R.; Tiedje, J.M.; Firestone, R.B. Assimilatory nitrate uptake in *Pseudomonas fluorescens* studied using nitrogen-13. Arch. Microbiol. 129:135–140; 1981.

Binkley, D.; Bell, R.; Sollins, P. Comparison of methods for estimating soil nitrogen transformations in adjacent conifer and alder-conifer forests. Can. J. For. Res. 22:858–863; 1992a.

Binkley, D.; Hart, S.C. The components of nitrogen availability assessments in forest soils. Adv. Soil Sci. 10:57–112; 1989.

Binkley, D.; Matson, P. Ion exchange resin bag method for assessing forest soil nitrogen availability. Soil Sci. Soc. Am. J. 47:1050–1052; 1983.

Binkley, D.; Sollins, P.; Bell, R.; Sachs, D.; Myrold, D. Biogeochemistry of adjacent conifer and alder-conifer stands. Ecol. 73:2022–2033; 1992b.

Bjarnason, S. Calculation of gross nitrogen immobilization and mineralization in soil. J. Soil Sci. 39:393–406; 1988.

Blackburn, T.H. Method for measuring rates of NH_4^+ turnover in anoxic marine sediments Appl. Environ. Microbiol. 37:760–765; 1979.

Boring, L.R.; Swank, W.T.; Waide, J.B.; Henderson, G.S. Sources, fates, and impacts of nitrogen inputs to terrestrial ecosystems: Review and synthesis. Biogeochemistry 6:119–159; 1988.

Bormann, F.H.; Likens, G.E.; Melillo, J.M. Nitrogen budget for an aggrading northern hardwood forest ecosystem. Science 196:981–983; 1977.

Bremner, J.M. Nitrogen-urea. In: Page, A.L., ed. *Methods of Soil Analysis. Part 2.* 2nd ed. Madison, WI: American Society of Agronomy; 1982:699–709.

Burge, W.D.; Broadbent, F.E. Fixation of ammonia by organic soils. Soil Sci. Soc. Am. Proc. 25:199–204; 1961.

Davidson, E.A.; Hart, S.C.; Firestone, M.K. Internal cycling of nitrate in soils of a mature coniferous forest. Ecology 73:1148–1156; 1992.

Davidson, E.A.; Hart, S.C.; Shanks, C.A.; Firestone, M.K. Measuring gross nitrogen mineralization, immobilization, and nitrification by ^{15}N isotopic pool dilution in intact soil cores. J. Soil Sci. 42:335–349; 1991.

Davidson, E.A.; Stark, J.M.; Firestone, M.K. Microbial production and consumption of nitrate in an annual grassland. Ecology 71:1968–1975; 1990.

Di Stefano, J; Gholz, H. A proposed use of ion exchange resin to measure nitrogen mineralization and nitrification in intact soil cores. Comm. Soil Sci. Plant Anal. 17:989–998; 1986.

Echevarria, G.; Morel, J.L.; Fardeau, J.C.; Leclerc-Cessac, E. Assessment of phytoavailability of nickel in soils. J. Environ. Qual. 27:1064–1070; 1998.

Eno, C.F. Nitrate production in the field by incubating the soil in polyethylene bags. Soil Sci. Soc. Proc. 24:277–279; 1960.

Frossard, E.; Sinaj, S. The isotope exchange kinetic technique: A method to describe the availability of inorganic nutrients. Applications to K, P, S and Zn. Isotop Environ. Health Stud. 33:61–77; 1997.

Genetet, I.; Martin, F.; Stewart, G.R. Nitrogen assimilation in mycorrhizas: Ammonium assimilation in the N-starved ectomycorrhizal fungus *Cenococcum graniforme*. Plant Physiol. 76:395–399; 1984.

Gibson, D.J. Spatial and temporal heterogeneity in soil nutrient supply measured using in situ ion-exchange resin bags. Plant Soil 96:445–450; 1986.

Glibert, P.M.; Lipschultz, F.; McCarthy, J.J.; Altabet, M.A. Isotope dilution models of uptake and remineralization of ammonium by marine plankton. Limnol. Oceanogr. 27:639–650; 1982.

Gordon, A.; Tallas, M.; Van Cleve, K. Soil incubations in polyethylene bags: Effect of bag thickness and temperature on nitrogen transformations and CO_2 permeability. Can. J. Soil Sci. 67:65–75; 1987.

Handley, L.L.; Raven, J.A. The use of natural abundance of nitrogen isotopes in plant physiology and ecology. Plant Cell Environ. 15:965–985; 1992.

Hart, S.C.; Firestone, M.K. Evaluation of three in situ soil nitrogen availability assays. Can. J. For. Res. 19:185–191; 1989.

Hart, S.C.; Nason, G.E.; Myrold, D.D.; Perry, D.A. Dynamics of gross nitrogen transformations in an old-growth forest: The carbon connection. Ecology 75:880–891; 1994a.

Hart, S.C.; Stark, J.M.; Davidson, E.A.; Firestone, M.K. Nitrogen mineralization, immobilization, and nitrification. In: Weaver, R.W.; Angle, S.; Bottomley, P.; Bezdicek, D.; Smith, S.; Tabatabai, A.; Wollum, A., eds. *Methods of Soil Analysis. Part 2. Microbiological and Biochemical Properties.* Madison, WI: Soil Science Society of America; 985–1018; 1994b.

He, Z.L.; Zhu, J. Transformation kinetics and potential availability of specifically-sorbed phosphate in soils. Nutr. cycl. agroecosyst. 51:209–215; 1998.

Herman, D.J.; Rundel, P.W. Nitrogen isotope fractionation in burned and unburned chaparral soils. Soil Sci. Soc. Am. J. 53:1229–1236; 1989.

Kirkham, D.; Bartholomew, W.V. Equations for following nutrient transformations in soils, utilizing tracer data. Soil Sci. Soc. Proc. 18:33–34; 1954.

Klubek, B.; Skujins, J. Gaseous nitrogen losses from ^{15}N-ammonium and plant material amended great basin desert surface soils. Geomicrobiol. J. 2:225–236; 1981.

Knowles, R.; Blackburn, T.H. Nitrogen isotope techniques. San Diego: Academic; 1993.

Kuo, S. Phosphorus. In: Sparks, D.L.; Page, A.L.; Helmke, P.A.; Loeppert, R.H.; Soltanpour, P.N.; Tabatabai, M.A.; Johnston, C.T.; Sumner, M.E., eds. *Methods of Soil Analysis. Part 3. Chemical Methods.* Madison, WI: Soil Science Society of America; 3:869–919; 1996.

Ladha, J.K.; Peoples, M.B.; Garrity, D.P.; Capuno, V.T.; Dart, P.J. Estimating dinitrogen fixation of hedgerow vegetation using the nitrogen-15 natural abundance method. Soil Sci. Soc. Am. J. 57:732–737; 1993.

Lajtha, K.; Michener, R., eds. *Stable Isotopes in Ecology.* Oxford: Blackwell; 1994.

Low, A.P.; Stark, J.M.; Dudley, L.M. Effects of soil osmotic potential on nitrification, ammonification, N-assimilation, and nitrous oxide production. Soil Sci. 162:16–27; 1997.

Lynch, J.M.; Whipps, J.M. Substrate flow in the rhizosphere. Plant Soil 129:1–10; 1990.

Mary, B.; Recous, S.; Robin, D. A model for calculating nitrogen fluxes in soil using ^{15}N tracing. Soil Biol. Biochem. 30:1963–1979; 1998.

Milchunas, D.G.; Lauenroth, W.K. Carbon dynamics and estimates of primary production by harvest, ^{14}C dilution, and ^{14}C turnover. Ecology 73:593–607; 1992.

Mosier, A.R.; Klemedtsson, L. Measuring denitrification in the field. In: Weaver, R.W.; Angle, S.; Bottomley, P.; Bezdicek, D.; Smith, S.; Tabatabai, A.; Wollum, A., eds. *Methods of Soil Analysis. Part 2. Microbiological and Biochemical Properties.* Madison, WI: Soil Science Society of America; 1047–1066; 1994.

Myrold, D.D.; Tiedje, J.M. Simultaneous estimation of several nitrogen cycle rates using ^{15}N: theory and application. Soil Biol. Biochem. 18:559–568; 1986.

Nadelhoffer, K.J.; Aber, J.D.; Melillo, J.M. Seasonal patterns of ammonium and nitrate uptake in nine temperate forest ecosystems. Plant Soil 80:321–335; 1984.

Nohrstedt, H.-O. Natural formation of ethylene in forest soils and methods to correct results given by the acetylene-reduction assay. Soil Biol. Biochem. 15:281–286; 1983.

Nommik, H.; Vahtras, K. Retention and fixation of ammonium and ammonia in soils. In: Stevenson, F.J., ed. *Nitrogen in Agricultural Soils.* Madison, WI: American Society of Agronomy; 1982:123–171.

Oremland, R.S.; Capone, D.G. Use of "specific" inhibitors in biogeochemistry and microbial ecology. Adv. Microbial Ecol. 10:285–383; 1988.

Oremland, R.S.; Culbertson, C.W. Evaluation of methyl fluoride and dimethyl ether as inhibitors of aerobic methane oxidation. Appl. Environ. Microb. 58:2983–2992; 1992.

Peterjohn, W.T.; Schlesinger, W.H. Nitrogen loss from deserts in the southwestern United States. Biogeochemistry 10:67–79; 1990.

Pichtel, J.R.; Dick, W.A. Influence of biological inhibitors on the oxidation of pyritic mine spoil. Soil Biol. Biochem. 23:109–116; 1991.

Raich, J.W.; Nadelhoffer, K.J. Belowground carbon allocation in forest ecosystems: Global trends. Ecology 70:1346–1354; 1989.

Rice, C.W.; Tiedje, J.M. Regulation of nitrate assimilation by ammonium in soils and in isolated soil microorganisms. Soil. Biol. Biochem. 21:597–602; 1989.

Robertson, G.P.; Vitousek, P.M. Nitrification potentials in primary and secondary succession. Ecol. 62:376–386; 1981.

Rudolph, J.; Koschorreck, M.; Conrad, R. Oxidative and reductive microbial consumption of nitric oxide in a heathland soil. Soil Biol. Biochem. 28:1389–1396; 1996.

Scheu, S.; Parkinson, D. Changes in bacterial and fungal biomass C, bacterial and fungal biovolume and ergosterol content after drying, remoistening and incubation of different layers of cool temperate forest soils. Soil Boil. Biochem. 26:1515–1525; 1994.

Schimel, D.S. *Theory and Application of Tracers.* San Diego, CA: Academic; 1993.

Schimel, J.P. Assumptions and errors in the $^{15}NH_4^+$ pool dilution technique for measuring mineralization and immobilization. Soil Biol. Biochem. 28:827–828; 1996.

Schimel, J.P.; Firestone, M.K. Inorganic N incorporation by coniferous forst floor material. Soil Biol. Biochem. 21:41–46; 1989.

Schimel, J.P.; Firestone, M.K.; Killham, K.S. Identification of heterotrophic nitrification in a sierran forest soil. Appl. Environ. Microbiol. 48:802–806; 1984.

Schimel, J.P.; Jackson, L.E.; Firestone, M.K. Spatial and temporal effects on plant-microbial competition for inorganic nitrogen in a California grassland. Soil Biol. Biochem. 21:1059–1066; 1989.

Schlesinger, W.H. *Biogeochemistry: An Analysis of Global Change.* San Diego, CA: Academic; 1991.

Schlesinger, W.H.; Peterjohn, W.T. Processes controlling ammonia volatilization from Chihuahuan desert soils. Soil Biol. Biochem. 23:637–642; 1991.

Shearer, G.; Duffy, J.; Kohl, D.H.; Commoner, B. A steady-state model of isotopic fractionation accompanying nitrogen transformations in soil. Soil Sci. Soc. Am. Proc. 38:315–322; 1974.

Shearer, G.; Kohl, D.H. N_2-fixation in field settings: Estimations based on natural ^{15}N abundance. Aust. J. Plant Physiol. 13:699–756; 1986.

Shearer, G.; Kohl, D.H.; Chien, S.H. The nitrogen-15 abundance in a wide variety of soils. Soil Sci. Soc. Am J. 42:899–902; 1978.

Sibbeson, E.A. Simple ion-exchange resin procedure for extracting plant available elements from soil. Plant Soil 46:665–669; 1977.

Sinaj, S.; Frossard, E.; Fardeau, J.C. Isotopically exchangeable phosphate in size fractionated and unfractionated soils. Soil Sci. Soc. Am. J. 61:1413–1417; 1997.

Sparks, D.L.; Page, A.L.; Helmke, P.A.; Loeppert, R.H.; Soltanpour, P.N.; Tabatabai, M.A.; Johnston, C.T.; Sumner, M.E., eds. *Methods of Soil Analysis. Part 3. Chemical Methods.* Madison, WI: Soil Science Society of America; 1996.

Stanford, G.; Smith, S.J. Nitrogen mineralization potentials of soils. Soil Sci. Soc. Am. Proc. 36:465–472; 1972.

Stark, J.M.; Firestone, M.K. Isotopic labeling of soil nitrate pools using nitrogen-15-nitric oxide gas. Soil Sci. Soc. Am. J. 59:844–847; 1995.

Stark, J.M.; Firestone, M.K. Kinetic characteristics of ammonium-oxidizer communities in a California oak woodland-annual grassland. Soil Biol. Biochem. 28:1307–1317; 1996.

Stark, J.M.; Hart, S.C. Diffusion technique for preparing salt solutions, Kjeldahl digests, and persulfate digests for nitrogen-15 analysis. Soil Sci. Soc. Am. J. 60:1846–1855; 1996.

Stark, J.M.; Hart, S.C. High rates of nitrification and nitrate turnover in undisturbed coniferous forests. Nature 385:61–64; 1997.

Steffens, D.; Sparks, D.L. Kinetics of nonexchangeable ammonium release from soils. Soil Sci. Soc. Am. J. 61:455–462; 1997.

Stevenson, F.J. Cycles of soil. New York: Wiley; 1986.

Subler, S.; Blair, J.M.; Edwards, C.A. Using anion exchange membranes to measure soil nitrate availability and net nitrification. Soil Biol. Biochem. 27:911–917; 1995.

Tabatabai, M.A. Soil enzymes. In: Weaver, R.W.; Angle, S.; Bottomley, P.; Bezdicek, D.; Smith, S.; Tabatabai, A.; Wollum, A., eds. *Methods of Soil Analysis. Part*

2. Microbiological and Biochemical Properties. Madison, WI: Soil Science Society of America; 2:775–834; 1994.

Tann, C.C.; Skujins, J. Soil nitrogenase assay by ^{14}C-acetylene reduction: Comparison with the carbon monoxide inhibition method. Soil Biol. Biochem. 17:109–112; 1985.

Tiedje, J.M. Ecology of denitrification and dissimilatory nitrate reduction to ammonium. In Zehnder, A.J.B., ed. *Biology of Anaerobic Microorganisms.* New York: Wiley; 1988:179–244.

Tietema, A.; Van Dam, D. Calculating microbial carbon and nitrogen transformations in acid forest litter with ^{15}N enrichment and dynamic simulation modelling. Soil Biol. Biochem. 28:953–965; 1996.

Van Cleve, K.; Coyne, P.I.; Goodwin, E.; Johnson, C.; Kelley, M. A comparison of four methods for measuring respiration in organic material. Soil Biol. Biochem. 11:237–246; 1979.

Vitousek, P.M.; Andariese, S.W. Microbial transformations of labeled nitrogen in a clear-cut pine plantation. Oecologia 68:601–605; 1986.

Weaver, R.W.; Angle, S.; Bottomley, P.; Bezdicek, D.; Smith, S.; Tabatabai, A.; Wollum, A., editors. *Methods of Soil Analysis. Part 2. Microbiological and Biochemical Properties.* Madison, WI: Soil Science Society of America; 1994.

Weaver, R.W.; Danso, S.K.A. Dinitrogen fixation. In: Weaver, R.W.; Angle, S.; Bottomley, P.; Bezdicek, D.; Smith, S.; Tabatabai, A.; Wollum, A., eds. *Methods of Soil Analysis. Part 2. Microbiological and Biochemical Properties.* Madison, WI: Soil Science Society of America; 2:1019–1046; 1994.

Wolf, D.C.; Legg, J.O.; Boutton, T.W. Isotopic methods for the study of soil organic matter dynamics. In: Weaver, R.W.; Angle, S.; Bottomley, P.; Bezdicek, D.; Smith, S.; Tabatabai, A.; Wollum, A., eds. *Methods of Soil Analysis. Part 2. Microbiological and Biochemical Properties.* Madison, WI: Soil Science Society of America; 2:865–906; 1994.

Wolf, D.C.; Skipper, H.D. Soil sterilization. In: Weaver, R.W.; Angle, S.; Bottomley, P.; Bezdicek, D.; Smith, S.; Tabatabai, A.; Wollum, A., eds. *Methods of Soil Analysis. Part 2. Microbiological and Biochemical Properties.* Madison, WI: Soil Science Society of America; 2:41–52; 1994.

Zou, X.; Valentine, D.W.; Sanford, R.L., Jr.; Binkley, D. Resin-core and buried-bag estimates of nitrogen transformations in Costa Rican lowland rainforests. Plant Soil. 139:275–283; 1992.

15

Biogenic Trace Gas Exchanges

Pamela Matson and Allen Goldstein

Biogenic trace gases are defined as those gases of biological origin whose atmospheric mixing ratios (concentrations by volume) are less than a few parts per million by volume (ppmv). In the past several decades, knowledge of trace gas exchanges between terrestrial or aquatic systems and the atmosphere, and of the biological, physical, and chemical processes that control them, has increased dramatically. The increased attention and research effort in this area stems primarily from the fact that the atmospheric concentrations of a number of trace gases are increasing. The increases of some of the less reactive gases such as nitrous oxide (N_2O) and methane (CH_4) are documented in the 20-year or longer record of atmospheric measurements at sampling stations throughout the world (e.g., Prinn et al. 1990, Steele et al. 1992) and by the long-term record provided through the analysis of gases trapped in glacial ice (e.g., Raynaud et al. 1988); increases in some reactive trace gases such as oxides of nitrogen (NO_x) and ozone have been determined via ground-based ambient concentration measurements, ground- or aircraft-based flux measurements and atmospheric models. The consequences of these atmospheric changes are felt at a variety of scales; some contribute to the radiative balance of Earth and hence climate change, and others have critical roles in regional and global atmospheric chemistry.

The understanding of the sources and sinks of the fluxes has depended on the contributions of a number of disciplines, including atmospheric chemistry, ecology, biogeochemistry, microbiology, soil physics and chemistry, meteorology, and hydrology. Exchanges of biogenic trace gases between surfaces and the atmosphere are controlled by the production and consumption of gases by plants and microbial processes, the physical transport through soils, sediments, or water, and the flux across the air–surface boundary. These biological and physical processes in turn depend on other biotic and abiotic properties and processes within ecosystems. If we want to use our understanding of trace gas fluxes to develop estimates at regional or global scales (see Chapter 18), and to develop predictive models of fluxes with future environmental and anthropogenic change (see Chapters 13 and 25), studies of trace gas exchange must be carried out in the context of ecosystem processes and properties (Matson and Harriss 1995). Clearly, the development of an understanding of trace gas fluxes requires far more than measurements of flux, and thus, ultimately, requires the use of many of the other methods described in this book.

Approaches for Estimation of Fluxes

There are a number of different approaches to measuring trace gas fluxes, each with its own advantages and limitations, each with a set of conditions or range of questions for which it is most appropriate. No single gas measurement technique works for all gases under all situations. Choice of the approach or combination of approaches depends on the scientific questions being addressed, the biophysical characteristics of the study site, the analytical capabilities for the gases of interest, and the

facilities and funding available to the investigator. In the following sections, we outline some of the most commonly used methods for estimation of trace gas exchange, including enclosure and micrometeorological approaches. We devote most of our attention to issues surrounding enclosure approaches, given that micrometeorological approaches are addressed in other chapters of this book. Our discussion of these approaches draws heavily on material published in *Biogenic Trace Gases: Measuring Emissions from Soil and Water* (Matson and Harriss 1995), and we direct interested readers to that volume and other literature cited here for more detailed information.

Enclosure Methods

Gas Exchange at the Soil–Air Interface

Gas transport across the soil–air interface is primarily a function of advection (mass flow) and diffusion (Nazaroff 1992; Livingston and Hutchinson 1995). Molecular diffusion across the interface is controlled by the trace gas concentration gradient and the diffusivity of the gas in the soil–water matrix. Rates of gas transport in soils and sediments are typically much reduced compared with those in air, because the physical structure (e.g., soil particles) increases the pathlength that gas molecules must travel to the atmosphere (tortuosity) and because soil water obstructs many of the diffusive pathways. Not surprisingly, then, soil textural differences affect the exchange of gases. Likewise, the presence of water in soils and sediments reduces the volume of air-filled pore spaces and decreases diffusivity, reducing advective transport and diffusional transport in the soils. Variation in these transport processes, together with differences in production and consumption of gases (Firestone and Davidson 1989), account for the large spatial and temporal variation for which trace gas fluxes are notorious. For complete discussion of the gas transport processes at the soil–atmosphere interface, see Livingston and Hutchinson (1995).

Enclosures cover the surface of soils or sediments in order to restrict the volume of air available for exchange, so that any net flux between the enclosed air and soil can be measured as a change in head-space gas concentration. Enclosures (also known as chambers) are typically low in cost and technology requirements and relatively easy to use. They are especially useful for addressing research questions on the biological, chemical, or physical controls of surface gas exchange. Because chambers are inexpensive and highly mobile, measurements at many different sites are possible, including sites remote from electricity and security. In addition, collection of gases from enclosures may be the only option for some gases for which field-suitable analytical sensors are not available or are prohibitively expensive for routine use.

Numerous terms have been used to describe different enclosure designs; we adopt the terminology used by Livingston and Hutchinson (1995), in which they describe systems in terms of being steady state or non–steady state, flow-through or non–flow-through, and vented or nonvented (Fig. 15.1). In steady state systems, the trace gas concentration gradient that controls molecular diffusion across the air–soil interface is held constant, typically by using an open-path circulation system to sweep the enclosed volume with a constant flow of external air; thus, the trace gas concentration is similar inside and outside the enclosure. In contrast, in a non–steady state system, the concentration within the enclosure gradually increases such that the concentration gradient is continuously diminishing. Thus, in non–steady state systems, a negative feedback on diffusion is possible, and the dimensions of the chambers and the time they are deployed have to be carefully selected to minimize that potential. Non–steady state systems may be most useful in air–soil systems with very low exchange rates (especially when ambient values are below the analytical system's detection limit), because they allow concentrations to increase over time. Steady state systems must have very high analytical precision because small concentration differences are multiplied by larger air flows. On the other hand, steady state systems cause less perturbation of the concentration gradient and may be more useful for high-frequency repeat measurements (Denmead 1979).

Enclosures are typically fit with a small-diameter vent designed to communicate atmospheric pressure changes to the enclosed volume and thus minimize the effects of the chamber on mass flow across the interface; in nonvented systems, advective transport is suppressed. In addition, venting also allows compensation for air sample with-

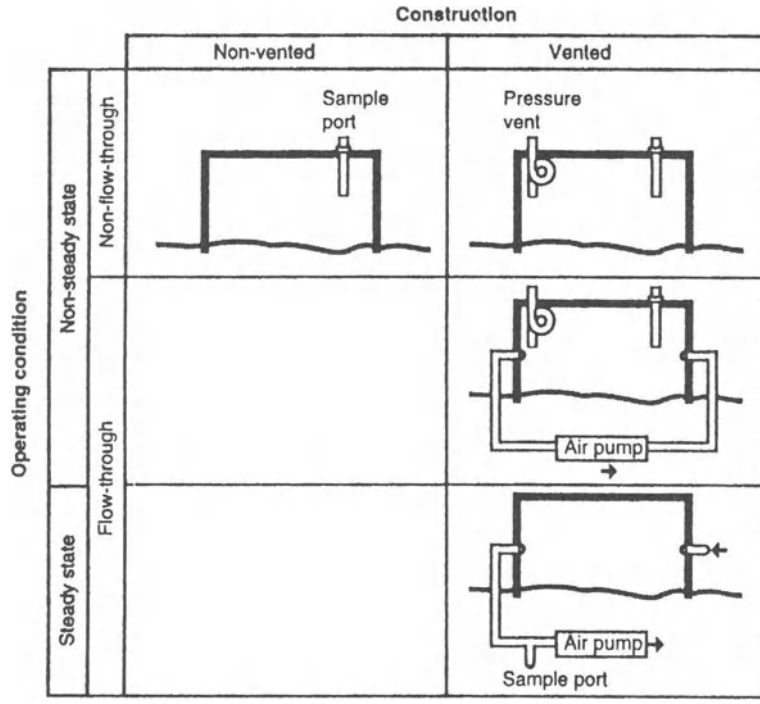

FIGURE 15.1. Classification system for enclosures. (From Livingston and Hutchinson [1995]. Used by permission of Blackwell Science Ltd.)

drawal during sampling and for possible reduction in volume during chamber placement. Guidelines for calculating vent diameter are presented in Mosier and Hutchinson (1981).

In addition to choice of primary enclosure type, decisions also have to be made about the chamber geometry and fabrication materials, deployment approaches, temperature control, light control, and sample collection and handling. No one chamber design is appropriate for all situations, so enclosures must be evaluated for each sampling situation and should be optimized for site characteristics and typical exchange rates. For a thorough review of these issues, see Livingston and Hutchinson (1995) and references cited therein. Only a few of the most critical points will be addressed here. The ratio of chamber volume to surface area covered is one of the most critical issues of chamber design. Generally speaking, a non–steady state chamber's volume-to-area ratio (i.e., in chambers with straight sides, height above the soil or water surface) should be small enough so that change in concentration in the enclosed area can be measured over a short period of time, but large enough to minimize the effects of disturbance of the enclosed surface. Volume-to-area ratios of field chambers are typically 15 cm or greater. Measurement periods should be chosen to maintain a constant rate of concentration change, so that fluxes can be modeled using linear regression and negative feedback on diffusion is minimized.

Another critical issue regarding chamber design concerns the use of single- versus double-component enclosures. Single-component systems are enclosures with attached bases and are deployed in a single step, but physical disturbance of the chamber site that often occurs during deployment (see below) can lead to inaccurate exchange rates; for example, gases can "pulse" from the soil when the chamber is inserted. In contrast, two-component systems are deployed in two steps, the first of which seals an open base to the surface. Because the base can be inserted from minutes to months prior to sampling, disturbance effects associated with placement are minimized. The enclosure top can then be sealed to the base without further disturbance effects. A variety of chamber designs have been used to accomplish the critical seal between the top and base (see Livingston and Hutchinson, 1995)

One of the most serious concerns about enclosure sampling of gas fluxes is that of soil distur-

bance, because soil disturbance influences the biological and physical processes that regulate gas production, consumption, and transport. Potential disturbances include inadvertent mixing of surface soil and establishment of channels for gas flow during insertion of enclosures or enclosure bases; altering soil permeability or inducing pressure gradients by trampling areas adjacent to enclosures; and disturbing vegetation within or adjacent to enclosures. With care, disturbance and its influence on gas flux measurements can be minimized. We recommend collection and analysis of a gas sample collected at time zero (t = 0) (collected immediately after the chamber is placed) to aid in detection of serious disturbance effects; time zero concentrations that are inordinately high relative to ambient may indicate significant disturbance.

Enclosure design and deployment are just the first steps in flux estimation. Air sample collection, transport, storage, and analysis also require the development of protocols and safeguards. Contamination of gases by the storage materials, loss or dilution due to leakage, and sorption onto walls of the storage container all must be evaluated for each gas of interest. Different syringe types vary in terms of leakage rate and must be tested to evaluate potential gas loss over time. Ideally, samples should be analyzed within several hours after collection. Glass containers may allow longer storage if logistics demand it, but they also have the potential for leakage and contamination (Brooks et al. 1993) and should be tested for specific uses and sample holding times. In the case of both syringes and glass containers, samples of known concentration should be handled, stored, and analyzed regularly in the same manner as samples as part of standard practice.

The rate of gas exchange per unit surface area can be calculated from a series of observed chamber air concentrations. Flux calculations require trace gas concentration observations as a function of time, enclosure basal area and volume, as well as temperature and pressure of the enclosed air at the time of sampling. In non–steady state systems, both linear and nonlinear models have been used to describe the relationship between concentration and time; determination of the appropriate model requires a reasonably large number of gas collections over time in each enclosure (for N_2O and CH_4, we recommend at least four collections over 20- to 30-minute sampling periods; for nitric oxide [NO] and carbon dioxide [CO_2], where in situ analysis and continuous measurement is straightforward, much more frequent measurements are taken over much shorter time periods). Livingston and Hutchinson (1995) present a rigorous set of guidelines for estimating exchange rates in both steady state and non–steady state systems, and discuss potential errors associated with estimations.

Trace gas fluxes typically have high spatial and temporal variability; indeed, this variability is one of the reasons that micrometeorological techniques, which integrate over whole ecosystems and allow for long-term continuous sampling, are the preferred approach in some situations. However, if the sampling design is carefully developed to match the characteristics of the site over time, and if appropriate ancillary measurements are carried out, the variability inherent in gas fluxes can often be used to increase understanding of the processes controlling fluxes. Indeed, enclosures are often uniquely useful for process studies because of the small domains over which observations are made. Focusing of sampling in areas assumed a priori to be "representative" or "typical" can lead to biased extrapolation estimates and erroneous conclusions. Sampling to explicitly include and evaluate on-site spatial and temporal variability provides an opportunity both to develop site averages that encompass natural variability as well as to increase understanding of the factors controlling fluxes. Spatial and geostatistical approaches have great advantages for extrapolation of fluxes to scales beyond which the measurements were made (Robertson 1987, Rossi et al. 1992); however, the intense data requirements associated with geostatistical approaches suggest they may be most useful in pilot studies that direct future sampling designs.

Just as there is enormous spatial and temporal variability within sites, cross-system variability has confounded regional and global estimates of trace gas exchange based on enclosure-based methods. Ironically, because of this great variability among ecosystems, enclosure methods are essential for regional- and global-scale evaluations of trace gas, as they are inexpensive, mobile, can be deployed widely in any geographical area, and can be used to study the factors controlling trace gas fluxes. Thus, they form the basis for regional and global budgets and models of N_2O, CH_4, NO_x, volatile

organic carbon (VOC) compounds, and sulfur (S) gas fluxes.

As with the within-site estimates, regional and global estimates can be improved by using a stratified sampling approach that partitions the region on the basis of coarse-scale environmental pattern (e.g., soil type, climatic type, vegetation type, etc.) (Matson and Vitousek 1990; Livingston et al. 1988; Matson et al. 1989; Bartlett et al. 1989, 1993; Matson et al. 1990) or management types (Bouwman 1994; Eichner et al. 1990; Matthews et al. 1994). Temporal variability must also be accounted for. Seasonal changes in fluxes driven by changes in radiation, temperature, precipitation, inundation patterns, and organic matter inputs are highly significant for many gases. In some systems, periods of high flux are very short-lived but account for a majority of the annual flux (e.g., Matson et al. 1990; Whalen and Reeburgh 1992; Matson et al. 1998).

Gas Exchange at the Water–Air Interface

The processes that control exchange of gases between freshwater and coastal marine ecosystems (including wetlands) and the atmosphere are somewhat more complicated than for soils. The pathways are: (1) diffusive and turbulent flow across the air–water interface, (2) ebullition (bubbling), and (3) transfers through emergent aquatic plants.

As with soils, gas transport at the air–water interface is controlled in part by the concentration gradient between water and air; in aquatic systems, however, turbulence is also an important factor. For slightly soluble gases, such as DMS, CH_4, and CO_2, diffusive flux (occurring by a combination of molecular diffusive and turbulent diffusive processes) can be calculated as the gas transfer velocity times the concentration gradient across the aqueous boundary layer (the $<$0.5-mm thick boundary layer below the air–water interface). The gas transfer velocity is a function of the physical processes (turbulence, molecular diffusion of the gas) and the viscosity of the water (Liss 1983; MacIntyre et al. 1995) and is empirically related to wind speed, heat fluxes, and wave characteristics (Wanninkhof 1992). The concentration gradient across the boundary layer is determined by the sources and sinks of the trace gases and by variation in solubility with temperature and salinity. Concentrations are also influenced by highly spatially and temporally variable processes, such as transport of gas-laden water from the thermocline, deep waters, hypolimnion, and sediments due to wind mixing, convective motions, or upwelling. For a discussion of the relationships between gas transfer velocity and hydrodynamic and other physical variables, such as wind speed, wind stress, surface waves, and turbulence parameters, see MacIntyre et al. (1995).

A number of direct and indirect methods are currently in use to determine gas flux across the water–air interface. Direct methods include the use of chambers and enclosures, and tracer methods. As in the soil situation, chambers are placed over the water surface (either moored or floating with the lip just below the surface), and change in concentration is measured in the head-space over time (Frankignolle 1988; Sebacher et al. 1983). In wetlands, coastal marshes, and mud flats, non–steady state chambers and flow-through chambers that are floating or sealed to the sediments have been widely used to estimate exchange of reduced sulfur gases, especially DMS and hydrogen sulfide (H_2S) (e.g., MacTaggart et al. 1987, Goldan et al. 1987, Morrison and Hines 1990, Castro and Galloway 1991), and of CH_4. The advantage of the chamber method is that gas fluxes are measured directly rather than being modeled or extrapolated on the basis of thermodynamic relationships with other known gas fluxes. The disadvantages are that the chamber isolates the water or sediments from such factors as wind shear, turbulence, and pressure fluctuations that affect gas transfer velocity. In addition, single-component systems are particularly problematic in sediments because chamber placement commonly causes bubble formation.

The deliberate tracer method evades the problems with disruption of physical processes experienced by chambers and enclosures. In it, a gaseous tracer such as sulfur hexafluoride (SF_6) is added to the water system and the change in concentration over time is measured. Where necessary, a nonvolatile tracer is added to the water body with the volatile tracer, in order to allow separation of the effects of dispersion versus gas transfer on change in concentration. Ideal volatile tracers should be nontoxic, nonreactive, and measurable at low concentrations. See MacIntyre et al. (1995) for a more detailed review of deliberate tracer methods.

A variety of indirect methods to estimate flux depend on estimation of gas transfer velocity using

empirically related variables, including wind speed and wind shear (e.g., Liu and Schwab 1987; Wanninkhof 1992), or turbulence parameters obtained from meteorological and irradiance measurements (e.g., Imberger 1985), along with measured saturation anomalies between surface water and the air above. This approach is appealing because of the relative ease of measuring wind speeds (the variable most commonly used in the empirical models), and because it, unlike the enclosure methods, can be used in any weather. Chemical input–output budgets have also been used to calculate gas transfer (reaeration) coefficients in rivers, in cases in which point sources of inputs with excess gases serve as inputs and careful measurements of concentration changes and flow downstream are possible (e.g., Clark et al. 1992).

As noted earlier, gas flux in freshwater and coastal marine ecosystems also occurs by ebullition, the one-way transport of gases from organic-rich reducing sediments to the atmosphere. Bubbles are formed in some sediments because the production of CH_4 raises the partial pressures of the dissolved gases above the hydrostatic pressure in the sediment (Chanton and Dacey 1991). Once formed, the bubbles can be released from the sediments, often due to some kind of perturbation, and can rise quickly through the water column to the atmosphere, bypassing the potentially oxidizing sediment–water interface, water column, or plant root system. As CH_4-rich bubbles are formed and released from sediments, they strip the sediments of other dissolved gases. Numerous studies, especially of CH_4 emissions in freshwater and coastal marine environments, have indicated that ebullition is a dominant pathway of flux in many ecosystems (e.g., Crill et al. 1988; Chanton and Martens 1988; Martens et al. 1992).

Ebullition has been measured using air-filled floating chambers and with submerged water-filled bubble traps; sampling has most often focused on emission of CH_4. The floating chamber collects gas diffusing through the water column in addition to bubbles; the two different transport mechanisms can be distinguished via measurement of abrupt changes in methane concentrations in the headspace (Fig. 15.2) (Chanton and Whiting 1995). Frequent (every 3 to 5 minutes) or continuous gas sampling is necessary for this approach to distinguish ebullition from diffusion (e.g., Miller and Oremland 1988; Bartlett et al. 1989, 1990; Devol et al. 1988). Large inverted funnels, fitted with tubing, filled with water, and suspended over sediments, have also been used to collect bubbles (e.g., Chanton et al. 1989; Keller and Stallard 1994). Bubble volume and gas samples can be collected remotely by syringe sampling at the other end of the tubing, at intervals from minutes to weeks after placement. As with the chamber approaches described earlier, sampling frequency and sample handling and storage protocols must be carefully tested (see Chanton and Whiting 1995 for more detailed descriptions of methods).

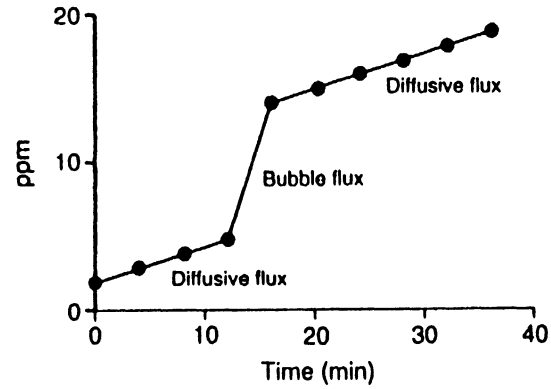

FIGURE 15.2. Abrupt change in methane concentrations over time indicates the capture of bubbles released from sediments. The smooth linear increases in methane concentrations represent diffusive flux from water. (From Chanton et al. [1995]).

While plants produce and emit volatile organic trace gases from their own metabolic processes (discussed later), they also serve as conduits for gases such as CH_4 that are produced microbially in organic-rich sediments where the aquatic macrophytes are rooted. Because of the often anaerobic conditions in the sediments, the plants must shunt oxygen through intercellular gas spaces (lacunae) in their stems and roots to allow root metabolic processes to proceed. In turn, reduced gases in the sediments can use the same transport system for escape to the atmosphere, effectively bypassing sediment–water and water–atmosphere interfaces. When they are present, emergent aquatic plants typically dominate gas exchange. A rich body of literature has documented the mechanisms of gas exchange and the situations in which it is most important (see

Chanton and Whiting 1995 for a review). Chambers are the most simple and widely used method for measuring gas emissions via plants. Although different designs are used, they are typically made of transparent film, Plexiglas, or polycarbonate, and some can be sealed together to cover plants up to 3 m in height. The chamber is typically deployed onto a collar that was previously placed in the sediment. Temperature control is usually necessary, and CO_2 concentration is often monitored and controlled as well. While these chamber systems have been principally used for estimation of CH_4, the fact that DMS is related to plant physiological processes suggests such chambers may be best for it and other plant-derived gases as well. However, because many sulfur compounds are easily adsorbed onto enclosure materials, care must be taken in choice of materials for the enclosure (Kuster and Goldan 1987). Chanton and Whiting (1995) discuss the various approaches and review the published research that has deployed the chambers.

Trace Gas Exchanges at Plant–Air Interfaces

Plants play a number of different roles with respect to biogenic trace gases, including providing a carbon or energy substrate for the microbial processes that lead to gas production or consumption, acting as conduits for gas transport, aerating the soil, and otherwise influencing the diffusivity of the soil. For some trace gases, plant tissues are the loci of production and emission. For example, a wide suite of VOC compounds are produced and emitted by plants. Isoprene and the monoterpenes are the most widely studied of the biogenically emitted VOCs (Fehsenfeld et al. 1992); however, many other VOCs, including a variety of alkenes, alcohols, and ketones, have been identified as plant emissions (Nemecek-Marshall et al. 1995; Goldstein et al. 1996; Guenther et al. 1996; Winer et al. 1983). Likewise, plants emit ammonia (NH_3), especially during tissue senescence and under conditions of high N availability (Schlesinger and Hartley 1992; Freney and Simpson 1983; Schjoerring 1991). Numerous reduced sulfur compounds are also emitted by plants (Renneberg 1991; Aneja and Cooper 1989; MacTaggart et al. 1987). These gases can play critical roles in atmospheric chemistry (Logan 1983; Chameides et al. 1988; Sillman et al. 1990; Brasseur and Chatfield 1991; Fehsenfeld et al. 1992).

A variety of techniques have been used to collect and analyze gases emitted from plants. Enclosures are often used for field measurements of flux. For measurements of monoterpenes and isoprene, an individual tree branch or several small plants are typically enclosed in a Teflon bag, sometimes fitted with a fan to mix the air (Zimmerman 1979; Winer et al. 1983; Lamb et al. 1987; Juuti et al. 1990; Lerdau et al. 1994). The bag is sealed, evacuated, and refilled, or purged, with VOC-free air. During enclosure, air flow is maintained through the bag; the head-space is sampled at the end of the enclosure period to determine gas concentration. Gas exchange chambers and leaf cuvettes also have been used to estimate VOC emissions from different species and under different environmental conditions (Isidorov et al. 1985; Tingey et al. 1987; Monson and Fall 1989). These systems function similarly to CO_2 gas exchange systems (but with different, more sensitive analytical systems required). Because concentrations are typically very low, many analytical methods require preconcentration of the gases via cryoconcentration or trapping on absorbents, followed by measurement with gas chromatography. For further description of these and other approaches, see Tingey et al. (1991). Micrometeorological approaches that estimate VOC exchange for whole ecosystems are increasingly being used (Knoerr and Mawry 1981; Lamb et al. 1985; Goldstein et al. 1996; Guenther et al. 1996).

Enclosure methods are also frequently used to estimate NH_3 and reduced S gas emissions (e.g., Denmead 1983; MacTaggart et al. 1987; Fehsenfeld 1995). In the case of NH_3, the gas is trapped on an acid medium (e.g., dried filter paper initially saturated with oxalic acid) and then measured as ammonium with colorimetry or ion chromatography (see Fehsenfeld 1995 for a recent review of trapping methods). Since NH_3 is readily absorbed on the materials used to make the chambers, the reliability of this approach under low flux conditions is questionable. Gradient diffusion techniques (discussed below) have been widely used for NH_3 in agricultural systems (Denmead 1983) and appear to be a better alternative under conditions suitable for micrometeorological approaches (see below). Fluxes of sulfur gases are measured almost exclusively with enclosures (MacTaggart et al. 1987; Fehsenfeld 1995), in which a purge gas flows

through the chamber and the increase in concentration of the gas is monitored, often after collection on filter or foil collectors (MacTaggart et al. 1987, Lamb et al. 1987).

Micrometeorological Approaches

While chambers and enclosures have advantages in that they are portable and inexpensive, micrometeorological approaches using towers or aircraft have other important advantages. With them, it is possible to measure fluxes without disturbance of the soil, plant, or water surface. Moreover, micrometeorological approaches inherently average over a surface area that increases with height of the measurements over the surface, and so represent integrated fluxes from a larger proportion of the ecosystem rather than from small plots within it. Micrometeorological approaches allow the examination of fluxes over continuous time scales from minutes to years. Finally, in the case of measurements over vegetation canopies, micrometeorological approaches allow the examination of vertical transport through the entire canopy, not just at a single interface. For gases such as CO_2 and NO_y that can be emitted or taken up at various points in the soil–canopy system, micrometeorological approaches are the only way to evaluate actual exchange between ecosystems and the atmospheric boundary layer. The concept and theories of micrometeorological approaches are described in detail in a number of books and chapters, including those by Lenshow (1995), Kaimal and Finnigan (1992), Baldocchi (1991), Baldocchi et al. (1988), and Lenshow and Hicks (1989). In this book, Chapters 11 and 13 present in-depth discussions of selected micrometeorological techniques and their use in water, energy, and CO_2 exchange. Thus, our discussion of micrometeorological approaches will be brief.

There are a variety of micrometeorological techniques for measuring trace gas fluxes. As with the enclosure approach, no single technique is best for all gases or all situations. For a discussion of eddy correlation, eddy accumulation, gradient and difference techniques, and mass balance and Bowen ratio techniques, we recommend the thorough descriptions and explanations of Lenshow (1995) and Baldocchi (1991) as well as the other chapters in this book. Micrometeorological approaches were originally designed to be used for flux measurements over horizontally homogeneous surfaces with long fetch and flat terrain. However, ecological questions are most often addressed in landscapes that are anything but homogeneous. Variations in vegetation type and cover, topography and parent material, soil type and fertility, soil moisture, to name only a few, all contribute to the enormous variation we see in ecological processes and trace gas flux. While this relatively fine-scale heterogeneity has been one of the factors impeding the use of micrometeorological approaches in ecology, new approaches are now being developed to evaluate the use of these techniques in the heterogeneous conditions of many natural ecosystems.

One way that surface heterogeneity is being addressed is through estimation of a flux footprint, which is the contribution of each distinct element of the surface area in the upwind source region to the vertical flux measured at a point above the surface. Flux footprints are typically estimated by analytic dispersion models (Horst and Weil 1992), and Langrangian stochastic dispersion models (Schuepp et al. 1990). Integrating the flux footprint to determine the effective source area for the sensor is fundamentally difficult for quantities that are carried by turbulent diffusion because the footprint is a constantly varying quantity that depends on characteristics of the air flow, including thermal stability and crosswind turbulence (Schmid 1994, 1997). The effective source area of a flux measurement increases strongly with increasing measurement height, and less strongly with increasing stability and crosswind turbulence. Tools for estimating the characteristic dimensions of the area responsible for the majority of the measured surface fluxes in heterogeneous environments have been developed (Schmid 1997). A conservative estimate of an appropriate fetch area during the day is 100 times the measurement height, with a larger fetch area at night.

Analytical Methods for Trace Gases

There is a wide array of analytical approaches available for the measurement of trace gas concentrations. Some of the instruments and analytical

methods are only useful for batch type collections typical of the non–flow-though type enclosure sampling; others have the continuous or fast-response-time capabilities and low detection limits required for some flow-through chamber designs or micrometeorological approaches (Table 15.1) (Crill et al. 1995; see also Fehsenfeld 1995). Today, not all gases can be evaluated with micrometeorological systems due simply to analytical limitations; on the other hand, rapid technological advances are, from year-to-year, changing the way trace gases can be measured (Kolb et al. 1995). Among the standard analytical methods in wide use today are chemical methods (e.g., CO_2 adsorption on soda lime, H_2S reacted with zinc [Zn] or cadmium [Cd] in solution), optical methods (e.g., NO and nitrogen dioxide [NO_2] measurement by chemoluminescent and flourescent techniques; infrared techniques for CO_2 and carbon monoxide [CO]), and chromatographic methods (gas chromatography with various detectors for the analysis of N_2O, CH_4, CO_2, VOCs, and a variety of S compounds). For recent descriptions of analytical methods and primary citations, see Crill et al. 1995 and Fehsenfeld 1995.

While these analytical techniques are likely to remain the mainstay of trace gas analysis in the immediate future, several relatively new techniques carry potential for analysis of trace gas fluxes. For example, photoacoustic infrared analysis systems have been used for continuous gas analyses in chamber systems (Ambus and Robertson 1998). LIDAR (light detection and ranging) systems can now measure water vapor and ozone differences through vertical profiles. Such measurements may be used in combination with estimates of convective velocity to measure flux (Davis 1992). Long-

TABLE 15.1. Techniques for standard methods of analysis.

Species	Technique*	Sample method	Detection limit	Ambient concentration
Carbon				
CH_4	GC-FID	Batch	10 ppbv	1.75 ppmv
	GFC with IR absorption	Continuous	10 ppbv	
CO	GC with HgO detector	Batch	1 ppbv	0.05–1 ppmv
	GC-FID with methanizer	Batch	10 ppb	
	HgO detector	Continuous	3 ppbv	
	GFC with IR absorption	Continuous		
CO_2	Non-dispersive IR adsorption	Continuous	3 ppmv	355 ppmv
	GC-FID with methanizer	Batch	1 ppbv	
	GC-TCD	Batch		
	Absorbtion and titration	Batch		
NMHC	GC-FID after concentration	Batch	50 pptv	0.1–50 ppbv
	GC-PID	Batch		
Nitrogen				
N_2O	GC-ECD	Batch	40 pptv	280–320 ppbv
NO	NO/O_3 chemiluminescence	Continuous	5 pptv	0.001–10 ppbv
NO_2, NO_x, NO_y	NO/O_3 chemiluminescence	Continuous	10 pptv	0.01–100 ppbv
NH_3	Denuder tubes		20 pptv	0.1–50 ppbv
	Condensation collection IC		20 pptv	
Sulpher				
SO_2	GC with S-doped FPD	Batch	3 pg S/sample	0.005–100 ppbv
	Condensation collection/IC	Batch	10 pptv	
	Gas/liquid exchange coil, HPLC	Batch	10 pptv	
H_2S	$AgNO_3$	Batch	0.2 ppb	1–500 pptv
	GC-PID	Batch	100 pptv	
Organo-S and H_2S	GC with S-doped FPD	Batch	3 pg S/sample	
	O_3 chemiluminescence	Batch	200 pptv	
	GC-ECD after fluorination	Batch	0.03 pg S/sample	

*ECD, electron capture detector; FPD, flame photometric detector; GC, gas chromatography; IC, ion chromatography; PID, photoionization detector.
(From Crill et al. [1995].)

path fourier-transform infrared spectrometry (e.g., Gosz et al. 1988) and tunable diode lasers (e.g., Zahniser et al. 1995) have also been developed for field measurements of gases and are being used in conjunction with eddy correlation and other flux estimate approaches for estimates of emissions of CH_4, N_2O, and other gases.

Multiple Approaches for Understanding and Estimating Fluxes

In the earlier days of trace gas studies, it was typical to study only one trace gas at a time and to use a single measurement approach. As the interdisciplinary science of biosphere–atmosphere interactions continues to mature, many investigators are evaluating fluxes of different gases in a single study, having found that knowledge of the dynamics of several gases offers insights into the functioning of the system and the factors controlling the emission of each gas. For example, N_2O (a nonreactive greenhouse gas) and NO_x (a very chemically reactive gas involved in air pollution) were rarely studied together in the field until around 1990, despite the fact that they are produced by the same microbial processes in soil. Now, studies that evaluate the fluxes of both gases (which requires the use of two different analytical systems) are commonly done and are providing insight into the role of microbial processes and soil physical characteristics such as water-filled pore space in controlling production and emission from soils to the atmosphere (e.g., Davidson 1992; Davidson 1993; Davidson et al. 1993; Matson et al. 1996; Matson et al. 1998). Moreover, studies of N gas exchanges today are typically accompanied by studies of microbial dynamics as well as edaphic and environmental characteristics. Similarly, N_2O and CH_4 emissions were typically studied by different groups in different ecosystems for different reasons, until researchers realized that the inverse relationship between the two gases in some ecosystems provides insight into the processes responsible for flux, and also suggests the potential for tradeoff in the gas emissions under different management practices and environmental changes (Mosier et al. 1991; Keller et al. 1986; Steudler et al. 1989).

Beginning in the late 1980s, a series of multidiscipline, multiapproach studies have evaluated trace gas exchange between terrestrial and aquatic ecosystems and the atmosphere, with an eye to not just estimating fluxes but also understanding the factors that lead to variability in fluxes across broad regions. The Amazon Boundary Layer Experiments (ABLE-2A and B) first attempted to integrate ground-based, tower-based, and aircraft-based measurements of gas flux (Harriss et al. 1988, 1990). The Arctic Boundary Layer Experiments (ABLE-3A and B) took this integration a step further, coordinating ecosystem characterization, enclosure-based measurements of CH_4 and other gas fluxes, and eddy correlation estimates of CH_4 flux on towers and aircraft (Harriss et al. 1992), ultimately allowing comparison of the measurement approaches across the different scales (Bartlett and Harriss 1993). More recently, studies such as BOREAS have expanded the concept to include multiple tower sites with accompanying ground-based soil, vegetation, and chamber measurements, and multiple aircraft systems for sensing fluxes at different scales (Sellers et al. 1995, Margolis and Ryan 1997).

Such massive efforts present wonderful opportunities for biogenic trace gas researchers. However, approaches that include measurements of multiple gases using a variety of techniques are becoming the norm for individual researchers or small teams of scientists as well. Moreover, studies that include not only trace gas measurements but evaluation of water, nutrient, and meteorological dynamics (described in many of the other chapters of this book) will ultimately improve our ability to develop and use ecosystem models that estimate trace gas flux (see Chapter 25), and to extrapolate our knowledge to regional and global scales (see Chapter 18).

References

Ambus, P.; Robertson, G.P. Automated near-continuous measurement of carbon dioxide and nitrous oxide fluxes from Soil. Soil Sci. Soc. Am. 62:394–400; 1998.

Aneja, V.P.; Cooper, W.J. Biogenic sulfur emissions: A review. In: Saltzman E.S.; Cooper W.J., eds. *Biogenic Sulfur in the Environment.* Washington, DC: American Chemical Society; 1989:2–13.

Baldocchi, D.D. Canopy control of trace gas emissions. In: Sharkey, T.D., Holland, E.A., Mooney, H.A., eds. *Trace Gas Emissions by Plants.* San Diego, CA: Academic; 1991:293–333.

Baldocchi, D.D.; Hicks, B.B.; Meyers, T.P. Measuring biosphere-atmosphere exchanges of biologically related gases with micrometeorological methods. Ecology 69(5):1331–1340; 1988.

Bartlett, D.S.; Bartlett, K.B.; Hartmann, J.M.; Harriss, R.C.; Sebacher, D.I.; Pelletier-Travis, R.; Dow, D.D.; Brannon, D.P. Methane emissions from the Florida Everglades: Patterns of variability in a regional wetland ecosystem. Global Biogeochemical Cycles 3:363–374; 1989.

Bartlett, D.S.; Crill, P.M.; Bonassi, J.A.; Richey, J.E.; Harris, R.C. Methane flux from the Amazon River floodplain: Emissions during rising water. J. Geophys. Res. 95:16,773–16,778; 1990.

Bartlett, K.B.; Harriss, R.C. Review and assessment of methane emissions from wetlands. Chemosphere 26:261–320; 1993.

Bouwman, A.F. *Direct Emission of Nitrous Oxide from Agricultural Soils.* Report nr 773004004. Bilthoven, Netherlands: National Institute of Public Health, Environmental Protection; 1994.

Brasseur, G.P.; Chatfield, R.B. The fate of biogenic trace gases in the atmosphere. In: Sharkey, T.D.; Holland, E.A.; Mooney, H.A.; eds. *Trace Gas Emissions by Plants.* San Diego, CA: Academic; 1991:1–27.

Brooks, P.D.; Atkins, G.J.; Herman, D.J.; Prosser, S.J.; Barrie, A. Rapid, isotopic analysis of selected soil gases at atmospheric concentrations. In: Harper, L.A., Mosier, A.R.; Duxbury, J.M.; Rolston, D.E.; eds. *Agricultural Ecosystem Effects on Trace Gases and Global Climate Change.* Volume Special Publication 55. Madison, WI: American Society of Agronomy; 1993:193–202.

Castro, M.S.; Galloway, J.N. A comparison of sulfur-free and ambient air enclosure techniques for measuring the exchange of reduced sulfur gases between the soils and the atmosphere. J. Geophys. Res. 96:15427–15437; 1991.

Chameides, W.L.; Lindsay, R.W.; Richardson, J.; Kiang, C.S. The role of biogenic hydrocarbons in urban photochemical smog: Atlanta as a case study. Science 241:1473–1475; 1988.

Chanton, J.P.; Dacey, J.W.H. Effects of vegetation on methane flux, reservoirs, and carbon isotopic composition. In: Sharkey, T.D.; Holland, E.A.; Mooney, H.A.; eds. *Trace Gas Emissions by Plants.* San Diego, CA: Academic; 1991:65–92.

Chanton, J.P.; Martens, C.S. Seasonal variations in ebullitive flux and carbon isotopic composition of methane in a tidal freshwater estuary. Global Biogeochem. Cycl. 2:289–298; 1988.

Chanton, J.P.; Martens, C.S.; Kelley, C.A. Gas transport from methane-saturated tidal freshwater and wetland sediments. Limnol. Oceanogr. 34:807–819; 1989.

Chanton, J.P.; Whiting, G.J. Trace gas exchange in freshwater and coastal marine environments: Ebullition and transport by plants. In: Matson, P.A.; Harriss, R.C.; eds. *Biogenic Trace Gases: Measuring Emissions from Soil and Water.* Cambridge, MA: Blackwell; 1995:98–125.

Clark, J.F.; Simpson, H.J.; Smethie, W.M.; Toles, C. Gas exchange in a contaminated estuary inferred from chlorofluoroocarbons. Geophys. Res. Lett. 19:1133–1136; 1992.

Crill, P.M.; Bartlett, K.B.; Wilson, J.O. Tropospheric methane from an Amazonian floodplain lake. J. Geophys. Res. 93:1564–1570; 1988.

Crill, P.M.; Butler, J.H.; Cooper, D.J.; Novelli, P.C. Standard analytical methods for measuring trace gases in the environment. In: Matson, P.A.; Harriss, R.C.; eds. *Biogenic Trace Gases: Measuring Emissions from Soil and Water.* Cambridge, MA: Blackwell; 1995:164–205.

Davidson, E.A. Sources of nitric oxide and nitrous oxide following wetting of dry soil. Soil Sci. Soc. Am. J. 56:95–102; 1992.

Davidson, E.A. Soil water content and the ratio of nitrous oxide to nitric oxide emitted from soil. In: Oremland, R.S. ed. *Biogeochemistry of Global Change: Radiatively Active Trace Gases.* New York: Chapman and Hall; 1993:369–386.

Davidson, E.A.; Matson, P.A.; Vitousek, P.M.; Riley, R.; Garcia-Mendez, G.; Maass, J.M. Processes regulating soil emissions of NO and N_2O in a seasonally dry tropical forest. Ecology 74:130–139; 1993.

Davis, K.J. *Surface Fluxes of Trace Gases Derived from Convective-Layer Profiles.* Ph.D. dissertation, University of Colorado, Boulder, CO; 1992.

Denmead, O.T. Chamber systems for measuring nitrous oxide emission from soils in the field. Soil Sci. Soc. Am. J. 43:89–95; 1979.

Denmead, O.T. Micrometeorological methods for measuring gaseous losses of nitrogen in the field. In: Freney, J.R.; Simpson, J.R.; eds. *Gaseous Loss of Nitrogen from Plant-Soil Systems.* The Hague, Netherlands: Martinus Nijhoff/W. Junk; 1983:133–157.

Devol, A.H.; Richey, J.E.; Clark, W.A.; King, S.L.; Martinelli, L.A. Methane emissions to the troposphere from the Amazon floodplain. J. Geophys. Res. 93:1583–1592; 1988.

Eichner, M.J. Nitrous oxide emissions from fertilized soils: Summary of available data. J. Environ. Qual. 19:272–280; 1990.

Fehsenfeld, F. Measurement of chemically reactive trace gases at ambient concentrations. In: Matson, P.A.; Harriss, R.C.; eds. *Biogenic Trace Gases: Measuring*

Emissions from Soil and Water. Cambridge, MA: Blackwell; 1995:206–258.

Fehsenfeld, F.; Calvert, J.; Fall, R.; Goldan, P.; Guenther, A.B.; Hewitt, C.N.; Lamb, B.; Liu, S.; Trainer, M.; Westberg, H. et al. Emissions of volatile organic compounds from vegetation and the implications for atmospheric chemistry. Global Biogeochem. Cycl. 6(4):389–430; 1992.

Firestone, M.K.; Davidson, E.A. Microbial basis of NO and N_2O production and consumption in soil. In: Andreae, M.O.; Schimel, D.S.; eds. *Exchange of Trace Gases Between Terrestrial Systems and the Atmosphere.* New York: Wiley; 1989:7–21.

Frankignoulle, M. Field measurements of air-sea CO_2 exchange. Limnol. Oceanogr. 33:313–322; 1988.

Freney, J.R.; Simpson, J.R. Volatilization of ammonia. In: Freney, J.R.; Simpson, J.R.; eds. *Gaseous Loss of Nitrogen from the Plant-Soil System.* The Hague, Netherlands: Dr. W. Junk; 1983:1–32.

Goldan, P.D.; Kuster, W.C.; Albritton, D.S.; Fehsenfeld, F.C. The measurement of natural sulfur emissions from soils and vegetation: Three sites in the eastern United States revisited. J. Atmos. Chem. 5:439–467; 1987.

Goldstein, A.H.; Fan, S.M.; Goulden, M.L.; Munger, J.W.; Wofsy, S.C. Emissions of ethene, propene, and l-butene by a midlatitude forest. J. Geophys. Res. 101:9,149–9,157; 1996.

Gosz, J.R.; Dahm, C.N.; Risser, P.G. Long-path FTIR measurement of atmospheric trace gas concentrations. Ecology 69(5):1326–1330; 1988.

Guenther, A.; Zimmerman, P.; Klinger, L.; Greenberg, J.L.; Ennis, C.; Davsi, K.; Pollock, M.; Westberg, H.; Allwine, G.; Geron, C. Estimates of regional natural volatile organic compound fluxes from enclosure and ambient measurements. J. Geophys. Res. 101:1345–1359; 1996.

Harriss, R.C.; Wofsy, S.C.; Bartlett, D.S. The Arctic boundary layer expedition (ABLE 3A): July–August 1988. J. Geophys. Res. 97:16383–16394; 1992.

Harriss, R.C.; Garstang, M.; Wofsy, S.C.; Beck, S.M.; Bendura, J.R.; Coelho, J.R.B.; Drewry, J.W.; Hoell, J.M.; Matson, P.A.; McNeal, R.J.; Molion, C.B.; Navarro, R.L.; Rabine, V.; Snell, R.L. The Amazon Boundary Layer Experiment (ABLE 2B): Wet season 1987. J. Geophys. Res. 95:16,721–16,736; 1990.

Harriss, R.C., Wofsy, S.C.; Garstang, M.; Browell, E.V.; Molion, L.C.B.; McNeal, R.J.; Hoell, J.M.; Jr.; Bendura, R.J.; Beck, S.M.; Navarro, R.L.; Riley, J.T.; Snell, R.L. The Amazon Boundary Layer Experiment (ABLE 2A): Dry season 1985. J. Geophys. Res. 93:1351–1360; 1988.

Horst, T.W.; Weil, J.C. Footprint estimation for scalar flux measurements in the atmospheric surface layer. Bound Lay. Meterol. 59:279–296; 1992.

Imberger, J. The diurnal mixed layer. Limnol. Oceanogr. 30:737–770; 1985.

Isidorov, V.A.; Zenkevich, I.G.; Ioffe, B.V. Volatile organic compounds in the atmosphere of forests. Atmos. Environ. 19:1–8; 1985.

Juuti, S.; Arey, J.; Atkinson, R. Monoterpene emission rate measurements from a Monterey pine. J. Geophys. Res. 95:7515–7519.; 1990.

Kaimal, J.C.; Finnigan, J.J. Atmospheric Boundary Layer Flows: Their Structure and Measurement. Oxford: Oxford Univ. Pr.; 1992.

Keller, M.; Kaplan, W.A.; Wofsy, S.C. Emissions of N_2O, CH_4, and CO_2 from tropical soils. J. Geophys. Res. 91:11791–11802; 1986.

Keller, M.M.; Stallard, R.F. Methane emission by bubbling from Gatun Lake, Panama. J. Geophys. Res. 99:8307–8319; 1994.

Knoerr, K.R.; Mawry, F.L. Energy balance/Bowen ratio techniques for estimating hydrocarbon fluxes. In: Bufalinin J.J.; Arnts, R.R.; eds. *Atmospheric Biogenic Hydrocarbons.* Stoneham, MA: Butterworth; 1981:35–52.

Kolb, C.E.; Wormhoudt, J.C.; Zahniser, M.S. Recent advances in spectroscopic instrumentation for measuring stable gases in the natural environment. In: Matson, P.A.; Harriss, R.C.; eds. *Biogenic Trace Gases: Measuring Emissions from Soil and Water.* Cambridge, MA: Blackwell; 1995:259–290.

Kuster, W.C.; Goldan, P.D. Quantitation of the losses of gaseous sulfur compounds to enclosure walls. Environ. Sci. Technol. 21:810–815; 1987.

Lamb, B.; Guenther, A.; Gay, D.; Westbert, H. A national inventory of biogenic hydrocarbon emissions. Atmos. Environ. 21:1695–1705; 1987.

Lamb, B.; Westerberg, H.; Allwine, G. Biogenic hydrocarbon emissions from deciduous and coniferous trees in the United States. J. Geophys. Res. 90:2380–2390; 1985.

Lenschow, D.H. Micrometeorological techniques for measuring biosphere-atmosphere trace gas exchange. In: Matson, P.A.; Harriss, R.C.; eds. *Biogenic Trace Gases: Measuring Emissions from Soil and Water.* Cambridge, MA: Blackwell; 1995:126–163.

Lenschow, D.H.; Hicks, B.B.; eds. *Global Tropospheric Chemistry: Chemical Fluxes in the Global Atmosphere.* Boulder, CO: National Center for Atmospheric Research; 1989.

Lerdau, M.; Dilts, S.B.; Westberg, H.; Lamb, B.K. Monoterpene emission from Ponderosa Pine. J. Geophys. Res. 99(D8):16609–16615; 1994.

Liss, P.S. Gas transfer: Experiments and geochemical implications. In: Liss, P.S.; Slinn, W.G.N.; eds. *Air-Sea Exchange of Gases and Particle.* Dordrecht, Netherlands: Reidel; 1983:241–298.

Liu, P.C.; Schwab, D.J. A comparison of methods for estimating u* from given uz and air-sea temperature difference. J. Geophys. Res. 92:6488–6494; 1987.

Livingston, G.P.; Hutchinson, G.L. Enclosure-based measurement of trace gas exchange: Applications and sources of error. In: Matson, P.A.; Harriss, R.C.; eds. *Biogenic Trace Gases: Measuring Emissions from Soil and Water.* Oxford: Blackwell; 1995:14–51.

Livingston, G.; Vitousek, P.M.; Matson, P.A. Nitrous oxide fluxes and nitrogen transformations across a landscape gradient in Amazonia. J. Geophys. Res. 93:1593–1599; 1988.

Logan, J.A. Nitrogen oxides in the troposphere: Global and regional budgets. J. Geophys. Res. 88:10,785–10,807; 1983.

MacIntyre, S.; Wanninkhof, R.; Chanton, J.P. Trace gas exchange across the air-water interface in freshwater and coastal marine environments. In: Matson, P.A.; Harriss, R.C.; eds. *Biogenic Trace Gases: Measuring Emissions from Soil and Water.* Cambridge, MA: Blackwell; 1995:52–97.

MacTaggart, D.L.; Adams, D.F.; Farwell, S.O. Measurement of biogenic sulfur emissions from soil and vegetation using dynamic enclosure methods: Total sulfur gas emissions via MFC/FD/FPD determination. J. Atmos. Chem. 5:417–437; 1987.

Margolis, H.A.; Ryan, M.G. A physiological basis for biosphere-atmosphere interactions in the boreal forest: An overview. Tree Physiol. 17:491–499; 1997.

Martens, C.S.; Kelley, C.A.; Chanton, J.P.; Showers, W. Carbon and hydrogen isotopic composition of methane from wetlands and lakes of the Yukon-Kuskokwim Delta and the Alaskan tundra. J. Geophys. Res. 97:16689–16703; 1992.

Matson, P.A.; Billow, C.; Hall, S. Fertilization practices and soil variations control nitrogen oxide emissions from tropical sugar cane. J. Geophys. Res. 101(D13):18533–18545; 1996.

Matson, P.A.; Harriss, RC; eds. *Biogenic Trace Gases: Measuring Emissions from Soil and Water.* Cambridge, MA: Blackwell; 1995.

Matson, P.A.; Harriss, R.C. Trace gas exchange in an ecosystem context: Multiple approaches to measurement and analysis. In: Matson, P.A.; Harriss, R.C.; eds. *Biogenic Trace Gases: Measuring Emissions from Soil and Water.* Cambridge, MA: Blackwell; 1995:1–13.

Matson, P.A.; Naylor, R.L.; Ortiz-Monasterio, I. Integration of environmental, agronomic, and economic aspects of fertilizer management. Science 280:112–115; 1998.

Matson, P.A.; Vitousek, P.M. Ecosystem approach to a global nitrous oxide budget. Bioscience 40(9):667–672; 1990.

Matson, P.A.; Vitousek, P.M.; Livingston, G.P.; Swanberg, N.A. Sources of variation in nitrous oxide flux from Amazonian ecosystems. J. Geophys. Res. 95:16789–16798; 1990.

Matson, P.A.; Vitousek, P.M.; Schimel, D.S. Regional extrapolation of trace gas flux based on soils and ecosystems. In: Andreae, M.O.; Schimel, D.S.; eds. *Exchange of Trace Gases Between Terrestrial Ecosystems and the Atmosphere.* New York: Wiley; 1989:97–108.

Matthews, E. Nitrogenous fertilizers: Global distribution of consumption and associated emissions of nitrous oxide and ammonia. Global Biogeochem. Cycl. 8(4):411–439; 1994.

Miller, L.G.; Oremland, R.S. Methane efflux from the pelagic regions of four lakes. Global Biogeochem. Cycl. 2:269–; 1988.

Monson, R.K.; Fall, R. Isoprene emission from Aspen leaves: The influence of environment and relation to photosynthesis and photorespiration. Plant Physiol. 90:267–274; 1989.

Morrison, M.C.; Hines, M.E. The variability of biogenic sulfur flux from a temperate salt marsh on short time and space scales. Atmos. Environ. 24A:1771–1779; 1990.

Mosier, A.R.; Hutchinson, G.L. Nitrous oxide emissions from cropped fields. J. Environ. Qual. 10:169–173; 1981.

Mosier, A.R.; Schimel, D.; Valentine, D.; Bronson, K.; Parton, W. Methane and nitrous oxide fluxes in native, fertilized, and cultivated grasslands. Nature 350:330–332; 1991.

Nazaroff, W.W. Radon transport from soil to air. Rev. Geophys. 30:137–160; 1992.

Nemecek-Marshal, M.; MacDonald, R.C.; Franzen, J.J.; Wojciechowski, C.L.; Fall, R. Methanol emission from plants. Plant Physiol. 108:1359–1368; 1995.

Prinn, R.G.; Cunnold, D.; Rasmussen, R. Atmospheric emissions and trends of nitrous oxide deduced from ten years of ALE-GAGE data. J. Geophys. Res. 95:18369–18385; 1990.

Raynaud, D.; Chappellaz, J.; Barnola, J.M.; Korotkevitch, Y.S.; Lorius, C. Climate and CH_4 cycle implications of glacial-interglacial CH_4 change in the Vostok ice core. Nature 333:655–657; 1988.

Rennenberg, H. The significance of higher plants in the emission of sulfur compounds from terrestrial ecosystems. In: Sharkey, T.D.; Holland, E.A.; Mooney, H.A.; eds. *Trace Gas Emissions by Plants.* San Diego, CA: Academic; 1991: 217–260.

Robertson, G.P. Geostatistics in ecology: interpolating with known variance. Ecology 68:744–748; 1987.

Rossi, R.E.; Mulla, D.J.; Journel, A.G.; Franz, E.H. Geostatistical tools for modeling and interpreting eco-

logical spatial dependence. Ecol. Monogr. 62(2):277–314; 1992.

Schjoerring, J.K. Ammonia emission from the foliage of growing plants. In: Sharkey, T.D.; Holland, E.A.; Mooney, H.A.; eds. *Trace Gas Emissions by Plants.* San Diego, CA: Academic; 1991:267–292.

Schlesinger, W.H.; Hartley, A.E. A global budget for atmospheric NH_3. Biogeochemistry 15(3):191–211; 1992.

Schmid, H.P. Source areas of scalars and scalar fluxes. Bound Lay. Meteorol. 67:293–318; 1994.

Schmid, H.P. Experimental Design for Flux Measurements: Matching Scales of Observations and Fluxes. Agric. For. Meteorol. 87:179–200; 1997.

Schuepp, P.H.; Leclerc, M.Y.; Macpherson, J.I.; Desjardins, R.L. Footprint prediction of scalar fluxes from analytical solutions of the diffusion equation. Bound. Lay. Meteorol. 50(N1–4):353–373; 1990.

Sebacher, D.I.; Harriss, R.C.; Bartlett, K.B. Methane flux across the air-water interface: Air velocity effects. Tellus 35B:103–109; 1983.

Sellers, P.; Hall, F.; Margolis, H.; Kelly, B. The Boreal Ecosystem-Atmosphere Study (BOREAS): An overview and early results from the 1994 field year. Bull. Am. Meteorol. Soc. 76(9):1549–1577; 1995.

Sillman, S.; Logan, J.A.; Wofsy, S.C. The sensitivity of ozone to nitrogen oxides and hydrocarbons in regional ozone episodes. J. Geophys. Res. 95:1837–1851; 1990.

Steele, L.P.; Dlugokensky, E.J.; Lang, P.M.; Tans, P.P.; Martin, R.C.; Masarie, K.A. Slowing down of the global accumulation of atmospheric methane during the late 1980's. Nature 358:313–316; 1992.

Steudler, P.P.; Bowden, R.D.; Melillo, J.M.; Aber, J.D. Influence of nitrogen fertilization on methane uptake in temperate forest soils. Nature 341:314–316; 1989.

Tingey, D.R.; Evans, R.C.; Bates, E.H.; Gumpertz, M.L. Isoprene emissions and photosynthesis in three ferns: The influence of light and temperature. Plant Physiol. 69:609–616; 1987.

Tingey, D.T.; Turner, D.P.; Weber, J.A. Factors controlling the emissions of monoterpenes and other volatile organic compounds. In: Sharkey, T.D.; Holland, E.A.; Mooney, H.A.; eds. *Trace Gas Emissions by Plants.* San Diego, CA: Academic; 1991:93–119.

Wanninkhof, R. Relationship between wind speed and gas exchange over the ocean. J. Geophys. Res. 97:7373–7382; 1992.

Whalen, S.C.; Reeburgh, W.S. Interannual variations in tundra methane emission: A 4-year time series at fixed sites. Global Biogeochem. Cycl. 6:139–159; 1992.

Winer, A.M.; Fitz, D.R.; Miller, P.R. *Investigation of the Role of Natural Hydrocarbons in Photochemical Smog Formation in California.* Report nr AO-056-32. Statewide Air Pollution Research Center, University of California, Riverside; California Air Resources Board; 1983.

Zahniser, M.S.; Nelson, D.D.; McManus, J.B.; Kebabian, P.L. Measurement of trace gas fluxes using tunable diode laser spectroscopy. Philosoph. Trans. R. Soc. Lond. A351:371–382; 1995.

Zimmerman, P.R. *Tampa Bay Area Photochemical Oxidant Study. Determination of Emission Rates of Hydrocarbons from Indigenous Species of Vegetation in the Tampa/St. Petersburg, Florida, Area.* Report nr EPA 904/9-77-028. Atlanta, GA: U.S. Environmental Protection Agency; 1979.

16

Ecosystem Nutrient Balance and Dynamics

Kate Lajtha

Introduction

Many attempts at balancing ecosystem-level nutrient budgets have been made in the past few decades using a variety of approaches, and for a variety of different purposes. Relatively simple mass balance equations have been used at the level of the watershed that might comprise single forested ecosystems (e.g., Binkley et al. 1982; Stohlgren et al. 1991; Likens and Bormann 1995; Hedin et al. 1995; Stottlemyer and Troendle 1992), or at the level of a larger-scale region (e.g., Gold 1990; Frink 1991; Jaworski et al. 1992; Howarth et al. 1996; Valiela et al. 1997) that might include different land uses and nutrient inputs. These budgets have been developed with varying efforts at measuring, or modeling, internal processes of nutrient retention and release.

The whole-ecosystem-level budget has a variety of purposes, including:

1. directly testing mechanistic models and understanding processes that control nutrient retention, turnover, and leaching in a field setting;
2. estimating processes by difference that are difficult to measure directly (such as weathering), or to test measurement methods for complex processes when the measurement techniques are called into question (such as dry deposition inputs, nitrogen fixation, or denitrification);
3. understanding controls on regional water quality;
4. in an experimental setting, understanding responses to watershed perturbations such as harvest, fire, or anthropogenic pollutant deposition (e.g., Likens et al. 1978; Pardo et al. 1995);
5. assessing the potential for long-term depletions in critical nutrient pools, such as cation stocks in forests affected by acidic deposition (e.g., Federer et al. 1989; Likens et al. 1996).

Each specific purpose may require a unique level of analysis and detail of measurement.

Often the lack of balance in an ecosystem budget has proven far more interesting than a budget that has balanced. For example, Bormann et al. (1977) found a higher rate of nitrogen (N) storage (as accumulation in biomass) plus loss (as streamwater) in the Hubbard Brook, NH, watershed than they found in inputs of N measured as bulk deposition. At the time, they suggested that the imbalance was probably due to unmeasured N_2 fixation. Thus the imbalance led to a testable hypothesis that directed future research, and later measurements showed that fixation inputs were unlikely to correct the imbalance. Only a portion of the imbalance could be corrected by improved methods of measuring atmospheric inputs such as dry deposition. However, when the imbalance was compared with the mass of N in the soil pool (7200 kg ha^{-1}), it became clear that a fluctuation of 0.5% in this pool would dwarf the budget imbalance, and thus much of the N uptake by vegetation probably came from a small net change in the mineral soil. This study showed the difficulty in comparing relatively well-quantified external fluxes with poorly quantified and considerably larger internal fluxes, and showed the importance of examining the common assumption of ecosystem steady state.

In this chapter I will review some of the basic methods and problems of creating whole-

ecosystem nutrient budgets, including budgets at the whole-watershed scale, at the smaller plot or landscape scale, and in systems without readily measurable hydrologic outflows, as well as uses of nitrogen-15 (^{15}N) tracer techniques to follow N in ecosystems. I will focus primarily on forested ecosystems, as there is relatively little data in other vegetation types at the watershed level (but see Dodds et al. (1996) for an analysis of tallgrass prairie watersheds).

Input–Output Ecosystem Budgets at the Watershed Scale

The most basic input–output budget for a forested catchment can be constructed by comparing measured atmospheric inputs to fluvial outputs for a watershed that meets the requirement of having relatively impermeable bedrock. Geochemists have used input–output budgets for decades to estimate weathering rates and mechanisms, generally assuming that biota have little effect on the cations measured in streamflow (e.g., Miller and Drever 1977; Johnson et al. 1968). However, ecosystem ecologists are generally more interested in those nutrient ions that have substantial interactions with both vegetation and the microbial community, making specific process-level inferences from input–output budgets alone more challenging. Using N as an example, lower outputs of N in streamwater than was input via atmospheric deposition could be attributed to microbial immobilization, losses to the atmosphere, uptake and storage in vegetation and soil organic matter, or a combination of several of these processes (Fig. 16.1). On the other hand, a simple input–output budget may find its greatest use in providing an independent check of the measurement of internal processes, such as dry deposition inputs (discussed below).

The interpretation of an input–output budget certainly requires some knowledge of internal forest characteristics. Time since stand initiation (Vitousek and Reiners 1975; Emmett et al. 1993; Lepistö et al. 1995; Pardo et al. 1995), fire history (Chorover et al. 1994; Grier 1975; Bayley and Schindler 1991), weathering rate and chemistry (Johnson et al. 1968; Reynolds and Johnson 1972; Miller and Drever 1977; Anderson 1988), and land use (McDowell et al. 1995) may all exert strong control over streamwater concentrations of nutrient ions, and these are often not controlled for in studies attempting to understand patterns of ecosystem nutrient retention. For example, attempts to find patterns of streamwater or soil solution output relating to pollutant deposition in N-saturated ecosystems have had mixed results (Johnson 1992; Tietema et

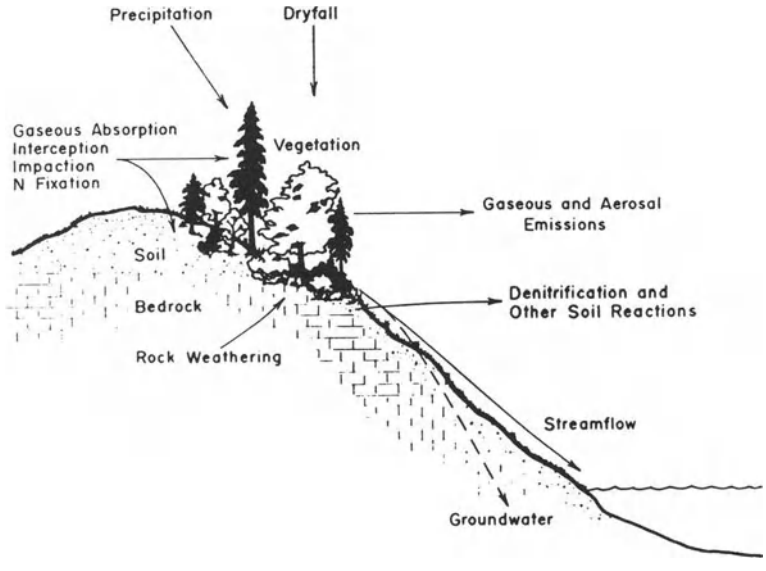

FIGURE 16.1. Major inputs and outputs of elements to a terrestrial watershed. (From Waring and Schlesinger [1985].)

al. 1995; Gundersen 1995; Dise and Wright 1995) in part due to internal differences among ecosystems that now are only beginning to be explored with more detailed process-level work on internal cycles and characteristics. Ecosystems may not be in steady state, or storage may not be constant from year to year; in these cases, caution must be taken in interpreting input–output budgets.

Atmospheric Inputs

One of the central concerns in obtaining an accurate input–output budget is errors associated with measurements of both the atmospheric inputs and the hydrologic outputs. Concerns with the different methods of estimating atmospheric deposition to a forested or otherwise complex watershed terrain are briefly outlined here and reviewed thoroughly in Rustad et al. (1994) and Lovett et al (1997). Further details and discussion of the available measurement techniques are given in Chapter 17. Most reports in the literature have used either wet-only deposition or else bulk deposition to measure total atmospheric inputs to an ecosystem. With the realization that dry and occult deposition may provide substantial percentages of the total inputs of specific elements, various techniques were developed to measure or model dry inputs, none of which have been generally accepted. Direct measurement techniques such as deposition to surrogate collectors have known inherent errors, as natural vegetation surfaces cannot be replicated or even modeled accurately. Current methodologies that use models and inferential techniques are strongly debated (Hicks et al. 1980, 1986, 1991). Inferential techniques include the use of towers, met stations, and surrogate surfaces and filters (see Chapter 17), and thus are expensive and require a high level of technical expertise compared with other techniques. Because no direct measurement of total deposition to a canopy has been found, these models cannot be independently verified, although as the models are refined and more catchment level budgets are constructed as secondary estimates of inputs, these techniques may prove to be the most sound. However, canopy type and structure, topographic exposure, elevation, and slope orientation all affect deposition inputs by wet, dry, and cloud water, making it difficult to determine deposition inputs to a complex terrain from a single collector at a field station (Lovett et al. 1997).

Some authors have used throughfall as a surrogate for deposition, as it is an integrator of dry, cloud, and wet deposition that actually reaches the vegetation, and a network of throughfall collectors over a large and variable landscape is more feasible than a large array of the more expensive deposition collectors (e.g., Gundersen 1995). However, although canopy uptake and leaching may be minimal for ions such as sulfate (SO_4^{2-}), sodium (Na^+) or chloride (Cl^-), they are significant processes for ions such as nitrate (NO_3^-) and ammonium (NH_4^+) (e.g. Lindberg et al. 1986; Friedland et al. 1991; Lovett et al. 1996) making throughfall estimates of total deposition less accurate. These processes may also vary among sites and vegetation types, depending on total rainfall and evergreen/deciduous differences, making simple corrections inaccurate. However, across a range of forest types and background N deposition rates at low elevations, Lovett and Lindberg (1993) calculated a reasonably constant net canopy N uptake of 16% of inputs ($r^2 = 0.89$), which has been used as a correction factor for throughfall estimates in similar sites. When an array of deposition collectors is not feasible, applying such corrections factors to other estimates of input may be the most accurate technique, with the understanding that changes in vegetation type, potential inputs from cloud water, etc., will certainly make the estimates less accurate.

Although no one method to determine atmospheric deposition to an ecosystem has received complete acceptance by the scientific community, studies that have calculated a catchment mass balance may offer an independent test for different methods of estimating dry deposition of various ions. For example, Hultberg and Grennfelt (1992) found good agreement between throughfall estimates of salt dry deposition and dry deposition calculated from a watershed mass balance. Rustad et al. (1994), however, found much higher estimates of dry deposition inputs of SO_4 and Cl from a catchment budget than from measured throughfall and canopy mass balance calculations. They suggested that the discrepancy was due to an error in their throughfall calculation, as occasional (and thus not sampled) superdominant conifers in the mixed hardwood and conifer forests at their study site in Maine could be extremely efficient scavengers of

dry and occult deposition. Lovett et al. (1992) also found that estimates of sulfur (S) deposition at Hubbard Brook were significantly higher using the catchment mass balance method compared to throughfall or inferential measurements. Similarly, Shepard et al. (1989) found that estimates of dry deposition inputs of S provided by a catchment level budget were significantly higher than estimates by regressions applied to wet-only deposition or models of atmospheric concentrations of S coupled to deposition velocities. Thus, although throughfall measures of dry deposition have the advantage of being relatively inexpensive and easy, they may underestimate true deposition. Although it is not clear which measurement technique is more accurate, the catchment budget can provide either verification of an independent measure or else evidence that a particular measurement approach is in error.

Stream Outputs

The classic small watershed approach to ecosystem budgets ideally uses long-term data from gauged streams as the major output measurement (Likens 1985). Techniques for sampling streams for representative seasonal and annual estimates of hydrology and nutrient flux can be found in Likens et al. (1977) and Stottlemyer (1987). A detailed discussion of stream gaging sites and types of stations can be found in Reinhart and Pierce (1964). Methods for accurate and precise hydrologic sampling are necessarily site- and climate-specific, and thus few set rules apply. Flumes might be needed for steep slopes where high sediment yields are common, while V-notch weirs are more accurate in systems without high sediment loads. While some sites use proportional, automatic samplers for collecting stream water, other sites such as Hubbard Brook have found that weekly grab samples are equally as accurate in their ecosystems (W. Martin, personal communication). A detailed analysis of sampling frequency requirements in different catchment types for accurate representation can be found in Semkin et al. (1994).

Multiple years of data are critical to reduce the chance that input–output budgets are biased by hydrologic and climatic variability (Williams and Melack 1997a), as the retention of nutrients within the ecosystem can change with variations in the hydrologic (Lajtha et al. 1995, Seely et al. 1998) or temperature regime (Mitchell et al. 1996). However, even long-term data cannot accurately determine climatic links to variations in stream water chemistry, and thus a paired, or replicated, watershed approach is a preferred goal if manipulative experiments are to be performed. Clearly, finding or measuring a control, or reference, watershed is not always possible, although most long-term ecological research (LTER) sites with watersheds make some attempt at replication. Experiments involving effects of forest harvest, sewage sludge disposal, or experiments within the stream ecosystems at the Hubbard Brook Experimental Forest provide some of the best examples of this approach. More often, a single control and a single manipulated watershed are measured, limiting true statistical power (Chorover et al. 1994) although differences might be large enough to be convincing even without much replication (e.g. Kahl et al. 1993). Paired-catchment data can be augmented with pre- and postdisturbance comparisons, but there is always the possibility that interannual variability could be falsely interpreted as an effect of the manipulation (Williams and Melack 1997b). Local "control" watersheds cannot, of course, serve as controls for the analysis of regional disturbances, such as climate change or increased anthropogenic deposition of nutrients or pollutants. In these cases, large regional assessments can be performed (e.g., Stoddard 1994) or else annual discharge-concentration relationships can be separated into trajectories of time, discharge, and ion concentration to determine processes that regulate streamwater concentrations (Williams and Melack 1997a). Due to funding and time constraints, however, most watershed studies are performed without much replication or over long time spans, and thus cannot reliably address biogeochemical trends.

Because stream water chemistry integrates many processes over a large spatial scale and often over a large and poorly understood time scale, it is difficult and often misleading to directly relate stream water chemistry to processes within the forest stand. However, most watershed budgets have attempted to attribute differences in inputs and outputs to retention processes within the terrestrial ecosystem. Denitrification of N leached from the terrestrial ecosystem can be significant, variable, and high, depending on the presence and charac-

teristics of a forest riparian zone, groundwater dynamics, and/or in-stream processing (Billen et al. 1991). Tietema and Verstraten (1991), for example, found that while streamwater N losses were only 21% of extremely high atmospheric inputs of N to an acid forest ecosystem in the Netherlands, 83% of the amount "retained" by the ecosystem was actually denitrified. A literature compilation by Hill (1996) found that denitrification of subsurface water inputs from agricultural and unsewered residential land uses through riparian zones ranged from 55 to 94% and were dependent on hydrologic flow paths and residence times. In an analysis of tallgrass prairie watersheds, Dodds et al. (1996) found that denitrification and ammonia volatilization were a large percentage of N inputs, and noted that large watersheds had a greater amount of time to immobilize or to denitrify N inputs than smaller watersheds, causing stream water concentrations of N to be lower. Holmes et al. (1996) also found stream water outputs to be a poor measure of N exports from the terrestrial ecosystem, and that denitrification was related to stream order and to organic inputs.

Although the simplest answer to this problem might be to directly measure denitrification losses as part of the internal cycling of N, the measurement of actual denitrification rates (rather than denitrification potentials) is fraught with difficulties. Denitrification is extremely variable in the terrestrial landscape, and is dependent on landscape position (Farrell et al. 1996; Groffman and Tiedje 1989) and the presence of rare "hot spots" (Christensen et al. 1990; Parkin 1987). Perhaps more importantly, the most common method for measuring denitrification, the acetylene blockage technique, has been called into question in recent years in both oxic and anoxic soils and sediments (Seitzinger et al. 1993; Bollmann and Conrad 1997) as acetylene appears to scavenge intermediate nitric oxide, and also blocks autotrophic nitrification and thus does not measuring coupled nitrification–denitrification. Although more complex methodologies are being developed for both terrestrial and aquatic soils and sediments, including N_2 flux and ^{15}N isotope pairing methods (cf. Nielsen et al. 1997; Joye et al. 1996; LaMontagne and Valiela 1995; Scholefield et al. 1997; Seitzinger et al. 1993; Van Luijn et al. 1996), no one technique has been accepted. Also, most denitrification at the watershed scale may take place primarily in riparian forest, stream, or lake sediments, and thus capturing the spatial scale of denitrification is extremely difficult.

Burns (1998) pointed out that denitrification was only one of many aquatic and in-stream processes that could reduce nutrient concentrations in streams. In his study of the Neversink River (Catskill Mountains, NY), diurnal variations in stream NO_3^- levels of up to 30% were consistent with uptake by photoautotrophs during daylight hours, and that both biological uptake and denitrification were important processes reducing stream NO_3^- over a reach by up to 29%. Clearly, stream NO_3^- concentrations integrate both terrestrial and aquatic retention processes. However, Burns (1998) points out the failure of many models of watershed response to atmospheric N deposition to acknowledge aquatic and in-stream processes, because many attribute all retention to terrestrial processes.

Other Budget Approaches

Johnson and Van Hook (1989) discussed some of the advantages and disadvantages of the watershed-level versus the stand-level approach to nutrient balance studies. Advantages of the watershed approach include little site disturbance and the fact that the system is viewed as a unit. Disadvantages include the fact that fluxes in the soil are rarely accounted for, and the requirement of impermeable bedrock is rarely met. The stand-level approach allows investigators to examine aboveground nutrient cycling, and has the advantages of reduced heterogeneity, estimates of within-soil processes, and a decoupling from aquatic processes (if that is a goal). Outputs can be measured using lysimeters, which have some decided disadvantages, including problems with interpreting the pool of soil water sampled and obtaining an accurate estimate of water flux.

Stand-Level Budgets Using Lysimetry

Ecosystem budgets have been conducted at scales smaller than the watershed in a variety of ways. Often when stream sampling is impossible or impractical, or unnecessary for the hypothesis being tested, a stand-level approach can be used, and ecosystem outputs can be estimated using lysimeters,

or soil water collectors (e.g., Binkley et al. 1992; Joslin et al. 1992; Joslin and Wolfe 1992; Johnson and Lindberg 1992; Mitchell et al. 1992; Likens et al. 1994; Johnson 1995). Lysimetry has been used in experimental settings where the experiments, such as fertilization with N, are performed on stands smaller than a watershed (e.g., Currie et al. 1996; Christ et al. 1995; Rustad et al. 1996; Magill et al. 1997; Gundersen 1998 and other nitrogen saturation experiment (NITREX) sites). In these studies, streamwater outputs would integrate over too large an area, making the fertilization signal hard to detect, and riparian or in-stream denitrification and processing could also confound results. Lysimetry is also used when streams are not present (e.g., Lajtha et al. 1995) due to high infiltration rates. Lysimetry is perhaps most appropriate when the soil solution per se needs to be measured in studies of the terrestrial part of a watershed. For example, questions concerning the role of plant uptake versus soil sorption in watershed-level studies of nutrient retention might best be answered using lysimeters so that confounding effects of stream or riparian zone denitrification are omitted. However, due to variable and significant in-stream processing of some nutrients such as N, lysimeter results should be used cautiously for predictions of stream or drinking water quality.

The term lysimeter has had several meanings in the soil science literature; for the purpose of this chapter, a lysimeter is a sampler, inserted into the soil, that collects in situ soil solution water. Lysimeters collect water either with (tension) or without (zero-tension) applied tension to extract water. Tension lysimeters are generally smaller and relatively easy to install. They are most commonly made of ceramic or Teflon and glass mixes with a fine pore size to filter the soil solution before it is extracted. In theory, tension can be applied to match that of the soil water moving via gravitational or matric flow, and thus these lysimeters should collect water from the soil matrix as well as saturated, or macropore flow. Zero-tension lysimeters (ZTLs) can only collect saturated flow, although this is, presumably, the majority of water flow through the soil. These are constructed to have significantly larger collection areas than tension lysimeters, whose collection area is not easily measured, and thus ZTLs have the advantage of sampling a known, potentially quite wide area. Because ZTLs should be relatively large, they are inserted into the soil via a soil pit adjacent to the soil column that is under investigation.

There are advantages and disadvantages to each type of lysimeter (summarized in Lajtha et al. 1999, along with a general description of purchasing or constructing different types of lysimeters). Zero-tension lysimeters are more difficult to install and cause more disturbance to a site, especially if they are to be installed at depth. They tend to collect significantly less soil water at depth, and thus investigators have generally restricted the use of ZTLs to surface horizons. A number of studies have compared concentrations of elements collected by these different types of lysimeters, and summaries can be found in Litaor (1988), Marques et al. (1996), and Lajtha et al. (1999). Although several studies have found that soil solutions collected with tension lysimeters had higher concentrations of many ions, as one would expect since they should collect a more tightly bound fraction of soil water, this varied a great deal depending on the ion examined and the site. In general, there have not been clear patterns of differences between lysimeter types across the many studies, although nitrate appears to often be elevated in tension versus zero-tension lysimeters.

Lysimeters collect soil solution, and thus are not, per se, flux measurements of ecosystem losses. Even ZTLs only collect a variable fraction of total solution flux. Measurements of solute concentration must be coupled with a water-balance model in order to calculate fluxes below the rooting zone. It is likely that this calculation introduces one of the larger errors in lysimetry; it is certainly easier to directly measure stream hydrology and water chemistry than to model water flux. Coupled ecosystem and hydrologic models must, of course, be customized to each site, and require significant knowledge about the climatology of the site (e.g., PnET-II [Aber et al. 1995], WaVES [Dawes and Hatton 1993]). Chloride and bromide have been used as inert tracers through ecosystems as a way of bypassing modeling water flux, although the Cl^- method has recently been called into question (Chorover et al. 1994).

It is critical to realize that there are few reasons to believe that soil solution leachates would or should match patterns of stream water chemistry. In theory, lysimeters placed below the rooting zone of an ecosystem collect soil water that would oth-

erwise leach from the system, and can no longer be affected by vegetation. In fact, significant denitrification, adsorption, and immobilization can take place in deep mineral soil (Qualls and Haines 1992). Several studies have examined both streamwater chemistry at the watershed scale and within-site soil solution chemistry with lysimeters (e.g., Sollins and McCorison 1981; Johnson et al. 1995; Fenn et al. 1996; Adams et al. 1997) although direct comparisons are rare. At one site in the Hubbard Brook Experimental Forest, long-term means of nitrate concentrations collected from the Bs horizon by lysimeters were higher than those found in streamwater, but differences were small (Fig. 16.2). There were no differences in dissolved organic carbon (DOC) concentrations, suggesting that the lysimeters represented streamwater fairly accurately, and that few removal processes operated below the Bs horizon. Similarly, Adams et al. (1997) measured both soil solution concentrations at different

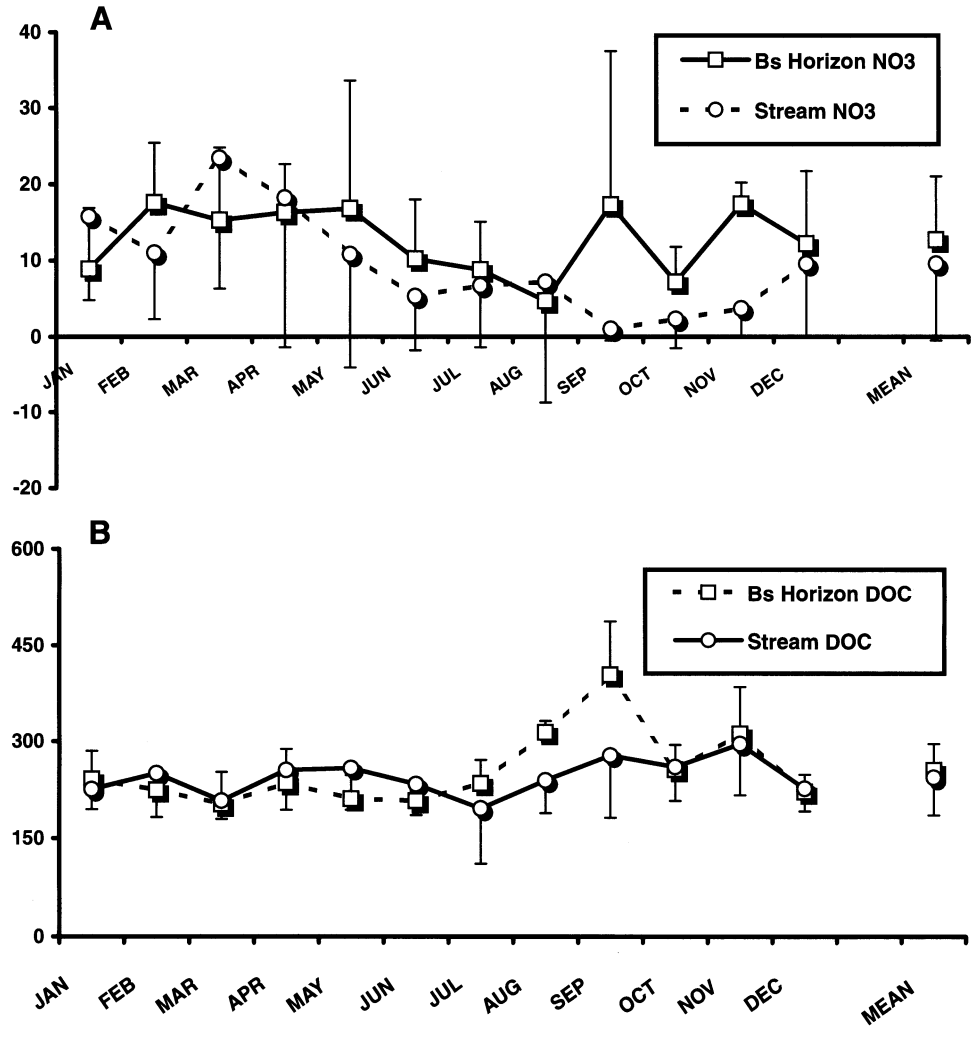

FIGURE 16.2. Long term (1984–1995) mean (±SD) monthly concentrations (μmol liter^{-1}) of nitrate and dissolved organic carbon in lower soil water (below the Bs horizon, measured using tension lysimetry) and in streamwater at the low elevation hardwood site (600 m) at the Hubbard Brook Experimental Forest, NH (Driscoll, unpublished data).

soil depths in zero-tension lysimeters and stream concentrations after fertilization in the Fernow Experimental Forest, West Virginia. C horizon soil solution concentrations of most elements appeared comparable to stream concentrations. Because soil solution concentrations declined with depth, soil solution concentrations from below the B horizon were higher than stream concentrations. This has implications for lysimetry studies, as many experiments have installed lysimeters below the B horizon, with the justification that the majority of roots rarely extend below the B horizon. Both the soil solution and stream water responded similarly to fertilization, although trends appeared more clearly in the stream water data. As part of the NITREX study, Kjonaas et al. (1998) compared plot-scale lysimetry and whole-catchment N export data both before and after N fertilization of a small catchment in Sweden. Although N losses measured using tension lysimeters were higher before N fertilization, losses at the plot and watershed scales were similar after fertilization. Curiously, although plot-scale lysimeters collected more dissolved organic nitrogen (DON), catchment-level runoff data showed greater dissolved inorganic nitrogen (DIN) levels, perhaps simply due to differences between the plot with installed lysimeters and the rest of the catchment. Finally, Seely et al. (1998) compared concentrations of different N species in lysimeters placed below the rooting zone in sandy soils and in groundwater outputs directly below the sites (Fig. 16.3). Concentrations of all N species declined with passage to groundwater, but the attenuation of DON was greater than the attenuation of either NO_3^- or NH_4^+, and the decline in DON in these soils below the rooting zone, and thus below a zone of any significant organic matter accumulation, was greater than the attenuation seen in upper mineral and organic zones. Although DON is generally the predominant form of N leaching from most forested watersheds (Hedin et al. 1995; Sollins and McCorison 1981; Johnson and Lindberg 1992), clearly budgets of DON and thus N will differ markedly depending on the output measurement used.

Such differences in the estimate of ecosystem outputs need to be noted in literature compilations, although many data syntheses, such as the European ECOFEE and ENSF compilations, have combined studies that use both lysimeter and stream water measures of output N (Gundersen 1995, Dise and Wright 1995). Studies of N saturation often address the question of eutrophication of surface or drinking water; clearly in these cases stream water outputs are the critical variable (e.g., Murdoch and Stoddard 1992; Stoddard 1994, Baron et al. 1994). Other studies of N saturation potential at the watershed level also analyze stream outputs (Durka et al. 1994; Hedin et al. 1995; Lepistö et al. 1995; Nodvin et al. 1995), and many conclusions about the relationship between N inputs and outputs, and current N saturation models (i.e. Aber 1992) have been made. Many studies, such as the European NITREX study or the U.S. Integrated Forest Study (IFS) network, measured losses of N compounds from either fertilized or unfertilized plots via lysimeters (Johnson and Lindberg 1992; Aber et al. 1993; Tietema et al. 1995; Gundersen and Rasmussen 1995; Kjonaas et al. 1998) and also draw conclusions about the relationship between N leaching and anthropogenic N loading. Because systematic errors can be introduced when merging results from these different types of ecosystem budgets, it will be important to keep leaching estimates separated by collection method.

Monolith Lysimetry and Sandbox Experiments

A completely different approach to the element mass-balance budget is to create an artificial ecosystem under field conditions. Isolated pits filled either with native soil or sand and variously instrumented to measure leaching losses have been used for decades in soil and agricultural research (e.g., Young et al. 1996) and are variously referred to as monolith lysimeters, weighing lysimeters, unconfined lysimeters, or sandboxes. These microecosystems can allow for a nearly complete budgeting of inputs and outputs. In the San Dimas lysimeter experiment (San Dimas Experimental Forest, Glendora, CA) (Ulery et al. 1995; Quideau et al. 1996), large earthen-walled pits were filled in 1937 with homogenized soil material that was sampled and archived at each 7.5 cm depth, and planted into different monocultures. These have been used for studies of weathering under different species, soil aggregate stability, and changes in soil C, N, and exchangeable cations over time, but these were not equipped to measure complete input and output budgets.

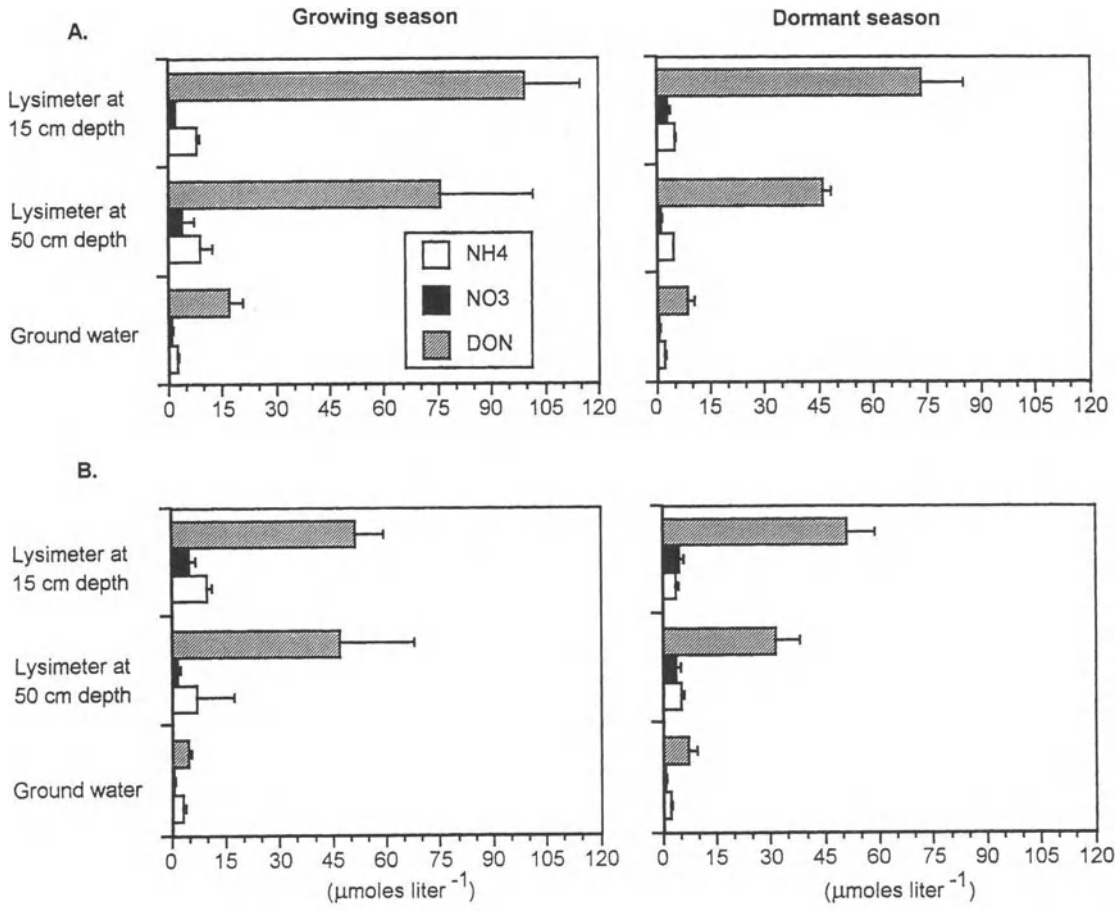

FIGURE 16.3. Mean concentrations of N species captured in zero-tension lysimeters and measured in groundwater during the growing season (April 15 to October 15) and dormant season (October 16 to April 14) over a 2-year period in a forested watershed developed on sandy substrates, Waquoit Bay, Cape Cod, MA. Values for two sites with different soil textures are shown: A, fine sand and B, loamy sand. (Redrawn from Seely et al. [1998].)

The Hubbard Brook "sandbox" experiment (Bormann et al. 1987; Bormann et al. 1993), was created in 1982 specifically to calculate complete plot-level element budgets. Large monolith lysimeters were dug to a depth of 1.5 m, lined with reinforced membranes on the sides and outfitted with bottom drains to measure output solution chemistry, filled with screened glacial outwash sand and 5 cm of topsoil, and planted with seeds or seedlings of known N content. Here an experimental ecosystem was created under field conditions where, in theory, all inputs and outputs could be measured. Even in these carefully controlled ecosystems, though, a balanced budget could not be made; pine sandboxes had an unexplained input of 54 kg N ha^{-1} yr^{-1} (Bormann et al. 1993). The authors argued against dry deposition inputs at this order of magnitude, and suggested that associative rhizosphere N_2 fixation could account for this imbalance. Although they measured rates of acetylene reduction in low-O_2 chambers in pitch and red pine rhizospheres, they declined to convert these direct measurements into annual or per-unit-area values of N_2 fixation, citing the uncertain ratio of C_2H_4 fixed to N_2 fixed and unknown O_2 concentrations in the actual rhizospheres. Thus rapid associative fixation could not be independently measured, and other studies of associative fixation have uniformly measured rates

of <1 kg N ha^{-1} yr^{-1} (Kapustka and Dubois 1987; Grant and Binkley 1987; Silvester 1989; Binkley 1996).

These studies suggest that a controlled, artificial ecosystem with known boundaries can yield important information about nutrient cycling processes that cannot be determined from the larger-scale whole-ecosystem budget approach where spatial variability is high and many processes cannot be measured at a spatially explicit scale. However, these experiments are expensive, are rarely replicated (San Dimas was not replicated by species), and take several decades before the first meaningful analyses can be made. The artificial nature of fill soil may have a large effect on process rates, making extrapolations to undisturbed ecosystems difficult. The small scale of the mesocosms also pose some limitations on interpretation, just as plot-scale studies cannot always be representative of ecosystem-level dynamics. Although the measured output from these mesocosms quite accurately represent the true outputs, only a narrow portion of an ecosystem is measured, as deep soil, groundwater, and riparian dynamics are not measured.

Nitrogen-15 Studies at the Ecosystem Scale

Because the watershed budget approach cannot trace internal movement or storage of ions, various authors through the years have used isotopes to follow the fate of ecologically relevant elements. The use of phosphorus-32 (^{32}P) or other radioactive tracers in large-scale experiments in natural terrestrial systems is not common (but see Caldwell et al. 1985), but ^{15}N has been added to natural ecosystems in a large number of studies either as enriched fertilizer (Mead and Pritchett 1975; Broadbent and Carleton 1978; Nadelhoffer et al. 1995; Koopmans et al. 1996; Jordan et al. 1997; Nadelhoffer et al. 1998b; Tietema et al. 1998, to name a few) or at background, throughfall input concentrations (White and Howes 1994; Stams et al. 1991; Koopmans et al. 1996; Buchmann et al. 1995, 1996; Seely and Lajtha 1997; Nadelhoffer et al. 1998a). Unfortunately, less than a handful have used ^{15}N at background throughfall input levels and have traced movement over long time periods and in a number of ecosystem pools, including output pools such as deep lysimeters.

Buchmann et al. (1995, 1996) used ^{15}N as a tracer at background levels in the Fichtelgebirge, Germany. Because there was a 20% decrease in the recovery of both $^{15}NO_3$ and $^{15}NH_4$ tracer after 15 months, they estimated that this reflected the amount of loss from the system via leaching. The highest retention of ^{15}N was in organic soil horizons, followed by mineral soils, uptake by understory herbs, and uptake by overstory trees. Quite similar patterns have since been seen in many other studies with ^{15}N tracer additions, where input–output budget studies alone could not have measured the retention rates in these different pools. Similarly Koopmans et al. (1996), using quite low as well as fertilizer levels of ^{15}N addition in N-saturated sites in the Netherlands, budgeted the added N into vegetation uptake, soil retention, and leaching losses, and found more uptake of label by trees in a Douglas fir site than in a Scots pine site. Seely and Lajtha (1997) added ^{15}N to throughfall to trace seasonal differences in N retention in a coastal watershed in the United States and to examine soil texture effects on N retention, and found patterns similar to those of Buchmann et al. (1995), but with much higher leaching losses.

Other studies using background levels of ^{15}N for other purposes, such as estimating nitrification rates, have not measured many internal pools, but have measured leaching losses of label (e.g., Stams et al. 1991). Similarly, Hart et al. (1993) compared the fate of deposited N in a grassland and a plantation forest using background-level ^{15}N tracer, but because the purpose of the experiment was to analyze internal N processes, the plot sizes used were too small to make ecosystem-level budgets. However, they were able to identify important retention mechanisms in the soils examined, and found that the grassland retained significantly more of the deposited N than the forest. In most of these studies the recovery of ^{15}N was relatively high initially, often close to 100%, but declined with time, suggesting that there might be a very real time limitation on following these experiments.

Other studies have used tracers in both reference and fertilized plots; such complete cross-system studies allow researchers to evaluate retention mechanisms under different fertilizer and climate

regimes. Nadelhoffer et al. (1998a) added ^{15}N to both reference and chronically fertilized stands at the Harvard Forest, Massachusetts, and found that tree uptake increased with fertilization; this pattern was not, however, observed by Tietema et al. (1998) in a series of lightly (3 to 6 kg N ha^{-1} yr^{-1}) to more heavily (20 to 91 kg N ha^{-1} yr^{-1}) fertilized NITREX sites. In this latter study, the percentage of ^{15}N applied that was taken up by trees (10 to 42%) after 1 year did not appear to be related to total fertilizer addition, although the efficiency of retention by organic soil horizons (11 to 47%) decreased with N addition as loss to leaching (0 to 50%) increased with N additions.

Labeled tracers have the advantage of allowing the researcher to trace the movement of an element through a plot-level ecosystem. However, there are several disadvantages to these techniques. Most studies have added tracer directly to the forest floor, thus ignoring canopy interactions. The size of the plots that can be used is necessarily small, as tracers tend to be expensive and, in the case of radioactive tracers, dangerous to use in levels that can leach out of the system. Another problem is the time course of study. Most studies can follow added label for a year or two at most due to the decreasing recovery of the tracer. Preston and Mead (1995) followed labeled litter for 7.5 years and found stabilization of the label after 3 years, but also found a low recovery (under 20%) with time. In contrast, White and Howes (1994) found 40% of added label remaining after 7 years in a salt marsh. Yet because so much of added N is immobilized in soil organic matter, this N could become available for uptake by vegetation or else lost from the system via leaching or denitrification at a later date, and thus these processes will be underestimated in short-term studies. Because there is continuous exchange between mineral and organic bound N-forms in soils, the label will begin to behave like the bulk of soil N (Knicker et al. 1997). However, with further refinement and perhaps through the use of models to track the further fate of label, these techniques will certainly add to the arsenal of methods that can be used in the calculation of ecosystem-level elemental budgets.

Acknowledgments This review benefited greatly from discussions with and reviews by Linda Pardo, Dan Binkley, Steve Perakis, C. Wayne Martin, Knute Nadelhoffer, and Charley Driscoll, who generously offered advice, references, data, and criticism.

References

Aber, J.D. Nitrogen cycling and nitrogen saturation in temperate forest ecosystems. Trends Ecol. Evolut. 7:220–223; 1992.

Aber, J.D.; Magill, A.; Boone, R.; Melillo, J.M.; Steudler, P.; Bowden, R. Plant and soil responses to chronic nitrogen additions at the Harvard Forest, Massachusetts. Ecol. Applic. 3:156–166; 1993.

Aber, J.D.; Ollinger, S.V.; Federer, C.A.; Reich, P.B.; Goulden, M.L.; Kicklighter, D.W.; Melillo, J.M.; Lathrop, R.G., Jr. Predicting the effects of climate change on water yield and forest production in the northeastern United States. Clim. Res. 5:207–222; 1995.

Adams, M.B.; Angradi, T.R.; Kochenderfer, J.N. Stream water and soil solution response to 5 years of nitrogen and sulfur additions at the Fernow Experimental Forest, West Virginia. For. Ecol. Manage. 95:79–91; 1997.

Anderson, D.W. The effect of parent material and soil development on nutrient cycling in temperate ecosystems. Biogeochemistry 5:71–97; 1988.

Baron, J.S.; Ojima, D.S.; Holland, E.A.; Parton, W.J. Analysis of nitrogen saturation potential in Rocky Mountain tundra and forest: Implications for aquatic systems. Biogeochemistry 27:61–82; 1994.

Bayley, S.E.; Schindler, D.W. The role of fire in determining stream water chemistry in northern coniferous forests. In: Mooney, H.A.; Medina, E.; Schindler, D.W.; Schulze, E.D.; Walker, B.H., eds. *Ecosystem Experiments. SCOPE 45.* New York: Wiley; 1991:141–165.

Billen, G.; Lancelot, C.; Meybeck, M. N, P, and Si retention along the aquatic continuum from land to ocean. In: Mantoura, R.F.C.; Martin, J.-M.; Wollast, R., eds. *Ocean Margin Processes in Global Change.* New York: Wiley; 1991:19–44.

Binkley, D. The influence of tree species on forest soils: Processes and patterns. In: Mead, D.J.; Cornforth, I.S., eds. *Proceedings of the Trees and Soil Workshop.* Agronomy Society of New Zealand Special Publication 10. Canterbury, NZ: Lincoln Univ Pr.; 1996:1–33.

Binkley, D.; Kimmins, J.P.; Feller, M.C. Water chemistry profiles in an early- and mid-successional forest in coastal British Columbia. Can. J. For. Res. 12:240–248; 1982.

Binkley, D.; Sollins, P.; Bell, R.; Sachs, D.; Myrold, D. Biogeochemistry of adjacent conifer and alder-conifer stands. Ecology 73:2022–2033; 1992.

Bormann, B.T.; Bormann, F.H.; Bowden, W.B.; Pierce, R.S.; Hamburg, S.P.; Wang, D.; Snyder, M.C.; Li, C.Y.; Ingersoll, R.C. Rapid N_2 fixation in pines, alder and locust: Evidence from the sandbox ecosystem study. Ecology 74:583–598; 1993.

Bormann, F.H.; Bowden, W.B.; Pierce, R.S.; Hamburg, S.P.; Voigt, G.K.; Ingersoll, R.C.; Likens, G.E. The Hubbard Brook sandbox experiment. In: Jordan, W.R.; Gilpin, M.E.; Aber, J.D., eds. *Restoration Ecology.* Cambridge: Cambridge Univ. Pr.; 1987:251–256.

Bollmann, A.; Conrad, R. Acetylene blockage technique leads to underestimation of denitrification rates in oxic soils due to scavenging of intermediate nitric oxide. Soil Biol. Biochem. 29:1067–1078; 1997.

Bormann, F.H.; Likens, G.E.; Melillo, J.M. Nitrogen budget for an aggrading northern hardwood forest ecosystem. Science 196:981–983; 1977.

Broadbent, F.E.; Carlton, A.B. Field trials with isotopically labelled nitrogen fertilizer. In: Nielson, D.R.; MacDonald, J.G., eds. *Nitrogen in the Environment.* New York: Academic; 1978:1–41.

Buchmann, N.; Gebauer, G.; Schulze, E.-D. Partitioning of ^{15}N-labeled ammonium and nitrate among soil, litter, below- and above-ground biomass of trees and understory in a 15-year-old *Picea abies* plantation. Biogeochemistry 33:1–23; 1996.

Buchmann, N.; Schulze, E.-D.; Gebauer, G. ^{15}N-ammonium and ^{15}N-nitrate uptake of a 15-year-old *Picea abies* plantation. Oecologia 102:361–370; 1995.

Burns, D.A. Retention of NO_3^- in an upland stream environment: A mass balance approach. Biogeochemistry 40:73–96; 1998.

Caldwell, M.M.; Eissenstat, D.M.; Richards, J.H.; Allen, M.F. Competition for phosphorus: Differential uptake from dual-isotope-labeled soil interspaces between shrub and grass. Science 229:384–386; 1985.

Chorover, J.; Vitousek, P.M.; Everson, D.A.; Esperanza, A.M.; Turner, D. Solution chemistry profiles of mixed-conifer forests before and after fire. Biogeochemistry 26:115–144; 1994.

Christ, M.; Zhang, Y.; Likens, G.E.; Driscoll, C.T. Nitrogen retention capacity of a northern hardwood forest soil under ammonium sulfate additions. Ecol. Applic. 5:802–812; 1995.

Christensen, S.; Simkins, S.; Tiedje, J.M. Spatial variation in denitrification: Dependency of activity centers on the soil environment. Soil Sci. Soc. Am. J. 54:1608–1613; 1990.

Currie, W.S.; Aber, J.D.; McDowell, W.H.; Boone, R.D.; Magill, A.H. Vertical transport of dissolved organic C and N under long-term N amendments in pine and hardwood forests. Biogeochemistry 35:471–505; 1996.

Dawes, W.R.; Hatton, T.J. *TOPOG_IRM. 1. Model description.* Canberra, Australia: CSIRO, Division of Water Resources, Canberra Laboratory, Institute of Natural Resources and Environment; 1993.

Dise, N.B.; Wright, R.F. Nitrogen leaching from European forests in relation to nitrogen deposition. For. Ecol. Manage. 71:153–161; 1995.

Dodds, W.K.; Blair, J.M.; Henebry, G.M.; Koelliker, J.K.; Ramundo, R.; Tate, C.M. Nitrogen transport from tallgrass prairie watersheds. J. Environ. Qual. 25:973–981; 1996.

Durka, W.; Schulze, E.-D.; Gebauer, G.; Voerkelius, S. Effects of forest decline on uptake and leaching of deposited nitrate determined from ^{15}N and ^{18}O measurements. Nature 372:765–726; 1994.

Emmett, B.A.; Reynolds, B.; Stevens, P.A.; Norris, D.A.; Hughes, S.; Gorres, J.; Lubrecht, I. Nitrate leaching from afforested Welsh catchments: Interactions between stand age and nitrogen deposition. Ambio 22:386–394; 1993.

Farrell, R.E.; Sandercock, P.J.; Pennock, D.J.; Van Kessel, C. Landscape-scale variations in leached nitrate: Relationship to denitrification and natural nitrogen-15 abundance. Soil Sci. Soc. Am. J. 60:1410–1415; 1996.

Federer, C.A.; Hornbeck, J.W.; Tritton, L.M.; Martin, C.W.; Pierce, R.S.; Smith, C.T. Long term depletion of calcium and other nutrients in eastern US forests. Environ. Manage. 13:593–601; 1989.

Fenn, M.E.; Poth, M.A.; Johnson, D.W. Evidence for nitrogen saturation in the San Bernardino Mountains in southern California. For. Ecol. Manage. 82:211–230; 1996.

Friedland, A.J.; Miller, E.K.; Battles, J.J.; Thorne, J.F. Nitrogen deposition, distribution and cycling in a subalpine spruce-fir forest in the Adirondacks, New York, USA. Biogeochemistry 14:31–55; 1991.

Frink, C.R. Estimating nutrient exports to estuaries. J. Environ. Qual. 20:717–724; 1991.

Gold, A.J.; DeRagon, W.R.; Sullivan, W.M.; Lemunyon, J.L. Nitrate-nitrogen losses to groundwater from rural and suburban land uses. J. Soil Water Conserv. 45:305–310; 1990.

Grant, D.; Binkley, D. Rates of free-living nitrogen fixation in some piedmont forest types. For. Sci. 33:548–551; 1987.

Grier, C.C. Wildfire effects on nutrient distribution and leaching in a coniferous ecosystem. Can. J. For. Res. 5:599–607; 1975.

Groffman, P.M.; Tiedje, J.M. Denitrification in north temperate forest soils: Relationships between denitrification and environmental factors at the landscape scale. Soil Biol. Biochem. 21:621–626; 1989.

Gundersen, P. Nitrogen deposition and leaching in European forests: Preliminary results from a data compilation. Water Air Soil Pollut 85:1179–1184; 1995.

Gundersen, P. Effects of enhanced nitrogen deposition in a spruce forest at Klosterhede, Denmark, examined by

moderate NH_4NO_3 addition. For. Ecol. Manage. 101:251–268; 1998.

Gundersen, P.; Rasmussen, L. Nitrogen mobility in a nitrogen limited forest at Klosterhede, Denmark, examined by NH_4NO_3 addition. For. Ecol. Manage. 71:75–88; 1995.

Hart, S.C.; Firestone, M.K.; Paul, E.A.; Smith, J.L. Flow and fate of soil nitrogen in an annual grassland and a young mixed-conifer forest. Soil Biol. Biochem. 25:431–442; 1993.

Hedin, L.O.; Armesto, J.J.; Johnson, A.H. Patterns of nutrient loss from unpolluted, old-growth temperate forests: Evaluation of biogeochemical theory. Ecology 76:493–509; 1995.

Hicks, B.B.; Hosker, R.P.J.; Meyers, T.P.; Womack, J.D. Dry deposition inferential techniques. I. Design and tests of a prototype meteorological and chemical system for determining dry deposition. Atmos. Environ. 25A:2345–2359; 1991.

Hicks, B.B.; Weseley, M.L.; Durham, J.L. *Critique of Methods to Measure Dry Deposition.* EPA-600/9-80-050. Washington, DC: U.S. Environmental Protection Agency (EPA); 1980.

Hicks, B.B.; Weseley, M.L.; Lindberg, S.E.; Bromberg, S.M., eds. *Proceedings of the Dry Deposition Workshop of the National Acid Precipitation Assessment Program, March 1986.* Oak Ridge, TN: NOAA/ATDD; 1986.

Hill, A.R. Nitrate removal in stream riparian zones. J. Environ. Qual. 25:743–755; 1996.

Holmes, R.M.; Jones, J.B.J.; Fisher, S.G.; Grimm, N.B. Denitrification in a nitrogen-limited stream ecosystem. Biogeochemistry 33:125–146; 1996.

Howarth, R.W.; Billen, G.; Swaney, D.; Townsend, A.; Jaworski, N.; Lajtha, K.; Downing, J.A.; Elmgren, R.; Caraco, N.; Jordan, T.; Berendse, F.; Freney, J.; Kudeyarov, V.; Murdoch, P.; Zhao-lang, Z. Regional nitrogen budgets and riverine N and P fluxes for the drainages to the North Atlantic Ocean: Natural and human influences. Biogeochemistry 35:75–139; 1996.

Hultberg, H.; Grennfelt, P. Sulphur and seasalt deposition as reflected by throughfall and runoff chemistry in forested catchments. Environ. Pollut. 755:215–222; 1992.

Jaworski, N.A.; Groffman, P.M.; Keller, A.A.; Prager, J.C. Watershed nitrogen and phosphorus balance: Upper Potomac River basin. Estuaries 15:83–95; 1992.

Johnson, D.W. Nitrogen retention in forest soils. J. Environ. Qual. 21:1–12; 1992.

Johnson, D.W. Soil properties beneath ceanothus and pine stands in the eastern Sierra Nevada. Soil Sci. Soc. Am. J. 59:918–924; 1995.

Johnson, N.M.; Likens, G.E.; Bormann, F.H.; Pierce, R.S. Rate of chemical weathering of silicate minerals in New Hampshire. Geochim. Cosmochim. Acta 32:531–545; 1968.

Johnson, D.W.; Lindberg, S.E., eds. *Atmospheric Deposition and Forest Nutrient Cycling: A Synthesis of the Integrated Forest Study.* New York: Springer-Verlag; 1992.

Johnson, D.W.; Swank, W.T.; Vose, J.M. Effects of liming on soils and streamwaters in a deciduous forest: Comparison of field results and simulations. J. Environ. Qual. 24:1105–1117; 1995.

Johnson, D.W.; Van Hook, R.I., eds. *Analysis of Biogeochemical Cycling Processes in Walker Branch Watershed.* New York: Springer-Verlag; 1989.

Jordan, M.J.; Nadelhoffer, K.J.; Fry, B. Nitrogen cycling in forest and grass ecosystems irrigated with ^{15}N-enriched wastewater. Ecol. Applic. 7:864–881; 1997.

Joslin, J.D.; Kelly, J.M.; Van Miegroet, H. Soil chemistry and nutrition of North American spruce-fir stands: Evidence for recent change. J. Environ. Quality 21:12–30; 1992.

Joslin, J.D.; Wolfe, M.H. Red spruce soil solution chemistry and root distribution across a cloud water deposition gradient. Can. J. For. Res. 22:893–904; 1992.

Joye, S.B.; Smith, S.V.; Hollibaugh, J.T.; Paerl, H.W. Estimating denitrification rates in estuarine sediments: A comparison of stoichiometric and acetylene based methods. Biogeochemistry 33:197–215; 1996.

Kahl, J.S.; Norton, S.A.; Fernandez, I.J.; Nadelhoffer, K.J.; Driscoll, C.T.; Aber, J.D. Experimental inducement of nitrogen saturation at the watershed scale. Environ. Sci. Technol. 27:565–568; 1993.

Kapustka, L.A.; Dubois; J.D. Dinitrogen fixation by cyanobacteria and associative rhizosphere bacteria in the Arapaho Prairie in the Sand Hills of Nebraska. Am. J. Bot. 74:107–113; 1987

Kjonaas, O.J.; Stuanes, A.O.; Huse, M. Effects of weekly nitrogen additions on N cycling in a coniferous forest catchment, Gardsjon, Sweden. For. Ecol. Manage. 101:227–250; 1998.

Knicker, H., Ludemann, H.-D.; Haider, K. Incorporation studies of NH_4^+ during incubation of organic residues by ^{15}N-CPMAS-NMR spectroscopy. Eur. J. Soil Sci. 48:431–441; 1997.

Koopmans, C.J.; Tietema, A.; Boxman, A.W. The fate of ^{15}N enriched throughfall in two coniferous forest stands at different nitrogen deposition levels. Biogeochemistry 34:19–44; 1996.

Lajtha, K.; Jarrell, W.; Johnson, D.W.; Sollins, P. Collection of soil solution. In: Robertson, P.; Coleman, D.; Bledsoe, C.; Sollins, P., eds. *Standard Soil Methods for Long-Term Ecological Research.* Oxford: Oxford Univ. Pr.; 1999.

Lajtha, K.; Seely, B.; Valiela, I. Retention and leaching losses of atmospherically-derived nitrogen in the ag-

grading coastal watershed of Waquoit Bay, MA. Biogeochemistry 28:33–54; 1995.

LaMontagne, M.G.; Valiela, I. Denitrification measured by a direct N_2 flux method in sediments of Waquoit Bay, MA. Biogeochemistry 31:63–83; 1995.

Lepisto, A.; Andersson, L.; Arheimer, B.; Sundblad, K. Influence of catchment characteristics, forestry activities and deposition on nitrogen export from small forested catchments. Water Air Soil Pollut. 84:81–102; 1995.

Lindberg, S.E.; Lovett, G.M.; Richter, D.D.; Johnson, D.W. Atmospheric deposition and canopy interactions of major ions in a forest. Science 231:141–145; 1986.

Likens, G.E. An experimental approach for the study of ecosystems. J. Ecol. 73:381–396; 1985.

Likens, G.E.; Bormann, F.H. *Biogeochemistry of a Forested Ecosystem.* New York: Springer-Verlag; 1995.

Likens, G.E.; Bormann, F.H.; Pierce, R.S.; Eaton, J.S.; Johnson, N.M. *Biogeochemistry of a forested ecosystem.* New York: Springer-Verlag; 1977.

Likens, G.E.; Bormann, F.H.; Pierce, R.S.; Reiners, W.A. Recovery of a forested ecosystem. Science 199:492–496; 1978.

Likens, G.E.; Driscoll, C.T.; Buso, D.C. Long-term effects of acid rain: response and recovery of a forest ecosystem. Science 272:244–246; 1996.

Likens, G.; Driscoll, C.; Buso, D.; Siccama, T.; Johnson, C.; Lovett, G.; Ryan, D.; Fahey T.; Reiners, W. The biogeochemistry of potassium at Hubbard Brook. Biogeochemistry 25:61–125; 1994.

Lindberg, S.E.; Lovett, G.M.; Richter, D.D.; Johnson, D.W. Atmospheric deposition and canopy interactions of major ions in a forest. Science 231:141–145; 1986.

Litaor, M.I. Review of soil solution samplers. Water Resourc. Res. 1988:727–733; 1988.

Lovett, G.M.; Bowser, J.J.; Edgerton, E.S. Atmospheric deposition to watersheds in complex terrain. Hydrol. Process. 11:645–654; 1997.

Lovett, G.M.; Likens, G.E.; Nolan, S.S. Dry deposition of sulfur to the Hubbard Brook Experimental Forest: A preliminary comparison of methods. In: Swarz, S.E.; Slinn, W.G.N., eds. *Precipitation Scavenging and Atmosphere-Surface Exchange.* Washington, DC: Hemisphere; 1992:1391–1402.

Lovett, G.M.; Lindberg, S.E. Atmospheric deposition and canopy interactions of nitrogen in forests. Can. J. For. Res. 23:1603–1616; 1993.

Lovett, G.M.; Nolan, S.S.; Driscoll, C.T.; Fahey, T.J. Factors regulating throughfall flux in a New Hampshire forested landscape. Can. J. For. Res. 26:2134–2144; 1996.

Magill, A.H.; Aber, J.D.; Hendricks, J.J.; Bowden, R.D.; Melillo, J.M.; Steudler, P.A. Biogeochemical response of forest ecosystems to simulated chronic nitrogen deposition. Ecol. Applic. 7:402–415; 1997.

Marques, R.; Ranger, J.; Gelhaye, D.; Pollier, B.; Ponette, Q.; Goedert, O. Comparison of chemical composition of soil solutions collected by zero-tension plate lysimeters with those from ceramic-cup lysimeters in a forest soil. Eur. J. Soil Sci. 47:407–417; 1996.

McDowell, W.H.; Lugo, A.E.; James, A. Export of nutrients and major ions from Caribbean catchments. J. North Am. Benthol. Soc. 14:12–20; 1995.

Mead, D.J.; Pritchett, W.L. Fertilizer movement in a slash pine ecosystem. I. Uptake of N and P and N movement in the soil. Plant Soil 43:451–465; 1975.

Miller, W.R.; Drever, J.I. Chemical weathering and related controls on surface water chemistry in the Absaroka Mountains, Wyoming. Geochim. Cosmochim. Acta 41:1693–1702; 1977.

Mitchell, M.J.; Burke, M.K.; Shepard, J.P. Seasonal and spatial patterns of S, Ca, and N dynamics of a northern hardwood forest ecosystem. Biogeochemistry 17:165–189; 1992.

Mitchell, M.J.; Driscoll, C.T.; Kahl, J.S.; Likens, G.E.; Murdoch, P.S.; Pardo, L.H. Climatic control of nitrate loss from forested watersheds in the northeast United States. Environ. Sci. Technol. 30:2609–2612; 1996.

Murdoch, P.S.; Stoddard, J.L. The role of nitrate in the acidification of streams in the Catskill Mountains of New York. Water Resourc. Res. 28:2707–2720; 1992.

Nadelhoffer, K.J.; Downs, M.R.; Fry, B. Sinks for ^{15}N-enriched additions to an oak forest and a red pine plantation. Ecol. Applic. 9:72–86; 1999a.

Nadelhoffer, K.J.; Downs, M.R.; Fry, B.; Aber, J.D.; Magill, A.H.; Melillo, J.M. The fate of ^{15}N-labelled nitrate additions to a northern hardwood forest in eastern Maine, USA. Oecologia 103:292–301; 1995.

Nadelhoffer, K.J.; Downs, M.R.; Fry, B.; Magill, A.; Aber, J. D Controls on N retention and exports in a fertilized watershed. Environ. Monitor. Assess. 55(1):187–210; 1999b.

Nielsen, T.H.; Well, R.; Myrold, D.D. Combination probe for nitrogen-15 soil labeling and sampling of soil atmosphere to measure subsurface denitrification activity. Soil Sci. Soc. Am. J. 61:802; 1997.

Nodvin, S.C.; Van Miegroet, H.; Lindberg, S.E.; Nicholas, N.S.; Johnson, D.W. Acidic deposition, ecosystem processes, and nitrogen saturation in a high elevation southern Appalachian watershed. Water Air Soil Pollut. 85:1647–1652; 1995.

Pardo, L.H.; Driscoll, C.T.; Likens, G.E. Patterns of nitrate loss from a chronosequence of clear-cut watersheds. Water Air Soil Pollut. 85:1659–1664; 1995.

Parkin, T.B. Soil microsites as a source of denitrification variability. Soil Sci. Soc. Am. J. 51:1194–1199; 1987.

Preston, C.M.; Mead, D.J. Long-term recovery in the soil profile of ^{15}N from Douglas-fir needles decomposing in the forest floor. Can. J. For. Res. 25:833–837; 1995.

Qualls, R.G.; Haines, B.L. Biodegradability of dissolved organic matter in forest throughfall, soil solution, and stream water. Soil Sci. Soc. Am. J. 56:578–586; 1992.

Quideau, S.A.; Chadwick, O.A.; Wood, H.B. Base cation biogeochemistry and weathering under oak and pine: A controlled long-term experiment. Biogeochemistry 35:377–397; 1996.

Reinhart, K.G.; Pierce, R.S. *Stream-Gaging Stations for Research on Small Watersheds.* Agriculture Handbook 268. Washington, DC: U.S.D.A. Forest Service; 1964.

Reynolds, R.C.; Johnson, N.M. Chemical weathering in the temperate glacial environment of the Northern Cascade Mountains. Geochim. Cosmochim. Acta 36:537–554; 1972.

Rustad, L.E.; Fernandez, I.J.; David, M.B.; Mitchell, M.J.; Nadelhoffer, K.J.; Fuller, R.B. Experimental soil acidification and recovery at the Bear Brook Watershed in Maine. Soil Sci. Soc. Am. J. 60:1933–1943; 1996.

Rustad, L.E.; Kahl, J.S.; Norton, S.A.; Fernandez, I.J. Underestimation of dry deposition by throughfall in mixed northern hardwood forests. J. Hydrol. 162:319–336; 1994.

Scholefield, D.; Hawkins, J.M.B.; Jackson, S.M. Development of a helium atmosphere soil incubation technique for direct measurement of nitrous oxide and dinitrogen fluxes during denitrification. Soil Biol. Biochem. 29:1345; 1997.

Seely, B.; Lajtha, K. Application of a ^{15}N tracer to simulate and track the fate of atmospherically-deposited N in the coastal forests of the Waquoit Bay Watershed, Cape Cod, MA. Oecologia 112:393–402; 1997.

Seely, B.; Lajtha, K.; Salvucci, G. The dynamics of N fluxes from canopy to ground water in a coastal forest ecosystem developed on sandy substrates. Biogeochemistry 42:325–343; 1998.

Seitzinger, S.P.; Nielsen, L.P.; Cafrey, J.; Christensen, P.B. Denitrification measurements in aquatic sediments: A comparison of three methods. Biogeochemistry 23:147–169; 1993.

Semkin, R.G.; Jeffries, D.S.; Clair, T.A. Hydrochemical methods and relationships for study of stream output from small catchments. In: Moldan, B.; Cerny, J., eds. *Biogeochemistry of Small Catchments.* Chichester, UK: Wiley; 1994:163–187.

Shepard, J.P.; Mitchell, M.J.; Scott, T.J.; Zhang, Y.M.; Raynal, D.J. Measurement of wet and dry deposition in a northern hardwood forest. Water Air Soil Pollut 48:225–238; 1989.

Silvester, W.B. Molybdenum limitation of asymbiotic nitrogen fixation in forests of Pacific Northwest America. Soil Biol. Biochem. 21:283–289; 1989.

Sollins, P.; McCorison, F.M. Nitrogen and carbon solution chemistry of an old growth coniferous forest watershed before and after cutting. Water Resourc. Res. 17:1409–1418; 1981.

Stams, A.J.M.; Bootlink, H.W.G.; Lutke-Schipholt, I.J.; Beemsterboer, B.; Woittiez, J.R.W.; Van Breemen, N. A field study on the fate of ^{15}N-ammonium to demonstrate nitrification of atmospheric ammonium in an acid forest soil. Biogeochemistry 13:241–255; 1991.

Stoddard, J.L. Long-term changes in watershed retention of nitrogen: Its causes and aquatic consequences. In: Baker, L.A., ed. *Environmental Chemistry of Lakes and Reservoirs.* Washington, DC American Chemical Society; 1994:223–284.

Stohlgren, T.J.; Melack, J.M.; Esperanza, A.M.; Parsons, D.J. Atmospheric deposition and solute export in giant sequoia–mixed conifer watersheds in the Sierra Nevada, California. Biogeochemistry 12:207–230; 1991.

Stottlemyer, R. Monitoring and quality assurance procedures for the study of remote watershed ecosystems. In: Boyle, T.P., ed. *New Approaches to Monitoring Aquatic Ecosystems.* ASTM STP 940. Philadelphia, PA: American Society for Testing and Materials; 1987:189–198.

Stottlemyer, R.; Troendle; C.A. Nutrient concentration patterns in streams draining alpine and subalpine catchments, Fraser Experimental Forest, Colorado. J. Hydrol. 140:179–208; 1992.

Tietema, A.; Emmett, B.A.; Gundersen, P.; Kjonaas, O.J.; Koopmans, C.J. The fate of ^{15}N-labelled nitrogen deposition in coniferous forest ecosystems. For. Ecol. Manage. 101:19–28; 1998.

Tietema, A.; Verstraten, J.M. Nitrogen cycling in an acid forest ecosystem in the Netherlands under increased atmospheric nitrogen inputs. Biogeochemistry 15:21–46; 1991.

Tietema, A.; Wright, R.F.; Blanck, K.; Boxman, A.W.; Bredemeier, M.; Emmett, B.A.; Gundersen, P.; Hultberg, H.; Kjonaas, O.J.; Moldan, F.; Roelofs, J.G.M.; Schleppi, P.; Stuanes, A.O.; Van Breemen, N. NITREX: The timing of response of coniferous forest ecosystems to experimentally-changed nitrogen deposition. Water Air Soil Pollut. 85:1623–1628; 1995.

Ulery, A.L.; Graham, R.C.; Chadwick, O.A.; Wood, H.B. Decade-scale changes of soil carbon, nitrogen, and exchangeable cations under chaparral and pine. Geoderma 65:121–134; 1995.

Valiela, I.; Collins, G.; Kremer, J.; Lajtha, K.; Geist, M.; Seely, B.; Brawley, J.; Sham; C.H. Nitrogen loading from coastal watersheds to receiving estuaries: New method and application. Ecol. Applic. 7:358–380; 1997.

Van Luijn, F.; Boers, P.C.M.; Lijklema, L. Comparison of denitrification rates in lake sediments obtained by the N_2 flux method, the ^{15}N isotope pairing technique and the mass balance approach. Water Res. 30:893–900; 1996.

Vitousek, P.M.; Fahey, T.; Johnson, D.W.; Swift, M.J. Element interactions in forest ecosystems: Succession, allometry and input-output budgets. Biogeochemistry 5:7–34; 1988.

Vitousek, P.M.; Reiners, W.A. Ecosystem succession and nutrient retention: A hypothesis. BioScience 25:376–381; 1975.

Waring, R.H.; Schlesinger, W.H. Forest ecosystems: Concepts and management. Orlando, FL: Academic; 1985.

White, D.S.; Howes, B.L. Long-term ^{15}N-nitrogen retention in the vegetated sediments of a New England salt marsh. Limnol. Oceanogr. 39:1878–1892; 1994.

Williams, M.R.; Melack, J.M. Atmospheric deposition, mass balances, and processes regulating streamwater solute concentrations in mixed-conifer catchments of the Sierra Nevada, California. Biogeochemistry 37:111–144; 1997a.

Williams, M.R.; Melack, J.M. Solute export from forested and partially deforested catchments in the central Amazon. Biogeochemistry 38:67–102; 1997b.

Young, M.H.; Wierenga, P.J.; Mancino, C.F. Large weighing lysimeter for water use and deep percolation studies. Soil Sci. 161:491; 1996.

17

Deposition of Nutrients and Pollutants to Ecosystems

Lars O. Hedin

Role of Atmospheric Deposition

Our view of how ecosystems depend upon atmospheric deposition has changed considerably over the past four decades. Early work primarily focused on the role of atmospheric nutrient sources in ecosystems that directly depend on precipitation as the dominant water source, such as ombrotrophic wetlands and surface waters that drain such wetlands (Tamm 1958; Gorham 1961). However this view changed dramatically in the 1970s, in response to suggestions that atmospheric deposition of strong mineral acids, or "acid rain," can affect nutrient cycles in a variety of ecosystems, including forests, wetlands, streams, rivers, and lakes (Odén et al. 1968; Likens and Bormann 1974; Gorham 1976; National Research Council 1986). These concerns about effects of acid rain (more appropriately termed "acid deposition") on European and North American ecosystems spurred an unprecedented effort during the 1970s and 1980s, aimed at improving our understanding of how nutrients, pollutants, and chemical elements enter ecosystems from the atmosphere. In fact, most modern methods and theories for studying atmospheric deposition derive from this period.

A picture gradually emerged, which emphasized the role that the atmosphere plays in delivering a host of different pollutants to ecosystems in industrial regions of the world (i.e., hydrogen ions [H^+], sulfate [SO_4^{2-}], nitrate [NO_3^-], ammonium [NH_4^+], ammonia [NH_3], sulfur dioxide [SO_2], nitrogen dioxide [NO_2], hydrochloric acid [HCl], heavy metals, and ozone [O_3]). We now also know that atmospheric deposition causes, or at least influences, some of our most challenging environmental concerns, including freshwater and soil acidification (Schindler 1988; Gorham 1989), soil base cation loss (Hedin et al. 1994; Hedin and Likens 1996), forest decline (Schultze 1989; Schulze et al. 1989; Gawal et al. 1996), ecosystem N saturation (Ågren and Bosatta 1988; Aber et al. 1998), estuarine eutrophication (Howarth et al. 1996), heavy metal accumulation (Gawal et al. 1996), and direct phytotoxic effects of O_3 and SO_2 (Lovett 1994).

There is also growing evidence that atmospheric deposition is important for maintaining ecosystem nutrient cycles in relatively unpolluted regions of the world. This means that, even in its unadulterated form, the unpolluted atmosphere can be an important source of nutrients to ecosystems. For example, studies in southern Chile point to the atmosphere as the source of nitrogen (N) and base cations for maintaining nutrient cycles in unpolluted temperate rain forests (Hedin et al. 1995; Hedin and Likens 1996; Perez et al. 1998). Others have proposed that atmospheric inputs of N, phosphorus (P), and base cations are important for tropical forests that grow on old soils (e.g., Prospero et al. 1981; Lewis 1981; Jordan 1985; Swap 1992; Lesack and Melack 1996; Kennedy et al. 1998; Chadwick et al. 1999). A recent study in the Hawaiian Islands (Chadwick et al. 1999) indicated that montane tropical rain forests on highly weathered soils depend on P inputs from the long-distance transport of P-containing dust aerosols, originating as far away as dry regions of China. Such long-distance transport of dust aerosols has also been implicated as a source of iron and other trace elements to low-productivity areas of the world's

oceans (Duce and Tindale 1991). Analogously, Cornell et al. (1995) proposed that atmospheric deposition of dissolved organic N (DON) might be a dominant source of new N in certain ocean areas.

These examples illustrate the fundamental importance of atmospheric deposition for understanding how ecosystems function in the world, and for understanding how human activities are impacting natural ecosystems. However, the examples also illustrate that our view of atmosphere–ecosystem interactions is still in a formative stage. Despite considerable progress, much remains to be understood about the link between ecosystems and the atmosphere.

Vectors of Delivery

Atmospheric nutrients and pollutants enter ecosystems via three main vectors of deposition, each subject to its own set of controlling factors and methods of measurement: (1) *Wet deposition* consists of chemical elements that enter via precipitation, mainly as dissolved solutes but also as particles entrained in raindrops; (2) *cloud deposition* consists of elements dissolved in cloud or fog droplets that impact onto terrestrial surfaces, such as leaves or branches; and (3) *Dry deposition* consists of aerosols and/or gases that are deposited directly onto surfaces of vegetation, soils, or water.

The relative contributions of these vectors can vary substantially among ecosystems and with time, due to factors that act along the path of transport from emission sources to deposition in ecosystems (e.g., Ollinger et al. 1993), and due to factors that are intrinsic to receiving ecosystems (e.g., leaf area, stomatal conductance, etc.). At the scale of individual ecosystems, the contributions by the different vectors depend on the exact chemical form (and thus reactivity) of nutrients or pollutants in the atmosphere and on local-scale meteorological and geographical conditions, such as topographic location and exposure (Miller et al. 1993; Lovett et al. 1997). Wet and dry deposition are typically the dominant deposition vectors with dry deposition becoming progressively more important in arid regions (Gilette et al. 1992). However, cloud deposition can be important in cloud-rich locations such as high-elevation forests (Lovett and Kinsman 1990; Johnson et al. 1991; Friedland et al. 1991; Schemenauer and Cereceda 1992a; Weathers and Likens, 1997), particularly since even small amounts of cloud water can contain high concentrations of pollutants and nutrients (Weathers, et al., 1988); Lin et al. 1995). A summary of factors that control the different vectors of atmospheric deposition is beyond the scope of this chapter; the reader is referred to a number of excellent texts and reviews (e.g., Finlayson-Pitts and Pitts 1986; Fowler et al. 1991; Graedel and Crutzen 1993; Duyzer and Fowler 1994; Lovett 1994; Taylor and Johnson 1994; Winner 1994; Moncrieff et al. 1997; Lovett et al. 1997; Sutton et al. 1998).

Many ecosystem-level questions demand an understanding of the total deposition of a nutrient or pollutant to an ecosystem. It is in these cases insufficient to measure only a single vector of deposition, and investigators must carefully consider each vector that is likely to be significant. However many studies report only wet deposition, primarily because this vector is less laborious and less expensive to estimate than cloud or dry deposition. Nevertheless, it is important to note that wet deposition will to varying degrees underestimate total nutrient deposition to an ecosystem. For example, Butler and Likens (1995) have found dry deposition to contribute as much as 34% of total S and 32% of total N deposition to forests in Ithaca, NY (also see Lovett 1994). This means that it is often difficult to gain a *comprehensive* understanding of atmospheric deposition to ecosystems. This difficulty has spurred the development of alternative approaches for inferring atmospheric deposition, including mass-balance flux techniques and natural abundance stable isotopic techniques. These alternative approaches are discussed at the end of this chapter.

Scales of Inquiry

It is often difficult to know how measures of atmospheric deposition at single locations scale to larger areas. Deposition rates depend on several local-scale factors, including forest edge effects (Weathers et al. 1992, 1995), orographic effects along elevational gradients (Fowler et al. 1991), canopy structure and topographic location in land-

scapes (Lovett 1994; Lovett et al. 1997), and local emission sources, such as farm operations (local enhancement of NH_3 deposition) or unpaved roads (local enhancement of base cation deposition) (Hedin and Likens 1996). In addition, different methodologies sample over different spatial scales. For example, a wet-deposition collector samples nutrient fluxes in rain and snow over a small (the diameter of the collector) and fixed location in a landscape. In contrast, micrometeorological measures of trace gas flux integrate fluxes over a larger area of a landscape (termed "footprint"); the exact size and location of this footprint varies over time as a function of local meteorological conditions. Such effects must be considered during the selection of appropriate sites and methods for studying atmospheric deposition. The aim is generally to select locations that are representative of the surrounding landscape, and thus are subject to as few local effects as possible. The aim is also to select methods in which the sampling footprint is well known.

Considerable information is needed to extrapolate from single locations to regional-scale patterns of atmospheric deposition. Spatial deposition patterns are typically derived from networks of sampling stations, either based on relatively straightforward isopleth mapping routines or from more complex geostatistical approaches that permit examination of underlying patterns of spatial variance. Such networks have been successful at describing regional patterns of wet deposition in North America and Europe, including the National Atmospheric Deposition Program/National Trends Network (NADP/NTN; over 200 stations in North America; URL address: http://nadp.sws.uiuc.edu) and the Cooperative Programme for the Monitoring and Evaluation of Long Range Air Pollutants In Europe (EMEP; 106 stations in 25 European countries). Much less is known, however, about regional patterns of dry or cloud deposition, mainly due to the inherent difficulties of estimating these vectors (e.g., Ollinger et al. 1993; Weathers et al. 1988).

Also temporal scales influence how we interpret atmospheric deposition. While rare, long-term records from single sites or networks have been valuable for understanding changes in deposition at scales of decades (e.g., Hedin et al. 1994; Likens et al. 1990).

Wet Deposition

Wet deposition occurs as rain or snow, and is estimated by combining measures of the chemistry and volume of individual precipitation events:

$$D_E = ([X]_E \times V_E)/10 \qquad (17.1)$$

where D is wet deposition for event E (in kg ha^{-1}), $[X]_E$ is concentration of element X in event E (in mg $liter^{-1}$), and V_E is the precipitation volume of event E (in cm of precipitation depth). Wet deposition can then be integrated over time, as the sum of individual deposition events over a period:

$$D_{total} = (D_1 + D_2 + \cdots + D_n) \qquad (17.2)$$

where D_{total} is the total wet deposition during the period of events 1 to n.

Precipitation volumes are typically measured by rain gauges that integrate precipitation depth over time, such as the mechanical Belfort®-type gauge, or the increasingly popular electronic tipping-bucket gauges. Precipitation chemistry is generally sampled by specialized collectors that minimize any risks for contamination of chemically dilute rain or snow. So-called "bulk precipitation collectors" are now rarely used, as they remain open at all times and therefore are sensitive to dust contamination during periods between precipitation events. Instead, most studies now employ so-called "wet-only" collectors (Fig. 17.1), which use a heated sensor to detect rain or snow events, and automatically open only during these events.

It is critically important to collect precipitation samples with minimal or no contamination from the collector itself, from any vegetation near the collector, or from the handling or shipping of water samples. The field collection vessel, and any bottles that hold the precipitation sample, must be composed of chemically inert materials (e.g., high-density polyethylene or Teflon) and must be thoroughly cleaned by washing in dilute acid followed by copious rinsing and leaching by ultrapure deionized water. Sample bottles should be closed tightly to prohibit any gaseous exchanges, refrigerated, and shipped to the analytical laboratory as soon as possible. It may be necessary to add a preservative (e.g., chloroform) to sample bottles to stabilize solutes that are subject to bacterial up-

FIGURE 17.1. Picture of wet-only collector used in the Swedish monitoring network, coordinated by the Meteorological Institute at the University of Stockholm. The lid of the collector is in the "open" position. (Photograph by Lars Hedin.)

take, such as organic acids, amino acids, or other forms of dissolved organic carbon (DOC) and DON (Keene, et al., 1989; Scudlark, et al., 1998). To minimize bacterial uptake or other chemical transformations within the collection vessel, it is preferable to limit sampling to as short a period as possible, down to single precipitation events. It is generally advisable to evaluate empirically the stability of a nutrient in question in the field collection vessel, in sample bottles, and with and without preservatives. Detailed procedures for assuring the quality of sample collection and handling, and for selecting an appropriate location for precipitation collectors, can be found in operator manuals for high-quality precipitation networks, such as NADP/AIRMoN (1997) and Bigelow and Dossett (1988).

Dry Deposition

Dry deposition is an exceedingly complex process that depends on a series of mechanisms that influence how aerosols and gases move from the atmosphere to deposition surfaces (e.g., Hicks et al. 1987; Fowler et al. 1991; Lovett 1994). The advective movement of aerosols and gases from the free atmosphere to the atmosphere within the ecosystem is affected by meteorological variables, including wind speed, wind direction, and stability of the air column. The subsequent movement of aerosols and gases to deposition surfaces (e.g., a leaf) is influenced by physical aerosol properties, such as diameter and mass. The final reactions between aerosols or gases and deposition surfaces depend on how physical and chemical properties of the aerosol or gas (e.g., propensity to adsorb to surfaces) interact with the physical, chemical, and biological properties of the deposition surface (e.g., the ability of leaf stomata to absorb the gas).

Despite this complexity, it is possible to discern some general trends in mechanisms of dry deposition as a function of aerosol size. Larger and heavier aerosol particles (approximately >5 μm in diameter) are mainly deposited by gravitational sedimentation and/or inertial impaction. In contrast, dry deposition of finer aerosols and gases (approximately 0.2 to 2 μm in diameter) chiefly occurs by molecular diffusion through the boundary layer of deposition surfaces, followed by physical or chemical absorption. Thus, while larger aerosols (e.g., Ca^{2+}-rich dust) are deposited by impaction onto surfaces, finer aerosols (e.g., SO_2 gas) depend on diffusion through the boundary layer and through stomatal openings of leaves, before they are deposited within stomatal cavities of leaves. In contrast, aerosols between 2 and 5 μm in diameter (the so-called "accumulation range") are less subject to dry deposition; these aerosols accumulate in the atmosphere and can be transported long distances before they eventually are removed by wet deposition processes.

The overall complexity of dry deposition means that it is difficult to conduct direct and comprehen-

sive measures of this process. Nitrogen is a good example since different atmospheric forms of N are deposited via different pathways, each subject to different mechanistic controls. For example, dry deposition of $(NH_4)_2SO_4$ aerosols primarily occurs by impaction onto surfaces, the gas nitrogen dioxide (NO_2) is mainly deposited inside stomatal cavities of plant leaves, while the gases NH_3 or nitric acid (HNO_3) are adsorbed directly onto vegetation and soil surfaces (Table 17.1). To estimate all forms of N deposition it is therefore necessary to measure several pathways and several aerosols. This means that selective techniques such as deployment of artificial dust-capturing surfaces, or leaf chambers to estimate gas absorption by live plant tissues, generally only measure part of total dry deposition.

Three broad approaches are presently used to estimate dry deposition to ecosystems: (1) measures based on micrometeorological techniques; (2) measures based on coupling empirical measures with model calculations; and (3) measures based on mass-balance calculations (see separate chapter below). Micrometeorological approaches depend on applying meteorological techniques to infer net fluxes of aerosols and gases from the atmosphere to ecosystems. Direct measures of atmospheric gas concentrations above an ecosystem (e.g., using a meteorological tower) can be translated mathematically into dry deposition fluxes in two ways. First, net fluxes can be calculated from combining measures of vertical concentration gradients with known or inferred diffusivity parameters (Hicks et al. 1987; Lovett 1994; Moncrieff et al. 1997; Sutton et al. 1997). The *aerodynamic* method infers net fluxes from such concentration gradients, and from knowledge of the exchange coefficient for the gas in question (e.g., Fowler and Unsworth 1979). The *Bowen ratio* method couples direct measures of vertical concentration gradients with measures of local energy balances, and assumes that the gases, temperature, and humidity are transferred predictably across the land–atmosphere interface (e.g., Lindberg et al. 1995). Second, net fluxes can be directly measured from concentrations of aerosols or gases in air parcels that move either upward or downward relative to a reference surface, in the so-called *eddy covariance* method (Hicks et al. 1987; Lovett 1994). Net land–atmosphere exchange is calculated from the integrated difference between upward versus downward fluxes for a given aerosol or gas.

A second approach combines empirical measures of aerosol and gas concentrations with efforts to model the deposition process. For example, the *big-leaf model* of Hicks et al. (1987) and the more recent *multi-leaf model* (Meyers et al. 1998) concep-

TABLE 17.1. Deposition velocities and mechanisms of deposition for different atmospheric aerosols and gases. (From Lovett [1994]).

Aerosol or gas	Dominant mechanism of deposition in terrestrial ecosystem	Typical range of deposition velocity ($cm\ sec^{-1}$)
Large particles (diam. >2 μm): e.g., soil dust or sea salt containing Ca^{2+}, Mg^{2+}, Si, Al^{4+}, Na^+, Cl^-, some SO_4^{2-}, and NO_3^-	Gravitational sedimentation and inertial impaction on exterior surfaces	0.5–2
Fine particles (diam. <2 μm): most SO_4^{2-} and NO_3^-, Pb, NH_4^+, and H^+	Diffusion across boundary layers and deposition on exterior surfaces	<0.5
Gases		
SO_2	Cuticular adsorption and stomatal uptake by exterior and interior surfaces of leaves	0.2–1 for dry foliage, stomata open; >1 for wet foliage
HNO_3	Adsorption primarily onto exterior surfaces, also interior leaf surfaces	1–5, perhaps greater
NO_2	Adsorption primarily onto interior leaf surfaces, also exterior surfaces	0.1–0.5 when stomata open
NH_3	Adsorption on exterior surfaces and interior of leaves	0.5–5, with highest values in humid conditions
O_3	Stomatal uptake and adsorption to interior leaf surfaces, also exterior surfaces	0.1–0.8

tualize dry deposition as a series of resistances that control the sequential movement of aerosols and gases from the free atmosphere to deposition surfaces (Fig. 17.2): (1) from the atmosphere to the boundary layer of the deposition surface or "big leaf" (R_a), (2) through the boundary layer to the surface (R_b), and (3) the eventual absorption of aerosols by a deposition surface (R_c).

The dry deposition flux ($-F$) can then be defined as the atmospheric concentration of an aerosol or gas (C) at a specific reference height, times the aerosol or gas deposition velocity (v_d), where v_d is the inverse of the sum of the individual resistances ($R_t = R_a + R_b + R_c$) (Hicks et al. 1987; Lovett 1984; Garland 1977):

$$-F = v_d/C = 1/R_t \qquad (17.3)$$

Deposition velocities differ greatly between different aerosols and/or gases, depending on the propensity of the aerosol or gas to react with terrestrial surfaces (see Table 17.1). For example, while NH_3 (g) is readily deposited on terrestrial surfaces (v_d up to 5 cm sec^{-1}), NH_4^+ exists mainly in fine aerosol particles with only a weak propensity for dry deposition ($v_d < 0.5$ cm sec^{-1}) (see Table 17.1).

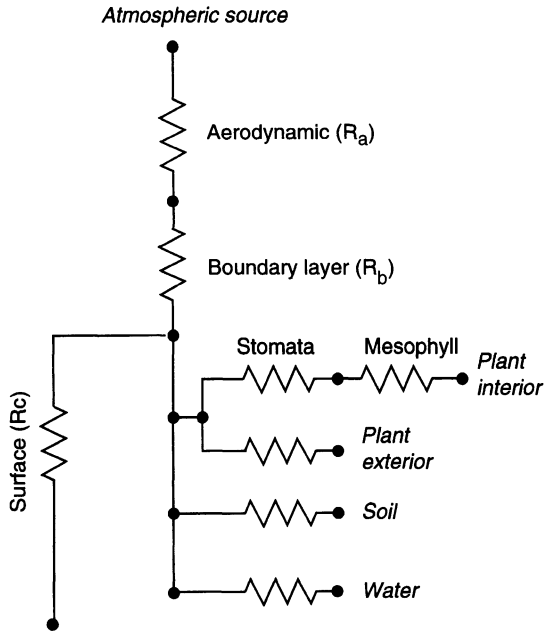

FIGURE 17.2. Sequentially coupled resistances in the "big-leaf model" of dry deposition. (From Lovett [1994].)

Dry deposition can then be inferred by combining empirical measures of aerosol or gas concentrations with a modeling formulation of the deposition process. While such models differ in structure and complexity, they are generally based on understanding how deposition velocities change as a function of meteorological parameters (e.g., light, temperature, or humidity) and canopy properties (e.g., surface area or structure). An excellent review of these models can be found in Lovett (1994).

Concentrations of aerosols and gases are measured either by air filtration and "denuder" methods, or by spectral absorption or emission methods. Filtration methods depend on passing a known amount of air through a filter system that removes the aerosol or gas in question. A series of filters are typically employed in so-called "filter packs," to stepwise remove large aerosols, fine aerosols, and reactive gases (e.g., HCl or HNO_3). The contents on each filter are dissolved in ultrapure deionized water, and subsequently analyzed by standard wet chemistry methods. These analyses do not provide information on the exact aerosol or gas composition, but identify the dissolved ionic forms (e.g., NH_4^+ vs. NO_3^-) of atmospheric constituents. Denuder systems depend on the chemical adsorption of gases onto coated glass tubes, for example in measuring air NH_3 concentrations by sorbing NH_3 (g) by acidic components in the coating. Other gases are measured spectrally, including SO_2, O_3, and NO and NO_2.

Cloud Deposition

Estimates of cloud deposition depend on two measures: the chemistry of cloud water and the rate of deposition of droplets to terrestrial surfaces. Two types of collectors are commonly used to sample cloud water for chemical analyses: passive collectors and active collectors. Passive collectors depend on wind to cause droplets to impact onto a mesh of polypropylene or Teflon strings that lead to a collection bottle (e.g., Schemenauer and Cereceda 1992a). In contrast, active cloud collectors use a motorized fan to create a consistent and strong

movement of air over the impact surfaces, which typically consist of Teflon strings that lead to a collection bottle (e.g., Weathers et al. 1988). Because it is important to exclude rain droplets as much as possible, active cloud collectors are typically designed to draw air in a manner (e.g., from below the collector) that protects from the entry of vertically falling droplets (Figure 17.3); such protection is more difficult to accomplish for passive collectors. At the conclusion of a sampling event, the collection bottle is closed and shipped to the laboratory for chemical analysis. The remaining cloud collector surfaces and Teflon strings must be thoroughly washed before being used again. Further descriptions of collection techniques can be found in Weathers et al. (1988), Schemenaurer and Cereceda (1992a, b), and Weathers and Likens (1997).

Cloud water input can be modeled from characteristics of the deposition surface and information on wind speed, liquid water content, and the size distribution of droplets during the deposition event (e.g., Lovett et al. 1982; Lovett and Reiners 1986; Lovett 1984). Alternatively, inputs of cloud water can also be empirically measured by a hydrologic canopy budget, with cloud deposition approximated as throughfall + stemflow during nonprecipitating cloud events. For cloud events with precipitation, cloud deposition can be calculated as: (throughfall + stemflow) − (wet deposition + canopy evaporation). Cloud deposition can then be calculated as the product between the concentration of a nutrient or pollutant in cloud water and the volume of water deposited during the event.

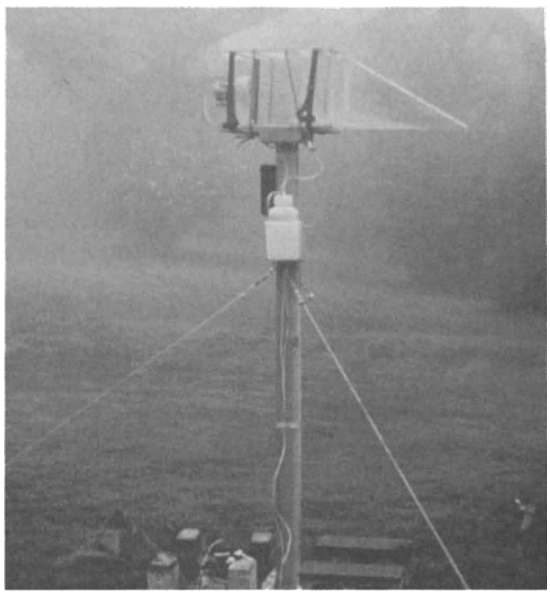

FIGURE 17.3. Picture of active cloud collector used in southern Chile. The Plexiglass frame ensures air flow through the teflon impact strings while protecting from precipitation droplets. (Photograph by Kathy Weathers.)

Mass-Balance Techniques

By applying mass balances to entire ecosystems, or parts of ecosystems (e.g., the forest canopy), it is possible to calculate deposition vectors that may be cumbersome or expensive to measure directly. The idea is to calculate the unknown vector by the mass balance of inputs, outputs, and change in internal storage of the ecosystem or subsystem of interest. Direct estimates of dry and/or cloud deposition are often difficult, time demanding, expensive, and can be associated with considerable uncertainties. The less complicated measures of wet deposition, throughfall and stemflow, and hydrologic nutrient losses, makes mass-balance techniques attractive for understanding total nutrient deposition in many ecosystems. It is important to note that the mass-balance approach is methodologically independent from modeling and/or inferential techniques for estimating dry and cloud deposition. This means that mass balances also can serve as independent and empirically derived checks on indirect modeling approaches (e.g., Butler and Likens 1995).

It is possible to establish mass balances at different scales in ecosystems. At the scale of entire watershed ecosystems, the approach depends on accurate measures of wet deposition, hydrologic and gaseous losses from the watershed, and changes in storage of a given nutrient or element within ecosystem pools. It is then possible to calculate dry (or dry + cloud) deposition as the difference between the sum of all output vectors and wet deposition, corrected for any observed change in internal storage during the measurement period (see Likens et al. 1990).

Canopy mass balances are based on measures of the chemistry and flux of water that passes through the forest canopy as throughfall and stemflow. The canopy mass balance is analogous to the watershed

balance: Dry deposition is calculated as the difference between nutrient outputs (fluxes in throughfall plus stemflow) and nutrient inputs by wet deposition, again corrected for any change in internal storage (e.g., Lovett 1994). This approach assumes that leaching of nutrients from tree tissues, and chemical reactions between nutrients supplied by wet deposition and tree tissues, are negligible. This is not always the case, as some nutrients are affected by internal canopy sinks and/or sources within canopies. For example, potassium K^+ is known to be released from live leafs and canopy K^+ budgets can be significantly compromised by this internal source.

Nevertheless, canopy mass balances are commonly used as alternative measures of dry deposition to forests. Butler and Likens (1995) adopted these techniques to estimate dry and total deposition of S and N to forests near Ithaca, NY. They found that canopy mass-balance techniques gave deposition values very similar to more standard inferential deposition velocity techniques used by the National Dry Deposition Network (now CASiNet). In contrast, Lovett et al. (1992) found important differences between inferential and mass-balance measures of S dry deposition to the Hubbard Brook Experimental Forest, NH.

While it is more difficult to establish mass balances at the scale of entire watersheds, such efforts can quantify dry deposition to larger areas within landscapes. For example, Likens et al. (1990) estimated dry S deposition from a 23-year record of watershed S fluxes at the Hubbard Brook Experimental Forest. Dry deposition was calculated as:

$$I_{dry} = O_{stream} + O_{gaseous} - I_{wet} - I_{weathering} + \Delta_{storage} \quad (17.4)$$

where I_{dry} = dry deposition input, O_{stream} is hydrologic output in streams that drain a watertight watershed, $O_{gaseous}$ is gaseous outputs as H_2S, I_{wet} is wet deposition input, $I_{weathering}$ is inputs due to mineral weathering, and $\Delta_{storage}$ is the net change in internal S stores in the ecosystem (primarily sorption/desorption of S in soils, and net plant uptake of S). Based on 23-year records of S bulk precipitation input, hydrologic losses, and knowledge about changes in internal S pools due to tree growth and immobilization reactions in soils, Likens et al. (1990) were able to assemble the following long-term mass balance, formatted as in Equation 17.4:

$$I_{dry} = 1040 + 20 - 705 - 40 + 120 \text{ eq } SO_4^{2-} \text{ ha}^{-1} \text{ yr}^{-1}$$

It can be seen that the watershed S mass balance is dominated by hydrologic outputs and wet deposition (in this case, measured as bulk deposition by Likens et al.). This budget illustrates the strong effect of human-induced atmospheric deposition on the S budget of a relatively undisturbed forest ecosystem. From this budget, Likens et al. calculated a long-term average dry deposition of S as approximately 435 eq $\text{ha}^{-1}\,\text{yr}^{-1}$, or as much as approximately 38% of total atmospheric S deposition to this forest.

Similar to the canopy mass balance, this watershed balance depends on how well the different inputs, outputs, and changes in internal stores of S are known. Likens et al. argued that these vectors were either relatively well known (e.g., hydrologic losses and wet deposition), or of negligible contribution to the overall S balance (e.g., gaseous hydrogen sulfide (H_2S) losses and changes in internal storage; +20 vs. +120 eq $\text{ha}^{-1}\,\text{yr}^{-1}$). However, this may not be the case for other elements, or for other ecosystems. The advantage of this approach is that it allows analysis of long-term dynamics, and that it explicitly compares dry deposition against other major fluxes of S in the ecosystem.

Stable Isotope and Other Tracer Techniques

Natural abundances of stable isotopes, and other watershed-scale tracers, are not commonly used to understand atmospheric deposition to terrestrial ecosystems. However, tracer techniques hold considerable promise for studying source-sink relationships across land–atmosphere interfaces in a manner that complements more traditional methods of study. Tracer techniques have the advantage that insights can be gained from a relatively limited set of samples. Some of the utility and robustness of tracer techniques stems from that, by nature, these approaches are based on measures of *intensive* quantities that do not depend on knowing boundaries of the ecosystem or measurement area (e.g.,

isotope ratios or concentrations). In contrast, the more traditional measures of deposition fluxes derive from *extensive* quantities (e.g., mass fluxes of nutrients) that depend directly on the size and boundaries of the system in question. Recent summaries by Kendall and McDonnell (1998), Kendall et al. (1995), and Macko and Ostrom (1994) discuss some of the prospects and difficulties of using stable isotopes to infer nutrient and element fluxes across the atmosphere–land interface.

For example, natural abundances of Sr isotopes have been used to understand Ca^{2+} cycling in ecosystems (Ca^{2+} isotopes are rarely used due to analytical difficulties, and due to less predictable patterns in biological and geological systems). Graustein and Armstrong (1983) took advantage of local differences in isotopic signals of strontium (Sr) associated with bedrock (assumed to reflect weathering inputs) and with atmospheric dust. By analyzing the natural abundance $^{87}Sr/^{86}Sr$ ratios in plant materials, Graustein and Armstrong could then deduce the exact mixture of the two putative sources (weathering vs. atmospheric sources) needed to produce the isotopic ratio measured in plant tissues. In this manner it is possible, if local conditions permit a clear separation among putative end-members, to quantify the degree to which atmospheric Sr deposition (and by extension other base cations) contribute to internal nutrient cycles of entire ecosystems. The technique has now been more widely employed in forested ecosystems (e.g., Åberg et al. 1989; Miller et al. 1993; Bailey et al. 1996; Dambrine et al. 1997; Kennedy et al. 1998). However, it should be cautioned that this approach, like other natural abundance isotope techniques, is associated with uncertainties and site-specific challenges. The approach assumes that the two end-members (weathering vs. atmospheric sources) are isotopically distinct, homogeneously mixed, and unvarying in time and space. Unfortunately, these assumptions are likely to be violated in many ecosystems. For example, the atmospheric end-member is typically neither homogeneous nor unvarying, but originates from heterogeneous mixtures of several sources that differ in $^{87}Sr/^{86}Sr$ signatures and that vary in relative contribution over ecological and geological time scales. Weathering is equally complex, often involving different combinations of primary and secondary minerals that may vary in both weathering rate and isotopic signature of weathered Sr. A final difficulty is that Sr typically does not behave identically to other cations, and that the magnitude of these differences among cations may, in turn, vary from site to site. Nevertheless, the approach can be quite useful in locations where end-members are clearly different, and where the underlying assumptions can be carefully examined.

Even greater difficulties exist in using ^{15}N isotopic signatures to study atmospheric N deposition to ecosystems. First, ^{15}N signatures are quite variable in wet deposition (Durka et al. 1994; Macko and Ostrom 1994). Second, ^{15}N signatures within forest ecosystems range greatly due to isotopic fractionation (systematic change in isotopic ratios) associated with the processes of N uptake, mineralization, denitrification, and other biological transformations (e.g., Hedin 1994; Macko and Ostrom 1994). To overcome the difficulties associated with such internal fractionation, Durka et al. (1994) employed a dual-label (^{15}N and ^{18}O) isotope approach to trace atmospheric NO_3^- inputs to forests in Germany. By simultaneously measuring the ^{15}N and ^{18}O signatures in NO_3^- in streams draining forests, they were able to more clearly separate the isotopic signatures of atmospherically deposited NO_3^- vs. NO_3^- produced by nitrification within the forest ecosystem. This study is an example of how relatively advanced isotopic analyses can be used to understand how atmospheric deposition impacts ecosystems (see Hedin 1994).

In a different application of watershed-scale tracers, Hedin et al. (1995) and Hedin and Hetherington (1996) used the dominance of sea-salt aerosols in the atmospheres of unpolluted temperate forests in southern Chile to quantify the role of atmospheric cation deposition. By assuming that chloride (Cl^-) acts as a conservative tracer in forested watersheds, Hedin et al. (1995) used sea-salt ratios of elements to Cl^- to subtract out the contribution of atmospheric deposition to element outputs in watershed streams. Such subtraction removed the majority of solutes in streams, indicating that these ecosystems depend closely on atmospheric deposition (also see Chadwick et al. [1999]).

Summary and Prospects

The past four decades have seen rapid developments in our abilities to measure atmospheric nutrient inputs to ecosystems. While there still is

much to learn about quantifying inputs to atmospheric ecosystems, it can be argued that some of the greatest challenges now lie at the interface between atmospheric deposition and ecosystem function. The time is right to develop better understanding of how atmospheric inputs affect and maintain the long-term function and sustainability of natural (and human-impacted) ecosystems throughout the world (see Chadwick et al. 1999).

References

Aber, J.; McDowell, W.; Nadelhoffer, K.; Magill, A.; Berntson, G.; Kamakea, M.; McNulty, S.; Currie, W.; Rustad, L.; Fernandez, I. Nitrogen saturation in temperate forest ecosystems: Hypotheses revisited. BioScience 48:921–934; 1998.

Ågren, G.I.; Bosatta, E. Nitrogen saturation of the terrestrial ecosystem. Environ. Pollut. 54:185–197; 1988.

Åberg, G.; Jacks, G.; Hamilton, P.J. Weathering rates and $^{87}Sr/^{86}Sr$ ratios: An isotopic approach. J. Hydrol. 109:65–78; 1989.

Bailey, S.W.; Hornbeck, J.W.; Driscoll, C.T.; Gaudette, H.E. Calcium inputs and transport in a base-poor forest ecosystem as interpreted by Sr isotopes. Water Resources Research 32:707–719; 1996.

Bigelow, D.S.; Dossett, S.R. *Instruction Manual: NADP/NTN Site Operation.* Fort Collins, CO: National Atmospheric Deposition Program/National Trends Network Coordinator, Natural Resource Ecology Laboratory, Colorado State University; 1998.

Butler, T.J.; Likens, G.E. A direct comparison of throughfall plus stemflow to estimates of dry and total deposition of sulfur and nitrogen. Atmos. Environ. 29:1253–1265; 1995.

Chadwick, O.A.; Derry, L.A.; Vitousek, P.M.; Huebert, B.J.; Hedin, L.O. Changing sources of nutrients during four million years of ecosystem development. Nature 397:491–497; 1999.

Cornell, S.; Rendell, A.; Jickells, T. Atmospheric inputs of dissolved organic nitrogen to the oceans. Nature 376:243–246; 1995.

Dambrine, E.; Loubert, M.; Vega, J.A.; Lissarague, A. Localisation of mineral uptake by roots using Sr isotopes. Plant Soil 192:129–132; 1997.

Duce, R.A.; Tindale, N.W. Atmospheric transport of iron and its deposition in the ocean. Limnol. Oceanogr. 36:1715–1726; 1991.

Durka, W.; Schultze, E.D.; Gebauer, G.; Voerkelius, S. Effects of forest decline on uptake and leaching of deposited nitrate determined from ^{15}N and ^{18}O measurements. Nature 372:765–767; 1994.

Duyzer, J.; Fowler, D. Modeling land-atmosphere exchange of gaseous oxides of nitrogen in Europe. Tellus B 46:353–372; 1994.

Finlayson-Pitts, B.J.; Pitts, J.M. *Atmospheric Chemistry: Fundamentals and Experimental Techniques.* New York: Wiley; 1986.

Friedland, A.J.; Miller, E.K.; Battles, J.J.; Thorne, J.F. Nitrogen deposition, distribution and cycling in a subalpine spruce-fir forest in the Adirondacks, New York, USA. Biogeochemistry 14:31–55; 1991.

Fowler, D.; Duyzer, J.H.; Baldocchi, D.D. Inputs of trace gases, particles and cloud droplets to terrestrial surfaces. Proc. R. Soc. Edinburgh 97B:35–59; 1991.

Fowler, D.; Unsworth, M.H. Turbulent transfer of sulphur dioxide to a wheat crop. Quart. Rev. R. Meteorol. Soc. 105:767–84; 1979.

Garland, J.A. The dry deposition of sulphur dioxide to land and water surfaces. Proc. R. Soc. Lond. 12:245–268; 1977.

Gawal, J.E.; Ahner, B.A.; Friedland, A.J.; Morel, F.M.M. Role for heavy metals in forest decline indicated by phytochelatin measurements. Nature 381:64–65; 1996.

Gillette, D.A.; Stensland, G.J.; Williams, A.L.; Barnard, W.; Gatz, D.; Sinclair, P.C.; Johnson, T.C. Emissions of alkaline elements calcium, magnesium, potassium, and sodium from open sources in the contiguous United States. Global Biogeochem. Cycl. 6:437–457; 1992.

Gorham, E. Factors influencing supply of major ions to inland waters, with special reference to the atmosphere. Geol. Soc. Am. Bull. 72:795–840; 1961.

Gorham, E. Acid precipitation and its influence upon aquatic ecosystems-an overview. Water Air Soil Pollut. 6:pp.457–481; 1976.

Gorham, E. Scientific understanding of ecosystem acidification: A historical review. Ambio 18:150–154; 1989.

Graedel, T.E.; Crutzen, P.J. The changing atmosphere. Sci. Am. 261:58–68; 1989.

Graustein, W.C.; Armstrong, R.L. The use of strontium-87/strontium-86 ratios to measure atmospheric transport into forested watersheds. Science 219:289–292; 1983.

Hedin, L.O. Stable isotopes, unstable forest. Nature 372:725–726; 1994.

Hedin, L.O.; Armesto, J.J.; Johnson, A.H. Patterns of nutrient loss from unpolluted, old-growth temperate forests: evaluation of biogeochemical theory. Ecology 76:493–509; 1995.

Hedin, L.O.; Granat, L.; Likens, G.E.; Buishand, T.A.; Galloway, J.N.; Butler, T.J.; Rodhe, H. Steep declines in atmospheric base cations in regions of Europe and North America. Nature 367:351–354; 1994.

Hedin, L.O.; Hetherington, E. Atmospheric and geologic constraints on the biogeochemistry of North and South American temperate rain forests. In: Lawford, R.G.; Alaback, P.B.; Fuentes, E. *High-Latitude Rainforests and Associated Ecosystems of the West Coast of the Americas.* New York: Springer-Verlag; 1996:57–74.

Hedin, L.O.; G.E. Likens. Atmospheric Dust and Acid Rain. Scientific American 275:88–92; 1996.

Hicks, B.B.; Baldocchi, D.D.; Meyers, T.P.; Hosker, R.P., Jr.; Matt, D.R. A preliminary multiple resistance routine for deriving deposition velocities from measured quantities. Water Air Soil Pollut. 30:75–90; 1987.

Howarth, R.W.; Billen, G.; Swaney, D.; Townsend, A.; Jaworski, N.; Lajhta, K.; Downing, J.A.; Elmgren, R.; Caraco, N.; Jordan, T.; Berendse, F.; Freny, J.; Kudeyarov, V.; Murdoch, P.; Zhao-Liang, Z. Regional nitrogen budgets and riverine N and P fluxes for the drainages to the North Atlantic Ocean: Natural and human influences. Biogeochemistry 35:75–139; 1996.

Johnson, D.W.; Van Miegroet, H.; Lindberg, S.E.; Todd, D.E. Nutrient cycling in red spruce forests of the Great Smoky Mountains. Can. J. For. Res. 21:769–787; 1991.

Jordan, C.F. *Nutrient Cycling in Tropical Forest Ecosystems: Principles and Their Applications.* New York: Wiley; 1985.

Keene, W.C.; Talbot, R.W.; Andreae, M.O.; Beecher, K.; Berresheim, H.; Castro, M.; Farmer, J.C.; Galloway, J.N.; Hoffmann, M.R.; Li, S.M.; Maben, J.R.; Munger, J.W.; Norton, R.B.; Pszenny, A.P.; Puxbaum, H.; Westberg, H.; Winiwarter, W. An intercomparison of measurement systems for vapor and particulate phase concentrations of formic and acetic-acids. J. Geophys. Res. Atmos. 94:6457–6471; 1989.

Kendall, C.; McDonnell, J.J. (eds.). *Isotope Tracers in Catchment Hydrology.* Amsterdam: Elsevier; 1998.

Kendall, C.; Sklash, M.G.; Bullen, T.D. Isotope tracers of water and solute sources in catchments. In Trudgill, S.T. *Solute Modelling in Catchment Systems.* New York: Wiley; 1995:262–303.

Kennedy, M.J.; Chadwick, O.A.; Vitousek, P.M.; Derry, L.A.; Hendricks, D.M. Changing sources of base cations during ecosystem development, Hawaiian Islands. Geology 26:1015–1018; 1998.

Lesack, L.F.W.; Melack, J.M. Mass balance of major solutes in a rainforest catchment in the Central Amazon: implications for nutrient budgets in tropical rainforests. Biogeochemistry 32:115–152; 1996.

Lewis, W.J. Precipitation chemistry and nutrient loading by precipitation in a tropical watershed. Water Resourc. Res. 17:169–181; 1981.

Likens, G.E.; Bormann, F.H. Acid rain: A serious regional environmental problem. Science 184:1176–1179; 1974.

Likens, G.E.; Bormann, F.H.; Hedin, L.O.; Driscoll, C.T. Dry deposition of sulfur: A 23-year record for the Hubbard Brook Forest ecosystem. Tellus 42B:319–329; 1990.

Lin, Z.Q.; Schuepp, P.H.; Schemenauer, R.S.; Kennedy, G.G. Trace-metal contamination in and on balsam fir (*Abies balsamea*) foliage in southern Quebec, Canada. Water Air Soil Pollut. 81:175–191; 1995.

Lindberg, S.E.; Kim, K.H.; Meyers, T.P.; Owens, J.G. Micrometeorological gradient approach for quantifying air-surface exchange of mercury-vapor—tests over contaminated soils. Environ. Sci. Technol. 29:126–135; 1995.

Lovett, G.M. Rates and mechanisms of cloud water deposition to a subalpine balsam fir forest. Atmos. Environ. 18:361–371; 1984.

Lovett, G.M. Atmospheric deposition of nutrients and pollutants in North America: An ecological perspective. Ecol. Applic. 4:629–650; 1994.

Lovett, G.M.; Bowser, J.J.; Edgerton, E.S. Atmospheric deposition to watersheds in complex terrain. Hydrol. Process. 11:645–654; 1997.

Lovett, G.M.; Kinsman, J.D. Atmospheric pollutant deposition to high-elevation ecosystems. Atmos. Environ. 24A:2767–2786; 1990.

Lovett, G.M.; Likens, G.E.; Nolan, S.S. Dry deposition of sulfur to the Hubbard Brook Experimental Forest: A preliminary comparison of methods. In: Schwartz, S.E.; Slinn, W.G.N., eds. *Precipitation Scavenging and Atmosphere-Surface Exchange. Vol. 3.* Washington, DC: Hemisphere; 1992:1391–1402.

Lovett, G.M.; Reiners, W.A. Canopy structure and cloud water deposition in subalpine coniferous forests. Tellus 38B:319–327; 1986.

Lovett, G.M.; Reiners, W.A.; Olsen, R.K. Cloud droplet deposition in subalpine balsam-fir forests: Hydrological and chemical inputs. Science 218:1303–1304; 1982.

Macko, S.A.; Ostrom, N.E. Pollution studies using stable isotopes. In: Lajtha, K.; Michener, R.H. *Stable Isotopes in Ecology and Environmental Science.* London: Blackwell; 1994:45–62.

Meyers, T.P.; Finkelstein, P.; Clarke, J.; Ellestad, J.G.; Sims, P.F. A multi-layer model for inferring dry deposition using standard meterological measurements. J. Geophysical Res. 103:645–666; 1998.

Miller, E.K.; Blum, J.D.; Friedland, A.J. Determination of soil exchangeable-cation loss and weathering rates using Sr isotopes. Nature 362:438–441; 1993.

Moncrieff, J.; Valentini, R.; Greco, S.; Seufert, G.; Ciccioli, P. Trace gas exchange over terrestrial ecosystems: Methods and perspectives in micrometeorology. J. Exp. Bot. 48:1133–1142; 1997.

NADP/AIRMON. *Site Operator's Manual for the NADP Atmospheric Integrated Research Monitoring Net-*

work. Fort Collins, CO: National Atmospheric Deposition Program/Atmospheric Integrated Research Monitoring Network; 1997.

National Research Council. *Acid Deposition: Long-Term Trends.* Washington, DC: National Academy; 1986.

Odén, S. The acidification of air and precipitation and its consequences on the natural environment. Swed. Nat. Sci. Res. Counc. Ecol. Committ. Bull. 1; 1968.

Ollinger, S.V.; Aber, J.D.; Lovett, G.M.; Millham, S.E.; Lathrop, R.G.; Ellis, J.M. A spatial model of atmospheric deposition for the northeastern U.S. Ecol. Applic. 3:459–472; 1993.

Prospero, J.M.; Nees, R.T.; Uematsu, M. Atmospheric transport of soil dust from Africa to South America. Nature 289:570–572; 1981.

Perez, C.A.; Hedin, L.O.; Armesto, J.J. Nitrogen mineralization in two unpolluted old-growth forests of contrasting biodiversity and dynamics. Ecosystems 1:361–373; 1998.

Schemenauer, R.S.; Cereceda, P. The quality of fog water collected for domestic and agricultural use in Chile. Journal of Applied Meteorology 31:275–290; 1992a.

Schemenauer, R.S.; Cereceda, P. Monsoon cloudwater chemistry on the Arabian peninsula. Atmos. Environ. 26A:1583–1587; 1992b.

Schemenauer, R.S.; Cereceda, P. A proposed standard fog collector for use in high-elevation regions. J. Appl. Meteorol. 33:1313–1322; 1994.

Schindler, D.W. Effects of acid rain on freshwater ecosystems. Science 239:149–157; 1988.

Schulze, E.D. Air pollution and forest decline in a spruce (*Picea abies*) forest. Science 244:776–783; 1989.

Schulze, E.-D.; Lange, O.L.; Oren, R. (eds.). Forest decline and air pollution. Berlin: Springer-Verlag; 1989.

Scudlark, J.R.; Russell, K.M.; Galloway, J.N.; Church, T.M.; Keene, W.C. Organic nitrogen in precipitation at the mid-Atlantic US coast: Methods evaluation and preliminary measurements. Atmos. Environ. 32:1719–1728; 1998.

Swap, P.; Garstang, M.; Greco, S.; Talbot, R.; Kallberg, P. Saharan dust in the Amazon basin. Tellus 44:133; 1992.

Sutton, M.A.; Burkhardt, J.K.; Guerin, D.; Nemitz, E.; Fowler, D. Development of resistance models to describe measurements of bi-directional ammonia surface-atmosphere exchange. Atmos. Environ. 32:473–480; 1998.

Tamm, C.O. *The Atmosphere.* 233–242 In: Ruhland, W. (ed.) *Encyclopedia of Plant Physiology.* Berlin: Springer-Verlag, 1958.

Taylor, G.E., Jr.; Johnson, D.W. Air pollution and forest ecosystems: A regional to global perspective. Ecol. Applic. 4:662–689; 1994.

Weathers, K.C.; Likens, G.E.; Bormann, F.H.; Bicknell, S.H.; Bormann, B.T.; Daube, B.C.; Eaton, J.S.; Galloway, J.N.; Keene, W.C.; Kimball, K.D.; McDowell, W.H.; Siccama, T.G.; Smiley, D.; Tarrant, R.A. Cloudwater chemistry from 10 sites in North-America. Environ. Sci. Technol. 22:1018–1026; 1988.

Weathers, K.C.; Lovett, G.M.; Likens, G.E. The influence of a forest edge on cloud deposition. 1415–1423 In: Schwartz, S.E.; Slinn, W.G.N. *Precipitation scavenging and atmosphere-surface exchange. Vol. 3.* Washington, DC: Hemisphere; 1992.

Weathers, K.C.; Lovett, G.M., Likens, G.E. Cloud Deposition to a spruce forest edge. Atmos. Environ. 29:665–672; 1995.

Winner, W.E. Mechanistic analysis of plant responses to air pollution. Ecol. Applic. 4:651–661; 1994.

18

Landscape and Regional Biogeochemistry: Approaches

Ingrid C. Burke

Introduction

Landscape- or regional-scale biogeochemistry is a subfield of biogeochemistry that focuses on the large-scale spatial variation in the fluxes and distribution of elements. The application of ecosystem ecology to such large spatial scales is inherently problematical because processes are difficult if not impossible to measure at these scales (Rosswall et al. 1988; Groffman and Wagenet 1994). Biogeochemical processes at such scales are important determinants of regional-to-global earth system dynamics, and are the best indication of atmosphere–biosphere interactions and economic processes that result from food and other natural resource production (Schimel et al. 1988; Matson et al. 1989; Burke et al. 1991; Riebsame et al. 1994; Walker 1994).

There are three general types of questions that are addressed in landscape or regional biogeochemistry. First, we seek to understand patterns in the distribution and flux of elements in currently existing landscapes or regions (discussed in section on pattern analysis). This type of study often utilizes the spatial and temporal variability that occurs across large scales to study the controls over biogeochemical processes (e.g., Jenny 1941; Lieth 1978; Meentemeyer et al. 1985; Zak et al. 1986; Groffman and Tiedje 1989; Burke 1989; Knapp et al. 1993; Schimel et al. 1991; and many others). For instance, a landscape or region may have strong variation in soil water availability, soil temperature, soil texture, and land use, all of which are important controls over net primary productivity, decomposition, soil organic matter, and trace gas flux. The landscape provides an experimental framework in which we can ask how these controls interact to influence the flux and distribution of elements. This experimental framework is simpler than conducting a manipulative analysis. It is also confounded however, since most of the major controls over biogeochemical processes (i.e., microclimate and soils) vary together across the landscape (Groffman et al. 1988; Burke 1989), making it difficult to isolate the influence of individual control factors.

In a second type of analysis, we address the biogeochemical connections among components of the landscape (discussed in section on spatially explicit analysis). In this case, components of the landscape are spatially dependent; changes in one place influence the flux and distribution of elements in another. Water is most often the important vector for transporting elements among landscape components, so this type of study often addresses the terrestrial–aquatic interface. Wind may also be an important vector, particularly for soil erosion. This type of study is fundamentally different from the pattern analysis described above because the biogeochemical processes studied are so-called "spatially explicit," or represent spatial redistribution within or among landscapes and regions.

Finally, in a third general type of study in landscape or regional biogeochemistry, we attempt to extrapolate our understanding the controls over biogeochemical pools and fluxes over large scales (discussed in section on extrapolating to regional or landscape scale). Landscapes and regions correspond with the scales at which many important processes and perturbations occur, including land-use management, fires, flooding, and some severe weather events. Simple empirical modeling or

simulation analysis is used to assess the current processes occurring at these scales, and the potential sensitivity of biogeochemical pools and fluxes to these types of perturbations.

In this paper, I review the most common methodologies for each of these three types of analyses in landscape and regional biogeochemistry, identify their strengths and weaknesses, and briefly note some of the new techniques available. My emphasis is on reviewing the approaches and strategies for designs in landscape- to regional-scale biogeochemistry, rather than describing the detailed methods. For each of the three major categories (pattern analysis, spatially explicit analysis, and extrapolating to landscape and regional scales), I will describe the approaches for field analyses and for modeling analyses.

Pattern Analysis: Design for Field Studies

To a large extent, empirical pattern analysis has provided much of our current knowledge of the controls over biogeochemical pools and fluxes. The early work of Dockuchaiev (1883), Shaw (1930), and Jenny (1941), made across large-scale regional gradients, had a substantial influence on the foundations of soil science and ecosystem ecology. Similarly, Lieth (1978) made great contributions with respect to our understanding of the controls over primary productivity, Meentemeyer (1984) over decomposition, and Matson and Vitousek (1987) over trace gas flux. The relationships generated from pattern analysis not only contribute to our knowledge of the biogeochemical processes and their controls, but also provide important predictive equations. For instance, the relationship generated by Sala et al. (1988) concerning primary productivity in grasslands is incorporated into the major biogeochemical simulation model for grasslands, Century (Parton et al. 1987). Many of these studies utilized large databases from multiple sources, which creates difficulties in that methods are often not consistent across studies. New empirical studies that address landscape- to regional-scale variation in biogeochemical pools that use consistent methods across such large gradients are often more useful. Here, I discuss several issues relevant to the design of such studies.

Stratified Sampling and Discrete Units

Most landscape biogeochemistry studies have utilized stratified random sampling, which requires an a priori discrete classification of landscapes or regions. Jeffers (1988) and Groffman (1991) suggest that this type of stratified sampling approach is the most appropriate and useful design for assessing the controls over biogeochemical processes, and for scaling up studies from the field to landscapes, regions, or the globe. In this type of design, investigators utilize prior information about the system, and stratify in such a way as to attempt to capture the major variation in the controls over biogeochemical processes in field units. Clearly, the decisions made at this point influence field results and propagate through to the scaling of field measurements to larger areas (Groffman 1991; O'Neill 1986).

Four basic types of a priori classification are usually made, and the choice both reflects the expertise of the investigator and results in some bias in the results. First, investigators may group landscape or regional units by vegetation type (e.g., Zak et al. 1986; Burke et al. 1989; Giblin et al. 1991; Valentine and Binkley 1992; Kielland 1995), and replicate by sampling several different stands representing each vegetation type. For example, Zak et al. (1986) stratified a forest landscape in Michigan by forest community type. In this landscape, previous research had defined four community types, sugar maple–basswood, sugar maple–red oak, and red oak–black oak, that were the product of site conditions, especially fertility. Second, groupings may be made by soil type (Lajtha and Schlesinger 1988; Groffman and Tiedje 1989; Groffman et al. 1992; Groffman and Hanson 1997), since soils integrate many of the processes important to biogeochemical cycling (Jenny 1980; Amundson and Jenny 1997). For example, Lajtha and Schlesinger (1988) stratified a desert landscape based upon its pedogenic age to evaluate large-scale controls over phosphorus availability. A third type of classification is particularly common in landscapes that are strongly driven by fluvial processes, in which two-dimensional representations of landscapes called "catenas" (Aandahl 1948; Jenny 1980) are divided into units such as summit, midslope (or backslope), and toeslope (or footslope) (Schimel et al. 1985; Schimel 1986; Aguilar et al. 1988; Groffman et al.

1993). More complex versions of landform classification (Swanson et al. 1988; Coppinger et al. 1991) may be used where elevation and aspect are as important as slope position. Finally, land-use management classifications are often used (e.g., Mosier et al. 1991; Reiners et al. 1994), sometimes in combination with one of the other grouping systems.

Once the classification system is chosen, investigators generally select replicate units for study, and conduct a standard field sampling program within the replicate units. Data are appropriately analyzed using analysis of variance type statistics. Special care needs to be taken with interpretation, since significance of the "class" or unit only implies that the investigator's a priori classification represents an axis of strong variability in biogeochemical processes. Since vegetation, soil, landform, and land use may all co-vary, it is not possible using this type of sampling regime to isolate the proximal controls over biogeochemical processes (Groffman et al. 1988). Two-way analysis of variance, utilizing overlapping classification schemes and sampling, can assist with this problem.

Use of an a priori discrete classification scheme in sampling landscape or regional scale patterns in biogeochemical pools and processes is the most common strategy, and it has substantial advantages (Matson et al. 1989). Ecologists are generally quite familiar with the appropriate variations on experimental design and statistical analysis, and the peer-review process is relatively simple as a result. Extrapolating from the sampled area to landscapes and/or regions is relatively simple (see section below), as long as the units chosen reflect most of the variation at the new scale.

Sampling Continuous Variation

An alternative approach to using discrete classes in characterizing landscape- to regional-scale patterns in biogeochemistry is to sample continuous variation in control factors and thus, response variables. Many of the classic papers that assess large-scale controls over biogeochemical processes are meta-data analyses, utilizing data from a large number of studies that cross relatively large gradients of temperature, precipitation, vegetation, and soils (e.g., Lieth 1978; Meentemeyer 1984; Meentemeyer et al. 1982, 1985; Matson and Vitousek 1987). The continuous variation in multiple control factors allows interactions among variables to be statistically evaluated across a range of values. This type of design has some strong advantages over the discrete approaches outlined above, in that regression equations can provide predictive models for use in other systems (e.g., Paruelo et al. 1998).

Two general types of field sampling designs are commonly used to capitalize on continuous variation in the controls over biogeochemical processes. In the first, one or more transects are arrayed along the major gradients, and sampling is conducted at regular or random intervals (e.g., Meentemeyer and Berg 1986; Yonker et al. 1988; Vitousek et al. 1994; Schimel et al. 1991; Knapp et al. 1993; Naiman et al. 1994; Pouyat et al. 1995; Johanson et al. 1995). Data may then be analyzed using regression or correlation analysis, analyzing the relationship between the independent variable(s) and the dependent biogeochemical factor of interest.

The second type of design for sampling continuous variation is to utilize a grid sampling scheme that permits continuous variation in all independent and dependent variables (Robertson 1987). This type of design is particularly powerful for testing for the spatial autocorrelation present in biogeochemical factors; the analysis is summarized in Robertson (1987). This design and analysis protocol permit the investigator to test for important spatial scales of variation and spatial dependence that may not be evident a priori (e.g., Robertson 1982, 1987; Robertson et al. 1988, 1997; Halvorson et al. 1994), and can not be assessed using the discrete approach outlined above. Alternatively, the continuous grid design may be analyzed using nonspatial multivariate techniques to evaluate the multidimensional relationships among the control factors and biogeochemical pools and processes. Multivariate techniques such as principal components analysis or factor analysis may be used to identify the shared variance in the data set, for interpretation of the major controls over distribution and flux (Burke 1989; Naiman et al. 1994). Simple multiple regression or correlation techniques may also be used (Groffman and Turner 1995) to characterize relationships, as in the transect design.

The continuous approaches offer several distinct advantages over the discrete approaches. First, the design is less closely the result of investigator bias (not requiring stratification), and more combina-

tions of control factors and response variables are likely to be sampled. Second, some substantial statistical power is gained; if all the assumptions of regression analysis are met, for instance, each sample (or composite) adds one degree of freedom. Third, the spatial dimension of landscapes or regions can be explicitly addressed through autocorrelation analysis. Fourth, patterns and processes that are not apparent to the investigator a priori may emerge from the autocorrelation analysis (e.g., Robertson et al. 1997). Finally, many relationships among the variables can be explored through multivariate analysis. These techniques are used much less commonly than the discrete approaches described above. The most likely explanations are the limitation imposed by the number of samples that need to be taken to conduct such analyses, the fact that many of the most sophisticated multivariate procedures do not produce predictive equations for application, and finally, a lesser familiarity with these geostatistical and multivariate techniques among most biogeochemists than the more traditional, agronomically based statistics such as analysis of variance.

Spatially Explicit Analyses

Field Analyses

Many of the key processes responsible for environmental degradation involve the movement of elements or compounds within and among components of landscapes and regions. Acid deposition, eutrophication, and pollutant transport are examples of important environmental problems that involve transport and concentration of substances, particularly in wetlands or aquatic areas. Identifying source landscape units and quantifying the rate of transport is often a major goal.

There are three basic approaches to quantifying source–sink relationships in landscapes or regions: simple measurements of pools and inference, use of natural abundance of isotopes to characterize sources and sinks, and use of a tracer to track movement.

In the first approach, investigators utilize an understanding of the hydrologic cycle to estimate nutrient movement through landscapes. In the classic watershed approach (Likens et al. 1977), detailed estimates are made of ecosystem-level biogeochemical budgets (inputs and internal cycling), and are combined with estimates of stream/river nutrient concentrations and streamflow to estimate total watershed hydrologic export of elements. This classic approach has unquestionably yielded our most important knowledge on the basic movement of elements and particulate matter through terrestrial systems to aquatic. In addition, it has contributed crucial information on how humans alter the landscape- to regional-scale fluxes of nutrients through direct disturbance (Likens et al. 1977; Bormann et al. 1974; Vitousek and Reiners 1975; Gorham et al. 1979), through altering atmospheric input (Likens et al. 1996), and landscape- (Peterjohn and Correl 1984; Hanson et al. 1994) to regional- and continental-scale impacts of humans on river export of nutrients to oceans (Peierls et al. 1991; Cole et al. 1993; Howarth et al. 1996). Multiple element analyses provide particularly powerful tools for exploring changes through time, since some of the most significant biogeochemical alterations may be reflected more in such relationships as cation/anion ratios than in single element trends (Likens et al. 1996).

A second approach is the use of stable isotopes to estimate sources, sinks, and net fluxes among compartments of the landscape or region. Elements in different pools exist with different "isotopic signatures" (δ isotope), which are characteristically determined by (1) the signature of the source pools and (2) the fractionation, or preferential processing of lighter isotopes, for a particular process. The basic approach is to identify the isotopic signatures of potential sources for the sink pool of interest, as well as the signature of this sink pool, and then to use mixing models to calculate the fractional contribution of each source (e.g., Shearer and Kohl 1993). The approach for ecosystem ecologists has been reviewed in detail (e.g., Peterson and Fry 1987; Lajtha and Michener 1994; Shearer and Kohl 1993), as it is used at scales from organismal to global, but has particular utility for scales such as landscape to regional, in which large-scale processes are very difficult to quantify. Geochemists have long used natural abundance patterns of isotopes to distinguish among important sources such as weathering, atmosphere, and pollution (e.g., Wadleigh et al. 1985; Abert 1995; Finley et al. 1995). One of the first applications by ecosystem

ecologists to assess large-scale movement of nutrients using the natural abundance of stable isotopes was an assessment of the source of nitrate (fertilizer vs. soil organic matter) in surface water of a cultivated watershed (Kohl et al. 1971). The work was met with a great deal of criticism regarding the usefulness of the technique in part because relatively few samples can be economically analyzed, even though the data may represent a very large watershed. Nonetheless, a great deal of recent work has elaborated on the techniques, better establishing variance estimates for the calculations (Shearer and Kohl 1993), and providing a better basis for understanding the strengths and limitations of the approach. Evaluation of $\delta^{13}C$ within organisms has provided important information on carbon (C) sources and fluxes in aquatic ecosystems (Peterson and Fry 1987; Fry 1991; Michener and Schnell 1994). Multiple isotope (e.g., C, sulfur [S], and nitrogen [N]) methods significantly improve upon our ability to assess and quantify sources and sinks (e.g., Fry 1991; Michener and Schell 1994).

Finally, a third approach to studying the two-dimensional redistribution of elements within landscapes and regions is using tracers. I distinguish this from the natural abundance methods above as being an approach in which the investigator releases an isotope or element into the environment, and then tracks its distribution at the landscape scale in space and time. Again, aquatic biogeochemists have taken the lead in this area. Two types of tracers are utilized, biologically active isotopes, and nonactive substitutes. Hutchinson and Bowen (1947) may have been the first to apply such a technique, in a tracer study of phosphorus-32 (^{32}P), in which they studied the sedimentation of ^{32}P from the epilimnion into the hypolimnion of a lake. For example, in a current large-scale comparison of N processing in streams, ^{15}N is released and tracked downstream in biological and inorganic pools to assess the biological cycling and spatial redistribution (Holmes, personal communication).

One approach that has proved useful is the analysis of soil movement using cesium-137 (^{137}Cs). Cesium-137 is not technically a tracer, in that the investigator does not apply it, however humans distributed it relatively uniformly over the landscape during the bomb tests of the 1950s. Because Cs is a cation that binds to cation exchange sites on clays (Tamura 1960) and is relatively inert (Schultz et al. 1960), its current distribution is thought to reflect the net redistribution of soils on a landscape since the 1950s (Ritchie and McHenry 1978; Martz and de Jong 1987; Schlesinger et al. 1989; Coppinger et al. 1991). A limitation of this method is that actual estimates of rates of soil movement are not possible, only indices of net movement of soil particles by wind or water.

Otherwise, for terrestrial systems, use of tracers for the two-dimensional movement of elements across landscapes does not have a rich literature. There is likely to be a great deal that can be contributed in methodological development in this area.

Modeling Movement

How are investigators modeling the movement of materials and energy across landscapes and regions? Clearly, the distribution of organic matter, inorganic nutrients, toxic materials, and sediments across landscapes and regions is largely the consequences of lateral and vertical movement of those materials. Models that truly incorporate spatial processes represent a very important advance in our ability to test our understanding of how systems function at large scales. However, just as field analysis of movement in ecosystem ecology has been somewhat limited, so has simulation analysis of movement (Costanza et al. 1990; Kareiva and Wennergren 1995). Many of the past efforts that address movement of materials across landscapes and regions were conducted by hydrologists and soil scientists studying erosion, and there is a significant literature on these models (e.g., Favis-Mortlock et al. 1996; Kirkby et al. 1996). The approach is to connect a spatial database to a model, as described above, but the model includes spatial processes in which materials or biota flow among individual cells. Rules and probabilities for movement may be governed by such features as topographic location (slope angle and aspect, location with respect to wind direction and force), vegetation type, soil type, and stochastic processes (e.g., fire) (Wallin et al. 1996). Transitions in states that influence the source/sink potential of a particular cell or group of cells may be implemented using a cellular automata approach (e.g., Hi and Reynolds 1997), a simple set of transition rules that can generate relatively complex patterns.

Results of spatial models may be tested against either field data (Costanza et al. 1990) or remotely sensed data (Burke et al. 1991). Testing simulated patterns against actual patterns is not a simple statistical procedure (Constanza et al. 1990), particularly since the spatial resolutions of simulated and observed data often differ. Constanza et al. (1990) apply goodness-of-fit tests to simulated results that are aggregated to multiple resolutions. This approach not only allows one to assess how well the spatial model performed at the simulated resolution, but also provides opportunities to test the most appropriate scale of application for the model.

Extrapolating to the Regional or Landscape Scale

Field Analysis

Many of the important questions associated with biogeochemistry today involve extrapolating our knowledge of biogeochemistry to landscape or regional scales (Walker 1994; Groffman and Wagenet 1994; Levin et al. 1997). For instance, we might ask what the large-scale impacts of human activities are on trace gas flux or soil C, or wish to know the level of primary productivity associated with a sociopolitical unit such as a county, state, or geographic region. Such estimates are critical for understanding the large-scale interactions of biogeochemical processes and atmospheric dynamics (Matson et al. 1989; Schimel et al. 1988) and their impacts on socioeconomic processes (Riebsame et al. 1994).

In all cases, the best large-scale value is one that is measured at the largest scale. Thus, gaseous exchange with the atmosphere is probably best estimated using either eddy correlation or eddy accumulation techniques (Chapter 11) or measurements from aircraft (Matson and Harriss 1988) which have footprints that correspond roughly to the landscape scale (hundreds of meters to kilometers). Similarly, hydrologic fluxes of elements may be estimated at relatively large scales, through the watershed approach, which can be nested to estimate efflux from small land areas to quite large regions (e.g., Howarth et al. 1996).

For many of the variables with which we work, however, such as net primary productivity and soil nutrient dynamics, it is not possible to directly estimate pools and fluxes at landscape to regional scales. The actual processes are generally measured in the field, at scales that correspond with <1 to 10 m in plot size (e.g., see Chapters 2, 4, 5, and 7). The key issues for landscape and regional studies are the processes by which we scale this information up to larger scales, or extrapolate, and by which we estimate the error of our estimates. (I distinguish here between extrapolation, or using small-scale measurements to assess large-scale fluxes and pools, and interpolation, the process of estimating values for places that were not measured.)

If stratified sampling has taken place, as described above, and an average value is available for each landscape or regional unit (e.g., soil type, land-use type, vegetation type), these averages can be aggregated based upon the known area of each unit and a weighted sum:

$$\sum_{i=1}^{n} P_i * A_i = Poolsize \qquad (18.1)$$

where P_i is the pool per unit area within landscape unit i, and A_i is the area of landscape unit i. If it is a flux that is being estimated, the value must be extrapolated to the appropriate time interval, then scaled as above. Land area of the units may be provided from remotely sensed or other digital data. The approach has been used to a large extent by scientists studying trace gas flux (e.g., Robertson and Rosswall 1986; Matthews and Fung 1987; Reiners et al. 1989; reviewed by Matson et al. 1989; Groffman et al. 1992), and by those studying small-scale soil nutrient variation associated with individual plants (e.g., Vinton and Burke 1995; Robles and Burke 1997). The method of extrapolation is logical and closely tied to the most common type of field sampling, as described above. However, it is riddled with sources of error that ecologists have not yet been successful at quantifying in an aggregate sense (O'Neill et al. 1979; Jeffers 1988; Rastetter et al. 1992). There is a significant literature on estimating error for scaling up temporal data (see Jeffers 1988), and for estimating error associated with maps (e.g., A in Equation 18.1) (Maling 1989). However, many of these errors must be aggregated for the extrapolated value, and we do not at this time have a simple set of equations for estimating

error or confidence intervals. Until ecologists have agreed upon appropriate formulae for estimating confidence intervals of such estimates, the variance for each of the elements of the extrapolation should be presented clearly.

Modeling

The major drawbacks to using the above extrapolation method are the limitations associated with classification errors. Multiple controls over biogeochemical pools and fluxes co-vary, as mentioned above, and the classification strategy does not allow those controls to be separated (Matson et al. 1989). An alternate approach is to utilize models that allow for continuous variation in the control factors to occur.

Either simple statistical models or simulation models may be utilized. In either case, there are three steps to the analysis (Costanza et al. 1990; Burke et al. 1991; Ollinger et al. 1993; Coleman et al. 1994). The first step is to obtain a georeferenced database of the major control factors over the biogeochemical pool or flux of interest, for the region or landscape of interest. Key decisions must be made regarding (1) which control factors will be incorporated and (2) what spatial and temporal resolution will be used. The decisions are interactive, and both are influenced as much by logistical constraints as by scientific construct of the system. For instance, georeferenced data on soils are available at specific resolutions, and one is generally not able to find scales more resolved. Land-use, vegetation, and net primary productivity data are often generated from satellite imagery (see Chapter 3). In the second step, the data are integrated into a geographic information system (GIS) (this may be industry-standard software or generated by the scientist), and a single scale of resolution for applying the model is selected when the data are "overlaid," or spatially registered with one another. In many cases, the choice will be to aggregate fine-scaled data to a coarser scale. Considerable attention must be paid to the algorithms used in scaling up data. A well-recognized problem is that if linear algorithms are used to scale information up to larger spatial units, significant error will result if those data are introduced into a model with nonlinearities (Cale et al. 1983; Burke et al. 1990; Rastetter et al. 1992; Pierce and Running 1995).

Finally, the model is applied to the layers of input data. The model may be very simple, such as a regression model, or a complex simulation model, as long as the control or input variables of choice are present in the GIS, and have the appropriate temporal resolution. Output variables of interest are stored in the GIS for mapping or analysis. At present, considerable effort is usually required to link simulation models with GIS, although several automated linkages are being developed (Coleman et al. 1994).

The process of extrapolating to landscape or regional scales represents the integration of many different types of scientific activities. For instance, modeling changes in regional C storage involves first, the integration of large number of field studies into a coherent body of knowledge, represented by the simulation model (Fig. 18.1). Simulation models must be rigorously tested in the field using separate data sets from those which generated them (Lauenroth et al. 1998). In some cases, pattern analysis studies have provided important information that is included in simulation models (Parton et al. 1987), or geographic data have provided important information for validating simulation models (Burke et al. 1989). Finally, large-scale simulations can be tested against large-scale measurements, such as eddy accumulation, as a means of increasing our confidence in such extrapolations.

Summary

During the past several decades, the number of tools and approaches for ecosystem ecologists has dramatically increased the opportunities for study of processes at landscape to regional scales. This activity is crucial for the discipline to apply our understanding to the scales most relevant to atmosphere–biosphere interactions, human impacts on the environment, and global change. Coupled with the difficulties of studying ecosystem processes at large scales is a current strong limitation in our ability to express error and uncertainty of our measurements and models. This combination of the high degree of societal need for our results, the relatively young state of our discipline at these scales, and our limitations in expressing uncertainty pro-

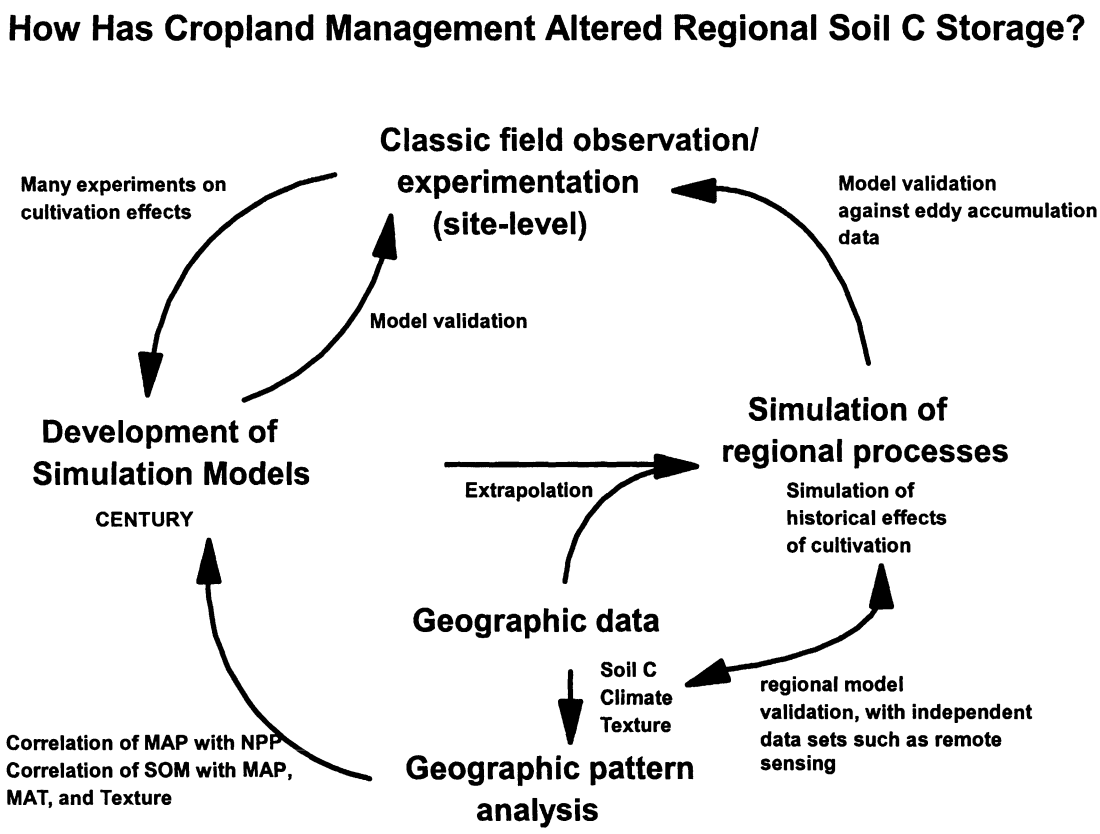
How Has Cropland Management Altered Regional Soil C Storage?
Classic field observation/ experimentation (site-level)
Many experiments on cultivation effects
Model validation against eddy accumulation data
Model validation
Development of Simulation Models
CENTURY
Simulation of regional processes
Extrapolation
Simulation of historical effects of cultivation
Geographic data
Soil C
Climate
Texture
regional model validation, with independent data sets such as remote sensing
Correlation of MAP with NPP
Correlation of SOM with MAP, MAT, and Texture
Geographic pattern analysis

FIGURE 18.1. The relationship among the scientific activities involved in assessing the effects of cropland management on regional C storage in the Great Plains of the United States (e.g., Parton et al. 1987; Sala et al. 1988; Cole et al. 1988; Burke et al. 1989, 1990; and many others).

vides a strong impetus for future work in landscape- to regional-scale ecosystem ecology.

Acknowledgments I wish to acknowledge the contributions of W. K. Lauenroth, H. Epstein, and P. Groffman to this manuscript, and the long-term contributions of W.A. Reiners to the ideas and review presented here. This work was supported by the National Science Foundation Shortgrass Steppe Long Term Ecological Research Project, the Environmental Protection Agency STAR program, and by the Great Plains Project (grant HD 33554 from the National Institute of Child Health and Human Development).

References

Aandahl, A.R. The characterization of slope positions and their influence on total nitrogen content of a few virgin soils of western Iowa. Soil Sci. Soc. Am. Proc. 13:449–54; 1948.

Aberg, G. The use of natural strontium isotopes as tracers in environmental studies. Water Air Soil Pollut. 79:309–322; 1995.

Aguilar, R.E.; Kelly, F.; Heil, R.D. Effects of cultivation on soils in Northern Great Plains rangeland. Soil Sci. Soc. Am. J. 52:1081–1085; 1988.

Amundson, R.; Jenny, H. Thinking of biology—On a state factor model of ecosystems. BioScience 47:536–543; 1997.

Bormann, R.H.; Likens, G.E.; Siccama, T.G.; Pierce R.S.; Eaton, J.S. The export of nutrients and recovery of stable conditions following deforestation at Hubbard Brook. Ecol. Monogr. 44:255–277; 1974.

Burke, I.C. Control of nitrogen mineralization in a sagebrush steppe landscape. Ecology 70:1115–1126; 1989.

Burke, I.C.; Kittel, T.G.F.; Lauenroth, W.K.; Snook, P.; Yonker, C.M.; Parton, W.J. Regional analysis of the

central great plains, sensitivity to climate variability. BioScience 41:685–692; 1991.

Burke, I.C.; Reiners, W.A.; Schimel, D.S. Organic matter turnover in a sagebrush steppe landscape. Biogeochemistry 7:11–31; 1989.

Burke, I.C.; Schimel, D.S.; Yonker, C.M.; Parton, W.J.; Joyce, L.A.; Lauenroth, W.K. Regional modeling of grassland biogeochemistry using GIS. Landsc. Ecology 4:45–54; 1990.

Burke, I.C.; Yonker, C.M.; Parton, W.J.; Cole, C.V.; Flach, K.; Schimel, D.S. Texture, climate, and cultivation effects on soil organic matter content in U.S. grassland soils. Soil Sci. Soc. Am. J. 53:800–805; 1989.

Cale, W.G.; O'Neill, R.V.; Shugart, H.H. Development and application of desirable ecological models. Ecol. Model. 18:171–186; 1983.

Cole, J.J.; Peierls, B.L.; Caraco, N.F.; Pace, M.L. Nitrogen loading of rivers as a human-driven process. In: McDonnell, M.J.; Pickett, S.T.A., eds. *Humans as Components of Ecosystems.* New York: Springer-Verlag; 1993:163–174.

Coleman, M.B.; Bearly, T.L.; Burke, I.C.; Lauenroth, W.K. linking ecological simulation models to geographic information systems: an automated solution. In: Michener, W.; Brunt, J., eds. *Environmental Information Management and Analysis: Ecosystem to Global Scales.* London: E. Taylor and Francis; 1994:397–412.

Coppinger, K.D.; Reiners, W.A.; Burke, I.C.; Olson, R.K. Net erosion on a sagebrush steppe landscape as determined by cesium-137 distribution. Soil Sci. Soc. Am. J. 55:254–258; 1991.

Costanza, R.; Sklar, F.H.; White, M.L. Modeling coastal landscape dynamics. BioScience 40:91–107; 1990.

Dockuchaiev, V.V. Russian chernozem. In: *Collected writings.* 3. Jerusalem (1967): Israel Progress in Science Transactions; 1883.

Favis-Mortlock, D.T.; Quinton, J.N.; Dickinson, W.T. The GCTE validation of soil erosion models for global change studies. J. Soil Water. Conserv. 51:396–401; 1996.

Finley, J.B.; Drever, J.I.; Turk, J.T. Sulfur isotope dynamics in a high-elevation catchment, West Glacier Lake, Wyoming. Water Air Soil Pollut. 79:227–241; 1995.

Fry, B. Stable isotope diagrams of freshwater food webs. Ecology 72:2293–2297; 1991.

Giblin, A.E.; Nadelhoffer, K.J.; Shaver, G.R.; Laundre, J.A.; McKerrow, A.J. Biogeochemical diversity along a riverside toposequence in arctic Alaska. Ecol. Monogr. 61:415–435; 1991.

Gorham, E.; Vitousek, P.; Reiners, W.A. The regulation of chemical budgets over the course of terrestrial ecosystem succession. Annu. Rev. Ecol. Syst. 10:53–584; 1979.

Groffman, P.; Hanson, G.C. Wetland denitrification: Influence of site quality and relationships with wetland delineation protocols. Soil Sci. Soc. Am. J. 61:323–329; 1997.

Groffman, P.M. Ecology of nitrification and denitrification in soil evaluated at scales relevant to atmospheric chemistry. In: Rogers, J.E.; Whitman, W.B., eds. *Microbial Production and Consumption of Greenhouse Gases: Methane, Nitrous Oxides, and Halomethanes.* Washington, DC: American Society for Microbiology; 1991:201–217.

Groffman, P.M.; Tiedje, J.M. Denitrification in north temperate forest soils: Spatial and temporal patterns at the landscape and seasonal scales. Soil Biol. Biochem. 21:613–620; 1989.

Groffman, P.M.; Tiedje, J.M.; Mokma, D.L.; Simkins S. Regional scale analysis of denitrification in north temperate forest soils. Landsc. Ecol. 7:45–53; 1992.

Groffman, P.M.; Tiedje, J.M.; Robertson, G.P.; Christensen, S. Denitrification at different temporal and geographical scales: Proximal and distal controls. In: Wilson, J.R., ed. *Advances in Nitrogen Cycling in Agricultural Ecosystems.* Wallingford, UK: CAB International; 1988.

Groffman, P.M.; Turner, C.L. Plant productivity and nitrogen gas fluxes in a tallgrass prairie landscape. Landsc. Ecol. 10:255–266; 1995.

Groffman, P.M., Wagenet, R.J. Advances and pitfalls in expressing land qualities at different scales. *Proceedings of the 15th World Congress of Soil Science.* Acapulco, Mexico; 1994:662–681.

Groffman, P.M.; Zak, D.R.; Christensen, S.; Mosier, A.; Tiedje, J.M. Early spring nitrogen dynamics in a temperate forest landscape. Ecology 74:1579–1585; 1993.

Halvorson, J.J.; Bolton, H.; Smith, J.L.; Rossi, R.E. 1994. Geostatistical analysis of resource islands under Artemisia tridentata in the shrub-steppe. Great Basin Naturalist 54:313–328.

Hanson, G.C.; Groffman, P.M.; Gold, A.J. Symptoms of nitrogen saturation in a riparian wetland. Ecol. Applic. 4:750–756; 1994.

Hi, H.; Reynolds, J.F. Modeling effects of spatial pattern, drought, and grazing on rates of rangeland degradation: A combined markov and cellular automaton approach. In: Quattrochi, D.A.; Goodchild, M.F., eds. *Scale in Remote Sensing and GIS.* Boca Raton, FL: CRC; 1997:211–230.

Howarth, R.W.; Billen, G.; Swaney, D.; Townsend, A.; Jaworski, N.; Lajtha, K.; Downing, J.A.; Elmgren, R.; Caraco, N.; Jordan, T. et al. Regional nitrogen budgets and riverine N and P fluxes for the drainages to the North Atlantic ocean: Natural and human influences. Biogeochemistry 35:75–139; 1996.

Hutchinson, G.E.; Bowen, V.T. A direct demonstration of the phosphorus cycle in a small lake. Proc. Natl. Acad. Sci. U.S.A. 33:148–153; 1947.

Jeffers, J.N.R. Statistical and mathematical approaches to issues of scales in ecology. In: Rosswall, T.; Woodmansee, R.G.; Risser, P.G., eds. *Scales and Global Change.* New York: Wiley; 1988:47–56.

Jenny, H. *Factors of Soil Formation: A System of Quantitative Pedology.* New York: McGraw-Hill; 1941.

Jenny, H. *The Soil Resource: Origin and Behavior.* New York: Springer-Verlag; 1980.

Johansson, M.-B.; Berg, B.; Meentemeyer, V. Litter mass-loss rates in late stages of decomposition in a climatic transect of pine forests. Long-term decomposition in a Scots pine forest. IX. Can. J. Bot. 73:1509–1521; 1995.

Kareiva, P.; Wennergren, U. Connecting landscape patterns to ecosystem and population processes. Nature 373:299–302; 1995.

Kielland, K. Landscape patterns of free amino acids in arctic tundra soils. Biogeochemistry 31:85–98; 1995.

Kirkby, M.J.; Imeson, A.C.; Bergkamp, G.; Cammeraat, L.H. Scaling up processes and models. J. Soil. Water Conserv. 51:391–395; 1996.

Knapp, A.K.; Fahnestock, J.T.; Hamburg, S.P.; Statland, L.B.; Seastedt, T.R.; Schimel, D.S. Landscape patterns in soil-plant water relations and primary production in tallgrass prairie. Ecology 74:549–560; 1993.

Kohl, D.H.; Shearer, G.B.; Commoner, B. Fertilizer nitrogen: Contribution to nitrate in surface water in a corn belt watershed. Science 174:1331–1334; 1971.

Lajtha, K.; Schlesinger, W.H. The biogeochemistry of phosphorus cycling and phosphorus availability along a desert soil chronosequence. Ecology 69:24–39; 1988.

Lajtha, L.; Michener, R.H., eds. *Stable Isotopes in Ecology and Environmental Science.* Oxford: Blackwell; 1994.

Lauenroth, W.K.; Canham, C.D.; Kinzig, A.P.; Poiani, K.A.; Kemp, W.M.; Running, S.W. Simulation modeling in ecosystem science. In: Pace, M.L.; Groffman, P.M. *Successes, Limitations, and Frontiers in Ecosystem Science.* New York: Springer-Verlag; 1998:404–415.

Levin, S.A.; Grenfell, B.; Hastings, A.; Perelson, A.S. Mathematical and computational challenges in population biology and ecosystems science. Science 275:334–343; 1997.

Lieth, H. primary productivity in ecosystems: Comparative analysis of global patterns. In: Lieth, H.F.H. *Patterns of primary production in the biosphere.* Stroudsburg, PA: Dowden, Hutchinson and Ross; 1978:300–321.

Likens, G.E.; Bormann, F.H.; Pierce, R.S.; Eaton, J.S.; Johnson, N.M. *Biogeochemistry of a Forested Ecosystem.* New York: Springer-Verlag; 1977.

Likens, G.E.; Driscoll, C.T.; Buso, D.C. Long-term effects of acid rain: Response and recovery of a forested ecosystem. Science 272:244–246; 1996.

Maling, D.H. *Measurements from Maps: Principles and Methods from Cartometry.* Oxford: Pergamon; 1989.

Martz, L.W.; de Jong, E. Using cesium-137 to assess the variability of net soil erosion and its association with topography in a Canadian prairie landscape. Catena 14:439–351; 1987.

Matson, P.A.; Harriss, R.C. Prospects for aircraft-based gas exchange measurements in ecosystem studies. Ecology 69:1318–1326; 1988.

Matson, P.A.; Vitousek, P.M. Cross-system comparisons of soil nitrogen transformations and nitrous oxide flux in tropical forest ecosystems. Global Biogeochem. Cyc. 1:163–170; 1987.

Matson, P.A.; Vitousek, P.M.; Schimel, D.S. Regional extrapolation of trace gas flux based on soils and ecosystems. In: Andreae, M.O.; Schimel, D.S., eds. *Exchange of Trace Gases Between Terrestrial Ecosystems and the Atmosphere.* Chichester, UK: Wiley; 1989:97–108.

Matthews, E.; Fung, I. Methane emission from natural wetlands: Global distribution, area, and environmental characteristics of sources. Global Biogeochem. Cyc. 1:61–86; 1987.

Meentemeyer, V. The geography of organic decomposition rates. Ann. Am. Assn. Am. Geogr. 74:551–560; 1984.

Meentemeyer, V.; Berg, B. Regional variation in rate of mass loss of *Pinus sylvestris* needle litter in Swedish pine forests as influenced by climate and litter quality. Scand. J. For. Res. 1:167–180; 1986.

Meentemeyer, V.; Box, E.O.; Thompson, R. World patterns and amounts of terrestrial plant litter production. BioScience 32:125–128; 1982.

Meentemeyer, V.; Gardner, J.; Box, E.O. World patterns and amounts of detrital soil carbon. Earth Surf. Proc. Land. 10:557–567; 1985.

Michener, R.H.; Schell, D.M. Stable isotope ratios as tracers in marine aquatic food webs. In: Lajtha, K.; Michener, R.H., eds. *Stable Isotopes in Ecosystems.* Oxford: Blackwell; 1994:114–137.

Mosier, A.R.; Schimel, D.; Valentine, D.; Bronson, K.; Parton, W. Methane and nitrous oxide fluxes in native, fertilized, and cultivated grasslands. Nature 350:330–332; 1991.

Naiman, R.J.; Pinay, G.; Johnston, C.A.; Pastor, J. Beaver influences on the long-term biogeochemical characteristics of boreal forest drainage networks. Ecology 75:905–921; 1994.

O'Neill, R.V.; DeAngelis, D.L.; Waide, J.B.; Allen, T.F.H. *A Hierarchical Concept of Ecosystems.* Princeton, NJ: Princeton Univ. Pr.; 1986.

O'Neill, R.V.; Hunsaker, C.T.; Jones, K.B.; Riitters, K.H.; Wickham, J.D.; Schwartz, P.M.; Goodman, I.A.; Jackson, B.L.; Baillargeon, W.S. Monitoring environmental quality at the landscape scale. BioScience 47:513–519; 1997.

Ollinger, S.V.; Aber, J.D.; Lovett, G.M.; Millham, M.E.; Lathrop, R.G.; Ellis, J.M. A spatial model of the atmospheric deposition for the northeastern U.S. Ecol. Applic. 3:459–472; 1993.

Parton, W.J.; Schimel, D.S.; Cole, C.V.; Ojima, D.S. Analysis of factors controlling soil organic matter levels in great plains grasslands. Soil Sci. Soc. Am. J. 51:1173–1179; 1987.

Paruelo, J.M.; Jobbagy, E.G.; Sala, O.E.; Lauenroth, W.K.; Burke, I.C. Functional and structural convergence of temperate grassland and shrubland ecosystems. Ecol. Applic. 8:194–206; 1998.

Peierls, B.L.; Caraco, N.F.; Pace, M.L.; Cole, J.J. Human influence on river nitrogen. Nature 350:386–387; 1991.

Peterjohn, W.T.; Correll, D.L. Nutrient dynamics in an agricultural watershed: Observations on the role of a riparian forest. Ecology 65:1466–1475; 1984.

Peterson, B.J.; Fry, B. Stable isotopes in ecosystem studies. Annu. Rev. Ecol. Syst. 18:293–320; 1987.

Pierce, L.L.; Running, S.W. The effects of aggregating sub-grid land surface variation on large-scale estimates of net primary production. Landsc. Ecol. 10:239–253; 1995.

Pouyat, R.V.; McDonnell, M.J.; Pickett, S.T.A. Soil characteristics of oak stands along an urban-rural land-use gradient. J. Environ. Qual. 24:516–526; 1995.

Rastetter, E.B.; King, A.W.; Cosby, B.J.; Hornberger, G.M.; O'Neill, R.V.; Hobbie, J.E. Aggregating fine-scale ecological knowledge to model coarser-scale attributes of ecosystems. Ecol. Applic. 2:55–70; 1992.

Reiners, W.A.; Bouwman, A.F.; Parsons, W.F.J.; Keller, M. Tropical rain forest conversion to pasture: Change in vegetation and soil properties. Ecol. Applic. 4:363–377; 1994.

Reiners, W.A.; Strong, L.L.; Matson, P.A.; Burke, I.C.; Ojima, D.S. Estimating biogeochemical fluxes across sagebrush-steppe landscapes with thematic mapper imagery. Remote Sens. Environ. 28:121–219; 1989.

Riebsame, W.E.; Galvin, K.A.; Young, R.; Parton, W.J.; Burke, I.C.; Bohren, L.; Knop, E. An integrated model of causes of and responses to environmental change: Land use/cover in the Central Great Plains. BioScience 44:350–356; 1994.

Ritchie, J.C.; McHenry, J.R. Fallout cesium-137 in cultivated and noncultivated north central United States watersheds. J. Environ. Qual. 7:40–44; 1978.

Robertson, G.P. Regional nitrogen budgets: Approaches and problems. Plant Soil 67:73–81; 1982.

Robertson, G.P. Geostatistics in ecology: Interpolating with known variance. Ecology 68:744–748; 1987.

Robertson, P.G.; Huston, M.A.; Evans, F.C.; Tiedje, J.M. Spatial variability in a successional plant community: Patterns of nitrogen availability. Ecology 69:1517–1524; 1988.

Robertson, G.P.; Klingensmith, K.M.; Klug, M.J.; Paul, E.A.; Crum, J.R.; Ellis, B.G. Soil resources, microbial activity, and primary production across an agricultural ecosystem. Ecol. Applic. 7:158–170; 1997.

Robertson, G.P.; Rosswall, T.H. Nitrogen in West Africa: The regional cycle. Ecol. Monogr. 56:43–72; 1986.

Robles, M.D.; Burke, I.C. Legume, grass, and Conservation Reserve Program effects on recovery of soil organic matter pools and nutrient availability. Ecol. Applic. 7:345–357; 1997.

Rosswall, T.; Woodmansee, R.G.; Risser, P.G., eds. *Scales and Global Change.* Chichester, UK: Wiley; 1988.

Sala, O.E.; Parton, W.J.; Joyce, L.A.; Lauenroth, W.K. Primary production of the central grassland region of the United States. Ecology 69:40–45; 1988.

Schimel, D.S. Carbon and nitrogen turnover in adjacent grassland and cropland ecosystems. Biogeochemistry 2:345–357; 1986.

Schimel, D.S.; Coleman, D.C.; Horton, K.A. Soil organic matter dynamics in paired rangeland and cropland toposequences in North Dakota. Geoderma 36:201–214; 1985.

Schimel, D.S.; Kittel, T.G.F.; Knapp, A.K.; Seastedt, T.R.; Parton, W.J.; Brown, V.B. Physiological interactions along resource gradients in a tallgrass prairie. Ecology 72:672–684; 1991.

Schimel, D.S.; Simkins, S.; Rosswall, T.; Mosier, A.R.; Parton, W.J. Scale and the measurement of nitrogen-gas fluxes from terrestrial ecosystems. In: Rosswall, T.; Woodmansee, R.G.; Risser, P.G., eds. *Scales and Global Change.* Chichester, UK: Wiley; 1988:179–193.

Schlesinger, W.H.; Tonteyn, P.J.; Reiners, W.A. Effects of overland flow on plant water relations, erosion, and soil water percolation on a Mojave Desert landscape. Soil Sci. Soc. Am. J. 53:1567–1572; 1989.

Schultz, R.K.; Overstreet, R.; Burshad, I. On the soil chemistry of cesium-137. Soil Sci. 89:16–27; 1960.

Shaw, C.E. Potent factors in soil formation. Ecology 11:239–245; 1930.

Shearer, G.; Kohl, D.H. Natural abundance of 15n: Fractional contribution of two sources to a common sink and use of isotope discrimination. In: Knowles, R.; Blackburn, T.H. *Nitrogen isotope techniques.* San Diego, CA: Academic; 1993:89–126.

Swanson, F.J.; Kratz, T.K.; Caine, N.; Woodmansee, R.G. Landform effects on ecosystem patterns and processes. BioScience 38:92–98; 1988.

Tamura, T. Selective sorption reaction of cesium with mineral soil. Nucl. Saf. 5:5:262–268; 1960.

Valentine, D.W.; Binkley, D. Topography and soil acidity in an arctic landscape. Soil Sci. Soc. Am. J. 56:1553–1539; 1992.

Vinton, M.A.; Burke, I.C. Interactions between individual plant species and soil nutrient status in shortgrass steppe. Ecology 76:1116–1133; 1995.

Vitousek, P.M.; Reiners, W.A. Ecosystem succession and nutrient retention: A hypothesis. BioScience 25:376–381; 1975.

Vitousek, P.M.; Turner, D.R.; Parton, W.J.; Sanford, R.L. Litter decomposition on the Mauna Loa environmental matrix, Hawaii patterns, mechanisms, and models. Ecology 75:418–429; 1994.

Wadleigh, M.A.; Veizer, J.; Brooks, C. Strontium and its isotopes in Canadian rivers: Fluxes and global implications. Geochim. Cosmochim. Acta 49:1727–1736; 1985.

Walker, B.H. Landscape to regional-scale responses of terrestrial ecosystems to global change. Ambio 23:67–73; 1994.

Wallin, D.O.; Swanson, F.J.; Marks, B.; Cissel, J.H.; Kertis, J. Comparison of managed and pre-settlement landscape dynamics in forests of the Pacific Northwest, USA. For. Ecol. Manage. 85:291–309; 1996.

Yonker, C.M.; Schimel, D.S.; Paroussis, E.; Heil, R.D. Patterns of organic carbon accumulation in a semiarid shortgrass steppe, Colorado. Soil Sci. Soc. Am. J. 52:478–483; 1988.

Zak, D.R.; Pregitzer, K.S.; Host, G.E. Landscape variation in nitrogen mineralization. Can. J. For. Res. 16:1258–1263; 1986.

Part 3

Manipulative Ecosystem Experiments

19

Nutrient Manipulations in Terrestrial Ecosystems

Valerie T. Eviner, F. Stuart Chapin III, and Charles E. Vaughn

Introduction

Nutrient addition experiments are the ecosystem manipulations that are undertaken most frequently, because they are relatively easy and inexpensive to perform. In addition, because of the widespread nature of nutrient limitation in terrestrial ecosystems (Vitousek and Howarth 1991), these experiments almost always show dramatic results. As with much of ecology, the roots of nutrient manipulation experiments come from agriculture, where fertilizer trials are regularly used to determine which nutrients most strongly limit plant growth and what the biological and economic returns are for different levels of nutrient addition.

Ecological Questions Addressed by Nutrient Addition

Most early nutrient addition experiments in ecology addressed questions that were similar to those of agronomists: Are nutrients limiting to plant growth, or which nutrients most strongly limit plant growth in a particular location? These experiments demonstrate that nutrients are among the factors that limit plant growth in most terrestrial ecosystems (Chapin 1980; Vitousek and Howarth 1991; Shaver et al. 1986), and that the particular nutrients that are limiting change through space and time. The extension of these site-specific patterns of nutrient limitation across the landscape have led to an understanding of large-scale ecological issues such as changes in nutrient availability and limitation through succession and soil development (Chapin et al. 1994; Vitousek and Farrington 1997; Walker and Syers 1976). Nutrient addition experiments have also been used to elucidate the roles of nutrients in determining plant community dynamics (Wedin and Tilman 1993; Berendse et al. 1992; Willems et al. 1993; Bobbink 1991), microbial characteristics (Lovell and Hatch 1998; Clarholm 1993; Stamford et al. 1997), and ecosystem processes (Bremer and Kurkmar 1997, Magill et al. 1997).

By using isotopically labeled fertilizer, it is possible to track the quantity of added nutrients that is readily available for plant uptake, versus the amount that is adsorbed, leached, lost as gas, immobilized by microbes, or incorporated into soil organic matter. Isotopes also enable us to follow the dynamics of the added nutrients through time, tracking how long they are retained and the mechanisms of retention. By comparing plant uptake of labeled (fertilizer-derived) and unlabeled (native soil–derived) nutrients, we can gain important insights into how nutrient additions alter nutrient cycling and the role of native soil nutrients in plant nutrition. Also, by tracing the relative uptake of labeled nutrients by different plant species, we can determine how plants compete for resources at different nutrient levels.

The role of nutrients as a control over ecosystem processes has recently received more attention due to concern over the effects of atmospheric deposition of nitrogen (N), and to a lesser extent, sulfur, (S), on ecosystems. Nutrient deposition can have profound effects on plant community composition (Aerts and Berendse 1998; Gunn 1995; Hogg et al.

1995), plant production (Aber et al. 1993), microbial communities (Arnolds 1989; Munzenberger et al. 1995), and biogeochemical cycles (Aber et al. 1993; Feijtel et al. 1989; Vitousek et al. 1997; van Breemen and van Dijk 1988; Friedland et al. 1991). Nutrient addition experiments are critical tools in helping ecosystem ecologists determine critical thresholds of system responses to increased atmospheric deposition. For example, N or S deposition can acidify the soil, leading to aluminum toxicity and a loss of essential nutrients such as calcium (Ca), which has been linked to the decline of forest systems (Lawrence et al 1995; Fernandez and Rustad 1990; Forsius et al. 1995; Wilson and Skeffington 1994).

The increase in nutrient deposition has made an understanding of ecosystem nutrient limitation and its thresholds critical in mitigating human perturbations of the global system. The ability of a system to retain N plays a crucial role at the regional and global scales. Nitrogen leaching into groundwater pollutes streams and lakes, while N trace gas losses can increase tropospheric ozone and contribute to stratospheric ozone depletion and global warming (Schlesinger 1997). The response of plant biomass to nutrient additions is critical in determining the capacity of terrestrial systems to serve as a carbon (C) sink for elevated carbon dioxide (CO_2) emissions.

Nutrient addition experiments are becoming increasingly important in addressing applied issues with important economic and health consequences. For example, Scandinavian tundra and forest tundra are typically dominated by lichens, which serve as the major winter food for reindeer, which in turn are an important cultural and economic resource for Saami people. Nutrient addition experiments show that lichens are extremely sensitive to N deposition. The results of these experiments suggest that the pollutants carried northward from eastern Europe seriously threaten the reindeer industry of Scandinavia (Woodin 1997).

The capacity of ecosystems to retain or "filter" nutrients is also an important applied issue that can be addressed by nutrient addition experiments. Wetlands and riparian zones have been suggested as natural filters for nutrient-rich waters from agriculture or sewage treatment plants (Jenssen et al. 1994; Rogers et al. 1991; Daniels and Gilliam 1996). Once the nutrient retention capacity of any ecosystem is exceeded, the nutrients leach into groundwater. Groundwater with a high nitrate concentration is a health concern, because the nitrate can be converted to nitrite, which is toxic in low-oxygen environments (such as a human fetus, where fetal hemoglobin is a strong competitor for oxygen) (Bouchard et al. 1992; Fan and Steinberg 1996).

Nature of Nutrient Limitation

It is not always clear exactly what is meant by the phrase nutrient limitation; it has been used to describe the response of various components of the overall ecosystem to nutrient additions. Historically, the most common test of nutrient limitation is to determine if the growth of a given plant community is limited by a particular nutrient. In this case, the initial growth response of plants indicates whether this plant community is nutrient-limited, and biomass measurements must be taken before the plant community changes. However, even though the overall community biomass may respond to one nutrient, some component species may be limited by others (Bobbink 1991; Jones and Martin 1964), and thus nutrient limitation within a given site can vary among patches with different species composition.

Altered nutrient supply usually changes competitive balance, leading to changes in species composition. For example, in Alaskan tussock tundra, most species responded favorably to nutrient addition for the first three years of the experiment, but after nine years, tall shrubs, which benefited most from the nutrient addition, produced a dense canopy that reduced the growth of mosses and evergreen shrubs (Chapin et al. 1995). Körner (Körner 1995; Körner and Larcher 1988; Körner 1989; Körner 1999) argues that this competitive exclusion of low-nutrient-adapted species following addition of nutrients implies that these species are not nutrient-limited. We argue that the concept of nutrient limitation for individual species or a given community is most useful as a gauge of the initial growth response of plants to nutrient addition prior to changes in competitive balance. In contrast, the changes in the plant community in response to nutrient additions must be incorporated into the concept of nutrient limitation of an ecosystem, since

the community shifts are a critical factor determining the response of the overall ecosystem net primary productivity (NPP) and biogeochemical processes to nutrient additions (Bowman et al. 1993). Thus, for questions addressing the overall ecosystem capacity to fix C, the nutrient saturation point of an ecosystem, or the overall response of a system to nutrient deposition—the duration of the experiment should be long enough to incorporate these community shifts, which can be the most significant mechanism driving overall ecosystem response to nutrient additions.

Commonly Limiting Nutrients

Which nutrients are limiting can often be predicted based on the age of the system, climate (especially how weathered or leached the soil is), soil texture, parent material, and vegetation type.

Most nutrient limitation experiments focus on nitrogen (N), phosphorus (P), and potassium (K). Nitrogen is the most commonly limiting nutrient to plant growth in temperate terrestrial systems (Vitousek and Howarth 1991). Phosphorus tends to be limiting in the lowland wet tropics (Tanner et al. 1998), on very old soils (Vitousek and Farrington 1997), and in legume-rich systems (Jones et al. 1983, 1990). Potassium tends to be limiting in areas of high precipitation, or very late in soil development (Tisdale et al. 1993). While N, P and K may be the most commonly limiting nutrients, it is not uncommon to find productivity limited by other nutrients such as calcium (Ca), magnesium (Mg), and sulfur (S). For example, California grasslands are often assumed to be N-limited, but many sites respond to P and S fertilization (Jones et al. 1983). Nitrogen, P, and K fertilizers often contain these other nutrients, so that some responses to these fertilizers may partially reflect responses to Ca, Mg, and S. This is especially true for legume-rich sites, which are often limited by nutrients such as S and P (Jones and Martin 1964; Jones et al. 1970).

Single Versus Multiple Nutrient Limitation

The simplest view of environmental limitation is that growth is limited by a single resource at any one time; another resource becomes limiting only when the supply of the first resource is increased above the point of limitation (Liebig's law of the minimum). Several processes contribute to the multiple resource limitation observed in most ecosystems: (1) Plants adjust both root/shoot allocation and nutrient uptake capacity to maximize capture of (and minimize limitation by) the most strongly limiting resource (Chapin et al. 1987; Rastetter and Shaver 1992). (2) Changes in environment (e.g., rainstorms, pulses of nutrient supply) change the relative abundance of resources so that different factors limit NPP at different times. (3) Different species in an ecosystem are limited by different resources, so that ecosystem-scale NPP responds to addition of more than one resource. Each of these processes contributes to the response of ecosystems to multiple resources.

Experimental Design

General Approach

The design of nutrient-addition experiments must be tailored to the question addressed. A single application of nutrients at high addition rates (e.g., 10 to 20 g N or P m^{-2}) is the simplest test of whether production of the ecosystem (or its dominant species) is limited by a particular nutrient at the time of nutrient application. The lack of response to low nutrient-addition rates could reflect lack of limitation by the nutrient applied or failure of the plants to gain access to the added nutrient due to chemical fixation (which frequently happens with phosphorus) or biological immobilization by soil microbes or vegetation on the ground surface (Chapin et al. 1986).

Experiments intended to examine the sensitivity of ecosystems to atmospheric deposition should use application rates that approximate natural deposition, which can range from considerably less that 1 g m^{-2} yr^{-1} to greater than 10 g m^{-2} yr^{-1} in industrialized areas. Low deposition rates typically occur on the west coasts of continents and other places remote from pollution sources. These additions should be added repeatedly to determine long-term response. One problem with these experiments is that control plots inevitably receive ambient deposition, so one can only test the impact of atmospheric deposition that is higher than ambient levels.

Experimental Setup

The appropriate design for nutrient addition experiments is similar to that of most field experiments. For example, many experiments use a randomized block design, in which replicate blocks are set out in "representative patches" of the ecosystem, with buffer strips between treatment plots. Each treatment is then randomly assigned within blocks. The size of the buffer strips depends on the mobility of the nutrient and the lateral root extension of the dominant plants. The most difficult task in implementing this design is in deciding what is a representative patch, and what is the domain over which the results can be generalized. The results of the experiment can only be rigorously generalized to the experimental area. For example, if the experiment is set out on a hillside, and patches of bare ground are avoided, the results can be generalized only to vegetated components of the ecosystem on that hillside. This would be an appropriate design for looking at the effect of nutrients on the competitive interactions among plants. In a study of this sort, inclusion of bare patches would only increase the variance without adding insight about competitive processes (Hobbie and Chapin 1998). If the experiment is intended to be generalized to a large region, either the replicate blocks must be dispersed over the entire region or the experiment must be repeated over the entire region. For example, to generalize about whether nutrient limitation changed through postglacial succession at Glacier Bay, Alaska, plots were distributed throughout a 100-km length of the bay, with 10 replicate blocks per successional stage but only one replicate block in each location (Chapin et al. 1994). In another series of studies conducted by several research groups, similar nutrient addition treatments were applied to tussock tundra throughout its range in Alaska, Britain, and Scandinavia (Tamm 1954; Goodman and Perkins 1968; Shaver and Chapin 1980; Shaver and Chapin 1995), demonstrating that growth of the dominant species (*Eriophorum vaginatum*) in this vegetation type was consistently nutrient-limited, but that the identity of the limiting nutrient varied regionally.

The extent of replication necessary in a nutrient-addition study depends on the magnitude and variability of nutrient limitation and the size of the nutrient addition. For experiments in which expected effects are large, a sample size of 4 to 6 may be adequate. However, if effects may be more subtle, as in isotope addition experiments or experiments simulating atmospheric deposition, or if the experiment deliberately incorporates substantial landscape heterogeneity (to increase the generalizability of results), larger sample sizes (e.g., 8 to 10) are essential. The actual experimental design chosen is usually a compromise between what is desirable and what is feasible.

Experimental Design

There are many factors to consider in designing a nutrient addition experiment, and the choices are specific to the question and system. There are many controls on the effectiveness of a given nutrient addition, including climate, soils, the potential of the vegetation to respond to nutrients, land use, date of germination relative to date of fertilization, limitation of other nutrients, and decreases in biomass due to diseases and herbivores (FAO 1987). These factors could confound the interpretation of nutrient-addition experiments by affecting the availability of nutrients added and the measurements of biomass response. These confounding factors can be minimized by carefully deciding the form of nutrient to add, the amount to add, the frequency and timing of additions, and when to measure the response variables.

The question to be addressed should guide which of these complicating issues to focus on. For example, when determining which nutrients are limiting at a given site, it is critical to add the different nutrients in forms with similar availabilities. Most N additions (ammonium [NH_4^+], nitrate [NO_3^-], urea) are immediately soluble and available for plant uptake. It would not be valid to compare the biomass response to these soluble N fertilizers with response to rock phosphate or elemental S, which have much slower nutrient supply rates. In addition, factors such as adsorption, trace gas loss, and leaching can prevent any of the added nutrients from being available to plants. These factors should be accounted for, and addition rates of different nutrients should be adjusted to ensure similar supply rates. This is especially crucial when comparing nutrient limitation across sites. Site differences in hydrology, soil adsorption, pH, and vegetation can

have large effects on partitioning, adsorption, volatilization, and leaching. Thus, a constant rate of fertilizer application may not add a consistent amount of nutrients to the plant-available pool, and site differences in response to fertilization may be due to the different availability of added nutrients, rather than due to differences in nutrient limitation.

The way that nutrients are added can influence plant uptake (Malhi et al. 1989), and the distribution of biomass and nutrients (Imo and Timmer 1992), which can have large impacts on the interpretation of results. The following sections present some general guidelines for designing a nutrient addition experiment, but for a complete review, Tisdale et al. (1993) is an invaluable reference.

Time Scale of Response

The interpretation of nutrient-addition experiments requires a clear understanding of the sequential response of different ecosystem processes to nutrient addition (Table 19.1) so that the appropriate response variable and time scale can be chosen.

1. After nutrients are applied, they must first reach the plant. If application rates are high, this movement to the plant may be virtually instantaneous. However, with low application rates, nutrients may be immobilized by surface mosses or soil microbes and never reach plants in detectable amounts. We expect chemical or biological immobilization of nutrients to be most pronounced in low-fertility soils.
2. Following plant uptake of nutrients, tissue nutrient concentrations typically increase before there is a growth response. If growth is seasonally programmed, is limited by the number of meristems, or occurs slowly due to environmental constraints, growth may lag behind the increased tissue concentration by as much as a year (Shaver and Chapin 1995). Still other plant responses, such as flowering, depend on initiation of floral meristems and are generally delayed even more than the growth response.
3. The initial growth response of plants reflects the limitation of growth of that given plant assemblage by nutrient supply.
4. The altered nutrient supply generally changes competitive balance (Tilman 1988), so that plants that are superior competitors in fertile soils begin to out-compete and may eventually eliminate species that were initially abundant under the original low-nutrient conditions. Incorporating these community shifts gives a measure of the overall ecosystem's potential to respond to nutrient additions.

TABLE 19.1. Typical time course of ecosystem responses to nutrient additions.

Process	Time scale
Diffusion through soil	Seconds to days
Microbial immobilization	Hours to year
Increased tissue concentration	Days to years
Increased plant growth	Weeks to years
Altered competitive balance	Months to decades
Altered species composition	Years to decades

Addition Rates

As discussed above, the experimental question will determine the magnitude of nutrient additions. However, deciding on addition rates becomes more difficult when considering the variation in the factors that influence the availability of added nutrients. In order to detect if a given nutrient is limiting across a number of sites, it may be advisable to add large amounts of fertilizer to ensure that plants can access some of the added nutrients on all sites. There is no need to be concerned about fertilizer additions being available to plants in deposition studies because differences in adsorption and loss are important variables that determine how a system responds to deposition. Thus, for deposition studies, a low, constant fertilization rate is desired across sites.

How to Add?

The timing of addition can be important in determining the availability of nutrient additions to plants. High loss rates can result from additions at times of high precipitation or low plant uptake. In general, the decision of when to add fertilizer should be dictated by the question, and then by a balance between timing of fertilizer availability, plant demands, and environmental conditions that affect loss.

Nutrients are typically added in solid form, although this can burn the surface vegetation. For example, mosses, lichens, and many evergreen shrubs are sensitive to high nutrient addition rates. However, addition of dissolved nutrients in a water solution is time consuming and can create artifacts if moisture is potentially limiting to growth.

Use of slow-release fertilizer (e.g., Osmocote or rock phosphate) is an excellent way to provide nutrients gradually, rather than in a single pulse. These fertilizers differ in the forms of nutrients present (ammonium vs. nitrate), the combinations of nutrients supplied, and in the rate of release. In other cases, pulsed nutrient input (as simulated by addition of soluble nutrients) may be more typical of natural ecosystem patterns (Cui and Caldwell 1997; Bilbrough and Caldwell 1997).

Ideally, the nutrients should be added to that component of the ecosystem where the processes naturally occur. For example, if the purpose is to trace N uptake by plants and soil microorganisms, isotopically labeled N should be distributed uniformly through the rooting zone rather than applied to the surface, where it might contaminate the plants or be immobilized by surficial vegetation (algae or mosses) or litter microbes. These experiments are most readily done with microcosms, in which the isotope can be injected into the soil using long "spinal-tap" needles that are soldered closed at the end but have holes drilled in the side of the needle (Jackson et al. 1989; Hungate et al. 1997). Nadelhoffer et al. (1995) have applied ^{15}N to the litter layer of forests to follow the fate of nutrients returned to the forest floor in litterfall.

Form of Nutrients Added

Nutrients should be added in a chemical form that reasonably approximates the form that is available in that ecosystem. For example, N might be added as nitrate in ecosystems with high nitrification rates or as urea or NH_4^+ in ecosystems with low nitrification rates. In N deposition experiments, it is important to choose the form of N that is being deposited at the study sites (e.g., NO_3^- in the eastern United States, NH_4^+ in the Netherlands), because these different forms of N can have very different effects on ecosystem and community response (Crabtree and Bazzaz 1993; Vaast and Zasoski 1992).

The form of added nutrients is important, because inappropriate choices can create unintended side effects. For example, addition of ammonium chloride or sodium nitrate can cause chloride or sodium toxicity, create osmotic problems at high levels, or alter soil pH. Two options are to add ammonium nitrate or to add two ammonium forms which differ in their pH effects (see below). Which form is chosen also determines the fate and retention of fertilizer, and effects on ecosystem and community dynamics.

Many fertilizers contain multiple elements. For example, most commercial phosphate fertilizers are made with sulfuric acid and contain enough sulfate to act as a S fertilizer in S-deficient soils. When choosing which form of fertilizer to use, pay careful attention to the other nutrients that are in the fertilizer; nutrients are commonly complexed to forms of other limiting nutrients (K, N, P, S, Ca), which could also play an important role in biomass response.

Practicality and economy are two other important considerations when choosing the appropriate form of fertilizer. For example, studies requiring large P inputs would necessitate as much as a 30-cm-deep layer of rock phosphate to achieve the desired P additions! Nutrient addition experiments that focus on agriculture or rangeland applications need to consider economy as well. Osmocote, or any other expensive nutrient source, would never be used by growers.

Nitrogen

Control of Fertilizer Nitrogen Availability

The major processes that decrease the fertilizer N available to plants are microbial immobilization, leaching loss, trace gas losses through nitrification and denitrification, ammonia volatilization, and adsorption of NH_4^+ on soil particles. To minimize loss through leaching and denitrification, it is best to avoid additions of N during very wet times. Ammonia (NH_3) volatilization can lead to substantial losses of added N, as high as 25 to 50% (Tisdale et al. 1993). Ammonia losses are especially high in systems with high soil pH, soil moisture around field capacity, high evaporation, and substantial plant residue at the surface of the soil. In such systems, N should be added as NO_3^- rather than as NH_4^+ or urea.

Fixation of NH_4^+ on minerals is not a permanent loss—it is often a temporary retention mechanism that decreases nitrification and leaching loss. Ammonium fixation on soil is most common on coarse clays and fine silt, especially on vermiculite and illite. Fixation increases with freezing and drying. Soils with high concentrations of K and Ca tend to have very low NH_4^+ adsorption.

Common Nitrogen Fertilizers

Nitrogen is commonly added as NH_4^+ salts, NO_3^- salts, or urea. Ammonium nitrate (NH_4NO_3) is a very common form of N fertilizer in nutrient addition experiments. Additions of this form ensure high N availability, without the confounding factor of adding other mineral nutrients, and it has little effect on soil pH. Disadvantages to using NH_4NO_3 are that it is more prone to denitrification and leaching than NH_4^+ salts, it must be stored carefully because it can absorb moisture and cake very easily, and, if it comes into contact with oxidizable C sources (such as fuel), it is very explosive, so it must be handled with care.

Ammonium salts have the best system retention of N in most cases, but they reduce pH and should not be used in acidic soils, except in combination with urea, which has the counteracting effect of raising pH. Care must also be taken in applying NH_4^+ salts to calcareous soils (Kissel et al. 1985); NH_4^+ salts that precipitate with Ca (fluoride [F^-], sulfate [SO_4^-], phosphate [PO_4^-]) can stimulate NH_3 volatilization and nitrification, leading to high loss rates of the N added. However, NH_4^+ additions with chloride (Cl^-), NO_3^-, and iodide (I^-) are suitable for application to calcareous soils (Tisdale et al. 1993). In addition, at high pH, additions of NH_4^+ can lead to the accumulation of nitrite (NO_2^-), which is toxic to plants and microbes. Ammonium sulfate is the most acidic N addition (Boswell 1985), and should be avoided in low pH soils. Ammonium phosphate can be used as a fertilizer in situations in which both N and P additions are required. Ammonium chloride (NH_4Cl) can be problematic because some plants are sensitive to it at relatively low concentrations, and at high concentrations, chloride can be toxic to all plants. This is especially an issue in long-term additions, or areas where Cl^- can accumulate quickly (such as arid regions with high evaporation).

Nitrate salts are not as acid as ammonium salts. Nitrate accompanied by base cations (e.g., sodium [Na^+], Ca^{2+}) can increase pH, and should be avoided in basic soils. Nitrate fertilizers are very soluble and mobile and are subject to high loss rates through leaching and denitrification. However, in some systems, long-term fertilization studies have seen higher plant yields in response to NO_3^- than NH_4^+ due to the negative effect of NH_4^+ on soil acidity (Koren'kov 1983). Common sources of nitrate are $NaNO_3$, KNO_3, and $Ca(NO_3)_2$.

Urea is one of the most common forms of N additions. It is relatively inexpensive and easy to handle, it has much less tendency to absorb moisture and cake than ammonium nitrate, and it is not prone to explosion. However, there are many problems associated with urea additions, and careful attention must be paid to the characteristics of a system before deciding that its use is appropriate. Urea should never be added to soils with high pH (pH greater than 7.5). As with ammonium applications, high pH can lead to nitrite accumulation, as well as high rates of ammonia volatilization. This can occur with urea applications even in acid or neutral soils, because urea can substantially increase soil pH (Bremner 1995).

Another problem associated with urea application is that it often contains biuret, an impurity that inhibits germination and seedling growth. Because of this, as well as the toxicity of high concentrations of NH_3 to plants, urea should not be added just before germination, or early in the growing season. Urea losses can be minimized by subsurface applications, rather than a broadcast surface application.

Another important option for N additions is slow-release fertilizers, which are the easiest way to apply N gradually and continuously. Slow-releasing N is available in a number of different forms, but it is most commonly supplied as urea, particularly in the slow-releasing fertilizers that do not also supply P and K (Hauck 1985).

How to Add Nitrogen Fertilizers

As discussed above, the form of N chosen will dictate what conditions minimize losses and negative effects of fertilizer N. In general, N fertilization is optimized when added at the time of peak plant uptake. Nitrate additions should be avoided in areas with high rainfall, or that are very wet, in order to

decrease losses through leaching and denitrification. Ammonium and urea additions should be avoided in very basic soils, in order to avoid ammonia volatilization and nitrite accumulation, and urea additions in acid and neutral soils should be carefully applied and monitored in order to minimize pH increases and its negative effects. Ammonium additions should also be avoided in very acid soils. High addition rates, or long-term additions will increase the effects of N salts on soil pH, and a form with little impact on pH, such as NH_4NO_3 should be used.

Phosphorus

Control of Phosphorus Fertilizer Availability

The availability of fertilizer P to plants is limited mostly by its solubility and its adsorption to soil minerals. Adsorption is especially high in soils with high clay contents and in weathered acid soils, which tend to have high concentrations of aluminum oxides and iron oxides. Adsorption is higher on 1:1 clays such as kaolinite than on 2:1 clays, such as montmorillonite. The pH is a critical factor determining adsorption. Although different minerals adsorb P maximally at different pHs, in most soils P availability is maximal at pH 5.5 to 6.5. The presence of divalent cations also can substantially increase P adsorption. For example, clays saturated with Ca^{2+} have higher adsorbed P than those with Na^+. Thus, calcareous soils often have low P availability. Phosphate can also compete with other ions for adsorption sites, so its adsorption is decreased in the presence of OH^-, $H_3SiO_4^-$, SO_4^-, and MoO_4^{2-}. Phosphorus adsorption is more permanent than N adsorption. Once P is adsorbed, it does not become available to plants at any great quantities. To make up for this, P fertilization must usually be high in order to cause any appreciable increase in P availability. For example, it is common to add P at half the rate that N is added, although plant tissue contains about 14 times more N than P.

In addition to adsorption, it is also necessary to consider precipitation of the phosphate ions. Adsorption usually occurs once phosphate enters the bulk soil, whereas precipitation occurs close to fertilizer granules. High concentrations of calcium, aluminum and iron could cause substantial precipitation, while the use of other fertilizer salts, such as $(NH_4)_2SO_4$, NH_4NO_3, NH_4Cl, KNO_3, K_2SO_4, and KCl, can decrease P precipitation.

It is important when comparing the response of growth to P fertilization among different sites, that one consider these different factors regulating P availability.

Common Phosphorus Fertilizers

There are two main types of P fertilizer: a water-soluble form that is immediately available to plants, and P in rock phosphate, which is slowly available in acid conditions.

Rock phosphate is a good way to provide a small, continuous supply of P to a system. The P supply to plants is optimized if rock phosphate is finely ground and mixed into the soil, but it is only effective in acid soils (pH <6.0). It is most effective in systems with warm, moist soils, and long growing seasons. Application rates must be high to achieve effective fertilization. It should be noted, however, that long-term studies have shown that even after 4 to 10 years, a single application of superphosphate can enhance P availability to a greater extent than fertilization with rock phosphate (Bolland et al. 1989).

The water-soluble forms offer the advantage of immediate availability of P, and are much more comparable to forms of other nutrient additions such as NH_4NO_3 and KCl. In general, there are very small differences in supply rate between the different water-soluble P fertilizers. Water-soluble P is often added as single superphosphate or triple superphosphate, which are calcium orthophosphates. These work well in nutrient limitation experiments as long as the site is not calcium limited. These have no effect on soil pH, and almost all of the P is water soluble and plant available. Single superphosphate contains substantial S, which is beneficial for combined-nutrient additions, but is not a satisfactory way to test for P limitation in soils that may also be S limited. Triple superphosphate, on the other hand, has very little S (0 to 1%) and is much better for such applications. Phosphorus is often added as ammonium phosphates, but this is not a satisfactory way to add P if trying to test for N versus P limitation.

Phosphorus can also be added as a slow release fertilizer. For example, Osmocote produces P_2O_5 pellets.

How to Add Phosphorus Fertilizer

Even with the best P fertilization management, plants often take up less than 25% of added P (Tisdale et al. 1993). In high-fixing soils, rather than adding P in one application, several smaller, more frequent applications can maximize plant P availability. If adding a water-soluble form, it is desirable to minimize contact with the soil, so large granules should be used. In contrast, very fine granules maximize release of phosphate from water-insoluble fertilizers (Young et al. 1985).

The best time to add water-soluble P is just before germination, because P availability rapidly decreases with time after fertilization (Bramley and Barrow 1992).

Potassium

Control of Fertilizer Potassium Availability

The availability of K fertilizer is determined by many different factors, and different soils can be drastically different in the amount of fertilizer needed to increase exchangeable K concentrations. Potassium, like NH_4^+, can be temporarily fixed onto soils. However, at very high pH, soil fixation can be permanent as K becomes trapped between the collapsed silicate layers of clays. Wet soils substantially increase K fixation, and K is gradually released as the soil dries. Adsorption characteristics of soils for K are opposite to those of P; the highest K fixation is seen in 2:1 clays with high illite, while 1:1 clays, such as kaolinite, do not fix substantial amounts of K. Fine soil textures increase fixation onto soil, while aluminum ion (Al^{3+}) concentrations decrease fixation. In very acid soils, high concentrations of Al^{3+} and magnesium ions (Mn^{2+}) inhibit plant K^+ uptake, and could interfere with growth response to fertilization. Leaching losses of K are relatively small in most soils, but could be substantial in sandy soils, or humid tropical soils with high rainfall.

Assessment of K limitation is more complicated than for other nutrients because it is not a simple function of K available in soil solution, but is more dependent on the ratio of K^+ to Ca^{2+} and Mg^{2+}, which compete with K^+ for entry into the plants. So in soils with high calcium and magnesium, higher amounts of K must be added to become available to plants. In addition, when adding a combination of nutrients that includes K, be sure to avoid adding other nutrients complexed with Ca or Mg (such as $CaSO_4$).

Common Potassium Fertilizers

All commonly used forms of K fertilizer are equally effective in supplying plant-available K. The major factor determining the appropriate choice depends on the other nutrients being tested or added. Potassium is most commonly added as KCl (muriate of potash), which is readily dissolved in water. There are some plants that are intolerant to Cl^-, in which case another form must be used. Potassium chloride also has limited applications in long-term fertilization, because Cl^- accumulation can be detrimental to plant growth or microbial activity. Potassium sulfate (K_2SO_4) is often used in Cl^--sensitive situations and is an appropriate choice for systems where S is not limiting to growth.

Potassium carbonate (K_2CO_3), potassium bicarbonate ($KHCO_3$), and potassium hydroxide (KOH) are very effective fertilizers, and when used on acid soils, they will decrease the leaching of cations. Potassium phosphates are good for gradual applications because they have more controlled solubility than the other forms of K fertilizer. Other forms that are commonly used are potassium magnesium sulfate and potassium nitrate. Long-term or high rates of K additions usually use potassium nitrate (KNO_3) or potassium pyrophosphate ($K_4P_2O_7$) in order to avoid salt accumulation problems. Unfortunately, because these are complexed with the two most commonly limiting nutrients, these forms can't be used to separately test K, N, and P limitation.

How to Add Potassium Fertilizer

Potassium fertilizers are most effective if added just before or at the time of germination or onset of growth. Higher leaching losses can occur if K is applied long before plant uptake will occur.

Sulfur

Control of Sulfur Fertilizer Availability

Sulfate (SO_4^{2-}), like nitrate, can be readily lost through leaching, especially in soils where monovalent cations predominate (K^+, Na^+). Adsorption

can be high in soils with high clay content and high concentrations of aluminum oxides and iron oxides. Adsorption increases at low pH, and is greater in soils with kaolinite than with illite or montmorillonite. This adsorption is readily reversible and will only affect short-term S availability, and probably increase long-term availability by preventing S leaching. Sulfate can also be removed from the plant-available pool by precipitating with calcium carbonate ($CaCO_3$).

Common Sulfur Fertilizers

Like phosphorus, S has two main forms of fertilizer, a readily available water-soluble form and a slowly available insoluble form.

Sulfate additions are immediately plant available, and supply rates are comparable with NH_4NO_3, KCl, and water-soluble P additions. Different forms of soluble S are approximately equal in their efficiency to supply S to plants, unless complexed with zinc (Zn), copper (Cu), or Mn. All forms of water-soluble S are complexed with other important nutrients (N, P, iron [Fe], Ca, K, Mg), so careful consideration of other limiting nutrients in a system must be made before deciding on which form of S fertilizer to use. Gypsum ($CaSO_4$) is one of the most common ways to add sulfur. It is also possible to add S as single superphosphate if a combined application with P is desired. In order to minimize S leaching loss, applications of sulphate should be made close to the time of peak plant uptake.

The second main form of S fertilizer is elemental sulfur (S_0), which is a water-insoluble solid. When finely ground and mixed with soils, it is oxidized to SO_4^{2-} by microbes. The relative effectiveness of S_0 application is determined by the particle size added, how and when it is added, the S_0 oxidizing characteristics of soil, and environmental conditions. Finer-size particles supply SO_4^{2-} at a faster rate. A mixture of S_0 particle sizes is sometimes desirable in order to achieve both rapid and long-lasting S availability. Dissolution of SO_4^{2-} is maximized if the pellets undergo wet–dry or freeze–thaw cycles. A way to maximize release of plant-available S is to use irregularly shaped, porous granules. Alternatively, S_0 can be applied with bentonite, a clay that absorbs water and causes the S_0 granules to disintegrate.

The timing of additions is crucial, S_0 must be added as far ahead of germination and growth initiation as possible (Beaton et al. 1985). Even when adding S_0 with bentonite or porous granules, a few months are needed for substantial release of plant-available S. Elemental sulfur applications are more efficient if they are incorporated into the soil. A possible problem associated with S_0 additions is acidification of the soil, but this can be avoided by making sure that the fertilizer is uniformly distributed (Beaton et al. 1985).

Isotopes

The use of isotopically labeled fertilizer allows ecologists to ask more refined, mechanistic questions. Isotopes can serve as an invaluable tool to check the efficiency of nutrient additions by tracking the fate of fertilizer additions, and thus helping to determine if the lack of response of a system to nutrient additions is mediated by low fertilizer availability due to adsorption, loss, or microbial immobilization (Drury and Beauchamp 1991). Isotopes can also be used to look at the long-term fate and availability of fertilizer (Preston and Mead 1994). Reciprocal transplants of litter from plots fertilized with labeled and unlabeled nutrients can help track recycling of fertilizer nutrients from the litter (Power et al. 1986).

Isotopes can also elucidate the mechanisms of ecosystem response to nutrient additions. Community composition changes may be explained by differences in resource competition at different nutrient levels, which can be determined by comparing labeled fertilizer uptake by different species (Nannipieri et al. 1985; Chang et al. 1996). Comparing amounts of labeled and unlabeled nutrients in soil and plant pools can elucidate how nutrient additions alter native soil nutrient availability (Pilbeam et al. 1997; Hart et al. 1986; Clinton and Mead 1994).

Isotopes can be particularly useful for studying system response to nutrient deposition. Isotopically labeled nutrients can elucidate the pathways and controls over nutrient movement through ecosystems, and can point to the mechanisms of ecosystem retention and loss (Nadelhoffer et al. 1995; Buchmann et al. 1996; Koopmans et al. 1996).

Isotopically labeled fertilizers are most commonly enriched. The minimum level of enrichment needed depends on how subtle the effects of a treatment are, and the rates of cycling and loss of nutrients, especially in relation to how long after addition the effects must be detected. For short-term experiments looking at more obvious changes, the less expensive isotopically depleted fertilizers or low-enrichment fertilizers can be used (see Power et al. 1986).

Nitrogen and S have stable isotopes that are valuable in fertilizer-labeled studies as well as in tracing the fate of atmospheric deposition. The radioactive N isotope has too short of a half-life to be useful in fertilizer applications. Phosphorus and S also have radioactive forms. The P isotope is short-lived, and is generally only used for short-term partitioning experiments and to assess soil adsorption (He and Zhu 1998). For a review of P isotope techniques, see Di et al. (1997). Of all of the nutrients, P fertilizer tends to be retained in the system for the longest amount of time, but due to the lack of a stable isotope, and the short half-lives of the radioactive isotopes, it is impossible to trace the fate of P fertilizer for any appreciable time.

Sulfur has both radioactive and stable isotopes, allowing much more flexibility in the types of questions that can be asked. Either form can be used to track the fate of fertilizer S (Shock et al 1983) and to determine the effect of S fertilization on S dynamics (Eriksen 1996; Ghani et al. 1993).

Nitrogen-15 is the most common isotopically labeled fertilizer used. It has been used in many studies to elucidate fate (Nannipieri et al 1985; Bristow et al. 1987), adsorption (Foster et al 1985), and long-term versus short-term fertilizer availability and dynamics (Preston and Mead 1994; Chabrol et al. 1988; see Schimel 1993 for a good review). It has also been used to trace the fate of fertilizer nutrients in litter over time (Power et al. 1986; Muller 1988). (For a review of ^{15}N fertilizer methods, see Hauck et al. 1994.)

The use of ^{15}N fertilizers has led to interesting findings. For example, it is often assumed that microbial immobilization of fertilizer is a short-term mechanism for ecosystem retention, and microbial N will eventually turn over and become available to plants. Several studies tracing the fate of ^{15}N fertilizer did not see this microbial N being made available to plants, even over an extended period of time (Proctor and Mead 1994; Rutherford and Juma 1992). Another surprising result from ^{15}N studies was that the ecosystem retention of ^{15}N in a jack pine forest was dominated by chemical fixation of $^{15}NH_3$, which was substantially higher than microbial immobilization (Foster et al. 1985).

While isotopes can be invaluable tools, interpretations must be made carefully. Studies of ^{15}N fertilizers have often shown that fertilizing increases plant uptake of unlabeled soil N, which has been attributed to increases in soil organic N mineralization (Pilbeam et al 1997) and increases in plant uptake rates (Leon et al. 1995). These increases in native organic N uptake may not necessarily be due to increased availability or uptake, but may be an artifact of fertilizer application. Microbes may have immobilized the flush of ^{15}N fertilizer, allowing native soil N that would normally be immobilized to be taken up by plants. This pool substitution could lead to an overestimate of the effect of fertilizer on N cycling, and an underestimate of nutrient uptake by plants in response to fertilization. (Hart et al 1986; Jenkinson et al. 1985). Interpretation of isotope data must also consider isotope fractionation in uptake and soil processes, especially when using depleted, or low-enrichment fertilizer. This is especially true in systems with even small amounts of NH_3 volatilization, which discriminates very strongly against ^{15}N, and will enrich the soil ^{15}N pool relative to the unlabeled pool. In such systems, the use of $^{15}NO_3$ rather than urea or ammonium is recommended (Nommik et al 1994).

These problems in interpretation of isotopic fertilization experiments can be minimized by using trace levels of highly enriched label to trace the natural movement of nutrients in ecosystems. For example, to resolve the question of whether the increase in unlabeled plant N described above is an artifact of fertilizer additions, or a result of N addition altering N cycling, unlabeled fertilizer additions could be followed by trace amounts of highly enriched ^{15}N to document nutrient partitioning and gross rates of nutrient transformations. Tracer additions should be high enough for the isotope to be detectable for the duration of the experiment, but not so high as to perturb natural process rates by "fertilization" (Jackson et al. 1989; Davidson et al. 1991). Low-level ^{15}N addition can determine rates of microbial immobilization in the absence of roots (Davidson et al. 1991; Hart et al. 1994); the parti-

tioning of inorganic N among plant uptake, microbial uptake, and chemical fixation in the presence of plants (Jackson et al. 1989; Norton and Firestone 1996; Recous et al. 1992; Hart et al. 1993); or the time course of N movement from the inorganic pool to microbes (including mycorrhizae) to plants (Buchmann et al. 1996).

Isotopes can be used in a variety of approaches. If the main objective of the study is to track fertilizer fate, these isotopically labeled fertilizers should be used. However, if the main objective of the study is to document changes in nutrient cycling in response to fertilization, it would be better to fertilize with unlabeled nutrients, and then add trace amounts of labeled nutrients to track the movement of the overall nutrient pool through the system, or to determine gross rates of nutrient transformations.

Alternatives to Nutrient Addition Experiments

Nutrient addition experiments are not the only way to assess nutrient limitation in ecosystems. For example, the N/P ratio in plant tissues is an excellent indicator of the type of nutrient limitation (Redfield 1958; van den Driessche 1974; Ingestad 1979; Aerts et al. 1992; Koerselman and Mueleman 1996). A plot of P concentration against the N concentration in unfertilized plots was an effective predictor of the biomass response to N vs. P (Fig. 19.1) (Koerselman and Mueleman 1996). At N/P ratios >16, the community biomass was P-limited, whereas at N/P ratios <14, N limited plant growth in all but one study. At N/P ratios between 14 and 16, plants responded to both N and P. The N/P ratio was a better predictor of nutrient response than was tissue concentration, which varied 3-fold for N and 16-fold for P. There was no clear relationship between the nutrient concentration in plant tissue and the nature of nutrient limitation (Koerselman and Mueleman 1996).

The effects of nutrients on ecosystem dynamics can also be elucidated through nutrient depletion experiments. Carbon-rich (low-nutrient) substrates, such as sawdust or starch, can be added to increase the C/N ratio of soils, leading to microbial immobilization of nutrients and a reduction in nutrient availability to plants (Yarie and Van Cleve 1996). Studies of ^{15}N fertilization have indicated that this N immobilized by microbes may not become available to plants, even after an extended period of time (Rutherford and Juma 1992; Jonasson et al. 1996). However, this approach should be used with caution, because labile C additions can also stimulate nutrient cycling and availability.

Other methods to decrease nutrients are harvesting of litter or plants, burning, and topsoil removal (Marrs 1985). These methods are appropriate only for certain questions and have substantial ecosystem effects in addition to the reduction in nutrient supply.

Another approach to studying the effects of nutrient additions has been to take advantage of depositional gradients of N and S. This approach has been used in many studies to look at the effects of deposition on plant communities and ecosystem processes (Randlett et al. 1992). Isotopes can be particularly helpful here, because N and S from atmospheric deposition have different isotopic sig-

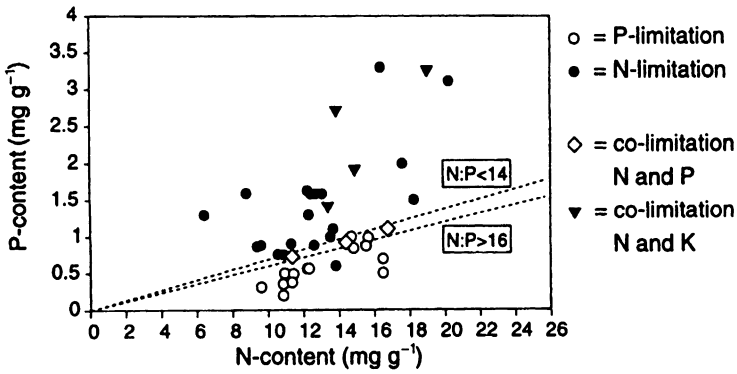

FIGURE 19.1. Vegetation N/P ratios can be used to predict N and P limitation. Vegetation with an N/P ratio less than 14 was N limited, an N/P higher than 16 indicated P limitation, and there was co-limitation of N and P when the N/P ratio was between 14 and 16. (From Koerselman and Mueleman 1996.)

natures than do soil N and S, and thus their fate can often be traced within the system (Koopsman et al. 1997).

Summary and Conclusions

Nutrient addition experiments can be used to address a variety of questions, including the role of nutrients in mediating ecosystem processes, nutrient effects on plant and microbial community dynamics, the limitations on plant growth and ecosystem production, and the response of ecosystems to increased atmospheric deposition of nutrients.

When designing a nutrient addition experiment, it is critical to minimize the impact of the fertilizer additions on soil pH, salt toxicity, and the supply of other potentially limiting nutrients that are not being tested (e.g., S, Ca). It is also important to understand whether a lack of response to fertilization is due to the absence of limitation for that nutrient, or the failure of the nutrient additions to become available to plants. This is especially important when comparing responses of plant growth to nutrient additions across sites, where factors controlling fertilizer availability could differ substantially.

Isotopes are an invaluable tool for attaining a mechanistic understanding of the fate and dynamics of nutrient additions. They can be used to test how much of the fertilizer becomes available to plants, elucidate mechanisms of nutrient retention and loss, detect changes in soil nutrient dynamics, and trace competitive uptake between different plant species and microbial groups. The incorporation of isotope methods into nutrient addition experiments should solidify our understanding of the controls of nutrients over all aspects of the ecosystem.

Acknowledgments This chapter is based on ideas developed under funding from the Bonanza Creek Long-Term Ecological Research Program (National Science Foundation BSR-9196130 and U.S. Forest Service PNW 96-5024-2-CA), a grant from the California Sustainable Agriculture Research and Education Program, a NASA Earth System Science Fellowship (ESS/97-0127), a National Science Foundation doctoral dissertation improvement grant (DEB-9801487), and funding from the Division of Agriculture and Natural Resources to the University of California Hopland Research and Extension Center.

References

Aber, J.D.; Magill, A.; Boone, R.; Melillo, H.M.; Steudler, P.; Bowden, R. Plant and soil responses to chronic nitrogen additions at the Harvard Forest, Massachusetts. Ecol. Applic. 3:156–166; 1993.

Aerts, R.; Wallen, B.; Malmer, N. Growth-limiting nutrients in *Sphagnum*-dominated bogs subject to low and high atmospheric nitrogen supply. J. Ecol. 80:131–140; 1992.

Aerts, R.; Berendse, F. The effect of increased nutrient availability on vegetation dynamics in wet heathlands. Vegetatio 76:63–69; 1988.

Arnolds, E. Former and present distribution of stipitate hydnaceous fungi (Basidiomycetes) in the Netherlands. Nova Hedwigia 48:107–142; 1989.

Beaton, J.C.; Fox, R.L.; Jones, M.B. Production, marketing, and use of sulfur products. In: Engelstad, O.P., ed. *Fertilizer Technology and Use.* 3rd ed. Madison, WI: Soil Science Society of America; 1985:416–454.

Berendse, F.; Elberse, W.T.H.; Geerts, R.H.M.E. Competition and nitrogen loss from plants in grassland ecosystems. Ecology 73:46–53; 1992.

Bilbrough, C.J.; Caldwell, M.M. Exploitation of springtime ephemeral N pulses by six Great Basin plant species. Ecology 78:231–243; 1997.

Bobbink, R. Effects of nutrient enrichment in Dutch chalk grassland. J. Appl. Ecol. 28:28–41; 1991.

Bolland, M.D.A.; Weatherly, A.J.; Gilkes, R.J. The long-term residual value of rock phosphate and superphosphate fertilizers for various plant species under field conditions. Fertil. Res. 20:89–100; 1989.

Boswell, F.C. Production marketing and use of nitrogen fertilizers. In: Engelstad, O.P., ed. *Fertilizer Technology and Use.* 3rd ed. Madison, WI: Soil Science Society of America; 1985:229–292.

Bouchard, D.C.; Williams, M.K.; Surampalli, R.Y. Nitrate contamination of groundwater: Sources and potential health effects. Am. Water Works Assoc. J. 84:85–90; 1992.

Bowman, W.D.; Theodose, T.A.; Schardt, J.C.; Conant, R.T. Constraints of nutrient availability on primary production in two alpine tundra communities. Ecology 74:2085–2097; 1993.

Bramley, R.G.V.; Barrow, N.J. The reaction between phosphate and dry soil. II. The effect of time, temperature and moisture status during incubation on the amount of plant available P. J. Soil Sci. 43:759–766; 1992.

Bremer, E.; Kuikman, P. Influence of competition for nitrogen in soil on net mineralization of nitrogen. Plant Soil 190:119–126; 1997.

Bremner, J.M. Recent research on problems in the use of urea as a nitrogen fertilizer. Fertil. Res. 42:321–329; 1995.

Bristow, A.W.; Ryden, J.C., Whitehead, D.C. The fate at several time intervals of ^{15}N-labeled ammonium nitrate applied to an established grass sward. J. Soil Sci. 38:245–254; 1987.

Buchmann, N.; Gebauer, G.; Schulze, E.-D. Partitioning of ^{15}N-labeled ammonium and nitrate among soil, litter, below- and above-ground biomass of trees and understory in a 15-year-old *Picea abies* plantation. Biogeochemistry 33:1–23; 1996.

Chabrol, M.; Powlson, D.S.; Hornby, D. Uptake by maize (*Zea mays* L.) of nitrogen from ^{15}N-labeled dazomet, ^{15}N-labeled fertilizer and from the soil microbial biomass. Soil Biol. Biochem. 20:517–523; 1988.

Chang, S.X.; Preston, C.M.; McCullough, K.; Weetman, G.F.; Barker, J. Effect of understory competition on distribution and recovery of ^{15}N applied to a western red cedar–western hemlock clear-cut site. Can. J. For. Res. 26:313–321; 1996.

Chapin, F.S., III. The mineral nutrition of wild plants. Annu. Rev. Ecol. Syst. 11:233–260; 1980.

Chapin, F.S., III, Vitousek, PM, Van Cleve, K. The nature of nutrient limitation in plant communities. Am. Naturalist 127:48–58; 1986.

Chapin, F.S., III; Bloom, A.J.; Field, C.B.; Waring, R.H. Plant responses to multiple environmental factors. BioScience 37:49–57; 1987.

Chapin, F.S., III; Walker, L.R.; Fastie, C.L.; Sharman, L.C. Mechanisms of primary succession following deglaciation at Glacier Bay, Alaska. Ecol. Monog. 64:149–175; 1994.

Chapin, F.S., III; Shaver, G.R.; Giblin, A.E.; Nadelhoffer, K.G.; Laundre, J.A. Response of arctic tundra to experimental and observed changes in climate. Ecology 76:694–711; 1995.

Clarholm, M. Microbial biomass P, labile P, and acid phosphatase activity in the humus layer of a spruce forest, after repeated additions of fertilizers. Biol. Fertil. Soils 16:287–292; 1993.

Clinton, P.W.; Mead, D.J. Competition for nitrogen between *Pinus radiata* and pasture. II. Trends in plant and soil processes. Can. J. For. Res. 24:889–896; 1994.

Crabtree, R.C.; Bazzaz, F.A. Seedling response of four birch species to simulated nitrogen deposition: ammonium vs. nitrate. Ecol. Applic. 3:315–321; 1993.

Cui, M.; Caldwell, M.M. A large ephemeral release of nitrogen upon wetting of dry soil and corresponding root responses in the field. Plant Soil 191:291–299; 1997.

Daniels, R.B.; Gilliam, J.W. Sediment and chemical load reduction by grass and riparian filters. Soil Sci. Soc. Am. J. 60:246–251; 1996.

Davidson, E.A.; Hart, S.C.; Shanks, C.A.; Firestone, M.K. Measuring gross nitrogen mineralization, immobilization, and nitrification by ^{15}N isotopic pool dilution in intact soil cores. J. Soil Sci. 42:335–349; 1991.

Di, H.J.; Condron, L.M.; Fossard, E. Isotope techniques to study phosphorus cycling in agricultural and forest soils: a review. Biol. Fertil. Soils 24:1–12; 1997.

Drury, C.F.; Beauchamp, E.G. Ammonium fixation, release, nitrification, and immobilization in high-fixing and low-fixing soils. Soil Sci. Soc. Am. J. 55:125–129; 1991.

Eriksen, J. Incorporation of S into soil organic matter in the field as determined by the natural abundance of stable S isotopes. Biol. Fertil. Soils 22:149–155; 1996.

Fan, A.M.; Steinberg, V.E. Health implications of nitrate and nitrite in drinking water: An update on methemoglobinemia occurrence and reproductive and developmental toxicity. Regul. Toxicol. Pharmacol. 23:35–43; 1996.

Feijtel, T.C.; Salingar, Y.; Hordijk, C.A.; Sweerts, J.P.R.A.; van Breemen, N.; Cappenberg, T.H.E. Sulfur cycling in a Dutch moorland pool under elevated atmospheric S-deposition. Water Air Soil Pollut 44:215–234; 1989.

Fernandez, I.J.; Rustad, L.E. Soil response to sulfur and nitrogen treatments in a northern New England (USA) low elevation coniferous forest. Water Air Soil Pollut. 52:23–40; 1990.

[FAO] Food and Agricultural Organization of the United Nations. *Fertilizer Strategies.* Rome:FAO; 1987.

Forsius, M.; Kleemola, S.; Starr, M.; Ruoho-Airola, T. Ion mass budgets for small forested catchments in Finland. Water Air Soil Poll. 79:19–38; 1995.

Foster, N.W.; Beauchamp, E.G.; Corke, C.T. Immobilization of nitrogen-15-labeled urea in a Jack Pine forest floor. Soil Sci. Soc. Am. J. 49:448–452; 1985.

Friedland, A.J.; Miller, E.K.; Battles, J.J.; Thorne, J.F. Nitrogen deposition, distribution and cycling in a subalpine spruce-fir forest in the Adirondacks, New York, USA. Biogeochemistry 14:31–55; 1991.

Ghani, A.; McLaren, R.G.; Swift, R.S. The incorporation and transformation of ^{35}S in soil: Effects of soil conditioning and glucose or sulphate additions. Soil Biol. Biochem. 25:327–335; 1993.

Goodman, G.T.; Perkins, D.F. The role of mineral nutrients in *Eriophorum* communities. III. Growth response to added inorganic elements in two *Eriophorum vaginatum* communities. J. Ecol. 56:667–683; 1968.

Gunn, J.M. Restoration and recovery of an industrial region: Progress in restoring the smelter-damaged land-

scape near Sudbury, Canada. New York: Springer-Verlag; 1995.

Hart, P.B.S.; Rayner, J.H.; Jenkinson, D.S. Influence of pool substitution on the interpretation of fertilizer experiments with ^{15}N. J. Soil Sci. 37:389–403; 1986.

Hart, S.C.; Firestone, M.K.; Paul, E.A.; Smith, J.L. Flow and fate of soil nitrogen in an annual grassland and a young mixed-conifer forest. Soil Biol. Biochem. 25:431–442; 1993.

Hart, S.C.; Nason, G.E.; Myrold, D.D.; Perry, D.A. Dynamics of gross nitrogen transformations in an old-growth forest: The carbon connection. Ecology 75:880–891; 1994.

Hauck, R. Slow-release and bioinhibitor-amended nitrogen fertilizers. In: Engelstad, O.P., ed. *Fertilizer Technology and Use.* 3rd ed. Madison, WI: Soil Science Society of America; 1985:294–322.

Hauck, R.D.; Meisinger, J.J.; Mulvaney, R.L. Practical considerations in the use of nitrogen tracers in agricultural and environmental research. In: Weaver, R.W.; Angle, J.S.; Bottomley, P.S., eds. *Methods of Soil Analysis. Part 2. Microbiological and Biochemical Properties.* Madison, WI: Soil Science Society of America; 1994:907–950.

He, Z.L.; Zhu, J. Transformation kinetics and potential availability of specifically-sorbed phosphate in soils. Nutr. Cycl. Agroecosyst. 51:209–215; 1998.

Hobbie, S.E.; Chapin, F.S., III. The response of tundra plant biomass, aboveground production, nitrogen, and CO_2 flux to temperature manipulation. Ecology 79:1526–1544; 1998.

Hogg, P.; Squires, P.; Fitter, A.H. Acidification, nitrogen deposition and rapid vegetational change in a small valley mire in Yorkshire. Biol. Conserv. 71:143–153; 1995.

Hungate, B.A.; Chapin, F.S., III; Zhong, H.; Holland, E.A.; Field, C.B. Stimulation of grassland nitrogen cycling under carbon dioxide enrichment. Oecologia 109:149–153; 1997.

Imo, M.; Timmer, V.R. Growth nutrient allocation and water relations of mesquite *Prosopis-Chilensis* seedlings at differing fertilization schedules. For. Ecol. Manage. 55:279–294; 1992.

Ingestad, T. Nitrogen stress in birch seedlings. II. N, K, P, Ca, and Mg nutrition. Physiol. Planta 45:149–157; 1979.

Jackson, L.E.; Schimel, J.P.; Firestone, M.K. Short-term partitioning of ammonium and nitrate between plants and microbes in an annual grassland. Soil Biol. Biochem. 21:409–415; 1989.

Jenkinson, D.S.; Fox, R.H.; Rayner, J.H. Interactions between fertilizer nitrogen and soil nitrogen, the so-called "priming" effect. J. Soil Sci. 36:425–444; 1995.

Jenssen, P.D.; Maehlum, T.; Roseth, R.; Braskerud, B.; Syversen, N.; Njos, A.; Krogstad, T. The potential of natural ecosystem self-purifying measures for controlling nutrient inputs. Mar. Pollut. Bull. 29:420–425; 1994.

Jonasson, S.; Vestergaard, P.; Jensen, M.; Michelsen, A. Effects of carbohydrate amendments on nutrient partitioning, plant and microbial performance of a grassland-shrub ecosystem. Oikos 75:220–226; 1996.

Jones, M.B.; Martin, W.E. Sulfate-sulfur concentration as an indicator of sulfur status in various California dryland pasture species. Soil Sci. Soc. Am. Proc. 28:539–541; 1964.

Jones, M.B.; Lawler, P.W.; Ruckman, J.E. Differences in annual clover response to phosphorus and sulfur. Agron. J. 62:439–442; 1970.

Jones, M.B.; Williams, W.A.; Vaughn, C.E. Soil characteristics related to production on subclover-grass range. J. Range Manage. 36:444–446; 1983.

Jones, M.B.; Demmend, M.W.; Vaughn, C.E.; Deo, G.P.; Dally, M.R.; Center, D.M. Effects of phosphorus and sulfur fertilization on subclover-grass pasture production as measured by lamb gain. J. Prod. Agric. 3:534–539; 1990.

Kissel, D.E.; Sander, D.H.; Ellis, R., Jr. Fertilizer-plant interactions in alkaline soils. In: Engelstad, O.P., ed. *Fertilizer Technology and Use.* 3rd ed. Madison, WI: Soil Science Society of America; 1995:153–196.

Koerselman, W.; Mueleman, A.F.M. The vegetation N:P ratio: A new tool to detect the nature of nutrient limitation. J. Appl. Ecol. 33:1441–1450; 1996.

Koopmans, C.J.; Tietema, A.; Boxman, A.W. The fate of ^{15}N enriched throughfall in two coniferous forest stands at different nitrogen deposition levels. Biogeochemistry 34:19–44; 1996.

Koopmans, C.J.; Van Dam, D.; Tietema, A.; Verstraten, J.M. Natural ^{15}N abundance in two nitrogen saturated forest ecosystems. Oecologia 111:470–480; 1997.

Koren'kov, D.A. *Nitrogen Fertilizers.* New Delhi: Oxonian Press; 1983.

Körner, C. The nutritional status of plants from high altitudes. A worldwide comparison. Oecologia 81:379–391; 1989.

Korner, C. Towards a better experimental basis for upscaling plant responses to elevated CO_2 and climate warming. Plant cell Environ. 18:1101–1110; 1995.

Korner, C. *Alpine Plant Life.* Heidelberg: Springer-Verlag; 1999.

Korner, C.; Larcher, W. Plant life in cold climates. In: Long, S.F., Woodward, F.I., eds. *Plants and Temperature.* Cambridge: The Company of Biol Ltd. Symp Soc Exp Biol 42:25–57; 1988.

Lawrence, G.B.; David, M.B.; Shortle, W.C. A new mechanism for calcium loss in forest-floor soils. Nature (Lond.) 378:162–165; 1995.

Leon, M.; Laine, P.; Ourry, A.; Boucaud, J. Increased uptake of native soil nitrogen by roots of *Lolium mul-*

tiflorum Lam. after nitrogen fertilization is explained by a stimulation of the uptake process itself. Plant Soil 173:197–203; 1995.

Lovell, R.D.; Hatch, D.J. Stimulation of microbial activity following spring applications of nitrogen. Biol. Fertil. Soils 26:28–30; 1998.

Magill, A.H.; Aber, J.D.; Hendricks, J.J.; Bowden, R.D.; Melillo, J.M.; Steudler, P.A. Biogeochemical response of forest ecosystems to simulated chronic nitrogen deposition. Ecol. Applic. 7:402–415; 1997.

Malhi, S.S.; Nyborg, M.; Solberg, E.D. Recovery of ^{15}N-labeled urea as influenced by straw addition and method of placement. Can. J. Soil Sci. 69:543–550; 1989.

Marrs, R.H. Techniques for reducing soil fertility for nature conservation purposes: A review in relation to research at Roper's Heath, Suffolk, England. Biol. Conserv. 34:307–332; 1985.

Muller, M.M. The fate of clover-derived nitrogen (^{15}N) during decomposition under field conditions: Effects of soil type. Plant Soil 105:141–147; 1988.

Munzenberger, B.; Schmincke, B.; Strubelt, F.; Huttl, R.F. Reaction of mycorrhizal and non-mycorrhizal scots pine fine roots along a deposition gradient of air pollutants in eastern Germany. Water Air Soil Pollut. 85:1191–1196; 1995.

Nadelhoffer, K.J.; Downs, M.R.; Fry, B.; Aber, J.D.; Magill, A.H.; Melillo, J.M. The fate of ^{15}N-labeled nitrate additions to a northern hardwood forest in eastern Maine, USA. Oecologia 103:292–301; 1995.

Nannipieri, P.; Ciardi, C.; Palazzi, T. Plant uptake, microbial immobilization, and residual soil fertilizer of urea-nitrogen in a grass-legume association. Soil Sci. Soc. Am. J. 49:452–457; 1985.

Nommik, H.; Pluth, D.J.; Larsson, K.; Mahendrappa, M.K. Isotopic fractionation accompanying fertilizer nitrogen transformations in soil and trees of a Scots pine ecosystem. Plant Soil 158:169–182; 1994.

Norton, J.M.; Firestone, M.K. N dynamics in the rhizosphere of *Pinus ponderosa* seedlings. Soil Biol. Biochem. 28:351–362; 1996.

Pilbeam, C.J.; McNeill, A.M.; Harris, H.C.; Swift, R.S. Effect of fertilizer rate and form on the recovery of ^{15}N-labeled fertilizer applied to wheat in Syria. J. Agric. Sci. 128:415–424; 1997.

Power, J.F.; Wilhelm, W.W.; Doran, J.W. Recovery of fertilizer nitrogen by wheat as affected by fallow method. Soil Sci. Soc. Am. J. 50:1499–1503; 1986.

Preston, C.M.; Mead, D.J. Growth response and recovery of ^{15}N-fertilizer one and eight growing seasons after application to lodgepole pine in British Columbia. For. Ecol. Manage. 65:219–229; 1994.

Randlett, D.L.; Zak, D.R.; Macdonald, N.W. Sulfate adsorption and microbial immobilization in northern hardwood forests along an atmospheric deposition gradient. Can. J. For. Res. 22:1843–1850; 1992.

Rastetter, E.B.; Shaver, G.R. A model of multiple element limitation for acclimating vegetation. Ecology 73(4):1157–1174; 1992.

Recous, S., Machet, J.M.; Mary, R. The partitioning of fertilizer-N between soil and crop: Comparison of ammonium and nitrate applications. Plant Soil 144:101–111; 1992.

Redfield, A.C. The biological control of chemical factors in the environment. Am. Sci. 46:205–221; 1958.

Rogers, K.H.; Breen, P.F.; Chick, A.J. Nitrogen removal in experimental wetland treatment systems: Evidence for the role of aquatic plants. Res. J. Water Pollut. Contr. Fed. 63:934–941; 1991.

Rutherford, P.M.; Juma, N.G. Effect of glucose amendment on microbial biomass, spelling fertilizer ^{15}N-recovery and distribution in a barley-soil-system. Biol. Fertil. Soils 12:228–232; 1992.

Schimel, D.S. *Theory and application of Tracers.* New York: Academic; 1993.

Schlesinger, W.H. *Biogeochemistry: An Analysis of Global Change.* New York: Academic; 1997.

Shaver, G.R.; Chapin, F.S., III. Response to fertilization by various plant growth forms in an Alaskan tundra: Nutrient accumulation and growth. Ecology 61:662–675; 1980.

Shaver, G.R.; Chapin, F.S., III, Gartner, B.L. Factors limiting seasonal growth and peak biomass accumulation in *Eriophorum vaginatum* in Alaskan tussock tundra. J Ecol. 74:257–278; 1986.

Shaver, G.R.; Chapin, F.S., III. Long-term responses to factorial NPK fertilizer treatment by Alaskan wet and moist tundra sedge species. Ecography 18:259–275; 1995.

Shock, C.C.; Jones, M.B.; Williams, W.A.; Center, D.M. Effect of sulfur fertilization on three annual range species I. Laughlin soil experiment. Agron. J. 75:515–520; 1983.

Stamford, N.P.; Ortega, A.D.; Temprano, F.; Santos, D.R. Effects of phosphorus fertilization and inoculation of Bradyrhizobium andmycorrhizal fungi on growth of Mimosa caesalpiniaefolia in an acid soil. Soil Biol. Biochem. 29:959–964; 1997.

Tamm, C.O. Some observations on nutrient turnover in a bog community dominated by *Eriophorum vaginatum* L. Oikos 5:189–194; 1954.

Tanner, E.V.J.; Vitousek, P.M.; Cuevas, E. Experimental investigation of nutrient limitation of forest growth on wet tropical mountains. Ecology 79:10–22; 1998.

Tilman, D. Plant strategies and the dynamics and function of plant communities. Princeton, NJ: Princeton Univ. Pr.; 1988.

Tisdale, S.L.; Nelson, W.L.; Beaton, J.D.; Havlin, J.L. Soil fertility and fertilizers. New York: Macmillan; 1993.

Vaast, P.; Zasoski, R.J. Effects of Va-mycorrhizae and nitrogen sources on rhizosphere soil characteristics growth and nutrient acquisition of coffee seedlings *Coffea arabica* L. Plant Soil 147:31–39; 1992.

van Breemen, N.; van Dijk, H.F.G. Ecosystem effects of atmospheric deposition of nitrogen in the Netherlands. Environ. Pollut. 54:249–274; 1988.

van den Driessche, R. Prediction of mineral nutrient status of trees by foliar analysis. Botan. Rev. 40:347–394; 1974.

Vitousek, P.M.; Howarth, R.W. Nitrogen limitation on land and in the sea: How can it occur? Biogeochemistry 13:87–115; 1991.

Vitousek, P.M.; Farrington, H. Nutrient limitation and soil development: Experimental test of a biogeochemical theory. Biogeochemistry 37:63–75; 1997.

Vitousek, P.M.; Aber, J.; Howarth, R.W.; Likens, G.E.; Matson, P.A.; Schindler, D.W.; Schlesinger, W.H.; Tilman, G.D. Human alterations of the global nitrogen cycle: Causes and consequences. Issues in Ecology. 1. 1997.

Walker, T.W.; Syers, J.K. The fate of phosphorus during pedogenesis. Geoderma 15:1–19; 1976.

Wedin, D.; Tilman, D. Competition among grasses along a nitrogen gradient: Initial conditions and mechanisms of competition. Ecol. Monogr. 63:199–229; 1993.

Willems, J.H.; Peet, R.K.; Bik, L. Changes in chalk-grassland structure and species richness resulting from selective nutrient additions. J. Vegetat. Sci. 4:203–212; 1993.

Wilson, E.J.; Skeffington, R.A. The effects of excess nitrogen deposition on young Norway spruce trees. I. The soil. Environ. Pollut. 86:141–151; 1994.

Woodin, S.J. Effects of acid deposition on arctic vegetation. In: Woodin, S.J.; Marquiss, M. eds. *Ecology of Arctic Environments.* Oxford: Blackwell; 1997:219–239.

Yarie, J.; Van Cleve, K. Effects of carbon, fertilizer and drought on foliar nutrient concentrations of taiga tree species in interior Alaska. Ecol. Applic. 6:815–827; 1996.

Young, R.D.; Westfall, D.G.; Colliver, G.W. Production, marketing and use of phosphorus fertilizers. In: Engelstad, O.P., ed. *Fertilizer Technology and Use.* 3rd ed. Madison, WI: Soil Science Society of America; 1985:324–376.

20

Biotic Manipulations of Aquatic Ecosystems

Daniel E. Schindler, Brian R. Herwig, and Stephen R. Carpenter

Introduction

Large-scale biotic manipulations have been performed in aquatic habitats to evaluate how ecosystem structure alters processes and dynamics. These experiments have involved either direct manipulation of species or the habitat structure that mediates species interactions. Manipulations at smaller experimental scales can not encompass the natural biology of wide-ranging species or the system-level heterogeneity that has critical effects on the interactions between community and ecosystem dynamics (e.g., Schindler et al. 1997). Manipulations of aquatic ecosystems are often used to explore the responses of possible management actions or, in fact, are large management experiments (e.g., Kitchell 1992; Hansson et al. 1998; Olson et al. 1998). In this chapter we review briefly some of the techniques used in controlled experimental settings and in natural resource management that have involved biotic manipulations of aquatic ecosystems. We also discuss some considerations for design of ecosystem experiments, and refer to important directions for future ecosystem research. We have limited our review to experiments in freshwater systems, and cite only selected examples of biotic manipulations. For more detailed descriptions of some of the methods we discuss, readers should consult Nielsen and Johnson (1983), Downing and Rigler (1984), and Cooke et al. (1993).

Manipulations of Species

Manipulations of species in ecosystems involve either supplementation or removal of existing populations, or introductions of novel species. Both types of manipulations usually aim to restructure food webs to determine the consequences for ecosystem processes. Although some manipulations have involved introduction of exotic species, we urge extreme caution in such experiments and encourage careful consideration of potential ecological damage that may result (Li and Moyle 1981).

Species Removals

Manipulations that remove a single species are difficult to perform. Most removals impact a broad spectrum of ecologically similar species. Elimination of fishes is usually accomplished by physical removal, application of chemical piscicides, or a combination of both (Meronek et al. 1996). Methods for physical removal include use of seines, gill nets, trawls, trap nets, electrofishing, angling, and water drawdowns. In shallow systems, the efficiency of electrofishing and seining can be improved by using blocking nets to minimize gear avoidance (Moss et al. 1996). These methods are generally labor intensive and are only moderately successful because of difficulties in removing all individuals from a population. Physical removal is most effective if spawning aggregations allow mass removal of the target species. Physical removal methods are preferred over chemical treatment if the fishes are to be transferred to another system, or temporary perturbation of the entire community, including nontarget species, is not desired.

Physical removal experiments should include a monitoring program that allows estimation of the magnitude of the manipulation. The easiest way to accomplish this is by monitoring the change in a

standardized catch rate as the removal manipulation proceeds (Fig. 20.1). Fisheries biologists have derived relatively straightforward methods of estimating abundance with such "depletion methods" (Hilborn and Walters 1992).

Application of chemicals such as rotenone or antimycin is very effective at removing fishes from aquatic systems. These piscicides can be purchased from aquaculture and fisheries supply companies who also provide detailed instructions for application. Chemical piscicides are usually not species-specific and often have detrimental effects on invertebrate communities (e.g., Cushing and Olive 1957; Anderson 1970). An exception to this is the removal of the sea lamprey from lakes by application of a toxicant that prevents development of ammocetes in natal streams, with only subtle effects on other fishes and invertebrates (Meyer and Schnick 1983). In the case of rotenone treatment, addition of about 1 mg liter^{-1} when water temperatures are about 20°C should produce a complete fish kill. Rotenone inhibits oxygen uptake in fish, causing them to swim to the surface within minutes of application where they can be netted and resuscitated by transfer to dilute solutions of methylene blue or potassium permanganate (Nielsen and Johnson 1983). In general, manipulations with piscicides require several weeks to months for invertebrates to recover following treatment. If a manipulation involves piscicide treatment followed by stocking, periodic monitoring with caged specimens should be used to establish degradation of the piscicide before restocking.

Removal of invertebrates from streams has been accomplished by application of chemical insecticides (e.g., Malathion; Wallace et al. 1986). In these experiments, perturbations to invertebrates were maintained for over 2 years. Chemical pesticides generally do not allow removal of individual taxa or functional groups. Application of insecticidal bacteria may allow more taxon-specific manipulations in aquatic ecosystems (e.g. Merritt et al. 1989; Wipfli and Merritt 1994). However, specificity of such treatments are limited to only a few functional groups (e.g., Simuliidae). In small ponds, physical removal of aquatic insect predators was successfully accomplished by repeated seining with fine mesh nets (Herwig and Schindler 1996).

Species Introductions

Stocking manipulations to enhance existing populations or introduce novel species to aquatic ecosystems have a long and impressive history in eco-

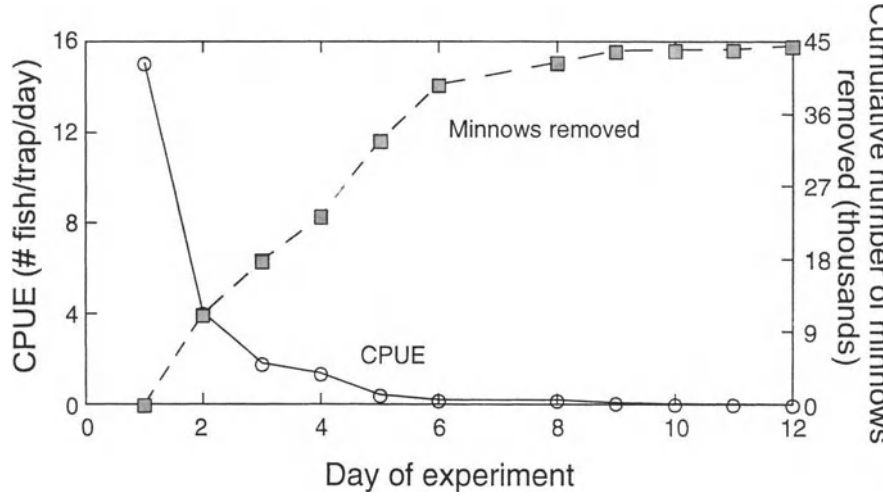

FIGURE 20.1. Changes in catch rate of minnows with galvanized minnow traps (CPUE), and cumulative number of individuals removed during an experimental manipulation to eliminate planktivorous fishes from Tuesday Lake, Michigan (Carpenter and Kitchell 1993a). Population size can be calculated by comparing the decrease in catch rate as a function of the number of fish removed at any time during the experiment, and serves to monitor the magnitude of the manipulation.

system experimentation (Northcote 1988). Unlike species removal experiments, stocking can be taxon-specific. Some knowledge of the natural history of the organism (e.g., spawning habitat, thermal requirements) should allow evaluation of whether the experimental system is habitable. The cheapest method to add new species is to introduce a small spawning stock and let nature take its course. This is especially effective when stocking piscivorous fishes into systems that lack other large predators (e.g., Carpenter and Kitchell 1993a; Brabrand and Faafeng 1993). In ecosystems with public access, cooperation with regulatory agencies to restrict exploitation may be needed to ensure successful introductions of game fishes (Kitchell 1992; Benndorf et al. 1988). Intensive stocking of juveniles can also establish the target species at the desired population density. This method can be very expensive because the cost of fish increases substantially with age (Madenjian et al. 1991). Manipulations to alter food web structure in systems dominated by omnivorous fishes with high reproductive capacity (e.g., carp, *Cyprinus carpio;* gizzard shad, *Dorosoma cepedianum;* roach, *Rutilis rutilis*), may require a combination of piscivore stocking and physical removal of resident species to alter community composition (e.g., Shapiro and Wright 1984; Kasprzak et al. 1993; Meijer et al. 1994; Hansson et al. 1998). Prey fish introductions to lakes with large predator populations are unlikely to be successful without removal of some of the predators.

Detailed descriptions of fish stocking techniques are found in Nielsen and Johnson (1983). General rules of thumb for minimizing stress to stocked fishes are: (1) stock when water temperature is cold, (2) prevent thermal shock by minimizing temperature differences between collection site, holding water, and stocking site, (3) keep holding water well aerated (>5 mg liter^{-1} O_2), (4) minimize handling stress during capture and holding, and (5) treat fish with a general external antibiotic or parasiticidal solution prior to stocking.

Ecosystem-scale stocking of invertebrates has not been done as often as fish stocking. Notable exceptions to this are the stocking of *Mysis relicta* throughout western North America and Scandinavia (Lasenby et al. 1986), amphipods (Hill et al. 1990) and calanoid copepods in alpine lakes (McNaught et al. 1999). In these experiments, relatively small numbers of reproductively mature individuals were collected with trawls or large nets, transported in cold water, and stocked into experimental ecosystems.

Inadvertent introductions of species to aquatic systems also represent potential learning opportunities at the ecosystem scale. For example, the rainbow smelt (*Osmerus mordax*) (Hrabik et al. 1998) and the rusty crayfish (*Orconectes rusticus*) (Capelli 1982) have invaded and greatly altered ecosystem structure in lakes throughout the upper Midwest in the United States. When coupled with small-scale experiments or process studies, invasions often offer insight into the mechanisms by which exotics alter ecosystem structure and function. However, studies of inadvertent introductions are not as powerful as direct ecosystem manipulations because species may be present for several years before being detected, and preinvasion and reference data may not be available for use in statistical analyses of the effects of invasion. Studies of inadvertent introductions and the effects of other human activities are most valuable when treated as case studies rather than as controlled experiments. Case studies at the ecosystem scale represent important opportunities for learning in ecosystem ecology and conservation (Schrader-Frechette and McCoy 1993), but are not an alternative to direct ecosystem manipulation.

Habitat Manipulations

Macrophyte Restoration and Removal in Lakes

Macrophyte manipulations have been an important arena for ecosystem experiments in systems where exotic plants have proliferated and often displaced native species, and others where native plants have been lost due to eutrophication and human development. Macrophyte manipulations are often performed to determine their effects on other processes such as eutrophication (Moss et al. 1996) and fish production (Carpenter et al. 1997). In systems with extensive macrophytes, plant removal is generally accomplished through water-level drawdown, dredging, mechanical cutting, raking and derooting, or application of herbicides (Cooke et al. 1993).

Mechanical methods and herbicides are probably the most effective, but are usually not taxon-specific. Consideration of the spatial pattern of macrophyte removal should be included in the experimental design because the geometry of remaining macrophyte beds may have important implications for how other parts of the system respond to manipulation. For example, the amount of edge habitat produced by mechanical cutting of macrophyte beds affects the nature of predator–prey interactions among littoral zone fishes and their prey (Trebitz and Nibbelink 1996). Water level regulation is viable in reservoirs where exposure of root systems to drying and/or freezing can have species-specific effects (Cooke et al. 1993).

Macrophyte introduction is usually accomplished by transplanting healthy cuttings, tubers, or rosettes to the system to be restored. This process is labor intensive and will only succeed if water and sediment chemistry are appropriate for the species of interest, and if light availability is high enough to support plant growth. In systems where large herbivores such as grass carp or waterfowl will impede macrophyte restoration, these must be removed or excluded from areas where macrophyte growth is desired (Lauridsen et al. 1993; Cooke et al. 1993).

Restoration of Other Structural Features

Manipulations of structural features of aquatic ecosystems have been designed to evaluate how habitat architecture affects ecosystem processes. Large woody debris and rock formations are important structural features of aquatic ecosystems (Johnson and Stein 1979; Harmon et al. 1986) that are a focus for ecosystem restoration (NRC 1992). Large woody debris has been depleted in many rivers and lakes due to loss of riparian trees and active removal from inshore habitats (Maser and Sedell 1994; Christensen et al. 1996). Loss of rock formations can result from channel straightening and simplification of fluvial systems, and from water-level change and structure removal in lakes. These losses of structural features have important implications for hydrology, nutrient cycling, and predator–prey interactions. Most experiments have been performed in streams with the goal of evaluating the effects on fish production. These manipulations have involved construction of crosschannel log sills (Gowan and Fausch 1996), boulder groupings, cobble-filled wire gabions, and other current deflectors (House and Boehne 1985; Moore and Gregory 1988), and replacement of large woody debris (Hilderbrand et al. 1998). Large-scale manipulation of structural features such as large woody debris to determine their effects on ecosystem processes is an important avenue for future research in all aquatic habitats and is critical to restoration of many aquatic ecosystems (Hilderbrand et al. 1998).

Wetland Restoration

Extensive loss of wetlands has focused the attention of scientists and managers on restoration of disturbed sites throughout North America and Europe (Zedler 1996). A call for experimental approaches through use of reference systems and extensive postmanipulation monitoring (Brinson and Rheinhardt 1996) likens mitigation efforts to ecosystem experiments. Although the methods of wetland restoration are extensive and often site-specific, some general principles are useful. Most wetland restoration projects involve restoration of the natural hydrology, elimination of contaminants and pollutants, and reestablishment of lost species (NRC 1992). Revegetation may require active seeding because of depleted seed banks in many restored wetlands (Galatowitsch and van der Valk 1996). The appropriate time frame to evaluate the result of a wetland restoration effort is debatable, but usually underestimated (Mitsch and Wilson 1996). By putting wetland restoration into an adaptive management context (Gunderson et al. 1995), the appropriate time frame becomes a dependent variable in these ecosystem manipulations.

Simulation Modeling, Manipulation Strength, and Statistical Power

Simulation modeling is a powerful tool for planning ecosystem experiments, exploring possible responses to manipulations, and interpreting results (Kitchell 1992; Carpenter and Kitchell 1993b; Scheffer 1997; Trebitz et al. 1997). Modeling is especially valuable in the implementation of management experiments because it helps crystallize

goals and hypotheses, and provides a mechanism with which to gain consensus among managers and scientists about experimental design and manipulation strength (Trebitz et al. 1997).

Ecosystem manipulations should be substantial and sustained to interpret responses in inherently variable natural systems. Substantial manipulations span the natural range of the independent variable. Sustained manipulations are continued for several generations or turnover times of the dependent variables.

Experiments to study trophic cascades in lakes illustrate these principles (Fig. 20.2). Trophic cascades derive from shifts in the fish community, which pass through the food web to affect primary producers (Carpenter and Kitchell 1993a). To produce a cascade, shifts in the fish community must be large enough to change the dominance of large-bodied *Daphnia* species. Large-bodied *Daphnia* have broad diets, rapid population growth that enables them to track changes in primary producers, and low rates of phosphorus excretion that exacerbate phosphorus limitation of primary producers. Therefore increases in large-bodied *Daphnia* reduce biomass of primary producers, while decreases in large-bodied *Daphnia* are followed by increased biomass of primary producers. The new zooplankton community must be sustained for months to years to yield a convincing change in primary producer biomass.

Simulation studies show that the probability of detecting responses of primary production depends on the nature of the manipulation (press pulse) (Bender et al. 1984) and the magnitude of change in piscivore biomass (see Figure 20.2). In press experiments, piscivore biomass was changed and held at the new level for 5 years. In pulse experiments, piscivore biomass was changed for only 1 year. In press experiments, the probability of detecting changes in primary producers was near maximal when piscivore biomass was changed by at least 3-fold (increased by a factor of 3, or decreased by a factor of a third). In pulse experiments, the probability of detecting effects of piscivore reductions was always low. For piscivore increases, pulse experiments were about as effective as press experiments if piscivore biomass was increased 5-fold or more. Experience from management-oriented biomanipulation experiments suggests that at least 75% of planktivorous fish should be removed from lakes to achieve the desired piscivore-dominated, clear water state (Hansson et al. 1998). In many cases, the strength of these manipulations is further enhanced by stocking piscivores at the same time

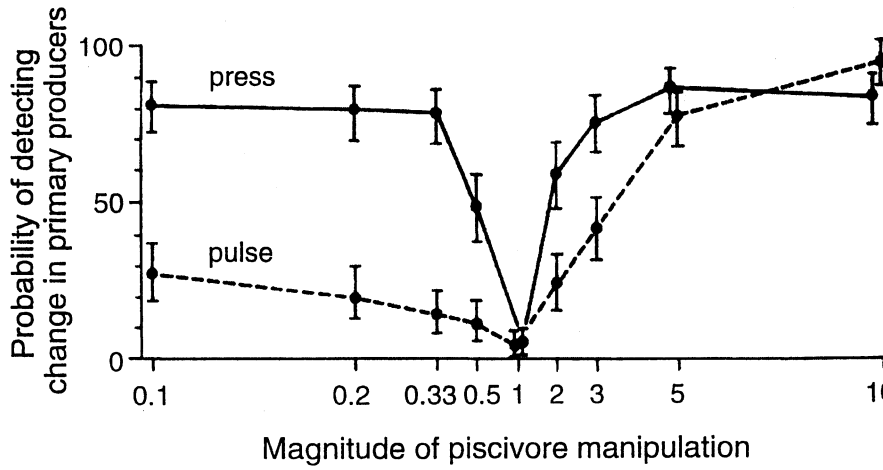

FIGURE 20.2. Probability of detecting changes in primary producers versus magnitude of piscivore manipulation (posttreatment piscivore biomass/pretreatment piscivore biomass). Probabilities were calculated by Monte Carlo analysis of a simulation model fit to results from whole-lake experiments, under the assumption that five lakes were manipulated and five lakes served as reference ecosystems. (Redrawn from Carpenter 1989. Copyright by the Ecological Society of America. Used by permission.)

that the planktivores are removed (Hansson et al. 1998).

Most biotic manipulations of aquatic ecosystems have been performed to estimate the magnitude and variability of responses (i.e., ecological significance) rather than to test null hypotheses (i.e., statistical significance) (Carpenter et al. 1995a). Although it would be valuable to repeat the same manipulation in several similar ecosystems (e.g., Bystrûm et al. 1998) this type of replication is often impossible. It is possible to measure the response in one manipulated ecosystem (Stewart-Oaten et al. 1986; Carpenter et al. 1989; Carpenter and Kitchell 1993a). To check alternative explanations for the results, reference systems or additional manipulations should be included in the experimental design (Stewart-Oaten et al. 1986; Walters et al. 1989).

In some situations, the null hypothesis of no response must be carefully considered. These situations raise questions of statistical power, or the probability of detecting an effect that genuinely exists (McAllister and Peterman 1992). Statistical power depends on the variance of the dependent variables, the minimum magnitude of response that the experiment is intended to detect, and number of replicates. Replication may occur in space (by manipulating several ecosystems) or in time (Stewart-Oaten et al. 1986; Walters et al. 1989, McAllister and Peterman 1992). Although consideration of statistical power is becoming more prevalent in the planning of replicated, small-scale experiments, statistical power has rarely been estimated for replicated ecosystem experiments. Where spatial replication is possible, two studies suggest that about 10 lakes (5 treatment, 5 reference) provide adequate power for experiments on trophic cascades and effects of habitat manipulation on fish growth (Carpenter 1989; Carpenter et al. 1995b). In cases in which temporal replication is employed, long time series before and after press treatments will maximize the prospects for detecting any effects that occur. Sequences of manipulation may increase the power. We are not aware of any formal power calculations for time series analyses of ecosystem experiments. Experience suggests that effects can be detected with time series of about 80 or more observations, provided that autocorrelation is small (Carpenter et al. 1989; Carpenter and Kitchell 1993b). In some situations, similar ecosystem experiments have been performed by different research teams on very different ecosystems. Joint analyses of these similar experiments (meta-analyses) could be very instructive.

Future Prospects

Field Guide to Keystones

Keystone species are central to understanding how ecosystem structure is linked to processes. Power et al. (1996) emphasize that keystones cannot be identified reliably on the basis of biomass, productivity, nutrient content, or other indices of dominance. The field mark of a keystone is high sensitivity of ecosystem processes to changes in the keystone's abundance. They define a keystone species as one "whose impact on its community or ecosystem is large, and disproportionately large relative to its abundance" (Power et al. 1996). A number of attributes of keystones are identifiable from basic ecology and natural history (Jones and Lawton 1995; Power et al. 1996). However, field experiments are necessary to determine which species are keystones and to measure their effects (Paine 1980). Keystone species will often be wide-ranging, long-lived species that control, or are controlled by, spatially extensive processes or processes with long turnover times. Impacts of keystone species are often transmitted through complex, indirect effects among interacting species (Power et al. 1996). Because indirect effects are often mediated by the behaviors of wide-ranging species and by habitat heterogeneity (Wootton 1994), many keystone interactions are impossible to study in small-scale or brief experiments. Ecosystem manipulation is the only real option for studying such keystone species.

Humans and Ecosystems

Humans are usually ignored or treated only as independent variables (sources of pollutants or agents of perturbation) in ecosystem experiments. In fact, humans are a dominant component of most ecosystems and interact (act as both independent and dependent variables) with other system components (McDonnel and Pickett 1993).

Some of the best examples of people as interactive ecosystem components come from fisheries

(Hilborn et al. 1995). Fisheries management involves fishers, fish, and the ecosystems in which they are embedded. Therefore, management experiments inevitably include the human dimension.

People are highly responsive top predators capable of restructuring lake fish communities and creating trophic cascades that alter entire food webs and ecosystem processes (Kitchell 1992; Carpenter and Kitchell 1993a). Lake Mendota, Wisconsin, was stocked with walleyes as part of a large biomanipulation experiment (Kitchell 1992). Publicity associated with the project attracted skilled anglers who accounted for increasing effort and catch rates from 1987 through 1989 (Fig. 20.3, Johnson and Carpenter 1994). Catch rates continued to rise in 1990. In 1991, catch rates dropped substantially. It is likely that declining catch rates were caused by high recruitment of forage fishes, which made artificial lures and live bait less attractive to walleyes. However, angler effort showed little response to low catch rates in 1991. By 1992, catch rates returned to high levels and angler effort continued to be relatively high. Sustained fishing despite declining catch rates is well known from commercial fisheries (Hilborn et al. 1995). The Lake Mendota experience shows that sport fishers, like commercial fishers, respond strongly to perceived opportunities and keep fishing during periods of low success.

Experiments that address the responses of people to changes in other ecosystem components as well as the effects of people on other ecosystem components have an important future in ecosystem ecology. Such experiments may lead to new crossdisciplinary linkages of ecology and social sciences.

Adaptive Management

Management agencies routinely perform large-scale manipulations of ecosystems. In most cases there is considerable uncertainty about the consequences of these management activities. In fact, environmental policies are research questions masquerading as answers (Gunderson et al. 1995). Environmental impact statements are hypotheses that are usually never tested (Orians 1986). Management activities or other human interventions are powerful manipulations from which we could learn a great deal if they were run as experiments.

In order to convert management actions to learning opportunities, information needs to be collected and interpreted. Experimentation involves monitoring both before and after the manipulation, of both manipulated and reference ecosystems if possible.

In order to manage adaptively, learning needs to be incorporated into future management actions. Adaptive management would provide institutional mechanisms for running experiments as partnerships of science and management, and integrating new knowledge into future management practice.

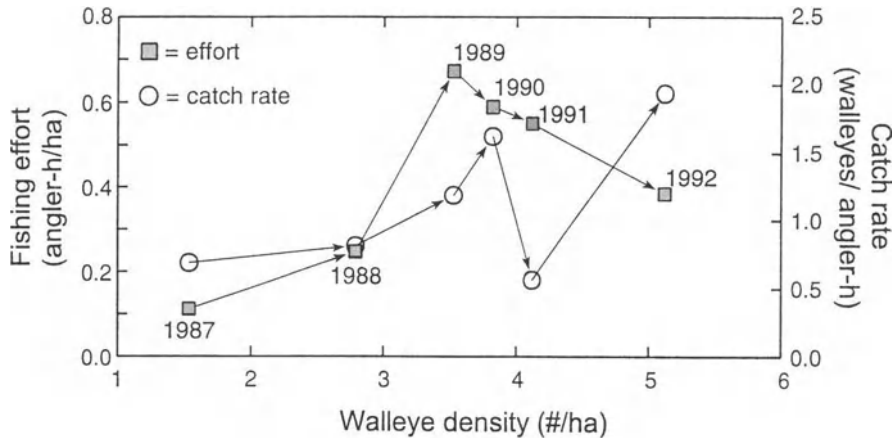

FIGURE 20.3. Fishing effort and catch rates by anglers, as a function of walleye (*Stizostedion vitreum vitreum*) density in Lake Mendota, Wisconsin, 1986 to 1992. Walleyes were stocked at the beginning of the fishing season in 1987, 1988, and 1989. (Data from Johnson and Carpenter 1994.)

Although the notion of using management activity as a learning exercise to improve future policies has been explicit since the 1970s, experience has been spotty and adaptive ecosystem management remains an important frontier of ecosystem science (Gunderson et al. 1995).

Many of the methods commonly used in biotic manipulations of aquatic ecosystems have not changed much in the past several decades. The current popularity of stable isotope tracers in ecological experiments is one example of a technique that has recently become more accessible to experimental ecologists. New techniques will certainly have important roles in future ecosystem experiments that involve biotic manipulations. However, we think that the development of interesting and relevant ecosystem experiments in the future will not be constrained by methodology. Instead, the development of large-scale experiments that span the scientific disciplines relevant to management, include human dimensions, and probe the functional importance of certain species to ecosystem functioning are the key to success of future ecosystem experiments.

Acknowledgments We thank Marty Berg for information about experiments in streams, and the National Sciences Foundation and the Wisconsin Department of Natural Resources for support. Sture Hansson, Dick Lathrop and David Lewis provided helpful reviews of the manuscript.

References

Anderson, R.S. Effects of rotenone on zooplankton communities and study of their recovery patterns in two mountain lakes in Alberta. J. Fish. Res. Board Can. 27:1335–1356; 1970.

Bender, E.A.; Case, T.J.; Gilpin, M.E. Perturbation experiments in community ecology: Theory and practice. Ecology 65:1–13; 1984.

Benndorf, J.; Schultz, H.; Benndorf, A.; Unger, R.; Penz, E.; Kneschke, H.; Kossatz, K.; Dumke, R.; Horning, U.; Kruspe, R.; Reichel, S. Food-web manipulation by enhancement of piscivorous fish stocks: Long-term effects in the hypertrophic Bautzen Reservoir. Limnologica (Berlin) 19:97–110; 1988.

Brabrand, A.; Faafeng, B. Habitat shift in roach (*Rutilus rutilus*) induced by pikeperch (*Stizostedion lucioperca*) introduction: Predation risk versus pelagic behavior. Oecologia 95:38–46; 1993.

Brinson, M.M.; Rheinnhardt, R. The role of reference wetlands in functional assessment and mitigation. Ecol. Applic. 6:69–76; 1996.

Bystrûm, P.; Persson, L.; Wahlstrûm, E. Competing predators and prey: Juvenile bottlenecks in whole-lake experiments. Ecology 79:2153–2167; 1998.

Capelli, G.M. Displacement of northern Wisconsin crayfish by *Orconectes rusticus* (Girard). Limnol. Oceanogr. 27:741–745; 1982.

Carpenter, S.R. Replication and treatment strength in whole-lake experiments. Ecology 70:453–463; 1989.

Carpenter, S.R.; Chisholm, S.W.; Krebs, C.J.; Schindler, D.W.; Wright, R.F. Ecosystem experiments. Science 269:324–327; 1995a.

Carpenter, S.R.; Cunningham, P.; Gafny, S.; Munoz del Rio, A.; Nibbelink, N.; Pellett, T.; Storlie, C.; Trebitz, A.; Wilson, K. Responses of bluegill to habitat manipulations: Power to detect effects. N. Am. J. Fish. Manage. 15:519–527; 1995b.

Carpenter, S.R.; Frost, T.M.; Heisey, D.; Kratz, T.K. Randomized intervention analysis and the interpretation of whole ecosystem experiments. Ecology 70:1142–1152; 1989.

Carpenter, S.R.; Kitchell, J.F., eds. *The Trophic Cascade in Lakes.* London: Cambridge Univ. Pr.; 1993a.

Carpenter, S.R.; Kitchell, J.F. Simulation models of the trophic cascade: Predictions and evaluations. In: Carpenter, S.R.; Kitchell, J.F., eds. *The Trophic Cascade in Lakes.* London: Cambridge Univ. Pr.; 1993b.

Carpenter, S.R.; Olson, M.; Cunningham, P.; Gafny, S.; Nibbelink, N.; Pellett, T.; Storlie, C.; Trebitz, A.; Wilson, K. Macrophyte structure and growth of bluegill (*Lepomis macrochirus*): Design of a multi-lake experiment. In: Jeppeson, E.; Christoffersen, K.; Søndergaard, M., eds. *The Role of Submerged Macrophytes in Structuring Lakes.* New York: Springer-Verlag; 1997.

Cooke, G.D.; Welch, E.B.; Peterson, S.A.; Newroth, P.R. *Restoration and Management of Lakes and Reservoirs.* 2nd ed. Boca Raton, FL: CRC; 1993.

Christensen, D.L.; Herwig, B.R.; Schindler, D.E.; Carpenter, S.R. Impacts of lakeshore residential development on coarse woody debris in north temperate lakes. Ecol. Applic. 6:1143–1149; 1996.

Cushing, C.E.; Olive, J.R. Effects of toxaphene and rotenone upon the macroscopic bottom fauna of two northern Colorado reservoirs. Trans. Am. Fish. Soc. 86:294–301; 1957.

Downing, J.A.; Rigler, F.H., eds. *A Manual on Methods for the Assessment of Secondary Productivity in Fresh Waters.* 2nd ed. Oxford: Blackwell; 1984.

Galatowitsch, S.M.; van der Valk, A.G. The vegetation of restored and prairie wetlands. Ecol. Applic. 6:102–112; 1996.

Gowan, C.; Fausch, K.D. Long-term demographic responses of trout populations to habitat manipulation in six Colorado streams. Ecol. Applic. 6:931–946; 1996.

Gunderson, L.H.; Holling, C.S.; Light, S.S. *Barriers and Bridges to the Renewal of Ecosystems and Institutions.* New York: Columbia Univ. Pr.; 1995.

Hansson, L.-A.; Annadotter, H.; Bergman, E.; Hamrin, S.F.; Jeppesen, E.; Kairesalo, T.; Luokkanen, E.; Nilsson, P.; Søndergaard, M. Biomanipulation as an application of food chain theory: Constraints, synthesis and recommendations for temperate lakes. Ecosystems 1:558–574; 1998.

Harmon, M.E.; Franklin, J.F.; Swanson, F.J.; Sollins, P.; Gregory, S.V.; Lattin, J.D.; Anderson, N.H.; Cline, S.P.; Aumen, N.G.; Sedell, J.R.; Lienkaemper, G.W.; Cromack, K., Jr.; Cummins, K.W. Ecology of coarse woody debris in temperate ecosystems. Adv. Ecol. Res. 15:133–302; 1986.

Herwig, B.R.; Schindler, D.E. Effects of aquatic insect predators on zooplankton in fishless ponds. Hydrobiologia 324:141–147; 1996.

Hilborn, R.; Walters, C.J. *Quantitative Fisheries Stock Assessment: Choice, Dynamics and Uncertainty.* New York: Chapman and Hall; 1992.

Hilborn, R.; Walters, C.J.; Ludwig, D. Sustainable exploitation of renewable resources. Annu. Rev. Ecol. Syst. 26:45–67; 1995.

Hilderbrand, R.H.; Lemly, A.D.; Dolloff, C.A.; Harpster, K.L. Design considerations for large woody debris placement in stream enhancement projects. N. Am. J. Fish. Manage. 181:161–161; 1998.

Hill, C.; Fürst, M.; Hammar, J. Introduction of the amphipods *Pallasea quadrispinosa* and *Gammaracanthus lacustris* into lakes in northern Sweden. Ann. Zool. Fennici 27:241–244, 1990.

House, R.A.; Boehne, P.L. Evaluation of instream enhancement structures for salmonid spawning and rearing in a coastal Oregon stream. N. Am. J. Fish. Manage. 5:283–295; 1985.

Hrabik, T.R.; Magnuson, J.J.; McLain, A.S. Predicting the effects of rainbow smelt on native fishes in small lakes: Evidence from long-term research on two lakes. Can. J. Fish. Aquat. Sci. 55:1364–1371; 1998.

Johnson, B.M.; Carpenter, S.R. Functional and numerical responses: A framework for fish-angler interactions? Ecol. Applic. 4:808–821; 1994.

Johnson, D.L.; Stein, R.A., editors. *Response of Fish to Habitat Structure in Standing Water.* Special Publication 6. Bethesda, MD: American Fisheries Society, North Central Division; 1979.

Jones, C.G.; Lawton, J.H. *Linking Species and Ecosystems.* New York: Chapman and Hall; 1995.

Kasprzak, P.; Krienitz, L.; Koschel, R. Changes in the plankton of Lake Feldberger Haussee (Germany, Maecklenburg-Vorpommern) in response to biomanipulation. Arch. Hydrobiol. 128:149–168; 1993.

Kitchell, J.F., ed. *Food Web Management: A Case Study of Lake Mendota.* New York: Springer-Verlag; 1992.

Lasenby, D.C.; Northcote, T.G.; Fürst, M. Theory, practice and effects of *Mysis relicta* introductions to North American and Scandinavian lakes. Can. J. Fish. Aquat. Sci. 43:1277–1284; 1986.

Lauridsen, T.L.; Jeppesen, E.; Andersen, F.O. Colonization of submerged macrophytes in shallow fish manipulated Lake Vaeng: Impact of sediment composition and waterfowl grazing. Aquat. Bot. 46:1–15; 1993.

Li, H.W.; Moyle, P.B. Ecological analysis of species introductions into aquatic systems. Trans. Am. Fish. Soc. 110:772–782; 1981.

McDonnel, M.J.; Pickett, S.T.A., Eds. *Humans as Components of Ecosystems.* New York: Springer-Verlag; 1993.

Madenjian, C.P., Johnson, B.M.; Carpenter, S.R. Stocking strategies for fingerling walleyes: An individual-based model approach. Ecol. Applic. 1:280–288; 1991.

Maser, C.; Sedell, J.R. *From the Forest to the Sea.* Delray Beach, FL: St. Lucie; 1994.

McAllister, M.K.; Peterman, R.M. Experimental design in the management of fisheries: A review. N. Am. J. Fish. Manage. 12:1–18; 1992.

McNaught, A.J.; Schindler, D.W.; Parker, B.R.; Paul, A.J.; Anderson, R.S.; Donald, D.B.; Agbeti, M. Restoration of the food web of an alpine lake following trout stocking. Limn Ocean 44:127–136; 1999.

Meijer, M-L.; van Nes, E.H.; Lammens, E.H.R.R.; Gulati, R.D.; Grimm, M.P.; Backx, J.; Hollebeek, P.; Blaauw, E.M.; Breukelaar, A.W. The consequences of a drastic fish stock reduction in the large and shallow Lake Wolderwijd, The Netherlands. Can we understand what happened? Hydrobiologia 275/276:31–42; 1994.

Meronek, T.G.; Bouchard, P.M.; Buckner, E.R.; Burri, T.M.; Demmerly, K.K.; Hatleli, D.C.; Klumb, R.A.; Schmidt, S.H.; Coble; D.W. A review of fish control projects. N. Am. J. Fish. Manage. 16:63–74; 1996.

Merritt, R.W.; Walker, E.D.; Wilzbach, M.A.; Cummins, K.W.; Morgan, W.T. A broad evaluation of B.T.I. for black fly (Diptera: Simuliidae) control in a Michigan river: Efficacy, carry and nontarget effects on invertebrates and fish. J. Am. Mosq. Control Assoc. 5:397–415; 1989.

Meyer, F.P.; Schnick, R.A. Sea lamprey control techniques: Past, present, and future. J. Gt. Lakes Res. 9:354–358; 1983.

Mitsch, W.J.; Wilson, R.F. Improving the success of wetland creation and restoration with know-how, time, and self-design. Ecol. Applic. 6:77–83; 1996.

Moore, K.M.S.; Gregory, S.V. Response of young-of-the-year cutthroat trout to manipulation of habitat structure in a small stream. Trans. Am. Fish. Soc. 117:162–170; 1988.

Moss, B.; Stansfield, J.; Irvine, K.; Perrows, M.; Phillips, G. Progressive restoration of a shallow lake: A 12-year experiment in isolation, sediment removal and biomanipulation. J. Appl. Ecol. 33:71–86; 1996.

[NRC] National Research Council. *Restoration of Aquatic Ecosystems.* Washington, DC: National Academy; 1992.

Nielsen, L.A.; Johnson, D.L. *Fisheries Techniques.* Bethesda, MD: American Fisheries Society; 1983.

Northcote, T.G. Fish in the structure and function of freshwater ecosystems: A "top-down" view. Can. J. Fish. Aquat. Sci. 45:361–379; 1988.

Olson, M.H.; Carpenter, S.R.; et al. Managing macrophytes to improve fish growth: A multi-lake experiment. Fisheries 23:6–12; 1998.

Orians, G. Ecology and environmental problem solving. Northwest Sci. 60:287–292; 1986.

Paine, R.T. Food webs: Linkage, interaction strength, and community infrastructure. J. Anim. Ecol. 49:667–685; 1980.

Power, M.E.; Tilman, D.; Estes, J.A.; Menge, B.A.; Bond, W.J.; Mills, L.S.; Daily, G.; Castilla, J.C.; Lubchenco, J.; Paine, R.T. Challenges in the quest for keystone species: Identifying keystone species is difficult-but essential to understanding how loss of species will affect ecosystems. BioScience 46:609–620; 1996.

Schindler, D.E.; Carpenter, S.R.; Cole, J.J.; Kitchell, J.F.; Pace, M.L. Influence of food web structure on carbon exchange between lakes and the atmosphere. Science 277:248–251; 1997.

Scheffer, M. *Ecology of Shallow Lakes.* New York: Chapman and Hall; 1997.

Shrader-Frechette, K.S.; McCoy, E.D. *Method in Ecology.* London: Cambridge Univ. Pr.; 1993.

Shapiro, J.; Wright, D.I. Lake restoration by biomanipulation: Round Lake, Minnesota, the first two years. Freshwat. Biol. 14:371–383; 1984.

Stewart-Oaten, A.; Murdoch, W.; Parker, K. Environmental impact assessment: 'Pseudoreplication' in time? Ecology 67:929–940; 1986.

Trebitz, A.S.; et al. A model of bluegill-largemouth bass interactions in relation to aquatic vegetation and its management. Ecol. Model. 94:139–156; 1997.

Trebitz, A.S.; Nibbelink, N. Effect of pattern of vegetation removal on growth of bluegill: A simple model. Can. J. Fish. Aquat. Sci. 53:1844–1851; 1996.

Wallace, J.B.; Vogel, D.S.; Cuffney, T.F. Recovery of a headwater stream from an insecticide induced community disturbance. J. North Am. Benthol. Soc. 5:115–126; 1986.

Walters, C.J.; Collie, J.S.; Webb, T. Experimental design for estimating transient responses to habitat alterations: Is it practical to control for environmental interactions? Can. Sp. Publ. Fish. Aquat. Sci. 105:13–20; 1989.

Wootton, J.T. The nature and consequences of indirect effects in ecological communities. Annu. Rev. Ecol. Syst. 25:443–466; 1994.

Wipfli, M.S.; Merritt, R.W. Effects of *Bacillus thuringiensis* var *israelensis* on nontarget benthic insects through direct and indirect exposure. J. North Am. Benthol. Soc. 13:190–205; 1994.

Zedler, J.B. Ecological issues in wetland mitigation: An introduction to the forum. Ecol. Applic. 6:33–37; 1996.

21

Biotic Manipulations Involving Belowground Animals

Diana H. Wall and O. James Reichman

Introduction

The experimental approach for the study of soil biota in ecosystems has evolved rapidly with the increase in our knowledge. From the mid 1960s to mid 1990s, the influence of soil biota on ecosystem processes in natural settings was determined primarily by manipulations with selected biocides. These were used to exclude specific groups of soil biota. More recently (mid-1990s to present), soil ecologists have assessed those experiments and found sufficient evidence to suggest that other experimental approaches are more appropriate for evaluating the relation between soil community structure and ecosystem processes. However, laboratory microcosms continue to be an additional experimental means for relating soil biota to ecosystem processes. Because of the constraints of the soil habitat and the complexity of biotic interactions, the approaches used for analyzing soil biota and ecosystem processes differ somewhat from the biotic manipulations in aquatic and aboveground ecosystems.

In this chapter, we first introduce the soil biota and the problems inherent in evaluating their role in ecosystem processes. We then discuss manipulations that exclude organisms and the more recent approaches using natural gradients as treatments and manipulations of the belowground habitat. Finally, we briefly discuss the experimental approach of combining field experiments with laboratory microcosms, which has proved invaluable for relating soil organisms to ecosystem processes. In all cases, we caution that the question being asked, the hypothesis being tested, and the organisms being studied will determine the approach to be used. We therefore have not described differences in experimental design, since these can differ significantly with organism size, abundance and habitat scale. Where possible, we indicate references for sampling and extraction methods and for determination of biomass for the different organisms.

Soil Biota

Experiments to determine the significance of biota in ecosystem functioning have most often involved aboveground organisms. Generally, aboveground species are more obvious and easier to manipulate than those that live belowground. Yet, in many systems more biomass occurs belowground, therefore knowledge of the soil organisms (including roots) and how they interact with aboveground biota to affect ecosystems is crucial for understanding overall ecosystem function.

The soil itself is a complex matrix with wide variation in physical and chemical properties. For example, in the United States, there are more than 2000 soil types, all varying in physical and chemical properties and above- and belowground biota. A further complicating aspect of belowground studies is the rich diversity of organisms that live in the soil (Dindal 1990; Coleman and Crossley 1996). The animate component within soils includes plant roots, vertebrates (from small snakes and salamanders to large mammals), invertebrates (including some of the most speciose taxa such as nematodes, mites, beetles, ants, and termites), algae, fungi, and microbes. The connections of these groups to

aboveground biota are numerous, making the above- and belowground systems interdependent. Numerous organisms that forage and seek mates aboveground spend a large majority of their time belowground in dens and nests, utilize soil biota for food, and/or have one stage of their life cycle in the soil.

Recent reviews have shown belowground vertebrates and invertebrates have different functions, some of them key to soil sustainability (Lavelle 1997; Brussaard et al. 1997; Hooper et al., in press). The invertebrates in soil can alter net primary productivity (NPP), soil structure, patterns of microbial activity, soil organic matter dynamics, and nutrient cycling (Mielke 1977; Grant et al. 1980; Cox 1984; Seastedt 1984; Anderson 1987; Huntly and Inouye 1988; Brown and Gange 1990; Verhoef and Brussaard 1990; Beare et al. 1992; Reichman et al. 1993; Heal et al. 1996; Lavelle 1997). For example, depending on the system, earthworms can increase water infiltration (Sharpley et al. 1979; Subler et al. 1997), but, in some cases, accelerate nitrate leaching (Subler et al. 1997). Soil invertebrates also have potential utility as indicators of pollution and other soil disturbance (Paoletti et al. 1991; Freckman and Ettema 1993; Blair et al. 1996; Niles and Freckman 1998). Vertebrates, whose contribution to functioning of soil systems is generally underrated, change soil structure and chemistry through wallowing and compaction (Lock 1972), tunneling and mixing of soil organic matter (Kalisz and Stone 1984; Anderson 1987), consuming roots (Reichman and Smith 1985, 1991; Reichman and Jarvis 1989), fracturing soil aggregates (Cortinas and Seastedt 1996), dispersing symbiotic fungi, microbes and invertebrates (Maser et al. 1978; Johnson 1996; Herrera et al. 1997), generating egg-laying sites (Huntly and Inouye 1988), and depositing feces and urine (Anderson 1987; Jaramillo and Detling 1992).

Difficulties in experimentally evaluating the role and influence of species in soil are magnified when one considers the variation in the soil biota. These difficulties include (1) size of the organisms (microscopic to 1.5 kg), (2) vast diversity of the species, many of which are undescribed (one group of soil microarthropods, the orabatid mites, are estimated to have about 20% of the species described, or 7000 described species in soils [Balogh and Balogh 1992]), (3) life spans (minutes to years), (4) the three-dimensional spatial scales over which the animals exist (μm to >10 m depth), and (5) the differences in their distribution over a landscape (nested and clumped underneath plants vs. evenly distributed). In addition, no single method exists for sampling all organisms in soil, making quantification between microscopic invertebrate taxa (protozoa, nematodes, tardigrades, rotifers, mites, springtails) problematic (Anderson and Ingram 1993; Hall 1996; Schinner et al. 1995; Blair et al. 1996; Coleman et al. 1999; Wall and Virginia 1999).

In the soil only vertebrates and larger visible macroinvertebrates (>10 mm in length, i.e., termites, ants, earthworms, millipedes) are easily studied at the species level. Most ecosystem experiments of microfauna (0.5 to 200 μm in length) and mesofauna (200 μm to 10 mm in length) have been at the functional or trophic group level. In contrast to aboveground systems, in which a high percentage of identified species with similar functions are placed into trophic groups, soil ecologists have trophic groups with a higher proportion of unidentified species with unknown life histories. Thus, functional groups of soil biota are designated as those organisms of similar morphology and function inferred from feeding habits of a few known species within the group (Freckman 1982; Coleman and Crossley 1996). This lack of knowledge associated with the species of functional groups affects our estimates of nutrient cycling through the soil food webs. Nevertheless, numerous studies at the functional group level and collaboration on ecosystem experiments with taxonomists, have contributed significantly to our understanding of soil biota and ecosystem functioning.

Soil biodiversity is structured into food webs that appear to exert a strong influence on ecosystem function (Moore and de Ruiter 1991; Heal et al. 1996; Swift and Anderson 1994). The majority of ecosystem research has concentrated primarily on microbial biomass and soil respiration, and neglected the contributions of soil protozoa, mycorrhizae, and invertebrates. These latter groups are abundant in soils and have many direct and indirect effects on ecosystem processes. They directly affect ecosystems by affecting plant community composition, as herbivores, as processors of organic matter, and as regulators by preying on other animal species. They indirectly affect processes as secondary consumers, regulating the rate of decomposi-

tion by transporting microbes and microinvertebrates, and by rearranging or chemically altering soil such that its properties are substantially different from unmanipulated soil. The approaches used in investigations of the effect of soil biota on ecosystem processes should consider direct and indirect effects, although the latter are much more difficult to test.

Exclusions as Biotic Manipulations

Species removals or exclusions have been used as biotic manipulations more often than species introductions. This is because (1) the species introduced could become invasive and (2) plant pathology research over the past 100 years has shown problems in establishing a beneficial species into a soil habitat. In soil experiments, exclusion generally refers to exclusion of a trophic group, a high-level taxonomic grouping such as an order or phylum (which could include many trophic groups), or animals of a certain size range. Removal of an organism at the species level from a soil is very difficult.

The exclusion of soil biota theoretically involves two steps, the actual removal of the target taxon and a means to keep it out. In soils, exclusion from a plot of land works better for vertebrates than invertebrates that are highly mobile (ants, termites, earthworms), or transferred by rain or wind (nematodes, mites, protozoa), or that have survival mechanisms that allow them to withstand any chemical exclusion. The physical removal of a soil organism is only effective where individuals are large (visible) and occur in low densities. For example, small mammals can be trapped and removed (Reichman and Smith 1985; Huntly and Inouye 1988). However, in the field it is almost impossible to remove all individual invertebrates from the soil by any of the methods we discuss. Therefore, for soil invertebrates and microflora, different types of exclusion methods, for example, litter bags and electroshocking soil, are often combined to assure the absence of animals (Seastedt et al. 1987; Couteaux et al. 1991). We urge caution in the selection of methods for removal of invertebrates, since the manipulation can affect other factors (e.g., soil physical and chemical properties) (Huhta et al. 1989; Coleman et al. 1999).

Physical Exclusion Methods

Invertebrate biota are removed by two methods—physical and chemical—and have been the subject of many reviews (Seastedt 1984; Freckman et al. 1986; Huhta et al. 1989; Coleman and Crossley 1996). The physical methods include barriers, litter bags (Crossley and Hoglund 1962; Coleman and Crossley 1996), autoclaving/steam sterilizing (Ingham et al. 1985), microwave (Ferris 1984; Huhta et al. 1989), liquid nitrogen (Sulkava et al. 1996), drying (Huhta et al. 1989), gamma irradiation (Griffiths 1987), and electroshocking for removing earthworms (Bohlen et al. 1995; Blair et al. 1996). Methods such as barriers, litter bags and electroshocking are used in the field to selectively exclude larger invertebrates (Blair et al. 1996; Coleman et al. 1999). Autoclaving, steam sterilizing, microwaving, freezing, drying, and gamma irradiation are all used to exclude as many groups of taxa as possible from soil removed from the field. Once the soil is removed from the experimental plot, it is taken to the laboratory, the method to remove the biota applied, and the soil reintroduced back into the field. The type of soil, the volume of soil, and the variation in the intensity and duration of the treatment all interact to determine the taxa that are removed. It is difficult, even with gamma irradiation, to remove all the soil organisms.

If the experiment has a temporal component, it is necessary to keep the target organisms initially excluded out of the plot. This is often achieved for vertebrates and invertebrates with physical barriers such as "fences" and trenches. Fences are small and narrow, generally made out of plastic or metal flashing that is driven into the soil to a depth sufficient to leave several centimeters remaining aboveground. Barriers for invertebrates, also termed microplots, cylinders, or enclosures, are "fences" composed of PVC, concrete, fiberglass, or another material. Essentially, these barriers prevent animals from moving into the experimental plot. Soil within the barriers is either left as is, or the target animals are removed from the soil by an additional exclusion method, such as soil sterilization, gamma irradiation, or others listed previously. Barriers can be circular, ranging from about 5 cm to 80 cm in diameter and 0.5 m in depth, or rectangular and can be inserted to a depth of 1 to 2 m depending on the soil type (Anderson et al. 1985;

Verhoef and de Goede 1985; Bohlen et al. 1995). The size of the barrier usually depends on the duration of the experiment and the size of the soil samples to be removed during the experiment. Barriers (microplots) have been successfully used in agriculture for analysis of soil pathogens of plants (Barker et al. 1979; Noling and Ferris 1985) and in ecology (enclosures) for excluding macrofauna (Anderson et al. 1985; Verhoef and de Goede 1985; Bohlen et al. 1995).

Litter bags are one of the primary experimental tools to evaluate the relationship between the biota and decomposition processes. These bags are usually made from a plastic-type window screen with a known mesh size. Different sized mesh is used to exclude various groups and sizes of animals. This type of "semipermeable membrane" can exclude organisms only in a hierarchical fashion (i.e., larger and larger holes will allow in all but even larger organisms, but not exclude smaller organisms) so it does not allow for a full factorial manipulation. For example, Tian et al. (1997), in a decomposition study of a continuous maize/cassava cropping system, used 0.5-mm mesh litter bags to allow access of microarthropods and 0.08-mm mesh bags to exclude them. Measured amounts of organic matter are placed in the bags for determining decomposition rates in ecosystem studies (Crossley and Hoglund 1962; Seastedt and Crossley 1980; Anderson and Ingram 1993; Andren et al. 1995). Bags are left on the soil surface or buried in the soil and retrieved over a period of time to quantify the animals as well as mass loss and nutrient status of the organic material. Santos and Whitford (1981) used litter bags in conjunction with biocides to exclude selected taxa.

Chemical Exclusions

Chemical or biocide manipulations were used for many years by soil ecologists for several reasons, including (1) they could easily be applied to soils in most ecosystems, (2) they appeared to be selective for groups of soil organisms (e.g., nematicides for nematodes, fungicides for fungi, insecticides for microarthropods, etc.), and (3) they were replicable over large-scale field plots.

However, in recent years (mid-1990 to present), ecologists have largely decreased biocide use as a means of soil biotic manipulation. This is because of increasing evidence showing considerable variation in the reliability of the chemicals for the specific targets. The evidence includes (1) nontarget effects on other biota, including humans (Freckman and Caswell 1985; Ingham 1985; Colinas et al. 1994; Ingham et al. 1994; Coleman and Crossley 1996; Coleman et al. 1999), (2) independent effects on other ecosystem parameters (NPP, root biomass), that are not listed by chemical companies, (3) groundwater contamination (impacts on animals living in the soil–water interface), and (4) degradation of the atmosphere. In addition, regulations on the use of current biocides, replacement of chemical formulations in formerly used biocides, numerous new chemicals, and removal of chemicals from the market have made gathering information on the impact of each chemical on the soil, the soil food web, and other ecosystem parameters increasingly costly in time, as well as affecting our ability to wisely interpret the results.

A synthesis of the numerous available chemicals in the United States and elsewhere that are presently listed for fungi, insects, nematodes, and bacteria, and documentation of their target and nontarget effects and their chemical degradation compounds is not within the scope of this chapter. We caution those who might wish to use a biocide to first check with authorities to see if the chemical is still registered for legal use, and suggest a thorough search in the soil ecology literature to identify nontarget effects and degradation products (see Ingham 1985; Colinas et al. 1994; Ingham et al. 1994).

The biocides differ considerably in their application and their effectiveness. The application method for the biocide in the field is dependent on the manufacturer's formulation; many are applied as a liquid or granular to the soil and others as a spray to the plant or soil. Some biocides are systemic and are translocated throughout the plant to the roots with unknown effects on the rhizosphere food web. The effectiveness of the biocide application for the target organism groups will vary with soil physical and chemical properties, the amount of rainfall, soil temperature, and the formulation of the biocide (Thomlin and Gore 1974; Thomason et al. 1983; Ingham 1985; Duncan and Noling 1998).

The side effect of biocides on nontarget organisms is the major reason that most soil ecologists have chosen other types of manipulations. However, in the past, herbicides, insecticides, and

nematicides have been employed to exclude large numbers of individuals (Santos and Whitford 1981; Ingham 1985; Seastedt et al. 1987; Brown and Gange 1990; Yeates et al. 1991; Beare et al. 1992). The nontarget effects may have been unknown or very reduced in those soils when the study was conducted. Additionally, biocides used in these studies may have been fairly effective across broad taxonomic groups, but would be less effective if a single species or group were the target. Yet, there is evidence that even within a broad taxonomic group, species can differ in their response to the biocide. For example, Freckman et al. (1980) found species within nematode trophic groups (plant parasites, bacterial feeders, fungal feeders, predators, omnivores) varied in their response to 1,3-dichloropropene, a nematicide that was used primarily to exclude plant parasitic nematodes. Some species were killed faster than others, irrespective of trophic group, and some species survived the chemical. Specific biocides can have broad impacts across the soil food web. For example, the fungicide Benomyl, which was widely used in ecosystem experiments, has a detrimental effect on earthworm populations (Edwards and Thompson 1973; Tomlin and Gore 1974; Greig-Smith 1992) and some species of protozoa. Insecticides including naphthalene and the nematicide carbofuran, reduce earthworm populations (Tomlin and Gore 1974; Ingham 1985; Colinas et al. 1994; Ingham et al. 1994). The nematicide carbofuran has also decreased mites, *Rhizobium* populations, field crickets, and springtails (see Ingham 1985). Of the biocides presently used in ecosystem studies for biotic manipulations, naphthalene "moth balls" (Seastedt and Crossley 1980), an insoluble volatile compound used since the early 1960s, is considered to have less impact on nontarget organisms. However, it also has to be carefully considered. When placed on the soil surface, it has been shown to affect not only moths, but fungi, protozoa, and earthworms as well (Ingham et al. 1994).

Compounds resulting from degradation of biocides can lead to other spurious results. For example, a compound applied to kill soil herbivores may break down into nitrogen or phosphorus compounds that cause a "fertilizer effect," or increased plant growth. Unless an investigator had information on the degradation products, the increased NPP could erroneously be attributed solely to exclusion of the herbivores.

Chemical manipulations have proven to be questionable for examining the role of soil biota in ecosystem processes for many reasons. We have no further recommendations and now elaborate on the important directions for future ecosystem studies of soil biota.

Natural Gradients as Treatments

Ecologists often use the range or natural variation in environmental and biotic conditions as independent variables to determine the effect of key factors on ecosystem processes. While these are not truly manipulative, they do have the effect of providing large-scale differences in the variable of interest.

For example, gradients of temperature or moisture can be employed to understand how these parameters impinge on the entire array of ecosystem processes. Even climatic variation can be used to analyze characteristics of ecosystems. Similarly, soil differences over short distances (Freckman and Virginia 1997) or large differences in soil features (Schimel et al. 1985; Schlesinger et al. 1990; Bragg 1995) have been used effectively to understand the relationship between abiotic and biotic processes. The soil features of interest may include parent material and soil nutrients such as nitrogen or carbon (see Schlesinger et al. 1990).

Geography can also be used to exclude various taxa from soil as a factor in soil ecosystem processes. This can occur on continental scales, such as comparisons between African and North American habitats (Reichman and Jarvis 1989), or for habitat differences within a region.

Another type of "natural" experiment that is useful for evaluating the effect of a species on an ecosystem process is the invasion of nonindigenous species. Exotic species, whether plants or animals, have invaded huge areas of the globe, and thus offer an unfortunate experiment for the effect of alternate conditions on an ecosystem. For example, in the northeastern United States, the spread of the exotic earthworm species (*Amynthas hawayanus* and *A. agrestis*) has decreased forest floor litter, changed soil properties and increased erosion (Burtelow et al. 1998). The introduction into Europe of the New Zealand flatworm, an obligate predator of lumbri-

cid earthworms, offers an opportunity to examine changes in nutrient retention in a number of ecosystems (Boag et al. 1998). Introduction of exotic soil animals that are plant pathogenic or parasitic can be especially problematic but offer opportunities for study of a single species on plant productivity in diverse ecosystems. The introduction from the colder German soils of a plant parasite, the sugar beet cyst nematode, *Heterodera schactii,* into the desert agricultural soils of California, resulted in a fast spread of this soil species, an adverse economic impact to sugar beet industry due to loss of NPP and root biomass, and enactment of quarantine procedures to prevent spread (Miller 1986). More recently, the plant parasitic nematode, *Belonolaimus longicaudatus,* has been introduced from soils of the southeastern United States to California, again causing detrimental impacts to plants and economic costs (Cherry et al. 1997).

Habitat Manipulations

Manipulations of habitat can involve altering the physical structure of the soil, transplanting soil and/or its inhabitants, excluding organisms, or excluding certain nutrients or water (Seastedt et al. 1987).

Physical Alteration

Alteration of the soil by using various tilling regimes often generates major findings about soil functional groups and ecosystem processes (Robertson et al. 1993; Robertson and Freckman 1995), as well as the impact on soil biodiversity (Swift and Anderson 1994; Heal et al. 1996). Plowing affects several features of the soil, including its friability, water infiltration, and nitrification (usually by breaking up soil aggregates) (Paustian et al. 1997). Manipulations can take place across entire fields or as plots within a field. Comparisons between the functional groups or species in nonaltered and altered soils and the rate of the ecosystem process provide a measure of the role of the organism.

The effects of the biota can also be examined by experimentally altering soil. For example, pocket gophers excavate extensive burrows belowground and deposit the tailings and nutrients on the soil surface as mounds. Experimentally, both the burrows and the mounds can be simulated by hand excavating and by piling soil of the appropriate type on the surface. Even the spatial pattern of such disturbances can be altered to evaluate the physical impact of the disturbance and how the pattern itself influences ecosystem processes (Reichman et al. 1993).

Experimental manipulation of fire regimes is often used to study the effects of burning on aboveground processes. However, fire also affects the soil and its inhabitants (Seastedt 1988; Seastedt and Reddy 1991; Blair 1997) by altering the temperature immediately (as the fire passes) or in the near term (by yielding dark ash, which absorbs light energy and insulates the soil). Furthermore, as a second order effect, the resulting plant community also alters the subsequent belowground community and its effect on ecosystem processes (Ojima et al. 1990). Following the fire, measuring the rate of litter decompositon (litter bags) and the response of the soil biota in the fire-manipulated versus unmanipulated soils provides information on the resilience and resistance of the system, and the redundancy of the soil food web.

Mechanical manipulations, such as soil warming, the addition or exclusion of water, and increasing carbon dioxide (CO_2) can be employed (Whitford et al. 1981; Freckman et al. 1987; Couteaux et al. 1991; Treonis and Lussenhop 1997).

Introductions and Transplants

One of the most effective types of manipulations involves reciprocal transplants of some organism or habitat feature of interest. For example, soil cores of similar sizes can be extracted from one location and transposed with cores from another area to determine the influence of native soil on the biotic and abiotic characteristics of each soil type (J. Blair, personal communication). In a subset of this type of transplant, soil may be extracted and sterilized and reintroduced into the same hole. Transplants are an especially effective type of manipulation if care is taken to treat all treatments similarly. Thus, in the reciprocal core transplant manipulation, controls that include simulated transplants within the same soil type must be used (i.e., core extracted and put back into the same hole).

Transplanting soil and plants can also be useful for determining the effect of aboveground vegetation on belowground processes. This happens on a

large scale when crops are planted (e.g., experiments with nitrogen-fixing bacteria) or when areas are reforested. Transplants of this type occur in many managed ecosystems, but unfortunately these are only rarely viewed as experimental opportunities. Recent attempts to restore degraded habitats may provide special opportunities to determine the effect of transplants on systems, especially if analyses are conducted prior to as well as after transplants take place. Smaller-scale, highly controlled transplants can be especially useful for identifying specific changes in ecosystem processes. These types of experiments can be used to determine the effect of plant species composition and diversity on belowground ecosystem processes (e.g., Monz et al. 1994). In some manipulation experiments, cylinders are driven into the soil, the cylinders containing the soil removed, and used in growth chamber experiments. Monz et al. (1994) removed more than 50 cylinders of soil and plants from the shortgrass steppe in Colorado to the Duke University, North Carolina, phytotron to test the impact of global change (elevated CO_2, moisture, and temperature) on soil mycorrhizae under controlled conditions.

A variation of transplanting plants is the reciprocal movement of organic material such as litter or thatch (Knapp and Seastedt 1986). This type of experiment increases the quantity of litter that the soil food web processes. In these studies, litter is raked from one location, added to another site, and then the decomposition and soil biotic results are compared with unmanipulated controls in which the litter is present. The shading factor of litter manipulation can be accomplished by using screens of different mesh size to filter light.

Among the most difficult types of ecosystem studies is evaluating the impact of aboveground animals (soil compaction, grazing, nutrient input) on soil, the soil biota, and on processes. Predator or prey densities can be "transplanted" or altered, by adding or subtracting either, to determine the effect on belowground processes. Vertebrates are often fenced or confined in some manner to facilitate the manipulation. For example, bison have been reintroduced into some prairie settings, and their effect on certain belowground ecosystem processes has been analyzed (James 1992; Seastedt 1995).

As appealing and productive as these approaches can be, they also carry significant liabilities. There is very little control over the independent variables, which also limits the opportunity for adequate replication. In addition, if comparisons are made over relatively large scales, such as between regions or continents, or along latitudinal or longitudinal gradients, the covariation of many variables can confound the results.

Resource Manipulations

Manipulation of water, sun, and nutrients or other chemicals can have a direct effect on ecosystems, but also indirectly influence processes by stimulating or inhibiting biotic variables in the system. For example, fertilizing or irrigating plants with overhead sprinklers to supplement rainfall may increase plant density and root biomass, and change root architecture and the resource quality of the plant. This can indirectly increase soil biotic competition for other resources, or the manipulation may provide additional food for consumers, which in their own right will impinge on ecosystem processes (Verhoef and Brussaard 1990; Swift and Anderson 1994).

Laboratory Studies

The ultimate biotic manipulation involves bringing the soil of the studied ecosystem into the laboratory or Ecotron (Naeem et al. 1994), isolating or manipulating the soil biotic organisms, and more effectively controlling climatic variables. There are obvious problems with such approaches, such as the inherent artificiality, and large systems are particularly difficult to simulate accurately. Yet, investigators familiar with the complexity of the soil system and its inhabitants frequently test hypotheses using a combination of experimental approaches: microcosm, mesocosm, greenhouse, phytotron, and field manipulations (see Moore et al. 1996; Naeem et al. 1994). However, although seemingly simpler and with fewer variables, laboratory microcosms and growth chambers are not without problems. Microscopic soil invertebrates and microorganisms can be introduced through the water source, through soil contamination (sweeping or splashing

soil into the experimental set-up), or through air, and confound experimental results. Laboratory and "phytotron" experimenters need to be aware of nontarget introductions. Nevertheless, the combination of manipulations, including laboratory or greenhouse, offers increased information on the role of soil biota in ecosystem processes.

Summary

Experimental manipulations of soil biota in ecological systems are difficult, especially in the field. Relatively few variables can be effectively controlled without introducing undue artificiality, and hence greater replication and attention to sample sizes may be required to overcome naturally occurring, variation-inducing, effects. All of the problems to which aboveground manipulations are susceptible are magnified in the microscopic habitats belowground. However, subterranean processes are among the most important in virtually all ecosystems, and hence ecologists must apply new techniques and technologies, and creatively address the important, unanswered questions in the soil. Molecular biology (van der Knaap et al. 1993; Clegg et al. 1995; Jones et al. 1997), image analysis systems, and isotopes (Boutton et al. 1983; Kuikman et al. 1989; Freckman et al. 1991; Briones et al. 1999; Hobbie et al. 1999; Yeates 1999), are offering new and exciting directions for evaluating soil organisms at the species or genus level and their roles in the functioning in ecosystems. In particular, the use of microbial tracers offers new strategies for understanding the interaction of microbial "species" with other soil biota and their effect on plants (Stephens et al. 1993; Clegg et al. 1995; Brimecombe et al. 2000). The challenge for ecologists is to identify those techniques useful in soil biology, such as identifying the flow of nitrogen through microarthropods using stable isotopes, or examining the distribution of soil biota related to water, temperature, and vegetation with geographic information system (GIS) techniques, that will allow us to increase our scale of understanding of the soil biota and ecosystem processes.

References

Anderson, D.C. Belowground herbivory in natural communities: A review emphasizing fossorial animals. Q. Rev. Biol. 62:261–286; 1987.

Anderson, J.M.; Huish, S.A.; Ineson, P.; Leonard, M.A.; Splatt, P.R. Interactions of invertebrates, microorganisms; tree roots in nitrogen; mineral element fluxes in deciduous woodland soils. In: Fitter, A.H.; Atkinson, D.; Read, D.; Usher, M.B., eds. *Ecological Interactions in Soil.* Oxford: Blackwell; 1985:377–392.

Anderson, J.M.; Ingram, J.S.I. *Tropical Soil Biology and Fertility. A Handbook of Methods.* 2nd ed. Wallingford, UK: CAB; 1993.

Andren, O.; Bengstsson, J.; Clarholm, M. Biodiversity and species redundancy among litter decomposers. In: Collins, H.P.; Robertson, G.P.; Klug, M.J., eds. *The Significance and Regulation of Soil Biodiversity.* Dordrecht, Netherlands: Kluwer; 1995:141–151.

Balogh, J.; Balogh, P. *The Oribatid Mite Genera of the World.* Vol. 1. Budapest: Hungarian National Museum Pr.; 1992.

Barker, K.R.; Daughtry, B.I.; Corbett, D.W. Equipment and techniques for establishing field microplots for the study of soilborne pathogens. J. Nematol. 11:106–107; 1979.

Beare, M.H.; Parmelee, R.W.; Hendrix, P.F.; Cheng, W.; Coleman, D.C.; Crossley, D.A., Jr. Microbial and faunal interactions and effects on litter nitrogen and decomposition in agroecosystems. Ecol. Monogr. 62:569–591; 1992.

Blair, J.M. Fire, N availability and plant response in grasslands: A test of the transient maxima hypothesis. Ecology 78:2359–2368; 1997.

Blair, J.M.; Bohlen, P.J.; Freckman, D.W. Soil invertebrates as indicators of soil quality. In: Doran, J.W.; Jones, A.J., eds. *Methods for Assessing Soil Quality.* Madison, WI: Soil Science Society of America; 1996:273–291.

Boag, B.; Yeates, G.W.; Johns, P.M. Limitations to the distribution and spread of terrestrial flatworms with special reference to the New Zealand flatworm (*Artioposthia triangulata*). Pedobiologia 42:495–503; 1998.

Bohlen, P.J.; Parmelee, R.W.; Blair, J.M.; Edwards, C.A.; Stinner, B.R. Efficacy of methods for manipulating earthworm populations in large-scale field experiments in agroecosystems. Soil Biol. Biochem. 27:993–999; 1995.

Boutton, T.W.; Arshad, M.A.; Tieszen, L.L. Stable isotope analysis of termite food habits in East African grasslands. Oecologia 59:1–6; 1983.

Bragg, T.B. The physical environment of Great Plains grasslands. In: Joern, A.; Keeler, K.H., eds. *The Changing Prairie.* Oxford: Oxford University Pr.; 1995:48–81.

Brimecombe, M.J.; DeLeij, F.A.A.M.; Lynch, J.M. Effect of introduced *Pseudomonas fluorescens* strains on soil nematode and protozoan populations in the rhizo-

sphere of wheat and pea. Microbiol. Ecol. 38:387–397; 2000.

Briones, M.J.I.; Ineson, P.; Sleep, D. Use of delta ^{13}C to determine food selection in collembolan species. Soil Biol. Biochem. 31(6):937–940; 1999.

Brown, V.K.; Gange, A.C. Insect herbivory below ground. Adv. Ecol. Res. 20:1–58; 1990.

Brussaard, L.; Behan-Pelletier, V.M.; Bignell, D.E.; Brown, V.K.; Didden, W.A.M.; Folgarait, P.I.; Fragoso, C.; Freckman, D.W.; Gupta, V.V.S.R.; Hattori, T.; Hawksworth, D.; Klopatek, C.; Lavelle, P.; Malloch, D.; Rusek, J.; Söderström, B.; Tiedje, J.M.; Virginia, R.A. Biodiversity and ecosystem functioning in soil. Ambio 26:563–570; 1997.

Burtelow, A.E.; Bohlen, P.J.; Groffman, P.M. Influence of exotic earthworm invasion on soil organic matter, microbial biomass and denitrification potential in forest soils of the northeastern United States. Appl. Soil Ecol. 9:197–202; 1998.

Cherry, T.; Szalanski, A.L.; Todd, T.C.; Powers, T.O. The internal transcribed spacer region of *Belonolaimus* (Nemata: Belonolaimidae). J. Nematol. 29:23–29; 1997.

Clegg, C.D.; Anderson, J.M.; Lappin-Scott, H.M.; Van Elsas, J.D.; Jolly, J.M. Interaction of a genetically modified *Pseudomonas fluorescens* with the soil feeding earthworm *Octolasion cyaneum* (Lumbricidae). Soil Biol. Biochem. 27:1423–1429; 1995.

Coleman, D.C.; Crossley, D.A., Jr. *Fundamentals of Soil Ecology.* New York: Academic; 1996.

Coleman, D.C.; Blair, J.M.; Elliott, E.T.; Wall, D.H. Soil invertebrates. In: Robertson, G.P.; Bledsoe, C.S.; Coleman, D.C.; Sollins, P., eds. *Standard Soil Methods for Long Term Ecological Research.* New York: Oxford University Pr.; 1999:349–377.

Colinas, C.; Ingham, E.; Molina, R. Population responses of target and non-target forest-soil organisms to selected biocides. Soil Biol. Biochem. 26:41–48; 1994.

Cortinas, M.R.; Seastedt, T.R. Short- and long-term effects of gophers (*Thomomys talpoides*) on soil organic matter dynamics in alpine tundra. Pedobiologia 40:162–170; 1996.

Couteaux, M.-M.; Mosseau, M.; Celerier, M.-L.; Bottner, P. Increased atmospheric CO_2 and litter quality: Decomposition of sweet chestnut leaf litter with animal food webs of different complexities. Oikos 61:54–64; 1991.

Cox, G. The distribution and origin of mima mound grasslands in San Diego County, California. Ecology 65:1397–1405; 1984.

Crossley, D.A., Jr.; Hoglund, M.P. A litter-bag method for the study of microarthropods inhabiting leaf litter. Ecology 43:571–573; 1962.

Dindal, D.L., ed. *Soil Biology Guide.* New York: Wiley; 1990.

Edwards, C.A.; Thompson, A.R. Pesticides and the soil fauna. Resid. Rev. 45:1–79; 1973.

Duncan, L.W.; Noling, J.W. *Agricultural Sustainability and Nematode Integrated Pest Management.* In: Barker, K.R.; Pederson, G.A.; Windham, G.L., eds. *Plant and Nematode Interactions.* Agronomy Monograph 36. Madison, WI: American Society of Agronomy, Crop Science Society of America, Soil Science Society of America; 1998:251–287.

Ferris, R.S. Effects of microwave oven treatment on microorganisms in soil. Phytopathology 74:121–126; 1984.

Freckman, D.W., ed. *Nematodes in Soil Ecosystems.* Austin, TX: Univ. Texas Pr.; 1982.

Freckman, D.W.; Caswell, E.P. Ecology of nematodes in agroecosystems. Annu. Rev. Phytopathol. 23:275–296; 1985.

Freckman, D.W.; Ettema, C.E. Assessing nematode communities in agroecosystems of varying human intervention. Agric. Ecosys. Environ. 45:239–261; 1993.

Freckman, D.W.; Slobodkin, L.B.; Taylor, C.E. Relation between species lists and tolerance to nematicides. In: Dindal, D.L., ed. *Soil Biology as Related to Land Use Practices.* Washington, D.C.: U.S. Environmental Protection Agency; 1980:34–42.

Freckman, D.W.; Virginia, R.A. Low diversity Antarctic soil nematode communities: Distribution and response to disturbance. Ecology 78:363–369; 1997.

Freckman, D.W.; Cromack, K., Jr.; Wallwork, J.A. Recent advances in quantitative soil biology. In: Mitchell, M.J.; Nakas, J.P., eds. *Microfloral and Faunal Interactions in Natural and Agroecosystems.* Dordrect, Netherlands: Martinus Nijhoff/Dr. W. Junk; 1986:399–422.

Freckman, D.W.; Whitford, W.G.; Steinberger, Y. Effect of irrigation on nematode population dynamics and activity in desert soils. Biol. Fertil. Soils 3:3–10; 1987.

Freckman, D.W.; Barker, K.R.; Coleman, D.C.; Acra, M.; Dyer, M.I.; Strain, B.R.; McNaughton, S.J. The use of the ^{11}C technique to measure plant responses to herbivorous soil nematodes. Funct. Ecol. 5:810–817; 1991.

Freckman, D.W.; Caswell, E.P. Ecology of nematodes in agroecosystems. Annu. Rev. Phytopathol. 23:275–296; 1985.

Grant, W.E.; French, N.R.; Folse, L.J. Effects of pocket gopher mounds on plant production in shortgrass prairie ecosystems. Southwestern Natur. 25:215–224; 1980.

Greig-Smith, P.W. *Ecotoxicology of earthworms.* Andover, MA: Intercept; 1992.

Griffiths, B.S. Growth of selected microorganisms and plants in soil sterilized by ethylene oxide or gamma-irradiation. Soil Biol. Biochem. 19:115–116; 1987.

Hall, G.S., ed. *Methods for the Examination of Organismal Diversity in Soils and Sediments.* Wallingford, UK: CAB; 1996.

Heal, O.W.; Struwe, S.; Kjoller, A. Diversity of soil biota and ecosystem function. In: Walker, B.; Steffen, W., eds. *Global Change and Terrestrial Ecosystems.* Cambridge, UK: Cambridge University Pr; 1996:385–402.

Herrera, J.; Kramer, C.L.; Reichman, O.J. Patterns of fungal communities that inhabit rodent food stores: Effect of substrate and infection time. Mycologia 89:846–857; 1997.

Hobbie, E.A.; Macko, S.A.; Shugart, H.H. Insights into nitrogen and carbon dynamics of ectomycorrhizal and saprotrophic fungi from isotopic evidence. Oecologia 118:353–360; 1999.

Hooper, D.U.; Dangerfield, J.M.; Brussaard, L.; Wall, D.H.; Wardle, D.A.; Bignell, D.E.; Brown, V.K.; Coleman, D.C.; Giller, K.E.; Lavelle, P.; van der Putten, W.H.; deRuiter, P.C.; Rusek, J.; Silver, W.; Tiedje, J.; Wolters, V.; Eggleton, P.; Masters, G.J. Interactions between above and belowground biodiversity in terrestrial ecosystems: patterns, mechanisms and feedbacks. BioScience (in press).

Huhta, V.; Wright, D.H.; Coleman, D.C. Characteristics of defaunated soil. I. A comparison of three techniques applied to two different forest soils. Pedobiologia 33:417–426; 1989.

Huntly, N.; Inouye, R. Pocket gophers in ecosystems: Patterns and mechanisms. BioScience 38:786–793; 1988.

Ingham, E.R. Review of the effect of 12 selected biocides on target and non-target soil organisms. Crop Protect. 4:3–32; 1985.

Ingham, R.E.; Trofymow, J.A.; Ingham, E.R.; Coleman, D.C. Interactions of bacteria, fungi, and their nematode grazers: Effects on nutrient cycling and plant growth. Ecol. Monogr. 55:119–140; 1985.

Ingham, E.R.; Coleman, D.C.; Crossley, D.A., Jr. Use of sulfamethoxazole-penicillin, oxytetracycline, carbofuran, carbaryl, napthalene and Temik to remove key organism groups in soil in a corn agroecosystem. J. Sustain. Agric. 4:7–30; 1994.

James, S. Localized dynamics of earthworm populations in relation to bison dung in North American tallgrass prairie. Soil Biol. Biochem. 24:1471–1479; 1992.

Jaramillo, V.J.; Detling, J. Small scale heterogeneity in a semi-arid North American grassland. II. Cattle grazing and simulated urine patches. J. Appl. Ecol. 29:9–13; 1992.

Johnson, C.N. Interactions between mammals and ecotmycorrhizal fungi. Trends Ecol. Evol. 11:503–507; 1996.

Jones, J.T.; Phillips, M.S.; Armstrong M.R. Molecular approaches in plant nematology. Fundam. Appl. Nematol. 20(1):1–4; 1997.

Kalisz, P.J.; Stone, E.L. Soil mixing by scarab beetles and pocket gophers in north-central Florida. J. Soil Sci. Soc. Am. 48:169–172; 1984.

Knapp, A.K.; Seastedt, T.R. Detritus accumulation limits productivity of tallgrass prairie. BioScience 36:662–668; 1986.

Kuikman, P.J.; van Vuren, M.M.I.; Van Veen, J.A. Effect of soil moisture regime on predation by protozoa of bacterial biomass and the release of bacterial nitrogen. Agric. Ecosys. Environ. 27:271–279; 1989.

Lavelle, P. Faunal activities and soil processes: adaptive strategies that determine ecosystem function. Adv. Ecol. Res. 27:93–132; 1997.

Lock, J.M. The effects of hippopotamus grazing on grasslands. J. Ecol. 60:445–467; 1972.

Maser, C.; Trappe, J.M.; Nussbaum, R.A. Fungal-small mammal interrelationships with emphasis on Oregon coniferous forests. Ecology 59:799–809; 1978.

Mielke, H. Mound building by pocket gophers: their impact on soils and vegetation in North America. J. Biogeogr. 4:171–180; 1977.

Miller, L.I. Economic importance of cyst nematodes in North America. In: Lamberti, F.; Taylor, C.E., eds. *Cyst Nematodes.* New York: Plenum; 1986:373–385.

Moore, J.C.; de Ruiter, P.C. Temporal and spatial heterogeneity of trophic interactions within belowground food webs: An analytical approach to understand multi-dimensional systems. Agric. Ecosys. Environ. 34:371–397; 1991.

Moore, J.C.; de Ruiter, P.C.; Hunt, H.W.; Coleman, D.C.; Freckman, D.W. Microcosms and soil ecology: Critical linkages between field studies and modeling food webs. Ecology 77:694–705; 1996.

Monz, C.A.; Hunt, H.W.; Reeves, F.B.; Elliott, E.T. The response of mycorrhizal colonization to elevated CO_2 and climate change in *Pascopyrum smithii* and *Bouteloua gracilis.* Plant Soil 165:75–80; 1994.

Naeem, S.; Thompson, L.J.; Lawler, S.P.; Lawton, J.H.; Woodfin, R.M. Declining biodiversity can alter the performance of ecosystems. Nature 368:734–737; 1994.

Niles, R.K.; Freckman, D.W. From the ground up: nematode ecology in bioassessment and ecosystem health. In: Barker, K.R.; Pederson, G.A.; Windham, G.L., eds. *Plant and Nematode Interactions.* Agronomy Monograph 36. Madison, WI: American Society of Agronomy, Crop Science Society of America, Soil Science Society of America; 1998:65–85.

Noling, J.W.; Ferris, H. Influence of *Meloidogyne hapla* on alfalfa yield and host population dynamics. J. Nematol. 17:415–422; 1985.

Ojima, D.S.; Parton, W.J.; Schimel, D.S.; Owensby, C.E. Simulated impacts of annual burning on prairie ecosystems. In: Collins, S.L.; Wallace, L.L., eds. *Fire in*

North American Tallgrass Prairies. Norman, OK: Univ. Oklahoma Pr.; 1990:118–132.

Paoletti, M.G.; Favretto, M.R.; Stinner, B.R.; Purrington, F.F.; Bater, J.E. Invertebrates as bioindicators of soil use. Agric. Ecosys. Environ. 34:341–362; 1991.

Paustian, K.; Collins, H.P.; Paul, E.A. Management controls on soil carbon. In: Paul, E.A.; Paustian, K.; Elliott, E.T.; Cole, C.V., eds. *Soil Organic Matter in Temperate Agroecosystems: Long-Term Experiments in North America.* Boca Raton, FL: CRC; 1997:15–49.

Reichman, O.J.; Benedix, J.H.; Seastedt, T.R. Animal generated disturbances and size hierarchies in a tallgrass plant community. Ecology 74:1281–1285; 1993.

Reichman, O.J.; Jarvis, J.U.M. The impact of three species of sympatric fossorial herbivorous mole-rats (Rodentia: Bathyergidae) on overlying vegetation. J. Mammal. 70:763–771; 1989.

Reichman, O.J.; Smith, S. Impact of pocket gopher burrows on overlying vegetation. J. Mammal. 66:720–725; 1985.

Reichman O.J.; Smith, S. Effects of simulated leaf and root herbivory on mortality, biomass, reproduction, and nutrient allocation in a biennial, *Tragopogon dubius.* Ecology 72:116–124; 1991.

Robertson, G.P.; Freckman, D.W. The spatial distribution of nematode trophic groups across a cultivated ecosystem. Ecology 76:1425–1433; 1995.

Robertson, G.P.; Crum, J.R.; Ellis, B.G. The spatial variability of soil resources following long-term disturbance. Oecologia 96:451–456; 1993.

Santos, P.; Whitford, W.G. The effects of microarthropods on litter decomposition in a Chihuahuan desert ecosystem. Ecology 62:654–663; 1981.

Schlesinger, W.H.; Reynolds, J.F.; Cunningham, G.L.; Huenneke, L.F.; Jarrell, W.M.; Virginia, R.A.; Whitford, W.G. Biological feedback in global desertification. Science 247:1043–1048; 1990.

Schimel, D.S.; Coleman, D.C.; Horton, K.A. Soil organic matter dynamics in paired rangeland and cropland toposequences in North Dakota. Geoderma 36:201–214; 1985.

Schinner, F.; Ohlinger, R.; Kandeler, E.; Margesin, R., eds. *Methods in Soil Biology.* Berlin: Springer-Verlag; 1995.

Seastedt, T.R. The role of microarthropods in decomposition and mineralization processes. Annu. Rev. Entomol. 29:25–46; 1984.

Seastedt, T.R. Mass, nitrogen, and phosphorous dynamics in foliage and root detritus of annually burned and unburned tallgrass prairie. Ecology 69:59–65; 1988.

Seastedt, T.R. Soil systems and nutrient cycles of the North America Prairie. In: Joern, A.; Keeler, K.H., eds. *The Changing Prairie.* Oxford: Oxford Univ. Pr.; 1995:157–174.

Seastedt, T.R.; Crossley, D.A., Jr. Effects of microarthropods on the seasonal dynamics of nutrients in forest litter. Soil Biol. Biochem. 12:337–342; 1980.

Seastedt, T.R.; Reddy, M.V. Fires, mowing, and insecticides effects on soil *Sternorrhncha* (Homoptera) densities in tallgrass prairie. J. Kansas Entomol. Soc. 64:238–242; 1991.

Seastedt, T.R.; Todd, T.C.; James, S.W. Experimental manipulations of soil arthropod, nematode, and earthworm communities in a North American tallgrass prairie. Pedobiologia 30:9–17; 1987.

Sharpley, A.N.; Syers, J.K.; Springett, J.A. Effect of surface casting earthworms on the transport of phosphorus and nitrogen in surface runoff from pasture. Soil Biol. Biochem. 11:459–462; 1979.

Stephens, P.M.; Davoren, C.W.; Ryder, M.H.; Doube, B.M. Influence of the lumbricid earthworm *Aporrectodea trapezoides* on the colonization of wheat roots by *Pseudomonas corrugata* strain 2140R in soil. Soil Biol. Biochem. 25:1719–1724; 1993.

Subler, S.; Baranski, C.M.; Edwards, C.A. Earthworm additions increased short-term nitrogen availability and leaching in two grain-crop agroecosystems. Soil Biol. Biochem. 29:413–421; 1997.

Sulkava, P.; Huhta, V.; Laasko, J. Impact of soil faunal structure on decomposition and N-mineralization in relation to temperature and moisture in forest soil. Pedobiologia 40:505–513; 1996.

Swift, M.J.; Anderson, J.M. Biodiversity and ecosystem function in agricultural systems. In: Schulze, E.-D.; Mooney, H.A., eds. *Biodiversity and Ecosystem Function.* Berlin: Springer-Verlag; 1994:15–38.

Tian, G.; Brussaard, L.; Kang, B.T.; Swift, M.J. Soil fauna-mediated decomposition of plant residues under constrained environmental and residue quality conditions. In: Cadisch, G.; Giller, K.E., eds. *Driven by Nature: Plant Litter Quality and Decomposition.* Wallingford, UK: CAB; 1997:125–134.

Thomason, I.J.; Freckman, D.W.; Luc, M. Perspectives in nematode control. Rev. Nematol. 6:315–323; 1983.

Tomlin, A.D.; Gore, F.L. Effects of six insecticides and a fungicide on the numbers and biomass of earthworms in pasture. Bull. Environ. Contam. Toxicol. 12:487–492; 1974.

Treonis, A.M.; Lussenhop, J. Rapid response of soil protozoa to elevated CO_2. Biol. Fertil. Soils 25:60–62; 1997.

van der Knaap, E.; Rodriguez, R.J.; Freckman, D.W. Differentiation of bacterial-feeding nematodes in soil ecological studies by means of arbitrarily primed PCR. Soil Biol. Biochem. 25:1141–1151; 1993.

Verhoef, H.A.; de Goede, R.G.M. Effects of collembolan grazing on nitrogen dynamics in a coniferous forest. In: Fitter, A.H.; Atkinson, D.; Read, D.; Usher, M.B., eds. *Ecological Interactions in Soil.* Oxford: Blackwell; 1985:297–317.

Verhoef, H.A.; Brussaard, L. Decomposition and nitrogen mineralization in natural and agroecosystems: the contribution of soil animals. Biogeochemistry 11:175–211; 1990.

Wall, D.H.; Virginia R.A. The world beneath our feet: Soil biodiversity and ecosystem functioning. In: Raven, P.; Williams, T.A., eds. *Nature and Human Society: The Quest for a Sustainable World. Proceedings of a National Academy of Sciences Forum Oct. 28–30, 1997.* Washington, DC: National Academy; 2000:225–241.

Whitford, W.G.; Freckman, D.W.; Elkins, N.Z.; Parker, L.W.; Parmelee, R.; Phillips, J.; Tucker, S. Diurnal migration and response to simulated rainfall in desert soil microarthropods and nematodes. Soil Biol. Biochem. 13:417–425; 1981.

Yeates, G.W. Effects of plants on nematode community structure. Annu. Rev. Phytopathol. 37:127–49; 1999.

Yeates, G.W.; Bamforth, S.S.; Ross, D.J.; Tate, K.R.; Sparling, G.P. Recolonization of methyl bromide sterilized soils under four different field conditions. Biol. Fertil. Soils 11:181–189; 1991.

22

Assessing the Effects of Acidification on Aquatic Ecosystems: Insights from Lake Experiments

Thomas M. Frost and Janet M. Fischer

Introduction

A large number of aquatic ecosystems worldwide are acidic. In some, acidity has been generated by natural causes such as geologic processes in volcanic regions, chemical actions of mosses in sphagnum bogs, and plant decay products in brown-water habitats (Hutchinson 1957). In many other cases, however, acid conditions have been caused by human activities, which frequently have substantial consequences for ecosystems. For example, some mining processes generate acidified lakes or streams that usually occur in fairly restricted areas (e.g., McKnight and Bencala 1988; Schrenk et al. 1998). Much more widespread are situations in which acidification has been generated by atmospheric deposition contaminated with sulfuric or nitric acid that has been produced by fossil fuel burning. Such acid deposition is a relatively recently recognized phenomenon that has had major environmental consequences, particularly in regions downwind of industrial or highly populated areas (Charles 1991).

The long-range transport of acid contamination creates environmental problems that are complex both scientifically and politically. As with other widespread environmental problems, ecologists have been called upon to evaluate the full range of effects caused by acidification. Experimental studies have played a major role in assessing the effects of this ecological stress. Investigations of problems such as acidification have also provided an opportunity to improve the understanding of basic ecosystem features, in large part through experimental investigations. In this chapter we describe the wide range of methods that have been developed to evaluate the effects of acidification on aquatic ecosystems, emphasizing experimental approaches in lakes. We review hydrologic, geologic, chemical, and biological aspects of acidification for aquatic ecosystems and illustrate some of the complexities of experimental work on the phenomenon of acidification.

The range of ecosystems effected by acidification is quite broad. We focus our chapter on lakes, even though stream and terrestrial habitats have certainly been influenced by acid effects in some regions and they have received a fair degree of experimental investigation. We have emphasized lakes in the interest of maintaining a reasonable degree of focus in this chapter. Many of the general features of lake responses to acidification are important for other ecosystems as well. Investigators with interests in other habitats should also consult Crosby et al. (1991), Elwood et al. (1991) and other related reports for information on acidification effects on streams (Jenkins et al. 1995) and related reports for terrestrial studies. It is also important to consider that the understanding of acidification's effects on ecosystems has not been derived solely from experimental work. Tremendous insights have been derived from comparative analyses across a range of diverse ecosystems (e.g., Confer et al. 1983; Dillon et al. 1987) and from paleolimnological investigations of historic conditions (Smol et al. 1984). As in other assessments of stress effects on ecosystems, overall evaluations must be based on a variety of different research approaches (e.g., Breitburg et al. 1999).

The Chemistry of Acidification

The acid level of a water sample is defined as its hydrogen ion activity. This is the concentration of active hydrogen ions, which is usually reported as pH, the logarithm (base 10) of the reciprocal of the concentration of free hydrogen ions (Wetzel 1983). Hydrogen ion activity is controlled by the dissociation of water molecules and their interactions with the diversity of other ions present in aqueous solutions. Natural waters typically exhibit pH levels between 4 and 10. Anthropogenic acidification has occurred when pH levels have been decreased due to inputs of sulfuric and/or nitric acid. Such inputs have the most adverse effects in waters with low acid-neutralizing capacity. These dilute waters have relatively little resistance to the changes caused by acid inputs. Waters that have been influenced by acid deposition usually exhibit a pH level of less than 6.5 prior to acid effects, which is then reduced sometimes to levels of 5.0 or lower.

It is important to keep in mind that all waters with pH values less than 7.0 can not be considered as acidic due to human activities, even in situations where organic acids do not control water chemistry. Carbonic acid exerts a major influence on natural waters. It is formed by the dissolution of carbon dioxide and its interactions with other ions, particularly calcium and magnesium (Stumm and Morgan 1981). Even pure distilled water exhibits a pH level of close to 5.6 when it comes into equilibrium with atmospheric carbon dioxide levels. Many freshwater ecosystems are substantially oversaturated with carbon dioxide (Cole et al. 1994), which generates naturally low pH conditions in some situations (Kratz et al. 1987). Actually, uncontaminated precipitation can exhibit pH values as low as 5.0 because it contains trace amounts of weak and strong acids (Schindler 1988). At the same time, precipitation with pH values down to 4.0 or lower has been observed in regions with high industrial contamination worldwide and these acid levels are clearly generated by human processes (Schindler 1988). As a consequence, there are numerous aquatic ecosystems with pH values below 5.0 that have been acidified through human activities. We have provided only a brief synopsis of acidification chemistry here and we suggest that researchers interested in the details of this chemistry consult Munson and Gherini (1991) for a much more thorough review.

What Controls the Anthropogenic Acidification of Aquatic Ecosystems?

Whether the pH of a particular habitat is lowered by acidic deposition depends upon the amount and form of acid loading within that region and the chemical and biological resistance to acid inputs that it receives.

A number of programs have been established to categorize the rates of acid loading that occur in regions worldwide. Within the United States, deposition is reported by the National Atmospheric Deposition Program (Husar et al. 1991), which reports specific rates for a network of sites throughout the country. When evaluating acid loading, it is important to consider the deposition of both sulfuric and nitric acids rather than just the pH of deposition because these acids have very different effects because of their specific chemistries and their processing by microorganisms (see discussion below). It is also important to consider that deposition can occur in both wet and dry forms. Dry deposition is particularly difficult to incorporate as a portion of input in a region's overall budget. The overall loading of acid within a region is estimated as rates of hydrogen ion, nitric acid, or sulfuric acid deposition. This quantity can be difficult to estimate but it is one key factor in evaluating acidification in a region.

The processes that influence acid deposition once it has fallen within a region are also complex. Controls on the ultimate fate of acids that have been loaded within a region are influenced by geology and hydrology, as well as by microbial processes that take place within it. Regions that are most sensitive to acid deposition's effects are underlain by geologic materials that are resistant to weathering and that are poor in carbonate minerals. Areas high in carbonate minerals are unlikely to be influenced by even high rates of acid deposition. For example, in the United States, although lakes in southern Wisconsin receive around five times more acid deposition than lakes in northern Wisconsin, these lakes are less likely to become acidified due to dif-

ferences in watershed geology. Lakes in southern Wisconsin are underlain by sedimentary materials containing substantial amounts of carbonates, while those in the north lie upon glacial till originating from the Laurentian Shield region of Canada, which is predominated by minerals that are resistant to weathering (Martin 1965).

Even in regions with resistant geologic materials, hydrology influences lake chemistry by determining the amount of time that water remains in contact with minerals before it reaches a lake or stream. A higher proportion of groundwater inputs in a lake's hydrologic budget will produce chemical conditions that provide greater resistance to acidification (Anderson and Bowser 1986). Just for a single lake, shifts in hydrology driven by climatic effects such as drought can substantially change acid–base chemistry and pH levels over a short time period (Webster et al. 1990). Hydrologic regimes with the highest proportions of inputs as precipitation generate situations with the highest potential for acidification.

Acid within a lake or stream, or being transported to a water body, can be neutralized by chemical and biological processes. Some minerals such as calcium carbonate can neutralize acid in water. Such direct chemical effects are measured as acid-neutralizing capacity, once termed alkalinity (Wetzel and Likens 1991). Biological processes can also neutralize the effects of acid. Much nitric acid can be neutralized by its uptake as a plant nutrient. This effect can be substantial in many aquatic habitats. Sulfuric acid can be neutralized by the reduction of sulfate to less oxidized forms by bacterial processes in anaerobic environments (Cook et al. 1986). Nitric acid can likewise be neutralized in anaerobic environments. The overall net effects of acid additions to lakes can, therefore, be much less than would be expected on the basis of hydrogen ions being added. Biological alkalinity generation can be substantial and must be factored into any predictions of the effects of acid loading within a region (Schindler 1986).

Ecological Consequences of Acidification

The effects of acidification on ecological processes are substantial and they can influence a wide range of lake features. Acid effects have been inferred from comparative surveys that have examined biological and chemical characteristics across series of lakes that exhibit different pH conditions (e.g., Schindler et al. 1989). Long-term patterns of acidification have also been inferred from paleolimnological studies (Smol et al. 1984). The clearest demonstrations of acidification effects have been through direct pH manipulations conducted at a variety of different scales. We emphasize these experimental studies here to help illustrate the value of such research approaches. We summarize smaller-scale experiments that have been used to assess acid effects and then describe experiments conducted at the scale of a whole ecosystem. We outline the range of the factors that must be considered in conducting and interpreting acidification experiments.

Smaller-Scale Experiments to Evaluate the Effects of Acidification

Smaller-scale experiments have been a powerful tool for studying the effects of acidification on aquatic communities (e.g., Havens 1992; Locke and Sprules 1993; Fischer 1997). While these studies lack the realism of acidification experiments conducted at the whole-lake scale, they have several advantages including (1) opportunities to compare several different acidified treatments (e.g., different levels of pH), (2) replication of experimental treatments, and (3) reduced costs of implementation.

In situ mesocosm experiments have been used to study the responses of lower trophic levels (bacteria, phytoplankton, and zooplankton) to acidification. Fishes have generally been excluded from these experiments because it is difficult to recreate natural densities and behaviors in mesocosms. Mesocosms are constructed of clear polyethylene (>4 mil) tubes that are suspended from floating rafts made from wood or PVC pipe. Mesocosm volumes range from less than 60 liters (Havens 1992) to 16,000 liters (Locke and Sprules 1993); however, most mesocosms are greater than 2000 liters. Some mesocosms are open to sediments (Arvola et al. 1986, Barmuta et al. 1990), while others are sealed at the bottom (Locke and Sprules 1993, Fischer

1997). The duration of such experiments should be planned carefully to avoid scale-dependent artifacts (e.g., excessive periphyton growth on mesocosm walls). Experiments in larger (>1000 liters) mesocosms can be run for longer periods of time (weeks or months) while smaller mesocosms (<1000 liters) should be terminated within a couple of weeks. Systematic considerations of the effects of mesocosm size are worthy assessments from a variety of perspectives (Petersen et al. 1997) and may have particular value in evaluating acidification effects.

Previous studies have employed a variety of experimental treatments to study the effects of acid on aquatic communities. Acid is generally added to mesocosms in a dilute form to avoid the temporary formation of highly acidic patches of water. Typically, sulfuric acid is used to lower pH in mesocosms (but see Barmuta et al. 1990 for an example of a combination of sulfuric and nitric acids). In most studies, acid is evenly mixed throughout the mesocosm. However, Locke and Sprules (1993) successfully manipulated pH in the epilimnion versus the whole water column of thermally stratified mesocosms. Interestingly, zooplankton communities responded similarly in the epilimnetic and whole water column acidification treatments suggesting that a high pH hypolimnetic refuge does not increase survival of acid-sensitive species. While most studies reduce pH to target levels in a single step, Havens (1992) allowed a 7-day acclimation period during which pH was reduced in small steps. Fischer (1997) compared zooplankton responses to a single sustained acidification (PRESS sensu Bender et al. 1984) versus multiple short-term acidification events (PULSE sensu Bender et al. 1984). Crustacean zooplankton responded similarly in PRESS and PULSE treatments, while some shorter-lived rotifer species exhibited recovery when the pH was raised in the PULSE treatment (Fischer, unpublished data). In all of these studies, interpretation of results was aided by the inclusion of an unacidified control treatment.

Community responses to acidification in mesocosm experiments occur through direct and indirect pathways. For example, several studies (Barmuta et al. 1990; Locke and Sprules 1993; Fischer 1997) have noted increases in acid-tolerant species such as *Bosmina longirostris* following decreases in their acid-sensitive competitors (e.g., *Holopedium gibberum* and *Daphnia* spp.). Several different approaches have been used to explore mechanisms driving community responses to acidification. Locke and Sprules (1993) used changes in body size, egg ratio, and lipid status to make inferences about the role of acid sensitivity and food web interactions in controlling zooplankton responses. Fischer (1997) applied first order autoregressive models (Ives 1995) to experimental data to differentiate the role of direct and indirect effects in zooplankton community responses to acidification. While most mesocosm studies have focused on community-level responses, Havens (1992) also monitored the effects of acidification on ecosystem parameters such as algal carbon assimilation rates and carbon transfer efficiency from algae to zooplankton.

Short-term experiments in smaller containers have the potential to reveal some of the mechanisms operating in responses to acidification. In particular, they can be used to test the direct response of smaller organisms to acid effects. Results of such experiments must be interpreted with caution, however. Results of standard laboratory experiments may not be very effective for predicting community responses at the whole-lake scale. In an explicit comparison of laboratory bioassays and a whole-lake acidification experiment, Gonzalez and Frost (1994) found that bioassays for one rotifer species correctly predicted the population's decrease in response to acid conditions. However, detrimental effects of acid conditions in bioassays occurred only when acid conditions were combined with reduced food availability. Rotifers were insensitive to acid conditions if they were fed ad libitum and incubated in the lake in 4-liter containers for 2 to 3 days, as is standard in many bioassay protocols. Discrepancies between small-scale and whole-lake responses were much more striking for a second rotifer species. Bioassays suggested that this species would decline under acid conditions. Instead, they increased to dominate rotifer biomass during the most acidified stage of the experiment (Gonzalez and Frost 1994). These rotifer results were consistent with the general observation that many population changes in the acidified lake were driven by indirect, food-web-related mechanisms rather than direct responses to acidification (Webster et al. 1992). Similarly, Fischer (1997) working with other zooplankton taxa quantified population

responses across a gradient of pH conditions in 10-liter containers incubated in situ for 7 days. Species known to respond to acidification through indirect pathways did not respond to acidification in these short-term experiments. In general, short-term experiments isolate the direct effects of experimental manipulations that happen quickly. They are less effective, however, in incorporating slower-acting indirect mechanisms that can operate within a lake. Thus, we view the combination of experiments conducted at different scales (e.g., beakers to whole lakes) as an effective approach for examining the effects of acidification on aquatic ecosystems (Frost et al. 1988).

Large-Scale Experiments to Evaluate the Effects of Acidification

As with other whole-ecosystem experiments (Carpenter et al. 1995), tremendous insights have been gained into the effects of acidification and into basic ecosystem processes through whole-lake acidification experiments. Such experiments can be designed to ask different basic questions about acidification. Extrapolation from any single experiment must be based on a fundamental understanding of the way that a manipulated lake interacts with its surrounding landscape, as well as the ways that it compares with other lakes. Detailed comparisons of a few whole-lake acidification experiments revealed a fair number of common features in their results (Schindler et al. 1991).

The most fundamental element of any large-scale experiment is the availability of a reference system or systems against which the conditions in a treatment system can be compared. Such comparisons allow inferences of manipulation effects against the background of natural variability (e.g., Schindler et al. 1991; Frost et al. 1988). Treatment lakes are paired against nearby reference lakes or are divided into treatment and reference basins using vinyl curtains (available from, for example, Environetics, Inc., Bridgeview, Ill. and FabriCraft, Syracuse, NY). Such situations have obvious limitations in terms of their replication, of course, and require the use of special statistical techniques (e.g., Carpenter et al. 1989; Rasmussen et al. 1993) that have some important limitations (Stewart-Oaten et al. 1992).

A whole-ecosystem acidification experiment can be designed to test either how much a lake would respond to a predetermined amount of acid loading (Rudd et al. 1990; Schindler 1988) or the effects of acidification to a particular target level on the organisms and processes within a lake (Schindler et al. 1985; Brezonik et al. 1993). The former experimental design revealed the importance of acid-neutralizing processes other than those associated with the immediate chemical response of a lake's water to the effects of added acid, a phenomenon that is responsible for the much less extensive occurrence of lake acidification than might have been anticipated based upon standard limnological measures (Schindler 1986). The latter design can be used to explore the consequences of levels of acidification that have occurred, such as might be important in developing management programs for regions effected by acidification.

Experiments to test the consequences of acidification must consider a wide range of factors when evaluating the consequences of decreasing pH levels. The proportional occurrence of nitric and sulfuric acids used in a manipulation must be considered because they have fundamentally different effects as they acidify an ecosystem (Rudd et al. 1988). The full range of biogeochemical responses to changes in pH conditions must also be factored into experimental designs. Some of the most dramatic organismal responses to reduced pH conditions have been associated with changes in the levels of aluminum (Al) (Cronan and Schofield 1979) and mercury (Hg) (Wiener et al. 1990) that have been generated by acidification. Increased Al levels result from changes in its solubility with acidification, whereas Hg increases have been driven by microbial processes coupled with biomagnification up a lake's food web. Likewise, the fundamental cycling of nitrogen was shut down by acidification to around pH 5.4, causing a progressive accumulation of ammonium (Rudd et al. 1988). The addition of even a single acid can induce multiple stresses and generate a wide range of changes that propagate from the initial stress (Frost et al. 1999). These changes not only include the biogeochemical shifts described above but also changes in physical lake properties such as light

absorbance (Schindler et al. 1996; Williamson et al. 1996; Yan et al. 1996a), as well as the fundamental interactions within a lake's food web mentioned earlier (Webster et al. 1992).

Acidification experiments must also consider the time necessary for the full range of chemical and biological effects to propagate through an ecosystem. For example, adult fishes have been shown to be relatively immune to acid effects while younger fishes (less than one year of age) are more sensitive. Effects on adult fish populations would only be detectable after a time period close to the life span of fishes, requiring an extended treatment period to detect the effects of changing fish populations (Schindler et al. 1985; Eaton et al. 1992). Such fish changes might be anticipated to have major consequences on a wide range of limnological features (Carpenter and Kitchell 1993). The degree of changes in chemical features have been shown to increase over the course of a pH manipulation to a certain level (Brezonik et al. 1993). It seems unlikely that the whole-lake experiments that have been conducted have been carried out for a long enough time that all acid responses have had an opportunity to reach their culmination. Longer experiments seem likely to exhibit a wider range of responses. One example of a pH time course from an acidification experiment in Little Rock Lake, Wisconsin, is illustrated in Figure 22.1. Some examples of Little Rock Lake results are also presented to illustrate the different time courses of responses by different zooplankton species (Figs. 22.2 and 22.3).

Whole-lake experiments have other limitations in addition to the time necessary for effects to play out. Not all of the interactions of a lake with its watershed can be incorporated in experimental designs. Water inputs and the materials that they can

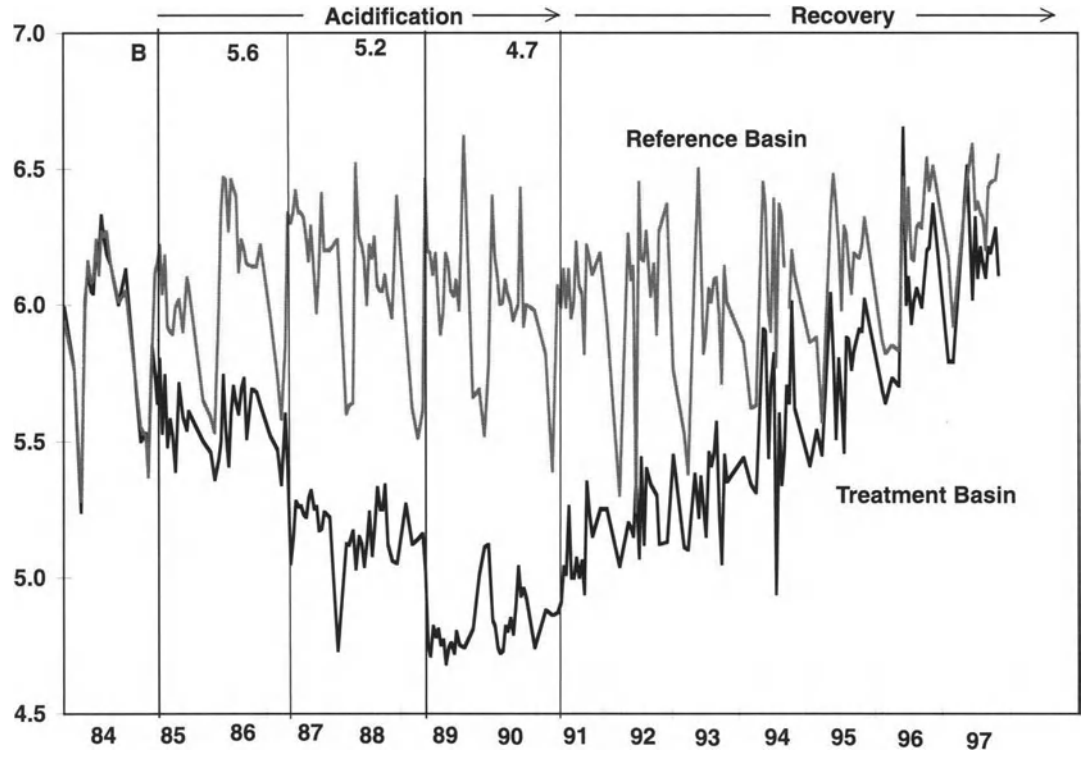

FIGURE 22.1. Time series of surface pH values in the treatment and reference basins of Little Rock Lake, Wisconsin, USA. The acidification phase of the experiment extended from 1984 through 1990. Since ice out in 1991, the treatment basin has been undergoing recovery. Methods are reported in Brezonik et al. (1993).

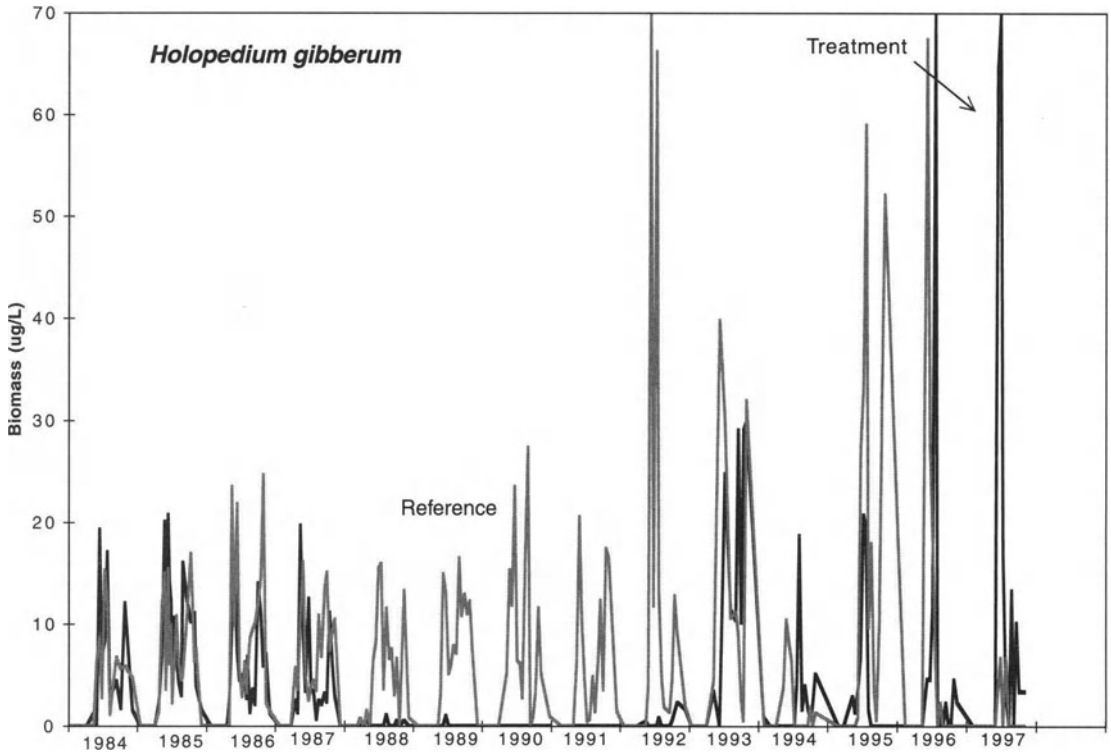

FIGURE 22.2. Time series of biomass values (μg liter^{-1}) for *Holopedium gibberum* in the treatment and reference basins of Little Rock Lake, Wisconsin, USA. The acidification phase of the experiment extended from 1984 through 1990. Since ice out in 1991, the treatment basin has been undergoing recovery. Methods for collecting these data are reported in Frost and Montz (1988).

transport are frequently not able to effectively simulate the effects of acid deposition. Time constraints can interact with watershed considerations. For example, the occurrence of a drought during the course of the Little Rock Lake experiment minimized any interactions of the lake with its surroundings, potentially exacerbating the rates of acidification produced by the manipulation (Frost et al. 1999). Despite these limitations, however, whole-lake manipulations provide the best opportunity to evaluate the full range of consequences of acidification.

Perceptions of the consequences of acidification vary depending upon the scale of the measures used to assess lake response. For example, in Little Rock Lake, total zooplankton biomass, a measure of the basic function of the zooplankton community, was much less influenced by acidification than was the zooplankton community composition (Frost et al. 1995). This reflects a basic feature of lake ecosystems in that collective ecosystem properties appear to be much less sensitive to the effects of stress than do populations of individual species. This occurs because there is a substantial amount of functional complementarity among the species that carry out a basic system function, a process that appears to occur in many different ecosystems (Frost et al. 1995). This raises an important issue in the choice of variable used to measure response in small- or large-scale acidification experiments. Responses by variables such as total zooplankton are going to be generally much less sensitive to a manipulation than responses by a sensitive species. Of course, an incorrect species choice may lead to a situation in which responses in an experimental variable may be difficult to detect, particularly against the background of natural daily, seasonal, and annual variability.

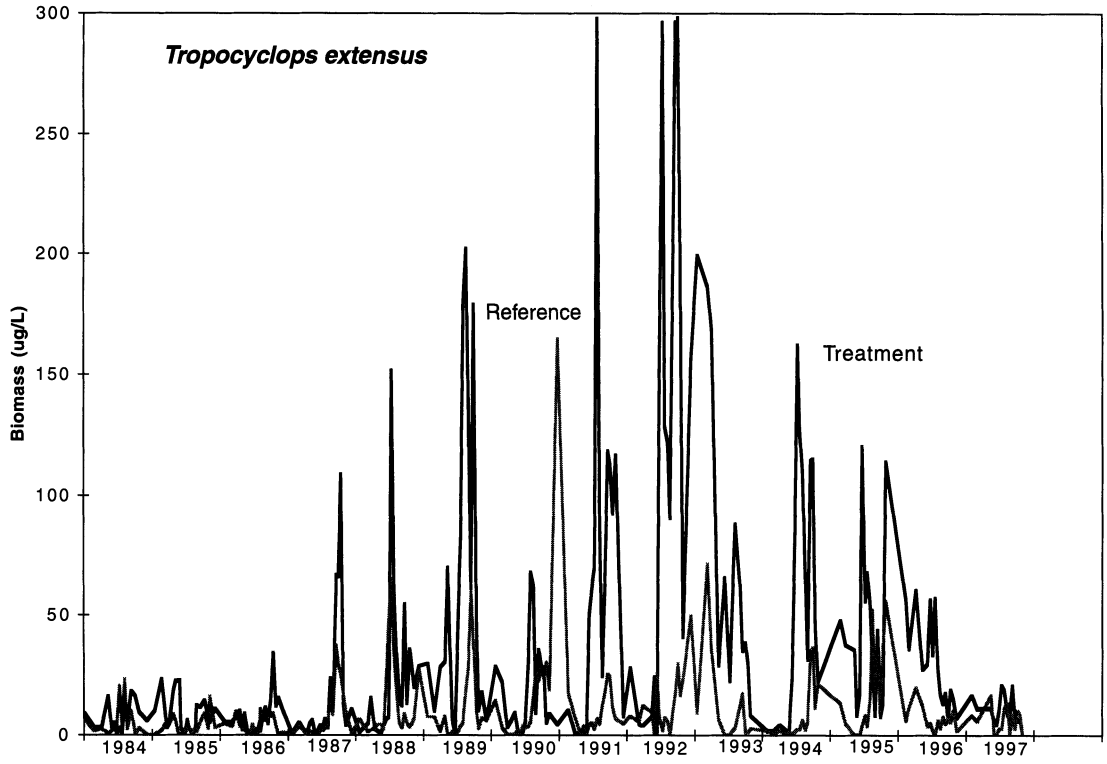

FIGURE 22.3. Time series of biomass values (μg liter^{-1}) for *Tropocyclops extensus* in the treatment and reference basins of Little Rock Lake, Wisconsin, USA. The acidification phase of the experiment extended from 1984 through 1990. Since ice out in 1991, the treatment basin has been undergoing recovery. Methods for collecting these data are reported in Frost and Montz (1988).

The results from Little Rock Lake also illustrate another feature that has been common to several whole-lake experiments. They provide an opportunity to examine a lake's recovery from acidification once acid additions have been completed. Chemically, conditions in Little Rock Lake returned to preacidification levels fairly quickly (see Fig. 22.1). Biological recovery has not followed the same pathway, however. In particular, zooplankton recovery has not taken place as quickly as chemical recovery (see Figs. 22.2 and 22.3). At the same time, and contrary to expectations, species that had exhibited high population abundance during acidification did not persist at their high levels but declined to premanipulation population levels (Frost et al. 1998). Other recovery experiments have taken lakes that had been acidified unintentionally by anthropogenic processes and increased their pH by the addition of a buffering agent such as lime (e.g., Andersson and Olsson 1985; Yan et al. 1996b). Such liming can also be used as a management tool in regions where widespread acidification of lakes has occurred. While liming does not allow for complete recovery of a lake, conditions are generally improved substantially. Comparisons between responses to stress and recovery from stress have an added benefit of exploring the basic forces that underlie a community. Whether biological recovery is simply slower than chemical recovery or whether a lake's community has been shifted into some alternate stable state remains to be seen. Given recent changes in acid loading, there may be more opportunities to examine recovery in large-scale experiments.

The wide-ranging utility of large-scale experimental manipulations is clear. They can provide valuable insights into the effects of a stress such as acidification and into fundamental characteristics of

ecosystems. It has been our goal in this chapter to illustrate these benefits and to point out some of the cautions that must be made when designing and interpreting acidification experiments.

Acknowledgments We thank Janet Blair and Tim Kratz for their assistance at a distance and Bob Howarth for his patience and encouragement in the development of this chapter. Support for its production was provided by the National Science Foundation through its Long-Term Research in Environmental Biology, Long-Term Ecological Research, and Post-Doctoral Research in Environmental Biology programs.

References

Anderson, M.P.; Bowser, C.J. The role of groundwater in delaying lake acidification. Water Resourc. Res. 22:1101–1108; 1986.

Andersson, F.; Olsson, B., eds. Lake Gardsjon: An acid lake and its catchment. Ecol. Bull. 37:1–336; 1985.

Arvola, L; Salonen, K.; Bergstrom, I.; Heinanen, A.; Ojala, A. Effects of experimental acidification on phyto-, bacterio-, and zooplankton in enclosures of a highly humic lake. Int. Rev. ges. Hydrobiol. 71:737–758; 1986.

Barmuta, L.A.; Cooper, S.D.; Hamilton, S.K.; Kratz, K.W.; Melack, J.M. Responses of zooplankton and zoobenthos to experimental acidification in a high-elevation lake (Sierra Nevada, California, U.S.A.) Freshwat. Biol. 23:571–586; 1990.

Bender, E.A.; Case, T.J.; Gilpin, M.E. Perturbation experiments in community ecology: Theory and practice. Ecology 65:1–13; 1984.

Breitburg, D.; Seitzinger, S.; Saunders, J., eds. The effects of multiple stressors on freshwater and marine aquatic ecosystems. Limnol. Oceanogr. 44 (3, part 2):739–972; 1999.

Brezonik, P.L.; Eaton, J.G.; Frost, T.M.; Garrison, P.J.; Kratz, T.K.; Mach, C.E.; McCormick, J.H.; Perry, J.A.; Rose, W.A.; Sampson, C.J.; Shelley, B.C.L.; Swenson, W.A.; Webster, K.E. Experimental acidification of Little Rock Lake, Wisconsin: Chemical and biological changes over the pH range 6.1 to 4.7. Can. J. Fish. Aquat. Sci. 50:1101–1121; 1993.

Carpenter, S.R.; Kitchell, J.F., eds. *The Trophic Cascade in Lakes.* Cambridge Studies in Ecology. New York: Cambridge Univ. Pr.; 1993.

Carpenter, S.R.; Chisholm, S.W.; Krebs, C.J.; Schindler, D.W.; Wright, R.F. Ecosystem experiments. Science 269:324–327; 1995.

Carpenter, S.R.; Frost, T.M.; Heisey, D.; Kratz, T.K. Randomized intervention analysis and the interpretation of whole-ecosystem experiments. Ecology 70:1142–1152; 1989.

Charles, D.F., ed. *Acidic Deposition and Aquatic Ecosystems: Regional Case Studies.* New York: Springer-Verlag; 1991.

Cole, J.J.; Caraco, N.F.; Kling, G.W.; Kratz, T.K. Carbon dioxide supersaturation in the surface waters of lakes. Science 265:1568–1570; 1994.

Confer, J.L.; Kaaret, T.; Likens, G.E. Zooplankton diversity and biomass in recently acidified lakes. Can. J. Fish. Aquat. Sci. 40:36–42; 1983.

Cook, R.B.; Kelly, C.A.; Schindler, D.W.; Turner, M.A. Mechanisms of hydrogen ion neutralization in an experimentally acidified lake. Liminol. Oceanogr. 31:134–148; 1986.

Cronan, C.S.; Schofield, C.L. Aluminum leaching in response to acid precipitation: Effects on high-elevation watersheds in the Northeast. Science 204:304–306; 1979.

Crosby, B.J.; Ryan, P.F.; Webb, J.R.; Hornberger, G.M.; Galloway, J.N. Mountains of Western Virginia. In: Charles, D.F., ed. *Acidic Deposition and Aquatic Ecosystems: Regional Case Studies.* New York: Springer-Verlag; 1991:297–318.

Dillon, P.J.; Reid, R.A.; de Grosbois, E. The rate of acidification of aquatic ecosystems in Ontario, Canada. Nature 329:45–48; 1987.

Eaton, J.G.; Swenson, W.A.; McCormick, J.H.; Simonson, T.D.; Jensen, K.M. A field and laboratory investigation of acid effects on largemouth bass, rock bass, black crappie, and yellow perch. Trans. Am. Fish. Soc. 121:644–658; 1992.

Elwood, J.W.; Sale, M.J.; Kaufmann, P.R.; Cada, G.F. The Southern Blue Ridge Province. In: Charles, D.F., ed. *Acidic Deposition and Aquatic Ecosystems: Regional Case Studies.* New York: Springer-Verlag; 1991:319–364.

Fischer, J.M. Zooplankton community responses to acidification: the role of rapid evolution and compensatory dynamics. Ph.D. disseration, University of Wisconsin, Madison, WI; 1997.

Frost, T.M.; DeAngelis, D.L.; Bartell, S.M.; Hall, D.J.; Hurlbert, S.H. Scale in the design and interpretation of aquatic community research. In Carpenter, S.R., ed. *Complex Interactions in Lake Communities.* New York: Springer-Verlag; 1988:229–258.

Frost, T.M.; Carpenter, S.R.; Ives, A.R.; Kratz, T.K. Species compensation and complementarity in ecosystem function. In Jones, C.G.; Lawton, J.H., eds. *Linking Species and Ecosystems.* New York: Chapman and Hall; 1995:224–239.

Frost, T.M.; Montz, P.K. Early zooplankton response to experimental acidification in Little Rock Lake, Wis-

consin, USA. Verh. Internat. Verein. Limnol. 23:2279–2285; 1988.

Frost, T.M.; Montz, P.K.; Kratz, T.K. Zooplankton community responses during recovery from acidification: Limited persistence by acid-favored species in Little Rock Lake, Wisconsin. Restor. Ecol. 6:336–342; 1998.

Frost, T.M.; Montz, P.K.; Kratz, T.K.; Badillo, T.; Brezonik, P.L.; Gonzalez, M.J.; Rada, R.G.; Watras, C.J.; Webster, K.E.; Wiener, J.G.; Williamson, C.E.; Morris, D.P. Multiple stresses from a single agent: Diverse responses to the experimental acidification of Little Rock Lake, Wisconsin. Limnol. Oceanogr. 44:784–794; 1999.

Gonzalez, M.J.; Frost, T.M. Comparisons of laboratory bioassays and a whole-lake experiment: Rotifer responses to experimental acidification. Ecol. Applic. 4:69–80; 1994.

Havens, K.E. Acidification effects on the algal-zooplankton interface. Can. J. Fish. Aquat. Sci. 49:2507–2514; 1992.

Hutchinson, G.E. *A Treatise on Limnology. Vol. I. Geography, Physics and Chemistry.* New York: Wiley; 1957.

Husar, R.B.; Sullivan, T.J.; Charles, D.F. Historical trends in atmosheric sulfur deposition and methods for assessing long-term trends in surface water chemistry. In: Charles, D.F., ed. *Acidic Deposition and Aquatic Ecosystems: Regional Case Studies.* New York: Springer-Verlag; 1991:65–82.

Ives, A.R. Predicting the response of populations to environmental change. Ecology 76:926–941; 1995.

Jenkins, A.; Ferrier, R.C.; Kirby, C., eds. *Ecosystem Manipulation Experiments: Scientific Approaches, Experimental Design and Relevant Results.* Ecosystems Research Report 20. Office for Official Publications of the European Communities: Luxembourg; 1995.

Kratz, T.K.; Cook, R.B.; Bowser, C.J.; Brezonik, P.L. Winter and spring pH depressions in northern Wisconsin lakes caused by increases in pCO_2. Can. J. Fish. Aquat. Sci. 44:1082–1088; 1987.

Locke, A.; Sprules, W.G. Effects of acidification on zooplankton population and community dynamics. Can. J. Fish. Aquat. Sci. 50:1238–1247; 1993.

Martin, L. *The Physical Geography of Wisconsin.* Madison, WI: Univ. Wisconsin Pr.; 1965.

McKnight, D.; Bencala; K.E. Diel variations in iron chemistry in an acidic stream in the Colorado Rocky Mountains, USA. Arct. Alp. Res. 20:492–500; 1988.

Munson, R.K.; Gherini, S.A. Processes influencing the acid-base chemistry of surface waters. In: Charles, D.F., ed. *Acidic Deposition and Aquatic Ecosystems: Regional Case Studies.* New York: Springer-Verlag; 1991:9–34.

Petersen, J.E.; Chen, Chung-Chi; Kemp, W.M. Scaling aquatic primary productivity experiments under nutrient- and light-limited conditions. Ecology 78:2326–2338; 1997.

Rasmussen, P.W.; Heisey, D.M.; Nordheim, E.V.; Frost, T.M. Time-series intervention analysis: Unreplicated large-scale experiments In: Scheiner, S.M.; Gurevitch, J., eds. *Design and Analysis of Ecological Experiments.* New York: Chapman and Hall; 1993:138–158.

Rudd, J.W.M.; Kelly, C.A.; Schindler, D.W.; Turner, M.A. Disruption of the nitrogen cycle in acidified lakes. Science 240:1525–1527; 1988.

Schindler, D.W. The significance of in-lake production of alkalinity. Water Air Soil Pollut. 30:931–944; 1986.

Schindler, D.W. Effects of acid rain on freshwater ecosystems. Science 239:149–157; 1988.

Schindler, D.W.; Mills, K.H.; Malley, D.F.; Findlay, D.L.; Shearer, J.A.; Davies, I.J.; Turner, M.A.; Linsey, G.A.; Cruikshank, D.R. Long-term ecosystem stress: The effects of years of experimental acidification on a small lake. Science 228:1395–1401; 1985.

Schindler, D.W.; Kasian, S.E.M.; Hesslein; R.H. Biological impoverishment in lakes of the midwestern and northeastern United States from acid rain. Environ. Sci. Tech. 23:573–580; 1989.

Schindler, D.W.; Frost, T.M.; Mills, K.H.; Chang, P.S.S.; Davies, I.J.; Findlay, D.L.; Malley, D.F.; Shearer, J.A.; Turner, M.A.; Garrison, P.J.; Watras, C.J.; Webster, K.E.; Gunn, J.M.; Brezonik, P.L.; Swenson, W.A. Comparisons between experimentally- and atmospherically-acidified lakes during stress and recovery. Proc. R. Soc. Edinb. 97B:193–226; 1991.

Schindler, D.W.; Curtis, P.J.; Parker, B.R.; Stainton, M.P. Consequences of climate warming and lake acidification for UV-B penetration in North American boreal lakes. Nature 379:705–708; 1996.

Schrenk, M.O.; Edwards, K.J.; Goodman, R.M.; Hamers, R.J.; Banfield, J.F. Distribution of *Thiobacillus ferrooxicans* and *Leptospriillum ferrooxidans:* Implications for generation of acid mine drainage. Science 279:1519–1522; 1998.

Smol, J.P.; Charles, D.F.; Whitehead, D.R. Mallomonadacean microfossils provide evidence of recent lake acidification. Nature 307:628–630; 1984.

Stewart-Oaten, A.; Bence, J.R.; Osenberg; C.W. Assessing effects of unreplicated perturbations: No simple solutions. Ecology 73:1396–1404; 1992.

Stumm, W.; Morgan, J.J. *Aquatic Chemistry.* 2nd ed. New York: Wiley; 1981.

Webster, K.E.; Newel, A.D.; Baker, L.A.; Brezonik, P.L. Climatically induced rapid acidification of a softwater seepage lake. Nature 347:374–376; 1990.

Webster, K.E.; Frost, T.M.; Watras, C.J.; Swenson, W.A.; Gonzalez, M.; Garrison, P.J. Complex biological responses to the experimental acidification of Little

Rock Lake, Wisconsin, USA. Environ. Pollut. 78:73–78; 1992.

Wetzel, R.G. *Limnology.* Philadelphia: Saunders; 1983.

Wetzel, R.G.; Likens, G.E. *Limnological Analyses.* 2nd ed. New York: Springer-Verlag; 1991.

Wiener, J.G.; Fitzgerald, W.F.; Watras, C.J.; Rada, R.G. Partitioning and bioavailability of mercury in an experimentally acidified Wisconsin lake. Environ. Toxicol. Chem. 9:909–918; 1990.

Williamson, C.E.; Stemberger, R.S.; Morris, D.P.; Frost, T.M.; Paulsen, S.G. Ultraviolet radiation in North American lakes: Attenuation estimates from DOC measurements and implications for plankton communities. Limnol. Oceanogr. 41:1024–1034; 1996.

Yan, N.D.; Keller, W.; Scully, N.M.; Lean, D.R.S.; Dillon, P.J. Increased UV-B penetration in a lake owing to drought induced acidification. Nature 381:141–143; 1996a.

Yan, N.D.; Keller, W.; Somers, K.M.; Pawson, T.W.; Girard, R.E. Recovery of crustacean zooplankton communities from acid and metal contamination: Comparing manipulated and reference lakes. Can. J. Fish. Aquat. Sci. 53:1301–1327; 1996b.

23

Large-Scale Water Manipulations

Paul J. Hanson

Introduction

Researchers predict that increasing levels of greenhouse gases in the atmosphere will cause a 1 to 3.5°C increase in average global temperatures and alter regional levels of precipitation (Kattenberg et al. 1996; Rind et al. 1990). Changes in global temperature and altered precipitation patterns may lead to dramatic changes in ecosystem productivity, biogeochemical cycling, and the availability of water resources (Kirschbaum and Fischlin 1996; Melillo et al. 1990). The responses of ecosystems to decreased water availability or increased occurrence of drought is considered a key issue in climate change scenarios (Wigley et al. 1984), because changes in the carbon sequestration potential of vegetation at the global scale may alter the accumulation of carbon dioxide (CO_2) in the atmosphere, potentially moderating or accelerating climate changes (Ojima et al. 1991; Wigley and Jones 1985). Because the actual direction and magnitude of expected changes in precipitation are highly uncertain, and consensus scenarios for regional climate change do not exist, manipulation experiments can play a significant role in clarifying the potential impacts of a range of climate change scenarios on highly valued ecosystems.

Controlled experiments in greenhouses and growth chambers have provided us with a large database of information concerning the impacts of moisture manipulations on the physiology and growth of forest tree seedlings and saplings (Ellsworth and Reich 1992; Hinckley et al. 1978; Kleiner et al. 1992; Kolb et al. 1990; Pezeshki and Chambers 1986). However, concerns remain as to the appropriateness of the extrapolation of small-scale and short-term data to mature tree responses in forest stands where existing data are limited largely to short-term responses to water stress (Cregg et al. 1989; Hinckley et al. 1978) or to a limited number of trees sampled or species observed (Dougherty and Hinckley 1981; Epron et al. 1992; Ginter-Whitehouse et al. 1983). Similar concerns and arguments can be made for the extrapolation of data for other ecosystems. In response to concerns over the validity of small-scale experimental response data for environmental assessments, several recent reviews (Graham et al. 1990; Mooney 1991; Mooney et al. 1991; Woodward 1992) have called for large-scale manipulation experiments as the appropriate means by which to study the impacts of changing climates on ecosystems.

This chapter outlines important methodological issues involved in the design and operation of large-scale precipitation manipulation experiments. Previous precipitation or water manipulation studies historically focused on scenarios of increasing or decreasing precipitation patterns and the resulting impacts on small plants or saplings grown in pots or small field plots (Hinckley et al. 1978; Kozlowski 1982). The primary objective of these studies was to determine the impact of irrigation or drought on plant growth or the harvest index of a particular crop. Irrigation methods for application to agricultural crops and forest plantations have been discussed previously (Hagan et al. 1967; Stewart and Nielsen 1990) and they will not be extensively reviewed here. Instead, this chapter focuses on precipitation manipulation methods that

have been used at the plot or stand level in natural ecosystems or forest plantations for studying the impacts of anthropogenic stressors (i.e., acid precipitation and/or climate change) on ecosystem and plant processes. Large-scale manipulations are defined in this chapter as those field experiments that are of sufficient size and complexity to handle questions of individual plant response as well as stand-level carbon, water, and nutrient cycling responses.

Active Versus Passive Manipulations

Precipitation manipulation studies can be divided into two general categories: active versus passive approaches. Active precipitation manipulation studies involve the use of above-canopy irrigation methods to supplement natural rainfall or add modified rainfall chemistries. Passive approaches employ understory troughs or complete "roofs" to intercept natural throughfall or rainfall for diversion away from treatment plots. The diverted water can be discarded or channeled to alternate plots for complementary irrigation. Studies described by Abrahamsen et al. (1977), Irving and Miller (1981), and Johnston et al. (1986) all employed active irrigation methods for use in small field studies of acid precipitation impacts on crops and tree seedlings. Active plot-scale irrigations were also employed by Sala and Lauenroth (1982) and more recently by Golluscio et al. (1998) to evaluate grassland ecosystems. A good example of the passive approach would be the throughfall displacement experiment described by Hanson et al. (1995, 1998) for manipulation of rainfall quantity in an upland oak forest. A combination of active and passive approaches was employed at the plot scale by the EXMAN (experimental manipulation) projects in forest ecosystems in Europe (Beier et al. 1995) and at the watershed scale (Moldan et al. 1995; Hultberg et al. 1993) for studies of the impact of rainfall chemistries on growth and nutrient cycling of plantation-grown conifers. Table 23.1 summarizes a number of field-based studies that have attempted with various rates of success to modify natural rainfall patterns against the backdrop of natural climate variability. Total control of water quantity and chemistry is easy to attain for small plants in greenhouses and growth chambers, but is much more difficult in the field. A notable attempt to achieve such control at the level of whole catchments is the CLIMEX project (Jenkins and Wright 1995) which uses a 1200-m^2 greenhouse to attempt complete control over system precipitation, temperature, and atmospheric CO_2 concentrations. A recent mesic grassland study (Fay et al., in press) combined passive rainfall collection and subsequent active redistribution to generate multiple pre-

TABLE 23.1. Studies designed to passively manipulate throughfall quantity or quality of forest stands or grasslands for evaluating impacts on plant and soil processes.

Location	Key genera	Stand age (yr)	Treatment	Manipulated area[a] (m^2)	Reference
Walker Branch, USA	*Quercus/Acer*	80–120	±33%	12,800	Hanson et al. 1995, 1998
Lake Gårdsjön, Sweden	*Picea*	80–100	na[b]	6300	Moldan et al. 1995 Hultberg et al. 1993
Klosterhede, Denmark	*Picea*	74	−100% and variable	1176	Gundersen et al. 1995 Beier et al. 1995 Rasmussen et al. 1995
Solling, Germany	*Picea*	60	variable	300	Lamersdorf et al. 1995
Konza Prairie, USA	Grassland	na	−30% altered timing	144	Fay et al. (in press)
Ballyhooly, Ireland	*Picea*	60	−100%	100	Lamersdorf et al. 1995
Springforbi, Denmark	*Picea*	14–21	−50 to −75%	46	Holstener-Jørgensen 1994
France	*Quercus*	32	−100%	14–25	Bréda et al. 1993; 1995
Canada	*Acer*	80	−100%	16 per tree	Pilon et al. 1996

[a]Area available for manipulating throughfall. This is typically the area under a roof, troughs or tarpaulin.
[b]Not applicable.

cipitation treatments at the plot scale, including normal precipitation quantity and timing, 30% reductions in precipitation, and 30% reductions and/or extended dry periods.

With this brief introduction to the general types of precipitation and ecosystem manipulations that have been reported, consideration will be given to methodological issues important for appropriate application of water manipulations to large-scale field studies.

Artificial Rainfall

Controlled studies designed to assess the effects of rain or mist chemistries on test plants must consider several chemical and physical design criteria if results are to meaningfully address effects appropriate to field conditions. Among the parameters traditionally considered important are those related to solution chemistry (pH, ionic composition), solution physics (drop size and velocity), and the temporal and spatial characteristics of precipitation events (uniform distribution, intensity, and volume). Artificial rainfall systems can be designed in a variety of ways to meet a variety of experimental goals. Simple irrigation systems consisting of dippers, watering cans, or hoses have been used to amend soil water and nutrient levels periodically. Automated drip irrigation systems function in the same way, but do not allow for the interaction between rain and foliage characteristic of natural rainfall. The addition of water and nutrients through overhead nozzles or rotating booms represents an additional step in complexity that allows for this contact.

The primary goal of any artificial rain system for use in controlled experiments should be to imitate the chemical and physical features of natural rain events in an appropriate temporal scale and under reasonable environmental conditions. A summary of the variables of ambient rainfall that have been incorporated into existing rain simulation systems is found in Table 23.2. Hanson et al. (1990) discuss the features of appropriate rainfall simulators in some detail. The key physical and chemical features of appropriate artificial rain are repeated here. Raindrop sizes should be maintained in the range between 0.1 and 1.0 mm for most rain simulations, dispensing nozzles directed upward to allow gravity to drive deposition should be positioned 2 to 3 m above the plant leaves to allow the raindrops to attain terminal velocity before impact (an important consideration for studies of foliar nutrient deposition/leaching).

TABLE 23.2. Important variables to consider when simulating rainfall additions and throughfall removal.

I. Artificial rainfall additions
A. Physical variables:
Drop size
Drop velocity
Rainfall distribution
Rainfall intensity
Reasonable quantities
B. Chemical variables:
Inorganic ions
Organic constituents
C. Temporal and environmental variables:
Time of day
Event frequency
Light, Temperature, Wind
II. Throughfall removal or redistribution
A. Physical variables:
Rainfall distribution
Rainfall intensity
Reasonable quantities
B. Chemical variables:
Inorganic ions
Organic constituents
C. Temporal and environmental variables:
Time of day (for redistribution of throughfall)
Light, Temperature, Wind

To ensure adequate control over the chemical integrity of rain solutions artificial rain systems should employ the following: water purification systems, adequate clean storage capacity, and apparatus for diluting stock solutions if mixing is conducted automatically. Among the chemical variables traditionally considered important are solution pH and ionic concentrations of several macro- and microelements.

Unfortunately, many of the key elements of good artificial rain additions make their application at the field scale costly and logistically difficult. As an alternative, researchers have typically defaulted to subcanopy additions of water and/or simulated throughfall chemistries via drip or pressurized nozzle approaches. Understory additions of supplemental rainfall are the logical approach as they are easier to operate and install, but they fall short of

being an accurate simulation of increased precipitation because they do not allow for the interaction of precipitation with canopy foliage, branches, and stems, and the concurrent uptake (NO_3, HN_4) or leaching (base cations and organics) of chemicals that takes place during normal rainfall events.

Throughfall Interception

As a passive means of modifying ecosystem water budgets, the interception of throughfall has proven very useful in a number of studies (see Table 23.1). Typical applications have used either complete understory roofs (Gundersen et al. 1995) or partial coverage of the ground area with gutters or troughs (Holstener-Jørgensen 1994; Hanson et al. 1995; Hanson et al. 1998) to manipulate the amount of water reaching the forest floor. The largest field manipulation of water attempted to date is the Walker Branch Throughfall Displacement Experiment (TDE) which includes 12,800 m^2 of manipulated area (Hanson et al. 1998; Hanson et al. 1995). The TDE was developed for an upland oak ecosystem located in the eastern United States (lat. 35°58′N, long. 84°17′W). Mean annual precipitation is 140 cm and mean temperature is 13.3°C. Depth to bedrock at this location is approximately 30 m. The site is dominated by *Quercus alba* L., *Quercus prinus* L., and *Acer rubrum* L., but it contains 16 other tree species with a total stand basal area that averages 20 to 25 $m^2\ ha^{-1}$. Briefly, the manipulations of throughfall levels reaching the forest floor are made with a system designed to passively transfer precipitation from one experimental plot to another. There are three plots in the TDE: one wet, one dry, and one ambient. Each 80 × 80 m plot is divided into one hundred 8 × 8 m subplots that serve as the locations for repetitive, nondestructive measurements of soil and plant characteristics. Throughfall precipitation is intercepted in ≈2000 subcanopy troughs (0.3 × 5 m), each suspended above the forest floor of the dry plot (≈33% of the ground area is covered) (Fig. 23.1A). The intercepted throughfall is then transferred by gravity flow across an ambient plot and distributed onto the wet treatment plot through paired drip holes spaced approximately 1 m apart in approximately 6-cm diameter PVC pipe.

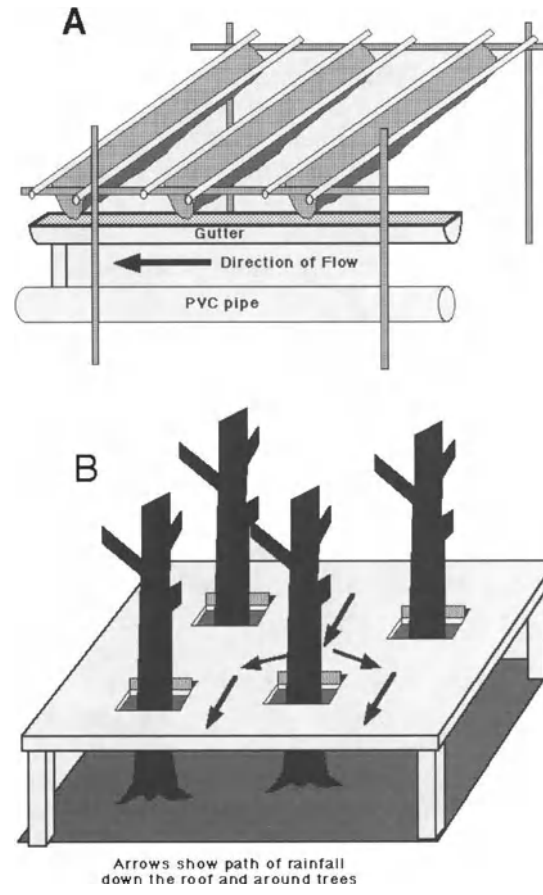

FIGURE 23.1. Schematic representations of the two types of throughfall collectors that have been used in large-scale water manipulations. A, A throughfall collection system designed to intercept a fractional amount (approximately 33%) of throughfall reaching the forest floor shown with collection gutters and transfer pipes (Hanson et al. 1995, 1998). B, An understory roof collection structure used to intercept 100% of the throughfall incident upon the forest floor (collars are used on individual trees to intercept stem flow, but are not shown).

Of the other throughfall manipulation studies listed in Table 23.1, the roofed catchment (Fig. 23.1B) located at Lake Gårdsjön, Sweden (Hultberg et al. 1993, Moldan et al. 1995) is the next largest in terms of total area manipulated (6400 m^2). However, the Lake Gårdsjön facility has not been applied to manipulations of throughfall quantity and drought. Instead they have been focusing on 100% removal of ambient throughfall chemis-

tries followed by similar quantities added back with altered chemistries. Other roofed catchment studies (Rasmussen et al. 1995; Beier et al. 1995) involve somewhat smaller manipulation areas (i.e., typically less than 500 m^2) and they most often use 100% removal of throughfall as the primary manipulation although the duration of the treatments is variable. In most cases in which 100% throughfall removal has been applied, attempts are made to resaturate the soils periodically, especially during dormant periods.

Pilon et al. (1996) report on the use of a sealed tarpaulin around the base of individual trees as a method to eliminate throughfall inputs to the root zone of trees, but their approach was not consistently effective in the first year of their study, and the tarpaulin approach had no effect on soil water content in the second year of their study. They point out that the presence of a tarpaulin directly on the soil surface does preclude normal evaporation processes. This is a serious limitation to the ground tarpaulin approach to throughfall manipulations.

In a recent study of grasslands (Fay et al., in press), investigators employed a number of permanently installed plastic greenhouse roofs (9×14 m) as simultaneous shields from ambient rainfall and throughfall collectors. Together with large rainfall collection tanks, pumps, irrigation nozzles, and barriers to horizontal rooting and water movement (7.6×7.6 m plots under each roof), their roofed plots represent a cost effective approach for manipulating both the quantity and timing of rainfall events over a 6×6 m treatment area.

Verification of Water Treatments

A key feature of any water manipulation experiment should be an adequate and comprehensive characterization of the soil water status. This is important both from the standpoint of verifying the treatments applied and for the characterization of the level of soil moisture stress experience by plants and microorganisms. Measurements of soil water status need to have adequate temporal resolution to cover important seasonal patterns, and for large-scale experiments, a clear understanding of the spatial variation in soil water status across the experimental site is essential. While these points may seem obvious, adequate soil water data are not always collected. For example, in the throughfall roof study conducted at Klosterhede, Denmark (Gundersen et al. 1995), natural throughfall was removed and replacement throughfall was added by a sprinkler system underneath the roof, and extensive measurements of the artificial throughfall reaching the forest floor were conducted both temporally and spatially. Unfortunately, neither soil water content or soil matric potential data were reported leaving us unsure of the soil water status during the experiment. As a result, direct comparisons of plant, decomposition, and nutrient cycling responses between the Klosterhede studies (Beier et al. 1995; Gundersen et al. 1995) and other large-scale water manipulation studies are hampered due to a lack of published data on soil water status. Future soil water manipulations should include adequate measurement approaches at appropriate spatial and temporal scales to avoid this problem.

Measurement Approaches

Soil water observations can be conducted using a variety of methods. Destructive gravimetric sampling, neutron probe measurements, and time domain reflectometry can be used for measurements of soil moisture content. Tensiometers and soil resistance blocks can provide a direct measurement of soil matric potential with appropriate calibration, and soil psychrometers can be installed in the field for a direct measurements of soil water potential. A detailed discussion of the advantages and disadvantages of each technique can be found in Chapter 13 and in a previous review by Rundel and Jarrell (1989). When not directly measured as matric or total soil water potential, measured soil water content data need to be translated into water potential terms (i.e., soil moisture retention curves) so that direct intercomparisons among studies can be facilitated. In many published studies it is difficult to judge the severity of drought because soil water content data are often not expressed as matric or total water potential.

Although destructive gravimetric sampling is often prohibited in an experimental setting where removal of soil over time may compromise the natural state of the soil profile, a certain amount of gravimetric soil sampling should always be conducted to complement (and if necessary calibrate)

the chosen nondestructive approach. For large-scale experiments that will include drought periods, tensiometers are not recommended as they are typically only functional over a limited range of soil matric potentials (-0.00 to -0.08 MPa). Neutron probe approaches have also fallen out of favor recently because they demand site-specific calibration and additional radiation protection procedures. Soil resistance blocks, soil psychrometers, and other electronically based sensors are the best choice for a study in which detailed temporal resolutions on the order of hours or days are required, but they would be expensive to replicate over large spatial scale. Autologging of any instrument becomes a problem when replicated over large spatial scales due to signal losses over long wire lengths and the disturbance associated with wire installation. Perhaps the best approach for measuring soil water status over large spatial scales (in the absence of proven remote sensing methods, see Chapter 13) is time domain reflectometry (Topp and Davis 1985).

Time domain reflectometry (TDR) has proven to be a cost effective and durable approach for making soil water content measurements in large-scale water manipulation studies (Hanson et al. 1995). However, since TDR is only a measurement of soil moisture content, complementary information on the relationship between soil water content and soil water potential for the experimental soils (i.e., a soil moisture release curve) is required to translate water content data to soil water or matric potential. Measured TDR yields water content for the bulk soil including coarse fraction (i.e., soil particles >2 mm), but soil moisture release curves are typically conducted on soils from which the coarse fraction has been removed. Therefore, bulk or raw TDR data (TDR_r) must be corrected for coarse fraction content before it is used in a soil moisture release curve to obtain soil water or matric potential information. Alternatively, soil moisture release curves including particle size classes greater than 2 mm should be generated. Paruelo et al. (1987) took the latter approach and showed that significant soil water could be held by the 2- to 11-mm coarse fraction of a Patagonian arid steppe soil. They also showed that large coarse fraction components (i.e., rocks >11 mm) decreased soil water holding capacity nearly proportionate to their volume.

To obtain soil water potential data from TDR_r for soils having large coarse fraction components (i.e., rocks assumed to contain zero water) Hanson et al. (1998) used the following calculation to correct TDR values (TDR_c) for application to their soil moisture release curves from sieved soil:

$$TDR_c = TDR_r/(100 - C_f) * 100 \quad (23.1)$$

where C_f is the appropriate mean coarse fraction for the soil. For their soil with a mean coarse fraction of 14.2% in the surface 35 cm, TDR_c values were typically 2 to 3% higher than observed TDR_r.

What is the appropriate depth for making soil water or matric potential measurements? Unfortunately, there is no simple answer to this question. Important criteria depend on the questions being addressed in a particular study and the nature of the soils being measured. If plant responses are a key component, one should consider measuring that portion of the soil profile that includes the "effective" rooting depth of the plants of interest. Multiple soil depths should be considered if time and money allow. A recent study contrasting water use by herbaceous and woody plant life-forms in a shortgrass steppe community (Dodd et al. 1998) showed that each uses water from different layers of the soil profile. In such a system it would be critical to collect water content data from multiple soil depths corresponding to the water use characteristics of the species of interest. Data on depth of water resources for plant function are available for a number of other ecosystems (Ehleringer et al. 1991; Flanagan et al. 1992; Gordon et al. 1989; White et al. 1985).

Dealing with Spatial Variation

Spatial variation in soil characteristics, species composition, vegetation cover, slope, and aspect all interact and lead to potentially significant spatial differences across sites used for large-scale manipulations. This pretreatment variation must be characterized and understood to ensure that observed differences in soil water status imposed by the treatment infrastructure are true treatments and not simply inherent patterns driven by variable site characteristics. Pretreatment data collections for soil water content and/or water potential should be available for at least one full year to characterize the soil water patterns across the experimental area of interest, and the temporal resolution of the pre-

treatment data should encompass periods of maximum and minimum soil water levels. Pretreatment data for other variables that might logically trend across a large experimental area (e.g., soil temperature) would also be useful.

An example of the use of pretreatment information as a base from which to judge the effectiveness of a large-scale TDE is provided by Hanson et al. (1998). They collected pretreatment measurements of soil water content by TDR at an 8 × 8 m grid across their experimental site (310 locations) from April 1992 through July 12, 1993, and they found significant pretreatment gradients in water content across their experimental area driven by slope position and soil coarse fraction. From these pretreatment observations a covariate matrix was developed based on an individual measurement's location according to the following equations:

$$Yij = \sum (Yijk)/n \quad (23.2)$$

$$Y = \sum (Yij)/n \quad (23.3)$$

$$CovYij = (Yij - Y)/sdY \quad (23.4)$$

where Yij is the mean annual value for a given location, Y is the grand mean for all locations and times, i and j are the horizontal and vertical coordinates of the experimental area, k is the month of the observation, and n is the number of observations for a given summation. As an illustration of the importance of understanding pretreatment patterns, Figure 23.2 shows a contour plot of winter and summer pretreatment soil water data for the TDE (Hanson et al. 1998) along with a graph of the corresponding covariate rankings based on Equation 23.4. They found that a single covariate rank based on an entire years' worth of data was not robust enough to apply to all subsequent dates. Instead, they used two covariate ranks: one for the dormant season when soil water conditions were near saturation and one for summer periods when soils were drier. The validity of the approach used by Hanson et al. (1998) was contingent on the assumption that there was no spatial autocorrelation

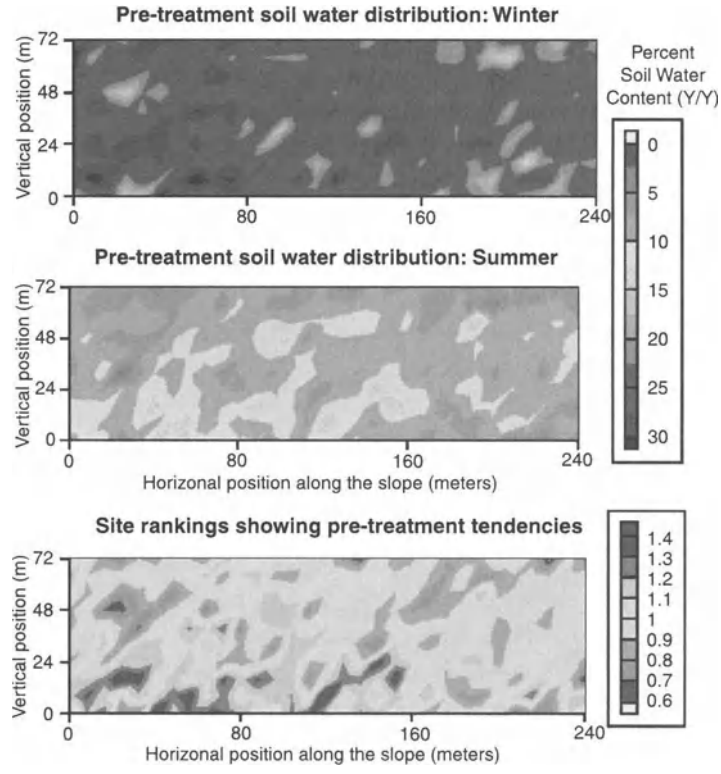

FIGURE 23.2. Winter and summer soil water content (% v/v) across the Walker Branch Throughfall Displacement Experiment area (Hanson et al. 1995) prior to the initiation of treatments (top two graphs) shown together with a contour plot of the derived covariate rankings (see Equation 23.4) for each of the measurement locations. Rankings greater than or less than one correspond to wetter versus drier than average pretreatment measurement positions.

among the individual rod pairs located 8 m apart. To evaluate this assumption, they constructed semivariograms (Turner et al. 1991) based on TDR measurements of soil water content at a 0.15-m spacing along both vertical and horizontal transects within the TDE area and demonstrated that beyond 4 to 5 m the individual soil water measurements could be considered independent.

Collection of Adequate Weather Data

All large-scale manipulation studies must collect adequate weather data to allow for the evaluation of impacts of the treatment infrastructure on uncontrolled environmental variables (i.e., air temperature, humidity). A complete set of variables to be monitored should include the following: incoming rainfall, irradiance, photosynthetic photon flux density, air temperature, and relative humidity or dewpoint. Understory climate data should also include photosynthetically active radiation (PAR) at ~1.5 m, air temperature, soil temperatures (multiple depths), and relative humidity. Collecting weather data at an hourly resolution is recommended, as many current process models of forest stand or ecosystem function demand this level of time resolution of weather input data sets.

Confounding Issues

Any experimental design involves compromises between ideal conditions and logistical reality. Gundersen (1995) discusses some of the common unintended consequences of large-scale manipulation studies in detail. Gundersen concludes that large manipulations often lead to modified microclimatic conditions (i.e., light, temperature, and humidity) due to the presence of experimental structures. Those studies using complete understory roofs (near 100% interception) do show temperature differences between roofed and control plots (Gundersen et al. 1995), but the sign of the differences is seasonally dependent. In the TDE, Hanson et al. (1995, 1998) originally anticipated that the presence of the troughs, gutters, and pipes might act as a radiation barrier or thermal blanket during periods of incomplete canopy leaf coverage and lead to changes in the understory microclimate. However, they found little evidence of any changes in air or soil (10 cm) temperatures during the growing season when the canopy is fully leafed out. Large gaps between collection troughs in the study design of the TDE probably allowed for adequate turnover and circulation of air around the trough infrastructure. Fay et al. (in press) found that soil temperatures under their grassland roofs were elevated 1.2 to 1.8°C over ambient conditions, and attributed the temperature increase to reduced nighttime radiative loss. The grassland roofs also reduced radiation reaching the plant canopy, and unroofed control plots were incorporated into the experimental design to assess the long-term impact of the altered light environment.

Unintentional modifications of rainfall chemical inputs also often accompany large-scale water manipulations. Chemicals derived from atmospheric dry and wet deposition and from canopy leaching are normally transferred to the forest floor in throughfall. In the attempt to modify the water budget of forest stands using understory troughs (Hanson et al. 1995) or roofs (Beier et al. 1995; Fay et al., in press; Gundersen et al. 1995; Rasmussen et al. 1995), unavoidable chemical transfers are also made. Rasmussen et al. (1995) showed that treatments in which 100% of the intercepted throughfall was extracted also removed significant potassium from the site, and they concluded that such a change would accumulate and become biologically significant over time. Hanson et al. (1998) stated that some changes in chemical inputs due to ±33% throughfall alterations on their upland oak site were taking place, but concluded that the biological impact for their system would be minimal. Even if the anticipated level of biological response to small changes in chemical inputs/outputs resulting from an experimental manipulation is expected to be small, some measurements of the level of chemical transfers taking place should be included.

Plot Size and Edge Effects

Small-scale water manipulation studies having manipulated areas less than 50 m^2 (Bréda et al. 1993, 1995; Fay et al., in press; Holstener-Jørgensen 1994) often use belowground barriers to root and

water migration to control edge effects. While this can be an effective and appropriate solution, it can also generate experimental artifacts for studies of large plants. Root barriers may reduce the "true" rooting volume and lead to unintended changes in root/shoot relationships of large trees. In experiments without barriers, the issue of water migration between plots and root growth beyond plot boundaries is a serious potential problem. Hanson et al. (1995, 1998) addressed this issue by choosing very large plots with predefined buffer zones to allow for potential overlap of water or roots. During the course of their experiment, incidental treefalls within treated plots showed that the effective rooting area under a tree was highly correlated with each tree's crown spread. This observation suggests that a conservative approach for edge effects would be to allow a minimum of two mean crown widths between water manipulation plots. However, this "rule-of-thumb" should not substitute for good surveys of the water distribution patterns throughout any large-scale water manipulation study.

Statistical Replication

Because of costs and logistics associated with stand- or catchment-level manipulation experiments, true replication is often very limited or lacking in large-scale water manipulation experiments. This lack of replication leads to the unfortunate consequence of researchers having to resort to subsampling within treated areas or "pseudoreplication" (Eberhardt and Thomas 1991). Recognizing pseudoreplication in any large-scale manipulation study design is critical (Hurlbert 1984). Without this recognition, simple differences in site characteristics might be overlooked and be totally confounded with the interpretation of the treatment response.

The practical and scientific need for large contiguous albeit unreplicated water manipulation structures must be preceded by serious evaluation of the uniformity of the pretreatment site variables (i.e., soil type and vegetation distribution, slope, etc.). Although unreplicated experimental designs are clearly not ideal, pseudoreplication has been recognized as a reasonable limitation and an acceptable approach when costly experimental designs are being initiated for answering scientific questions that can not be addressed at smaller scales (Eberhardt and Thomas 1991). Eberhardt and Thomas (1991) recommend that unreplicated experiments be supported by adequate sampling of site environmental parameters (including climatic conditions), comparable ambient areas, and pretreatment observation of critical variables.

Conclusions

Large-scale water manipulation experiments represent the only logical choice for scientific questions demanding an understanding of integrated responses of plants and soils in a natural microclimate. Large-scale manipulations were defined as field experiments that are of sufficient size and complexity to handle questions of individual plant response, interplant interactions, as well as stand-level carbon, water, and nutrient cycling responses. Because large-scale manipulations are intended to retain all features of natural forest stands or ecosystems except those being manipulated (i.e., precipitation inputs), extreme care must go into the planning and design of the experimental approach so that normal physical, chemical, and climatic features of the forests or ecosystems are retained.

A commitment to multi-year maintenance and operation of large-scale water manipulation facilities should be demonstrated during the planning and design of such studies. Maintaining large-scale manipulations over multiple years minimizes the initial costs of construction to levels that are comparable to more traditional experimental designs. Multi-year studies also provide an opportunity to see the impacts of a given manipulation against natural year-to-year variations in weather, thus expanding the scope of the planned manipulations. Finally, it is important to understand that sustained treatments on large-scale water manipulation studies may be the only way that we can detect responses that are normally manifested only slowly in a natural ecosystem (e.g., changes in stored carbohydrates or nutrient cycling processes).

Acknowledgments This research is sponsored by the Program for Ecosystem Research, Environmental Sciences Division, Office of Health and Envi-

ronmental Research, U.S. Department of Energy under contract DE-AC05-96OR22464 with Lockheed Martin Energy Research Corporation. Publication 4893, Environmental Sciences Division, Oak Ridge National Laboratory.

References

Abrahamsen, G.; Bjor, K.; Teigen, O. *Field Experiments with Simulated Acid Rain in Forest Ecosystems. 1. Soil and Vegetation Characteristics, Experimental Design, and Equipment.* Res. Rep. 4, 1432 NISK, Aas-NLH, Norway; 1977.

Beier, C.; Gundersen, P.; Hansen, K.; Rasmussen, L. Experimental manipulations of water and nutrient input to a Norway spruce plantation at Klosterhede, Denmark. II. Effects on tree growth and nutrition. Plant Soil 168–169:613–622; 1995.

Bréda, N.; Cochard, H.; Dreyer, E.; A. Granier. Water transfer in a mature oak stand (*Quercus petraea*): Seasonal evolution and effects of a severe drought. Can. J. For. Res. 23:1136–1143; 1993.

Bréda, N.; Granier, A.; Barataud, F.; Moyne, C. Soil water dynamics in an oak stand. I. Soil moisture, water potentials and water uptake by roots. Plant Soil 72:17–27; 1995.

Cregg, B.M.; Halpin, J.E.; Dougherty, P.M.; Teskey, R.O. Comparative physiology and morphology of seedling and mature forest trees. In: Noble, R.D.; Martin, J.L.; Jensen, K.F., eds. *Air Pollution Effects on Vegetation Including Forest Ecosystems.* Washington, DC: U.S. Department of Agriculture; 1989:111–118.

Dodd, M.B.; Lauenroth, W.K.; Welker, J.M. Differential water resource use by herbaceous and woody plant life-forms in a shortgrass steppe community. Oecologia 117:504–512; 1998.

Dougherty, P.M.; Hinckley, T.M. The influence of a severe drought on net photosynthesis of white oak (*Quercus alba*). Can. J. Bot. 59:335–341; 1981.

Eberhardt, L.L.; Thomas, J.M. Designing environmental field studies. Ecol. Monogr. 61:53–73; 1991.

Ehleringer, J.R.; Phillips, S.L.; Schuster, W.S.F.; Sandquist, D.R. Differential utilization of summer rains by desert plants. Oecologia 88:430–434; 1991.

Ellsworth, D.S.; Reich, P.B. Water relations and gas exchange of *Acer saccharum* seedlings in contrasting natural light and water regimes. Tree Physiol. 10:1–20; 1992.

Epron, D.; Dreyer, E.; Bréda, N. Photosynthesis of oak trees [*Quercus petraea* (Matt.) Liebl.] during drought under field conditions: Diurnal course of net CO_2 assimilation and photochemical efficiency of photosystem II. Plant Cell Environ. 15:809–820; 1992.

Fay, P.A.; Carlisle, J.D.; Knapp, A.K.; Blair, J.M.; Collins, S.L. Altering rainfall timing and quantity in a mesic grassland ecosystem: design and performance of rainfall manipulation shelters. Ecosystems (in press).

Flanagan, L.B.; Ehleringer, J.R.; Marshall, J.D. Differential uptake of summer precipitation among co-occurring trees and shrubs in a pinyon-juniper woodland. Plant Cell Environ. 15:831–836; 1992.

Ginter-Whitehouse, D.L.; Hinckley, T.M.; Pallardy, S.G. Spatial and temporal aspects of water relations of three tree species with different vascular anatomy. For. Sci. 29:317–329; 1983.

Golluscio, R.A.; Sala, O.E.; Lauenroth, W.K. Differential use of large summer rainfall events by shrubs and grasses: A manipulative experiment in the Patagonian steppe. Oecologia 115:17–25; 1998.

Gordon, D.R.; Welker, J.M.; Menke, J.W.; Price, K.J. Competition for soil water between annual plants and blue oak (*Quercus douglasii*) seedlings. Oecologia 79:533–541; 1989.

Graham, R.L.; Turner, M.G.; Dale, V.H. How increasing CO_2 and climate change affect forests. BioScience 40:575–587; 1990.

Gundersen, P. Unintended differences between natural and manipulated forest plots. In: Jenkins, A.; Ferrier, R.C.; Kirby, C., eds. *Ecosystem Manipulation Experiments: Scientific Approaches, Experimental Design and Relevant Results.* Ecosystem Research Report 20. Luxembourg: Commission of the European Communities; 1995:335–343.

Gundersen, P.; Andersen, B.R.; Beier, C.; Rasmussen, L. Experimental manipulations of water and nutrient input to a Norway spruce plantation at Klosterhede, Denmark. I. Unintended physical and chemical changes by roof experiments. Plant Soil 168–169:601–611; 1995.

Hagan, R.M. et al., eds. *Irrigation of Agricultural Lands.* Agronomy Monograph 11, Madison, WI: American Society of Agronomy; 1967.

Hanson, P.J.; McLaughlin, S.B.; Garten, C.T., Jr. Application of artificial rain in experimental systems: Methods, results of case studies, and future needs. In: Payer, H.D.; Pfirrmann, T.; Mathy, P., eds. *Environmental Research with Plants in Closed Chambers.* Air Pollution Research Report 26, Commission of the European Communities; 1990:223–233.

Hanson, P.J.; Todd, D.E.; Edwards, N.T.; Huston, M.A. Field performance of the Walker Branch Throughfall Displacement Experiment. In: Jenkins, A.; Ferrier, R.C.; Kirby, C., eds. *Ecosystem Manipulation Experiments: Scientific Approaches, Experimental Design and Relevant Results.* Ecosystem Research Report 20. Luxembourg: Commission of the European Communities; 1995:307–313.

Hanson, P.J.; Todd, D.E.; Huston, M.A.; Joslin, J.D.; Croker, J.; Augé, R.M. *Description and Field Performance of the Walker Branch Throughfall Displacement Experiment: 1993–1996.* ORNL/TM-13586. Oak Ridge, TN: Oak Ridge National Laboratory; 1998.

Hinckley, T.M.; Lassoie, J.P.; Running, S.W. Temporal and spatial variations in the water status of forest trees. For. Sci. Monogr. 20;1978.

Holstener-Jørgensen, H.; Holmsgaard, E. Effects of irrigation and drought on growth of young Norway spruce on east Danish moraine. For. Landsc. Res. 1:127–142; 1994.

Hultberg, H.A.; Andersson, B.I.; Moldan, F. The covered catchment: An experimental approach to reversal of acidification in a forest ecosystem. In: Rasmussen, L.; Brydges, T.; Mathy, P., eds. *Experimental Manipulations of Biota and Biogeochemical Cycling in Ecosystems.* Ecosystem Research Report 4, Commission of the European Communities; 1993:46–54.

Hurlbert, S.H. Pseudoreplication and the design of ecological field experiments. Ecol. Monogr. 54:187–211; 1984.

Irving, P.M.; Miller, J.E. Productivity of field-grown soybeans exposed to acid rain and sulfur dioxide alone and in combination. J. Environ. Qual. 10:473–478; 1981.

Jenkins, A.; Wright, R.F. The CLIMEX project: Performance of the experimental facility during the first year of treatment, In: Jenkins, A.; Ferrier, R.C.; Kirby, C., eds. *Ecosystem Manipulation Experiments: Scientific Approaches, Experimental Design and Relevant Results.* Ecosystem Research Report 20. Commission of the European Communities; 1995:323–327.

Johnston, J.W., Jr.; Shriner, D.S.; Abner, C.H. Design and performance of an exposure system for measuring the response of crops to acid rain and gaseous pollutants in the field. J. Air Pollut. Contr. Assoc. 36:894–899; 1986.

Kattenberg, A.; Giorgi, F.; Grassl, H.; Meehl, G.A.; Mitchell, J.F.B.; Stouffer, R.J.; Tokioka, T.; Weaver, A.J.; Wigley, T.M.L. Climate models: Projections of future climate. In: Houghton, J.T., et al., eds. *Climate Change 1995. The Science of Climate Change.* New York: Cambridge Univ. Pr.; 1996:283–357.

Kirschbaum, M.U.F.; Fischlin, A. Climate change impacts on forests. In: Watson, R.T.; Zinyowera, M.C.; Moss, R.H., eds. *Climate Change 1995. Impacts, Adaptations and Mitigation of Climate Change: Scientific-Technical Analysis.* New York: Cambridge Univ. Pr.; 1996:95–129.

Kliener, K.W.; Abrams, M.D.; Schultz, J.C. The impact of water and nutrient deficiencies on the growth, gas exchange and water relations of red oak and chestnut oak. Tree Physiol. 11:271–287; 1992.

Kolb, T.E.; Steiner, K.C.; McCormick, L.H.; Bowersox, T.W. Growth response of northern red-oak and yellow-poplar seedlings to light, soil moisture and nutrients in relation to ecological strategy. For. Ecol. Manage. 38:65–78; 1990.

Kozlowski, T.T. Water supply and tree growth. Part I. Water Deficits. For. Abstr. 43:57–95; 1982.

Lamersdorf, N.P.; Beier, C.; Blanck, K.; Bredemeier, M.; Cummins, T.; Farrel, E.P.; Rasmussen, L.; Ryan, M. Reactions of soil solution chemistry to drought: Results of experiments within the EXMAN project. In: Jenkins, A.; Ferrier, R.C.; Kirby, C., eds. *Ecosystem Manipulation Experiments: Scientific Approaches, Experimental Design and Relevant Results.* Ecosystem Research Report 20. Commission of the European Communities; 1995:86–95.

Melillo, J.M.; Callaghan, T.V.; Woodward, F.I.; Salati, E.; Sinha, S.K. Effects on Ecosystems. In: Houghton, J.T.; Jenkins, G.J.; Ephraums, J.J., eds. *Climate Change. The IPCC Scientific Assessment.* New York: Cambridge Univ. Pr.; 1990:282–310.

Moldan, F.; Hultberg, H.; Andersson, A. Gårdsjön covered catchment experiment: Changes in runoff after three years of throughfall exclusion. In: Jenkins, A.; Ferrier, R.C.; Kirby, C., eds. *Ecosystem Manipulation Experiments: Scientific Approaches, Experimental Design and Relevant Results.* Ecosystem Research Report 20. Commission of the European Communities; 1995:113–118.

Mooney, H. Biological response to climate change: An agenda for research. Ecol. Applic. 1:112–117; 1991.

Mooney, H.A.; Drake, B.G.; Luxmoore, R.J.; Oechel, W.C.; Pitelka, L.F. Predicting ecosystem responses to elevated CO_2 concentrations. BioScience 41:96–104; 1991.

Ojima, D.S.; Kittel, T.G.F.; Rosswall, T.; Walker, B.H. Critical issues for understanding global change effects on terrestrial ecosystems. Ecol. Applic. 1:316–325; 1991.

Paruelo, J.M.; Aguiar, M.R.; Golluscio, R.A. Soil water availability in the Patagonian arid steppe: Gravel content effect. Arid Soil Res. Rehab. 2:67–74; 1987.

Pezeshki, S.R.; Chambers, J.L. Stomatal and photosynthetic response of drought-stressed cherrybark oak (*Quercus falcata* var. *pagodaefolia*) and sweet gum (*Liquidambar styraciflua*). Can. J. For. Res. 16:841–846; 1986.

Pilon, C.E.; Côté, B.; Fyles, J.W. Effect of an artificially induced drought on leaf peroxidase activity, mineral nutrition and growth of sugar maple. Plant Soil 179:151–158; 1996.

Rasmussen, L.; Beier, C.; Andersen, B.R. Effects of experimental manipulations with biogeochemical cycles in a Norway spruce plantation in Denmark: The Dan-

ish part of the EXMAN project. In: Jenkins, A.; Ferrier, R.C.; Kirby, C., eds. *Ecosystem Manipulation Experiments: Scientific Approaches, Experimental Design and Relevant Results.* Ecosystem Research Report 20. Commission of the European Communities; 1995:96–103.

Rind, D.; Goldberg, R.; Hansen, J.; Rosenzweig, C.; Ruedy, R. Potential evapotranspiration and the likelihood of future drought, J. Geophys. Res. 95(D7):9983–10004; 1990.

Rundel, P.W.; Jarell, W.M. Water in the environment. In: Pearcy, R.W.; Ehleringer, J.R.; Mooney, H.A.; Rundel, P.W., eds. *Plant Physiological Ecology: Field Methods and Instrumentation,* New York: Chapman and Hall; 1989:29–56.

Sala, O.E.; Lauenroth, W.K. Small rainfall events: An ecological role in semiarid regions. Oecologia 53:301–304; 1982.

Stewart, B.A.; Nielsen, D.R., eds. *Irrigation of Agricultural Crops.* Agronomy Monograph 30. Madison, WI: American Society of Agronomy; 1990.

Topp, G.C.; Davis, J.L. Measurement of soil water content using time domain reflectometry (TDR): A field evaluation. Soil Sci. Soc. Am. J. 49:19–24; 1985.

Turner, S.J.; O'Neill, R.V.; Conley, W.; Conley, M.R.; Humphries, H.C. Pattern and scale: Statistics for landscape ecology. In: Turner, H.G.; Gardner, R.H. *Quantitative Methods in Landscape Ecology: The Analysis and Interpretation of Landscape Heterogeneity.* New York: Springer-Verlag: 1991:17–49.

White, J.W.C.; Cook, E.R.; Lawrence, J.R.; Broecker, W.S. The D/H ratios of sap in trees: Implications for water sources and tree ring D/H rations. Geochim. Cosmochim. Acta 49:237–246; 1985.

Wigley, T.M.L.; Briffa, K.R.; Jones, P.D. Predicting plant productivity and water resources. Nature 312:102–103; 1984.

Wigley, T.M.L.; Jones, P.D. Influences of precipitation changes and direct CO_2 effects on streamflow. Nature 314:149–152; 1985.

Woodward, F.I. Tansley Review 41. Predicting plant responses to global environmental change. New Phytol. 122:239–251; 1992.

24

Ecosystem Climate Manipulations

Karin P. Shen and John Harte

Introduction

Human activities such as fossil fuel burning and deforestation are expected to cause global climate change of a rate and magnitude unmatched in the historical record. Results from climate modeling studies indicate that the earth is likely to experience an increase in global average temperature of several degrees Celsius by the end of the next century (IPCC 1995). This temperature increase, and other associated climate changes, will have far-reaching effects on the natural environment and human society.

Impending climate change will affect ecosystems, and ecosystem responses can in turn exert strong feedbacks to climate. Mathematical modeling and paleoclimatic studies have explored potential ecosystem response to climate change. Since the early 1980s, there have been hundreds of laboratory investigations of climate change impacts on soil and plants. Field manipulation studies of global warming have been fewer in number, and of these only a small fraction have been on an ecosystem level.

In this chapter, we discuss laboratory and field manipulation methods for studying ecosystem response to global climate change. We focus our discussion on whole-ecosystem methods, and our emphasis on terrestrial ecosystems reflects the general emphasis of past work. We begin with a brief review of global warming and model predictions, discuss the use of paleoclimatology and simulation models, and then review ecosystem climate manipulation methods. We conclude with recommendations for successful manipulation studies.

Global Climate Change and Ecosystems

Greenhouse gases, while relatively transparent to incoming solar radiation, warm Earth's surface by trapping outgoing infrared radiation. Such gases include water vapor, carbon dioxide (CO_2), methane (CH_4), nitrous oxide (N_2O), and chlorofluorocarbons (CFCs). Decades-long records of atmospheric measurements from sampling stations around the world reveal steady increases in the tropospheric concentrations of all of these gases (Keeling and Whorf 1998; Ross and Elliott 1996; Schimel et al. 1995). These increases are unambiguously attributable to human activities.

Concomitant with the increasing greenhouse gas concentrations, global average temperature has increased 0.3 to 0.6°C within the last century (IPCC 1995). Mathematical models of global climate (general circulation models, GCMs) allow prediction of the magnitude and distribution of climate change due to anthropogenic greenhouse gas and aerosol emissions. Comparison of model output with the past 100-year climate record indicates that observed patterns of change are generally consistent with predictions. As anthropogenic greenhouse gas emissions are unlikely to abate in the coming decades, it is almost certain that the earth will experience continued global warming.

General circulation model studies indicate that continuing emissions will likely increase global mean average temperature by between 1 and 3.5°C by the year 2100 (IPCC 1995), with the major source of uncertainty being the estimation of cli-

mate feedback responses to the direct effect of increasing infrared absorption in the atmosphere. This temperature increase is expected to be heterogeneous in both time and space. Winter temperatures are expected to increase more than summer temperatures and the polar regions are expected to warm more than lower latitudes. Significant precipitation increases are expected at high latitudes and smaller changes (of either sign) at lower latitudes. Other expected effects of global warming include increased evaporation, stratospheric cooling, rising sea level, changes in cloud cover, changes in soil temperature and moisture levels, and changes in the intensity and frequency of storms and droughts.

One of the most critical meteorological parameters governing terrestrial ecosystem function is soil moisture, which in turn is linked to temperature, precipitation, humidity, the pattern of snow melt, the distribution of vegetation, and extreme weather events. General circulation models can yield only broad speculations regarding impacts of increased greenhouse gases on soil, especially soil moisture. All models predict increased soil moisture in high northern latitudes in winter. Most models predict increased aridity in midlatitude land areas in summer, mainly due to enhanced summertime evaporation (Hansen et al. 1988a; Hansen et al. 1988b; Manabe and Weatherald 1987). Also, snowpacks will melt earlier and summer depletion of the soil moisture reservoir will begin earlier (Hartmann 1990; Kattenberg and Maskell 1995). In areas with marginal soil moisture or seasonal drought, it is likely that the probability and intensity of drought will increase. Summer soil moisture reductions and increased probability of summer drought, particularly in midlatitudes, would have serious implications for agriculture and water resource allocation. Summer soil moisture in northern midlatitudes increases in some regions, however, when aerosol effects are included in the model, in contrast to the decrease found in greenhouse-gas-only simulations (Kattenberg and Maskell 1995).

Global warming could have far-reaching effects on the biosphere, and while GCMs attempt to predict the magnitude and scope of such warming, specific information regarding the potential impacts on natural systems remains limited. Little is known about the detailed consequences of rapid climate change on ecological processes. Soil conditions and the response of ecosystems will depend on local changes in temperature (including its rate of change), precipitation, soil moisture, and extreme weather events. Predicting the consequences of a small change in overall mean temperature for whole-ecosystem function is therefore going to be very difficult. Furthermore, a major difficulty in predicting the direct ecological consequences of global warming is that there is massive local heterogeneity of temperature within the same ecosystem at any given time. Current models are unable to make reliable estimates of changes in the critical parameters on the required local scales. The consequences of changes in global mean temperature for the structure and function of terrestrial ecosystems are largely unknown.

One approach to modeling the biosphere is to link a GCM with a land surface process model (Dickinson et al. 1986; Harvey and Schneider 1985; Randall et al. 1996; Sato et al. 1989; Sellers et al. 1986; Sud et al. 1990; Verseghy et al. 1993). The land surface components of coupled climate models range from simple schemes to complex representations of soil and vegetation (Gates et al. 1995). Developing a land surface model that can interact and evolve with the atmosphere as it changes (two-way interaction) is an active research area in climate modeling. All GCM simulations to date have ignored vegetation changes, and nearly all current land surface schemes involve only one-way atmosphere–biosphere interaction. Henderson-Sellers and McGuffie (1994) made the first attempt to include the terrestrial biosphere as an interactive component of a global model applied to estimating the sensitivity of the climate to a doubling of the atmospheric concentration of CO_2. There is also avid interest in developing a comprehensive land surface scheme that integrates biophysical, biogeochemical, and ecosystem dynamical processes. Some recent land surface schemes incorporate biogeochemical and ecological knowledge and, when coupled with atmosphere–ocean GCMs, will be capable of modeling biological and physical responses to global change (Sellers et al. 1997). For example, the IBIS (integrated biosphere simulator) model of Foley et al. (1996) combines land surface biophysics with terrestrial carbon fluxes and global vegetation dynamics.

Developing biosphere models to couple with GCMs is one way to learn about ecosystem consequences of global warming. Another is using observed statistical associations of organisms with specific climate conditions, combined with GCM predictions, to determine how current species' ranges may be altered by global warming. Because vegetation is a dominant factor in structuring ecosystems, most studies have focused on how climate influences the distribution of vegetation (Davis and Zabinski 1992; Woodward 1992). Present geographical ranges for species of interest are compared with climate zone maps to determine the bounding values of temperature and moisture that correspond to each species' range limit. Pollen and fossil records reveal distributions under past climates. Global circulation model predictions of global warming are then used to predict future locations of suitable climates for each species, yielding a quantitative estimate of the range displacement. Such studies indicate large potential displacements in geographical ranges (Davis and Zabinski 1992). Because many species will not be able to adjust rapidly enough, and because migration may be impeded by human settlements, these studies imply reductions in geographical range and thus in population size.

Although studies involving mechanistic models or statistical associations are valuable, they have many limitations. Model evaluation and improvement are hampered by a lack of appropriate observed data (Dickson 1995; Gates et al. 1995). Developing better models and thus better predictions requires the grounding of laboratory and especially field studies of ecosystem response to climate change. It is to these that we now turn.

Methods of Ecosystem Climate Manipulation

Response of ecosystems to future climate change can be assessed with experiments that manipulate environmental variables (e.g., temperature, CO_2, or light levels) in a manner that mimics climate change. This can be done in a laboratory growth chamber, or by a variety of field methods. To date, the majority of manipulation studies have involved enhanced CO_2 concentration, have taken place in a growth chamber, and have focused on a single species. Recently, long-term field manipulations of whole-ecosystem response (or representative samples of ecosystems) to climate change have become more common.

Laboratory Methods: Growth Chambers

Laboratory growth chambers manipulate environmental variables, including temperature, moisture, and light (intensity, spectrum, and day length). These studies have largely been limited to soil processes or to response of a single species (e.g., Hunt et al. 1996). Ecosystem studies in small laboratory chambers, referred to as "microcosms," can comprise intact field samples, but more typically are communities "assembled" in the laboratory. Verhoef (1996) lists some considerations for the design and implementation of microcosm experiments. Growth chambers have many advantages. They enable precise control of environmental conditions, and are easier to understand than complex, real-world systems. Chamber studies are easily replicable and repeatable and generate quick results, making statistically significant findings more likely, and the costs can be modest. Chamber studies give mechanistic insights and so can be helpful in developing simulation models.

Unfortunately, as a result of their inherently small spatial scale and their assemblage history, over time laboratory chamber ecosystems tend to diverge considerably from real-world ecosystems (Dudzik et al. 1979). Some processes and organisms are too large, wide-ranging, or slow to include in a growth chamber study, while others change so quickly that they may reach unrealistic rates or population densities in the course of a microcosm experiment (Carpenter 1996).

Mesocosm experiments, one step up from microcosms, are conducted in larger, more versatile growth chambers. Körner and coworkers have designed mesocosm experiments with tropical (Körner and Arnone 1992) and spruce ecosystems (Hattenschwiler and Körner 1996). A notable mesocosm facility is the Ecotron (Lawton 1996; Lawton et al. 1993), a collection of integrated growth chambers that can be used to study community and ecosystem response to climate change. The Ecotron attempts to construct, maintain, and manipulate entire model ecosystems and simulta-

neously monitor population dynamics and ecosystem processes. The ecosystems in the Ecotron are not intact, real ecosystems, but carefully constructed, "artificial" ecosystems. Nevertheless, these artificial systems are modeled on real communities and embody many essential features of natural communities. The Ecotron has been used to study relationships between biotic diversity, climate change, and ecosystem processes (e.g., Naeem et al. 1994).

Results from growth chamber studies can provide guidance for field work and mathematical model development. There have been attempts to combine laboratory studies with concurrent field investigations (e.g., Rawat and Purohit 1991). This is an encouraging trend, as growth chamber manipulations, whether micro- or mesocosm, are of limited usefulness without the context of field studies (Carpenter 1996; Lawton et al. 1993; Verhoef 1996).

Field Manipulations: General Considerations

The most beneficial studies for understanding ecosystem response to global climate change are large-scale, long-term (up to 10 years or more) field manipulations. Such studies provide context for laboratory work and aid in designing and testing dynamical models. Methods vary with the type of ecosystem under study and the manipulation variable. We limit our discussion to whole-ecosystem climate (primarily warming) and ultraviolet-B (UV-B) radiation manipulations, and begin with some basic considerations.

Global warming will be neither uniform nor constant over the globe, and, because of differences in soil and vegetation, not all systems will respond similarly to climate change. Site selection criteria have therefore included anticipated level of local climate change and likely sensitivity of dominant vegetation and biogeochemical processes to climate change (NSFESP 1991). Field manipulations of climate require careful planning of experimental design and monitoring. The size of the experiment will depend on the system as well as the method; for example, while experimental plots may be fairly small in an Arctic tundra site and still encompass a representative portion of the entire ecosystem (Debevec and Maclean 1993), this may not be the case in other systems. It has been suggested that plot size should be large enough to encompass the rooting system of several individuals of the dominant plant species (NSFESP 1991). Treatments should be spaced to avoid the treatment effect influencing the control and should be as identical as possible to the controls, ideally differing only in the variable to be manipulated. This may necessitate using a "dummy" experimental set-up on the control plots, which does not involve the climate manipulation but introduces the same unintended effects as the treatment apparatus.

Climate manipulation experiments alter many ecosystem characteristics. Key parameters to monitor are those that integrate several aspects of ecosystem function and are especially sensitive to climate change. Because there is significant diurnal variation in most soil and vegetation processes, and because fine root and organic matter profiles vary with depth, it is desirable to monitor soil temperature and moisture at least several times a day and at more than one depth. Other key soil parameters include carbon stocks, nitrogen (total and available inorganic), at least one measure of soil microbial activity (such as bottle respiration, field CO_2 fluxes, or actual active microbial counts), and nitrogen mineralization (NSFESP 1991). Key vegetation parameters include phenology, above- and below-ground biomass, leaf area index, stomatal conductance, water use efficiency, photosynthetic rates, and community composition (presence or absence).

Replication of climate manipulations over a natural landscape-scale climatic gradient, such as a mountain slope, can be useful (NSFESP 1991). Topographic gradients provide a means of looking at ecosystem response to climatic variation over longer time scales than are accessible in manipulation experiments, and have been used as surrogates for field manipulations (see, for example, Burke et al. 1995; Lashof 1989; Stanton et al. 1994; Tate 1992; Townsend et al. 1995; Vitousek and Matson 1991). Most gradient studies have focused on soil carbon because of the important potential role of climate-induced carbon release from ecosystems as a feedback to climate (e.g., Trumbore et al. 1996). Adaptations to climate along a topographic gradient are characterized by many time constants, making the substitution of differences over a topographic gradient for changes expected from future global warming problematic. Microbes and insects may adapt quickly, whereas physical

and chemical soil properties will adapt more slowly. The carbon content of soil along a gradient may vary because of differences in the amount of time that has elapsed since soil formation began, differences in vegetation communities with differing litter quality, and differing microbial activity due directly to temperature and moisture. In one study, soil mesofaunal abundance and diversity showed dramatically different responses to manipulated soil microclimate, to interannual soil microclimate variation, and to spatial variation in soil microclimate along a gradient (Harte et al. 1995b). Chapin et al. (1995) found that longer-term responses (9 years) in a passive greenhouse experiment showed closer correspondence to patterns of vegetation distribution along environmental gradients than did shorter-term (3 year) responses. Further study of ecosystem responses to manipulated and natural climate variation can help to identify when and how gradient analyses can substitute for manipulation experiments (Pacala and Hurtt 1993; Vitousek and Matson 1991).

Reciprocal transplants and common garden designs (e.g., Anderson et al. 1996) permit study of selected climate factors, and can augment surrogate gradient studies. For example, a reciprocal soil transplant would interchange soil from a cool spot and a warm spot on the gradient, thus reducing the confounding influences of physical and chemical differences in soil on response to climate change. Climate influence on vegetation communities can also be explored. Jensen (1993) used a common garden design to estimate the relative effects of source-site climate and transplant-site climate on white fir (*Abies concolor*) sapling growth rates. The transplant scheme has its limitations, not the least of which is the intrinsically small scale. Reciprocal transplants do not provide a whole-ecosystem perspective, but rather, may be used in conjunction with techniques which give information at larger scales.

Field Manipulations: Warming Experiments

The object of most manipulation experiments is to alter one or more climate parameters, such as air or soil temperature, precipitation, radiation, or timing of snowmelt. Changing any one of these, however, can affect some or all of the others as well, and such secondary meteorological responses are not always intended or predictable. Parameters of direct concern to ecologists, such as soil moisture, are likely to be jointly influenced by all of these secondary responses to the directly manipulated parameter. In this section, we discuss experimental approaches for direct warming of ecosystems, and discuss secondary responses as well.

Greenhouses

The simplest and most prevalent method of increasing temperature is a passive greenhouse. Passive greenhouses have been deployed across a variety of habitats, primarily at high latitude or high elevation, including Arctic tussock tundra, Antarctic fellfield, subalpine meadows, Tibetan plateau, and temperate grassland. Greenhouses are typically used to elevate temperature, although they have also been used to manipulate other climate variables, such as water (soil moisture and humidity), light (level and spectral quality), and CO_2. Greenhouses generally achieve a temperature increase of about 2 to 6°C above ambient, depending on the design and objectives of the study. In general, greenhouses are inexpensive (which facilitates replication), simple to build, and low maintenance. They can be used in remote areas without electrical power, and in long-term simulations. Chapin et al. (1995), for example, ran a greenhouse manipulation study for 9 growing seasons in an Arctic tundra community. Greenhouses are seldom left in place during the winter months, however, as they have typically been deployed in harsh climates and cannot withstand winter conditions.

Greenhouses come in a variety of sizes and designs, from a variety of open-topped designs, to horticultural cloches, to dome tents, to screens, to classic greenhouses with glass, plastic, or fabric panels (Fig. 24.1). An appropriate control might be an open plot shaded with the same material (Debevec and Maclean 1993). The choice of materials is as important as structural design; Debevec and Maclean (1993) found significant differences in temperature elevation, light attenuation, and gas transmission among different combination of greenhouse materials. Kennedy (1995a) lists several recent studies and notes their greenhouse design and the temperature elevation achieved. The International Tundra Experiment (ITEX) (e.g.

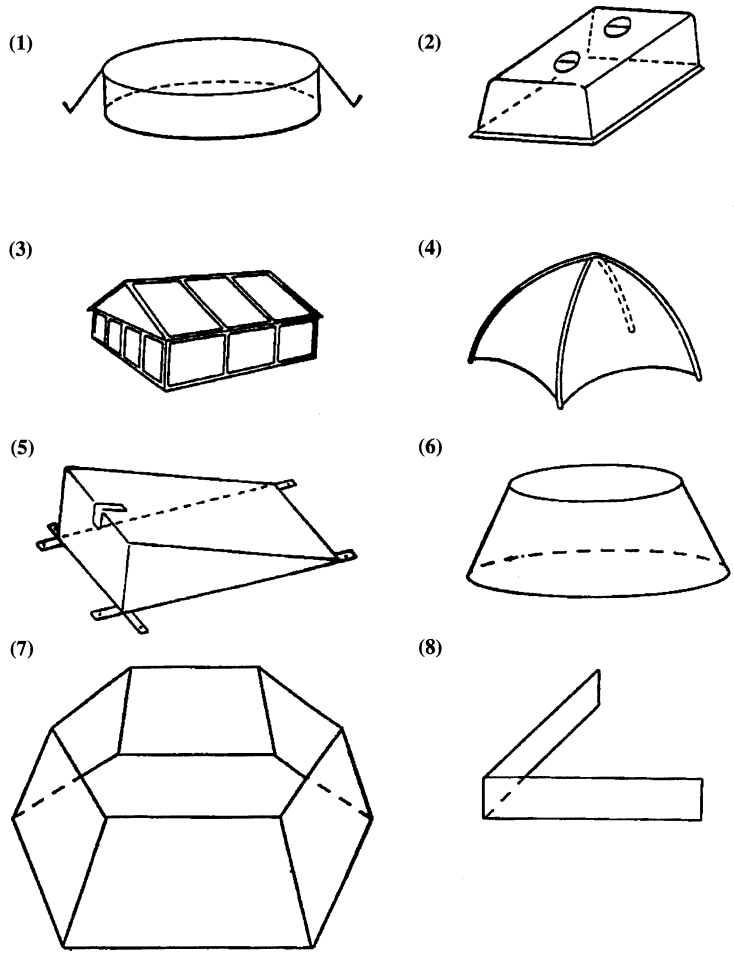

FIGURE 24.1. Greenhouse designs used in ecological field research: (1) Open-topped or fabric-covered chambers (e.g., Strathdee et al. 1993); (2) traditional horticultural cloche (e.g., Wynn-Williams 1990); (3) multiple-paneled greenhouse (e.g., Debevec and Maclean 1993); (4) geodesic dome-shaped tent (e.g., Coulson et al. 1993); (5) folding perspex greenhouse (e.g. Wynn-Williams 1992); (6) Open-topped cone (e.g. Klein 1998); (7) Open-topped hexagon (e.g., Marion et al. 1997); (8) the ITEX corner (e.g., Marion et al. 1997). (Figures 1 to 5 modified from Kennedy 1995b).

Klein 1998; Marion et al. 1997) uses three different kinds of open-topped greenhouses (see Figure 24.1): a cone design, a hexagon design, and the ITEX "corner." The use of standard greenhouse designs in ITEX across several different ecosystems facilitates comparison of results.

Despite their many advantages and the frequency of their use in climate change studies, passive greenhouses have several limitations. It has been argued that passive greenhouses may inadequately simulate climate change (Kennedy 1995a; Kennedy 1995b), and that the nature and magnitude of the temperature increase cannot be well controlled. "Active cloches" have been used to achieve a controlled temperature elevation (Oechel et al. 1992). Norby et al. (1997) and Edwards and Norby (1998) used evaporative coolers and in-line heaters with a feedback control system to maintain air temperatures within open-top chambers. An analysis of temperature data within and outside of a greenhouse deployed in maritime Antarctica (Kennedy 1995a) found that the greenhouse induced an amplified daily range of air temperatures and particularly increased summer temperatures, in opposition to GCM predictions. Secondary microclimate effects are usually examined only after the experiment has been concluded, with no prior effort made to control for unwanted effects.

Greenhouses affect not only temperature, but also moisture, gas composition, snow cover (and therefore growing season), light (intensity and spectral quality), and wind speed. A greenhouse blocks precipitation and reduces diffusion and turbulent mixing, thus suppressing upward vapor

transport during the day and impeding dew formation at night. In some situations it may be possible to avoid unwanted microclimate effects. In the CLIMEX facility (Beerling and Woodward 1994), for example, ambient precipitation is gathered and distributed inside the greenhouse, and Chapin et al. (1995) argued that uneven microtopography allowed air circulation beneath their tundra greenhouses, reducing blockage of gas exchange. In general, though, greenhouses significantly and unavoidably modify microclimate, and usually not in ways that conform to global warming predictions. Greenhouses also have undesired impacts on the contained vegetation. The wind protection they provide reduces mechanical damage caused by ice crystal abrasion, flailing, and wind pruning, as well as surface heat loss and evaporation (Kennedy 1995b). A greenhouse can be a barrier to pollinators, dispersal agents, grazers, and pathogens. Greenhouse-induced changes in light and snow cover affect photosynthesis, canopy morphology, and phenology (NSFESP 1991). These effects, as well as unintentional microclimate effects, increase the difficulty of attributing observed ecosystem changes to temperature elevation alone, or to the combination of microclimate changes expected under global warming.

Despite their shortcomings, greenhouses, if carefully planned and designed, can be useful in studying effects of warming. There are frequently situations in which there are no other alternatives, such as in remote or powerless areas (Chapin et al. 1995; Kennedy 1994). Improving greenhouse applications requires careful microclimate control and monitoring, with microclimate modification achieved through appropriate selection of design and materials. Open-topped greenhouse designs may be one of the best. Marion et al. (1997) note that open-top greenhouses are able to achieve a significant temperature effect, while minimizing most of the unwanted ecological effects.

Warming Soil Directly: Buried Wires in Soil

An alternative to greenhouses is electrical resistance wire buried in the soil. This technique was first attempted by Rykbost et al. (1975), who buried wires 92 cm deep in cropland; they were not attempting to simulate climate warming, but rather were testing the feasibility of using waste heat water from power plants to boost crop production. The applications to global warming manipulations were apparent, and the technique has since been used by others for that purpose. Van Cleve et al. (1983; 1990) used buried electrical cables to heat 400 m^2 of Alaskan black spruce forest soil to approximately 9°C above ambient. Peterjohn et al. designed (1993) and applied (1994) a system of heating cables buried 10 cm deep and 20 cm apart in a temperate deciduous forest soil. Using thermostats, they maintained a nearly steady soil temperature elevation of 5°C above ambient over a variety of environmental conditions. To recreate their design, Peterjohn et al. (1993) suggest a power density of at least 67 W m^{-2}, and nesting experimental plots within a larger heated area. They also recommend creating two types of control plots, one with non-heating wires to mimic the disturbance caused by the installation and presence of the wires, and one completely undisturbed.

Buried wires can, if desired, achieve a constant, controlled temperature elevation above ambient with suitable electronic control. They do not cause as many unintended microclimate effects as greenhouses, such as blocking precipitation and wind. Although they require electricity, and therefore cannot be used in powerless areas, they are not too complicated or costly, and can be applied in many kinds of systems. Buried wires are one of the best options for soil warming manipulations in forest ecosystems. While this would not constitute a ecosystem-level manipulation, Peterjohn et al. (1993) contend that warming entire ecosystems may be unnecessary if (and this is a big if) changes in soil processes are the dominant ecological response to warming.

The use of buried wires has drawbacks for ecosystem warming, such as disturbance of the turf and soil to install the wires. Although Peterjohn et al. (1994) found that disturbing the soil seemed to have no effects on daily average temperatures, other soil and ecosystem processes, such as gas diffusion, water transport, mesofaunal activity, and rooting may still be affected. Comparison with appropriate control sites may help to cancel out these effects. Year-round simulations are not realistic, as midwinter applications of heat via buried soil cables under a snowpack are obviously inappropriate (NSFESP 1991). Also, the apparatus may cause fires, as has happened in the experiments of Peter-

john and coworkers. Another serious criticism of this technique is that it creates an unrealistic vertical temperature profile in the soil, affecting aboveground ecosystem components only indirectly and deeper soil more than surface soil. This is opposite to global warming, which involves increased transfer of heat to the soil from above. Buried wires do not warm foliage and thus do not provide a whole-ecosystem warming method. Despite the important role of soil in ecosystem function, a soil-only warming experiment is not a sufficient substitute for a whole-ecosystem manipulation.

Warming Soil Directly: Fluid-Filled Pipes at the Soil Surface

A method similar to buried electrical wires but with fewer disadvantages is heating the soil surface with warming pipes. Hillier et al. (1994) used a system of fluid-filled, stainless steel pipes at the soil surface to produce a continuous, constant temperature differential. They used this pipe system in a meadow in southern England to manipulate the length of the growing season and to simulate a milder winter. Each warmed plot was paired with an unheated reference plot of similar vegetation structure and with a dummy pipe network to cancel out shading effects introduced by the apparatus. The pipe network was supported by a metal grid, which also functioned in the lateral dissipation of heat, creating a more uniform temperature distribution.

There are several advantages to this type of system. Unlike buried electrical wires, this method does not create an unrealistic vertical temperature profile in the soil, nor disturb the soil surface or low-lying vegetation. And unlike greenhouses, there is not blocked precipitation, reduced wind, or light attenuation. The apparatus can be used to produce heating or cooling, enabling a greater variety of climate manipulation scenarios. For bare soil or low-lying vegetation, this method is a good one for manipulating foliage as well as soil temperature. For elevating temperature in ecosystems with taller plants, Hillier et al. (1994) mention the use of infrared heaters suspended over the vegetation, to which we now turn.

Increasing Downward Radiation: Overhead Heaters

In global warming, the total heating effect is the sum of the direct infrared (IR) radiative effect of increased greenhouse gas concentrations and the resulting feedback effects involving the hydrologic cycle, atmospheric circulation, and, in ways that are less well understood, the biota, all operating from local to global spatial scales. Although elevated greenhouse gas levels result in surface warming because of both enhanced downward IR and because warmer air convects and conducts more heat to ecosystems, the consequences of both the direct and feedback effects on surface warming can be simulated by raising the downward IR radiation level appropriately.

Manipulating radiation can be preferable to other warming methods for many reasons. Increasing the downward IR radiation mimics the "top down" nature of heating that actually occurs under an atmosphere with increased levels of greenhouse gases. Nijs et al. (1996) found that applying heating from above maintains the natural temperature gradients within the canopy. Infrared lamps transfer heat noninvasively, and there are few unintended effects on microclimate. Year-round manipulations are possible, although in areas with very deep winter snowpack, the heaters may become covered if mounted too low, thus temporarily creating an unrealistic warming scenario. Greenhouses, buried wires, and surface pipes all have greater problems with application in winter, however, so comparatively, overhead heaters are a better option.

Overhead IR lamps can be thermostated to achieve a constant increase in soil temperature, but there is no reason to believe that forcing a continuous, constant temperature increase would realistically simulate the effects of global warming. In fact, if soils dry under global warming, then the temperature effect on soil of global warming should vary diurnally (Harte et al. 1995b). Seasonal variation is also predicted by GCMs (Kattenberg and Maskell 1995). Use of a constant level of downward IR allows investigation of the temporal variability in soil temperature response, as well as the subsequent ecosystem responses.

At the midrange of GCM forecasts, the net surface warming due to both the direct effect of an equivalent doubling of CO_2 plus the contribution of major feedbacks is simulated by enhancing downward IR radiation by 20 to 30 W m^{-2} (Harte et al. 1995b). To achieve daily-averaged soil temperature increases as high as 6°C at 10 cm soil depth, such as is sometimes attained in greenhouse studies, fluxes of up to 60 to 80 W m^{-2} would be

needed. To simulate global warming in the field, this energy input is best applied to the vegetation canopy using overhead energy sources, and whenever possible, should be provided throughout the year, so that changes such as the early initiation of snowmelt and lengthening of the growing season can be examined. The application of energy from above constitutes an ecosystem-level warming experiment, as opposed to a soil-only warming experiment, and leads to warmer foliage as well as soil.

The use of overhead heaters for ecosystem warming was first applied by Harte et al. (1995b) in a montane meadow in Colorado, in the United States. Since 1991, the downward IR radiation over five treatment plots has been increased, night and day, year-round, with infrared heaters suspended 2.5 m above the ground from a frame consisting of towers and cables (Fig. 24.2). The heaters are designed and spaced to produce a nearly uniform temperature increase over the treatment plots, but not to significantly influence the nearby control plots. No dummy heaters were installed over the control plots, but shadowing effects of the heaters were determined to be minimal. The experimental manipulation had significant microclimate and biotic responses, discussed in detail elsewhere (Harte et al. 1995a,b; Harte and Shaw 1995; Loik and Harte 1996; Saleska et al. 1999; Torn and Harte 1996). Soil temperature response to increased radiation varied throughout the day; during midday the solar gain on the drier heated-plot soils resulted in a maximum temperature increment. Forcing a constant temperature elevation, rather than constant energy input, would have eliminated the possibility of capturing variations in temperature response that may actually occur from the direct effect of global warming and that may be ecologically important.

Nijs et al. (1996) also used overhead heaters for ecosystem warming in a perennial ryegrass system

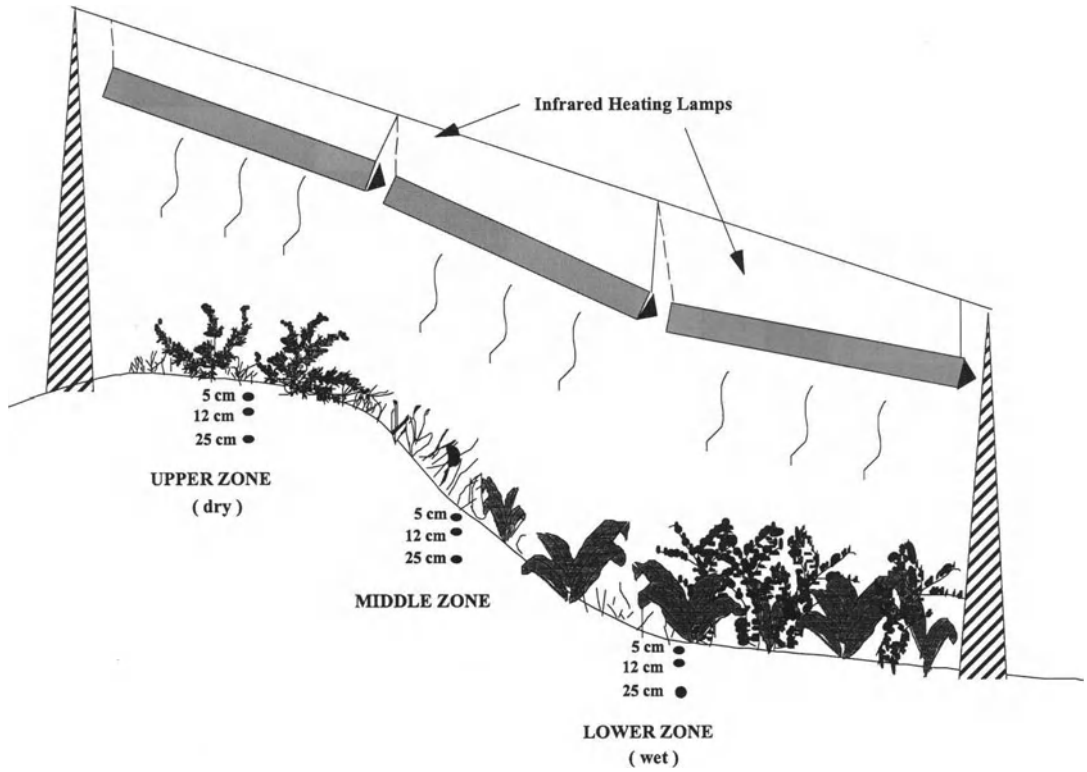

FIGURE 24.2. Overhead infrared heater assemblage (Kalglo, Inc.) used by Harte et al. (1995b) to warm a subalpine meadow ecosystem in Colorado.

in Switzerland, choosing to achieve a fixed 2.5°C temperature differential between adjacent heated and control plots by continually adjusting the IR heater output. In their experiment, called Free Air Temperature Increase (FATI—in analogy to the FACE experiments of enhanced CO_2—although this a misnomer since IR heaters do not directly warm the intervening air), they used large heaters, one per plot, mounted vertically at the plot edge and angled to irradiate downward over the plot. Their control plots had dummy heaters (no output) to cancel out shading effects. They screened out radiation below 800 nm to avoid unwanted photomorphogenic effects. An alternative to filtering is to select heaters designed to emit radiation essentially only in the IR portion of the spectrum. Nijs and coworkers were interested in the effect of the experimental design on canopy and leaf temperatures and thus only ran their study for a period of weeks. In another warming experiment, Bridgham et al. (1995) used overhead heaters to investigate effects of global warming on trace gas fluxes in bog ecosystems in Minnesota, in the United States. Rather than apply the manipulation in situ, they established large mesocosms (2.2 m^2 and 0.6 m in depth) with intact vegetation communities, and placed them in containers for manipulation by the heaters. Though not technically an in situ field study, this comes close to an actual ecosystem manipulation, and has the advantages of convenience and easier access.

Overhead heaters can be applied in many ecosystems, and are relatively easy to install in tundra, desert, meadow, and agricultural systems. Since IR heaters do not directly heat the air, this technique cannot simulate the convective heating effect of global warming. It would be impractical to use suspended heaters for whole-ecosystem warming in forests, because of the need to suspend them over the canopy. Moreover, a dense canopy would virtually eliminate the possibility of soil warming. Indeed, no method of controlled heating of whole dense forests has been demonstrated, but forest soil heating can be achieved either by heating wires or pipes at the soil surface, set to provide a constant power output, or by IR lamps suspended under the canopy.

Field Methods: Other Climate Variables

Global warming will alter many climatic variables besides temperature. Changes in amount and duration of winter snowpack, amount and distribution of rainfall, cloud cover, and soil moisture are some effects relevant to ecosystem processes.

Changes in snow depth and the duration of the snowmelt period can limit the distribution of plant species and may induce a variety of growth responses, including changes in morphology, flowering, and seed-set, as well as taxonomic shifts toward more opportunistic species. Snow fences provide a simple and inexpensive means of locally altering snowpack. Snow shoveling has also been employed to alter snow depth (Dunne 1996). Snow fences have been used in long-term experiments at the LTER site at Niwot Ridge, Colorado, U.S.A. (Brooks et al. 1996; Walker 1991). Brooks et al. found that the installation of a 2.6 $\times$ 60 m snow fence at this site resulted in a snowpack significantly deeper and longer lasting than before construction of the fence. Sturges (1989) examined the effect of induced snow accumulation on mountain big sagebrush by installing a snow fence 3.8 m tall. Chapin and Shaver (1996) used snow fences to determine the effects of shortened growing season in a tussock tundra ecosystem. They erected a 40-m long, 1.5-m tall snow fence perpendicular to the prevailing winter wind and parallel to the slope of their field site, creating late-lying snowdrifts and shortening the growing season by 2 weeks. Galen and Stanton (1995) also used snow fences to alter growing season length. Tabler (1980) discusses geometry and density of drifts formed by snow fences. Although snow fences exert a dramatic local impact on snow accumulation, their effects cannot be precisely controlled. As we have discussed, greenhouses and buried resistance wires also have major drawbacks for winter application. Infrared lamps provide a useful way to simulate effects of global warming on winter snow cover, but the melt pits they produce may accumulate wind-blown snow and thus unrealistically increase total snowmelt water available to the heated plots.

Global warming will also affect rainfall patterns. Although soil moisture is affected by direct warming, the combined effect on soil moisture of both an altered thermal regime and altered precipitation rates has not been investigated at field scale. Tarpaulins have been used to intercept rainfall on experimental plots in a savanna ecosystem in Arizona, U.S.A., to investigate the impact of global change on seedling recruitment (MacPherson 1995) and on montane meadow plots along an elevational gra-

dient (Dunne 1996). A major drawback of this approach is the physical effort needed to deploy the tarpaulins on rapid response, or shading if they are left in place. Additional rainfall is, of course, readily simulated by artificial watering. In the Throughfall Displacement Experiment (Hanson and Edwards 1996), soil moisture in an upland oak forest in eastern Tennessee, U.S.A., is manipulated by intercepting throughfall with subcanopy troughs suspended above the forest floor of the dry plots and transferring it by gravity flow across an ambient plot for subsequent distribution onto the wet treatment plots.

Field Methods: Enhancing UV-B Radiation

Separate from the issue of global warming, stratospheric ozone depletion from emissions of chlorofluorocarbons and other anthropogenic compounds also poses a threat to ecosystems. The natural stratospheric ozone layer attenuates solar UV-B radiation (290 to 320 nm), and therefore depleting the ozone layer increases penetration of UV-B radiation to the earth's surface. UV-B radiation affects plant chemistry and physiology (Caldwell et al. 1989), as well as plant morphology and competition (Barnes et al. 1995). Terrestrial plants are especially vulnerable due to their obligatory requirement for sunlight for photosynthesis (Greenberg et al. 1996).

There have been hundreds of studies of the impacts of elevated solar UV-B radiation on plants (for a summary, see Caldwell and Flint 1994). Very few have dealt with multiple species, much less plant communities or whole ecosystems. Most have been short-term studies in greenhouses or growth chambers, but these often overestimate the UV-B radiation effects (Mark et al. 1996). Results of several studies suggest that different species of plants show large differences in sensitivity to UV-B radiation (Rau and Hofmann 1996), making it difficult to extrapolate results from chamber studies of single-species response to UV-B radiation alteration to whole-ecosystem response. As is the case with ecosystem manipulations of climate, there is a relative scarcity of whole-ecosystem, long-term field manipulations of UV-B radiation (Barnes et al. 1995; Caldwell and Flint 1994; Flint and Caldwell 1996).

Field studies of UV-B radiation have taken one of three approaches: excluding UV-B radiation by filtering sunlight, transplanting to high altitudes (where UV-B radiation intensity is greater due to reduced screening from natural ozone), or enhancing ambient UV-B radiation artificially. Excluding UV-B radiation in the field is done with a shade or greenhouse. Exclusion experiments are simpler and cheaper than enhancement manipulations, and if carefully conducted, can suggest whether ambient UV-B radiation is influential (Caldwell and Flint 1994). They cannot be used to realistically simulate ozone depletion, however, since extrapolating results from UV-B radiation exclusion experiments to enhanced levels of UV-B radiation is not necessarily justified. The effects of elevated UV-B radiation can also be examined by studying plant responses at high elevation or in low latitudes, since the amount of UV-B radiation reaching the earth's surface increases with altitude above sea level and with lower latitudes (Rau and Hofmann 1996). Controls can be obtained by suitable filtering of excess radiation (Tevini et al. 1989) or by comparison with plant response in lowland areas (Dohring et al. 1996). These studies have the advantage of realistic spectrum characteristics of solar enhancement, but it is difficult to attribute differences in plant response at different locations to UV-B radiation enhancement alone, and not genetic, climatic, or soil differences between sites.

Field manipulations enhance global UV-B radiation by supplementing ambient sunlight using fluorescent lamps. Conceptually, the use of overhead lamps for UV-B radiation enhancement is similar to the use of overhead IR lamps for global warming studies. Determining the proportional UV-B radiation increase associated with various decreases in stratospheric column ozone is typically accomplished with a mathematical radiative transfer model (e.g., Bjorn and Murphy 1985; Green 1983; Green et al. 1980; Rundel 1986). Since a reduction of the ozone layer results in a very specific increase in solar UV-B radiation in a wave band of only about 30 nm, the fluorescent lamps for UV-B radiation field manipulations must be filtered in order to screen out wavelengths below 290 nm (e.g., Flint and Caldwell 1996; Mackerness et al. 1996). Different screening techniques and materials can also be used to obtain different kinds of treatments, such as to remove or supplement UV-B radiation.

(e.g., Adamse and Britz 1996). Ideally, these lamps should automatically vary the output as the background sunlight level changes (e.g., Barnes et al. 1995; Fiscus et al. 1996; Olszyk et al. 1996), although some studies have kept a constant output for a set amount of daylight hours (e.g., Olszyk et al. 1996). Only a few field experiments of UV-B radiation enhancement have considered the plant community or ecosystem level, and none has been long-term. Barnes et al. (1995) examined the effects of increased UV-B radiation resulting from a 20% decrease in stratospheric ozone on canopy photosynthesis and light competition in wheat and wild oat in Utah, U.S.A., using a modulated fluorescent lamp system, suspended 40 cm above the experimental plants. Fiscus et al. (1996) used fluorescent lamps suspended in open-topped field chambers to study response of soybean to three levels of UV-B radiation corresponding to various changes in the total column ozone thickness.

The use of UV lamps in the field is costly, and plagued with problems. The lamps and filters do not provide ideal simulations of solar UV-B radiation (for a detailed analysis, see Caldwell et al. 1986). There are problems of optical degradation, aging, and temperature sensitivity, and also geometrical constraints which prevent an accurate UV-B radiation enhancement simulation. An added difficulty is that since relatively small amounts of energy are involved in these manipulations, and the UV-B radiation phenomena are so wavelength-specific, small discrepancies can result in substantial inaccuracies (Caldwell and Flint 1994). Although there is a need for ecosystem-level field studies of UV-B radiation impacts of stratospheric ozone depletion, the use of UV-B enhancing lamps is problematic for long-term field studies. We encourage the reader to consult the work of Caldwell and coworkers for more information before undertaking field manipulations of this kind.

General Recommendations

As a prerequisite to undertaking a climate manipulation study, ecologists should familiarize themselves with the science of global warming and the latest climate model predictions for changes in temperature, precipitation, and other variables. The best place to begin is the most recent report by the Intergovernmental Panel on Climate Change (IPCC 1995)

There is a need for large-scale, long-term field studies of ecosystem response to global and regional change, including warming, moisture changes, elevated CO_2, and increased UV-B radiation. Large-scale, whole-ecosystem experiments are the best means of examining the individual and net effects of the different feedbacks within the system. In addition to their own worth, field manipulations provide context for the many smaller-scale (time and space), single-species studies that exist. Experiments may need to run for several years before trends become discernible (Coulson et al. 1996). Whenever possible, long-term field studies should be year-round, in order to capture the entire annual cycle of response.

There is no single ecosystem manipulation method that will be appropriate in all situations. For whole-ecosystem warming manipulations in relatively low canopy systems, the use of overhead IR heaters to increase radiant energy input to ecosystems is probably the best option. As discussed above, it is preferable for many reasons to maintain a constant power output rather than a thermostated temperature rise. Climate manipulations should incorporate monitoring of microclimate throughout the experiment, on an appropriately fine spatial and temporal scale, and researchers should examine variance and extremes in addition to mean values so as to gain insight to diel and seasonal variations in microclimate response to the treatment.

The task of extrapolating experimental results on ecosystem responses to climate change on the scale of plots to that of landscapes or continents is now widely accepted as one of the central challenges facing global change science (e.g., Anderson 1992; Ehleringer and Field 1993; Lubchenco 1991; Rosswall et al. 1988). Predicting community and ecosystem responses to environmental changes from study of individual physiological processes requires consideration of the time scales over which physiological processes exert their effects (Chapin and Shaver 1996). Problems of small scale size in field studies may sometimes be circumvented by combining information from laboratory, field, and modeling studies (e.g., Harte et al. 1992). Comparing results from ecosystem field manipulations and from correlation analysis along elevational gradients can generate insights into how transient re-

sponse to climate change may be related to long-term response to differing climate conditions. Thus, field manipulation experiments should not be performed in isolation, but in tandem with a variety of laboratory and other field techniques and development of mechanistic and statistical models.

Simulation models of soil and ecosystem processes can be used to integrate experimental findings into existing large-scale ecosystem models, and ecosystem climate manipulation experiments offer a sensitivity analysis and testing of current models of ecosystem function in various biomes (NSFESP 1991). Ecosystem climate manipulations provide an unparalleled opportunity to calibrate and validate mechanistic models, a great virtue since lack of suitable observations is inhibiting the evaluation of universal land surface schemes (Gates et al. 1995). For example, in the meadow warming experiment of Harte et al. (1995b), Shen (1998) calibrated a microclimate model with soil temperature and moisture data from control plots, then validated the model against the treatment minus control difference. This constitutes a rigorous validation against an independent data set, something rarely possible but much desired in modeling studies.

Ecosystem field studies combining more than one manipulation (warming, CO_2, UV, moisture, or other stresses) are becoming more common (e.g., Beerling and Woodward 1994; Chapin et al. 1995; Nijs et al. 1996; Repo et al. 1996; Tissue and Oeschel 1987). Cost may be an issue, as long-term field studies of enhanced CO_2 concentration or UV-B radiation are difficult and expensive, and some manipulations are problematic to design and implement. The complication of confounding factors (i.e., difficulty attributing an observed response to a particular forcing variable) can be reduced with an appropriate factorial design, provided a sufficiently large area of habitat is available for experimentation. Both single-variable and combined-variable manipulations have merits and pitfalls, and each yields information not extractable from the other.

Most ecosystem climate manipulations have focused on alpine, subalpine, Arctic, and sub-Arctic ecosystems, because global climate change is predicted to be especially pronounced in these types of systems, and also because these systems are considered to be especially sensitive to changes. There is much to be learned from ecosystem manipulations in other regions, such as midlatitudes and tropics. Future work might beneficially target these gaps.

References

Adamse, P.; Britz, S.J. Rapid fluence-dependent responses to ultraviolet-B radiation in cucumber leaves: The role of UV-absorbing pigments in damage protection. J. Plant Physiol. 148:57–62; 1996.

Anderson, J.E.; Williams, J.; Kriedemann, P.E.; Austin, M.P.; Farquhar, G.D. Correlations between carbon isotope discrimination and climate of native habitats for diverse eucalypt taxa growing in a common garden. Aust. J. Plant Physiol. 23:311–320; 1996.

Anderson, J.M. Responses of soils to climate change. In: Woodward, F.I., ed. *Global Climate Change: The Ecological Consequences.* Advances in Ecological Research. Vol. 22. New York: Academic Press, 1992:163–210.

Barnes, P.W.; Flint, S.D.; Caldwell, M.M. Early-season effects of supplemented solar UV-B radiation on seedling emergence, canopy structure, simulated stand photosynthesis and competition for light. Global Change Biol. 1:43–53; 1995.

Beerling, D.J.; Woodward, F.I. The climate change experiment (CLIMEX): Phenology and gas exchange responses of boreal vegetation to global change. Global Ecol. Biogeogr. Lett. 4:17–26; 1994.

Bjorn, L.O.; Murphy, T.M. Computer calculation of solar ultraviolet radiation at ground level. Physiol. Vegetat. 23:555–561; 1985.

Bridgham, S.D.; Pastor, J.; Updegraff, K.; Janssens, J.A.; Malterer, T.J. [Abstract] Paper presented at the Ecological Society of America Annual Meeting, Snowbird, Utah, July 30 to August 3, 1995.

Brooks, P.D.; Williams, M.W.; Schmidt, S.K. Microbial activity under alpine snowpacks, Niwot Ridge, Colorado. Biogeochemistry 32:93–113; 1996.

Burke, I.C.; Elliott, E.T.; Cole, C.V. Influence of macroclimate, landscape position, and management on soil organic matter in agroecosystems. Ecol. Applic. 5:124–131; 1995.

Caldwell, M.M.; Camp, L.B.; Warner, C.W.; Flint, S.D. Action spectra and their key role in assessing biological consequences of solar UV-B radiation change. In: Worrest, R.C.; Caldwell, M.M., eds. *Stratospheric Ozone Reduction, Solar Ultraviolet Radiation, and Plant Life.* Berlin: Springer-Verlag; 1986.

Caldwell, M.M.; Flint, S.D. Stratospheric ozone reduction, solar UV-B radiation and terrestrial ecosystems. Climat. Change 28:375–394; 1994.

Caldwell, M.M.; Teramura, A.H.; Tevini, M. The changing solar ultraviolet climate and the ecological consequences for higher plants. Trends Ecol. Evolut. 4:363–367; 1989.

Carpenter, S.R. Microcosm experiments have limited relevance for community and ecosystem ecology. Ecology 77:677–680; 1996.

Chapin, F.S.; Shaver, G.R. Physiological and growth responses of arctic plants to a field experiment simulating climatic change. Ecology 77:822–840; 1996.

Chapin, F.S.; Shaver, G.R.; Giblin, A.E.; Nadelhoffer, K.J.; Laundre, J.A. Responses of arctic tundra to experimental and observed changes in climate. Ecology 76:694–711; 1995.

Coulson, S.; Hodkinson, I.D.; Strathdee, A.; Bale, J.S.; Block, W.; Worland, M.R.; Webb, N.R. Simulated climate change: the interaction between vegetation type and microhabitat temperatures at Ny-Alesund, Svalbard. Polar Biol. 13:67–70; 1993.

Coulson, S.J.; Hodkinson, I.D.; Webb, N.R.; Block, W.; Bale, J.S.; Strathdee, A.T.; Worland, M.R.; Wooley, C.; Worland, M.R.; Wooley, C. Effects of experimental temperature elevation on high-arctic soil microarthropod populations. Polar Biol. 16:147–153; 1996.

Davis, M.B.; Zabinski, C. Changes in geographical range resulting from greenhouse warming: Effects on biodiversity in forests. In: Peters, R.L.; Lovejoy, T.E., eds. *Global Warming and Biological Diversity.* New Haven, CT: Yale Univ. Pr.; 1992:297–308.

Debevec, E.M.; Maclean, S.F. Design of greenhouses for the manipulation of temperature in tundra plant communities. Arctic Alp. Res. 25:56–62; 1993.

Dickinson, R.E.; Henderson-Sellers, A.; Kennedy, P.J.; Wilson, M.F. *Biosphere-Atmosphere Transfer Scheme (BATS) for the NCAR Community Climate Model.* Boulder, CO: National Center for Atmospheric Research; 1986.

Dickson, D. Aerosols role simulated in new global warming model. Nature 374:487–487; 1995.

Dohring, T.; Kofferlein, M.; Thiel, S.; Seidlitz, H.K. Spectral shaping of artificial UV-B irradiation for vegetation stress research. J. Plant Physiol. 148:115–119; 1996.

Dudzik, M.; Harte, J.; Jassby, A.; Lapan, E.; Levy, D.; Rees, J. Some considerations in the design of aquatic microcosms for plankton studies. Int. J. Environ. Stud. 13:125–130; 1979.

Dunne, J. Personal Communication, University of California, Berkeley, CA, 1996.

Edwards, N.T.; Norby, R.J. Below-ground respiratory responses of sugar maple and red maple saplings to atmospheric CO_2 enrichment and elevated air temperature. Plant Soil 206:85–97; 1998.

Ehleringer, J.; Field, C. *Scaling Physiological Processes: Leaf to Globe.* San Diego, CA: Academic; 1993.

Fiscus, E.L.; Booker, F.L.; Miller, J.E. Response of soybean bulk leaf water relations to ultraviolet-B irradiation. J. Plant Physiol. 148:63–68; 1996.

Flint, S.D.; Caldwell, M.M. Scaling plant ultraviolet spectral responses from laboratory action spectra to field spectral weighting factors. J. Plant Physiol. 148:107–114; 1996.

Foley, J.A.; Prentice, I.C.; Ramankutty, N.; Levis, S.; Pollard, D.; Sitch, S.; Haxeltine, A. An integrated biosphere model of land surface processes, terrestrial carbon balance, and vegetation dynamics. Global Biogeochem. Cycl. 10:603–628; 1996.

Galen, C.; Stanton, M.L. Responses of snowbed plant species to changes in growing-season length. Ecology 76:1546–1557; 1995.

Gates, W.L.; Henderson-Sellers, A.; Boer, G.J.; folland, C.K.; McAvaney, B.J.; Semazzi, F., Smith, N., Weaver, A.J.; Zeng, Q.-C. Climate models: Evaluation. In: Houghton, J.T.; Meira Filho, L.G.; Callander, B.A.; Harris, N.; Kattenberg, A.; Maskell, K., eds. *Climate Change 1995: The Science of Climate Change.* Cambridge: Cambridge Univ. Pr.; 1995: 483–516.

Green, A.E.S. The penetration of ultraviolet radiation to the ground. Physiol. Plant 58:351–359; 1983.

Green, A.E.S.; Cross, K.R.; Smith, L.A. Improved analytic characterization of ultraviolet skylight. Photochem. Photobiol. 31:59–65; 1980.

Greenberg, B.M.; Wilson, M.I.; Gerhardt, K.E.; Wilson, K.E. Morphological and physiological responses of *Brassica napus* to ultraviolet-B radiation: Photomodification of ribulose-1,5-bisphosphate carboxylase/oxygenase and potential acclimation processes. J. Plant Physiol. 148:78–85; 1996.

Hanson, P.J.; Edwards, N.T. Personal Communication, Oak Ridge, TN, 1996.

Hansen, J.; Fung, I.; Lacis, A.; Rind, D.; Lebedeff, S.; Ruedy, R.; Russell, G. Global climate changes as forecast by the Goddard Institute for Space Studies three-dimensional model. J. Geophys. Res. 93:9341–9364; 1988a.

Hansen, J.; Rind, D.; DelGenio, A.; Lacis, A.; Lebedeff, S.; Prather, M.; Reudy, R.; Karl, T. Regional greenhouse climate effects. In: *Coping with Climate Change. Proceedings of the Second North American Conference on Preparing for Climate Change.* Washington, DC: Climate Institute; 1988b.

Harte, J.; Jensen, D.; Torn, M.S. The nature and consequences of indirect linkages between climate change and biological diversity. In: Peters, R.; Lovejoy, T., eds. *Global Warming and Biological Diversity.* New Haven, CT: Yale Univ. Pr.; 1992.

Harte, J.; Rawa, A.; Price, V. Effects of manipulated soil microclimate on mesofaunal biomass and diversity. Soil Biol. Biogeochem. 28:313–322; 1995a.

Harte, J.; Shaw, R. Shifting dominance within a montane vegetation community: Results of a climate-warming experiment. Science 267:876–880; 1995.

Harte, J.; Torn, M.S.; Chang, F.R.; Feifarek, B.; Kinzig, A.P.; Shaw, R.; Shen, K. Global warming and soil microclimate: Results from a meadow-warming experiment. Ecol. Applic. 5:132–150; 1995b.

Hartmann, D.L. Modeling climate change. In: MacDonald, G.J.; Sertorio, L., eds. *Global Climate and Ecosystem Change.* NATO ASI Series B: Physics. Vol. 240, New York: Plenum; 1990.

Harvey, L.D.D.; Schneider, S.H. Transient climate response to external forcing on 100–104 year timescales. 1. Experiments with globally-averaged, coupled, atmosphere, land, and ocean energy balance models. J. Geophys. Res. 90:2191–2206; 1985.

Hattenschwiler, S.; Korner, C. System-level adjustments to elevated CO_2 in model spruce ecosystems. Global Change Biol. 2:377–387; 1996.

Henderson-Sellers, A.; McGuffie, K. Land-surface characterization in greenhouse climate simulations. International J. Climatol. 14:1065–1094; 1994.

Hillier, S.H.; Sutton, F.; Grime, J.P. A new technique for the experimental manipulation of temperature in plant communities. Funct. Ecol. 8:755–762; 1994.

Hunt, H.W.; Elliott, E.T.; Detling, J.K.; Morgan, J.A.; Chen, D.X. Responses of a C-3 and a C-4 perennial grass to elevated CO_2 and temperature under different water regimes. Global Change Biol. 2:35–47; 1996.

[IPCC] Intergovernmental Panel on Climate Change. *Climate Change 1995: The Science of Climate Change.* Cambridge: Cambridge Univ. Pr.; 1995.

Jensen, D.B. *Population Differentiation in Tree-Ring Growth Responses of White Fir (Abies concolor) to Climate: Implications for Predicting Forest Responses to Climate Change.* Doctoral thesis, University of California, Berkeley, CA; 1993.

Kattenberg, A.; Maskell, K. Climate models: Projections of future change. In: Hougton, J.T.; Meira Filho, L.G.; Callender, B.A.; Harris, N.; Kattenberg, A.; Maskell, K., eds. *Climate Change 1995: The Science of Climate Change.* Cambridge: Cambridge Univ. Pr.; 1995:285–357.

Keeling, C.D.; Whorf, T.P. Atmospheric CO_2 records from sites in the SIO air sampling networked. In: *Trends: A Compendium of Data on Global Change.* Oak Ridge, TN: Carbon Dioxide Information Analysis Center, Oak Ridge National Laboratory; 1998.

Kennedy, A.D. Simulated climate change: a field manipulation study of polar microarthropod community response to global warming. Ecography 17:131–140; 1994.

Kennedy, A.D. Temperature effects of passive greenhouse apparatus in high-latitude climate change experiments. Funct. Ecol. 9:340–350; 1995a.

Kennedy, A.D. Simulated climate change: Are passive greenhouses a valid microcosm for testing the biological effects of environmental perturbations? Global Change Biol. 1:29–42; 1995b.

Klein, J. Personal Communication, University of California, Berkeley, CA, 1998.

Korner, C.; Arnone, J.A. Responses to elevated carbon dioxide in artificial tropical ecosystems. Science 257:1672–1675; 1992.

Lashof, D.A. The dynamic greenhouse: Feedback processes that may influence future concentrations of atmospheric trace gases and climatic change. Climat. Change 14:213–242; 1989.

Lawton, J.H. The Ecotron facility at Silwood Park: The value of big bottle experiments. Ecology 77:665–669; 1996.

Lawton, J.H.; Naeem, S.; Woodfin, R.M.; Brown, V.K.; Gange, A.; Godfray, H.J.C.; Heads, P.A.; Lawler, S.; Magda, D.; Thomas, C.D.; Thompson, L.J.; Young, S. The Ecotron: A controlled environmental facility for the investigation of population and ecosystem processes. Philos. Trans. R. Soc. Lond. [Biol.] 341:181–194; 1993.

Loik, M.E.; Harte, J. High-temperature tolerance of *Artemisia tridentata* and *Potentilla gracilis* under a climate change manipulation. Oecologia 108:224–231; 1996.

Lubchenco, J. The sustainable biosphere initiative: An ecological research agenda. A report from the Ecological Society Of America. Ecology 72:371–412; 1991.

Mackerness, S.A.H.; Butt, P.J.; Jordan, B.R.; Thomas, B. Amelioration of Ultraviolet-B-induced down-regulation of MRNA levels for chloroplast proteins, by high irradiance, is mediated by photosynthesis. J. Plant Physiol. 148:100–106; 1996.

MacPherson, G. Personal communication, University of Arizona, Tucson, AZ, 1995.

Manabe, S.; Weatherald, R.T. Large-scale changes of soil wetness induced by an increase in atmospheric carbon dioxide. J. Atmos. Sci. 44:1211–1235; 1987.

Marion, G.M.; Henry, G.H.R.; Freckman, D.W.; Johnstone, J.; Jones, G.; Jones, M.H.; L vesque, E.; Molau, U.; Molgaard, P.; Parsons, A.N.; Svoboda, J.; Virginia, R.A. Open-top designs for manipulating field temperature in high-latitude ecosystems. Global Change Biol. 3(Supl. 1):20–32; 1997.

Mark, U.; Sailemark, M.; Tevini, M. Effects of solar UVB radiation on growth, flowering and yield of central and southern european maize cultivars (*Zea mays l*). Photochem. Photobiol. 64:457–463; 1996.

Naeem, S.; Thompson, L.J.; Lawler, S.P.; Lawton, J.H.; Woodfin, R.M. Declining biodiversity can alter the performance of ecosystems. Nature 368:734–737; 1994.

Nijs, I.; Kockelbergh, F.; Teughels, H.; Blum, H.; Hendrey, G.; Impens, I. Free Air Temperature Increase (FATI): A new tool to study global warming effects on plants in the field. Plant Cell Environ. 19:495–502; 1996.

Norby, R.J.; Edwards, N.T.; Riggs, J.S.; Abner, C.H.; Wullscleger, S.D.; Gunderson, C.A. Temperature-controlled open-top chambers for global change research. Global Change Biol. 3:259–267; 1997.

[NSFESP] National Science Foundation, Ecosystem Studies Program. Soil-warming experiments in global change research, Woods Hole, MA, September 27 and 28, 1991.

Oechel, W.C.; Riechers, G.; Lawrence, W.T.; Prudhomme, T.J.; Grulke, N.; Hastings, S.J. CO_2LT: An automated, null-balance system for studying the effects of elevated CO_2 and global climate change on unmanaged ecosystems. Funct. Ecol. 6:86–100; 1992.

Olszyk, D.; Dai, Q.J.; Teng, P.; Leung, H.; Luo, Y.; Peng, S.B. UV-B effects on crops: Response of the irrigated rice ecosystem. J. Plant Physiol. 148:26–34; 1996.

Pacala, S.; and Hurtt, G. Terrestrial vegetation and climate change: Integrating models and experiments. In: Kareiva, P.; Kingsolver, P.; Huey, R., eds. *Biotic Interactions and Global Change.* Sunderland, MA: Sinauer; 1993: 57–74.

Peterjohn, W.T.; Melillo, J.M.; Bowles, F.P.; Steudler, P.A. Soil warming and trace gas fluxes: Experimental design and preliminary flux results. Oecologia 93:18–24; 1993.

Peterjohn, W.T.; Melillo, J.M.; Steudler, P.A.; Newkirk, K.M.; Steudler, P.A.; Newkirk, K.M.; Bowles, F.P.; Aber, J.D. Responses of trace gas fluxes and N availability to experimentally elevated soil temperatures. Ecol. Applic. 4:617–625; 1994.

Randall, D.A.; Dazlich, D.A.; Zhang, C.; Denning, A.S.; Sellers, P.J.; Tucker, C.J.; Bounoua, L.; Los, S.O.; Justice, C.O.; Fung, I. A revised land surface parameterization (SIB2) for GCMs. 3. The greening of the Colorado State University general circulation model. J. Climate 9:738–763; 1996.

Rau, W.; Hofmann, H. Sensitivity to UV-B of plants growing in different altitudes in the Alps. J. Plant Physiol. 148:21–25; 1996.

Rawat, A.S.; Purohit, A.N. CO_2 and water vapour exchange in 4 alpine herbs at 2 altitudes and under varying light and temperature conditions. Photosyn. Res. 28:99–108; 1991.

Repo, T.; Hanninen, H.; Kellomaki, S. The effects of long-term elevation of air temperature and CO_2 on the frost hardiness of Scots pine. Plant Cell Environ. 19:209–216; 1996.

Ross, R.J.; Elliott, W.P. Tropospheric water vapor climatology and trends over North America: 1973–93. J. Climate 9:3561–3574; 1996.

Rosswall, T., Woodmansee, R.G.; Risser, P.G. Scales and global change, Chichester, England: Wiley; 1988.

Rundel, R. Computation of spectral distribution and intensity of solar UV-B radiation. In: Worrest, R.C.; Caldwell, M.M., eds. *Stratospheric Ozone Reduction, Solar UV, and Plant Life.* NATO ASI Series G. Vol. 8. New York: Plenum; 1986:49–62.

Rykbost, K.A.; Boersma, L.; Mack, H.J.; Schmisseur, W.E. Yield response to soil warming: Agronomic crops. Agron. J. 67:733–738; 1975.

Saleska, S.; Harte, J.; Torn, M. Effect of experimental ecosystem warming on CO_2 fluxes in a montane meadow. Global Change Biol. 5:125–142; 1999.

Sato, N.; Sellers, P.J.; Randall, D.A.; Schneider, E.K.; Shukla, J.; Kinter, J.L.; Hou, Y.T.; and Albertazzi, E. Effects of implementing the Simple Biosphere Model in a general circulation model. J. Atmos. Sci. 46:2757–2782; 1989.

Schimel, D.; Alves, D.; Enting, I.; Heimann, M.; Joos, F.; Raynaud, D.; Wigley, T.; Prather, M.; Derwent, R.; Enhalt, D.; Fraser, P.; Sanhueza, E.; Zhou, X.; Jonas, P.; Charlson, R.; Rodhe, H.; Sadavisan, S.; Shine, K.P.; Fouquart, Y.; Ramaswamy, V.; Solomon, S.; Srinivasan, J.; Albirtton, D.; Derwent, R.; Isakson, I.; Lal, M.; Wuebbles, D. Radiative forcing of climate. In: Houghton, J.T.; Meira Filho, L.G.; Callender, B.A.; Harris, N.; Kattenberg, A.; Maskell, K., eds. *Climate Change 1995: The Science of Climate Change.* Cambridge: Cambridge Univ. Pr.; 1995:65–132.

Sellers, P.J.; Dickinson, R.E.; Randall, D.A.; Betts, A.K.; Hall, F.G.; Berry, J.A.; Collatz, G.J.; Denning, A.S.; Mooney, H.A.; Nobre, C.A.; Sato, N.; Field, C.B.; Henderson-Sellers, A. Modeling the exchanges of energy, water, and carbon between continents and the atmosphere. Science 275:502–509; 1997.

Sellers, P.J.; Mintz, Y.; Sud, Y.C.; Dalcher, A. A simple biosphere model (SiB) for use within general circulation models. J. Atmos. Sci. 43:505–530; 1986.

Shen, K.P. A modelling study of experimental warming of a sub-alpine meadow. Doctoral thesis, University of California, Berkeley, CA, 1998.

Stanton, M.L.; Rejmanek, M.; and Galen, C. Changes in vegetation and soil fertility along a predictable snowmelt gradient in the mosquito range, Colorado, USA. Arctic Alp. Res. 26:364–374; 1994.

Strathdee, A.T.; Bale, J.S.; Block, W.C.; Coulson, S.J.; Hodkinson, I.D.; Webb, N.R. Effects of temperature elevation on a field population of *Acyrthosiphon svalbardicum* (hemiptera, aphididae) on Spitsbergen. Oecologia 96:457–465; 1993.

Sturges, D.L. Response of mountain big sagebrush to induced snow accumulation. J. Appl. Ecol. 26:1035–1041; 1989.

Sud, Y.C.; Sellers, P.J.; Mintz, Y., Chou, M.D.; Walker, G.K.; Smith, W.E. Influence of the biosphere on the global circulation and hydrologic cycle: a GCM simulation experiment. Agric. For. Meteorol. 52:133–180; 1990.

Tabler, R.D. Geometry and density of drifts formed by snow fences. J. Glaciol. 26:405–419; 1980.

Tate, K.R. Assessment, based on a climosequence of soils in tussock grasslands, of soil carbon storage and release in response to global warming. J. Soil Sci. 43:697–707; 1992.

Tevini, M.; Mark, M.; Saile, M. Plant experiments in growth chambers illuminated with natural sunlight. In: Payer, H.D.; Pfirrman, T.; Mathy, P., eds. Environmental Research with Plants in Closed Chambers, Brussels: Commission of the European Communities; 1989:240–251.

Tissue, D.T.; Oeschel, W.C. Response of *Eriphorum vaginatum* to elevated CO_2 and temperature in the Alaskan Arctic tundra. Ecology 76:721–733; 1987.

Torn, M.S.; Harte, J. Methane consumption by montane soils: Implications for positive and negative feedback with climatic change. Biogeochemistry 32:53–67; 1996.

Townsend, A.R.; Vitousek, P.M.; Trumbore, S.E. Soil organic matter dynamics along gradients in temperature and land use on the island of Hawaii. Ecology 76:721–733; 1995.

Trumbore, S.E.; Chadwick, O.A.; Amundson, R. Rapid exchange between soil carbon and atmospheric carbon dioxide driven by temperature change. Science 272:393–396; 1996.

Van Cleve, K.; Dyrness, C.T.; Viereck, L.A.; Fox, J.; Chapin, F.S.; Oeschel, W. Tiaga ecosystems in interior Alaska. BioScience 33:39–44; 1983.

Van Cleve, K.; Oechel, W.C.; Hom, J.L. Response of black spruce (*Picea mariana*) ecosystems to soil temperature modification in interior Alaska. Can. J. For. Res. 20:1530–1535; 1990.

Verhoef, H.A. The role of soil microcosms in the study of ecosystem processes. Ecology 77:685–690; 1996.

Verseghy, D.L.; McFarlane, N.A.; Lazare, M. CLASS: A Canadian land surface scheme for GCMs. 2. Vegetation model and coupled runs. Int. J. Climatol. 13:347–370; 1993.

Vitousek, P.M.; Matson, P.A. Effects of tropical deforestation on global and regional atmospheric chemistry—Comment. Climat. Change 19:159–162; 1991.

Walker, B.H. Ecological consequences of atmospheric and climate change. Climat. Change 18:301–316; 1991.

Woodward, I.F. A review of the effects of climate on vegetation: Ranges, competition, and composition. In: Peters, R.L.; Lovejoy, T.E., eds. *Global Warming and Biological Diversity.* New Haven: Yale Univ. Pr.; 1992:105–123.

Wynn-Williams, D.D. Microbial colonization processes in Antarctic fellfield soils: An experimental overview. Proc. NIPR Symp. Polar Biol. 3:164–178; 1990.

Wynn-Williams, D.D. Plastic cloches for manipulating natural terrestrial environments. In: Wynn-Williams, D.D., ed. *BIOTAS Manual of Methods for Antarctic Terrestrial and Freshwater Research.* Cambridge: Scientific Committee on Antarctic Research; 1992.

Part 4

Synthesis and Conclusions

25

Ecosystem Modeling

Herman H. Shugart

Introduction

In the usual usage, ecological models are mathematical expressions developed to be analogous, in some sense, with an ecosystem of interest (Table 25.1). The models of principal interest here are those are used to integrate information and to produce predictions of responses of ecosystems to change. With an abruptly increasing availability of computer power in terms of speed, cost, and magnitude of computation over the past two decades, there has been an explosive development of the application of computer models in ecology as well as in other sciences. New computer software allows scientists to explore complex dynamic equations using small (but powerful) computers in the same manner that an earlier generation of ecologists used paper as "scratch pads" to sketch data patterns and dynamic interrelations. The mathematical techniques used in developing and analyzing ecological models have been treated in several books (e.g., Caswell et al. 1972; Smith 1974; Odum 1983; Jørgensen 1986; Beltrami 1987; Yodzis 1989; Shugart 1998) and are the focus of several ecological journals.

Dale (1970) enumerated four phases of ecosystem analysis:

1. Lexical phase—determining system entities or parts.
2. Parsing phase—choosing the types of relationships among the parts that are of interest.
3. Modeling phase—specifying the mechanisms by which these interrelationships take place.
4. Analysis phase—investigating the properties of the model so produced (including validation of the model of the ecosystem).

These can be used as a framework to discuss the broad topic of ecosystem modeling.

Lexical Phase

The determination of the parts of an ecosystem is often considered the simplest aspect of ecosystem studies involving modeling, but it often proves to be critical to later applications of models. The parts of an ecosystem can be classified taxonomically into categories such as individuals, populations, species, genera, etc. (Dale 1970). They can also be grouped according to structural criteria such as life-form criteria (e.g., trees, shrubs, grass) or functional criteria (herbivores, carnivores, decomposers).

Considerations in defining the parts of the system are involved with the objectives of a given study and the intent of other phases of the systems analysis process. A principal simplification for the mathematical models used in ecology involves ignoring sources of system heterogeneity. For example, models of population growth typically use the numbers of individuals in a population as a state variable and ignore the statistics of the ages and sexes in the population. This is done even in the face of commonsense intuition that the ages and sexes in a population should have important consequences on birth and death rates. Similarly, models of element cycles ignore the spatial heterogeneity that seems a dominant feature of terrestrial

TABLE 25.1. Descriptions of different types of models commonly used in ecosystem analysis.

Type of Model	Description
Conceptual models	Diagrams or descriptions of the important connections among the components of an ecosystem
Microcosms	Small (usually small enough to fit on a laboratory bench) physical and biological analogs to a larger ecosystem of interest
Population models	Usually systems of differential or difference equations that compute the change in the numbers of individuals in a population
Community models	Often of similar structure to population models but including terms that involve interactions with other populations
Compartment models	Usually systems of differential or difference equations that follow the transfer of elements, energy, or other material through an ecosystem
Multiple commodity models	Compartment models that treat the interactive transfers of several different materials through an ecosystem
Individual-based models	Models in which the dynamic changes in the individuals in an ecosystem are used as a basis to understand larger system dynamics

ecosystems. Food web models represent transfers of material as relative constant flows from one homogeneous compartment to another despite the nonhomogeneous distributions of prey and predators. One of the most important considerations in developing ecosystem models is what relationships will be emphasized in the parsing phase of the model development.

Parsing Phase

Science progresses by simplifying the systems under consideration. In experimental science, one attempts to simplify by controlling to as great a degree as possible, all extraneous factors with respect to a given experimental objective. Similarly, the formulation of a dynamic model is embedded with assumptions involving which factors can be left out of one's accounting of system dynamics. Models are simplifications of more complex realities. It can be surprising, the degree to which successful models of a wide range of ecological interactions assume unimportant aspects that one rationally might think otherwise. The central issue is often, "At what scale is it appropriate to leave a given process out of an ecosystem model?"

The factors to be considered in understanding how the parts of an ecosystem interact often include transfers of material or energy among the parts of the ecosystem. This emphasis is to some degree born of historical interests in ecosystem ecology. According to McIntosh (1985), a now famous paper, "The Trophic-Dynamic Aspect of Ecology," published posthumously by Raymond Lindeman in 1942, represents the birth of ecosystem ecology. Lindeman synthesized data on the biomass of different feeding or trophic levels from three lakes in Minnesota and characterized a lake in terms of the transfer of energy from one part of the system to another. One of Lindeman's principal contributions was to identify a fundamental dynamic process (energy flow) with which the seasonal trophic relations of animals could be integrated into the long-term process of community changes (Cook 1977).

Elements of Lindeman's work had been developed and discussed earlier (McIntosh 1985). The importance of energetics (Lotka 1925), the progressive removal of energy through the steps of a food chain on the basis of thermodynamics (Semper 1881; Petersen 1918), the lake as an interactive system (Forbes 1897; Thienemann 1918; Allee 1934) were all developed prior to Lindeman. The uniqueness of the Lindeman paper (1942) was a product of the creativity and theoretical richness of his work and of the timing of the publication. Even so, Lindeman's contribution was not extensively influential until the 1950s (Wiegert 1988). At that time, E.P. Odum (1953) produced an ecology textbook organized around the concepts of ecosystems and their structure and function. By the 1960s, there was an explosive development in ecosystem ecology (McIntosh 1985). Because of the central importance of understanding the trophic dynamics of ecosystems ("ecoenergetics"), Odum in 1968 could state, "*Ecoenergetics is the core of ecosystem analysis.*"

This historical emphasis in ecological energetics and, subsequently, the transfer of elements among ecosystem components has tended to dominate the

commodities used in ecosystem models. Initially, models were univariate (they considered the transfer of energy or nutrients but not both), but over time, multiple commodity models have become more prevalent.

Modeling Phase

There is a myriad of different mathematical approaches that have been applied to the formulation of ecological models. However, two related mathematical formulations are most often used to predict the change in the state variables of a system. In the first, the difference equation, the change in the state variable at a given time t (denoted Δx_t) over a fixed interval of time (Δt) is used to compute the new value of the state variable at the next time $t + \Delta t$ (denoted $x_{t+\Delta t}$). The resultant equations are of the form:

$$x_{t+\Delta t} = x_t + \Delta x_t \text{ or } \Delta x_t = x_{t+\Delta t} - x_t \quad (25.1)$$

The emphasis is on the quantitative value on the condition or state of each of the parts and on determining how these states change over time. The change in the quantitative measure of the parts is as change in a state variable represented by such an equation. This will be made more explicit in the examples that follow.

In a difference equation, the incremental change of the state variable can be measured over the interval Δt as:

$$\frac{\Delta x}{\Delta t} = \frac{x_{t+\Delta t} - x_t}{\Delta t} \quad (25.2)$$

If the interval of time (Δt) is made smaller until it approaches zero (denoted $t \rightarrow 0$), then the change in x over the time interval is the slope of x versus time at time t. This is denoted dx/dt and is the differential equation for the instantaneous change of x with time. Differential equations are the second mathematical formulation typically used to simulate changes in the state variables of a dynamic system.

Both difference and differential equations are deterministic. If one knows the values of the state variables of the system (and any external factors from outside the system that operate to change these state variables), then one can predict the future state of the system.

As a well-known example of an ecological application of a differential equation model, consider a simple population in a relatively unchanging environment. The state variable of interest is the population density of the population, N. In this simple case, one could predict the changes in the population by keeping track of the births and deaths of the individuals that make up the population over some time interval. One can represent the number of individuals in the population by a simple difference equation,

$$N_{t+\Delta t} = N_t + B_t - D_t \quad (25.3)$$

where $N_{t+\Delta t}$ is the population at time $t + \Delta t$, B_t is the number of individuals born between time t and time $t + \Delta t$, and D_t is the number of individuals dying between time t and time $t + \Delta t$.

If instead of the change of the population over an interval (Δt), we consider the rate at which the population is changing (the slope of the curve when one plots population change against time), the differential equation most frequently used to represent population change is:

$$\frac{dN}{dt} = (b - d)N \text{ or } \frac{dN}{dt} = rN \quad (25.4)$$

where b is the proportion of the population giving birth, d is the proportion of the population dying, and r is $(b - d)$ and is called the intrinsic rate of population increase.

The rate that the number of individuals are born into a population is a function of the size of the population (larger populations tend to have more births than small populations, etc.) and the simplest relationship that expresses this relation is to assume that the number of individuals born is a constant proportion of the population. A similar situation holds for the death of individuals over a time interval with a simple assumption being that the number dying is a constant proportion of the population.

This representation (Eq. 25.4) of change in populations has been know for quite some time. The increase in a population implied by Equation 25.5 over time can be solved analytically to obtain:

$$N_t = N_0 e^{rt} \quad (25.5)$$

where N_0 is the size of the population at time 0 and N_t is the size of the population at time t.

Recall that in Equation 25.4, the intrinsic rate of increase of the population r was defined as the dif-

ference in the birth rate constant and the death rate constant ($r = b - d$). This implies that the rate of population birth and death is a fixed proportion of the number of individuals in the population. As populations get large with respect to space or resources available to them, one would expect the proportion of individuals dying to increase due to such effects as stress, shortages of food or space, etc. One might also expect a depression in the proportion of females in the population giving birth to diminish for much the same reasons. These factors are termed density-dependent factors in that they are conditions that alter the rate of population growth as a function of the population density.

A Simple Population Model

A simple case of how the births and deaths in a population might be effected by density of the population would be to assume that the decrease in birth rate is a linear function of population density. A similar assumption could be made for the population death rate. The population growth as a function of time under these assumptions would be:

$$\frac{dN}{dt} = \{(b - b_{dd}N) - (d + d_{dd}N)\}N \quad (25.6)$$

where b is the proportion of the population giving birth, b_{dd} is the density related change in the proportion of the population giving birth, d is the proportion of the population dying, and d_{dd} is the density related change in the proportion of the population dying.

One can rearrange the terms of this equation to obtain:

$$\frac{dN}{dt} = \{(b - d) - (b_{dd} + d_{dd})N\}N \quad (25.7)$$

If the expression $b_{dd} + d_{dd}$ is replaced by a new expression so that:

$$b_{dd} + d_{dd} = \frac{r}{K}$$

Then the differential equation describing the change of the population becomes:

$$\frac{dN}{dt} = \left(r - \frac{r}{K}\right)N \text{ or} \quad (25.8)$$

$$\frac{dN}{dt} = rN\left(1 - \frac{1}{K}N\right) \quad (25.9)$$

Population ecologists refer to this equation as the logistic equation or the Verhulst-Pearl equation (Fig. 25.1). The dynamics of the equation are considerably different from the equation for the exponential increase of a population (Equations 25.4 and 25.5). A population behaving as described by the logistic equation will rise or fall to K over time (see Fig. 25.1). K is called the carrying capacity and is associated with concepts that are well ingrained in the vocabulary of population biology and wildlife management—so much so that it has taken to be a tangible property of a given habitat or location. For example, wildlife managers are involved with knowing the carrying capacity of a given area with regard to a deer herd or other managed animal population. The carrying capacity concept applied in wildlife biology is derived directly from the logistic equation (Equation 25.9). There are important limitations in the behavior of populations implied by the logistic equation. Important among these is that the expected condition of the population over time is an unchanging population at the carrying capacity (see Fig. 25.1).

This simple example illustrates several aspects that are found in other, more elaborate developments of ecological modeling. The lexical phase would involve the identification of the numbers of individuals in the population as the system's parts of interest and not considering sex ratios, individual maturity, age structure of the population, etc. as germaine to this particular modeling exercise. The parsing phase would identify population growth and limitations on growth as the phenomena of interest. The modeling phase would involve the specification of the r and K parameters in the models.

Compartment Models and Material Flow

Food chains and food webs initially emphasized the energy-related aspects of feeding relations in ecological systems. The understanding of transfers of energy in and out of plants and animals was (and is) an important topic for physiologists and physiological ecologists. There was an important cross-seeding of techniques from physiological researchers developed in the 1930s. These mathematical techniques were intended to quantify the dynamics of various substances moving through the vertebrate body (Shugart and O'Neill 1979). These systems-oriented methods evolved from laboratory

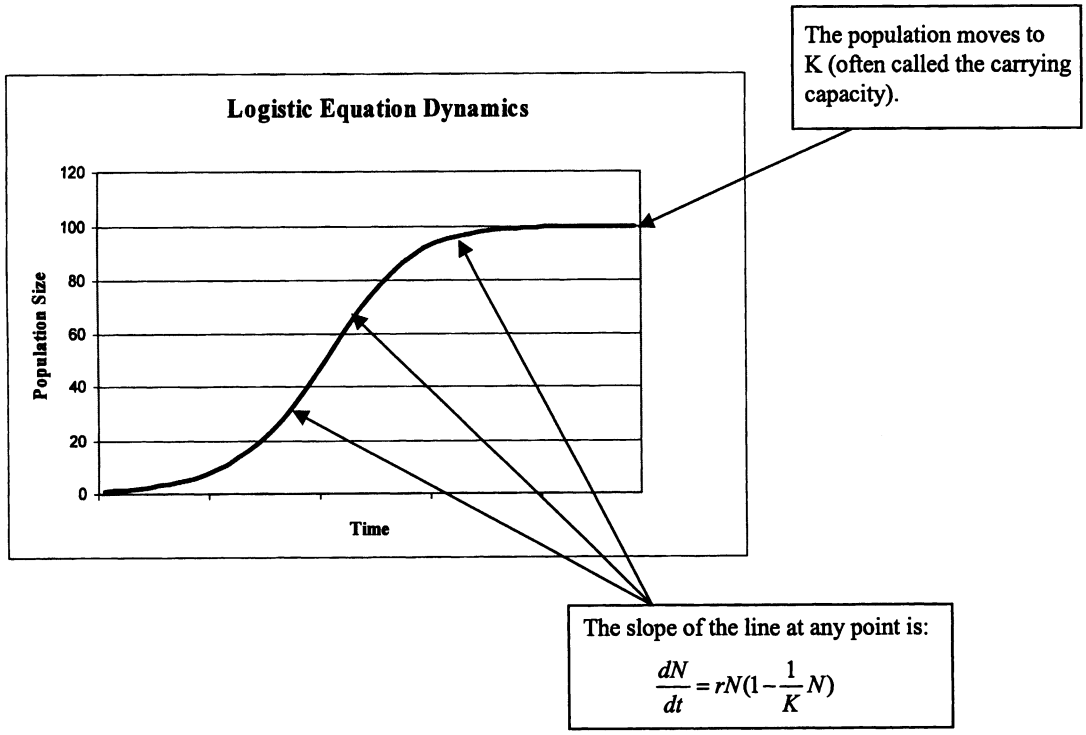

FIGURE 25.1. Dynamics of the logistic equation.

experiments involving following the movements of "tracers." Initially, these tracers were dyes. Radioisotope tracers were increasingly used following the "atomic-age" availability of isotopes for experimental purposes in the early 1950s. A typical tracer experiment might involve injecting a dye in an artery and noting the time required for the dye to reappear in an adjacent vein. The focus of such an experiment might be to estimate the rate of blood circulation. As the dye dilutes and is mixed through the entire body, one might also use the degree of dilution to estimate the total volume of blood.

A mathematical theory was developed for the tracer experiments (Teorell 1937; Zilversmit et al. 1943) that eventually became known as tracer kinetics or compartment modeling (Hearon 1953; Solomon 1949; Sheppard and Householder 1951). Mathematical aspects of this topic will be discussed in this chapter in the context of ecological modeling (also see Shugart and O'Neill [1979] for a compilation of classic examples). In tracer kinetics, the body is divided into a mutually exclusive set of "compartments" (e.g., blood, bone, liver, etc.). The change in the material in each component is related to changes in the other components as flows of material from one compartment to another. The analogy between this approach and conceptualizations of energy or nutrients flowing through the components of an ecosystem is the basis for a large body of ecological modeling.

At present, an area of great importance in ecosystem studies is determining the magnitudes and the controlling factors for ecosystem element cycles (or food webs). In such studies, the important parts of the ecosystem are represented as "compartments." The changes in compartments are the result of the fluxes of material out (to other compartments or out of the system) or in (from other compartments or from outside the system). The compartments are the state variables of the ecosystem. The changes in these state variables are each represented by one of the equations in an interacting set of differential equations.

The fluxes of materials from one compartment to another can, in some cases, be extremely difficult to measure. Often the fluxes are estimated using

procedures that amount to assuming that the materials going in and out of a compartment are equal. This is true when the amount of material in the compartment is constant. In other cases, fluxes are measured by assuming that rates of transfer noted in laboratory experiments or in small field experiments and applied to larger systems.

The formulation of element cycling compartment diagrams (or models) involves subtle, underlying assumptions about the constancy of ecosystems and the extrapolation of observations to larger spatial scales. For these reasons, ecosystems, such as watersheds, in which some of the fluxes can be measured directly have great scientific importance (Bormann and Likens 1979).

Formulation of Compartment Models for Ecosystem Studies

The usual application of compartment models in ecology involves the internal and external transfers of nutrients and energy in ecosystems. A straightforward introduction to these models is through the terms and procedures associated with estimating the parameters of the model. The fundamental unit of a compartment model is the single compartment and the associated flows of material or energy in and out of the compartment:

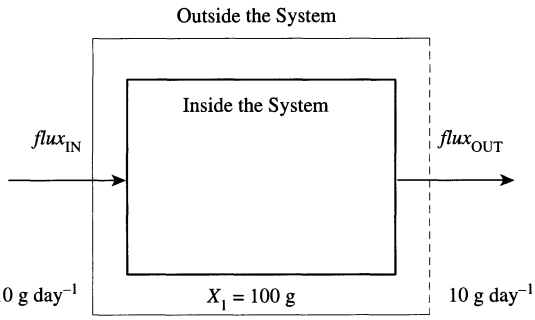

This representation is typical of that used in compartment modeling in general. In the case shown above, the compartment is in a state of equilibrium—the amount of material going in and out is the same. Thus, the amount of material in the compartment is not changing. The lack of change in the state of the system under these conditions is the origin of the term steady state. Also, the balance of inflows and outflows inspires the term equilibrium. In the usual case, the material flowing through the system is conserved (neither created nor destroyed in the process), and the two terms (equilibrium, steady state) describe an equivalent condition.

The compartment (X_1) contains 100 g of the material of interest. The flux into the example compartment from outside the system is 10 g day^{-1} and the flux from the compartment outside the system is also 10 g day^{-1}. Note that the dotted line defines what is considered to be inside and outside the system. This defines the system of interest and amounts to an ecosystem definition. A differential equation representing this compartment is:

$$\frac{dX_1}{dt} = \text{Flux}_{\text{in}} - \text{Flux}_{\text{out}} \qquad (25.10)$$

In simple compartment models, the loss from a compartment is taken to be a constant proportion of the amount of the material in the compartment and this proportion is called the transfer coefficient or the rate constant. It is important to point out the difference in the rate of change and the rate constant. The rate of change is dimensioned in units of material per unit time (in the example, g day^{-1}); the rate constant is dimensioned in units of time^{-1} (in the example, day^{-1}). In compartment model notation, form of the differential equation used to model material flows is:

$$\frac{dX_1}{dt} = f_1 - \lambda_{11}X_1 \qquad (25.11)$$

where f_1 is the input to compartment X_1 (g day^{-1}) from outside the system and λ_{11} is the rate constant for compartment X_1 losses (day^{-1})

Note that the input from outside the system is a rate of input dimensioned in g day^{-1} and the loss from compartment X_1 is the product of the contents of the compartment (g) and a rate constant (units of day^{-1}) and, thus, as a product is also dimensioned in g day^{-1}. The value of the rate constant in this equation can be calculated from the flux out of the system (10 g day^{-1}) and the equilibrium value of the compartment (100 g). Because $\lambda_{11}X_1$ = 10 g day^{-1} and X_1 = 100 g, then λ_{11} = 10 g day^{-1}/X_1 = 10 g day^{-1}/100 g = 0.1 day^{-1}.

Even a simple system (such as the one described in Equation 25.10) provides some useful concepts for understanding the flow of materials through a

system. One important measure is the time constant (or turnover time)—the time needed for the amount of material flowing through the compartment at equilibrium to equal the amount of material in the compartment. The time constant is often denoted with T (for an entire system) or T_i (for the i^{th} compartment in a system).

Complexity in a compartment model arises in the linking together of compartments representing parts of the system. A simple case, the linking two compartments, might be represented as:

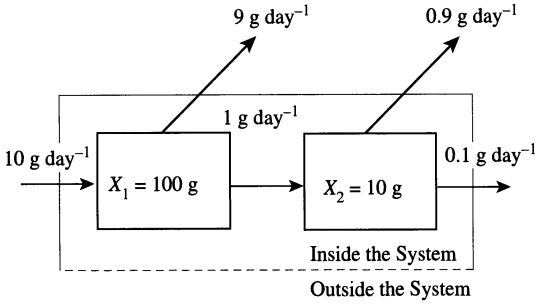

With the corresponding pair of differential equations being:

$$\frac{dX_1}{dt} = f_1 - \lambda_{11}X_1 \qquad (25.12)$$

$$\frac{dX_2}{dt} = \lambda_{12}X_1 - \lambda_{22}X_2 \qquad (25.13)$$

where f_1 is the input to compartment X_1 (g day^{-1}) from outside the system or the forcing to compartment X_1, λ_{11} is the rate constant for compartment X_1 losses (day^{-1}), λ_{12} is the rate constant for the transfer of material from X_1 to X_2 (day^{-1}), and λ_{22} is the rate constant for compartment X_2 losses (day^{-1}).

As an example of the dynamics associated with compartment model representation of ecosystems, consider the classic study of the energy flow in the Silver Springs ecosystem developed by Odum (1955). In this study, the transfers of energy in a spring in Florida were quantified with respect to the amounts of energy in different parts of the system (compartments) and the flows of energy into, within, and out of the system. The pattern of energy flow is shown as a compartment model in Figure 25.2.[1] The system of differential equations representing the fluxes of energy flow is:

$$\frac{dX_1}{dt} = f_1 - \lambda_{11}X_1 \qquad (25.14)$$

$$\frac{dX_2}{dt} = f_2 + \lambda_{12}X_1 - \lambda_{22}X_2 \qquad (25.15)$$

$$\frac{dX_3}{dt} = \lambda_{23}X_2 - \lambda_{33}X_3 \qquad (25.16)$$

$$\frac{dX_4}{dt} = \lambda_{34}X_3 - \lambda_{44}X_4 \qquad (25.17)$$

$$\frac{dX_5}{dt} = \lambda_{15}X_1 + \lambda_{25}X_2 + \lambda_{35}X_3 + \lambda_{45}X_4 - \lambda_{55}X_5 \qquad (25.18)$$

where f_i is the input to compartment X_i (kcal m^{-2} yr^{-1}) from outside the system and λ_{ii} is the rate constant for compartment X_i losses (yr^{-1}). When i $\neq$ j: λ_{ij} is the rate constant for the transfer of energy from X_i to X_j (yr^{-1}).

The notation used allows the rate constants to be expressed as a matrix. Using the notation $dX_i/dt = \dot{X}_i$, the system of equations can be expressed in matrix form as:

$$\begin{bmatrix}\dot{X}_1\\ \dot{X}_2\\ \dot{X}_3\\ \dot{X}_4\\ \dot{X}_5\end{bmatrix} = \begin{bmatrix}\lambda_{11} & 0 & 0 & 0 & 0\\ \lambda_{12} & \lambda_{22} & 0 & 0 & 0\\ 0 & \lambda_{23} & \lambda_{33} & 0 & 0\\ 0 & 0 & \lambda_{34} & \lambda_{44} & 0\\ \lambda_{15} & \lambda_{25} & \lambda_{35} & \lambda_{45} & \lambda_{55}\end{bmatrix}\begin{bmatrix}X_1\\ X_2\\ X_3\\ X_4\\ X_5\end{bmatrix} + \begin{bmatrix}f_1\\ f_2\\ 0\\ 0\\ 0\end{bmatrix} \qquad (25.19)$$

or using the values for rate constants calculated from the information from Figure 25.2:

$$\begin{bmatrix}\dot{X}_1\\ \dot{X}_2\\ \dot{X}_3\\ \dot{X}_4\\ \dot{X}_5\end{bmatrix} = \begin{bmatrix}-6.08 & 0 & 0 & 0 & 0\\ 1.01 & -15.81 & 0 & 0 & 0\\ 0 & 1.79 & -6.19 & 0 & 0\\ 0 & 0 & .33 & -2.11 & 0\\ .84 & 5.14 & .74 & .66 & -191.58\end{bmatrix} \cdot \begin{bmatrix}X_1\\ X_2\\ X_3\\ X_4\\ X_5\end{bmatrix} + \begin{bmatrix}20810\\ 486\\ 0\\ 0\\ 0\end{bmatrix} \qquad (25.20)$$

In the matrix representation of the model, the empty

[1]Note that in Figure 25.2 and the text that follows, kilocalories are used to conform to the original paper; 1 kilocalorie = 4184 Joules.

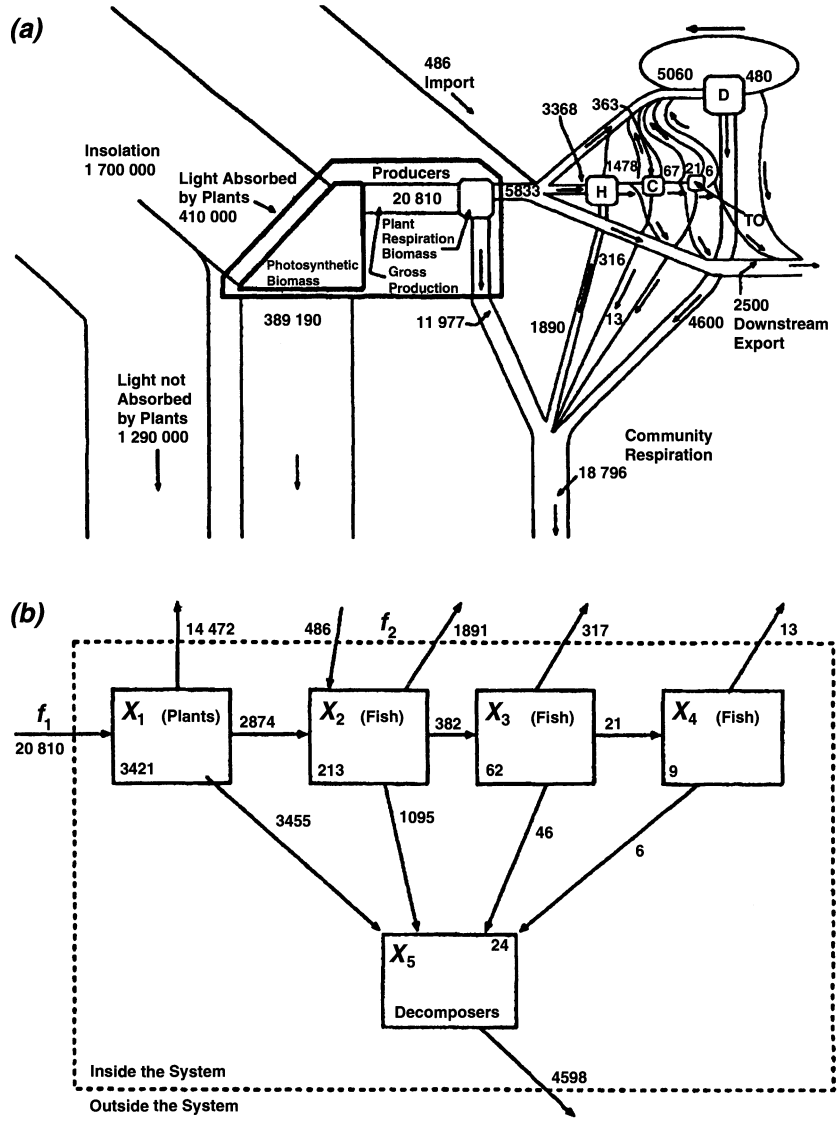

FIGURE 25.2. Energy flow in a clear spring in Florida as represented by Odum (1955). A, Flows of energy in the spring as represented from Odum (1955). B, Compartment model of energy flow in the system. Values in the compartments represent the steady state or equilibrium values of energy in each compartment determined by Odum in units of kcal m^{-2}; values beside each arrow represent the fluxes of energy in the systems (kcal m^{-2} yr^{-1}). Numerical values follow Patten's (1971) computation of energy fluxes based on the original Odum (1955) paper.

or zero entries in the rate constant matrix make up what is referred to as the structure of the model.

Commonly, compartment models are solved by using numerical techniques on a digital computer. Numerical methods for solving the differential equations representing the material or energy flows in a compartment model involve determining the values of the derivative at some starting point. These derivatives are then applied to determine an approximate value for the state variables a short interval later, recalculating the derivatives at this new point in time, and approximating the state variables over the next short interval. There are several methods for correcting for inaccuracies in this ap-

proximation and to vary the calculation interval to optimize computational speed to solve the appropriate and desired accuracy of approximation (see Patten 1971; Beltrami 1987).

Figure 25.3 illustrates the dynamic response of the Silver Springs model in Equation 20.20 under several diagnostic conditions. Figure 3A shows what is termed the forced response of the system. In this case, the dynamics of the system is determined for a case in which the initial values or initial conditions of the compartments are all set to zero. The inputs of the system or forcings are set to their normal values. The dynamics that are shown are analogous to a case in which the material (or energy) going into a system is labeled in some way from a particular time onward and the dynamics of this new, labeled material as it replaces the old, unlabeled material is followed.

Figure 25.3B illustrates the free response of the Silver Springs model. In this case, the compartment state variables begin the simulation with the values that one would expect them to have at equilibrium, and the input terms in the equations are set to zero. The dynamics are analogous to those expected if all material in the system were labeled and the rate at which this labeled material was flushed out of the system is equaled by the input of new, unlabeled material. Figure 25.3C is the impulse response of the system. This response has its analog in a rapid injection of labeled material into an otherwise unlabeled system.

Compartment models are appealing for ecological studies for several reasons. First, they are mathematically tractable. The procedures for estimating the parameters for such models are well developed in several fields (applied mathematics, physics, engineering). Historically, these invited procedures were transferred to ecosystem studies. Compartment models also appeared to predict certain aspects of ecological systems, particularly the movement of radioactive materials through a variety of aquatic and terrestrial ecosystems. The development of the atomic bomb, nuclear industry and concern about radioactive pollution inspired considerable interest in the movement of radioisotopes through ecosystems. The experimental (and in some cases, accidental) application of isotopes to laboratory and field systems ("radioecology") was an important aspect of ecology in the 1950s and 1960s. For materials such as radioisotopes and trace substances of various kinds, compartment models have proven to have reasonable predictive ability (given an appropriate parameterization).

Analysis Phase

The analysis phase of ecosystem modeling tends to focus on two questions:

1. How credible is the model as a representation of the ecosystem? This leads to issues of model validation.
2. What do features of the models tell us about the real system? This leads to considerations of the theoretical implications of formal analyses of the models and to application of the models to predict changes in the system under novel and/or future conditions.

The complexity of these considerations can be great, but it is worthwhile to identify some of the key issues.

Model Validation

In determining model credibility, Mankin et al. (1977) and Shugart (1984) divided model testing into two basic types of procedures (verification and validation) and saw model application as a measure of a model's usefulness. In verifying a model, the model is tested on whether it can be made consistent with some set of observations. In validation procedures, a model is tested on its agreement with a set of observations independent of those observations used to structure the model and estimate its parameters. When testing a model, it can be important that it can simulate ecosystem change under the constraint that all parameters in the model are realistic (Shugart 1984).

Sensitivity Analysis

The basic aim of sensitivity analysis is to document the pattern of variation in the state variables or system responses to small changes in the model parameters. The usual objective of sensitivity analysis is to determine which parameters in a model are "important" with respect to developing better measurements. Sensitivity analysis also provides insights into theories on system structure and control

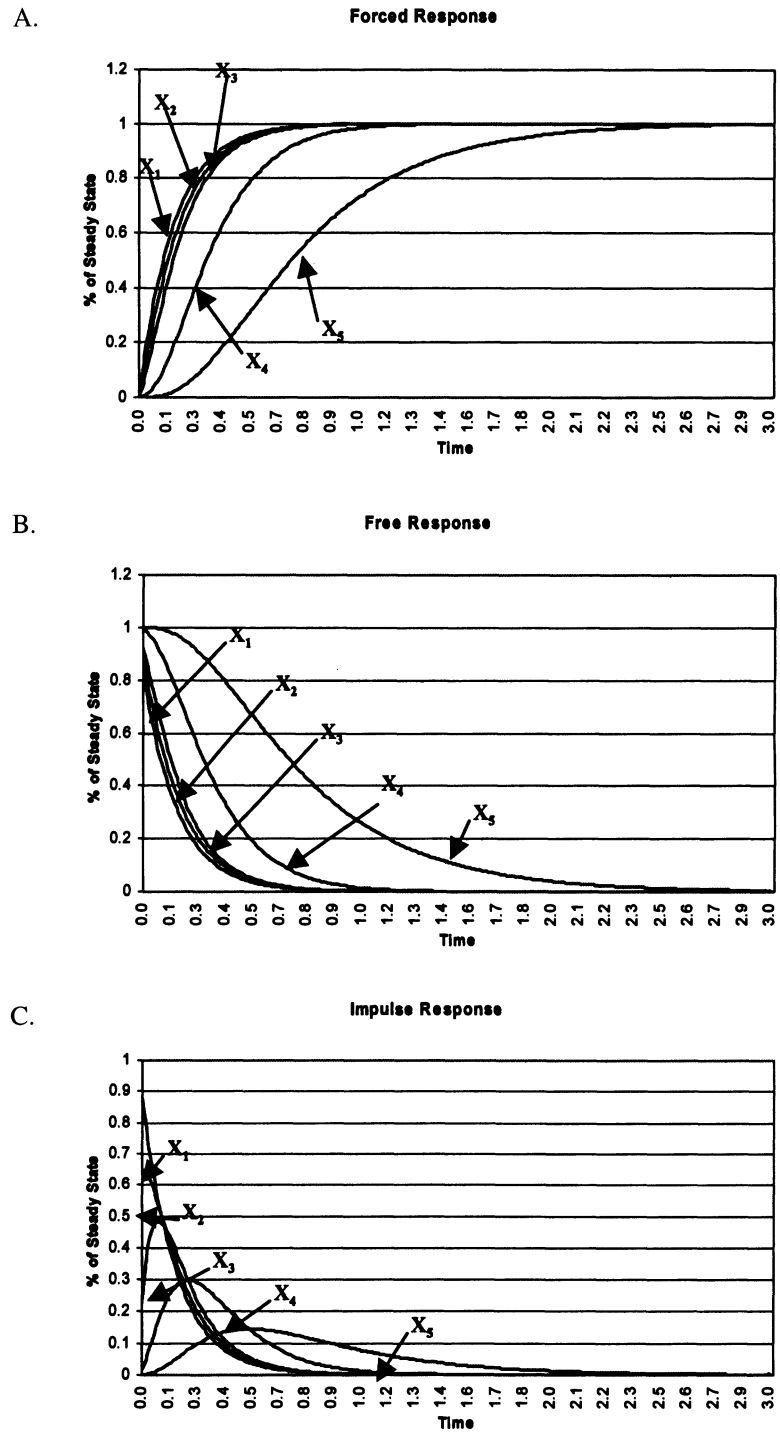

FIGURE 25.3. Dynamic responses of the Silver Springs, FL, compartment model. A, Forced response; B, free response; C, impulse response.

of system behavior. The basic concept of determining how a system changes in response to changes in the parameters is intuitively appealing. It mimics the sort of experimental manipulations that one would like to be able to perform to better understand how a system works.

Stability Analysis

The fundamental concern in analyzing the stability of a system is the long-term response of the system to an external change or a perturbation. Clearly, this is a topic of interest in considering the response of ecosystems to changes in the environment. There are two rather different mathematical traditions and associated methods for determining stability of dynamic systems. The first is appropriate only for linear systems and originates from some of the greats of physics and mathematics (Newton, Euler, Laplace, Lagrange, Maxwell). The second applies to linear and nonlinear systems and was the doctoral dissertation of a Russian mathematician, A.M. Lyapunov (Timothy and Bona 1968).

Linear stability analyses is involved with the response of the system to perturbations or changes in inputs. In linear systems, a system is stable if its response to an impulse function approaches zero as time approaches infinity (DiSephano et al. 1967). There are a number of methods that can be used to determine the stability of linear systems. Linear compartment models in which the material being transferred from one compartment to another are conserved and are stable because the structure of the matrix of parameters for the models.

One method that has been applied in several ecosystems to determine stability of systems is the procedure known as "loop analysis" (Levins 1974; Yodzis 1989). Loop analysis is derived from criteria for determining the stability of linear systems called the Routh-Hurwitz criteria (Timothy and Bona 1968). The appealing aspect of loop analysis is that it allows one to determine from the structure of interactions whether a linear system will be unstable. This finding is independent of the particular parameter values (other than their signs) that are involved. One cannot use the analysis to prove that a system is stable (which can depend on the magnitudes as well as the signs of the parameters). Applications of loop analysis to nonlinear systems are usually couched on the assumption that the system behaves in a linear manner, at least under the conditions being considered.

The second approach to the problem of systems stability was that of A.M. Lyapunov. In this case, stability concepts could be applied to nonlinear (as well as linear) systems. Lyapunov recognized two sorts of stability. The first sort of stability in a Lyapunov sense concerned whether or not the systems would return to the vicinity its former state following a small perturbation. In a system that is stable, any (small) perturbation on a system within ε of the state of the system at some time (t_0) produces a response from the system ($x_{r(t)}$) that is bounded within a distance δ of the unperturbed response ($x_{(t)}$) of the system. In a system that is asymptotically stable, the difference between the perturbed system dynamic and the unperturbed system dynamic goes to zero after a sufficiently long time.

Future Directions: Multiple Commodity Models and Individual-Based Models

In a field as creative as ecosystem modeling, it is sometimes difficult to predict future directions of development. Two areas that seem to be developing both theoretical and practical innovations are both products of increased computational power. These are complex models simulating multiple commodities (light, water, nutrients) and models that simulate ecosystem structural change by simulating each individual of the dominant organisms in the community.

Multiple Commodity Models

Multiple commodity models are a logical outgrowth of compartment models described above. The models used in ecosystem studies often have similar internal assumptions that are a part of the rationale for scaling the models to larger space and longer time scales. These assumptions are also a basis for the organization of available data on ecosystem performance into dynamic models. Important among these assumptions are:

1. *Generality:* The concept that ecosystems function in accordance to some overarching rules that control structure and/or function. Examples

might be the relation between ecosystem productivity and climatic indices (Rosenzweig 1968; Leith 1975; Box 1978), or the regularities in decomposition rates across ecosystems (Meentemeyer 1978).

2. *Optimality:* The concept that processes in ecosystems will (over time) tend to optimize (or, in some cases, maximize) such attributes as leaf area index, net primary productivity, or internal energy fluxes. Two frequently invoked principles are *limiting or critical factors*—the concept that a particular internal variable, such as soil nitrogen or canopy water flux, is the keystone factor controlling the fluxes and changes in the terrestrial ecosystems, and *stoichiometry*—the concept that physical and chemical processes in ecosystems will tend to maintain certain ratios in the concentrations of critical nutrient elements, carbon and water.
3. *Equilibrium seeking:* The assumption, either built into the model formulations or used to estimate model parameters, that ecosystems seek an equilibrium. Models based on conservation of mass, energy, etc. maintain balances of input and outputs, and lead naturally to an assumption of equilibrium-seeking behavior.

Many of this class of models "scale-up" the response of processes as they are understood at the smaller scale to the landscape- or regional-system response. For example, one might assume that the fluxes of heat, water, and carbon dioxide (CO_2) associated with the functioning of a single leaf are duplicated by the sum of the responses of the billions of individual leaves comprising a vegetated landscape. In some cases, the underlying assumption of homogeneous landscape models is that the mathematical structure of particularly biophysical and chemical reactions at the landscape level resemble those observed at a detailed level (perhaps with some differences in the model parameters). These models are usually the type of ecological models linked to other models of ocean or atmospheric dynamics to assess the feedbacks among these major Earth systems (Ojima 1992).

There is a rich array of models of this class. For example, most models of element cycling in watersheds or other ecosystems tend to view the processes as being homogeneous within the system of definition. Indeed, traditional ecosystem models were often referred to as point models because they simulated the dynamics of ecosystems with no explicit references to spatial heterogeneity. Two types of these models that have been widely applied in the context of changing environmental conditions are those that simulate a regional plant canopy and those that are focused on the storage and transfer of material.

Canopy Process Models

Plant physiologists have made considerable progress in understanding the dynamic response of individual leaves to their environment. Much of this work was initially developed looking at the response of leaves (over minutes or seconds) in small chambers in which the temperature, vapor pressure deficit and other important variables for understanding leaf function were measured and/or controlled. Canopy process models (e.g., Running and Coughlan 1988) simulate the flux of CO_2 and water from plant canopies over time scales of seconds to a day. In general, these models are extensions of leaf-level models of photosynthesis (e.g., Farquhar et al. 1980) and transpiration (e.g., Penman 1948; Monteith 1972) applied to whole canopies. The models do not consider individual plants, but view the canopy as a single, multilayer unit with a fixed structure (i.e., leaf area). Photosynthesis and transpiration are simulated by estimating microclimatic variation and stomatal conductance for the canopy (or canopy layers).

Material Transfer Models

One "standard" ecosystem model is the compartment model of the transfer of material or energy into an ecosystem, through the components of an ecosystem and, eventually, out of the ecosystem. More complex, often nonlinear material transfer models were developed during the International Biological Program (IBP) in the early 1970s. The IBP models were a heterogeneous collection of models and modeling approaches that emphasized understanding natural productivity. Many of these models have evolved toward present day applications. An example is the CENTURY model, which was developed as a soil-process-related section of the IBP Grassland Biome ELM model (Parton 1978). The CENTURY model (Parton et al. 1987) was developed to simulate soil organic matter dy-

namics and plant production in grazed grasslands and agroecosystems. The CENTURY model simulates the dynamics of carbon (C), nitrogen (N), and phosphorus (P) in soil–plant systems using monthly time steps. The input data required for the model include soil texture, monthly precipitation, maximum and minimum air temperatures, and plant lignin content. By the late 1980s, the CENTURY model had been used to simulate regional patterns of soil C, N, and P and plant production for the U.S. central grasslands region and the impact of management practices on agroecosystems (Parton et al. 1987, 1988).

Combined Models of Change in Structure and Material Flow

Recently, models that combine the biophysical understanding found in canopy process models with the transport of matter associated with material transport models have come to the fore in studies of large-scale environmental change. For example, the Forest-BGC model (Running and Coghlan 1988; Running and Nemani 1988; Running et al. 1989) for hydrology and plant canopy function has been melded to an individual-tree-based forest model to provide a capability to simulate the change in forest structure over time (Friend et al. 1993). The resultant model, HYBRID, also uses a more detailed photosynthesis model, PGEN (Friend 1991), to improve the representation of mechanisms for photosynthesis production and allocation. As another example, the DOLY model (Woodward et al. 1995) is a global scale terrestrial model that combines predicting primary productivity and the phytogeographical problem of predicting leaf area across continents. The model has features associated with canopy process models, such as a model representation of the bulk biochemical features of photosynthesis, the dependence of CO_2 exchange, temperature and moisture changes on the stomatal conductance, and the role of canopy conductance on evapotranspiration and soil water losses. The involvement of N with the photosynthesis process and the dynamics of the uptake and allocation of N is also simulated. The model can be used to simulate the global distributions of leaf areas and net primary productivity under present and altered climates.

Individual-Based Models

In the past two decades or so, a broad range of ecologists (animal behaviorists, population biologists, community and ecosystems ecologists) has independently created a diverse array of individual-based models (Huston et al. 1988). The catalyst for this development was undoubtedly the increased availability and power of digital computers—the necessary tools to solve most of these models. The earliest such models were developed by population ecologists (Holling 1961, 1964; Rohlf and Davenport 1969) interested in incorporating animal behavior into population models and foresters interested relating tree growth to forest yield. The dynamics of populations when represented by individual-based models can differ significantly from an equivalent state-variable representation of the same system (Lomnicki 1988; Huston et al. 1988; DeAngelis and Gross 1992).

Increasingly, models that simulate the dynamics of ecological systems by accounting for changes in each of a large number of individuals in the system have been developed and applied in population and ecosystems ecology (Huston et al. 1988; DeAngelis and Gross 1992). Huston et al. (1988) point out that one advantage of such models is that two implicit assumptions associated with the more traditional state-variable approach used in ecological modeling populations are not necessary. These are the assumptions that (1) the unique features of individuals are sufficiently unimportant to the degree that individuals are assumed to be identical, and (2) the population is "perfectly mixed" so that there are no local spatial interactions of any important magnitude. Most ecologists are interested in variation in individuals (a basis for the theory of evolution and a frequently measured aspect of plants and animals) and appreciate spatial variation as being quite important.

These assumptions seem particularly inappropriate for trees, which are sessile and which vary greatly in size over their life span. This may be one of the reasons that tree-based forest models are among the earliest and most widely elaborated of this genre of models. The effects of spatial pattern have been well known from practical experience in agronomy and forestry for some time. In many agricultural (and forestry) experiments, the determination of spacing of plants has a profound effect on

the thinning response and the size of the individuals in a crop.

Among the earliest individual-based models in ecology were models of forests based on the growth of the individual trees that comprise the forest stand. These models were developed by quantitatively oriented foresters and were focused from their inception toward practical issues in production forestry.

An important subcategory of individual-organism-based tree models that have been widely used in ecological (as opposed to traditional forestry applications) are the so-called "gap" models (Shugart and West 1980). The first such model was the JABOWA model (Botkin et al. 1972; Botkin 1993) developed for forests in New England. Several gap models for a wide range of forests (and eventually, grasslands and savannas) were subsequently developed (Shugart, et al. 1992; Urban and Shugart 1992) for a wide range of locations. The earlier versions were developed with an interest in using models for interecosystems comparison (Shugart 1984) and adhered relatively closely to the JABOWA formulation. More recent models have diverged, particularly in the addition of spatial competition among trees, a range of modifications to allow simulation of a wider range of environmental conditions, and additional biological and/or physiological mechanisms.

Conclusions

Ecosystem modeling has been treated in this chapter with an emphasis on the historical roots of the topic and with simple familiar examples of some of the more common approaches the model development. Ecology has become increasingly quantitative over its recent history, and this has lead to a "trendy" exploration of a wide array of mathematical approaches in ecological studies. It is important to realize that the fundamental issues in ecological modeling go to issues of determining what are the logical parts of the ecosystem, knowing how these parts significantly interact, and using this information to posit theories about the nature of ecosystems. The mathematics is in support of these larger and essentially scientific objectives.

The principal examples used in this presentation have been differential equations used to model the interactions of a population or the movement of materials through ecosystems. These examples were chosen to both demonstrate the dynamics of these interactions and to illustrate development or analysis of a dynamic model. This chapter was intended to provide an introduction to some of the considerations in developing ecological models. The treatment of many important topics in the area of ecological modeling has been intentionally brief. There are several texts on the topics of systems and mathematical approaches in ecology, and several of these are noted as citations in the text.

References

Allee, W.C. Concerning the organization of marine coastal communities. Ecol. Monogr. 5:541–554; 1934.

Beltrami, E. *Mathematics for Dynamic Modeling.* Orlando, FL: Academic; 1987.

Bormann, F.H.; Likens, G.E. *Pattern and Process in a Forested Ecosystem.* New York: Springer-Verlag; 1979.

Botkin, D.B. *Forest Dynamics: An Ecological Model.* Oxford: Oxford Univ. Pr.; 1993.

Botkin, D.B.; Janak, J.F.; Wallis, J.R. Some ecological consequences of a computer model of forest growth. J. Ecol. 60:849–872; 1972.

Box, E.O. Geographical dimensions of terrestrial net and gross primary productivity. Radiat. Environ. Biophys. 15:305–322; 1978.

Caswell, H.; Koenig, H.E.; Resh, J.A.; Ross, Q.E. An introduction to systems science for ecologists. In: Patten, B.C., ed. *Systems Analysis and Simulation in Ecology.* Vol. II. New York: Academic; 1972:3–80.

Cook, R.E. Raymond Lindeman and the trophic-dynamic concept in ecology. Science 198:109–122; 1977.

Dale, M.B. Systems analysis and ecology. Ecology 51:2–16; 1970.

DeAngelis, D.L.; Gross, L.J., eds. *Individual-Based Models and Approaches in Ecology: Populations, Communities and Ecosystems.* New York: Chapman and Hall; 1992.

DiStefano, J.J., III, Stubberud, A.R.; Williams, I.J. *Schaum's Outline of Theory and Problems of Feedback and Control Systems.* New York: McGraw-Hill; 1967.

Farquhar, G.D.; von Caemmerer, S.; Berry, J.A. A biochemical model of photosynthetic CO_2 fixation in leaves of C3 species. Planta 149:78–90; 1980.

Friend, A.D. Use of a model of photosynthesis and leaf microenvironment to predict optimal stomatal conductance and leaf nitrogen partitioning. Plant Cell Environ. 14:895–905; 1991.

Friend, A.D.; Shugart, H.H.; Running, S.W. A physiology-based model of forest dynamics. Ecology 74:792–797; 1993.

Hearon, K.Z. The kinetics of linear systems with special reference to periodic reactions. Bull. Math. Biophys. 15:121–141; 1953.

Holling, C.S. Principles of insect predation. Annu. Rev. Entomol. 6:163–182; 1961.

Holling, C.S. The analysis of complex population processes. Can. Entomol. 96:335–347; 1964.

Huston, M.; DeAngelis, D.L.; Post, W.M. New computer models unify ecological theory. BioScience 38:682–691; 1988.

Jørgensen, S.E. *Fundamentals of Ecological Modeling.* Amsterdam; Elsevier; 1986.

Levins, R. The quantitative analysis of partially specified systems. Ann. N.Y. Acad. Sci. 231:123–138; 1974.

Lieth, H. Modeling the primary productivity of the world (pp. 237–263). In: Leith, H.; Whittaker, R.H., eds. *Primary Productivity of the Biosphere.* New York: Springer-Verlag; 1975:237–263.

Lindeman, R.L. The trophic-dynamic aspect of ecology. Ecology 23:399–418.

Lomnicki, A. *Population Ecology of Individuals.* Princeton, NJ: Princeton Univ. Pr.; 1988.

Mankin, J.B.; O'Neill, R.V.; Shugart, H.H.; Rust, B.W. The importance of validation in ecosystem analysis. In: Innis, G.S., ed. *New Directions in the Analysis of Ecological Systems. Part I.* LaJolla, CA: Simulation Councils of America, 1977:63–71.

McIntosh, R.P. *The Background of Ecology: Concept and Theory.* Cambridge: Cambridge Univ. Pr.; 1985.

Meentenmeyer, V. Macroclimate and lignin control of litter decomposition rates. Ecology 59:465–472; 1978.

Montieth, J.L. Solar radiation and productivity in tropical ecosystems. J. Appl. Ecol. 9:747–766; 1972.

Odum, E.P. *Fundamentals of Ecology.* Philadelphia: Saunders; 1953.

Odum, E.P. Energy flow in ecosystems: A historical review. Am. Zool. 8:11–18; 1968.

Odum, H.T. Trophic structure and productivity of Silver Springs, Florida. Ecol. Monogr. 27:55–112; 1955.

Odum, H.T. *Systems Ecology.* New York: Wiley; 1983.

Ojima, D., ed. *Modeling the Earth System.* Boulder, CO: UCAR/Office for Interdisciplinary Earth Studies; 1992.

Parton, W.J. Abiotic section of ELM. In: Innis, G.S., ed. *Grassland Simulation Model.* Ecological Studies 26. New York: Springer-Verlag; 1978:31–53.

Parton, W.J.; Schimel, D.S.; Cole, C.V.; Ojima, D. Analysis of factors controlling soil organic levels of grasslands of the Great Plains. Soil Sci. Soc. Am. J. 51:1173–1179; 1987.

Parton, W.J., Stewart, J.W.B.; and Cole, C.V. Dynamics of C, N, P and S in grassland soils: A model. Biogeochemistry 5:109–131; 1988.

Patten, B.C. A primer for ecological modeling and simulation with analog and digital computers. In: Patten, B.C.; ed. *Systems Analysis and Simulation in Ecology.* Vol. I. New York: Academic; 1971:4–121.

Penman, H.L. Natural evaporation from open water, soil and grass. Proc. R. Soc. Lond. A 193:120–145; 1948.

Petersen, C.G.J. *The Sea Bottom and Its Production of Fish Food.* Reports of the Danish Biological Station. No. 25. 1918:1–62.

Rohlf, F.J.; Davenport, D. Simulation of simple models of animal behavior with a digital computer. J. Theor. Biol. 23:400–424; 1969.

Rosenzweig, M.L. Net primary productivity of terrestrial communities: Prediction from climatological data. Am. Nat. 102:67–74; 1968.

Running, S.W.; Coughlan, J.C. A general model of forest ecosystem processes for regional applications I. Hydrological balance, canopy gas exchange and primary production processes. Ecol. Model. 42:125–154; 1988.

Running, S.W.; Nemani, R.R. 1988. Relating seasonal patterns of the AVHRR vegetation index to simulated photosynthesis and transpiration of forests in different climates. Remote Sens. Environ. 24:347–367; 1988.

Running, S.W.; Nemani, R.R.; Peterson, D.L.; Band, L.E.; Potts, D.F.; Peirce, L.L.; Spanner, M.A. Mapping regional forest evapotranspiration and photosynthesis by coupling satellite data with ecosystem simulation. Ecology 70:1090–1101; 1989.

Semper, K. *Animal Life as Affected by the Natural Conditions of Existence.* New York: Appleton; 1881.

Sheppard, C.W.; Householder, A.S. The mathematical basis of the interpretation of tracer experiments in closed, steady-state systems. J. Appl. Phys. 22:510–520; 1951.

Shugart, H.H. *A Theory of Forest Dynamics: The Ecological Implications of Forest Succession Models.* New York: Springer-Verlag; 1984.

Shugart, H.H.; *Terrestrial Ecosystems in Changing Environments.* Cambridge: Cambridge Univ. Pr.; 1998.

Shugart, H.H.; O'Neill, R.V., eds. *Systems Ecology.* Stroudsburg, PA: Dowden, Hutchinson and Ross; 1979.

Shugart, H.H.; Smith, T.M.; Post, W.M. The application of individual-based simulation models for assessing the effects of global change. Annu. Rev. Ecol. Syst. 23:15–38; 1992.

Shugart, H.H.; West, D.C. Forest succession models. BioScience 30:308–313; 1980.

Smith, J.M. *Models in Ecology.* Cambridge: Cambridge Univ. Pr.; 1974.

Solomon, A.K. Equations for tracer experiments. J. Clin. Invest. 28:1297–1307; 1949.

Teorell, T. Kinetics of distribution of substances administered to the body. Arch. Int. Pharmacodyn. 57:205–240; 1937.

Thienemann, A. *Lebengemeinschaft und Lebensraum.* Naturwissenshaft Wocheschrift, N.F. 17:282–290; 297–303; 1918.

Timothy, L.K.; Bona, E. *State Space Analysis: An Introduction.* New York: McGraw-Hill; 1968.

Urban, D.L.; Shugart, H.H. Individual-based models of forest succession. In: Glenn-Lewin, D.C.; Peet, R.K.; Veblen, T.T., eds. *Plant Succession: Theory and Prediction.* London: Chapman and Hall; 1992:249–293.

Wiegert, R.G. The past, present and future of ecological energetics. In: Pomeroy, L.R.; Alberts, J.J., eds. *Concepts of Ecosystem Ecology.* New York: Springer-Verlag; 1988:29–56.

Woodward, F.I.; Smith, T.M.; Emanuel, W.R. A global land primary productivity and phytogeography model. Global Biogeochem. Cycl. 9:471–490; 1995.

Yodzis, P. *Introduction to Theoretical Ecology.* New York: Harper and Row; 1989.

Zilversmit, D.B.; Entenmann, C.; Fishler, M.C. On the calculation of turnover time and turnover rate from experiments involving the use of labeling agents. J. Gen. Physiol. 26:325–331; 1943.

26

Stoichiometric Analysis of Pelagic Ecosystems: The Biogeochemistry of Planktonic Food Webs

James J. Elser

Introduction

For a pelagic ecosystem scientist in the field, whether in a 40-m oceanographic research vessel cruising the central Pacific or in an inflatable dinghy bobbing in a Minnesota kettle lake, the objects of interest are underneath and out of sight. In this way it might be said that pelagic ecology has more in common with soil ecology than soil ecology has with aboveground ecology. Whether or not this is true might be judged by comparison of various contributions to this volume. In any case, because direct observation is infrequent for both pelagic and soil ecologists, the major players and the processes that connect them are sometimes largely abstractions in ecosystem approaches to pelagic and soil systems. Perhaps because pelagic systems enforce abstraction, many of ecology's most influential concepts and theories, such as the trophic dynamics concept (Lindeman 1942), resource ratio competition theory (Tilman 1982), the trophic cascade (Carpenter et al. 1985), and the multidimensional niche (Hutchinson 1961), have their roots in the water. Indeed, a dominant concept in ecosystem science is that of the watershed, often with a lake at its terminus (Likens 1985). Our current understanding of the general patterns in the distribution and dynamics of organisms and of physical and chemical conditions in the subsurface pelagic world has been hard-won and obtained via a combination of hard work and technical advancement.

In this chapter, I describe some new aspects of the interrelationships between physical, chemical, and biological factors influencing pelagic ecosystem function, with a primary emphasis on food web dynamics and nutrient cycling. This involves a central focus on individual organisms in pelagic ecosystems, the microscopic and potentially enigmatic plankton, and how the interplay between ecosystem conditions and the physiological requirements of the plankton influences ecological dynamics. My emphasis is on a synthesis of a suite of new observations regarding the complex interactions among these players, observations that have arisen by application of a new way of thinking about ecological dynamics, "ecological stoichiometry" (sensu Reiners 1986; Elser et al. 1996; Hessen 1997). It is my hope that this presentation will document the connections between the pelagic food web and the hydrodynamic and geochemical environment in which it is imbedded. I assume that the reader has familiarity with well-known aspects of pelagic ecosystems, such as the biological components of pelagic food webs (bacteria, protozoans, phytoplankton, metazoan zooplankton); patterns of thermal stratification, light penetration, and photosynthetic response; the role of nutrients in eutrophication; and analysis of trophic interactions from energetic perspectives. By describing new findings obtained via stoichiometric approaches I hope to show that integration of these findings with our existing, but potentially incomplete, frameworks may permit us to understand pelagic ecosystems comprehensively from wind to water to the food web itself. Thus, my primary goal is not to describe specific methods of measurement or manipulation in pelagic ecosystems; many of the specific approaches useful in ecological stoichiometry have already been described in previous chapters that are aimed at the

individual components of stoichiometric relationships (e.g., energy, carbon, nitrogen, or phosphorus). Instead, I try to summarize new "methods" of thinking about ecosystems and thus to motivate future studies to elaborate on these preliminary ideas and refine the analyses necessary to test them.

Biogeochemical Structure of Planktonic Food Webs

In pelagic ecosystems, energy and materials move through the feeding relationships of various size-structured components of the planktonic food web that eventually lead to higher predators such as fish (Fig. 26.1). Much of this processing is mediated by herbivores, with varying efficiency, but considerable trophic processing also involves the consumption of detrital organic matter from various sources. The factors that determine the abundance and rates of production of food web components have fascinated pelagic ecologists since the days of Lindeman (1942) and before. Given the importance of fisheries resources as a source of food for humans and of food web structure in affecting water quality, achieving a more accurate and predictive understanding of pelagic food web dynamics must be one of the most important priorities of aquatic ecosystem scientists. In this section, I describe in detail some views of how an understanding of the contrasting nutritional features of major food web components can help us understand the structure and dynamics of pelagic food webs. Here I emphasize the algae and their macrozooplankton consumers, but will give some attention to bacteria and various protozoans in a later section.

At the base of pelagic food webs are autotrophic phytoplankton of a bewildering array of sizes, shapes, and taxonomic affiliations. The basic ecology of this group is well described elsewhere (Reynolds 1984; Harris 1986; Morris 1980). In the context of this chapter, I emphasize the nutritional flexibility and variability of phytoplankton autotrophs, a situation with strong parallels to the physiological plasticity exhibited by higher plants in terrestrial systems.

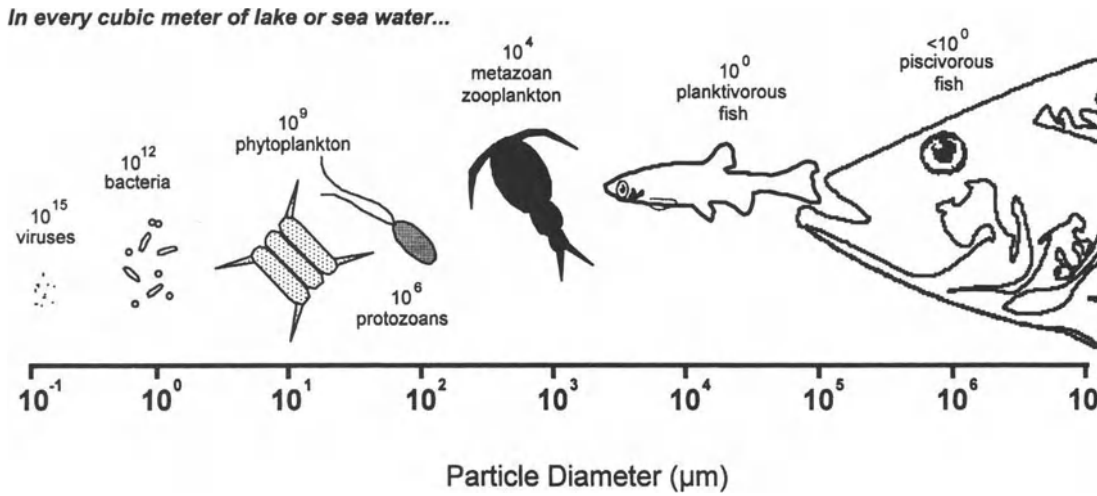

FIGURE 26.1. Components of a typical pelagic food web. Microbial processes are dominated by the activities of bacteria and protozoans. Autotrophic production by phytoplankton is passed to higher trophic levels with strongly varying efficiency. This chapter focuses on how stoichiometric relationships between resources (light, nutrient elements) and algal needs affect the rates and quality of autotrophic production, between organic and inorganic resources and bacterial needs affect the rates and quality of microbial production, and between the energy and nutrient content of food affects the success and production of various consumers (such as microzooplankton and metazoan herbivores). Furthermore, methods of stoichiometric analysis provide a means for assessing the feedbacks between consumers and producers via the stoichiometry of nutrient recycling.

The flexibility of phytoplankton lies at both the intraspecific and interspecific levels. When a given species is grown under chemostat conditions in which growth rate, light, temperature, and nutrient supply ratios are altered, the chemical composition of cellular biomass changes dramatically in predictable ways. A very large literature on these responses exists; I highlight major findings here. First, algae growing at differing rates in chemostats (i.e., growing at various degrees of nutrient limitation) generally have strongly altered elemental composition. More specifically, if algal growth rate is limited by a single nutrient X, then cellular carbon (C)/X ratio increases with decreasing growth rate (Goldman et al. 1979; Healey and Hendzel 1980) (Fig. 26.2A). Second, algae "are what they eat" in terms of macronutrient supply. That is, at any given growth rate, when the nitrogen/phosphorus (N/P) ratio of the inflow medium is changed, cellular N/P responds in parallel (due to luxury accumulation of the nonlimiting nutrient), so that high supply N/P ratios generate algal biomass with high N/P ratio and vice versa (Rhee 1978). Third, algae "are what they eat" in terms of their response to light intensity as well (Fig. 26.2B). That is, at a fixed growth rate under nutrient limitation, increased light intensity raises the C/X ratio (where X is the limiting nutrient) (Healey 1985; Rhee and Gotham 1981; Smith 1983). Thus, algal biomass also comes to reflect the balance of supply of light and limiting nutrient. Finally, these physiological responses vary from species to species according to the competitive abilities of individual taxa as algal species differ in terms of nearly all of the physiological parameters that determine the growth response to resource supply (Tilman 1982; Andersen 1997) (Fig. 26.2C). For example, the N and P composition at zero growth rate (the so-called "optimal N/P ratio" or N/P_{opt}) (Tilman 1982) differs considerably among species, with blue-green algae having low N/P_{opt} (and thus being good competitors for N but weak competitors for P) while green algae and diatoms have high N/P_{opt} (and thus compete well when P is scarce compared with N).

From the work just reviewed we see that algal elemental composition is a function of the severity of nutrient limitation (in terms of decreased growth rate), the identity of the limiting nutrient, the nutrient composition of the supply, ambient light intensity, and algal species identity. Thus, the key message from the literature on the nutritional physiology of algae is that we should expect to find considerable variation in the elemental composition of algal biomass at the base of pelagic food webs. Indeed this is what we see when we look at C/nutrient ratios in suspended organic matter in lakes and oceans (Fig. 26.3) (Elser and Hassett 1994; Sterner and Hessen 1994). From an ecosystem perspective, what this means is that primary production is a highly heterogeneous process in biogeochemical terms. Additional data supporting this connection have recently been analyzed by Sterner et al. (1997) who documented strong variation in the C/P of suspended organic matter at the base of pelagic food webs in Canadian Shield lakes. Specifically, they found that small, sheltered lakes had very high C/P ratios in particulate matter, while large, well-mixed lakes (including Lake Superior) had particulate matter with lower, more balanced C/P composition. Sterner and colleagues propose an explanation for these patterns, the "light/nutrient hypothesis," arguing that hydrodynamic conditions change dramatically as lakes increase in surface area, modifying the light and P supply balance experienced by algae in the surface mixed layer and thus the C/P ratio of organic matter production. They also describe a suite of ecological consequences of variation in the stoichiometry of autotroph production, including effects on the strength of the microbial food web, the species composition of the zooplankton (due to food quality effects discussed below), and the strength of "top down" effects in the food web. Experimental support for the effect of light/nutrient balance in regulating algal C/P and grazer success has been produced (Urabe and Sterner 1996; Sterner et al. 1998). These findings suggest that to better understand physical–biological coupling in the pelagic zone we need to move away from our tendency to consider energy flow and nutrient cycling as distinct topics. Energy and nutrients are linked in intimate and critical ways, and a future challenge will be to develop frameworks that integrate both energy and matter in a single system.

Terrestrial ecosystem scientists may recognize a close parallel between the C/P ecophysiology of phytoplankton just described and the influential concepts of "nutrient use efficiency" (Vitousek 1982) and "nutrient productivity" (Agren 1988)

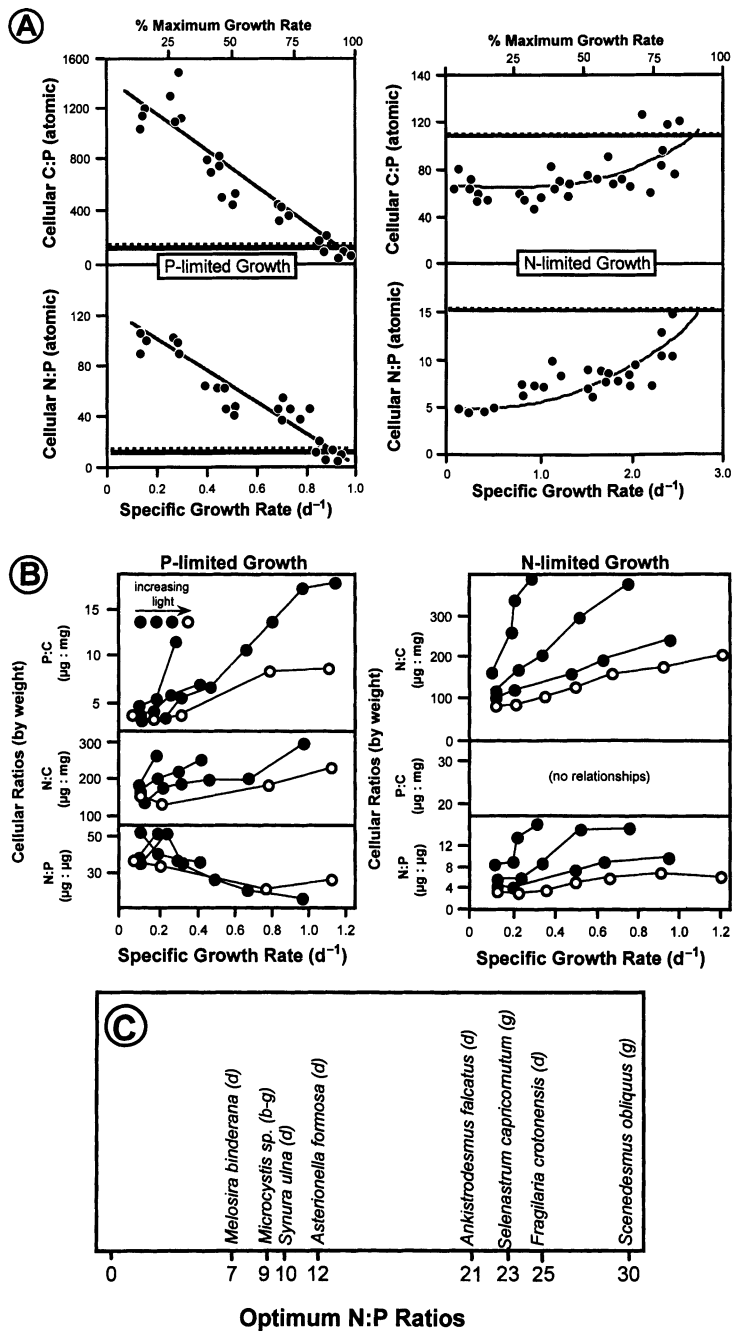

FIGURE 26.2. Sources of variation in the elemental composition of autotrophic production in pelagic ecosystems. A, Physiological responses to the severity of nutrient limitation. Cellular nutrient content (in terms of C/P and N/P ratios) in response to dilution rate in P-limited (left) and N-limited (right) chemostats. Note that in the N-limited chemostats, cellular N/P decreased more rapidly than cellular C/P with decreasing N-limited growth rate, indicating that cellular C/N increased with increasing severity of N-limitation. (From Goldman et al. [1979]. Reprinted by permission from *Nature*. Copyright © 1979 Macmillan Magazines Ltd.) B, Physiological responses to light intensity under nutrient limitation. Note that at any given severity of nutrient limitation (i.e., dilution rate), cellular nutrient/C ratio decreases (C/nutrient increases) with increasing light intensity. (From Healey [1985].) C, Interspecific differences in "optimal" N/P ratios of various freshwater phytoplankton species. An "optimal" N/P ratio is the ratio of the minimal cell quotas for N and P for a given species. These differences imply that the elemental composition of mixed-species autotroph biomass will reflect the species mixture present as well as their physiological condition. d = diatom, g = green alga, b-g = blue-green alga/cyanobacterium. (From Tilman [1982]. Copyright © 1982 by Princeton University Press. Reprinted by permission of Princeton University Press.)

that have been useful in analysis of the ecosystem consequences of terrestrial plant nutrition. This suggests that stoichiometric analysis might serve as an integrative theory with which we can analyze how ecosystem processes linked to autotrophs operate across terrestrial and aquatic ecosystems (Sterner et al. 1997).

Next, I consider the effects of variation in elemental composition of phytoplankton on the rest of the planktonic food web. Addressing these effects

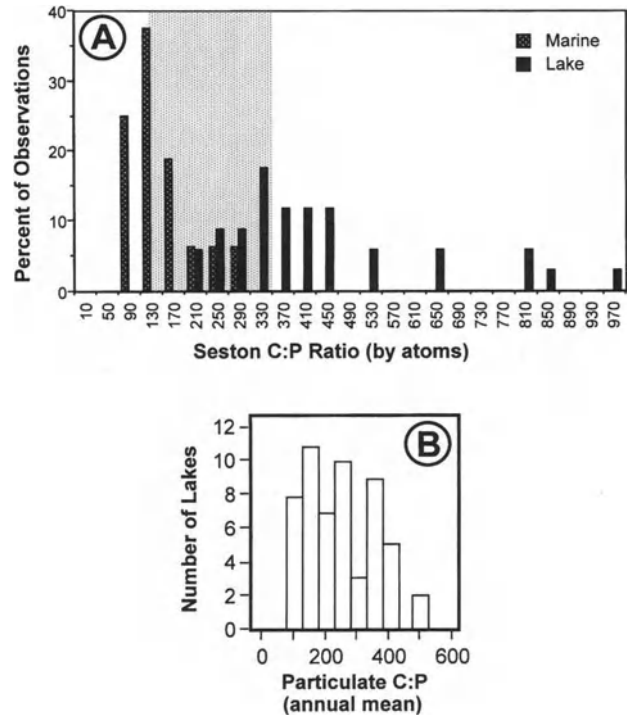

FIGURE 26.3. Frequency histograms for the distribution of C/P ratio in suspended particulate matter (seston) in lakes and oceans. A, Data from direct sampling reported by Elser and Hassett (1994). B, Data for lakes compiled from the literature by Hecky and others (1993). (From Sterner and Hessen [1994].)

requires an understanding of the nutritional ecology of herbivorous zooplankton.

The ecological response of herbivorous zooplankton to the quantity of food available in pelagic ecosystems has been a dominant theme in pelagic ecology for decades, with much effort focused on testing and elaborating the "size-efficiency hypothesis" of Brooks and Dodson (1965). This work has emphasized size-dependent differences in food acquisition, utilization, and production among taxa as an explanation for the apparent competitive superiority of large zooplankton species (such as *Daphnia*) under conditions of low predation pressure. Many excellent reviews of this topic already exist (Hall et al. 1976; Lampert and Schober 1980; DeMott 1989) and emphasize differences among species in food collection strategies and food processing under conditions of varying food abundance. These studies have done much to clarify our understanding of the factors regulating zooplankton succession and production. Clearly, food quantity is a critical aspect of the lives of zooplankton in many habitats. Here I wish to emphasize an additional and potentially under-appreciated factor regulating zooplankton dynamics, the impact of nutritional quality of available food. As we will see, an appreciation of the role of food quality as indexed by algal nutrient content provides a potentially key mechanism by which the multiplicity of factors that regulate algal elemental composition (reviewed briefly above) have ramifications for the rest of the food web.

Sterner and Hessen (1994) have recently reviewed available evidence regarding the influence of food quality on zooplankton dynamics. Their analysis emphasizes the extreme variability of elemental and biochemical composition of algae, contrasting that variability with the narrow requirements for building herbivore biomass, pointing out that different herbivore species can have strongly contrasting elemental composition but intraspecific variation is modest (Fig. 26.4A). They summarized data indicating only minor differences between species in N composition (in terms of percentage of N or C/N) but strong differences in phosphorus composition (in terms of percentage of P or C/P and N/P). Of particular potential interest to freshwater zooplankton ecologists is the fact that the keystone

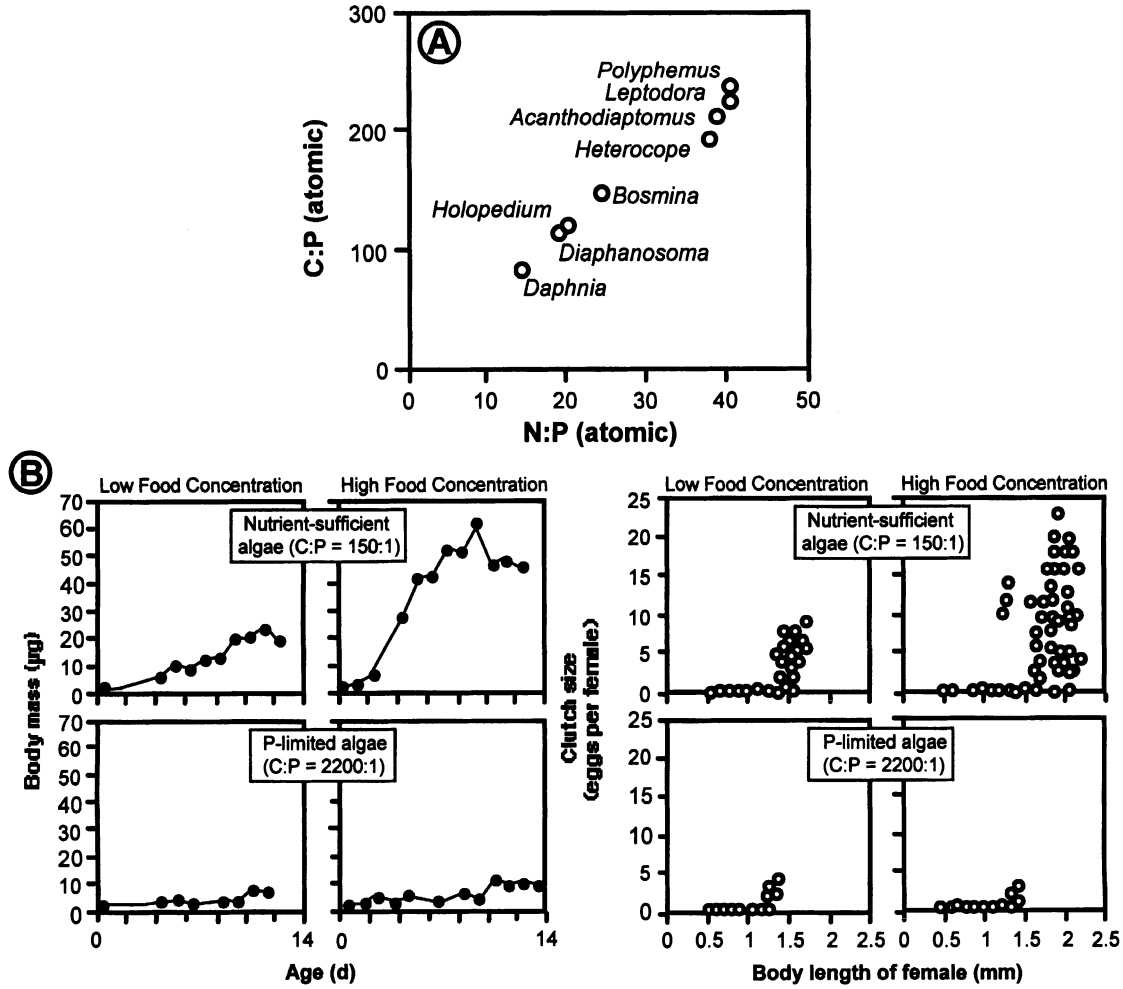

FIGURE 26.4. A. Variation in the elemental composition (in terms of C/P and N/P ratios) of various freshwater zooplankton species. (From Sterner and Hessen [1994].) B, Selected data from a study of the response of a high phosphorus animal (*Daphnia obtusa*) to a diet of P-limited (high C/P) *Scenedesmus*. Note that P-limited algae caused severe reductions in growth (left) and reproduction (right), even when provided at high abundance. (From Sterner et al. [1993].)

herbivore in lakes, *Daphnia,* appears to be a genus with unusually high body phosphorus content. Furthermore, feeding studies indicate that body elemental composition in zooplankton taxa appears closely regulated, changing little in response to altered food abundance or diets of P-rich or P-deficient algae (Andersen and Hessen 1991). Zooplankton "are *not* what they eat." These stringent somatic requirements apparently exact a severe cost when stoichiometric food quality deteriorates. For example, *Daphnia* growth and reproduction plummet when animals are fed P-limited algae with high C/P ratio (Fig. 26.4B) (Sterner et al. 1993). Sterner and Hessen (1994) elaborate on the many ways that herbivores deal with their nutritional environment, from alterations in feeding rates and selectivity to digestive processes that adjust assimilation of various food components, but the bottom line is that the dietary challenges imposed by nutrient-poor food can strongly affect individual growth and population dynamics, thus affecting community structure, the rate of secondary production, as well

as recycling of potentially limiting nutrient elements from the food. Thus, in the work synthesized by Sterner and Hessen (1994), imbalance between herbivore requirements and food elemental composition is seen to have effects at a variety of levels of ecological integration, from individual behavior to ecosystem processes.

Our understanding of the importance of food quality on zooplankton dynamics and the rest of the pelagic ecosystem has been considerably refined even in the brief period since the review of Sterner and Hessen (1994) appeared (Sterner and Schulz 1998). Evidence for the role of certain essential fatty acids (highly unsaturated fatty acids, or HUFA) in constraining zooplankton growth when feeding on moderately nutrient-stressed algae has been produced (Müller-Navarra 1995) but Sundbom and Vrede (1997) have shown that these fatty acid effects are most likely only under conditions of moderate P stress when algal C/P is 150–300:1. Above that ratio, direct mineral P limitation of grazer growth is more likely. Furthermore, since the fatty acid profiles vary considerably among various algal species, potential HUFA effects are enhanced by the monospecific conditions of laboratory studies but are less likely under field conditions, where many algal species are on the menu. The first direct evidence for mineral limitation of *Daphnia* growth has recently been produced. Urabe et al. (1997) showed via an ingenious experimental design that much of the reduced growth of *Daphnia* fed high C/P algae (C/P ~1200) can be recovered by briefly soaking animals in solutions with high concentrations of mineral phosphate (PO_4). Animals were apparently able to relieve their P-limitation by taking up PO_4-P through the gut (a phenomenon with the discomfiting name of "anal drinking"!). While this mechanism is clearly not relevant in natural situations, this experiment does provide direct evidence that reduced growth of *Daphnia* when fed high C/P algae reflects a real mineral limitation by P. These data come from laboratory studies. However, there is accumulating evidence that the deleterious effects of poor food quality associated with P-limitation of algal growth may be widespread in natural systems (DeMott and Gulati 1999; MacKay and Elser 1998). It now seems clear that food of high C/P ratio is manifestly unsuitable for many grazers, especially animals with high body P contents that must acquire disproportionately more P from their diet in order to construct their P-intensive biomass.

The observation of characteristic differences in elemental composition among various zooplankton species has inspired considerable speculation and, more recently, tests assessing the physiological, cellular, and evolutionary bases of those differences. These include efforts to interpret the strong variation in body phosphorus content that has been documented. Why do animals such as daphnids and calanoid copepods, organisms of similar body size, similar habitat, and reasonably close taxonomic affiliation, have such drastically different body phosphorus contents (around 1.2 to 1.8% P in *Daphnia,* ~0.3 to 0.5% P in adult copepods)? Hessen and Lyche (1991) were first to speculate that these differences might be associated with differences between these groups in body RNA content, arguing that RNA is a P-rich molecule known to vary considerably among organisms. This idea was echoed by Sterner and Hessen (1994), who suggested that if the RNA hypothesis were supported, it would be "possible to see a clear thread extending all the way from molecular biology to ecosystem function."

That thread is beginning to be woven into a more substantive fabric. Elser et al. (1996) delved in considerable detail into the elemental composition of biomolecules and cellular structures, showing that major biomolecules (especially proteins and nucleic acids) differ little in terms of percentage of N but strongly in terms of percentage of P. This result that makes it easier to understand the relative uniformity of N composition of cellular structures and whole organisms along with the strong variation observed in percentage of P. Elser et al. (1996) established that the ribosome, the cellular structure of protein synthesis and thus animal growth, is the most P-rich of major cellular structures considered, and thus argued that animal elemental composition (especially percentage of P but also N/P) was strongly linked to body growth rate due to the high demand for ribosomes and P-rich RNA during rapid growth. They also produced evidence from literature studies showing negative correlations between body-specific growth rate and body N/P ratio in *Daphnia* and *Drosophila.* New data specific to this hypothesis have recently been produced by Main et al. (1997), who showed in studies of five cladoceran species that percentage of N changed little with body growth rate but percentage of P

increased rapidly and N/P declined (Fig. 26.5). Direct evidence that high P-content of various zooplankton taxa is associated with increased RNA allocation has recently been produced (Vrede et al. 1998; Dobberfuhl 1999). Thus, steps toward the integration of multiple levels of organization, from molecules and cells to ecosystems, have begun to be made by application of methods of stoichiometric thinking.

Above, we saw that, from an ecosystem perspective, the process of primary production is biogeochemically heterogeneous, with that heterogeneity arising largely due to intraspecific responses of physiologically plastic algae to environmental conditions. Here, we see that the process of secondary production is also biogeochemically heterogeneous, but that heterogeneity is driven not by physiological responses of individual herbivore taxa but instead largely by the mix of species, low or high in P, present in the community.

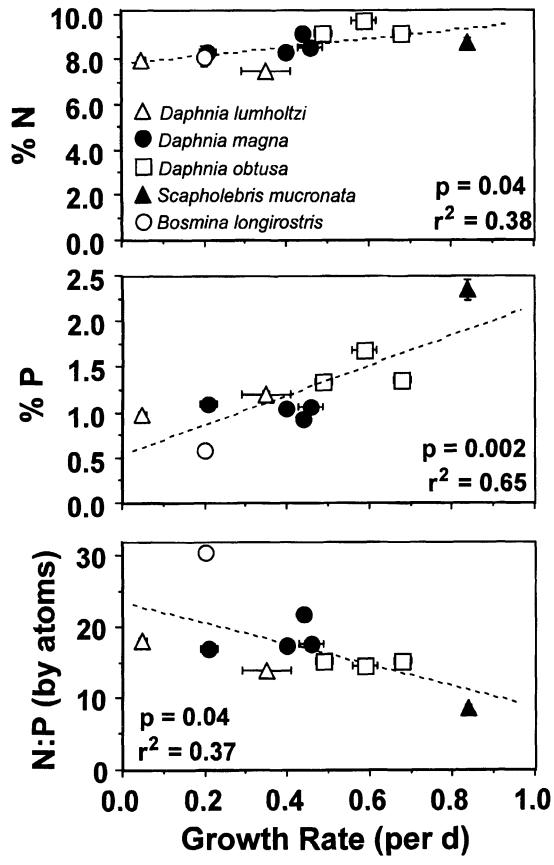

FIGURE 26.5. The connection between body elemental composition and body growth rate in freshwater zooplankton. P-rich, low N/P taxa are taxa with high specific growth rates. (From Main et al. [1997].)

To this point, I have emphasized the ecological stoichiometry of primary and secondary production, two important aspects of trophic dynamics and thus of direct concern in ecosystem study. Another major aspect of ecosystem study is nutrient cycling and, while the theme of the work described above is clearly linked to nutrient dynamics, I have not yet discussed how the stoichiometry of autotrophs and grazers affects nutrient cycling itself, an effect that will feed back in interesting ways to the extent that grazer nutrient release is an important source of nutrients to the algae. The facts that algal elemental composition varies, that zooplankton elemental composition differs among species, and that individual zooplankters homeostatically regulate their elemental composition at fixed levels imply that the rates and ratios of nutrient recycling by grazing zooplankton should vary dramatically because of the law of conservation of matter. These issues have recently been reviewed (Elser and Urabe 1999); I touch on the highlights here. The stoichiometry of consumer-driven nutrient recycling has been analyzed in several theoretical frameworks, including ones considering C/P ratios and rates of P-release (Olsen et al. 1986; Hessen and Andersen 1992) and one focusing on N/P ratios of released nutrients as affected by food and grazer N/P ratios (Sterner 1990). Results of Sterner's efforts are shown in Figure 26.6A. The N/P ratio of recycled nutrients is predicted to be a function of food N/P ratio (but in a nonlinear way) as well as of grazer N/P ratio (low N/P grazers generate high N/P release ratios relative to high N/P grazers, as intuition would predict). Stoichiometric nutrient release models have found strong empirical support via the field studies of Urabe, who showed that, in a lake with a relatively fixed grazer N/P ratio, release N/P ratio was a function of the N/P ratio of ingested food (Figure 6B) (Urabe 1993) and, in a separate study in a lake in which food N/P ratio was relatively constant, that release N/P ratio was a negative function of grazer N/P ratio (Figure 6C) (Urabe et al. 1995).

Thus, stoichiometric processes operate also in the realm of consumer-driven nutrient cycling and to the extent that grazers are important nutrient

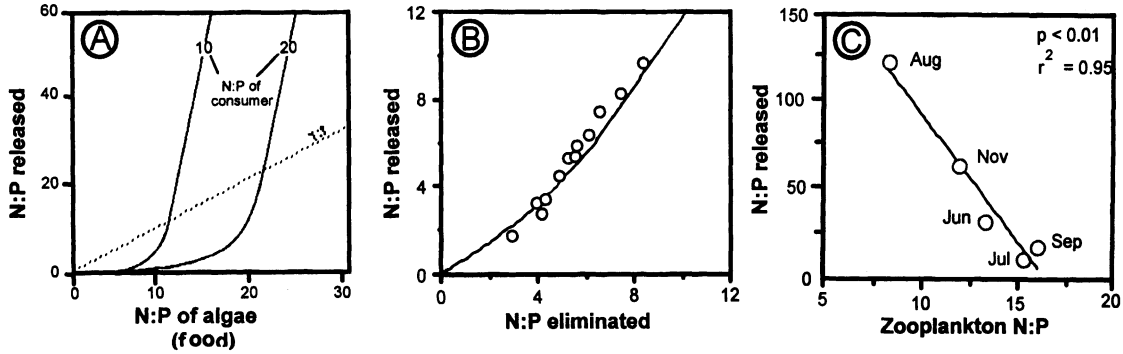

FIGURE 26.6. Theory and test of stoichiometric nutrient release by consumers. A, Predicted N/P ratio of nutrient release by a consumer as a function of food N/P ratio (x-axis) and body N/P of the consumer (predictions for a low N/P animal [10:1] and a high N/P animal [20] are shown). The theory predicts that, holding consumer N/P constant, relative release rates of N and P by consumers are a nonlinear function of food N/P ratio and that, holding food N/P constant, release N/P is a negative function of body N/P of the consumer. (From Sterner [1990].) B, Relationship between measured N/P release ratio by zooplankton as a function of food N/P in a Japanese pond. The solid line indicates the relationship predicted by the model of Sterner (1990). (Data from Urabe [1993].) C, Relationship between measured N/P ratio of nutrient release by zooplankton communities and the N/P ratio of the zooplankton assemblage. The study was performed in Lake Biwa and the N/P of available food was generally constant during the study period. (Data from Urabe et al. [1995].)

sources for algae (and, as mentioned above, they frequently are), we would expect feedbacks between nutrient availability and grazer dynamics (Elser and Urabe 1999). Indeed, the stoichiometric perspective successfully explained shifts in the identity (N vs. P) of the nutrient limiting phytoplankton growth in the whole-lake experiments reported by Elser et al. (1988). Phytoplankton growth was limited by P when the zooplankton were dominated by *Daphnia* (as described above, a low N/P animal and thus likely to produce high N/P recycling ratio) but was limited by N when high N/P copepods were the dominant grazer (Sterner and others 1992). In this study, grazers clearly operated as key sources of potentially limiting nutrients and their feedback to the algae was to shift the identity of the limiting nutrient. However, feedbacks may not always be of this type, as under various conditions zooplankton can also be major nutrient sinks (Andersen 1997). In such situations, grazers may not alter the identity of the limiting nutrient (as observed by Elser et al. 1988) but instead may amplify limitation by that nutrient if they strongly sequester limiting element in their own biomass. These feedback effects are complex and have only recently been modeled by Andersen (1997), whose model will be discussed below.

Dynamics Under Stoichiometric Constraints: The Andersen Model

The work just reviewed reveals a complex set of interactions in which nutrient supply affects autotroph physiological status, which in turn affects grazer success and nutrient release, coming full circle to feed back on algal nutritional status. Sorting through these feedbacks to understand their implications for pelagic food webs and nutrient processing is a difficult task made more difficult by our current lack of theoretical models that incorporate stoichiometric constraints and consequences. This deficiency has recently been alleviated by the development of the first set of "stoichiometrically explicit" models of pelagic trophic interactions and nutrient cycling by Andersen (1997). I refer to these models as "stoichiometrically explicit" as a parallel to the now widespread phrase "spatially explicit." Spatially explicit ecological theory considers the constraints that space and rates of movement

through space place on ecological dynamics. Similarly, a "stoichiometrically explicit" theory of trophic interactions and nutrient cycling would operate within the constraints that the first law of thermodynamics operating on energy and multiple elements imposes on growth rates, biomass, and nutrient release.

Andersen's approach considers the dynamics of a phosphorus–autotroph–grazer system under conditions in which algal C/P ratio varies with P-limited growth rate, grazer growth rate varies in proportion to food quantity or quality as appropriate, and grazer nutrient release is governed by mass balance. Algal growth is modeled via the familiar "Droop equation," which expresses P-limited algal growth rate in terms of cellular P/C ratio. Importantly, grazer growth and reproduction are modeled via expressions that assess whether animal growth is limited by food abundance or by food quality, comparing the rates of C and P ingestion relative to current requirements of the animal. Finally, the rate of P released by the grazer is modeled as the difference between ingested P and P incorporated into new biomass.

Incorporating these simple and biologically realistic assumptions has profound consequences for predicted dynamics. Those consequences are perhaps best appreciated by considering the isoclines for grazer and autotroph populations, which are peculiarly hump-shaped (Fig. 26.7). For the algal isocline, the rising portion in the middle of the curve corresponds the region of saturation of feeding response of individual grazers but the isocline comes down to the x-axis (the algal axis) as a result of the constraint of total P in the system. That is, given that algae have a physiological minimal P/C ratio, algal biomass in terms of C has an upper limit set by the total amount of P in the system divided by that minimal P/C ratio. Even more interesting is the grazer isocline, which is also hump-shaped due to the constraints of matter. The first intersection of the zooplankton isocline with the algal axis is the conventional food quantity threshold; but what generates the second intersection? This intersection is a direct result of the realization that grazer biomass is also constructed of P. That is, given that the total amount of P in the system is fixed, as algal biomass increases there is less and less P available to build grazer biomass!

The shape of these isoclines generates two primary configurations of ecological interest that are a function of species characteristics and environmental conditions. In the first (panel A in Fig. 26.7), algae and grazer isoclines have one positive intersection (point A1) in the positive phase plane. This intersection is a locally stable equilibrium point but, beyond its immediate vicinity, stable limit cycles are predicted. In this situation, the equilibrium point with zero grazers (point A2) is locally unstable (i.e., the system is invasible by grazers). Alternatively, conditions might generate the situation shown in panel B in Figure 26.7, in which there are now two positive intersections. Andersen's analysis shows that the second positive intersection (point B2) is locally unstable and, importantly, that the grazer extinction equilibrium (B3) is now locally stable. Dynamics of the algae–grazer system in this scenario are highly unstable.

What determines whether the interaction resembles panel A or panel B? Andersen's analysis showed that whether or not the interaction lies in the realm of stable or unstable dynamics with the possibility of grazer extinction depends on a few key parameters of algal and zooplankton physiology. Specifically, his analysis shows that transitions between panel A versus panel B in Figure 26.7 occur as a function of:

$$g'' = g^*(Q_a/\theta) \qquad (26.1)$$

where g^* is the growth capacity of the grazer species, Q_a is the minimal P/C of the algae (i.e., algal P/C when algal growth rate is zero under P limitation), and θ is the elemental composition (P/C) of the grazer. When g'' is high, it is more likely that the system will be in a situation like that in panel A of Figure 26.7 in which the zooplankton–phytoplankton interaction is stable. Such a situation will occur when grazer P content (θ) is low (as such animals are less sensitive to the food quality effects that bend the grazer isocline) and Q_a is high (as this means that algal biomass at zero growth rate will be lower for a given P input). On the other hand, situations dominated by algal species with superior competitive abilities for P (lower Q_a) or grazers with higher P contents (higher θ) reduce g'', favoring unstable dynamics that promote grazer extinction (panel B in Figure 26.7). Thus, predicted dynamics may differ considerably for different grazer species, which we now know have potentially

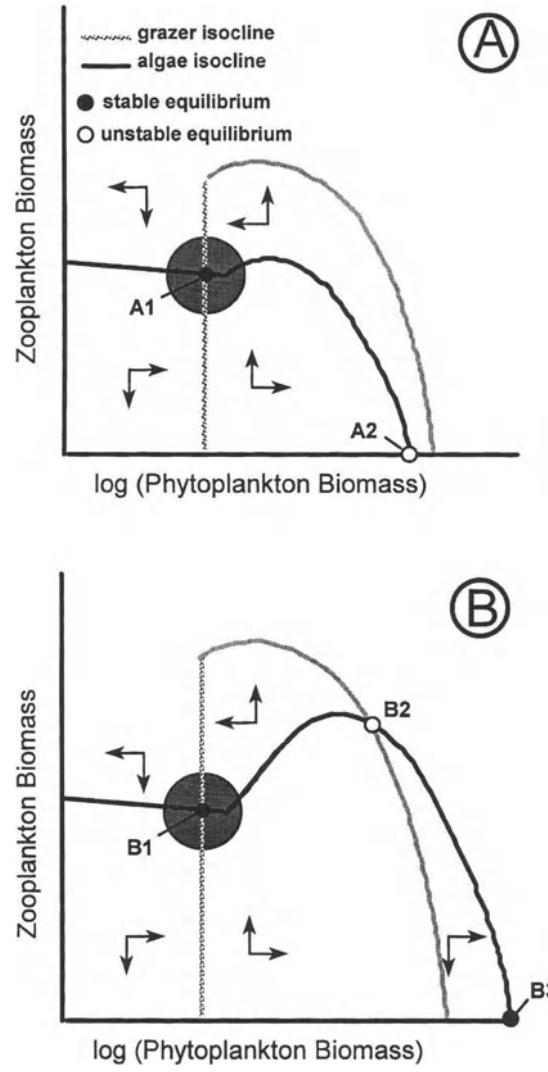

FIGURE 26.7. Exemplary growth isoclines for algae and grazer in the stoichiometrically explicit model of Andersen (1997). Panel A illustrates an example, more likely at low nutrient levels and/or when the grazer is a low-P animal, in which only one intersection in the positive phase plane exists. In this scenario, algae–grazer dynamics are attracted to the locally stable equilibrium point (A1) if the system starts in the shaded area or are entrained into stable limit cycles otherwise. In this scenario, the grazer extinction point (point A2) is locally unstable. Panel B illustrates an example, more likely at higher P levels and/or when the grazer is a high-P animal, in which three intersections in the positive phase plane exist. As in panel A, the first intersection (point B1) is locally stable but now a second, alternative, equilibrium (B2) exists but is locally unstable. Importantly, in this scenario the third point, a grazer extinction point (B3), is locally stable and thus deterministic extinction of the grazer is a possibility. Andersen's analysis shows that algae–grazer dynamics under situations like panel B are extremely erratic and very sensitive to initial conditions.

strongly divergent P composition (θ). Taxa with low P composition (such as *Bosmina* or calanoid copepods in freshwater systems) may enjoy stable dynamics due to favorable food quality conditions sustained by rapid P release while P-rich taxa (such as *Daphnia*) may undergo erratic dynamics and frequent local extinction. This last point may be of key interest in understanding variation in secondary production and fisheries performance, as the species with the highest potential for transforming primary production into secondary production (high P species with high growth rates, e.g., *Daphnia*) are predicted to be the taxa with the most unstable dynamics.

How might changes in ecosystem conditions affect these dynamics? Briefly, Andersen's analysis shows that fertilization destabilizes the interaction between algae and grazers, increasing the likelihood of grazer extinction by shrinking the domain of attraction of the stable equilibrium point A1. In addition, intuition suggests that light intensity should also alter the dynamical landscape of the phosphorus–algae–grazer system, as increased light intensity tends to make it harder for algae to match P atoms with fixed C, thus increasing the realm under which food quality impacts are felt. Thus, changes in nutrient inputs and/or light intensity can alter the stoichiometry of the grazer–algae

interaction and generate alternative community states.

The alternative states generated by changes in light and/or nutrient supplies appear to be qualitatively different worlds of interaction. The first state, which I will call the "quantity world," is in the vicinity of equilibrium point B1 (see Fig. 26.7B) and is a world where actively growing algae are kept in check by high grazing rates; grazers are constrained by low food quantity and regenerate P at high rates. This is the world where most conventional food web theory holds and where most of our intuition about trophic interactions has been developed. However, there appears to be a second world of interaction that may be lurking in many ecosystems, generating confusion in food web ecologists. I refer to this world as the "quality world," the part of the phase plane at or near the locally unstable equilibrium point B2 and influenced by the locally stable point B3. In the quality world, algae are growing at low, P-stressed rates and are fed upon by low biomasses of zooplankton grazers whose growth rates are strongly limited by food quality and whose rates of P-release are extremely low. Furthermore, the entire system is at risk of collapse to the locally stable grazer extinction point. In this world, much of our ecological intuition is strangely inaccurate. Here, high grazer growth capacity is disadvantageous to the grazer as high body P composition increases the likelihood of extinction. Grazers are no longer a source of nutrients for algae via P recycling but instead are a sink. In the quality world, grazers are not in competition with each other for food and instead intraspecific (Sommer 1992) or even interspecific facilitation (Urabe 1995) are possibilities. Facilitation occurs because increased cropping of algae potentially raises per capita algal nutrient supply and thus improves food quality and therefore growth for each grazer. The situation in the quality world involves unconventional interactions but appears consistent with observations from P-stressed lakes on the Canadian Shield (Elser et al. 1998; Hassett et al. 1997; Sterner and others 1997). It seems imperative to better understand what environmental factors affect algal nutritional status and thus shift the pelagic food web between the quantity and quality worlds. The balance of light and nutrient supplies discussed earlier (Sterner et al. 1997) may be a place to start. New theoretical work incorporating stoichiometric constraints seems critical as well.

What About the Microbes?

At this point of the chapter many of my pelagic colleagues may be tapping their fingers, impatient with my emphasis on phytoplankton–macrozooplankton interactions and waiting for a discussion of how the critically important transformations mediated by microbes (bacteria, protozoa) are incorporated into this way of thinking. Unfortunately, I have little room left here to describe exciting work by which similar principles have been elucidated for processes operating in the microbial realm, but in this section I will briefly summarize some of the most important findings in this area. Much of this work supports the idea that supplies of energy and key materials jointly affect the microbial food web. Thus, stoichiometric thinking may help illuminate the general principles of energy and material cycling that are common to the microbial and conventional food webs, and thus help to unify these sometimes divergent approaches.

First, as for the autotrophic algae, bacterial elemental composition is not fixed and instead varies considerably with environmental conditions and growth rate (Vadstein et al. 1988; Chrzanowski and Kyle 1996). Here, the basic principles are roughly the same: under P-limited conditions, bacterial C/P ratio is inversely proportional to growth rate (Chrzanowski and Kyle 1996). Stoichiometry also appears important in the bacteria–flagellate interaction, as rates of nutrient release are strongly linked to both the elemental composition of the bacteria and of the bacterivore (Eccleston-Parry and Leadbeater 1995; Jurgens and Gude 1990; Caron et al. 1988; Goldman et al. 1985, 1987; Nakano 1994). Furthermore, mixotrophic bacterivores appear to respond adaptively to changes in their nutritional environment. For example, studies by Nygaard and Tobiesen (1993) and Rothhaupt (1996) show that mixotrophs shift between bacterivorous and autotrophic modes of nutrition depending on relative supplies of light, inorganic P, and prey bacteria.

Microbial processing of detrital materials is also strongly dependent on the elemental composition

of the detrital material being metabolized (Tezuka 1989, 1990; Hessen 1994). For example, Tezuka (1989) showed that mineralization of N and P (i.e., release of N and P into dissolved forms) by bacteria was strongly dependent on the elemental composition of the detrital material. When detritus was derived from P-limited algae and thus had high C/P and low C/N ratios, bacterial activity resulted in release of inorganic N but no release of inorganic P, as P was apparently retained by P-limited bacteria. Conversely, when N-limited algae with high C/N and low C/P ratios were used as a source of detrital material, bacteria freely mineralized P but retained N. Field studies also support the key role of stoichiometry in determining the role of bacteria in nutrient cycling in pelagic systems. For example, Elser et al. (1995a) showed that when the N/P ratio of bacteria-sized particles (<1.0 μm) was less than 20, bacteria immobilized inorganic N, but when N/P was greater than 20, bacteria released N. Thus, pelagic bacteria were sinks or sources of N in the internal N cycle depending on their current physiological condition. In the same lakes, experiments using naturally derived organic substrates from algae varying in their nutritional status showed that the C, N, and P demands of the bacteria varied considerably during the growing season, closely tracking bacterial population development during growth and stationary phases (Chrzanowski et al. 1997). These studies show that under natural conditions, bacterial demands for key elements are highly variable and that the natural environment rarely provides organic energy and important nutrient elements at rates and proportions best suited for maximal bacterial growth.

The work just briefly outlined identifies similarities in key principles regulating ecological dynamics in the microscopic and macroscopic worlds. That is, at the bottom of the microbial food web is a food base, the bacteria, that (like algae in the conventional food chain) has a strongly varying elemental composition linked to its growth status. Analytical and theoretical approaches that ignore potential variation in the elemental composition of bacteria may lead investigators astray. Somewhat unique to the microbial food web is that organisms at the base, the bacteria, are heterotrophic. Nevertheless, bacterial activities also operate within a stoichiometric framework, as illustrated by shifts in source/sink function with changes in growth status and substrate composition. Stoichiometric principles also hold during microbial trophic interactions, as bacteria are fed upon by consumers whose rates of nutrient release are a function of both food and consumer elemental composition. Food quality effects on protozoan growth are, to my knowledge, not yet documented but seem likely given the realities of mass balance and the possibility of poor matches between protozoan demands and the composition of nutrient-stressed bacteria. The work summarized above illustrates that stoichiometric mechanisms are fully at play in the microbial realm. Application of stoichiometric thinking may help integrate our approaches to microscopic and macroscopic ecology.

Methodological Issues

Progress in understanding pelagic ecosystem dynamics in stoichiometric terms has been relatively rapid, pursued by a number of investigators internationally. Nevertheless, limitations on further progress remain. Some of these are conceptual and theoretical while others are technological. With respect to the latter, progress in understanding the stoichiometric relations of some key pelagic players under field conditions, such as bacteria, protozoa, and small metazoans, is limited by our ability to make reliable determinations of their elemental composition. Such limitations may be solved by improved methods of isolating appreciable numbers of these taxa from field samples and by improved methods of elemental analysis capable of providing accurate data on small sample sizes. Furthermore, we need better methods of characterizing the elemental composition of all of the individual particles (bacteria, various algal species, detritus, protozoa) that contribute to suspended particulate matter, the base of pelagic food webs. Some studies have made initial attempts via X-ray microanalysis (Olsen and others 1986) but currently such procedures are too laborious for routine application. Analysis of materials isolated by flow cytometry of live samples may be an alternative means, but this technology is currently too expensive and cumbersome for routine application.

The work reviewed above with reference to algal C/P ratios and the light/nutrient hypothesis suggests close coupling between hydrodynamic processes

and the stoichiometry of planktonic food webs. Physical limnologists and oceanographers have the advantage of being able to generate hydrodynamic data at high spatial and temporal resolution, while most biological data are only available on coarse scales due to methodological limitations. The situation is the same for stoichiometric data, as analytical methods for elemental composition are slow and labor-intensive. One methodology that holds promise for reducing the mismatch between the intensities of hydrodynamic and stoichiometric observations is near-infrared reflectance spectroscopy (NIRS). Developed largely for food product analysis, this approach analyzes the infrared signatures produced by covalent bond structures of organic materials and, when properly calibrated, provides information on elemental composition (C, N, P) as well as on composition of major biomolecules (protein, lipid, carbohydrate, nucleic acid). Furthermore, the analysis is rapid (<5 minutes per sample) and nondestructive so that the sample remains for archiving or for analysis of other constituents. The approach has recently been applied in a limnological setting by Malley et al. (1993), who found good agreement between particulate samples analyzed by NIRS and by conventional elemental analysis. They also successfully analyzed sediment samples and Malley indicates that the approach should be applicable to mixed or species-specific zooplankton samples. Thus, NIRS may allow real-time, high-intensity observations of stoichiometric properties in limnological and oceanographic settings, reducing sample analysis costs at the same time.

Improved methodological and analytical capabilities may greatly facilitate analysis of pelagic ecosystems in stoichiometric terms. However, technical issues are not the primary constraint on progress in this realm. More important will be the rate at which pelagic scientists begin to apply the conceptual and theoretical tools described in this chapter (and elsewhere) to incorporate the role of stoichiometric constraints into their view of nutrient cycling and trophic dynamics.

Applications

How might improved understanding of pelagic ecosystems obtained via stoichiometric analysis be usefully applied in addressing problems of human concern? We have already seen how the model of Andersen (1997) has direct application to problems of eutrophication involving increased P loading to lakes. Indeed, stoichiometric approaches are already in direct application in a major project that seeks to analyze and model eutrophication processes in the Mediterranean Sea, the Baltic Sea, and the Northeast Atlantic Ocean (COMWEB project). Stoichiometric thinking may be particularly important in understanding and making accurate predictions concerning the impacts of perturbations that, as human influences often do, alter more than one key factor at a time. For example, consider the effects of global climate change on water column structure, hydrodynamics, and nutrient dynamics in pelagic ecosystems. Stoichiometric analysis suggests that climate change effects on hydrodynamics may push many pelagic ecosystems from the "quantity" world to the "quality" world, with potentially serious consequences for food web performance. First, consider marine systems where it has been suggested that global warming may create warmer and shallower (and thus brighter) surface mixed layers with more sluggish circulation and thus reduced nutrient availability (Broecker 1982; Mullin 1993; Rowe and Baldauf 1995; Karl et al. 1995). For example, El Niño conditions in the North Pacific subtropical gyre were associated with a shallower, less turbulent mixed layer, a shift from N- to P-limitation of production, and increased seston C/P (Karl et al. 1995, 1997). This response is consistent with the data for the lake-size series analyzed by Sterner et al. (1997) indicating that reduced turbulence in pelagic ecosystems may accentuate autotroph C/nutrient imbalance, conceivably impairing secondary production. This possibility is particularly intriguing given recently documented long-term declines in marine zooplankton biomass (Roemmich and McGowan 1995). Next, consider lakes. Climate change may affect lakes in the same way as described above for oceanic water columns: creating shallower, brighter mixed layers with reduced nutrient supplies, elevating C/nutrient ratios of primary production and imposing stoichiometric constraints on food web performance. A potential example of this can be seen in the study of Schindler et al. (1990) of a boreal forest lake during a 20-year period of climatic warming. During this period, watershed runoff decreased, resulting in lower inputs of colored dissolved organic carbon (DOC)

(and thus clearer water and a brighter mixed layer) as well as in reduced P loading. Thus, climatic warming in this case simultaneously disrupted *both* the light and phosphorus economies of the lake, a perturbation whose ecological consequences might best be understood via stoichiometric approaches.

Implications

What does the work synthesized in this chapter imply for the ways in which we study pelagic ecosystems? There is a mixture of good and bad news. Some bad news is that it indicates that some familiar models of nutrient cycling and trophic interactions in pelagic food webs, as well as the intuition about pelagic ecosystem dynamics we have developed via those models, are of restricted domain, incomplete, or simply wrong. As noted by Andersen (1997), some of these models take liberties with the first law of thermodynamics and nearly all completely ignore the effects of food quality on consumer success. Some good news is that incorporating ecological stoichiometry into models of trophic interactions and nutrient cycling is reasonably straightforward (though the outcomes are complex!) and the work of Andersen (1997) is a big step forward. Really good news is the possibility that many aspects of pelagic ecosystem structure and function that have previously been puzzling or unexplainable may ultimately be found to be linked to stoichiometric influences once these effects are incorporated into our thinking and study plans. For example, trophic interaction models that incorporate only the effects of food quantity on herbivore success invariably predict that alterations in top trophic levels will alter primary producer abundance via the trophic cascade. However, observations suggest that the strength of trophic cascades varies considerably among lakes (DeMelo et al. 1992; Brett and Goldman 1996; Elser et al. 1995b). Ecological stoichiometry can reconcile this mismatch between existing theory and observation, as the model of Andersen (1997) delineates the stoichiometric conditions for strong, stable trophic cascades. A recent whole-lake food web experiment supports the existence of stoichiometric constraints on trophic cascades (Elser et al. 1998). Additional bad news is that several parameters that are apparently critical to understanding trophic dynamics and nutrient cycling within the pelagic food web, such as the elemental composition of suspended particulate matter and of various important grazers, are not routinely measured in pelagic ecosystem studies. Fortunately, these parameters are relatively easy and only moderately expensive to analyze. Of greater difficulty and expense is the implication that pelagic ecosystem scientists might understand their systems better if they also measured *fluxes* of multiple elements in their study systems. Such measurements are in fact relatively laborious and expensive and achieving a complete picture of the flows of multiple materials in pelagic food webs will be difficult. Recent advances in network analysis (e.g., Gaedke and Straile 1994) may facilitate such studies, as network analysis makes it possible to obtain a reasonably complete picture of the flows of multiple materials in a trophic network given a restricted set of observations of key pools and pathways. Brave ecological theorists might be able to take the next step by abducting more sophisticated tools from theoretical chemistry where they are used to analyze complex reaction networks constrained by chemical reality (Masuda 1990; Clarke 1992).

Despite Reiners' stimulus almost 15 years ago (Reiners 1986), ecological stoichiometry is only now becoming a self-identifying field. Many of the most basic data have yet to be collected and we have only a sketchy idea of how the stoichiometric structure of various pelagic ecosystems varies. We also have little idea whether or not patterns of ecological stoichiometry differ for pelagic versus benthic versus lotic versus terrestrial habitats. Discovering those patterns may an important next step in producing an integrated and predictive ecosystem science built on first principles rather than habitat-specific paradigms. To that end, I close this chapter with a message for the adventurous ecologists from beyond the pelagia who have braved this chapter to its very end. The principles of stoichiometric analysis and understanding I have delineated here, such as the links between elemental composition and growth in both autotrophs and grazers or the role of multiple mass balance in consumer production and nutrient release, are broad and founded in basic biology and thermodynamics. How do you imagine these processes to unfold in your grassland, your stream, your soil, your forest canopy? New methods of thinking accompanied by new methods of

measurement may make it possible to develop a single framework that incorporates the common principles regulating nutrient cycling and trophic dynamics in all ecosystems.

Acknowledgments. Jotaro Urabe, Tom Andersen, Tom Chrzanowski, and Mike Pace provided useful comments on early versions of this material. I thank Bob Howarth and Osvaldo Sala for the invitation to prepare this chapter. I am also grateful to Jotaro Urabe and staff at the Center for Ecological Research, Kyoto University, for providing a productive working atmosphere when the first draft of this chapter was produced. My stay in Japan was supported by Kyoto University and National Science Foundation (NSF) INT-9602466. Many of these data and ideas were generated due to studies supported by NSF grants DEB-9119269 and DEB-9527322.

References

Agren, G.I. Ideal nutrient productivities and nutrient proportions in plant growth. Plant Cell Environ. 11:613–620; 1988.

Andersen, T. *Pelagic Nutrient Cycles: Herbivores as Sources and Sinks.* Berlin: Springer-Verlag; 1997.

Andersen, T.; Hessen, D.O. Carbon, nitrogen, and phosphorus content of freshwater zooplankton. Limnol. Oceanogr. 36:807–814; 1991.

Brett, M.T.; Goldman, C.R. A meta-analysis of the trophic cascade. Proc. Nat. Acad. Sci. USA 93:7723–7726; 1996.

Broecker, W.S. Ocean chemistry during glacial time. Geochim. Cosmochim. Acta 46:1689–1705; 1982.

Brooks, J.L.; Dodson, S.I. Predation, body size, and composition of plankton. Science 150:28–35; 1965.

Caron, D.A.; Goldman, J.C.; Dennett, M.R. Experimental demonstration of the roles of bacteria and bacterivorous protozoa in plankton nutrient cycles. Hydrobiologia 159:27–40; 1988.

Carpenter, S.R.; Kitchell, J.F.; Hodgson, J.R. Cascading trophic interactions and lake productivity. BioScience 35:634–639; 1985.

Chrzanowski, T.H.; Kyle, M. Ratios of carbon, nitrogen, and phosphorus in *Pseudomonas fluorescens* as a model for bacterial element ratios and nutrient regeneration. Aquat. Microb. Ecol. 10:115–122; 1996.

Chrzanowski, T.H.; Kyle, M.; Elser, J.J.; Sterner, R.W. Element ratios and growth dynamics of bacteria in an oligotrophic Canadian shield lake. Aquat. Microb. Ecol. 11:119–125; 1997.

Clarke, B.L. Stoichiometric network analysis of the oxalate-persulfate-silver oscillator. J. Chem. Phys. 97:2459–2472; 1992.

DeMelo, R.; France, R.; McQueen, D.J. Biomanipulation: Hit or myth? Limnol. Oceanogr. 37:192–207; 1992.

DeMott, W.R. The role of competition in zooplankton succession. In: Sommer, U., ed. *Plankton Ecology.* Berlin: Springer-Verlag; 1989:195–252.

DeMott, W.R.; Gulati, R.D. Phosphorus limitation in *Daphnia:* Evidence from a long-term study of three hypereutrophic Dutch lakes. Limnol. Oceanogr. 44:1557–1564; 1999.

Dobberfuhl, D.R. *N:P Stoichiometry in Crustacean Zooplankton: Phylogenetic Patterns, Physiological Mechanisms, and Ecological Consequences.* Ph.D. thesis, Arizona State University, Tempe, AZ, 1999.

Eccleston-Parry, J.D.; Leadbeater, B.S.C. Regeneration of phosphorus and nitrogen by four species of heterotrophic nanoflagellates feeding on three nutritional states of a single bacterial strain. Appl. Environ. Microbiol. 61:1033–1038; 1995.

Elser, J.J.; Chrzanowski, T.H.; Sterner, R.W.; Mills, K.H. Stoichiometric constraints on food-web dynamics: A whole-lake experiment on the Canadian Shield. Ecosystems 1:120–136; 1998.

Elser, J.J.; Chrzanowski, T.H.; Sterner, R.W.; Schampel, J.H.; Foster, D.K. Elemental ratios and the uptake and release of nutrients by phytoplankton and bacteria in three lakes of the Canadian Shield. Microb. Ecol. 29:145–162; 1995a.

Elser, J.J.; Dobberfuhl, D.; MacKay, N.A.; Schampel, J.H. Organism size, life history, and N:P stoichiometry: Towards a unified view of cellular and ecosystem processes. BioScience 46:674–684; 1996.

Elser, J.J.; Elser, M.M.; MacKay, N.A.; Carpenter, S.R. Zooplankton-mediated transitions between N and P limited algal growth. Limnol. Oceanogr. 33:1–14; 1988.

Elser, J.J.; Hassett, R.P. A stoichiometric analysis of the zooplankton-phytoplankton interaction in marine and freshwater ecosystems. Nature 370:211–213; 1994.

Elser, J.J.; Luecke, C.; Brett, M.T.; Goldman, C.R. Effects of food web compensation after manipulation of rainbow trout in an oligotrophic lake. Ecology 76:52–69; 1995b.

Elser, J.J.; Urabe, J. The stoichiometry of consumer-driven nutrient cycling: Theory, observations, and consequences. Ecology 80:735–751; 1999.

Gaedke, U.; Straile, D. Seasonal changes of trophic transfer efficiencies in a plankton food web derived from biomass size distributions and network analysis. Ecol. Model. 75/76:435–445; 1994.

Goldman, J.C.; Caron, D.A.; Andersen, O.K.; Dennett, M.R. Nutrient cycling in a microflagellate food chain.

I. Nitrogen dynamics. Marine Ecol. Prog. Ser. 24:231–242; 1985.

Goldman, J.C.; Caron, D.A.; Dennett, M.R. Nutrient cycling in a microflagellate food chain. IV. Phytoplankton-microflagellate interactions. Marine Ecol. Prog. Ser 38:75–87; 1987.

Goldman, J.C.; McCarthy, J.J.; Peavey, D.G. Growth rate influence on the chemical composition of phytoplankton in oceanic waters. Nature 279:210–215; 1979.

Hall, D.J.; Threlkeld, S.T.; Burns, C.W.; Crowley, P.H. The size-efficiency hypothesis and the size structure of zooplankton communities. Annu. Rev. Ecol. Syst. 7:177–208; 1976.

Harris, G.P. *Phytoplankton Ecology: Structure, Function, and Fluctuation.* London: Chapman and Hall; 1986.

Hassett, R.P.; Cardinale, B.; Stabler, L.B.; Elser, J.J. Ecological stoichiometry of N and P in pelagic ecosystems: Comparison of lakes and oceans with emphasis on the zooplankton-phytoplankton interaction. Limnol. Oceanogr. 41:648–662; 1997.

Healey, F.P. Interacting effects of light and nutrient limitation on the growth rate of *Synechococcus linearis* (Cyanophyceae). J. Phycol. 21:134–146; 1985.

Healey, F.P.; Hendzel, L.L. Physiological indicators of nutrient deficiency in lake phytoplankton. Can. J. Fish. Aquat. Sci. 37:442–543; 1980.

Hecky, R.W.; Campell, P.; Hendzell, L.L. The stoichiometry of carbon, nitrogen, and phosphorus in particulate matter of lakes and oceans. Limnol. Oceanogr. 38:709–724; 1993.

Hessen, D.O. The effect of substrate stoichiometry on microbial activity and carbon degradation in humic lakes. Environ. Internat. 20:67–76; 1994.

Hessen, D.O. Stoichiometry in food webs: Lotka revisited. Oikos 79:195–200; 1997.

Hessen, D.O.; Andersen, T. The algae-grazer interface: Feedback mechanisms linked to elemental ratios and nutrient cycling. Arch. Hydrobiol. Beih. Ergeb. Limnol. 35:111–120; 1992.

Hessen, D.O.; Lyche, A. Inter- and intraspecific variations in zooplankton element composition. Arch. Hydrobiol. 121:343–353; 1991.

Hutchinson, G.E. The paradox of the plankton. Am. Nat. 85:137–145; 1961.

Jurgens, K.; Gude, H. Incorporation and release of phosphorus by bacteria and phagotrophic flagellates. Marine Ecol. Prog. Ser. 59:271–284; 1990.

Karl, D.; Letelier, R.; Tupas, L.; Dore, J.; Christian, J.; Hebel, D. The role of nitrogen fixation in biogeochemical cycling in the subtropical North Pacific Ocean. Nature 388:533–538; 1997.

Karl, D.M.; Letelier, R.; Hebel, D.; Tupas, L.; Dore, J.; Christian, J.; Winn, C. Ecosystem changes in the North Pacific subtropical gyre attributed to the 1991–92 El Niño. Nature 373:230–234; 1995.

Lampert, W.; Schober, U. The importance of "threshold" food concentrations. In: Kerfoot, W.C., ed. *Evolution and Ecology of Zooplankton Communities.* Hanover, NH: Univ. Pr. New England; 1980:264–267.

Likens, G.E., ed. *An Ecosystem Approach to Aquatic Ecology: Mirror Lake and Its Environment.* New York: Springer; 1985.

Lindeman, R.L. The trophic dynamic aspect of ecology. Ecology 23:399–418; 1942.

MacKay, N.A.; Elser, J.J. Factors potentially preventing trophic cascades: Food quality, invertebrate predation, and their interaction. Limnol. Oceanogr. 43:339–347; 1998.

Main, T.; Dobberfuhl, D.R.; Elser, J.J. N:P stoichiometry and ontogeny in crustacean zooplankton: A test of the growth rate hypothesis. Limnol. Oceanogr. 42:1474–1478; 1997.

Malley, D.F.; Williams, P.C.; Stainton, M.P.; Hauser, B.W. Application of near-infrared reflectance spectroscopy in the measurement of carbon, nitrogen, and phosphorus in seston from oligotrophic lakes. Can. J. Fish. Aquat. Sci. 50:1779–1785; 1993.

Masuda, M. Stoichiometric relations of complex chemical reaction networks and stoichiometric number theory: A criterion for preserving overall stoichiometry in reduced mechanisms. J. Chem. Phys. 92:6030–6035; 1990.

Morris, I., ed. *The Physiological Ecology of the Phytoplankton.* Berkeley, CA: Univ. California Pr.; 1980.

Müller-Navarra, D. Evidence that a highly unsaturated fatty acid limits *Daphnia* growth in nature. Arch. Hydrobiol. 132:297–307; 1995.

Mullin, M.M. Webs and scales: Physical and ecological processes in marine fish recruitment. Seattle, WA: Univ. Washington Pr.; 1993.

Nakano, S. Carbon:nitrogen:phosphorus ratios and nutrient regeneration of a heterotrophic flagellate fed on baceria with different elemental ratios. Arch. Hydrobiol. 129:257–271; 1994.

Nygaard, K.; Tobiesen, A. Bacterivory in algae: A survival strategy during nutrient limitation. Limnol. Oceanogr. 38:273–279; 1993.

Olsen, Y.; Jensen, A.; Reinertsen, H.; Borsheim, K.Y.; Heldal, M.; Langeland, A. Dependence of the rate of release of phosphorus by zooplankton on the P:C ratio in the food supply, as calculated by a recycling model. Limnol. Oceanogr. 31:34–44; 1986.

Reiners, W.A. Complementary models for ecosystems. Am. Nat. 127:59–73; 1986.

Reynolds, C.S. *The Ecology of Freshwater Phytoplankton.* Cambridge: Cambridge Univ. Pr.; 1984.

Rhee, G. Effects of N:P atomic ratios and nitrate limitation on algal growth, cell composition, and nitrate uptake. Limnol. Oceanogr. 23:10–25; 1978.

Rhee, G.-Y.; Gotham, I.J. The effect of environmental factors on phytoplankton growth: Light and the interactions of light with nitrate limitation. Limnol. Oceanogr. 26:649–659; 1981.

Roemmich, D.; McGowan, J. Climatic warming and the decline of zooplankton in the California Current. Science 267:1324–1326; 1995.

Rothaupt, K.O. Laboratory experiments with a mixotrophic chrysophyte and obligately phagotrophic and phototrophic competitors. Ecology 77:716–724; 1996.

Rowe, G.T.; Baldauf, J.G. Biofeedback in the ocean in response to climate change. In: Woodwell, G.M.; MacKenzie, F.T., eds. *Biotic Feedbacks in the Global Climatic System: Will the Warming Feed the Warming?* Oxford: Oxford Univ. Pr.; 1995:233–245.

Schindler, D.W.; Beaty, K.G.; Fee, E.J.; Cruikshank, D.R.; DeBruyn, E.D.; Findlay, D.L.; Linsey, G.A.; Shearer, J.A.; Stainton, M.P.; Turner, M.A. Effects of climatic warming on lakes of the central boreal forest. Science 250:967–970; 1990.

Smith, V.H. Light and nutrient dependence of photosynthesis by algae. J. Phycol. 19:306–313; 1983.

Sommer, U. Phosphorus-limited *Daphnia:* Intraspecific facilitation instead of competition. Limnol. Oceanogr. 37:966–973; 1992.

Sterner, R.W. The ratio of nitrogen to phosphorus resupplied by herbivores: Zooplankton and the algal competitive arena. Am. Nat. 136:209–229; 1990.

Sterner, R.W.; Clasen, J.; Lampert, W.; Weisse, T. Carbon:phosphorus stoichiometry and food chain production. Ecol. Lett. 1:146–150; 1998.

Sterner, R.W.; Elser, J.J.; Fee, E.J.; Guildford, S.J.; Chrzanowski, T.H. The light:nutrient ratio in lakes: The balance of energy and materials affects ecosystem structure and process. Am. Nat. 150:663–684; 1997.

Sterner, R.W.; Elser, J.J.; Hessen, D.O. Stoichiometric relationships among producers, consumers, and nutrient cycling in pelagic ecosystems. Biogeochemistry 17:49–67; 1992.

Sterner, R.W.; Hagemeier, D.D.; Smith, W.L.; Smith, R.F. Phytoplankton nutrient limitation and food quality for *Daphnia.* Limnol. Oceanogr. 38:857–871; 1993.

Sterner, R.W.; Hessen, D.O. Algal nutrient limitation and the nutrition of aquatic herbivores. Annu. Rev. Ecol. Syst. 25:1–29; 1994.

Sterner, R.W.; Schulz, K.L. Zooplankton nutrition: Recent progress and reality check. Aquat. Ecol. 33:1–19; 1998.

Sundbom, M.; Vrede, T. Effects of fatty acid and phosphorus content of food on the growth, survival, and reproduction of *Daphnia.* Freshwat. Biol. 38:665–674; 1997.

Tezuka, Y. The C:N:P ratio of phytoplankton determines the relative amounts of dissolved inorganic nitrogen released during aerobic decomposition. Hydrobiologia 173:55–62; 1989.

Tezuka, Y. Bacterial regeneration of ammonium and phosphate as affected by the carbon:nitrogen: phosphorus ratio of organic substrates. Microb. Ecol. 19:227–238; 1990.

Tilman, D. *Resource Competition and Community Structure.* Princeton, NJ: Princeton Univ. Pr.; 1982.

Urabe, J. N and P cycling coupled by grazers' activities: Food quality and nutrient release by zooplankton. Ecology 74:2337–2350; 1993.

Urabe, J. Effects of zooplankton on seston stoichiometry: Magnitude, direction, and implications. Abstracts, ASLO Annual Meeting Reno, NV, 1995.

Urabe, J.; Classen, J.; Sterner, R.W. Phosphorus-limitation of *Daphnia:* Is it real? Limnol. Oceanogr. 42:1436–1443; 1997.

Urabe, J.; Nakanishi, M.; Kawabata, K. Contribution of metazoan plankton to the cycling of N and P in Lake Biwa. Limnol. Oceanogr. 40:232–241; 1995.

Urabe, J.; Sterner, R.W. Regulation of herbivore growth by the balance of light and nutrients. Proc. Nat. Acad. Sci. USA 93:8465–8469; 1996.

Vadstein, O.; Jensen, A.; Olsen, Y.; Reinertsen, H. Growth and phosphorus status of limnetic phytoplankton and bacteria. Limnol. Oceanogr. 33:489–503; 1988.

Vitousek, P. Nutrient cycling and nutrient use efficiency. Am. Nat. 119:553–572; 1982.

Vrede, T.; Andersen, T.; Hessen, D.O. Phosphorus distribution in three crustacean zooplankton species. Limnol. Oceanogr. 44:225–229; 1998.

Index

Above-canopy irrigation, 342
Aboveground net primary productivity (ANPP), 31–43
  errors associated with estimates of, 37–41
  fast turnover ecosystems, 33–36
  optimal methodology, 41
  slow turnover ecosystems, 33–36
Absorbed photosynthetically active radiation (APAR)
  constraints on conversion to biomass, 46
  definition, 45
  NPP algorithm, 50
relation to NDVI, 45
Absorbents, 241
Acer, 154, 342, 344
Acetylene inhibition technique, 92, 253
Acidification. *See also* Atmospheric deposition; Hydrogen ions; pH
  acid rain, 265
  aquatic ecosystems, 330–340
  chemistry of, 331
  experiments, large-scale, 334–338
  experiments, smaller-scale, 332–333
  recovery, 335
Acridine orange (AO), 140–141
Adaptive management, 314
ADAR, 13
Advanced spaceborne thermal emission and reflection radiometer (ASTER), 14
Advanced synthetic aperture radar (ASAR), 17
Advection/decomposition model, 133
Advective transport, 236
Aerial photography, 11–13, 22
Aerial remote sensing, 12–18
Aerodynamic method, 166, 167, 269
Aerosols, 265–266, 268, 269, 353
Agriculture, 291–292, 341. *See also* Crops
Air
  density of, 170
  EMEP, 367
  FATI, 362
  interface with soil, 236–242
  interface with water, 239–241
Airborne laser profiling systems, 19
Airborne synthetic aperture radar systems, 19
Aircraft-based techniques, 19, 175–176, 242
Albedo, MODIS sampling, 14
Algae, 318, 391, 399. *See also* Planktonic systems
Aluminum (Al), 269, 292, 299, 334
Amazon Boundary Layer Experiments (ABLE-2A and B), 244
Amino acids, 144
Aminopeptidases, 145
Ammonia (NH_3), 221
  bacterial nitrate reduction, 91
  chemical inhibitors of assimilation, 218
  mechanism of adsorption, 269
  methods of analysis, 243
  plant emissions, 241
  in the redox sequence, 86–87
  trapping of, 241
  volatilization, 253, 296
Ammonia accumulation in closed incubations, 90
Ammonium chloride (NH_4Cl), 297
Ammonium ions (NH_4^+)
  atmospheric deposition, 270
  canopy uptake and leaching, 251
  fixation on minerals, 297
  nutrient addition experiments, 294
  production by decomposition, 104
Ammonium nitrate (NH_4NO_3), 297
Ammonium sulfate [$(NH_4)_2SO_4$], 269
Amynthas agrestis, 322
Amynthas hawayanus, 322
Anaerobic respiration, inhibitors of, 218
Analysis phase, ecosystem modeling, 381
Anderson model, 397–404

Animals. *See also specific animals*
belowground, 318–329
indicators of water source, 194–195
Anoxic bag incubations, 94
Anoxic jar incubations, 89–90
ANPP. *See* Aboveground net primary productivity
Anthropogenic effects. *See also specific effects*
acidification of ecosystems, 330, 331
ecosystem manipulations, 313–314
on species ranges, 355
regional-scale nutrient fluxes, 280
Antimycin, 309
AO (acridine orange), 140–141
APAR. *See* Absorbed photosynthetically active radiation
Apoblasts, 201
Arctic Boundary Layer Experiments (ABLE-3A and B), 244
Arthropods, 152, 153–154
ASAR (advanced synthetic aperture radar), 17
Ash, in soil, 59
Assimilation, definition, 115
ASTER (advanced spaceborne thermal emission and reflection radiometer), 14
Atmospheric boundary layers (ABLs), 161–163, 169, 175–177
Atmospheric deposition
acidification of ecosystems, 330–340
ecosystem nutrient budgets, 251–252
natural levels, 293
role of, 265–276
scales of inquiry, 266–267
Autotrophs, 45, 218, 219, 392
AVHRR, 22
AVHRR GAC, 13
AVIRIS, 13, 15

BABH, Basal area at breast height, 37
Backscatter, 9, 16, 19, 24
Bacteria. *See also* Microbes
abundance and biomass, 139–143
active versus inactive cells, 141–142
carbon cycling, 138–150
electroreceptors, 86
flow cytometry, 141
food replication, 401
growth efficiency (BGE), 144
production (BP), 143
respiration (BR), 144
sample preservation, 141
secondary production, 138–139
substrate uptake and turnover, 144–146
Balloons, photography from, 12
Band-to-band registration, 13
Barriers, species exclusions, 320
Basal area at breast height (BABH), 37
Belonolaimus longicaudatus, 323
Belowground net primary production (BNPP), 58–71
carbon balance, 62–63
example calculations, 60
ingrowth cores, 60–61
isotopic estimation of, 61–62
minirhizotrons, 63–65
Monte Carlo simulations, 66–67
nitrogen balance, 63
uncertainty in estimates, 65–69
Benomyl, 322
Benthic flux chambers, 89
Benthic respiration, 90–91
BGE (bacterial growth efficiency), 144
Big-leaf model, deposition, 269–270
Biocides, species manipulation, 321–322
Biogenic compounds, 174, 235–248
Biogeochemical processes
extrapolating values, 282–283
landscape and regional, 277–278
modeling movements, 281–283
planktonic food webs, 389–406
response to nutrient additions, 293
Biomass
aboveground estimates, 35–36
accumulation of error, 38
bacterial, 139–143
belowground change, 58
coefficients of variation for BNPP input variables, 67–68
direct measurement, 23
frequency of sampling, 155–156
Holopedium gibberum, 336
indirect estimation, 23–24
nutrient addition experiments, 294
production, 38
radar backscatter saturation, 24
relation to productivity, 31–32
seasonal patterns, 33–35
understory, 37
Biome classes, 49
Biome parameter look-up table (BPLUT), 46, 48
BIOME-BGC simulations, 46–49
BIOPAK software, 23
Biotic manipulations. *See also* Transplants
aquatic ecosystems, 308–317
belowground animals, 318–329
food webs, 308
keystone species, 313
species exclusions, 320
species introduction and transplants, 323–324
Bioturbation, 88
Blood, 194
Body elemental composition, 396

Bogs plant decomposition, 127
Bone, 194–195
Boreal ecosystem-atmosphere study (BOREAS), 244
Bosmina longirostris, 333
Bottles, 73, 74–75, 77–79, 88–89
Bowen ratio method, 166, 167–168, 269
Branches, 9, 37
Bromide ions (Br^-), 254
Bubbles. *See* Ebullition
Buried bag techniques, 218, 219
Burning, 323. *See also* Combustion

C/P ratios, 391–392, 393–394, 395, 396–398, 401
C_3 photosynthetic pathways
  carbon isotope use, 123, 192, 194
  climatic conditions, 49
  decomposition rates, 113
  PAR conversion efficiency, 46
  seasonal productivity, 35
C_4 photosynthetic pathways
  carbon isotope use, 123, 194
  climatic conditions, 49
  decomposition rates, 113
  PAR conversion efficiency, 46
  seasonal productivity, 35
Caged plots, 152–154
Calcium (Ca)
  isotopic techniques, 273
  as limiting nutrient, 293
  mechanism of deposition, 269
  and NH_4^+ absorption, 297
  release by decomposition, 104
  soil loss, 292
Calcium carbonate ($CaCO_3$), 88–89
Caliche, 194
Canopies
  architecture models, 8–10
  atmospheric mixing, 166
  capacitance, 35
  descriptors, 8
  estimation of biomass, 24
  estimation of cover, 9
  fluxes, 161–180
  height of, 19
  light, interactions with, 8
  micrometeorological methods, 161
  nitrogen uptake, 251
  reflectance, 13
  SAR imagery of cover, 17
  three-dimensional structure of, 24–25
Canopy process models, 384
Canopy sublayers (CSLs), 162
Capacitance, in double sampling, 35
Carbofuran, 322
Carbon (C). *See also* Carbon cycling; Dissolved inorganic carbon; Dissolved organic carbon; Particulate organic carbon; Soil organic carbon
  BIOME-BGC simulations, 46–49
  ^{12}C from SOM pools, 126
  ^{13}C experiments, 113
  ^{13}C organic matter analysis, 188
  ^{13}C plant components, 127
  ^{14}C technique in aquatic systems, 75–79
  ^{14}C as tracer, 117
  $\delta^{13}C$ with depth, 123–128
  $\delta^{13}C$ within organisms, 281
  $\delta^{13}C$ with soil depth, 121
  $\delta^{13}C$ in tree rings, 193
  ecosystem flow, 32, 33
  estimated annual balance, 164
  isotopes in SOM, 119–128
  isotopic abundance, 182
  isotopic estimates of BNPP, 61–62
  isotopic ratios, 190
  long-term mineralization in soil, 112
  plant budgets, 61
  sequestration potential of vegetation, 341
  soil storage, 284
  soil stores, 104–106
  well-mixed box models, 119–123
Carbon balance, estimation of BNPP, 62–63
Carbon cycling
  global studies, 44
  large-scale validation, 54
  pelagic ecosystem methods, 138–150
  pelagic environments, 139
  processes in soil, 118
  SOM transformations, 119
Carbon dioxide (CO_2)
  and global warming, 341, 353
  and primary production, 72
  atmospheric $\delta^{18}O$, 193
  benthic flux measurements, 88–89
  canopy process models, 384
  canopy profiles, 163
  carbonic acid formation, 331
  daily changes, 79
  density in air, 170
  estimating primary production, 73
  global flasks network, 53–54
  global flux, 44
  habitat manipulations, 323
  heterotrophic decomposition, 118
  infrared gas analysis, 110, 112
  methods of analysis, 243
  production by decomposition, 104
  sampling periods, 238
  seasonal soil efflux, 164
  soil respiration, 118

Carbon dioxide (CO_2) (*continued*)
SOM fractionations, 111–113
super sinks for, 221
vertical profiles, 162
Carbon isotope models, SOC, 124–126
Carbon monoxide (CO), 243
Carbonates, 75, 331–332
Carbonic acid, 331
CASI airborne sensor, 13
Catenas, 278–279
Cation deposition, 273
CCD (charge coupled device), 12
Cell size, and biomass, 142–143
Cellulose, 110, 186–187, 193–194
CENTURY model, 106, 384–385
Cesium (Cs), 281
Channel straightening, 311
Charge coupled device (CCD), 12
Cherry pickers, 12
CHH, SIR-C, 18
Chloride ions (Cl^-), 254
Chlorine (Cl), deposition, 251, 269
Chlorofluorocarbons (CFCs), 353
Clay, 201, 206, 298
Clearcuts, 18
Climate. *See also* Weather
C isotope fractionations, 122
constraints on NPP, 54
ecosystem manipulations, 353–369
field manipulations, 356–357, 357–362
GCM model, 353–355
global change, 353–355
global warming, effect of, 341
litter fall sampling, 36
manipulation experiments, 356–357
modeling, 353, 373–388
and PAR conversion efficiency, 46
reconstruction, 193–194
simulation of warming, 359–360
Climatology, NASA Data Assimilation Office input, 50–51
CLIMEX projects, 342–343, 359
Closed-path analyzers, 170, 171
Cloud deposition, 266, 270–271
Coastal marshes, 239
Coastal Zone Color Scanner, 82
Combustion, 104–105, 110, 188
Community models, ecosystem, 374
Compartment models, ecosystem, 374, 376–381
Compensatory growth, 154–156
COMWEB project, 402
Conceptual models, ecosystem, 374
Condition, stand structure, 8
Conditional sampling (CS), 174
Conifers, surface area, 20
Conservation of mass, 62
Consumption, 151–154, 216
Continuous models, canopy architecture, 9
Continuous sampling, 238, 279
Convection, 239
Convective boundary layers (CBLs). *See* Atmospheric boundary layers (ABLs)
Cooperative Programme for the Monitoring and Evaluation of Long Range Air Pollutants in Europe (EMEP), 267
Cover, 8, 22–23
Cows, consumption by, 152
Crickets, 322
Critical factors, ecosystem modeling, 384
Crops
carbon isotope studies, 122
litter decomposition, 108
smooth aerodynamic surfaces, 49
soil carbon storage, 284
Crowns, 9, 12, 13
Cryoconcentration, 241
Cryogenic vacuum line, 185
CTC (5-cyano-2,3-ditolyl tetrazolium chloride), 142
Current deflectors, aquatic, 311
5-Cyano-2,3-ditolyl tetrazolium chloride (CTC), 142

Daedalus, 13
Daphnia, 312, 333, 394, 397
DAPI (4′6-diamidino-2-phenylindole), 140–141
DBH. *See* Diameter at breast height
DBL (diffusive boundary layer), 89
Decomposition
advection/decomposition model, 133
bogs plants, 127
definition, 104
diffusion/decomposition model, 133
and energy flow, 32
heterotrophic, 118
labeling plant material, 224
litter, 36
and organic matter dynamics, 104–116
rate variation, 104
Deforestation, and global warming, 353
Delivery vectors, atmospheric deposition, 266
Delta notation, definition, 181
Denitrification. *See also* Nitrification
bacterial nitrate reduction, 91
chemical inhibitors, 218
equation, 87
leached nitrogen, 252–253
nitrogen formation, 88
Density flotation gradients, 105
Density fractionation, 111

Deposition
acidification of ecosystems, 330–340
atmospheric, 265–276
big-leaf model, 269–270
ecosystem nutrient budgets, 251–252
multi-leaf model, 269–270
National Atmospheric Deposition Program, 267, 331
natural levels, 293
nitrogen, 292
and throughfall, 251
Destructive gravimetric sampling, 345
Deuterium, 185–186
DFAA (dissolved free amino acids), 145
Diameter at breast height (DBH), 24, 36, 37, 40
4′6-Diamidino-2-phenylindole (DAPI), 140–141
DIC. *See* Dissolved inorganic carbon
Dielectric constants, 16
Diffusion, 236–242. *See also* Gases
Diffusion/decomposition model, 133
Diffusive boundary layer (DBL), 89
Digital photography, 12, 21–22
Dimethyl sulfide (DMS), 239
DIN (dissolved inorganic nitrogen), 256
Diode lasers, tunable, 244
Dissolved free amino acids (DFAA), 145
Dissolved inorganic carbon (DIC), 75–79, 138–139
Dissolved inorganic nitrogen (DIN), 256
Dissolved neutral monosaccharides (DNMS), 145
Dissolved organic carbon (DOC), 138, 146, 255, 402–403
Dissolved organic nitrogen (DON), 118–119, 256, 266
Distance, use of rangefinders, 11
DMS emissions, 239, 241
DNA, measurement of bacterial production, 143
DNMS. *See* dissolved neutral monosaccharides
DOC. *See* Dissolved organic carbon
DOLY model, 385
DON. *See* Dissolved organic nitrogen
Dot grids, 12
Double sampling techniques, 35–36
Douglas fir, 10, 14
Dowels, decomposition studies, 110
Droop equation, 398
Droughts, 341
Dry deposition, 266, 268–270, 271, 331
Drying, 320
Dust aerosols, 265–266

Earth Observing System (EOS), 14, 44–57
Earthworms, 119, 322
Ebullition, 88, 239
ECD (electronic capture detectors), 243
ECOFEE, N data, 256
Ecosystem modeling, 373–388
Ecotron, 324, 356
Eddy accumulation methods, 166, 282–283
Eddy correlation methods, 282–283
Eddy covariance flux towers, 54
Eddy covariance methods, 166
atmospheric deposition, 269
correction terms, 169–170
evaluation of systems, 173–174
sensors, 170–172
systems, 165
theory, 168–169
Eddy diffusivity, 167
Edge effects, 35, 266–267, 349
El Niño, 402
Electrofishing, 308
Electromagnetic cover area measurement, 22
Electromagnetic rangefinders, 11
Electron acceptors, 86–87, 90–91
Electron transport system (ETS), 142
Electron transport system activity (ETSA), 90
Electronic capture detectors (ECD), 243
Electroshocking, 320
EMEP (Cooperative Programme for the Monitoring and Evaluation of Long Range Air Pollutants in Europe), 267
Enclosures, 236–242
Energy flow
balance at surfaces, 167–168
benthic sediments, 86
compartment models, 378–381
ecosystem schematics, 32
phytoplankton communities, 73
and primary productivity, 31
in spring, 380
ENSF, N data, 256
Environmental impact statements, 314
ENVISAT, 17
EOS. *See* Earth Observing System
Epifluorescent microscopy, 140–141
Equilibrium seeking, 384
Errors leading to overestimation (ELOs), 38
Errors leading to underestimation (ELUs), 37
ERS-1, 17
ERS-2, 17
Esterases, 145
Estuaries, 80–81
ETS (electrotransport system), 142
ETSA (electron transport system activity), 90
Eutrophication, 72
Evaporation, 170, 183–184
Evapotranspiration (Et), 192
EXMAN projects, 342
Exoenzymes, 145, 218

Farming, 267. *See also* Agriculture; Crops
FATI (free air temperature increase), 362
Feathers, 194–195

Fermentation, 86
Ferrous carbonate ($FeCO_3$), 89, 90
Ferrozine, 93
Fertilizers
  isotopically labeled, 300–302
  nitrogen availability, 296–297
  nutrient addition experiments, 296
  phosphorus, 298–300
  potassium, 299
  sulfur, 299–300
  trials, 291
Fetch, definition, 164
Fetch/height ratio, 165
Film, photographic, 11, 12
Filter paper, 110, 204
Fire, 323. *See also* Combustion
Fish, 309–310, 335
Fisheries, 313–314
Fishing, 314
Flame photometric detectors (FPDs), 243
Flooding, spectral analysis, 18
Flow cytometry, 141–142
Fluid-filled pipes, 360
Flumes, 252
Fluorochromes, 140–142
Flux footprints, 164–165, 166, 242
Fluxes, 161–180
FLUXNET, tower operation, 54
Fog, 266
Foliage, 8, 9, 19–21, 25. *See also* Leaves
Food webs
  alteration of structure, 310
  biogeochemistry, 389–406
  and compartment models, 376–378
  human manipulation, 314
  planktonic, 390–397
  rhizosphere, 321–322
  species manipulations, 308
  whole-lake, 403
Footprints, definition, 12, 165
Forest-BGC model, 385
Forests. *See also* Trees
  aerodynamic surfaces, 49
  biomass estimation, 23–24
  decline in Ca, 292
  deposited N, 258
  diffusive transport in soil, 124
  discrimination of, 23
  heat tables, 36
  input-output budget for catchment, 250
  irrigation, 341
  litter decomposition, 108
  manipulated throughfall quality, 342
  spectral analysis, 18
  structure of canopies, 8
  tropical, 37
  turbulence over, 166
Fossil fuels, 330
Fossil records, 355
FPAR. *See* Fraction of absorbed photosynthetically active radiation
FPDs (flame photometric detectors), 243
Fractal models, 8, 9
Fraction of absorbed photosynthetically active radiation (FPAR), 14, 21, 45, 49
Free Air Temperature Increase (FATI), 362
Freeze/thaw, SAR imagery, 17
Freezing, species removal, 320
Fulvic acid, 105
Fungi, soil, 318
Fungicides, 321–322

Gap fraction methods
  data, 8
  estimation of cover, 22
  indirect measurement, 21
  instruments for analysis, 11
  LAI, derivation of, 21
Gap models, 386
Gas chromatography (GC), 110, 243
Gases. *See also* Trace gases; *specific gases*
  advective movement, 268
  deposition, 266, 269
  soil–air interface, 236–239
  water surface, 80–81
  water–air interface, 239–241
Gaussian plume approach, 165
General circulation models (GCM), 353–355
General Oceanic Go-Flo bottles, 78
Geographic information systems (GIS), 283
Geometrical optical models, 9
Gill propeller anemometer, 171
Global positioning systems (GPS), 11, 13
Global Terrestrial Observing System (GTOS), 53
Global warming
  aerosols, effect of, 353
  carbon dioxide (CO_2), 341, 353
  deforestation, 353
  DOC, 402–403
  effect on climate, 341
  GCM models, 353–355
  greenhouse gases, 341, 353
  infrared radiation, 353
  nitrous oxide, 359
  rainfall patterns, 362
  simulation of, 359–360
  species ranges, 355
  trace gas losses, 292
  ultraviolet radiation, 363–364
Glucose, 145

Glucosidases, 145
GPP. *See* Gross primary productivity
GPS (global positioning system), 11, 13
Grab samples, 252
Grassland Biome ELM model, 384
Grasslands
  aboveground biomass, 35
  biogeochemical simulation model, 278
  deposited N, 258
  energy flow, 32
  estimation of ANPP, 33
  litter decomposition, 108
  manipulation of throughfall, 342, 345
  overestimation of productivity, 39–40
  photosynthetic pathways, 49
  smooth aerodynamic surfaces, 49
Gravimetric measurements, 201–202
Grazers, 154–156, 397–400
Greenhouse gases, 341, 353. *See also specific gases*
Greenhouses, 357–359
Gross consumption rates, 226
Gross primary productivity (GPP)
  daily estimates, 51–52
  definition, 31, 72
  EOS, 44–57
  light and dark bottle technique, 74–75, 77–79
  oceans, contribution of, 72
Gross production rates, 226
Groundwater, 184, 257
Growth, respiration costs, 52–53
Growth chambers, 355–356
GTOS (Global Terrestrial Observing System), 53

Habitat manipulations, 310–311, 323
Harvesting techniques, 35
Heat, 90, 167–168, 174. *See also* Global warming; Temperature
Heat balance method, 208–209
Heat pulse method, 208
Heavy metals, 265
Height
  BABH, 37
  canopy, 19
  DBH, 24, 36, 37, 40
  fetch/height ratio, 165
  vegetation architecture, 12
Helsinki University of Technology scatterometer (HUTSCAT), 17
Hemicellulose, 187. *See also* Cellulose
Hemispherical photographs, 8, 9, 10, 11
Herbicides, 311
Herbivory, 151–157
Heterodera schactii, 323
Heterotrophic nitrification, 217–218
High-pressure flowmeters (HPFM), 210
Highly unsaturated fatty acids (HUFA), 395
Holopedium gibberum, 333, 336
Horizontal stand descriptors, 8
HPFM (high-pressure flowmeters), 210
Hubbard Brook Experimental Forest, 249–252, 255
HUFA (highly unsaturated fatty acids), 395
Human interventions
  acidification of ecosystems, 330
  ecosystem manipulations, 313–314, 353
  regional-scale nutrient fluxes, 280
  and species ranges, 355
Humic acid, 105
Humin, 105
HUTSCAT (Helsinki University of Technology scatterometer), 17
HYBRID model, 385
Hydraulic conductance, 209
Hydrochloric acid (HCl), 221, 265
Hydrogen (H_2), 182, 189, 191
Hydrogen ions (H^+), 265, 269, 331. *See also* Acidification; pH
Hydrogen sulfide (H_2S), 88, 93, 95, 243
Hydrologic sampling methods, 252
Hydroxylates, 86
Hypolimnion, 239

IBIS (integrated biosphere simulator), 354
IBP (International Biological Program), 33, 384
IC (ion chromatography), 243
IERs (ion exchange resins), 221–222
IFS (Integrated Forest Study), 256
In situ diel, 73, 79–81
Individual-based models, 374, 385–386
Infrared gas analyzers (IRGA), 110, 170, 172–173
Infrared radiation, 353, 360–362
Infrared range finders, 11
Ingrowth cores, 60–61
Input–output ecosystem budgets, 250–253
INSAR (interferometry SAR), 19
Insecticides, 321–322
Insects, adaptation, 356
Integrated biosphere simulator (IBIS), 354
Integrated Forest Study (IFS), 256
Interferometry, 17–18, 19
International Biological Program (IBP), 33, 384
International Tundra Experiment (ITEX), 357–358
Inundation patterns, 17
Invertebrates, 309, 318, 319, 320–321. *See also specific invertebrates*
Ion chromatography (IC), 243
Ion exchange resins (IERs), 221–222
Irgalan Black, 140

Iron (Fe)
atmospheric deposition, 265
benthic fluxes, 88
chemical inhibitors of oxidation, 218
in ecosystem control, 78
organotrophic reduction, 91
in the redox sequence, 86–87
reduction in benthic sediments, 92–95
reduction equation, 87
Irradiation, 218–220, 320
Irrigation, 341, 343–344
Isopiestic thermocouple psychrometry, 203
Isoprene, 241
Isotopes. *See also* Radioisotopes; Stable isotopes
atmospheric deposition, 272–273
BNPP estimation, 61–62
kinetic effects, 121–122
label fertilizers, 291
movement of sink pool, 225
natural abundances, 181, 230–231
nutrient addition experiments, 300–302
nutrient flow measurement, 225–229
nutrients transformations measurement, 223–225
ocean water, 183
in precipitation, 132
soil-to-plant fractionation, 131
in SOM, 128
transpiration ratios, 192
Isotopic methods. *See also* Radioisotopes; Stable isotopes
dilution, 224–229
exchange kinetic technique, 225–226
fractionation, 121–122
mass-balances, 271
multi-box isotope models, 126–128
pairing methods, 253
production in aquatic systems, 75–79
ratio mass spectrometry, 181–184
stable isotope ratio analyses, 181–198
tracers, 258–259
well-mixed one box models, 129–132
ITEX (International Tundra Experiment), 357–358

JABOWA model, 386
JERS-1, 17

Katabatic drainage, 169
Keystone factors, 384
Keystone species, 313
Kinetic isotope effect, 121–122

LADs (leaf angle distributions), 9, 25
LAI. *See* Leaf area index
Lakes, 310–312, 330–340, 390
Land surface temperature, 14
Land-use management, 278
Landcover, 17, 23, 46, 50
LANDSAT, 13, 22
LANDSAT 7, 14
LANDSAT Thematic Mapper (TM), 13, 18
Landscapes, 278–279, 280
Langrangian stochastic dispersion models, 242
Laser vegetation imaging sensor (LVIS), 12
Lasers
airborne profiling systems, 19
altimetry, 12, 20
diode, 244
LVIS, 12
penetration, 12, 21
rangefinders, 11
SLICER altimetry, 20
Lead (Pb), 269
Leaf angle distributions (LADs), 9, 25
Leaf area index (LAI)
and APAR, 45
definition, 36
direct measurement, 20
estimation of cover, 9
FPAR, relation to, 49
geometrical optical methods, 24
indirect measurement, 21
NDVI estimation, 22
satellite mapping of, 54
Leaves. *See also* Foliage
area, 8, 22–23
canopy architecture models, 8–9
capacitance, 35
consumption, 153–154
optical properties, 13
organic matter sampling, 186–189
production estimates, 36–37
sampling considerations, 187
total area, 8
tracing of, 20
turnover time, 36
water extraction, 185
water sampling, 184
Lenses, photographic, 11–12
Leucine, 143, 144
Lexical phase, climate modeling, 373–374
LHH, SIR-C, 18
LHV, SIR-C, 18
Lichens, 292
LIDAR (light detection and ranging), 12, 19, 243
Light
interactions with canopies, 8
and leaf production, 36
light/nutrient hypothesis, 391, 401–402
monochromatic, 12

Light detection and ranging (LIDAR), 12, 19, 243
Lignins, 49, 127, 187
Lindeman, Raymond, 374
Line quantum sensors, 11
Litter
  collection of, 110
  decomposition, 106–110
  definition, 23
  pools, 32, 34–35
  woody detritus decomposition, 109
Litter bags, 107–108, 320–321
Litterfall, 36, 40
Loam, 201
Logistic equation dynamics, 377
Lolium rigidum, 152
Long-path fourier-transform infrared spectrometry, 243–244
Long-term ecological research (LTER), 252
Loop analysis, 383
LTER (long-term ecological research), 252
LVIS (laser vegetation and imaging sensor), 12
Lysimetry, 253–258

Macronutrients, 391
Macrophytes, 310–311
Magnesium (Mg), 88, 269, 293, 299
Manganese (Mn), 86–87, 91, 92–95
Marine snow, 79
Marshes, 127
MAS, 13
Mass water content, 199
Mass water content of soils (q_m), 201–202
Mass water percentage, 199
Mass-balance techniques, 271–272
Material flow, 376–378, 378–381, 385
Material transfer models, 384–385
Mean residence time (MRT), 225
Mercury (Hg), 334
Mesocosms, 332–333, 355–356
Meteoric water lines (MWL), 183
Methane (CH_4)
  early studies, 244
  ebullition, 88
  fluxes, 240
  methods of analysis, 243
  in the redox sequence, 86–87
Methanogenesis, 86–87, 96
Methanotrophy, 218
Methylene blue, 309
4-Methylumbelliferyl (MUF), 145
Microautoradiography, 142
Microbes, 138–150, 318, 356, 400–401. *See also* Bacteria; Planktonic systems
Microcosms, 355–356, 374
Micrometeorological techniques, 161, 242, 267
Microwave radiometers, 201, 206–207
Microwaves, 9, 14–18, 21, 320
Migration, 195, 355
Mineral horizons, 110, 119
Mineralization
  assays, 89–90
  benthic flux measurements, 88–89
  carbon, 87, 112
  definition, 215
  nitrogen, 218
  organic matter, 86
  oxygen, 88–89
  phosphorous, 218–219
Minirhizotrons, 63–65, 67–68
Minnows, 309
Missing sink question, 44
Mites, 322
Modeling phase, ecosystem modeling, 375
MODIS (moderate resolution imaging spectroradiometer), 14, 45
Monarch butterflies, 195
Monochromatic light, 12
Monolith lysimeters, 256–258
Monoterpenes, 241
Monte Carlo analysis, 65–69
Moorlands, 168
Mortality, 376
Mössbauer spectroscopy, 93
Moth balls. *See* Naphthalene
Mud flats, 239
MUF (4-methylumbelliferyl), 145
Multi-box isotope models, 126–128
Multi-leaf model, deposition, 269–270
Multiple commodity models, 374
Multiple community models, 383–386
Multispectral imagery, 22
Multispectral scanners, 13–14
Multivariate techniques, 279

N/P ratios, 391–392, 393, 394, 395–397, 302
NADP. *See* National Atmospheric Deposition Program
Naphthalene, 322
NASA (National Aeronautics and Space Administration), 12, 14, 44, 50–51
National Atmospheric Deposition Program, 331
  AIRMoN, 268
  National Trends Network (NADP/NTN), 267
Natural abundance methods, 230–231
NCP (net community productivity), 31
NDVI (normalized difference vegetation index), 22, 24, 45
Near-infrared (NIR), 12, 13
Near-infrared reflectance spectroscopy (NIRS), 402

NEE (net ecosystem exchange), 54, 163–164
Nematicides, 321–322
Nematodes, 152
NEP (net ecosystem productivity), 31, 72, 73
Net community productivity (NCP), 31
Net ecosystem exchange (NEE), 54, 163–164
Net ecosystem productivity (NEP), 31, 72, 73
Net fine root production (NFRP), 58–59, 62–63, 64
Net primary productivity (NPP)
  aboveground (ANPP), 31–43
  annual estimation, 52–53
  availability of data, 53
  belowground (BNPP), 58–71
  definition, 31
  errors and estimation, 37–41
  final algorithm, 51–53
  from the EOS, 44–57
  global, 44–49, 53–55
  logical and data flow diagrams, 51, 52
  multiple nutrient limitation, 293
  nutrient additions, response to, 293
  soil invertebrates, 319
  soil respiration, 118
  spatial variability, 44
Net production rates, 215
Net radiometers, 168
Neutron probe measurements, 345
New Zealand flatworm, 322–323
NFRP (net fine root production), 58–59, 62–63, 64
NIR (near-infrared), 12, 13
Nitrate (NO_3^-)
  atmospheric deposition, 265, 269
  bacterial reduction, 91–92
  canopy uptake and leaching, 251
  conversion to nitrites, 292
  inhibitors of assimilation, 218
  isotope dilution experiments, 228
  nutrient addition experiments, 294
  production, 216
  streamwater and Bs horizon, 255
Nitric acid (HNO_3), 269, 330, 332
Nitric neutralization, 332
Nitric oxide (NO), 243
Nitrification. *See also* Denitrification
  autotrophic inhibitors, 218
  benthic flux measurements, 88
  estimated rate of, 258
  heterotrophic, 217–218
  isotope dilution measurement, 226–227
  by urea, 296
Nitrogen (N). *See also* Denitrification; Nitrification; Nitrogen fixation
  addition to soil, 292
  atmospheric deposition, 251–252, 265, 273
  balance, 67–68
  balance and dynamics, 249–264
  benthic fluxes, 92
  BIOME-BGC simulations, 47, 49
  cycling, 128, 334
  $\delta^{15}N$ and soil age, 130
  $\delta^{15}N$ with soil depth, 121
  ecosystem scale, 258–259
  estimation of NFRP, 63, 64
  fertilizers, 296–298, 301
  fixation, 118, 218, 225, 230–231, 257
  formation during denitrification, 88
  isotope dilution experiments, 225–226
  isotope pairing methods, 253
  leaching, 292
  as limiting nutrient, 293
  lysimetry of groundwater, 257
  mass-balance calculations, 272
  mineralization, 218
  nutrient flow, 223–224
  of nitrogen cycling, 132
  precipitation, 132
  ratio to lignin, 49
  soil loss pathways, 118–119
  soil-to-plant fractionation, 131
  SOM, 113, 119, 128, 132–134
  tracers, 281
  well-mixed one box model, 129–132
Nitrogen dioxide (NO_2), 265, 269
Nitrogen oxide (NO), 238
Nitrogen saturation experiment (NITREX) sites, 254, 256, 259
Nitrous oxide (N_2O), 174, 243, 244, 359
NMHC, 243
NOAA, 22
Non-methane hydrocarbons, 174
Nonphotosynthetic vegetation (NPV), 23
Normalized backscatter coefficient (σ_0), 16
Normalized difference vegetation index (NDVI), 22, 24, 45
NPP. *See* Net primary productivity
NPV (nonphotosynthetic vegetation), 23
NS001, 13
Nutrient-addition experiments
  addition rates, 295
  alternatives to, 302–303
  experimental design, 293–300
  form of nutrients added, 296
  historical, 291–292
  timescale of response, 295
  timing of addition, 295–296
Nutrients
  atmospheric deposition, 265–276
  balance and dynamics, 249–264

barriers to loss, 117
budgets, 221
constraint on leaf area, 46
delivery vectors, 266
efficiency, 391–392
human disturbances, 280
inhibitors of transformation, 218
limitations, 292–293
manipulations, 291–307, 324
substrate analogs, 222–223
super sinks, 221–222
terrestrial ecosystem cycles, 216
transformations, 215–234

Oceans
color satellites, 82
food webs, 390
in situ diel estimation of GPP, 79, 80–81
isotopic composition of water, 183
Oligonucleotides probes, 142
Optimality, 384
Organic matter sampling, 186–189
Orographic effects, 266–267
Osmocote, 296, 298–299
Overestimation errors (OE), 38, 39
Overhead heaters, 360–362
Oxic zones, 90–91
Oxygen (O_2)
consumption in sediments, 90–91
daily changes, 79
exchange, 80–81
isotopic abundance, 182
light and dark bottle technique, 74–75
measurement of primary production, 73
organic matter, 189
respiration pathway, 87
total benthic mineralization, 88–89
water, 186
Winkler titration, 75
Oxygen/nitrate ratios, 88
Ozone (O_3), 243, 265, 269, 292
Ozone layer, 363

PAR. *See* Photosynthetically active radiation
Parsing phase, climate modeling, 374–375
Particulate organic carbon (POC), 145
Pattern analysis, 278
PCA (principal component analysis), 146
Pedogenic carbonates, 194
Pee Dee Belemnite (PDB), 182
Pelagic ecosystems, 138–150, 389–406
Peltier thermocouple psychrometry, 203
Peptidases, 145
Perpendicular vegetation index (PVI), 22–23
PFDs (flame photometric detectors), 243
PGEN model, 385
pH, 296, 297, 298, 331. *See also* Acidification; Hydrogen ions
Phosphoric acid, 215
Phosphorous (P)
deposition, 265
fertilizers, 298–300
as limiting nutrient, 293
mineralization, 218–219
nutrient transformations, 225
^{32}P tracer, 281
precipitation in soils, 298
transformation rates, 218, 219, 220
Photoacoustic infrared analysis systems, 243
Photography, 11–12, 21–22
Photoionization detector (PID), 243
Photosynthetically active radiation (PAR)
absorbed energy, 31
conversion efficiency (ε), 45–46
ε in the NPP algorithm, 50
inference of, 13
measurement of, 11
parameterization of ε, 46–49
Phytomass, 8, 17
Picea, 342
PID (photoionization detector), 243
Pin oak *(Quercus ellipsoidalis),* 154
Piscicides, 308–309
Piscivores, 310, 312
Piston velocity, 80–81
Planktonic systems. *See also specific components*
bacteria respiration, 143–146
biogeochemistry of food webs, 389–406
carbon cycling, 138–150
mortality estimation, 73
primary production, 72–73
Plant canopy analyzers, 36
Plant pressure chambers, 203–204
Plant–air interfaces, 241–242
Plants
compensatory growth, 154–156
gas emissions by, 241
gas exchange, 239
seasonality of digestibility, 152
transplanting, 323–324
water fluxes, 207–210
water resource partitioning, 189–190
water sampling, 184
whole root/shoot hydraulic conductance, 209–210
Plowing, 323
POC (particulate organic carbon), 145
Point and line intercepts, 22
Pollen records, 355

Pollutants. *See also specific pollutants*
atmospheric deposition, 265–276
delivery vectors, 266
effect on soil invertebrates, 319
modeling of, 165
Polycarbonate filters, 140
Population models, 374, 376, 377
Populus deltoides, 10, 14
Populus nigra, 10, 14
Potassium (K)
fertilizers, 299
as limiting nutrient, 293
and (NH_4^+) absorption, 297
production by decomposition, 104
release, 272
Potassium carbonate (K_2CO_3), 299
Potassium chloride (KCl), 299
Potassium hydroxide (KOH), 221, 299
Potassium nitrate (KNO_3), 299
Potassium permanganate ($PMnO_4$), 299
Potassium pyrophosphate ($K_4P_2O_7$), 299
Precipitation. *See also* Rainfall
and atmospheric deposition, 265
changes in patterns, 341
CLIMEX facility, 342–343, 359
isotopic composition, 183
nitrogen loss isotope fractionation, 132
predicted increases, 354
TDEs, 344, 347, 348
throughfall, 251, 342, 343, 344–345
volume measurement, 267–268
Predators, transplanted, 324
PRESS treatments, 333
Pressure chambers, 203–204, 210
Prey, transplanted, 310, 324
Primary productivity. *See also* Gross primary productivity; Net primary productivity
in aquatic ecosystems, 72–85
herbivores, effect of, 154–156
reaction, 72
schematic carbon flow, 33
Principal component analysis (PCA), 146
Production, definition, 32
Profiling radar scatterometers, 19
Pseudoreplication, 349
Pulse laser systems, 11
PULSE treatments, 333
Pulse-labeling techniques, 223
PVI (perpendicular vegetation index), 22–23
Pyrites, 88

Quantum light sensors, 9
Quartz bottles, 75
Quartz combustion furnace, 188
Quercus, 154, 342, 344

Radar, SAR, 17
Radar interferometry, 17–18
Radar profilers, 17, 23
Radar remote sensing, 14–18
Radar scatterometers, 8
RADARSAT, 17
Radiative transfer, 9
Radioisotopes. *See also* Isotopes; Isotopic methods; Stable isotopes
decomposition rates, 113
material flow, 377
production measurements, 143–144
SOM turnover studies, 117–137
sulfate reduction, 95–96
tracers of nitrogen cycling, 132
Rain forests, 265
Raindrop size, 343
Rainfall, 343–344, 362. *See also* Precipitation
Raleigh distillation effects, 133, 193
Rangefinders, 11
Reciprocal transplants, 109–110
Redox zonation, 86–87
Reflectances, 45
Relaxed eddy accumulation (REA), 174
Remote sensing, 8, 21
Reoxidation, 88
Representative sampling, 184
Rhizobium, 322
Riparian zones, 292, 311
Rivers, 79–81. *See also* Streams
RNA hypothesis, 395
Rock formations, 311
Rock phosphate, 296, 298
Roots
barriers to, 349
belowground biomass estimation, 59–60
estimated turnover, 62
measurement of length, 63–64
within soil, 318
whole-plant hydraulic conductance, 209–210
Rotenone, 309
Rotifers, 333
Roughness sublayer (RSL), 162, 167, 168
Routh-Hurwitz criteria, 383

Salinity, and trace gas solubility, 239
Sample collection
organic matter, 186–189
plot shape, 35
soil, 59, 254
soil water, 184
streams, techniques for, 252–253
trace gases, 174, 238
water, 184

wet deposition, 267–268
xylem water, 184
Sampling
conditional, 174
considerations, 187
continuous, 238, 279
designs, 279–280
destructive gravimetric, 345
double, 35–36
frequency, 40, 155–156
hydrologic methods, 252
instrument noise and, 171
MODIS, 14
representative, 184
size of quadrats, 35
stratified, 282–283
stratified random, 278–279
San Dimas Experimental Forest, 256
Sand, 89, 201
Sandbox experiments, 256–258
Sap, 208–209
Sap-feeders, 152
SAR (synthetic aperture radar), 17, 23
Satellite-born radiometers, 8
Satellites, 13–14, 22, 82. *See also specific projects*
SBLs (surface boundary layers), 161–163
Scatterometers, 16–17
SeaWiFS, 82
Secondary productivity, 31
Sediments
and benthic respiration in, 86–103
carbon mineralization pathways, 87
heat production by, 90
POC in, 145
redox reactions, 87
retrieved course, 89
Seebeck effect, 203
Seeding, 311
Seedlings, 362
Seines, 308, 309
Senescence, 32, 34–35, 241
Sensible heat flux, 174
Sensitivity analysis, 381–383
Shadows analysis, 12
Shoots, 209–210
Shrubland vegetation, 19–20, 23–24, 33, 35, 37
Shrubs, 12, 19
Sieving, wet, 105
Silver Springs model, 381
Simulation modeling, 229–230, 311–313
SIR-C, 18
SIR-C/X-SAR, 17
Size fractionation, 111
Size-efficiency hypothesis, 393
SLICER laser altimetry, 20
Snowmelt, 362
Sodium (Na), 269
Sodium *p*-nitrophenyl phosphate, 222
Software, 23
Soil. *See also* Soil organic matter; Soil water
acidification, 265
age, 130
biota, 318–320
biotic manipulations, 318–319
carbon cycling processes, 118
carbon mineralization, 112
carbon storage, 284
CENTURY soil organic matter model, 106
chemical properties, 357
direct warming, 359–360
food webs, 319–320
isotope dilution techniques, 226–229
laboratory studies, 324
landscapes, 278
lysimeter sampling, 254
matric potentials, 202, 345
mesofauna, 357
nitrogen cycling processes, 128
nitrogen flux, 133
organic matter dynamics, 104–116
respiration, 163
snow, effect of, 362
spatial variation, 346–348
surface roughness, 16
temperature, 356
tilling, 323
transplanting, 323
volumetric samples, 59
water potential, 199–207
Zobler soil texture database, 46
Soil heat flux plates, 168
Soil organic carbon (SOC), 123–125, 127
Soil organic matter (SOM)
additions to, 118
biological fractions, 111–113
$\delta^{15}N$ and depth, 132–134
definition, 110
internal transfers, 119
losses from, 118–119
mathematical models, 117–137
multi-box isotope models, 126–128
physical fractionation, 110–111
pools, 104–106, 117–118
stable nitrogen ratios, 128
transformations, 119
well-mixed one box model of N isotopes, 129–132
Soil psychrometers, 345
Soil resistance blocks, 345, 346

Soil water
  constraint on leaf area, 46
  content, 199
  extraction, 185
  manipulations, 357
  partitioning by plants, 189–190
  potential, 199
  reservoir, 354
  sampling, 184
  stress, 345
Solar energy, 45
SOM. *See* Soil organic matter
Sonic anemometers, 172, 174, 175
Source–sink relationships, 280
Spatial autocorrelation, 279
Species
  biotic manipulations, 308–310, 320–322
  global warming and ranges, 355
  introduction, 323–324
  keystone, 313
  transplants, 323–324, 357
Spectral analysis, 18, 23
Spectral vegetation indices (SVI), 45
Spodosols, 124, 134
SPOT, 13
SPOT HRV, 22
Springtails, 322
Stability analysis, 383
Stable isotopes, 181–198, 272–273, 280–281. *See also* Isotopes; Isotopic methods; Radioisotopes
Stand-level analyses, 12, 253–258
Stand-to-stand scale models, 9
Standard mean ocean water (SMOW), 182
Standard substrates, decomposition studies, 109–110
Standing dead compartments, 32, 34–35
Stands, 7–26
Stems, 8, 24–25, 185, 186–189
Steppes, 32, 37
Sterilization, 218–220, 320
Stocking, 309–310
Stoichiometry, ecological, 389–406
Stomata, 268
Stratified sampling, 278–279, 282–283
Streams, 79–81, 184, 252–253, 309
Strontium (Sr), 273
Sugar maple *(Acer saccharum),* 154
Sulfates, 87, 95–96, 251, 265, 269
Sulfides, 86–87, 88, 93
Sulfur (S)
  addition to soil, 292
  analysis, 243
  deposition, 252
  fertilizers, 299–300
  gas exchange, 239
  gas fluxes, 241
  inhibitors of oxidation, 218
  labeled fertilizers, 301
  as limiting nutrient, 293
  mass-balance calculations, 272
  nutrient-addition experiments, 294
  plant emissions, 241
Sulfur dioxide (SO_2), 243, 265, 268
Sulfur hexafluoride (SF_6), 239
Sulfuric acid (H_2SO_4), 221, 330, 332
Super sinks, 221–222
Surface boundary layers (SBLs), 161–163
Surface elevations, 17
Surface reflectance, 14, 15
SVI (spectral vegetation indices), 45
Swardstick, 19
Symplast, 201
Synthetic aperture radar (SAR), 17, 23
SYTO 13, 141

Tannins, 152
Taylor's frozen turbulence model, 171
TDR (time domain reflectometry), 204–206
TDEs (throughfall displacement experiments), 344, 347, 348
Temperature. *See also* Climate; Global warming; Heat
  climate manipulations, 357–362
  daily changes, 79
  reconstruction, 193
  soil, 356
  trace gas solubility, 239
  vertical profiles, 162
Tensiometers, 345, 346
Thermal dissipation, 209
Thermoclines, 239
Thermocouple psychrometry, 203
Throughfall, 251, 342–345
Throughfall displacement experiments (TDE), 344, 347, 348
Thymidine, 143
Timber, 12, 36, 37. *See also* Forests; Trees
Time domain reflectometry (TDR), 201, 204–206, 345–348
Topographic gradients, 356
Total root carbon allocation (TRCA), 62–63
Tower-based flux measurements, 162–163, 242
Trace gases. *See also* Gases
  analytical methods, 242–244
  biogenic, 235–248
  conditional sampling, 174
  estimation of fluxes, 235–242
  exchange at plant–air interfaces, 241–242
  history analysis, 244
  preconcentration, 241
Trace metals, 75, 78

Tracers. *See* Isotopic methods; Radioisotopes
Transpiration, 192
Transplants, 109–110, 323–324, 357
Trap nets, 308
Trawls, 308
TRCA (total root carbon allocation), 62–63
Tree rings, 187, 193–194
Trees. *See also* Forests; Timber
  biomass estimation, 37
  crown diameter, 12
  error in estimates of growth, 40
  fractal models of, 9
  height estimation, 19
  mortality estimation, 40
  three-dimensional structure of canopies, 25
  vectorization method, 25
  2,3,5-Triphenyltetrazolium chloride, 222
Trophic cascades, 312
Tropocyclops extensus, 337
Tundra, 108, 292, 356
Turbulences, 239
Twigs, 36–37

Ultrasonic rangefinders, 11
Ultraviolet radiation, 356, 363–364
Understory light sensors, 11
Upper system boundary (USB), 163
Urea, 296

V-notch weirs, 252
Vapor pressure deficit (VPD), 51
VCL (vegetation canopy LIDAR), 12
Vegetation. *See also* Plants; *specific types*
  carbon sequestration potential, 341
  classification of landscapes, 278
  definition of structure, 7
  transplants, 357
  visual estimation, 8
Vegetation canopy LIDAR (VCL), 12
Vertical descriptors, 8
Vertical leaf area distribution, 25
Vertical stereo photographic pairs, 19
Videography, 12–13, 63
Volatile organic carbon (VOC), 238–239, 241
Volumetric water content of soils (θ_v), 199, 200, 201–202

Walker Branch Throughfall Displacement Experiments (TDEs), 344, 347
Walleye *(Stizostedion vitreum vitreum),* 314
Warming. *See* Global warming; Temperature
Water. *See also* Soil water; Xylem water
  acid levels, 331
  availability and uptake, 199–214
  biogeochemistry, 277
  canopy capacitance, 35
  carbonic acid in, 331
  chemical potential, 200–201
  ecosystem-level relations, 181–198
  in the environment, 199–201
  grassland productivity, 33
  hydrogen concentrations, 185–186
  isotope pulse dynamics, 191–192
  manipulation studies, 311, 324, 341–352
  ^{18}O measurement, 73
  oxygen concentrations, 185–186
  and radar backscatter, 16
  recycling, 193
  regional quality, 249
  resource partitioning, 189–190
  sample collection and storage, 184–185
  short-term use, 189–192
  sources, 194–195
  use efficiency, 192
  vacuum line separation, 188
  verification of treatments, 345–348
Water drawdowns, 308
Water potential, 201, 202–204
Water stress, 192, 345
Water vapor, 162, 243
Water–air interface, 239–241
Watersheds, 250–253, 280
Weather, 348. *See also* Climate
Well-mixed box models, 119–123
Well-mixed one box models, 129–132
Wells, 184
Wet deposition, 266, 267–268
Wetlands, 239, 292, 311
Whole-ecosystem-level budget, 249
Wind
  eddy covariance, 168
  friction velocity, 167
  greenhouses, effect of, 359
  landscape scale biogeochemistry, 277
  oxygen exchange, 80–81
  trace gas concentrations, 239
Winkler titration, 75
Wires, soil warming, 359–360
Wood. *See* Timber
Woody debris, 109, 311
Würgler bags, 94

X-ray microanalysis, 401
Xylem water, 184, 191–192, 208–209

Zero-tension lysimeters, 254
Zinc (Zn), 78
Zobler soil texture database, 46
Zooplankton, 333, 334, 393–396